A Formal Modeling Approach to Understanding Stone Tool Raw Material Selection in the African Middle Stone Age:

A Case Study from Pinnacle Point, South Africa

by

Simen Oestmo

A Dissertation Presented in Partial Fulfillment
of the Requirements for the Degree
Doctor of Philosophy

Approved April 2017 by the
Graduate Supervisory Committee

Curtis W. Marean, Chair
C. Michael Barton
Kim Hill
Marco A. Janssen
Todd Surovell

ARIZONA STATE UNIVERSITY

May 2017

ABSTRACT

The South African Middle Stone Age (MSA), spanning the Middle to Late Pleistocene (Marine Isotope Stages (MIS) 8-3) witnessed major climatic and environmental change and dramatic change in forager technological organization including lithic raw material selection. *Homo sapiens* emerged during the MSA and had to make decisions about how to organize technology to cope with environmental stressors, including lithic raw material selection, which can effect tool production and application, and mobility.

This project studied the role and importance of lithic raw materials in the technological organization of foragers by focusing on why lithic raw material selection sometimes changed when the behavioral and environmental context changed. The study used the Pinnacle Point (PP) MSA record (MIS6-3) in the Mossel Bay region, South Africa as the test case. In this region, quartzite and silcrete with dramatically different properties were the two most frequently exploited raw materials, and their relative abundances change significantly through time. Several explanations intertwined with major research questions over the origins of modern humans have been proposed for this change.

Two alternative lithic raw material procurement models were considered. The first, a computational model termed the Opportunistic Acquisition Model, posits that archaeological lithic raw material frequencies are due to opportunistic encounters during random walk. The second, an analytical model termed the Active-Choice Model drawn from the principles of Optimal Foraging Theory, posits that given a choice, individuals will choose the most cost effective means of producing durable cutting tools in their environment and will strategically select those raw materials.

An evaluation of the competing models found that lithic raw material selection was a strategic behavior in the PP record. In MIS6 and MIS5, the selection of quartzite was driven by travel and search cost, while during the MIS4, the joint selection of quartzite and silcrete was facilitated by a mobility strategy that focused on longer or more frequent stays at PP coupled with place provisioning. Further, the result suggests that specific raw materials and technology were relied on to obtain food resources and perform processing tasks suggesting knowledge about raw material properties and suitability for tasks.

Til Mamma, alltid i mitt hjerte

ACKNOWLEDGMENTS

First, I want to acknowledge my advisor, Curtis W. Marean for giving me this opportunity and supporting me throughout this research process. I would also like to thank him for his generous sharing of project vehicles, project equipment including computer facilities, lab space, and storage space both at Arizona State University and in Mossel Bay, South Africa. I would like to acknowledge my committee members Michael Barton, Kim Hill, Marco Janssen, and Todd Surovell for their contributions to making this research possible and for comments on previous drafts. I would also like to thank Geoff Clark and Arjun Heimsath. I am forever grateful to Kyle Brown for his guidance and inspirational peptalks when I started this journey. I am also grateful to Haley Cawthra and Kerstin Braun for their gracious sharing of marine geophysics and speleothem data respectfully. This effort would not have been possible without their contributions.

This research would also not have been possible without the MAPCRM team at the Dias Museum, directed by Betina du Plessis. She and her team work tirelessly to maintain the lab and its collections, always providing lab space for analysis. They also provide superb field support as one of the greatest excavation teams on the planet.

Thank you to friends and colleagues including Benjamin Schoville, Terry Ritzman, Jayne Wilkins, Hope Williams, Jocelyn Bernatchez, Jake Harris, and many others that have been supportive along the way and kept me going.

This research was made possible by two fellowship awards for PHD directed studies from the Norway-America Association and American-Scandinavian Foundation's Haakon Styri Scholarship and Andrew E. and G. Norman Wigeland Fund, a Graduate

Education Dissertation Fellowship from ASU's Graduate Education College, and a Doctoral Dissertation Research Improvement Grant from the National Science Foundation (#1602347).

I would like to thank my family, including the Norwegian side (Mom, Dad, Even, Solvei, Mina, and Fride) and the American side (Cinda, George, Murray, Carla, and Clay) for their encouragement and support during the course of this endeavor. Finally, I would like to express my highest praise and heartfelt appreciation to my wife Tove for her unwavering belief in me, and for always being the proverbial 'rock' I could lean on in times of need. Thank you for always being supportive and enduring this long journey with me.

TABLE OF CONTENTS

Page

CHAPTER Page

CHAPTER Page

LIST OF TABLES

Table Page

Table Page

Table Page

Table Page

Table Page

Table Page

Table Page

Table Page

Table Page

Table Page

Table Page

Table Page

Table Page

Table Page

Table Page

Table Page

Table Page

Table Page

Table Page

Table Page

Table Page

Table Page

Table Page

Table Page

Table Page

Table Page

Table Page

Table Page

Table Page

Table Page

Table Page

Table Page

Table Page

Table Page

Table Page

LIST OF FIGURES

Figure Page

Figure Page

Figure Page

Figure Page

Figure Page

Figure Page

Figure Page

Figure Page

Figure Page

Figure Page

Figure Page

Figure Page

Figure Page

CHAPTER 1: PROJECT INTRODUCTION

Introduction

The South African Middle Stone Age (MSA), spanning the Middle to Late Pleistocene witnessed major climatic and environmental change and dramatic change in forager technological organization including stone tool raw material selection. The MSA lasted from ~300 ka, maybe as early as 500 ka to ~35 ka (Deino and McBrearty 2002, Herries 2011, Johnson and McBrearty 2010, Marean and Assefa 2005, Tryon and McBrearty 2002), spanning minimally Marine Isotope Stage 8 (MIS8) to MIS3. Genetic research (Fagundes et al. 2007, Gronau et al. 2011, Henn et al. 2011, Relethford 2008), the fossil record (Bräuer, Deacon, and Zipfel 1992, Day 1969, Hublin 1992, White et al. 2003), and the archaeological record (Clark et al. 2003, Marean 2010b, McBrearty and Brooks 2000, Shea 2008) strongly suggest that modern humans emerged during the Middle to Late Pleistocene, coinciding with the African MSA.

These prehistoric hominin hunter-gatherers lived in a dynamic world wherein survival depended upon decisions about how to organize technology to cope with environmental stressors. Since anatomically and behaviorally modern *Homo sapiens* emerged during the MSA, any decisions these forager groups made that enabled the continued survival of the human lineage are of particular interest. When organizing technology, potentially crucial decisions were made about raw material choice for stone tool production and application. The raw material selection stage is potentially important as it can set the range of possibilities for the later tool production and tool application. Because stone tools are the most predictably durable aspect of the archaeological record and were an important part of prehistoric technology, they provide an excellent

opportunity to study the technological organization of prehistoric foragers in relation to environmental challenges.

Following the Oldowan, decisions regarding stone tool raw material selection, the changing use, and co-use of different stone tool raw materials is well known from a wide range of environmental and climatic contexts, time-periods, and 'cultures' (Andrefsky Jr 1994, Bamforth 1990, Bar-Yosef 1991, Braun et al. 2009, Clark 1980, Goldman-Neuman and Hovers 2012, Jelinek 1991, Kuhn 2004, 1991, Stout et al. 2005). However, there is disagreement about why raw material patterns change, and the role and importance of stone raw material choice in the technological organization of foragers (Ambrose and Lorenz 1990, Binford and Stone 1985, Binford 1979, Brantingham 2003, Clark 1980, Deacon 1989, Gould 1985, Gould and Saggers 1985, Kuhn 2004, Mackay 2008, McCall 2007, Stout 2002, Torrence 1986, Wurz 1999).

Based upon Optimal Foraging Theory (OFT) models (Stephens and Krebs 1986) it is often assumed that all species of animals, including humans, are utility efficient (Alexander 1996, Krebs and Davies 1984) and choices are made to achieve maximum return on investments of time and energy (Bleed 1986, Nelson 1991, Torrence 1983). Raw material choices may also have been made due to style preference (Close 2002, Mackay 2011, Sackett 1982, 1986) and symbolic value (Clendon 1999, Gould, Koster, and Sontz 1971, Wurz 1999), which may be motivated by other goals. This dissertation focuses on two broader questions. First, what is the role and importance of stone raw materials in the technological organization of foragers? Second, why did some prehistoric foragers, while having several stone raw material options available, change their lithic raw material preference when the behavioral and environmental context changed?

To address these two broader questions this dissertation investigates raw material selection by early anatomically modern human foragers who lived in the Mossel Bay region (**Figure 1**) on the south coast of South Africa during the South African MSA.

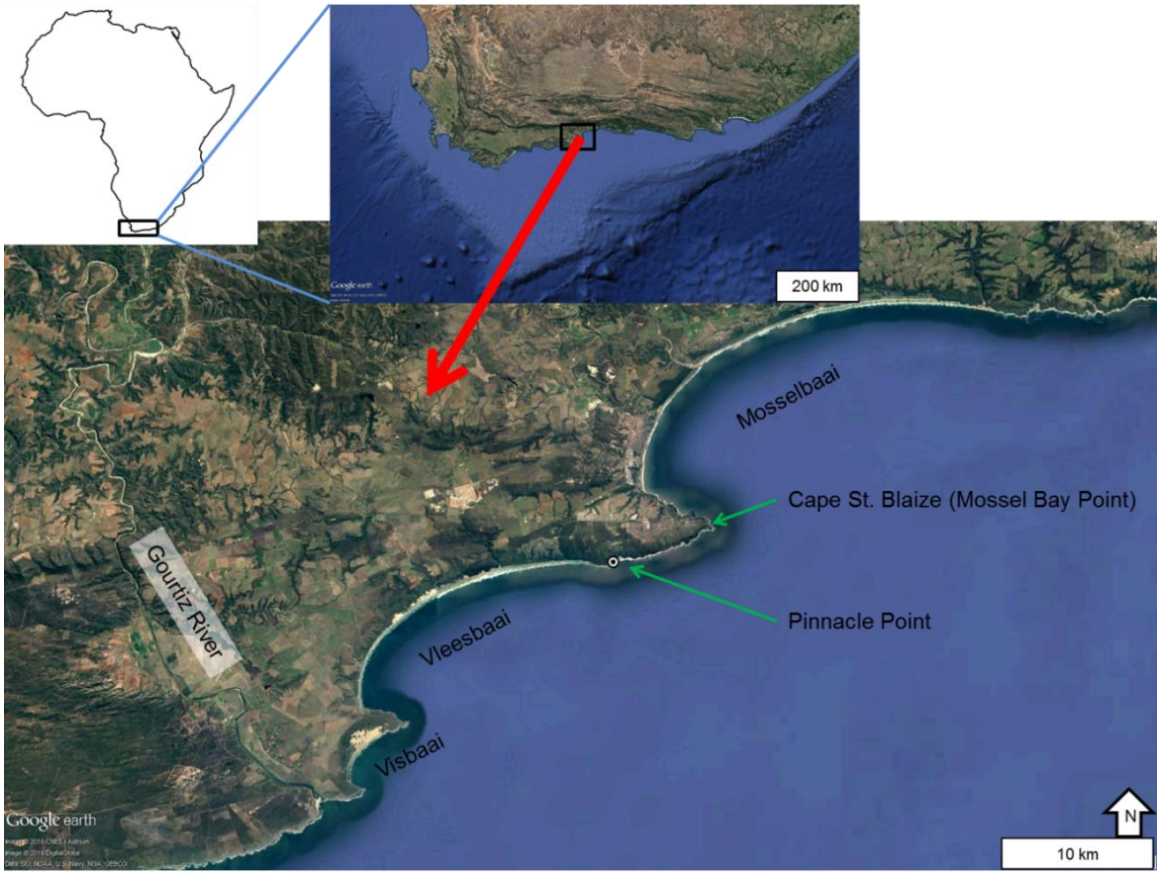

Figure 1. The location of the Mossel Bay region. Location of Pinnacle Point also shown. Satellite Imagery from Google Earth Pro 7.1.5.1557.

The Mossel Bay region has several MSA sites (**Figure 2**) that combined yield a long archaeological sequence that is well suited for the study of raw material selection during important periods of human evolution. The archaeological sequences from these sites have been excavated with great precision, are thoroughly dated (Brown et al. 2012, Brown et al. 2009, Jacobs 2010, Marean et al. 2010, Marean et al. 2007), and are complemented by local paleoclimatic and paleoenvironmental records of high resolution

(Albert and Marean 2012, Bar-Matthews et al. 2010, Braun et al. ms, Copeland et al. 2015, Esteban et al. 2016, Fisher et al. 2010, Marean et al. 2014, Matthews et al. 2011, Matthews, Marean, and Nilssen 2009, Rector and Reed 2010). In addition, the local geology is well understood (Cawthra et al. 2015, Malan and Viljoen 2008, Pickering et al. 2013, Roberts et al. 2012, Thamm and Johnson 2006, Viljoen and Malan 1993), and thorough surveys for stone raw material sources have been undertaken (Brown 2011, Oestmo et al. 2014).

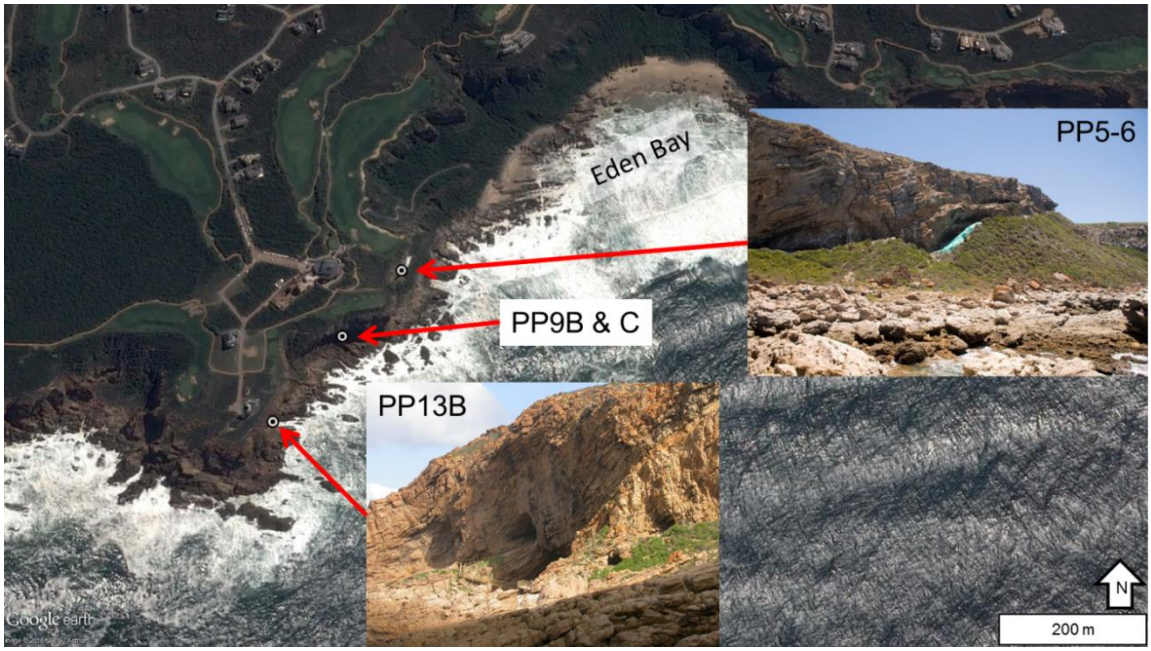

Figure 2. Location of Pinnacle Point sites. Satellite Imagery from Google Earth Pro 7.1.5.1557. Images of localities by the author.

The MSA stone tool record from the Mossel Bay region ranges from ~164-48 ka, which temporally overlaps a wide range of stone tool variation along with some notable technologies including the early microlithic (Brown et al. 2012) and Howiesons Poort (Brown et al. 2012, Brown et al. 2009) at site Pinnacle Point 5-6 (PP5-6). In addition to the Still Bay that is of similar age to the early microlithic and is observed at nearby localities, they figure heavily in the study of the origin of modern human behavior

(Brown et al. 2012, Deacon 2001, Henshilwood and Dubreuil 2011, Henshilwood and Marean 2003, Klein 2000, McBrearty and Brooks 2000, Shea 2011). In the early microlithic, Still Bay, and Howiesons Poort foragers shifted to a regular use of fine-grained raw materials in addition to the use of more coarse-grained quartzite, and the reasons for this are debated (Ambrose 2006, Ambrose and Lorenz 1990, Brown 2011, Deacon 1989, Mackay 2008, McCall and Thomas 2012, McCall 2006, Minichillo 2006, Wurz 1999).

The PP13B and PP9 records that precede the PP5-6 record shows a long record of procurement of quartzite from cobble beaches or other secondary sources (Thompson, Williams, and Minichillo 2010). In the PP5-6 record there is a marked increase in the selection of silcrete early in the MIS5 part of the sequence, and then particularly during MIS4 that coincides with an increase in procurement from primary outcrop sources, and the shift to a more blade-based technology (Brown 2011, Wilkins et al. 2017). This study investigates the following questions to help clarify why there is a change in raw material frequencies in the early microlithic and Howiesons Poort stone tool technologies at PP5-6. First, are the lithic raw material frequencies observed in the Pinnacle Point MSA record due to opportunistic behavior or strategic choice? Second, if strategically chosen, in what contexts, environmentally and/or behaviorally, was it more efficient to use quartzite rather than silcrete to produce and use stone tools?

Two mutually exclusive models facilitate testing of hypotheses about raw material selection and creating expectations that can be applied to the archaeological record at Pinnacle Point. First, a computational model of stone tool raw material procurement termed the Opportunistic Acquisition Model (OAM) is evaluated. The OAM posits that

archaeological raw material type frequencies are due to opportunistic encounters with stone sources during random-walk (see Brantingham (2003)) in the environment. Second, an analytical resource-choice model termed the Active-Choice Model (ACM) drawn from OFT is presented, which posits that a forager when selecting a stone raw material will try to maximize the amount and duration of tool cutting edge produced per unit time investment in producing the tool. While there may be other variables important to raw material choice, our formal models must begin simply and then expand later, and tool cutting edge is a widely recognized variable of interest (Braun 2005, Brown 2011, Mackay 2008). The study of raw material selection is well suited to the OFT approach because raw material decisions are part of a tool making process where the decisions can be modeled as optimization problems (Kuhn 1994, Metcalfe and Barlow 1992, Surovell 2009).

To evaluate hypotheses drawn from the OAM and ACM, model outcomes under three different model conditions (MIS4, MIS5, and MIS6) are compared to archaeological raw material frequency data from PP13B, PP9, and PP5-6 at Pinnacle Point. To identify the conditions that could shift raw material frequencies under the different MIS conditions I compare the model outcomes under two derived environmental effects (coastline position and raw material source distribution, and vegetation type) and one derived behavioral effect (mobility rate and strategy) to archaeological frequencies.

Following the evaluations of the hypotheses, a sensitivity analysis of each model is conducted to examine the robustness of the model outcomes with respect to changes in parameter values. Additionally, one model constraint assumption is tested, which is what

effect the presence of offshore silcrete sources during lower sea-levels has one the raw material frequencies. The sensitivity analysis (one-factor-at-the-time – OFAT) for the OAM includes: 1) changing the amount of time the forager can move about the landscape; 2) simulating what happens when Pinnacle Point is not an exclusive site on the landscape but instead one of three that the forager can return too; 3) changing independent behavioral variables one at the time to look at the effects on raw material outcome; 4) changing behavioral variables wholesale to simulate curated, expedient, and site caching behavior. For the ACM, the sensitivity analysis includes changing the assumed currency. The two alternative currencies are the amount and duration of cutting edge on blades produced per unit time investment in producing the blade, and the amount of blades and duration of cutting edge on those blades produced per unit time investment in producing the blade.

Intellectual merit and broader impacts

In the social sciences, there is an ongoing growth in the development of formal modeling of human behavior and social and cultural systems. This research significantly contributes to archaeological method and theory. Changing raw material patterns are evident in many if not most archaeological sequences in any time-period, and although some previous studies (e.g. Brantingham 2006, 2003, Pop 2015) present formal models to address this issue, a more comprehensive methodological framework using two mutually exclusive formal models that specifically target raw material selection is missing in the archaeological literature. To rectify this, this project produces a framework of two formal models (one computational and one analytical) of raw material selection that can be

applied to other examples of tool resource choice regardless of raw material type in archaeological sequences throughout the world. Formal models are important tools in any scientific enterprise and their strength lay in the fact that they are logically grounded, thus making it is easier to pinpoint why a model is supported or not. All models must begin simply, and this research, through its use of two simple models, illustrates how formal models can be applied to questions of technological change and the procurement of materials and thus contributes to that ongoing development of social science modeling.

This study explores the formative period of modern human origins, where our human ancestors faced climatic and environmental change, to explore how raw material choices were developed and elaborated in one of the most ancient and longest living of human technologies: stone tool technology. The two formal models (one computational and one analytical) of raw material selection presented here, employ several independent methods (agent-based computational modeling, analytical modeling, and experimental archaeology) that build on efforts by Barton and Riel-Salvatore (2014), Brantingham (2003, 2006), and Surovell (2009). This investigation differs from previous studies with an informal approach (e.g. Ambrose and Lorenz 1990, Binford and Stone 1985, Brown 2011, Gould and Saggers 1985, McCall 2006, Minichillo 2006) because it simultaneously considers different hypotheses and the effects independent variables have on raw material selection, is formal (analytical and computational), and calculates net-return rates of raw material selection as the environmental and behavioral context changed by using high-resolution climate/environmental data from the Mossel Bay region. The study provides net-return rates on stone tool raw material selection that will be integrated into the 'Paleoscape model' project for the Mossel Bay region and contribute to the

comprehensive model of hunter-gatherer resources (Franklin et al. 2015, Marean et al. 2015).

Additionally, this research makes significant contributions to the Modern Human Origins debate. The project aims to settle a debate concerning rapid shifts in raw material selection that is evident at the onset of new climatic and environmental conditions in the late Pleistocene during the African Middle Stone Age (MSA). This research will provide needed clarity as to whether lithic raw material selection was a strategic behavior or if other lifestyle constraints caused the observed raw material pattern. Moreover, the research will highlight if the cultural adaptive response to climatic and environmental change in the MSA was driven by a mobility strategy that precluded any specific investment in stone technology and only prioritized moving people to the food resources, or if the response was an increased reliance on technological innovation facilitated by strategic selection of raw materials that demanded technical insight in raw material characteristics.

Organization of dissertation

Chapter 2 provides a literature review starting with the concept of technological organization and how it is linked to the concepts of mobility systems and foraging strategies. It then reviews informal and formal models that have been proposed to explain technological change when corresponding with behavioral and/or environmental change. Then the chapter turns to raw material selection, the role and importance of raw materials in the technological organization of foragers, and the concept of raw material quality including a summary of examples of ethnographic observations of raw material selection.

This is followed by a review of the application of mechanical testing to lithic raw material, and the examination of other claims for why raw materials are selected. At the end of the chapter, I organize the models that have been proposed for explaining why raw materials change in the archaeological record into a framework with two broad categories called ‘Non preference-based change’ and ‘Preference-based change’.

Chapter 3 provides a review of raw material selection in the African Early (ESA) and Later Stone Age (LSA), and then a thorough review of the evidence for raw material selection from the Middle Stone Age (MSA) record from South Africa. At the end of the chapter, I present the existing informal models proposed to explain raw material selection and thus change in archaeological raw material frequencies in the South African MSA.

Chapter 4 provides an in-depth overview of the geology of the Mossel Bay region presents pertinent data on lithologies and sources types that are pertinent to this study. Both onshore and offshore data are presented.

Chapter 5 outlines the models and hypotheses evaluated in this study. This is followed by a full presentation of the Opportunistic Acquisition Model (OAM) and Active-Choice Model (ACM). The OAM is presented using the ODD (Overview, Design concepts, and Details) protocol for presenting agent-based models. Then the ACM is presented. The ACM has two variants called the (ACM-P (sequential encounter and embedded procurement; travel and search time-cost is excluded) and the ACM-R (simultaneous encounter and direct procurement; travel and search time-cost is included) and both are detailed. A description of the variables needed to calculate the net-return rates used in the ACM is presented. After presenting the models, the model conditions and model condition variables are described. The model conditions are Marine Isotope

Stages 6, 5, and 4, while the model condition variables are coastline position and raw material source distribution, vegetation type, and mobility rate and strategy. Then the hypotheses drawn from both models are presented. This is followed by the presentation of a testing framework that will be used to evaluate the model outcomes for both the OAM and the ACM. Finally, predicted relationships between time-costs and the three different model condition variables are presented. The predicted relationships show how different time-costs potentially relates to model conditions variables thus can potentially explain archaeological raw material frequencies during the different model conditions.

Chapter 6 presents the methods used in this study. It starts by detailing how the Opportunistic Acquisition Model (OAM) was constructed. The building blocks of the OAM include geological and geophysical data, raw material survey data, GIS analysis, and agent-based modeling. Second, I describe how the variables needed for both variants of the Active-Choice Model were obtained. Methods used to obtain estimates of variable values includes a stone tool reduction experiment, a raw material quality and fracture mechanics experiment, published data, raw material survey data, and GIS analysis. The chapter ends with describing how archaeological data were recorded and analyzed, including artifact metric attributes, raw material frequency, cortex type, cutting edge/mass ratios, and the ratio of retouch frequency to artifact volumetric density.

Chapter 7 presents the archaeological record from Pinnacle Point (PP). It starts with summarizing the site chronologies and stratigraphy of PP13B, PP9, and PP5-6. Then the stone tool data from these sites that are relevant for evaluating archaeological expectations are presented. Stone tool data are first presented by MIS designation using the major stratigraphic aggregate from the three different sites. Then all three sites will be

presented together at the stratigraphic aggregate level. Additionally, raw material frequency data on the sub-aggregate level from PP5-6 are presented.

Chapter 8 presents the Opportunistic Acquisition Model (OAM) modeling results. First, the raw material frequency result of same-day return simulations are presented and compared to archaeological frequencies under the different model conditions. Second, the model outcome of simulations where the forager can move for longer time away from the Pinnacle Point locality are presented (the first round of the one-factor-at-the-time (OFAT1) sensitivity analysis) and compared to the archaeological raw material frequencies under the different model conditions. Then I evaluate Hypothesis 1 (H_1) drawn from the OAM. The first step in the evaluation was to investigate the assumption whether it is realistic to move randomly in relation to raw material sources in the Mossel Bay region. The key criterion examined is the time without raw material in the toolkit. The next step was to evaluate H_1 based on the result of the same-day return simulations and the results of the OFAT1 sensitivity analysis. Following the discussion of these results, a set of results from round 2 (OFAT2), 3 (OFAT3), and 4 (OFAT4) of the sensitivity analysis is presented with subsequent discussions of those results. The goal of the sensitivity analysis was to gauge the effect different model parameters have on the raw material output thus checking the robustness of the initial Hypothesis 1 evaluation conclusion.

Chapter 9 first presents the obtained measurements and estimates of the variables needed in the Active-Choice model (ACM). Starting with the currency variables, *e* (cutting edge per mass) and *d* (cutting edge durability), then looking at the actual currency, which is *e* times *d* (cutting edge per mass multiplied by the duration of use

before dulling). This followed by the presentation of the t_s (raw material travel and search time-cost), t_p (raw material procurement time-cost), m_1 (wood fuel for heat-treatment travel and search time-cost), m_2 (heat-treatment time-cost), and m_3 (flake manufacturing time-cost) variables.

Chapter 10 presents the net-return rates under all model conditions for both the ACM-P (sequential encounter and embedded procurement; travel and search time-cost is excluded) and ACM-R (simultaneous encounter and direct procurement; travel and search time-cost is included) variants are presented. Raw material rankings are created based on the net-return rates and compared to archaeological raw material frequencies under five different model conditions. Then the model outcomes under three different model condition variables are presented to understand whether changes in individual time-costs drive the net-return rates and thus explain the archaeological raw material frequencies. The presentation of the model outcomes allows for a ranking that can be used compare to archaeological frequencies. Then, the comparison to the archaeological frequencies, which allows for testing predicted relationships between time-costs and model condition variables, are presented.

The last section of the chapter presents the evaluation of Hypothesis 2 (H_2) and Hypothesis 3 (H_3) from the Active-Choice Model (ACM) using two alternative currencies. The AMC-P (embedded procurement; excludes travel and search time-cost) net-return rates are used to evaluate H_2, while ACM-R (direct procurement; includes travel and search time-cost) net-return rates are used to evaluate H3. Both these currencies are then used to gauge whether individual time-costs under the three different model condition variables can explain archaeological raw material frequencies.

Chapter 11 discusses potential issues and problems with the Active-Choice Model and the Opportunistic Acquisition Model.

Chapter 12 presents a synthesis and discussion of the results of both models and put the results in a broader context.

Chapter 13 presents the conclusions of this study.

CHAPTER 2: LITERATURE REVIEW

Introduction

The focus of this chapter will be on reviewing the broader theoretical, experimental, and archaeological context that the concept and act of lithic raw material selection are based in. The raw material selection stage in lithic manufacture is potentially important as it can set the range of possibilities for the later tool production and tool application. However, lithic raw material selection is only one facet of how hunter-gatherers organize their technology, which makes it necessary to discuss the concept of technological organization and how it is linked to hunter-gatherers movement and subsistence strategies. Thus, this dissertation takes an organizational approach (c.f. McCall 2012) to investigate technological change.

In this chapter, I will first review the concept of technological organization and how it is linked to the concepts of mobility systems and foraging strategies. A summary then follows of proposed informal models to explain technological change when corresponding with behavioral and/or environmental change. Then I will provide a review of optimal foraging theory and its application to archaeology, followed by a summary of formal models that have been utilized to explain technological change when corresponding with behavioral and/or environmental change. Then the chapter turns to raw material selection with a focus on the role and importance of raw materials in the technological organization of foragers. This is followed by a review of the concept of raw material quality and the application of mechanical testing to lithic raw materials. Then I examine other claims for why raw materials are selected by including a summary of examples of ethnographic observations of raw material selection. At the end of the

chapter, I organize the models that have been proposed to explain raw material frequencies in archaeological records and why sometimes the raw material frequencies change.

Technological organization, mobility systems, and foraging strategies

Prehistoric hunter-gatherers lived in a dynamic world, where on a yearly, monthly, weekly, and even daily basis the weather changed, and seasons came and went, which in turn had a potential effect on the subsistence base. Moreover, through the lifetime of an individual hunter-gatherer or over a couple of generations, the climate changed and the environment was altered drastically by geophysical processes such as coastline change and biological processes such as vegetation change, which in turn could change the subsistence base. Thus, in any given environmental context, a hunter-gatherer group had to make decisions about how to organize technology that could affect survivorship of the group in an environment, potentially including raw material selection, when they faced problems such as time stress (Torrence 1983), energy costs (Bleed 1986), mobility requirements (Binford 1979, Kelly 1988, Shott 1986, Torrence 1983), resource procurement scheduling (Binford 1979), risk management (Bousman 1993, Torrence 1989), and raw material availability (Andrefsky Jr 1994, Bamforth 1986, Gould and Saggers 1985, Kelly 1988). These problems were all obstacles to achieving maximum return on investments of time and energy (Bleed 1986, Nelson 1991, Torrence 1983).

Nelson (1991: 57) defined technological organization as "the selection and integration of strategies for making, using, transporting, and discarding tools and the materials needed for their manufacture and maintenance." Technological organization

can also refer to a tactic, which is the means to implementing strategies. Moreover, Nelson (1991: 58) defined strategies as "problem-solving processes that are responsive to conditions created by the interplay between humans and their environment." or differently, strategies are a set of contingent rules for how to behave on specified constraint values. Insights into the technological organization of a prehistoric forager group can be gained by using sequence models in archaeology by studying the steps taken to produce tools (Bleed 2001). Several studies suggest that stone tool production is affected by the mobility strategy of a given forager group (Andrefsky 1991, Bamforth 1991, 1990, Kelly 1988, Parry and Kelly 1987, Torrence 1989, 1983). This suggests that aspects of the technological organization of a forager group can act as a proxy for mobility and foraging strategies. What this means is that by studying technological organization it is possible to infer about forager mobility and foraging strategies. Faunal and floral remains can also provide evidence for mobility and foraging strategies (see Winterhalder and Smith 2000 for review). By using multiple proxies, it is possible to build a more robust and complete picture of foraging strategies.

Mobility is one of the distinguishing characteristics of hunter-gatherers (Kelly 1995: 111) and should be considered an important research focus because many aspects of a hunter-gatherer's life such as resource foraging, religion, kinship, trade, artistic, and personal obligations are influenced by mobility (Kelly 1992: 48). It is important to point out however that these connections between mobility and hunter-gatherer lifeways are often hypothetical and rarely empirically demonstrated. The emphasis on foraging life and mobility does not imply that mobility is seen as being the deterministic factor on hunter-gatherer lifeways, but rather that the aspects of hunter-gatherer life and mobility

are inter-linked. Kelly (1983: 277) defined hunter-gatherer mobility strategies as "the way in which hunter-gatherers move about a landscape over the course of a year." This is different daily foraging in which resources are acquired." In addition, Kelly (1983: 277) defined mobility strategies as "one facet of the way in which hunter-gatherers organize themselves in order to cope with problems of resource acquisition." As Kelly (1992: 60) put it: "there are no Gardens of Eden on earth, no single locales that can provide for all human needs. Mobility-residential, logistical, long-term, and migration was the first means humans used to overcome this problem. Changes in the way humans choose to be mobile dramatically affect other aspects of human life, from demography to enculturation. Theoretically, then, mobility must be critical to understanding human evolutionary change." The challenge is how to operationalize methods in the form of models to gauge mobility and linked concepts such as food and resource procurement in the archaeological record.

Binford created much of the theoretical foundation for explaining technological change and organization and its link to mobility systems and foraging strategies (Binford 1980, 1979, 1978, 1977). Binford presented dichotomies where he conceptualized a range of different technological strategies that the hunter-gatherer could utilize to cope with environmental problems and resource distribution (Brown 2011).

In 1977, based on observations of Nunamiut gear use during hunting trips, Binford presented preliminary expectations for the technological composition of archaeological assemblages. Binford (1977) documented that gear that was transported on hunting trips almost always was returned back to their residential camp and that even broken equipment seldom failed to make it back. Tools that did not make it were either

lost or purposefully discarded, while equipment left at task-specific localities reflected the result of work that had been done there. He introduced the concepts of 'curated' and 'non-curated' technology but the two hypothetical extremes were used without regard to procurement strategy (Brown 2011). The Nunamiut 'curated' their equipment according to Binford.

Later, in 1979 Binford introduced the concepts of 'household' and 'personal' gear that is distinct from 'situational' gear. Household and personal gear were classified as gear made for anticipated or scheduled tasks, while situational gear was classified as gear made and used out of necessity due to unanticipated events (Binford 1979). Household and personal tools were made of materials that have been deliberately selected for that purpose, meaning materials suited for that task, and such household and personal tools were curated. On the other hand, situational gear was made expediently on the spot and made out of materials available on the landscape or materials that have been stored and was intended to be used for another purpose. Binford proposed that this difference between household/personal and situational gear can explain how intra-assemblage variation can be partly explained by convergence. Thus, planned tools and expediently made tools may be used for the same purpose but they were produced differently (Brown 2011).

Based on his fieldwork observation, Binford (1979) asserted that raw material procurement was usually embedded in other subsistence activities that the hunter-gatherers had scheduled. Further, he contended that raw material acquisition rarely happens by direct and devoted forays with the sole purpose of collecting stones. Instead, he proposed, the variability in the proportion of stones in the archaeological assemblages

is the function of the scale of the habitat that has been exploited from the locality but also the function of discard of tools that have been previously manufactured at some other locality. The Nunamiut were observed to always collect raw materials when they encounter them during scheduled subsistence activities. The encountered raw materials were then stored on the landscape at locations that the Nunamiut would likely visit again during other scheduled activities (Binford 1979).

Although it was important that Binford used ethnographic observations (direct observation leading to empirical data on forager behavior) to build his expectations for archaeological assemblages it is important to note that Binford was observing the use of rifles, steel knives, and sleds among other things. These objects have very different use-lives compared to objects used by Stone Age hunter-gatherers. Curation (maintenance) of a steel knife is different than curation of a stone tipped knife.

In 1980, Binford (1980), following Beardsley et al. (1956) and Murdock (1967), demonstrated that hunter-gatherer mobility maps onto variation in the environment. One of the proxies that Binford used for the environment was the effective temperature (ET) measure, which although is sensitive to seasonality, was used to show that there is a systematic relationship between environments and hunter-gatherer settlement types. Then, while looking at ethnographic data about hunter-gatherers, Binford divided the variability in hunter-gatherer foraging strategies into two broad strategies, called foragers and collectors, and then described the probable archaeological signature of each settlement type (Binford 1980).

The forager strategy rests on the concept of residential mobility (Binford 1980). In short, residential mobility is the movement of the entire group from one location to

another, where the hunter-gatherers move the consumers, themselves, to the resources. The foragers use an encounter-based strategy, and gather food on a daily basis and seldom store food. Resource distribution and group size determine the number of residential moves. Group size and duration of stay and seasonal use of camps will all have an effect on the archaeological visibility of residential mobility. Localities, which Binford called sites where resources were extracted, should have a low density of archaeology. Residential mobility is expected in landscapes where resources are homogeneously distributed and available year-round, and thus maximum foraging efficiency will result from dispersing the group to resource locations (Kelly 1995: 120). Year-round resource availability does not mean that all resources are available at all times but rather that there are no parts of the year that are characterized by no resource availability.

The collector strategy is tied to logistical mobility (Binford 1980). Logistical mobility is the movement of a subset of the entire residential group to and from a key residential location in order to perform specific tasks. The key residential locations are not necessarily defined by food (Kelly 1995: 120). Although collectors usually exhibit residential mobility, they typically obtain resources through special trips and they store food. Logistical mobility is expected when resources are patchily distributed on the landscape and temporally punctuated. Such resources were often predictable on the landscape and seasonally abundant. The logistical trips occur when the group is located away from critical resources but it is not practical or possible to move the whole group from the current place to where the resource occurs. In situations where access to food resources is restricted by seasonality, hunter-gatherers have a need for obtaining critical

resources in a shorter period of time. Binford proposed that if several critical resources need to be obtained during the same short period of time it would lead to more logistical mobility. A hunter-gatherer group will obtain maximum foraging efficiency in such a situation by aggregation at key residential sites and sending out foraging parties (Kelly 1995: 120). Archaeologically, resource extraction sites may reflect similar or repetitive site function due to many recurring visits through time (Brown 2011).

Kelly (1983), following Binford (1980), investigated mobility strategies further by focusing on how they relate to the environmental resource structure. Kelly used five different variables to measure dimensions of mobility, one example being the average distance moved per residential move (Kelly 1995, Kelly 1983). The different dimensions were analyzed in relation to the gross abundance and distribution of food, using effective temperature (ET) and primary biomass as their measurements. Kelly demonstrated several patterns between residential mobility and the environmental resource structure. One example is that there is a strong positive relationship between the average distance moved per residential move and measures of ET, which in this case Kelly related to seasonality (Kelly 1983).

Informal models for understanding technological change

Many informal models have been developed to explain technological variability not only in terms of lithics but all technology used by a foraging group when the changes correspond with changes in the behavioral and/or environmental context. The early ethnographic studies by Binford are the foundation for much of the body of theory that these models are based on (Shott 1986). The models are developed with the goal to

explain technological change that has been observed in the archaeological record (Kelly 1992). What these models have in common is that either they deal with technological organization and technological choices directly or they deal with concepts such as risk, foraging strategies, and population size that all are potentially linked to technological organization and choices foragers make about technology. Binford's foundational work, summarized above, resulted in studies of technological organization systems with focus on different factors including optimization of technology (Bleed 1986), time stress (Torrence 1983), amelioration of risk (Bamforth and Bleed 1997, Bousman 1993, Collard et al. 2012, Collard et al. 2011, Torrence 1989), technological strategies associated with settlement systems (Kuhn 2004, 1991), population size (Collard, Buchanan, and O'Brien 2013, Collard et al. 2013), and curated and expedient technologies (Bousman 1993, Nelson 1991). Common for most of these studies following Binford is that they take a cost/benefit or risk avoidance approach when trying to understand technological variability (Brown 2011). It is important to note that these concepts are likely all linked and this needs to be taken into consideration. What follows is a discussion and summary of the most important work relating to these concepts and technological organization and I draw on Brown's (2011) comprehensive review of these works when appropriate.

Early efforts focused on the concept of time-stress and the optimization of technology (Torrence 1983, Bleed 1986). Torrence (1983) proposed that technology used for subsistence should vary according to two factors related to time stress: the severity and the character of time stress. Scheduling of toolmaking with respect to the overall requirement of the subsistence activity should influence technological variability. Binford's embedded procurement, according to Torrence, is a good example where time

scheduled for tool making and maintenance is built into other activities. She further proposed that the time available to accomplish tasks should be inversely correlated with the diversity and complexity in a tool assemblage because tools that are more specialized perform tasks more efficiently. The presence of complex and modular tools may indicate forward investment in the production of compound tools or modular tools, which facilitated easy replacement of parts when time is at a minimum (Brown 2011). Using this foundation, Torrence (1983) ranked time stress encountered by ethnographic hunter-gatherers using ethnographic data from Oswalt (1973). Time stress was ranked according to latitude and seasonality, which were used as a proxy for time stress. She found that as latitude increases so do tool diversity and complexity (both in number of components per tool and per toolkit). She used this linear relationship to propose that time stress and scheduling conflict in higher latitudes where availability of resources are seasonally controlled are at least partially responsible for the level of investment of technology observed in the ethnographic data (Brown 2011). A problem with using Oswalt's (1973) study is that the concepts of tool diversity and complexity are both subjective. Diversity is based on the number of subjectively identified tools, while tool complexity is based on the number of subjectively identified tool components. Thus, calculations of tool diversity and complexity can be skewed depending on how many tool types or parts one recognizes in a tool system.

Bleed (1986) took a different approach. He used principles of modern engineering and ethnographic observations to predict the most efficient or optimal design of weapons and tools within the forager versus collector framework created by Binford (1979). He defined efficiency as the output of a technology divided by its cost. Bleed then created a

distinction between ‘reliable’ and ‘maintainable’ tools. Reliable tools are designed to always work when they are needed and tend to be overbuilt to minimize failure and be able to function well below their maximum capacity, which is facilitated by having many redundant components and typically having a built-in backup system. A specialist with a toolkit designed to be able to handle all situations that can arise during repairs performs maintenance at scheduled events in advance of use. Reliable technologies are more likely to be adopted by collectors since they have scheduled resource acquisition where food resources need to be acquired in bulk during narrow and predictable time windows, and that the predictable nature of the food resources allows predictable downtime for scheduled maintenance of tools in advance of resource extraction (Brown 2011). Bleed contended that the Nunamiut that Binford studied used reliable technology particularly in terms of maintenance of tools in advance of hunting. Bleed cited the observations of periods of intensive equipment preparation prior to hunts, the carrying of multiple rifles for caribou hunting, and repair kits with the possibility to fix a range of problems. An issue with comparing the reliable technology concept with Binford’s study is the fact that the Nunamiut used rifles, which is not comparable to weaponry used by Stone Age hunter-gatherers.

Conversely, ‘maintainable’ tools are simpler in design and construction, consist of relatively fewer parts than reliable tools, and are created to be easily repaired or to be easily repurposed for a different use (Bleed 1986). Because the failure of one part results in the failure of the whole tool, the repair kit is more specialized and incorporates spares for parts that might be expected to fail. However, maintainable tools may still work when compromised and can be easily adapted for another unanticipated use. Maintainable tools

are typically repaired by the user as they break and not during scheduled events in advance of subsistence activities (Brown 2011). Bleed used the !Kung and Yanomami groups, considered to be foragers, as an example of hunter-gatherers that used maintainable technology. Both groups use modular-based hunting kits that are simple and lightweight with no redundancy in design, and they carry repair kits with modular parts. Although there is observed specialized tips among the Yanomama they have to be repaired after each shot so they can be used again.

Based on this, Bleed (1986) proposed that the best means for evaluating efficiency in design of hunting technology is to look at scheduling of tool use and the cost of failure. One could envision situations where both reliable and maintainable design elements could be incorporated into a single system. However, reliable systems are typically very costly to build, maintain, and transport. This may be the case but not when using rifles as the example as Bleed did with the Nunamiut. A rifle might be costly in monetary terms but the forager does not have to procure all the different parts of the weapon and manufacture it. The rifle comes ready-made. This needs to be kept in mind. Nevertheless, according to Bleed, when the cost of failure is high (e.g. failure to capture prey can lead to starvation due to lack of alternative resources to extract), meaning that the risk is high, the hunter-gatherer should use reliable tools. On the other hand, when the cost of failure is low (risk is low), the hunter-gatherer should rely on maintainable tools because they are less costly to manufacture and transport. Bleed (1986) contended, in disagreement with Torrence, that latitude is not always a good predictor of the type of technology in the past because the Central Eskimo toolkit in terms of maintainability is very similar to the !Kung and Yanomama. That is not to say that the Central Eskimo and

the !Kung had the same technology but that their technology was built on similar principles of maintainability, and available opportunistic hunting opportunities. Further, he proposed based on his observations that hunter-gatherers in the past would alter their technology to reach an optimal solution in their environmental context (Brown 2011).

Torrence (1989) took Bleed's reliable and maintainable tools concepts and proposed that they should be treated as separate variables and not as a continuum. She proposed that human mobility is not necessarily associated with choice of technological strategy but rather that technological strategy is more likely associated with tool use frequency, prey mobility, and the temporal and spatial availability of prey. According to Torrence, hunter-gatherers will invest in technology and will make a greater diversity of tools when the risk of failure is high (if the forager risks going without food because the food resource will not be available for a considerable amount of time (e.g. seasonal availability) then the risk of failing to extract such a resource is high – the forager might face starvation). Technology for hunting mobile prey is the most complex, while plant-gathering tools are the least complex because hunter-gatherers that have broad diets are under less stress and typically have plant foods in their diets, and they invest less in technology (Brown 2011). Additionally, Torrence pointed out that some of the most complex tools, what Oswalt (1973) called untended facilities for trapping and disabling prey, are very seldom found in the archaeological record due to poor preservation. This is a good point. However, preservation has most likely also eroded away evidence for more complex technology linked to plant or other edible organic food processing.

Others, however, contend that it is not the case that hunter-gatherers that have broad diets are under less stress (Broughton 1997, 1994, Broughton and Grayson 1993,

Hawkes and O'Connell 1992). Broad diets reflect more stress as the forager has to pursue lower ranking prey items to maintain the caloric budget. A plausible effect of having to pursue lower ranked prey due to decline in returns from high-ranked prey is investment in technology to be able to handle such prey (Bright, Ugan, and Hunsaker 2002, Knecht 1993, Kuhn and Stiner 2001, Ugan, Bright, and Rogers 2003).

Torrence (1989) made another important point by cautioning against viewing technological complexity as a linear trend in time. She pointed out several examples in the more recent archaeological record where more formal tools have been replaced by more expedient technologies made from lower quality materials. To her, risk and the severity of loss condition the investment in technology. Risk and severity of loss can be assessed by looking at the abundance of alternative resources, which according to her were plant-resources. Torrence (1989) argued that risk arises whenever a hunter-gatherer group is dependent on mobile prey, which may only be available on a seasonal basis. She divided tools into two classes: tools that are good at minimizing resource variation in space, and tools that are good at coping with temporal variability.

Using that framework Torrence (1989) then proposed that when hunter-gatherers were selecting raw materials they would choose the least costly raw materials suited for the intended task. An example of this is that maintainable tools may require materials that are more amenable to recycling. Torrence argued that raw material choice is not independent of tool use. She disagreed that raw material availability (c.f. Andrefsky 1994) has an influence on selection, and she viewed the total technological system including raw material choice as a way to solve a problem. Bamforth and Bleed (1997) echoed that view and contended that the raw material selection stage of stone tool

technology was potentially very important because it could set the range for what types of tool-forms and flaking outcome that could be produced. Bamforth and Bleed's arguments will be discussed further in a later part of this chapter when discussing the role and importance of raw materials in technological organization.

In an effort to coalesce earlier work by Torrence, Bleed and others, Bousman (1993) tried to unite foraging theory with the concept of technological organization. He pointed out that patch and prey foraging models from optimal foraging theory do not include the input of technology and that archaeologists need a uniform body of theory to explain why past technologies changed. Because patch and prey foraging models normally lack the input of technology, Bousman (1993) proposed that technology should be included in the search and handling costs due to the need for tools when humans are foraging. Based on this, he proposed similarly to Torrence (1989) that diet-breadth should increase if technology costs are minimized and conversely should decrease when technologies that are more expensive are utilized. As noted above, this has been contested by researchers using prey-choice models drawn from Optimal Foraging Theory (e.g. Broughton 1997, 1994, Broughton and Grayson 1993, Hawkes and O'Connell 1992).

Further, Bousman (1993) proposed that the resource structure of a given environment should be characterized by abundance, temporal availability, and spatial distribution of the resources. This created needed nuance to how archaeologists discuss the characteristics of resources in the environment. He proposed that the predictability of food resources should be viewed in terms of constancy, which is when resources are spatially and temporally stable all year round, and contingency, which is when resources are predictable but only seasonally available. Shellfish are examples of food resources

that have a degree of constancy, while seasonal fish runs have a degree of contingency. This is an important point. Resources that have a low degree of both constancy and contingency have low predictability.

Based on this way of characterizing resource structure Bousman predicted expected technological patterns for Binford's (1980) foragers versus collectors framework. Foragers were proposed to be time-minimizers favoring extending the use life of extractive technology and work to reduce production and maintenance costs of the repair kit. The forager pattern is associated with more spatially disbursed and less predictable resources. Conversely, collectors spend more time investing and maintaining extractive tools and the associated repair kit and are associated with a predictable resource structure (Brown 2011). Bousman proposed that depending on the resource structure, the forager and collector patterns could alternate and coexist.

Similar to Torrence, Bousman (1993) assessed risk based on the outcome of food collection. However, he contended that costs and benefits of technology could be manipulated in different ways. Bousman proposed that toolmakers have four primary strategies to increase the efficiency in terms of time allocation and handling costs. 1) The toolmakers can decrease the production time by making expedient tools, which are tools defined by minimal alteration. If such an expedient strategy is planned then either raw materials need to be readily available in terms of abundance on the landscape or available at pre-stocked caches of stone. 2) The toolmakers can increase the use life of the tools by making maintainable tools as defined by Bleed (1986). The life of such tools is extended by repair or resharpening. The cost of raw material acquisition is reduced by maintaining the tools. 3) Efficiency can be increased by creating reliable tools as defined by Bleed

(1986). When the risk of failure is high (meaning that failure to extract the particular resource leads to the forager having to wait a long time to get a similar chance) and when food resource packages are big and can be obtained in bulk then toolmakers should use reliable tools. However, reliable tools are costly and require a lot of planning. 4) The toolmakers can increase production volume to increase the efficiency of tools (e.g. increase the amount of cutting edge produced per unit of stone). Technologies that are more efficient can increase the yield of tools from a given amount of raw material. Bousman proposed that this type of strategy can decrease raw material acquisition costs.

Building on the work of Bleed and Binford, Bousman (1993) proposed that the concept of curated tools should be subdivided into maintainable tools and reliable tools. The characteristics of curated tools should include tools that are made and planned in advance of use, tools that are transported maintained, flexible, reshaped, and tools that are stored (Brown 2011). He proposed a hypothetical triangle where maintainable, reliable, and expedient technologies are the three corners but they do not necessarily represent mutually exclusive strategies. There are two reasons for why the strategies are not mutually exclusive: (1) stone types will greatly influence tool use-life and curation rates for all tools made regardless of strategy; (2) raw material availability, which constrains what can be accessed to make tools regardless of strategy, is a function of mobility range size and pattern, natural abundance, and potentially material exchange (Bousman, 1993).

A different approach to looking at technological variability is to look at how the mobility and foraging strategy affected the archaeological assemblages in terms of diversity; whether tools were curated or used expediently when linked to specific

mobility strategies. Shott (1986) following Binford (1980) conducted a study aimed at technological organization and mobility. He investigated the relationship between assemblage diversity and relative mobility. Shott (1986) used artifact data and mobility information from many ethnographically described hunter-gatherer groups. He found that artifact diversity has an inverse relationship with residential mobility, where artifact diversity decreases as mobility increases (Shott 1986).

Parry and Kelly (1987) who focused on the relationship between the relative abundance of formal and expedient stone tools in relation to mobility strategies and hunter-gatherer sedentism presented a similar finding. Sedentism is a term closely linked to hunter-gatherer mobility, and many archaeologists tend to see sedentism as emerging on a continuum of residential mobility and see sedentism as an important social and behavioral threshold (Kelly 1992). Parry and Kelly (1987) demonstrated a general trend from formal tool use to expedient tool use relative to mobile and sedentary populations in the North American prehistory. They showed that, as hunter-gatherer groups became more sedentary, their technological organization became more expedient, in which the groups relied less on formal tools and conserving raw materials (Parry and Kelly 1987).

Kuhn (1991) following Parry & Kelly (1987), used the amount of retouch on stone tools, which Kuhn saw as a proxy for how formal a tool technology was, to investigate mobility when studying Italian Mousterian Middle Paleolithic assemblages. Kuhn demonstrated a positive relationship between short occupation span and high frequency of retouch. Frequent moves with a residential mobility system put pressure on curating materials to prevent shortfalls. However, Kuhn (1991) also showed that raw-

material availability, differential transport of raw materials and tool functions all affected stone tool variability, and thus the technological organization.

Riel-Salvatore and Barton (2004) proposed a new methodology to study the technological organization of hunter-gatherer groups in relation to their mobility strategies. Using volumetric artifact density from excavations and the frequency of retouched tools within a given lithic assemblage, they gauged if tool assemblages resulted from a residential or logistical mobility strategy (Riel-Salvatore and Barton 2004). This approach was different from past ones as it relied on palimpsests of assemblages to understand technological variability. Using palimpsests is important as it limits the inherent variability of technological change or change in site use in the short term, which both can be subject to taphonomic bias. Instead, a palimpsests approach gives a view of the long-term technological adaptation and mobility strategy at a site (Barton and Riel-Salvatore 2014).

To link assemblage composition and mobility strategy, they used the concepts of curated and expedient tools following Nelson (1991), which articulated a clear difference between curated and expedient lithic assemblages in the archaeological record. The two concepts occupy the ends of a continuum of economic behavior where curated assemblages are recognized by highly conservative use of raw materials and a high frequency of retouch, and expedient assemblages resulting from a liberal use of raw materials and a relatively low frequency of retouch (Riel-Salvatore and Barton 2004). Relying on a behavioral ecology theoretical framework (Bird and O'Connell 2006, Winterhalder and Smith 2000) and optimal use of tool utility under different mobility

strategies, they align curated assemblages with residential mobility and expedient assemblages with logistical mobility on a continuum (Riel-Salvatore and Barton 2004).

Overall, these informal models created to gauge mobility in the archaeological record share the strength of being easy to operationalize because they are general in form and thus easy to apply to archaeological contexts. Although grounded in a behavioral ecology theoretical framework and concerned with optimization of currencies relative to some constraint, these informal models are empirically built on ethnographical and other archaeological data, which have helped make the concepts operational and testable. These informal models set the foundation for a better understanding of technological variability and organization and its connection to mobility and foraging strategies.

From informal to formal modeling

A problem with most of these previous studies is that they developed propositions by building verbal arguments based on archaeological patterns and sometimes ethnographic observations, and then tested those patterns with interpretations of archaeological data (Surovell 2009: 10). The risk arising from this is that the chain of inference about proposed human behavior in the archaeological record becomes circular if observed archaeological patterns are tested against a model built on interpretations of archaeological data. It is important to note that although some of the informal models were built using ethnographic observations (e.g. Binford 1980, 1979, 1977, Shott 1986) there is a lack of empirical tests using ethnographic data of either key assumptions or predicted relationships in most of these cases. Further, the models are so generalized that it can be unclear whether the predictions follow directly from implied goals, currencies,

and constraints (Bird and O'Connell 2006, Surovell 2009). One can risk creating and applying a model that lacks a logical foundation due to imperfect or at least unsubstantiated premises (Surovell, 2009: 2). It is worth noting however that all models (formal or informal) began as informal ideas, concepts, and frameworks. Nevertheless, Kelly (1995: 56) argued: "at present, then, many interpretations of stone tools assemblages as indicators of mobility are subjective, intuitive, and sometimes contradictory."

Some of the contradictions can arise from the data itself. There are several problems and limitations in linking aspects of technological organization such as frequency of retouched tools recovered today or raw material selection with past ecological behaviors such as mobility and foraging strategies. The first set of problems are caused by taphonomic processes starting with the discard behavior of the foragers (Binford 1977), and then post-depositional processes acting on the assemblages (Bernatchez 2010, Dibble et al. 1997, Enloe 2006, Kuman 1989, Lenoble and Bertran 2004, Lenoble, Bertran, and Lacrampe 2008, McPherron, Dibble, and Goldberg 2005, Oestmo et al. 2014, Schiffer 1975), and finally, the recovery methods of archaeologists (Lombard 2008b, Marean et al. 2004). These three sets of problems are not exclusive to informal models but also apply to formal models. However, a problem that is more associated with informal models is the use of subjectively created artifact classes and typologies. One example is the model created by Shott (1986) where artifact diversity was found to be inversely correlated with mobility. The measure of artifact diversity is obviously subjective and depends on how many artifact types one has built into a typological or classification system. When using typologies an archaeologist runs the risk

of having automatic prior assumptions about what a technology should look like or what it constitutes. This risks defining measures that ensure the outcome that is proposed. Ideally, when drawing a hypothesis from operational variables that are subjectively defined the hypothesis should be blind-tested.

A good example of contradictory results is the use of the concept of curation to investigate mobility strategies by Binford (1977, 1973) and Bamforth (1986). Binford (1977: 35) proposed that a greater reliance on curation was the optimal solution to the problem of moving food to the consumers because it increased tool efficiency in terms of the work output relative to the investment in manufacturing (Binford 1977). Conversely, Bamforth (1986) contended that raw-material availability is the ultimate conditioning factor on stone tool maintenance and recycling (retouch) (Bamforth 1986: 40). Bamforth (1986) found when testing his model against both ethnographical and interpretation of archaeological data that high rates of stone tool maintenance and recycling were in some cases more associated with foraging strategies as opposed to collecting strategies.

These differing results when using the same concept highlights a serious problem with informal models. Binford and Bamforth had different and implicit assumptions and did not define curation specifically. As noted above, Binford studied steel knives, rifles, and sleds among other things used by the Nunamiut, which of course have different use-lives compared to stone tools. They both tested their predictions against archaeological data and some ethnographic observations and found their hypotheses to be supported. However, there are no direct systematic observations of any group making and using stone tools where we also know mobility patterns and foraging strategies. Thus, there is a risk of being right for the wrong reason since there is no reason to trust the validity of the

theoretical model (Surovell 2009: 11). Further, because many informal models do not have explicit predictions that have to follow the assumptions it potentially makes the models not logically valid (Surovell 2009: 2).

Based on this, this study advocate for the formalization of models that tries to explain technological variation or aspects of technological organization. This study is far from being the first to attempt such an approach. Most of these models are grounded in an Optimal Foraging Theory (OFT) model framework or in the broader overlaying Behavioral Ecology (BE) theory. What follows is a review and summary of attempts to formalize such models.

Optimal foraging theory (OFT) and its applications to archaeology

The study of how a hunter-gatherer group organizes technology is well suited to an OFT framework (Charnov 1976, Charnov and Orians 1973, Krebs and Davies 1984, Maynard Smith 1978, Stephens and Krebs 1986) because decisions about raw material selection, procurement, tool production (including heat-treatment), and use must be made at virtually every stage of the process, and those decisions can be modeled as optimization problems (Surovell 2009). Formal models from OFT is a subset of models from Behavioral Ecology (BE), and are tools that can help a researcher formulate testable hypotheses about potential fitness-related trade-offs individuals could face in a given socio-ecological context (Bird and O'Connell 2006). In other words, they offer a framework for researchers to organize testable propositions about behavior (Bird and O'Connell 2006). Specifically, models from OFT are designed to test hypotheses about individual behavior under a specified set of conditions (Bird and O'Connell 2006).

A formal model is a model that is constructed mathematically, built from equations, expressions, algorithm, or code. Formal models have the advantage of having explicit predictions that must derive from their assumptions, making them logically valid (Surovell 2009: 2). By nature, mathematical formal models entail causal relations that have unambiguous predictions (Surovell 2009). Additionally, the behavioral ecology and OFT grounding and the mathematical construct should result in more objective models compared to verbally constructed informal models.

It is important to note that the "models themselves are never tested" (Bird and O'Connell 2006: 146). Instead, "it is the situation-specific assumptions" or hypotheses that the given model application require that will be tested. These assumptions or hypotheses apply to the fitness-related goal of behavior, the decision variable that is associated with achieving that goal, the trade-offs linked with the decision variable, one or more currencies used to evaluate the trade-offs, and the constraints that define or limits the agent's situational response (Bird and O'Connell 2006: 146). When modeled as a series of dependent relationships, the assumptions (hypotheses) enable the researcher to generate predictions about behavior under the given circumstances (Bird and O'Connell 2006: 146). If there is a mismatch between predicted and archaeologically inferred behavior it implies "either that one or more of the specific hypotheses about goals, decision variables, trade-offs, currencies, and constraints are wrong" and thus needs reassessment, or it might imply that the model itself is "inappropriate to the behavioral question being addressed" (Bird and O'Connell 2006: 146). Additionally, a mismatch can happen because instead of testing against direct observations of behavior the testing is

against archaeologically inferred behavior where the inferences themselves are potentially erroneous.

It is useful here to summarize the most well-known OFT model, the Prey Choice Model (PCM) (Bird and O'Connell 2006, Emlen 1966, MacArthur and Pianka 1966). Bird and O'Connell (2006: 147) give a good summary of the PCM so I draw on their summary below. The PCM makes a distinction between search and handling, which are two mutually exclusive aspects of foraging. Bird and O'Connell (2006) defined handling as including all activities associated with pursuit, capture or collection that happens after whatever is targeted is encountered. A more useful definition of handling when applying the PCM to non-edible resources such as lithic raw materials is all the time required after a resource is encountered and before the utility of a resource can be realized. It also includes activities associated with prepping the prey for consumption. For this study, that means the manufacturing part of stone tool production. The PCM is designed to address whether a hunter-gatherer should handle the encountered prey or continue to search for another prey that might give the hunter-gatherer a better return relative to time spent searching for, collecting, and processing (Bird and O'Connell 2006). To be able to answer this question, Bird and O'Connell (2006: 147) stated that the PCM assumes that the goal of the foraging activity is to maximize the rate of energy capture, which is the currency. A more precise description is that the PCM assumes rate maximization of nutrient capture but t to be able to operationalize the PCM the currency was simplified to energy capture. The decision the agent faces is whether to handle a particular prey when encountered or to move on to search for another prey that might yield a higher net-return rate, which is the trade-off (Bird and O'Connell 2006). Further, the PCM operated under

the constraints that the agent can estimate or knows the encounter or post-encounter return rate relative to the handling cost of all potential prey types. In addition, the agent searches in a landscape where types of prey are mixed and the chance of encounter is random relative to the abundance of the prey types (Bird and O'Connell 2006: 147).

The PCM posits that if an agent wants to maximize foraging efficiency, the post-encounter profitability of a targeted item needs to be "equal to or greater than the expected overall foraging net return, including search." Further, the model predicts that the prey that has the highest rank will always be taken when encountered, while prey types that are less profitable are added to the diet in descending rank order until the on-encounter return from the prey type with the next lowest-rank falls below the expected return from searching for and handling all resources of higher rank (Bird and O'Connell 2006: 147). All such resources that fall below will by definition decrease the average return of the environment as a whole, which means that they "will be bypassed consistently in favor for a continued search for profitable prey" (Bird and O'Connell 2006: 147). In addition, the PCM also predicts that the post-encounter profitability of a given prey type and the rate at which all higher-ranked prey types are encountered controls the inclusion of a given prey type rather than the abundance of a given prey type or the encounter rate (Bird and O'Connell 2006: 147).

There is evidence for the assumption that living organisms are designed to be optimizers (Alexander 1996, Krebs and Davies 1984) because natural selection favors behaviors that maximize fitness, rewarding optimization within a given environmental context (Surovell 2009). However, it is important to note that (1) nothing is never perfectly maximized, and (2) it is not always the case that an organism maximizes any

specified currency other than fitness because of tradeoffs and realities of biological mechanisms. Currencies and other fitness-related goals can conflict, which can lead to inevitable tradeoffs. Nevertheless, a number of studies show that aspects of hunter-gatherer behavior can be better understood in the context of optimal foraging theory (Hawkes, Hill, and O'Connell 1982, Hill et al. 1987, Hill and Hawkes 1983, O'Connell and Hawkes 1981, Smith 1991, Smith 1981, Winterhalder 1981). However, whether the concept of optimality behavior can be applied to hunter-gatherers has been debated and critiqued (Bishop 1983, Dawkins 2006, Jochim 1983, Keene 1983, Lee 1979, Sahlins 1976, Schrire 2009). Those against argue that optimal foraging models treat cultural factors as trivial (Bishop, 1983), and dehumanize the behavior of foragers (Schrire, 2009), or obscures the difference between the needs of an individual and the needs of the society (Keene, 1983). These are important concerns. Another concern, the assumption that the forager has perfect knowledge about the environment and encounter rates with prey items, which is inter-linked with the concept of risk as it pertains to the effect of risk on a forager's utility or fitness and thus optimal choice between strategies (Smith 1991, Smith and Boyd 1990) will be discussed further below (*Chapter 11*).

Applications of OFT models to the archaeological record have focused on six general issues (Bird and O'Connell 2006):

1) Diet breadth change among hunter-gatherers and the question of intensification (e.g., Basgall 1987, Bayham 1979, Beaton 1991b, Botkin 1980, Bouey 1987, Broughton 2004, 2002, 1999, 1997, 1994, Cannon 2000, Edwards and O'Connell 1995, Erlandson 1991, Glassow 1996, Glassow and Wilcoxin 1988, Grayson 1991, Hildebrandt and Jones 1992, Jones and Richman 1995, Kennett 2005, Kennett and Kennett 2000, Mannino and

Thomas 2002, Nagaoka 2002, O'Connell, Jones, and Simms 1982, Raab and Bradford 1997, Raab and Larson 1997, Raab 1996, Raab et al. 1995, Raab 1992, Raab and Yatsko 1992, Perlman 1980, Porcasi, Jones, and Raab 2000, Simms 1987, Stiner and Munro 2002, Stiner, Munro, and Surovell 2000, Stiner et al. 1999, Szuter and Bayham 1989, Wolgemuth 1996, Yesner 1989).

2) The origins and diffusion of domestication of plants and animals (e.g., Alvard and Kuznar 2001, Diehl 1997, Dominguez 2002, Foster 2003, Gremillion 2004, Hawkes and O'Connell 1992, Keegan and Butler 1987, Keegan 1986, Kennett and Winterhalder 2006, Layton, Foley, and Williams 1991, Piperno and Pearsall 1998, Redding 1988, Russell 1988, Winterhalder and Goland 1997, Wright 1994).

3) Central place foraging (e.g.,Barlow and Metcalfe 1996, Bettinger, Mahli, and McCarthy 1997, Bird et al. 2002, Cannon 2003, Elston and Zeanah 2002, Metcalfe and Barlow 1992, Lupo 2001, Lupo and Schmitt 1997, O'Connell and Marshall 1989, Orians and Pearson 1979, Zeanah 2004, 2000),

4) Colonization processes and competitive exclusion among hunter-gatherers (e.g., Beaton 1991a, Bettinger and Baumhoff 1982, Keegan 1995, Keegan and Diamond 1987, Kennett, Anderson, and Winterhalder 2006, Kelly 1999, Meltzer 2002),

5) Animal skeletal element transport (see Marean and Cleghorn 2003 and references therein), and

6) Links between foraging and technology. Compared to the other issues such as diet breadth and origins of domestication, links between foraging and technology have received relatively little attention (Bird and O'Connell 2006). Although, as stated above, many early studies on technological organization and its link to foraging behavior used a

BE framework they did not use formal models with explicitly stated goals, currencies, decisions, trade-offs, and constraints (Bird and O'Connell 2006). However, applying OFT to technological choices has several issues: 1) there is no theory to predict the suite of alternative technologies that will arise. Instead one can only evaluate alternative technologies that are known to exist; 2) Adaptation of technology is affected by cognitive mechanisms other than just those that evaluate rate gain maximization. Such cognitive mechanisms include social learning prejudices (Bandura 1977) and signaling (Gurven et al. 2009, Bird, Smith, and Bird 2001) that can both affect which technologies are chosen regardless of gain rates. 3) In addition, the evolution of cultural preferences in tandem with functionally optimal technologies sometimes requires cultural group selection (Soltis, Boyd, and Richerson 1995, Henrich 2004). These issues need to be taken into account when applying an OFT framework to technological choices. Models derived from the OFT or BE framework that have focused on links between foraging and technology pertain to this dissertation and will be summarized and discussed in the following section.

Formal models for understanding technological change

The formal models reviewed below can be divided into two broader categories: 1) analytical optimization models, 2) simulation-based models that utilize agent-based models or other computer-based tools to understand technological or behavioral change. In the first category, some of the models have investigated investment in technology or focused on time-costs linked to technology as a part of the rate maximization equation. These will be the focus of a summary and review below. Others have focused on why

certain core types such as Levallois core technology prevail across large spans of time and space (Brantingham and Kuhn 2001), or when one should field-process a stone nodule instead of bringing the whole nodule back to a campsite (Beck, Taylor, and Jones 2002, Metcalfe and Barlow 1992). Additionally, work by Surovell (2003, 2009) has focused on creating a behavioral ecology framework for lithic technology.

Surovell (2009, 2003) built on the previous formal models by Kuhn (1994) and others (e.g. Brantingham and Kuhn 2001, Metcalfe and Barlow 1992) to create a whole suite of new formal models aimed at building a stronger foundation for lithic technology, technological organization and mobility strategy studies in behavioral ecology. I will review one of his models here. Surovell (2009) called it the "Mean Per Capita Occupation Span" model, and it models artifact accumulation where the goal is to derive archaeological measures of occupation span and reoccupation of sites using only attributes of technological organization (Surovell 2009: 58). Surovell (2009: 58) stated, "Because occupation span and the frequency of residential mobility are inversely related, measures of occupation by their very nature are also measures of mobility." Thus, these measures of mobility can then be used as independent variables for the investigation of technological variability or technological organization (Surovell 2009: 58).

Surovell (2009: 68) defined the concept of "mean per capita occupation span as "the average length of stay per site occupant." and (2009: 70) argued that it is more useful than occupation span because it should be independent of the number of occupations. Moreover, Surovell (2009: 70) argued, "If the archaeological record is seen as the product of individual agents operating in time and space, and the behavioral phenomena we wish to study are the cumulative product of individuals, then the per

capita measure should be a more accurate reflection of the by-products of those behaviors."

Surovell (2009: 74) constructed the model with two main variables; transported and locally acquired artifacts. The model assumes that a forager arrives at a site with a transported toolkit, and upon arrival, the forager replenishes the toolkit to some optimum size of artifacts with locally acquired raw materials (Surovell 2009: 74). All things being equal; the model predicts that as occupation span is lengthened, artifacts acquired locally will increasingly dominate archaeological assemblages. Thus, short-term occupation of a site should equate to a relatively high proportion of transported artifacts, while long-term occupation of a site should equate to a relatively low proportion of non-locally acquired artifacts (Surovell 2009: 77). Because the size of a transported toolkit is limited (a forager only has so much space to carry things), it influences the discard rates of transported artifacts into a site. Thus, the ratio of local to nonlocal raw materials represented by transported and locally acquired tools should provide a proxy measure for mean occupation span per site occupant (Surovell, 2009). Support for this proposition was found with archaeological data from both North America and Australia.

A limitation with the occupation span models is that it relies on the proper identification of local versus non-local raw materials. Surovell's study cases from North America and Australia involves distinct raw materials with well-known proveniences on the landscape (Surovell, 2009). However, the distinction of what is local and what is non-local materials in the South African Middle Stone Age (MSA) record has been debated, where the identification of silcrete being an exotic non-local raw material features prominently (Ambrose 2006, 2002, Ambrose and Lorenz 1990, Minichillo 2006). The

original argument that silcrete was an exotic and non-local material was based on the observation of its rise in frequency during the Marine Isotope Stage (MIS5) to MIS4 transition, which was argued to indicate that foragers changed how they moved about the landscape (Ambrose and Lorenz 1990).

However, two different studies have changed that perception. 1) Minichillo (2006) argued that silcrete and other fine-grained raw materials as observed in the Klasies River record are local raw materials obtained from secondary sources, mainly cobble beaches. This suggested that these exotic raw materials could be obtained inexpensively in terms of time-cost (Minichillo, 2006). An outcome of this was more pressure to conduct more detailed provenience studies of raw material to be able to discern which raw materials are local and which are not, and to highlight whether raw materials come from primary sources or secondary sources. 2) In the second important study, Brown et al. (2009) showed that silcrete at Pinnacle Point has been heat-treated. They showed that the appearance of silcrete as fine-grained and 'exotic' as observed in the archaeological record from PP5-6 is due to heat-treatment. Prior to this finding, it had been hard to source silcrete because the archaeological silcrete seldom looked like the silcrete found on the landscape. The finding that foragers heat-treated silcrete showed that what appeared as a fine-grained non-local raw material without any clear proveniences on the landscape could instead be local silcrete that was heat-treated to improve the quality.

Combined these two findings show that what constitute local and non-local raw materials in the MSA record at Pinnacle Point, and potentially elsewhere is complex. The "Mean Per Capita Occupation Span" model appears to be an excellent avenue to look independently at mobility in the archaeological record at Pinnacle Point but in the

absence of proper identification of what constitutes local and non-local raw materials, this study will not attempt to utilize Surovell's model.

OFT-derived models

The following review will focus on formal models that have investigated investment in technology, or focused on the time-costs of technology as a part of the rate-maximization equation.

An early formal model dealing with technological organization and mobility in the first category is the "Mobile Toolkits" model created by Kuhn (1994). The model explored two different technological trade-offs in the design of mobile toolkits. The alternative technological strategies have associated costs and benefits that can be modeled with respect to a currency and thus to define optimizing behaviors (Surovell 2009: 16). The two central questions asked by the model (Kuhn 1994: 426) were that if one assumes that mobile toolkits are designed to maximize durability, functionality, and versatility at the same time as minimizing weight, 1) should a group of foragers carry cores (mostly unused mass of raw materials) or tools/tool blanks?; 2) should they transport a few large tools or a number of small tools? Kuhn (1994: 438) stated that the major assumption of his model is that when a forager is making tools for more or less continuous transport the predominant concern is to maximize potential utility relative to the cost of transport. More specifically the model assumes a currency of utility divided by mass, and the goal of the model is to find the technological solution that maximizes this quantity for a toolkit. Utility is defined as the potentiality to produce usable flake edges, measurable relative to a minimum usable size for tools and cores (Surovell 2009: 16).

Kuhn (1994) derived two predictions. First, mobile toolkits should contain tools or tool blanks rather than cores because of more usable flake edge per unit mass. Secondly, transported tool blanks should optimally be between 1.5 and 3 times bigger than their minimum usable size. This result is based on the assumption that utility is proportional to artifact length, which in turn is assumed to be proportional to the potential for resharpening or renewal. Kuhn (1994: 439) did not test his model against ethnographical or archaeological data but states that it is "one potential avenue for recognizing even more fundamental limitations in how we think humans behave." Kuhn's model stands today as perhaps the only model put forward that uses an explicit currency combined with trade-offs and time-cost in an attempt to predict technological change. Because of the inherent detail needed in testing Kuhn's model it has not been applied to archaeological records because of a lack necessary resolution in the archaeological data.

Elston and Brantingham (2002) focused on microlithic technology and its role in hunter-gatherer adaptive strategies by looking at tool design and risk. This is different from previous studies, which have focused on origins, technological lineages, and cultural history. They contrasted organic points that have microblade insets with simple organic points and flaked stone points by outlining the general costs and benefits of the different designs. In addition, by using the Z-score model (a risk sensitivity model) they focused on the relative advantages of wedge-shaped and split-pebble microcores. Based on ethnographic and archaeological data they found that bone and wooden points equipped with microblades are significantly more expensive to manufacture than simple stone or organic points. However, in terms of risk of failure, they perform much better, and the points with microblade insets are much easier to repair. To Elston and

Brantingham risk of failure refers to the probability of shortfalls in finding and extracting resources in a given environment. Thus under certain climatic and demographic circumstances, microlithic technology should be preferred. Blade cores such as wedge-shaped and split-pebble also have trade-offs, and Elston and Brantingham (2002) proposed that the most expensive forms should be adopted in high latitude environments despite their costs because they provide advantages in tool maintenance such as ease of repair. They reviewed the role of microlithic technology as a risk-minimizing strategy (strategy to minimize the risk of shortfalls in capture food resources) of arctic and sub-arctic large game hunters in Northern Asia. They proposed that microlithic technology provided aid to provisioning efforts through long winters with diminished food resources that were hard to access. The use of microlithic technology minimized the risk of failure to capture sufficient resources. The role of microlithic technology as a risk-minimizing strategy helped it spread in the Northeast during the Late Upper Pleistocene (Elston and Brantingham 2002).

Ugan and colleagues (2003) building on the work of Bright et al. (2002) proposed a technological investment model. In their model, intensification of technology is treated as a series of decisions. These decisions are related to how tools are used and how extra time and energy used on technology has an effect on search and handling time for food resources. They proposed that the costs associated with technological investment are as important to consider as the potential benefits. Further, they cautioned that diminishing returns could result from continued investment in technology (Ugan, Bright, and Rogers 2003). The goal to be achieved in their model is to maximize the net-return rate of food resources in the most efficient way possible (Brown 2011). They proposed that there is a

critical balance between time costs resulting from search and handling time cost and time costs associated with improvement of technology. Further, they proposed that search and handling and technological improvement are two mutually exclusive activities. Using their model, they found that there is a positive relationship between technological investment and amount of time spent handling a food resource. Investment should increase with the amount of time spent in handling. The tradeoff is that the time spent on investment reduces the time that can be spent searching (Ugan, Bright, and Rogers 2003). The study highlighted the potential conflict between time spent on improving technology and the time needed to procure energy resources. However, tool work can be done at night, during periods of bad weather, during time spent waiting for people, or conditions to change. Hence, if tool work is timed properly it does not have to be conducted during potential foraging time and thus the two activities are not mutually exclusive.

Further, Ugan and colleagues (2003) contend that the use-life of an artifact affects the time that mobile hunter-gatherers would have available to forage, and based on that they proposed at least three ways that technological investment can manifest itself. The hunter-gatherers can decide to invest in high-quality materials and construction that result in artifacts with longer use-lives. Alternatively, the hunter-gatherers can invest in expedient tool manufacture and spend most of the time on maintenance to extend tool use-life. The third strategy is to replace the entire tool on a regular basis (Brown 2011). They contended that technological investment cost could be decreased by embedding the cost in other activities such as embedding raw material procurement into daily foraging movement. This is similar to my point above that tool work can be embedded with duties performed in the evening and at night at a campsite or performed when waiting out

adverse weather conditions. However, if tool work is embedded in such a way the optimal solutions arrived on by Ugan et al. (2003) will change.

Bettinger et al. (2006) disagreed with Ugan and colleagues' (2003) explanation for how technological investment occurs and proposed an alternative model of technological intensification. Because not all tools perform the same task they cautioned against using a single gain curve when comparing rates of procurement function. In their model, they used points and lines to connect between different curve functions of gain and manufacture time to be able to predict when a hunter-gatherer should switch to a more expensive technology (Brown 2011). Bettinger and colleagues (2006) asserted that it would not make sense for a hunter-gatherer to invest in a technology that yields a lower net-return rate than a cheaper technology. Thus, a hunter-gatherer should keep using an inexpensive technology if a more expensive technology does not yield a higher net-return rate (Brown 2011). Their model also predicted that when diffusion or transmission of ideas introduces a new technology that increases net-return rates than the existing technologies if retained should revert to cheaper and simpler designs (Bettinger, Winterhalder, and McElreath 2006).

A big issue with both Bettinger and Ugan's studies is that they both present very little testing of their concepts using ethnographic data. Central assumptions have not been grounded in observed behaviors or experiments. For example, the proposition that search and handling and technological improvement are two mutually exclusive activities is most likely wrong. That proposition could have been checked by comparing it to ethnographically observed behavior.

Mackay and Marvick (2011) also considered technological time-costs when applied to stone tool manufacture. They created a model where it is assumed that there is a positive correlation between technological cost and improvement in resource capture. The model showed, similar to ethnographic observations of the relationship between subsistence risk and technological complexity, that the viability of technologies with increased time costs is constrained by the resource abundance across the landscape. They found that it is more likely that costly technologies should be pursued in landscapes with fewer resources. This is because improvements that might arise from investing in costly technologies are most likely going to be marginal when the net-return is already high. This result mirror earlier observations about the relationship between risk and technological complexity (c.f. Bousman 1993, Torrence 1989).

However, increased investment in technology is not the only way to mitigate risk related to fewer resources. Establishing and maintaining social networks providing information among scattered social groups that can act as a safety net in situations of resource scarcity is another way to mitigate risk (Whallon 2006). Additionally, ethnographic observations suggest that technology does not have to be complex and costly to be able to survive in a resource-poor environment. Ethnographic observations from the Western Central desert in Australia, for example, show that the toolkit consisted of three types of tools: 1) multipurpose tools that were lightweight and easy to carry; 2) appliances that can be left where they were used, and reused at a later time if needed; 3) instant tools that are created on the spot using local raw materials and discarded expediently on the landscape (Gould 1978, Gould, Koster, and Sontz 1971). It is

important to note here that nothing is known about the economies and net-return rates associated with a different toolkit in this Australian example.

Mackay and Marvick (2011) compared the ethnographic observations and the hypothetical models they created to archaeological changes in technological costs from three late Pleistocene sites (Diepkloof, Elands Bay Cave, and Klein Kliphuis). Based on their findings they proposed that while costly technologies are generally pursued under global glacial conditions, at the peak of glacial conditions there is a reversion to technological systems with minimum cost (Mackay and Marwick 2011). Specifically, they proposed that this most likely reflects a switch in the optimization goal from the focus on gaining maximum resource net-return rates to instead focusing on maximizing early resource acquisition and/or a focus on maximizing the number of subsistence encounters.

However the proposition that there is a reversal at the peak of glacial conditions is not clear-cut in South Africa. The argument hinges on that the evidence uncovered so far is representative for the overall technology. It is possible and highly likely that with more excavations the technology organization during the peak of glacial and in interglacial periods will reflect more complex and thus costly technology. Evidence from Sibudu in the Eastern Cape shows that in the moderate interglacial MIS3 there is no simple reversal to a less costly technology but instead increased variability in technology (Conard and Will 2015, Will, Bader, and Conard 2014). Additionally, the assumption that glacial conditions during the MSA in South Africa presents the forager with fewer resources is also potentially wrong.

One pressing problem with the models reviewed above is that they treat technology as a single monolithic entity. Most technologies consist of several components made up of several types of materials, which all require separate actions to acquire and process. By concocting technology into one entity of costs and benefits one risks washing out what parts of the technology are costly to procure and manufacture and which ones are not. To obtain a better estimate of the cost of technology one should look at the currency and cost of single raw materials needed in the technology. Once a web of cost and benefits for each raw material is obtained then one can combine these to calculate the full cost of technology that can be used to understand benefits and costs of technology in food-getting activities. By looking at raw materials needed for a particular technology individually one will get a clearer picture of which parts were more important in the overall technological organization.

Formal simulation models

Brantingham (2003) challenged the argument that changes in stone tool raw material frequencies in archaeological assemblages can be considered a reliable proxy for hunter-gatherer adaptive variability (Féblot-Augustins 1993, Kuhn 1995, Mellars 1996). He further challenged the traditional explanations that changes in raw material usage frequencies is due to mobility and procurement strategies that co-vary with climate/environmental change (Ambrose and Lorenz 1990, Binford and Stone 1985, Kuhn 2004), selection of certain raw materials for their physical properties (Braun et al. 2009, Gould and Saggers 1985, Minichillo 2006), changes in demography (Clark 1980), the preference for appearance or color (Akerman, Fullagar, and van Gijn 2002, Clendon

1999, Stout 2002), symbolic value (Wurz 1999), and style (Close 2002). Brantingham (2003) presented a neutral model using agent-based computational simulation. He showed that his neutral model can explain most patterning observed in raw material use.

In the neutral model, one forager with a mobile toolkit of fixed capacity is randomly placed on the environment. At each time step, the forager moves to one of the nearest eight neighboring cells or stays in the present cell, with equal probability (=1/9). At each time step, a fixed amount of raw material is consumed dependent only upon its frequency in the mobile toolkit. If a raw material source is encountered, the toolkit is re-provisioned up to its maximum capacity before moving again at random. If no raw material source is encountered, the forager moves immediately at random. Simulations are run until 200 unique raw material sources are encountered, or the edge of the simulation world is reached (Oestmo, Janssen, and Marean 2016). The model is replicated in Netlogo by (Janssen and Oestmo 2013).

Brantingham (2003) presented three important results. 1) The raw material richness in an assemblage should always be less than the available range of raw materials on the landscape. 2) The model predicted that the mobile toolkit of a forager should mostly consist of raw materials that can be encountered in close proximity to the site. 3) Raw materials from distant sources should be minimally represented (Brantingham 2003). Brantingham (2003: 506) asserted that in order to demonstrate the deliberate selection of raw materials, patterning must be shown to be different from the results of the neutral model, which provides a baseline for comparison where archaeologists can be certain that an observed raw material pattern is not the result of strategic selection.

However, a problem with Brantingham's model is that it simulates what is being carried not what is being discarded and observable in an assemblage.

Pop (2015) contested that Brantingham's model in its original form is suited to identify archaeological patterns because it can only simulate processes that govern toolkit composition and these processes differ substantially from the processes that influences discard records (Pop, 2015). In Pop's study, archaeological sites or assemblages are demonstrated to not offer an adequate proxy for the average composition of ancient forager toolkits. He pointed out that richness of assemblage is by itself a poor predictor of site occupation history. Additionally, Pop showed that practice of calculating archaeological raw material frequencies from distances to sources is flawed. An issue with Pop's study is that because site occupation history is also an archaeological interpretation, using one to predict the other is not a valid test. The only way this would be a valid test, I propose, is to base the relationship on ethnographically observed populations.

Neverthelss, Pop's (2015) work is important as it calibrates Brantingham's model. His revised model predicted that: 1) raw materials from any given source should always occur in similar quantities at archaeological sites with similar access costs, and it should happen regardless of direction of access. Major deviation in the archaeological record from this expectation can only be explained by behaviors affecting mobility patterns. 2) The most heavily utilized (meaning curated or retouched) raw material will be from relatively isolated sources. Deviation from this pattern suggests avoidance of that raw material source. 3) Because there is a sharp decline in raw material abundance with increasing distance to source, large sites will only form at or very near to raw material

sources. Deviation from this expectation is only explainable by behaviors resulting from biased, non-random movement. 4) The probability of observing a given number of raw material types in an archaeological assemblage depends on the distance between assemblage and source, and the distance between the source and neighboring sources. Deviation from modeled frequencies is indicative of behaviors that resulted in targeted procurement or avoidance of particular raw material types. 5) Maximum transfer distances and the ratio of maximum to median transport-distances that have been observed in an assemblage should be smaller under conditions of low source densities compared to conditions where source densities are higher. Deviation from these expectations can indicate mobility patterns that are biased, or it may reflect factors such as lithic recycling. 6) The number of unique raw materials should be low under conditions of low source densities. Deviation reflects preference or avoidance of certain raw materials. Given these predictions Pop (2015) argued that a requirement to accurate interpretation of the model output is high-resolution raw material sourcing data. The research presented in this study attempts to apply Brantingham's random walk approach to a real landscape with high-resolution data on source locations and extents. Pop's third prediction will be tested when appropriate below in *Chapter 12*.

Following up on his early work (2003), Brantingham (2006) addressed the problem of being able to translate patterns of archaeological raw material frequencies into quantitative characteristics of forager mobility. He pointed out that it is a challenging problem because forager mobility is interlinked with a number of potential variables including raw material quality and abundance, individual movement and technological decisions, which makes it hard to analyze mobility independent of those variables. He

proposed a formal model of forager mobility that is based on a well-known stochastic process from biology called the Lévy walk (Brantingham 2006, Shlesinger, Zaslavsky, and Klafter 1993, Viswanathan et al. 2002). Lévy walks are based on a simple equation that states that the probability of a move of a certain length (L) is commanded by a negative power-law with properties defined by an exponent (u). Moves of length L are straight-line paths between two stops along a single route. Foraging stops can be "interpreted as turning points along a continuous path that represents a single foraging bout, temporary camps or resting spots for special-purpose activity groups" during logistical forays, or residential camps used by hunter-gatherers using a residential mobility strategy (Brantingham 2006: 437). Thus, the Lévy walk processes can represent both daily foraging bouts and residential moves that the forager group makes. Lévy walk is generated from the power-law distribution when forager moves between two points in incremental steps corresponding to a minimum possible step, which is also called the characteristic step length. However, the probability distribution can also generate Lévy flights, which are instances of the forager jumping instantaneously between two points that are separated by distance L (Brantingham 2006).

From a forager perspective, the Lévy walk allows the forager to detect foraging targets at the end point of Lévy paths or at intermediate steps between them. Conversely, the Lévy flight allows the forager to only detect targets at the end of individual flights. Short distance moves tend to be most common as the density of the probability distribution is concentrated around lower values of L, while long-distance moves occur with finite probability (Brantingham 2006: 437-438). He pointed out that studies of a diverse set of organisms such as dinoflagellates, honey bees, albatross, deer, and howler

monkeys have shown that Lévy walks describe the empirical frequency distribution of move lengths for these organisms (Bartumeus et al. 2003, Boyer et al. 2004, Ramos-Fernandez et al. 2004, Viswanathan et al. 1999, Viswanathan et al. 1996). Because of this Brantingham (2006) proposed based on a theoretical and empirical basis that one can also expect that the movement of human foragers can be structured similarly. Specifically, Brantingham (2006) asserted that this model, in combination with neutral assumptions about raw material procurement and use (Brantingham 2003), could be used to recover detailed quantified information about organization of mobility from raw material transport distances and provide potential currencies for comparative studies of mobility strategies. The results of his formal modeling are consistent with informal models presented in the past that have suggested that greater mean and maximum stone transport distances reflect increased planning depth and greater optimization of mobility and risk sensitivity (Brantingham 2006). Brantingham's formal model was supported by recent ethnographic observations by Raichlen et al. (2014) that show that the movement-pattern of Hadza foragers (both sexes) approximate a Levy walk.

Brantingham (2006) noted that his model does not imply that hunter-gatherers calculated probabilities to structure their mobility. The rationale behind modeling hunter-gatherer mobility as a Lévy process, he contended, is linked to how one brings individuals and food resources together at the same time and place, which is a fundamental ecological problem faced by all organisms (Cashdan 1992, Potts 1988, Stephens and Krebs 1986). When studying non-human organisms some ecologists favored the assumption that foragers do not have any prior knowledge about the resource distribution across the landscape (Viswanathan et al. 2002, Viswanathan et al. 1999), and

argued that the organisms have evolved behaviors that approximate a Lévy random search because these behaviors offer an optimal solution to finding heterogeneously distributed resources (i.e. patchy) (Brantingham 2006). Based on this Brantingham proposed that it is not unreasonable to expect that hunter-gatherers would deploy a Lévy search strategy when entering new environments for which they did not have any prior information about the resource structure. However, once information was gathered about the environment then random search would no longer be necessary. Brantingham (2006: 450) pointed out that a Lévy search strategy can provide an adequate explanation of hunter-gatherer mobility for those cases when foragers have moved to new environments because we lack information about why hunter-gatherers moved to certain locations at different distances, which is a function of the lack of scale discernible from the archaeological record. However, one issue an archaeologist faces is that it is very challenging, if not impossible, to pinpoint in the archaeological record at what point a foraging group first moved into a new environment and at which point the foragers had enough knowledge about their surroundings to stop using random search. The implementation of the Levy walk is beyond the scope of the study presented here but will be the focus of a future study.

Barton and Riel-Salvatore (2014) conducted agent-based modeling to simulate how lithic assemblages form. They pointed out that studying formation processes is important as they are the key link between the materials being studied and the behavior that archaeologists want to understand (Barton and Riel-Salvatore 2014). They focused on four variables that can affect the formation of lithic assemblages, and systematically evaluate the individual and combined effect of the length of stay at sites, distribution of

raw materials, differences in site activities, and movement patterns on assemblages over different time intervals. Barton and Riel-Salvatore found that when you increase the access to raw materials you decrease the frequency of retouched lithics. On the other hand, tasks that require more use of lithics results in assemblages with a higher frequency of retouched lithics. Further, Barton and Riel-Salvatore (2014) found that the length of stay under any mobility strategy has an effect on the density of lithic accumulation, while it has little effect on the composition of an assemblage. Similarly, they found that mobility patterns have a limited effect on the composition of an assemblage. However, when they coupled mobility pattern with place provisioning or individual provisioning, which are associated with logistical and residential mobility strategies respectively (Kuhn 2004), they found that it has a significant effect on the compositions of assemblages. Another important finding was that lithic palimpsests resulting from multiple occupations might provide better information about hunter-gatherer ecology and adaptability than assemblages that have resulted from single or few occupations (Barton and Riel-Salvatore 2014).

They contended that the model experiments support their interpretation (Barton et al. 2011, Riel-Salvatore, Popescu, and Barton 2008, Riel-Salvatore and Barton 2004) that the relationship between retouched artifact frequency and density is a robust proxy for hunter-gatherer land-use strategies. The pattern should be most apparent for archaeological sites that have alternating occupations between LMS (logistical mobility strategy) base camps and RMS (residential mobility strategy) residential camps. They argued that place provisioning that usually goes along with logistical mobility drives the

distinctive patterns observed in lithic assemblages accumulated at localities that have periodically acted as LMS base camps (Barton and Riel-Salvatore 2014).

Their modeling predicted the quantitative signature for localities that served exclusively as RMS residential camps and/or LMS resource extraction camps based on the composition of the assemblage. This signature is a positive relationship between retouched frequency and artifact density, which is the opposite of localities that have been used as LMS base camps and RMS residential camps on an alternating basis (Barton and Riel-Salvatore 2014).

It is important to note that Barton and Riel-Salvatore utilized retouch frequencies reported from European Middle and Upper Paleolithic assemblages. The retouch frequencies from South African MSA assemblages are relatively low (e.g. Brown, 2011; Singer and Wymer, 1981). No study has explicitly compared the amount of retouch frequency between the Middle Paleolithic and Middle Stone Age assemblages but the relative lack of retouch in the MSA record is curious and warrants more research. It could be that access to raw materials was so prevalent due to either abundance or lack of competitions because of low population numbers that it let the foragers be more expedient overall with raw materials. Because of this, Barton and Riel-Salvatore's model might not be as useful for MSA records as it will likely suggest that most MSA assemblages are due to have been used as LMS base camps and RMS residential camps on an alternating basis. However, the simulation predictions they presented will be contrasted against the Pinnacle Point record in conjunction with the discussion and synthesis of model results in *Chapter 12*. The predictions are: 1) increase in access to raw materials decreases the frequency of retouched lithics; 2) tasks that require more use of

lithics results in assemblages with a higher frequency of retouched lithics; 3) length of stay regardless of mobility strategy affects the density of lithic accumulation but at the same time has little effect on the composition of an assemblage; 4) mobility patterns have a limited effect on the composition of an assemblage; 5) when mobility pattern is coupled with place provisioning or individual provisioning it has significant effect on assemblage composition (Barton and Riel-Salvatore, 2014).

Issues with formal models

Because the formal models have such explicitly stated assumptions, currencies, constraints, and goals, they are increasingly harder to operationalize and apply to the archaeological record. Metcalfe and Barlow (1992: 352) argued that testing their "field processing model" would be very hard to do rigorously because it would require estimates of different parameters of their model at a level of precision unlikely to ever be available in the archaeological record. Kuhn (1994) did not test his model either. However, as Surovell (2009) showed, it is possible to test formal models and find support for them by carefully selecting proxy measures of currencies and constraints to test the models. However, these proxies need to be verified by ethnographic observations.

However, Surovell (2009: 20) argued that because there is a reliance on proxy measures of currencies and constraints to test formal models in lithic technology, uncertainties will start to compound that could make the formal mathematical models lose their formality because it cannot be demonstrated that the assumptions have been met. This, of course, is a problem but the utility of formal models are not that they are

easily operationalized and tested, which they are not, but that they have a sound logical foundation (Surovell 2009: 20).

Conversely, an advantage with computer-based simulation models is that, if model assumptions about human behavior and environmental context that are based on direct ethnographic and physical, observations respectfully are used, they allow for the investigation of human behavioral variation. This is because one can simulate long time-periods, and variables associated with human behavior and/or environmental context can be changed one at the time. This is important because lithic technology is largely an extinct technology, and direct observations of the accumulation of lithic assemblages over similar timeframes comparable to those observed in the archaeological record are not achievable (Barton and Riel-Salvatore, 2014).

The last point to consider when using a mathematical view of the world is that mathematical models are simple views of the complex world, where assumptions are often simplified (Surovell 2009: 21). However, as Winterhalder and Smith (1992: 13-14) put it "simple is not simple-minded. Simple models are a necessary, not temporary or primitive stage of scientific development." This same notion goes for simulation models. By starting simple and by investigating the interconnectedness of the variables one can potentially get a better understanding of what the causal factors are. These causal factors can be verified with ethnographic observations creating a causal model for behavioral change and then that model can be applied to the archaeological record. Once the simple causal model is understood it is possible to build more complex models with more variables.

The preceding review of informal and formal models to understand technological organization systems has highlighted that if you are choosing a model to investigate mobility strategies and want to apply it to a given archaeological assemblage you have a dilemma. On one side, informal models offer you the ease of operationalizing and applicability to the archaeological record, however, they can be potentially illogical because predictions do not follow ambiguous assumptions. On the other side, formal models offer you a logical foundation with explicit predictions following assumptions, however, they are very hard to operationalize and apply to the archaeological record because their explicitly stated currencies, assumptions, constraints, and goals would require estimates of at a level of resolution unlikely ever to be available in the archaeological record.

Although there are models presented above that are hard to test with archaeological data or ethnographic observations potentially making them scientifically less valid, there are, however, some models such as Dibble's cortex model (Lin, McPherron, and Dibble 2015, Dibble et al. 2005) and Barton's retouch frequency model (Barton 1991) that are specified for archaeological materials. The cortex model has been experimentally tested and verified several times and has been found to be a robust method (Douglass and Holdaway 2011, Douglass et al. 2008, Holdaway et al. 2008, Douglass 2010, Lin et al. 2010, Parker 2011). In addition, the successful application of the method to multiple different assemblages (Holdaway, Douglass, and Fanning 2013, Douglass 2010, Douglass et al. 2008, Ditchfield et al. 2014, Holdaway, Wendrich, and Phillipps 2010, Dibble et al. 2012, Brown 2011, Phillipps 2012) suggest that the differences in cortex composition among lithic assemblages can provide an objective and

quantitative way of comparing prehistoric variations in movement and technology (Lin, McPherron, and Dibble 2015).

The important takeaway from the discussion on formal models is that a model that only deals with living people and the calories that they expend with no consideration of the material record they produce and discard is poorly specified for the archaeological record regardless of whether it is expressed as a narrative (informal model), computer algorithm (e.g. agent-based model simulation) or as an equation. Put another way, for a model to be useful for the archaeologist the model needs to produce explicit outcomes or expectations that are testable by direct comparison to the archaeological record. This dissertation takes such an approach and presents two formal models that produce outcomes that can be tested by comparison to the archaeological record.

Raw material selection

Of the formal models reviewed above, only Brantingham (2006, 2003) and Pop (2015) explicitly proposed processes for why raw materials change in the archaeological record. However, several informal models have been proposed for why raw materials change. In the following sections, I review and summarize research that has focused on the role and importance of raw materials in the technological organization of foragers. Then I move to discuss why raw materials are selected starting with the concept of quality and how it can be quantified by using mechanical tests. This is followed by a review of other hypotheses for why raw materials are selected and thus potentially why raw material frequencies change in archaeological records. At the end, I organize the different models that been

proposed for why raw materials change into a framework subdivided into two broader categories called ‘Non preference-based change’ and ‘Preference-based change’.

The role and importance of raw materials in technological organization

Following the Oldowan, a wide range of environmental and climatic contexts, time-periods, and ‘cultural traditions’ have yielded a pattern of changing use, and co-use of coarse-grained and fine-grained stone tool raw materials (e.g., Andrefsky 1994, Bamforth 1990, Bar-Yosef 1991, Braun et al. 2009, Clark 1980, Goldman-Neuman and Hovers 2012, Jelinek 1991, Kuhn 2004, 1991). However, the explanation for this variation and the significance of stone raw materials in the technological organization of foragers are heavily debated. Generally, the arguments can be divided into two camps. Some argue that raw materials are directly procured (Gould 1985, Gould and Saggers 1985), perhaps for their physical properties linked to functional needs (Mackay 2008, Minichillo 2006, Stout 2002), or symbolic (Clendon 1999, Gould, Koster, and Sontz 1971, Wurz 1999) and stylistic needs (Close 2002, Mackay 2011, Sackett 1986, 1982). The other argument is that raw materials are acquired during an embedded and encounter-based procurement strategy (Binford and Stone 1985, Binford 1979), where the changing frequencies are either due to changes in the mobility strategy affecting the foraging range size (Ambrose and Lorenz 1990, Kuhn 2004, 1991, McCall 2007) or changes in the natural availability of raw materials on the landscape (Brantingham 2003, Brown 2011, Volman 1981). Changes in raw material usage frequencies have also been hypothesized to be linked to changes in demography (Clark 1980) and trade and exchange (Akerman, Fullagar, and van Gijn 2002, Deacon 1989, Torrence 1986, Wurz 1999). Similar possibilities need to

be kept in mind when investigating raw material selection and why raw material frequencies change in the archaeological record.

The direct procurement versus embedded procurement is a useful heuristic framework to contrast raw material selection behavior but it is useful to note that, for example, the Australian record shows that the most likely scenario for a raw material selection strategy is a mix of both direct and embedded procurement in addition to trade and exchange (Akerman 2007, Akerman, Fullagar, and van Gijn 2002). Examples from the Australian record show that special stones used for circumcision were mostly directly procured using special task groups or traded for, while other stone was procured while moving for other purposes (Gould 1978).

Binford's (1980, 1979) models, particularly his proposition that raw material procurement always should be embedded with other resource extraction activities were not always well received. The ensuing debate between Binford (Binford and Stone 1985:1) and Gould (Gould 1985, Gould and Saggers 1985, Sackett 1986) is called the "righteous rocks debate". Gould and Saggers (1985) contended that Binford's embedded and encounter-based procurement strategy model is inflexible, and they pointed to Gould's ethnographic observations in addition to archaeological patterns that both show clear evidence of direct procurement of lithic raw materials. Using the localities of James Creek East and West, Gould and Saggers (1985) conducted experiments showing that non-local materials that were selected for adze production were superior for woodworking compared to local materials. Conversely, they found that at James Creek West, the local materials were suitable for specific purposes and thus the preferential selection of those materials is reflected in the archaeological sequence. Gould and

Saggers' (1985) main argument was that factors other than an encounter-based strategy can explain raw material preference at certain localities. However, they did agree with Binford that many examples of exotic or non-local stone materials can be explained by embedded procurement.

Following the 'righteous rock debate', Bamforth and Bleed (1997) focused on the role of raw material selection in the technological organization of hunter-gatherers. They proposed that the stage that includes the selection and procurement of raw materials is critical because it sets the range of possibilities for how a hunter-gatherer produces tools and how the tools can later be used. They pointed out that once raw materials are acquired, it can be used to produce the most complex flaked stone tools in an hour by a skilled knapper. They used a conceptual framework based on risk and the potential cost of failure of the tool, and they balance the decisions made by hunter-gatherers regarding procurement, production, and use (Brown 2011). Bamforth and Bleed argued that the cost of failure can be high or low in each of these different decisions. Hunter-gatherers should avoid technological strategies where the cost of failure is unacceptably high, which should lead to the selection of strategies that minimizes failure. However, the strategy of minimizing risk to find food resources at the expense of greater mean return rates is not part of any empirically supported model in foraging theory (Brown 2011). When considering the concept of risk, they argued that if suitable stone is not available when needed it can result in the failure of tool production scheduling, which in turn can result in the canceling of the intended activity. An important thing to note is that cost and risk of canceling the intended activity can be compared directly to efficiency and procurement costs and benefits. Canceling the intended activity is just a part of the overall income

equation. Further, special efforts to procure stone could be costly and interfere with other activities. However, hunter-gatherers may need to bear these costs in situations where high failure rates linked to production requires access to large amounts of raw materials and increased efforts in procurement (Bamforth and Bleed 1997).

To define how ethnographic groups manage risk they used the number of tools as the proxy for technological diversity, and number of tool parts as the proxy for technological complexity (Bamforth and Bleed 1997). They found, similar to Torrence (1983) that in higher latitudes the risk and the cost of failure increase because there is a general lack of alternative food sources. They posited that if alternative food sources are taken into account when hunter-gatherers are targeting mobile prey, then increasing latitude results in greater toolkit diversity but not necessarily toolkit complexity. A critical thing to note again concerning Bamforth and Bleed's (1997) and Torrence's (1983) studies is that tool classes are potentially subjective in nature, and the same is true for tool parts. This can skew the calculation of complexity.

Distance-decay models

Two aspects that can affect the role and importance of raw materials in the technological organization is the availability of raw materials and the distance to source (Andrefsky Jr 1994, Goodyear 1989, Kuhn 1991). How distance to source affects technological variability is best understood by using the distance-decay concept (Blumenschine et al. 2008). The concept holds that raw materials from non-local, distant sources, or that are costly to obtain will be represented in lower frequencies (Renfrew 1969), show more evidence of conservation (Bamforth 1990, Neeley and Barton 1994), be found in smaller

sizes (Ambrose 2002), and be in a more finished form compared to local materials (Géneste 1985).

Several studies have been presented that are versions of distance-decay models, and the made the case for the importance of geographic setting and distance to source in interpreting assemblage variability (e.g. Géneste 1985, Féblot-Augustins 1997, Bamforth 1986, Andrefsky 1994). In an early study that supports the distance-decay concept Géneste (1985) examined Middle Paleolithic (MP) assemblages from sites in the Perigord region of France. He demonstrated that local raw materials were mostly represented by all phases of reduction, while non-local materials were mostly represented as finished and discarded tools. Based on this he argued that the makers of the Mousterian technology had a dual strategy of provisioning places and provisioning individuals. Places (e.g. campsites, home bases, central places) were provisioned with local raw materials that were used more expediently, while individuals were provisioned with curated and maintained tools made on non-local raw materials (Géneste 1985).

Following Geneste's study, studies by Bamforth (1986) and Andrefsky (1994) and Feblot-Augustins (1997) presented more data supporting the distance-decay argument. In a classic study, Andrefsky (1994) focused on the availability of raw materials and how it determines the technological organization of hunter-gatherers and the resulting lithic technology. Andrefsky hypothesized that it was the relative abundance of raw materials on the landscape and quality of the available raw materials that determined whether an archaeological assemblage would be formal or informal in nature. He argued against using settlement system as a factor explaining changes between formal (curated) and informal (expedient) tool use. He defined raw material quality in terms of

flakeability, which can be further defined as the suitability of a stone to facilitate the production of formal tools that require craftsmanship. The problem with formal tools is that it is a subjective designation based on a given typology. In the South African MSA record, there are few formal tools compared to unretouched and expediently flaked tools. Nevertheless, the MSA record suggests that flakeability was a preferred quality driving the selection of raw materials (Brown et al. 2009, Mackay 2008). Stone raw materials that are fine-grained usually meet that definition (Brown 2011).

Andrefsky (1994) used three archaeological examples from the western United States that showcase both sedentary and mobile site occupations. He showed that raw material availability and abundance, and not settlement system are the most important factors determining assemblage composition. Andrefsky (1994) showed that when the hunter-gatherer faced a situation where raw materials regardless of quality were locally abundant then they made the majority of the tools on local materials, although formal tools were made more commonly with high-quality materials. Conversely, when the hunter-gatherers faced a situation where local materials were scarce and of relatively lower quality they used the local materials to make expedient tools, while the majority of the tools were imported as formal tools made on non-local materials. These formal tools were conserved, maintained, re-sharpened, and used again for a variety of tasks (Andrefsky 1994). The important point made by the work by Andrefsky and others is that availability of raw materials and the intended tool use both need to be considered as important factors alongside mobility and time stress when discussing technological variability.

However, several studies have argued that constraints on raw material availability do not explain technological variability (e.g. Kuhn 2004, 1991, Milliken 1998). Kuhn (1991) investigated the intensity of lithic reduction at two Mousterian sites in Italy called Guattari and Sant'Augostino. At both sites, there was evidence for the use of small flint pebbles, which limited the size of debitage and the use of the Levallois reduction technique. While the Guattari site has unworked pebbles in the vicinity of it Sant' Augostino does not. Kuhn put forward a hypothesis that the decision to reuse or economize stone material relates to the cost of raw material acquisition. To test his hypothesis, Kuhn used indices of core size, frequency of tools with multiple edges, ratios of retouched to unretouched tools, and scraper reduction to estimate the intensity of core reduction and tool maintenance. The archaeological record at Guattari showed the expected pattern of greater intensity of core reduction but tools where not reduced as intensely. Based on this he contended that the intensity of core reduction is associated with raw material availability but not tool reduction and that the differential conservation of non-local 'exotic' raw materials is more likely due to mobility strategy and extended tool use than with the cost of raw material acquisition. Kuhn then proposed that sites that are occupied for longer durations are more amenable to lowering costs by stockpiling raw materials using embedded procurement. According to Kuhn (1991), this would result in a more expedient use of non-local material than can be expected from a simple distance decay model (Brown 2011).

Following up on his earlier paper, Kuhn (2004) focused on provisioning strategies to explain changes in raw material use in the Upper Paleolithic site of Űçağızlı in Turkey. He found that there is a continuity of raw material selection throughout the sequence.

Change is visible in the steady increase of the use of flint from secondary to primary sources and the increased transfer distances that occurred with the shift from episodic to more intensive occupation of the cave at 12 ka. Scrapers made from non-local materials from distant sources that are found in the layers that reflect intensive occupation, actually are less reduced than scrapers that are made on local materials that are found in layers reflecting less intensive occupations. This result is similar to his findings in a MP context that limited support for the distance-decay premise.

Using the record from Űçağızlı, Kuhn outlined three potential provisioning strategies that the hunter-gatherers may have designed to overcome supply constraints. In the first strategy, the individual is provisioned with finished transportable formal tools. This strategy is appropriate for hunter-gatherers that have a mobility system with frequent moves, which requires the population to keep weight at a minimum (Kuhn 1994). In the second strategy, it is the location that is provisioned. If hunter-gatherers make more frequent use of a cave or if they are more sedentary it makes more sense to keep lithic raw materials in ready supply. In the third strategy, Kuhn (2004) described the provisioning of unplanned activities. In this strategy, materials are provisioned for tools that are made as needed. Further, Kuhn showed that the occupants of Űçağızlı over time changed their provisioning strategy from focusing on provisioning individuals when the site was occupied less intensively to provisioning the site when the site was more intensively occupied. According to Kuhn this shift in provisioning strategy would allow fewer restrictions on conserving raw materials leading to a more expedient use of scrapers. Conclusively, Kuhn (2004) asserted that changes in raw material economy should correspond with changes in settlement system and provisioning strategies. This

argument has been supported by simulation work done by Barton and Riel-Salvatore (2014) that showed, using agent-based modeling, that assemblage composition is strongly affected by mobility strategy in conjunction with place or individual provisioning.

An important lesson from the studies in support for and against the distance-decay concept is that we should be investigating multiple variables within a larger settlement system instead of just looking at single conditioners of technology such as raw material availability, time stress, risk, or mobility system (Milliken 1998).

The preceding discussion highlights arguments for or against whether raw material abundance and distance to source have an effect on technological organization of a hunter-gatherer, in turn affecting the composition of an archaeological assemblage. However, the discussion does not highlight why hunter-gatherers select a raw material, and thus potentially why raw material frequencies change in the archaeological record.

Raw material quality

Archaeologists and modern knappers most often cite quality as a key feature that drives raw material selection (Brantingham et al. 2000). Knappers today usually emphasize replicating formal tools and not producing tools needed for their own fitness or survival; this has led to a bias towards the ease of flaking being considered the most important raw material quality (Brown 2011, Luedtke 1992, Magne 2001). Similarly, archaeologist's definition of raw material quality has been based on stone grain size (Goodyear 1989) and ease of shaping and reduction (Andrefsky 1994). Goodyear (1989) used stone grain size to define quality. The advantage of using fine-grained raw materials according to Goodyear is that it provides a reliable isotropic fracture and increases the control over

core reduction. Goodyear (1989) argued that fine-grained stones can be reduced with minimal undesired breakage due to the plasticity of the material. Andrefsky (1994), similar to Goodyear, defined quality based on how easily a stone material can be shaped and retouched. To him, fine-grained materials provide the knapper with greater control over the reduction process compared to coarse-grained materials, which are more difficult to shape. It has also been proposed that the size of the raw material package may play a part in the consideration of raw material quality as the nodule size or configuration of the raw material may constrain the technological approach to core reduction (Brantingham et al. 2000, Hiscock et al. 2009, Kuhn 1991)

Ethnographic observations have also highlighted how quality was defined by traditional people with knowledge of stone tool making. In an early account, Nelson (1916) noted that Ishi, a Yahi Californian Native American, favored glass when making bifacial projectile points because of its superior workability. Heider (1967) observed the Dugum Dani of the West New Guinea highlands and noted that they prefer harder black stone over softer speckled stone when making ground stone axes and adze heads. However, they do not provide any names for their raw materials for what archaeologists would classify as different types of raw materials. Binford and O'Connell (1984) while observing Alywaran tool makers in the Australian Central Desert noted that the Alywaran men look for purity of color and smooth texture when selecting stone raw materials. They deliberately select and prepare materials to create men's knives, and avoid materials found at the surface as they consider that material to be rotten and thus will not fracture properly. To find good materials, they not only investigated the flaking properties of the

quartzite materials in the quarry area by striking off large test flakes but also considered previously knapped waste products (Binford and O'Connell 1984).

Stout (2002) summarized ethnographic observations of how Irian Jaya adze makers in Indonesia select and describe raw materials. Among the raw materials, the Irian Jaya use are metamorphosed basalt and andesitic basalt, which they quarry during several days in groups led by expert craftsmen. The prospective raw material source cobbles and boulders are evaluated according to crystalline structure, grain size, and internal flaws. The quarry group breaks up the boulders using large hammerstones and sometimes by fire, which is a process that can take all day (Stout 2002). As the quarry group creates cores and flake blanks they are shared, while early-stage ('roughed out') adzes are stockpiled and wrapped in leaves and carried back to the village. Ultimately, the adzes are finished by a group by knapping and grinding at the village. Although the Irian Jaya have a complex vocabulary to describe and teach the adze production process, including how to identify the desired properties of potential nodules prior to core preparation, they do not have formal names for the raw materials. This suggested that the classification of the raw materials is less important than the act of identifying the physical and aesthetic properties of the raw materials (Stout 2002).

In a more recent ethnographic study, Arthur (2010) studied how Ethiopian Konso women make scrapers from stone and glass for hide-working. Traditionally, the Konso women preferred chalcedony, which they had to travel a distance of 25 kilometers to acquire. They preferred chalcedony because it was homogeneous and easy to flake. They avoided stone that fell apart easily and broke into small pieces. After the 1970s chalcedony was partly replaced by glass and local quartz and quartz crystal.

In summary, the ethnographic observations suggest that the tool makers considered quality with respect to both flaking properties and the suitability to the intended task (Brown 2011). The tool makers knew and thought about fundamental differences that can occur in the manufacture and performance quality of raw materials. However, preferences associated with non-functional stone properties were only understood after mechanical properties were evaluated. The quality traits considered being important to archaeologists and modern knappers such as homogeneity, fracture predictability, and edge durability are grounded in fracture mechanics theory (Cotterell and Kamminga 1992, Erdogan 2000). These traits can be quantified in actualistic experiments and standardized laboratory tests (Brown 2011). Brown (2011) provided a comprehensive review of the methods used to characterize lithic raw materials and I will draw on his review below.

Mechanical testing of lithic stone properties

Brown (2011) pointed out that researchers have several variables to test when it comes to evaluating and comparing the physical properties of stone raw materials. These include stone hardness, toughness, abrasion resistance, uniformity, elasticity, and stiffness (Domanski, Webb, and Boland 1994). Goodman (1944) used stone hardness and toughness in an early ground-breaking study where she mechanically tested lithic stone properties. She identified two major hurdles a researcher faces when wanting to quantify the fracture properties of a raw material. The first hurdle is that archaeologists and geologists often do not identify and describe stone in a similar way. Second, when a researcher wants to attempt to test raw materials to rank them according to physical

properties these tests should be constructed so that they mimic conditions of human flaking and tool use. Goodman addressed the observation that prehistoric hunter-gatherers and ethnographically observed hunter-gatherers did not always select the raw material that was the easiest to flake. She argued that when describing the range of properties that could be desirable to prehistoric toolmakers a researcher should evaluate a variety of variables. To that effect, Goodman used raw material density, hardness, toughness, and resiliency to rank flint, obsidian, quartzite, fossilized wood, and tuff.

Hardness, toughness, abrasion resistance, uniformity, elasticity, and stiffness all evaluate a material's resistance to applied pressure (Brown 2011). This resistance is given in units of pound-force per square inch (PSI) or in megapascals (MPa). However, the manner of the directionality of the applied force simulates different aspects of how a tool is manufactured or used (Brown 2011). A problem with these tests is that they generally show the variability within similar lithologies and might only be useful for statistical comparison on a regional basis or across single localities (Luedtke 1992). In a study comparing chert from volcanic and sedimentary origins, Domanski and colleagues (1994) found that the mechanical properties can vary greatly (Brown 2011).

However, the homogeneity, grain size, and isotropism of a sample also control mechanical properties (Cotterell and Kamminga 1992). What these variables have in common is that they are used in uniformity studies (Brantingham et al. 2000, Braun et al. 2009, Domanski, Webb, and Boland 1994, Domanski and Webb 1992) that seek to quantify the frequency or the encounter rate of flaws in a given mass of stone (Brown 2011). Two early examples of such uniformity studies are by Domanski et al. (1994) that ranked stone raw materials by the number of samples that fail during preparation, and

Brantingham and colleagues (2000) that ranked raw material quality by tabulating visible flaws and crystal impurities to calculate an impurity encounter rate.

However, two tests that are better at tracking flakeability (the ease of which a stone can be fractured) are the fracture toughness and rebound hardness tests (Domanski and Webb 1992). Domanski et al. (Domanski, Webb, and Boland 1994) stated that fracture toughness is the resistance of a material to fracture propagation. To test toughness a researcher notches one end of a core shaped like a cylinder and then apply and simultaneously measure the force required to pull apart the notched side and completely fracture the core. Lower values indicate that it is relatively easy to initiate fractures in the stone, and they are approached in glass or obsidian (Brown 2011).

Sevillano (1997) showed that published fracture toughness values for quartzites generally ranges between 2.0-4.0 MPa $m^{1/2}$, which is on average higher than chert values that ranges between 1.2-1.8 MPa $m^{1/2}$ (Sevillano 1997), untreated silcrete that ranges between 2.0-2.5 MPa $m^{1/2}$ (Domanski, Webb, and Boland 1994), heat-treated silcrete that ranges between 1.4-1.8 MPa $m^{1/2}$ (Domanski, Webb, and Boland 1994), and quartz that ranges between 0.3-2.1 MPa $m^{1/2}$ (Atkinson 1984). This study follows Brown (2011) in arguing that abovementioned values provide a good relative scale of flaking quality for materials found in the Mossel Bay region. What the values above indicate are that untreated silcrete may overlap in flaking quality with quartzite. However, the flaking quality of heat-treated silcrete is close to chert (Brown 2011). A caveat is that heat-treated silcrete also overlaps with quartz.

Rebound hardness, on the other hand, is an estimate of the resistance of a raw material to strain or deformation. Hardness is usually measured using a Schmidt hammer

(Goudie 2006). Hardness is heavily influenced by how homogeneous or pure a stone is, which means that it represents a measure of fracture predictability (Braun et al. 2009). Noll (2000) argued that stone raw materials with higher rebound values are stiffer, which makes them fracture easier and predictably (Braun et al. 2009). In an important study, Braun and colleagues (2009) found that rebound hardness correlates with other measures of hardness and elasticity but do not seem to correlate well with abrasion-resistance.

Raw material stiffness, an important variable for evaluating the performance of blade manufacture, can also be measured using Young's Modulus (Domanski, Webb, and Boland 1994). Young's Modulus measures how resistant a material is to deformation when a compressive load is gradually increased to the point of material failure by calculating stress curves (Domanski, Webb, and Boland 1994). Greater material stiffness is reflected in high values of Young's Modulus. To measure Young's Modulus a researcher divides the amount of the compressive load required to fracture the raw material by the cross-sectional area of the sample core (Domanski, Webb, and Boland 1994). It has been found that heat-treatment of certain lithologies such as chert and silcrete can increase the overall stiffness of the raw material, which results in an increased flakeability (Brown et al. 2009, Domanski, Webb, and Boland 1994, Domanski and Webb 1992, Webb and Domanski 2008).

Fracture toughness, rebound hardness, and Young's Modulus all evaluate strain on material associated with tool manufacture but they do not test what the strain on the material is during use. The Los Angles (Kahraman and Fener 2007) and Taber Abrasion (Braun et al. 2009) tests are two methods available to test the abrasion resistance of a material. In both methods, blocks of material are subjected to controlled amounts of

abrasive force. A researcher then measures the percentage of lost material resulting from the tests. Noll (2000) noted that less resistant materials yield greater percentage values. The demonstration by Braun and colleagues (2009) that abrasion resistance and rebound hardness are not always correlated is very important. It suggests that when hunter-gatherers select raw materials they might have to choose between increased flakeability (high rebound hardness) and increased durability (low percentage of material loss).

Brown (2011) contended that on average quartzite is more difficult flake compared to other raw materials such as silcrete, chert, and quartz. This assertion is supported by other studies that argued that coarse granular raw materials such as quartzite are less desirable for the production of small blades because they are increasingly susceptible to step fracture terminations and limits the potential for reshaping and retouch (Kuhn 1989, Webb and Domanski 2008). Given the result by Braun and colleagues (2009) that abrasion resistant and rebound hardness is not necessarily correlated, the higher fracture toughness values of quartzite might point to advantages in using it (Brown 2011). A correlation between critical strain, meaning where catastrophic fracture occurs from strain, fracture toughness, Young's Modulus, and edge toughness has been demonstrated (McCormick 1985). Materials that have been shown to have high fracture toughness values and lower overall Young's Modulus values will have edges that are more wear-resistant because edge toughness (wear-resistance) increases with critical strain, which is correlated with fracture toughness and Young's Modulus (Brown 2011). Further, edge toughness is also positively correlated with edge angle, where a decrease in the edge angle (acuter) decreases edge toughness (McCormick and Almond 1990). In sum, edge toughness (strength) is an advantage that quartzite has over other finer-grained

raw materials such as heat-treated silcrete, chert, and quartz. However, edge strength is not the same as edge sharpness, which is dependent on the grain size of the material (Brown 2011). The finer-grained materials, which are more brittle and less resistant to strain induced fracture have the sharpest edges (McCormick and Almond, 1990). Heat-treatment of silcrete should thus reduce edge toughness but create sharper and more brittle edges (Crabtree 1967, Wilke, Flenniken, and Ozbun 1991) because of the decreased fracture toughness and/or increased Young's Modulus (Beauchamp and Purdy 1986, Brown et al. 2009, Domanski, Webb, and Boland 1994). **Table 1** summarizes the different raw material qualities that have been highlighted to be attractive qualities when selecting a raw material and which physical measurements that account for those qualities.

Table 1. Raw material properties by physical measurements

	Physical Measurements							
Raw Material Properties	High Fracture Toughness & Low Stiffness (Young's Modulus)	Low Fracture toughness	Higher Fracture Toughness	Increased Rebound Hardness	Increased Stiffness (Young's Modulus)	Abrasion Resistant	Increased Edge Angle	Finer Grain Size
Easy to Flake (Flakeability)		X[b]		X[d]	X[e]			
More Durable			X[c]			X[f]		
Increased Edge Sharpness								X[h]
Increased Edge Toughness/Wear-Resistance	X[a]						X[g]	

a b (Brown 2011); c (Braun et al. 2009, Sevillano 1997); d (Noll 2000); e (Brown et al. 2009, Domanski, Webb, and Boland 1994, Domanski and Webb 1992, Webb and Domanski 2008); f (Braun et al. 2009, Noll 2000); g (McCormick and Almond 1990); h (McCormick and Almond, 1990).

Given these qualities, edge strength (toughness), edge sharpness, overall durability, and flakeability, quartzite and heat-treated silcrete offer two different choices. One choice is to select quartzite, which would give you improved edge strength but at the

cost of decreased flakeability. Jones (1979) and Noll (2000) noted a more durable edge on ESA hand axes made on quartzite. On the other, if silcrete is selected and heat-treated then you gain flakeability and edge sharpness, potentially at the cost of decreased edge strength (Brown 2011).

In summary, it strengthens the results of the mechanical testing that ethnographic observations also suggest strategic or deliberate selection of raw materials for physical properties. However, it is important to note that the concept of stone quality is subjective and depends upon the intended use of the tool (Brown 2011). However, researchers can rank materials based on mechanical properties such as hardness, elasticity, and edge durability (Braun et al. 2009, Domanski, Webb, and Boland 1994, Noll 2000). This type of ranking will be useful for predicting the materials that should be selected for different tasks (Brown 2011). However, the range of materials in the local environment and the local knowledge of source locations will limit the raw material selectivity (Brown 2011).

Other factors influencing raw material selection and frequency

Although raw materials sometimes are selected by an individual for specific qualities linked to mechanical properties and are procured either during direct or embedded procurement, other factors such as such as stylistic (Close 2002, Mackay 2011, Sackett 1986, 1982) or symbolic needs (Clendon 1999, Gould, Koster, and Sontz 1971, Wurz 1999) might influence why some raw materials are selected over others, thus potentially change raw material frequencies in archaeological records. Additionally, others factors linked to whole populations or groups over longer time scales such as demographic change (Clark 1980) and trade and/or exchange (Akerman, Fullagar, and van Gijn 2002,

Torrence 1986) might also explain why raw material usage frequencies change in the archaeological record.

In the first group of alternative factors, Gould et al. (1971) observed that the aborigines under study tend to place aesthetic value on chert with different colors and texture. Aborigines from Warburton prefer white chert, while the Nyatunyatjara and northern Ngatatjara prefer yellowish quartzites and creamy yellow chert. Gould and colleagues (1971) noted that these preferences appears not to be driven by the actual working qualities of the different materials but instead is a reflection of the close 'totemic' tie each man has to the region he was born in and he claims totemic decent from. Further, they noted that a man feels a sense of kinship to these localities and value them as a part of themselves (Gould, Koster, and Sontz 1971). According to Gould et al. the raw materials are not sacred but they observe that the materials are carried over long distances by their owners. Similarly, ethnographic observations by Clendon (1999) showed that shiny and semitranslucent stone was chosen for the production of some stone tools in order to imbue them with aesthetic value and to derive magic and curative powers from that value. The observations of Gould and colleagues and Clendon suggest that hunter-gatherers sometimes choose raw materials that have symbolic value to them. However, questions remain about how frequent raw materials are subject to direct selection based on style, totemic ties, or color; how frequent are they in an assemblage? These are very hard questions to answer and will be crucial to address in future studies. For example, one needs to come up with a way to quantify what are potentially semi-precious stones in an assemblage.

Close (2002) investigated the size and shape of backed microblades from North African assemblages dating to the late upper Paleolithic. She (2002) found that when selecting raw materials for making backed microblades that the distance to the source and the type of raw material did not have a profound effect on the size and shape of the tools. The research by Close (2002) suggested to her that among these groups the cultural constraints on the size and shape of tools and the use of tools in 'face to face' group interactions suggests that the main driver behind raw material selection (or the lack of raw material preference) was style preference. It is important to point out that Closes' arguments are all inferred from archaeological data. It is not clear how Close was able to infer 'face to face' group interactions.

In the other group of alternative factors, which are linked to whole groups of people over longer time scales, Akerman et al. (2002) contended that the selection of raw materials to make Kimberly points in Australia was driven by trade and exchange of the points themselves. They noted that Aborigines that they observed did not pay any regard to real or perceived physical capabilities of the raw materials that they used to make points. That is, they did not select the raw materials for edge strength or edge durability for example. Instead, semitranslucent and shiny stones were selected so that some of the Kimberly points could be of value in trade and exchange with other groups. This ethnographic observation suggests that the trade and exchange of raw materials can have an effect on archaeological raw material frequencies.

Clark (1980) argued that the change from one raw material to another in archaeological sequences in Africa might be due to changes in demography. He used the raw material frequency data from both South and North African LSA and MSA sites to

argue that the changing raw material preference is due to the replacement of technological tradition at the sites, and not perhaps an evolution of a single developing tradition.

In summary, all these factors, either linked to individual selection of raw materials or population or group-wide behaviors, need to be taken into account when discussing why archaeological raw material frequencies change.

Models for why raw materials change

Given the multiple hypotheses and models that have been proposed to explain why forager select certain raw materials and why raw material frequencies change in the archaeological record it is here useful to create a systematic framework that highlights how the different factors can change the raw material frequencies. Brown (1999) presented a useful model framework that categorized the different models in this respect. Brown (1999: 57) divided the models into an "Encounter Based Procurement" model category and a "Deliberate Procurement" model category. Both sets of model categories had two variants each. The "Encounter Based Procurement" model category included a "Natural Availability" variant and a "Mobility-linked" variant, whereas the "Deliberate Procurement" model category had a "Symbolic" variant and a "Functional" variant.

Below I build on and modify Brown's framework but make two important changes. 1) The two main model categories are renamed to 'Non preference-based change' and 'Preference-based change'. This is because it allows for the inclusion of other hypotheses proposed about raw material change and selection that are linked to whole populations or groups of people over longer time-spans and not just individual

actions. 2) The ‘Non preference-based change’ model category include three variants called ‘Natural availability’, ‘Mobility-Linked’, and ‘New tranport abilities/Carrying costs’, while the ‘Preference-based change’ model category includes three variants called ‘Utilitarian’, ‘Non-functional’, and ‘Social learning/Culture’.

Non preference-based change

In this model category, which is similar to Brown’s (1999) “Encounter-Based Procurement” model category, raw material change in the archaeological record is the result of the availability of raw materials that are encountered on the landscape either due to availability of new sources or changes in mobility system that result in the forager encountering new sources of raw materials. This model category can be viewed as an example of ‘embedded procurement’ as proposed by Binford (1979). The forager when moving about the landscape acquires raw materials opportunistically. However, a third variant can also be envisioned and that is the introduction of new transport abilities, which can change the carrying costs.

Natural availability

In the ‘Natural Availability’ variant, changes in environmental and climatic conditions with accompanying natural processes result in the alternating exposure and cover-up of potential raw materials sources on the landscape, which influences the availability of raw materials. However, erosion of raw material sources without replacement can also affect the availability of sources. In this variant, the frequency of raw materials in the archaeological record is due to abundance and availability of sources on the surrounding

landscape. Thus, changes in archaeological raw material frequencies are due to changes in the natural availability and abundance of raw material sources on the landscape (c.f. Andrefsky 1994, Brown 2011, Volman 1981).

Mobility-linked

In the second variant called "Mobility-linked", archaeological raw material frequencies are linked to the foraging range size, foraging pattern, and frequency of residential moves of foragers. When foraging range size increases it can change the type of raw materials that are encountered. Conversely, as foraging range size decreases it can limit the availability of some resources because some sources would be rarely visited. Thus, raw material availability co-varies with changes in human mobility strategies. Changes to foraging pattern to included new areas, while precluding old ones can also change the type of raw material that are encountered. Additionally, the changes in the frequency of residential moves can alter the type of raw materials that are encountered as new residential sites can be situated more frequently close to new raw material sources. Thus, in this variant, raw material frequencies in the archaeological record can be due to foraging range size and pattern or the frequency of residential moves. It follows then that change in archaeological raw material frequencies can result from changes in foraging range size, pattern, or frequency of residential moves (c.f. Ambrose and Lorenz 1990, Kuhn 2004, 1991, McCall 2007, McCall and Thomas 2012).

New transport abilities/Carrying costs

In this variant archaeological raw material frequencies are linked to changes in the transport abilities or the carrying costs of a group. The introduction of technologies such as bags, baskets, sleds, watercrafts or the use of horses can lower the cost of carrying or transporting raw materials, in turn, affecting what is transported back to and discarded at the site. Archaeological raw material frequencies are due to the ability to transport raw materials that is possessed by a forager group. Thus, when changes in transport abilities/carrying cost occur it changes the archaeological raw material frequencies.

Preference-based change

In the 'Preference-based change' model category, it is posited that changes in the archaeological raw material frequencies can be due to three different possibilities: 1) Changes in the strategic selection of raw materials that takes advantage of raw material qualities for a specific functional or utilitarian purpose; 2) Changes in the selection due to symbolic properties of the raw materials; 3) Changes in social learning or cultural aspects performed by the group in the form of traditions of tool procurement and use or trade and exchange of materials,

The selection for symbolic value seemingly does not belong to this model. The question whether symbolic value is something that is deliberately selected is linked to the debate about function versus culture. This debate was most famously undertaken by Binford (1966, 1973) and Bordes (1970) in the 1960's and 70's. However, ethnographic examples from Australia shows that raw materials were directly procured for qualities linked to symbolic value (e.g. Clendon 1999). Therefore the 'Non-functional' model

variant presented in the ‘preference-based change’ model category should be seen as a strategy that targets a raw material for a specific quality regardless of whether that quality is linked to function/utility or symbolic value.

Utilitarian

In the ‘Utilitarian’ variant, the changing proportion of raw materials that are used to create tools results from the changing functional/utilitarian requirements of the technological strategy that is employed (c.f. Gould 1985, Gould and Saggers 1985, Mackay 2008). When selecting a raw material for a utilitarian purpose the forager can exploit new resource making new tools with new requirements and use the tools in new ways. Conversely, the forager can also exploit old resources making new tools with new requirements and use the tools in new ways. Different raw materials present the forager with tradeoffs (e.g. abundance of raw material, flakeability, edge sharpness, edge toughness). By strategically selecting a raw material for a utilitarian purpose the forager also faces costs linked to travel and search, procurement, and manufacturing. Depending on the utility (e.g. flakeability, edge strength, edge sharpness) that is being sought, the forager selects whatever raw material has the lowest cost in terms of search, procurement, manufacture, and use given the climatic or environmental context. Thus, the raw material with the highest net-return rate of utility is selected. In this variant, archaeological raw material frequencies are due to the strategic selection of the raw material with the highest net-return rate of the sought-after utility. Changes in the archaeological frequencies are due to changes in the net-return rates of raw materials, which can be affected by the environmental and/or behavioral context of the forager (c.f. Mackay 2008).

Non-functional

In the "Non-functional" variant, the selection of raw materials and the changing proportions of raw materials reflect changes in the symbolic needs of the tool maker. The symbolic value of the final product is determined by raw material selection. In this variant, archaeological raw materials frequencies change because of changes in the symbolic value of raw materials (c.f. Clendon 1999, Gould et al. 1971, Wurz 1999).

Social learning/Culture

In this variant, raw material frequencies are linked to endogenous culturally transmitted preference or horizontal transmission of preference introduced from outside. Changes to the traditions of a group (vertically transmitted and relatively stable in a group), which are enforced by social learning can be brought on from inside the group, maybe due to a new discovery and invention. A change in the culturally transmitted preference of a raw material, perhaps needed for a new tool, leads to a change in raw material selection. Alternatively, raw material change is due to the influx of change from the outside either by trade or exchange or dominance by a new group (c.f. Akerman et al. 2002, Deacon 1989, Torrence 1996). Thus, in this variant, changes in archaeological raw material frequencies are the result of endogenous changes in culturally transmitted preference or due to horizontal transmission of change introduced from outside.

This model framework that outlines models that propose why raw material frequencies change in the archaeological record will be the used when I below present the archaeological evidence for raw material selection and change in the South African Middle Stone Age.

CHAPTER 3: RAW MATERIAL SELECTION IN THE AFRICAN STONE AGE

Introduction

In this chapter, I will first briefly look at raw material selection and technological organization in the African Early (ESA) and Later Stone Age (LSA), and then I will thoroughly review the evidence for raw material selection and technological organization from the Middle Stone Age (MSA) record from South Africa and Lesotho. At the end of this chapter, I will present a framework for different models that have been proposed to explain raw material change in the South African MSA.

It is has been argued that the African continent has a greater diversity of stone materials available for stone tool manufacturing compared to Western Europe. Because of this raw material selection has figured prominently in studies of hominin technological variability in Africa (Brown 2011, Clark 1980). Goodwin and Van Riet Lowe (1929, 1929) divided the African Stone Age into three major phases based at a general level by the presence of large core tools in the ESA, prepared cores with flakes and blades as the products in the MSA, and microlithic, scraper and flake tool technologies in the LSA. In other words, the overall pattern in the African Stone age is a long and punctuated progression from larger and cruder to smaller and refined tools, and increased complexity in core reduction techniques, which reveals an elevated depth of planning (Brown 2011). Lithic raw material preference changes over time from the preference of tougher and durable materials through the ESA and most of the MSA towards an increased use of fine-grained and what has been argued to be higher quality raw materials in the late MSA and early LSA (Ambrose 2002, Brown 2011).

Earlier Stone Age

The ESA dates from as early as 3.3ma (Harmand et al. 2015, McPherron et al. 2010) or at least 2.6ma (Delagnes and Roche 2005, Roche 1999, Semaw et al. 2003, Semaw 2000, 1997, Stout et al. 2010, Stout et al. 2005) to approximately 500ka with the onset of blade production and hafting of points (Herries 2011, Johnson and McBrearty 2010, Porat et al. 2010, Wilkins and Chazan 2012, Wilkins et al. 2012) but definitively 300ka-250ka (Marean and Assefa 2005). The ESA was potentially the result of the behavior of at least 4 hominin species including *A. afarensis*, *H. habilis*, H. erectus, and *H. heidelbergensis*. The ESA can be classified as core-tool technology but flake removals were also utilized, and the ESA can be divided into three major periods, the 'Lomekwian' dating from at least 3.3ma to perhaps 2.6ma (Harmand et al. 2015), the Oldowan dating from 2.6ma to 1.8ma (Semaw et al. 2003, Semaw 2000, 1997), and the Acheulian dating from 1.8ma to perhaps 500ka (Herries 2011, Lepre et al. 2011).

Broadly, the Oldowan (post-Lomekwian) can be characterized by the production of simple flaked pieces and detached pieces made on river cobbles resulting from erosion of volcanic deposits (Brown 2011). The earliest evidence of the ESA all comes from Eastern African sites in Kenya, Tanzania, and Ethiopia but evidence is also found for the Oldowan and Acheulian in Southern Africa at sites such as Sterkfontein, Swartkrans, and Wonderwork Cave. Leakey (1971) originally defined the Oldowan as being typologically diverse with some specialized tool forms. However, Toth (1985) showed that most flakes could be viewed as stages in a continuum, while Potts (1991) proposed that much of the variability observed in the Oldowan is attributable to morphology of the raw material package, form and reduction degree (Brown 2011).

It has been previously proposed that the ESA does not show a lot of evidence for cognitive complexity (Ambrose 2001). However, more recent research shows that the makers of the Oldowan in some cases selected and transported materials in a preferential manner (Braun et al. 2009, Braun, Plummer, et al. 2008, Braun, Rogers, et al. 2008, Goldman-Neuman and Hovers 2012, Harmand 2009, Stout et al. 2005). Several studies have shown that early hominins preferentially selected raw materials due to certain qualities or properties such as having few flaws and not being weathered (Schick and Toth 1993), being fine-grained and easy to flake (Stout et al. 2005), and being abrasion-resistant, predictable, and having few impurities (Braun et al. 2009, 2008). The work by Braun and colleagues (2008) showed that non-local raw materials were transported as far as 10 kilometers. Harmand (2009) showed that occupants at Lokalaei 1 and 2c localities in West Turkana preferentially selected medium-grained phonolite. Goldman and Hovers (2012) investigated Oldowan localities in the Makaamitalu basin in Hadar, Ethiopia. They found that at A.L. 894 the hominins selected against non-homogeneous materials, while at A.L. 666 the hominins selected high-quality raw materials and procured rare materials from unknown sources.

Following the Oldowan is the Acheulian period. The Acheulian spans from 1.8ma to 500ka (Herries, Curnoe, and Adams 2009, Lepre et al. 2011) and it marks the introduction to true bifacial shaping technology usually recognized in the form of the hand axe or the cleaver core tool. However, the Acheulian also includes flake tools and unmodified flakes and scrapers. Compared to the Oldowan, the regular shape of the hand axe has been used as evidence to argue that hominins making Acheulian technology had advanced cognition in both planning and tool making (Delagnes and Roche 2005). Early

studies of the tool diversity and the cultural implications of the hand axe form and shape argued that it reflects cultural traditions (Isaac 1975, Noll 2000). However, raw material selection by the makers of the Acheulian has been heavily studied to understand inter-assemblage variability (Sharon 2008). Isaac (1986) and Clark (1980) contended for a similar approach in the form of residual analyses where the goal is to remove the effects that raw materials have on the finished tool before discussing whether different biface shapes and forms indicate different cultural traditions. Clark argued that we should try to separate those material-based aspects of the Acheulian technology that can be easily tested such as the primary form of the raw material, distance and quantity of materials on the landscape, material texture or fabric of material from those aspects that are harder to test such as range of variability expected within and between groups, mental templates, and task-specific demands (Brown 2011). Clark's argument still holds, and this study focuses on the material-based aspects of the South African Middle Stone Age that are potentially easier to test.

Using Isaac and Clark's approach early experimental studies aimed to understand the relationship between raw material diversity and edge characteristics (Brown 2011). Jones (1979) found that experimentally created bifaces made on quartzite are excellent for butchery because the edges do not dull easily. However, the quartzite did not allow for careful retouch. Given that, Jones proposed that tools made on finer-grained materials that have been retouched to keep the edge sharp are not refined. Instead, Jones contended that it takes the same level of skill to manufacture bifaces on coarse-grained quartzite as it does with finer-grained materials (Brown 2011).

Later efforts have sought to rate raw materials based on their mechanical properties to better understand technological variability. Noll (2000) used Taber abrasion (resistance to abrasive force), rebound hardness (flakeability) and uniaxial compressive strength (material stiffness) tests to rate igneous stone available surrounding the Acheulian site of Olorgesaile in Kenya. Noll found that cutting edge seemed to be more important than symmetry, while the frequency of raw materials has significant effect on tool thickness, scar stepping, and edge angle (Brown 2011). In conclusion, Noll (2000) proposed that the raw materials at Olorgesaile were selected for hardness and strength and that the large cutting tools were manufactured to provide its makers with long cutting edges. Sharon (2008) found that makers of hand axes and cleavers at a suite of Acheulian sites in Africa and Western Asia preferred durable materials. Sharon's (2008) research alongside others (Braun et al. 2009, Stout et al. 2005) suggested that hominins that created Oldowan and Acheulian assemblages sometimes selected durable materials even though raw materials that were more predictable were available (Brown 2011). This, in combination with the evidence of relatively long-distance transport of some materials (Braun, Plummer, et al. 2008, Clark and Kurashina 1979), implies that the ability to preferentially select materials for specific mechanical properties is a trait shared by all hominin toolmakers (Brown 2011).

Later Stone Age

The following review of the LSA will focus on the South African record. The LSA can be broadly defined as a microlithic, scraper, and flake tool technology. The LSA in the Cape can be divided into four major industries, the Robberg Industry dating from 22ka to

12ka (Deacon 1978), the Oakhurst formerly known as Smithfield A and generally recognized in the eastern Cape dating from 12ka to 8ka (Mitchell 2002), the Albany generally recognized on the southern cape dating from 12ka to 8 ka (Deacon 1978), and the Wilton dating from 8ka to 2ka (Deacon and Deacon 1999, Deacon 1978). In addition, after the Wilton more informal technologies appear that sometimes are termed the Smithfield or the 'macrolithic' that date from 2ka to contact (Deacon and Deacon 1999).

The Robberg is well represented at three sites: Nelson Bay Cave (NBC) in Plettenberg Bay (Deacon 1978), Rose Cottage Cave (RCC) in the Free State (Wadley 1996), and Sehonghong (SHH) in Lesotho (Carter, Mitchell, and Vinnicombe 1988, Mitchell 1996, 1995). The Robberg assemblages are characterized by microlithic bladelets with no retouch that are made on blade cores and a small number of backed tools and scrapers (Brown 2011). There are also bone tools at Nelson Bay Cave. However, undescriptive flakes and debitage represent the vast majority of the assemblages. Not surprisingly, the raw material preferences between the sites are different. At Nelson Bay Cave on the south coast, quartz was the preferred raw material (**Figure 3**), followed by quartzite and some silcrete (Deacon 1978). However, the raw material frequencies change in a moderately vectored way through time with quartz decreasing while quartzite and silcrete increase. At Rose Cottage Cave and Sehonghong located in the Free State and mountainous Lesotho respectively the preferred material was Opaline (Mitchell 1995, Wadley 1996). In terms of the blade technology, Mitchell (1995) argued that the presence of crested blades in the Robberg suggests standardized blade reduction, while Deacon (Deacon 1995a) argued that the small blades in the Robberg and the Howiesons Poort was both made by indirect percussion (punch).

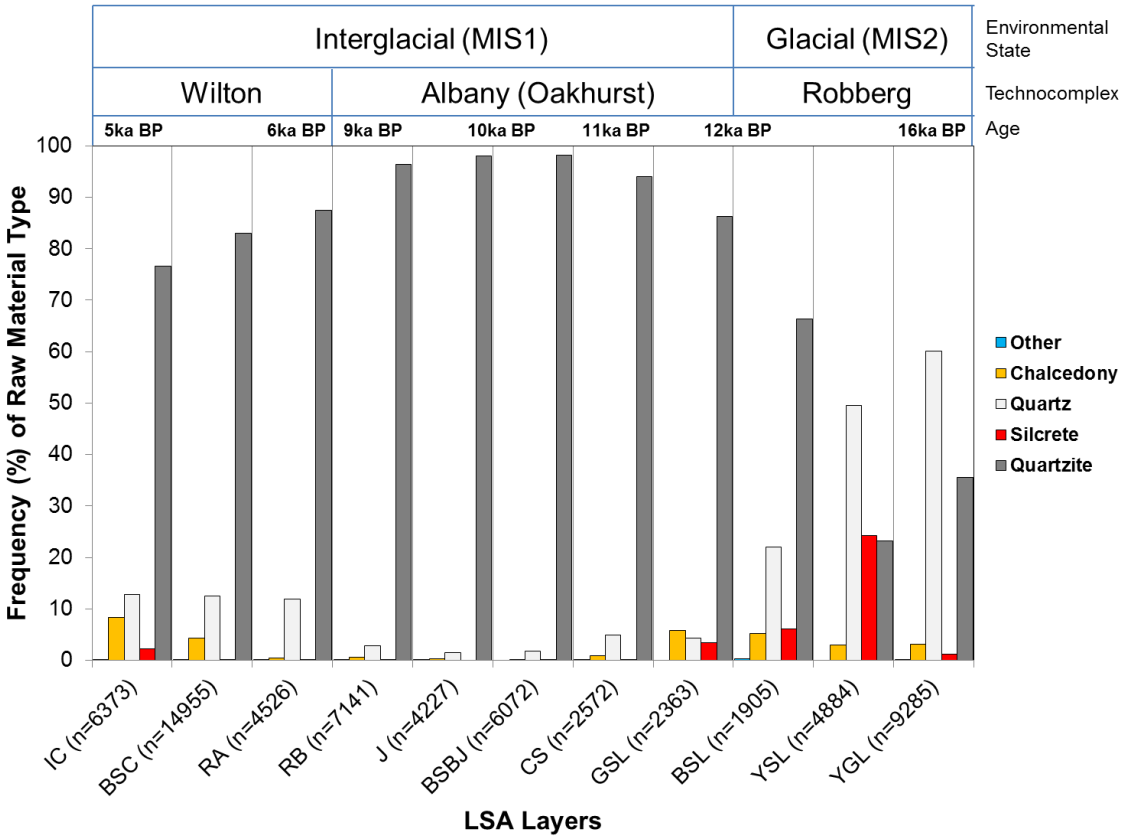

Figure 3. Relative Frequencies of raw materials from LSA layers for all stone artifacts at Nelson Bay Cave (NBC). Frequencies are shown in comparison to comparable glacial and inter-glacial states (Marine Isotope Stages). Raw material frequencies and ages from Deacon (1978).

Following the Robberg is the Oakhurst, also known as Smithfield A. The Oakhurst industry was named after the rock shelter near Wilderness and is characterized by round endscrapers, duckbill scrapers, some polished bone and a few backed pieces (Deacon and Deacon 1999). Mostly the Oakhurst assemblages are made on more coarse-grained raw material than the preceding Robberg and the following Wilton (Deacon 1978, Mitchell 2002). The Oakhurst has been divided into regional variants including the Albany in the Southern Cape and Lockshoek in the Karro (Deacon and Deacon 1999). At Nelson Bay Cave quartzite dominates the Albany (Oakhurst) levels with more than 90% of the artifacts made on Quartzite (**Figure 3**). At Boomplaas (BP) the Albany layers show

the highest percentage of quartzite during the LSA in its sequence (Deacon 1978, Mitchell 2002). A reasonable argument for the lack of fine-grained materials in the Oakhurst is that the fine-grained materials were replaced by bone tools that are found in Oakhurst assemblages (Brown 2011).

The Wilton follows the Oakhurst and it applies to mid to late Holocene microlithic assemblages (Barham and Mitchell 2008). These assemblages can be subdivided into Classic Wilton (Mid-Holocene) dating from 8ka to 4.5ka and the Late Holocene Wilton dating from 4.5ka to 2ka (Deacon and Deacon 1999). The Late Holocene Wilton is also termed the Interior Wilton, Late Wilton or Post-Classic Wilton (Deacon and Deacon 1999). Classic Wilton is characterized by a wide range of microliths, borers, small scrapers, double scrapers, ornaments, and polished bones, while the Late Holocene Wilton showcases fewer segments but an increase in bladelets (Brown 2011). At Nelson Bay Cave quartzite was the preferred raw material (**Figure 3**), while Opaline was the dominant raw material at Rose Cottage Cave (Wadley 2000). However, at the type-site quartz, silcrete and chalcedony are all preferred materials in all artifact categories (Deacon 1972).

After the Wilton, there is a lot of variability in terms of artifact size and raw material use but at least two kinds of assemblages are identified (Deacon and Deacon 1999, Orton 2008). Both types of assemblages reflect a decrease in the percentage of formal tools and reduced diversity of raw materials. The first type of assemblage is sometimes termed the Smithfield, which have pottery and stone tools made on fine-grained materials such as indurated shale, chalcedony, quartz and silcrete. If the assemblage includes long scrapers with backed bladelets it is called Smithfield.

Boomplaas has an assemblage post-dating the Wilton that consists of faunal remains reflecting pastoralism and small scrapers and backed blades made on fine-grained raw materials (Deacon and Deacon 1999) The second type of assemblage sometimes termed the 'marcolithic' precedes and is contemporary with the Smithfield. The 'macrolithic' assemblages have no pottery and they exhibit large unretouched flakes made on coarse-grained raw materials such as quartzite. At NBC, the assemblage that post-dates the Wilton consists of large and informal stone tools (Deacon and Deacon 1999). It has been argued that this change to a very informal technology with less formal tools and less raw material diversity is the result of changes in activity (Deacon and Deacon 1999, Schrire and Deacon 1989) but it could also be the result of imposed territory constraints imposed by expanding pastoralists (Jerardino 2007, Smith et al. 1991).

Southern African Middle Stone Age

Compared to the rest of the countries in southern Africa the MSA record from South Africa and Lesotho is very rich. There are sites that have yielded both stratified ESA and MSA layers such as Montagu Cave (Keller 1973, 1970) and sites that have a sequence from the ESA to the LSA such as Cave of Hearths (Mason 1957, McNabb and Sinclair 2009, van Riet Lowe 1954). A great number of sites have yielded stratified MSA and LSA layers; in South Africa: Blombos cave, Boomplaas Cave, Nelson Bay Cave, Rose Cottage Cave, and Die Kelders Cave 1. In Lesotho: Sehonghong, Melikane, Moshebi's Shelter, and Ntloana Tsoana. There have been at least 5 proposed nomenclature systems for the MSA in South Africa (Goodwin 1929, Goodwin and Van Riet Lowe 1929, Goodwin 1928, Lombard et al. 2012, Sampson 1974, 1972, Volman 1984, Wurz 2002).

Today the recognized stone age sequence in South Africa combining Volman's (1984), Wurz's (2002), and Lombard and colleagues' (2012) nomenclatures goes roughly like this: ESA, early MSA, Klasies River (MSA I or MSA 2a), Mossel Bay (MSA II or MSA 2b), pre-Still Bay, Still Bay, Howiesons Poort, post- Howiesons Poort (Sibudan, late MSA or MSA 3), final MSA (MSA 4 or MSA IV), and LSA. Important to note that this is not likely the consensus nomenclature but it will be used as the nomenclature in this study.

The first one to define the MSA in southern Africa was A.J.H. Goodwin, which in 1928 after looking at numerous artifacts he could not assign to either the ESA or the LSA, decided to make an intermediate sub-stage in the Stone Age called the Middle Stone Age (MSA). He noticed that there were assemblages that did not have the large hand-axes and cleavers of the ESA or the microliths of the LSA and that these assemblages were dominated by a flake-based technology (Goodwin 1928). Goodwin (1928) outlined a system that grouped the MSA into several groups of industries and variations. Goodwin (1928: 99-100) stated that the term industry could only be used when a group of tools was definable and certain, and the term variation would be used when there were uncertainties about the specific tool group relations to the other tool groups or if there was a lack of data accumulated. One of the tool morphologies he used to separate variations were points. Goodwin separated the MSA into 8 groups; these were the Glen Grey variation, Mossel Bay variation, Still Bay variation, Howiesons Poort variation, Pietersburg variation, Hagenstad variation, Alexandersfontein variation, and Sawmills variation (Goodwin 1928). Even though there were all these different industries and variations Goodwin (1929) stated that they all shared certain features: convergent

flakes, use of points and facetted flake butts. He argued that they all had a common origin point up north and had all been influenced by the Mousterian (Goodwin 1929: 143). The assemblages Goodwin used for his classification came from either selected surface collections or excavations where the excavator had no proper training. This resulted in a classification system that was based on selected tool types.

Through the 1930's up to the 1970's several new sites were excavated. Two sites that became important at the time were the Cave of Hearths in the Transvaal (Mason 1957, McNabb and Sinclair 2009, van Riet Lowe 1954) and Skildergat Cave in the Southern Cape (Jolly 1948, 1947). The Cave of Hearths yielded a MSA sequence that was unparalleled at that time and gave the first long MSA sequence in the Transvaal (Volman 1981). The Cave of Hearths clearly showed that the MSA was stratified between the ESA and the LSA (McNabb and Sinclair 2009). Skildersgat Cave (now named Peers Cave) is located in the Western Cape. This cave, which was excavated several times, was crucial at the time to understand the relationship between the Howiesons Poort and Still Bay variations (Jolly 1948, 1947). Other sites that were excavated and contributed to understanding the MSA sequence were: Tunnel Cave and Skildergat Kop (Malan 1955), Howiesons Poort Rock Shelter (Deacon 1995b), Mwulu's Cave (Tobias 1949), Bushman Rock Shelter (Louw 1969, Vogel 1969), Peers' Shelter (Goodwin and Peers 1953), Border Cave (Beaumont, de Villiers, and Vogel 1978, Butzer, Beaumont, and Vogel 1978, Grün et al. 2003, Grün and Beaumont 2001, Grün, Beaumont, and Stringer 1990), and Boomplaas Cave (Deacon 1979, Deacon et al. 1983, Deacon, Deacon, and Brooke 1976).

In the 1970's Garth Sampson (1974, 1972) designed a new nomenclature for the MSA in Southern Africa. Using a chronology based on statistical analysis of lithic assemblages from several sites he structured the MSA into, from oldest to newest, the Pietersburg complex, the Bambata complex, and the Howiesons Poort and Umguzan related assemblages (Magosian) (Sampson 1974). Sampson's nomenclature soon came under critique because of a steadily increasing radiocarbon database, which suggested that the MSA assemblages were far older than suspected, and the fact that the transitional Magosian had inconsistent radiocarbon ages (Klein 1970).

Following the original excavations and publication of the Klasies River assemblages by Singer and Wymer (1982) Volman (1984) introduced a new nomenclature for the MSA in Southern Africa. Based on the descriptions Singer and Wymer gave about the different stratified layers and the change in raw material and tool types throughout the sequence Volman introduced a sequence that he argued could be used for any MSA assemblage south of the Limpopo River (Volman 1984: 200-209):

- MSA 1: Characterized by a high percentage of convergent flake cores and small broad flakes that rarely shows evidence of faceting. Denticulates are the most abundant retouched tool, while there are no retouched points and scrapers with retouch are rare. Volman assigned MSA 1 assemblages to MIS6.
- MSA 2a & 2b: Characterized by large narrow flakes and blades that decrease in average length from MSA 2a to MSA 2b. There is an increase in the abundance of retouched artifact types from MSA 2a to MSA 2b.

Denticulates are common in MSA 2a, while retouch points are common in MSA 2b. Volman assigned MSA 2a and 2b assemblages to MIS5e-5a.

- Howiesons Poort: Characterized by a high percentage of retouched tools in the form of segments, trapezoids, and allied backed or truncated pieces, while flakes are not usually facetted, and they are smaller and broader compared to flakes in MSA 2. Additionally, there is an increase in the use of fine-grained material in contrast to preceding and following MSA phases. The Howiesons Poort contains scrapers and variable proportions of unifacially and bifacially retouched points. Volman assigned Howiesons Poort assemblages to MIS4.
- MSA 3: Characterized by the same types of artifacts as in MSA 2 assemblages; very similar to MSA 2b. There is a trend towards large flake-blades in the final stage of the phase. Volman assigned MSA 3 assemblages to MIS3.

In 2002, Sarah Wurz (2002) designed a new nomenclature system for the MSA in southern Africa. She bases her system on the KRM sequence. It is not a widely used nomenclature so I will not outline its details but one important thing Wurz did was to add the Still Bay technological phase to her nomenclature, wedged between Volman's stage MSA 2b and the Howiesons Poort (Wurz 2002).

The most updated nomenclature is presented by Lombard et al. (2012). They subdivided the MSA into eight South Africa and Lesotho (SAL) technocomplexes.

- The earliest technocomplex is the early Middle Stone Age, which they argued lasted between 300 ka to 130 ka coinciding with MIS8 to MIS6.

- The Klasies River technocomplex dates from 130 to 105 ka and is the same as the MSA I at Klasies River or MSA 2a generally. It coincided with MIS5d and 5e.
- The Mossel Bay technocomplex followed, known as MSA II at Klasies River and MSA 2b generally. It dates to 105 ka to 77 ka and it coincided with MIS5a to 5c.
- The Mossel Bay was followed by a technocomplex informally termed the pre-Still Bay, dating from 90 ka to 72 ka. This technocomplex, they argued, coincided with MIS5 to MIS4 transition.
- The Still Bay dates from 77 ka to 70 ka and coincided with the MIS5a to MIS4 transition.
- The Howiesons Poort followed and it dates from 66 ka to 58 ka coinciding with MIS4 to MIS3 transition.
- Following the Howiesons Poort is the Sibudu technocomplex, which is known as the late MSA/post-Howiesons Poort or MSA 3 generally, or MSA III at Klasies River. It coincided with MIS3.
- Finally, they have the final Middle Stone technocomplex that they date from 40 ka to 20 ka. It is known as MSA IV at Klasies River or MSA 4 generally. It coincided with the MIS3 to MIS2 transition.

In the late 1990's and 2000's several new sites started to be excavated, with higher attention to detail and where state of the art dating techniques are being applied to date their sequences. These new sites have improved our understanding of the MSA and I will review them here focusing on raw material selection and technological organization. The

focus here will be on sites that have been dated with the single-grain OSL technique (e.g., Jacobs, Roberts, et al. 2008a) and that have a well-understood stratigraphy yielding relatively high-resolution data on lithic technology. I will omit open-air sites.

I will first review sites from western South Africa and the Cape region (**Figure 4**): Klasies River (KRM), Blombos Cave (BBC), Diepkloof Rockshelter (DRS), Die Kelders Cave 1 (DK1), Nelson Bay Cave (NBC), Klein Kliphuis (KKH), Klipdrift Shelter (KDS), Apollo 11 (AP), and then I will shift my focus to eastern and central South Africa and Lesotho and review the following sites: Sibudu (SIB), Rose Cottage Cave (RCC), Sehonghong (SHE), Umhlatuzana (UHM), and Ntloana Tsoana (NT) (**Figure 4**).

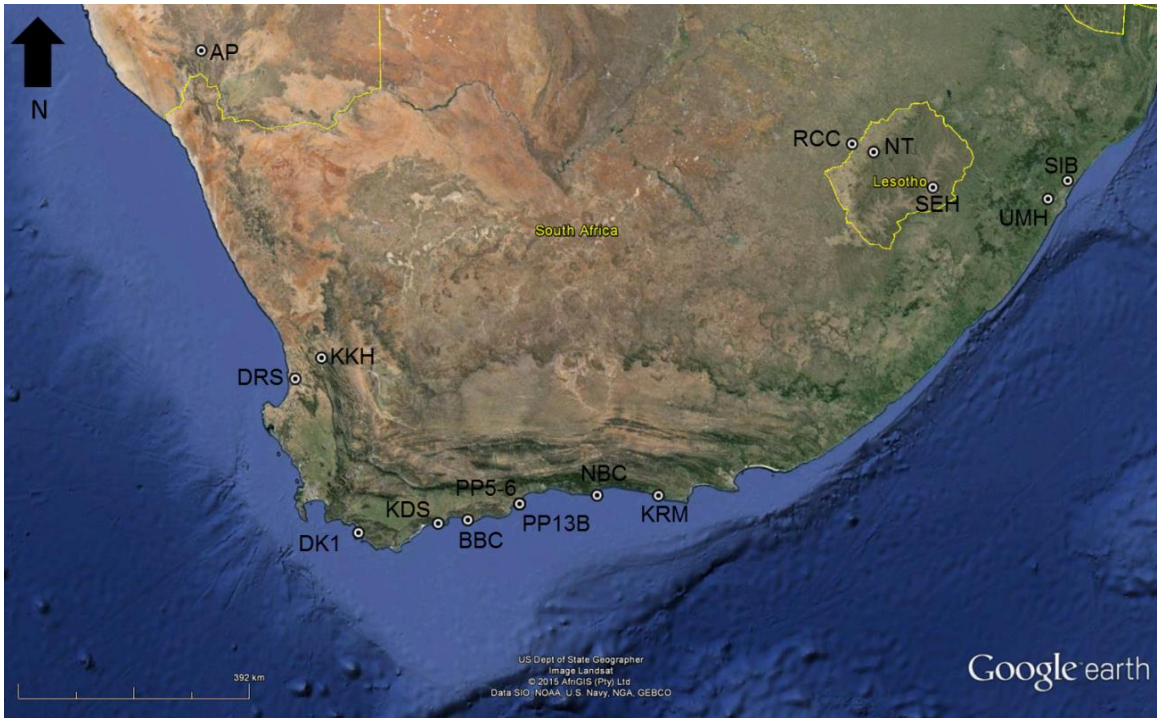

Figure 4. The geographic location of MSA sites with well-stratified and well-described deposits. Satellite image from Google Earth. AP: Apollo 11, DRS: Diepkloof Rock Shelter, KKH: Klein Kliphuis, DK1: Die Kelders Cave 1, BBC: Blombos Cave, PP5-6: Pinnacle Point 5-6, PP13B: Pinnacle Point 13B, NBC: Nelson Bay Cave, KRM: Klasies River, RCC: Rose Cottage Cave, NT: Ntloana Tsoana, UHM: Umhlatuzana, KDS: Klipdrift Shelter, SIB: Sibudu.

Klasies River (KRM)

Klasies River is a cave complex on the coast in the Eastern Cape Province, which was first excavated by Singer and Wymer (1982) in 1966-1968 and then by Deacon in the Mid 1980's (Deacon and Geleijnse 1988), and is presently being excavated by Sarah Wurz. The site has yielded a deeply stratified MSA to LSA sequence. Singer and Wymer (1982) divided the MSA into five different stages based on tool typology, stratigraphy, and raw material change (**Figure 5**):

- MSA I: Characterized by large numbers of finely struck flake-blades of local quartzite and a fair quantity of pointed flake-blades of fine quality. Many of the flake-blades are thin and symmetrical and the striking platform has been reduced and rounded, the thinned platforms suggest that indirect percussion was used to make the flake-blades (Singer and Wymer 1982: 112). The cores reflect systematic work, and well-developed single and double platform cores outnumber the irregular types. Some of the points had been reworked into denticulates and points.
- MSA II: Characterized by a decline in the quality of the flake-blades, a rise in the number of pointed flake-blades and a corresponding decrease in the number of worked points. However, denticulates and scrapers are the most common specialized form. Quartzite dominates the assemblage, while there is a slight increase in the use of non-local rock at the end of the stage (**Figure 5**). There is no increase in single platform cores even though there is an increase in struck flake-blades.

- Howiesons Poort (HP): Characterized by a drastic reduction in both size and number of flake-blades made on the local quartzite, while the number of flakes and segments made on non-local rock are drastically increased. New tool types such as crescents, trapezes, triangles, obliquely blunted points appear. Diffuse bulbs and striking platforms on flakes made on non-local rock suggest the use of indirect percussion. Gravers and scrapers are present and are neatly made on local quartzite. While local quartzite is still being used for flake-blade production, there is a marked increase in the use of non-local silcrete and other raw fine-grained raw materials (**Figure 5**).
- MSA III (Post- Howiesons Poort): Characterized by being very similar to MSA II. It has the same artifact classes with the addition of a few small unifacial points. However, some of the worked points are more specialized than those from earlier MSA stages, especially flake-blades that are steeply backed or worked all along one edge, which make them effective cutting knives. Quartzite dominates the assemblage (**Figure 5**).
- MSA IV: Characterized by being clearly related to other MSA stages. Flake-blades are less common, but there is an increase in the number of pointed flake-blades. The size ranges of the flake-blades are more typical of the Howiesons Poort flake-blades. Single platform cores more numerous than double platform cores, but irregular and undeveloped cores are most common (Singer and Wymer 1982).

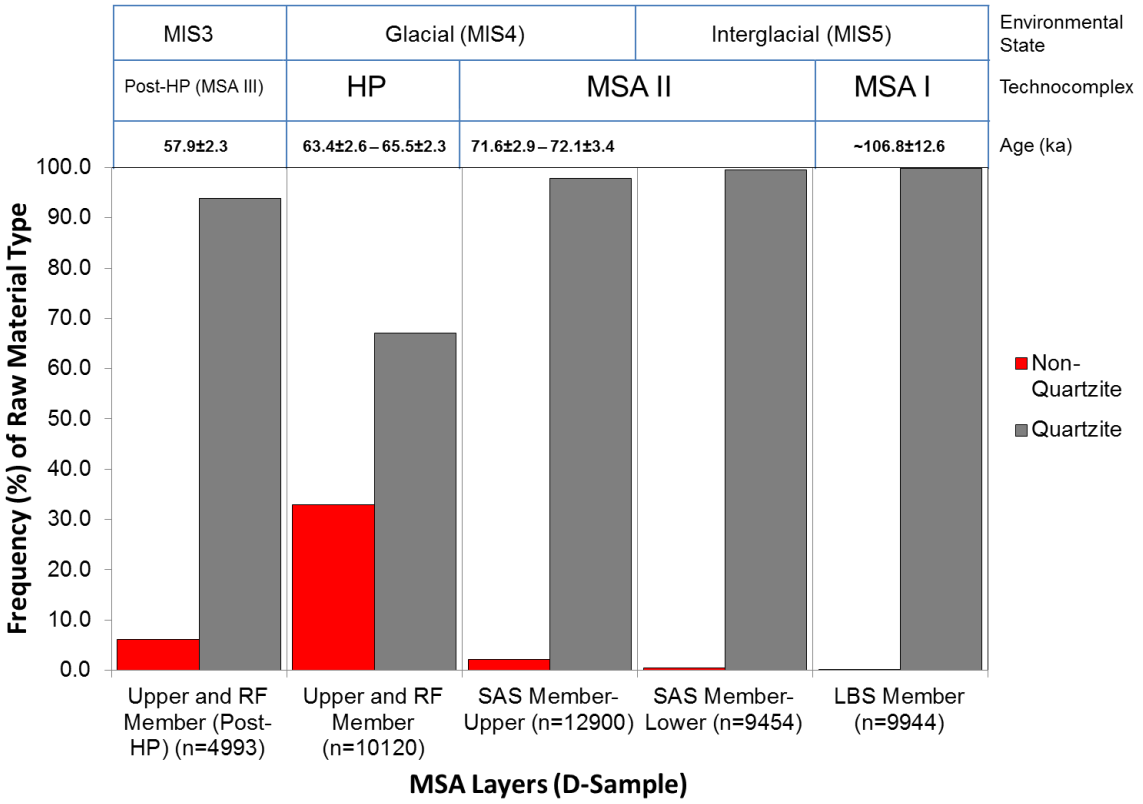

Figure 5. Relative frequencies of raw materials from MSA layers at Klasies River. Frequencies are shown in the context of glacial and inter-glacial states (Marine Isotope Stages). The designation of the different layers to specific Marine Isotope Stages is solely based on the OSL ages. Raw material frequencies are from Wurz (2002) and stratigraphic designations from Singer and Wymer (1982) and Deacon and Geleijnse (1988). OSL ages from Jacobs et al. (2008a) and Feathers (2002). Non-quartzite raw materials include silcrete, quartz, chert, chalcedony, and other CCS rocks.

Klasies River was first dated by correlating the different stages to the global marine isotope stages (MIS) by Butzer (1978). Klasies River has since been dated with OSL by Feathers (2002), who dated the bottom of the MSA I stage to about ~110 ka and the top of the MSA to about ~50 ka. A recent re-dating of selected layers puts the Howiesons Poort stage at between 65.5±1.9–63.4±2.2 ka, a minimum date for the MSA II stage at 72.1±3.1ka, and the start of the MSA III stage at 57.9±1.9 ka (Jacobs and Roberts 2008, Jacobs, Roberts, et al. 2008a). Research at KRM had three effects on the archaeology at that time after the first excavations by Singer and Wymer. First, it

provided a deeply stratified sequence, which gave birth to new ways of classifying the MSA. Second, the site became tied to the global marine isotope stages, which provided the researchers with relative dates for the sequence and a chance to look at stone tool technology variability versus environmental change. Third, it showed that the Howiesons Poort stage was well stratified between two MSA stages. Following the Singer and Wymer 1982 publication, Thackeray and Kelly (1988) looked at technological change over time. They argued that there is no major technological change throughout the MSA sequence only subtle stylistic shifts (Thackeray and Kelly 1988). Wurz (2002) investigated variability; she argued that the variability seen throughout the sequence is the result of changes between the dominant blade and/or point technological convention (traditions) through time. Sarah Wurz and collaborators studied the end products (Wurz et al. 2003); they argued that the MSA I and MSA II stages represent distinct technological traditions aimed at producing different end-products. Others took a multivariate approach to understanding the variability and emergence of the Howiesons Poort within the MSA (McCall 2006). McCall found that the Howiesons Poort assemblage correlates strongly with blade production. A study by Villa et al. (2010) suggested that the backed pieces in the Howiesons Poort had been hafted, and was an innovative way of hafting spears tips. They proposed that the disappearance of the Howiesons Poort at the onset of MIS3 was not linked to population contraction and isolation causing the collapse of social networks. Instead, they proposed that the internal evolution and process of change in the Howiesons Poort was associated with changes in the environment and subsistence base.

Blombos Cave (BBC)

In 1992, Christopher Henshilwood started excavating Blombos Cave, which is located in the Southern Cape (Henshilwood et al. 2001). This cave site has yielded some very important data concerning the origins of modern human behavior (Archer et al. 2015, d'Errico and Henshilwood 2007, d'Errico et al. 2005, Henshilwood et al. 2011, Henshilwood, d'Errico, and Watts 2009, Henshilwood et al. 2004, Henshilwood et al. 2002, Mourre, Villa, and Henshilwood 2010). The site is well-stratified with an Aeolian sand dune (67.8±4.2 ka) separating the MSA and LSA (Jacobs, Duller, and Wintle 2003, Jacobs, Wintle, and Duller 2003, Jacobs et al. 2012). Several TL (Tribolo 2003) and OSL (Henshilwood et al. 2011, Jacobs et al. 2006, Jacobs et al. 2012) dates have been taken to establish a well-defined MSA sequence. Because of the accuracy of single-grain OSL dates, I will use the work by Jacobs (Henshilwood et al. 2011, Jacobs et al. 2012). The MSA sequence is divided into 3 phases (from youngest to oldest): BBC M1a and b, BBC M2, and BBC M3). The description of the lithic assemblages from Henshilwood et al. (2001) follows.

The youngest phases, BBC M1a and b, are OSL dated to between 74.9±4.3 and 72.5±4.6 ka (Jacobs et al. 2012). The cores in this phase are mostly made on quartz and silcrete, but also some quartzite. More than 60 % of the detached pieces are made on silcrete; quartz is the second most common. Overall, silcrete is the preferred raw material in the M1 phase (**Figure 6**). Cortical silcrete is mostly of cobble origin. Curved flakes with small-lipped platforms and widening flakes that are the products soft-hammer bifacial retouch dominate the assemblages. Approximately 50 % of the retouched tools are bifacially flaked points or parts of them, unbroken points are elongated and most have

two opposed points to give them a lanceolate or narrowly elliptic leaf shape. The bifacial points are made on both silcrete and quartzite. Henshilwood et al. (2001: 429) argued that these bifacial points are 'Still Bay' points. Villa et al. (2009) investigated the Still Bay points from the BBC M1 layers and argue that wear evidence suggests that some of the points were hafted axially and used as spear tips. Scrapers are also a significant component. End scrapers are more numerous than side scrapers.

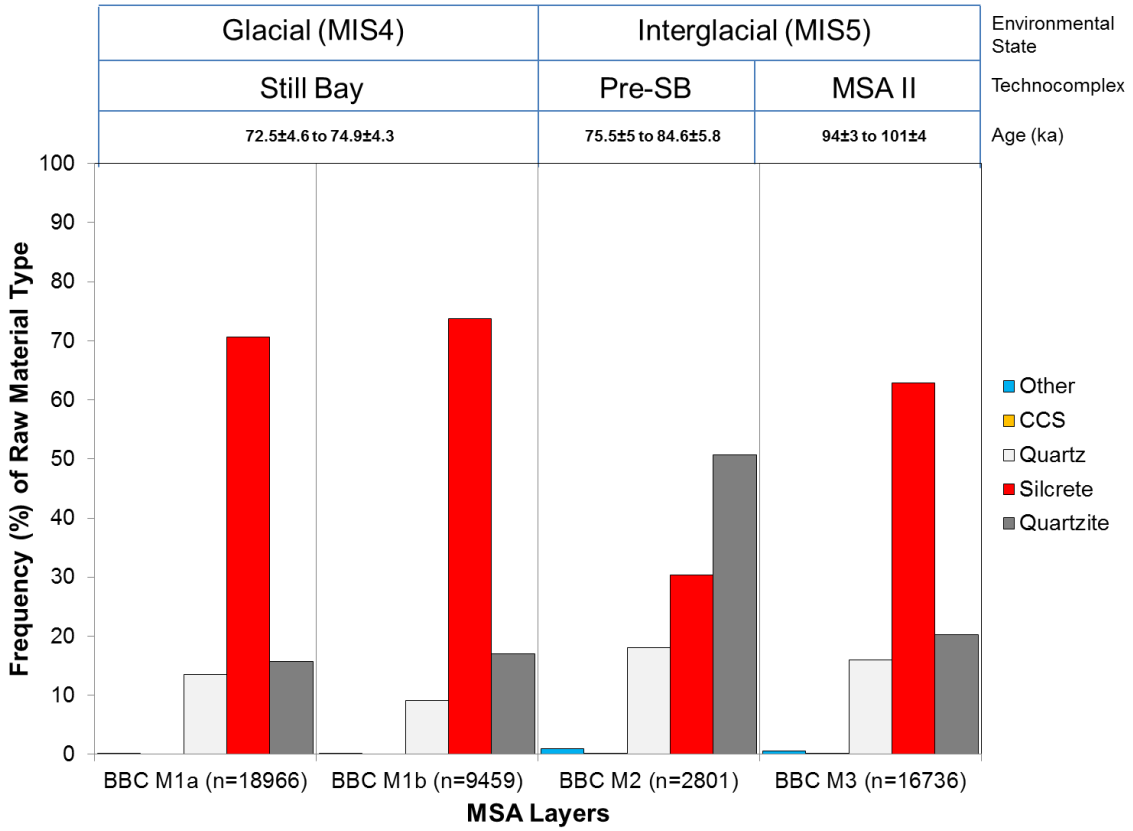

Figure 6. Relative frequencies of raw materials from MSA layers at BBC. Frequencies are shown in the context of glacial and inter-glacial states (Marine Isotope Stages). The designation of the different layers to specific Marine Isotope Stages is solely based on the OSL ages. Raw material frequencies and stratigraphic designations from Henshilwood et al. (2001) and ages from Henshilwood et al. (2011) and Jacobs et al. (2012).

The BBC M2 phase has OSL dates ranging between 84.6±5.8 ka and 75.5±5 ka (Henshilwood et al. 2011, Jacobs et al. 2012). Overall, the M2 assemblage is dominated

by quartzite followed by silcrete (**Figure 6**). The cores are mostly made on quartz. The silcrete cores from this phase are similar to the ones in BBC M3 but the quartz cores are irregular and nugget-like and many are less than 4 cm in maximum dimension. Flakes are predominantly on quartz and they differ from BBC M1 in having well-developed hard-hammer bulbs of percussion. There is a low frequency of bifacially flaked points. An assessment of more retouched tools is difficult to attain since they are almost all made on quartz (Henshilwood et al. 2001).

The oldest phase, BBC M3, is dated by OSL to between 101±4 to 94±3 ka (Henshilwood et al. 2011). The cores are predominantly for the production of flakes rather than flake-blades. There is an almost even split between silcrete and quartz cores with quartz being the most dominant. In plan-view, the silcrete cores show that flake removals are mostly centripetal with prominent bulbs of percussion probably achieved by hard-hammer percussion. The majority of the silcrete and quartzite cores are exhausted. In BBC3, 60 % of the detached pieces are silcrete. Hard-hammer flakes with a pronounced bulb of percussion are standard and prepared cores that are typical of MSA are abundant. Flake-blades are uncommon. There are no bifacially flaked points and the number of retouched artifacts is very low. There is a higher percentage of denticulates than in overlaying phases. The dating of the site puts the BBC M2 and M3 phases in Volman's (1984) MSA 2b lithic Stage.

Diepkloof Rock Shelter (DRS)

Diepkloof Rock Shelter is located approximately 180 kilometers north of Cape Town on the west coast of South Africa (Parkington et al. 2013). It is an inland site located 18

kilometers from the coast and overlooks the Verlorenvlei River that drain out in Elands Bay. Excavations at the site have been intermittent since 1973 and continue presently (Parkington et al. 2013, Porraz, Parkington, et al. 2013). The excavations have yielded 3.1 meters of deposits. Although the lithics from early excavation of the site have been studied (Mackay 2009, Porraz et al. 2008, Rigaud et al. 2006), I will focus on the more recent publication provided by Porraz et al. (2013) because it presents the most comprehensive lithic analysis to date. The current research team also provides the most up to date stratigraphic description (Porraz, Parkington, et al. 2013, Porraz, Texier, et al. 2013). However, the dating of the site is controversial and has implications for the span and timing of the different technocomplexes within the MSA sequence (Jacobs and Roberts 2017, 2015, 2008, Jacobs, Roberts, et al. 2008a, Porraz, Parkington, et al. 2013, Tribolo et al. 2013, Tribolo et al. 2009). Jacobs' single-grain methodology and dating has been independently verified at PP5-6 (Ciravolo, 2016; Smith et al., 2015), and she has published two re-analyses of her own samples (2017, 2015). Additionally, the Pinnacle Point OSL chronologies have been blind tested with U-Th dating in two separate caves and found to be concordant (Bar-Matthews et al., 2010; Marean et al., 2010). For this reason, I here use Jacobs' OSL ages when available (Jacobs and Roberts 2017, 2015, Jacobs, Roberts, et al. 2008a) alongside Porraz and colleagues lithic description.

The following is summarized from Porraz (2013). From the newest excavation, there are 53 stratigraphic units spanning from Noel (at the base) to Claude. The SUs are then grouped into technocomplexes based on age, patterns of raw material selection, blank production, and tool manufacture. In addition, the technocomplexes are sometimes divided into sub-phases. The sequence of technocomplexes goes as follows: MSA-MIKE,

Pre-Still Bay, Still Bay, Early HP, MSA-JACK, Intermediate HP, Late HP, and Post-HP. HP refers to Howiesons Poort,

MSA-MIKE (Stratigraphic units Mike and Lauren)

At the bottom of the sequence is a technocomplex termed MSA-MIKE (Stratigraphic units Mike and Lauren). Local materials (90%) dominate it with quartzite being over 86.3% of the assemblage. MSA-MIKE contains a low percentage of formal tools. The techno-economic aspect of the assemblage represents on-site knapping activities because all phases of the reduction sequence are present. However, the products made on non-local materials such as silcrete and hornfels have been introduced to the site as isolated products in the form of triangular flakes and blades.

Pre-Still Bay (Stratigraphic unit Lynn)

The assemblage is dominated by local quartzite (64.5%) followed by silcrete (15.4%) and then quartz (11.9%). Irregular flakes and laminar blanks dominate the assemblages. There is a correlation between distance and quality of raw material sources exploited to create certain tools and the intensity of reduction of the tools (Porraz, Parkington, et al. 2013). The tools that are made on quartzite are dominated by denticulates and notches, while tools that are made on silcrete and other fine-grained materials are more frequent and are more intensely retouched.

The Still Bay (Stratigraphic units Leo to Keeno)

This assemblage is dominated by quartzite (68.9%) followed by silcrete (14.7%) and then quarts (7%) and YB silcrete (7.6%). The amount of non-local rocks increases coupled with a decrease in the use of local rocks as the phase approaches the early HP technocomplex. The lithic assemblage is dominated by bifacial shaping reduction debris and debitage. The bifacial pieces are lanceolate in general morphology and are made on different raw materials. Porraz et al. (2013) argued that the bifacial pieces and/or bifacial shaping flakes were circulated, curated by Still Bay inhabits, and then transported during forays. Local quartzite was the main raw material but only a few bifacial products made on local quartzite are in the finished tool form. Conversely, bifacial tools made on fine-grained rocks are more extensively reduced and also transported over longer distances.

The Early-HP (Stratigraphic units Kegan to Jess)

This lithic assemblage is characterized by two distinct sub-phases termed ‘Kerry’ and ‘Kate’. ‘Kerry’ is dominated by exotic fine-grained silcrete (53.6%) followed by quartzite (25.3%) and quartz (11.7%), while ‘Kate’ is dominated by local quartzite (34.6%) then followed by quartz (29.7%) and silcrete (28.2%). The production was aimed at blade and bladelet production. Geometric backed tools are present but the dominant formal tool class is *pieces esquillees*, which are produced on different blank forms and on different raw materials. There is also a small frequency of bifacial pieces and shaping flakes. This part of the sequence was attributed to the Still Bay by earlier analyses (Porraz et al. 2008, Rigaud et al. 2006, Tribolo et al. 2009).

MSA-JACK (Stratigraphic units Jude and Jack)

In these assemblages locally available quartzite (45.4%) and quartz (32.9%) were preferred, followed by silcrete (10.3%) and hornfels (8.3%). The production is geared towards flake production. The flake products are very variable in size and morphology. The production is either in the form of a Levallois-like or non-invasive flaking strategy. Usually large backed pieces are present.

Intermediate- HP *(Stratigraphic units Joy to Fred)*

This assemblage is subdivided into two sub-phases termed 'Jeff' and 'Fiona'. 'Jeff' is dominated by fine-grained silcrete (47.1%) followed by quartzite (20%), then YB Silcrete (19.1%), and quartz (10.7%). 'Fiona' is dominated by Silcrete (60.7%), followed by quartz (19%), and then quartzite (10.3%). The two sub-phases were divided based on the difference in mean blade dimensions. The aim of the production in both phases is blades using a laminar core reduction system. There is a high frequency of strangulated-notched pieces, while denticulates and *pieces esquillees* are also present. Geometric backed pieces are present in relatively low frequencies compared to the early-HP.

The Late-HP (Stratigraphic units Frans to Debbie)

The Late-HP assemblage is subdivided into two sub-phases termed 'Frans' and 'Eric'. 'Frans' is dominated by silcrete (48.8%) followed by quartz (22.5%), and then quartzite (12.3%) and hornfels (10.8%). Sub-phase 'Eric' is dominated equally by quartz (40.6%) and silcrete (39.1%) followed by quartzite (7.8%) and YB silcrete (6.1%). Overall, typical Howiesons Poort core forms dominate the assemblage. The Late-HP displays an

increased frequency of geometrics, which represents about 50% of the formal tools. The geometrics are divided equally between truncated pieces and segments.

The Post-HP (Stratigraphic units Danny to Claude)

This assemblage is dominated by the use of silcrete (43.5%) followed by quartz (19.9%) and quartzite (19.5%), and then YB silcrete (12.1%). The production is aimed at laminar products including Howiesons Poort-type debitage. The formal tools are dominated by scrapers but unifacial points, denticulates, notches, and some rare backed pieces are present.

Diepkloof chronology

Tribolo et al. (2013) provided an OSL age of 100±10 ka for the lower MSA layer called 'Noel', and a similar OSL age of 100±10 ka is also given for the Pre-Still Bay (layer 'Lynn'). However, Jacobs and Roberts (2015) provided the ages of 93.3±4.4 and 88.2±4.4 for the lower MSA layers. The Still Bay (layer 'Logan') is OSL dated to 70.9±2.3 by Jacobs et al. (2008a), while the early-HP (layer 'Kerry') OSL dates to 73.6±2.5 ka (Jacobs, Roberts, et al. 2008a). The 'Kerry' layer, which contains backed pieces, is potentially a similar early emergence of backed blade technology as seen at PP5-6 with the 'early microlithic' in the SADBS stratigraphic aggregate (Brown et al. 2012, Wilkins et al. 2017). Further, Jacobs et al. (2008a) provided OSL ages for the intermediate-HP (layer 'John') at 63.3±2.2 ka, while the late-HP is given an OSL date of 61.8±1.7 (Layer 'Edgar'). Finally, Jacobs provided two OSL ages of 55.4±2.0 ka and 47.7±1.7 ka for the post-HP (layers 'Anne' and 'Allie' respectfully).

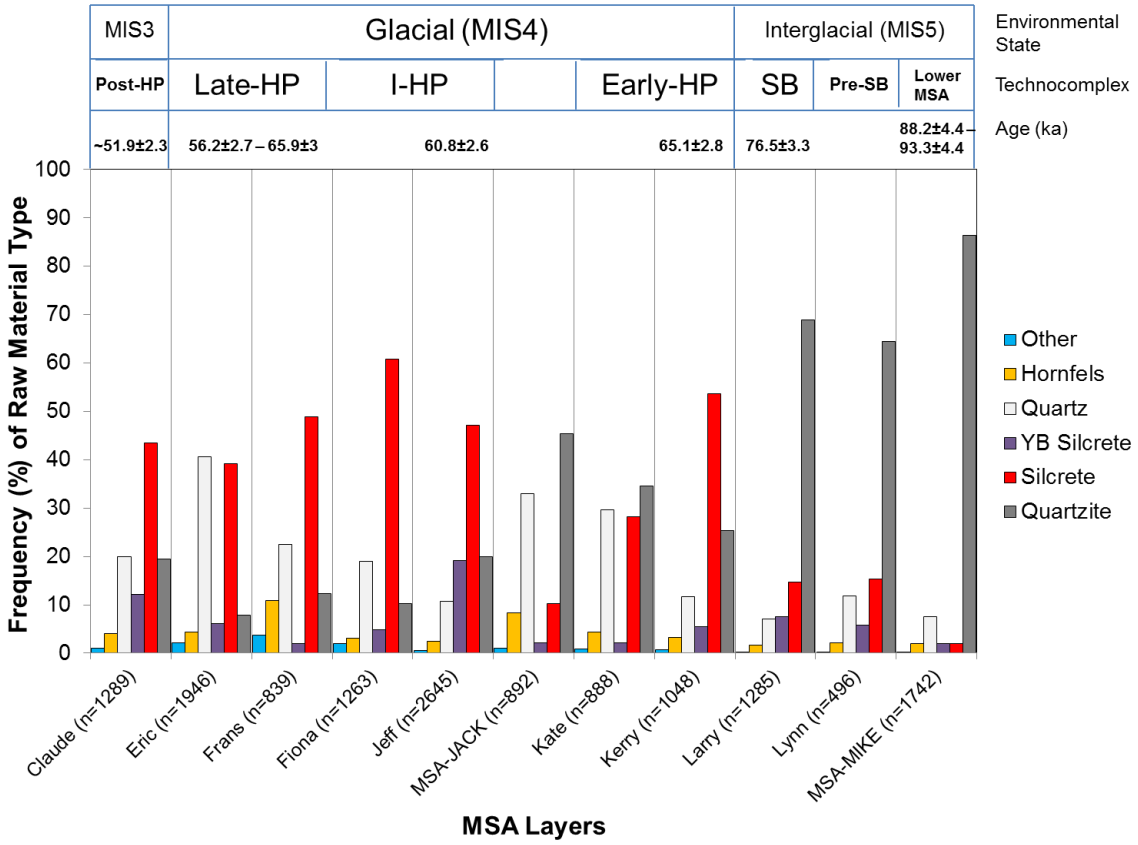

Figure 7. Relative frequencies of raw materials from MSA layers at Diepkloof Rock Shelter. Frequencies are shown in the context of glacial and inter-glacial states (Marine Isotope Stages). The designation of the different layers to specific Marine Isotope Stages is solely based on the OSL ages. Raw material frequencies and stratigraphic designations from Porraz et al. (2013) and ages from Jacobs and Roberts (2015).

Diepkloof raw material procurement

In terms of raw material procurement, the selection of local (less than 20 kilometers) versus non-local (more than 20 kilometers) raw materials varies throughout the sequence. The local versus non-local designation is based on geological surveys conducted at two scales. At the first scale, 20 km perimeters around Diepkloof were surveyed to document the full spectrum of available raw materials. At the second scale, the survey focused on the greater west coast region mostly directed at documenting silcrete sources (Porraz et al., 2013b). In the MSA-Mike, Pre-Still Bay, and the Still Bay the local materials

dominate (**Figure 7**). The pattern changes drastically in the early-HP (layer 'Kerry') where non-local materials dominate. In the early-HP (layer 'Kate') and the MSA-Jack technocomplexes, local materials are again preferred. However, from the Intermediate-HP to the post-HP technocomplex non-local materials dominate again. Porraz et al. (2013) argued that the drastic shift to non-local materials in the Howiesons Poort is suggestive of behaviors consistent with a provisioning of place model (Kuhn 1995). Further, the shift is interpreted to suggest higher predictability and control of desired resources. However, the HP backed pieces do not seem to be in a response to a modification in hunting weapons and they were not designed for a specific task (Igreja and Porraz 2013).

Die Kelders Cave 1(DK1)

Die Kelders Cave 1 refers to a cave complex located on the Walker Bay coast of the southern Cape. The first excavations of Die Kelders Cave 1 (DK1) were conducted by Schweitzer (1979, 1974, 1970) from 1969 to 1973. Although Schweitzer was not overly concerned with the MSA but mainly focused on the LSA, he was surprised to find MSA lithics beneath a sterile sand layer that signaled the beginning of the LSA sequence (Schweitzer 1979). In 1991 to 1995 additional excavations of the MSA deposits were conducted (Marean 2000, Marean et al. 2000). Volman analyzed the MSA lithics from the Schweitzer excavations (Grine, Klein, and Volman 1991, Volman 1981), while Thackeray (2000) investigated the new assemblage of lithics and found that they were very comparable with Volman's study. What follows is a summary from Grine et al. (1991) and Volman (1981). Volman noted that most of the lithics come from even-

numbered layers (4, 6, 8, 10, 12, 14), separated by odd-numbered layers with few artifacts (5, 7, 9, 11, 13). Throughout the sequence, there is evidence for centripetal reduction, and there are some cores with elongated, parallel and sub-parallel scars. In addition, convergent flakes are common in all layers. Overall, there is a low frequency of retouched pieces. The few retouched pieces usually take the form of notches or edge-damaged pieces. The earlier and later MSA layers yield longer and narrower flakes compared to the middle MSA layers, which yield shorter and broader flakes.

Volman noted that quartzite, quartz, and silcrete were the only raw materials that were used. Overall, quartzite is used throughout the sequence (**Figure 8**) but in levels 11 and 12 there is an increase in the use of silcrete (Volman 1981).

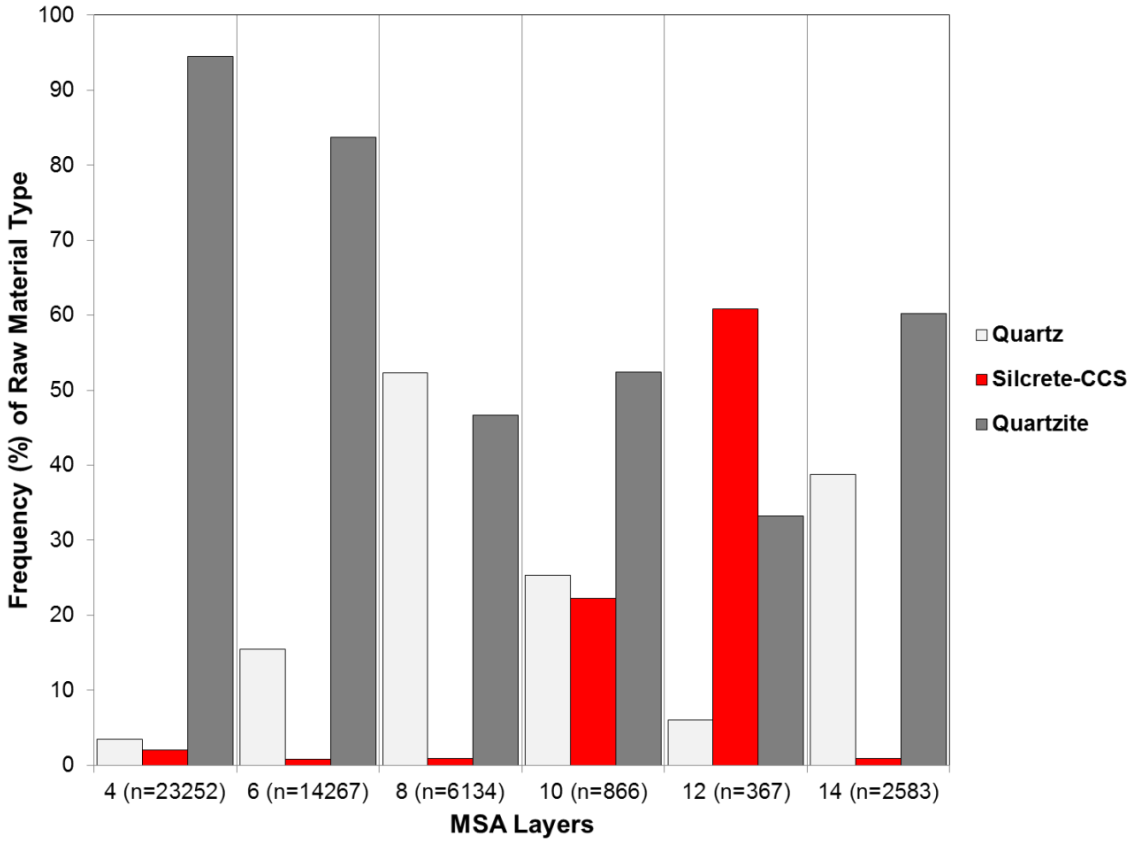

Figure 8. Relative frequencies of raw materials from MSA layers at Die Kelders Cave 1. Raw material frequencies and stratigraphic designations from Volman (1981).

There is, however, no increase or presence of typical Howiesons Poort-like tools such as backed pieces or notched-blades in the corresponding layers with increased silcrete. Whereas Volman (1981) argued that all raw materials were reduced the same way, Thackeray (2000) argued that most of the silcrete blades are smaller. Further, Thackeray argued that the small size of the silcrete blades results from a difference in size of the available nodule. Most of the silcrete cores are small and irregular or centripetally prepared, while the majority of the quartzite cores are centripetally prepared with some cores showing evidence of flake and flake-blade removal. Thus, there is more variability in the reduction strategies that previously argued (Brown 2011).

No convincing dating regime with single-grain OSL dating has been undertaken at DK1. However, Feathers and Bush (2000) used several dating techniques such as TL, IRSL, and single and multi-aliquot OSL that yields dates ranging from 70.3±5.8 to 59.4±5 for Layers 11 and 13. The single-aliquot OSL age of Layer 11 is 70.3±5.8, while Layer 13 has single-aliquot OSL age of 58.6±5.4 (Feathers and Bush 2000). In addition, the ESR ages suggest an average age of the deposits of 70±4 ka (Schwarcz and Rink 2000). These results suggest that layer 12, which has a drastic increase in the use of fine-grained silcrete, might date to the Howiesons Poort or Still Bay. However, as noted above layer 12 does note exhibit any lithic technology such as backed pieces or bifacial points.

Nelson Bay Cave (NBC)

Nelson Bay Cave is located on the Robberg Peninsula on the south coast of South Africa. Ray Inskeep excavated first in 1964-1966, 1970-1971, and 1979 (Inskeep and Avery 1987), and then Klein excavated in 1970 and 1971 (Klein 1972). The MSA deposits

begin with pre- Howiesons Poort MSA (levels 10-7), followed by the Howiesons Poort (level 7 to crust layers). Above the MSA, after a sterile occupation layer, the LSA follows, represented by the Robberg, Albany (Oakhurst), and Wilton industries. In his dissertation, Volman (1981) described the MSA lithics from Klein's excavation. Below I will summarize his findings. Overall, quartzite is the most abundant raw material (usually above 90% in all levels) followed by quartz, silcrete and other crypto-crystalline silicates including chert variants (**Figure 9**). Only in the Howiesons Poort is there a moderate increase in the use of silcrete, quartz, and crypto-crystalline silicates (**Figure 9**). Volman assigned pre-Howiesons Poort MSA level 8 to MSA 2b, Levels 9 and 10 as MSA 2a. The pre-Howiesons Poort is associated with long and narrow flakes, retouched points and sidescrapers, while the Howiesons Poort is associated with small flakes, some unifacial points, and retouched segments, triangles, trapezoids, other backed pieces, and denticulated endscrapers. In addition, there are multiple-notched and strangulated pieces. The backed tools are made on similar frequencies of quartzite and fine-grained raw materials. Some strangled and multiple-notched pieces were made on silcrete and chert but quartzite was used to make all other formal tools.

Overall, Volman (1981) described a low ratio of primary cortical flakes to cores within the Cave. He suggested that the primary reduction occurred outside the cave, leaving only successfully prepared cores to be transported into the cave. There is an absence of single-removal prepared cores. Once in the cave, the cores were highly reduced suggesting that once prepared, the cores were nearly exhausted. The majority of the cores were centripetal with single and multiple platform cores facilitating the production of parallel and sub-parallel flakes.

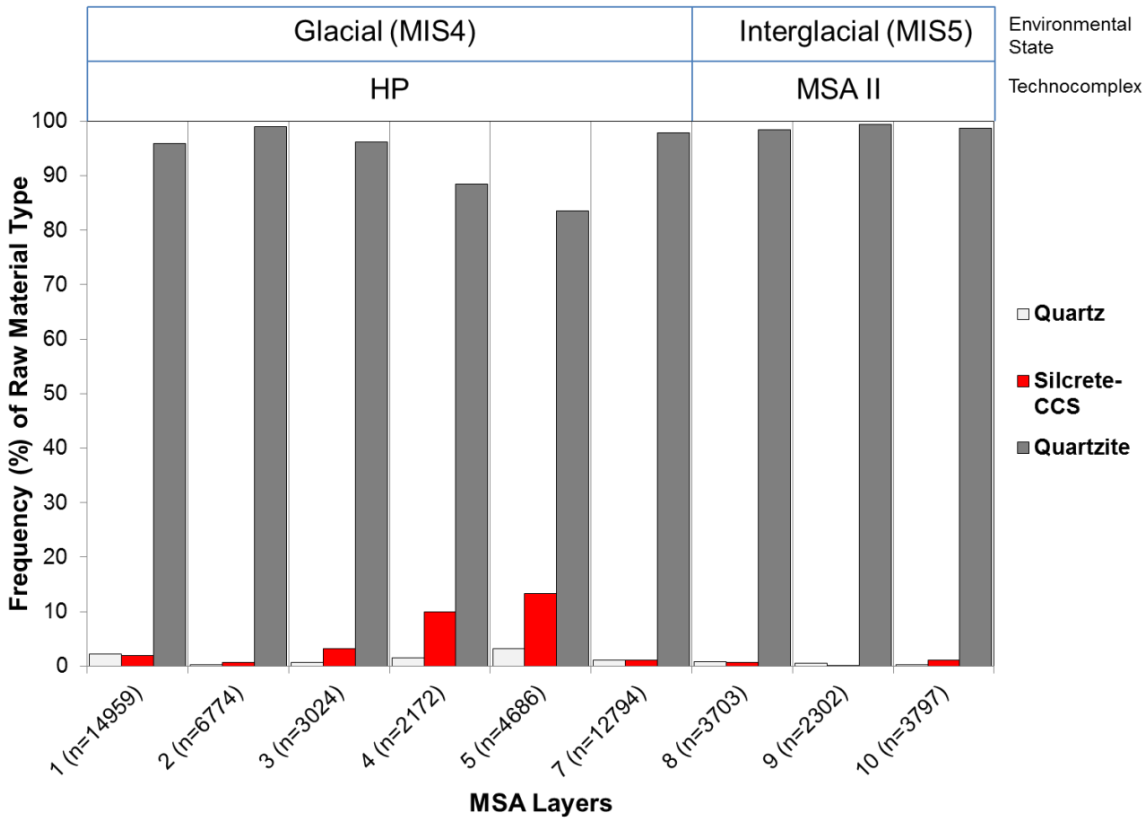

Figure 9. Relative frequencies of raw materials from MSA layers at Nelson Bay Cave. Frequencies are shown in the context of glacial and inter-glacial states (Marine Isotope Stages). The designation of the different layers to specific Marine Isotope Stages is here based on the technocomplexes. Raw material frequencies and stratigraphic designations from Volman (1981).

Although no ages are available, work by Jacobs et al. (2008a) showed that other Howiesons Poort assemblages are tightly constricted to between 65-60 ka at a range of other MSA sites all over South Africa. This suggests that the Howiesons Poort assemblage at Nelson Bay Cave can be dated to this age range.

Klein Kliphuis (KKH)

Klein Kliphuis (little rock house) was first excavated in 1984 and again in 2006 and is located low on the north-facing slope of Spitskop, a hill at the junction of the Kliphuis

and Olifants Rivers (Jacobs, Roberts, et al. 2008a, Mackay and Welz 2008, Mackay 2006). The site is 60 km from the present coastline. The MSA layers (D, D1, D2, and D3) from the original excavation are subdivided into somewhat arbitrary units, although Mackay (2006) noted that the excavators tried to follow changes in soil color and composition. Mackay (2006) described the lithics from the 1984 excavations. Layer D is dominated by quartz (61.2%) followed by silcrete (10.3%). There are some backed artifacts and an increased prevalence of bipolar core reduction. Layer D1 is 35.4% quartz, 37.3% quartzite, and 18.1% silcrete. Flakes discarded in this layer are heavier, longer, wider, and thicker on average compared to the other MSA layers. Unifacial points are present and there are no backed artifacts. Layer D2 is dominated significantly by silcrete (80.2%) followed by other crypto-crystalline silicates (CCS) (10.1%). There is an increased prevalence of backed artifacts, a high frequency of elongated artifacts (blades), a use of dorsal ridges to control flaking, and a high instance of platform cores. Layer D3 is 59.8% silcrete followed by 26.2% quartz. There are fewer backed artifacts than in layer D2 but very similar otherwise.

Jacobs et al. (2008a, b) in their supplementary material provided OSL ages for the sequence and a short summary of the 2006 excavation. Unfortunately, their stratigraphy division is not directly compatible with the early excavations. All the layers that corresponded to the Pleistocene are denoted D where any subdivisions are denominated with roman numerals. Layers were dug in 25mm spits. The transition from Howiesons Poort to post-Howiesons Poort occurs in Dvi7 and Dvi6. The original D2 unit is more or less equivalent to the Dvi unit from the new excavation, which is bracketed with two

OSL ages from 66.0±3.4 ka to 55.2±2.0 ka. This supports Mackay's (2006) assertion that the D2 unit represents the Howiesons Poort.

Klipdrift Shelter (KDS)

Klipdrift Shelter is located in the De Hoop Nature Reserve on the south coast of South Africa at a height of 19 meters above sea level. Excavations commenced in 2011 and revealed MSA occupations (Henshilwood et al. 2014). The uppermost layers are OSL dated to 51±3.3 ka, the middle layer is OSL dated to 65±4.8 ka to 59.4±4.6 ka, while the lowermost currently excavated layer dates to 71.6±5.1 ka. The ages of the middle occupation layers and the lithic component are compatible with a Howiesons Poort designation (Henshilwood et al. 2014). A description of the Howiesons Poort lithic assemblages was presented by Henshilwood et al. (2014). The tools of the Howiesons Poort layers are typical of the Howiesons Poort with formal tools composed of backed tools, notched tools, borers, retouched blades, and points. However, only 5% of the assemblage is retouched. Significant changes occur in terms of raw material frequency and tool production. In the lowest layers (PCA, PBE, PBD) silcrete dominates and is used to produce blades. There is also a relatively high prevalence of notched tools, the presence of strangulated blades and highly standardized truncated blades. In the two overlaying layers (PBC, PBA/PBB) quartz usage increases significantly, and the main tool group is backed tools including typical segments. In the uppermost layers (PAZ and PAY) quartzite and calcrete become more abundant; there is an increase in blade size and the emergence of an independent and structured Levallois-based flake production coinciding with a decrease in the frequency of backed tools. Henshilwood et al. argued

that the pattern of change throughout the Howiesons Poort sequence at KDS echoes patterns observed with the Howiesons Poort at Klasies River (Villa et al. 2010, Wurz 2000), and in the Intermediate and late Howiesons Poort layers at Diepkloof Rock Shelter (Porraz, Parkington, et al. 2013, Porraz, Texier, et al. 2013)

In terms of raw material procurement, the closest known potential silcrete source is 10 km to the north, while quartzite and sometimes quartz are most likely of a local origin. In terms of tool production, quartz, silcrete, and other CCS rocks are almost entirely devoted to the production of blades. Quartzite was expediently reduced and was used to produce both flakes and blades with direct hard hammer percussion.

Apollo 11 (AP)

Although not in South Africa, AP is a cave site situated in the Huns Mountains in southwestern Namibia and was excavated by Wendt in the late 1960's and early 1970's (Wendt 1976, 1974). Wendt (1976: 7) describes the artifact assemblages from the MSA layers as follows from bottom to top:

- Layer H: The basal layer has several large points and flake-blades in addition to a number of true medium to small-sized blades. Only a few retouched artifacts with notched/denticulated/serrated edges and coarse ventral retouch are present.
- Layer G: Blades in this layer are on average larger than in the overlying Layer F. There are numerous retouched flakes and blades in addition to a few burins and unifacial and bifacial points. This layer is OSL dated to 70.7±2.1 ka and

the artifact assemblage is classified as Still Bay, similar to the Still Bay industry of the Western and Southern Cape (Jacobs, Roberts, et al. 2008a).

- Layer F: This layer has facies of blade industries, and the blades are frequently snapped and on average smaller than in the underlying Layer G. There are variously retouched blades and flakes but also several burins, backed blades, backed points, a few large "crescents" and several partially unifacial points present. Wendt (1976: 7) stated that this layer has certain affinities with the Howiesons Poort. Jacobs et al. (2008a) OSL dated this layer to 63.2±1.9 ka, which falls within the range of other Howiesons Poort layers dated in their research.
- Layer E: The top of the MSA sequence consists of several distinct horizons with a low artifact density. The horizons contain blades assigned to the MSA but it lacks other typical tools. The layer radiocarbon dates to between 46 400±2500 years BP at the bottom to 26 300±400 BP at the top. A rock fall horizon that separates Layer E from F is OSL dated to 57.9±1.9 ka (Jacobs, Roberts, et al. 2008a).

Sibudu Cave (SIB)

Sibudu is located 40km north of Durban in the KwaZulu-Natal Province. It was first excavated by Mazel in 1983, but the in-progress excavation at the cave started in 1998 led by Lyn Wadley (2004) but is today led by Nick Conard (Conard, Porraz, and Wadley 2012, Will, Bader, and Conard 2014). The MSA sequence at this site from bottom to top is the: pre-Still Bay industry, Still Bay, Howiesons Poort, post-Howiesons Poort

('Sibudan'), late MSA, and final MSA (Jacobs, Roberts, et al. 2008a, b, Jacobs, Wintle, et al. 2008, Wadley 2007, 2005, Wadley and Jacobs 2004).

A short description of the pre-Still bay artifacts is offered in the supporting material to Jacobs et al. (Jacobs, Roberts, et al. 2008b). It is described as a flake rather than a blade industry and the raw material used are local dolerite and non-local hornfels. Wadley (2007) reports that the Still Bay retouched tools are on local dolerite, with non-local hornfels, quartz, and quartzite also being used. Hornfels does not occur within a 10 km radius of the site. In the Still Bay, 48 % of all retouched tools and 54 % of points and bifacial tools are made from dolerite, while 76 % of all flake, blade, and chunk classes are also made on dolerite. Other raw material types are hornfels, quartz, and quartzite. Further, 42 % of the retouched tools are bifacially worked. Few whole specimens of bifacial points are found, but both distal and proximal ends are found. Other retouched tools include unifacial points, a segment, and a crescent. The assemblage is flake rather than blade oriented. Cores are rare but there are two radially worked cores, one cylindrical core and one core with opposed platforms. Residue analysis on the Still Bay double-pointed bifacial artifacts suggests they were used as butcher knives rather than hunting weapons (Lombard 2006).

From the Howiesons Poort layers, Lombard (2008a) reported that there are no retouched points and the segments and other backed pieces are the formal tools. The majority of the backed tools are made on dolerite and hornfels, but there are some quartz artifacts. Some of the quartz is used to produce a laminar technology that emphasizes small bladelets. It is argued that there is a deliberate production of microliths using the quartz (de la Peña and Wadley 2014). There are a higher proportion of blades and more

large sandstone flakes than in overlaying MSA layers. Experimental work and residue analysis suggest that the backed segments and crescents were hafted and created a multi-component tool used for hunting (Lombard 2008a, Lombard and Pargeter 2008).

Wadley and Jacobs (2004) and Jacobs et al. (Jacobs, Roberts, et al. 2008b, a) described the post-Howiesons Poort, late MSA, and final MSA. In the post-Howiesons Poort quartz is a preferred raw material and there are no backed blades and segments, which separates it from the late and final MSA. There are few technological and typological changes occurred throughout this phase. During the late MSA unifacial points made mostly on dolerite and hornfels occur in high frequencies and their tip angle falls within the range considered suitable for spearheads. Residue analysis on these points suggests they were hafted onto bone or wooden shafts and used as hunting weapons (Lombard 2005, 2004). The final MSA contains examples of hollow-based bifacial stone points, and small bifacial and unifacial points, as well as sidescrapers and segments. Dolerite and hornfels are the main raw materials used. The sequence at Sibudu has several OSL dates: The pre-Still Bay is dated from 77.2±2.1 - 72.5±2.0 ka, the Still Bay to 70.5±2.0 ka, the Howiesons Poort from 61.7±1.5 to 64.7±1.9 ka, the post-Howiesons Poort to 58.5±1.4 ka, the late MSA to 48.0±1.4 ka, and the final MSA to 38.6±1.9 ka (Jacobs, Roberts, et al. 2008a, Jacobs, Wintle, et al. 2008). The Still Bay and Howiesons Poort ages fit within the range of dated Still Bay and HP assemblages at other sites (Jacobs, Roberts, et al. 2008a).

More recent excavations led by Conard have expanded the sample of the post-Howiesons Poort. Conrad and colleagues (Conard, Porraz, and Wadley 2012, Will, Bader, and Conard 2014) renamed the post-Howiesons Poort (layers BSP-BM) into a

‘cultural-taxonomic’ unit termed the ‘Sibudan’. They argued that the Sibudan dates to roughly 58ka reflecting many occupations over a short amount of time (Jacobs, Wintle, et al. 2008, Wadley and Jacobs 2006, Wadley 2013a). Will et al. (2014) found that the new assemblage under study is dominated by dolerite (62%) followed by Hornfels (34%). These frequencies are very different from the post-Howiesons Poort assemblage studied by Wadley, which is dominated by quartz (Jacobs and Roberts 2008). This discrepancy might suggest inter-site variation in raw material usage. This is possible because Conard and Wadley excavated different areas of the site. Will et al. (2014) noted that the dolerite is a local material most likely procured from a dolerite dyke in the sandstone cliff located some hundred meters away from the site. The local dolerite is an igneous, granular-appearing rock with varying grain size and mineral composition. The material is hard, rough, and homogenous. The hornfels is the most fine-grained material at SIB and yields favorable knapping characteristics and a sharp but potentially fragile edge. The closest known potential source of the hornfels is an outcrop located ~15-20 km to the south (Will, Bader, and Conard 2014). Overall, Will et al. (2014) noted that the lithic assemblage from the BSP-BM layers indicates a consistent pattern of raw material procurement in terms of both variety and abundance. Both dolerite and hornfels were reduced in the same manner and the tool makers used the same approach when producing blanks with both raw materials. The hornfels is more reduced, which is correlated with its longer transport distance and higher quality. The non-local raw material frequency varies between 25-38% and Will et al. (2014) argued that variability might be due to differential access to sources or changes in mobility. The older layers (BM, IV) are more reduced with higher flake blank to core ratios and smaller debitage products. Will et al. (2014)

argued that the subtle differences between the lower and upper layers in terms of reduction intensity and debitage sizes are either due to site use intensity, or change in access to raw material sites, or change in mobility system, or a combination of any of these factors.

Rose Cottage (RCC)

Rose Cottage Cave is located in the eastern Free State Province and was first excavated by Malan between 1943 and 1946, and then by Beaumont in 1962. Two recent excavations in the late 1980's to the late 1990's were undertaken by Wadley (1997) and Harper (1997). The unpublished assemblages excavated by Malan were analyzed by Wadley and Harper in 1989. They recognize a pre-Howiesons Poort assemblage, a Howiesons Poort assemblage, and a post-Howiesons Poort assemblage (Wadley and Harper 1989). The pre-Howiesons Poort industry is dominated by points, large flakes, and large parallel-sided flake-blades (Wadley and Harper (1989). The dominant raw material is opaline but tuff and siltstone is also common. Towards the end of the industry, knives are more dominant and there are as many backed tools as points. The opaline and tuff almost certainly come from the Caledon river some 8 km away (Harper 1997). Wadley and Harper (1989: 31) stated that there is a strong possibility that the pre-Howiesons Poort industry is related to the MSA 2b assemblages described by Volman (1984), which is found at sites in the Southern Cape. The Howiesons Poort industry at Rose Cottage Cave is dominated by backed tools and a wide range of tool types. There is an increase in the use of opaline and an increase in the percentage of small flakes and both small and large irregular flake-blades. Wadley and Harper (1989: 31) argued that the

Howiesons Poort at Rose Cottage Cave has all the attributes of a 'classic' Howiesons Poort industry. They note some difference between RCC and other sites; fewer segments or trapezoids in contrast to Border Cave, KRM, and NBC (Wadley and Harper 1989). The post-Howiesons Poort industry has some rare backed pieces, but is dominated by scrapers and has many points and knives. There are many small flakes and a relatively high proportion of irregular flakes. Wadley and Harper (1989: 31) argued that the post-Howiesons Poort industry might be equivalent to MSA 3 industries from other sites such as Border Cave and Klasies River. Further, Wadley and Harper (1989) noted that throughout the whole MSA sequence there is a gradual progression from large to small flakes, a decline in the percentages of parallel-sided flake-blades, and a continuous increase in irregular flake-blades. Recent OSL dating by Jacobs and collaborators (2008a) dated the Howiesons Poort industry to between 65.0±1.9 ka and 63.0±1.9 ka and the post-Howiesons Poort industry to 56.0±2.3 ka. These dates fit with OSL dates for the MSA 3 (post-Howiesons Poort) and the Howiesons Poort at other sites (Jacobs, Roberts, et al. 2008a). A recent study by Soriano and colleagues (2007) looked at the blade technology and tool forms of the Howiesons Poort and post-Howiesons Poort at Rose Cottage Cave. They concluded that the blade production in Howiesons Poort was a real technical innovation but was not made by using indirect percussion (Soriano, Villa, and Wadley 2007).

Umhlatuzana (UMH)

Umhlatuzana was first excavated in 1985 by Kaplan. It is a north-facing shelter located 100m above the Umhlatuzana River in KwaZulu-Natal (Lombard et al. 2010, Kaplan

1990, Kaplan 1989). The MSA sequence at Umhlatuzana can be divided into the Pre-Howiesons Poort, Howiesons Poort, and Late MSA. A summary of the stone assemblages from Lombard et al. (2010) follows. Pre-Howiesons Poort (levels 28-25): This technocomplex has been given an OSL age of 70.5±4.7 ka. Lombard et al. (2010) argued that the high frequency of bifacial foliate and serrated points and its age designates it as a Still Bay assemblage. Quartz dominates the raw material frequency with 80.5% followed by hornfels (18.3%). The Howiesons Poort (layers 24-22) has an OSL age of 60±3.5 ka and is dominated by quartz (76.9%) followed by hornfels (22.3%). The late-MSA (layers 21 to 19) has an OSL age of 41.9±2.6 ka and is dominated by 99% debitage, chips, chunks, and flakes. Hornfels is the dominant raw material (61%) followed by quartz (34.5%).

Sehonghong (SEH)

Sehonghong is a rock shelter located in the Sehonghong valley in Eastern Lesotho. Carter (1988) excavated it in 1971. The site has an archaeological sequence going from the MSA to the LSA. Carter et al. (1988) divided the MSA sequence into four phases (oldest to youngest): MSA 3, 5, 6, and 9. I will here focus on the artifact assemblage descriptions of the MSA 5 and 3 phases because they have been dated by using OSL. A description of the MSA 5 and 3 phases from Carter et al. (1988) follows:

- In the MSA 3 the most dominant raw material is opalines (55%) followed by hornfels (40%). Almost all cores are irregular but some cylindrical cores occur. No bladelet or prepared cores are present, while two backed flakes and

one segment occur in the assemblage. The MSA 3 phase is OSL dated to between 57.6±2.0 ka and 46.5±2.3 ka ago (Jacobs, Roberts, et al. 2008a).

- In the MSA 5 hornfels is the dominant raw material (57 %) followed by opaline (36%). There are some blades, bladelet, and Levallois cores, but most cores are irregular. Scrapers and knives are the most abundant common formal tool types. The MSA 5 phase is OSL dated to between 31.6±1.2 ka and 30.3±3.3 ka ago.

The OSL date and the artifact assemblage from the MSA 3 layer suggest that it belongs to Volman's stage MSA III (Volman 1984). But the occurrence of backed flakes and a segment, and considering the error on the OSL date of 59.9 ka, suggests that the MSA 3 might be an Howiesons Poort layer (Jacobs, Roberts, et al. 2008a).

Ntloana Tsoana (NT)

Ntloana Tsoana is a rock shelter located in the Masaru district in Western Lesotho. It was excavated in 1989 (Mitchell and Steinberg 1992). The MSA sequence is divided into three stratigraphic units named (oldest to youngest): CBS, HBL, and GWS. I will focus on the CBS and HBL stratigraphic units because they have been dated by OSL (Jacobs, Roberts, et al. 2008a).

- The CBS unit is dominated by opalines (45%) and tuff (40%), while other raw materials including siltstone, hornfels, chert, quartz, quartzite, sandstone and petrified wood are also present. Irregular cores are most abundant but there some few blade and bladelet cores. Formal tools are rare but slightly more abundant than in the overlying HBL. Backed pieces are the most common formal tool

category, which includes backed segments, backed blades, backed flakes, and obliquely backed blades. Other formal tools include points, knives, and scrapers. The CBS unit is OSL dated to 60.9±2.5 ka (Jacobs, Roberts, et al. 2008a).

- In the HBL unit Tuff (50%) is dominant followed by opalines (38%), and hornfels (6%). Other raw materials are chert, quartz, quartzite, and sandstone. Irregular cores are most abundant, while the cores are larger than those from the underlying CBS unit. There are some rare examples of prepared, blade, and bladelet cores. Facetted platforms are more common than in the CBS unit. The percentages of formal tools are very low but unifacial points and knives are most abundant with some scrapers and backed pieces. The HBL unit is OSL dated to 56±1.4 ka.

The MSA sequence from NT is comparable to the MSA sequence at RCC 40 km to the west. Both sites have post-Howiesons Poort layers that OSL dates to approximately 56 ka and they have Howiesons Poort layers that date to between 60 to 65 ka (Jacobs, Roberts, et al. 2008a, Mitchell and Steinberg 1992).

Summary of MSA raw material selection and technological organization

Several generalizations arise from the MSA records from South Africa and Lesotho. In the southern Cape, quartzite is the preferred raw material during the early MSA (MIS5), 'Klasies River', and 'Mossel Bay' technocomplexes but silcrete and other fine-grained raw materials become increasingly important during the Still Bay and Howiesons Poort technological (MIS4) entities at some sites (**Figure 10**). However, some sites show this pattern more than others do. At Diepkloof Rock Shelter and Blombos Cave this pattern is clearly visible (**Figure 10**). The four sites highlighted in **Figure 10** are particularly

important because they have long archaeological sequences. Additionally, these particular sites show raw material frequencies that include quartzite and non-quartzite raw materials such as silcrete and quartz.

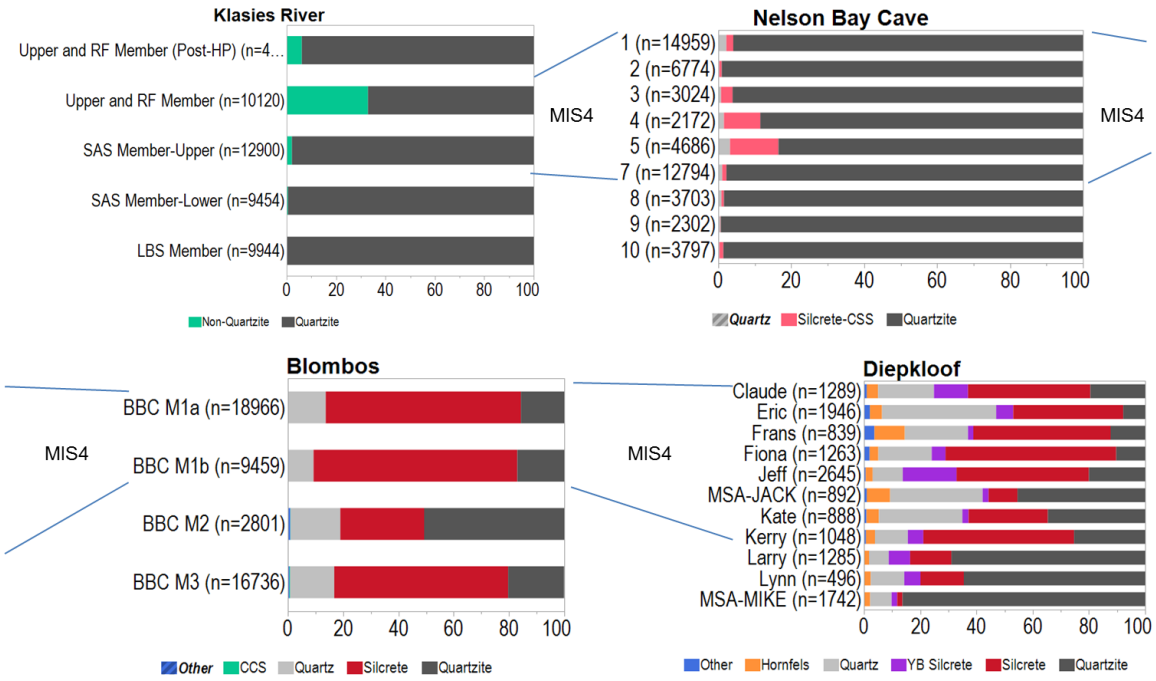

Figure 10. Composite figure of MSA raw material frequencies at Klasies River, Nelson Bay Cave, Blombos, and Diepkloof. Stratigraphic aggregates corresponding to MIS4 is highlighted.

The OSL dating of these sites shows that the change in raw material frequencies occurs at the MIS5 to MIS4 boundary (Brown et al. 2012, Jacobs and Roberts 2015, Jacobs et al. 2012, Jacobs and Roberts 2008, Jacobs, Roberts, et al. 2008a). In this dissertation I will build on previous research (Brown 2011, Brown et al. 2012, Brown et al. 2009) and highlight that the record for PP 5-6 shows an exaggerated increase in fine-grained materials such as silcrete comparable to Blombos Cave (**Figure 6**) and Diepkloof Rock Shelter (**Figure 7)**, and perhaps Die Kelders Cave 1 (**Figure 8**). In fact, silcrete dominates the assemblages from MIS 4 at these three sites. The dominance of silcrete exceeds that at other south coast sites such as Klasies River (**Figure 5**) and Nelson Bay

Cave (**Figure 9**).Outside the Cape in sites such as Sibudu, Rose Cottage Cave, Ntloana Tsoana, Sehonghong, and Umhlatuzana raw materials such as dolerite, hornfels, quartz and opaline are used in varying frequencies but also at these sites there is an increase of fine-grained raw materials such as opaline during the MIS5 to MIS4 transition. The pattern is not as pronounced as in the coastal sites in the Cape.

The materials chosen to manufacture backed pieces in the Howiesons Poort and bifacial points in the Still Bay somewhat mirror the raw material that dominates the rest of the assemblages during the same technocomplexes. At Blombos Cave, Still Bay points are mainly made on silcrete (Henshilwood et al. 2001), while at Diepkloof Rock Shelter the production of Still Bay points are dominated by local quartzite but few are in finished form (Porraz, Texier, et al. 2013). In the Howiesons Poort, the backed pieces at PP5-6 are made mainly on silcrete (Brown et al. 2012), whereas quartzite dominates the backed piece assemblages at Klasies River (Singer and Wymer 1982, Wurz 2002) and Nelson Bay Cave (Volman 1981).

The argument that post-Howiesons Poort industries (MIS3) reflect a return to a rudimentary prepared-core flaking strategy based on quartzite (e.g., Singer and Wymer 1982, Volman 1981) has been contested with data from new excavations. Evidence from Sibudu (Will, Bader, and Conard 2014), Diepkloof Rock Shelter (Porraz, Texier, et al. 2013), and PP5-6 (Brown et al. 2012, Brown et al. 2009) suggest that there was much more variability in the post-Howiesons Poort than previously acknowledged. However, some sites such as Klasies River, Nelson Bay Cave, and Die Kelders Cave 1 exhibit quartzite-dominated technology in MIS3.

Existing informal models of raw material change

As discussed above in *Chapter 2*, there is consensus on what mechanisms can cause changes in raw material frequencies at a general level including direct procurement due to physical qualities needed for specific tasks or qualities linked to symbolic values, embedded procurement, trade/exchange, and demographic change. In the South African MSA that was reviewed above, there are examples of major changes in raw material frequencies especially at the MIS5 to MIS4 transition. This transition coincides with a shift in technology as well with the introduction of symmetrical bifacial points and microlithic technology as expressed in the early microlithic (SADBS) at PP5-6, and Still Bay and Howiesons Poort technocomplexes.

However, there is no consensus as to what caused the raw material shifts observed with the early microlithic (SADBS), Still Bay and Howiesons Poort in the South African Middle Stone Age (Ambrose 2006, Brown 2011, Minichillo 2006). At least six different competing informal models for the shift in raw material use have been proposed including hypotheses linked to increased mobility (Ambrose and Lorenz 1990, McCall 2007, McCall and Thomas 2012), trade/exchange (Deacon 1989), symbolic value (Wurz 1999), functional demands (Mackay 2008), changing cost of wood fuel for heat-treatment (Brown and Marean 2010), and changing availability of raw materials (Brown 2011, Volman 1981).

As discussed in the preceding chapter, explanations for changes in raw material frequencies can be divided into two broad camps: 'Non preference-based change' (also called encounter-based procurement) or 'Preference-based change'. In the following subsections, I will summarize the six informal models that have been proposed to explain

the change in raw materials between MIS5 and MIS4. I will do so by categorizing them under the framework outlined above at the end of *Chapter 2*.

Natural Availability

An example of the 'Natural availability' variant of the 'Non preference-based change' model category is work by Volman (1981). He proposed that as the global temperatures fluctuate in MIS5 and MIS4, potential high-quality raw materials on the coastal shelf on the southern coast of South Africa became available when the coastal shelf was exposed. New access to raw materials explains why silcrete is more frequently procured during MIS4.

Brown (2011) built on the proposed relationship between an exposed coastal shelf and the change in raw materials. Brown (2011) presented a model termed the "Site-context Model" that proposed that the differential use of quartzite and fine-grained lithic raw materials in the MSA is possibly linked to the position of PP5-6 on the landscape in relation to the position of the coastline for a given time interval. Compared to a "Mobility-linked" variant of the encounter-based models where people increase their movement, Brown pointed out that in the "Site Context Model" it is the relative context of the site on the landscape that is moving. During warm periods, the site is located next to the coast, while during cold periods PP5-6- is located as far as 30 to 40 km inland. Brown (2011) posited that during coastal occupations of PP5-6, the makers of the MSA tools likely gathered locally available quartzite from cobble beaches. The reshuffling and replenishing of the active beaches by ocean swell, tidal activity, and storm surges provide a regular source for new materials. Other secondary context raw materials such as silcrete

may also be found in lower frequencies at these beaches creating a pattern at PP5-6 that reflects a selection of materials locally available in secondary context.

Conversely, during colder periods, Brown (2011) posited that when the coastline is regressing and PP5-6 is an inland site the toolmakers would still have access to cobbles but high-quality materials would be depleted quickly. This is because there is no active energy source to replenish the cobble source. Brown asserted that since the distance to a secondary source increases it leads to the increased attractiveness of terrestrial sources. Brown and colleagues (2011, 2009) proposed that one strategy to reduce the search cost during inland occupations is to improve the flaking quality of more locally available silcrete through heat-treatment.

The "Site Context Model" assumed that the primary sources of raw materials on the landscape did not change position since the MSA. Further, it is assumed that the dynamic cobble beaches hypothesized to be a major source of quartzite cobbles for MSA tool manufacture will move closer and farther away from PP5-6 as the coastline shifts during the interglacial and glacial cycles. In addition, the "Site Context Model" assumed that materials are chosen based on distance to source as a proxy measure for procurement cost. The model assumed that all materials have equal value and the selection of materials was strictly based on procurement cost. Because the model links the selection of silcrete with changes in the distance to secondary sources of quartzite, and the distance to primary silcrete sources does not change through time, the model assumptions are made to evaluate the potential baseline effects of coastline movement on stone tool raw materials. An important additional assumption of the "Site Context" model is that there are no submerged silcrete sources within 8 to 10 km to PP5-6. The study presented here

will test that constraint assumption and will investigate what effect that a potential silcrete source on the now submerged plain has on the raw material frequencies.

Brown (2011) presented a set of text expectations for the model. During interglacial conditions when the coastline is near Brown expects that there should be a greater use of quartzite, more beach cobble cortex, a lower percentage of heat-treated silcrete, more cortical products, larger flaking products, and lower cutting edge to mass ratios. For glacial conditions when the coastline is far away, Brown (2011) expected that there should be an increase in materials from inland sources, more primary cortex, higher percentages of heat-treated silcrete, less cortical flaking products, smaller products, and higher ratios of cutting to mass. Brown found mixed support for his expectations. Some expectations like increased cobble cortex in layers dating to MIS5 when cobble beaches are present in close vicinity to PP5-6 was met. However, expectations about increased use of materials from outcrop sources during MIS4 were not met in most stratigraphic units. The expectation about smaller tools during MIS4 was not met either in most stratigraphic units.

Another informal model that is an example of a 'Natural availability' variant is the "Wood-fuel availability" model proposed by Brown and Marean (2010). Although not specifically dealing with the availability of stone resource it instead deals with the changing abundance and availability of wood-fuel needed to heat-treat silcrete. They (2010) proposed that the shift to increased heat-treatment of silcrete during MIS4 occurs simultaneously with a shift to more summer rain and a vegetation type that includes more C4 grass. They stated that climates and vegetation with these characteristics have more trees suitable for heat-treatment since C4 grasslands normally have abundant acacias and

these trees typically provide high-quality wood. They proposed that the appearance and disappearance of silcrete are constrained by the abundance and availability of wood suitable for heat-treatment. More precisely, what they proposed was that when the cost to procure wood fuel to heat-treat silcrete increases, the selection of silcrete decreases. During MIS4 there was an increase in summer rains and woody vegetation that decreased the cost of procuring wood fuel, which made committing to heat-treatment a viable technology (Brown and Marean 2010).

Mobility-linked

Ambrose and Lorenz's (1990) application of Dyson-Hudson and Smith's (1978) ecological model of resource structure is an example of the 'Mobility-linked' variant of the 'Non preference-based change' model category. Ambrose and Lorenz (1990) proposed an inverse relationship between exotic non-local raw materials and stone tool source abundance and predictability. In their model, technological change is the result of a change in foraging range size, the degree of information sharing, and territoriality. The changes are proposed to have happened due to the fluctuation in the abundance and predictability of stone tool raw material sources. Ambrose and Lorenz argued that the Howiesons Poort occurred during a period in MIS4 when the climate was cooler and drier, and point to faunal remains that suggest that there was a shift to more open grassland. They proposed that the resource base was less predictable but more abundant. The human response to this is to increase mobility and this leads to a corresponding increase in the frequency of non-local raw materials encountered on the landscape. Ambrose and Lorenz's (1990) model is an example of Binford's (1979) 'embedded

procurement strategy' model, which suggests that all tool raw materials are procured during other subsistence activities. They rejected the argument that the changing procurement pattern of raw materials is the result of a change in technology (Brown 2011).

McCall (2007) and later McCall and Thomas (2012) presented a similar argument to Ambrose and Lorenz. They proposed that the emergence of the biface-dominated Still Bay technocomplex is related to increased mobility, which took the foragers away from lithic raw material sources. Increased mobility resulted from environmental change at the transition from MIS5 to 4, which led to a decline in plant productivity, lower densities of food resources and increased foraging territory size. In turn, the ecological changes led to a reorganization of the mobility strategy of the foragers and new strategies to supply raw materials (McCall 2007).

McCall and Thomas (2012) proposed that the increased selection of exotic and non-local raw materials in the Howiesons Poort technocomplex was due to the acquisition of such materials during long distance logistical hunting trips. They argued that the Howiesons Poort tool makers manufactured specialized and reliable tools that were used in a technological organization system that indicates longer-term residential occupations and logistical targeting of resources that were predictable, clumped and perhaps distant. They argued that the tools and weapons that Howiesons Poort segments and backed pieces were incorporated into fit within Bleed's (1986) concept of reliable tools.

Utilitarian

Mackay (2008) offered an informal model that is an example of a 'Utilitarian' variant of the 'Preference-based change' model category. Mackay (2008) proposed that environmental and climate conditions during MIS4 pressured the makers of the Howiesons Poort technocomplex to maximize the recovery of edge length from a given mass of stone. Mackay contended that MSA toolmakers gradually intensified efforts to locate raw materials that would facilitate maximization of cutting edge to mass. He (2008) proposed that towards the end of MIS4 when the selective pressure eased it diminished the requirement for fine-grained materials. Mackay (2008) argued, in contrast to model variants in the 'Non preference-based change' model category, that raw material selection was not a function of the distance to source but rather a function of the need for materials that could facilitate the manufacture of thin flake and blade blanks that allowed for a higher cutting edge to mass ratio, thus conserving core volume. The informal model proposed by Mackay is most aligned with Gould, Saggers, and colleagues' (1985, 1985, 1971) argument that archaeological stone tool raw material patterns represent evidence for deliberate selection of specific raw materials due to functional properties, which makes some raw materials better than others for a specific task.

Non-functional

Wurz (1999) performed a comparative metric analysis of backed artifacts resulting from Deacon's excavation of Klasies River finding only marginal differences in terms of size between backed artifacts made all types of raw materials. She pointed out that although there was an overall increase in the use of non-local materials, and the selection of these

materials was deliberate and significant, she found no functional difference in the way the local and non-local materials were used. All raw materials were used in the same manner. Thus, to Wurz, the advantage of using non-local materials was interpreted as being symbolic or provided by the artifact maker. Wurz's hypothesis is an example of the 'Non-functional' variant of the 'Preference-based change' model category. She proposed that the non-local stone or backed artifacts in the Howiesons Poort made on non-local materials have an abstract value that is unrelated to the physical properties of the rock, except the color of the rock.

Social learning/Culture

Deacon (1989) presented a competing informal model to Ambrose and Lorenz. Deacon's hypothesis is an example of a 'Social learning/Culture' variant of the 'Preference-based change' model category. Deacon argued that the selection of exotic and non-local raw materials during the Howiesons Poort technocomplex resulted from reciprocal exchange of hunting equipment similar to observed behavior in San hunter-gatherer groups. Further he proposed that reciprocal exchange was a means for coping with environmental stress that was brought on by colder climates during MIS4. Deacon proposed that this aspect of raw material selection supports his argument that anatomically modern humans in the MSA were behaviorally modern.

Summary

Two of the model variants presented above will be explicitly tested. The 'Natural availability' variant of the 'Non preference-based' model category will be tested with the

Opportunistic Acquisition Model (OAM), while the 'Utilitarian' variant of the 'Preference-based' model category will be tested with the Active-choice Model (ACM). However, by changing model variables in the OAM the 'Mobility-linked' variant will be evaluated as well. Testing of the 'New transport abilities/Carrying costs', 'Non-functional', and 'Social learning/Culture' variants is beyond the scope of this study.

CHAPTER 4: GEOLOGY OF THE MOSSEL BAY REGION AND STONE RAW MATERIAL SOURCES

General overview

To evaluate the two different formal models presented in this dissertation requires an understanding of the local geology of the Mossel Bay region as it pertains to potential primary and secondary context sources for stone tool raw materials. Brown (2011) presented an overview of the Mossel Bay region geology in this respect and I will summarize his overview in the following subsections. Stone tool raw material sources that will be discussed here were identified by field work by Brown and this author (2014). In addition, Brown based his designation of potential sources on published literature of the geology in the Mossel Bay region. **Figure 11** shows the distribution and extent of important geological formations visible during interglacial conditions discussed in more detail below.

Brown pointed out that even though no geochemical sourcing work has been done owing to the challenges associated with the positive identification of a specific location in space from which archaeological materials originated from, it is possible to assign probability to a source area or region (Shackley 1998). Because of this Brown (2011) stated that the potential source materials highlighted by him are discussed in terms of their geological distribution and general proximity to PP.

Elements of the Cape Supergroup, which formed as a thick wedge in a deep trough associated with the Gondwana breakup, are the primary context bedrock exposures in the Mossel Bay region (Malan and Viljoen 2008). The Cape Supergroup dates from 550 ma to 330 ma, is up to 10 km thick, and is divided into the Table

Mountain, Bokkeveld, and Witteburg groups (Thamm and Johnson 2006). Only the Table Mountain and Bokkeveld groups are represented in the Mossel Bay region. The Table Mountain Group consists of sheets of sandstone with some alternating beds of shale and conglomerates (Thamm and Johnson 2006).

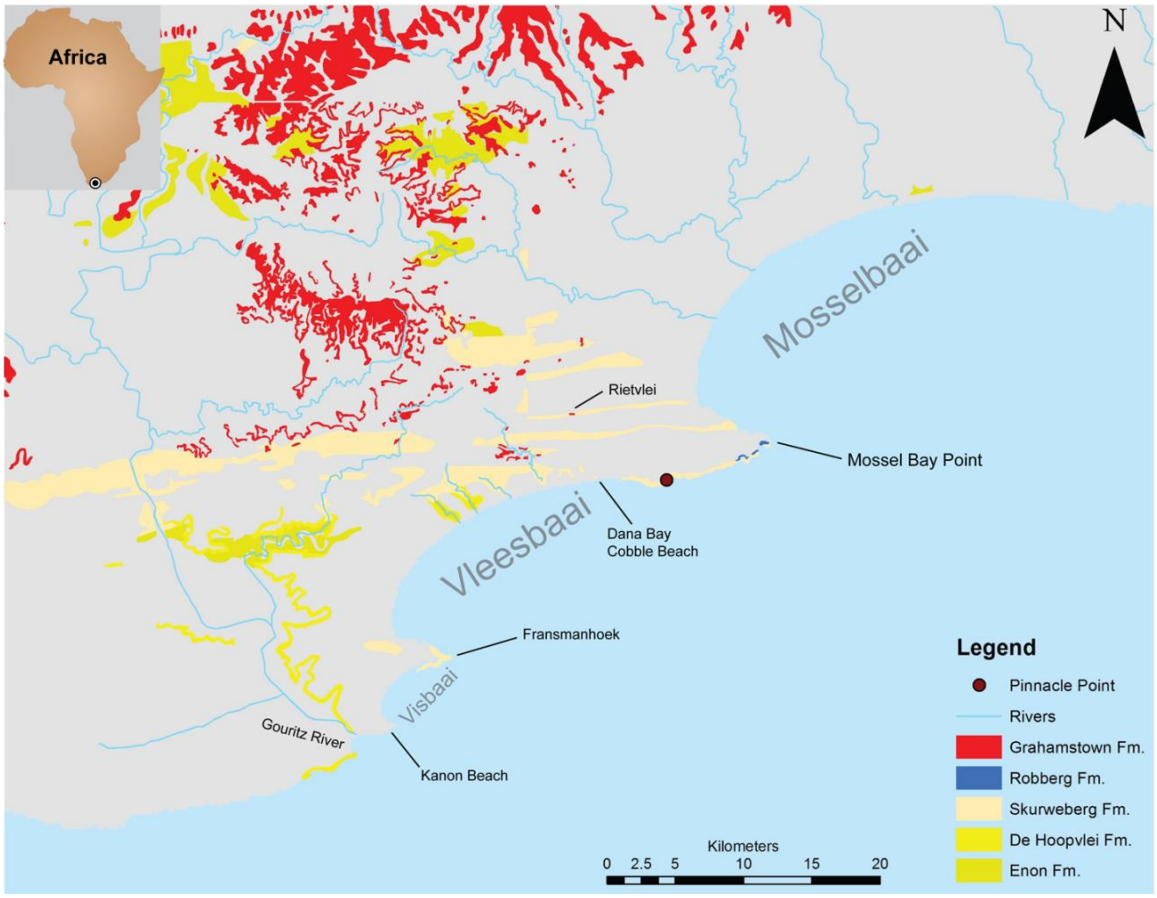

Figure 11. Geology map of the Mossel Bay region during interglacial conditions. The map shows the distribution and extent of important geological formation of interest in this study.

In the area surrounding PP, the Table Mountain Group is well represented by the Skurweberg and Baviaanskloof formations of the Nardouw Subgroup and by the Ceres Subgroup. The PP cave and rock shelters occur in Skurweberg quartzitic sandstone. The Nardouw and Ceres Subgroups occur as thick cross-bedded layers that are composed of former marine and fluvial sediments (Thamm and Johnson 2006). Overlaying the Table

Mountain group is the Bokkeveld group, which consists of alternating sandstone and mud/siltstone layers. The Bokkeveld layers were deposited during episodes of coastline transgression and regression. This action shifted deposition from lower energy deltaic environments to more high-energy wave-influenced marine environments (Thamm and Johnson 2006).

The below-ground geology of the now submerged Agulhas Bank in the vicinity of the Mossel Bay region consists of sandstone elements of the Table Mountain Group and Robberg Formation sandstone of the Uitehage Group. Further out, at -20 masl to over -80 masl the subsurface deposits are Cretaceous deposits. Multibeam bathymetry and side-scan sonar show that a low-relief plains landscape occurred between PP5-6 and the coastline when sea levels where lower than present (Cawthra et al. 2015). The presence of offshore quartzite-outcrops and eroded outcrops, and shelf sand would have provided a substrate for the creation of both sandy and rocky shorelines during lower sea level stands (Cawthra et al. 2015). **Figure 12 and 13** shows the interpreted distribution and extents of wave ravinement surfaces, cover sand, rivers and floodplains, and hardgrounds during MIS4 and MIS6 respectfully.

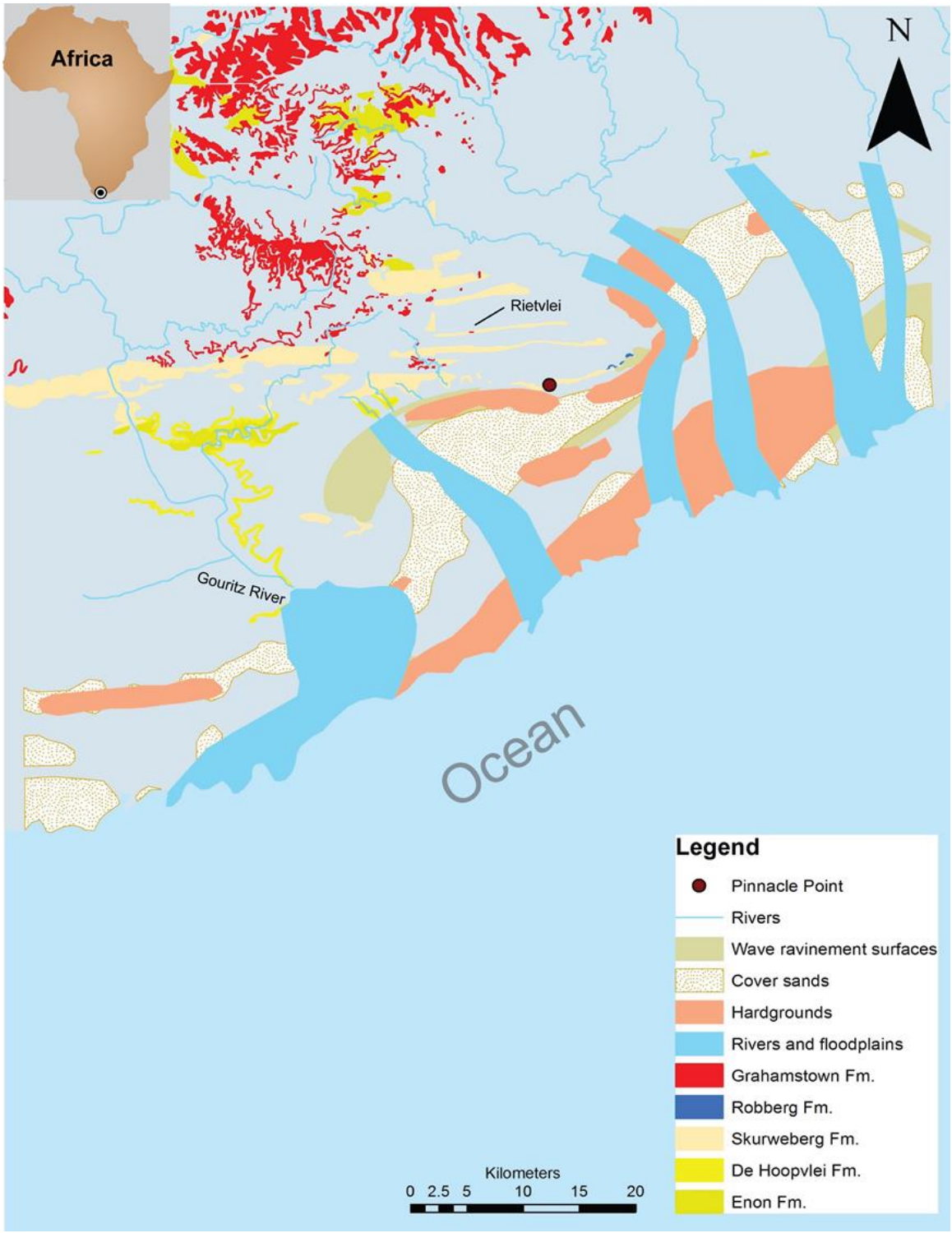

Figure 12. Geology map of the Mossel Bay region during MIS4. The map shows the distribution and extent of important geological occurrences on the exposed Agulhas platform. Distance to the coastline from Pinnacle Point is ~15km.

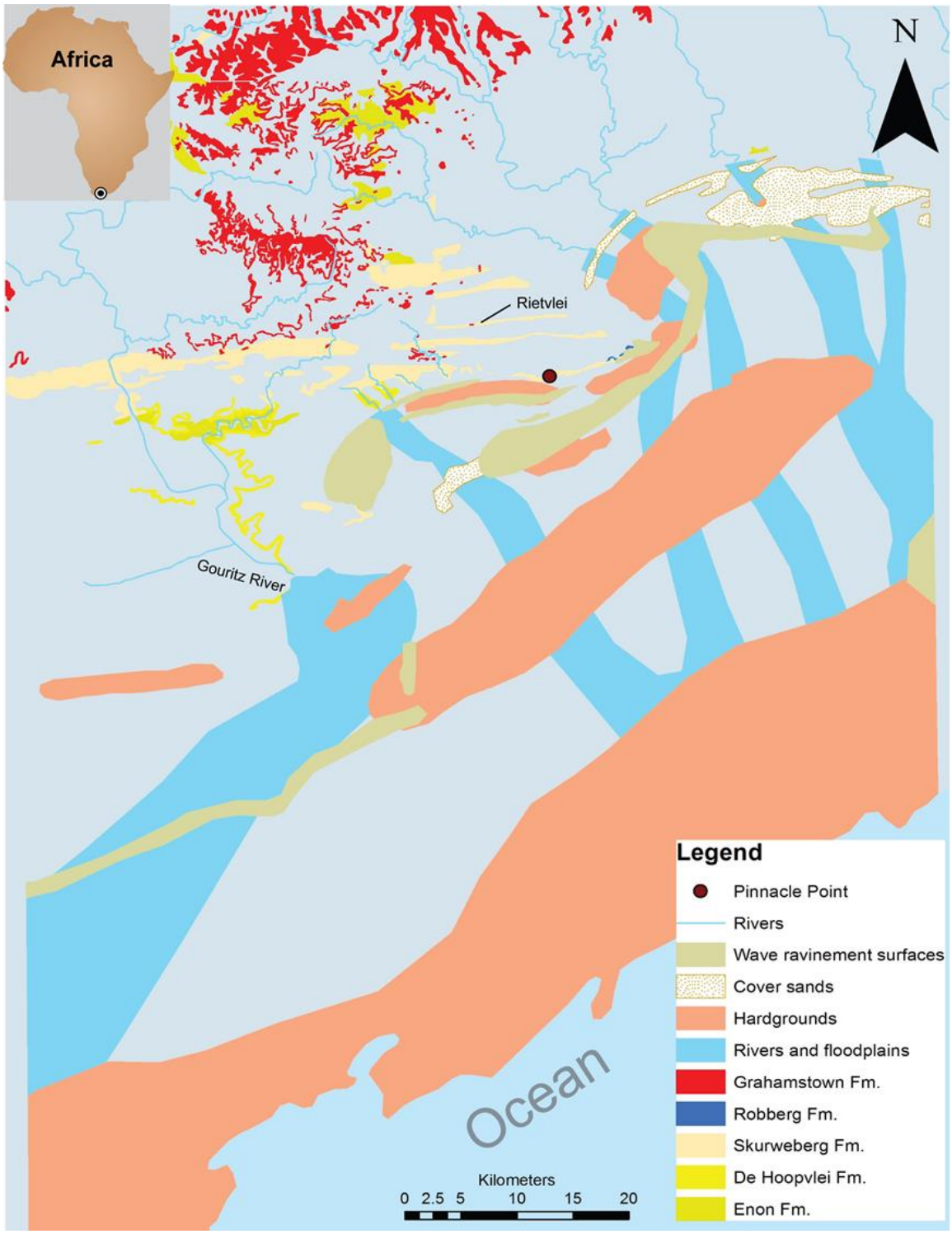

Figure 13. Geology map of the Mossel Bay region during MIS6. The map shows the distribution and extent of important geological occurrences on the exposed Agulhas platform. Distance to the coastline is ~42km.

The breakup of Gondwana and the following developing of land surfaces also had an effect on the formation and distribution of silcrete (Partridge, Botha, and Haddon 2006). After Gondwana underwent rifting, the land surfaces above and below the Great Escarpment underwent parallel erosion due to warm and wet conditions during the Cretaceous. This resulted in more or less continuous and flat surfaces on the seaward and inland sides of the escarpment, which is also called the "African Surface" (King 1948). Following the late Cretaceous, the 'African Surface' was capped and cemented by ferricrete, calcrete and most extensively by silcrete (Grahamstown Formation) along the southern coast (Partridge, Botha, and Haddon 2006). It has been argued that the 'African Surface' is most likely the product of multiple erosional episodes that resulted in a non-uniform and multi-level topography (Marker and McFarlane 1997). An example of the change in elevation of the silcrete-capped surface is found in the Riversdale-Albertinia area where the silcretes are located at 300 meters above sea level (masl) in the north and slopes down to less than 120 masl in the southeast (Summerfield 1981). Brown (2011) pointed out that the environmental conditions, mechanism, and timing of the processes that led to the formation of silcrete on the cape coast are not well understood. Silcrete appears to have formed at different elevations, and it has been proposed that the silcrete at different elevations have different formation ages (Marker and McFarlane 1997, Roberts 2003). Brown (2011) noted that silcrete formation research has several challenges including 1) there is a lack of modern analogs for modern silcrete formation (Roberts 2003); 2) competing hypotheses of formation drawn from the fact that silcrete will precipitate at both low and high soil PH (Partridge, Botha, and Haddon 2006); 3) a

lack of published absolute dates from weathering profiles of silcrete from southern Africa (Roberts 2003).

One proposed model for silcrete formation was presented by Summerfield (1983), who argued that silcrete forms during low pH environments, based on the apparent co-precipitation of silica and titanium. Summerfield argued that the precipitation happened in a humid and well-vegetated tropical environment. Alternatively, precipitation of silica happened due to cooler temperatures and increased aridity in the late Cretaceous that resulted in raised soil pH (Partridge and Maud 1987). However, there seems to be a consensus that silcrete formed multiple times during humid environments because soil pH was lowered resulting in silica precipitation due to increased ground water and dense vegetation, and because coastal-belt silcretes formed during the Miocene/Pliocene (Roberts 2003, Summerfield 1981).

Brown (2011) noted that the term ‘silcrete’ describes the eventual outcome of pedogenic processes that have formed in association with degraded bedrock. This degraded bedrock is termed ‘weathering profile silcrete’. The parent geology of a given local area therefore heavily influences the physical properties of the resulting silcrete (Roberts 2003, Summerfield 1981). However, while parent geology influences the formation if silcrete it does not heavily influence the mineralogy of the silcretes (Summerfield 1981). Most silcretes are predominantly composed of silica dioxide, with minor percentages of titanium, iron (goethite or hematite), and assorted other trace elements (Brown 2011) The silcrete in the southern coastal belt and in the exposures closest to the Mossel Bay region generally occur in association with weathered Bokkeveld clay/silt profiles (Summerfield 1981). Silcretes farther to the north occur in

the Buffelskloof formation sandstone/conglomerates of the Uitenhage group, in Kirkwood formation silt and mudstones of the Uitenhage group, and also within weathered profiles of the Cape Granite Suite (Brown 2011).

Brown (2011) noted that silcrete can be characterized as being either 'globular' where the rounded masses are surrounded by uncemented sediment, or 'conglomerate' where silcrete and quartz pebbles are cemented together, or 'massive' where the materials are homogeneous, fine-grained and relatively hard compared to the other types (Frankel 1952, Summerfield 1981). Massive silcretes often contain a lighter and more 'powdery' material termed rind (Summerfield 1981). The rind is undesirable for experimental flaking because it does not fracture predictably (Brown 2011). Another way to classify silcrete is according to the fabric of the material by using petrographic thin sections (Brown 2011). Brown (2011: 79) noted that "Summerfield (1981) defined four different silcrete fabrics: 'grain-supported' (GS), 'matrix supported' (M), 'floating' (F), and 'conglomerate' (C)." Summerfield's (1981) classification is based on the relative proportions of cementing silica matrix (M fabric), inclusive quartz grains (F fabric), the inclusion of previously cemented materials (C fabric), and the presence and absence of pre-existing structure (GS fabric) (Brown 2011).

Because parent geology does not heavily influence the mineralogy, geochemically fingerprinting silcrete is very challenging (Brown 2011, Summerfield 1981). Brown (2011) noted that it is challenging because the subsamples from the same weathering profile may show more variability in the composition of trace elements than compared to samples from widely separate exposures of differing geology (Corkill 1999). However, more recent work in Botswana (Nash et al. 2016, Nash, Coulson, Staurset, Ullyott, et al.

2013), the Western Cape (Nash, Coulson, Staurset, Smith, et al. 2013), and in Australia (Cochrane et al. 2016) has been more successful.

Primary context quartzite sources

Table Mountain Group sandstones outcrop throughout the Mossel Bay region with the Skurweberg formation being very prominently displayed. However, most of this quartzite is coarse-grained, cross-bedded, and does not fracture in a predictable manner (Brown 2011). At PP, the local Skurweberg quartzite is yellowish-grey to light brown in color, crumbly and coarse in texture (Brown 2011). Some Table Mountain sandstones are outcropping in drainages that dissect Vleesbaai but this material is also coarse-grained (Oestmo et al. 2014).

Presently, there are two good sources of primary context quartzite in the Mossel Bay region (**Figure 14**): The closest source is Robberg formation sandstone towards the Mossel Bay point. Robberg formation sandstones from the more recent Uitenhage Group that dates to 145 ma to 65 ma is highly indurated, which means that it has been hardened by heat or the introduction of cementing siliceous materials (Shone 2006). Robberg quartzite outcrops at the base of Cape St. Blaize Cave (CBC) at Mossel Bay point, and occurs intermittently to the west towards the PP site complex. The closest known outcrop of Robberg quartzite to PP is ~5.3 km away. The Robberg quartzites are very fine-grained with individual sand grains often only visible with magnification. The quartzite is generally light and ranges from grey to red to brown. The exposure below Cape St. Blaize Cave exhibits distinctive dark red and grey "Leopard spots" (Brown 2011). Thompson and Marean (2008) noted that based on cortex type present in the MSA

assemblage from Cape St. Blaize Cave, the local outcrop appears to be have been preferentially selected over secondary context beach cobbles. Brown (2011) noted that surface scatters of MSA artifacts along the Cape St. Blaize trail seem to be concentrated near outcrops of Robberg quartzite. Schoville and Brown (2010) stated that this material is very suitable for experimental production of flakes and blades.

Figure 14. An example of a primary outcrop of quartzite. Quartzite of Skurweberg formation located at Fransmanhoek located about 23 km southwest of PP along coast.

The second potential outcrop source is located at Fransmanhoek at the southeastern tip of Vleesbaai located some 24 km away when following the coastline (**Figure 14**). This material is coarser than the Robberg formation quartzite but is of higher quality than the local Skurweberg around the PP sites. The quartzite is light in color ranging from grey to blue with red bands and flakes conchoidally.

With lower sea levels, there would have been increased access to Table Mountain sandstones and Robberg Formation sandstones to the west of Cape St. Blaize as now submerged outcrops extend for 1.5 km. These outcrops form an offshore extension of the cliff feature that extends from PP to Mossel Bay point and would have been the only additional outcrop available on the low-relief plains landscape during lower sea level stands (Cawthra et al. 2015).

Primary context silcrete sources

Silcrete sources from a variety of parent geological formations are available and abundant to the Northwest of PP (**Figure 15**). Brown sampled silcrete from the Grahamstown formation of the Bokkeveld group, Kirkwood Formation of the Uitehage Group, and the Cape Granite Suite (Brown 2011, Brown et al. 2009). Brown found that almost all the silcrete he sampled, regardless of parent geology, yield materials of suitable quality for flaking once the materials have been heat-treated (Brown 2011, Brown et al. 2009). He noted, however, that some locations require more search time to procure suitable nodules. Brown (2011) also noted that compared to other MSA sites where the sources of the silcrete are not known and the silcrete is assumed to be non-local or exotic, the silcrete in the Mossel Bay region would have been abundant and recognizable to MSA tool makers as close as 8.5 km from PP.

Brown (2011: 80) argued using four lines of evidence that there would be no available silcrete sources on the now submerged Agulhas Bank during lower sea levels in the Pleistocene: 1) “The Agulhas Bank would have been submerged during the Post-Cretaceous periods when silcrete on the higher land surfaces formed”; 2) more recent

Pleistocene sea level transgressions would have created terraces that would have likely planed off any southern extensions of the deeply weathered profiles that the silcrete would have formed on; 3) There are no observed silcrete outcrops below 140 masl in the Mossel Bay region; 4) based on elevations of known silcrete exposures, there is no evidence to suggest that coastline movement during the Pleistocene resulted in an overlap between the coastline and silcrete outcrops that would have created silcrete-rich cobble beaches.

Figure 15. An example of a primary outcrop of silcrete. Note the pavement-like surface in the forefront. This silcrete source is an example of a Grahamstown formation silcrete and it is located 56 km north of PP.

Conversely, marine geophysical work by Dr. Haley Cawthra shows that there are prominent erosional surfaces (hardgrounds) interpreted as either calcretes or silcretes on

the inner shelf of the now submerged Paleo-Agulhas plain (Cawthra, pers comm.), which extends on average for 8km in the Mossel Bay region (Cawthra et al. 2015) (**Figures 12-13**). These hardgrounds formed during long exposures during lower sea stands. The case for offshore silcrete is based on several lines of evidence: 1) Silcrete has been found in inshore cores at depths of -50 masl (Rogers 1980); 2) on the south coast, the onshore silcrete mostly overlies Bokkeveld Group and Enon formation elements. Often these silcretes might later be covered by aeolianites on the south coast between Bredarsdorp and Cape Agulhas; 3) when aeolianites directly overly cretaceous rocks then silcrete is typically not found; 4) there are a limited amount of aeolianites near the present onshore cliffs and before the -40 masl coastline. The formation of silcrete on the offshore shelf could be possible if there was exposure in the Miocene. The silcrete could have formed if there was a high ground water table, fluvial drainages for entrapment and exposure and aridity for the formation processes to take place (Cawthra, pers comm.).

Other primary context lithologies

Quartz can be found locally as vein quartz in the Skurweberg formation (**Figure 16**) (Minichillo 2005, Thompson, Williams, and Minichillo 2010), and angular quartz is very frequently found associated with silcrete from the Bokkeveld group (Brown 2011). Brown (2011) noted that crystalline quartz and other semi-precious raw materials are known to form in pegmatites of the Cape Granite Suite. Examples from the PP5-6 assemblage show that almost all samples with cortex exhibit outcrop cortex. The closest Cape Granite Suite formation with pegmatite occurs some 21 km from PP near the town of George, thus sets a minimum radius for the direct procurement or transfer of this type

of raw material (Ferré and Améglio 2000, Walker and Mathias 1946). The closest known occurrence of cherts in primary context is two sedimentary formations in the southern Karoo Basin more than 100 km away. These two formations are the southern facies of the Prince Albert Formation of the Ecca Group and the Abrahamskraal Formation of the Beaufort Group (Brown 2011, Catuneanu et al. 2005, Johnson et al. 2006, Johnson et al. 1996).

Figure 16. An example of a primary outcrop of milky vein quartz. This one formed in Skurweberg formation outcrops close to surf zone at Pinnacle Point.

Secondary context sources

Brown noted that while primary context raw material sources receive a lot of attention due to the possibility of geochemical tracing, secondary sources, on the other hand, are

often overlooked (Shackley 1998). Because the secondary sources are often overlooked it has led to some raw materials to be termed exotic and non-local although they might originate from a local secondary source (Brown 2011, Minichillo 2006). The Mossel Bay region would have presented a prehistoric hunter-gatherer with a range of secondary sources including active cobble beaches and river drainages, static fossil river/beach terraces, and ancient alluvial gravels that occur in stratified formations (Brown 2011).

Cobble beaches

Surveys by Brown (2011) and this author (2014) have mapped the presence of several modern coastal cobble beaches with nodules suitable for stone tool manufacture in the Mossel Bay region (**Figure 17**). They occur at the following locations in decreasing walking distance to PP: Kanon Beach near the Gouritz River mouth (c. 27 km southwest of PP along coast); Fransmanhoek (c. 25 km southwest of PP along coast); Mossel Bay point (c. 6.8 km to the east); Dana Bay (5 km west of PP); and Eden Bay (directly adjacent to PP sites). The local Eden Bay beach is dominated by Skurweberg formation quartzite, which has been found to not fracture in a predictable manner (Brown 2011). However, with increased search time and a lot of material testing, it is possible to find suitable material for tool manufacture (Brown 2011, Minichillo 2005). Minichillo (Minichillo 2005) also noted the occurrence of small quartz nodules (4%) at Eden Bay during a quantitative survey.

The materials at the Mossel Bay point cobble beach are relatively homogeneous in nature and appear to derive from the locally outcropping Robberg formation quartzite (Brown 2011). Most of the materials that are found on the beach or in the intertidal zone

are sub-angular in nature, which suggests it is more recent detachments from the Robberg exposures that make up the Mossel Bay Point (Brown 2011).

The closest cobble beach to Pinnacle Point that consistently provides good quality raw materials is located at Dana Bay (~5 km west of Pinnacle Point). Brown (2011) visited this location over a four year period to collect materials for experimental MSA stone tool manufacturing. During two procurement bouts lasting 1 hour each, Brown collected 91 cobbles that included 86 (95%) fine quartzite cobbles, four hornfels cobbles (4%), and 1 silcrete nodule (1%) (Brown 2011). Brown's survey showed that silcrete is available at the Dana Bay cobble beach in unpredictable quantities. Brown found that he would encounter his own tested nodules the next time he visited the source but sufficient turnover and reshuffling of cobbles had also provided a supply of new cobbles. Brown noted that cobbles are not always available at the Dana Bay beach owing to the fact that it is frequently covered by beach sand. Brown (2011) observed the lack of cobbles when visiting the source for two straight years but he could not recover any cobbles the second year due to covering beach sands. This modern observation of the covering of a cobble beach yields a good example of how beach cobble availability during the Pleistocene could have been unpredictable (Brown 2011).

The cobble beaches or perhaps boulder beaches at Fransmanhoek (**Figure 17**) yield quartzite cobbles and boulders of good quality that are very suitable for tool manufacture. The presence of well-rounded boulders is a testament to the homogeneous nature of this material. The production of cobbles seems to be the result of erosion of the local high-quality Skurweberg formation quartzite (Oestmo et al. 2014).

Figure 17. An example of a cobble/boulder beach. This one at Fransmanhoek, some 25 km southwest of PP along the coast.

The marine geophysics work by Cawthra suggests that at lower sea level stands when the coastline was 1 km further out and more compared to today's conditions there were readily available cobbles belonging to extensive wave-ravinement surfaces within Vleesbaai, and around the Skurweberg and Robberg formation quartzite that outcrop to the east of the Mossel Bay Point (Cawthra et al. 2015) (**Figures 12-13**). The cobbles in Vleesbaai are most likely the result of erosion of outcropping Table Mountain sandstones that today is visible as subdued sandstones (Cawthra et al. 2015).

The wave-ravinement surfaces are associated with a regional marine flooding event across the rapidly drowning continental shelf. Using seismic methods the surfaces were sampled offshore of the Great Brak River in Mossel Bay (Cawthra 2014) and offshore of Vleesbaai (Cawthra, Personal comment) where they are exposed beneath

modern marine sands. The surfaces are composed of well-rounded cobbles and boulders and are interpreted to be the transgressive ravinement of the Holocene transgression. Erosion by wave action in the surf zone acts as a winnowing agent, eroding bedrock and resulting in the formation of these lag deposits (Nordfjord et al. 2009, Posamentier 2002). Similar wave ravinement surfaces have been described off the South African east coast (Cawthra, Uken, and Ovechkina 2012, Green 2009, Hay 1984), and offshore of the Wilderness Embayment (Cawthra et al. 2014).

Brown (2011) stated that though it has been easy to find modern primary and secondary sources for silcrete, quartzite, hornfels, and quartz, it has been harder to find sources for raw materials commonly referred to as 'CCS' (cryptocrystalline silicates) including chert, opaline, and chalcedony. Following Brown (2011) and recent geological convention, I will use the term 'chert' for all crypto- and microcrystalline silicates that fracture conchoidally including chalcedony but not including silcrete. As noted above, no local source of chert has been discovered by systematic pedestrian and vehicle survey in the Mossel Bay region. This is not unexpected as the local geology does not exhibit geological formations that contain chert (Thamm and Johnson 2006). The closest known occurrence of primary-context chert is over 100 km away in the southern Karoo basin, where the Gourtiz River and its tributaries have cut through geological formations containing chert. Archaeological examples from PP5-6 exhibit pebble and cobble cortex suggesting that they could have been water transported over long distances (Brown 2011). Several drainages dissect the Mossel Bay region but only the Gouritz River extends north of the Cape Super Group in the present day and thus cuts through the aforementioned primary context cherts.

Gouritz River

The Gouritz River and its tributaries extend 250 km inland and cut through six major geological entities. Brown has been unsuccessful in finding chert in the Gouritz drainage but several massive river bars containing river rolled cobbles offers good probability for finding chert. Brown (2011) argued that long stretches of the Gouritz, which today is lined with fine silt and sand that could obscure more cobble beds, could have been exposed in the past following high-water volume scouring of the drainage. In addition, at the mouth of the drainage, there is an extensive cobble and boulder beach. A visit to cobble-rich terraces along the Gouritz River in the Little Karoo by Brown and this author identified MSA primary lithic reduction areas. These areas contained chert artifacts with rolled cobble cortex suggesting that these materials where available in the drainage in prehistoric times.

Brown's surveys showed that the Gouritz transports a wide variety of raw materials in the shape of cobbles from the interior to the coastline. Additionally, survey of the river terraces in the Little Karoo also shows that MSA tool makers used the Gouritz river terrace deposits as sources for stone tool materials. However, Brown (2011) pointed out that it is not known if Pinnacle Point MSA tool-makers would have made a 60 km round trip to procure chert in the Gouritz River drainage. He argued that, alternatively, the foragers could wait for raw materials to be transported down the coastline. The swell direction of the Agulhas current in the Mossel Bay region is predominantly from the Southwest (Lavrenov 1998). Brown cited a study from the Oregon coast (Allan, Hart, and Tranquili 2006) that showed that cobbles driven by stronger winter wave action traveled farther than 285 meters in 8 months. If the cobbles

being deposited into the Indian Ocean by the Gouritz River underwent similar high-energy wave transport, Brown hypothesized that a sample of the cobbles would have been available at the different Mossel Bay region cobble beaches to the east of Gouritz River Mouth. Brown pointed to Kanon beach, located some 2 km to the east of the mouth of the Gouritz River, where he found 6 chert nodules of sufficient size to produce cores seen in the PP5-6 assemblage (Brown 2011).

Brown also argued that silcrete cobbles found at Dana Bay could be the result of the same phenomena. However, I would argue based on my survey that the silcrete at Dana Bay most likely is coming from the Blinde River that dissects Vleesbaai and cuts through several Bokkeveld Group silcretes by the modern day N2. Silcrete is then transported down the Blinde River and deposited in the Indian Ocean, and then subsequently wave rolled over to Dana Bay. This could have occurred during glacial periods such as MIS4 also but the silcrete cobbles would have been deposited at a beach now submerged by the ocean.

In addition to the Gouritz drainage, there are several small drainages that dissect Vleesbaai adjacent to the Pinnacle Point sites. Quartzite cobbles suitable for flaking are available in these currently low energy non-perennial streambeds. The cobbles are formed on material that has been eroded out by the dissecting drainages into the Enon and De Hoopvleei conglomerates that occur in drainages and are the likely sources for the cobbles (Oestmo et al. 2014). An additional source of chert unrelated to the Gouritz River appears to be riverbeds and conglomerates by the Hartenbos River located 10 km to the north of Pinnacle Point (Minichillo 2005).

Conglomerates

Another type of secondary context material is conglomerates (**Figure 18**). Brown (2011) pointed out that conglomerates are a possible source for quartzite cobbles when exposed in eroded profiles. They are also a potential source for beach cobbles where sea level transgressions could have churned up the formations. Cobble deposits in a conglomerate are found at several locations across the Mossel Bay region. These local conglomerate occurrences have yet to yield materials from outside the Cape Super Group (Shone 2006) and therefore they are an unlikely source for non-quartzite materials.

Figure 18. An example of a conglomerate. This one is likely to be an exposure of Enon Formation. The exposure is located in one of the drainages dissecting Vleesbaai. Jake Harris appears for scale.

The two conglomerates of interest to this dissertation are the Enon Formation of the Uitenhage Group, approximately contemporary to the Robberg Formation, and the De

Hoopvlei formation of the Bredasdorp Group (Brown 2011, Roberts et al. 2006, Shone 2006). Brown (2011) noted that the Enon Formation is found in thick beds in the Mossel Bay region, and is modeled to have formed in alluvial fans (Shone 2006). It consists primarily of quartzite and slate pebbles and cobbles set in an iron-rich limonite matrix. This matrix has a bright red appearance. Notable occurrences of this conglomerate are in an exposed profile of two drainages that dissect Vleesibaai (12-13 km west of Pinnacle Point), and in the town of Vleesbaai (21.5 km to the southwest along the coastline). I have also observed this conglomerate on the Cape St. Blaize Trail between Mossel Bay Point and Pinnacle Point.

The second conglomerate of interest is the De Hoopvlei formation, which is more localized compared to the Enon formation conglomerate. However, it does occur in the same drainages that dissect Vleesbaai (12-13 km west of Pinnacle Point) and it occurs on the Cape St. Blaize hiking trail midway between Pinnacle Point and Mossel Bay Point (5.5 km to the east) (Brown 2011). Brown (2011) noted that this conglomerate on the hiking trail occurs as well-cemented clasts, and appears to have been utilized as a source for quartzite in past based on the large amount of debitage on the ground.

Summary of raw material distribution

To the MSA toolmakers at the Pinnacle Point sites, low-quality quartzite was easily procured from the local Eden Bay beach. However, high-quality quartzite required either increased search time at the Eden Bay beach, or transport of 5 km to the west from the Dana Bay cobble beach when present, or transport of between 5.5 to 6.8 km to the east from the De Hoopvlei conglomerate or Robberg formation quartzite. Silcrete is rare in the

vicinity of the Pinnacle Point sites and would have required either increased search time at the Dana Bay cobble beach 5 km to the west when it was present or transport of 8.5 km from the closest known primary context silcrete source located at Rietvlei near the N2 to the northwest. The procurement of quartz required either search for abundant veins in the local Skurweberg sandstone, or through increased search at the local Eden Bay beach, or transport of at least 8.5 km from an occurrence of quartz associated with silcretes formed on Bokkeveld shales. Chert was likely available at local beaches but observed cherts are found at riverbeds and cobble beaches that are located 10 km and 27 km away, respectfully. Crystalline quartz in primary context is available at Cape Granite Suite formations 21 km away.

The knowledge of the potential raw material sources across the landscape allows for modeling of raw material procurement by hunter-gatherers. Below, two such models will be outlined: the Opportunistic Acquisition Model (OAM) and the Active-Choice Model (ACM).

CHAPTER 5: MODELS, MODEL CONDITIONS, AND HYPOTHESES

Introduction

The six informal models discussed in *Chapter 3* show that there is no consensus on why and how raw materials were acquired in the MSA. This dissertation will attempt to create some clarity to this debate and will use the Mossel Bay region (**Figure 1**) as the test case for understanding raw material selection in the MSA. To test my research questions I will consider and contrast two mutually exclusive formal models that facilitate testing hypotheses about raw material selection and creating expectations that can be applied to the MSA record in the Mossel Bay region.

Opportunistic Acquisition Model (OAM)

The OAM is a computational neutral model of stone tool raw material procurement (Brantingham 2003) and posits that archaeological raw material frequencies are due to opportunistic encounters with stone sources during random walk in the environment. The core foundation of a neutral model consists of two parts: 1) all same-level components of a system are identical in terms of their elemental behaviors, 2) and the impact that the environment has on the expression of those same elemental behaviors is identical (Bell 2001, Brantingham 2003, Gotelli and Graves 1996). In order to demonstrate that stone tool raw material patterns are due to strategic targeting, patterning must be shown to be different from the result of a neutral model, which discards the assumption that differences between raw material properties necessarily influence procurement decisions, and how stone tools in toolkits are maintained and discarded (Brantingham 2003). Specifically, a neutral model provides a baseline for comparison where archaeologists

can be certain that observed stone tool raw material patterns are not the result of selective choice based on quality and abundance, time and energy optimization associated with procurement of stone from spatially distant sources, planning depth that embed raw material procurement into greater foraging and mobility strategies, and risk minimization that results in quantities and forms of materials that are energetically economical and are least likely to fail (Brantingham 2003).

The OAM is an example of a 'Natural Availability' model variant in the 'Non preference-based change' model category or Binford's (1979) embedded procurement model. In the neutral model as originally presented by Brantingham (2003, see also Janssen and Oestmo 2013), the forager engages in random walk in a landscape with randomly distributed raw material sources. In the OAM, raw material procurement is embedded into the foraging movement; any material that is encountered will be procured if there is room in the toolkit, and raw materials are discarded at a fixed rate (Brantingham 2003).

Model description – ODD (Overview, Design concepts, and Details) protocol

This is a model description following the ODD protocol (Grimm et al. 2010). The ODD protocol is used to present a standardized description of individual-based and agent-based models. Primarily, the ODD aims to make model descriptions more understandable and complete, which can help an agent-based model be less subject to criticism that it cannot be reproduced. The OAM is an application of the neutral model of stone tool raw material procurement by Brantingham (2003) to a real landscape with real stone source locations

and the location of a known archaeological locality. Hereby, raw material refers to stone tool raw materials while sources refer to potential stone tool raw material sources.

Overview

Purpose: Apply Brantingham's neutral model to a real landscape with real locations of potential sources. The sources are represented as their sizes during current conditions, and from marine geophysics surveys, and the agent starts at an archaeological site at Pinnacle Point (PP), South Africa. Depending on whether the movement strategy ("movement-scenario") at the start is set to "return-to-starting-location" or "move-to-closest-locality" the agent either returns to Pinnacle Point, Vleesbaai or Cape St. Blaize Cave when it has exhausted the movement budget (all available ticks to move; a tick is one time step in the model). Once the agent has returned to a locality, it discards raw materials based on a discard probability function, and then it starts another foraging bout.

State variables and scales: The agent is foraging according to a random walk procedure after starting at the Pinnacle Point locality and has a toolkit of a fixed size. Three coastline configurations can be simulated: 1) The Mossel Bay coastline observed in the region today represents MIS5 (interglacial conditions) (**Figure 19**). 2) The average coastline during MIS4 represents moderate glacial conditions (**Figure 20**). 3) The average coastline during MIS 6 represents strong glacial conditions (**Figure 21**). The potential sources are distributed on the landscape according to their actual location and their real scale based on surveys of their locations, while the location and extent of potential sources on the now submerged coastal shelf are based on marine geophysics

surveys. The landscape during interglacial conditions has 74996 patches and 40 sources (**Figure 19**).

Figure 19. OAM interglacial raw material sources. Mossel Bay region during interglacial conditions with sources represented as their close to real size and distributed according to their real locations, and one forager (yellow figure) starting at known archaeological localities (purple houses).

During MIS4, the landscape has 121018 patches and depending on whether the closest potential offshore silcrete source is projected 49 or 50 sources (**Figure 20**). During MIS6 conditions, the landscape has 202186 patches and depending on whether the closest potential offshore silcrete source is projected 55 or 56 sources (**Figure 21**).

Figure 20. OAM MIS4 raw material sources. Mossel Bay region during MIS4 moderate glacial conditions with sources represented as their close to real size and distributed according to their real locations, and one forager (yellow figure) starting at known archaeological localities (purple houses). The map on the left shows material sources without the closest hardground assumed to be a silcrete source on the Paleo-Agulhas plain. The map on the right shows material sources including the closest hardground (red) assumed to be a silcrete source on the Paleo-Agulhas plain. Coastline 15km further out compared to interglacial conditions.

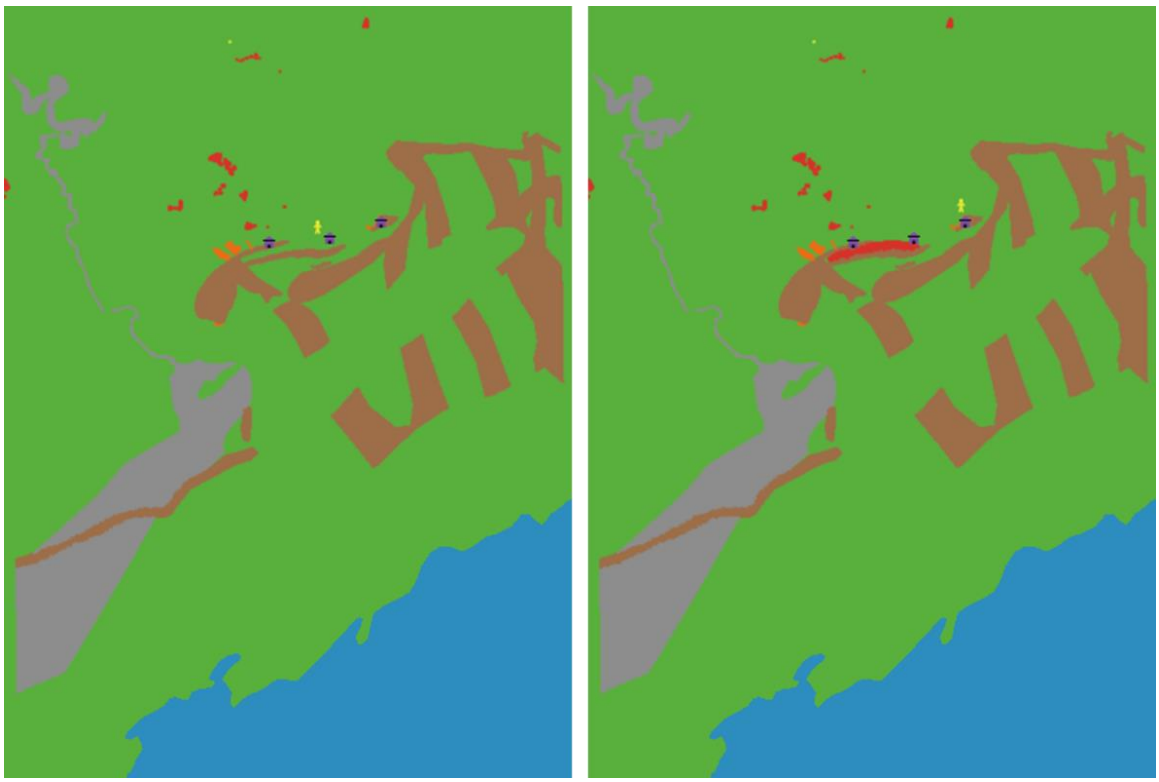

Figure 21. OAM MIS6 raw material sources. Mossel Bay region during MIS6 glacial conditions with sources represented as their close to real size and distributed according to their real locations, and one forager (yellow figure) starting at known archaeological localities (purple houses).The map on the left shows material sources without the closest hardground assumed to be a silcrete source on the Paleo-Agulhas plain. The map on the right shows material sources including the closest hardground (red) assumed to be a silcrete source on the Paleo-Agulhas plain. Coastline 42km further out compared to interglacial conditions.

Process overview and scheduling: **Figure 22** shows the main structure of the scheduling of activities in the model. One agent with a mobile toolkit of fixed capacity is placed at the Pinnacle Point locality on the landscape. Before moving, the agent is given a moving budget ("totticks"), movement strategy ("movement-scenario"), probability of discard on the landscape ("probdiscard"), and probability of discard at an archaeological locality ("probdiscardcamp"). The size of the moving budget indicates how long the agent can stay away from Pinnacle Point. The agent then moves randomly. At each time step, the agent moves to one of the nearest eight neighboring cells or stays in the present cell, with

equal probability (=1/9). Each time step one raw material unit is potentially consumed (discarded) dependent only upon on a probability of a discard function ("probdiscard") and the frequency of the specific raw material in the mobile toolkit. The probability of discard is set as a base parameter to be the same as the probability of discard in Brantingham's original neutral model (see *Chapter 6* for procedure). While moving, the agent will continue to evaluate if it has more ticks in its moving budget. If a source is encountered, the agent checks if the toolkit has room, if it has room the toolkit is re-provisioned up to its maximum capacity before moving again at random. If no source is encountered, the agent moves immediately at random. If the agent has no more ticks in the moving budget ("totticks") the agent move directly back to Pinnacle Point if the movement-scenario is "return-to-starting-locality", while the agent moves to the closest locality that could be Vleesbaai, Cape St. Blaize cave or Pinnacle Point if the movement-scenario is "move-to-closest-locality". If the agent has returned to Pinnacle Point or the other two localities, all raw materials are potentially discarded dependent only upon a probability of discard at the locality function ("probdiscardcamp"). The probability of discard at the campsite is set as a base parameter to be the same as the probability of discard in Brantingham's original neutral model (see *Chapter 6* for procedure). Each raw material unit still present in the toolkit when returning to a site is separately considered in sequence. Thus, the chance of one specific raw material type to end up in the archaeological assemblage depends on the frequency of the specific raw material in the mobile toolkit. Once the agent has discarded raw materials at the locality, the agent will start a new foraging bout with a fresh moving budget and a fresh toolkit.

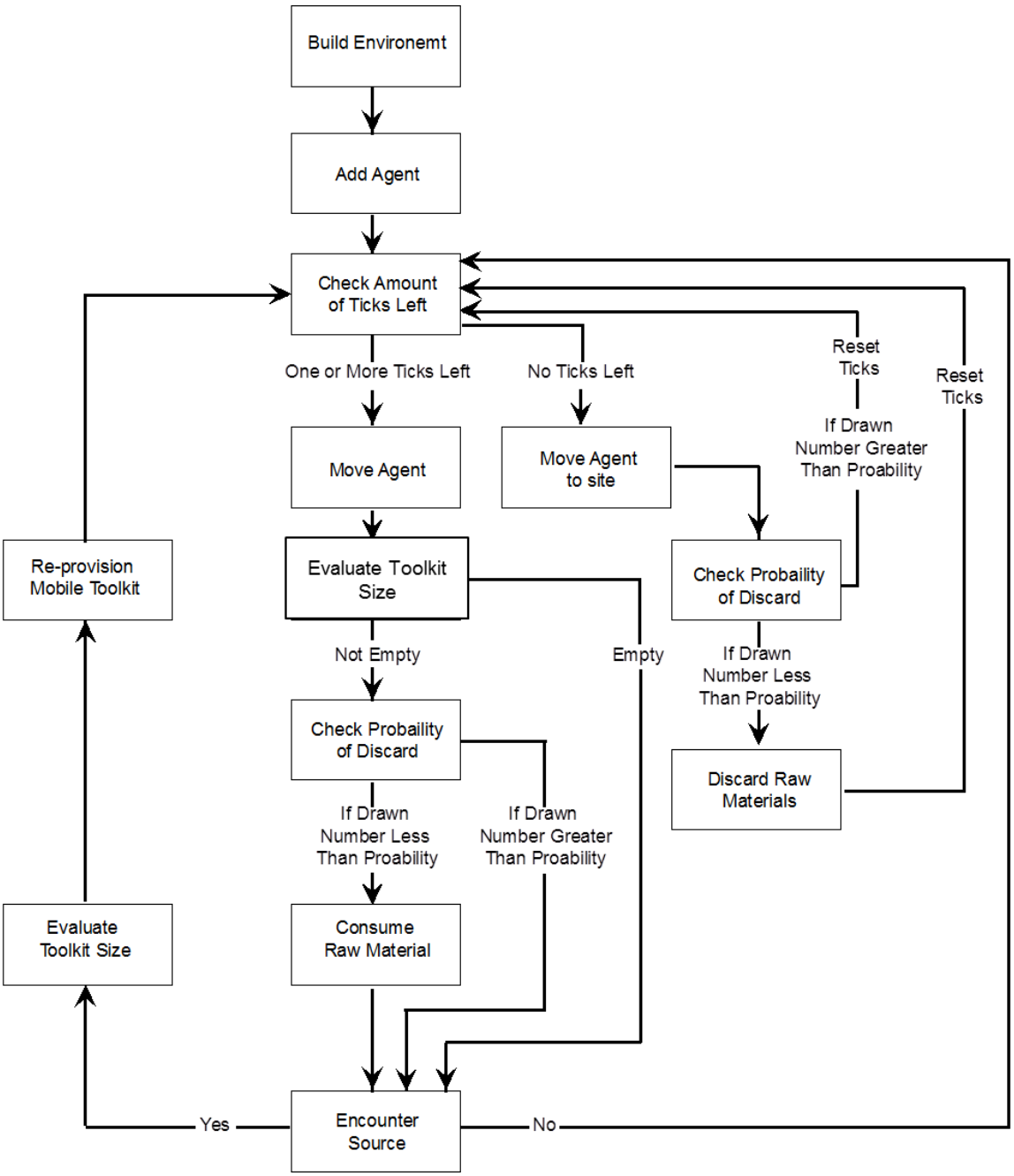

Figure 22. Overview over OAM steps and scheduling. Based on Figure 5 from Brantingham (2003).

Design concepts

<u>Basic principles:</u> Which general concepts, theories, hypotheses, or modeling approaches are underlying the model's design? There is debate whether changes in stone tool raw

material frequencies in an archaeological assemblage can be considered a reliable proxy for human forager adaptive variability (Brantingham 2003, Féblot-Augustins 1993, Kuhn 1995, Mellars 1996). Brantingham (2003) pointed out that a commonly made argument is that raw material richness, transport distances, and the character of transported technologies should signal four behaviors. *First*, it should signal raw material selection variation due to material quality and abundance. Then, *secondly*, it should signal time and energy cost optimization associated with raw material procurement from spatially dispersed sources. *Thirdly*, it should signal planning depth that combines raw material procurement with other forager activities such as food procurement. *Fourth* and finally, it should signal risk minimization resulting in raw material transportation strategies focusing on quantities and forms that are energetically economical and least likely to fail.

To test if raw material richness, transport distance, and the character of transported technologies in an archaeological assemblage is the result of adaptive behavior, Brantingham (2003: 487) presented a behaviorally neutral agent-based model that involves "…a forager engaged in a random walk within a uniform environment." The neutral model relies on the core principle that within a system, all same-level parts or factors are the same both in terms of their internal behaviors, and the impact that the environment has on those behaviors (Brantingham 2003). Brantingham's (2003: 491) model provides a baseline for comparison where archaeologists can test their "observed patterns in raw material richness, transport distance, and both quantity-distance and reduction intensity-distance relationships" against a model that simulates raw material patterns that are not the result of adaptation. Here Brantingham's model is applied to a

real landscape with real source locations. A baseline neutral model result is created that can be compared to an archaeological record.

Emergence: What key results or outputs of the model are modeled as emerging from the adaptive traits, or behaviors, of individuals? Relative frequency of raw materials deposited at site Pinnacle Point ("ppmaterialcamp-list"). Relative frequency of raw materials collected on the landscape ("materialcol-list"). Time steps without raw materials in the toolkit ("timesteps-empty").

Adaptation: What adaptive traits do the individuals have? What rules do they have for making decisions or changing behavior in response to changes in themselves or their environment? The agent will randomly move until the movement-budget ("totticks") is exhausted. When the allotted "totticks" are exhausted the agent moves directly back to Pinnacle Point if the "movement-scenario" is set to "return-to-starting-locality" or whatever locality is the closest if the "movement-scenario" is set to "move-to-closest-locality." The higher the allotted "totticks" budget the longer the agent randomly moves without moving back to any site. The agent picks up raw material if toolkit has room.

Objectives: If adaptive traits explicitly act to increase some measure of the individual's success at meeting some objective, what exactly is that objective and how is it measured? The objective of the agent is to move about the landscape at random and if encountering a raw material source the agent will fill up the toolkit to maximum capacity with that raw material type. The agent moves until movement-budget is used up, which at that point the

agent returns to either the Pinnacle Point locality if the movement scenario is set to "return-to-starting-locality" or whichever locality is the closest if the movement-scenario is set to "move-to-closest-locality." Once at Pinnace Point or at the other localities, the objective is to deposit raw materials. The amount of raw material at a locality will be measured by a relative frequency of raw material deposited at Pinnacle Point ("ppmaterialcamp-list").

Learning: Many individuals or agents (but also organizations and institutions) change their adaptive traits over time as a consequence of their experience? If so, how? The agent does not learn.

Prediction: Prediction is fundamental to successful decision-making; if an agent's adaptive traits or learning procedures are based on estimating future consequences of decisions, how do agents predict the future conditions (either environmental or internal) they will experience? The agent does not predict.

Sensing: What internal and environmental state variables are individuals assumed to sense and consider in their decisions? The agent can sense whether there is a source on the patch it occupies. The agent can sense the amount and distribution of raw materials in its toolbox. The agent can sense that its moving budget ("totticks") is depleted such that it needs to move back towards Pinnacle Point or to the other two localities.

Interaction: *What kinds of interactions among agents are assumed? Are there direct interactions in which individuals encounter and affect others, or are interactions indirect, e.g., via competition for a mediating resource?* There are no interactions between agents.

Stochasticity: *What processes are modeled by assuming they are random or partly random?* Before the agent has exhausted all of its ticks in the moving budget ("totticks"), the agent moves randomly at all times, and decisions on use of raw materials are done randomly. Discard of raw materials on the landscape and discard of raw materials at a locality are controlled by a probability function. At each time-step, the agent will draw a random number between 0-1, depending on the probability of discard ("probdiscard"), if the drawn number is below the probability of discard number the agent will discard one raw material unit. When returning to a locality, the agent will draw a random number, depending on the probability of discard at a locality ("probdiscardcamp"); if the drawn number is below the probability of discard number, the agent will discard a raw material. Every raw material unit present in the toolkit is subjected to the same random draw. For both probability functions, the higher the probability of discard number (0.000-1), the higher the chance of discarding a raw material. When the Movement-scenario is set to "move-to-closest-locality" it introduces randomness to the raw material frequency output at Pinnacle Point because the agent does not always move back there. The chance of the agent returning to Pinnacle Point is based on the chance of being close enough at the end of the movement budget.

Collectives: *Do the individuals form or belong to aggregations that affect, and are affected by, the individuals?* No.

Observation: *What data are collected from the ABM for testing, understanding, and analyzing it, and how and when are they collected?* Three sets of data were collected from each simulation run: 1) Relative frequency of raw materials discarded at site Pinnacle Point. 2) Relative frequency of raw materials collected while moving on the landscape. 3) Time-steps without raw material in agent toolkit. Relative frequency of raw materials is collected by having an agent depositing procured raw materials still present in the toolkit when returning to Pinnacle Point. The raw material units to be discarded depend on the "probdiscardcamp" function. Each remaining raw material unit in the toolkit is subjected to the same random draw of a number. If the random number is less than the "probdiscardcamp" number the raw material unit is discarded. The chance of one specific raw material type to be deposited at the archaeological locality depends on the frequency of that type in the toolkit. When "probdiscardcamp" is increased there is an increased chance of raw materials in toolkit being deposited at Pinnacle Point. Raw materials being collected while moving only depends on the chance of encountering a raw material source on the landscape and if there is room in the toolkit. Time-steps without raw materials are collected by calculating at each time step if the agent has any raw materials in the toolkit.

Details

<u>Initialization:</u> What is the initial state of the model world, i.e., at time t = 0 of a simulation run? **Table 2** provides the variables used in the application of the model.

Table 2: OAM model variables

Variable description	Variable	Units	Model Variables/Range
Simulated world size in *X* dimension	X	grid cells	421
Simulated world size in *Y* dimension	Y	grid cells	571
x-coordinate position of raw material/foragers	x	grid cells	Sources at real locations, foragers at 31
y-coordinate position of raw material/foragers	y	grid cells	Sources at real locations, foragers at 114
Number of agents moving about the landscape	nr-agents	arbitrary units	Minimum =1; Maximum = 10
Toolkit size	toolkit	arbitrary units	Minimum = 1; maximum = 100
Type of movement strategy used to return to locality	Movement-scenario	arbitrary units	return-to-starting-locality; move-to-closest-locality
Starting locality used by agent	Starting-Locality	arbitrary units	PP, VBB, CSB
Landscape	Landscape	arbitrary units	Interglacial, MIS4, MIS6
Source distribution on the landscape	SourceDistribution	arbitrary units	default; PlusClosestSilcrete
Number of unique raw material sources	n	sources	33 (IG), 49 (MIS4), 50 (MIS4PlusClosestSilcrete), 55 (MIS6), 56 (MIS6PlusClosestSilcrete)
Raw material type/source label	rm	materialtype	0, 1, 2…7
Raw material unit from any source	i	arbitrary units	1
Quantity of material from source *i* in mobile toolkit	v_i	arbitrary units	Minimum = 0; maximum = 100
Total material of all types in mobile toolkit	sumv	arbitrary units	Minimum = 0; maximum = 100
Probability of discarding material of source *i* in toolkit	probdiscard	arbitrary units	(0.000, 1.0)
Probability of discarding material of type rm in toolkit, min and max amount	∑materialtype / sumv	arbitrary units	Minimum = 0; maximum = 100
Maximum forager move length at each time step	l	grid cells	1
Distance traveled in *N* time steps; per maximum move length	N	meters	200 meters
An observed number of simulated time steps	totticks	ticks	Minimum = 1; maximum = 2000
Probability of discard material of source *i* in mobile toolkit at locality	probdiscardcamp	arbitrary units	(0.000, 1.0)
Probability of discard material of type rm in mobile toolkit at locality	∑materialtype / sumv	arbitrary units	Minimum = 0, Maximum = 100
Amount of foraging trips undertaken per one model run	maxnrtrips	nrtrips	Minimum = 0, Maximum = 1000

Input data: *Does the model use input from external sources such as data files or other models to represent processes that change over time?* The model uses ascii data files that contain map information such as coastline configuration and source locations. These ascii files are projected in Netlogo using the GIS extension.

Submodels: *What, in detail, are the submodels that represent the processes listed in 'Process overview and scheduling'? What are the model parameters, their dimensions, and reference values? How were submodels designed or chosen, and how were they parameterized and then tested?* The toolkit is simulated as a vector "vi" where each element represents the amount of raw material in the toolkit of unique material types. The maximum size of the toolkit is 100, and the sum of the elements of vi (quantity of material sources of any type in mobile toolkit) has to be smaller or equal to 100 or what the size of the toolkit has been set at when a simulation is started. The amount of material added to the toolbox when a material source is encountered is 100 - ∑i vi (100 raw material units minus the sum of all raw material units already present in toolkit), meaning that the toolbox is filled up to the maximum capacity.

With each time step, one unit of material is potentially consumed (discarded) from the toolbox. The probability that a material unit is consumed depends on the probability of discard function ("probdiscard") while the probability of one specific raw material type to be discarded depends on ∑materialtype / sumv (sum of one specific raw material type in toolkit divided by the sum of all raw material types in toolkit), meaning that it is relative to the frequency of one type compared to all available raw material types in the toolkit. Material sources do not deplete in the environment during the duration of

the simulation. The agent will monitor its moving budget when moving, if the agent has exhausted the moving budget ("totticks") the agent moves either back to the Pinnacle Point locality if the moving-scenario is set to "return-to-starting-locality" or the agent moves to the locality closest to it when done moving if the moving-scenario is set to "move-to-closest-locality." At any locality, the agent discards raw materials from the toolkit depending on the "probdiscardcamp" function. Each remaining raw material unit in the toolkit is subjected to the same random draw of a number. If the random number is less than the "probdiscardcamp" number, the raw material unit is discarded. The chance of one specific raw material type to be deposited at the archaeological locality depends on ∑materialtype / sumv (sum of one specific raw material type in toolkit divided by the sum of all raw material types in toolkit).

Model implementation: The application of the neutral model is implemented in Netlogo 5.2.

Active-Choice Model (ACM)

The Active-Choice Model (ACM) is an analytical resource-choice model, which presumes that given a choice, individuals will choose the most cost-effective means of producing cutting tools in their environment. The ACM posits that a forager when selecting a stone raw material will try to maximize the utility that is gained from the tool per unit time investment in the tool. It considers the time-cost (in minutes) of the following three aspects of raw material selection: (1) travel and search (t_s), (2) procurement (t_p), and (3) manufacturing (m). The utility of the tool is measured in cutting

edge available multiplied by the duration of use, or cm-min (centimeters multiplied by minutes of use before dulling) of tool cutting edge. The ACM is a 'Utilitarian' variant in the 'Preference-based change' model category as present above in *Chapter 2*.

Critical to the ACM are the assumptions that foragers optimize their behavior in most cases, and that foragers are aware of the two choices of stone tool raw material (quartzite or silcrete) facing them at the start of each foraging bout. In addition, there are two other observations that are critical to the development of the ACM. First, silcrete in the Mossel Bay region was heat-treated to make it more flakeable (Brown et al. 2009), and this created more edge and perhaps better edge per unit of source material collected. Second, quartzite has been found to be more durable compared to more fine-grained raw materials (Jones 1979), though it is important to note that silcrete has not been directly tested for durability. This probably means that quartzite edges can be utilized for more minutes of cutting before being discarded. Two variants of the ACM will be considered: ACM-P (sequential encounter and embedded procurement; travel and search time-cost is not included because the forager embedded raw material procurement into normal foraging movement) and ACM-R (simultaneous encounter and direct procurement; travel and time-cost is included in the costs to select a material because the forager makes a special trip to procure a material either from a central location or at a distance from the source). In both model variants, a net utility gain rate can be calculated for both quartzite (q) and silcrete (s).

ACM-P

In the ACM-P, the precise location of raw material does not determine movement because procurement is embedded, and stone sources are encountered sequentially. The forager moves as specified in the OAM but then may extract only one of the two raw material raw materials (quartzite or silcrete) due to its higher net-return rate upon encounter (and partially depending on the encounter rate with both source types). If $P_q > P_s$ (P stands for post-encounter net-return rate) a forager will ignore silcrete (s) when it is found, and continue foraging until quartzite (q) is encountered. If waiting to encounter the highest profitability source will lead the forager to run out of tool material, then the forager is expected to sometimes exploit the lower profitability source as well. This is similar to the sequential encounter and prey-choice model (Charnov and Orians 1973, Stephens and Krebs 1986), where one type of raw material might be ignored if the costs of using it are so high that it would be more efficient to continue searching and only extract the other raw material type when encountered. However, search time is cost-free in this variant because the foragers will be moving in search of food or other resources regardless.

The profitability of acquisition when sequentially encountering each source type (ACM-P) can be expressed as follows:

$P=e*d/(t_p+m)$,

where

P = rate of edge use production per time investment. P can be P_q (quartzite) or P_s (silcrete).

e = cutting edge; cm of usable cutting edge produced from a unit weight of core material.

d = durability; minutes of cutting use before dulling per cm of edge.

t_p = procurement time; time to procure the source material by extracting it from its natural placement per unit of weight of core material.

m = manufacturing time per unit of weight of core material; time to manufacture the desired tool or object (can include time to travel and search for wood fuel for heat-treatment (m_1) per unit weight of core material. time to heat-treat the material prior to flaking (m_2) per unit weight of core material, time to reduce the core to useable edge from a unit weight of core material (m_3), or other manufacturing processes such as time to retouch the material to preferred shape.

(See **Table 3** for further details and operationalization of model variables).

ACM-R

The above equation can also be modified, however, to estimate the overall efficiency of utility gain when targeting a source type from a central place or a campsite. In this variant called ACM-R, the forager has complete information about the location of raw material sources and makes decisions from a central place/campsite or at a distance about which source to visit and exploit (**Figure 23**). This is a simultaneous encounter model (Stephens and Krebs 1986, Waddington and Holden 1979), similar to the habitat choice model of (Smith 1991). The raw material with the highest net-return of a utility currency would be exploited while the other raw material would be ignored. Hence special forays will be conducted to obtain silcrete (s) if $R_s > R_q$ (R stands for net-return rate when all travel and search time is included). The simultaneous encounter model requires the net-return rate of each raw material type to include the travel and search time if the raw material types

are not encountered during normal foraging movement. In other words, the ACM-R simulates a direct procurement strategy where the forager targets a resource and deviates from its normal movement to procure that resource.

In the ACM-R, the time to travel and search (t_s) for the source material per unit weight of core material, and to transport it back to the manufacturing site is added into the equation. Hence: $R=e*d/(t_s+t_p+m)$,

where

R = rate of edge use production per time investment. R can be R_q (quartzite) or R_s (silcrete).

t_s = travel and search time; time to travel and search for material and to transport back to manufacturing site per unit of weight of core material.

(See **Table 3** for further details and operationalization of model variables).

This measure of the efficiency return will determine which raw material type should be exploited when the forager knows beforehand where they are located, and must make a special trip out to obtain the raw material.

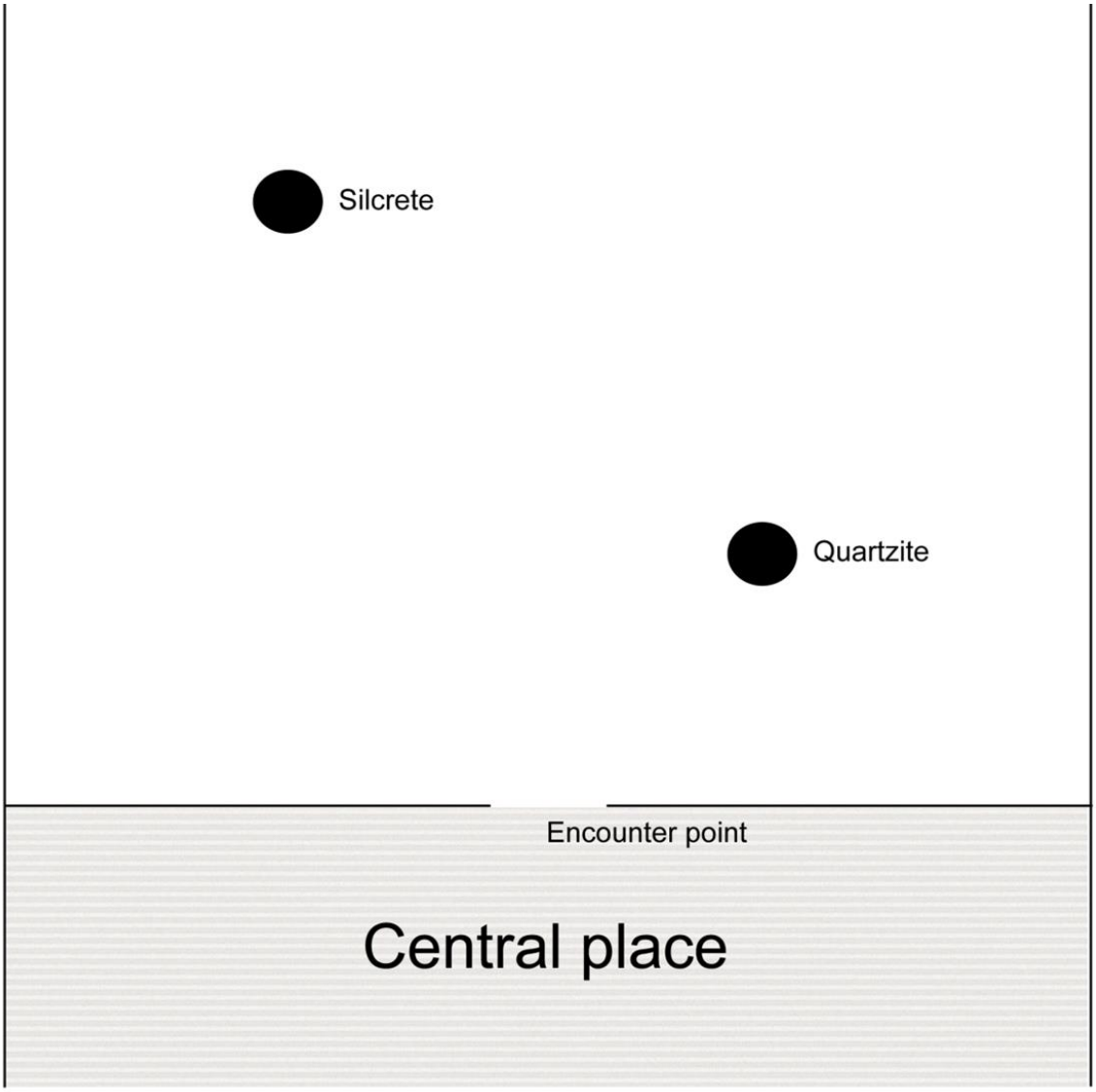

Figure 23. Depiction of simultaneous encounter model. Locations of raw materials are known beforehand and the forager at the encounter point, which in this case is the central place, decides to travel to and extract whichever source provides greatest net return rate of utility. Figure modified from Stephens and Krebs (1986).

Table 3. ACM Model variables.

Model Variable	Definition
P and R	P and R are the currencies the forager wants to maximize. In this model, the currency is cutting edge (*e*)*edge durability (*d*) divided by time cost invested in the tool (T_S + T_P + *m*). The P and R rate for each raw material is calculated by measuring the variables described below for both the two different model conditions (Table 3).
Cutting Edge (*e*)	A cutting edge (e) is any edge of a stone tool that is not broken or snapped, part of the tool platform, or part of the raw material rind (specifically associated with silcrete). Values of e (cm/kg) are quantified by a stone tool analysis conducted on data from the actualistic stone tool reduction study described below.
Durability (*d*)	Values of *d* (min) will be measured as minutes that a tool cutting edge can be used before dulling during cutting activities. Values of d (min) are quantified by a controlled cutting edge abrasion experiment to get values of how long a cutting edge lasts before dulling.
Travel and Search (t_s)	Raw material travel and search (t_s) is here defined as extra travel and search that occurs outside of the time-cost of normal hunting-gathering movement. Values of ts (min/kg) are quantified by using ethnographic data and a GIS analysis.
Procurement (t_p)	Raw material procurement (t_p) is here defined as the act of obtaining suitable raw materials at the source. Values of t_p (min/kg) are quantified by using survey data from raw material sources in the Mossel Bay region.
Manufacture (*m*)	*m* will be measured as three different sub-variables. When heat-treatment is included in the manufacturing process, *m* includes search and procurement time-costs of wood fuel (m_1) and the actual heat-treatment time-cost (m_2). Flaking time-cost (m_3) is the time to reduce the core to useable edge from a unit weight of core material. Values of wood fuel search and procurement time-cost (min/kg) will be quantified using a combined GIS and agent-based modeling analysis. Values of the actual heat-treatment (min/kg)) will be based on published experiments of silcrete heat-treatment (Brown et al. 2009, Schmidt et al. 2015, Schmidt et al. 2013). Values of flake manufacturing time (min/kg) will be quantified by a stone tool analysis conducted on data from the actualistic stone tool reduction study.

Model conditions and variables

This dissertation will examine the way three model variables (coastline position and raw material source distribution, vegetation type, and foraging mobility strategy and rate) from three different model conditions affect predicted raw material use patterns according to each model. Coastline position and raw material source distribution are viewed as one variable because, depending on coastline position, more potential raw material sources are exposed on the now submerged Paleo-Agulhas plain. **Table 4** shows details of all three model conditions, which are marine isotope stages (MIS4, MIS5, and MIS6), while **Figure 24** shows the coastline position for each MIS used in this study.

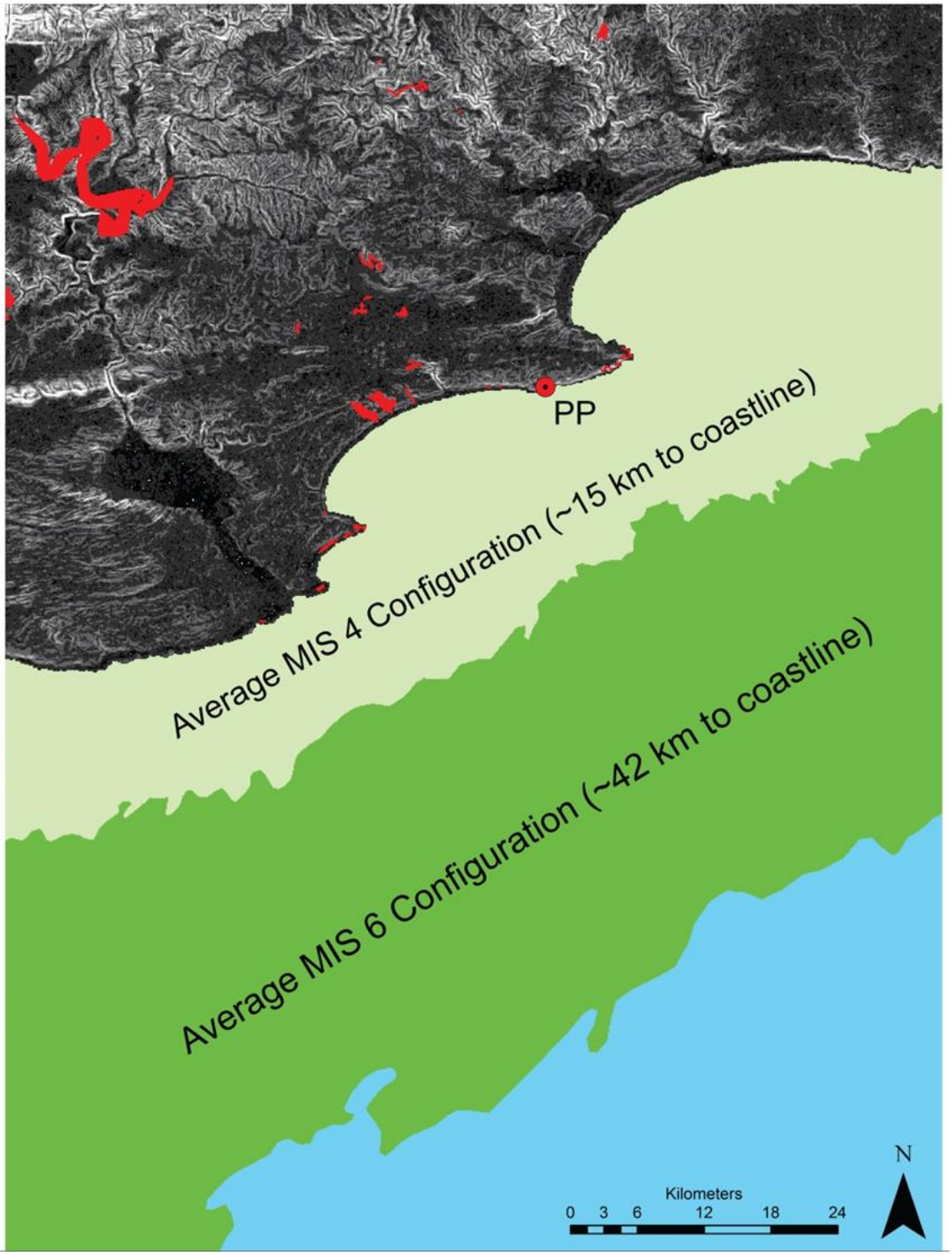

Figure 24. Depiction of coastline configuration used in the three different model conditions.

All three model conditions have different expressions of the same variables that can hypothetically affect the outcome of raw material frequencies in the OAM, and P (post-encounter net-return rates) or R (net-return rate when travel and search cost is included) for both raw materials in the ACM. These three marine isotope stages were chosen because they cover the majority of site occupations at Pinnacle Point between ~165-50 ka, and reflect three different states of site distance to the coastline (**Figure 24**) and raw material source distribution, vegetation types, and hypothetical foraging mobility strategies. In addition, the first major change in raw material selection in the Cape occurs roughly coincident with a shift from warmer conditions (MIS5) with quartzite dominating to glacial conditions (MIS4) with a rise in silcrete (Brown et al. 2012, Brown et al. 2009, Henshilwood 2012, Henshilwood and Dubreuil 2011, Villa et al. 2010, Wurz 2013).

Table 4. Model conditions.

Marine Isotope Stage	Climate and environmental condition	Date range [a]	Avg. average distance to coastline (km) [b]
MIS6	Strong Glacial	186-130 ka	42 km
MIS5	Interglacial	130-74 ka	1 km
MIS4	Moderate Glacial	74-57 ka	15 km

Note. [a] Marine Isotope Stage date ranges from Barham and Mitchell (Barham and Mitchell 2008) and Jouzel et al. (Jouzel et al. 2007). [b] Avg. average distance to coastline (km) calculated from the full age range of a Marine Isotope Stage. Data from Fisher et al. (2010).

To elaborate the model conditions and variables needed for this study I use data from four major sources: Speleothem data (Bar-Matthews et al. 2010, Braun et al. ms), strontium isotope data (Copeland et al. 2015), faunal data (Rector and Reed 2010), and sea-level curve modeling (Fisher et al. 2010). These four types of data are particularly important as they provide estimates of environmental and climatic context during all three model conditions. Specifically, speleothem data (oxygen and carbon isotopes) can

act as a proxy for rainfall regime and accompanying vegetation type during different climatic conditions, which is important when trying to reconstruct whether vegetation types with more tree species are present, which can give an estimate of the availability of wood fuels in the environment. The faunal data can support the speleothem data by highlighting the feeding adaptation of an animal community. In addition, the faunal data in conjunction with a strontium isotopic analysis can highlight migration or movement patterns of animals. Finally, the sea-level curve modeling can provide estimates of distance to coastline during glacial periods. Below I review how estimates of climatic and environmental data have been obtained in the four sources of data.

Bar-Matthews et al. (2010) analyzed multiple overlapping speleothems from Crevice Cave at Pinnacle Point. Crevice Cave is located approximately midway between PP13B and PP5-6, or 150 meters from PP5-6. They used U-Th dating to date the samples from 90 ka to 53 ka from a time-period when Crevice Cave was sealed by a dune. They report 152 growth laminae that they have sampled, providing extremely high-resolution δ18O and δ13C isotopic curves. Braun et al. (ms) extended that composite record from Crevice Cave to cover the time-period between 463 and 41 ka using speleothem samples from Staircase Cave and PP29.

Changes in the δ18O are proposed to be controlled by alternating moisture sources more so than temperature changes (Braun et al. ms). Further, changes in δ18O are also argued to be the result of variation in summer and winter rainfall regime by comparing the δ18O values to modern rainfall samples that were systematically collected from Mossel Bay (Braun et al. ms, Bar-Matthews et al. 2010). Changes in the δ13C are interpreted to be the result of fluctuations in the proportions of C3 shrubby vegetation and

C3 grasses, and the influx of C4 grasses. The C3 shrubby vegetation and C3 grasses are relatively depleted in δ13C, similar to modern Proteoid and Restioid Fynbos communities, while the C4 grasses are relatively enriched in δ13C and may be representing grassier Fynbos or thicket vegetation. The vegetation type is mostly dependent on rainfall amount and season and atmospheric CO_2 concentration (Braun et al. ms).

Bar-Matthews et al. (2010) compared their samples against a Holocene δ13C record from Pinnacle Point and a mixed C3/C4 signal from Cango Cave speleothem (Talma and Vogel 1992). The Crevice Cave δ18O and δ13C curves are correlated, which is interpreted to mean that when δ18O values are low it indicates more winter rainfall correlated with an increase in C3 vegetation, while when δ18O values are high it indicates more summer rainfall that correlates with an increase in C4 grasses, as would be expected.

Braun et al. (ms) using the extended record subdivided the speleothem composite record into two glacial-interglacial cycles to analyze the climate and environmental variability. They found that there was a decoupling between rainfall source, temperatures, and vegetation during glacial and transitional phases manifested by a low correlation between δ18O and δ13C. However, different glacials (MIS4 and MIS6) show distinct patterns due to the Agulhas current and precession. On the other hand, peak interglacial shows a stronger correlation between δ18O and δ13C, meaning that rain sources, vegetation, and temperatures co-varied. Braun and colleagues (ms) found that there is no one-to-one correlation between variables such as temperature, rainfall source and vegetation and glacial or interglacial periods.

Fisher et al. (2010) presented a GIS-based model for the position of the southern African coastline. The model takes into account the topography of the submerged and gently sloping Agulhas Bank and the sea cliffs at Pinnacle Point and the global sea level curve. Fisher and colleague's' approach is a major upgrade from prior 2-dimensional models that calculate the distance to coast using vertical sea height and distance from a single point to the coastline. Their model is dynamic providing estimates of distance to coastline in 1500 kyr increments. The model was tested by using strontium isotopes from Pinnacle Point speleothem, which is used as a proxy for distance to coastline, and shellfish abundance at PP13B and Blombos Cave, which is used to check if the distance to coastline is within the daily foraging range of ethnographically described hunter-gatherer.

Rector and Reed (2010) investigated the faunal remains from MSA assemblages from PP13B and a carnivore assemblage from PP30 in an attempt to reconstruct the environment of MIS6 and MIS5 at a localized geographical scale. They used 53 modern communities that sample a range of African habitats to establish the relationship between mammalian community structure and habitat to facilitate comparison with the fossil assemblages. Fossil assemblages from 25 levels of eight sites on the South African Coast are used to provide examples of Fynbos habitats. Four fossil carnivore dens of Pleistocene age are used to provide a comparison to the PP30 assemblage. To compare the PP assemblages to the other fossil assemblages and the modern communities, they used two different approaches to reconstruct habitat. In the univariate analysis, they compared the number of species in each substrate and the trophic category at each site by habitats in a one-way ANOVA. They tested the null hypothesis that different habitats

have the same number of species in each adaptation category. In the multivariate analyses, they compared the proportions of the adaptations found in mammalian communities from fossil sites to data from extant habitats using a correspondence analysis. Plotting the Pinnacle Point fossil sites using the variation from modern habitats allowed the identification of the most similar analog based on the proximity in the plot (Rector and Reed 2010).

Copeland and colleagues (2015) investigated ungulate movement patterns using strontium isotopes from enamel sampled from fossil fauna from PP13B and PP30. They presented a bioavailable $^{87}Sr/^{86}Sr$ isoscape for the Mossel Bay region that includes 171 sampling sites. Their analysis showed that Pleistocene ungulates from Pinnacle Point preferred the Paleo-Agulhas plain habitats to the habitats north of the current modern coastline. The ungulates avoided dissected plain, foothill, and mountain habitats more than 15km north of the modern coastline. This further suggested that the Pinnacle Point ungulates did not migrate from the coast to the interior (south to north). However, the strontium isotopic evidence is not able to falsify the hypothesis that large grazers migrated east-west on the Paleo-Agulhas Plain (Copeland et al. 2015).

MIS4 conditions

Coastline position and raw material source distribution variable

Based on the sea level curve modeling by Fisher et al. (2010), the coastline during MIS4 is close to the Pinnacle Point sites, and within or near the daily foraging radius of hunter-gatherers. Estimates from Fisher et al. (2010) put the average coastline configuration during MIS4 15 km away from the Pinnacle Point sites. Two raw material distribution

scenarios will be considered here based on marine geophysics work. In the first one, while wave-ravinement surfaces containing quartzite are present it is assumed that no silcrete sources are present on the low relief Paleo-Agulhas Plain (Cawthra et al. 2015). In this scenario, the closest primary context quartzite is 5.3 km from Pinnacle Point, while the closest primary context silcrete is 8.5 km away at Rietvlei. In the second scenario, in addition to the wave-ravinement surfaces, it is assumed that silcrete outcrops become available on the low-relief Paleo-Agulhas Plain (Cawthra et al. 2015). In this scenario, the closest primary context quartzite is 5.3 km from Pinnacle Point, while the closest primary context silcrete is 0.8 km away. For both scenarios, however, following Brown (2011) is is assumed here that cobble beaches that formed during interglacial periods such as MIS5 are depleted in high-quality raw materials by normal foraging activity and/or buried due to the lack of dynamic ocean swells, tidal forces, and storm surges acting on the stationary and inactive cobble beaches.

Vegetation type variable

During MIS4, the proportions of summer rain increases in the Mossel Bay region due to high precession parameters that included increased summer insolation on the southern hemisphere, which leads to a strong continental summer heat low (thermal low) that periodically connected with northward shifted westerlies to form tropical-temperate troughs that bring tropical rain (Braun et al. ms), which is accompanied by a vegetation type that includes C4 grasses and more trees such as acacias (Bar-Matthews et al. 2010).

Forager mobility rate and strategy variable

During MIS4 when the submerged coastal platform is uncovered due to lower sea levels (Fisher et al. 2010) and a summer rainfall regime dominates (Bar-Matthews et al. 2010), which brings C4 grasses with it, it is here assumed following Marean (2010b) and Copeland et al. (2015) that there is an increase in migratory animals feeding on the C4 grasslands. During MIS4, the forager groups living at Pinnacle Point have access to predictable marine resources because the coastline is within or near to the daily foraging radius. In addition, the coastal band is wider than during MIS5 potentially allowing for bigger populations of animals (Marean 2016). The combination of access to a larger population of migratory animals and access to predictable coastal resources increases the attractiveness of the Mossel Bay region. The hypothetical resulting mobility rate and strategy involved a decreased number of residential moves, making the groups more sedentary. Increased conservation of raw materials during MIS4 at PP5-6 potentially suggests limited access to raw material sources due to fewer moves that could intercept them (Brown 2011). Additionally, sedimentological work by Karkanas et al. (2014) suggests site occupation that is more intensive during MIS4 at PP5-6.

MIS5 conditions

Coastline position and raw material source distribution variable

Based on the sea level curve modeling by Fisher et al. (2010) the coastline is close to or at the present position, and easily within the daily foraging radius of hunter-gatherers (Fisher et al. 2010). Estimates from Fisher and colleagues put the coastline during MIS5 on average 1 km away from the Pinnacle Point sites. For ease of modeling, I will use the

current coastline configuration. Cobble beaches occur directly adjacent to the Pinnacle Point sites, and at Dana Bay, Mossel Bay Point, Fransmanhoek, and Kanon Beach. The dynamic forces of ocean swells, tidal forces, and storm surges help produce and replenish hi-energy cobble beaches present in close vicinity to Pinnacle Point. Closest primary context quartzite is 5.3 km from Pinnacle Point, while the closest primary context silcrete is 8.5 km away. Quartz is available in close vicinity (100-200 meters) to the Pinnacle Point locality as veins in the local Skurweberg Fm.

Vegetation type variable

During MIS5e with warm temperatures, the prevailing rainfall regime on the south coast is summer rainfall (Braun et al., ms). Post MIS5e, during the rest of MIS5 the temperature decreased and the prevailing rainfall regime changed to winter rainfall (Bar-Matthews et al. 2010, Braun et al. ms). The winter rainfall regime is accompanied by a C3 photosynthesis dominant vegetation type called Fynbos (Rebelo et al. 2006). The C3 dominant Fynbos is depleted in trees (O'Brien 1993, Van Wyk and Van Wyk 1997). The C3 signal is also supported by the faunal assemblage from PP13B and PP30 (Rector and Reed 2010).

Forager mobility rate and strategy variable

During MIS5, a forager group at Pinnacle Point would hypothetically conduct more residential moves than during moderate glacial periods due to a combination of restricted migratory animal availability and a higher abundance of predictable marine resources available within the daily foraging radius. A narrower width of the Agulhas plain

hypothetically restricts the abundance of migratory animals during interglacial periods (Marean 2016). Sedimentological work suggests less intensive occupation of PP5-6 during MIS5 compared to MIS4 (Karkanas et al. 2014). The hypothetical resulting mobility rate and strategy utilized more frequent moves between inland and coastal areas to intercept coastal resources during low spring tides.

MIS6 conditions

Coastline position and raw material source distribution variable

During MIS6 the coastline is far away from the Pinnacle Point sites, only reachable after multiple days of travel. Estimates from Fisher et al. (2010) put the coastline during MIS6 on average 42 km away from the Pinnacle Point sites. Similar to MIS4 conditions, two raw material distribution scenarios will be considered here based on marine geophysics work. In the first one, while wave-ravinement surfaces containing quartzite are present it is assumed that no silcrete sources are present on the low relief Paleo-Agulhas plain (Cawthra et al. 2015). In this scenario, the closest primary context quartzite is 1.4 km from Pinnacle Point, while the closest primary context silcrete is 8.5 km away at Rietvlei. In the second scenario, in addition to the wave-ravinement surface, it is assumed that silcrete outcrops become available on the low relief Paleo-Agulhas plain (Cawthra et al. 2015). In this scenario, the closest primary context quartzite is 1.4 km from Pinnacle Point, while the closest primary context silcrete is 0.8 km away. However, as with MIS4 conditions, following Brown (2011), it is assumed that any previous interglacial cobble beaches are depleted in high-quality raw materials and/or buried.

Vegetation type variable

The speleothem record suggests that the vegetation was stable C3 throughout MIS6. There was decoupling between rainfall source and vegetation manifested by low correlation between δ18Oc and δ13C. There was a gradual increase of Indian Ocean rainfall and likely only affected the coastal regions during winter, which was most likely related to changing dynamics of the Agulhas current. The faunal assemblage from PP13B and PP30 suggest that there was a mosaic habitat that consisted of both C3 and C4 vegetation (Rector and Reed 2010). The PP30 assemblage shows that large mammals such as alcelaphines and springbok dominate the large faunal assemblage suggesting open grassy habitats. This habitat type was most likely present on the exposed Paleo-Agulhas plain at lower sea levels (Copeland et al 2015). However, the presence of grysbok and Southern reedbuck indicate a cape floral region ecosystem is present too in addition to floodplains. This habitat was most likely always present in the interior regardless of the presence of an exposed Paleo-Agulhas plain (Marean et al. 2014).

Forager mobility rate and strategy variable

During MIS6 when the submerged coastal platform is uncovered due to lower sea levels (Fisher et al. 2010) and although C3 grasses dominates (Braun et al. ms), it is here assumed following Marean (2010b) and Copeland et al. (2015) that there is an increase in migratory animals feeding on the Paleo-Agulhas plain. During MIS6, the groups living at Pinnacle Point loose access to predictable coastal resources within the daily foraging radius. The coastal plain is wider compared to MIS4 resulting in the increase of the population of migratory animals. The increased width of the coastal shelf makes the

migratory animals a dense but unpredictable resource. The combination of less access to migratory animals and no daily access to predictable coastal resources hypothetically increased the frequency of residential moves to find resources.

Research hypotheses

Hypothesis 1 (H_1)

H_1 will be drawn from the OAM and states that opportunistic encounters during random walk in the environment result in a raw material usage frequency similar to the archaeological record. *Prediction:* I predict that opportunistic encounters during random walk in the environment will create a raw material pattern similar to the archaeological record. This is because it can be assumed either that random walk in the environment can be an optimal way to move or that there is no difference in utility currency profitability between the lithic raw materials. *Archaeological implications:* If *H_1* is supported, it minimally suggests that the observed raw material usage frequency reflects availability and abundance of raw materials in the environment (c.f. Brown 2011, Volman 1981). Further, it suggests that raw material procurement was embedded (e.g. Binford, 1979; Binford and Stone, 1985) in the overall forager movement and that raw material was opportunistically procured at any chance. This might imply expedient procurement, use, and discard of raw materials, suggesting that stone raw materials did not play a significant role in the technological organization and were insignificant. Support for *H_1* might indicate that the response to climatic and environmental change was a mobility strategy that involved targeting food resources that disregarded stone raw material

differences to obtain such resources; investment in stone tool technology was not a priority or needed.

Hypothesis 2 (H_2)

Drawn from the Active-Choice Model (ACM), I propose to test two alternative hypotheses. The *alternative hypothesis (H_2)* drawn from the ACM-P variant states that the archaeological stone raw material usage frequency is due to the selection of the raw material with the highest post encounter net-return of cm-min tool cutting edge (P) unless waiting to encounter the high profitability stone source will lead the forager to run out of tool material. *Prediction:* the raw material with the highest post encounter P rate will be selected. The switch from one raw material to another depends on which material has the highest P rate. *Archaeological implications:* if H_2 is supported it minimally suggests that during embedded procurement foragers strategically selected the raw material with the highest post-encounter net-return rate of cm*min cutting edge available in the environment. This supports a 'Utilitarian' model of raw material selection and change (c.f. Mackay 2008). Further, it suggests that other lifestyle constraints controlled the mobility strategy and foraging movement but that stone raw materials played a role in the technological organization of the foragers because stone raw materials were strategically chosen when encountered. Support for H_2 suggests that the act of encountering raw materials was embedded within the greater mobility strategy (c.f. Binford, 1979; Binford and Stone, 1985). Thus, support for H_2 suggests that the response to a given climatic and environmental context was relatively complex. There was a need for a mobility system that targeted food resources (disregarding the location of lithic raw material sources) that

relied on investment in a specific stone raw material and technology that could be used to extract such resources.

An implication of seeking raw materials with the highest net-return rate (highest rank) is that if raw materials show up in the archaeological record that under the given environmental context does not have the highest net-return rate (lower rank) selecting these raw materials did not minimize opportunity-cost for the forager. If lower ranked materials show up in the archaeological record it might suggest that foragers made specific trips (c.f. Gould, 1985; Gould and Saggers, 1985) or utilized embedded procurement to obtain these raw materials for other reasons such as symbolic needs (Clendon, 1999; Gould et al., 1971; Wurz, 1999), or stylistics needs (Close, 2002; Mackay, 2011; Sackett, 1982, 1986).

Hypothesis 3 (H_3)

The other *alternative hypothesis (H_3),* which is drawn from the ACM-R model variant, states that the archaeological stone raw material usage frequency is due to the selection of the raw material with the highest net-return of cm-min tool cutting edge (R) when all travel and procurement time-costs are considered. *Prediction:* the raw material with highest R rate will be selected. The switch from one raw material to another depends on which material has the highest R rate given the current environmental conditions. *Archaeological implications:* if H_3 is supported it minimally suggests that the foragers are strategically selecting the raw material with the highest net-return of cm*min cutting edge that is available in the environment when all travel and search costs are included. This supports a 'Utilitarian' model of raw material selection and change (c.f. Mackay

2008). Further, this suggests that stone tool raw materials played an important part in the technological organization because the raw material was travel and searched for at added cost (c.f. Gould, 1985; Gould and Saggers, 1985). Traveling and searching for a raw material suggests planning of the stone procurement activities because travel and search time needs to be included in the greater foraging mobility strategy. Hence, support for H_3 suggests that the response to climatic and environmental conditions was to use specific stone raw materials obtained during direct procurement and to manufacture technology to obtain food resources and/or performing processing tasks, which suggests increased knowledge about raw material characteristics and how to use them.

As with H_2, an implication of seeking raw materials with the highest net-return rate is that if raw materials show up in the archaeological record that under the given environmental context does not have the highest net-return rate selecting these raw materials did not minimize opportunity-cost for the forager. This can suggest raw material selection, through either direct or embedded procurement, for other reasons such symbolic (Clendon, 1999; Gould et al., 1971; Wurz, 1999) or stylistic needs (Close, 2002; Mackay, 2011; Sackett, 1982, 1986).

Alternative hypotheses

Alternatively, finding no support for any of the above stated hypotheses will strengthen informal models that has proposed that the observed variation in raw material frequencies is due to factors such as shifts in the geographical range of foragers (Clark 1980) and/or trade and exchange (Deacon 1989), which both are examples of the 'Social learning/Culture' variant in the 'Preference-based change' model category. Further

testing of these informal models cannot be done in this study but requires separate studies such as identifying how far raw materials have traveled. Other researchers are working on this problem (e.g. Nash, Coulson, Staurset, Smith, et al. 2013).

Model condition variables – Testing framework for model outcomes

The hypothesis drawn from the Opportunistic Acquisition Model (OAM) is only evaluated under coastline position and raw material source distribution variable. Model outcomes are directly compared to archaeological frequencies to evaluate whether the state of the coastline position and raw material source distribution during an MIS explains the archaeological raw material frequencies. The initial test is conducted using simulations of same-day returns (one daily foraging radius) of the agent to the Pinnacle Point locality. Then the outcomes of four rounds of a one-factor-at-a-time (OFAT) post-hoc sensitivity analysis are compared to the archaeological frequency data to evaluate the robustness of the same-day return results.

To evaluate the two hypotheses drawn from the Active-Choice Model (ACM) the net-return rates from both the ACM-P and ACM-R will be presented. The net-return rates of the raw materials are then used to rank the materials and the ranking is compared to the archaeological raw material frequencies. Comparisons between the rankings based net-return rates under the different model conditions (Marine Isotope Stages) and archaeological frequency data from the same MIS at Pinnacle Point are used to test Hypothesis 2 (derived from ACM-P) and 3 (derived from ACM-R)

To identify the conditions that would shift the optimal decision from one raw material type to another under different MIS conditions I compare the model outcomes to

archaeological frequencies under two derived environmental effects (coastline position and raw material source distribution, and vegetation type) and one derived behavioral effect (mobility rate and strategy).

The following steps were taken to test predicted relationships between time-costs and model conditions variables (outlined below) under the different model conditions that can explain changes in archaeological raw material frequencies at Pinnacle Point. First, net-return rates from the different model condition variables are presented, which allows for a ranking that can be used to compare to archaeological frequencies. Then, the comparison to the archaeological frequencies allows for testing of the predictions outlined for each model condition variable. If the raw material with the highest ranking under a model condition variable is the same as the raw material with the highest frequency in the archaeological record, the predicted relationship between time-cost and model condition variable is supported.

The coastline position and raw material source distribution predictions are based on distance to closest known source and raw material abundance on the landscape during the different model conditions. The predictions linked to vegetation type come from assumed change in vegetation type based on speleothem and faunal data, published literature on wood fuel travel and search cost and cost of heat-treatment. Mobility rate and strategy predictions come from archaeological observations and experimental data on raw material conservation and tool manufacture. How all the variables used to calculate the net-return rates were obtained is presented below in *Chapter 6*. It is important to note that the coastline position and raw material source distribution variable and vegetation type variable are not direct environmental variables; rather they are inferred from sea-

level modeling, modern raw material source locations and extents, and climate proxy data respectfully. The mobility rate and strategy variable is even more inferred because it is based on changes in the two derived environmental variables.

For both models (OAM and ACM), two different scenarios in regards to a Paleo-Agulhas plain silcrete source are assessed for the coastline position and raw material distribution variable for both models. This allows for testing the effect that a constraint assumption has on the raw material frequencies. In one scenario, it is assumed that there is no silcrete source on the Paleo-Agulhas Plain during MIS4 and MIS6, while in the other scenario it is assumed that the closest identified hardground to Pinnacle Point is a silcrete source available during MIS4 and MIS6.

ACM – Predicted relationships between time-costs and model condition variables

Coastline position and raw material source distribution

MIS4 – Without Paleo-Agulhas plain silcrete: The travel and search time-cost (t_s) to acquire quartzite is increased because of the depletion and/or disappearance of local quartzite cobble beaches leaving the closest quartzite source 5.3km away (**Figure 25**).

Expected net-return rate result: The increase in quartzite t_s time-cost is great enough to decrease the net-return rate for quartzite (Rq) to fall below the net-return rate for silcrete (Rs).

MIS4 – With Paleo-Agulhas plain silcrete: The travel and search time-cost (t_s) to acquire quartzite is increased, while the t_s time-cost to acquire silcrete is decreased because of the depletion and/or disappearance of local quartzite cobble beaches and the addition of the

close Paleo-Agulhas silcrete source only ~800 meters away (**Figure 26**). *Expected net-return rate result:* The combination of an increase in quartzite t_s time-cost and decrease in silcrete t_s time-cost is great enough to decrease the net-return rate for quartzite (Rq) to fall below the net-return rate for silcrete (Rs).

MIS5: The travel and search time-cost (t_s) to acquire quartzite is low relative to the t_s time-cost to acquire silcrete because of the availability of local quartzite cobble beaches (closest is ~400 meters away) and an 8.5km distant silcrete source (**Figure 25 and 26**). *Expected net-return rate result:* The difference between the low quartzite t_s time-cost and high silcrete t_s time-cost is great enough to decrease the net-return rate for silcrete (Rs) to fall below the net-return rate for quartzite (Rq).

MIS6 – Without Paleo-Agulhas plain silcrete: The travel and search time-cost (t_s) to acquire quartzite is only increased slightly compared to MIS5 conditions because, even though close cobble beaches were depleted and/or disappeared, there was an addition of available wave-ravinement surfaces on the Paleo-Agulhas plain only 1.5 km from PP (**Figure 25**). *Expected net-return rate result:* The slight increase in quartzite t_s time-cost is not great enough to decrease the net-return rate for quartzite (Rq) to fall below the net-return rate for silcrete (Rs).

MIS6 – With Paleo-Agulhas plain silcrete: The travel and search time-cost (t_s) to acquire quartzite increases slightly compared to MIS5, while the t_s time-cost to acquire silcrete decreases because of the depletion and/or disappearance of local quartzite cobble beaches

leaving the closest quartzite source 5.3km away and the addition of the close Paleo-Agulhas silcrete source only ~800 meters away (**Figure 26**). *Expected net-return rate result:* The combination of a slight increase in quartzite t_s time-cost and decrease in silcrete t_s time-cost is great enough to decrease the net-return rate for quartzite (Rq) to fall below the net-return rate for silcrete (Rs).

- *Archaeological implications if any of the predicted relationships are supported:* Raw material travel and search (t_s) time-cost determine selection. It lends support to Torrence's (1989, 1983) assertion that the cost of procurement drives the raw material selection if the qualtiy of the raw material being selected is good enough.

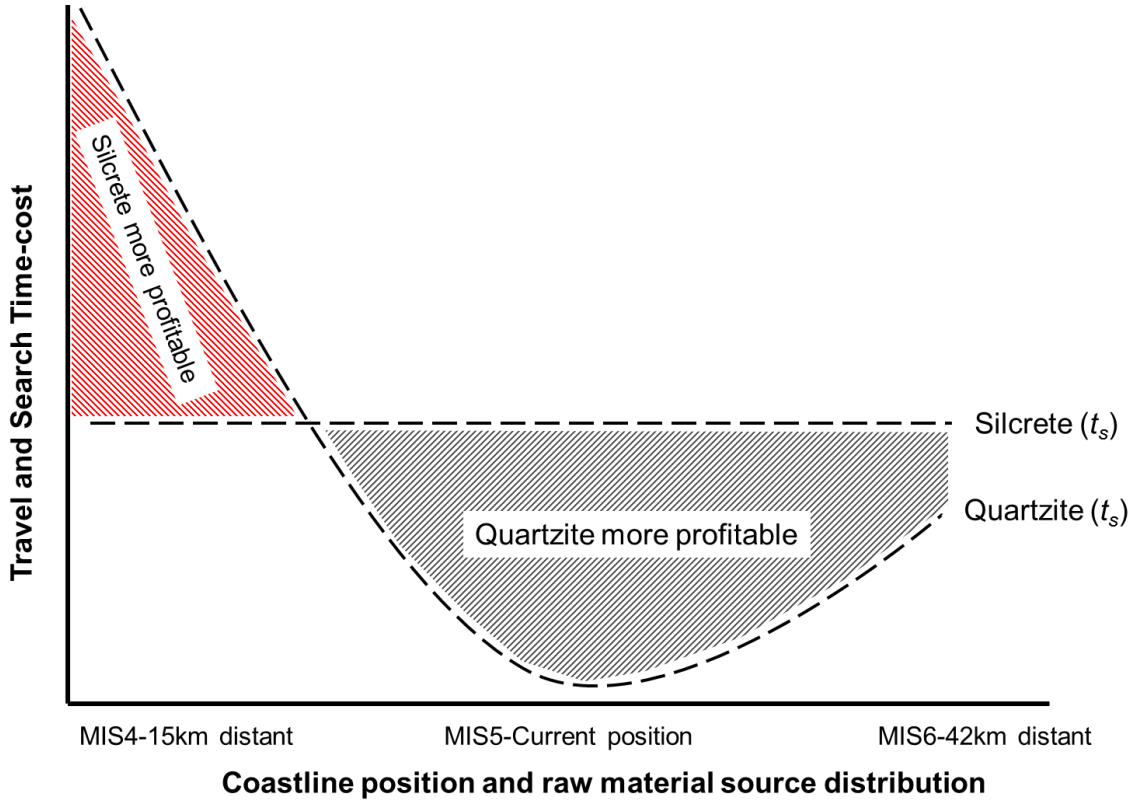

Figure 25. Predicted relationship between travel and search time-cost (t_s) to acquire quartzite and silcrete and model condition variable when no Paleo-Agulhas plain silcrete source is assumed to be present.

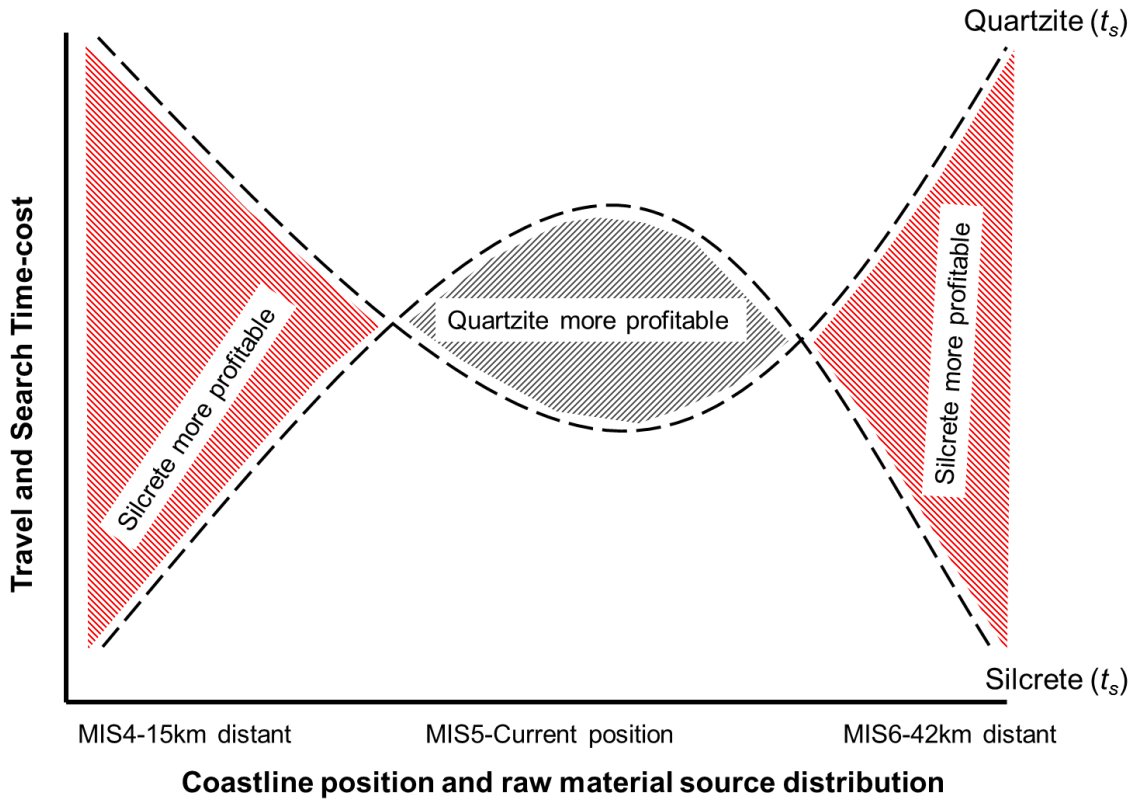

Figure 26. Predicted relationship between travel and search time-cost (t_s) to acquire quartzite and silcrete and model condition variable when the presence of a Paleo-Agulhas plain silcrete source is assumed.

Vegetation type

Two different heat-treatment methods are considered when evaluating the effect of this variable: the sand-bath method (Brown et al. 2009) hereby referred to as the insulated method, and the ember method (Schmidt et al. 2013) hereby referred to as the exposed method. In addition, a scenario where silcrete is not heat-treated is also considered. This scenario will allow for testing if the omission of heat-treatment affects the net-return of silcrete. In the insulated method, it is here assumed that wood-fuel travel and search time-cost (m_1) is not embedded in the time-cost of normal foraging movement, while time-cost of the actual heat-treatment (m_2) is embedded in the time-cost of normal forager camp activities. In the exposed method, it is assumed that m_1 time-cost is embedded in the

normal time-cost of foraging movement, while the m_2 time-cost is additional to the time-cost of normal forager camp activities.

MIS4: under the insulated method scenario, the availability of more trees in the C4 component of the vegetation type decreases the manufacturing time-cost (*m*) for silcrete because m_1 time-cost is decreased and the m_2 time-cost is not additional to time-cost of normal forager camp activities (**Figure 27**). *Expected net-return rate result:* The decrease in *m* time-cost is not great enough to decrease the net-return for silcrete (Ps) to fall below the net-return rate for quartzite (Pq).

Under the exposed method scenario, the vegetation type has no effect on the manufacturing time-cost (*m*) because the m_1 time-cost is embedded into the normal foraging movement. While the m_2 time-cost is additional to time-cost of normal forager camp activities regardless of environmental conditions **(Figure 27**). *Expected net-return rate result:* Combined, the *m* time-cost is not great enough to decrease the net-return for silcrete (Ps) to fall below the net-return rate for quartzite (Pq).

MIS5: Under the insulated method scenario, the dominance of C3 vegetation depleted in trees increases the manufacturing time-cost (*m*) for silcrete because m_1 time-cost is increased while the m_2 time-cost is not additional to time-cost of normal forager camp activities (**Figure 27**). *Expected net-return rate result:* The increase in *m* time-cost is great enough to decrease the net-return for silcrete (Ps) to fall below the net-return rate for quartzite (Pq).

Under the exposed method scenario, the change in vegetation type has no effect on the manufacturing time-cost (*m*) because the m_1 time-cost is embedded into the normal foraging movement. While the m_2 time-cost is additional to time-cost of normal forager camp activities regardless of environmental conditions **(Figure 27**). *Expected net-return rate result:* Combined, the *m* time-cost is not great enough to decrease the net-return for silcrete (Ps) to fall below the net-return rate for quartzite (Pq).

MIS6: under the insulated method scenario, the dominance of C3 vegetation type depleted in trees increases the manufacturing time-cost (*m*) for silcrete because m_1 time-cost is increased, while the m_2 time-cost is not additional to time-cost of normal forager camp activities (**Figure 27**). *Expected net-return rate result:* The increase in m time-cost is great enough to decrease the net-return for silcrete (Ps) to fall below the net-return rate for quartzite (Pq).

Under the exposed method scenario, the change in vegetation type has no effect on the manufacturing time-cost (*m*) because the m_1 time-cost is embedded into the normal foraging movement. While the m_2 time-cost is additional to time-cost of normal forager camp activities regardless of environmental conditions **(Figure 27**). *Expected net-return rate result:* Combined, the *m* time-cost is not great enough to decrease the net-return for silcrete (Ps) to fall below the net-return rate for quartzite (Pq).

- *Archaeological implications if any predicted relationships are supported:* Time-cost of heat-treatment as part of the manufacturing (*m*) variable determines selection. In addition, it supports the informal "wood fuel availability" model that proposes that the increase or decrease of heat-treated silcrete is constrained by the

abundance of wood fuels, which fluctuates with the dominating rainfall regime and resulting vegetation types, thereby changing the cost of the manufacture of silcrete (Brown and Marean 2010).

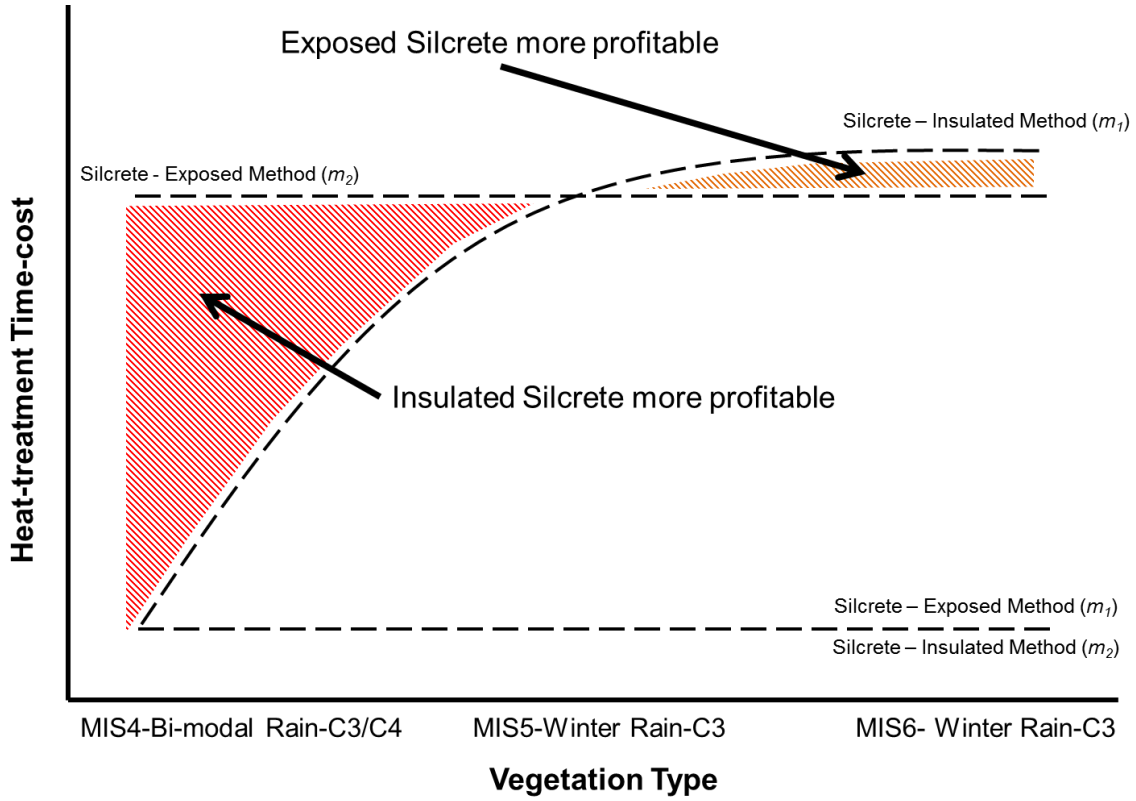

Figure 27. Predicted relationship between heat-treatment time-cost (m_1 and m_2) to acquire wood fuel for heat-treatment (m_1) and heat-treating (m_2) and model condition variable.

Mobility rate and strategy

MIS4: The hypothetical residential mobility system with less frequent moves and more sedentary behavior due to the assumed attractiveness of PP during MIS4 puts a premium on having raw materials that can be optimized in terms of cutting edge per mass in case of shortfall in finding new raw materials due to infrequent moves or due to length of stays at PP. This hypothetical mobility rate and strategy increases the manufacturing time-cost (*m*) for quartzite because flaking outcomes for coarse-grained quartzite are assumed less

predictable (Mackay 2008) yielding a lower *e* value and a higher value of flake manufacturing time-cost (m_3) relative to silcrete (**Figure 28**). *Expected net-return rate result:* The higher *m* time-cost and lower measured *e* value of quartzite is great enough to decrease the net-return rate for quartzite (P or Rq) to fall below the net-return rate for silcrete (P or Rs).

MIS5: The hypothetical residential mobility system with frequent moves during MIS5 does not put a premium on having a raw material that can be optimized in terms of cutting edge per mass due to the chance of encountering new raw material sources such as cobble beaches when moving to intercept the coastline. This mobility rate and strategy make the manufacturing time-cost (*m*) for quartzite irrelevant even though flaking outcomes for coarse-grained quartzite are assumed less predictable (Mackay 2008) yielding a lower *e* value and a higher value of flake manufacturing time-cost (m_3) relative to silcrete (**Figure 28**).

MIS6: The hypothetical residential mobility system with frequent moves and shorter duration stays at PP during MIS6 because of the extensive Paleo-Agulhas plain, which leads to ungulates on the plain being a dense but unpredictable resource does not put a premium on having a raw material that can be optimized in terms of cutting edge per mass due to the chance of encountering new raw material sources when moving about the landscape. This mobility rate and strategy make the manufacturing time-cost (*m*) for quartzite irrelevant even though flaking outcomes for coarse-grained quartzite are

assumed less predictable (Mackay 2008) yielding a lower *e* value and a higher value of flake manufacturing time-cost (m_3) relative to silcrete (**Figure 28**).

- *Archaeological implications if the predicted relationship is supported:* The amount of raw material cutting edge per mass (*e*) and manufacturing time-cost (*m*) determine selection. Further, it supports similar assertions by Gould and Saggers (1985, 1985) who argued that foragers select raw materials specifically for their qualities.

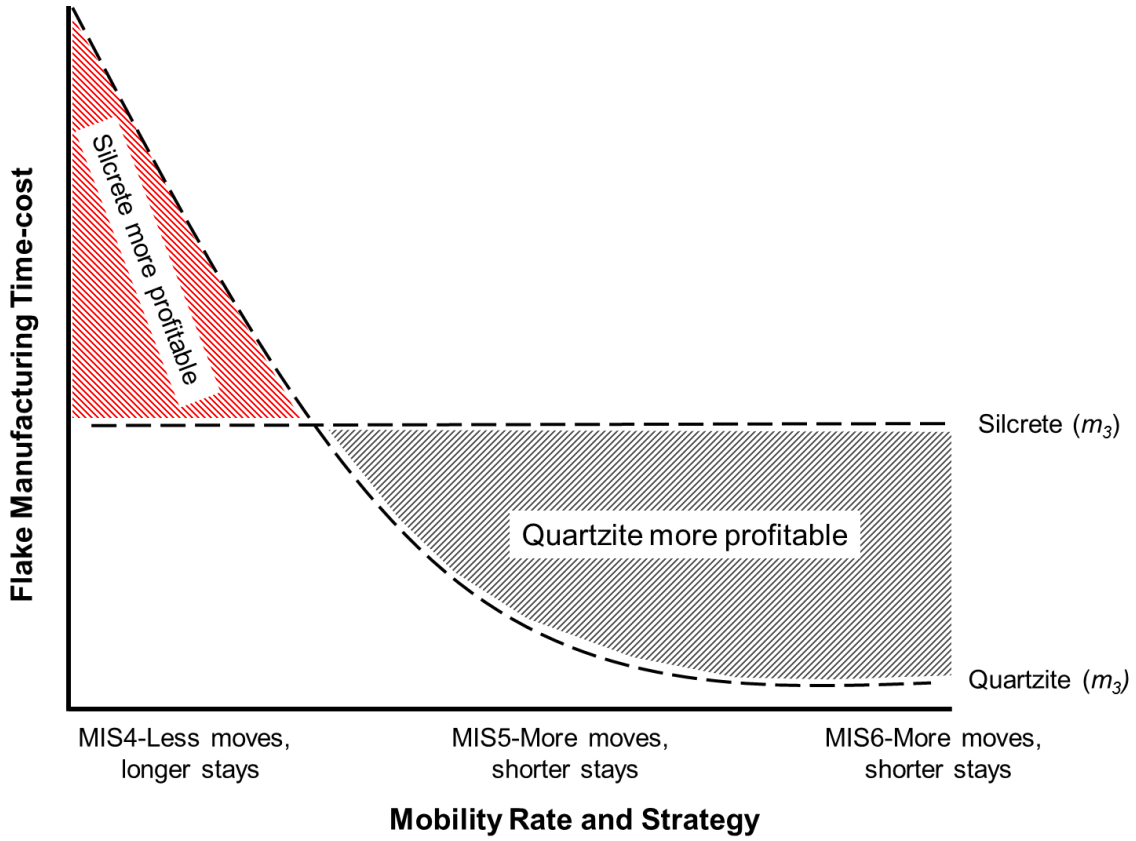

Figure 28. Predicted relationship between flake manufacturing time-cost (m_3) to manufacture quartzite and silcrete and model condition variable.

CHAPTER 6: METHODOLOGY

Introduction

The models presented in this study require a range of methodological steps to be operationalized. Below I describe these steps starting by detailing how the Opportunistic Acquisition Model (OAM) was constructed. The building blocks of the OAM include geological and geophysical data, raw material survey data, GIS analysis, and agent-based modeling. Second, I describe how the variables needed for both variants of the Active-choice Model (ACM) were obtained. Methods used to obtain estimates of variable values includes a stone tool reduction experiment, a raw material quality and fracture mechanics experiment, published data, raw material survey data, and GIS analysis.

Building the Opportunistic Acquisition Model

The OAM is at its core a type of agent-based model (ABM). Because the OAM does not entail any agent to agent interaction it is not a 'pure' agent-based model. To build the ABM the author collaborated with Dr. Marco Janssen, an expert on agent-based modeling (e.g. Delre et al. 2010, Salau et al. 2012, Janssen and Ostrom 2006), at Arizona State University. The author used the free Netlogo (Wilensky 1999) software platform for the modeling and conducted the modeling on computers at ASU. ABM is a useful tool because a collection of autonomous decision-making entities or 'agents' (in our case representing foragers) can be modeled as they interact with a constrained environment -- in this case representing a landscape (Axelrod and Tesfatsion 2006, Bonabeau 2002, Railsback and Grimm 2012, Gilbert 2007). Each agent individually assesses its situation and makes decisions based on a set of rules. An ABM is an algorithmic way of describing

the world, meaning that it consists of describing a system from the perspective of its constituent units, and ABM is ideal to use for calculating time-cost in our case because our foragers have decisions to make (Bonabeau 2002). An ABM was used to evaluate the OAM during both strong glacial and interglacial conditions against the archaeological record.

To build the OAM several steps were taken. 1) Brantingham's (2003) neutral model of stone procurement was replicated in Netlogo. 2) GIS was used to combine raw material source data with actual physical environmental map data. 3) Netlogo was used to run simulations with projected maps imported from the GIS. Each of these steps is detailed below.

Recreating Brantingham's neutral model

Brantingham's (2003) original model was created in a program called RePast. To facilitate the analysis in this study the neutral model was recreated in Netlogo (Janssen and Oestmo 2013) (**Figure 29**), a low-threshold and streamlined ABM software. The ODD protocol (Overview, Design concepts, and Details) of the recreated neutral model can be found in Appendix B.

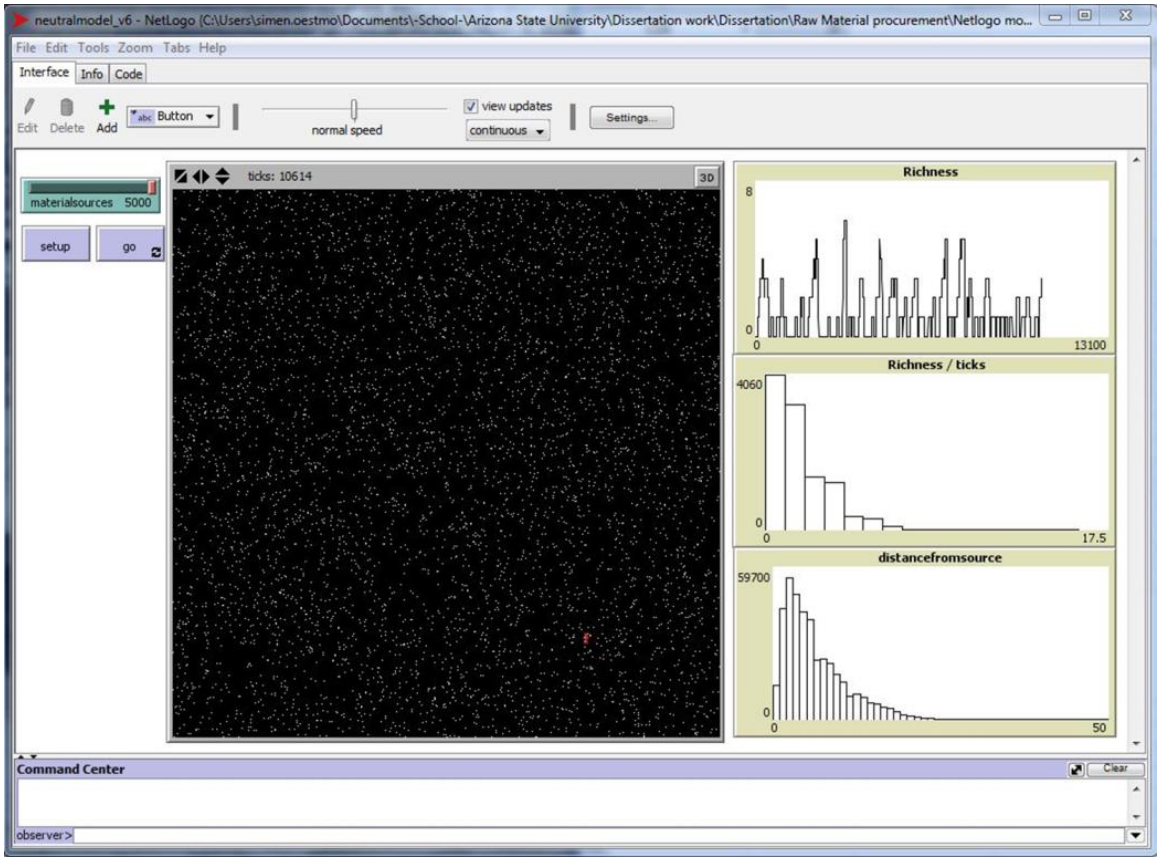

Figure 29. Screenshot of Brantingham's neutral model. Brantingham's (2003) neutral model was recreated by (Janssen and Oestmo 2013) in Netlogo (Wilensky 1999).

Modeling the effect of spatial clustering of raw material sources

After recreating the neutral model in Netlogo, a pilot study (Oestmo, Janssen, and Marean 2016) was undertaken to evaluate if random walk as a procurement strategy is a realistic assumption and to explore two limitations observed in the original neutral model by Brantingham (2003). In the original model, each raw material location is randomly distributed across the landscape without clustering and each location represents a unique raw material, while both are unrealistic assumptions. The pilot study explored how spatial clustering of source locations (**Figure 30**) affects the raw material pattern outcome.

Figure 30 show the three different clustering conditions that were used by Oestmo et al.

(2016) to gauge what effect spatial clustering of raw material sources have on the neutral model outcomes. The ODD for the spatial clustering model is in Appendix C.

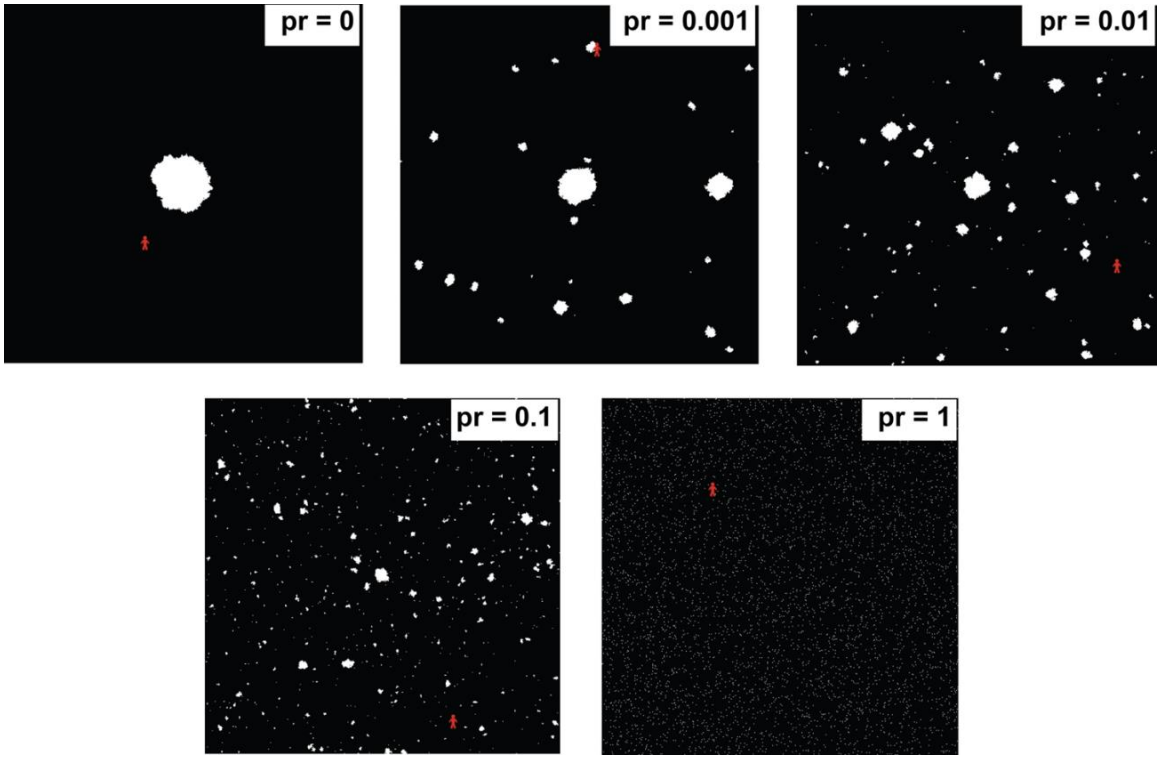

Figure 30. Effect of spatial clustering of raw material sources. Reprinted from Oestmo et al. (2016). pr stands for probability of random distribution of sources. At pr=0 all the sources are clustered together in the middle, while at pr=1 all the sources are randomly distributed across the whole landscape with single source joined together.

Oestmo et al. (2016) addressed three different model outcomes, raw material richness (number of different raw material types), distance materials move before being discarded, and steps that the agent takes without raw materials in the toolkit. The two first model outcomes were used to evaluate the effect of spatial clustering on the neutral model outcomes. The number of steps taken without raw materials in the toolkit was used to evaluate whether the criticism that a forager can never engage in random walk in an environment is a valid criticism (Brantingham 2003).

To address the second limitation noted above, that 5000 unique raw materials on an extended landscape is unrealistic, a second round of model simulations were run with only 20 unique raw materials distributed among the 5000 raw material locations. By chance, this can lead to clusters on the landscape where the majority of the raw materials distributed next to each other are of the same type.

Oestmo et al. (2016) simulated in addition to the original random walk behavior two other walk behaviors: 'seeking walk' and 'wiggle walk'. The wiggle walk simulates movement forward one cell at the time but at each time step the forager changes the direction by taking a left turn using a degree based on a drawn uniform distribution between 0 and 90 degrees, and then taking a right turn using a degree based on a uniformed distribution between 0 and 90 degrees. The seeking walk behavior is an analogy for returning to a stone cache at a central location. Seeking walk behavior models that the forager moves towards the closest material sources if the level of raw material in the toolkit is below a certain limit. Oestmo et al. (2016) used zero material in the toolkit as the limit, which means that anytime the toolkit is empty the forager will seek the nearest raw material source.

The pilot study did not rule out using the OAM as a model of foraging behavior, and a more rigorous test of its viability will be against an actual archaeological raw material frequency outlined below. The result of the pilot study will be discussed in *Chapter 8* where Hypothesis 1 drawn from the Opportunistic Acquisition Model is evaluated.

Neutral model application

Following the pilot study that investigated the effect of spatial clustering, when applying the OAM to the Mossel Bay Region, the physical locations of potential raw material sources were used, and different stone raw material types were distributed among those sources according to surveys (Brown 2011, Oestmo et al. 2014). The OAM was then evaluated by directly comparing the raw material frequency pattern resulting from random walk in the Mossel Bay region during MIS4, MIS5, and MIS6 model conditions to the archaeological sequence from Pinnacle Point (PP).

Three major steps were taken to be able to apply Brantingham's neutral model to an actual landscape and use physical positions and extents of raw material sources. 1) Several pedestrian surveys combined with manual in-field testing of flakeability of raw material were conducted (Brown 2011, Minichillo 2005, Oestmo et al. 2014). 2) Data containing the physical location and extents of raw material sources was combined with actual physical environmental data. GIS was used to project geological maps, coastline configurations, and raw material source locations in one project. 3) Maps from the GIS were imported into Netlogo for ABM simulations. An evaluation of model predictions and hypothesis testing was first conducted followed by a post-hoc sensitivity analysis (Broeke, van Voorna, and Ligtenberg 2016, Cariboni et al. 2007, Saltelli et al. 2004, Thiele, Kurth, and Grimm 2014) to evaluate how different model parameters affected the model outcome.

Raw material survey

To be able to model how a random walk in an actual environment would affect the raw material frequencies at archaeological localities, the locations and extents of potential raw material sources in the Mossel Bay region were needed. Data from raw material surveys over several years were used (Brown 2011, Oestmo et al. 2014) including a raw material survey conducted in March of 2012 by Brown and by Dr. Jayne Wilkins and this author in July of 2016. **Figure 31** shows a survey grid map of the Mossel Bay region highlighting areas of the landscape where systematic pedestrian and vehicle survey have been conducted.

The methods used during these pedestrian and vehicle surveys varied somewhat but the core components remained the same. Generally, by using available geological maps, topographic maps, and road maps the surveyor and one or more assistants would drive to a grid square and then follow internal roads in a grid square area to find geological formations of interest noted beforehand. If possible, all such areas would be visited if landowners granted access. At all sources, the GPS coordinates were recorded. The surveys focused on three different major source types: Outcrop (e.g. cliff and pavement surfaces), secondary (e.g. cobble beach and river deposits), and conglomerates. These source types were approached slightly differently but the data on cortex roundness (well-rounded to very angular), clast size (max length and mass), clast shape (e.g. tabular, spherical), and raw material type (e.g. quartzite, silcrete, quartz) were all recorded.

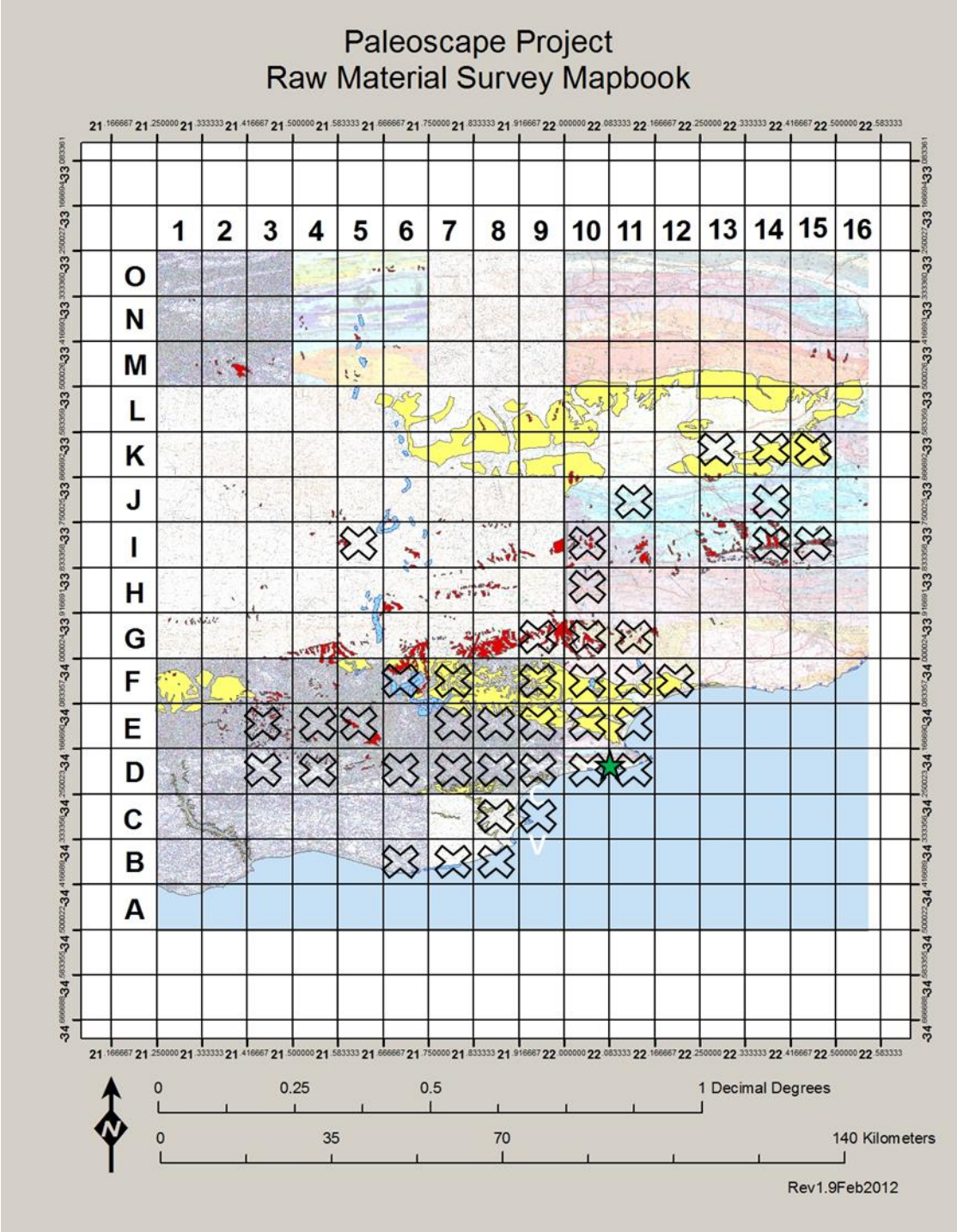

Figure 31. Survey grid map of the Mossel Bay region. The green star at the boundary between grid squares D10 and D11 marks the location of Pinnacle Point. Crosses in grid squares indicate that these squares have been visited and surveyed. Yellow-colored shapes indicate formations that have been geologically identified to be conglomerates. Red-colored shapes indicate formations that have been geologically identified to be silcrete. Light blue-colored shapes indicate positions of river cobble bars or coastal cobble beaches.

The collection of data at secondary sources was the most complex due to the potential variance in all the data categories. At the secondary sources, one or more sampling squares (25 by 25 cm) were laid down on the surface of clasts (**Figure 32**). The distance between multiple sampling-squares was determined based on the scale of the sampled area. Each clast (above 50mm) visible at the surface within a square was recorded and each clast was broken using a geological hammer so that interior characteristics such as flaws and banding could be recorded. Once the initial surface layer was collected a second and potential third layer was recorded the same way.

Figure 32. Raw material survey in progress. Location: Dana Bay cobble beach.

GIS data

To simulate strong interglacial conditions, already acquired actual physical environmental data for the Mossel Bay region was imported into ArcMap 10.4. The interglacial coastline configuration came from Mucina and Rutherford (2006). Source locations were based on GPS coordinates captured during surveys (Brown 2011, Oestmo et al. 2014). To create source extents, the GPS coordinate of sources were projected on top of an onshore geological map showing the underlying geology. The polygon of the underlying geology corresponding to the GPS point was then traced to create the extent of the potential source. This resulted in polygon shapefiles in ArcMap of the potential sources.

Distance to coastline estimations were based on the coastline distances calculated in the coastline model (Fisher et al. 2010). To create the MIS4 and MIS6 coastline configurations the distance estimates from Fisher et al (2010) were superimposed on a bathymetric map of the Mossel Bay region. Using the measure distance tool in ArcMap a line was traced from Pinnacle Point outwards directly perpendicular to the bathymetric elevation lines that are running northeast to southwest. The bathymetric elevation line located closest to the end of the measured distance line at 15km and 42 km was chosen as the new coastline for both MIS4 and MIS6 respectfully (**Figure 24**).

Estimated raw material source locations and extents on the submerged offshore platform were based on high-resolution marine geophysics survey data (Cawthra et al. 2015) provided by SACP4 member Dr. Hayley Cawthra from the South African Council for Geoscience (funded by the NGS). To create shapefiles showing superficial offshore geology and potential raw material sources in the Mossel Bay region a combination of

reports on mapping projects in the Mossel Bay region from the Council for Geoscience (CGS) and data from side-scan sonar was used (Cawthra et al. 2015).

Other environmental data such as drainage, vegetation, and slope was considered for input in the model but was not included. Drainage and vegetation data was not included to keep the model as simple as possible. A pilot run using slope data found that there would not be enough difference in slope to significantly affect human mobility due to the resolution used in the modeling.

For all GIS datasets, a set sequence of events was undertaken to conform the data to the same scale and raster resolution allowing for export of ascii files that were usable by Netlogo. All datasets were first imported into one ArcMap project where the coordinate system was set to WGS84. First, a clip box was created that set the outline of the region that was going to be simulated. All source shapefiles and coastline configuration shapefiles were cut by this clip box to create matching map sizes. Secondly, the clip box was then converted to a raster dataset with a raster size of 200, meaning that each raster cell was 200 by 200 meters. This resolution was chosen so that adequate resolution was provided in the model while still being able to project the whole Mossel Bay region in Netlogo. Third, all the clipped source and coastline configuration shapefiles were converted to raster using the same extent and raster size as the clip box raster, and they were snapped to the clip box raster to ensure identical raster map size and position. Fourth, the clipped raster maps were exported as ascii files allowing for easy import into Netlogo.

In total, three coastline configuration maps were created and exported, MIS4 (moderate glacial), MIS5 (Interglacial), and MIS6 (strong glacial). Each of these maps

had two data variables: land and ocean. Five raw material maps were produced. One for interglacial (MIS5) conditions (**Figure 33**), two for MIS4 conditions (**Figure 34**), and two for MIS6 conditions (**Figure 35**). These five maps had one variable (raw material) subdivided into raw material source types.

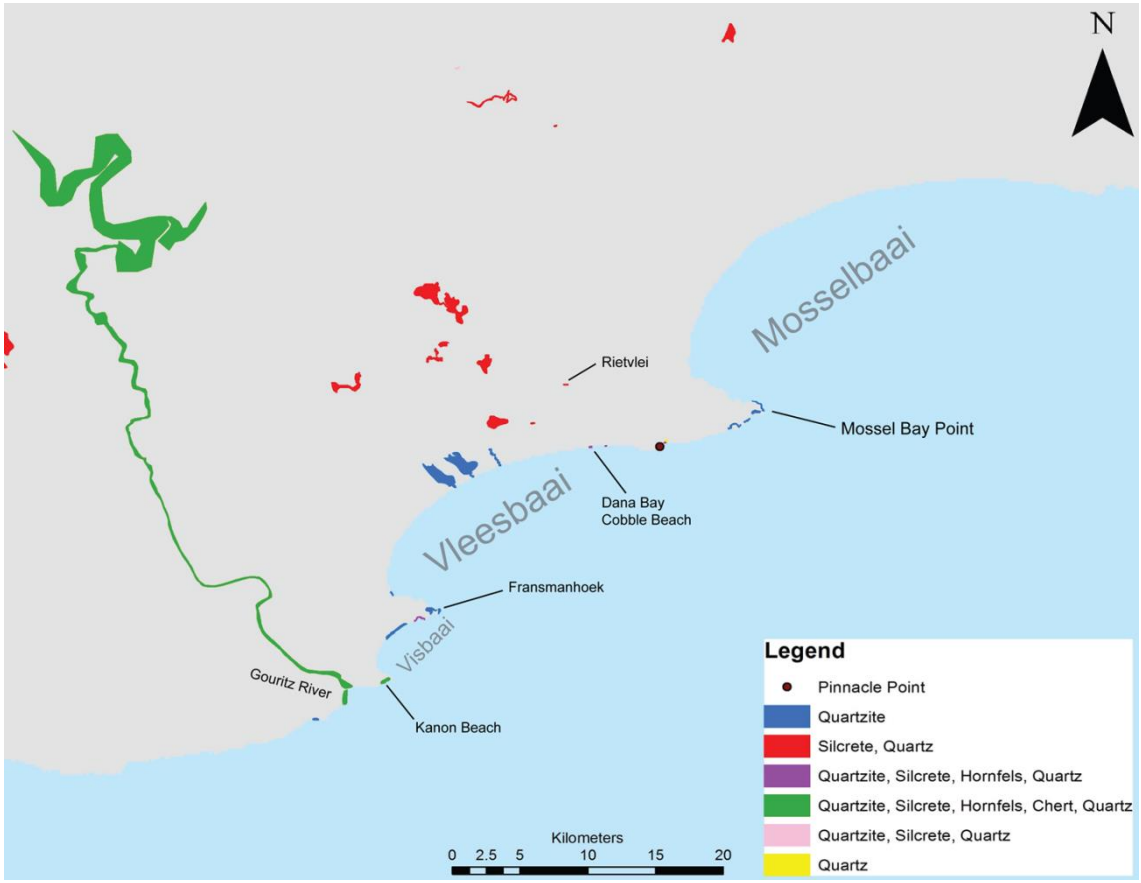

Figure 33. Interglacial raw material sources. Mossel Bay region during interglacial conditions with sources represented as their close to real size and distributed according to their real locations.

The major difference between the raw material distribution maps for MIS4 and MIS6 was the presence or absence of a hardground assumed to be a silcrete source on the Paleo-Agulhas plain that would be available during lower sea levels. This particular hardground was selected to be modeled because of its particular close proximity to Pinnacle Point.

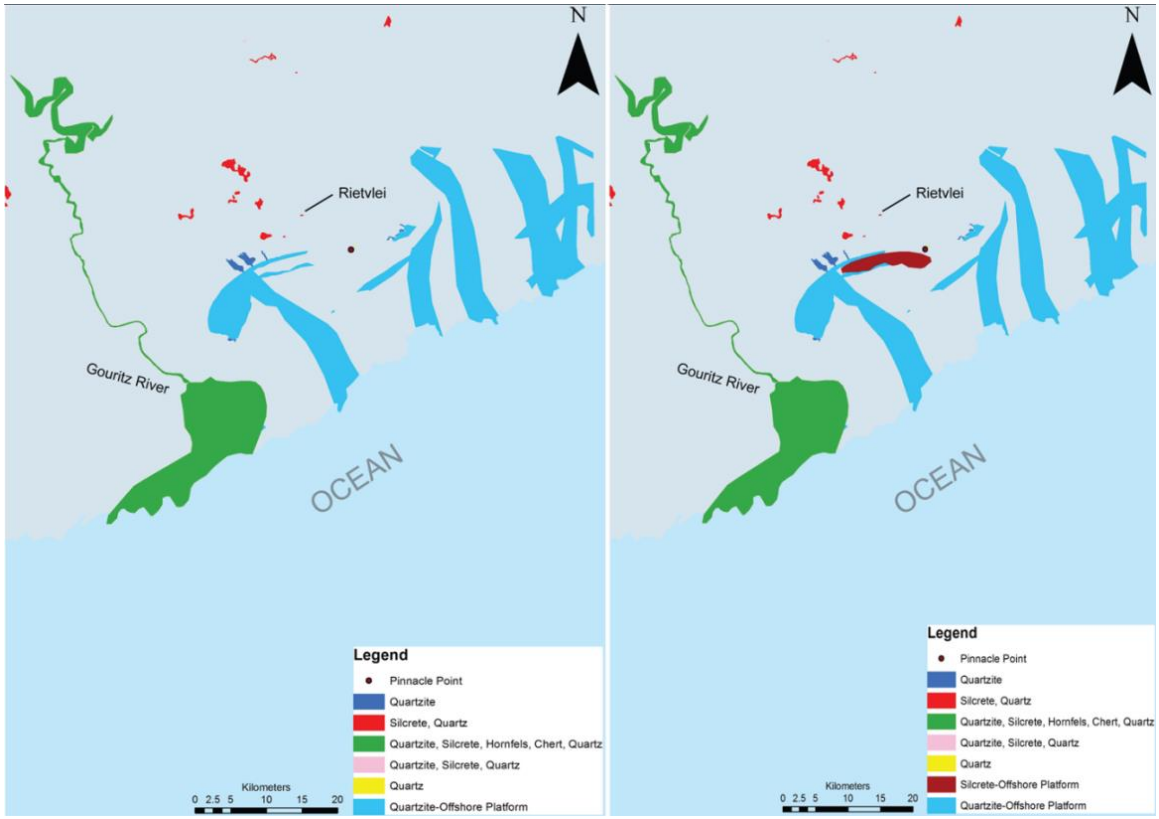

Figure 34. MIS4 raw material sources. Map shows the location of potential raw material source types used during MIS4 modeling conditions. Map on the left shows material sources without the closest hardground assumed to be a silcrete source on the Paleo-Agulhas plain. Map on the right shows material sources including the closest hardground (Burgundy) assumed to be a silcrete source on the Paleo-Agulhas plain. Distance to coastline from Pinnacle Point is ~15km.

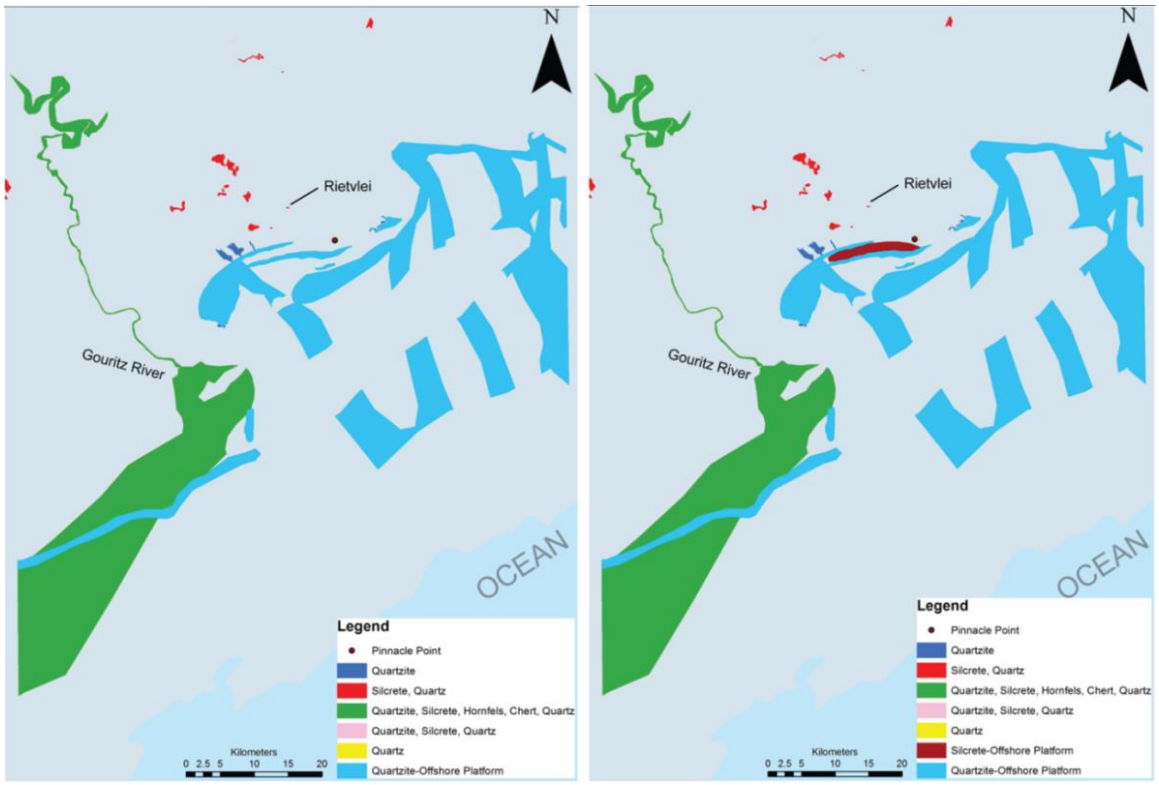

Figure 35. MIS6 raw material sources. Map shows the location of potential raw material source types used during MIS6 modeling conditions. Map on the left shows material sources without the closest hardground assumed to be a silcrete source on Paleo-Agulhas plain. Map on the right shows material sources including the closest hardground (Burgundy) assumed to be a silcrete source on the Paleo-Agulhas plain. Distance to coastline from Pinnacle Point is ~42km.

Netlogo application

Ascii files created in ArcMap were imported and employed in Netlogo using the GIS extension (**Figures 36-38**). All model simulations were run with the 'behaviorspace' function. Data were exported as Excel files for statistical analysis.

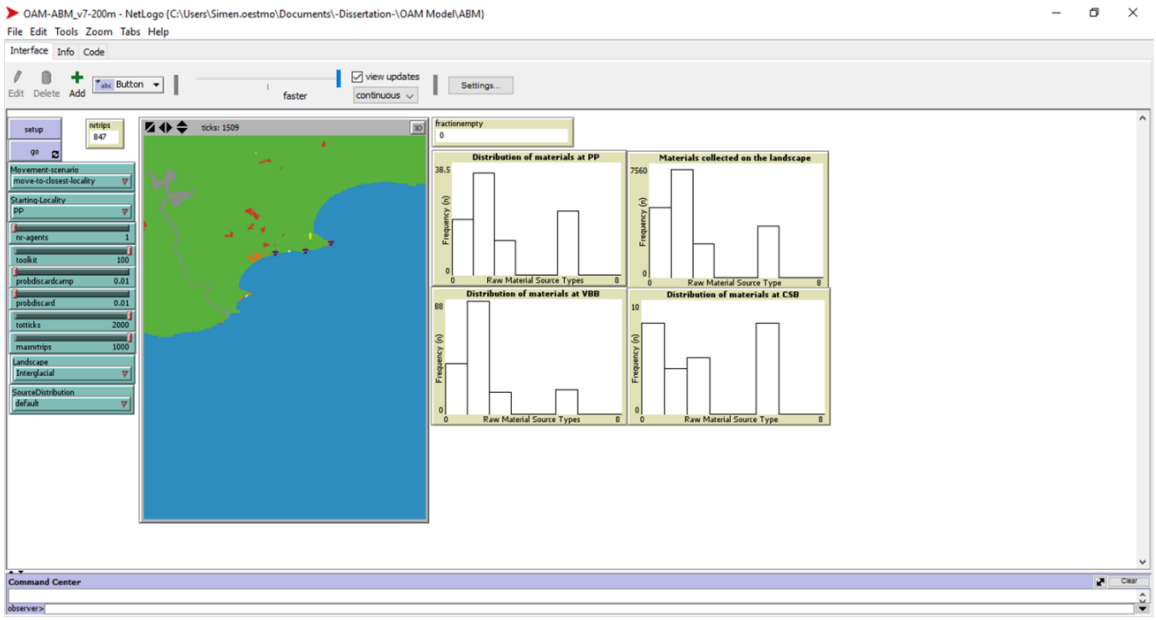

Figure 36. Interglacial raw material sources projected in Netlogo.

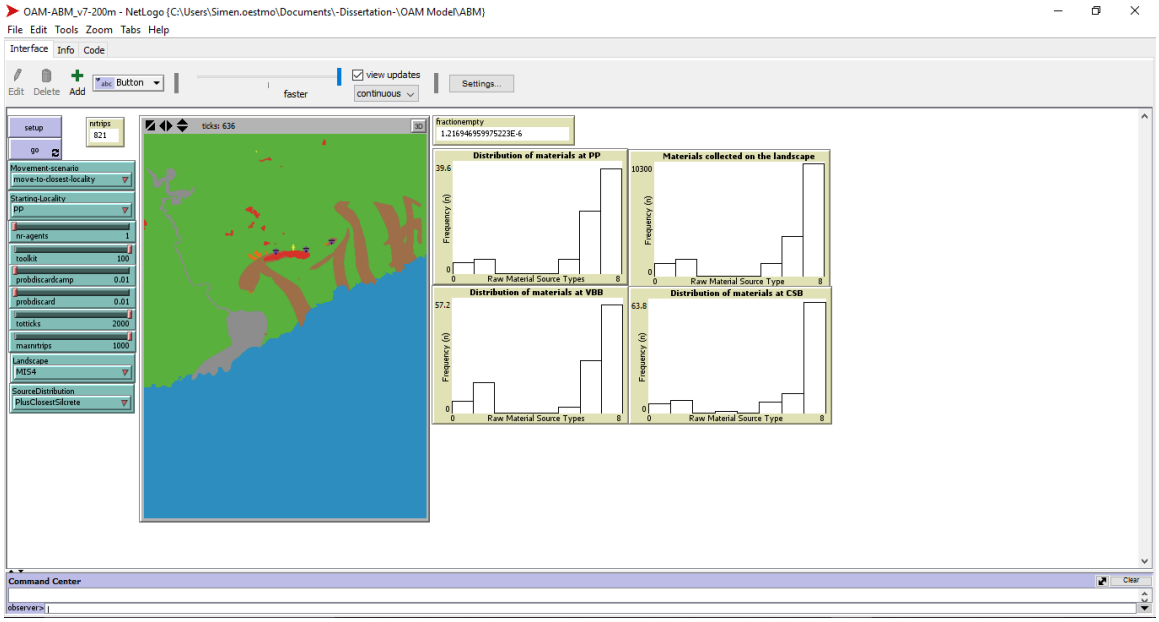

Figure 37. MIS4 raw material sources projected in Netlogo. This example shows the raw material source distributions including the closest hardground assumed to be a silcrete source on the Paleo-Agulhas Plain.

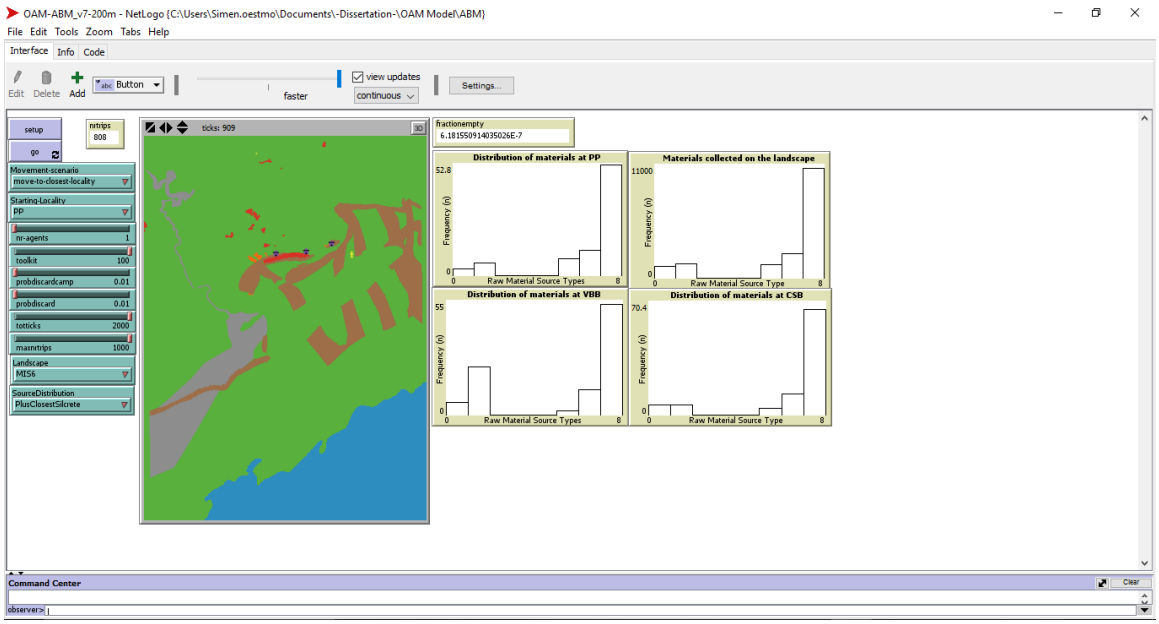

Figure 38. MIS6 raw material sources projected in Netlogo. This example shows the raw material source distributions including the closest hardground assumed to be a silcrete source on the Paleo-Agulhas plain.

OAM analytical methods – Base settings

The analysis of the OAM output was performed in several steps. First, the coastline position and raw material distribution variable outcomes were compared to archaeological frequencies under all five model conditions to test Hypothesis 1. In this initial test, only same-day returns of the agent were considered. 'Same-day returns' refers to one single foraging day of movement (~70-100 "totticks", assuming a walking pace of 3.5 to 2.5km/hr (Binford 2001, Marlowe 2010, Marlowe 2006)) where the agent starts and returns to the same locality in one day. This was undertaken by running the model (see **Table 2** for model variables) at base variable settings (**Table 5**). Same-day return simulations were run 1000 times. Because "maxnrtirps" were set to 1000 trips that means that the raw material frequency outcome from each model simulation resulted from 1 million foraging trips. The "probdiscard" and "probdiscardcamp" values used in all three

model conditions were set by using the following formula (count of sources/patches) / (5000/250000). This formula made the discard probability be similar to the probability of encountering a raw material source in Brantingham's (2003) original neutral model, which was 0.02 (5000 sources / 250000 patches).

Table 5. OAM Base variable settings

Model Condition	Model Variable	Base Variable Setting
MIS4	Movement-scenario	return-to-starting-locality
MIS4	Starting-Locality	PP
MIS4	nr-agents	1
MIS4	toolkit	100
MIS4	probdiscard	0.02
MIS4	probdiscardcamp	0.02
MIS4	totticks	100
MIS4	maxnrtrips	1000
MIS4	Landscape	MIS4
MIS4	SourceDistribution	default or PlusClosestSilcrete
MIS5	Movement-scenario	return-to-starting-locality
MIS5	Starting-Locality	PP
MIS5	nr-agents	1
MIS5	toolkit	100
MIS5	probdiscard	0.03
MIS5	probdiscardcamp	0.03
MIS5	totticks	100
MIS5	maxnrtrips	1000
MIS5	Landscape	Interglacial
MIS5	SourceDistribution	default
MIS6	Movement-scenario	return-to-starting-locality
MIS6	Starting-Locality	PP
MIS6	nr-agents	1
MIS6	toolkit	100
MIS6	probdiscard	0.01
MIS6	probdiscardcamp	0.01
MIS6	totticks	100
MIS6	maxnrtrips	1000
MIS6	Landscape	MIS6
MIS6	SourceDistribution	default or PlusClosestSilcrete

OAM analytical methods – Sensitivity analysis

To evaluate the robustness of the model outcome in comparison to the archaeological frequency data a sensitivity analysis was performed (Broeke, van Voorna, and Ligtenberg 2016, Cariboni et al. 2007, Saltelli et al. 2004, Thiele, Kurth, and Grimm 2014). This sensitivity analysis followed a one-factor-at-a-time (OFAT) approach (Broeke, van Voorna, and Ligtenberg 2016). When using an OFAT sensitivity analysis a set of base settings for the model variables are selected and then one variable is varied keeping all other variables fixed. An OFAT sensitivity analysis is used to reveal the form of the relationship between the changing variable and the model output given that all the other variables are at their base value (Broeke, van Voorna, and Ligtenberg 2016). An OFAT analysis, for example, can show whether the response between the changing variable and the outcome is linear or nonlinear, whether there are tipping points where the model outcome responds dramatically to a small change in the varied variable (Broeke, van Voorna, and Ligtenberg 2016). An OFAT analysis has the potential to increase the understanding of model mechanisms (Broeke, van Voorna, and Ligtenberg 2016). All four rounds of the OFAT were conducted on Hypothesis 1 (H_1) after the initial evaluation using base settings.

In the first round of the OFAT, the effect of increasing the amount of time allowed by the forager to be away from PP was modeled. This was accomplished by varying the "totticks" (movement-budget) variable. To examine the effect of increasing the amount of both time and distance the forager can move away from PP, effectively increasing residential mobility or foraging range size, "totticks" values of 50, 100, 500, 1000, 1500, and 2000 were simulated. This allowed for testing H_1 under both same-day

returns (~70-100 “totticks”, assuming a walking pace of 3.5 to 2.5km/hr (Binford 2001, Marlowe 2010, Marlowe 2006)) and up to ~15-20 foraging days away from Pinnacle Point (~2000” totticks”, assuming a walking pace of 3.5 to 2.5km/hr (Binford 2001, Marlowe 2010, Marlowe 2006)). **Table 6** shows simulations that were run in OFAT round one. All settings were kept the same as the base settings except for the changes in ”totticks”. The simulations in the first round of the OFAT were run 1000 times, meaning that the raw material frequency outcome from each model simulation resulted from 1 million foraging trips.

Table 6. OFAT round one simulation overview.

Model Condition	Movement-scenario variable	SourceDistribution variable	Totticks values simulated
MIS4	return-to-starting-locality	default	50 100 500 1000 1500 2000
MIS4	return-to-starting-locality	PlusClosestSilcrete	50 100 500 1000 1500 2000
MIS5	return-to-starting-locality	default	50 100 500 1000 1500 2000
MIS6	return-to-starting-locality	default	50 100 500 1000 1500 2000
MIS6	return-to-starting-locality	PlusClosestSilcrete	50 100 500 1000 1500 2000

In the second round of the OFAT (OFAT2), the effect of having two more foraging localities (represented by two actual archaeological MSA localities) to return too was modeled. The factor of having more than two localities to return too introduced randomness to the model and simulated Pinnacle Point as being just one of three localities that the forager can access on the landscape. **Table 7** shows simulations that were run in OFAT2. All settings were kept the same as the base settings except for the changes in “totticks” and changing the “Movement-Scenario” to “move-to-closest-locality”. The simulations in the second round of the OFAT were run 1000 times,

meaning that the raw material frequency outcome from each model simulation resulted from 1 million foraging trips.

Table 7. OFAT round two simulation overview.

Model Condition	Movement-scenario variable	SourceDistribution variable	totticks values simulated
MIS4	move-to-closest-locality	default	50 100 500 1000 1500 2000
MIS4	move-to-closest-locality	PlusClosestSilcrete	50 100 500 1000 1500 2000
MIS5	move-to-closest-locality	default	50 100 500 1000 1500 2000
MIS6	move-to-closest-locality	default	50 100 500 1000 1500 2000
MIS6	move-to-closest-locality	PlusClosestSilcrete	50 100 500 1000 1500 2000

In the third round of the OFAT (OFAT3), a test of the effect of changing of the probability of discard of raw materials on the landscape, the effect of changing the probability of discard of raw materials in the campsite, and the effect of changing the toolkit size on the raw material frequency output at Pinnacle Point was modelled. This round focused on what happens to the raw material frequency output at Pinnacle Point when the probability of discard on the landscape is lowered or raised; what happens to the raw material frequency output at Pinnacle Point when the probability of discard at Pinnacle Point is lowered and raised; what happens to the raw material frequency output at Pinnacle Point when the toolkit size is lowered from the original 100. **Table 8** shows the simulations that were run in OFAT3. All settings were kept the same as the base settings except for changes in the "probdiscard", "probdiscardcamp", and "toolkit." Additionally, totticks was set to 100 to simulate same-day returns. Simulations changing these variables one at the time were run under both movement-scenarios and both scenarios where Paleo-Agulhas silcrete is available or not. The simulations in the third

round of the OFAT were run 100 times, meaning that the raw material frequency outcome from each model simulation resulted from 100 000 foraging trips. OFAT3 simulations were only run 100 times after early test runs showed that the range of variance was narrow.

Table 8. OFAT round three simulation overview.

Model Condition	Movement-scenario variable	SourceDistribution variable	probdiscard values simulated
MIS4	return-to-starting-locality	default	0.001 0.1 0.5 0.75 0.95
MIS4	return-to-starting-locality	PlusClosestSilcrete	0.001 0.1 0.5 0.75 0.95
MIS4	move-to-closest-locality	default	0.001 0.1 0.5 0.75 0.95
MIS4	move-to-closest-locality	PlusClosestSilcrete	0.001 0.1 0.5 0.75 0.95
MIS5	return-to-starting-locality	default	0.001 0.1 0.5 0.75 0.95
MIS5	move-to-closest-locality	default	0.001 0.1 0.5 0.75 0.95
MIS6	return-to-starting-locality	default	0.001 0.1 0.5 0.75 0.95
MIS6	return-to-starting-locality	PlusClosestSilcrete	0.001 0.1 0.5 0.75 0.95
MIS6	move-to-closest-locality	default	0.001 0.1 0.5 0.75 0.95
MIS6	move-to-closest-locality	PlusClosestSilcrete	0.001 0.1 0.5 0.75 0.95
Model Condition	**Movement-scenario variable**	**SourceDistribution variable**	**probdiscardcamp values simulated**
MIS4	return-to-starting-locality	default	0.001 0.1 0.5 0.75 0.95
MIS4	return-to-starting-locality	PlusClosestSilcrete	0.001 0.1 0.5 0.75 0.95
MIS4	move-to-closest-locality	default	0.001 0.1 0.5 0.75 0.95
MIS4	move-to-closest-locality	PlusClosestSilcrete	0.001 0.1 0.5 0.75 0.95
MIS5	return-to-starting-locality	default	0.001 0.1 0.5 0.75 0.95
MIS5	move-to-closest-locality	default	0.001 0.1 0.5 0.75 0.95
MIS6	return-to-starting-locality	default	0.001 0.1 0.5 0.75 0.95
MIS6	return-to-starting-locality	PlusClosestSilcrete	0.001 0.1 0.5 0.75 0.95
MIS6	move-to-closest-locality	default	0.001 0.1 0.5 0.75 0.95
MIS6	move-to-closest-locality	PlusClosestSilcrete	0.001 0.1 0.5 0.75 0.95
Model Condition	**Movement-scenario variable**	**SourceDistribution variable**	**toolkit values simulated**
MIS4	return-to-starting-locality	default	5 10 50 75 100
MIS4	return-to-starting-locality	PlusClosestSilcrete	5 10 50 75 100
MIS4	move-to-closest-locality	default	5 10 50 75 100
MIS4	move-to-closest-locality	PlusClosestSilcrete	5 10 50 75 100
MIS5	return-to-starting-locality	default	5 10 50 75 100
MIS5	move-to-closest-locality	default	5 10 50 75 100
MIS6	return-to-starting-locality	default	5 10 50 75 100
MIS6	return-to-starting-locality	PlusClosestSilcrete	5 10 50 75 100

MIS6	move-to-closest-locality	default	5 10 50 75 100
MIS6	move-to-closest-locality	PlusClosestSilcrete	5 10 50 75 100

In the final and fourth round of the OFAT (OFAT4), three different scenarios of hunter-gatherer technological behavior were examined for their effect on the raw material frequency at Pinnacle Point: expedient, site caching, and conservative behaviors.

Expediency as technological strategy refers to "minimized technological effort under conditions where time and place of use are highly predictable" (Nelson 1991: 64). In the simulations of expedient behavior, it was assumed that the forager does not want, or needs, or cares whether it retains raw materials at any time step when moving about the landscape and does not need to conserve raw materials when returned to a locality. Once at a locality the forager discards or uses everything it has without concern for preserving material for future use (Nelson 1991). This type of behavior is linked to scenarios where the forager has decreased its residential mobility, become more sedentary making less frequent moves (Parry and Kelly 1987, Riel-Salvatore and Barton 2004). (Nelson 1991: 64) noted that expedient technological behavior relies on at least three conditions: 1) planning of stockpiling or caching of raw materials, or anticipated undertaking of activities where the raw materials are located (Bamforth 1986, Parry and Kelly 1987); 2) time available to manufacture tools as part the activity of their use, indicates no time stress (Torrence 1983); 3) increased occupations or regular reuse of the place where raw material are available in order to take advantage of the stockpile or cache (Parry and Kelly 1987).

Site caching or stock-piling technological behavior refers to the act of storing raw materials at a planned place in anticipation of future use (Nelson 1991). In the

simulations of site caching behavior, it was assumed that the forager wanted to not lose or discard raw materials when moving about the landscape but when returned to a locality it would dump all the collected raw materials still present in the toolkit. This type of behavior is linked to expedient behavior scenarios where there are often visited localities that functioned as home-bases where stone is cached for future use or provisioned to multiple people (Kuhn 1992, Nelson 1991).

A conservative or curated technological strategy refers to the "caring for tools and toolkits that can include advanced manufacture, transport, and reshaping" (Nelson 1991: 62). In the simulations of conservative behavior, it was assumed that the forager did not want to lose or discard raw materials when moving about the landscape with a limited toolkit size. When returning to a locality the forager also does not want to lose or discard raw materials. This type of behavior is linked to situations where the forager has increased its residential mobility, moving camp often, or where there is a need to provision individuals with gear that serves as a hedge against a variety of eventualities such as lack of raw materials, time, or facilities for repair at the time and place of use (Kuhn 1992, 1991, Nelson 1991, Parry and Kelly 1987, Riel-Salvatore and Barton 2004).

Table 9 shows the simulations that were run in OFAT3. All settings were kept the same as the base settings except for changes in the "probdiscard", "probdiscardcamp", and "toolkit". They were changed at the same time to a fixed value. Simulations running these behaviors were run under both movement-scenarios and both scenarios where Paleo-Agulhas silcrete is available or not. The simulations in the fourth round of the OFAT were run 100 times, meaning that the raw material frequency outcome from each model simulation resulted from 100 000 foraging trips. OFAT4 simulations were run 100

times because test runs showed that the range variance in the outcomes was sufficiently narrow.

Table 9. OFAT round four simulation overview.

Behavior	Model Condition	Movement-scenario variable	SourceDistribution variable	probdiscard setting	probdiscardcamp setting	toolkit setting
Expedient	MIS4	return-to-starting-locality	default	0.99	0.99	100
Expedient	MIS4	return-to-starting-locality	PlusClosestSilcrete	0.99	0.99	100
Expedient	MIS4	move-to-closest-locality	default	0.99	0.99	100
Expedient	MIS4	move-to-closest-locality	PlusClosestSilcrete	0.99	0.99	100
Expedient	MIS5	return-to-starting-locality	default	0.99	0.99	100
Expedient	MIS5	move-to-closest-locality	default	0.99	0.99	100
Expedient	MIS6	return-to-starting-locality	default	0.99	0.99	100
Expedient	MIS6	return-to-starting-locality	PlusClosestSilcrete	0.99	0.99	100
Expedient	MIS6	move-to-closest-locality	default	0.99	0.99	100
Expedient	MIS6	move-to-closest-locality	PlusClosestSilcrete	0.99	0.99	100

Behavior	Model Condition	Movement-scenario variable	SourceDistribution variable	probdiscard	probdiscardcamp	toolkit setting
Site Caching	MIS4	return-to-starting-locality	default	0.001	0.99	100
Site Caching	MIS4	return-to-starting-locality	PlusClosestSilcrete	0.001	0.99	100
Site Caching	MIS4	move-to-closest-locality	default	0.001	0.99	100
Site Caching	MIS4	move-to-closest-locality	PlusClosestSilcrete	0.001	0.99	100
Site Caching	MIS5	return-to-starting-locality	default	0.001	0.99	100
Site Caching	MIS5	move-to-closest-locality	default	0.001	0.99	100
Site Caching	MIS6	return-to-starting-locality	default	0.001	0.99	100
Site Caching	MIS6	return-to-starting-locality	PlusClosestSilcrete	0.001	0.99	100
Site Caching	MIS6	move-to-closest-locality	default	0.001	0.99	100
Site Caching	MIS6	move-to-closest-locality	PlusClosestSilcrete	0.001	0.99	100

Behavior	Model Condition	Movement-scenario variable	SourceDistribution variable	probdiscard	probdiscardcamp	toolkit setting
Conservative	MIS4	return-to-starting-locality	default	0.001	0.001	10

Conservative	MIS4	return-to-starting-locality	PlusClosestSilcrete	0.001	0.001	10
Conservative	MIS4	move-to-closest-locality	default	0.001	0.001	10
Conservative	MIS4	move-to-closest-locality	PlusClosestSilcrete	0.001	0.001	10
Conservative	MIS5	return-to-starting-locality	default	0.001	0.001	10
Conservative	MIS5	move-to-closest-locality	default	0.001	0.001	10
Conservative	MIS6	return-to-starting-locality	default	0.001	0.001	10
Conservative	MIS6	return-to-starting-locality	PlusClosestSilcrete	0.001	0.001	10
Conservative	MIS6	move-to-closest-locality	default	0.001	0.001	10
Conservative	MIS6	move-to-closest-locality	PlusClosestSilcrete	0.001	0.001	10

OAM analytical methods – Statistical analysis

All excel table outputs from the OAM were formatted the same way. A data conversion was conducted because the raw material frequency output created by the OAM is not strictly a pure raw material frequency but instead a frequency of the eight raw material source types that the agent has encountered. The raw material source type output was formatted to reflect individual raw material type frequencies by using published raw material survey data (Brown 2011, Oestmo et al. 2014) plus data from Brown's 2012 survey and Wilkins and this author's 2016 survey that contained the percentage of a specific raw material type at raw material source. This conversion based on survey data was applied to secondary sources such as the cobble beaches and the Gouritz River as they contain multiple types of raw materials. The average of the raw material frequency survey data from Eden Bay, Dana Bay, and Fransmanhoek was applied to output results where the agent had encountered and discarded material from those sources. The average frequency survey data from Kanon Beach, Gouritsmond Beach, and Gourtiz River was applied to the output results when the agent had encountered and discarded materials

from those sources (**Table 10**). Silcrete primary sources were assumed to yield 99% silcrete and 1% quartz to the agent when encountered based on surveys by Brown (2011). Quartzite primary sources were assumed to only contain quartzite. River flood plains and wave-ravinement surfaces present on the Paleo-Agulhas plain when the sea level was lower were assumed to only contain quartzite. The one hardground assumed to be a silcrete source on the Paleo-Agulhas plain was assumed to only contain silcrete. Primary quartz sources were assumed to only contain quartz. After this conversion was conducted the frequency data was run in JMP Pro 12 (Hodgson 2015), statistical software, to create descriptive statistics, and to test if the sample populations were significantly different.

Table 10. Source raw material frequencies.

Sources	Source Type	Quartzite %	Silcrete %	Hornfels %	Quartz %	Chert or Chalcedony %
Eden Bay, Dana Bay, Fransmanhoek,	Cobble Beach	98.5	0.6	0.4	0.5	0
Kanon beach, Gourtismond, Gourtiz River	Cobble Beach and River Deposits	95.8	0.97	0.6	1.6	0.97

To test the OAM model outcomes under the coastline position and raw material distribution variable, two separate testing procedures were conducted. In both procedures, the OAM raw material frequency (percent of overall assemblage) output data using the base variable settings were first created. In the first procedure, the frequencies were compared to archaeological frequency data by comparing the mean value and 95% confidence intervals against bootstrapped archaeological raw material frequencies. The median raw material frequency of the different raw materials was investigated to check if the outcomes were significantly different, meaning that the frequencies were outside the

95% confidence intervals of each other. In the second procedure, the model frequencies were used to create a ranking where the raw material with the highest frequency obtained the highest rank. The ranking was then compared to the archaeological raw material frequencies. Similarly, the outcomes from all OFAT sensitivity analysis rounds were tested using the same two procedures.

Obtaining variable estimates for the Active-Choice Model

Table 11 re-summarizes the variables needed in both variants of the Active-Choice Model (ACM). **Table 3** defines the variables. Below follows a description of how each of these variables were obtained.

Table 11. ACM variables

Model Variable
P and R
Cutting Edge (*e*)
Durability (*d*)
Travel and Search Time (t_s)
Procurement Time (t_p)
Manufacture Time (*m*) - Wood fuel travel and search (m_1), Heat-treatment ($_m2$), Flake manufacturing (m_3)

Cutting edge per mass experiment

A stone tool reduction experiment was conducted in collaboration with Dr. Kyle S. Brown to obtain measurements of the cutting edge (e) and flake manufacturing (m_3) variables needed to calculate the net-return rates from both ACM variants.

It has been shown archaeologically and experimentally that a flint-knapper can efficiently manage the amount of flake cutting edge/mass by altering the exterior

platform angle and by controlling the flake platform area (Davis and Shea 1998, Dibble 1997, Dibble and Rezek 2009, Pelcin 1998). The control of these flake variables has important implications for core maintenance and thus raw material economy (Brown 2011, Dibble 1997). It is expected that more expedient use of a raw material will result in a lower cutting edge length/mass ratio compared to more conservative use that seeks to maximize the cutting edge length/mass ratio (Braun 2005, Brown 2011). The optimal strategy to achieve a high cutting edge length/mass ratio, meaning that more raw material is conserved, is to increase the exterior platform angle while minimizing the ratio of platform width to platform thickness (Braun 2005, Brown 2011).

For the pilot study, quartzite and silcrete raw material samples were collected from primary outcrops and secondary sources during surveys of the Mossel Bay region conducted by Brown. Subsequently, thirty-six samples were precut into similar sized and shaped blocks to minimize shape and size variance (20 quartzite and 16 silcrete) (**Figure 39**).

Figure 39. Flaking experiment. A) Sample of blocks ready to be knapped. B) Dr. Kyle S. Brown knapping a block. C) Assemblage of purposefully detached products from a block, in order top left to bottom right.

Half of the silcrete blocks were heat-treated using temperature and duration specifications outlined by Brown et al. (2009) (**Figure 40**). After heat-treatment, Brown then reduced each block (both quartzite and silcrete) for 14 min using direct percussion with a hard-hammer cobble, while this author videotaped the process, collected, and bagged in sequence every product above 14mm that Brown purposely detached from the block (**Figure 39**). A product refers here to all flakes, blades, points, or fragments thereof that were purposefully detached from a raw material block. After each flaking bout, this author collected the rest of the reduction-waste in a single bag.

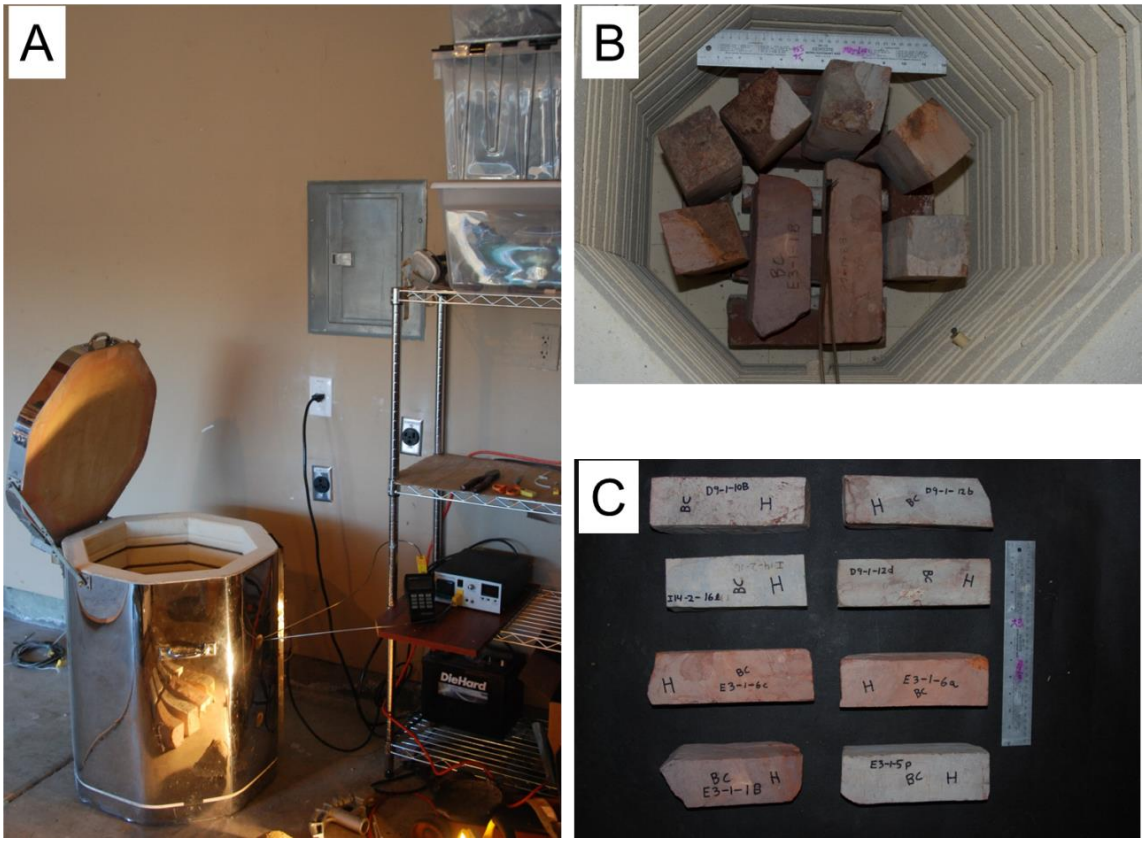

Figure 40. Heat-treatment of silcrete. A) Kiln and temperature-controller setup. B) Sample blocks in the kiln ready to be heat-treated. C) Sample blocks after heat-treatment.

The cutting edge length (cm) was measured on all complete and broken flakes above 14 mm in maximum dimension from the pilot study (See **Table 3** for the definition of cutting edge) to quantify the *e* values for both raw materials (Quartzite and both heat-treated silcrete and untreated silcrete). The *e* values were measured directly and accurately by tracing the outline of the cutting edge (Braun 2005). The weight of all complete flakes and all broken reduction debris were recorded to quantify the m_3 time-cost values for both raw materials. To quantify the cutting edge length (mm) / mass (g) rates (Braun 2005, Mackay 2008), the measurements of all complete flakes above 14mm in maximum dimension from the *e* value measurements were used, while each complete flake that was collected in sequence during each flaking bout was weighted.

In total, 1241 purposefully detached products or product fragments were measured from quartzite blocks. Additionally, 1374 debitage pieces denoted as ‘extra’ were also measured. The ‘extra’ pieces were all debitage or fragments above 14mm not purposefully detached from the block but that were collected at the end as part of the waste resulting from the reduction of a raw material block. In addition, 23 cores or core fragments were measured. For untreated silcrete, 438 purposefully detached products or product fragments were measured. The untreated silcrete blocks yielded 547 ‘extra’ and 9 core or core fragments. Heat-treated silcrete blocks yielded 597 purposefully detached products or product fragments, 1016 ‘extra’ pieces, and 9 core or core fragments.

Cutting edge durability experiment

A Taber Linear Abraser (**Figure 41**) and a TESC sharp edge tester (**Figure 42**) were used to calculate the length of time the edge of a tool lasts when cutting a material (*d*), which is needed in the ACM. There are multiple ways that stone tools could have been used, but one behavior that is universal among hunter-gatherers is butchery of animals. Animals are exploited for several reasons but mostly to extract resources such as food or materials for tools and clothing. However, the acquisition, sharing, and consumption of meat have great personal, social and symbolic significance among living humans (Bicchieri 1972, Clark 1972, Coon 1971, Lee and DeVore 1968, Milo 1994, Ortega Y Gasset 1972).

The TESC sharp edge tester (https://sharpedgetester.com/set50) provides an objective pass/fail test to judge the sharpness of an edge. Typically, a sharpness measurement takes a couple of seconds to perform and requires no special training.

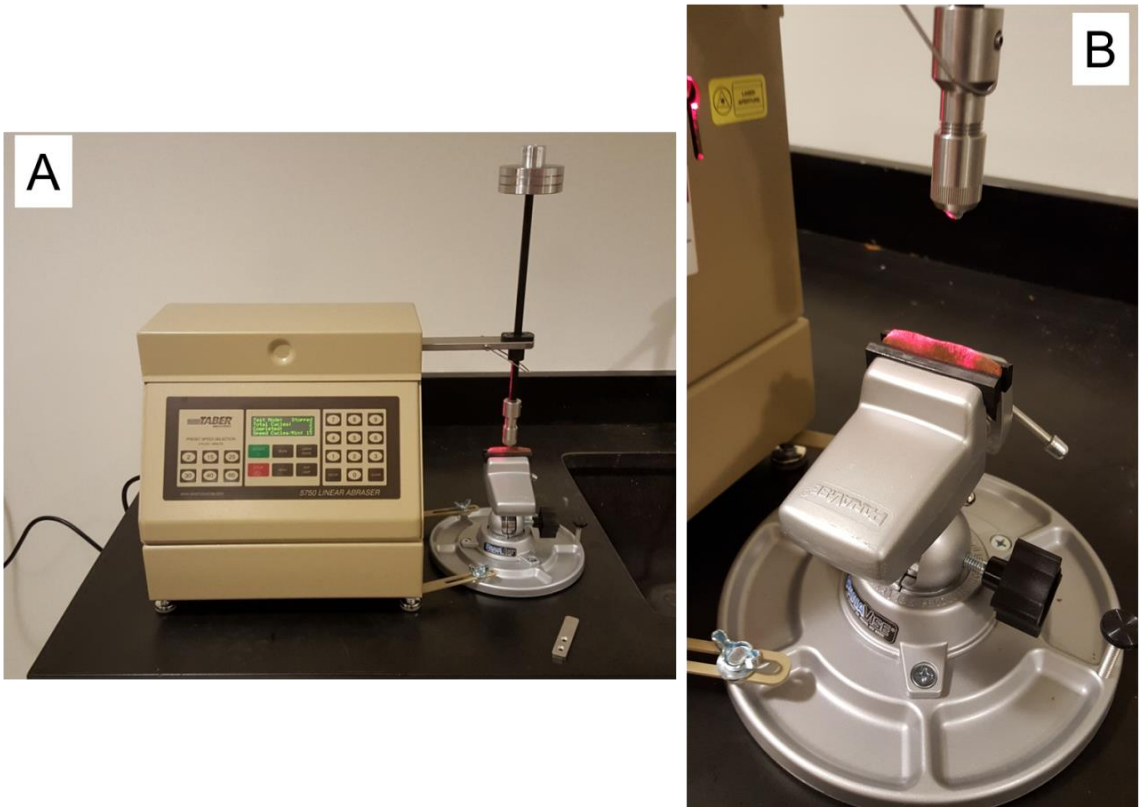

Figure 41. Taber Linear Abraser setup. A) Machine fully assembled. Note the horizontal arm with attached free-floating vertical boom with weights and abrasion tip on the right, B) Universal sample holder allowing for holding the stone tool with edge up. Note the red light, which is the guiding laser to allow for aligning the stone tool edge with the path of the abrader.

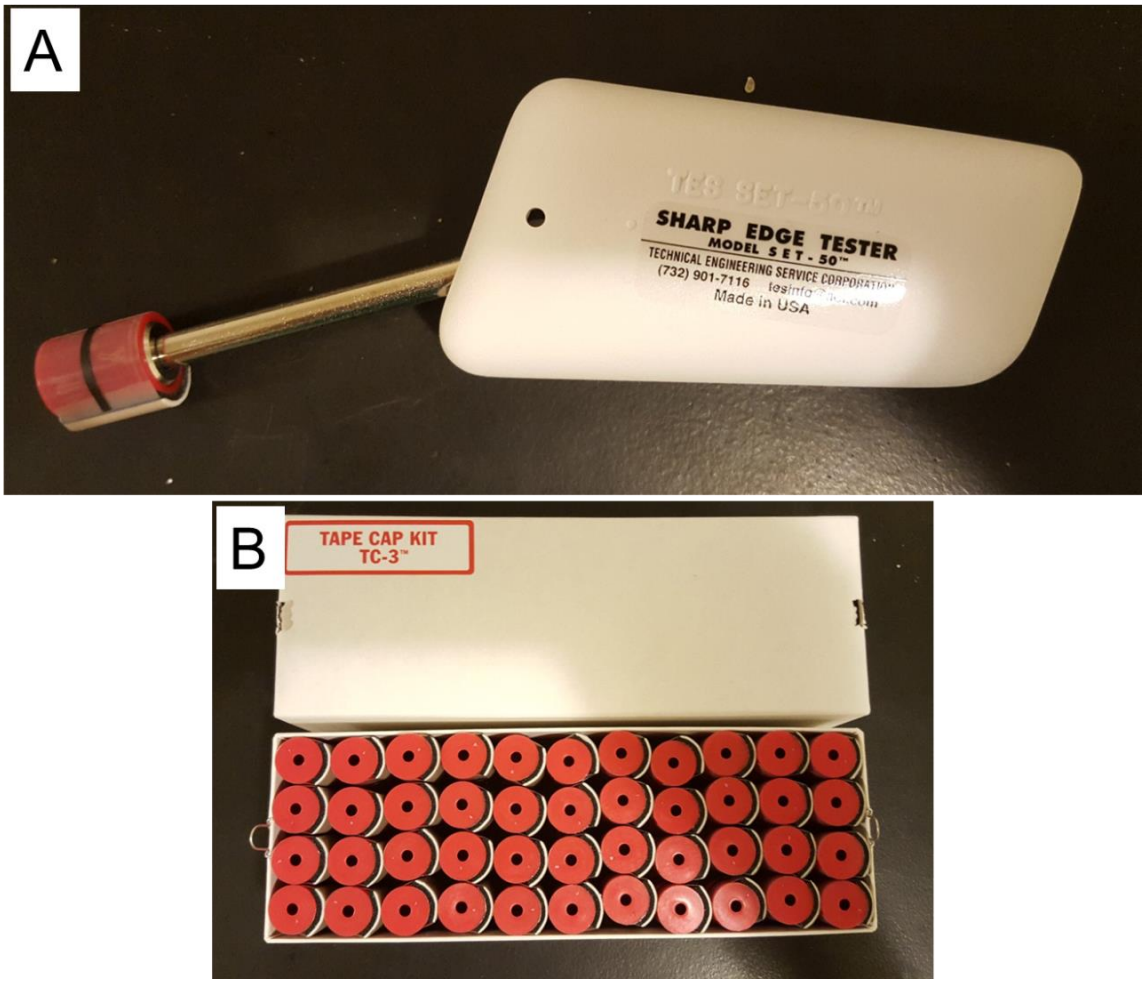

Figure 42. TESC sharp edge tester. A) Sharp Edge Tester Model SET-90. B) Tape caps in TC-3 kit.

The Taber Linear Abraser (http://www.taberindustries.com/linear-abraser) provided a standardized and replicable method to create consistent damage on a tool cutting edge. It is engineered to test either contoured or flat surface. It incorporates a horizontal arm that reciprocates in a linear motion. Attached to the end of the arm is a free-floating test system that is placed onto the stone tool cutting edge at the start of each test. As the arm with the free-floating system cycles back and forth, a spline shaft raises or lowers as the abrader attachment follows the contours of the cutting edge being tested. A stainless steel bit was used as the abrasion material to control for abrasion material on

all samples. The goal of the experiment was to measure the length of time the edge of a tool lasts when cutting a material, which is effectively a measure of raw material durability. The experiment was conducted in a controlled lab environment at ASU. The author randomly selected 140 complete tools for both quartzite and silcrete (70 untreated and 70 heat-treated) from the pilot study for this experiment.

Each stone tool sample had a straight edge controlling for documented variation in edge attrition associated with edge shape (Collins 2008) and had a standardized size based on archaeological material from the Mossel Bay region and the pilot study (length: 40-80 mm). Several steps were taken to obtain the *d* value. 1) Three edge angle measurements along the 2 cm part of the edge to be abraded were measured using the caliber technique (Dibble and Bernard 1980, Eren and Lycett 2016, Key and Lycett 2015). The average of the three measurements was recorded as the edge angle for each tool. The edge angles from the randomly selected tools ranged from ~15 to 60 degrees. 2) Photos of dorsal and ventral sides plus dorsal and ventral close-ups of the 2cm abrasion part were taken (**Figure 43**). 3) A tool sample was placed in the sample vice of the Taber linear abrader and then a TESC testing cap was used to record whether the tool could cut the testing cap before being abraded. 4) The linear abrader bit was placed on the tool edge at one end of the 2 cm testing area (**Figure 43**), and then the abrader was run for 2 seconds. 5) The sharpness test was redone using a TESC testing cap. If the sample failed to cut the TESC testing cap the sample was removed and re-photographed the same way as before abrasion. If the sample could still cut the cap, the abrasion bit was lowered back onto the edge and the abrader was run for 3 seconds. 6) A cycle of retesting with a TESC testing cap and abrading the edge more (5 seconds at the time) was conducted until the

edge could not cut the TESC testing cap. All samples were photographed again after being abraded the same way as before abrasion. 6) The mass (grams) of the sample after abrasion was measured.

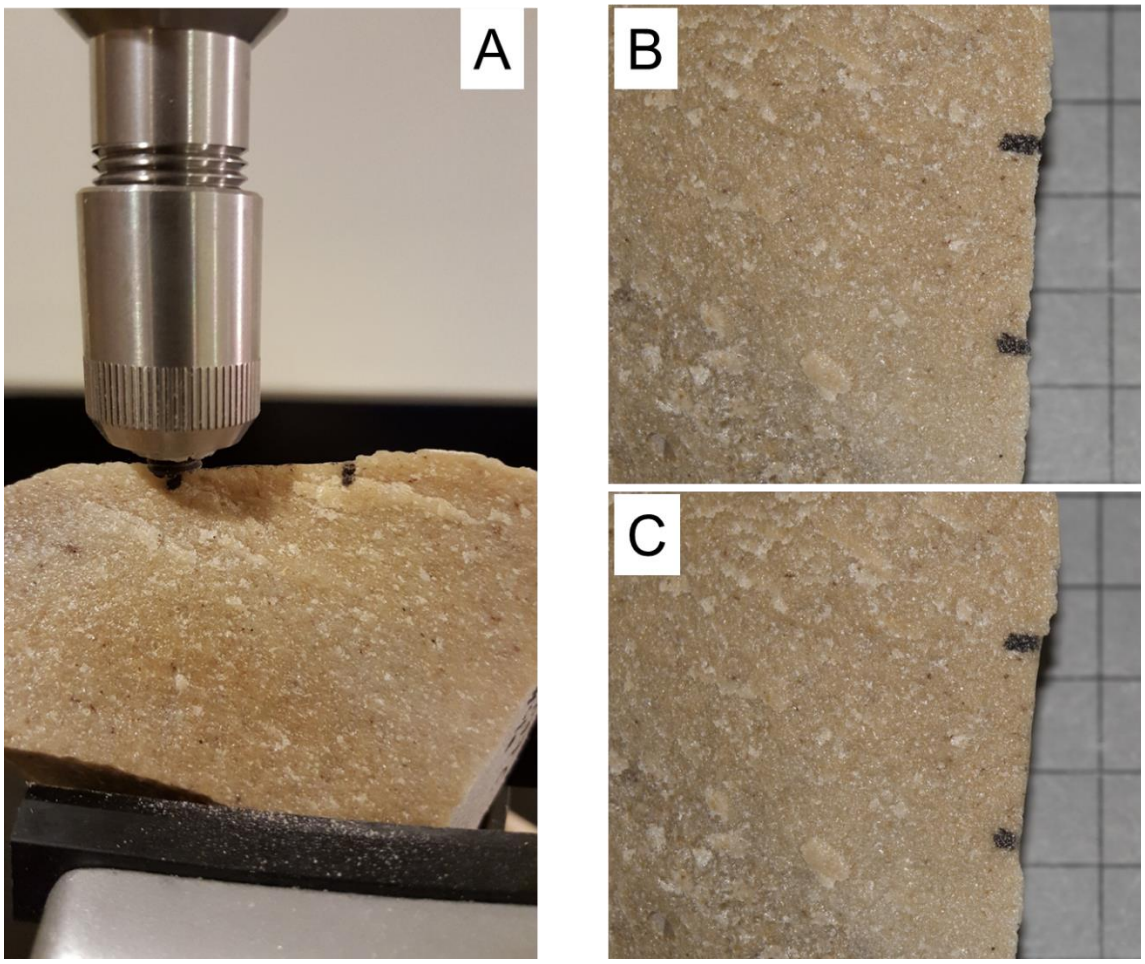

Figure 43. Edge abrasion. A) Abrasion tip resting on stone tool edge. Note, two black marks that show the 2cm area to be abraded. B) Ventral side of the sample before abrasion. C) Same sample after abrasion.

After abrading all samples and measuring their time to dullness (durability), the relationship between edge angle (degrees) and time to dullness (minutes) was examined using regression analysis. For quartzite and heat-treated silcrete samples there were significantly moderate (r= 0.3 to 0.5) relationships between edge angle and durability, while for untreated silcrete samples there was a significantly strong (r=0.5 to 1)

relationship between edge angle and durability. **Figure 44** shows the significant moderate relationship for all quartzite samples (r^2=0.5233; p=<0.0001). **Figure 45** shows the significant strong relationship for all untreated silcrete samples (r^2=0.6472; p=<0.0001). **Figure 46** shows the significant moderate relationship for all heat-treated silcrete samples (r^2=0.450; p=<0.0001).

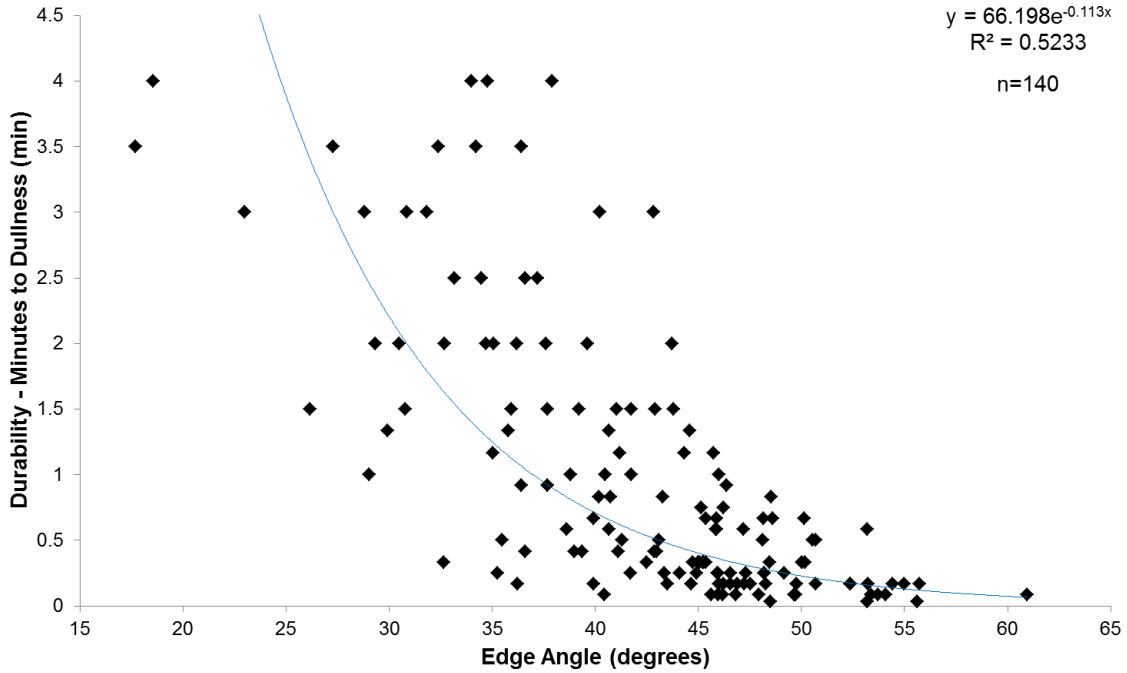

Figure 44. Relationship between edge angle and durability (time to dullness in minutes) for quartzite tools.

The linear regression results showed that all three raw material sample types do not exhibit the same relationship between edge angle and durability. Quartzite and untreated silcrete samples can best be explained by an exponential relationship where an increase in edge angle exponentially increases the time to dullness (minutes). Heat-treated silcrete samples can be best explained by a linear relationship. The difference in relationships between the samples suggests that quartzite and untreated silcrete should have exponentially increased time to dullness as the edge angles get acuter relative to

heat-treated silcrete samples. What that means is that heat-treated silcrete should be at a disadvantage in terms of time to dullness when only acute edge angles are considered. A subsample was selected to quantify the *d* variable (average edge angle: ~0-40 degrees) using edge angles similar to edge angles ethnographically observed on tools used for butchery (Gould, Koster, and Sontz 1971). In total, measurements from 54 quartzite samples, 28 untreated silcrete samples, and 35 heat-treated silcrete samples were used for quantifying the *d* variable.

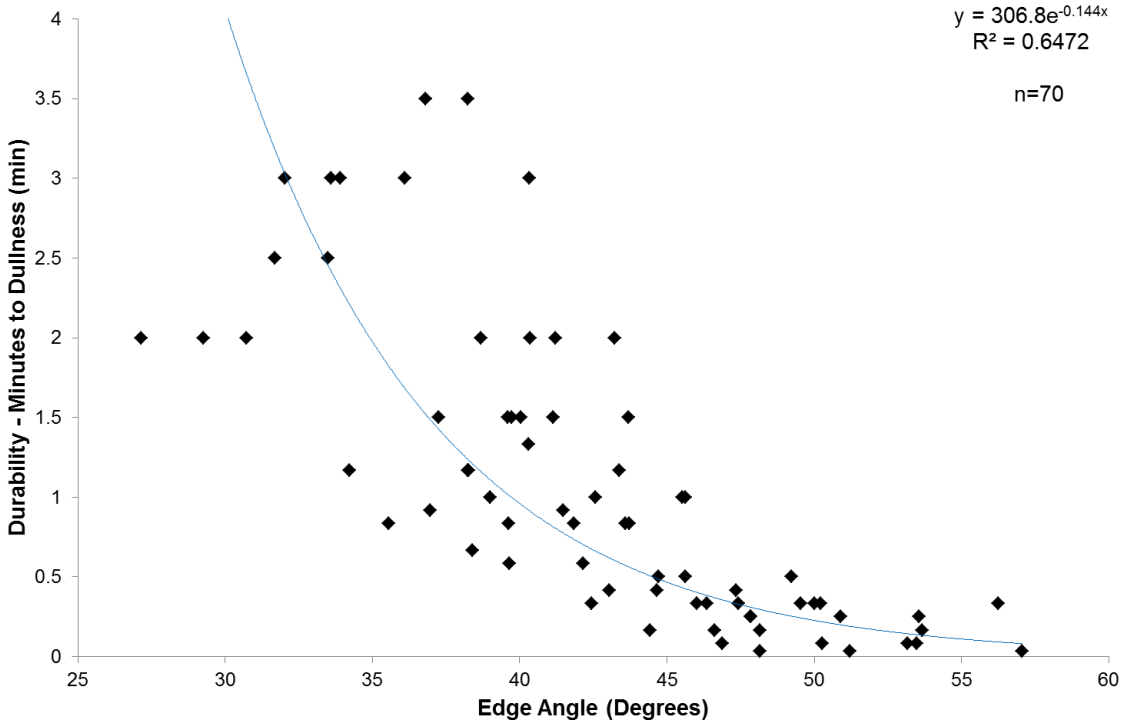

Figure 45. Relationship between edge angle and durability (time to dullness in minutes) for untreated silcrete tools.

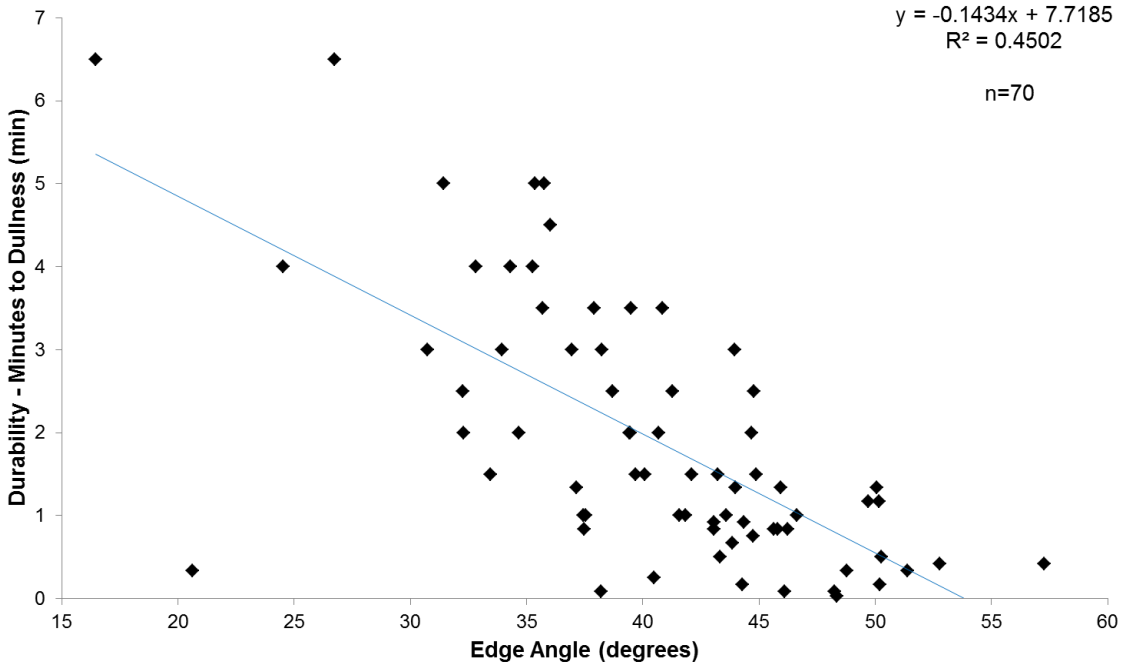

Figure 46. Relationship between edge angle and durability (time to dullness in minutes) for heat-treated silcrete tools.

Travel and search cost

To calculate the travel and search time cost (t_s) needed in the ACM-R several steps were taken. 1) Geological maps of the Mossel Bay region were georectified and projected in ArcMap 10.4. 2) Using GPS coordinates of the potential raw material sources obtained by extensive raw material surveys (Brown 2011, Oestmo et al. 2014) these sources were created into polygon shapefiles and projected in the same map space. Then the location of the Pinnacle Point sites was projected on the same map. A centroid location located halfway between PP5-6 and PP13B was used as the representative location for all Pinnacle Point sites. Using the measure distance tool the distance between Pinnacle Point and the closest Quartzite and silcrete source during all different model conditions obtained. Then, assuming a walking pace of 3.5 km/hr (Marlowe 2010, Marlowe 2006) the search and travel time-cost (t_s) for each source were calculated (time =

distance/speed). **Table 12** shows the distance to and from the closest known quartzite and silcrete sources during MIS5 and the travel and search time (min) values for t_s used in the ACM-R variant. **Table 13** shows the distance to sources and the travel and search time (min) values for t_s for sources during MIS4 and MIS6 used in the ACM-R variant. Note that the analysis considered both the scenario with an offshore hardground assumed to be a silcrete source and the scenario where no offshore silcrete is present.

Table 12. Summary of GIS calculations and survey data on travel and search time-cost.

Model Condition	Raw Material	Closest Source	Travel Distance To and From Closest Source(km)	Assumed Walking Pace (km/hr)*	Travel and search time (min) (t_s)
MIS5	Quartzite	Eden Bay	0.7	3.5	12.7
MIS5	Silcrete	Rietvlei	17	3.5	291.4

*walking pace from Marlowe (2010, 2006).

Table 13. Summary of GIS calculations and survey data on travel and search time-cost during MIS4 and MIS6 conditions.

Model Condition	Raw Material	Closest Known Source	Travel Distance To and From Closest Source(km)	Assumed Walking Pace (km/hr)*	Travel and search time (min) (t_s)
MIS4	Quartzite	Robberg Formation	10.5	3.5	180
MIS6	Quartzite	Wave-ravinement surface	2.9	3.5	48.8
MIS4&MIS6-With a Paleo-Agulhas pain silcrete source	Silcrete	Submerged Hardground	1.6	3.5	28
MIS4&MIS6-Without a Paleo-Agulhas pain silcrete source	Silcrete	Rietvlei	17	3.5	291.4

*walking pace from Marlowe (2010, 2006).

Procurement cost

Procurement time in this study is the time it takes to find a rock suitable for knapping after a raw material source is encountered. To calculate the procurement time-cost (t_p) needed in the ACM, survey data collected by Brown in 2012 was used. Brown, when encountering a source, measured the time (in minutes) it took to find suitable raw material to flake. **Table 14** shows the T_p values used in both variants of the ACM.

Table 14. Summary of survey data on procurement time-cost.

Model Condition	Raw Materials	Number of Surveyed Sources (n=)	Type of source	Average Procurement Time (min) (t_p)
MIS5	Quartzite	1	Primary Quartzite	5.4
MIS5	Silcrete	8	Primary Silcrete	8.1
MIS4 & MIS6	Quartzite	7	Secondary Quartzite (cobble beach)	5
MIS4 & MIS6	Silcrete	8	Primary Silcrete	8.1

Manufacturing cost – Wood fuel travel and search cost and heat-treatment cost

Ethnographic and cultural anthropology literature was surveyed to obtain estimates of wood fuel travel and search time cost (m_1). Observations from traditional and rural societies from across Africa (Biran, Abbot, and Mace 2004, Brouwer, Hoorweg, and Van Liere 1997, Fleuret and Fleuret 1978, Madubansi and Shackleton 2007, Tabuti, Dhilliona, and Lye 2003) were used to estimate the average time-cost that traditional groups accrue when procuring wood fuel for consumption.

Tabuti et al. (2003) showed that women in Bulamogi County, Uganda search for and collect firewood between 2-3hours (120-180 minutes) and walk rarely more than 2km to forage wood. Biran and colleagues (2004) noted that Malawian women living

around Lake Malawi National Park use on average ~4 hours (241 minutes) to search for and collect firewood and walk on average 4.2 km to forage wood. However, wood collecting does not happen every day. The mean daily time spent collecting wood is 63 minutes. Further, Biran and colleagues (2004) noted that Maasai women living in Simanjiro, Tanzania use on average 1.5 hours (90 minutes) to search for and collect firewood, and walk on average 2.2 km to forage wood. Here the mean daily time is 10 minutes. Brouwer et al. (1997) reported on a survey from the Ntcheu District in Malawi. They find that in four different villages that the collection distances people walk to obtain firewood on average ranges between 1.1 to 4 km, while the average time spent searching for and collecting firewood ranges between 2-5 hours (120-300 minutes). Madubansi and Shackleton (2007) reported that people living in the Bushbuckridge Lowveld in South Africa use on average between ~4-4.5 hours (~239-268 minutes) to search for and collect firewood per wood collection trip.

Table 15 shows the $m_1$values used in both variants of the ACM. To keep the m_1 calculations similar to the t_s variable a walking pace of 3.5km/hr was used (Marlowe 2010, Marlowe 2006). It was assumed that the exposed heat-treatment method does not require extra wood fuel in addition to the normal load brought home during daily foraging trips, meaning that during daily wood foraging trips the wood collected then also is enough to heat-treat the silcrete. Conversely, it was assumed that the insulated heat-treatment method requires at least twice as much wood fuel as collected during a normal wood collecting foraging trip thereby resulting in a doubling of the search and travel time to procure the wood. Additionally, it was assumed that during MIS4 when there is an increase in C4 grasses with a component of trees it lowered the search and travel cost for

wood fuel to be more comparable to the exposed method even through twice as much wood fuel is needed.

Table 15. Summary of wood fuel travel and search time-cost.

Model Condition	Heating Scenario	Assumed Walking Pace (km/Hr)*	Wood Fuel Travel and Search Time (min) (m_1)	Comment
MIS5	Insulated	3.5	180	20kg wood fuel needed, 3 hours Travel and Search
MIS4	Insulated	3.5	90	20kg wood fuel needed, 1.5 hours Travel and Search
MIS6	Insulated	3.5	180	20kg wood fuel needed, 3 hours Travel and Search
MIS5	Exposed	3.5	90	10kg wood fuel needed, 1.5 hours Travel and Search
MIS4	Exposed	3.5	90	10kg wood fuel needed, 1.5 hours Travel and Search
MIS6	Exposed	3.5	90	10kg wood fuel needed, 1.5 hours Travel and Search

*walking pace from Marlowe (2010, 2006).

Heat-treatment time-cost (m_2) was obtained from heat-treatment experiments conducted by Brown (2009) and Schmidt and colleagues (2015, 2013). **Table 16** shows the m_2 values used in both variants of the ACM. During the insulated method, time will be spent starting the fire but after that the fire can be left to itself because the silcrete is buried in the sand below the hearth and does not need extra attention. Conversely, during the exposed method extra attention needs to be paid to the samples, as they are placed directly in the ash cone below flames or underneath coals in direct contact with heat. Because there is an increased risk of destroying the samples (Wadley and Prinsloo 2014), more time needs to be spent monitoring the fire.

Table 16. Summary of heat-treatment time-cost.

Heat-treatment method	Heat-treatment time (min) (m_2)	Comment
Insulated	15	15 min needed to start fire
Exposed	50	50 min annealing needed

ACM analytical methods

To evaluate the ACM outcomes under the coastline positions and raw material source distribution, vegetation type, and mobility rate and strategy variables and test predictions for each variable, the ACM experimental data were bootstrapped 10000 times using a simple bootstrapping procedure. The bootstrapped standard errors were used to create 95% confidence intervals around the means to statistically investigate if the outcomes were significantly different. To be able to conduct a bootstrap variance is needed. For the e (cutting edge per mass), d (cutting edge durability), and m_3 (flake manufacturing time-cost) variables the variance was created organically by the different experimental outcomes. For the t_s (travel and search time-cost), t_p (procurement time-cost), m_1 (wood fuel travel and search time-cost) and m_2 (heat-treatment time-cost) variables variance was created by taking variable estimate for a model condition and dividing it by the total flaked core mass of each individual raw material block used in the flaking experiment. For quartzite that meant 20 measurements of for example travel and search time-cost (e.g. 12.7 minutes travel and search / 1.96 kg total flaked core mass = 6.47 travel and search time (min) per total flaked core mass (kg)).

The resource-choice model equations outlined above were used to calculate which raw material net-return rate is the greatest during different model conditions. Pq and Ps, and Rq and Rs were solved for by plugging in the measurements from the GIS analysis,

field survey data, flaking experiment and edge durability experiment. The data was bootstrapped 10000 times using a simple bootstrap procedure. The bootstrapped standard errors were used to calculate 95% confidence intervals around the means to statistically investigate the different outcomes of the net-return rate.

Archaeological data

The archaeological material originates in stone tool assemblages from PP5-6, PP9, PP13B (Brown 2011, Brown et al. 2012, Brown et al. 2009, Thompson, Williams, and Minichillo 2010, Wilkins et al. 2017, Wilkins et al. 2014). This data has been coded during several coding sessions. This author conducted a statistical analysis on the coded data, focusing on summarizing raw material frequency, artifact type frequency, artifact metric attributes, cortex type frequency, cutting edge length/mass ratio, and the ratio of frequency of retouch to artifact volumetric density. The data was summarized at different levels of resolution: all data was first summarized by marine isotope stages for the different localities, and then the data was summarized by stratigraphic aggregates at the different localities, Finally, for raw material frequencies, the data was summarized at the sub-aggregate level.

Raw material percentages are typically presented based on artifact counts. However, tallying raw material frequency by count is susceptible to taphonomic bias due post-depositional breakage of artifacts and on-site flaking of a given raw material package, which can overemphasize the contribution a raw material type has to the overall raw material frequency (Brown 2011, 1999). Total mass (kg) of each raw material in a given assemblage should reflect what has been transported and deposited at a locality,

acting as a proxy measure for the cost of transporting raw material to the site, instead of what has been flaked thereby increasing the count of a particular raw material or fragmented after being deposited at a locality (Brown 2011). Because the models evaluated in this study deal with procurement and transport of raw materials, the frequencies resulting from tallying by mass will be reported.

Cortex type is potentially a useful indicator of the source of a raw material. The roundness of a cortex of a raw material clast reflects the amount of reworking and/or transport by kinetic energy (Stow 2007). Generally, when the kinetic energy is increased it results in clasts with more rounded cortex (Stow 2007). Field observations in the Mossel Bay region suggests that high-energy environments such as cobble beaches and active stream beds produce on average more clasts with well-rounded to rounded cortex (also referred to as cobble cortex), while fixed geological structures such as cliffs or outcrops tend to produce cortex that is more sub-angular to very angular (also referred to as outcrop cortex) (Oestmo et al. 2014).

The cutting edge length/mass ratio was estimated for all complete artifacts with a maximal dimension greater than 14mm using the CE/M ratio equation formulated by Mackay (2008). As mentioned above, cutting edge per mass ratio is a proxy for flaking efficiency (Braun 2005, Brown 2011, Mackay 2008). Flaking efficiency is in this study referring to the degree to which a cutting edge of a stone tool is maximized for the amount of raw material used (Andrefsky Jr 1994, Bar-Yosef and Kuhn 1999, Braun 2005, Clark 1987, Hofman 1987, Mackay 2008, Nelson 1991, Parry and Kelly 1987, Sheets and Muto 1972, Wilkins et al. ms). It is not referring to the degree to which a cutting edge is maximized for a given mass of raw materials after retouch (Eren, Greenspan, and

Sampson 2008), and it does not refer to the maximization of usable blanks (Jennings, Pevny, and Dickens 2010).

The ratio of frequency of retouched artifacts to artifact volumetric density will be based on methods developed by Riel-Salvatore and Barton et al. (Barton, 1998; Riel-Salvatore and Barton, 2004; Riel-Salvatore et al., 2008). Barton (1991, 1990) suggested that the shape and the frequency of retouched tools may be related more to the intensity of which a site was occupied or reoccupied rather than being either the residue of ethnic groups (Bordes 1973, Bordes, Kelley, and Cinq-Mars 1969) or the result of different functions (Binford 1979, 1973). Building on that argument, Riel-Salvatore, Barton, and colleagues (Barton, 1998; Riel-Salvatore and Barton, 2004; Riel-Salvatore et al., 2008) created a method that incorporates measures of artifact volumetric density and relative frequency of retouched pieces. Because they assumed that there is a direct relationship between relative frequency of retouched tools and artifact volumetric density, and that they analyze whole assemblages including tools and debitage, and that they view morphological variability of retouched lithics as a function of the variations in the length and nature of use life of the retouch lithics, they can use their method as a heuristic device to reconstruct time-averaged land-use patterns (Riel-Salvatore et al. 2008). In their model, a higher frequency of retouched tools and low artifact volumetric density are associated with residential mobility because residentially mobile foragers are assumed to conserve their raw materials by curation due to raw material scarcity, which can be due to both their mobility pattern and relative abundance of raw material sources. On the other hand, a low frequency of retouched tools and high artifact volumetric density is associated with logistical mobility because logistically mobile foragers are assumed to

not conserve their raw materials due to raw material abundance, which can be due to local availability, embedded procurement, and stockpiling of raw materials at the site (Riel-Salvatore and Barton 2004). Their method offers, because of its focus on mobility and technological organization, "a means to assess whether technological changes are paralleled by changes in mobility strategies, as they can legitimately be expected to be." (Riel-Salvatore et al. 2008: 405).

A Bonferroni correction was not used in the analysis of the archaeological data because a single false positive in this set of tests is not a problem. The Bonferroni correction is useful when only a few multiple comparisons are undertaken and you are testing to see if one or two might be significant. However, in this case, where there are a large number of multiple comparisons and where many are potentially significant the Bonferroni correction can lead to a very high rate of false negatives (http://www.biostathandbook.com/multiplecomparisons.html).

To evaluate H_1, H_2 and H_3, and test model predictions for the different model conditions variables the archaeological raw material frequency data were bootstrapped 10000 times using a simple bootstrap procedure. Data from stratigraphic aggregates and sub-aggregates were used to allow for potential variance in raw material frequency. The bootstrapped standard errors were used to create 95% confidence intervals around the means to statistically investigate if the raw material frequencies were different.

To support Hypothesis 1 (H_1), the archaeological quartzite, silcrete and quartz frequencies needed to be statistically similar to any model simulation outcome from the OAM during any model condition or the ranking of model raw material frequencies need to match the ranking archaeological raw material frequencies. To support either

Hypothesis 2 (H_2) or Hypothesis 3 (H_3), the raw material with the highest frequency during any model condition (MIS4, MIS5, and MIS6) needed to be equivalent to the raw material with the highest net-return rate during the same model conditions.

Methods summary

The models presented in this study require a range of methodological steps to be operationalized. The building blocks of the OAM include geological and geophysical data, raw material survey data, GIS analysis, and agent-based modeling. A specific set of steps needs to be executed: 1) build the GIS dataset that includes the geological and geophysical data; 2) export this data to Netlogo for simulations; 3) after simulations the output data needs to be formatted and adjusted based on raw material survey data to be able to obtain raw material frequencies usable for comparison with archaeological data.

The ACM used a stone tool reduction experiment, a raw material quality and fracture mechanics experiment, published data, raw material survey data, and GIS analysis to obtain estimates of variable values. For this model, the sequence of events is not tightly constrained except that a standard stone tool attribute analysis (length, width, mass etc.) needs to be undertaken first, then the durability experiment can be undertaken to obtain time to dullness of the edges. Estimates of the other model variables can be obtained at any time in any sequence.

CHAPTER 7: PINNACLE POINT ARCHAEOLOGICAL RECORD

Site chronology and stratigraphy overview

Pinnacle Point (PP) is a geographical location centered on a small headland about 10 km west of the Mossel Bay point (**Figure 1**). The coastal cliff between Pinnacle Point and Mossel Bay point is heavily dissected and displays a range of caves and rock shelters. The rockshelters and caves are formed in the quartzitic cliffs that belong to the Table Mountain Sandstone Group (Karkanas and Goldberg 2010, Marean et al. 2004, Pickering et al. 2013). Archaeological excavations have been ongoing since 2000 with early work focusing on PP13B, then PP9 and lately at PP5-6 (Marean et al. 2004). The Pinnacle Point caves and rock shelters are argued to have formed roughly 1 ma ago (Pickering et al. 2013). Presently the archaeological record dates from ~162 ka to 51 ka (Brown et al. 2012, Jacobs 2010, Karkanas et al. 2015). It is possible to extend that record backward and forward in time. However, due to high sea-level stands during MIS11 any deposits in caves or rock shelters lower than +20 m prior to MIS11 will be limited but there are some present in PP13G and Opera House Cave (Pickering et al. 2013) in addition to PP9.

Excavated sediments at Pinnacle Point sites are at the coarsest scale divided into stratigraphic aggregates (StratAggs). The StratAggs are defined based on broad-scale sedimentological change. StratAggs are horizontally continuous entities that represent a sedimentologically homogeneous set of formation processes but can be composed of thinner layers dominated by either anthropogenic or geogenic processes. The formation processes are recognized based on field observations, micromorphology, and GIS-based analysis of the structure of plotted finds provenience (Brown et al. 2012, Karkanas et al. 2015, Oestmo and Marean 2015, Wilkins et al. 2017). StratAggs are further subdivided

into sub-aggregates (SubAggs), which captures more subtle changes in sedimentation and normally are predominantly geogenic or anthropogenic in formation process. SubAggs are horizontally continuous beyond a 1x1 square and typically present themselves as palimpsests of combustion features with a high density of artifacts that are interstratified with geogenic units (Wilkins et al. 2017). Within SubAggs even smaller units of stratigraphic units called StratUnits are present. The StratUnits represents small stratigraphic lenses and features and capture the most subtle sedimentological changes in terms of color and texture (Marean et al. 2004, Oestmo and Marean 2015). A StratUnit does not typically extend horizontally beyond a 50x50 cm quadrant. When a StratUnit does extend beyond a quadrant it is further divided into Lots. A Lot represents the smallest unit within the stratigraphic grouping system used at Pinnacle Point and is the scale of which excavation occurs at Pinnacle Point. All excavated finds are piece-plotted using a total station, which yields a 3D provenience of each find (Marean 2010b, Marean et al. 2004, Oestmo and Marean 2015).

In the following sections, I will provide a summary of the relevant major StratAggs at sites PP13B, PP9, and PP5-6 using already published data. The summaries will be given in connection with available age estimates allowing for an MIS designation. After the stratigraphy and chronology overview, I will present the stone tool data from these sites that are relevant for evaluating archaeological expectations resulting from testing predictions derived from the model condition variables and the testing of the hypotheses presented earlier. Stone tool data will be presented first by MIS Designation using the major StratAggs from the three different sites. Then the data will be presented

by StratAggs from the three different sites. When applicable the data will also be presented by SubAggs.

PP13B

Excavations at PP13B started in 2000 and concluded in 2008, and have yielded a complex depositional and erosional history (Marean et al. 2010, Marean et al. 2004). PP13B is located roughly 300 meters to the southwest of PP5-6 (**Figure 2**). The excavations have yielded the earliest secure date of shellfish consumption by modern humans (Marean et al. 2007), early securely dated modified pigments (Marean et al. 2007, Watts 2010), the presence of heat-treatment of silcrete (Brown et al. 2009), and the potential use of shells as symbolic objects (Jerardino and Marean 2010). Thompson et al. (2010) reported on the lithics from the sequence. They argued that the PP13B sequence shows little size-related change over time but there is evidence for varying reduction strategies between the different areas that have been excavated.

Excavations at PP13B have focused on three areas called: Northeastern, Eastern, and Western. Below I will summarize the context of the stratigraphic aggregates/units that contain archaeology present at these three areas. The stratigraphy and artifact context summary will follow from Marean et al. (2010), Bernatchez (2010), Karkanas and Goldberg (2010), and Herries and Fisher (2010), while the stone tool summary comes from Thompson et al. (2010).

Northeastern area

LC-MSA Lower: Compared to the overlaying LC-MSA Middle and Upper sedimentary units, the LC-MSA Lower sediments are the archaeologically richest and are the least cemented (Marean et al. 2010). The sediments contain multiple lenses of carbonaceous materials that appear heavily burnt and magnetic susceptibility (MS) testing of these lenses show presence of anthropogenic activity (Herries and Fisher 2010, Marean et al. 2010). Some of these combustion features are in situ and appear very fine with hearth cleanout separating them while others have been disturbed by trampling (Karkanas and Goldberg 2010, Marean et al. 2010). Three OSL ages result in a weighted mean age of 162±5ka making these sediments date to MIS6 (Jacobs 2010, Marean 2010b). The lithic assemblage is dominated by quartzite, with blades more common than points. There are few 'Levallois' flakes. There are slightly more plain platforms than facetted platforms. Retouch is rare. Prepared cores are the most common core type (Thompson, Williams, and Minichillo 2010).

LC-MSA Middle: The sediments contain multiple lenses of dark organic matter and ash that contain charcoal and *in situ* hearths. There is some evidence of trampling and cobbles and roof fall is common (Karkanas and Goldberg 2010, Marean et al. 2010). Comparable to the underlying LC-MSA Lower the MS signal and lithic density is moderate, while marine shellfish densities are high (Herries and Fisher 2010, Marean et al. 2010). The sediments have an OSL age of 125 ± 5ka (Jacobs 2010) indicating that the sediments belong close to the transition from MIS6 to MIS5 (Marean et al. 2010). The presence of shellfish in the deposits suggests a date in the later part of the transition perhaps to MIS5e (Jacobs 2010, Marean et al. 2010).

LC-MSA Upper (Lower Dune): These sediments cap the anthropogenic sequence and are composed of multiple heavily cemented layers. There are several phases of cementation. These cementation events postdate the deposition of the layers in the LC-MSA sequence and they both stabilized and hardened the archaeological deposits and the two aeolian dunes that sealed the deposits (Karkanas and Goldberg 2010, Marean et al. 2010). Compared to the LC-MSA Middle and LC-MSA Lower deposits the lithic density and the MS are both lower (Herries and Fisher, 2010), which suggest a decrease in occupation intensity (Marean et al. 2010). There is some evidence of slight aeolian activity, very low energy water flow and gravity (Bernatchez 2010, Karkanas and Goldberg 2010, Marean et al. 2010).

Summarized from Marean et al. (2010) three layers are recognized within the aggregate: 1) a lower, harder sandy and silty layer with multiple lenses of black to dark brown organic matter that lays directly on top of the richer archaeological deposits of the underlying LC-MSA Middle. 2) A sandy horizon with a weighted mean OSL age of 126 ± 4 ka (Jacobs 2010) that contains a lens with shellfish, which suggest that this layer dates to MIS5e (Marean et al. 2010). 3) A dune that caps the LC-MSA Upper deposits and has a weighted mean OSL age of 93 ± 4 ka (Jacobs 2010). This dune closed the cave to human occupation (Karkanas and Goldberg, 2010; Marean et al. 2010). Further, a flowstone that caps the ~93 ka dune has a U-Th date of ~92 ka proving a minimum age of the LC-MSA Upper (Marean et al. 2010, Marean et al. 2007).

Thompson et al. (2010) noted that the LC-MSA Middle and Upper lithics assemblages are dominated by quartzite but there is an increase in silcrete use compared

to underlying LC-MSA Lower. Facetted platforms are more common as well as blades compared to points. There are few formal tools.

Eastern area

Lower Roof Spall: The Lower Roof Spall (Roof Spall-Lower) sediment are stratified on top of the bedrock and is an MSA horizon consisting of a clast supported matrix primarily made up by roof spall, and cemented patches and sand in some places (Karkanas and Goldberg 2010, Marean et al. 2010). Archaeological finds are sparse. Two OSL ages both at 110 ± 4 ka (Jacobs 2010) indicate that these deposits date to MIS5 (Marean et al. 2010).

Upper Roof Spall and Shelly Brown Sand Facies: The Upper Roof Spall (Roof Spall-Upper) and Shelly Brown Sand aggregates overlap and blend together. The sediments consist of connected or isolated thin burning layers that are sometimes visible in the matrix as stratified small, thin, well-preserved hearths (Karkanas and Goldberg 2010). These hearths sometimes have lithics and fauna associated with them, laying in and besides the hearths. The hearths have distinct layering consisting of bands of ash, charcoal, and reddish-colored baked sediments (Karkanas and Goldberg 2010). Overall, lithics, fauna, and shell artifacts are dense in these deposits. The MS signal is also high (Herries and Fisher 2010). Where the Shelly Brown Sand aggregate is positively recognized the density of shellfish is particularly high. Six OSL ages indicate that these sediments have an adjusted maximum age of 98 ka and an adjusted minimum age of 91 ka (Jacobs 2010), which indicates that the archaeological remains where deposited during MIS5 (Marean et al. 2010).

The lithics assemblages from the eastern area during MIS5 are dominated by quartzite. Facetted platforms are slightly more common. Blades are also more common than points. Prepared and point cores occur. There is evidence for rare scraper retouch but other than that there are very few formal tools (Thompson et al. 2010).

Western area

LB Silt: The sediments of the LB Silt aggregate are poorly sorted silty sands with significant guano input (Marean et al. 2010). There is a stabilizing surface and increased organic input towards the top of the layer that leads to archaeological layers. However, artifact density and MS (Herries and Fisher 2010) are both low. An OSL age of 157 ± 8 ka (Jacobs 2010) indicates that these deposits date to MIS6 (Marean et al. 2010).

Thompson and colleagues (2010) note that the lithics assemblage from the western area that dates to MIS6 is dominated by quartzite. Points are more common accompanied by a higher frequency of point cores, while bladelets are infrequent. There are slightly more plain platforms than facetted platforms. There is evidence for rare scraper retouch as well as other types of retouch.

Dark Brown Sand Facies (DB Sand) – DB Sand 4(a-c): The DB Sand facies are defined based on their dark greasy brown sandy characteristics. The dark layers are interstratified with lighter brown to gray sandy horizons (Karkanas and Goldberg 2010, Marean et al., 2010). There are low to moderate artifact density but the dark nature of the material and sediments suggest burning, which is supported by the MS signal (Herries and Fisher 2010). All the sediments have a strong Aeolian sand input (Karkanas and Goldberg 2010, Marean et al. 2010). More specifically, the DB Sand 4 aggregates (a, b,

and c) are a set of dark brown lenses stratified within the LBG Sands with DB Sand 4c at the base (Karkanas and Goldberg 2010, Marean et al. 2010). There is a slight increase in artifact density compared to the underlying LB Silt but the MS signal remains low (Herries and Fisher 2010). Numerous skeletal remains of large animals (size 4) are present in association with several hammerstones in the DB Sand 4 (Marean et al. 2010). The surface of DB Sand 4c consists of decayed organic matter that suggests exposure for a long time, further indicating a living surface (Karkanas and Goldberg 2010, Marean et al. 2010). DB Sand 4b shows evidence for the first real charcoal and burnt bone layer in the western area. DB Sand 4a has abundant charcoal and suggests in situ burning (Karkanas and Goldberg 2010, Marean et al. 2010). An OSL age of 159 ± 7 ka (Jacobs 2010) indicates that the DB Sand 4 dates to MIS6 (Marean et al. 2010).

The Light Brown Gray Sand Facies (LBG Sand): The LBG Sand consists of lighter brown to gray sediments that are stratified below the DB Sand that is situated below DB Sand 3 (Karkanas and Goldberg 2010, Marean et al. 2010). One single LBG Sand layer was first recognized (LBG Sand 1) but now it is further subdivided into LBG Sand 2-4 where LBG Sand 2 is stratified under DB Sand 4a and so forth. Artifact density is lower in the LBG Sand layer than in DB Sand 4 lenses, and the sediments are less greasy (Karkanas and Goldberg 2010, Marean et al. 2010). In the LBG Sand 1 the sediments consist of decalcified sediments of Aeolian sand with a guano input (Karkanas and Goldberg 2010, Marean et al. 2010). The lower LBG Sand layers (2-4) consist of a mixture of roof spall and Aeolian sand and guano input (Karkanas and Goldberg 2010, Marean et al. 2010). Two OSL ages in LBG Sand 1 at the contact with the overlying DB

Sand 3 have ages of 127 ± 7 ka and 122 ± 5 ka (Jacobs 2010) indicating that LBG Sand 1 dates to MIS5 (Marean et al. 2010).

Dark Brown Sand Facies (DB Sand) – DB Sand 3 and 2: The DB Sand 3 and 2 aggregates are not disturbed by subsidence events or cutting that occurred in the underlying layers and they are draped over the slumped LBG Sand 1 presenting a clean contact, which likely represents an erosion event (Karkanas and Goldberg 2010, Marean et al. 2010). DB Sand 3 is a dark greasy horizon that includes dense MSA material. It stands out visually due to its dark color and it is laterally extensive. It is stratigraphically underlain by the much lighter LBG Sand 1 (Marean et al. 2010). The sediments of DB Sand 3 consist of significant amounts of charcoal and burnt bone (Karkanas and Goldberg 2010). A Uranium-Thorium (U-Th) age of 102 ± 0.08 (Marean et al. 2010) in DB Sand 2 and the three OSL ages from LBG Sand deposits that overlays DB Sand 4 ranging from 127 ± 7 to 98 ± 4 ka (Jacobs 2010) indicates that DB Sand 3 and 2 dates to MIS5 (Marean et al. 2010).

Light Brown Sand Facies (LB Sand): LB Sand sediments are the light brown materials situated below the surface that have a high artifact density. The LB Sand 1 is situated above the dark greasy horizons of DB Sand 2, while LB Sand 2 is situated below (Marean et al. 2010). The lithic density is higher compared to the DB Sand units but the MS signal is lower (Herries and Fisher 2010). The sediments are coarse-grained with a high frequency of 1 to 5 cm roof spall (Karkanas and Goldberg 2010, Marean et al. 2010). An OSL age of 90 ± 4 ka (Jacobs 2010) from DB Sand 3 in the middle of the interstratified sequence and an OSL age of 90 ± 4 from just above DB Sand 3 indicates that the LB Sand facies dates to MIS5 (Maren et al. 2010).

The lithics assemblages from the western area that date to MIS5 are dominated by quartzite. Facetted platforms are more common than plain platforms. Prepared cores are common. Points are more common as well as point cores being more common than blade cores. There are very few formal tools (Thompson et al. 2010).

PP9

PP9 is a coastal cave complex situated roughly 200 meters northeast of PP13B and contains both archeological and geological deposits, as well as fossil micromammal accumulations (**Figure 2**). The archaeological sediments were excavated under the direction of Dr. Andy Herries. Information about PP9 is very limited except for a study focusing on micromammals (Marean et al. 2004, Matthews et al. 2011). The little information provided about the dating and stratigraphy of PP9 will be summarized from Matthews et al. (2011). Micromammals were analyzed from facies accumulated close to the transition from MIS6 to MIS5 with OSL ages of between 130±9 and120±7 ka (Matthews et al. 2011). The PP9 cave complex consists of a number of smaller separate cavities called PP9A-E. The archaeological material comes from PP9B and C. The archaeological material from these two deposits will be sampled in the analysis presented below. PP9B was excavated in 2006 and its sediments consist of eroded raised beach deposits, MSA occupation horizons, and sterile capping dune (Matthews et al. 2011). PP9C lies directly above PP9B and was excavated in 2006. PP9C contains a complex stratigraphy with series of geological deposits and MSA occupations (Matthews et al., 2011).

PP5-6

PP5-6 is a rockshelter located approximately130 meters from the PP9B and PP9C complex and 300 meters from PP13B (**Figure 2**). PP5-6 consists of two main sections, PP5-6 North and PP5-6 South. PP5-6 North is the focus of this study and consists of one connected excavated area called the Long Section. The Long Section is a ~30 meter cone of sediment that built up against the cliff face under a rock shelter. The sediment stack rests on a dune that is at least 4 meters thick, and probably is the same dune that sealed many of the caves on the western side of Pinnacle Point ~90 ka (Brown et al. 2012, Karkanas et al. 2015, Wilkins et al. 2017). The rockshelter follows a southwest-trending fault breccia. Along the back wall of the shelter, an erosion gully has formed in the past removing a large chunk of the original deposits resulting in the creation of a west-facing cliff-face. This west-facing cliff-face is one of two major sections of the long-section (Brown et al. 2012, Brown et al. 2009, Karkanas et al. 2015, Wilkins et al. 2017). The other section is south-facing and it resembles a catastrophic detachment of sediment, most likely due to high sea-stands (Karkanas et al., 2015). In total, the excavated portion of the Long Section has exposed a >14m high continuous section of MSA deposits (Brown et al. 2009, Brown et al. 2012, Karkanas et al. 2015, Wilkins et al. 2017).

The Long Section consists of 12 major StratAggs. Below follows a summary of the StratAggs at PP5-6, from bottom to the top. The stratigraphy and artifact context summary will follow from Karkanas et al. (2015), Brown et al. (2012), and Wilkins et al. (2017). The chronology of PP5-6 is based on more than 65 single-grain OSL age estimates by Zenobia Jacobs (Brown et al. 2012, Brown et al. 2009, Karkanas et al. 2015). Karkanas et al. (2015) provided updated weighted mean OSL ages and those ages

are used here when available. The Pinnacle Point OSL chronologies have been blind tested with U-Th dating in two separate caves and found to be concordant (Bar-Matthews et al. 2010, Marean et al. 2010). Additionally, the Pinnacle Point 5-6 OSL chronology has been tied to the Toba eruption and subsequent eruption downfall - The Toba eruption dates to 74 ka and Toba tephra shards were discovered in the SADBS and ALBS StratAggs (concordant with their OSL age estimates) (Ciravolo 2016, Smith et al. 2015).

Yellow Brown Sand (YBS)

The YBS is an aeolian dune at the base of the Long Section. The dune is at least 4 meters thick. There is no evidence for anthropogenic input except for rare artifacts close to the contact with the overlying YBSR StratAgg. The YBS corresponds with an aeolian event recognized at other Pinnacle Point sites and it tightly constrained to ~90 ka (Bar-Matthews et al. 2010, Jacobs 2010, Marean et al. 2010).

Yellowish Brown Sand and Roofspall (YBSR)

The YBSR is OSL dated to 89 ± 5 ka, belongs to MIS5, and consists of roof spall rich sediments with lenses of combustion features that represent single intact hearth structures interbedded with geogenic layers containing roof spall with little anthropogenic input. The aggregate is ~ 1.25 meters thick.

Light Brown Sand and Roofspall (LBSR)

The LBSR dates to 81 ± 4 ka, belongs to MIS5 and is 4.5 meters thick. The sediments of LBSR is very similar to the YBSR in that it consists of roofspall, lenses of combustion

features representing single intact hearth structures interbedded with layers of roofspall lacking in anthropogenic input.

Ashy Light Brown Sand (ALBS)

The ALBS dates to 72 ± 3 ka and is the oldest aggregate in MIS4 at PP5-6. ALBS sediments are 0.8 meters thick. It consists of aeolian sand with ash-rich combustion microfacies in the lower part that was deposited after rock fall, perhaps a roof collapse.

Shelly Ashy Dark Brown Sand (SADBS)

The SADBS dates to 71 ± 3 ka, belongs to MIS4 and is 0.7 meters thick. The SADBS is divided into a Lower (SADBS Lower) and Upper (SADBS Upper) part. The sediments consist of thick deposits of trampled combustion microfacies representing cumulative palimpsests of hearth features that are not individually discernable. This StratAgg has yielded the oldest microliths in the world (Brown et al. 2012).

Orange Brown Sand 1 (OBS1)

The OBS 1 dates to 69 ± 3 ka, belonging to MIS4 and is 0.7 meters thick. The sediments of OBS1 consist of aeolian sand layers interstratified with thin layers of trampled and reworked palimpsests of combustion features.

Shelly Gray Sand (SGS)

The SGS dates to 64 ± 3ka, belonging to MIS4 and is 0.3 meters thick. The SGS consists of palimpsest of concentrated input of trampled and reworked combustion features.

Orange Brown Sand 2 (OBS2)

The OBS2 dates to 63 ± 3 ka, belonging to MIS4 and is 1 meter thick. OBS2 sediments consist of aeolian sand layers interstratified with palimpsests of reworked combustion features.

Dark Brown Compact Sand (DBCS)

The DBCS is the debris flow that truncates BAS, OBS2, SGS, and OBS1. It has lithics artifacts consistent with the strict definition of the Howiesons Poort technocomplex that likely derives from OBS2 (Brown et al. 2012). The OSL age of 62 ± 3 ka supports this assessment. The DBCS belongs to MIS4.

Black Ashy Sand (BAS)

The BAS sediment is a thick black layer that is rich in burnt finds. It sits directly on top of the OBS2, and is horizontally extensive.

Black Brown Compact Sand and Roofspall (BBCSR)

The BBCSR dates to 52 ± 3 ka, belonging to MIS3, and is < 0.5 meters thick. The BBCSR consists of alternating bands of brown (geogenic) and black (anthropogenic) sediments.

Northwest Remnant (NWR)

The NWR sits directly on top of the BBCSR and dates to 59 ± 3 ka (Brown, 2011) and belongs to MIS3. The NWR sediments are similar to that of the DBCS. There is an absence of shellfish, but the sand component is finer in texture (Brown, 2011).

Reddish Brown Sand and Roofspall (RBSR)

The RBSR dates to 51 ± 2 ka, belonging to MIS3 and is 2.75 meters thick. The RBSR sediments consist of aeolian sand with a paleosol at the top with centimetric and decametric roofspall. This aggregate drapes the entirety of the northern part of the Long Section. The artifact density is low.

Stratigraphic aggregate to MIS designation

In the following lithic analysis, the StratAggs described above were lumped into marine isotope stages based on mean OSL estimates. MIS5 consists of YBSR and LBSR, MIS4 consists of ALBS through DBCS, while MIS3 consists of BBCSR/BAS through RBSR. The BBCSR and the BAS StratAggs are combined in this study due to a limited amount of stone tools available for analysis from either StratAgg. In total 22861 lithics from the Pinnacle Point locality was used in the following analysis. The PP13B assemblage consisted of 5608 lithics, the PP9 assemblage of 154 lithics, while the PP5-6 assemblage consisted of 17099 lithics.

Stone tool data – grouped by site and Marine Isotope Stage (MIS)

Raw material frequency

Figure 47 shows the frequencies of raw material types in assemblages by site and MIS designation. The raw material frequencies are tallied by artifact count (**Table 17**).

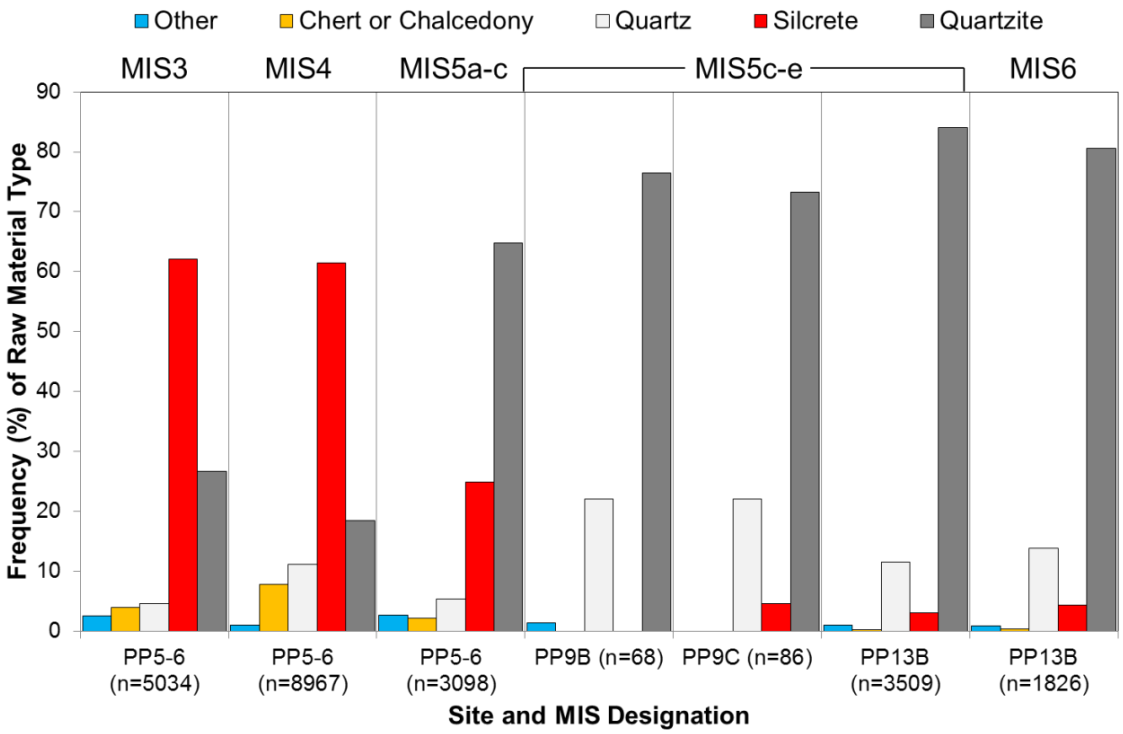

Figure 47. Frequency of raw material type in assemblage tallied by artifact count by site and MIS designation. The age of assemblages increases along the x-axis (from left to right).

Several observations can be made from **Figure 47**. Quartzite dominates the MIS6 assemblage from PP13B, and the MIS5 assemblages from PP13B, PP9B, PP9C, and PP5-6. The frequency of quartzite is significantly different from silcrete in all these assemblages (Every sample: Fisher's exact test – Two-tailed p=<0.00001). The increase in silcrete from MIS5 to MIS4 is significant (Fisher's exact test – Two-tailed p=<0.00001). During MIS4 there is significantly more silcrete than quartzite (Fisher's

exact test – Two-tailed p=<0.00001).This is followed by a significant decrease in the selection of silcrete in MIS3 compared to MIS4 (Fisher's exact test: Two-tailed p=<0.00001). However, during MIS3 there is still significantly more silcrete than quartzite (Fisher's exact test: Two-tailed p=<0.00001).

Another observation is that the quartz frequency relative to other raw materials is greatest in the MIS5 and MIS6 assemblages from PP13B and in the MIS5 assemblages from PP9B and PP9C. In the PP5-6 assemblages, quartz rises to the highest frequency relative to other raw material during MIS4. Additionally, chert (chalcedony) also rises to its highest frequency during MIS4 at PP5-6.

Table 17. Count of raw material type by site and MIS designation.

Site/MIS Designation	Other (n=)	Chert or Chalcedony (n=)	Quartz (n=)	Silcrete (n=)	Quartzite (n=)	Total (n=)
PP5-6-MIS3	126	203	235	3126	1344	5034
PP5-6-MIS4	92	707	1005	5509	1654	8967
PP5-6-MIS5	83	68	168	772	2007	3098
PP9B-MIS5	1	0	15	0	52	68
PP9C-MIS5	0	0	19	4	63	86
PP13B-MIS5	34	11	406	108	2950	3509
PP13B-MIS6	16	6	253	80	1471	1826
Total (n=)	352	995	2101	9599	9541	22588

Figure 48 shows the raw material frequencies using mass (kg) for sites and MIS designation (**Table 18**). Quartzite still dominates the MIS5 (91.8%) and MIS6 (92.4%) assemblages at PP13B and the MIS5 assemblages at PP9B (79.84%) and PP9C (92.5%), and PP5-6 (83.3%). There is, however, a change in the frequencies in the MIS4 and MIS3 assemblages at PP5-6. During MIS3 (64.2%) and MIS4 (52.3%) there is more quartzite than silcrete in terms of total artifact mass (kg). This means that although raw material count suggests that silcrete dominates the MIS4 assemblage when tallying by mass (kg),

which should reflect what has actually been transported to the locality, quartzite is the dominant raw material type. Another observation is that the relative frequency of quartz has decreased in all assemblages except for PP9B (20.1%). This suggests that in the other assemblages the elevated quartz frequency is due to many small fragments driving the frequency up.

Figure 49 shows a regression analysis between artifact count and mass for quartzite, quartz, and silcrete in each MIS assemblage. Two observations can be made: 1) Silcrete counts are strongly correlated with mass (R^2=0.959). An increase in mass results in a sharp increase in counts. The slope of the regression result for silcrete values shows that it is steeper than the result for quartz and quartzite. What this means is that an increase in the mass of silcrete lithics leads to an increased artifact count compared to quartzite and quartz. What drive this pattern, in particular, are the values from MIS3 and MIS4, which exhibit increased count values but low mass values. 2) Counts of quartzite lithics are also strongly correlated with mass (R^2=0.7683). However, quartzite values during MIS3 and MIS4 very different from silcrete values. Although mass values are similar the counts of lithics are much lower (**Tables 17-18**). This supports the assertion made above that when using counts as the means to calculating raw material frequency it overestimates what has actually be transported into the site. The increased count in silcrete can be attributed to increased fragmentation. However, if this is the case the fragmentation would equally affect quartzite as well resulting in an increased count. A second explanation for the increased count in silcrete is a more conservative reduction approach to the material, where the focus is on gaining as much cutting edge per unit of raw material as possible. This will be explored further below.

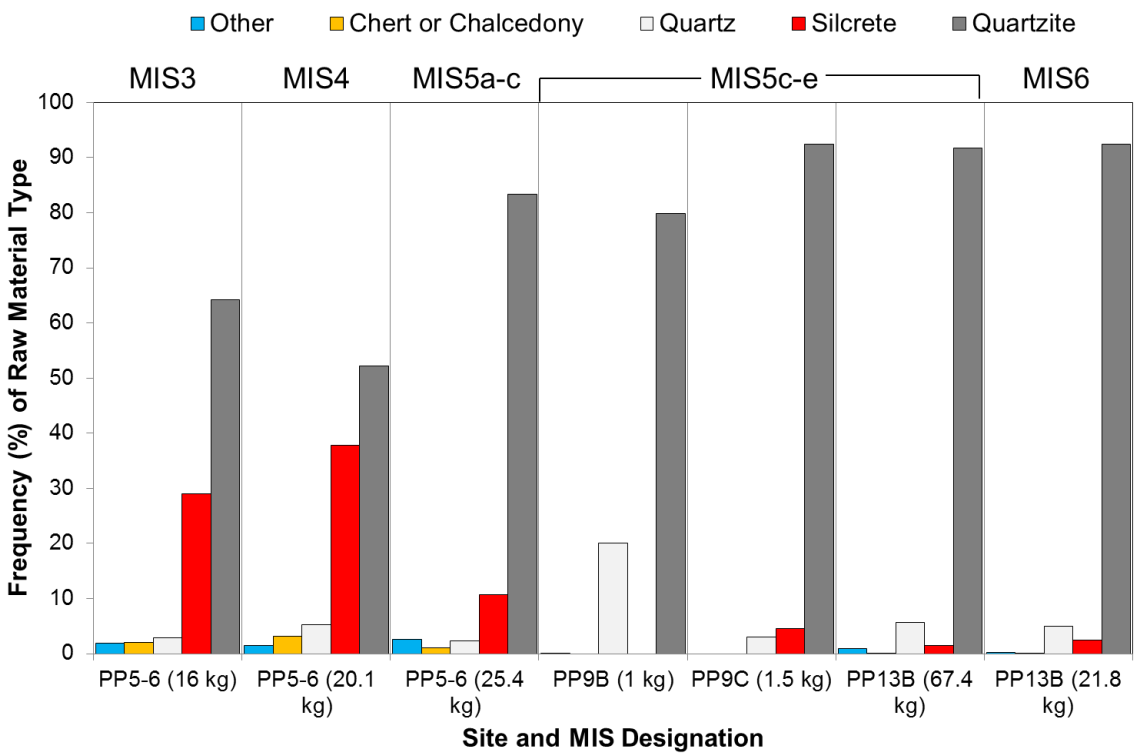

Figure 48. Frequency of raw material type in assemblage tallied by artifact mass (kg) by site and MIS designation. The age of assemblages increases along the x-axis (from left to right).

Table 18. Raw material type tallied by artifact mass (kg) by site and MIS designation.

Site/MIS Designation	Other (kg)	Chert or Chalcedony (kg)	Quartz (kg)	Silcrete (kg)	Quartzite (kg)	Total (kg)
PP5-6-MIS3 (n=5034)	0.311	0.327	0.452	4.641	10.270	16.001
PP5-6-MIS4 (n=8967)	0.285	0.645	1.063	7.614	10.508	20.115
PP5-6-MIS5 (n=3098)	0.666	0.280	0.594	2.706	21.194	25.439
PP9B-MIS5 (n=68)	0.001	0.000	0.206	0.000	0.818	1.025
PP9C-MIS5 (n=86)	0.000	0.000	0.046	0.069	1.423	1.539
PP13B-MIS5 (n=3509)	0.586	0.059	3.860	1.037	61.836	67.377
PP13B-MIS6 (n=1826)	0.041	0.016	1.068	0.535	20.125	21.786
Total (kg)	1.889	1.326	7.288	16.603	126.174	153.280

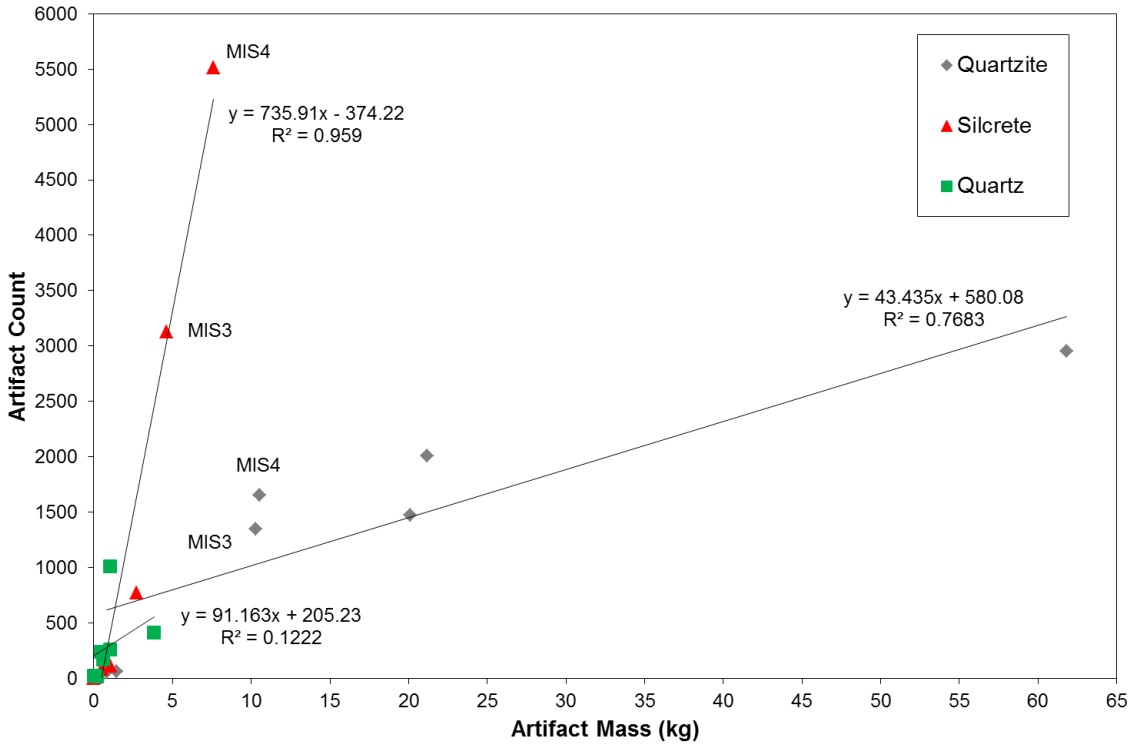

Figure 49. Regression analysis of artifacts counts against artifact mass (kg) for quartzite, quartz, and silcrete in MIS assemblages. Each single point represents a MIS assemblage.

By using the sub-aggregate (PP5-6) or stratigraphic aggregate (PP9B, PP9C, and PP13B) raw material frequencies from each MIS one can bootstrap the different raw material frequencies to obtain 95% confidence intervals around each mean raw material frequency. This can then be used to test whether a mean raw material frequency from an MIS is significantly different from the mean frequency of another in the same MIS. The MIS3 assemblage consists of sub-aggregate frequencies from RBSR (n=2), NWR (n=3), and BBCSR/BAS (n=6), The MIS4 assemblage consists of sub-aggregate frequencies from OBS2 (n=9), DBCS (n=9), SGS (n=6), OBS1 (n=8), SADBS Upper (n=9), SADBS Lower (n=2), and ALBS (n=3), while the MIS5 assemblage consists of sub-aggregate frequencies from LBSR (n=26) and ALBS (n=5), the PP9B and PP9C assemblage frequencies in addition to PP13B stratigraphic aggregate frequencies from LB Sand 1,

DB Sand 2, LB Sand 3, DB Sand 3, Shelly Brown Sand, Roof Spall-Upper, Roof Spall-Lower, LBG Sand 1, LC-MSA Upper, and LC-MSA Middle. The MIS6 assemblage consists of PP13B stratigraphic aggregate frequencies from DB Sand 4a, LBG Sand 2, DB Sand 4b, DB Sand 4c, LC-MSA Lower, LB Silt-G, and LB Silt.

Figure 50 shows the mean frequencies of quartzite, silcrete, and quartz with 95% confidence intervals resulting from a bootstrap of the standard error 10000 times. Starting in the MIS6, quartzite is significantly more frequent than quartz and silcrete, which have statistically similar frequencies. In the aggregates from MIS5, quartzite is significantly more frequent than silcrete and quartz. However, silcrete is now significantly more frequent than quartz (**Table 19**). From MIS5 to MIS4 the frequency of silcrete increases, while the frequency of quartzite decreases. The frequencies of silcrete and quartzite during MIS4 are significantly different from the silcrete and quartzite frequencies during MIS5. However, during MIS4 the frequencies of quartzite and silcrete are statistically similar (**Table 19**). When moving into MIS3, the frequency of quartzite increases again, while silcrete decreases. During MIS3, all three raw material frequencies are significantly different from each other (**Table 19**). The frequency of quartz is statistically similar across all four marine isotope stages (**Table 19**). Another interesting observation is that the frequency of silcrete during MIS5 is statistically similar to the frequency of quartz during MIS4 (**Table 19**).

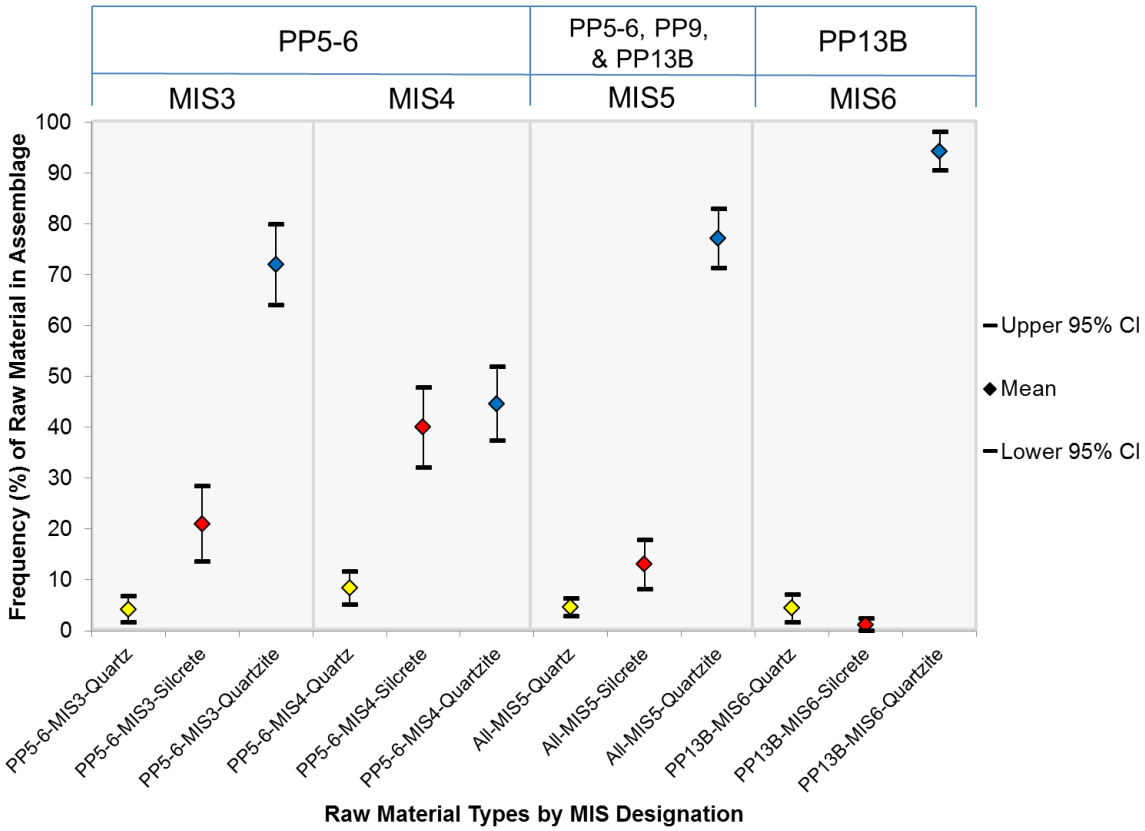

Figure 50. Bootstrapped raw material frequencies at Pinnacle Point by site and MIS designation. The plot shows the mean and the upper and lower 95% confidence intervals for quartz, quartzite, and silcrete. The age of assemblages increases along the x-axis (from left to right).

Table 19. Summary statistics and bootstrap test results for quartz, silcrete, and quartzite at PP5-6 by MIS Designation.

	PP5-6-MIS3-Quartz	PP5-6-MIS3-Silcrete	PP5-6-MIS3-Quartzite	PP5-6-MIS4-Quartz	PP5-6-MIS4-Silcrete	PP5-6-MIS4-Quartzite	All-MIS5-Quartz	All-MIS5-Silcrete	All-MIS5-Quartzite	PP13B-MIS6-Quartz	PP13B-MIS6-Silcrete	PP13B-MIS6-Quartzite
n (aggregate samples)	11	11	11	46	46	46	43	43	43	7	7	7
First Quartile	0.9	8.9	61.9	1.2	13.8	5.2	0.1	0.9	64.3	1.7	0	87.6
Min	0.4	2.6	47.2	0	0	0	0	0	26.9	0	0	87.6
Median	2.5	21.7	69.4	3.7	39.1	43.0	2.6	6.4	83.7	2.1	0	97.9
Mean	4.2	21.0	72.0	8.4	40.0	44.6	4.6	13.0	77.2	4.4	1.1	94.3

Max	15.3	39.2	90.0	66.1	96.6	96.5	24.9	64.8	100	9.4	5.0	100
Third Quartile	7.4	34.2	85.8	10.5	62.8	68.2	6.9	21.2	92.8	9.3	2.6	98.3
SD	4.5	12.8	13.8	11.8	27.5	25.5	6.0	16.5	20.0	3.9	2.0	5.4
Boot strapped SE	1.3	3.8	4.1	1.7	4.0	3.7	0.9	2.5	3.0	1.4	0.7	1.9
Margin of error (95% CI)	2.6	7.4	8.0	3.3	7.9	7.3	1.8	4.8	5.9	2.7	1.3	3.8
Bootstrapped Upper 95% CI	6.8	28.4	80.0	11.7	47.9	51.9	6.4	17.9	83.1	7.1	2.4	98.1
Bootstrapped Lower 95% CI	1.6	13.6	64.0	5.1	32.1	37.4	2.8	8.2	71.3	1.7	0	90.6

**Bootstrapped 10000 times*

Stone artifact type frequency

Figure 51 shows the frequencies of artifact types in assemblages according to site and MIS designation. **Table 20** shows the counts of the different artifact types.

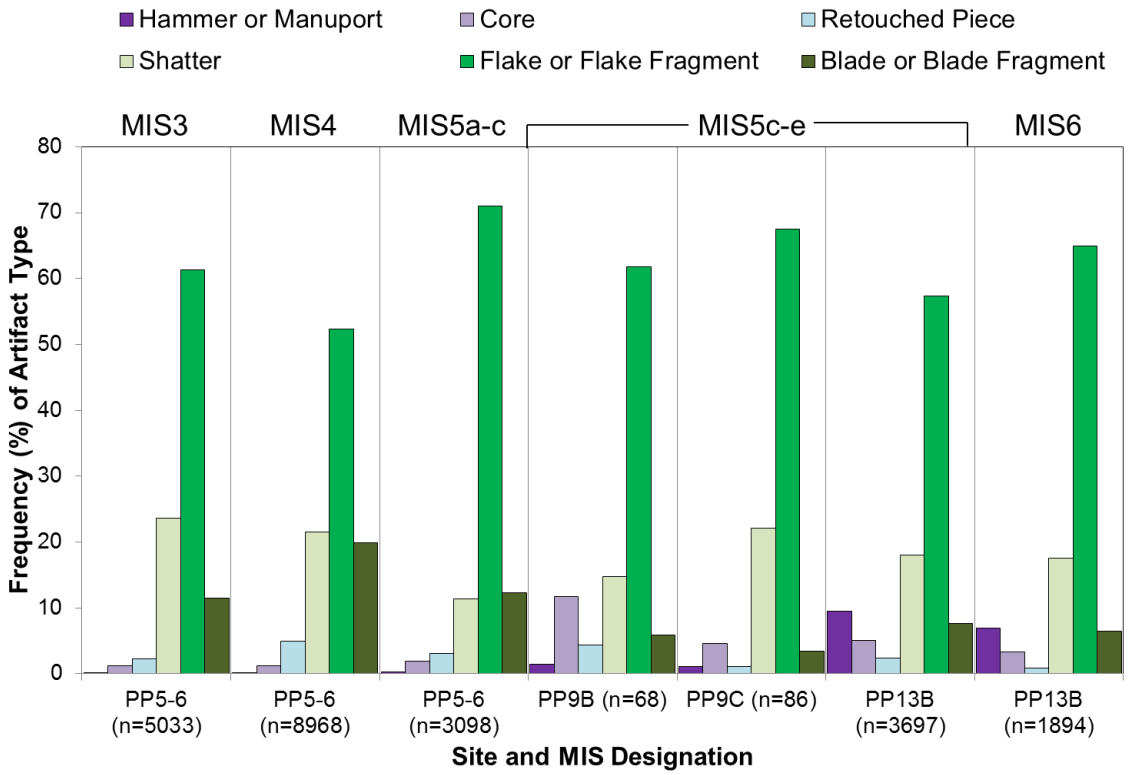

Figure 51. Frequency of artifact type in assemblage based on counts by site and MIS designation. The age of assemblages increases along the x-axis (from left to right).

There are several observations available from **Figure 51** and **Table 20**. Flake and flake fragments dominate all the assemblages (52.3% to 71%). In all assemblages there

are significantly more flakes and flake fragments than blades and blade fragments (Every sample: Fisher's exact test – Two-tailed p=<0.00001). Blade and blade fragments are always a small component of the total assemblage (3.5% to 19.9%). However, there is a significant increase in complete blades and blade fragments in MIS4 compared to MIS5 (Fisher's exact test: Two-tailed p=<0.00001). This is followed by a significant decrease in blades and blade fragments in MIS3 compared to MIS4 (Fisher's exact test: Two-tailed p=<0.00001).

Table 20. Count of artifact type by site and MIS designation.

Site/MIS Designation	Hammer or Manuport (n=)	Core (n=)	Retouched Piece (n=)	Shatter (n=)	Flake or Flake Fragment (n=)	Blade or Blade Fragment (n=)	Total (n=)
PP5-6-MIS3	7	59	113	1189	3088	577	5033
PP5-6-MIS4	8	113	440	1927	4693	1787	8968
PP5-6-MIS5	9	61	95	354	2199	380	3098
PP9B-MIS5	1	8	3	10	42	4	68
PP9C-MIS5	1	4	1	19	58	3	86
PP13B-MIS5	350	189	89	666	2119	284	3697
PP13B-MIS6	131	63	16	332	1230	122	1894
Total (n=)	507	497	757	4497	13429	3157	22844

By tallying artifact types by mass the shift to more blade production still holds in MIS5, MIS4, and MIS3 at PP5-6 compared to the older assemblages at PP9 and PP13B (**Figure 52** and **Table 21**). Additionally, the frequencies of cores and hammer or manuports at PP9 and PP13B increase. That means that more of the raw materials at those sites are contained to cores and hammerstones or manuports. The MIS5 record from PP9 and PP13B, and the MIS6 record from PP13B suggest knapping on more locally acquired raw materials such as quartzite, while the MIS5, MIS4, and MIS3 record from

PP5-6 suggest an increase in stone tool production on non-local raw materials such as silcrete.

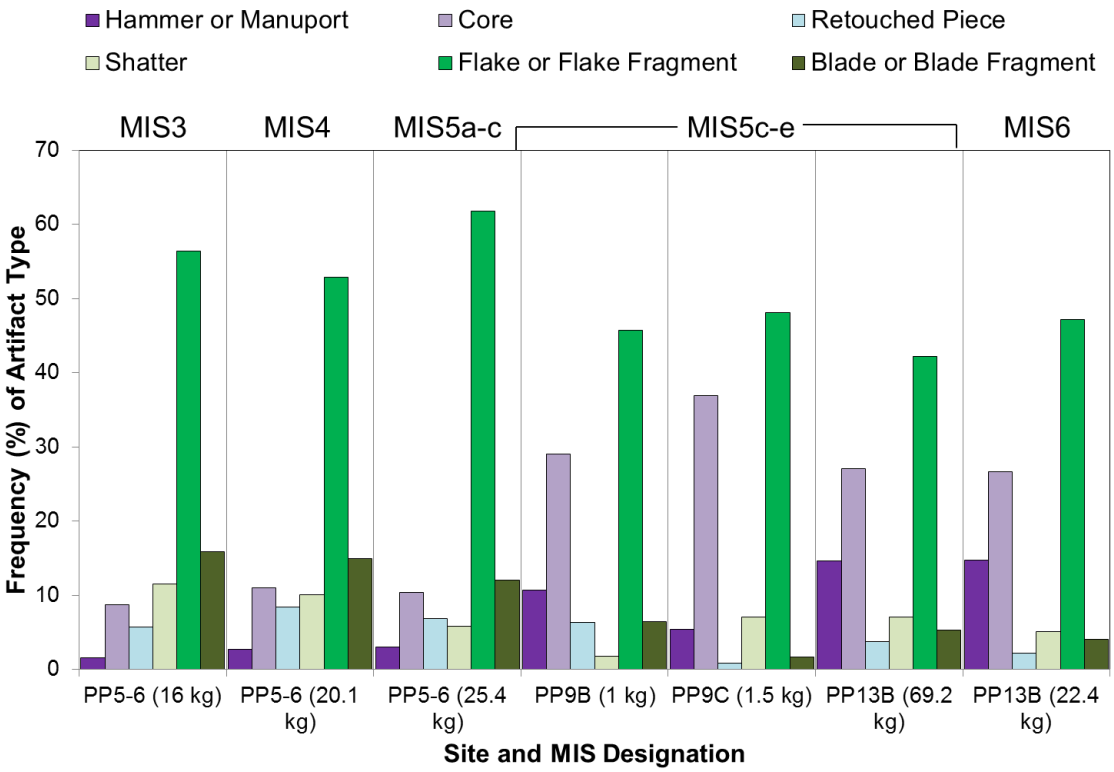

Figure 52. Frequency of artifact type in assemblage based on mass by site and MIS designation. The age of assemblages increases along the x-axis (from left to right).

Table 21. Artifact type tallied by mass (kg) by site and MIS designation.

Site/MIS Designation	Hammer or Manuport (kg)	Core (kg)	Retouched Piece (kg)	Shatter (kg)	Flake or Flake Fragment (kg)	Blade or Blade Fragment (kg)	Total (kg)
PP5-6-MIS3 (n=5028)	0.3	1.4	0.9	1.8	9.0	2.5	16.0
PP5-6-MIS4 (n=8960)	0.5	2.2	1.7	2.0	10.6	3.0	20.1
PP5-6-MIS5 (n=3094)	0.8	2.6	1.7	1.5	15.7	3.1	25.4
PP9B-MIS5 (n=68)	0.1	0.3	0.1	0.0	0.5	0.1	1.0
PP9C-MIS5 (n=86)	0.1	0.6	0.0	0.1	0.7	0.0	1.5
PP13B-MIS5 (n=3700)	10.1	18.7	2.6	4.9	29.2	3.7	69.2
PP13B-MIS6 (n=1888)	3.3	6.0	0.5	1.1	10.6	0.9	22.4
Total (kg)	15.2	31.8	7.5	11.5	76.4	13.3	155.8

When looking at what the complete blades of the assemblages are made of it shows a big shift in the materials used to make the blades (**Figure 53** and **Table 22**). During MIS5 there are significantly more complete blades made on quartzite than silcrete (Fisher's exact test: Two-tailed p=0.026). However, in the following MIS4 there is a significant increase in the usage of silcrete in MIS4 compared to MIS5 (Fisher's exact test: Two-tailed p=<0.00001). During MIS4 there are significantly more complete blades made on silcrete than quartzite (Fisher's exact test: Two-tailed p=<0.00001). This is followed by a significant decrease in complete blades made on silcrete during MIS3 compared to MIS4 (Fisher's exact test: Two-tailed p=<0.00001) but silcrete still dominates the production of blades compared to quartzite (Fisher's exact test: Two-tailed p=0.0004).

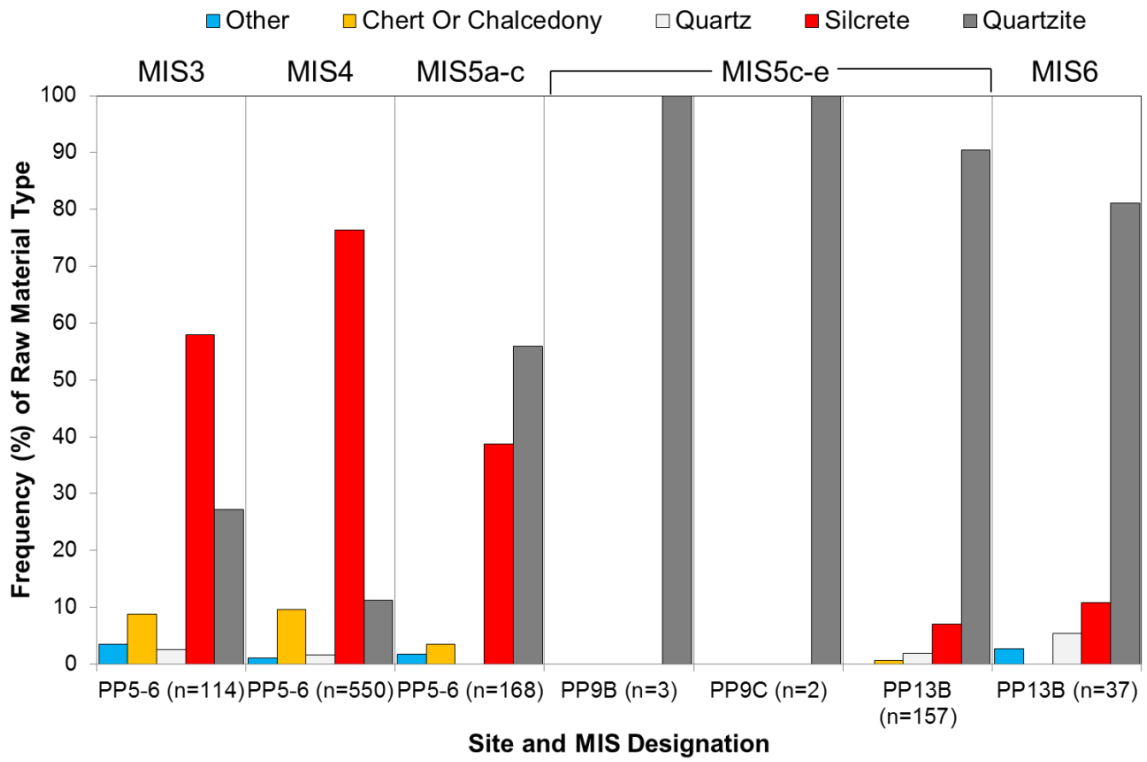

Figure 53. Frequency of complete blades made on all raw material types in assemblage by site and MIS designation. The age of assemblages increases along the x-axis (from left to right).

Table 22. Count of complete blades made on all raw material types by site and MIS designation.

Site/MIS Designation	Other (n=)	Chert Or Chalcedony (n=)	Quartz (n=)	Silcrete (n=)	Quartzite (n=)	Total (n=)
PP5-6-MIS3	4	10	3	66	31	114
PP5-6-MIS4	6	53	9	420	62	550
PP5-6-MIS5	3	6	0	65	94	168
PP9B-MIS5	0	0	0	0	3	3
PP9C-MIS5	0	0	0	0	2	2
PP13B-MIS5	0	1	3	11	142	157
PP13B-MIS6	1	0	2	4	30	37
Total (n=)	14	70	17	566	364	1031

Stone artifact metrics

Figure 54 shows the maximum dimension (mm) of all artifacts by site and MIS designation. **Supplementary Table B1** shows the summary statistics for each artifact assemblage, while **Supplementary Table B2** shows the Kruskal-Wallis test result and the uncorrected pairwise Mann-Whitney comparisons of the artifact assemblages. The median maximum dimension of MIS6 artifacts is significantly smaller than the following MIS5 artifacts (Mann-Whitney p=<0.00001). The median maximum dimension of MIS5 artifacts from PP13B is statistically similar in maximum dimension to PP9B (Mann-Whitney p=0.3641) and PP9C artifacts (Mann-Whitney p=0.5336). The median maximum dimension of MIS5 artifacts from PP5-6 is significantly larger than the MIS6 artifacts from PP13B (Mann-Whitney p=<0.00001) and the MIS3 and MIS4 artifacts from PP5-6 (Both: Mann-Whitney p=<0.00001). The median maximum dimension of MIS4 artifacts from PP5-6 is significantly smaller than MIS3 artifacts from PP5-6 (Mann-Whitney p=0.017).

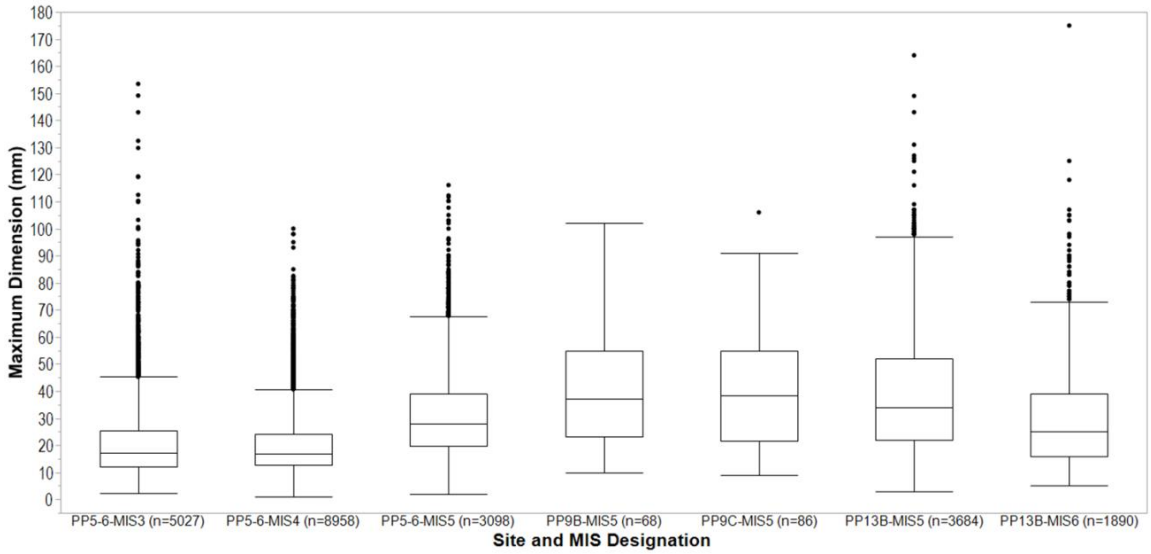

Figure 54. Boxplot of maximum dimension (mm) of all artifacts classes made on all raw material types by site and MIS designation. The age of assemblages increases along the x-axis (from left to right).

Figure 55 shows the maximum dimension (mm) of all quartzite and silcrete artifacts by site and MIS designation. **Supplementary Table B3** shows the summary statistics for each artifact assemblage, while **Supplementary Table B4** shows the Kruskal-Wallis test result and the uncorrected pairwise Mann-Whitney comparisons of the artifact assemblages. One pattern is instantly visible for the PP5-6 assemblages. The maximum dimension (mm) of silcrete artifacts are significantly smaller than the maximum dimension (mm) of quartzite artifacts in MIS3, MIS4 and MIS5 (All assemblages: Mann-Whitney p=<0.00001). This is different from the PP13B assemblages where the MIS6 silcrete artifacts are not significantly different from the quartzite artifacts (Mann-Whitney p=0.2189), and MIS5 silcrete artifacts are not significantly different from MIS6 quartzite (Mann-Whitney p=0.06) and silcrete artifacts (Mann-Whitney p=0.5125). The MIS3 quartzite artifacts from PP5-6, MIS5 quartzite artifacts from PP5-6,

PP9B, and PP9C have the largest maximum dimension (mm) values (**Supplementary Table B4**).

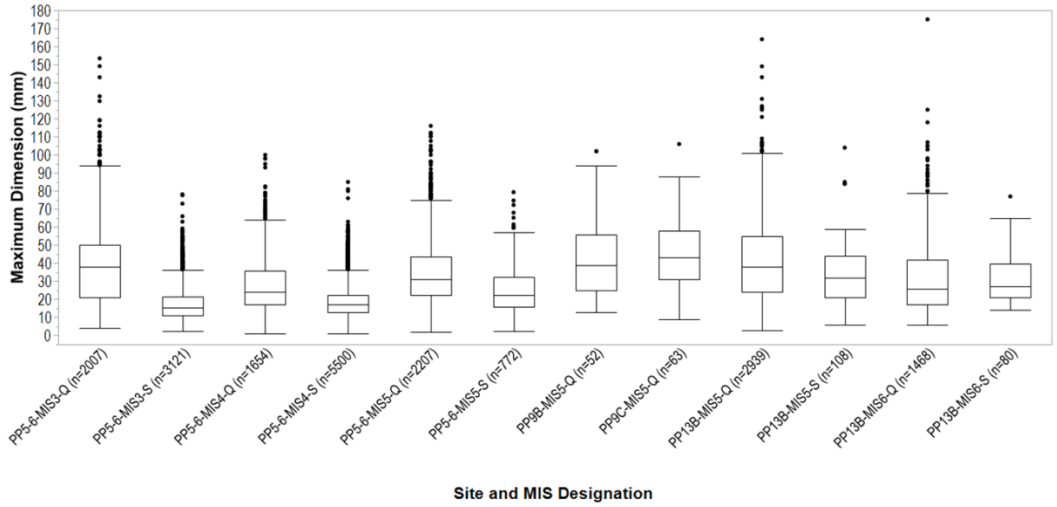

Figure 55. Boxplot of maximum dimension (mm) of all artifact classes made on quartzite (Q) and silcrete (S) by site and MIS designation. The age of assemblages increases along the x-axis (from left to right).

Figure 56 shows the maximum thickness (mm) of all artifacts by site and MIS designation. **Supplementary Table B5** shows the summary statistics for each artifact assemblage, while **Supplementary Table B6** shows the Kruskal-Wallis test result and the uncorrected pairwise Mann-Whitney comparisons of the artifact assemblages. MIS3 and MIS4 artifacts from PP5-6 are significantly thinner than artifacts from all other assemblages (All assemblages: Mann-Whitney p=<0.00001). The median maximum thickness (mm) of MIS5 artifacts from PP5-6 is significantly different from artifacts from all other assemblages expect from MIS5 artifacts from PP9C (Mann-Whitney p=0.4740). The maximum thickness (mm) of MIS5 artifacts from PP9C is not significantly different from aforementioned MIS5 artifacts from PP5-6 but also MIS5 artifacts from PP9B and PP13B and MIS6 artifacts from PP13B (**Supplementary Table B6**).

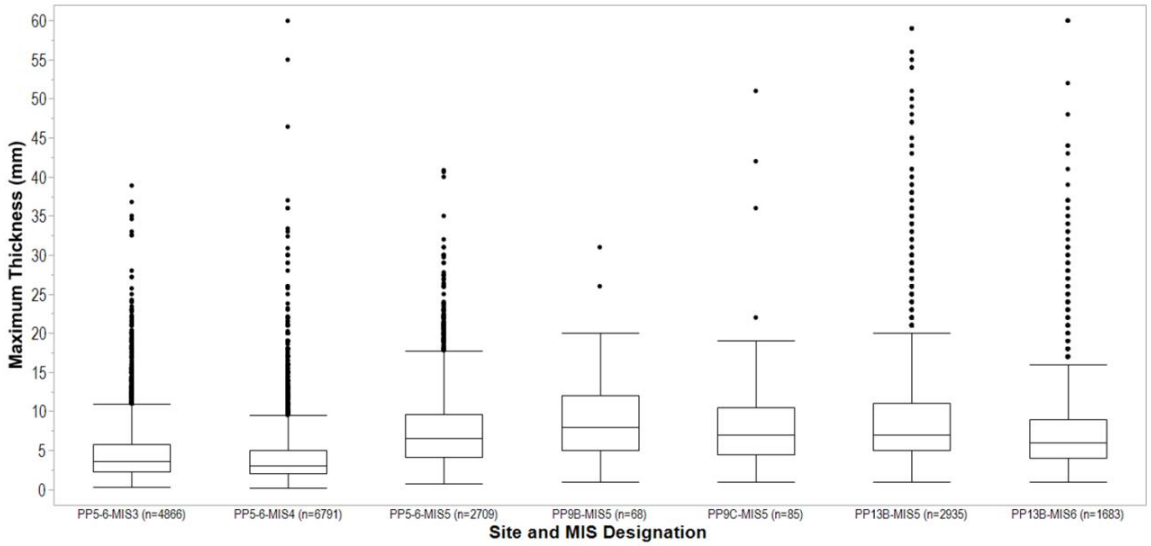

Figure 56. Boxplot of maximum thickness (mm) of all artifact classes made on all raw material types by site and MIS designation. The age of assemblages increases along x-the axis (from left to right).

Figure 57 shows the maximum thickness (mm) of all quartzite and silcrete artifacts by site and MIS designation. **Supplementary Table B7** shows the summary statistics for each lithic artifact assemblage, while **Supplementary Table B8** shows the Kruskal-Wallis test result and the uncorrected pairwise Mann-Whitney comparisons of the artifact assemblages. A similar pattern to the maximum dimension values is observable. The maximum thickness (mm) of silcrete artifacts from MIS3, MIS4, and MIS5 is significantly smaller than artifacts from all other assemblages (all assemblages: Mann-Whitney p=<0.00001), except for MIS5 silcrete stone tools from PP5-6 that is statistically similar to MIS5 silcrete stone tools from PP13B (Mann-Whitney p=0.08).

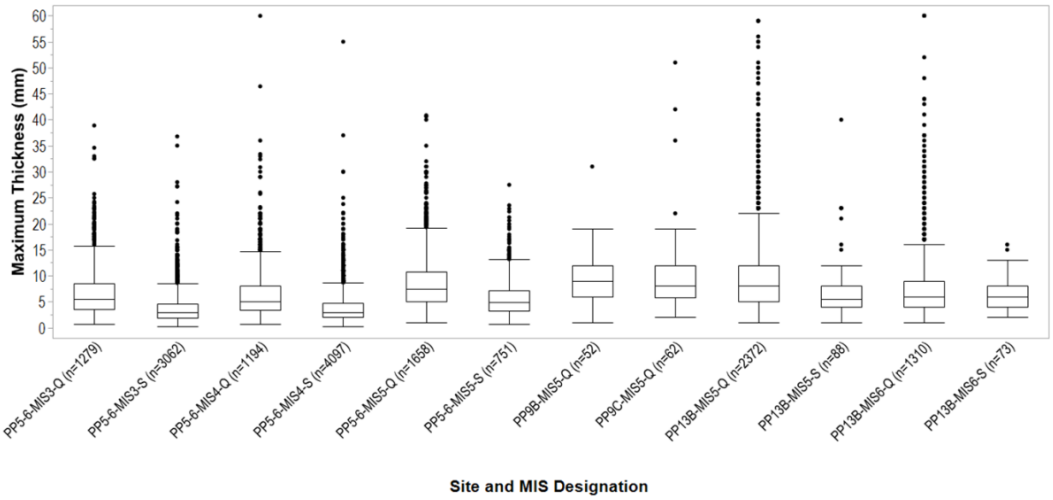

Figure 57. Boxplot of maximum thickness (mm) of all artifact classes made on quartzite (Q) and silcrete (S) by site and MIS designation. The age of assemblages increases along the x-axis (from left to right).

Figure 58 shows the technological length (mm) of all complete flakes and blades by site and MIS designation. **Supplementary Table B9** shows the summary statistics for each flake and blade assemblage, while **Supplementary Table B10** shows the Kruskal-Wallis test result and the uncorrected pairwise Mann-Whitney comparisons of the flake and blade assemblages. The technological length of complete flakes and blades from MIS3 and MIS4 at PP5-6 is significantly smaller than flakes and blades from the older assemblages (all assemblages: Mann-Whitney p=<0.00001). MIS5 complete flakes and blades from PP5-6 have a median technological length that is significantly different from artifacts from all other assemblages except for complete flakes and blades from the MIS6 assemblage at PP13B (**Supplementary Table B10**). The MIS5 assemblages from PP9B, PP9C, and PP13B have the highest median technological length (mm) values, and they are statistically similar (**Supplementary Table B10**).

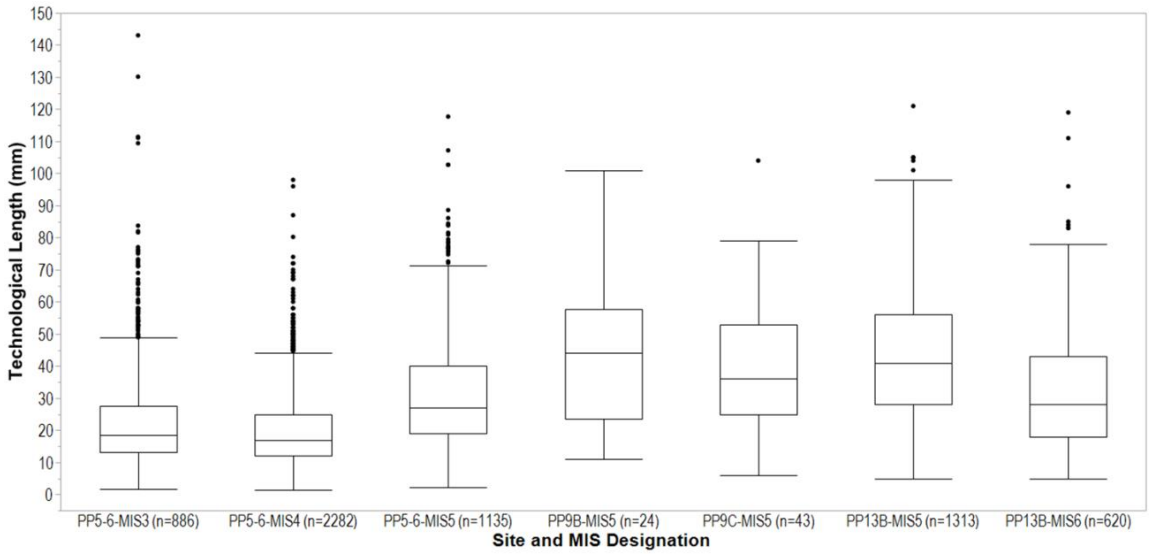

Figure 58. Boxplot of technological length (mm) of all complete flakes and blades made on all raw material types by site and MIS designation. The age of assemblages increases along the x-axis (from left to right).

Figure 59 shows the technological length (mm) of all complete quartzite and silcrete artifacts by site and MIS designation. **Supplementary Table B11** shows the summary statistics for each artifact assemblage, while **Supplementary Table B12** shows the Kruskal-Wallis test result and the uncorrected pairwise Mann-Whitney comparisons of the artifact assemblages. The median technological length (mm) of silcrete artifacts in MIS3, MIS4, and MIS5 are all significantly smaller than the quartzite artifacts in the same assemblages (all assemblages: Mann-Whitney p=<0.00001). The median technological length (mm) of MIS5 quartzite artifacts from PP9B, PP9C, and PP13B is the largest, and are all statistically similar (**Supplementary Table B12**). The median technological length (mm) of MIS6 quartzite artifacts is statistically similar to the MIS6 silcrete artifacts (Mann-Whitney p=0.8692).

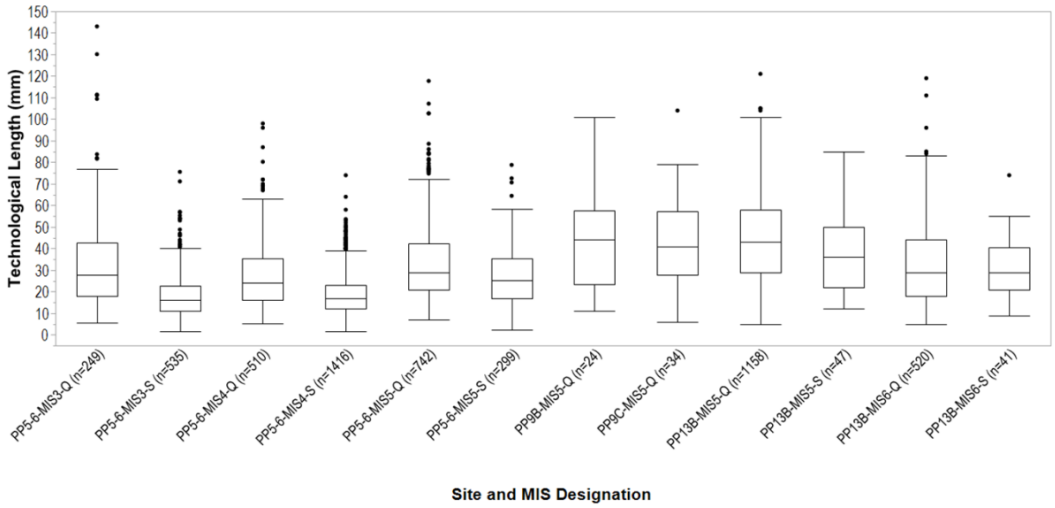

Figure 59. Boxplot of technological length (mm) of all complete flakes and blades made on quartzite (Q) and silcrete (S) by site and MIS designation. The age of assemblages increases along the x-axis (from left to right).

Figure 60 shows the technological width (mm) of all complete artifacts by site and MIS designation. **Supplementary Table B13** shows the summary statistics for each artifact assemblage, while **Supplementary Table B14** shows the Kruskal-Wallis test result and the uncorrected pairwise Mann-Whitney comparisons of the artifact assemblages. Similar to the technological length (mm) statistics, the median technological width of the MIS3 and MIS4 artifacts from PP5-6 are significantly smaller than artifacts from all other assemblages (all assemblages: Mann-Whitney p=<0.00001). MIS6 artifacts from PP13B is significantly smaller than the MIS5 artifacts from PP13B (Mann-Whitney p=<<0.00001). The median technological width (mm) of MIS5 artifacts from PP9B, PP9C, and PP13B is the largest, and they are statistically similar (**Supplementary Table B14**).

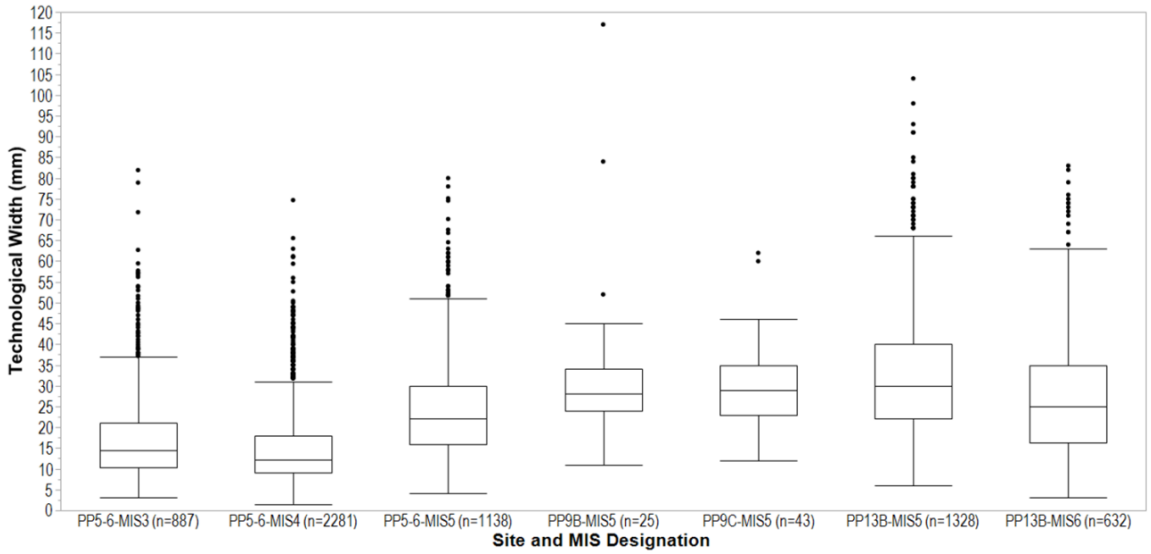

Figure 60. Boxplot of technological width (mm) of all complete flakes and blades made on all raw material types by site and MIS designation. The age of assemblages increases along the x-axis (from left to right).

Figure 61 shows the technological width (mm) of all complete quartzite and silcrete artifacts by site and MIS designation. **Supplementary Table B15** shows the summary statistics for each artifact assemblage, while **Supplementary Table B16** shows the Kruskal-Wallis test result and the uncorrected pairwise Mann-Whitney comparisons of the artifact assemblages. The median technological width (mm) of silcrete artifacts in MIS3, MIS4, and MIS5 are all significantly smaller than the quartzite artifacts in the same assemblages (all assemblages: Mann-Whitney p=<0.00001). The median technological width (mm) of MIS5 quartzite artifacts from PP9B, PP9C, and PP13B is the largest, and are all statistically similar (**Supplementary Table B16**). The median technological width (mm) of MIS5 complete quartzite artifacts from PP5-6 is statistically similar to MIS5 silcrete artifacts from PP13B, and MIS6 quartzite and silcrete artifacts from PP13B (**Supplementary Table S16**). The median technological width (mm) of

MIS6 quartzite artifacts is statistically similar to the MIS6 silcrete artifacts (Mann-Whitney p=0.9590).

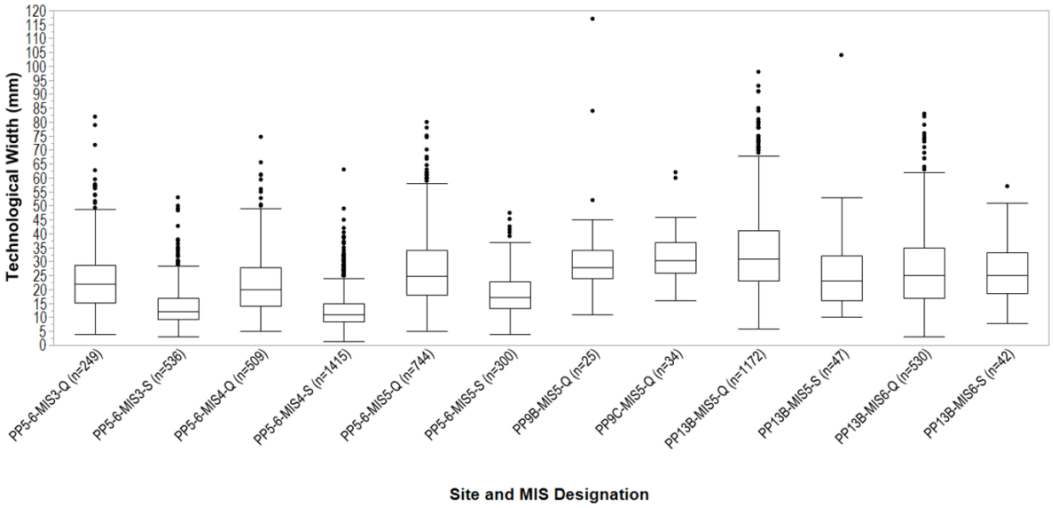

Figure 61. Boxplot of technological width (mm) of all complete flakes and blades made on quartzite (Q) and silcrete (S) by site and MIS designation. The age of assemblages increases along the x-axis (from left to right).

Cortex type frequency

Cortex type is potentially a useful indicator of from where a raw material was collected. It can be looked at two ways. One can look at the overall strategy regardless of raw material and one can look at the raw material-specific strategy to gauge whether different strategies were used for different raw materials. In the Pinnacle Point sequence, cobble cortex dominates overall, which suggests mostly procurement of raw materials from high-energy cobble beaches or stream beds (**Figure 62**). **Table 23** shows the count of cortex type by site and MIS designation. While cobble cortex dominates overall throughout the sequence there is, however, a significant increase overall in outcrop cortex in MIS4 (53.5%) compared to MIS5 (46.5%) (Fisher's exact test: Two-tailed p=<0.00001). This increase in outcrop cortex is enough to make there be significantly more outcrop cortex than cobble cortex (Fisher's exact test: Two-tailed p=<0.00001).

This is followed by a significant decrease in outcrop cortex during MIS3 compared to MIS4 (Fisher's exact test: Two-tailed p=<0.00001). During MIS3 there is significantly more cobble cortex than outcrop cortex (Fisher's exact test: Two-tailed p=<0.00001).

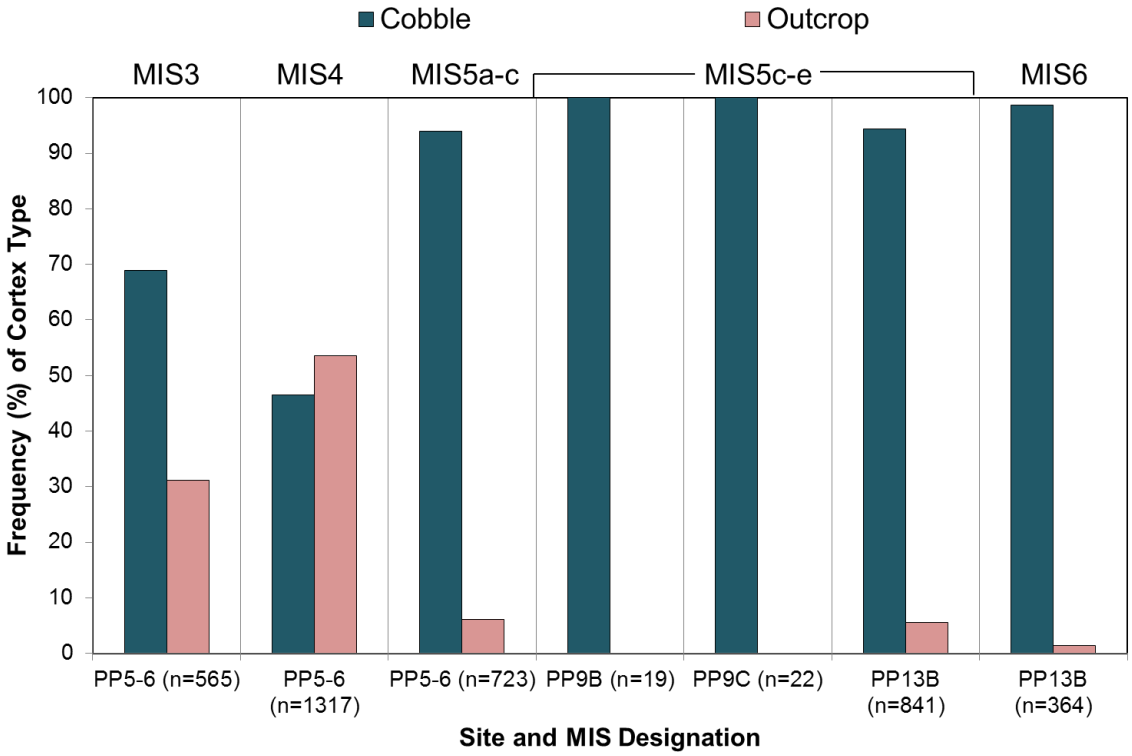

Figure 62. Frequency of cortex type on all raw materials in assemblage by site and MIS designation. The age of assemblages increases along the x-axis (from left to right).

Table 23. Count of cortex type on all raw materials by site and MIS designation.

Site/MIS Designation	Cobble (n=)	Outcrop (n=)	Total (n=)
PP5-6-MIS3	389	176	565
PP5-6-MIS4	612	705	1317
PP5-6-MIS5	679	44	723
PP9B-MIS5	19	0	19
PP9C-MIS5	22	0	22
PP13B-MIS5	794	47	841
PP13B-MIS6	359	5	364
Total (n=)	2874	977	3851

Above, the overall strategy of raw material procurement was investigated, which suggested that regardless of raw material, secondary sources were targeted more frequently throughout the sequence except for during MIS4 where outcrop dominates overall. However, when investigating the cortex type of quartzite and silcrete lithics separately several observations can be made (**Figure 63** and **Table 24**). During MIS6 and MIS5 at PP13B, and MIS5 at both PP9 sites quartzite and silcrete are dominated by cobble cortex. However, when moving into MIS5 at PP5-6, there is a slight increase in outcrop cortex on silcrete lithics but overall there is significantly more cobble cortex than outcrop cortex on both quartzite and silcrete (Fisher's exact test: both raw materials: Two-tailed p=<0.00001). During MIS4 there is a significant increase in outcrop cortex for both silcrete and quartzite during MIS4 compared to MIS5 (Fisher's exact test: Quartzite: Two-tailed p=<0.00001; Silcrete: Two-tailed p=<0.00001). However, what drives the overall pattern of more outcrop cortex during MIS4 is that there is significantly more outcrop cortex than cobble cortex on silcrete lithics (Fisher's exact test: Two-tailed p=<0.00001). Although there is a significant increase in outcrop cortex on quartzite lithics during MIS4 compared to MIS5 there is still significantly more cobble cortex than outcrop cortex on quartzite (Fisher's exact test: Two-tailed p=<0.00001). This is followed by a significant decrease in outcrop cortex on silcrete and quartzite during MIS3 compared to MIS4 (Fisher's exact test: quartzite: Two-tailed p=0.038; silcrete: Two-tailed p=<0.00001). Similar to MIS4, during MIS3 there is significantly more outcrop cortex than cobble cortex on silcrete (Fisher's exact test: Two-tailed p=<0.00001), while there is significantly more cobble cortex than outcrop cortex on quartzite (Fisher's exact test: Two-tailed p=<0.00001).

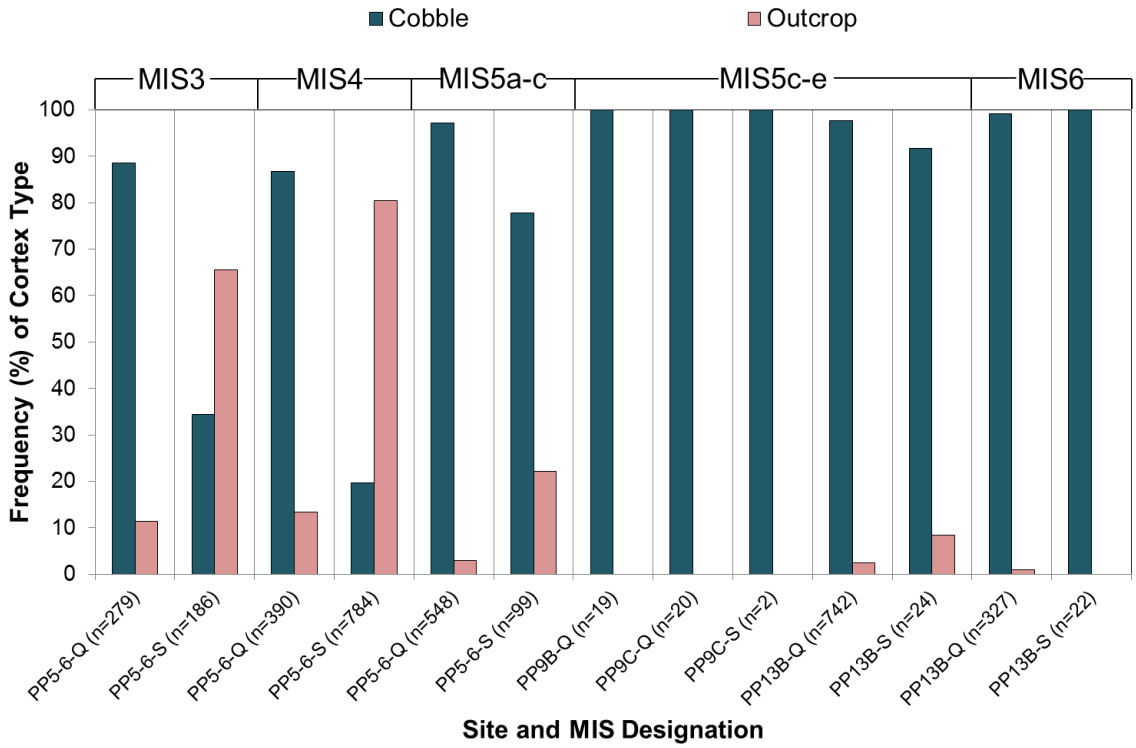

Figure 63. Frequency of cortex type on quartzite and silcrete artifacts in assemblage by site and MIS designation. Q=quartzite; S=Silcrete. The age of assemblages increases along the x-axis (from left to right).

Table 24. Count of cortex type on quartzite and silcrete lithics by site and MIS designation.

Site/MIS Designation	Cobble (n=)	Outcrop (n=)	Total (n=)
PP5-6-MIS3-Quartzite	247	32	279
PP5-6-MIS3-Silcrete	64	122	186
PP5-6-MIS4-Quartzite	338	52	390
PP5-6-MIS4-Silcrete	154	630	784
PP5-6-MIS5-Quartzite	532	16	548
PP5-6-MIS5-Silcrete	77	22	99
PP9B-MIS5-Quartzite	19	0	19
PP9C-MIS5-Quartzite	20	0	20
PP9C-MIS5-Silcrete	2	0	2
PP13B-MIS5-Quartzite	724	18	742
PP13B-MIS5-Silcrete	22	2	24
PP13B-MIS6-Quartzite	324	3	327
PP13B-MIS6-Silcrete	22	0	22
Total (n=)	2545	897	3442

Figure 64 shows that frequencies of cobble cortex on quartzite and silcrete co-vary in all assemblages. This is particularly true in the PP13B and PP9 assemblages. However, when moving into the MIS5 assemblage at PP5-6 the increase in outcrop cortex on silcrete is much sharper compared to quartzite. The increase in MIS4 is even more different but both raw materials have an increase in outcrop cortex. In MIS3, both raw materials have a decline in outcrop cortex but again the decline is sharper in silcrete.

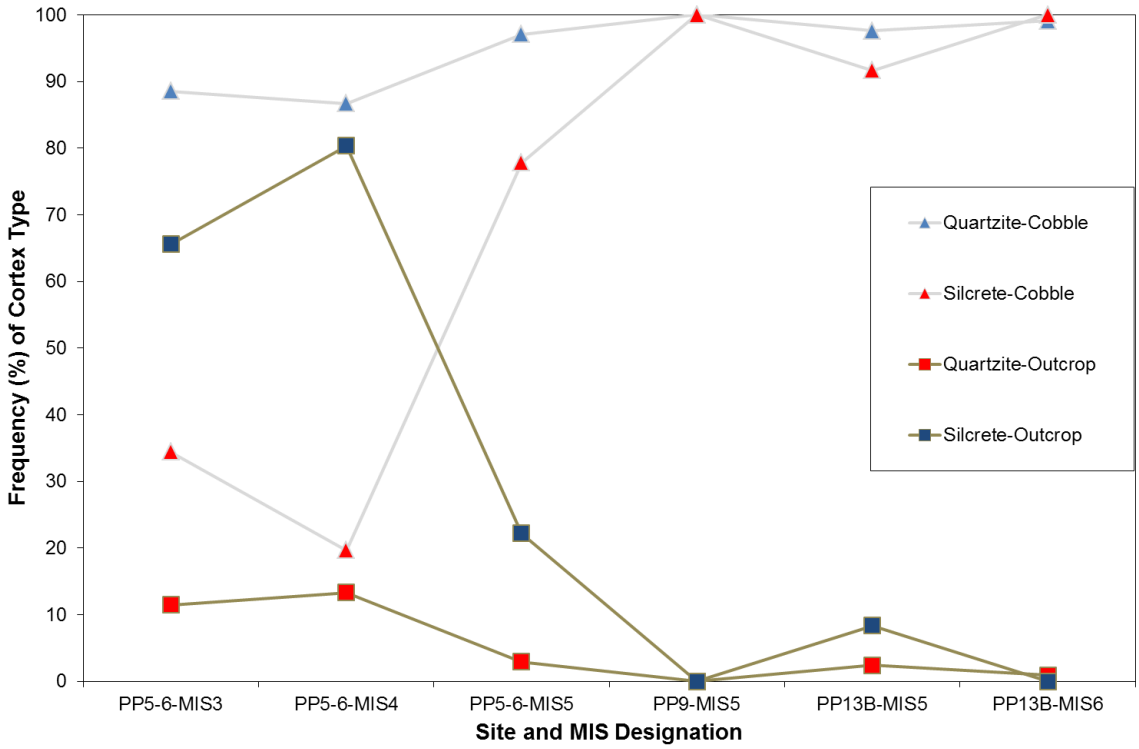

Figure 64. Timeline plot showing frequencies of cobble or outcrop cortex on quartzite and silcrete. The age of assemblages increases along the the x-axis (from left to right).

Cutting edge per mass ratio

Cutting edge per mass ratio (CE/M) is a proxy for flaking efficiency (Braun 2005, Brown 2011, Mackay 2008). **Figure 65** and **Table 25** show that MIS3 and MIS4 complete flakes and blades have higher values of CE/M. **Supplementary Table B17** shows that the median CE/M values of MIS3 and MIS4 complete flakes and blades at PP5-6 is

significantly larger than artifacts from all other assemblages (all assemblages: Mann-Whitney p=<0.00001). The median CE/M values of MIS5 artifacts from PP5-6 are statistically similar to MIS5 artifacts from PP9B and MIS6 artifacts from PP13B (**Supplementary Table B17**). Median CE/M values of MIS5 artifacts from PP9B, PP9C, and PP13B is the lowest and they are statistically similar (**Supplementary Table B17**).

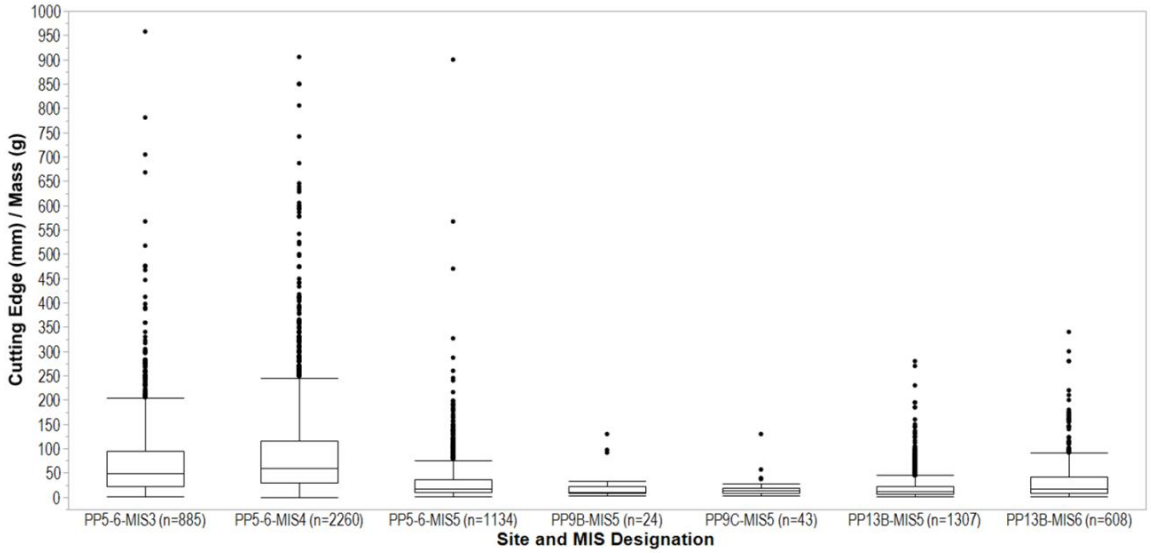

Figure 65. Boxplot with outliers showing distribution of Cutting Edge (mm) / Mass (m) (CE/M) values for all raw materials by site and MIS designation. The age of assemblages increases along the x-axis (from left to right).

Table 25. Cutting edge (mm) / Mass (g) (CE/M) descriptive statistics for all raw materials by site and MIS designation.

	PP5-6-MIS3	PP5-6-MIS4	PP5-6-MIS5	PP9B-MIS5	PP9C-MIS5	PP13B-MIS5	PP13B-MIS6
N	885	2260	1134	24	43	1307	608
Min	1.35	0.16	1.48	3.45	3.43	1.73	1.22
Max	957.73	905.50	900.00	130.00	130.00	280.00	340.00
Mean	78.35	91.57	31.52	24.58	17.81	20.05	32.71
Std. error	3.10	2.09	1.44	6.78	3.12	0.71	1.68
Variance	8487.71	9909.22	2355.89	1102.31	419.12	652.23	1724.18
Stand. dev	92.13	99.55	48.54	33.20	20.47	25.54	41.52
Median	49.94	60.00	17.75	11.01	13.12	11.74	17.02
25 prcntil	21.95	28.92	9.46	8.17	7.73	6.88	9.16
75 prcntil	94.93	116.67	36.28	22.94	19.13	22.18	42.19

Figure 66 and **Table 26** shows that complete flakes and blades made on silcrete from MIS3, MIS4, and MIS5 at PP5-6 have the highest median CE/M values (all assemblages: Mann-Whitney *p*=<0.00001). The median CE/M values of MIS5 quartzite artifacts from PP9B, PP9C, and PP13B is the largest, and are all statistically similar (**Supplementary Table B18**). The median CE/M values of MIS3 and MIS4 quartzite artifacts from PP5-6 are statistically similar to MIS5 and MIS6 silcrete artifacts from PP13B (**Supplementary Table B18**). The median CE/M of MIS5 complete quartzite artifacts from PP5-6 is statistically similar to MIS5 quartzite artifacts from PP9B and PP9C (**Supplementary Table B18**). The median CE/M values of MIS6 quartzite artifacts from PP13B are statistically similar to the MIS5 and MIS6 silcrete artifacts from PP13B (**Supplementary Table B18**).

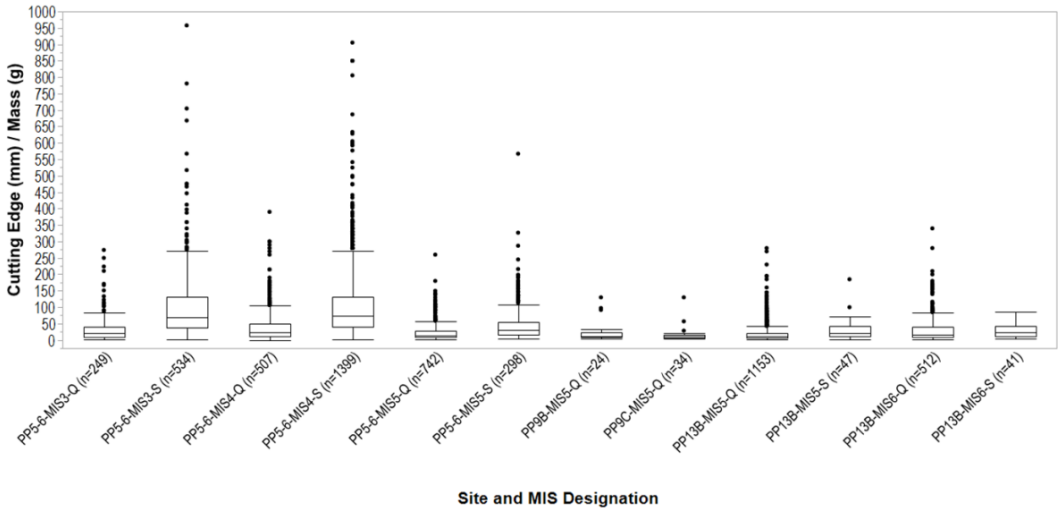

Figure 66. Boxplot with outliers showing distribution of Cutting Edge (mm) / Mass (g) (CE/M) values for quartzite and silcrete by site and MIS designation. Q=Quartzite; S=Silcrete. The age of assemblages increases along the x-axis (from left to right).

Table 26. Descriptive statistics of Cutting edge (mm) / Mass (m) (CE/M) for quartzite (Q) and silcrete (S) by site and MIS designation.

	PP5-6-MIS3-Q	PP5-6-MIS3-S	PP5-6-MIS4-Q	PP5-6-MIS4-S	PP5-6-MIS5-Q	PP5-6-MIS5-S	PP9B-MIS5-Q	PP9C-MIS5-Q	PP13B-MIS5-Q	PP13B-MIS5-S	PP13B-MIS6-Q	PP13B-MIS6-S
N	249	534	507	1399	742	298	24	34	1153	47	512	41
Min	2.14	1.35	0.16	1.55	1.48	3.04	3.45	3.43	1.73	1.93	1.22	3.86
Max	274.2	957.7	390.2	905.5	260.0	567.1	130.0	130.0	280.0	185.0	340.0	85.0
Mean	32.91	101.10	41.04	105.71	22.60	48.31	24.58	16.36	19.19	29.92	31.31	27.79
Std. error	2.52	4.54	2.19	2.76	0.91	3.30	6.78	3.81	0.75	4.61	1.71	3.45
Variance	1576.5	10982.9	2428.9	10664.4	613.2	3249.2	1102.3	492.4	645.8	997.4	1502.3	488.5
Stand. dev	39.71	104.80	49.28	103.27	24.76	57.00	33.20	22.19	25.41	31.58	38.76	22.10
Median	20.22	68.86	23.97	72.86	14.21	30.14	11.01	11.96	11.00	19.52	16.21	21.94
25 prcntil	9.58	38.30	11.62	40.14	8.07	17.01	8.17	7.45	6.59	10.07	8.75	11.17
75 prcntil	40.54	132.54	49.29	132.50	28.23	54.50	22.94	15.57	21.36	41.43	39.07	41.72

Retouch frequency versus artifact volumetric density

The ratio of retouch frequency to artifact volumetric density is here used as a tool to understand technological organization and land-use patterns (Barton 1998, Riel-Salvatore and Barton 2004, Riel-Salvatore, Popescu, and Barton 2008). **Figure 67** and **Table 27** show that the MIS4 assemblage from PP5-6 has both the highest retouched frequency and the lowest artifact density compared to the other assemblages. The MIS4 assemblage plots towards the curated end of the curation-expediency continuum. The MIS3 assemblage from PP5-6 tends towards the curated end but the retouch frequency and the artifact volumetric density is three times as low as the MIS4 assemblage. The MIS5 assemblage from PP5-6 tends towards the expedient end of the continuum with seven times lower retouch frequency and four times lower artifact volumetric density. The MIS5 and MIS6 assemblages from PP13B are at the expedient end of the continuum.

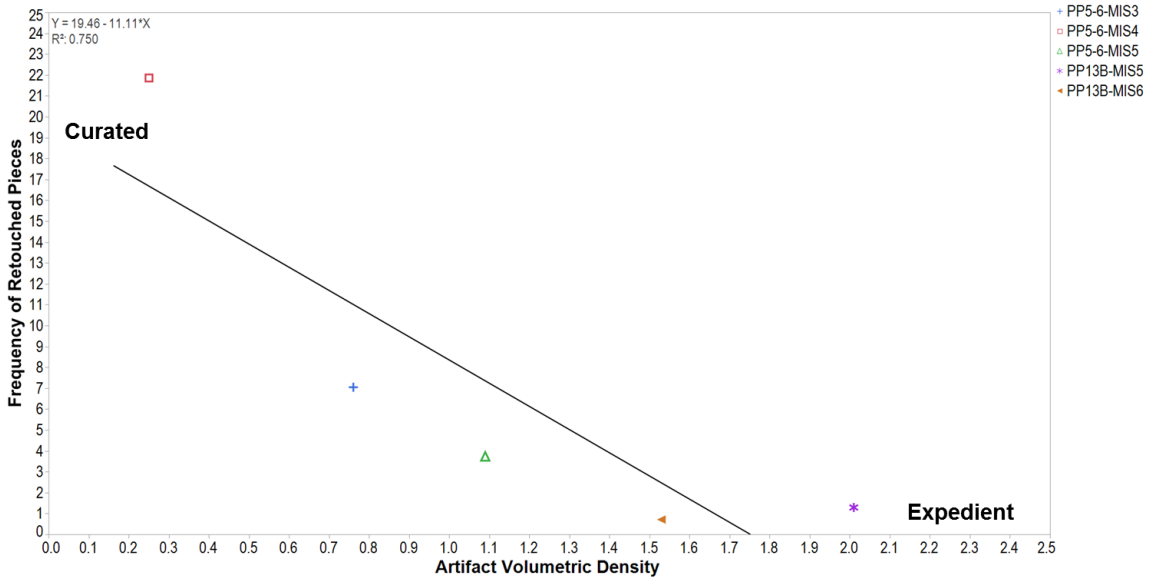

Figure 67. Linear regression between frequency of retouched pieces per total artifact mass (kg) from each marine isotope stage and artifact volumetric density (total artifact mass (kg) per total sediment volume (m^3)) from each marine isotope stage.

Table 27. Marine Isotope Stage summary data for retouched piece frequency, total artifact mass (kg), and sediment volume (m^3).

Site and MIS Designation	Total Artifact Mass (kg)	Retouched Pieces (n=)	Sediment Volume (m^3)	Frequency of retouched pieces (Retouch piece count / artifact mass (kg))	Artifact Density (Artifact Mass (kg) / Sediment Volume (m3))
PP5-6-MIS3	16.00	113	21.13	7.06	0.76
PP5-6-MIS4	20.12	440	79.81	21.87	0.25
PP5-6-MIS5	25.44	95	23.34	3.73	1.09
PP13B-MIS5	69.25	89	34.46	1.29	2.01
PP13B-MIS6	22.41	16	14.62	0.71	1.53

Marine Isotope Stage summary

Quartzite is the dominant raw material in terms of mass (kg) throughout the Pinnacle Point sequence. However, from MIS5 to MIS4 at PP5-6 there is significant increase in the use of silcrete. Silcrete frequency decreases slightly in MIS3 but is still more frequent compared to MIS5. When stone tool type frequencies are based on counts flakes and flake fragments dominate the stone tool artifact classes throughout the Pinnacle Point

sequence. However, as with the silcrete increase in MIS4, there is a similar significant increase in blade and blade fragments in MIS4 at PP5-6. The blades in the PP9B, PP9C, and PP13B assemblages are most frequently made on quartzite. However, silcrete increases as a preferred material to make blades in the MIS5 assemblage at PP5-6. During MIS4 and MIS3, the blades are most frequently made on silcrete. When the stone tool artifact type frequencies are based on mass (kg), the increase in blades in MIS5, MIS4, and MIS3 at PP5-6 is still present. However, the frequencies of cores and hammerstone/manuports in PP9 and PP13B assemblages increase. This means that a greater percentage of raw materials that have been transported to the sites are bound up in unused material.

The stone artifacts from MIS3 and MIS4 assemblages at PP5-6 are smaller and thinner than the lithics from the other assemblages. The maximum dimension and thickness of the MIS5 stone artifacts at PP5-6 is similar to the MIS6 stone artifacts from PP13B. The MIS5 lithics from PP9B, PP9C, and PP13B are longest and thickest in the sequence. When looking at quartzite and silcrete lithics separately silcrete stone artifacts from the MIS3, MIS4, and MIS5 at PP5-6 are significantly smaller and thinner than quartzite and silcrete lithics from all other assemblages, while the quartzite stone artifacts from MIS3, MIS4, and MIS5 at PP5-6 are more similar to the quartzite and silcrete stone artifacts from the other assemblages.

The technological lengths and widths of complete flakes and blades show a very similar pattern to the maximum dimension and thickness results. MIS3 and MIS4 stone artifacts from PP5-6 are shorter and narrower than stone tools from all other assemblages.

The silcrete stone artifacts from MIS3, MIS4, and MIS5 at PP5-6 are shorter and narrower than quartzite and silcrete lithics from all other assemblages.

The relative cortex frequency suggests that throughout the Pinnacle Point sequence, raw materials were mostly procured from high-energy environments such as cobble beaches and/or streambeds, or alternatively from conglomerates that include well-rounded clasts. However, in MIS4 at PP5-6 there is evidence that the dominant procurement strategy for silcrete shifted to focusing on fixed primary sources such as cliffs or outcrops. There is also an increase in outcrop cortex on quartzite but not enough to be the dominant strategy for that material. This pattern also holds in MIS3 at PP5-6; silcrete is dominated by outcrop cortex but in a smaller frequency compared to MIS4, whereas quartzite is dominated by cobble cortex with a small decrease in outcrop cortex.

MIS3 and MIS4 stone artifacts at PP5-6 were flaked more efficiently than lithics from all other assemblages. The MIS5 lithics from PP5-6 were flaked similarly in terms of efficiency compared to MIS6 stone artifacts from PP13B. MIS5 stone artifacts from PP9B, PP9C, and PP13B were flaked less efficiently. The flaking efficiency of MIS3, MIS4, and MIS5 silcrete stone artifacts are the highest comparable to quartzite and silcrete lithics from all other assemblages. The flaking efficiency of both quartzite and silcrete stone artifacts from MIS5 and MIS6 assemblages at PP13B is very similar.

The retouch frequency to artifact volumetric density ratio method suggests that the MIS4 assemblage at PP5-6 is due to curated behavior. The ratios of the MIS3 and MIS5 assemblages at PP5-6 indicate that they are a mix of curated and expedient behavior. The ratios of the MIS5 and MIS6 assemblages at PP13B suggest that they are due to expedient behavior.

Stone tool data – grouped by stratigraphic aggregate/unit

In the following section, the pertinent archaeological data (raw material frequency, lithic type frequency, cortex type frequency, technological length, cutting edge per mass ratios, and retouch frequency per artifact density ratios) will be presented by StratAggs (stratigraphic aggregates) from the localities in question. Additionally, raw material frequency from PP5-6 will be presented by SubAggs (sub-aggregates) to present an even higher resolution raw material frequency from that site.

Raw material frequency

Figure 68 and **Tables 28** (corresponding counts of raw materials in each StratAgg can be found in **Supplementary Table B19)** show that quartzite is the dominant raw material throughout the PP13B sequence in terms of transported mass (kg) (75.8% to 100%). Quartz is the second dominant raw material (0% to 13.4%), while silcrete frequencies only rise to prominence in the LC-MSA Lower (5%), LC-MSA Middle (5.8%), LC-MSA Upper (9.3%), and LB Sand 2 (6.4%) based on artifact mass (kg).

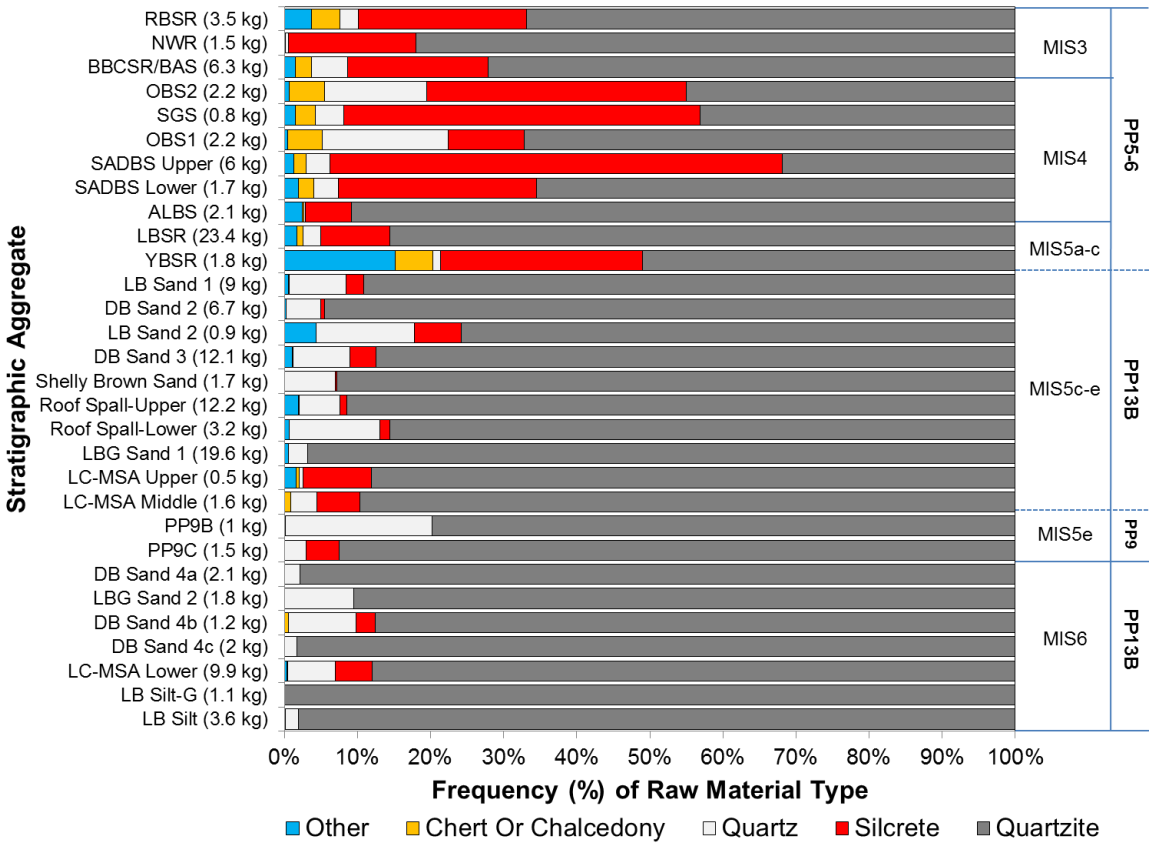

Figure 68. Relative frequency of raw material type in assemblage tallied by artifact mass (kg) by stratigraphic aggregates. The age of assemblages decreases along the y-axis (oldest at bottom).

Table 28. Raw material type tallied by mass (kg) for PP13B stratigraphic aggregates.

Stratigraphic aggregate	Other (kg)	Chert Or Chalcedony (kg)	Quartz (kg)	Silcrete (kg)	Quartzite (kg)	Total (kg)
LB Sand 1 (n=356)	0.045	0.011	0.709	0.216	8.045	9.03
DB Sand 2 (n=249)	0.012	0.000	0.321	0.030	6.285	6.65
LB Sand 2 (n=57)	0.039	0.000	0.121	0.058	0.685	0.90
DB Sand 3 (n=674)	0.128	0.019	0.942	0.432	10.603	12.12
Shelly Brown Sand (n=199)	0.000	0.001	0.118	0.002	1.581	1.70
Roof Spall-Upper (n=964)	0.233	0.011	0.677	0.115	11.132	12.17
Roof Spall-Lower (n=303)	0.022	0.000	0.394	0.043	2.720	3.18
LBG Sand 1 (n=464)	0.099	0.001	0.518	0.005	18.952	19.58
LC-MSA Upper (n=59)	0.007	0.002	0.002	0.044	0.415	0.47
LC-MSA Middle (n=184)	0.000	0.014	0.057	0.092	1.418	1.58
DB Sand 4a (n=36)	0.000	0.000	0.046	0.000	2.082	2.13
LBG Sand 2 (n=86)	0.001	0.000	0.172	0.000	1.657	1.83
DB Sand 4b (n=47)	0.000	0.006	0.109	0.030	1.024	1.17
DB Sand 4c (n=22)	0.000	0.000	0.034	0.000	1.955	1.99

LC-MSA Lower (n=1522)	0.037	0.010	0.642	0.496	8.718	9.90
LB Silt-G (n=16)	0.000	0.000	0.000	0.000	1.114	1.11
LB Silt (n=91)	0.003	0.000	0.065	0.001	3.488	3.56
Total (kg)	0.627	0.075	4.928	1.564	81.874	89.07

The record from PP9B and PP9C show that quartzite is the dominant raw material throughout at both PP9B (79.8%) and PP9C (92.5%) in terms of transported mass (kg) (**Figure 68** and **Table 29**; corresponding counts of raw materials at each site can be found in **Supplementary Table B20**). Quartz is the second dominant raw material (20.1% at PP9B), while silcrete is found at low frequency at PP9C (4.5%).

Table 29. Raw material type tallied by mass (kg) for PP9B and PP9C.

Cave Site	Other (kg)	Chert or Chalcedony (kg)	Quartz (kg)	Silcrete (kg)	Quartzite (kg)	Total (kg)
PP9B-MIS5 (n=68)	0.0009	0	0.2056	0	0.818	1.0245
PP9C-MIS5 (n=86)	0	0	0.0462	0.0694	1.4233	1.5389
Total (kg)	0.0009	0	0.2518	0.0694	2.2413	2.5634

At PP5-6 there is great variability in the raw material frequencies throughout the sequence at the StratAgg level based on what has been transported to the site (**Figure 68** and **Table 30**; corresponding counts of raw materials in each StratAgg can be found in **Supplementary Table B21**). Several interesting observations can be made from **Figure 68**. In the three earliest stratigraphic aggregates YBSR (51%), LBSR (85.6%), and ALBS (90.9%), and in the SADBS Lower (65.5%) and OBS1 (67.2%) StratAggs quartzite dominates, while silcrete is dominant in the interstratified SADBS Upper (61.9%) and SGS (48.8%) StratAggs. The following OBS2 (45.1%), BBCSR/BAS (72.2%), NWR (81.9%), and RBSR (66.9%) StratAggs are dominated by quartzite. Quartz only rises to a relatively high frequency (~ ≥5%) in terms of mass (kg) in OBS1 (17.2%), OBS2

(13.9%) and BBCSR (5%). Materials such as hornfels and indurated shale designated as 'other' raw materials only rise to relatively high frequencies (~ ≥5%) in the YBSR StratAgg (15.1%). Chert (Chalcedony) has elevated frequencies (~ ≥4%) in YBSR (5.2%), OBS1 (4.7%), OBS2 (4.9%), and RBSR (4%).

Table 30. Raw material type tallied by mass (kg) for PP5-6 stratigraphic aggregates.

Stratigraphic aggregate	Other (kg)	Chert or Chalcedony (kg)	Quartz (kg)	Silcrete (kg)	Quartzite (kg)	Total (kg)
RBSR (n=552)	0.127	0.138	0.086	0.801	2.332	3.484
NWR (n=275)	0.0001	0.002	0.01	0.266	1.25	1.526
BBCSR/BAS (n=3309)	0.097	0.133	0.311	1.206	4.527	6.273
OBS2 (n=1194)	0.014	0.105	0.300	0.768	0.974	2.161
SGS (n=339)	0.011	0.021	0.030	0.368	0.325	0.754
OBS1 (n=725)	0.011	0.105	0.383	0.232	1.495	2.226
SADBS Upper (n=3783)	0.076	0.100	0.198	3.735	1.925	6.034
SADBS Lower (n=294)	0.032	0.034	0.056	0.450	1.086	1.658
ALBS (n=316)	0.051	0.005	0.005	0.130	1.901	2.092
LBSR (n=2811)	0.399	0.188	0.576	2.211	20.055	23.429
YBSR (n=280)	0.266	0.092	0.018	0.487	0.899	1.763
Total (kg)	1.0841	0.923	1.973	10.654	36.769	51.4

Only stratigraphic aggregates with 10 or more stone artifacts are included.

Raw material frequency – Sub-aggregate data from PP5-6

In the following text, the analysis will focus on individual SubAggs within each StratAgg and MIS Designation at PP5-6. I start with the earliest deposits. During MIS 5 at PP5-6, quartzite dominates throughout and there is decreasing raw material variability with younger sediments. **Figure 69** and **Table 31** (corresponding counts of raw materials in each sub-aggregate can be found in **Supplementary Table B22**) show that quartzite is the dominant raw material in all sub-aggregates (45.5% to 100%) except for in Kirsty (26.9%), Elizabeth Sand and Roof spall (28.4%), Tove Sand and Roofspall (46.8%), and Logan Sand and Roofspall 2 (33.9%). Chert (Chalcedony) dominates in Kirsty (29.3%).

Silcrete dominates in Elizabeth Sand and Roofspall (48.2%), Tove Sand and Roofspall (49.7%), and Logan Sand and Roofspall 2 (64.8%). Quartz has relatively increased frequencies (~ ≥5%) in Simen Red (7.1%), Arnold Red (25%), Logan Red (16.4%), Logan Sand and Roofspall 1 (15.2%), Sondra Red (4.9%), Luke Shell (6.1%), and Cobus Shell (12.7%).

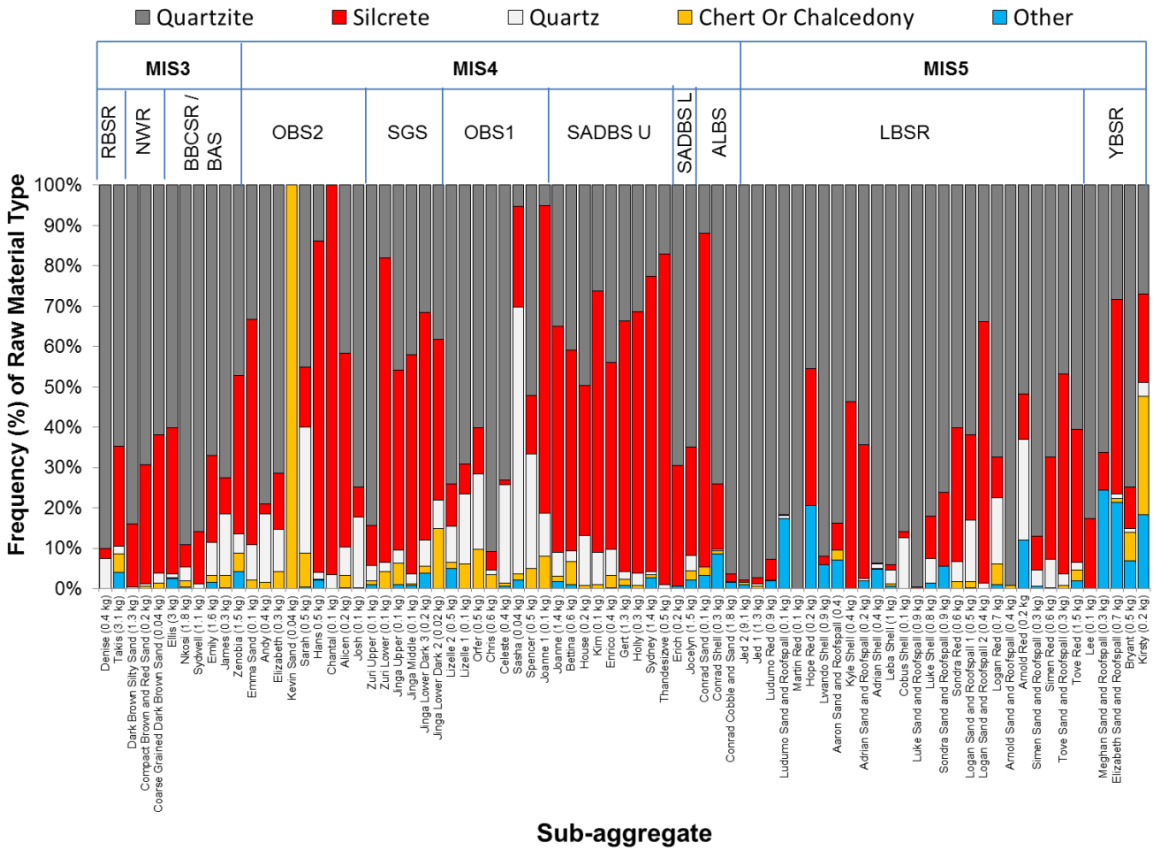

Figure 69. Relative frequency of raw material type tallied by artifact mass (kg) at PP5-6 by sub-aggregates during MIS3, MIS4, and MIS5. The age of assemblages increases along the x-axis (from left to right). Only sub-aggregates with 10 or more stone artifacts are included.

Other than Kirsty (29.3%), chert (chalcedony) only rises to relatively elevated frequencies (~ ≥5%) in Bryant (7.2%) and Logan Red (5.2%). 'Other' raw materials such as hornfels and indurated shale have very varied frequencies but rise to relatively elevated frequencies (~ ≥5%) in Kirsty (18.4%), Bryant (6.8%), Elizabeth Sand and

Roofspall (21.4%), Meghan Sand and Roofspall (24.3%), Arnold Red (12.1%), Sondra Sand and Roofspall (5.5%), Aaron Sand and Roofspall (7.15), Lwando Shell (6%), Hope Red (20.6%), and Ludumo Sand and Roofspall (17.3%).

Table 31. Raw material type tallied by artifact mass (kg) at PP5-6 by MIS5 sub-aggregates.

Stratigraphic aggregate	Sub-aggregate	Other (kg)	Chert or Chalcedony (kg)	Quartz (kg)	Silcrete (kg)	Quartzite (kg)	Total (kg)
LBSR	Jed 2	0.081	0.062	0.005	0.047	8.868	9.062
LBSR	Jed 1	0.000	0.006	0.008	0.019	1.265	1.299
LBSR	Ludumo Red	0.018	0.000	0.002	0.048	0.873	0.941
LBSR	Ludumo Sand and Roofspall	0.021	0.000	0.001	0.000	0.101	0.124
LBSR	Martin Red	0.000	0.000	0.000	0.000	0.104	0.104
LBSR	Hope Red	0.040	0.000	0.000	0.066	0.089	0.195
LBSR	Lwando Shell	0.052	0.000	0.000	0.017	0.797	0.866
LBSR	Aaron Sand and Roofspall	0.029	0.010	0.000	0.027	0.336	0.402
LBSR	Kyle Shell	0.000	0.000	0.000	0.196	0.228	0.424
LBSR	Adrian Sand and Roofspall	0.004	0.000	0.001	0.066	0.127	0.197
LBSR	Adrian Shell	0.020	0.001	0.005	0.001	0.407	0.435
LBSR	Leba Shell	0.006	0.006	0.035	0.014	0.959	1.020
LBSR	Cobus Shell	0.000	0.000	0.012	0.001	0.080	0.093
LBSR	Luke Sand and Roofspall	0.000	0.000	0.000	0.004	0.865	0.868
LBSR	Luke Shell	0.010	0.000	0.047	0.082	0.644	0.784
LBSR	Sondra Sand and Roofspall	0.047	0.000	0.000	0.157	0.648	0.851
LBSR	Sondra Red	0.000	0.010	0.028	0.193	0.351	0.583
LBSR	Logan Sand and Roofspall 1	0.001	0.008	0.081	0.114	0.332	0.536
LBSR	Logan Sand and Roofspall 2	0.000	0.000	0.005	0.236	0.123	0.364
LBSR	Logan Red	0.006	0.034	0.107	0.065	0.439	0.651
LBSR	Arnold Sand and Roofspall	0.000	0.002	0.000	0.000	0.343	0.346
LBSR	Arnold Red	0.027	0.000	0.055	0.025	0.114	0.221
LBSR	Simen Sand and Roofspall	0.002	0.000	0.011	0.024	0.254	0.292
LBSR	Simen Red	0.000	0.001	0.043	0.152	0.403	0.599
LBSR	Tove Sand and Roofspall	0.000	0.002	0.009	0.154	0.145	0.309
LBSR	Tove Red	0.028	0.040	0.026	0.478	0.878	1.450
YBSR	Lee	0.000	0.000	0.000	0.019	0.092	0.111
YBSR	Meghan Sand and Roofspall	0.060	0.000	0.000	0.023	0.162	0.245
YBSR	Elizabeth Sand and Roofspall	0.143	0.006	0.008	0.322	0.190	0.669
YBSR	Bryant	0.032	0.034	0.004	0.048	0.355	0.474
YBSR	Kirsty	0.031	0.050	0.006	0.038	0.046	0.171

Total (kg)	0.657	0.271	0.501	2.637	20.620	24.686

Only sub-aggregates with 10 or more stone tools are included.

Figure 69 and **Table 32** (corresponding counts of raw materials in each SubAgg can be found in **Supplementary Table B23**) show that there is great variability in raw material frequencies in the MIS4 SubAggs. Several observations can be made. Quartzite is dominant in the two early ALBS sub-aggregates (Conrad Cobble and Sand: 96.5%; Conrad Shell: 74.1%) and in the two SADBS Lower aggregates (Jocelyn: 65%; Erich: 69.5%). Silcrete dominates in the SADBS Upper aggregates (46.4% to 82%) except for in House (37.2%). In the OBS1 stratigraphic aggregate, quartzite dominates in all sub-aggregates (52.1% to 90.9%) except for Joanne 1 (5.1%) and Sasha (5.3%). Silcrete dominates in Joanne 1 (76.2%) and quartz dominates in Sasha (66.1%). The frequencies in the SGS sub-aggregates are dominated by silcrete (39.7% to 75.5%) except for in Zuri Upper (9.9%) and Jinga Upper (44.65%). Quartzite dominates in Zuri Upper (84.4%) and Jinga Upper (45.8%). In the following OBS2, the raw material frequencies are very variable. Quartzite dominates in sub-aggregates Josh (74.8%), Sarah (45.1%), Elizabeth (71.4%), and Andy (79.1%). Silcrete dominates in Alicen (48%), Chantal (96.6%), Hans (82.2%), and Emma Sand (55.9%). Kevin Sand is dominated by Chert (Chalcedony) (100%).

In addition to Sasha where quartz dominates the assemblage (66.1%), Quartz has relatively elevated frequencies (~ ≥10%) in House (12.4%), Joanne 1 (10.6%), Spencer (28.5%), Celeste (24.5%), Orfer (11.4%), Lizelle 1 (17.4%), Josh (17.5%), Sarah (31.2%), Elizabeth (10.5%), and Andy (17.4%). Other than Kevin Sand (100%), chert (chalcedony) has relatively increased frequencies (~ ≥5%) in Bettina (5.7%), Joanne 1

(8.1%), Spencer (5%), Orfer (9.7%), Lizelle 1 (6%), Jinga Lower Dark 2 (14.9%), Jinga Upper (5.2%), and Sarah (8.4%).

Table 32. Raw material type tallied by artifact mass (kg) at PP5-6 by MIS4 sub-aggregates.

Stratigraphic aggregate	Sub-aggregate	Other (kg)	Chert or Chalcedony (kg)	Quartz (kg)	Silcrete (kg)	Quartzite (kg)	Total (kg)
OBS2	Emma Sand (n=53)	0.000	0.001	0.006	0.038	0.023	0.069
OBS2	Andy (n=135)	0.000	0.006	0.070	0.010	0.323	0.409
OBS2	Elizabeth (n=97)	0.000	0.011	0.030	0.040	0.202	0.283
OBS2	Kevin Sand (n=47)	0.000	0.038	0.000	0.000	0.000	0.038
OBS2	Sarah (n=488)	0.002	0.042	0.157	0.075	0.227	0.505
OBS2	Hans (n=219)	0.011	0.001	0.009	0.443	0.074	0.539
OBS2	Chantal (n=20)	0.000	0.000	0.003	0.083	0.000	0.086
OBS2	Alicen (=99)	0.000	0.005	0.010	0.071	0.062	0.148
OBS2	Josh (n=33)	0.000	0.000	0.015	0.006	0.063	0.084
SGS	Zuri Upper (n=37)	0.001	0.001	0.005	0.013	0.113	0.134
SGS	Zuri Lower (n=68)	0.000	0.006	0.003	0.106	0.025	0.141
SGS	Jinga Upper (n=56)	0.001	0.007	0.005	0.063	0.064	0.140
SGS	Jinga Middle (n=40)	0.001	0.001	0.003	0.073	0.057	0.135
SGS	Jinga Lower Dark 3 (n=120)	0.007	0.003	0.012	0.106	0.059	0.188
SGS	Jinga Lower Dark 2 (n=16)	0.000	0.002	0.001	0.006	0.006	0.016
OBS1	Lizelle 2 (n=35)	0.008	0.002	0.014	0.016	0.116	0.156
OBS1	Lizelle 1 (n=20)	0.000	0.007	0.019	0.008	0.076	0.110
OBS1	Orfer (n=114)	0.000	0.047	0.092	0.056	0.294	0.489
OBS1	Chris (n=55)	0.001	0.018	0.007	0.026	0.513	0.564
OBS1	Celeste (n=87)	0.002	0.003	0.085	0.004	0.253	0.345
OBS1	Sasha (n=33)	0.001	0.001	0.028	0.011	0.002	0.042
OBS1	Spencer (n=301)	0.000	0.022	0.128	0.065	0.234	0.449
OBS1	Joanne 1 (n=77)	0.000	0.005	0.007	0.047	0.003	0.062
SADBS Upper	Joanne (n=372)	0.023	0.020	0.079	0.761	0.474	1.356
SADBS Upper	Bettina (n=339)	0.006	0.035	0.016	0.305	0.250	0.611
SADBS Upper	House (n=92)	0.000	0.001	0.022	0.065	0.087	0.176
SADBS Upper	Kim (n=58)	0.000	0.001	0.008	0.064	0.026	0.098
SADBS Upper	Enrico (n=161)	0.001	0.012	0.025	0.177	0.168	0.381
SADBS Upper	Gert (n=717)	0.010	0.018	0.026	0.793	0.430	1.277
SADBS Upper	Holly (n=193)	0.000	0.002	0.008	0.170	0.082	0.262
SADBS Upper	Sydney (n=1492)	0.037	0.012	0.010	1.015	0.314	1.388
SADBS Upper	Thandesizwe (n=356)	0.000	0.000	0.004	0.386	0.080	0.470
SADBS Lower	Erich (n=79)	0.001	0.000	0.000	0.055	0.127	0.182

SADBS Lower	Jocelyn (n=215)	0.031	0.034	0.056	0.396	0.959	1.476
ALBS	Conrad Sand (n=19)	0.002	0.002	0.000	0.058	0.008	0.071
ALBS	Conrad Shell (n=54)	0.022	0.002	0.001	0.041	0.189	0.254
ALBS	Conrad Cobble and Sand (n=243)	0.026	0.001	0.004	0.031	1.704	1.767
Total (kg)		0.194	0.369	0.968	5.683	7.687	14.901

Only sub-aggregates with 10 or more artifacts are included.

A separate StratAgg called DBCS also belongs to the MIS4 designation based on OSL dating as noted above. It is overlaying the SGS but is most likely derived from materials from the BAS, OBS2, and SGS. **Figure 70** and **Supplementary Table B24** (corresponding counts of raw materials in each sub-aggregate can be found in **Supplementary Table B25**) show that both quartzite and silcrete are the dominant raw materials throughout the DBCS sequence in terms of transported mass (kg).

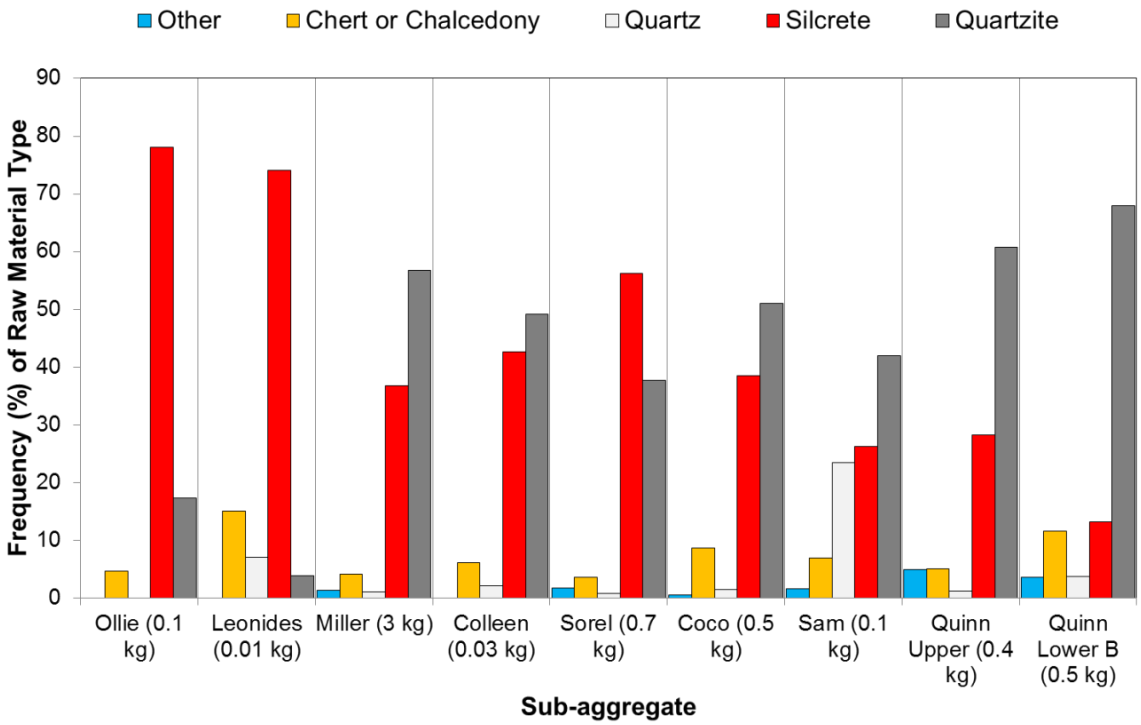

Figure 70. Frequency of raw material type in assemblage tallied by artifact mass (kg) at PP5-6 by DBCS sub-aggregates during MIS4. The age of assemblages increases along the x-axis (from left to right).

Quartzite dominates SubAggs Quinn Lower-B (68%), Quinn Upper (60.1%), Sam (41.9%, Coco (51%), Colleen (49.1%), Miller (56.8%), while silcrete dominates Sorel (56.2%), Leonides (74.1%), and Ollie (78%). Quartz has relatively elevated frequencies (~ ≥5%) in Sam (23.4%) and Leonides (7%). Chert (Chalcedony) has relatively elevated frequencies (~ ≥5%) in all aggregates (5% to 15.1%) except for Sorel (3.5%), Miller (4.1%), and Ollie (4.7%). 'Other' raw material types only rise to a relatively elevated frequency (~ ≥3%) in Quinn Lower B (3.6%) and Quinn Upper (4.9%).

During MIS3, quartzite is the dominant raw material in every SubAgg in terms of what has been transported (47.2% to 90%) (**Figure 69** and **Table 33**; corresponding counts of raw materials in each SubAgg can be found in **Supplementary Table B26**). Silcrete has elevated frequencies in Dark Brown Silty Sand (15.5%), Compact Brown and Red Sand (29.5%), Coarse Grained Dark Brown Sand (34.2%), Zenobia (39.2%), Emily (21.7%), Ellis (36.3%), and Takis (24.8%), while quartz has elevated frequencies (~ ≥5%) in James (15.3%), Emily (8.1%), and Denise (7.4%). Chert (Chalcedony) and 'other' raw materials such as hornfels and indurated shale only rise to a relatively high frequency (~ ≥4%) in Zenobia (Chert: 4.5%; 'other': 4.3%) and Takis (Chert: 4.5%; 'other': 4.1%).

Table 33. Raw material type tallied by artifact mass (kg) at PP5-6 by MIS3 sub-aggregates.

Stratigraphic aggregate	Sub-aggregate	Other (kg)	Chert or Chalcedony (kg)	Quartz (kg)	Silcrete (kg)	Quartzite (kg)	Total (kg)
RBSR	Denise (n=26)	0.000	0.000	0.026	0.009	0.319	0.354
RBSR	Takis (n=523)	0.127	0.138	0.060	0.773	2.013	3.111
NWR	Dark Brown Silty Sand (n=207)	0	0.0006	0.01	0.205	1.11	1.33
NWR	Compact Brown and Red Sand (n=57)	0.0001	0.0009	0	0.048	0.11	0.164

NWR	Coarse Grained Dark Brown Sand (n=11)	0	0.0005	0	0.013	0.023	0.037
BBCSR/BAS	Ellis (n=1867)	0.076	0.005	0.025	1.071	1.776	2.954
BBCSR/BAS	Nkosi (n=178)	0.006	0.030	0.062	0.101	1.630	1.829
BBCSR/BAS	Sydwell (n=108)	0.001	0.000	0.012	0.145	0.953	1.110
BBCSR/BAS	Emily (n=521)	0.024	0.027	0.127	0.338	1.044	1.560
BBCSR/BAS	James (n=36)	0.001	0.008	0.037	0.022	0.178	0.245
BBCSR/BAS	Zenobia (n=599)	0.065	0.069	0.073	0.600	0.722	1.529
Total (kg)		0.3001	0.279	0.432	3.325	9.878	14.223

Only sub-aggregates with 10 or more stone artifacts are included.

Bootstrapped raw material frequencies

By using the raw material frequencies from StratAggs or SubAggs from each MIS designation one can bootstrap the different raw material frequencies to obtain 95% confidence intervals around each mean raw material frequency. If StratAggs are used, which is the case with PP13B data then that data can be used to test whether a mean raw material frequency from a Marine Isotope Stage is significantly different from the mean frequency of another in the same Marine Isotope Stage. If SubAggs are used, which is the case with PP5-6 data then that data can be used to test whether a mean raw material frequency from a StratAgg is significantly different from the mean frequency of another in the same StratAgg.

The MIS5 assemblage from PP13B consists of 10 StratAgg samples (LB Sand 1, DB Sand 2, LB Sand 2, DB Sand 3, Shelly Brown Sand, Roof Spall-Upper, Roof Spall-Lower, LBG Sand 1, LCA-MSA Upper, and LC-MSA Lower, while the MIS6 assemblage from PP13B consists of seven StratAggs (DB Sand 4a, LBG Sand 2, DB Sand 4b, DB Sand 4c, LC-MSA Lower, LB Silt-G, and LB Silt. From PP5-6 six SubAggs were used from the BBCSR/BAS StratAgg, nine from the OBS2 StratAgg, six

from SGS, eight from OBS1, nine from SADBS Upper, five from SADBS Lower and ALBS combined, 26 from LBSR, and five from YBSR.

Figure 71 shows the mean frequencies of quartzite, silcrete, and quartz with 95% confidence intervals resulting from the bootstrap of the standard error 10000 times. In both the MIS5 and MIS6 assemblages at PP13B, quartzite is significantly more frequent than silcrete and quartz (**Table 34**). Additionally, in both MIS5 and MIS6, silcrete and quartz frequencies are statistically similar to each other in each assemblage and between both assemblages (**Table 34**). The silcrete frequency from the MIS5 assemblage at PP13B is statistically similar to the silcrete frequencies from the OBS1 and SADBS Lower/ALBS StratAggs at PP5-6, while the quartzite frequency is statistically similar to the quartzite frequency from the SADBS Lower/ALBS StratAgg (**Tables 34-35**).

At PP5-6 during MIS5, quartzite is significantly more frequent than silcrete and quartz in LBSR, while in the older YBSR quartzite and silcrete has statistically similar frequencies (**Figure 71** and **Table 35**). From LBSR in MIS5 to SADBS Lower/ALBS in MIS4, the frequency of silcrete increases, while the frequency of quartzite decreases. However, in the SADBS Lower/ALBS, the frequency of quartzite and silcrete are statistically similar.

When moving into the SADBS Upper the frequency of silcrete increases further while the quartzite frequency drops making the frequencies significantly different (**Table 35**). In next three aggregates, OBS1, SGS, and OBS2 in MIS4, quartzite and silcrete frequencies are statistically similar. In both OBS1 and OBS2, quartz frequencies are also statistically similar to silcrete frequencies (**Table 35**). When moving into MIS3, the frequency of quartzite increases again, while silcrete decreases making the two

frequencies significantly different. However, the quartz frequency is statistically similar to the silcrete frequency (**Table 35**). The frequency of quartz is relatively low in all StratAggs expect for in OBS1 and OBS2 stages (**Table 35**).

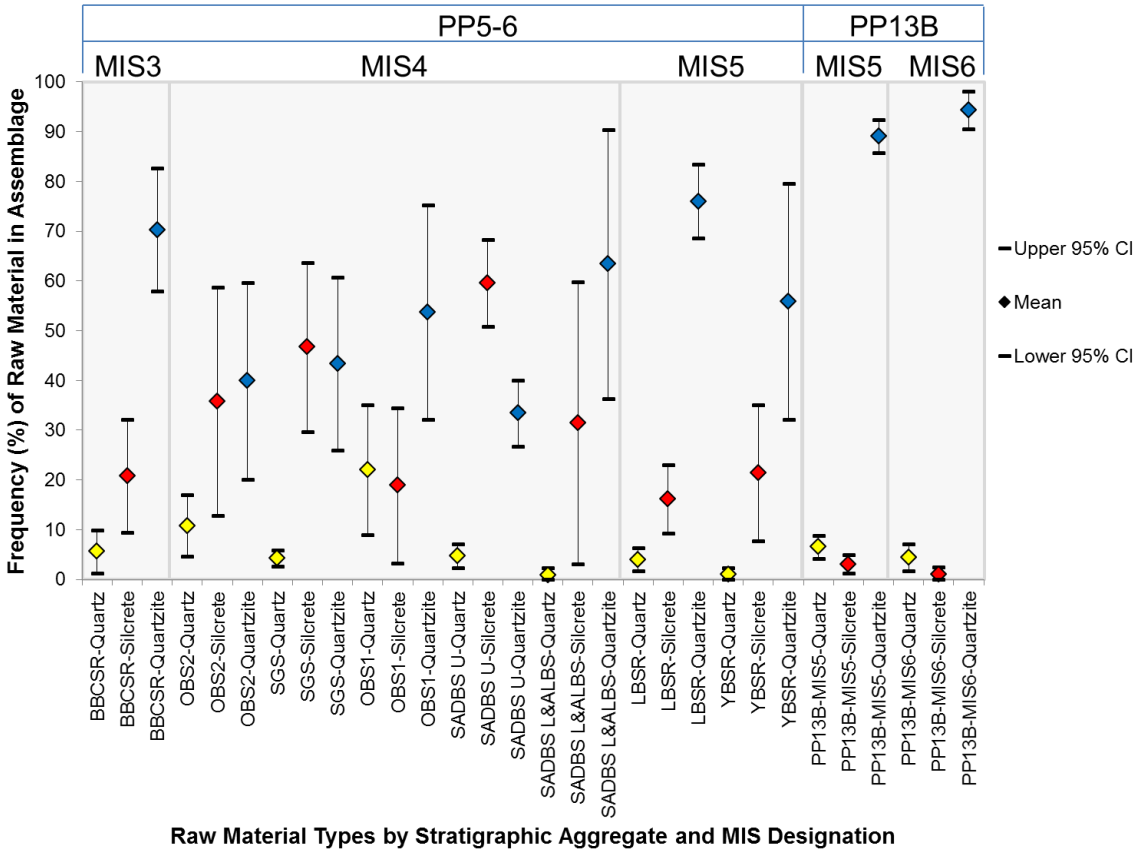

Figure 71. Bootstrapped raw material frequencies at PP13B by MIS designation and at PP5-6 by stratigraphic aggregate and MIS Designation. Plot shows the mean and the upper and lower 95% confidence intervals for quartz, quartzite, and silcrete. From PP5-6 only stratigraphic aggregates with five or more sub-aggregates with available raw material data are included. The age of assemblages increases along the x-axis (from left to right).

Another interesting observation is that the frequencies of quartzite and silcrete have overall greater margins of error during MIS4 compared to MIS3 and MIS5, which reflects a greater variance in what raw material in terms of mass was transported most frequently to PP5-6 relative to other raw materials. A shorter length between the upper and lower 95% CI bars indicates that a given raw material is the most frequently

transported material in terms of mass to PP5-6 across several SubAggs (**Table 35**). The only two StratAggs that do not showcase wide margins of error on all three raw materials are SADBS Upper, which shows that more silcrete in terms of mass is consistently transported more frequently to PP5-6 than quartzite and quartz, and LBSR, which shows that quartzite in terms of mass is consistently transported more frequently to PP5-6 than silcrete and quartz (**Table 35**). Additionally, the MIS5 and MIS6 assemblages from PP13B have narrow margins of error on all three raw materials (**Table 34**).

Table 34. Summary statistics and bootstrap test results for quartz, silcrete, and quartzite at PP13B by MIS Designation.

	PP13B-MIS5-Quartz	PP13B-MIS5-Silcrete	PP13B-MIS5-Quartzite	PP13B-MIS6-Quartz	PP13B-MIS6-Silcrete	PP13B-MIS6-Quartzite
n (aggregate samples)	10	10	10	7	7	7
First Quartile	3.352	0.375	86.993	1.709	0.000	87.621
Min	0.468	0.026	75.800	0.000	0.000	87.621
Median	6.256	1.862	89.412	2.148	0.000	97.852
Mean	6.545	3.046	89.153	4.413	1.085	94.341
Max	13.395	9.336	96.815	9.391	5.006	100.000
Third Quartile	8.989	5.981	93.287	9.331	2.551	98.291
SD	4.071	3.182	5.794	3.913	1.972	5.371
Boot strapped SE*	1.196	0.937	1.691	1.396	0.682	1.917
Margin of error (95% CI)	2.344	1.837	3.315	2.736	1.337	3.757
Bootstrapped Upper 95% CI*	8.889	4.883	92.468	7.150	2.423	98.097
Bootstrapped Lower 95% CI*	4.202	1.209	85.838	1.677	0.000	90.584

**Bootstrapped 10000 times*

Table 35. Summary statistics and bootstrap test results for quartz, silcrete, and quartzite at PP5-6 by stratigraphic aggregate.

	n aggregate frequencies	First Quartile	Min	Median	Mean	Max	Third Quartile
YBSR-Quartzite	5	27.676	26.941	66.214	55.833	83	78.799
YBSR-Silcrete	5	9.825	9.455	17.318	21.434	48	35.100
YBSR-Quartz	5	0.000	0.000	0.889	1.089	3	2.277
LBSR-Quartzite	26	60.476	33.900	81.899	76.023	100	93.748
LBSR-Silcrete	26	1.160	0.000	9.143	16.109	65	33.008
LBSR-Quartz	26	0.000	0.000	1.050	4.005	25	5.158
SADBS L&ALBS-Quartzite	5	38.448	11.910	69.446	63.384	96	85.290
SADBS L&ALBS-Silcrete	5	8.935	1.740	26.828	31.459	83	56.298
SADBS L&ALBS-Quartz	5	0.000	0.000	0.250	0.880	4	2.074
SADBS U-Quartzite	9	24.459	17.078	33.675	33.397	50	42.422
SADBS U-Silcrete	9	48.103	37.228	62.126	59.581	82	68.932
SADBS U-Quartz	9	1.456	0.742	3.168	4.676	12	68.932
OBS1-Quartzite	8	16.954	5.060	64.584	53.700	91	73.798
OBS1-Silcrete	8	5.300	1.077	10.970	18.866	76	22.419
OBS1-Quartz	8	9.424	1.214	18.063	22.005	66	22.419
SGS-Quartzite	6	28.190	18.007	40.173	43.357	84	55.447
SGS-Silcrete	6	32.241	9.858	49.463	46.741	76	61.211
SGS-Quartz	6	2.441	2.206	3.592	4.251	7	6.650
OBS2-Quartzite	9	0.000	0.000	41.749	39.896	79	73.079
OBS2-Silcrete	9	4.971	0.000	14.888	35.722	97	69.078
OBS2-Quartz	9	2.597	0.000	8.709	10.798	31	17.253
BBCSR-Quartzite	11	56.904	47.223	69.758	70.305	89	86.642
BBCSR-Silcrete	11	8.020	5.507	17.373	20.764	39	36.997
BBCSR-Quartz	11	0.992	0.860	4.089	5.574	15	9.898

SD	Boot strapped SE*	Margin of error (95% CI)	Bootstrapped Upper 95% CI*	Bootstrapped Lower 95% CI*
26.361	12.108	23.731	79.564	32.102
15.820	6.993	13.707	35.140	7.727
1.368	0.611	1.197	2.286	0.000
19.748	3.777	7.403	83.425	68.620
18.368	3.497	6.853	22.963	9.256
6.377	1.197	2.345	6.350	1.660
31.216	13.813	27.073	90.458	36.311
30.691	14.442	28.306	59.765	3.152
1.623	0.715	1.402	2.282	0.000
10.438	3.395	6.654	40.051	26.744
13.813	4.442	8.707	68.288	50.875
13.813	1.232	2.416	7.091	2.260
31.997	10.960	21.482	75.182	32.219
24.268	7.993	15.667	34.532	3.199
19.841	6.649	13.032	35.037	8.973
22.360	8.873	17.390	60.748	25.967
21.878	8.674	17.000	63.741	29.740
2.064	0.834	1.635	5.886	2.615
30.985	10.071	19.740	59.636	20.156
36.241	11.708	22.949	58.671	12.774
9.814	3.137	6.148	16.946	4.651
15.800	6.341	12.429	82.734	57.876
14.250	5.771	11.310	32.074	9.454
5.451	2.182	4.276	9.851	1.298

**Bootstrapped 10000 times.* Only stratigraphic aggregates with five or more sub-aggregates with available raw material data are included.

Stone tool artifact type frequency

In terms of the frequency of stone artifact types at PP13B, several observations can be made (**Figure 72** and **Table 36**). Flakes and flake fragments dominated throughout the sequence (42.5% to 70.2%) with a few exceptions, LBG Sand 1 (35.8%), DB Sand 4c

(31.6%), LB Silt-G (38.9%), and LB Silt (31.3%). There are more cores (0.5% to 27.8%) and hammerstones/manuports (1.8% to 55.3%) in the MIS6 StratAgg. There is a tendency towards a higher blade frequency in the MIS5 StratAggs (2.5% to 24.6%) compared to the MIS6 StratAggs (0% to 8.2%). There is significantly more blade and blade fragments in MIS5 StratAggs compared to MIS6 StratAggs (Fisher's exact test – Two-tailed p=<0.00001).

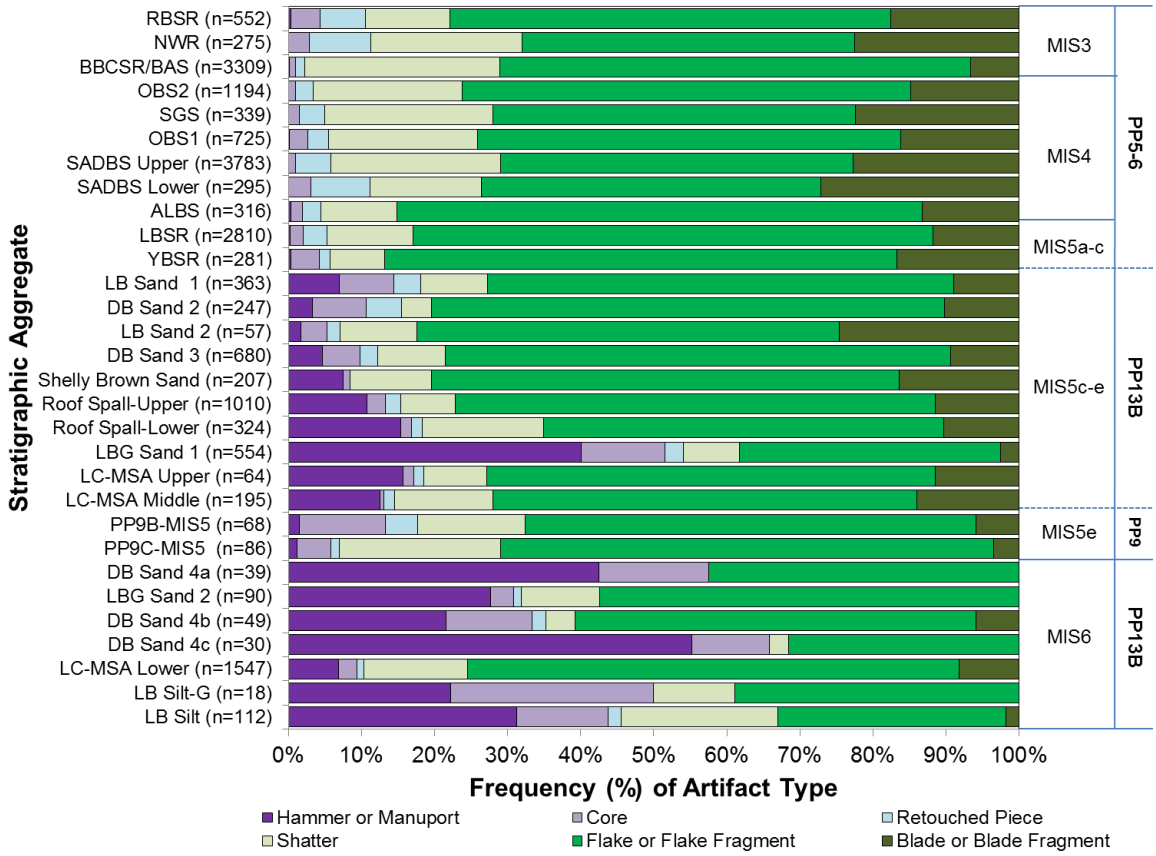

Figure 72. Relative frequency of stone artifact type at PP13B, PP9B, PP9C, and PP5-6 by stratigraphic aggregate. The age of assemblages decreases along the y-axis (oldest at bottom).

At PP9B and PP9C flakes and flake fragments dominated both PP9B (61.8%) and PP9C (67.4%) assemblages (**Figure 72** and **Table 37**). There are more cores at PP9B (11.8%) compared to PP9C (4.7%) but the frequencies are not statistically different

(Fisher's exact test – Two-tailed p=0.3876). There is a tendency towards a higher blade frequency in PP9B (5.9%) compared to PP9C (3.5%) but again, the frequencies are not statistically different (Fisher's exact test – Two-tailed p=1.0000).

When moving into MIS5 at PP5-6 several observations can be made (**Figure 72** and **Table 38**). Flake and flake fragments dominated throughout the sequence (48.2% to 71.85). However, the tendency towards higher blade frequencies that started in MIS5 StratAggs at PP13B and at both PP9 sites continue into MIS5 StratAggs at PP5-6. The frequency of blades and blade fragments are even more pronounced in MIS4 StratAggs (13.3% to 27.1%) compared to MIS3 (6.6% to 17.6%) and MIS5 (11.7% to 16.7%) StratAggs. There is a significant increase in blade and blade fragments in SADBS Lower compared to the ALBS (Fisher's exact test: Two-tailed p=0.0007). This is followed by a significant increase in blade and blade fragments in SADBS Upper compared to SADBS Lower (Fisher's exact test: Two-tailed p=<0.00001).

Another observation to be made is the decline in the frequencies of cores and hammerstones/manuports of the total assemblages as the archaeological sediments gets younger (**Figure 72**). However, both PP9 sites are exceptions with lower frequencies of hammerstones/manuports compared to most MIS5 and MIS6 StratAggs from PP13B.

Table 36. Count of stone artifact types by class at PP13B by stratigraphic aggregate.

Stratigraphic aggregate	Hammer or Manuport (n=)	Core (n=)	Retouched Piece (n=)	Shatter (n=)	Flake or Flake Fragment (n=)	Blade or Blade Fragment (n=)	Total (n=)
LB Sand 1	17	26	13	76	209	22	363
DB Sand 2	8	18	12	51	137	21	247
LB Sand 2	2	1	1	14	28	11	57
DB Sand 3	26	34	16	98	468	38	680
Shelly Brown Sand	8	2	0	24	142	31	207
Roof Spall-Upper	68	26	22	175	625	94	1010

Roof Spall-Lower	33	5	5	108	146	27	324
LBG Sand 1	167	75	16	74	212	10	554
LC-MSA Upper	6	1	1	11	40	5	64
LC-MSA Middle	15	1	3	35	116	25	195
DB Sand 4a	16	6	0	2	15	0	39
LBG Sand 2	22	3	1	17	47	0	90
DB Sand 4b	9	6	1	10	21	2	49
DB Sand 4c	13	4	0	3	10	0	30
LC-MSA Lower	29	25	11	274	1090	118	1547
LB Silt-G	4	5	0	2	7	0	18
LB Silt	35	14	2	24	35	2	112
Total (n=)	478	252	104	998	3348	406	5586

Table 37. Count of stone artifact types by class at PP9B and PP9C.

Cave Site	Hammer or Manuport (n=)	Core (n=)	Retouched Piece (n=)	Shatter (n=)	Flake or Flake Fragment (n=)	Blade or Blade Fragment (n=)	Total (n=)
PP9B	1	8	3	10	42	4	68
PP9C	1	4	1	19	58	3	86
Total (n=)	2	12	4	29	100	7	154

Table 38. Count of stone artifact types by class at PP5-6 by stratigraphic aggregate.

Stratigraphic aggregate	Hammer or Manuport (n=)	Core (n=)	Retouched Piece (n=)	Shatter (n=)	Flake or Flake Fragment (n=)	Blade or Blade Fragment (n=)	Total (n=)
RBSR	2	22	34	64	333	97	552
NWR	0	8	23	57	125	62	275
BBCSR/BAS	4	28	41	885	2131	220	3309
OBS2	0	12	28	244	733	177	1194
SGS	0	5	12	78	168	76	339
OBS1	1	18	21	148	420	117	725
SADBS Upper	2	36	183	878	1824	860	3783
SADBS Lower	0	9	24	45	137	80	295
ALBS	1	5	8	33	227	42	316
LBSR	7	50	91	332	2000	330	2810
YBSR	1	11	4	21	197	47	281
Total (n=)	18	204	469	2785	8295	2108	13879

Only stratigraphic aggregates with 10 or more stone artifacts are included.

Raw Material Frequency - Complete blades

When investigating what the complete blades are made on, quartzite dominates at PP13B, while a small frequency of the complete blade is made on silcrete (**Figure 73** and **Table 39**). At PP9B and PP9C all the complete blades are made on quartzite (**Table 40**). However, at PP5-6 silcrete dominates the complete blades, while the second dominant raw material is quartzite (**Figure 73** and **Table 41**).

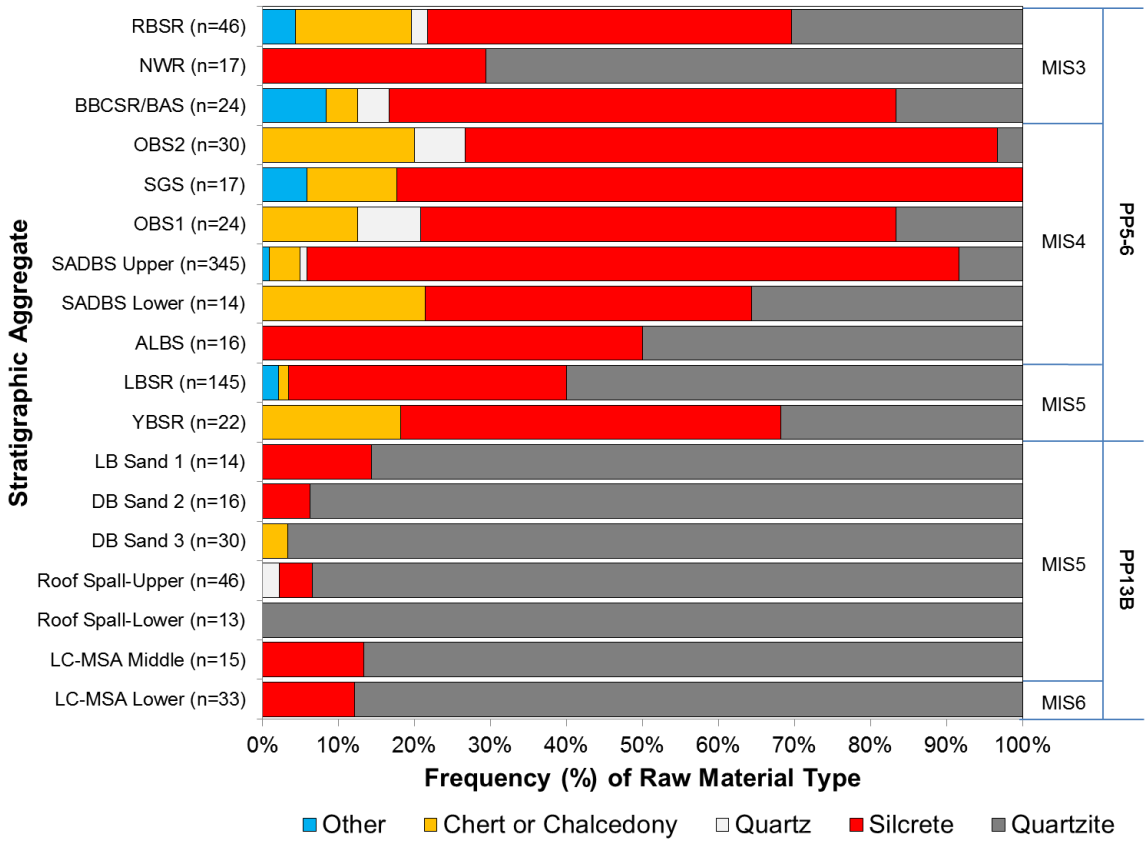

Figure 73. Frequency of raw material types used to make complete blades at PP13B and PP5-6 by stratigraphic aggregate. The age of assemblages decreases along the y-axis (oldest at bottom).

Silcrete dominates in YBSR (50%), SADBS Lower (42.9%), SADBS Upper (85.8%), OBS1 (62.5%), SGS (82.4%), OBS2 (70%), BBCSR/BAS (66.7%), and RBSR (47.8%). Quartzite dominates in the LBSR (60%), while quartzite and silcrete are tied in

the ALBS (50% each). There is a significant increase in silcrete used to produce blades in the SADBS Upper stratigraphic aggregate compared to the underlying SADBS Lower (Fisher's exact test: Two-tailed p=<0.00001). In all aggregates where silcrete dominates except for YBSR, SADBS Lower, and RBSR, the count of silcrete blades are significantly larger than the count of quartzite (all samples: Fisher's exact test – Two-tailed test p= <0.05). During the YBSR, SADBS Lower, and the RBSR the count of quartzite and silcrete blades are statistically similar. During the LBSR, when quartzite dominates the count of quartzite blades is significantly larger than the count of silcrete blades (Fisher's exact test – Tow-tailed p=0.0051). During the ALBS, the count of quartzite and silcrete is statistically similar.

Count frequencies of chert (chalcedony) blades has elevated frequencies (~ ≥10%) in YBSR (18.2%), SADBS Lower (21.4%), OBS1 (12.5%), SGS (11.8%), OBS2 (20%) and RBSR (15.2%). The count of quartz blades rises to elevated frequencies (~ ≥5%) in OBS1 (8.3%) and OBS2 (6.7%). Frequencies of blades made on 'other' raw materials such as hornfels and indurated shale only rise to elevated frequencies (~≥5%) in SGS (5.9%) and BBCSR (8.3%).

Table 39. Count of complete blades made on all raw material types at PP13B by stratigraphic aggregate.

Stratigraphic aggregate	Other (n=)	Chert or Chalcedony (n=)	Quartz (n=)	Silcrete (n=)	Quartzite (n=)	Total (n=)
LB Sand 1	0	0	0	2	12	14
DB Sand 2	0	0	0	1	15	16
DB Sand 3	0	1	0	0	29	30
Roof Spall-Upper	0	0	1	2	43	46
Roof Spall-Lower	0	0	0	0	13	13
LC-MSA Middle	0	0	0	2	13	15
LC-MSA Lower	0	0	0	4	29	33
Total (n=)	0	1	1	11	154	167

Only stratigraphic aggregates with 10 or more complete blades are included.

Table 40. Count of complete blades made on all raw materials at PP9B and PP9C.

Cave Site	Other (n=)	Chert or Chalcedony (n=)	Quartz (n=)	Silcrete (n=)	Quartzite (n=)
PP9B	0	0	0	0	3
PP9C	0	0	0	0	0
Total (n=)	0	0	0	0	3

Table 41. Count of complete blades made on all raw materials at PP5-6 by stratigraphic aggregate.

Stratigraphic aggregate	Other (n=)	Chert or Chalcedony (n=)	Quartz (n=)	Silcrete (n=)	Quartzite (n=)	Total (n=)
RBSR	2	7	1	22	14	46
NWR	0	0	0	5	12	17
BBCSR/BAS	2	1	1	16	4	24
OBS2	0	6	2	21	1	30
SGS	1	2	0	14	0	17
OBS1	0	3	2	15	4	24
SADBS Upper	3	14	3	296	29	345
SADBS Lower	0	3	0	6	5	14
ALBS	0	0	0	8	8	16
LBSR	3	2	0	53	87	145
YBSR	0	4	0	11	7	22
Total (n=)	11	42	9	462	159	683

Stone tool technological length

Figure 74 shows the technological lengths of complete flakes and blades in stratigraphic aggregates at PP13B. **Supplementary Table B27** shows the summary statistics. Complete lithics from LC-MSA Upper are significantly shorter than stone artifacts from most other StratAggs, except for Shelly Brown Sand, LBG Sand 2, LC-MSA Lower, and LB Silt (**Supplementary Table B28**). Complete flakes and blades from LC-MSA Lower are significantly shorter than lithics from most other StratAggs, except for LC-MSA Upper. At PP9B and PP9C the median of technological length (mm) of complete stone artifacts from PP9B and PP9C are statistically similar (**Figure 74** and **Supplementary Tables B29-30**).

At PP5-6 several observations can be made (**Figure 74** and **Supplementary Tables B31-32**: Complete lithics from the OBS2 are significantly shorter than stone artifacts from all other StratAggs at PP5-6 (**Supplementary Table B32**). The technological length of stone artifacts in the YBSR is significantly smaller than lithics from the overlying LBSR (**Supplementary Table B32**). The technological length of the LBSR and ALBS stone artifacts are statistically similar. The length of the complete lithics from SADBS Upper, OBS1, and SGS are statistically similar (**Supplementary Table B32**). RBSR stone artifacts are significantly larger than the underlying BBCSR/BAS stone artifacts but they are statistically similar to SADBS Lower, ALBS, and YBSR stone artifacts (**Supplementary Table B32**).

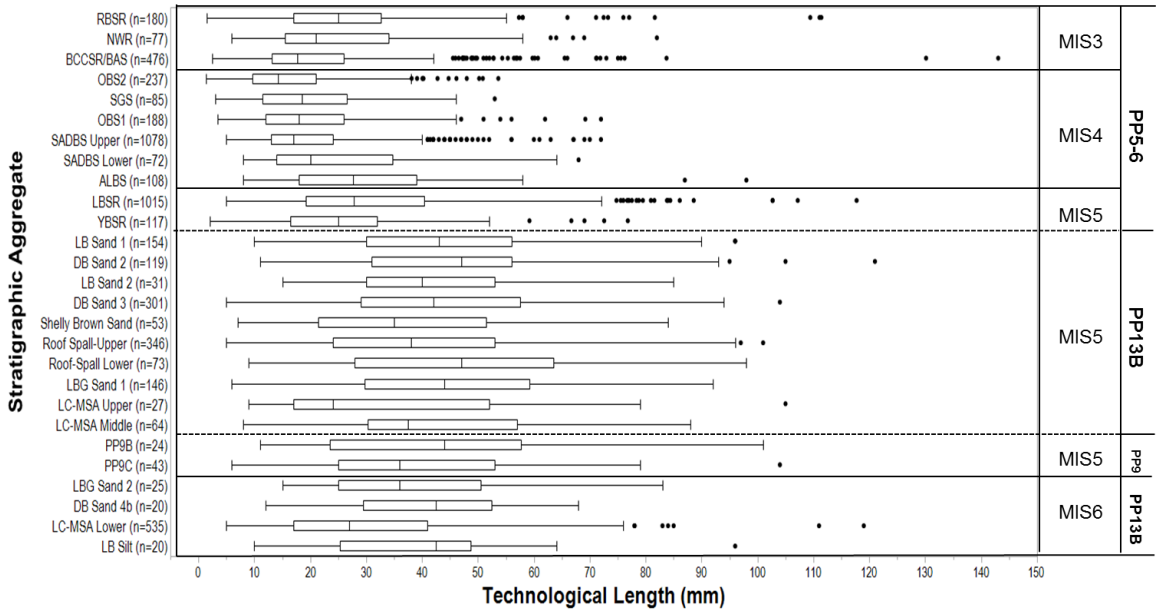

Figure 74. Boxplot of technological length (mm) of all complete flakes and blades made on all raw material types at PP13B, PP9B, PP9C, and PP5-6 by stratigraphic aggregate. The age of assemblages decreases along the y-axis (oldest at bottom). Only stratigraphic aggregates with 10 or more complete flakes and blades are included.

Stone tool technological length – Quartzite versus silcrete

Figure 74 above shows a trend towards complete flakes and blades with shorter technological lengths as the assemblages get younger. **Figure 75** shows a boxplot of technological length of complete stone tools when quartzite and silcrete lithics are viewed separately. At PP13B (**Supplementary Table B33** shows the descriptive statistics for each stratigraphic aggregate) silcrete from Roof Spall-Upper, quartzite from LC-MSA Upper, and both quartzite and silcrete from LC-MSA Lower have complete flakes and blades with the lowest median technological length. The median technological length (mm) of LC-MSA Lower complete flakes and blades made on quartzite and silcrete are significantly different than quartzite and silcrete artifacts from most assemblages except for quartzite from Shelly Brown Sand, silcrete from Roof Spall-Upper, quartzite from LC-MSA Upper, and quartzite from LBG Sand 2 (**Supplementary Table B34**).

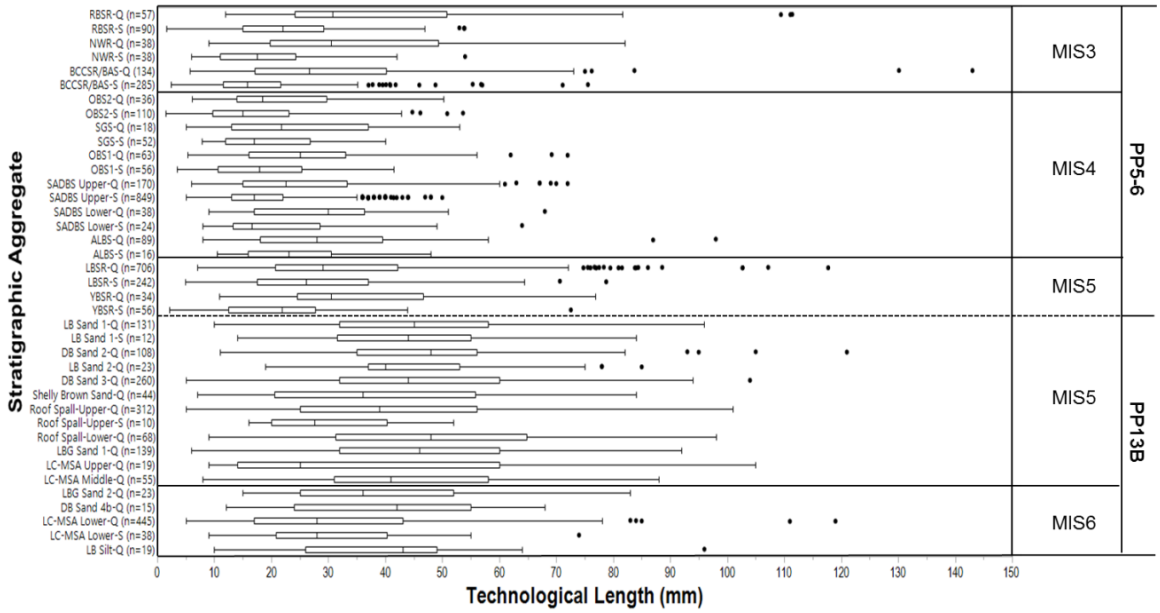

Figure 75. Boxplot of technological length (mm) of all complete flakes and blades made on quartzite (Q) and silcrete (S) at PP13B and PP5-6 by stratigraphic aggregate. The age of assemblages decreases along the y-axis (oldest at bottom). Only stratigraphic aggregates with 10 or more complete flakes and blades are included.

In each assemblage at PP5-6, the median technological length of complete silcrete flakes and blades is significantly smaller than the length of quartzite stone artifacts except for in the SGS and ALBS StratAggs (**Supplementary Tables B35-36**). Complete quartzite stone artifacts from the RBSR are significantly larger than both complete quartzite and silcrete lithics from all other aggregates except for quartzite stone artifacts from the NWR, LBSR, and the YBSR StratAggs.

Cortex type frequency

At PP13B, overall, there is significantly more outcrop cortex in MIS5 StratAggs compared to MIS6 StratAggs (Fisher's exact test: Two-tailed p=<0.00001) (**Figure 76** and **Table 42**). In each single StratAgg, the frequency of outcrop cortex is significantly lower than the frequency of cobble cortex (all assemblages: Mann-Whitney p=<0.00001). There is a significant increase in outcrop cortex in the Roof Spall-Lower aggregate compared to the underlying LBG Sand 1 (Fisher's exact test – Two-tailed p=<0.00001).

Table 43 shows the count of cobble and outcrop frequency for PP9B and PP9C. Overall, there is significantly more outcrop cortex than cobble cortex in at both caves (both caves: Fisher's exact test – Two-tailed p=<0.00001). In fact, there is no outcrop cortex recorded at either cave site.

At PP5-6, during MIS5 StratAggs (LBSR and YBSR) there is significantly more cobble cortex than outcrop cortex (Fisher's exact test: Two-tailed p=<0.00001) (**Figure 76** and **Table 44**). This pattern continues in the ALBS, the oldest stratigraphic aggregate in MIS4 (Fisher's exact test: Two-tailed p=<0.00001). In SADBS Lower there is no significant difference between the frequency of cobble cortex and outcrop cortex

(Fisher's exact test: Two-tailed p=1.0000). However, there is a significant increase in outcrop cortex in the SADBS Upper compared to SADBS Lower (Fisher's exact test: Two-tailed p=<0.00001). During the SADBS Upper there is significantly more outcrop cortex than cobble cortex (Fisher's exact test: Two-tailed p=<0.00001). Following the SADBS Upper, all stratigraphic aggregates except for the SGS (Fisher's exact test: Two-tailed p=0.3123) contains significantly more cobble cortex than outcrop cortex (Fisher's exact test: Two-tailed p=<0.00001).

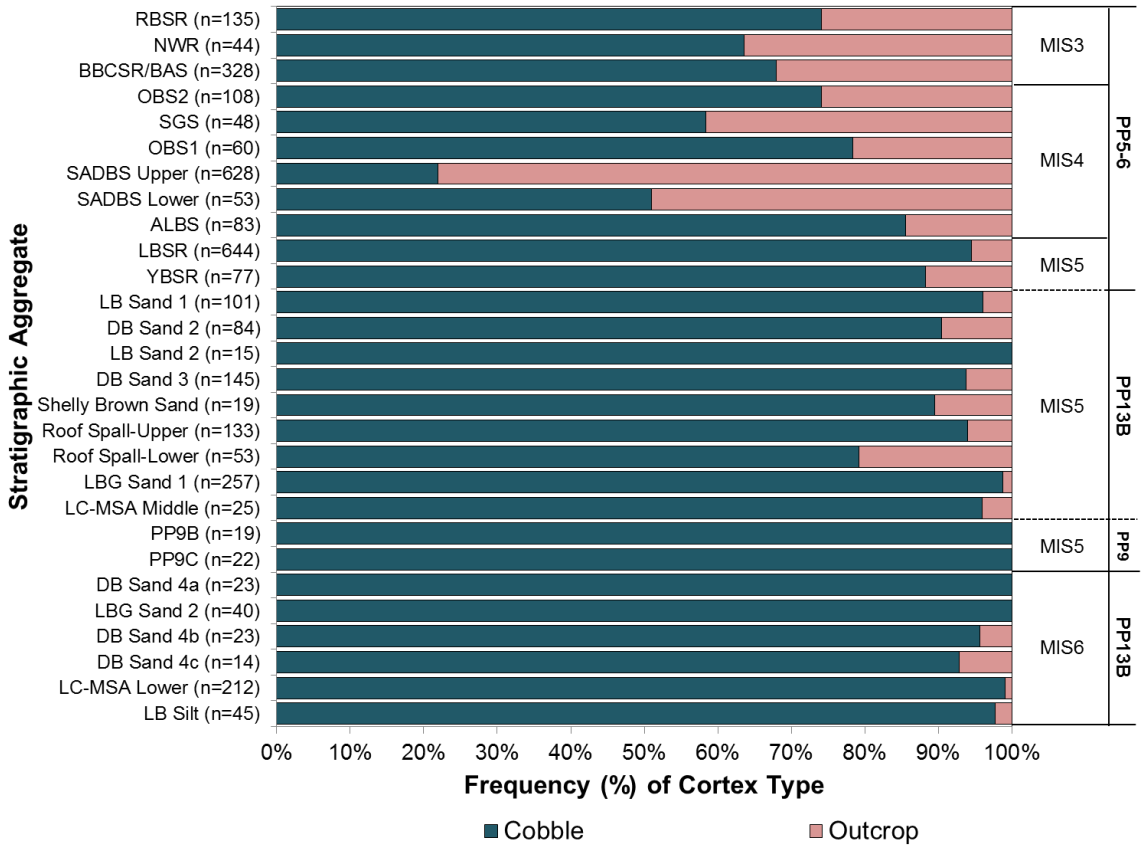

Figure 76. Relative frequency of cortex types at PP13B, PP9B, PP9C, and PP5-6 by stratigraphic aggregate. The age of assemblages decreases along the y-axis (oldest at bottom). Only stratigraphic aggregates with 10 or more lithics with cortex are included.

Table 42. Count of cortex types at PP13B by stratigraphic aggregate.

Stratigraphic aggregate	Cobble (n=)	Outcrop (n=)	Total (n=)
LB Sand 1	97	4	101
DB Sand 2	76	8	84
LB Sand 2	15	0	15
DB Sand 3	136	9	145
Shelly Brown Sand	17	2	19
Roof Spall-Upper	125	8	133
Roof Spall-Lower	42	11	53
LBG Sand 1	254	3	257
LC-MSA Middle	24	1	25
DB Sand 4a	23	0	23
LBG Sand 2	40	0	40
DB Sand 4b	22	1	23
DB Sand 4c	13	1	14
LC-MSA Lower	210	2	212
LB Silt	44	1	45
Total (n=)	1138	51	1189

Only stratigraphic aggregates with 10 or more stone tools with cortex recorded are included.

Table 43. Count of cortex types at PP9B and PP9C.

Cave Site	Cobble (n=)	Outcrop (n=)	Total (n=)
PP9B	19	0	19
PP9C	22	0	22
Total (n=)	41	0	41

Table 44. Count of cortex types at PP5-6 by stratigraphic aggregate.

Stratigraphic aggregate	Cobble (n=)	Outcrop (n=)	Total (n=)
RBSR	100	35	135
NWR	28	16	44
BBCSR/BAS	223	105	328
OBS2	80	28	108
SGS	28	20	48
OBS1	47	13	60
SADBS Upper	138	490	628
SADBS Lower	27	26	53
ALBS	71	12	83
LBSR	609	35	644
YBSR	68	9	77
Total (n=)	1419	789	2208

Cortex type frequency – Quartzite versus silcrete

The investigation of the overall strategy in terms of procuring from cobble sources or outcrop sources show that during MIS5 and MIS6 at PP13B, and during MIS5 at PP9B and PP9C cobble cortex dominates throughout but this is not the case at PP5-6. When investigating the cortex type of quartzite and silcrete stone artifacts separately which can indicate if different strategies were used for the two materials several observations can be made (**Figure 77).** At PP5-6, silcrete stone tools have consistently higher frequencies of outcrop cortex than quartzite stone artifacts, while quartzite lithics have consistently higher cobble cortex frequencies compared to silcrete stone artifacts (**Table 45**). In the YBSR there is significantly more outcrop cortex than cobble cortex on both quartzite and silcrete (Fisher's exact test: Two-tailed p=<0.00001). In the LBSR, there is significantly more outcrop cortex than cobble cortex on quartzite (Fisher's exact test: Two-tailed p=<0.00001), while the frequency of cobble and outcrop cortex on silcrete is statistically similar (Fisher's exact test –Two-tailed p=0.6636).

During MIS4, silcrete lithics have significantly more outcrop cortex than cobble cortex in the SGS and SADBS Upper (both samples: Fisher's exact test –Two-tailed p=<0.01), while the frequency of cobble and outcrop cortex on silcrete is statistically similar in the ALBS, SADBS Lower, OBS1, and the OBS2 (all samples: Fisher's exact test –Two-tailed p=>0.09). Conversely, during MIS4 quartzite artifacts have significantly more cobble cortex than outcrop cortex in all aggregates (all samples: Fisher's exact test –Two-tailed p=<0.001) except SADBS Lower (Fisher's exact test – Two-tailed p=0.3770). Moving into MIS3, silcrete has significantly more outcrop cortex than cobble cortex in the BBCSR/BAS (Fisher's exact test –Two-tailed p=<0.00001), while in the

RBSR and NWR the frequency of cobble and outcrop cortex on silcrete is statistically similar (Fisher's exact test: RBSR – Two-tailed *p*=0.0988; NWR – Two-tailed *p*=0.0654). Quartzite stone artifacts have significantly more cobble cortex than outcrop cortex in the RBSR, NWR, and BBCSR/BAS (RBSR and BBCSR/BAS: Fisher's exact test – Two-tailed *p*=<0.00001; NWR: Two-tailed *p*=0.0021).

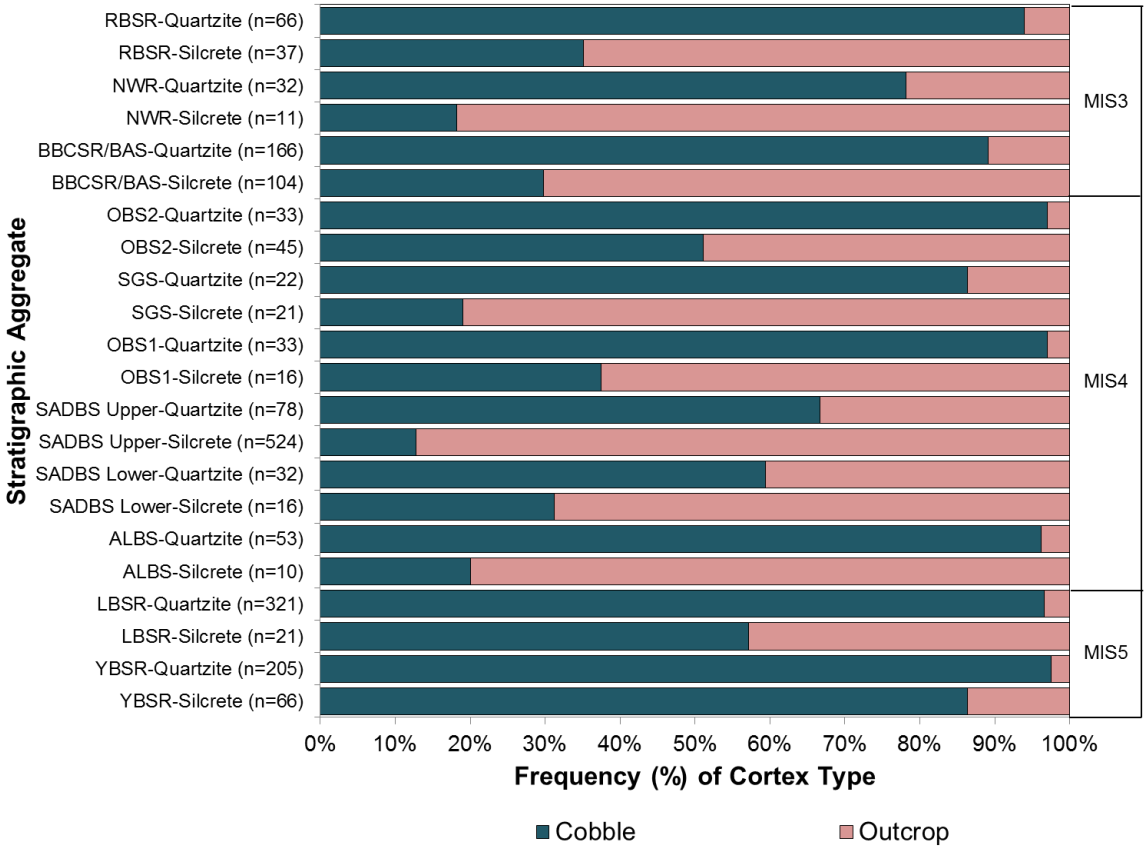

Figure 77. Relative frequency of cortex types on quartzite and silcrete artifacts at PP5-6 by stratigraphic aggregate. The age of assemblages decreases along the y-axis (oldest at bottom).

Table 45. Count of cortex types on quartzite and silcrete artifacts at PP5-6 by stratigraphic aggregate.

Stratigraphic aggregate	Cobble (n=)	Outcrop (n=)	Total (n=)
RBSR-Quartzite	62	4	66
RBSR-Silcrete	13	24	37
NWR-Quartzite	25	7	32
NWR-Silcrete	2	9	11

BBCSR/BAS-Quartzite	148	18	166
BBCSR/BAS-Silcrete	31	73	104
OBS2-Quartzite	32	1	33
OBS2-Silcrete	23	22	45
SGS-Quartzite	19	3	22
SGS-Silcrete	4	17	21
OBS1-Quartzite	32	1	33
OBS1-Silcrete	6	10	16
SADBS Upper-Quartzite	52	26	78
SADBS Upper-Silcrete	67	457	524
SADBS Lower-Quartzite	19	13	32
SADBS Lower-Silcrete	5	11	16
ALBS-Quartzite	51	2	53
ALBS-Silcrete	2	8	10
LBSR-Quartzite	310	11	321
LBSR-Silcrete	12	9	21
YBSR-Quartzite	200	5	205
YBSR-Silcrete	57	9	66
Total (n=)	1172	740	1912

Cutting edge per mass (CE/M)

Figure 78 and **Supplementary Table B37** show low values of CE/M overall throughout the PP13B sequence. **Supplementary Table B38** shows that the median CE/M values of LC-MSA Upper complete flakes and blades are significantly larger than CE/M values from complete flakes and blades from all other assemblages, except for complete lithics from the Shelly Brown Sand and LC-MSA Lower StratAggs. The median CE/M values of complete flakes and blades from the LBG Sand 1 aggregate are significantly smaller than the CE/M values from complete stone artifacts from all other assemblages except for LBG Sand 2, DB Sand 4b, and LB Silt (**Supplementary Table B38**). At PP9B and PP9C, the median CE/M values of complete flakes and blades from both sites are statistically similar, and the mean values are similar to most MIS5 and MIS6 values from PP13B (**Figure 78** and **Supplementary Tables B39-40)**.

When moving into MIS5 at PP5-6 the CE/M values increase. However, throughout the PP5-6 sequence there is variability (**Figure 78** and **Supplementary Tables B41-42).** The median CE/M values of SADBS Upper and OBS2 complete flakes and blades are significantly larger than the CE/M values from complete flakes and blades from all other assemblages. On the other hand, the median CE/M values of ALBS, LBSR, and YBSR complete stone artifacts are statistically similar, and the values are significantly smaller than the CE/M values from stone artifacts from all other aggregates (**Supplementary Table B42)**.

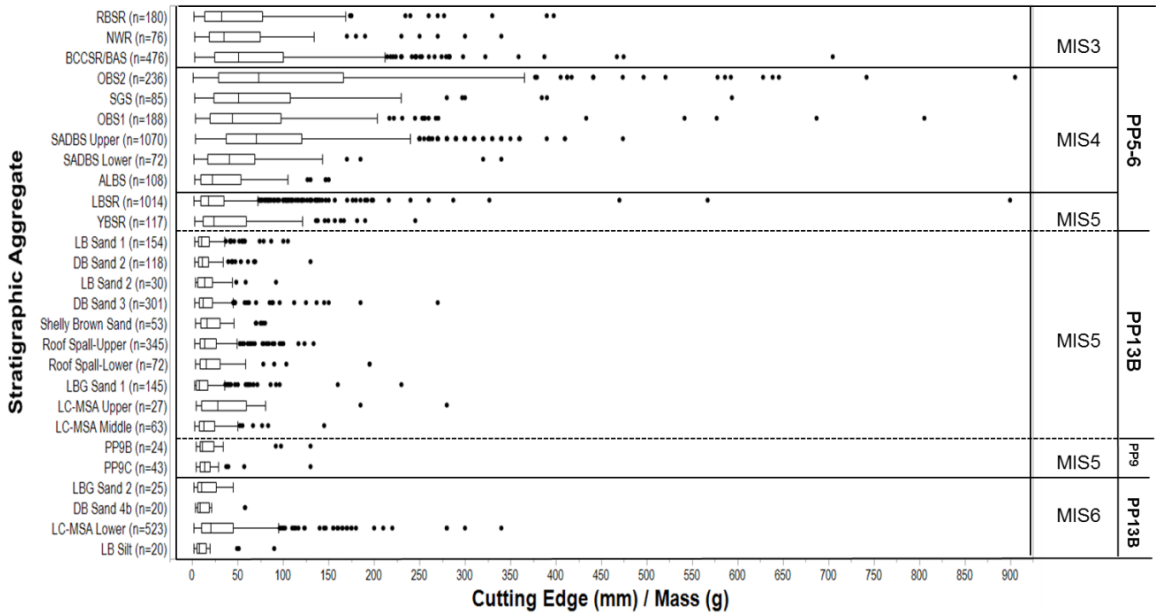

Figure 78. Boxplot showing distribution of Cutting edge / Mass (CE/M) values for all raw materials at PP13B, PP9B, PP9C, and PP5-6 by stratigraphic aggregate. The age of assemblages decreases along the y-axis (oldest at the bottom). Only stratigraphic aggregates with 10 or more complete flakes and blades are included.

Cutting edge per mass (CE/M) – Quartzite versus silcrete

Figure 79 and **Supplementary Table B43** shows that complete flakes and blades made on silcrete overall do not have higher CE/M values compared to complete quartzite stone artifacts in the same StratAgg. The three sample populations with the highest median

CE/M values are complete silcrete flakes and blades from Roof Spall-Upper and LC-MSA Lower, and complete quartzite flakes and blades from LC-MSA Upper (**Supplementary Table B44**). The CE/M values of silcrete artifacts from LB Sand 1 are statistically similar to CE/M values from complete quartzite lithics from the same StratAgg (**Supplementary Table B44**). The complete silcrete stone artifacts from LC-MSA Lower have statistically similar CE/M values to complete quartzite stone artifacts from the same StratAgg (**Supplementary Table B44**). However, the median CE/M value of complete silcrete flakes and blades from Roof Spall-Upper is significantly larger than the values of complete quartzite stone artifacts from the same StratAgg (Mann-Whitney: p=0.02).

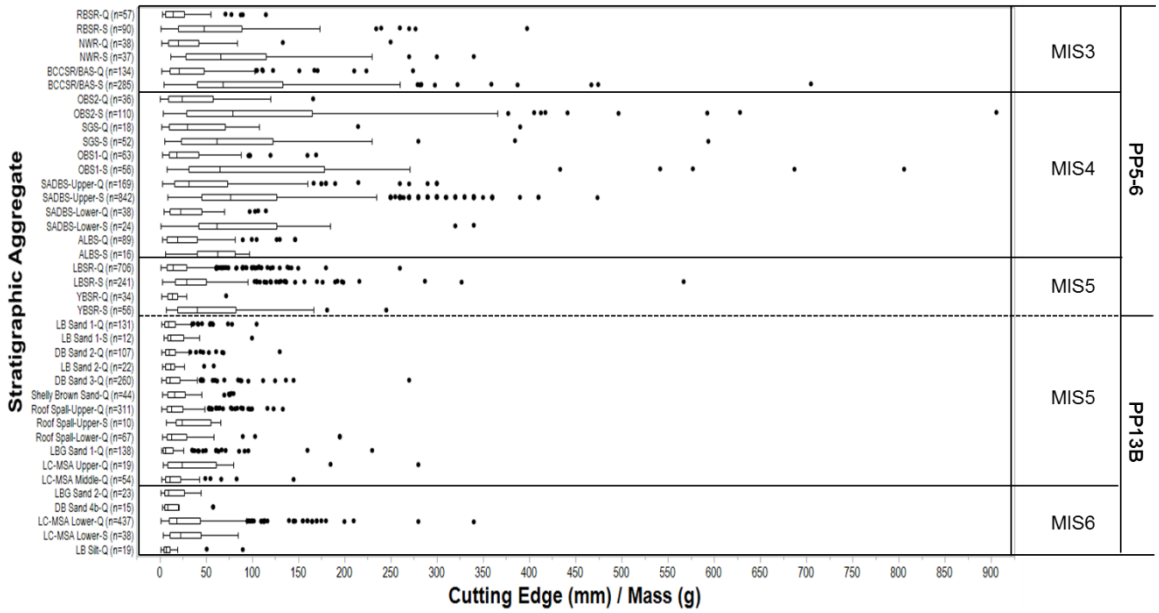

Figure 79. Boxplot showing distribution of Cutting edge / Mass (CE/M) values for quartzite and silcrete at PP13B and PP5-6 by stratigraphic aggregate. The age of assemblages decreases along the y-axis (oldest at the bottom). Only stratigraphic aggregates with 10 or more complete flakes and blades are included.

At PP5-6 complete flakes and blades made on silcrete overall have higher CE/M values compared to quartzite artifacts in the same StratAgg (**Figure 79** and

Supplementary Table B45). In each assemblage, the median CE/M values of complete silcrete flakes and blades are significantly smaller than the CE/M values from complete quartzite stone artifacts (**Supplementary Table B46**). Complete flakes and blades made on silcrete from the OBS2 and SADBS Upper have the highest median CE/M values (**Supplementary Table B46**). Conversely, complete flakes and blades made on quartzite from the RBSR, LBSR, and YBSR have the lowest median CE/M values (**Supplementary Table B46**).

Retouch frequency versus artifact volumetric density

Figure 80 and **Table 46** show that at PP13B, StratAggs have a wide spread of retouch frequency and artifact volumetric density values. MIS6 StratAggs LBG Sand 2, DB Sand 4b, LB Silt, and LB Sand 2 have the lowest combined retouch frequency and artifact volumetric density, which makes them plot towards the expedient end of the continuum. The MIS5 StratAgg LBG Sand 1 also has a low combined retouch frequency and artifact volumetric density. Towards the middle of the continuum the DB Sand 2, DB Sand 3, and LB Sand 2 StratAggs can be observed suggesting a less expedient behavior in these StratAggs. In the middle of the continuum the StratAggs Roof Spall-Upper, Roof Spall-Lower, LC-MSA Upper, LC-MSA Middle, LB Sand 1, and LC-MSA Lower is found. The behavior in these StratAggs suggests comparatively less expedient behavior.

PP5-6 aggregates have a wide spread of retouch frequency and artifact volumetric density values **(Figure 80** and **Table 47)**. Overlapping in the middle of the continuum with the PP13B StratAggs and plotting towards the expedient end several PP5-6 StratAggs can be observed. The BBCSR/BAS have the lowest combined retouch

frequency and artifact volumetric density, which makes it plot towards the expedient end of the continuum. In the middle, StratAggs YBSR, ALBS, LBSR, NWR, and SADBS Lower can be observed. Towards the curated end of the continuum the SGS, OBS1, and RBSR are found. At the curated end of the continuum, the SADBS Upper and OBS2 StratAggs can be observed suggesting a curated behavior in those aggregates.

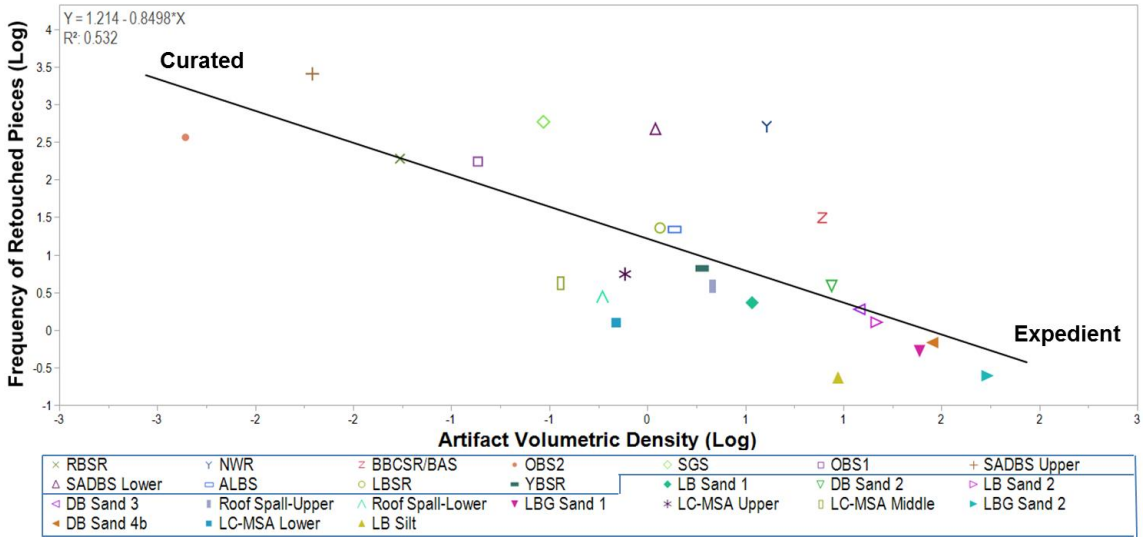

Figure 80. Linear regression using logged values between frequency of retouched pieces per total artifact mass (kg) from PP13B and PP5-6 stratigraphic aggregates and artifact volumetric density (total artifact mass (kg) per total sediment volume (m^3)) from PP13B and PP5-6 stratigraphic aggregates. Upper box of figure legend indicates PP5-6 stratigraphic aggregates, while lower box indicates PP13B stratigraphic aggregates.

Table 46. PP13B stratigraphic aggregate summary data for retouched piece frequency, total artifact mass (kg), and sediment volume (m^3).

Stratigraphic aggregate	Total Artifact Mass (kg)	Retouched Pieces (n=)	Sediment Volume (m^3)	Frequency of Retouched Pieces (Retouch piece count / artifact mass (kg))	Artifact Volumetric Density (Artifact Mass (kg) / Sediment Volume (m^3))
LB Sand 1	9.05	13	5.301	1.44	1.71
DB Sand 2	6.65	12	2.596	1.80	2.56
LB Sand 2	0.90	1	0.281	1.11	3.21
DB Sand 3	12.16	16	4.114	1.32	2.96
Roof Spall-Upper	12.30	22	8.816	1.79	1.40
Roof Spall-Lower	3.23	5	4.055	1.55	0.80
LBG Sand 1	21.11	16	5.265	0.76	4.01

LC-MSA Upper	0.48	1	0.533	2.10	0.89
LC-MSA Middle	1.60	3	2.501	1.87	0.64
LBG Sand 2	1.84	1	0.325	0.54	5.66
DB Sand 4b	1.18	1	0.276	0.84	4.29
LC-MSA Lower	9.99	11	11.709	1.10	0.85
LB Silt	3.78	2	1.430	0.53	2.65

Table 47. PP5-6 stratigraphic aggregate summary data for retouched piece frequency, total artifact mass (kg), and sediment volume (m^3).

Stratigraphic aggregate	Total Artifact Mass (kg)	Retouched Pieces (n=)	Sediment Volume (m^3)	Frequency of Retouched Pieces (Retouch piece count / artifact mass (kg))	Artifact Volumetric Density (Artifact Mass (kg) / Sediment Volume (m^3))
RBSR	3.484	34	12.308	9.758	0.283
NWR	1.526	23	0.830	15.077	1.839
BBCSR/BAS	9.227	41	3.780	4.443	2.441
OBS2	2.161	28	22.803	12.957	0.095
SGS	0.754	12	1.280	15.925	0.589
OBS1	2.226	21	5.295	9.433	0.420
SADBS Upper	6.034	183	33.393	30.329	0.181
SADBS Lower	1.663	24	1.595	14.432	1.042
ALBS	2.092	8	1.823	3.824	1.147
LBSR	23.428	91	21.963	3.884	1.067
YBSR	1.763	4	1.333	2.269	1.323

Site summaries

PP13B summary

Quartzite is the dominant raw material in terms of mass (kg) throughout the PP13B sequence. Quartz has relatively increased frequencies in LC-MSA Lower, DB Sand 4b, LBG Sand 2, Roof Spall-Lower, DB Sand 3, and LB Sand 2. Silcrete has relatively increased frequencies in LC-MSA Middle, LC-MSA Upper, and LB Sand 2. Flakes and flake fragments dominate the stone artifact type classes throughout the PP13B sequence. However, overall there are more blade and blade fragments in the MIS5 StratAggs. The frequency of blade and blade fragments increases to relatively high frequencies in several

MIS5 StratAggs such as LC-MSA Middle, LC-MSA Upper, Roof Spall-Lower, Roof Spall-Upper, Shelly Brown Sand, and LB Sand 2. Conversely, there are more hammerstones/manuports, and cores in the MIS6 StratAggs. The LB Silt, LB Silt-G, DB Sand 4c, DB Sand 4b, LBG Sand 2, and DB Sand 4a StratAggs have relatively high frequencies of hammerstones/manuports and/or cores. DB Sand 4c has a higher frequency of hammerstones/manuports than flake and flake fragments, while DB Sand 4a has relatively similar frequencies of flake and flake fragments and hammerstones/manuports. In MIS5, the LBG Sand 1 StratAgg has similar frequencies of flake and flake fragment and hammerstones/manuports. The complete blades are throughout the PP13B sequence mostly made on quartzite. However, in the LC-MSA Lower, LC-MSA Middle and LB Sand 1 about 10% of the blades are made on silcrete.

The stone artifacts from the LC-MSA Upper and LC-MSA Lower StratAggs are smaller in terms of technological length than lithics from the other aggregates. When looking at quartzite and silcrete stone artifacts separately silcrete artifacts from the LB Sand 1 and LC-MSA Lower StratAggs are not significantly smaller in terms of technological length than quartzite from the same aggregates. The silcrete stone artifacts from the Roof Spall-Upper are significantly smaller than the quartzite stone artifacts from the same aggregate.

The relative cortex frequency suggests that throughout the PP13B sequence raw materials were mostly procured from high-energy environments such as cobble beaches and/or streambeds, or alternatively from conglomerates that include well-rounded clasts. Outcrop cortex has relatively increased frequencies in the Roof Spall-Lower, Shelly Brown Sand, and DB Sand 2 StratAggs.

Complete flakes and blades from the LC- MSA Lower and LC-MSA Upper StratAggs were flaked more efficiently than stone artifact from all other assemblages. The MIS5 stone artifacts from PP5-6 were flaked similarly in terms of efficiency compared to MIS6 stone artifacts from PP13B. MIS5 stone artifacts from PP9B, PP9C, and PP13B were flaked less efficiently. The flaking efficiency of complete silcrete flakes and blades from LC-MSA Lower, Roof Spall-Upper, and LB Sand 1 are similar to the flaking efficiency of quartzite in the same aggregates.

The retouch frequency to artifact (stone tools) volumetric density ratios show that comparatively to PP5-6 StratAggs, the PP13B StratAggs tend to reflect behavior that is more expedient. MIS6 StratAggs LBG Sand 2, DB Sand 4b, LB Silt, and LB Sand 2 have the lowest combined retouch frequency and artifact volumetric density, which makes them plot towards the expedient end of the continuum. Additionally, the MIS5 StratAgg LBG Sand 1 also has a low combined retouch frequency and artifact volumetric density. Further, the rest of the StratAggs from PP13B plot towards the middle of the continuum overlapping with several PP5-6 StratAggs.

PP9 summary

Quartzite is the dominant raw material in terms of mass (kg) at both PP9B and PP9C. Quartz has a relatively increased frequency at PP9B, while silcrete is present at PP9C. Flakes and flake fragments dominate the stone tool artifact classes at both PP9B and PP9C. However, there are relatively more cores at PP9B and a slightly higher frequency of blade and blade fragments. The complete flakes and blades from PP9B and PP9C are similar in size, in terms of technological length. The relative cortex frequency suggests

that at both PP9B and PP9C raw materials were mostly procured from high-energy environments such as cobble beaches and/or streambeds, or alternatively from conglomerates that include well-rounded clasts. Complete flakes and blades from PP9B and PP9C were flaked similarly in terms of efficiency.

PP5-6 summary

Quartzite is the dominant raw material in terms of mass (kg) throughout the PP5-6 sequence, expect for in the SADBS Upper where significantly more silcrete was transported to site in terms of mass compared to quartzite. Silcrete has relatively increased frequencies in most StratAggs except for LBSR, ALBS, and OBS1. The frequency of silcrete in MIS4 overall is significantly higher than the frequency of silcrete in both the underlying MIS5 aggregates and in the overlaying MIS3 aggregates. However, at the level of StratAgg only in SADBS Upper is the silcrete frequency significantly different from the quartzite frequency. In all other MIS4 aggregates (SADBS Lower, ALBS, OBS1, SGS, and OBS2), the quartzite and silcrete frequencies are statistically similar. Quartzite and silcrete frequencies are also statistically similar in the YBSR, while in the LBSR and BBCSR/BAS quartzite is significantly more frequent than silcrete. Quartz has relatively increased frequencies in OBS1 and OBS2 making the frequencies statistically similar to silcrete frequencies in those two aggregates. In addition, the quartz frequency in the BBCSR/BAS is statistically similar to the silcrete frequency. Chert (chalcedony) is uncommon throughout, while ‘other’ raw materials such as hornfels and indurated shale only have a relatively elevated frequency in the YBSR.

When looking at the sub-aggregate level, during MIS3, quartzite is dominant in all sub-aggregates in terms of transported mass (kg). Silcrete rises to relatively elevated frequencies in Zenobia, Emily, Ellis, and Takis. Quartz only rises to a relatively elevated frequency in James. Chert (chalcedony) and 'other' raw materials are uncommon throughout. In the NWR, like the other MIS3 aggregates, quartzite dominates, while silcrete is the second most dominant material. Quartz, chert, and 'other' raw materials are very uncommon.

MIS4 sees a lot of variability in terms of raw material frequency. Quartzite dominates in the sub-aggregates of the ALBS, and SADBS Lower except for in Conrad Sand. In the SADBS Upper there is a switch to a preference for silcrete and silcrete dominance extends into the OBS1 in the Joanne 1 sub-aggregate. Overall, in OBS1 there is a preference for quartzite. However, sub-aggregate Sasha is dominated by quartz, and quartz has relatively elevated frequencies in all OBS1 sub-aggregates except for Chris. In the SGS there is again a switch to a preference for silcrete. Silcrete dominates in all SubAggs except for in Zuri Upper, where quartzite is most frequent. In the following OBS1 stratigraphic aggregates there is a lot of variability in terms of raw material preference. Sub-aggregates Josh, Sarah, Elizabeth, and Andy are dominated by quartzite, while silcrete dominates in Alicen, Chantal, Hans, and Emma Sand. Kevin Sand is totally dominated by chert (Chalcedony). Quartz has relatively elevated frequencies in Josh, Sarah, Elizabeth, and Andy. In the DBCS, quartzite dominates in all sub-aggregates except for Sorel, Leonides, and Ollie where silcrete is dominant. Quartz only rises to a relatively elevated frequency in Sam, while chert (chalcedony) only rises to a relatively elevated frequency in Leonides.

During MIS5 quartzite dominates throughout except for sub-aggregate Kirsty (YBSR), Tove Sand and Roofspall and Logan Sand and Roofspall 2 (LBSR). Kirsty is dominated by chert (chalcedony) whereas Tove Sand and Roofspall and Logan Sand and Roofspall 2 are dominated by silcrete. Silcrete has also relatively elevated frequencies in Kirsty (YBSR) Elizabeth Sand and Roofspall (YBSR), Lee (YBSR), Tove Red (LBSR), Simen Red (LBSR), Logan Sand and Roofspall 1(LBSR), Sondra Red (LBSR), Sondra Sand and Roofspall (LBSR), Adrian Sand and Roofspall (LBSR), Kyle Shell (LBSR), and Hope Red (LBSR). The frequency of quartz varies throughout but it has relatively elevated frequencies in Arnold Red (LBSR), Logan Red (LBSR), Logan Sand and Roofspall 1 (LBSR), and Cobus Shell (LBSR). Other than in the Kirsty sub-aggregate, chert (chalcedony) is relatively uncommon in all other MIS5 sub-aggregates. 'Other' raw materials such as hornfels and indurated shale on the other hand have relatively elevated frequencies in multiple sub-aggregates such as Kirsty (YBSR), Elizabeth Sand and Roofspall (YBSR), Meghan Sand and Roofspall (YBSR), Arnold Red (LBSR), Hope Red (LBSR), and Ludumo Sand and Roofspall (LBS).

Flakes and flake fragments dominate the stone tool artifact classes throughout the PP5-6 sequence. However, overall there is an increase in the production of blades in the MIS4 StratAggs. Particularly, in SADBS Lower, SADBS Upper, and SGS the frequency of blades and blade fragments are relatively elevated. The complete blades are throughout the PP5-6 sequence mostly made on silcrete except for in the LBSR aggregate and in the ALBS where the frequency of quartzite blades and silcrete blades are statistically similar. In the MI3 StratAggs, the frequency of blades made on quartzite increase but enough to be more frequent than blades made on silcrete.

The lithics from the SADBS Upper and OBS2 StratAggs are smaller in terms of technological length than stone tools from the other aggregates. When looking at quartzite and silcrete lithics separately silcrete lithics from each stratigraphic aggregate are significantly smaller in terms of technological length than quartzite lithics from the same aggregates.

The relative cortex frequency suggests that in the PP5-6 sequence raw materials were mostly procured from high-energy environments such as cobble beaches and/or streambeds, or alternatively from conglomerates that include well-rounded clasts except for in the SADBS Upper aggregates where outcrop cortex dominates. There is a tendency towards more outcrop cortex starting in the SADBS Lower aggregate and all aggregates from then on compared to the older ALBS, LBSR, and YBSR aggregates. When looking at quartzite and silcrete artifacts separately, silcrete artifacts always have a higher outcrop cortex frequency than quartzite in every aggregate. In MIS4 and MIS3 the frequency of cortex type on silcrete is dominated by outcrop cortex except in OBS2 where the frequency of cobble and outcrop cortex is similar. Quartzite only has relatively elevated outcrop cortex frequencies in SADBS Lower and SADBS Upper. However, there is still significantly more cobble cortex than outcrop cortex on quartzite in those aggregates.

Complete flakes and blades from the SADBS Upper and the OBS2 stratigraphic aggregates were flaked more efficiently than lithics from all other assemblages. Lithics from the ALBS, LBSR, and YBSR were flaked the least efficient compared to lithics from the other aggregates. Overall, lithics from the MIS4 aggregates have been flaked the most efficiently compared to MIS5 and MI3 aggregates. When comparing the flaking efficiency of complete silcrete flakes and blades the result is that silcrete lithics always

have been flaked more efficiently than quartzite lithics from the same aggregates. Silcrete stone artifacts from the OBS2 and SADBS Upper have the highest values of CE/M indicating that they have been flaked the most efficiently in the sequence, while quartzite lithics from the RBSR, LBSR, and YBSR have the lowest CE/M values suggesting that they were flaked the least efficiently in the sequence.

The retouch frequency to artifact volumetric density ratio method suggests that the SADBS Upper and OBS2 assemblages at PP5-6 are due to curated behavior. However, assemblages from OBS1, SGS, and RBSR can be considered more curated compared to assemblages from SADBS Lower, ALBS, LBSR, and YBSR. The ratio of the BBCSR/BAS assemblage suggests that it is due to expedient behavior.

Pinnacle Point Sequence – Archaeology summary

The PP13B and PP9 sequences show that quartzite stone tools made on cobbles dominate the lithic assemblages. There is relatively little change in flaking efficiency between aggregates, and there is little difference between quartzite and silcrete artifacts in the PP13B and PP9 part of the sequence. Although quartzite dominates throughout the Pinnacle Point sequence in terms of transported materials to the localities, there is a shift to silcrete as the most transported material in terms of mass in the SADBS Upper aggregate. This increase in silcrete is correlated with an increase in blade products and the increase in procurement of silcrete from outcrop sources. The majority of the blades are made on silcrete. Additionally, the flaking efficiency of both quartzite and silcrete increases in the SADBS upper aggregate, and this pattern of increased flaking efficiency persists throughout MIS4. However, the flaking efficiency of silcrete is significantly

higher than quartzite in all the MIS4 aggregates. The retouch frequency to artifact volumetric density ratio also suggests that the SADBS Upper and OBS2 assemblages particularly but also perhaps the OBS1 and SGS assemblages are due to curated behavior potentially resulting from increased residential mobility and/or raw material scarcity.

CHAPTER 8: OPPORTUNISTIC ACQUISITION MODEL HYPOTHESIS EVALUATION AND SENSITIVITY ANALYSIS

Introduction

In the section below modeling data from the Opportunistic Acquisition Model (OAM) will be presented from all five model conditions: MIS4 conditions with or without a Paleo-Agulhas plain silcrete source, MIS5 conditions, and MIS6 with or without a Paleo-Agulhas plain silcrete source. These five model conditions have five different states of coastline position and raw material source distribution. I will first test Hypothesis 1 (H_1) drawn from the Opportunistic Acquisition Model (OAM) using the outcomes of same-day return simulations and the one-factor-at-a-time (OFAT) round one (OFAT1) model outcomes that simulated raw material frequency outcomes at different movement-budgets. These tests are conducted by comparing model raw material outcomes with archaeological raw material frequencies. Following the initial test of Hypothesis 1 I ask if it is realistic to move randomly in relation to raw material sources in an environment. The key criterion that is looked at is the time without raw material in the toolkit. Then H_1 is evaluated further by a one-factor-at-a-time (OFAT) sensitivity analysis. The goal of the sensitivity analysis is to gauge the effect different model parameters have on the raw material output thus testing the robustness of the initial Hypothesis 1 evaluation.

Hypothesis 1 – Same-day return outcomes

Hypothesis 1 (H_1) states that opportunistic encounters during random walk in the environment result in a raw material usage frequency similar to the archaeological record. Because it can be assumed either that random walk in the environment can be an optimal

(or realistic) way to move or that there is no difference in utility currency profitability between the lithic raw materials, the prediction is that opportunistic encounters during random walk in the environment will create a raw material pattern similar to the archaeological record.

The first test of Hypothesis 1 under the coastline position and raw material source distribution variable only consider the result of model runs with a movement budget (TT= totticks) value= 100, which if assuming a walking pace of 3.5 to 2.5 km/hr (Binford, 2001; Marlowe, 2010; Marlowe, 2006) can be argued to reflect a daily foraging radius of a forager (same-day return).

MIS4 conditions without a Paleo-Agulhas plain silcrete source

Figure 81 and **Table 48** show that quartz has the highest frequency while quartzite has the second highest frequency during same-day returns during MIS4 conditions without a Paleo-Agulhas plain silcrete source. Silcrete was not deposited at all at PP. None of the model raw material frequencies match the archaeological frequencies. The model predicts more quartz than what is represented in the archaeological record, while silcrete and quartzite are both underpredicted. There is also no ranking match (**Supplementary Table B47**). This result does not support Hypothesis 1.

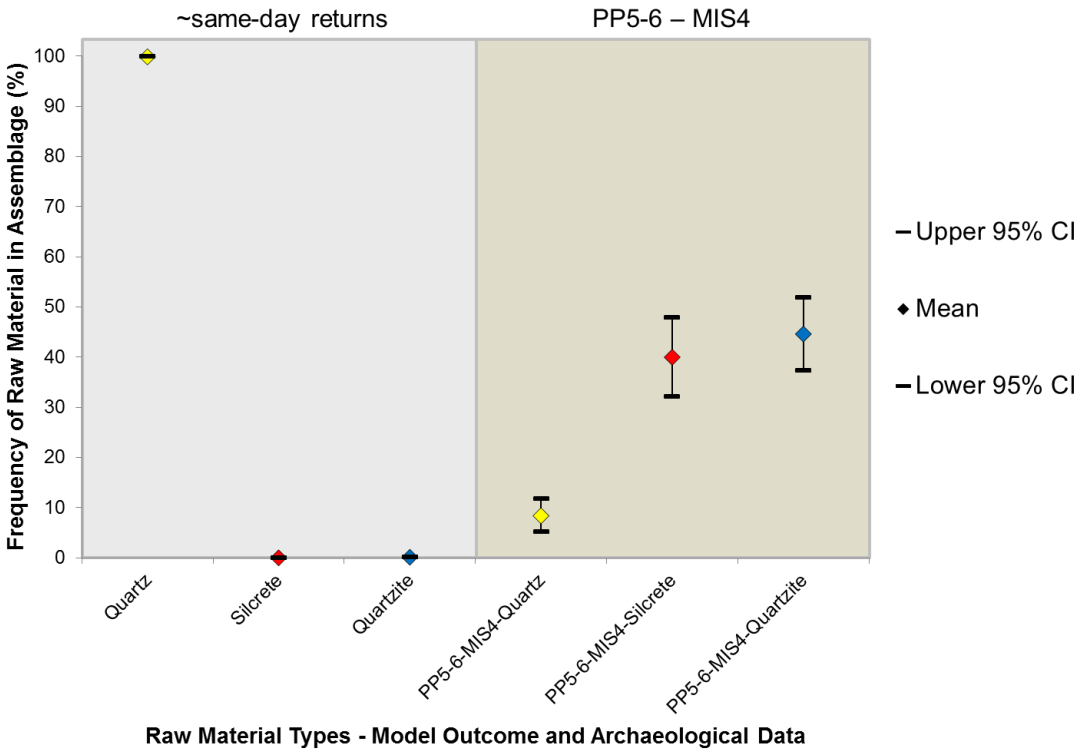

Figure 81. Comparison between same-day return modeling outcomes during MIS4 model conditions without a Paleo-Agulhas plain silcrete source and bootstrapped MIS4 archaeological raw material frequency data from PP5-6. Plot shows the mean and the upper and lower 95% confidence intervals for raw material frequencies.

Table 48. Summary statistics and test results for same-day return simulations of MIS4 conditions without a Paleo-Agulhas plain silcrete source compared to MIS4 archaeological raw material frequency data from PP5-6.

	Quartz	Silcrete	Quartzite	PP5-6-MIS4-Quartz	PP5-6-MIS4-Silcrete	PP5-6-MIS4-Quartzite
n (number of assemblages)	1000	1000	1000	46	46	46
First Quartile	99.85	0.00	0.00	1.21	13.79	5.19
Min	98.34	0.00	0.00	0.00	0.00	0.00
Median	100.00	0.00	0.00	3.73	39.13	43.00
Mean	99.89	0.00	0.11	8.39	40.00	44.63
Max	100.00	0.00	1.66	66.11	96.55	96.45
Third Quartile	100.00	0.00	0.15	10.53	62.77	68.24
SD	0.23	0.00	0.23	11.83	27.52	25.54
SE	0.01	0.00	0.01	1.67*	4.01*	3.71*
Margin of error (95% CI)	0.01	0.00	0.01	3.28	7.85	7.27
Upper 95% CI	99.90	0.00	0.13	11.66*	47.85*	51.90*

Lower 95% CI	99.87	0.00	0.10	5.11*	32.15*	37.35*

*Margins of error (95% CI) for archaeological data were obtained by bootstrapping the standard errors 10000 times.

MIS4 conditions with a Paleo-Agulhas plain silcrete source

Figure 82 and **Table 49** show that quartz has the highest frequency while silcrete has the second highest frequency during same-day returns during MIS4 conditions without a Paleo-Agulhas plain silcrete source. Quartzite has a very low frequency. The model predicts much more quartz than what is represented in the archaeology, while quartzite is underpredicted. However, the silcrete frequency from the model statistically matches the archaeological silcrete frequency. There is also no ranking match (**Supplementary Table B48**). Overall, this result does not support Hypothesis 1.

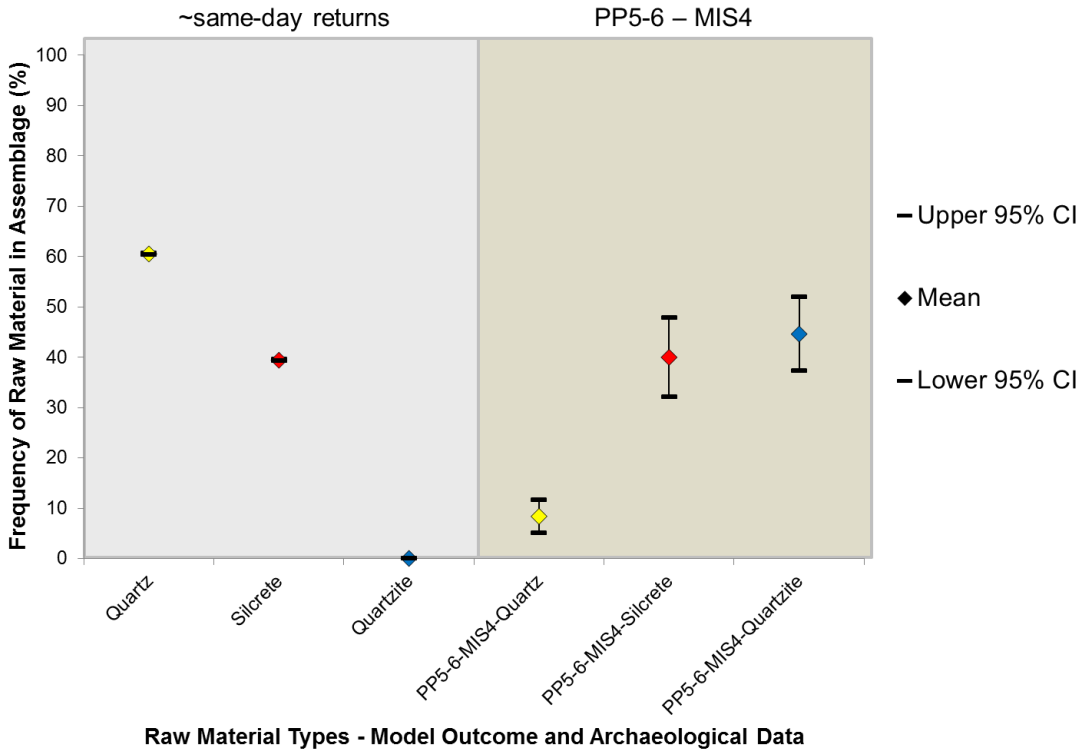

Figure 82. Comparison between same-day return modeling outcomes during MIS4 model conditions with a Paleo-Agulhas plain silcrete source and bootstrapped MIS4 archaeological raw material frequency data from PP5-6. Plot shows the mean and the upper and lower 95% confidence intervals for raw material frequencies.

Table 49. Summary statistics and test results for same-day return simulations of MIS4 conditions with a Paleo-Agulhas plain silcrete source compared to MIS4 archaeological raw material frequency data from PP5-6.

	Quartz	Silcrete	Quartzite	PP5-6-MIS4-Quartz	PP5-6-MIS4-Silcrete	PP5-6-MIS4-Quartzite
n (number of assemblages)	1000	1000	1000	46	46	46
First Quartile	58.65	37.65	0.00	1.21	13.79	5.19
Min	52.24	30.43	0.00	0.00	0.00	0.00
Median	60.45	39.52	0.00	3.73	39.13	43.00
Mean	60.54	39.42	0.04	8.39	40.00	44.63
Max	69.57	47.61	0.79	66.11	96.55	96.45
Third Quartile	62.29	41.32	0.00	10.53	62.77	68.24
SD	2.78	2.77	0.10	11.83	27.52	25.54
SE	0.09	0.09	0.00	1.67*	4.01*	3.71*
Margin of error (95% CI)	0.17	0.17	0.01	3.28	7.85	7.27
Upper 95% CI	60.71	39.59	0.05	11.66*	47.85*	51.90*
Lower 95% CI	60.37	39.25	0.03	5.11*	32.15*	37.35*

*Margins of error (95% CI) for archaeological data were obtained by bootstrapping the standard errors 10000 times.

MIS5 conditions

Figure 83 and **Table 50** show that quartz has the highest frequency while quartz has the second highest frequency during same-day returns during MIS5 conditions. Silcrete has a very low frequency. None of the model raw material frequencies match the archaeological frequencies except for silcrete that matches the frequency of silcrete from the MIS5 record at PP13B. The model predicts more quartz than what is represented in the MIS5 record at PP5-6 and PP13B, and in the total MIS5 assemblage at Pinnacle Point, while quartzite and silcrete are underpredicted. There is also no ranking match (**Supplementary Table B49**). This result does not support Hypothesis 1.

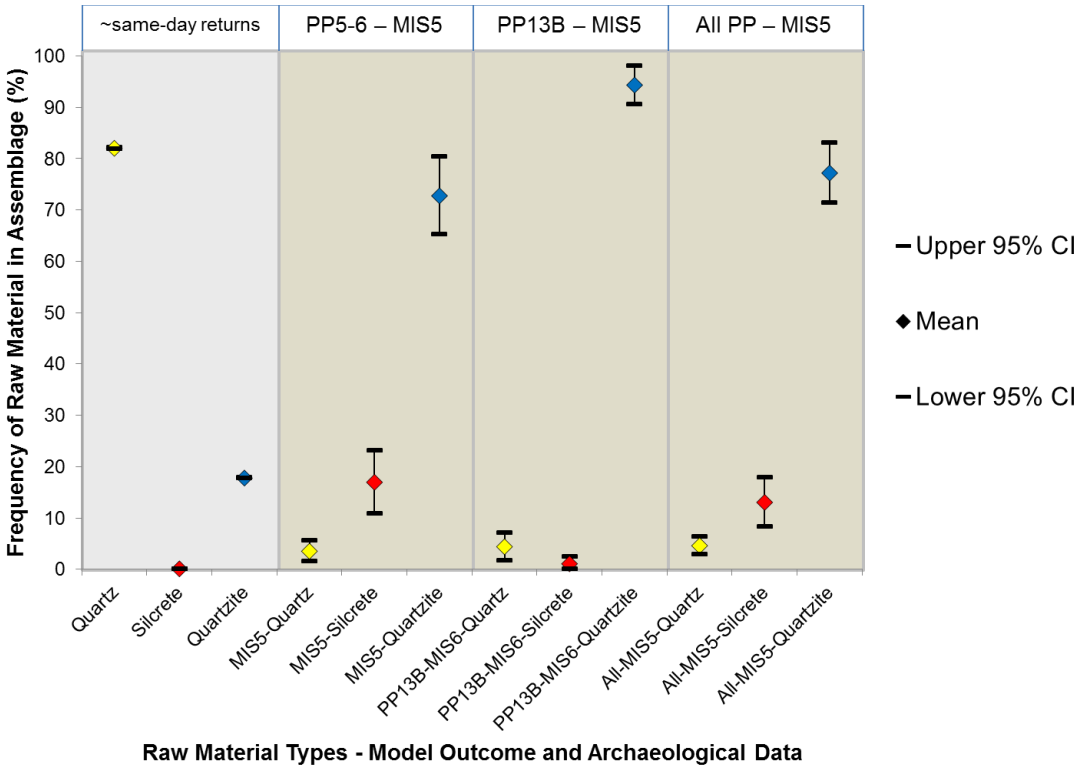

Figure 83. Comparison between same-day return modeling outcomes during MIS5 model conditions and bootstrapped MIS5 archaeological raw material frequency data from PP5-6, PP13B, and all MIS5 assemblages from the PP sequence including PP5-6, PP13B, PP9B, and PP9C. Plot shows the mean and the upper and lower 95% confidence intervals for raw material frequencies.

Table 50. Summary statistics and test results for same-day return simulations of MIS5 conditions compared to MIS5 archaeological raw material frequency data from PP5-6, PP13B, PP9B, and PP9C.

	Quartz	Silcrete	Quartzite	MIS5-Quartz	MIS5-Silcrete	MIS5-Quartzite	PP13B-MIS6-Quartz	PP13B-MIS6-Silcrete	PP13B-MIS6-Quartzite	All-MIS5-Quartz	All-MIS5-Silcrete	All-MIS5-Quartzite
n (number of assembl ages)	1000	1000	1000	31	31	31	7	7	7	43	43	43
First Quartile	80.63	0.10	16.46	0.00	1.45	60.24	1.71	0.00	87.62	0.10	0.95	64.30
Min	75.65	0.06	10.42	0.00	0.00	26.94	0.00	0.00	87.62	0.00	0.00	26.94
Median	82.14	0.11	17.69	0.89	10.19	76.11	2.15	0.00	97.85	2.65	6.44	83.74

Mean	82.03	0.11	17.79	3.53	16.97	72.77	4.41	1.09	94.34	4.61	13.05	77.20
Max	89.47	0.15	24.10	24.87	64.83	100.00	9.39	5.01	100.00	24.87	64.83	100.00
Third Quartile	83.38	0.12	19.17	3.92	32.95	92.83	9.33	2.55	98.29	6.95	21.21	92.83
SD	2.02	0.01	2.00	5.94	17.85	21.79	3.91	1.97	5.37	6.03	16.45	20.01
SE	0.06	0.00	0.06	1.03*	3.14*	3.85*	1.40*	0.68*	1.92*	0.90*	2.46*	3.00*
Margin of error (95% CI)	0.13	0.00	0.12	2.03	6.16	7.55	2.74	1.34	3.76	1.76	4.82	5.87
Upper 95% CI	82.15	0.11	17.92	5.56*	23.12*	80.32*	7.15*	2.42*	98.10*	6.37*	17.86*	83.07*
Lower 95% CI	81.90	0.11	17.67	1.51*	10.81*	65.21*	1.68*	0.00*	90.58*	2.85*	8.23*	71.33*

*Margins of error (95% CI) for archaeological data were obtained by bootstrapping the standard errors 10000 times.

MIS6 conditions without a Paleo-Agulhas plain silcrete source

Figure 84 and **Table 51** show that quartz has the highest frequency while quartzite has the second highest frequency during same-day returns during MIS6 conditions without a Paleo-Agulhas plain silcrete source. Silcrete was not deposited at all in the simulated Pinnacle Point assemblage. The model predicts much more quartz than what is represented in the archaeology, while quartzite is underpredicted. However, the silcrete frequency from the model statistically matches the archaeological silcrete frequency. There is also no ranking match (**Supplementary Table B50**). Overall, this result does not support Hypothesis 1.

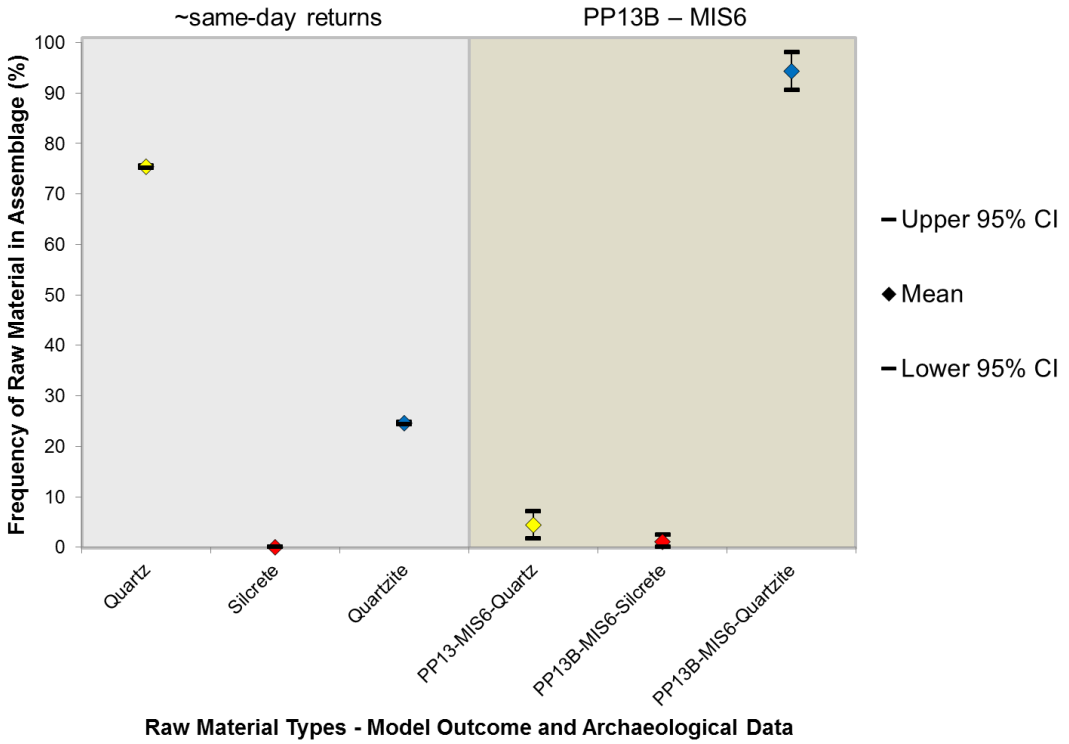

Figure 84. Comparison between same-day return modeling outcomes during MIS6 model conditions without a Paleo-Agulhas plain silcrete source and bootstrapped MIS6 archaeological raw material frequency data from PP13B. Plot shows the mean and the upper and lower 95% confidence intervals for raw material frequencies.

Table 51. Summary statistics and test results for same-day return simulations of MIS6 conditions without a Paleo-Agulhas plain silcrete source compared to MIS6 archaeological raw material frequency data from PP13B.

	Quartz	Silcrete	Quartzite	PP13-MIS6-Quartz	PP13B-MIS6-Silcrete	PP13B-MIS6-Quartzite
n (number of assemblages)	1000	1000	1000	7	7	7
First Quartile	73.10	0.00	22.17	1.71	0.00	87.62
Min	65.00	0.00	15.67	0.00	0.00	87.62
Median	75.79	0.00	24.21	2.15	0.00	97.85
Mean	75.41	0.00	24.59	4.41	1.09	94.34
Max	84.33	0.00	35.00	9.39	5.01	100.00
Third Quartile	77.83	0.00	26.90	9.33	2.55	98.29
SD	3.55	0.00	3.55	3.91	1.97	5.37
SE	0.11	0.00	0.11	1.40*	0.68*	1.92*
Margin of error (95% CI)	0.22	0.00	0.22	2.74	1.34	3.76
Upper 95% CI	75.63	0.00	24.81	7.15*	2.42*	98.10*
Lower 95% CI	75.19	0.00	24.37	1.68*	0.00*	90.58*

*Margins of error (95% CI) for archaeological data were obtained by bootstrapping the standard errors 10000 times.

MIS6 conditions with a Paleo-Agulhas plain silcrete source

Figure 85 and **Table 52** show that quartz has the highest frequency while silcrete has the second highest frequency during same-day returns during MIS4 conditions without a Paleo-Agulhas plain silcrete source. Quartzite has a low frequency. None of the model frequencies statistically match the archaeological frequencies. The model predicts more quartz and silcrete than what is represented in the archaeology, while quartzite is underpredicted. There is also no ranking match (**Supplementary Table B51**). This result does not support Hypothesis 1.

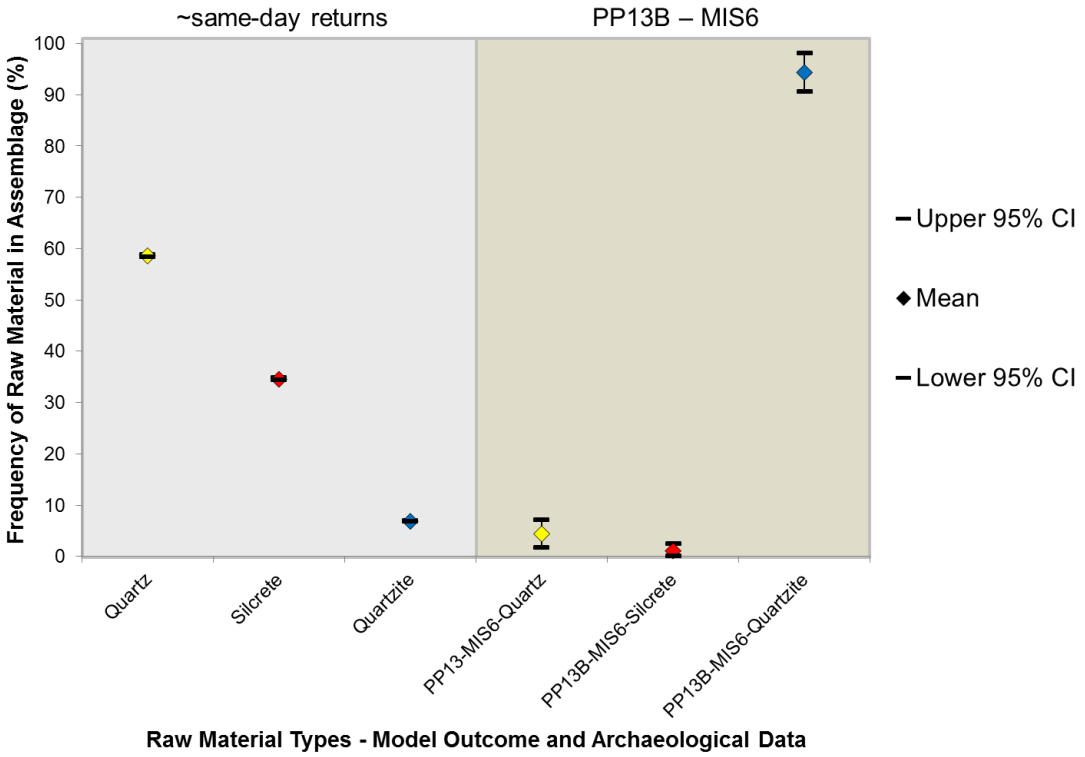

Figure 85. Comparison between same-day return modeling outcomes during MIS6 model conditions with a Paleo-Agulhas plain silcrete source and bootstrapped MIS6 archaeological raw material frequency data from PP13B. Plot shows the mean and the upper and lower 95% confidence intervals for raw material frequencies.

Table 52. Summary statistics and test results for same-day return simulations of MIS6 conditions with a Paleo-Agulhas plain silcrete source compared to MIS6 archaeological raw material frequency data from PP13B.

	Quartz	Silcrete	Quartzite	PP13-MIS6-Quartz	PP13B-MIS6-Silcrete	PP13B-MIS6-Quartzite
n (number of assemblages)	1000	1000	1000	7	7	7
First Quartile	56.24	31.92	5.75	1.71	0.00	87.62
Min	46.67	23.34	1.86	0.00	0.00	87.62
Median	58.57	34.58	6.73	2.15	0.00	97.85
Mean	58.60	34.54	6.86	4.41	1.09	94.34
Max	71.18	45.87	16.76	9.39	5.01	100.00
Third Quartile	61.21	36.98	7.78	9.33	2.55	98.29
SD	3.81	3.68	1.72	3.91	1.97	5.37
SE	0.12	0.12	0.05	1.40*	0.68*	1.92*
Margin of error (95% CI)	0.24	0.23	0.11	2.74	1.34	3.76
Upper 95% CI	58.84	34.77	6.96	7.15*	2.42*	98.10*
Lower 95% CI	58.37	34.31	6.75	1.68*	0.00*	90.58*

*Margins of error (95% CI) for archaeological data were obtained by bootstrapping the standard errors 10000 times.

OFAT1 modeling outcomes - Effect of increased movement budget

MIS4 conditions without a Paleo-Agulhas plain silcrete source

Figure 86 and **Table 53** compare model outcomes from MIS4 conditions without a Paleo-Agulhas plain silcrete source with MIS4 archaeological raw material frequencies from PP5-6. When the movement budget (TT=totticks) is increased, the frequency of silcrete is increased. However, the same is true for quartzite. Conversely, the frequency of quartz decreases with an increased movement-budget. When ~20 foraging days (TT=2000) are simulated, quartzite is the most frequent followed by quartz, while silcrete has the lowest frequency. All the frequencies are significantly different from each other during each type of movement budget (TT=totticks) simulation except for when TT=50 and TT=100 are simulated then silcrete and quartzite frequencies are statistically similar. Looking across the simulations of different movement budgets the model outcomes does not match the archaeological frequencies at any time. There is also no ranking match

during any of the movement budgets (**Supplementary Table B52**).This result does not support Hypothesis 1.

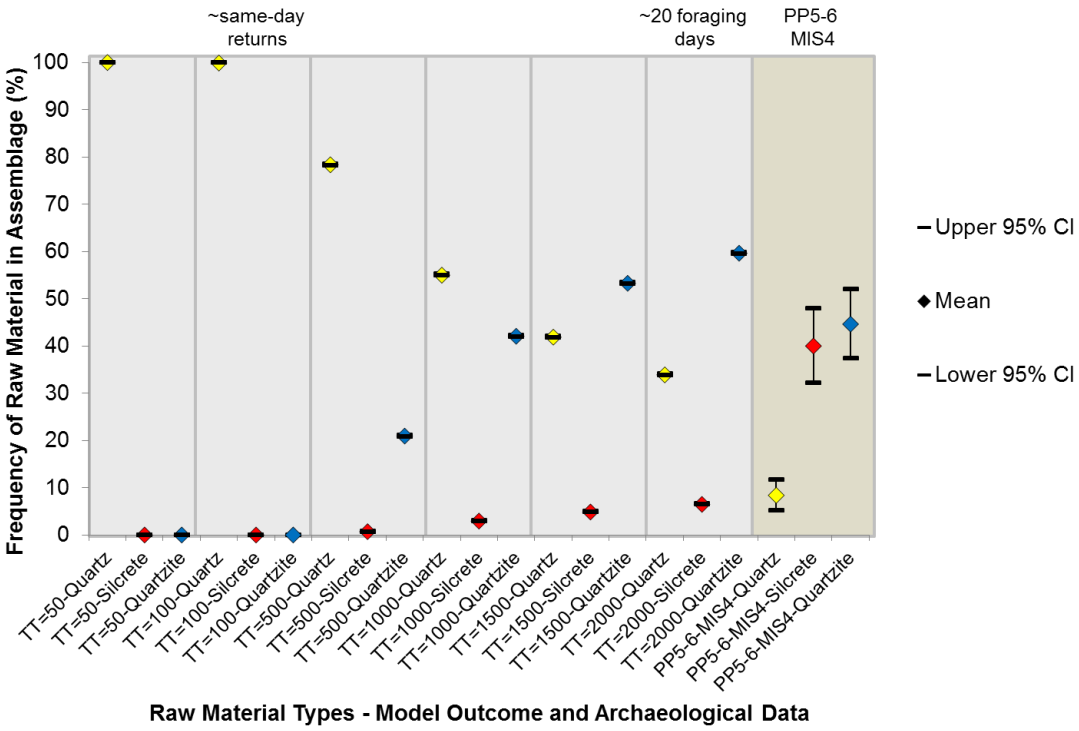

Figure 86. Comparison between OFAT1 modeling outcomes using different movement budgets (TT values) during MIS4 model conditions without a Paleo-Agulhas plain silcrete source and bootstrapped MIS4 archaeological raw material frequency data from PP5-6. Plot shows the mean and the upper and lower 95% confidence intervals for raw material frequencies.

Table 53. Summary statistics and test results for OFAT1 simulations of MIS4 conditions without a Paleo-Agulhas plain silcrete source compared to MIS4 archaeological raw material frequency data from PP5-6.

	TT=50-Quartz	TT=100-Quartz	TT=500-Quartz	TT=1000-Quartz	TT=1500-Quartz	TT=2000-Quartz	PP5-6-MIS4-Quartz
n (number of assemblages)	1000	1000	1000	1000	1000	1000	46
First Quartile	100.00	99.85	76.75	53.14	40.19	32.20	1.21
Min	100.00	98.34	70.36	46.56	34.36	27.03	0.00
Median	100.00	100.00	78.46	55.11	41.84	33.77	3.73
Mean	100.00	99.89	78.36	54.99	41.87	33.89	8.39
Max	100.00	100.00	84.87	63.38	50.53	40.78	66.11
Third Quartile	100.00	100.00	79.93	56.80	43.52	35.53	10.53
SD	0.00	0.23	2.37	2.69	2.51	2.43	11.83

SE	0.00	0.01	0.07	0.09	0.08	0.08	1.67*
Margin of error (95% CI)	0.00	0.01	0.15	0.17	0.16	0.15	3.28
Upper 95% CI	100.00	99.90	78.50	55.16	42.03	34.04	11.66*
Lower 95% CI	100.00	99.87	78.21	54.82	41.72	33.74	5.11*
	TT=50-Silcrete	**TT=100-Silcrete**	**TT=500-Silcrete**	**TT=1000-Silcrete**	**TT=1500-Silcrete**	**TT=2000-Silcrete**	**PP5-6-MIS4-Silcrete**
n (number of assemblages)	1000	1000	1000	1000	1000	1000	46
First Quartile	0.00	0.00	0.33	2.30	4.13	5.59	13.79
Min	0.00	0.00	0.00	0.51	1.82	3.32	0.00
Median	0.00	0.00	0.64	2.89	4.83	6.42	39.13
Mean	0.00	0.00	0.70	2.95	4.86	6.48	40.00
Max	0.00	0.00	3.12	6.78	8.92	10.38	96.55
Third Quartile	0.00	0.00	0.97	3.50	5.57	7.32	62.77
SD	0.00	0.00	0.49	0.95	1.12	1.25	27.52
SE	0.00	0.00	0.02	0.03	0.04	0.04	4.01*
Margin of error (95% CI)	0.00	0.00	0.03	0.06	0.07	0.08	7.85
Upper 95% CI	0.00	0.00	0.73	3.01	4.93	6.56	47.85*
Lower 95% CI	0.00	0.00	0.67	2.89	4.79	6.40	32.15*
	TT=50-Quartzite	**TT=100-Quartzite**	**TT=500-Quartzite**	**TT=1000-Quartzite**	**TT=1500-Quartzite**	**TT=2000-Quartzite**	**PP5-6-MIS4-Quartzite**
n (number of assemblages)	1000	1000	1000	1000	1000	1000	46
First Quartile	0.00	0.00	19.28	40.29	51.51	58.06	5.19
Min	0.00	0.00	14.80	34.16	45.68	52.83	0.00
Median	0.00	0.00	20.84	41.96	53.36	59.64	43.00
Mean	0.00	0.11	20.94	42.06	53.26	59.63	44.63
Max	0.00	1.66	28.64	49.75	60.13	66.67	96.45
Third Quartile	0.00	0.15	22.53	43.93	55.01	61.27	68.24
SD	0.00	0.23	2.34	2.64	2.61	2.46	25.54
SE	0.00	0.01	0.07	0.08	0.08	0.08	3.71*
Margin of error (95% CI)	0.00	0.01	0.15	0.16	0.16	0.15	7.27
Upper 95% CI	0.00	0.13	21.08	42.23	53.43	59.79	51.90*
Lower 95% CI	0.00	0.10	20.79	41.90	53.10	59.48	37.35*

*Margins of error (95% CI) for archaeological data were obtained by bootstrapping the standard errors 10000 times.

MIS4 conditions with a Paleo-Agulhas plain silcrete source

Figure 87 and **Table 54** compare model outcomes from MIS4 conditions with a Paleo-Agulhas plain silcrete source with MIS4 archaeological raw material frequencies from PP5-6.By increasing the movement budget (TT=totticks) the frequency of silcrete is

increased, however at TT=1500 and 2000 the silcrete frequency starts to decrease. Quartzite increases steadily up to TT=2000. Conversely, the frequency of quartz decreases with increased movement budget (TT=totticks) values. When ~20 foraging days (TT=2000) are simulated, silcrete is the most frequent raw material followed by quartzite, while quartz has the lowest frequency. All frequencies are significantly different from each other during each type of movement budget (TT=totticks) simulation.

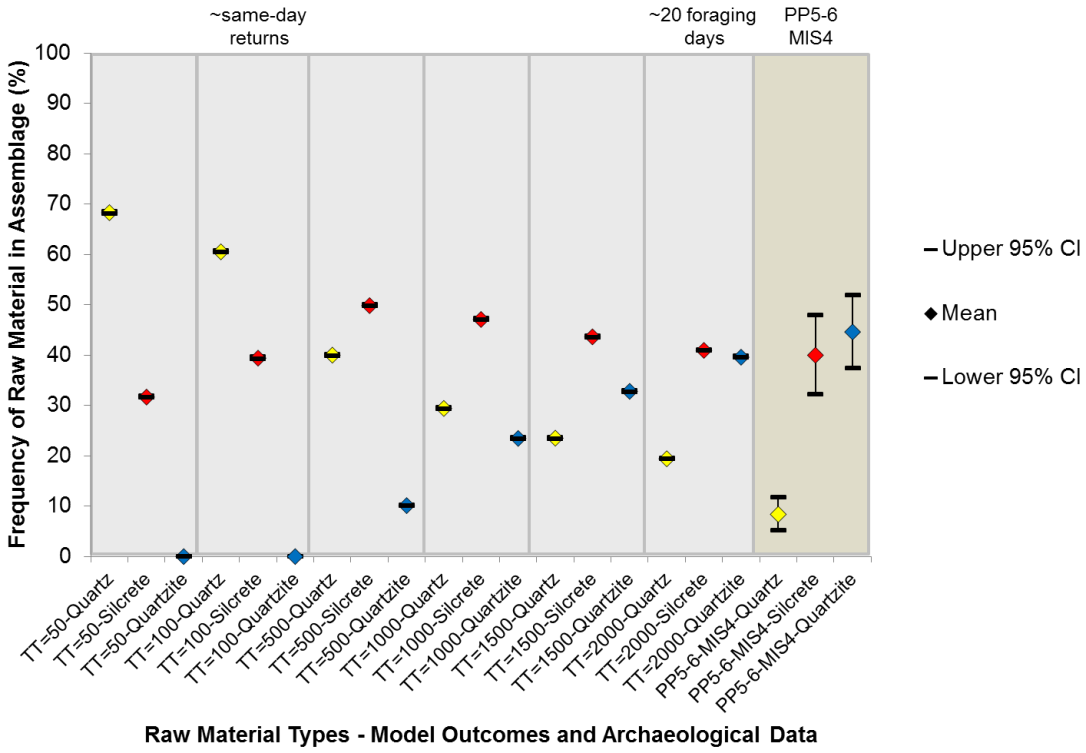

Figure 87. Comparison between OFAT1 modeling outcomes using different movement budgets (TT values) during MIS4 model conditions with a Paleo-Agulhas plain silcrete source and bootstrapped MIS4 archaeological raw material frequency data from PP5-6. Plot shows the mean and the upper and lower 95% confidence intervals for raw material frequencies.

Looking across the simulations of different movement budgets the silcrete frequencies do not match the archaeological silcrete frequencies at TT=50 and TT=500 simulations but do match at TT=1000 and TT=1500 simulations. When ~20 foraging

days (TT=2000) of movement are simulated, both quartzite and silcrete frequencies from the model statistically match the archaeological frequencies, while quartz does not. The model predicts a higher quartz frequency than the observed archaeological frequency. There is also no ranking match during any of the movement budgets (**Supplementary Table B53**).This result does not support Hypothesis 1.

Table 54. Summary statistics and test results for OFAT1 simulations of MIS4 conditions with a Paleo-Agulhas plain silcrete source compared to MIS4 archaeological raw material frequency data from PP5-6.

	TT=50-Quartz	**TT=100-Quartz**	**TT=500-Quartz**	**TT=1000-Quartz**	**TT=1500-Quartz**	**TT=2000-Quartz**	**PP5-6-MIS4-Quartz**
n (number of assemblages)	1000	1000	1000	1000	1000	1000	46
First Quartile	66.25	58.65	38.36	28.03	22.12	18.28	1.21
Min	59.25	52.24	31.71	22.92	16.94	14.03	0.00
Median	68.36	60.45	40.01	29.36	23.55	19.43	3.73
Mean	68.32	60.54	40.02	29.43	23.52	19.43	8.39
Max	77.23	69.57	48.41	37.51	29.68	24.15	66.11
Third Quartile	70.49	62.29	41.57	30.82	24.93	20.64	10.53
SD	2.99	2.78	2.39	2.16	2.02	1.71	11.83
SE	0.09	0.09	0.08	0.07	0.06	0.05	1.67*
Margin of error (95% CI)	0.19	0.17	0.15	0.13	0.13	0.11	3.28
Upper 95% CI	68.50	60.71	40.17	29.56	23.65	19.54	11.66*
Lower 95% CI	68.13	60.37	39.87	29.29	23.40	19.33	5.11*
	TT=50-Silcrete	**TT=100-Silcrete**	**TT=500-Silcrete**	**TT=1000-Silcrete**	**TT=1500-Silcrete**	**TT=2000-Silcrete**	**PP5-6-MIS4-Silcrete**
n (number of assemblages)	1000	1000	1000	1000	1000	1000	46
First Quartile	29.51	37.65	48.34	45.58	42.06	39.36	13.79
Min	22.77	30.43	41.65	38.33	36.25	33.52	0.00
Median	31.64	39.52	49.92	47.01	43.68	41.04	39.13
Mean	31.68	39.42	49.85	47.10	43.65	40.96	40.00
Max	40.75	47.61	58.71	54.37	51.75	48.33	96.55
Third Quartile	33.75	41.32	51.41	48.71	45.28	42.49	62.77
SD	2.99	2.77	2.44	2.34	2.34	2.31	27.52
SE	0.09	0.09	0.08	0.07	0.07	0.07	4.01*
Margin of error (95% CI)	0.19	0.17	0.15	0.14	0.14	0.14	7.85
Upper 95% CI	31.87	39.59	50.00	47.25	43.80	41.11	47.85*

Lower 95% CI	31.50	39.25	49.70	46.96	43.51	40.82	32.15*
	TT=50-Quartzite	**TT=100-Quartzite**	**TT=500-Quartzite**	**TT=1000-Quartzite**	**TT=1500-Quartzite**	**TT=2000-Quartzite**	**PP5-6-MIS4-Quartzite**
n (number of assemblages)	1000	1000	1000	1000	1000	1000	46
First Quartile	0.00	0.00	9.13	22.17	31.20	37.97	5.19
Min	0.00	0.00	6.01	16.95	21.73	32.41	0.00
Median	0.00	0.00	10.05	23.51	32.85	39.64	43.00
Mean	0.00	0.04	10.13	23.47	32.82	39.61	44.63
Max	0.00	0.79	15.61	29.57	39.41	46.09	96.45
Third Quartile	0.00	0.00	11.11	24.72	34.43	41.12	68.24
SD	0.00	0.10	1.45	1.96	2.33	2.28	25.54
SE	0.00	0.00	0.05	0.06	0.07	0.07	3.71*
Margin of error (95% CI)	0.00	0.01	0.09	0.12	0.14	0.14	7.27
Upper 95% CI	0.00	0.05	10.22	23.59	32.97	39.75	51.90*
Lower 95% CI	0.00	0.03	10.04	23.35	32.68	39.46	37.35*

*Margins of error (95% CI) for archaeological data were obtained by bootstrapping the standard errors 10000 times.

MIS5 conditions

Figure 88 and **Table 55** compare model outcomes from MIS5 conditions with MIS5 archaeological raw material frequencies from PP5-6, PP9B, PP9C, and PP13B. As the movement budget (TT=totticks) is increased, the frequency of silcrete is increased at the same time as quartzite increases. Conversely, the frequency of quartz decreases with increased movement budget (TT=totticks). When ~20 foraging days (TT=2000) are simulated, quartzite is the most frequent raw material followed by quartz, while silcrete has the lowest frequency. All the frequencies are significantly different from each other during each type of movement budget (TT=totticks) simulation.

Looking across the simulations of different movement budgets the quartz and quartzite frequencies do not match the archaeological frequencies at any time. The model predicts higher quartz frequencies at any movement budget than the observed archaeological frequencies, while it predicts lower quartzite frequencies at any movement

budget than the observed archaeological frequencies. Silcrete frequencies from TT=2000 simulations statistically match the silcrete frequency from PP5-6 during MIS5, whereas the silcrete frequency from TT=1500 simulations statistically matches the silcrete frequencies from both PP5-6 and the total PP MIS5 assemblage. TT=50, 100, and 500 silcrete frequencies statistically match the silcrete frequency from PP13B. There is also no ranking match during any of the movement budgets (**Supplementary Table B54**).This result does not support Hypothesis 1.

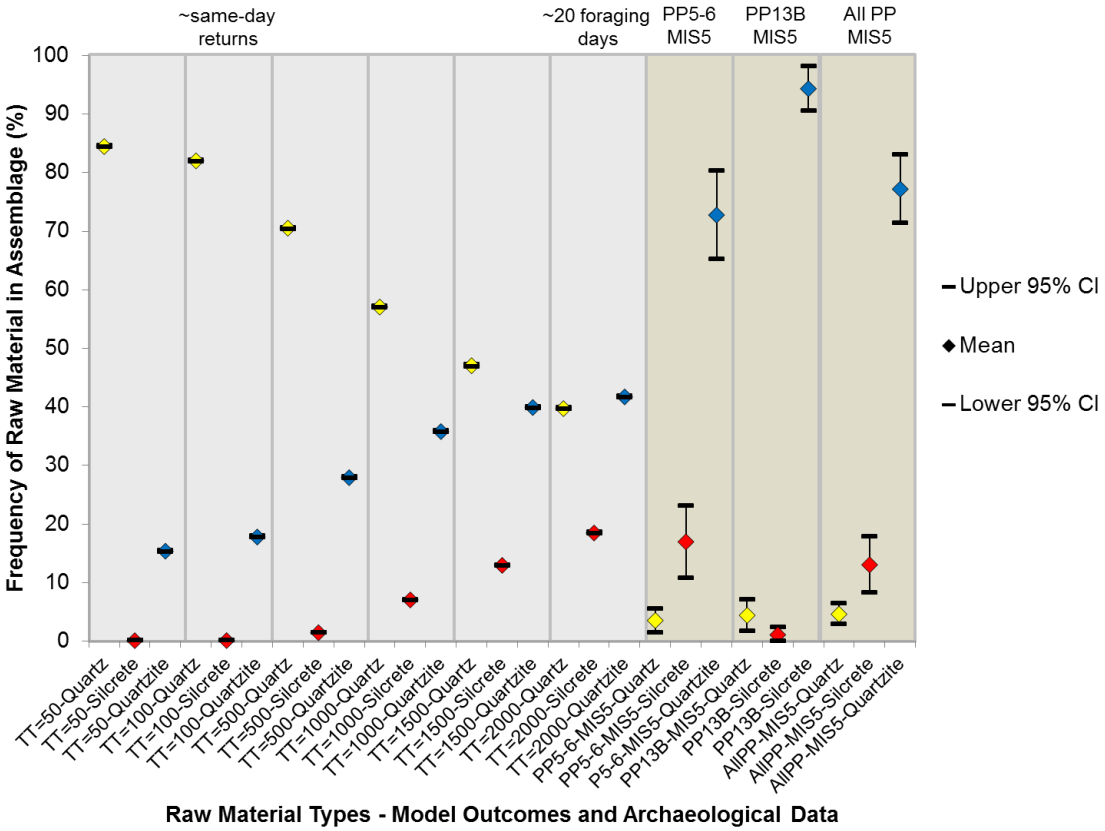

Figure 88. Comparison between OFAT1 modeling outcomes using different movement budgets (TT values) during MIS5 model conditions and bootstrapped MIS5 archaeological raw material frequency data from PP5-6, PP13B, and all MIS5 assemblages from the PP sequence including PP5-6, PP13B, PP9B, and PP9C. Plot shows the mean and the upper and lower 95% confidence intervals for raw material frequencies.

Table 55. Summary statistics and test results for OFAT1 simulations of MIS5 conditions compared to MIS5 archaeological raw material frequency data from PP5-6, PP13B, PP9B, and PP9C.

	TT=50-Quartz	TT=100-Quartz	TT=500-Quartz	TT=1000-Quartz	TT=1500-Quartz	TT=2000-Quartz	PP5-6-MIS5-Quartz	PP13B-MIS5-Quartz	AllPP-MIS5-Quartz
n (number of assemblages)	1000	1000	1000	1000	1000	1000	31	7	43
First Quartile	83.15	80.63	69.05	55.38	45.45	38.19	0.00	1.71	0.10
Min	77.10	75.65	63.79	49.60	40.38	32.27	0.00	0.00	0.00
Median	84.52	82.14	70.53	57.05	47.12	39.73	0.89	2.15	2.65
Mean	84.47	82.03	70.53	57.06	47.05	39.72	3.53	4.41	4.61
Max	90.66	89.47	77.54	63.66	55.27	47.61	24.87	9.39	24.87
Third Quartile	85.82	83.38	72.04	58.67	48.52	41.22	3.92	9.33	6.95
SD	2.07	2.02	2.22	2.33	2.30	2.33	5.94	3.91	6.03
SE	0.07	0.06	0.07	0.07	0.07	0.07	1.03	1.40	0.90
Margin of error (95% CI)	0.13	0.13	0.14	0.14	0.14	0.14	2.03	2.74	1.76
Upper 95% CI	84.60	82.15	70.66	57.20	47.19	39.86	5.56	7.15	6.37
Lower 95% CI	84.34	81.90	70.39	56.91	46.90	39.57	1.51	1.68	2.85
	TT=50-Silcrete	**TT=100-Silcrete**	**TT=500-Silcrete**	**TT=1000-Silcrete**	**TT=1500-Silcrete**	**TT=2000-Silcrete**	**PP5-6-MIS5-Silcrete**	**PP13B-Silcrete**	**AllPP-MIS5-Silcrete**
n (number of assemblages)	1000	1000	1000	1000	1000	1000	31	7	43
First Quartile	0.09	0.10	1.03	6.18	11.85	17.20	1.45	0.00	0.95
Min	0.06	0.06	0.14	3.19	7.65	12.21	0.00	0.00	0.00
Median	0.09	0.11	1.40	7.09	12.88	18.50	10.19	0.00	6.44
Mean	0.09	0.11	1.45	7.05	12.95	18.47	16.97	1.09	13.05
Max	0.14	0.15	4.11	11.85	17.94	25.51	64.83	5.01	64.83
Third Quartile	0.10	0.12	1.81	7.88	14.05	19.66	32.95	2.55	21.21
SD	0.01	0.01	0.58	1.26	1.63	1.89	17.85	1.97	16.45
SE	0.00	0.00	0.02	0.04	0.05	0.06	3.14	0.68	2.46
Margin of error (95% CI)	0.00	0.00	0.04	0.08	0.10	0.12	6.16	1.34	4.82
Upper 95% CI	0.09	0.11	1.49	7.13	13.05	18.59	23.12	2.42	17.86
Lower 95% CI	0.09	0.11	1.42	6.97	12.85	18.36	10.81	0.00	8.23
	TT=50-Quartzi	**TT=100-**	**TT=500-**	**TT=1000-**	**TT=1500-**	**TT=2000-**	**P5-6-MIS5-**	**PP13B-Silcrete**	**AllPP-MIS5-**

	te	Quartzite	Quartzite	Quartzite	Quartzite	Quartzite	Quartzite		Quartzite
n (number of assemblages)	1000	1000	1000	1000	1000	1000	31	7	43
First Quartile	14.04	16.46	26.47	34.31	38.37	40.12	60.24	87.62	64.30
Min	9.25	10.42	21.01	29.56	32.44	34.41	26.94	87.62	26.94
Median	15.33	17.69	27.97	35.84	39.94	41.79	76.11	97.85	83.74
Mean	15.37	17.79	27.92	35.79	39.91	41.72	72.77	94.34	77.20
Max	22.67	24.10	34.54	44.82	47.43	49.03	100.00	100.00	100.00
Third Quartile	16.68	19.17	29.41	37.32	41.46	43.32	92.83	98.29	92.83
SD	2.05	2.00	2.17	2.27	2.31	2.33	21.79	5.37	20.01
SE	0.06	0.06	0.07	0.07	0.07	0.07	3.85	1.92	3.00
Margin of error (95% CI)	0.13	0.12	0.13	0.14	0.14	0.14	7.55	3.76	5.87
Upper 95% CI	15.50	17.92	28.06	35.93	40.05	41.86	80.32	98.10	83.07
Lower 95% CI	15.25	17.67	27.79	35.65	39.76	41.57	65.21	90.58	71.33

*Margins of error (95% CI) for archaeological data were obtained by bootstrapping the standard errors 10000 times.

MIS6 conditions without a Paleo-Agulhas plain silcrete source

Figure 89 and **Table 56** compare model outcomes from MIS6 conditions without a Paleo-Agulhas plain silcrete source with MIS6 archaeological raw material frequencies from PP13B. When the movement budget (TT=totticks) is increased, the frequency of silcrete is increased at the same time as quartzite increases, while the frequency of quartz decreases. An interesting observation is that the quartzite frequency increases rapidly from 24.6% to 53.7% when going from TT=100 to TT=500. When ~20 foraging days (TT=2000) are simulated, quartzite is the most frequent followed by quartz, while silcrete has the lowest frequency. All the frequencies are significantly different from each other during each type of movement budget (TT=totticks) simulation.

Looking across the simulations of different movement budgets, the quartz and quartzite frequencies never match the archaeological frequencies, while the silcrete

frequencies match the archaeological frequencies at TT=50, 100, 500, and 1000. When ~20 foraging days (TT=2000) of movement are simulated, none of the model frequencies statistically matches the archaeological frequencies. The model predicts a lower quartz frequency than the observed archaeological frequency, while it predicts higher quartzite and silcrete values than the observed archaeological frequencies. There is also no ranking match during any of the movement budgets (**Supplementary Table B55**).The result does not support Hypothesis 1.

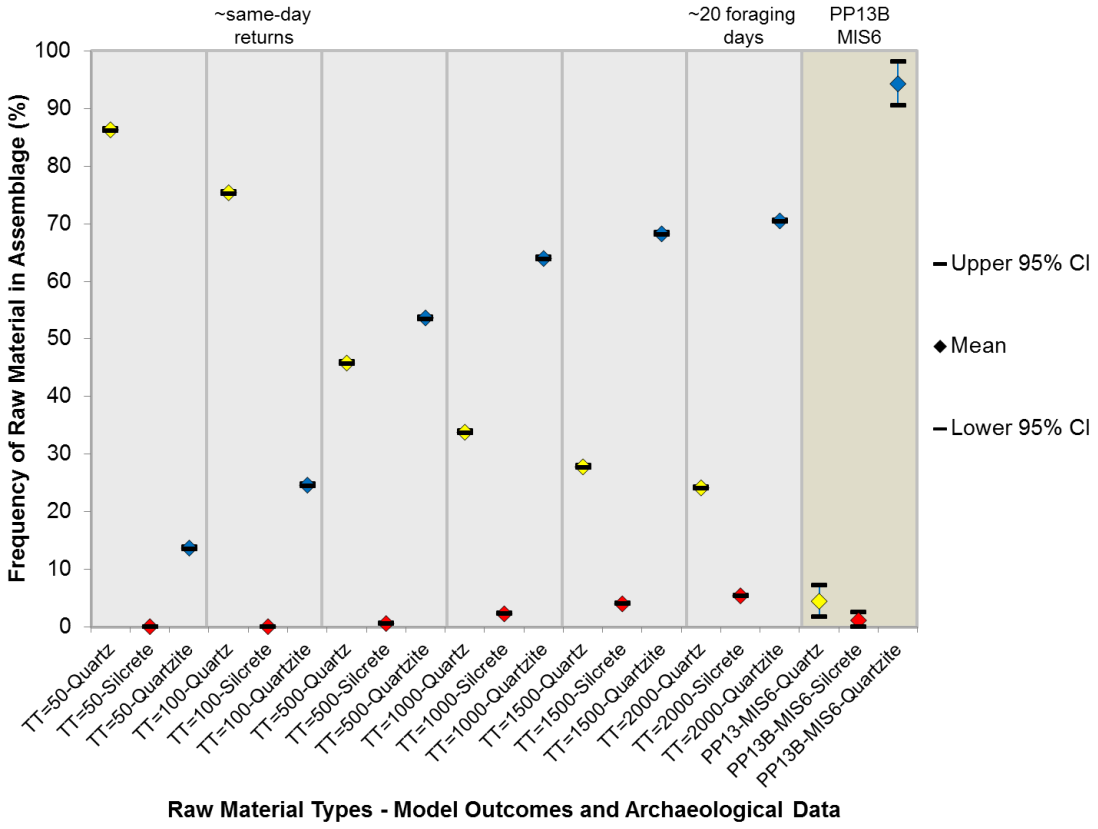

Figure 89. Comparison between OFAT1 modeling outcomes using different movement budgets (TT values) during MIS6 model conditions without a Paleo-Agulhas plain silcrete source and bootstrapped MIS6 archaeological raw material frequency data from PP13B. Plot shows the mean and the upper and lower 95% confidence intervals for raw material frequencies.

Table 56. Summary statistics and test results for OFAT1 simulations of MIS6 conditions without a Paleo-Agulhas plain silcrete source compared to MIS6 archaeological raw material frequency data from PP13B.

	TT=50-Quartz	TT=100-Quartz	TT=500-Quartz	TT=1000-Quartz	TT=1500-Quartz	TT=2000-Quartz	PP13-MIS6-Quartz
n (number of assemblages)	1000	1000	1000	1000	1000	1000	7
First Quartile	84.59	73.10	43.55	31.70	25.86	22.34	1.71
Min	73.16	65.00	35.90	23.54	17.44	15.97	0.00
Median	86.73	75.79	45.82	33.85	27.68	24.15	2.15
Mean	86.35	75.41	45.81	33.79	27.77	24.12	4.41
Max	94.72	84.33	56.69	43.70	37.64	33.75	9.39
Third Quartile	88.61	77.83	48.06	35.77	29.66	25.83	9.33
SD	3.29	3.55	3.25	2.99	2.84	2.59	3.91
SE	0.10	0.11	0.10	0.09	0.09	0.08	1.40*
Margin of error (95% CI)	0.20	0.22	0.20	0.19	0.18	0.16	2.74
Upper 95% CI	86.55	75.63	46.01	33.97	27.95	24.28	7.15*
Lower 95% CI	86.14	75.19	45.61	33.60	27.59	23.96	1.68*
	TT=50-Silcrete	**TT=100-Silcrete**	**TT=500-Silcrete**	**TT=1000-Silcrete**	**TT=1500-Silcrete**	**TT=2000-Silcrete**	**PP13B-MIS6-Silcrete**
n (number of assemblages)	1000	1000	1000	1000	1000	1000	7
First Quartile	0.00	0.00	0.27	1.52	3.12	4.42	0.00
Min	0.00	0.00	0.00	0.00	0.65	1.32	0.00
Median	0.00	0.00	0.54	2.07	3.86	5.33	0.00
Mean	0.00	0.00	0.54	2.23	3.97	5.36	1.09
Max	0.00	0.00	3.04	6.45	8.62	10.90	5.01
Third Quartile	0.00	0.00	0.87	2.81	4.81	6.18	2.55
SD	0.00	0.00	0.48	0.97	1.18	1.37	1.97
SE	0.00	0.00	0.02	0.03	0.04	0.04	0.68*
Margin of error (95% CI)	0.00	0.00	0.03	0.06	0.07	0.09	1.34
Upper 95% CI	0.00	0.00	0.57	2.29	4.04	5.44	2.42*
Lower 95% CI	0.00	0.00	0.51	2.17	3.89	5.27	0.00*
	TT=50-Quartzite	**TT=100-Quartzite**	**TT=500-Quartzite**	**TT=1000-Quartzite**	**TT=1500-Quartzite**	**TT=2000-Quartzite**	**PP13B-MIS6-Quartzite**
n (number of assemblages)	1000	1000	1000	1000	1000	1000	7
First Quartile	11.39	22.17	51.39	61.92	66.45	68.77	87.62
Min	5.28	15.67	43.02	54.60	59.15	60.52	87.62
Median	13.27	24.21	53.63	63.95	68.27	70.52	97.85
Mean	13.65	24.59	53.65	63.98	68.26	70.52	94.34
Max	26.84	35.00	63.37	75.07	77.64	79.87	100.00
Third Quartile	15.41	26.90	55.89	66.07	70.25	72.47	98.29
SD	3.29	3.55	3.24	3.05	2.90	2.83	5.37

SE	0.10	0.11	0.10	0.10	0.09	0.09	1.92*
Margin of error (95% CI)	0.20	0.22	0.20	0.19	0.18	0.18	3.76
Upper 95% CI	13.86	24.81	53.85	64.17	68.44	70.69	98.10*
Lower 95% CI	13.45	24.37	53.45	63.79	68.08	70.34	90.58*

*Margins of error (95% CI) for archaeological data were obtained by bootstrapping the standard errors 10000 times.

MIS6 conditions with a Paleo-Agulhas plain silcrete source

Figure 90 and **Table 57** compare model outcomes from MIS6 conditions with a Paleo-Agulhas plain silcrete source with MIS6 archaeological raw material frequencies from PP13B. As the movement budget (TT=totticks) is increased, the frequency of silcrete is increased but at TT=1000, 1500, and 2000 simulations the frequency of silcrete decreases. The frequency of quartzite, on the other hand, increases rapidly from TT=100 to TT=500 and steadily increases with increased movement-budget after that. Conversely, the quartz frequency decreases with increased movement budget (TT=totticks). When ~20 foraging days (TT=2000) are simulated, quartzite is the most frequent raw material followed by silcrete, while quartz has the lowest frequency. All the frequencies are significantly different from each other during each type of movement budget (TT=totticks) simulation.

Looking across the simulations of different movement budgets the frequencies do not match the archaeological frequencies at any time including when ~20 foraging days (TT=2000) of movement are simulated. During all movement budget simulations, the model predicts higher quartz and silcrete frequencies than the observed archaeological frequencies, while it predicts a lower quartzite frequency than the archaeological frequency. There is also no ranking match during any of the movement budgets (**Supplementary Table B56**). This result does not support Hypothesis 1.

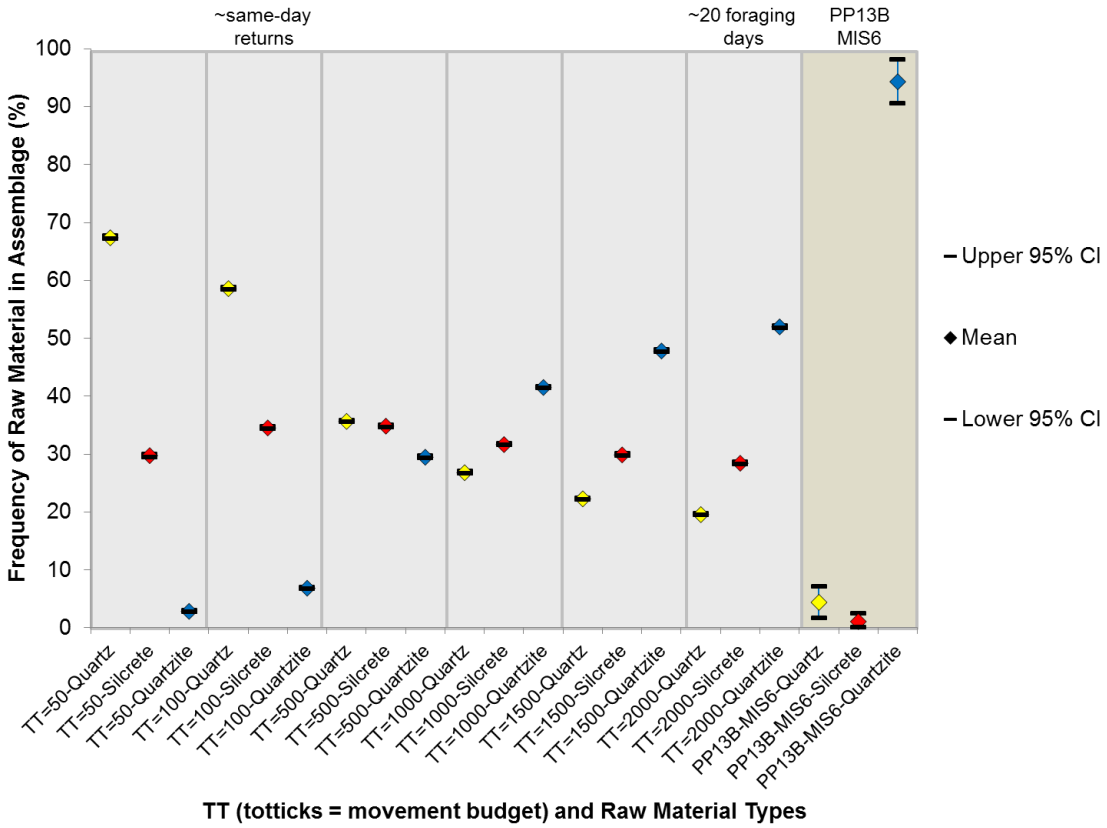

Figure 90. Comparison between OFAT1 modeling outcomes using different movement budgets (TT values) during MIS6 model conditions with a Paleo-Agulhas plain silcrete source and bootstrapped MIS6 archaeological raw material frequency data from PP13B. Plot shows the mean and the upper and lower 95% confidence intervals for raw material frequencies.

Table 57. Summary statistics and test results for OFAT1 simulations of MIS6 conditions with a Paleo-Agulhas plain silcrete source compared to MIS6 archaeological raw material frequency data from PP13B.

	TT=50-Quartz	TT=100-Quartz	TT=500-Quartz	TT=1000-Quartz	TT=1500-Quartz	TT=2000-Quartz	PP13B-MIS6-Quartz
n (number of assemblages)	1000	1000	1000	1000	1000	1000	7
First Quartile	64.56	56.24	33.53	24.80	20.56	17.97	1.71
Min	52.88	46.67	25.91	18.78	15.86	12.92	0.00
Median	67.93	58.57	35.53	26.94	22.21	19.49	2.15
Mean	67.39	58.60	35.67	26.81	22.29	19.57	4.41
Max	79.32	71.18	43.53	34.20	30.04	26.98	9.39
Third Quartile	70.54	61.21	37.72	28.74	23.91	21.16	9.33
SD	4.40	3.81	3.02	2.76	2.55	2.36	3.91
SE	0.14	0.12	0.10	0.09	0.08	0.07	1.40
Margin of error (95% CI)	0.27	0.24	0.19	0.17	0.16	0.15	2.74

Upper 95% CI	67.66	58.84	35.86	26.98	22.45	19.72	7.15
Lower 95% CI	67.11	58.37	35.48	26.64	22.13	19.42	1.68
	TT=50-Silcrete	**TT=100-Silcrete**	**TT=500-Silcrete**	**TT=1000-Silcrete**	**TT=1500-Silcrete**	**TT=2000-Silcrete**	**PP13B-MIS6-Silcrete**
n (number of assemblages)	1000	1000	1000	1000	1000	1000	7
First Quartile	26.63	31.92	32.85	29.75	27.94	26.54	0.00
Min	18.83	23.34	26.41	23.73	21.81	20.41	0.00
Median	29.11	34.58	34.88	31.66	29.88	28.45	0.00
Mean	29.76	34.54	34.85	31.66	29.89	28.44	1.09
Max	43.84	45.87	44.11	40.66	38.20	39.09	5.01
Third Quartile	32.48	36.98	36.90	33.51	31.75	30.26	2.55
SD	4.33	3.68	2.95	2.77	2.78	2.59	1.97
SE	0.14	0.12	0.09	0.09	0.09	0.08	0.68
Margin of error (95% CI)	0.27	0.23	0.18	0.17	0.17	0.16	1.34
Upper 95% CI	30.02	34.77	35.03	31.84	30.06	28.60	2.42
Lower 95% CI	29.49	34.31	34.66	31.49	29.71	28.28	0.00
	TT=50-Quartzite	**TT=100-Quartzite**	**TT=500-Quartzite**	**TT=1000-Quartzite**	**TT=1500-Quartzite**	**TT=2000-Quartzite**	**PP13B-MIS6-Quartzite**
n (number of assemblages)	1000	1000	1000	1000	1000	1000	7
First Quartile	1.93	5.75	27.52	39.47	45.82	49.84	87.62
Min	0.30	1.86	22.19	33.12	37.10	42.61	87.62
Median	2.66	6.73	29.50	41.46	47.85	51.98	97.85
Mean	2.86	6.86	29.48	41.53	47.82	51.99	94.34
Max	14.51	16.76	39.21	51.63	56.92	62.76	100.00
Third Quartile	3.37	7.78	31.31	43.56	49.85	53.98	98.29
SD	1.48	1.72	2.80	2.94	3.01	2.99	5.37
SE	0.05	0.05	0.09	0.09	0.10	0.09	1.92
Margin of error (95% CI)	0.09	0.11	0.17	0.18	0.19	0.19	3.76
Upper 95% CI	2.95	6.96	29.66	41.71	48.01	52.18	98.10
Lower 95% CI	2.77	6.75	29.31	41.35	47.64	51.80	90.58

*Margins of error (95% CI) for archaeological data were obtained by bootstrapping the standard errors 10000 times.

OAM – Same-day return outcomes and OFAT round 1results summary

Hypothesis 1 was not supported under any of the five different model conditions when considering only same-day returns to Pinnacle Point. The model persistently predicted more quartz than what is found in the archaeological record at Pinnacle Point (**Table 58**). Quartzite also never matches the archeological frequency of quartzite. Silcrete was found

to match the archaeological frequency of silcrete during MIS4 and MIS6 conditions without a Paleo-Agulhas silcrete source and during MIS5 conditions (**Table 58**).

When looking at the OFAT1 outcomes the comparison of the model outputs under different model conditions and the archaeological raw material frequencies show coastline position and raw material source distribution does not explain the archaeological raw material pattern (**Table 58**).

Table 58. Summary of whether model outcomes are the same as archaeological frequency data.

Model Condition Variable	Model Condition	Same-Day Returns Quartzite Frequency Same as Archaeology	Same-Day Returns Silcrete Frequency Same as Archaeology	Same-Day Returns Quartz Frequency Same as Archaeology	OFAT 1 Quartzite Frequency Same as Archaeology at Any Time	OFAT 1 Silcrete Frequency Same as Archaeology at Any Time	OFAT 1 Quartz Frequency Same as Archaeology at Any Time
Coastline Position and Raw Material Distribution	MIS4 without a Paleo-Agulhas Silcrete Source	Not Met	Not Met	Not Met	Not Met	Not Met	Not Met
Coastline Position and Raw Material Distribution	MIS4 with a Paleo-Agulhas Silcrete Source	Not Met	Met	Not Met	Met	Met	Not Met
Coastline Position and Raw Material Distribution	MIS5	Not Met	Met	Not Met	Not Met	Met	Not Met
Coastline Position and Raw Material Distribution	MIS6 without a Paleo-Agulhas Silcrete Source	Not Met	Met	Not Met	Not Met	Met	Not Met
Coastline Position and Raw Material Distribution	MIS6 with a Paleo-Agulhas Silcrete Source	Not Met	Not Met	Not Met	Not Met	Not Met	Not Met

Increasing and decreasing the movement budget thereby increasing and decreasing the range size of the forager does not result in a model output that matches the archaeological frequencies. The closest the model simulations come to match the archaeological pattern is under MIS4 conditions with a Paleo-Agulhas plain silcrete source when both quartzite and silcrete frequencies at TT=2000 statistically match the archaeological frequencies. However, the quartz frequency does not statistically match the archaeological frequency (**Table 58**). When looking at ranking comparisons there is also no match during same-day return simulations or during OFAT1 simulations. Overall, the results from same-day return simulations and OFAT1 presents no support for Hypothesis 1.

Is random walk a realistic raw material procurement strategy?

As noted previously the archaeological record indicates that hunter-gatherers changed their selection for stone tool raw materials even when several types of stone materials were available. Records from a wide range of environmental and climatic contexts, time-periods, and 'cultures' show the changing use, and co-use of different stone tool raw materials (e.g. Andrefsky Jr 1994, Bamforth 1990, Bar-Yosef 1991, Clark 1980, Jelinek 1991, Kuhn 2004, 1991). There is debate about what explains changing raw material selection and whether changing raw material frequencies in the archaeological record can be considered a reliable proxy for human forager adaptive variability (Brantingham 2003, Féblot-Augustins 1993, Kuhn 1995, Mellars 1996). Many hypotheses have been put forward to explain the changes in raw material usage frequency. These hypotheses include climate and environmental change and its co-variability with mobility and

procurement strategies (Ambrose and Lorenz 1990, Binford and Stone 1985, Kuhn 2004), direct selection of certain raw materials for their physical properties (Braun et al. 2009, Gould and Saggers 1985, Minichillo 2006), demographic change (Clark 1980), color or appearance preference (Akerman, Fullagar, and van Gijn 2002, Clendon 1999, Stout 2002), symbolic value (Wurz 1999), and style (Close 2002). These were all outlined above in *Chapter 2* and categorized into either 'Non Preference-based change' or 'Preference-based change' model categories.

Brantingham (2003) put forward an alternative to these hypotheses. He presented a neutral model that he argues explains some of the observed patterns in the record of raw material abundance. To demonstrate the deliberate selection of raw materials, he argued that patterning in the archaeological record must be shown to be different from the result of the neutral model. The neutral model provides a baseline for comparison where archaeologist can be certain that observed raw material patterns are not the result of strategic selection (Brantingham, 2003).

Oestmo and colleagues (2016) agreed with that sentiment but they highlighted that Brantingham (2003: 505) pointed out that an appropriate criticism of the neutral model is that a "forager could never engage in a random-walk foraging strategy and could never ignore the differences between stone raw material types." Oestmo et al. (2016) explored if such a criticism is valid and they followed Brantingham's (2003) suggestion that quantitative development of the observations presented in his study requires calibration of the ABM to run in simulated worlds built around the known geographic distribution of actual raw material sources. Oestmo et al. (2016) partly addressed Brantingham's suggestion by exploring two major limitations of the neutral model. The

first limitation is that raw material sources are distributed randomly without any clustering across the model landscape, which is not the case on most real landscapes where the locations of raw material sources are controlled by the underlying geological structure and geophysical processes. They suggested that an example of such structures and processes, which they draw from their own research region (Mossel Bay Region), are coastal cliffs and embayed beaches that potentially can produce cobbles beaches along a stretch of coastline. These cobble beaches appear clustered due to the geological structures and geophysical processes of the landscape.

The second limitation addressed by Oestmo et al. (2016) was the unrealistic assumption that each raw material location in the model (n=5000) represents a unique raw material. Five thousand raw material sources are possible across an extended landscape but not 5000 unique raw materials. They further argued that it is more likely that a smaller amount of raw materials such as 1-25 is represented by the 5000 source locations. Additionally, they note that the 1-25 unique raw materials are not randomly distributed in isolation away from the same type raw materials. They pointed out that not only are source locations clustered due to the underlying geological structure and geophysical processes but that several sources of the same material can be available in a cluster, depending on the geological formation.

The result of the study by Oestmo et al. (2016) showed that both the ‘seeking walk’, which is a simplified analogy for a forager that returns to a stone cache, and the random walk behavior both show that increased clustering of the raw material sources leads to increased time without raw materials in the toolkit. They noted, however, that time between procurement instances and time without materials in the toolkit have

different implications. On one hand, if the forager can stockpile a cache at a central location and can return to such a place then the forager can go extended periods without procuring raw material because it could return to the cache to fill up on raw materials. Conversely, if the forager engages in random walk and the random walk takes the forager away from the central location and never or very seldom returns directly to a stone cache then random walk is potentially an unrealistic or at least risky strategy because there is a high probability that the foragers will run out of materials (Oestmo, Janssen, and Marean 2016).

Based on the result of their study, Oestmo et al. (2016) predicted two things should hold true when the random walk model approach (the process of randomly walking while only picking up a raw material if one is encountered by chance, and discarding a raw material unit a set probability) is tested on real source locations with real extents in the Mossel Bay Region. First, raw material richness should be low comparatively to the default neutral model as the actual number of unique raw materials on the landscape in the Mossel Bay region is low. This prediction holds true due to the fact that only 5-6 raw materials (quartz, quartzite, silcrete, chert or chalcedony, hornfels, and silicified shale) are recognized broadly in the Mossel Bay region. Second, as the forager is moving about the landscape of the Mossel Bay region, the time spent without any raw materials in the toolkit will be high, in order of days and weeks. They proposed that if the second prediction holds true, then an alternative procurement strategy needs to be evaluated that meets the demands of the stone tool economy.

Presented below are the results of the second prediction that as the agent is moving across a real landscape (Mossel Bay region), and given the assumptions of the

random walk model, the time spent without any raw material in the toolkit will be high, on the order of days and weeks. The five different model conditions show different outcomes in regards to time without raw material in toolkit at different movement budget values (TT=totticks). None of the model conditions exhibit results that are consistent with the predictions outlined in Oestmo, Janssen, and Marean (2016). In all movement budget (totticks) simulations under all the five model conditions, the forager never goes above 1% of the time without raw material in the toolkit (**Supplementary Figures A1-A5 –** Raw data can be found in **Supplementary Tables B57-B66)**. If one assumes a leisurely pace of 2.5 km/hr and daily movement of up to 8 hours, then if the agent only moves TT=50 this translates to about 4 hours of foraging movement. Given this, 1% of 4 hours (240 minutes) is equal to (240 minutes*1/100) 2.4 minutes. In other words, when a forager conducts the foraging movement in a random fashion in regards to stone raw material sources for a half a foraging day, the agent is only without raw materials for ~2.4 minutes. Given the same pace and daily max movement budget of 8 hours, when the agent moves the full amount it is only without stone raw material for ~5 minutes during that period.

What this suggests is that under assumptions of a random walk model as presented by Brantingham, random walk is a realistic procurement strategy for stone tool raw materials when the forager is moving in the Mossel Bay Region. Further tests of the effect that changing the discard probability has on the time the forager spends without raw material in the toolkit should be undertaken. One can predict that by lowering the discard probability that time spent without raw material in the toolkit will decrease. However, it is beyond the scope of this study.

OAM – Hypothesis 1 evaluation

Knowing that random walk in relation to raw material sources can be considered a realistic mobility strategy to procure stone raw materials in the MBR. H_1 can now be evaluated. Below an evaluation using results from same-day return simulations during all the five different model conditions, and the results of round one of the sensitivity analysis (OFAT 1) is presented.

As noted above, in the first round of the OFAT (OFAT1), the effect of increasing the amount of time allowed by the forager to be away from PP was modeled. This was accomplished by varying the movement-budget (totticks) variable. This examined the effect of increasing the amount of both time and distance the forager can move away from Pinnacle Point, effectively increasing residential mobility. Movement budget (TT=totticks) values of 50, 100, 500, 1000, 1500, and 2000 were simulated. This allowed for testing H_1 under both same-day returns (~70-100 "totticks", assuming a walking pace of 3.5 to 2.5km/hr (Binford 2001, Marlowe 2010, Marlowe 2006)) and up to ~15-20 foraging days away from Pinnacle Point (~2000" totticks", assuming a walking pace of 3.5 to 2.5km/hr (Binford 2001, Marlowe 2010, Marlowe 2006)).

Given the failed prediction that the forager would be without raw materials in the toolkit for extended periods of time, up to days and weeks, during random walk in the environment of the Mossel Bay region, opportunistic acquisition is a realistic foraging strategy in terms of obtaining stone tool raw materials in the Mossel Bay region. However, the modeling outcomes from same-day return and OFAT1 (effect of increased movement budget) simulations of the coastline position and raw material source distribution variable show that H_1 is not supported under any of the five model conditions

(MIS4 with or without a Paleo-Agulhas plain silcrete source, MIS5, and MIS6 with or without a Paleo-Agulhas plain silcrete source). This suggests that the raw material frequencies observed in the Pinnacle Point record are not due to the distribution and availability of raw material sources in the Mossel Bay region or due to changes to foraging range size as exemplified by changing the movement budget that can lead to encounters with new and different raw material sources.

Further, it suggests that opportunistic behavior does not explain the raw material pattern; it suggests that raw material procurement was not embedded into the overall foraging movement. This can imply that expedient procurement, use, and discard of raw materials was not a preferred raw material strategy, and that stone tool raw material did play a significant role in the technological organization of the foragers. Whether expedient behavior in regards to raw material economy can result in model raw material frequencies that are statistically similar to the archaeological frequencies will be addressed in OFAT round 4 below.

The evaluation of Hypothesis 1 (H_1) suggests that other factors than opportunistic acquisition resulted in the raw material pattern observed at Pinnacle Point. The outcome suggests that the response to climatic and environmental change as observed in the changing coastline position and raw material source distribution was not a mobility strategy involving targeting food resources that disregarded stone tool raw material differences and where investment in stone tool technology was not a priority to obtain the food resources.

The results above do not rule out other hypotheses that the raw material pattern can be due to factors such as shifts in the geographical range of foragers (Clark, 1980)

and/or trade and exchange (Deacon 1989, Wurz 1999), which both examples of the 'Social learning/Culture' variant in the 'preference-based change' model category as outlined above. Further testing of these informal models cannot be done in this study but requires separate studies such as identifying how far these raw materials have traveled. Other researchers are working on this problem (e.g. Nash, Coulson, Staurset, Smith, et al. 2013).

To check the robustness of the initial evaluation of H_1 an expanded sensitivity analysis was also conducted. A number of factors can be argued to have an influence on the outcome of the H_1 evaluation, and warrant further examination: 1) the assumption that Pinnacle Point is an exclusive locality on the landscape where all foraging bouts start and end is most likely wrong. By using Pinnacle Point as the central place for each foraging bout the foraging pattern is restricted to the areas surrounding Pinnacle Point. 2) The assumptions about probability of discard on the landscape or at the campsite (Pinnacle Point) and the size of the toolkit are potentially incorrect. As noted in the methods chapter (*Chapter 6*), this analysis uses the same discard probability and toolkit size as used by Brantingham (2003). It is possible that different values of these factors can change the model outcome of same-day simulation to be similar to the archaeological raw material pattern. 3) The simple random walk using Brantingham's (2003) assumptions as a whole (base settings) is potentially incorrect. More complex behaviors that use discard probability and toolkit size assumptions that simulate either conservative, expedient, or site caching behavior are potentially more realistic. Below the results of simulations addressing these factors are presented starting with the assumption that Pinnacle Point is the exclusive locality that the forager can return too.

One-factor-at-the-time (OFAT) sensitivity analysis results

OFAT round 2 – Pinnacle Point only one of three localities to return too

As stated in the methods chapter (*Chapter 6*), in the second round of the OFAT (OFAT2), the effect of having two more central localities (represented by two actual archaeological MSA localities) to return too was modeled. The factor of having more than two localities to return too introduced randomness but also realism to the model and simulated Pinnacle Point as being just one of three localities that the forager can access on the landscape. By adding two more localities, the foraging pattern of the forager is also altered because the area around two more places on the landscape will now be more frequently visited.

MIS4 conditions without a Paleo-Agulhas plain silcrete source

Figure 91 and **Supplementary Table B67** compare the MIS4 archaeological raw material frequencies from PP5-6 with simulation results of MIS4 conditions without a Paleo-Agulhas plain silcrete source. The frequencies resulting from same-day returns do not statistically match the archaeological frequencies. In fact, the model result suggests that quartz should be the most frequent material, while the archaeology shows that quartz is the least frequent raw material. Looking across the simulations of different movement budgets, the model outcomes never match the archaeological frequencies. There is also no ranking match during any of the movement budgets (**Supplementary Figure B68**).

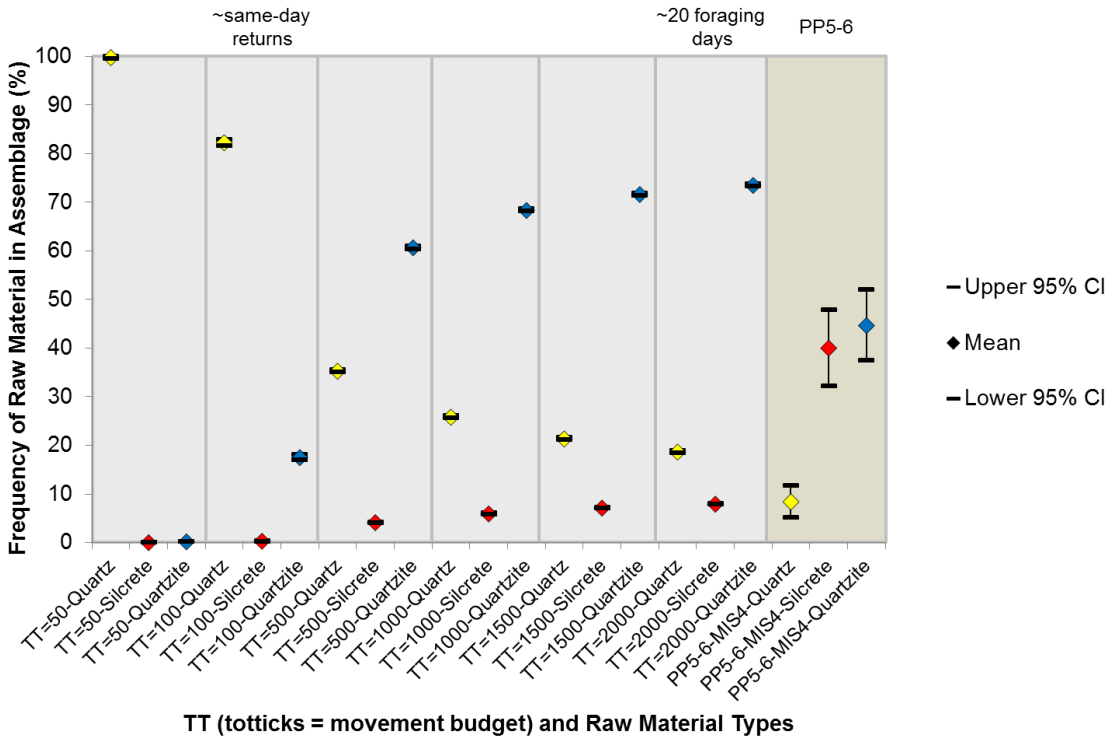

Figure 91. Comparison between OFAT2 outcomes using different movement budgets (TT values) during MIS4 model conditions without a Paleo-Agulhas plain silcrete source where the agent moves to the closest locality when the movement budget (totticks) is exhausted and bootstrapped MIS4 archaeological raw material frequency data from PP5-6. Plot shows the mean and the upper and lower 95% confidence intervals for the raw materials deposited at the both the simulated PP locality and at PP5-6.

MIS4 conditions with a Paleo-Agulhas plain silcrete source

When considering MIS4 conditions when a Paleo-Agulhas plain silcrete source is present, the quartzite and quartz frequencies resulting from same-day returns do not statistically match the archaeological frequencies, while the silcrete frequencies do statistically match (**Figure 92** and **Supplementary Table B69)**. Looking across the simulations of different movement budgets the silcrete frequencies match the archaeological silcrete frequencies at all TT simulations except for TT=50, while the quartz frequency statistically matches the archaeological quartz frequency during TT=1500 and TT=2000 simulations, and the quartzite frequency statistically matches the

archaeological quartzite frequency during TT=500 simulations. That means that during TT=500 simulations the model is close to explaining the archaeological raw material frequencies. However, the model predicts a higher quartz frequency than what is observed in the archaeological record. There is also no ranking match during any of the movement budgets (**Supplementary Figure B70**).

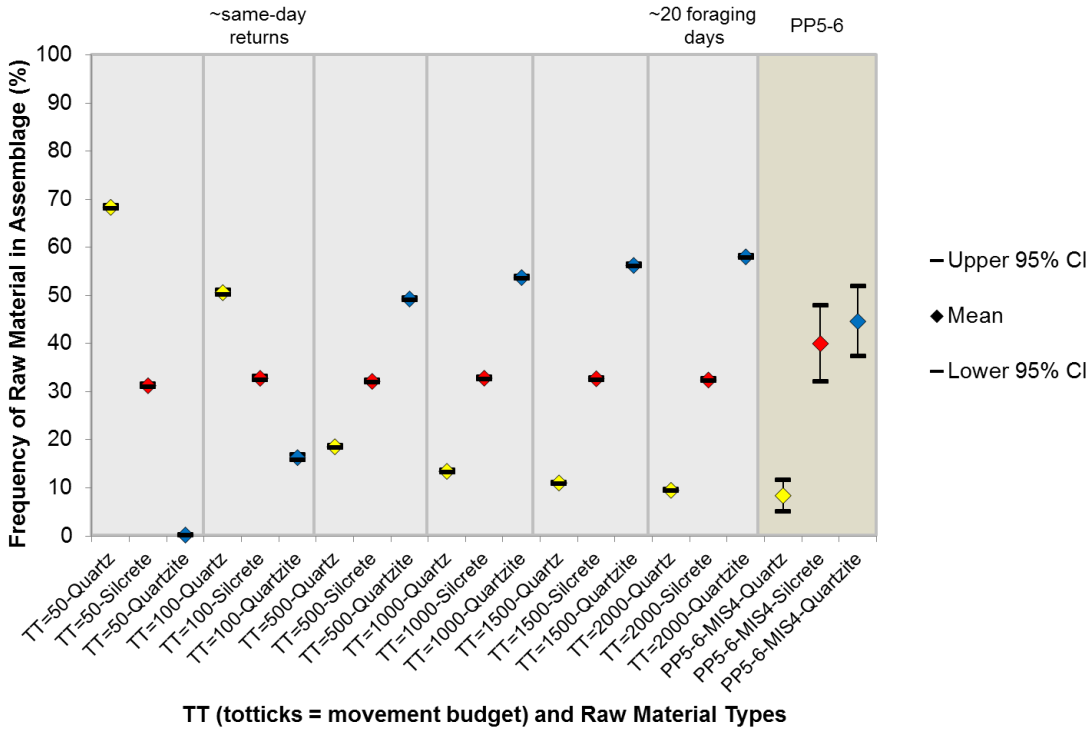

Figure 92. Comparison between OFAT2 outcomes using different movement budgets (TT values) during MIS4 model conditions with a Paleo-Agulhas plain silcrete source where the agent moves to the closest locality when the movement budget (totticks) is exhausted and bootstrapped MIS4 archaeological raw material frequency data from PP5-6. Plot shows the mean and the upper and lower 95% confidence intervals for the raw materials deposited at the both the simulated PP locality and at PP5-6.

MIS5 conditions

During MIS5 conditions quartz and quartzite raw material frequencies resulting from same-day returns again do not statistically match the archaeological frequencies, while the silcrete frequency does statistically match the MIS5 silcrete frequency from PP13B

(**Figure 93** and **Supplementary Table B71)**. Looking across the simulations of different movement budgets the quartz and quartzite frequencies do not match the archaeological frequencies at any time, while the silcrete frequency from TT=1000 and TT=1500 simulations statistically match the silcrete frequency from PP5-6, whereas the silcrete frequency from TT=500 simulations statistically match silcrete frequencies from both PP5-6 and the total Pinnacle Point MIS5 assemblage. TT=50 and TT=100 silcrete frequencies statistically match the silcrete frequency from PP13B. There is no ranking match during any of the movement budgets (**Supplementary Table B72**).

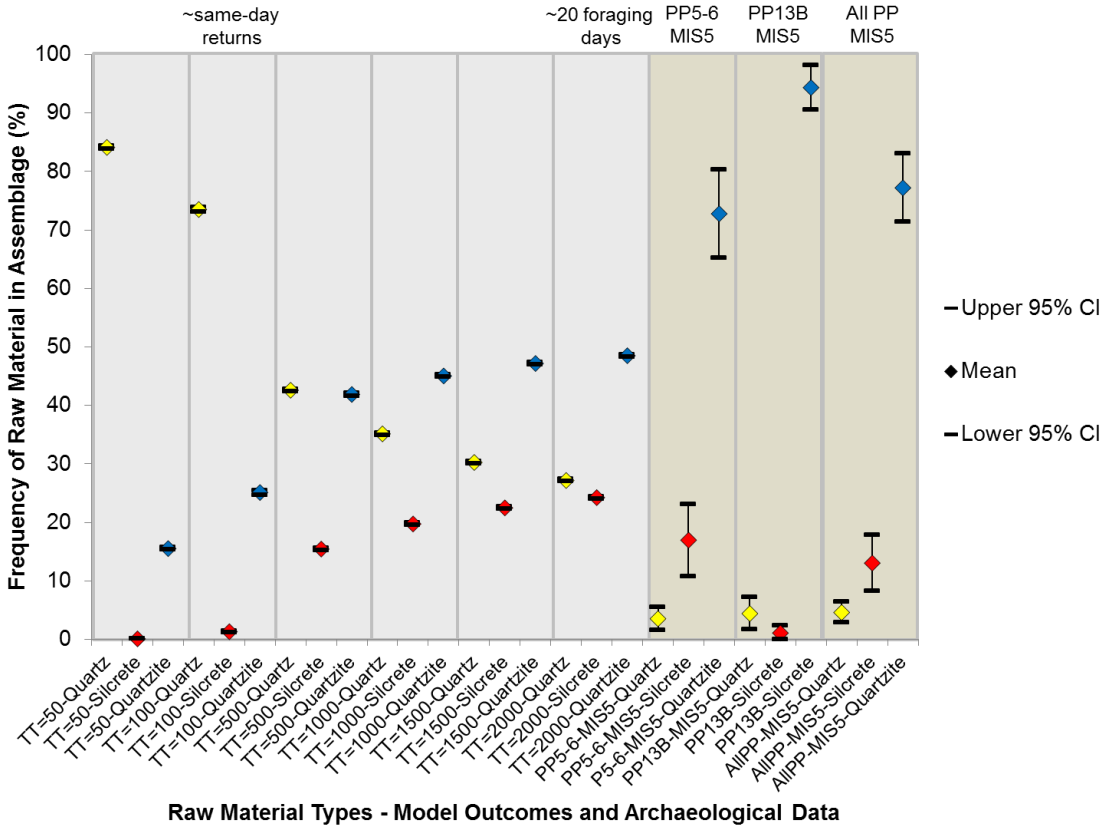

Figure 93. Comparison between OFAT2 outcomes using different movement budgets (TT values) during MIS5 model conditions where the agent moves to the closest locality when the movement budget (totticks) is exhausted and bootstrapped MIS5 archaeological raw material frequency data from PP5-6, PP13B, and all MIS5 assemblages from the PP sequence including PP5-6, PP13B, PP9B, and PP9C. Plot shows the mean and the upper and lower 95% confidence intervals for the raw materials deposited at the both the simulated PP locality and at PP5-6, PP9B, PP9C, and PP13B.

MIS6 conditions without a Paleo-Agulhas plain silcrete source

Figure 94 and **Supplementary Table B73** compare the MIS6 archaeological raw material frequencies from PP13B with simulation results of MIS6 conditions without a Paleo-Agulhas plain silcrete source.

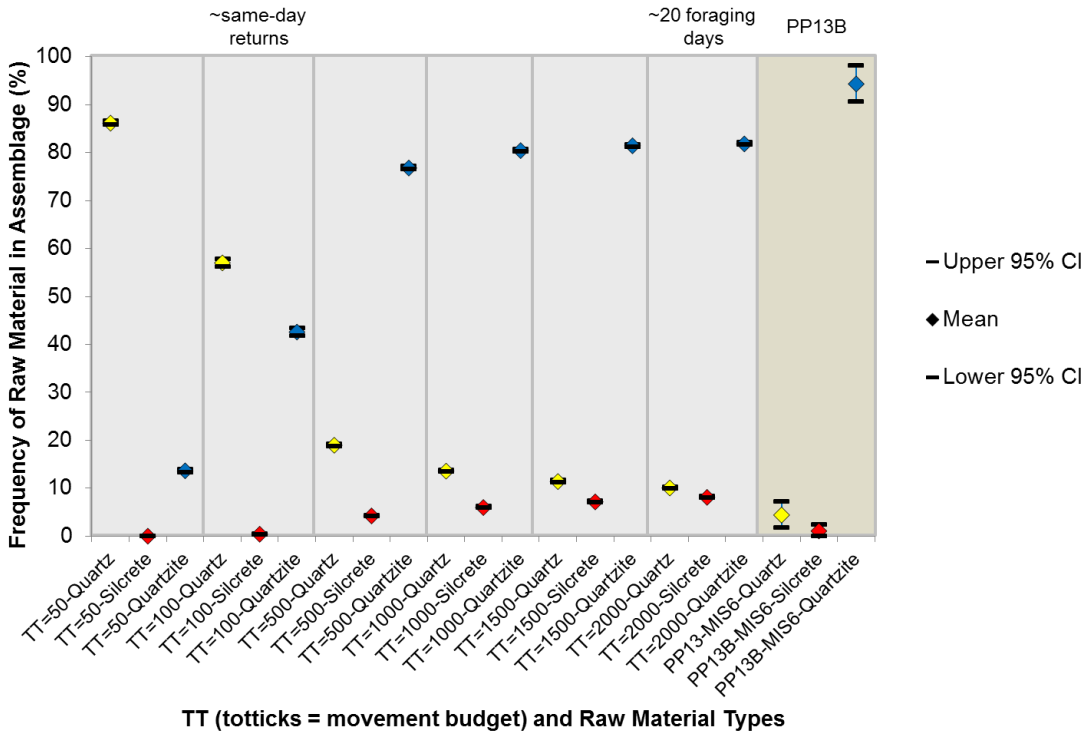

Figure 94. Comparison between OFAT2 outcomes using different movement budgets (TT values) during MIS6 model conditions without a Paleo-Agulhas plain silcrete source where the agent moves to the closest locality when the movement budget (totticks) is exhausted and bootstrapped MIS6 archaeological raw material frequency data from PP13B. Plot shows the mean and the upper and lower 95% confidence intervals for the raw materials deposited at the both the simulated PP locality and at PP13B.

The quartz and quartzite frequencies resulting from same-day returns do not statistically match the archaeological frequencies, while the silcrete frequency does match the archaeological frequency. Looking across the simulations of different movement budgets, the quartz and quartzite frequencies never match the archaeological frequencies, while the silcrete frequencies match the archaeological frequencies at TT=50

and TT=100. Although the frequencies of quartzite and quartz move in a direction of compatibility with the archaeological record as the movement budget is increased, the model underpredicts the amount of quartzite and over predicts the amount of quartz at TT=2000. There is no ranking match during any of the movement budgets (**Supplementary Table B74**).

MIS6 conditions with a Paleo-Agulhas plain silcrete source

When considering MIS6 conditions when a Paleo-Agulhas plain silcrete source is present, all the raw material frequencies resulting from same-day returns do not statistically match the archaeological frequencies (**Figure 95** and **Supplementary Table B75)**. Looking across the simulations of different movement budgets the frequencies do not match the archaeological frequencies at any time including when ~20 foraging days (TT=2000) of movement are simulated. As with simulations where Pinnacle Point is the exclusive locality that is accessible to foragers, during all movement budget simulations, the model predicts higher quartz and silcrete frequencies than the observed archaeological frequencies, while it predicts a lower quartzite frequency than the archaeological frequency. There is no ranking match during any of the movement budgets (**Supplementary Table B76**).

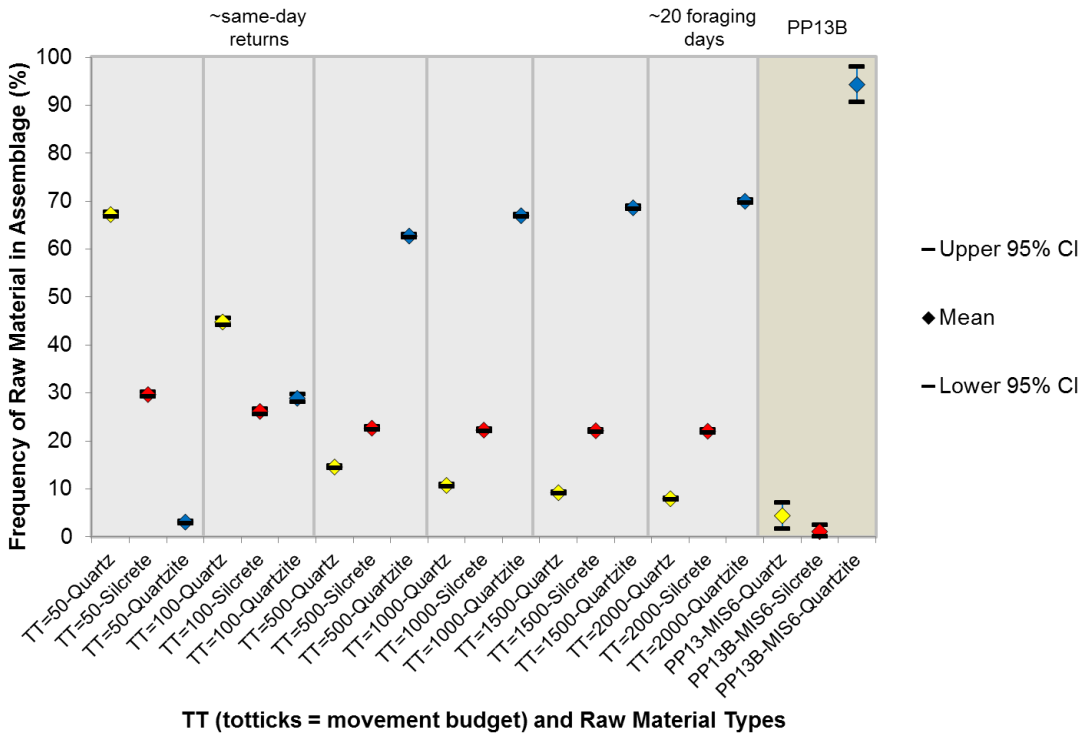

Figure 95. Comparison between OFAT2 outcomes using different movement budgets (TT values) during MIS6 model conditions without a Paleo-Agulhas plain silcrete source where the agent moves to the closest locality when the movement budget (totticks) is exhausted and bootstrapped MIS6 archaeological raw material frequency data from PP13B. Plot shows the mean and the upper and lower 95% confidence intervals for the raw materials deposited at the both the simulated PP locality and at PP13B.

The introduction of two more localities for the agent to be able to return too, which in effect changes the foraging pattern of the forager, injects a more realistic scenario where the agent is not fully dependent on Pinnacle Point as a home base or central location but instead Pinnacle Point is just one of three localities on the landscape that the forager can access. One can argue that this scenario thus more closely simulates residential mobility (Binford 1980) where the forager can move from site to site freely and is only dependent on whether the random walk takes the forager close to a locality at the end of a foraging bout. In addition, all simulations using a movement budget of TT-500 or more implies that the forager will set up a campsite on the landscape every 8 hours

of foraging regardless of the location until the movement budget is exhausted. We do not see these campsites in the model but they are there unless the forager stayed at any of three sites every day of every week and only moved between them, which they do not when they randomly walk.

The combination of more sites to return too and increased movement budget can create a situation where the forager starts at one site then moves out on the landscape for 5-20 days depending on the movement budget (TT=500 to TT=2000 and assuming a movement speed of 2.5 km/hr) only to return to a different site than it started at. When the forager subsequently moves again it can travel across the landscape for another 5-20 days and return to another site different from the two first ones. This type of movement I would argue resembles residential mobility.

The results above show that the under a more realistic scenario where Pinnacle Point is not an exclusive locality and the foraging pattern is extended to included areas around two more localities, the Opportunistic Acquisition Model (OAM) does not explain the archaeological raw material pattern during any model conditions. However, what if the model parameters themselves are changed making the agent more or less conservative with the raw material in the toolkit that is also of a varying size?

OFAT round 3 – Changing discard probabilities and toolkit size

In the third round of the OFAT (OFAT3), a test of the effect of changing the probability of discard of raw materials on the landscape, the effect of changing the probability of discard of raw materials in the campsite, and the effect of changing the toolkit size on the raw material frequency output at Pinnacle Point was modelled. This round focused on

what happens to the raw material frequency output at Pinnacle Point when the probability of discard on the landscape is lowered or raised, what happens to the raw material frequency output at Pinnacle Point when the probability of discard at Pinnacle Point is lowered and raised, and what happens to the raw material frequency output at Pinnacle Point when the toolkit size is lowered from the original 100.

These changes to the model parameters where considered both when Pinnacle Point is an exclusive locality and when Pinnacle Point is one of three localities that the forager can return too. This allows for evaluating whether the introduction of a more residential mobility strategy with more possible localities open to the forager changes the raw material frequency model outcomes. It is important to note here though that the simulations reported on below only consider same-day returns to a locality. This simulates what the raw material frequencies would look like when the forager will always return to a locality in close vicinity to the starting point every day. When the simulations use Pinnacle Point as an exclusive locality, the forager always returns there after a day's foraging movement, while during simulations where Pinnacle Point is one of three localities the forager can hypothetically switch locality at the end of each day without any intervening stops at other localities or potential 'stops' on the landscape.

Return to starting locality simulations

MIS4 conditions without a Paleo-Agulhas plain silcrete source

Supplementary Figure A6 and **Supplementary Tables B77-B79** compare the MIS4 archaeological raw material frequencies from PP5-6 with simulation results of MIS4 conditions without a Paleo-Agulhas plain silcrete source. The frequencies resulting from

same-day returns do not statistically match the archaeological frequencies under any parameter setting of ProbDiscardCamp (PDC), ProbDiscard (PD), or Toolkit size. The results of all settings for all three model-parameters predicts that quartz should be the most frequent material, while the archaeology shows that quartz is the least frequent raw material of the three. There is no ranking match (**Supplementary Table B80**).

MIS4 conditions with a Paleo-Agulhas plain silcrete source

When considering MIS4 conditions when a Paleo-Agulhas plain silcrete source is present, the quartzite and quartz frequencies from PDC, PD, and Toolkit size simulations do not statistically match the archaeological frequencies at any model parameter setting during same-day returns (**Supplementary Figure A7** and **Supplementary Tables B81-B83)**. However, silcrete frequencies from PDC, PD, and Toolkit size simulation do match the archaeological frequencies during PDC=0.001, PD=0.1, and Toolkit sizes 100, 75, 50, and 10 model parameters settings (**Supplementary Figure A8**, and **Supplementary Tables B81-B83**). This means that when the forager is more conservative compared to the base setting (0.02) with its discard of material at Pinnacle Point the frequency of silcrete statistically matches the archaeological frequency, while under all other model parameter settings, the model predicts a silcrete frequency that is lower than the archaeological frequency. The result of the simulations of the probability of discard on the landscape (PD) model parameter shows that when the agent is being more conservative with discard on the landscape compared to the base-setting (0.02) the frequency of silcrete matches the archaeological frequency, while under a lower PD setting (0.001) the model predicts a lower silcrete frequency than observed

archaeologically. Under higher PD settings than 0.01, the model predicts silcrete frequencies that are higher than the archaeological frequency. The Toolkit size parameter simulations show that frequency of silcrete matches the archaeological frequency even when you lower the toolkit size to half and even a tenth of the original size. Only when you have a Toolkit size of five does the model predict a silcrete frequency that is higher than the archaeological frequency.

Considering all this, it is important to note that quartzite and quartz frequencies do not match the archaeological frequency at any time, which means that changing the model parameters during MIS4 conditions with a Paleo-Agulhas plain silcrete source does not lead to model outcomes that match the archaeological frequencies overall. There is no ranking match (**Supplementary Table B84**).

MIS5 conditions

During MIS5 conditions, the quartzite and quartz frequencies from PDC, PD, and Toolkit size simulations do not statistically match the archaeological frequencies at any model parameter setting during same-day returns from any archaeological site (**Supplementary Figure A8** and **Supplementary Tables B85-B87)**. However, silcrete frequencies from PDC, PD, and Toolkit size simulation do match the archaeological frequencies from PP13B under all settings of PDC, PD, and Toolkit size (**Supplementary Figure A8**, and **Supplementary Tables B85-B87**).

Again, considering all this, it is important to note that quartzite and quartz frequencies do not match the archaeological frequency at any time, which means that changing the model parameters during MIS5 conditions does not lead to model outcomes

that match the archaeological frequencies overall. There is no ranking match (**Supplementary Table B88**).

MIS6 conditions without a Paleo-Agulhas plain silcrete source

Supplementary Figure A9 and **Supplementary Tables B89-B91** compare the MIS6 archaeological raw material frequencies from PP13B with simulation results of MIS6 conditions without a Paleo-Agulhas plain silcrete source. The quartzite and quartz frequencies from PDC, PD, and Toolkit size simulations do not statistically match the archaeological frequencies at any model parameter setting during same-day returns from any archaeological site. However, silcrete frequencies from PDC, PD, and Toolkit size simulation do match the archaeological frequencies from PP13B under all settings of PDC, PD, and Toolkit size.

As with the MIS5 results, this shows that changing the model parameters during MIS6 conditions without a Paleo-Agulhas plain silcrete source does not lead to model outcomes that match the archaeological frequencies overall. There is no ranking match (**Supplementary Table B92**).

MIS6 conditions with a Paleo-Agulhas plain silcrete source

When considering MIS6 conditions when a Paleo-Agulhas plain silcrete source is present, all the raw material frequencies from PDC, PD, and Toolkit size simulations do not statistically match the archaeological frequencies from PP13B at any model parameter setting during same-day returns (**Supplementary Figure A10** and

Supplementary Tables B93-B95). There is also no ranking match (**Supplementary Table B96**).

Overall, the results of all simulations when Pinnacle Point is an exclusive locality under all five model conditions show that changing how conservative a forager is with raw material discard on the landscape or at the campsite, or changing the size of the toolkit do not result in a raw material frequency model output that matches the archaeological frequencies. Again, it is important to note that only same-day returns were considered. In the following section, Pinnacle Point will be only one of three localities that the forager can access.

Move to closest locality simulations

MIS4 conditions without a Paleo-Agulhas plain silcrete source

Supplementary Figure A11 and **Supplementary Table B97-B99** compare the MIS4 archaeological raw material frequencies from PP5-6 with simulation results of MIS4 conditions without a Paleo-Agulhas plain silcrete source. The frequencies resulting from same-day returns for any of the raw materials do not statistically match the archaeological frequencies under any parameter setting of ProbDiscardCamp (PDC), ProbDiscard (PD), or Toolkit size. The results of all settings for all three model-parameters predicts that quartz should be the most frequent material, while the archaeology shows that quartz is the least frequent raw material. There is no ranking match (**Supplementary Table B100**).

MIS4 conditions with a Paleo-Agulhas plain silcrete source: When considering MIS4 conditions when a Paleo-Agulhas plain silcrete source is present, the quartzite and quartz frequencies from PDC, PD, and Toolkit size simulations do not statistically match the archaeological frequencies at any model parameter setting during same-day returns (**Supplementary Figure A12** and **Supplementary Tables B101-B103)**. However, silcrete frequencies from PDC, PD, and Toolkit size simulation do match the archaeological frequencies during PDC=0.001, PD=0.1, and Toolkit sizes 100, 75, 50, and 10 model parameters settings (**Supplementary Figure A12**, and **Supplementary Tables B101-B103**). Similar to simulations when Pinnacle Point is the exclusive locality to return too, when the forager is more conservative compared to the base setting (0.02) with its discard of material at any locality, the frequency of silcrete statistically matches the archaeological frequency. While under all other model parameter settings, the model predicts a silcrete frequency that is lower than the archaeological frequency. The result of the simulations of the probability of discard on the landscape (PD) model parameter show that when the agent is being more conservative with discard on the landscape compared to the base-setting (0.02) the frequency of silcrete matches the archaeological frequency, while under a lower PD setting (0.001) the model predicts a lower silcrete frequency than observed archaeologically. Under higher PD settings than 0.01, the model predicts higher silcrete frequencies that are higher than the archaeological frequency. The simulations of the toolkit size parameter show that frequency of silcrete matches the archaeological frequency even when you lower the toolkit size to half and even a tenth of the original size. Only when you have a toolkit size of five does the model predict a silcrete frequency that is higher than the archaeological frequency.

Considering all this, it is important to note that quartzite and quartz frequencies do not match the archaeological frequency at any time, which means that changing the model parameters during MIS4 conditions with a Paleo-Agulhas plain silcrete source does not lead to model outcomes that match the archaeological frequencies overall. There is no ranking match (**Supplementary Table B104**).

MIS5 conditions: During MIS5 conditions, the quartzite and quartz frequencies from PDC, PD, and Toolkit size simulations do not statistically match the archaeological frequencies at any model parameter setting during same-day returns from any archaeological site (**Supplementary Figure A13** and **Supplementary Tables B105-B107)**. However, silcrete frequencies from PDC, PD, and Toolkit size simulation do match the archaeological frequencies from PP13B under all settings of PDC, PD, and Toolkit size (**Supplementary Figure A13**, and **Supplementary Tables B105-B107**).

Again, considering all this, it is important to note that quartzite and quartz frequencies do not match the archaeological frequency at any time, which means that changing the model parameters during MIS5 conditions does not lead to model outcomes that match the archaeological frequencies overall. There is no ranking match (**Supplementary Table B108**).

MIS6 conditions without a Paleo-Agulhas plain silcrete source

Supplementary Figure A14 and **Supplementary Tables B109-B111** compare the MIS6 archaeological raw material frequencies from PP13B with simulation results of MIS6 conditions without a Paleo-Agulhas plain silcrete source. The quartzite and quartz

frequencies from PDC, PD, and Toolkit size simulations do not statistically match the archaeological frequencies at any model parameter setting during same-day returns from any archaeological site. However, silcrete frequencies from PDC, PD, and Toolkit size simulation do match the archaeological frequencies from PP13B under all settings of PDC, PD, and Toolkit size.

As with the MIS5 conditions results, changing the model parameters during MIS6 conditions without a Paleo-Agulhas plain silcrete source do not lead to model outcomes that match the archaeological frequencies overall. There is no ranking match (**Supplementary Table B112**).

MIS6 conditions with a Paleo-Agulhas plain silcrete source

When considering MIS6 conditions when a Paleo-Agulhas plain silcrete source is present, all the raw material frequencies from PDC, PD, and Toolkit size simulations do not statistically match the archaeological frequencies from PP13B at any model parameter setting during same-day returns (**Supplementary Figure A15** and **Supplementary Tables B113-B115**). There is no ranking match (**Supplementary Table B116**).

Overall, what the results of all simulations when Pinnacle Point is only one of three localities available to the forager under all five model conditions suggest is that changing how conservative a forager is with raw material discard on the landscape or at the campsite, or changing the size of the toolkit does not result in a raw material frequency model output that matches the archaeological frequencies. Again, it is important to note that only same-day returns were considered.

Taken together, both the simulations that treat Pinnacle Point as an exclusive locality and the simulations where Pinnacle Point is only one of three available localities show that altering how conservative the forager is and how large the toolkit of the forager is during same-day returns do not change the raw material frequency outcomes in such a way to match up with the archaeological frequencies. Further, this suggests that the H_1 evaluation using both simple same-day returns and OFAT1 results presented above is robust.

Given the results of OFAT2 and OFAT3, the initial evaluation of H_1 is robust but questions remain about how the model outcomes respond when the assumption about the base-settings of PDC, PD, and Toolkit size are all changed at once. Will the model outcomes change and match the archaeological frequencies when the model parameters in question are changed to reflect foraging behaviors that are based on ethnographic observations and archaeological data?

OFAT round 4 – Changing toolkit size, raw material consumption and discard strategy simultaneously

In the final and fourth round of the OFAT (OFAT4) as noted above, three different scenarios of hunter-gatherer technological behavior are examined for their effect on the raw material frequency at Pinnacle Point: expedient, site caching, and conservative behaviors.

Expediency as a technological strategy refers to "minimized technological effort under conditions where time and place of use are highly predictable" (Nelson 1991: 64). This type of behavior is linked to scenarios where the forager has decreased its residential

mobility, become more sedentary making less frequent moves (Parry and Kelly 1987, Riel-Salvatore and Barton 2004). Nelson (1991: 64) noted that expedient technological behavior relies on at least three conditions: 1) planning of stockpiling or caching of raw materials, or anticipated undertaking of activities where the raw materials are located (Bamforth 1986, Parry and Kelly 1987); 2) time available to manufacture tools as part of the activity of their use, which indicates no time stress (Torrence 1983); 3) increased occupations or regular reuse of the place where raw material are available in order to take advantage of the stockpile or cache (Parry and Kelly 1987).

Site caching or stockpiling technological behavior refers to the act of storing raw materials at a planned place in anticipation of future use (Nelson 1991). This type of behavior is linked to expedient behavior scenarios where there are often visited localities that functioned as home bases where stone is cached for future use or provisioned to multiple people (Kuhn 1992, Nelson 1991).

A conservative or curated technological strategy refers to the "caring for tools and toolkits that can include advanced manufacture, transport, and reshaping" (Nelson 1991: 62). This type of behavior is linked to situations where the forager has increased its residential mobility, moving camp often, or where there is a need to provision individuals with gear that serves as a hedge against a variety of eventualities such as lack of raw materials, time, or facilities for repair at the time and place of use (Kuhn 1992, 1991, Nelson 1991, Parry and Kelly 1987, Riel-Salvatore and Barton 2004).

These changes to every model parameters simultaneously were again both considered when Pinnacle Point is an exclusive locality and when Pinnacle Point is one of three localities that the forager can return too. Again, this allows for evaluating

whether the introduction of a more residential mobility strategy and a change in the foraging pattern with more possible localities open to the forager changes the raw material frequency outcomes from the model. However, compared to OFAT3 where only same-day returns were considered, here different values of movement budget (TT=totticks) were simulated. This allows for simulations of what happens when the forager can move freely across the landscape for extended periods of time and either always return to Pinnacle Point when it is treated as an exclusive campsite or by chance returning to one of three localities only depending on the proximity to any given locality at the end of a foraging bout.

Return to starting locality simulations

MIS4 conditions without a Paleo-Agulhas plain silcrete source: **Figure 96** and **Supplementary Tables B117-B119** compare the MIS4 archaeological raw material frequencies from PP5-6 with simulation results of MIS4 conditions without a Paleo-Agulhas plain silcrete source. The quartzite frequency resulting from conservative behavior simulations statistically match the archaeological frequencies under TT=1000, TT=1500, and TT=2000 movement budgets, while quartz and silcrete frequencies never match the archaeological frequencies under any movement budget.

When considering expedient behavior, the quartz frequency statistically matches the archaeological quartz frequency under TT=1000, TT=1500, and TT=2000 movement budgets. Quartzite and silcrete frequencies never match the archaeological frequencies under any movement budget. Finally, when considering the site caching behavior, none of the raw material frequencies match the archaeological frequencies under any

movement budget. There is also no ranking match for any behavior during any movement budget (**Supplementary Table B120**).

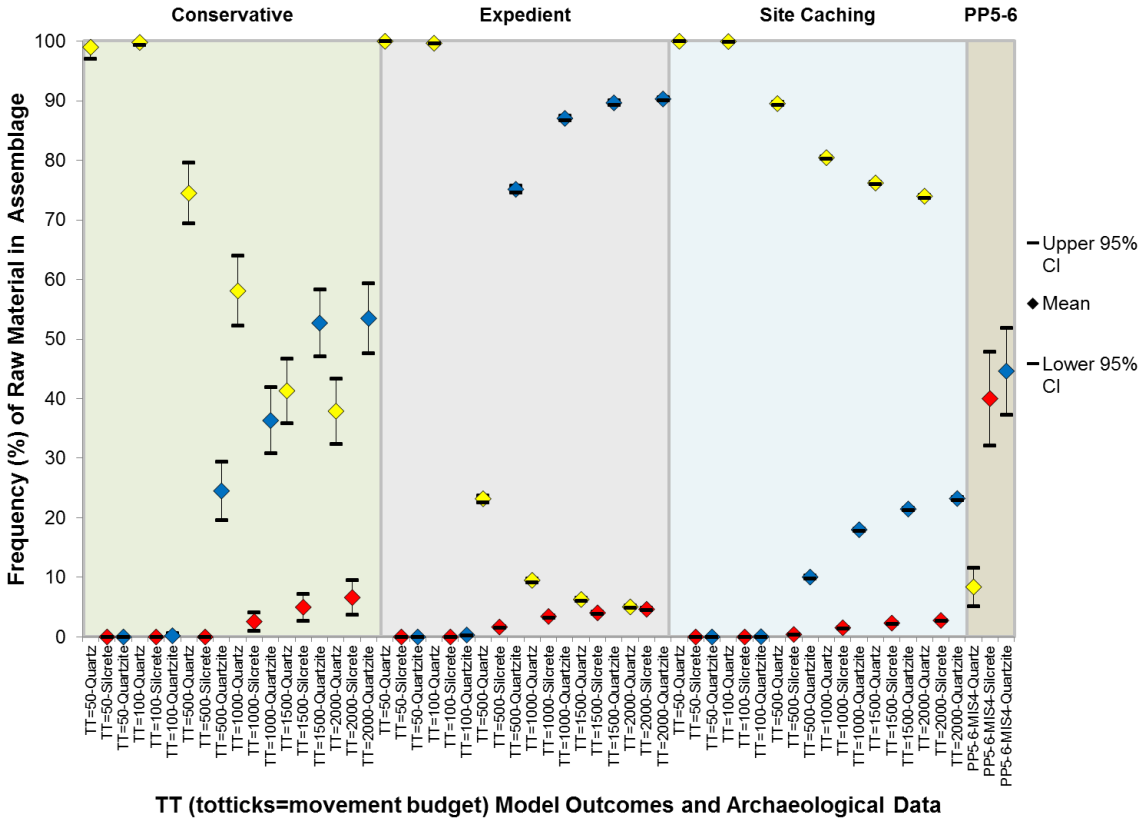

Figure 96. Comparison between OFAT4 outcomes using different movement budgets (TT values) for expedient, conservative, and site caching behaviors during MIS4 model conditions without a Paleo-Agulhas plain silcrete source where the agent returns to the starting locality (PP) and bootstrapped MIS4 archaeological raw material frequency data from PP5-6. Plot shows the mean and the upper and lower 95% confidence intervals for the raw materials deposited at the both the simulated PP locality and at PP5-6.

MIS4 conditions with a Paleo-Agulhas plain silcrete source

When considering MIS4 conditions when a Paleo-Agulhas plain silcrete source is present, the quartzite frequency resulting from conservative behavior simulations statistically match the archaeological frequencies under a TT=2000 movement budget, while the quartz frequency never matches the archaeological quartz frequencies under any movement budget. However, the silcrete frequency statistically matches the

archaeological frequency under all movement budgets (**Figure 97** and **Supplementary Tables B121-B123**).

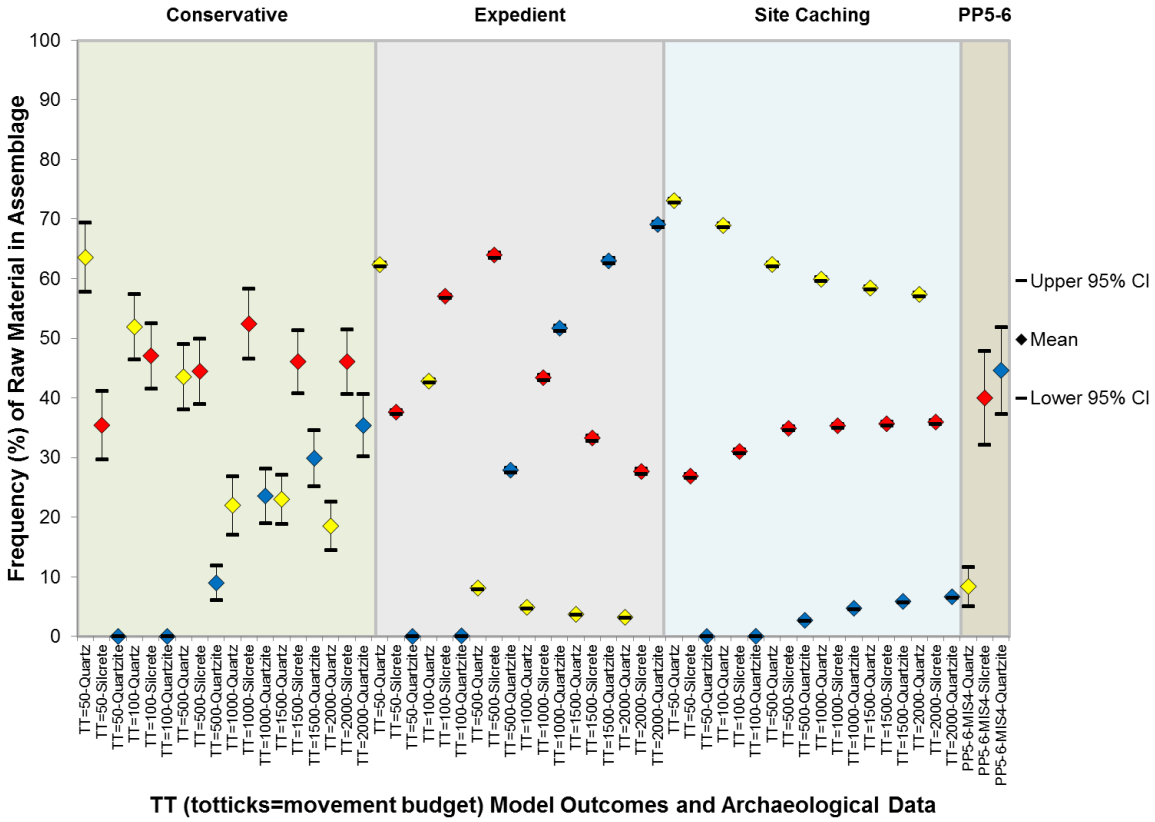

Figure 97. Comparison between OFAT4 outcomes using different movement budgets (TT values) for expedient, conservative, and site caching behaviors during MIS4 model conditions with a Paleo-Agulhas plain silcrete source where the agent returns to the starting locality (PP) and bootstrapped MIS4 archaeological raw material frequency data from PP5-6. Plot shows the mean and the upper and lower 95% confidence intervals for the raw materials deposited at the both the simulated PP locality and at PP5-6.

When considering expedient behavior, the quartzite frequency statistically matches the archaeological quartzite frequency under a TT=1000 movement budget, while the quartz frequency matches the archaeological frequency under a TT=500 movement budget. The silcrete frequency statistically matches the archaeological frequency under TT=50, TT=1000, TT=1500 movement budgets. The simulation of site caching behavior shows that both quartzite and quartz frequencies never matches the

archaeological frequencies under any movement budget, while the silcrete frequency matches the archaeological frequency under TT=500, TT=1000, TT=1500, and TT=2000 movement budgets. Taken together, the results of simulating all three foraging behaviors it is important to note that not at any time do all three materials match the archaeological frequencies under the same movement budget. There also is no ranking match for any behavior during any movement budget (**Supplementary Table B124**).

MIS5 conditions

During MIS5 conditions, the quartz frequency resulting from simulations of conservative behaviors never statistically match the archaeological frequencies from any of the archaeological sites. The silcrete frequencies from TT=50, TT=100, and TT=500 movement budget match the archaeological frequency from PP13B, while the silcrete frequency from a TT=1000 movement budget matches the archaeological frequency from the total MIS5 aggregate. Additionally, the silcrete frequency from TT=1500 and TT=2000 movement budgets matches the archaeological frequencies from PP5-6 and the total MIS5 aggregate (**Figure 98** and **Supplementary Tables B125-B127**).

When considering expedient behavior, the quartzite and quartz frequencies never statistically match the archaeological frequencies under any movement budget. The silcrete frequencies from TT=50 and TT=100 movement budgets statistically match the archaeological frequency from PP13B, the frequency from TT=1000 matches the archaeological frequency from the total MIS5 aggregate, while the frequency from TT=1500 matches the archaeological frequency from PP5-6. The simulation of site caching behavior shows that both quartzite and quartz frequencies never matches the

archaeological frequencies under any movement budget, while the silcrete frequencies from TT=50, TT=100, TT=500, and TT=1000 matches the archaeological frequency from PP13B.

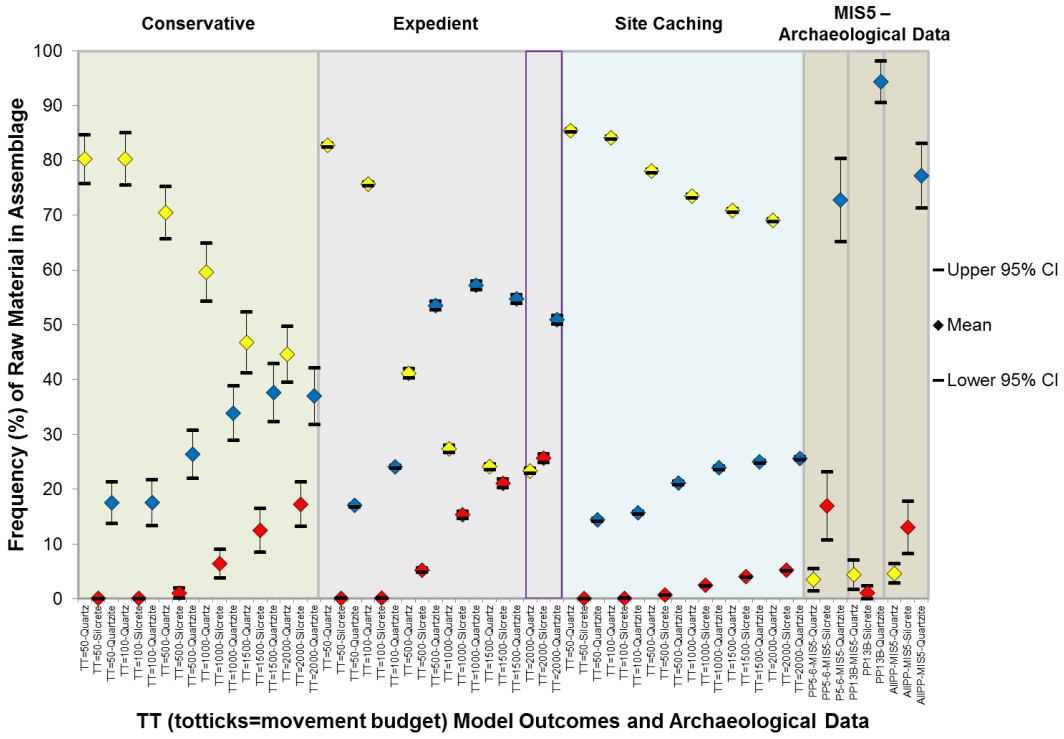

Figure 98. Comparison between OFAT4 outcomes using different movement budgets (TT values) for expedient, conservative, and site caching behaviors during MIS5 model conditions where the agent returns to the starting locality (PP) and bootstrapped MIS5 archaeological raw material frequency data from PP5-6, PP13B, and all MIS5 assemblages from the PP sequence including PP5-6, PP13B, PP9B and PP9C. Plot shows the mean and the upper and lower 95% confidence intervals for the raw materials deposited at the both the simulated PP locality and at PP5-6, PP9B, PP9C, and PP13B. Purple bar indicates a ranking match.

Again, considering all this, it is important to note that the results of simulating all three foraging behaviors show that not at any time do all three materials match the archaeological frequencies under the same movement budget, which means that changing

the foraging behavior during MIS5 conditions does not lead to model outcomes that match the archaeological frequencies overall.

There is, however, a ranking match between expedient behavior simulations using a movement budget of TT=2000 and MIS5 archaeological frequencies from PP5-6 and the total MIS5 aggregate (**Supplementary Table B128**). A purple bar in **Figure 98** indicates the ranking match. However, the quartzite model frequency at this movement budget is 51% of the assemblage while the archaeological quartzite frequency is 73% of the assemblage at PP5-6 and 77% of the assemblage in the total MIS5 aggregate. This is not a good fit. Additionally, the model quartz frequency is 23% of the assemblage while the archaeological quartz frequency is 3.5% of the assemblage at PP5-6 and 5% of the assemblage in the total MIS5 aggregate.

MIS6 conditions without a Paleo-Agulhas plain silcrete source

Figure 99 and **Supplementary Tables B129-B131** compare the MIS6 archaeological raw material frequencies from PP13B with simulation results of MIS6 conditions without a Paleo-Agulhas plain silcrete source. The quartzite and quartz frequencies resulting from conservative behavior simulations never statistically match the archaeological frequency, while the silcrete frequencies from all movement budgets match the archaeological frequency from PP13B.

When considering expedient behavior, the quartz frequency statistically matches the archaeological quartz frequency under TT=1000, TT=1500, and TT=2000 movement budgets. Similarly, the quartzite frequencies from TT=500, TT=1000, TT=1500 and TT=2000 movement budgets statistically match the archaeological frequency from

PP13B. Additionally, the silcrete frequencies from TT=50, TT=100, TT=500, and TT=1000 movement budget match the archaeological frequency from PP13B. The simulation of expedient behavior during MIS6 conditions without a Paleo-Agulhas plain silcrete source shows that during a movement budget of TT=1000 (oranger bar in **Figure 99** indicates frequency match) all three of the raw material frequencies match with their respective raw material frequencies at PP13B (**Figure 99** and **Supplementary Tables B129-B131**).

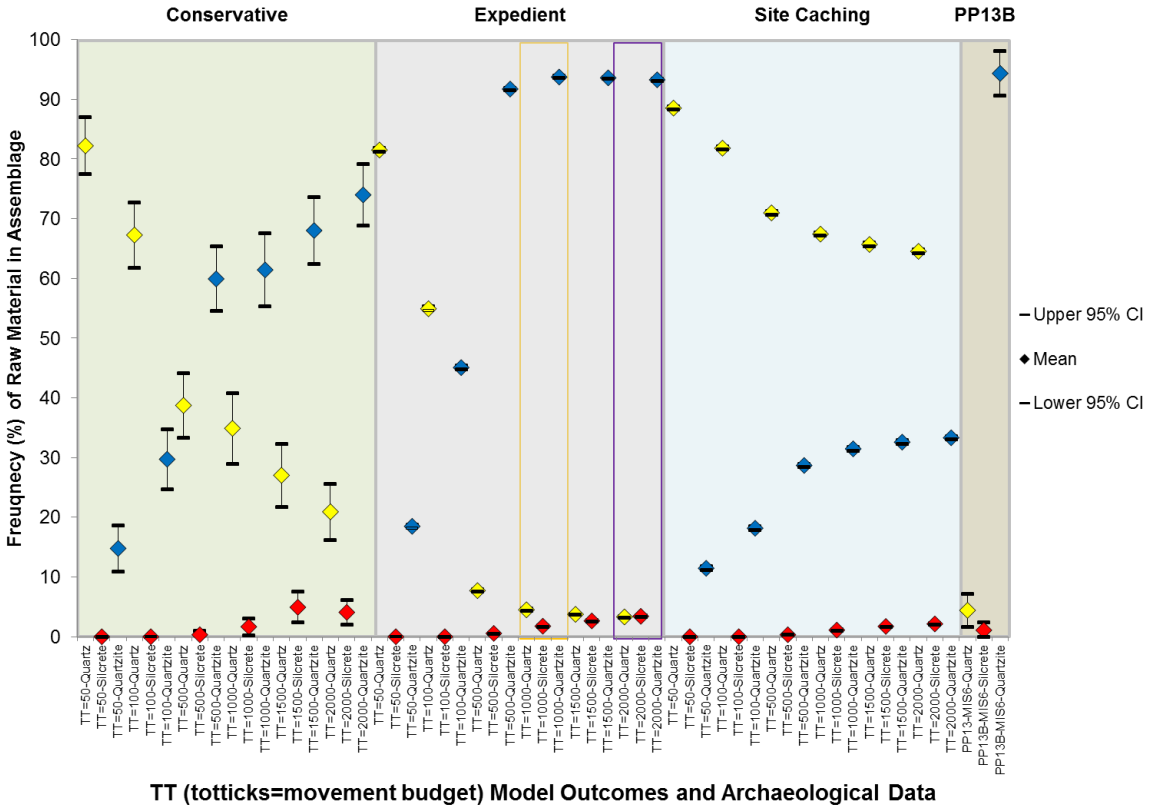

Figure 99. Comparison between OFAT4 modeling outcomes using different movement budgets (TT values) for expedient, conservative, and site caching behaviors during MIS6 model conditions without a Paleo-Agulhas plain silcrete source where the agent returns to the starting locality (Pinnacle Point) and bootstrapped MIS6 archaeological raw material frequency data from PP13B. Plot shows the mean and the upper and lower 95% confidence intervals for the raw materials deposited at both the simulated Pinnacle Point locality and at PP13B. Orange bar indicates frequency match; Purple bar indicates a ranking match.

Quartzite and quartz frequencies never match the archaeological frequencies under any movement budget when considering site caching behavior, while the silcrete frequencies from all movement budgets do match the archaeological frequency from PP13B.

The simulations of conservative and site caching behavior showed no overall match between model frequencies and archaeological frequencies. However, the simulations of expedient behavior provide a statistical match between model and archaeological frequencies when the movement budget is set to TT=1000. Assuming a leisurely walking pace of 2.5 km/hr (Binford, 2001) and a daily foraging time budget of 8 hours, a TT=1000 movement budget suggests a total foraging distance of 200km over the course of 10 foraging days before returning to Pinnacle Point. This result supports H_1 and suggests that opportunistic acquisition explains the raw material pattern during MIS6 if one does not assume that there is a silcrete source on the Paleo-Agulhas plain. Further, it suggests that the raw material pattern seen during MIS6 is the result of expedient behavior. The frequency match result is supported by a ranking match between expedient behavior using a movement budget of TT=2000 and MIS6 archaeological frequencies from PP13B (**Supplementary Table B132**). A purple bar in **Figure 99** indicates the ranking match. This ranking is a good fit. This is because the model quartzite frequency is 93.3% of the assemblage while the archaeological quartzite frequency is 94.3% of the MIS6 assemblage at PP13B. The model quartz frequency is 3.3% of the assemblage while the archaeological quartz frequency is 4.4% of the assemblage. Finally, the model silcrete frequency is 4% of the assemblage while the archaeological silcrete frequency is 1.1% of the MIS6 assemblage at PP13B.

MIS6 conditions with a Paleo-Agulhas plain silcrete source

When considering MIS6 conditions when a Paleo-Agulhas plain silcrete source is present, none of the raw material frequencies statistically match the archaeological frequencies under any movement budget (**Figure 100** and **Supplementary Tables B133-B135**).

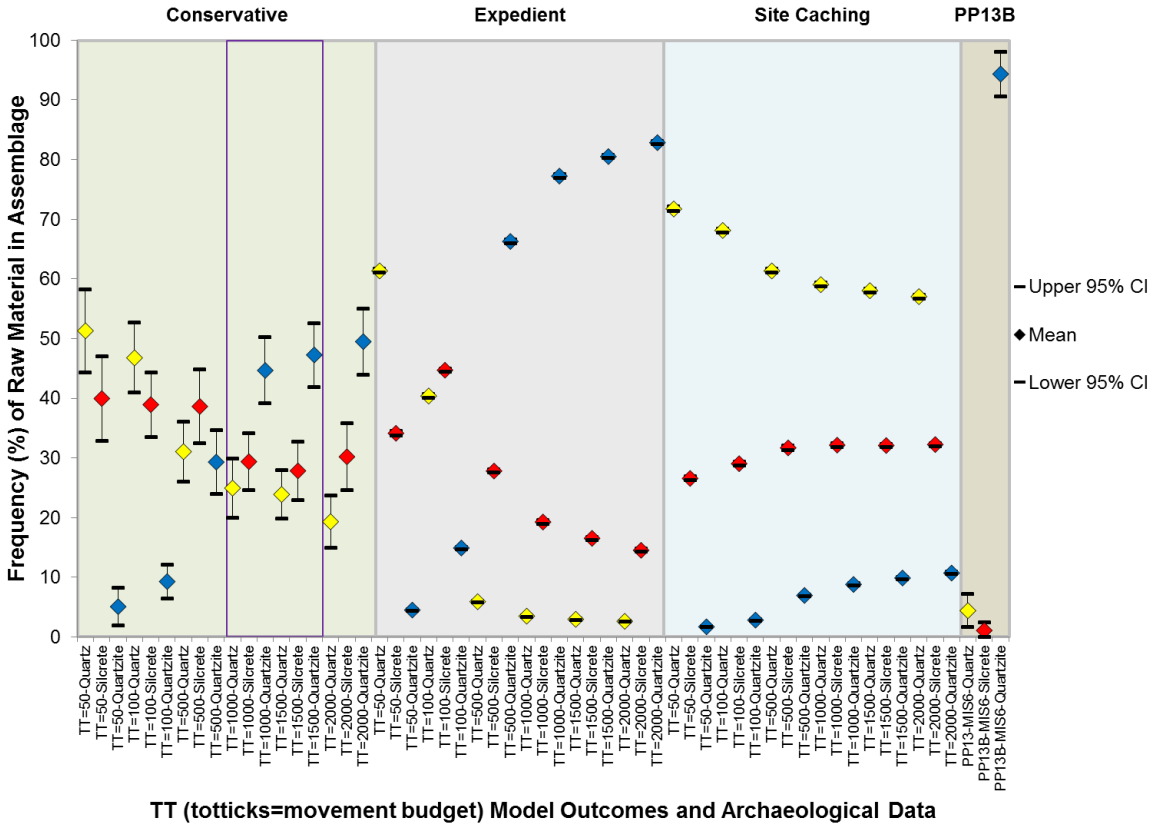

Figure 100. Comparison between OFAT4 outcomes using different movement budgets (TT values) for expedient, conservative, and site caching behaviors during MIS6 model conditions with a Paleo-Agulhas plain silcrete source where the agent returns to the starting locality (PP) and bootstrapped MIS6 archaeological raw material frequency data from PP13B. Plot shows the mean and the upper and lower 95% confidence intervals for the raw materials deposited at the both the simulated PP locality and at PP13B. Purple bar indicates a ranking match.

When considering expedient behavior, the quartzite and silcrete frequencies never match the archaeological frequencies from PP13B under any movement budget, while the

quartz frequencies from TT=500, TT=1000, TT=1500, and TT=2000 movement budgets match the archaeological frequency. The silcrete frequency statistically matches the archaeological frequency under TT=50, TT=1000, TT=1500 movement budgets. The simulation of site caching behavior shows that none of the raw material frequencies match the archaeological frequencies from PP13B under any movement budget. Together, the results of simulating all three foraging behaviors show that not at any time do all three materials match the archaeological frequencies under the same movement budget.

However, there is a ranking match between the conservative behavior using a movement budget of TT=1000 and TT=1500 and MIS6 archaeological frequencies from PP13B (**Supplementary Table B136**). A purple bar in **Figure 100** indicates the ranking match. This ranking is not a good fit. This is because the model quartzite frequency is 44.5% to 47% of the assemblage while the archaeological quartzite frequency is 94.3% of the MIS6 assemblage at PP13B. Both quartz and silcrete are overpredicted. The model quartz frequency is between 24-25% of the assemblage while the archaeological quartz frequency is 4.4% of the assemblage. Finally, the model silcrete frequency is between 28-30% of the assemblage while the archaeological silcrete frequency is 1.1% of the assemblage at PP13B.

Overall, what the results of all simulations under all five model-conditions suggest is that simulating different foraging behaviors that are based on ethnographic observations and archaeological data do not produce raw material frequency outputs that match the archaeological frequencies. There is, however, one exception. Simulations of expedient behavior during MIS6 conditions without a Paleo-Agulhas plain silcrete source

using a TT=1000 movement budget do produce a coherent raw material frequency output that matches the archaeological frequencies from PP13B. This result is also backed up by a ranking match between expedient behavior using a movement budget of TT=2000 and MIS6 archaeological frequencies from PP13B. To test whether this result is robust, I present below the results of simulations where Pinnacle Point is just one of three localities when the forager engages in any of the three foraging behaviors.

Move to closest locality simulations

MIS4 conditions without a Paleo-Agulhas plain silcrete source

Figure 101 and **Supplementary Tables B137-B139** compare the MIS4 archaeological raw material frequencies from PP5-6 with simulation results of MIS4 conditions without a Paleo-Agulhas plain silcrete source. The quartzite frequency resulting from conservative behavior simulations statistically match the archaeological frequencies under TT=500, TT=1000, TT=1500, and TT=2000 movement budgets, while quartz frequencies from TT=1500 and TT=2000 movement budgets match the archaeological frequencies. However, the silcrete frequency never matches the archaeological frequency from PP5-6 under any movement budget.

When considering expedient behavior, none of the raw material frequencies statistically matches the archaeological frequencies from PP5-6 under any movement budgets. Finally, when considering the site caching behavior, the quartz and silcrete frequencies never matches the archaeological frequencies under any movement budget, while the quartzite frequency from a TT=1000 movement budget matches the

archaeological frequency from PP5-6. There is also no ranking match for any behavior during any movement budget (**Supplementary Table B140**).

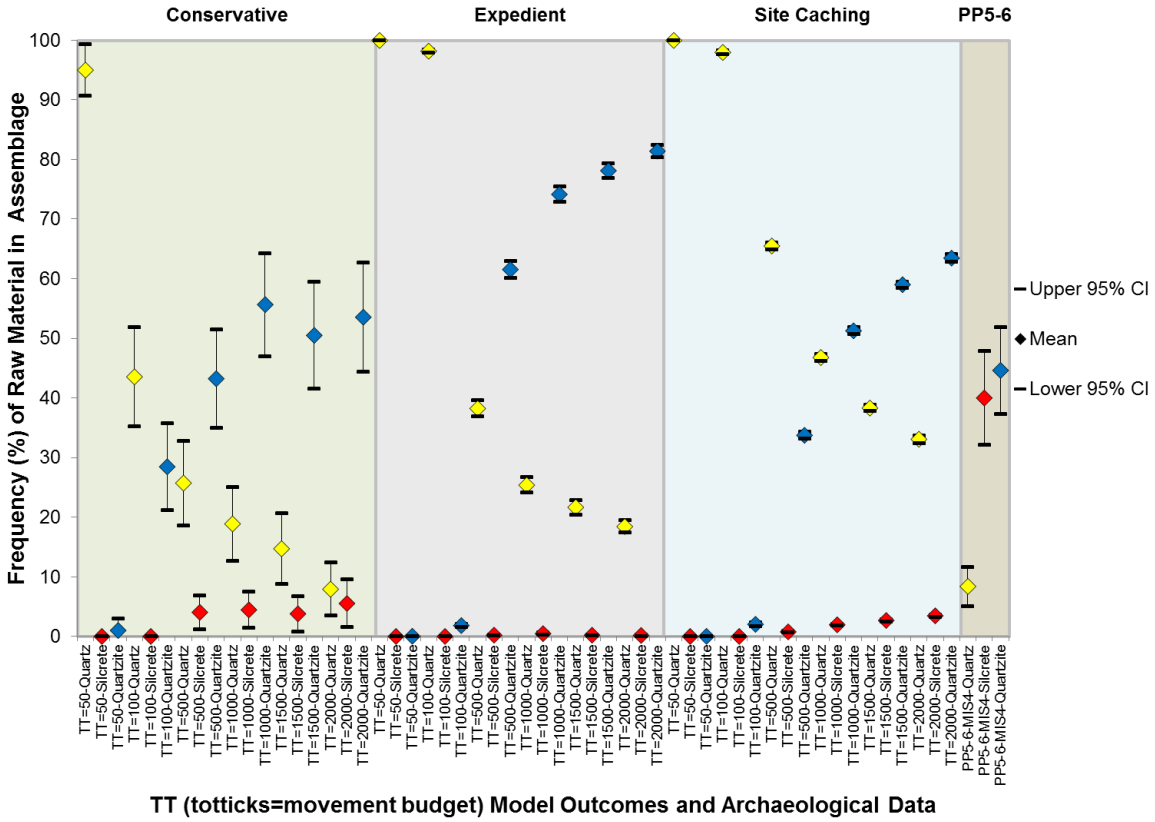

Figure 101. Comparison between OFAT4 outcomes using different movement budgets (TT values) for expedient, conservative, and site caching behaviors during MIS4 model conditions without a Paleo-Agulhas plain silcrete source where the agent moves to the closest locality when the movement budget (totticks) is exhausted and bootstrapped MIS4 archaeological raw material frequency data from PP5-6. Plot shows the mean and the upper and lower 95% confidence intervals for the raw materials deposited at the both the simulated PP locality and at PP5-6.

MIS4 conditions with a Paleo-Agulhas plain silcrete source

During MIS4 conditions when a Paleo-Agulhas plain silcrete source is present, the quartzite and quartz frequencies resulting from conservative behavior simulations statistically match the archaeological frequencies under TT=500, TT=1000, TT1500, and TT=2000 movement budgets, while the silcrete frequency from a TT=50 movement

budget matches the archaeological frequency from PP5-6 (**Figure 102** and **Supplementary Tables B141-B143**). When considering expedient behavior, the quartzite frequency statistically matches the archaeological frequency under a TT=2000 movement budget, while the quartz frequency matches the archaeological frequency from PP5-6 under TT=500, TT=1000, TT=1500, and TT=2000 movement budgets. The silcrete frequency statistically matches the archaeological frequency under a TT=50 movement budget.

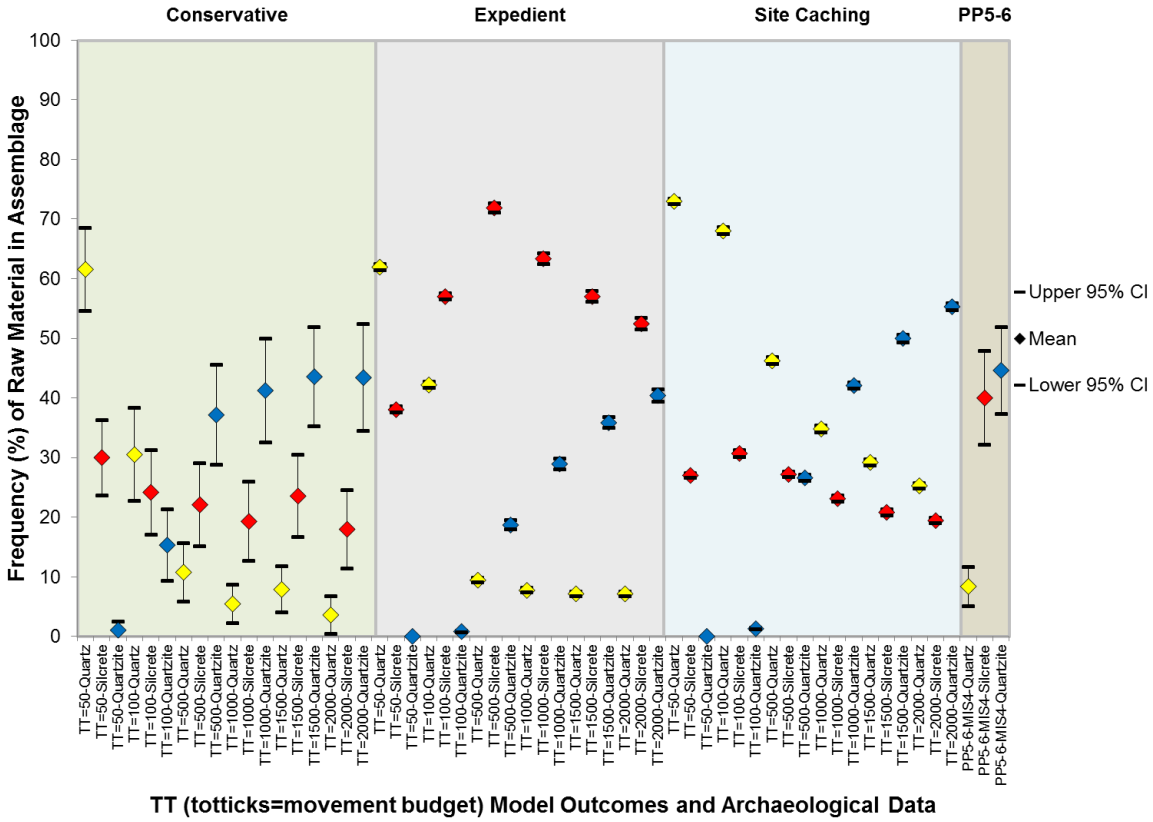

Figure 102. Comparison between OFAT4 outcomes using different movement budgets (TT values) for expedient, conservative, and site caching behaviors during MIS4 model conditions with a Paleo-Agulhas plain silcrete source where the agent moves to the closest locality when the movement budget (totticks) is exhausted and bootstrapped MIS4 archaeological raw material frequency data from PP5-6. Plot shows the mean and the upper and lower 95% confidence intervals for the raw materials deposited at the both the simulated PP locality and at PP5-6.

The simulation of site caching behavior shows that both quartz and silcrete frequencies never match the archaeological frequencies under any movement budget, while the quartzite frequency matches the archaeological frequency under TT=1000 and TT=1500 movement budgets. The results of simulating all three foraging behaviors show that the three materials never match the archaeological frequencies under the same movement budget. Neither, conservative, expedient, or site caching behavior seem to explain raw material frequencies during MIS4 at PP5-6 if a silcrete source is assumed to be present on the Paleo-Agulhas plain. There is also no ranking match for any behavior during any movement budget (**Supplementary Table B144**).

MIS5 conditions

During MIS5 conditions, the quartz and quartzite frequencies resulting from simulations of conservative behaviors never statistically match the archaeological frequencies from any of the archaeological sites under any movement budget. The silcrete frequencies from TT=50 and TT=100 movement budgets match the archaeological frequency from PP13B, while the silcrete frequency from TT=500, TT=1000, TT=1500, and TT=2000 movement budget matches the archaeological frequency from PP5-6 and the total MIS5 aggregate (**Figure 103** and **Supplementary Tables B145-B147)**. When considering expedient behavior, the quartzite and quartz frequencies never statistically match the archaeological frequencies from any site under any movement budget. The silcrete frequencies from every movement budgets statistically match the archaeological frequency from PP13B.

The simulation of site caching behavior shows that both quartzite and quartz frequencies never match the archaeological frequencies from any site under any movement budget. The silcrete frequencies from TT=50 and TT=100 movement budgets match the archaeological frequency from PP13B, while the frequency from TT=1500 and TT=2000 match the archaeological frequency from PP5-6 and the total MIS5 aggregate. Additionally, the silcrete frequency from TT=1000 also matches the archaeological silcrete frequency from the total MIS5 aggregate.

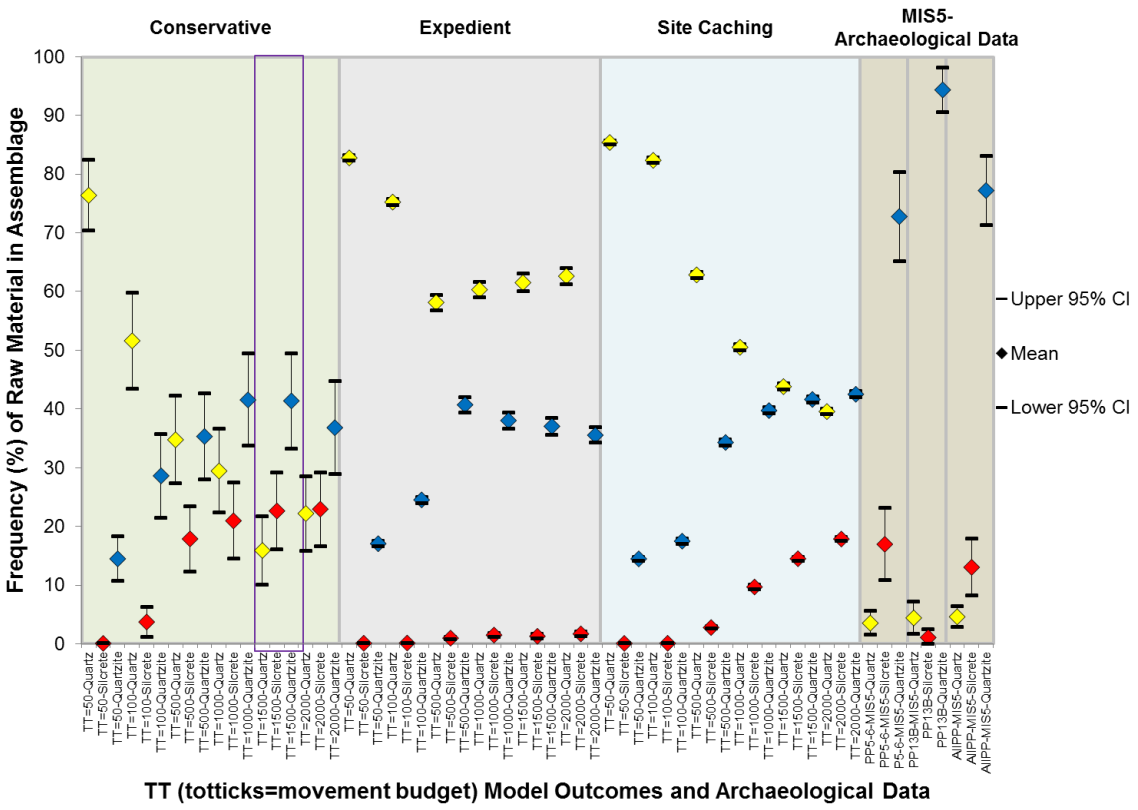

Figure 103. Comparison between OFAT4 outcomes using different movement budgets (TT values) for expedient, conservative, and site caching behaviors during MIS5 model conditions where the agent moves to the closest locality when the movement budget (totticks) is exhausted and bootstrapped MIS5 archaeological raw material frequency data from PP5-6, PP13B, and all MIS5 assemblages from the PP sequence including PP5-6, PP13B, PP9B, and PP9C. Plot shows the mean and the upper and lower 95% confidence intervals for the raw materials deposited at the both the simulated PP locality and at PP5-6, PP9B, PP9C, and PP13B. Purple bar indicates a ranking match.

There is, however, a ranking match between expedient behavior simulations using a movement budget of TT=1500 and MIS5 archaeological frequencies from PP13B (**Supplementary Table B148**). A purple bar in **Figure 103** indicates the ranking match. However, this match is not a good fit because the quartzite model frequency at this movement budget is 41.4% of the assemblage while the archaeological quartzite frequency is 94.3% of the assemblage at PP13B. Additionally, quartz and silcrete frequencies are overpredicted. The model quartz frequency is 16% of the assemblage while the archaeological quartz frequency is 4.4% of the assemblage at PP13B. The model silcrete frequency is 23% of the assemblage while the archaeological silcrete frequency is 1.1% of the MIS5 assemblage at PP13B.

Again, similar to simulations when Pinnacle Point is treated as an exclusive locality, the results of simulating all three foraging behaviors show that all three materials never match the archaeological frequencies under the same movement budget, which means that changing the foraging behavior during MIS5 conditions does not lead to model outcomes that match the archaeological frequencies overall.

MIS6 conditions without a Paleo-Agulhas plain silcrete source

Figure 104 and **Supplementary Table B149-B51** compare the MIS6 archaeological raw material frequencies from PP13B with simulation results of MIS6 conditions without a Paleo-Agulhas plain silcrete source. The quartzite frequencies resulting from conservative behavior simulations never statistically match the archaeological frequency from PP13B under any movement budget, while the silcrete frequencies from all

movement budgets match the archaeological frequency from PP13B. The quartz frequencies from TT=1000, TT=1500, and TT=2000 movement budgets match the archaeological frequency from PP13B.

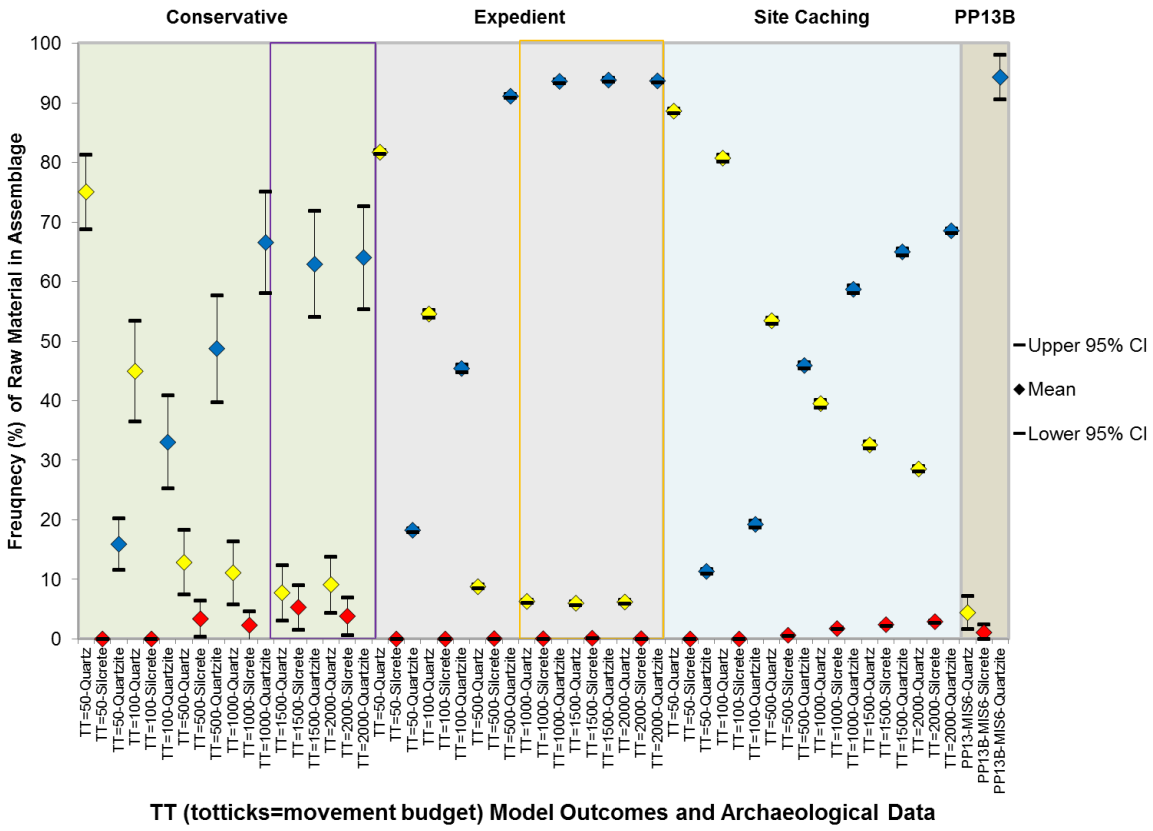

Figure 104. Comparison between model OFAT4 modeling outcomes using different movement budgets (TT values) for expedient, conservative, and site caching behaviors site during MIS6 model conditions without a Paleo-Agulhas plain silcrete source where the agent moves to the closest locality when the movement budget (totticks) is exhausted and bootstrapped MIS6 archaeological raw material frequency data from PP13B. Plot shows the mean and the upper and lower 95% confidence intervals for the raw materials deposited at the both the simulated Pinnacle Point locality and at PP5-6. Orange bar indicates frequency match; Purple bar indicates a ranking match.

When considering expedient behavior, the quartz frequency statistically matches the archaeological quartz frequency under TT=1000, TT=1500, and TT=2000 movement budgets, which is the same as simulations where Pinnacle Point is an exclusive locality. Similarly, the quartzite frequencies from TT=500, TT=1000, TT=1500 and TT=2000

movement budgets statistically match the archaeological frequency from PP13B. Additionally, the silcrete frequencies from all movement budgets match the archaeological frequency from PP13B. The simulation of expedient behavior during MIS6 conditions without a Paleo-Agulhas plain silcrete source when Pinnacle Point is only one of three localities accessible to the forager show that with movement budgets between TT=1000 and TT=2000 all three of the raw material frequencies match with their respective raw material frequencies at PP13B (**Figure 104** and **Supplementary Tables B149-B151**). Orange bar in **Figure 104** indicates the frequency matches.

Finally, when considering the site caching behavior, the quartzite and quartz frequencies never match the archaeological frequencies under any movement budget, while the silcrete frequencies from TT=50, TT=100, TT=500, TT=1000, and TT=1500 movement budgets do match the archaeological frequency from PP13B.

The simulations of conservative and site caching behavior showed no overall match between model frequencies and archaeological frequencies. However, the simulations of expedient behavior when Pinnacle Point is only one of three localities accessible to the forager provide a statistical match between model and archaeological frequencies when the movement budget is set to between TT=1000 and TT=200. Assuming a leisurely walking pace of 2.5 km/hr (Binford, 2001) and a daily foraging time budget of 8 hours, a TT=1000 movement budget indicates a total foraging distance of 200km over the course of 10 foraging days before returning to one of three localities. A movement budget set to TT=2000 indicates a total foraging distance of 400km over the course of 20 foraging days before returning to any of the sites. This result strengthens the outcome from simulations where Pinnacle Point is the exclusive locality. Both results

support H_1 and suggest that scenarios, where the forager are moving widely on the landscape and only return to either one of three localities between 10 to 20 days, explain the raw material pattern during MIS6. This type of pattern can suggest movement between the interior and the coast, perhaps intersecting the coast to procure coastal resources at spring tides (Marean 2014).

However, the ranking procedure produces a different result because there is a ranking match between conservative behavior using a movement budget of TT=1500 and TT=2000 and MIS6 archaeological frequencies from PP13B (**Supplementary Table B152**). A purple bar in **Figure 104** indicates the ranking match. This ranking is not a good fit. This is because the model quartzite frequency is 63% to 64% of the model assemblage while the archaeological quartzite frequency is 94.3% of the MIS6 assemblage at PP13B. Both quartz and silcrete are overpredicted. The model quartz frequency is 8% to 9% of the assemblage while the archaeological quartz frequency is 4.4% of the assemblage. Finally, the model silcrete frequency is 3.8% to 5.3% of the assemblage while the archaeological silcrete frequency is 1.1% of the assemblage at PP13B.

MIS6 conditions with a Paleo-Agulhas plain silcrete source

When considering MIS6 conditions when a Paleo-Agulhas plain silcrete source is present, the silcrete and quartzite frequencies never statistically match the archaeological frequencies from PP13B under any movement budget. The quartz frequencies from TT=500, TT=1000, TT=1500, TT=2000 movement budgets do match the archaeological frequency from PP13B (**Figure 105** and **Supplementary Tables B153-B155**). When

considering expedient behavior, again the silcrete and quartzite frequencies never match the archaeological frequencies from PP13B under any movement budget, while the quartz frequencies from TT=500, TT=1000, TT=1500, and TT=2000 movement budgets match the archaeological frequency from PP13B.

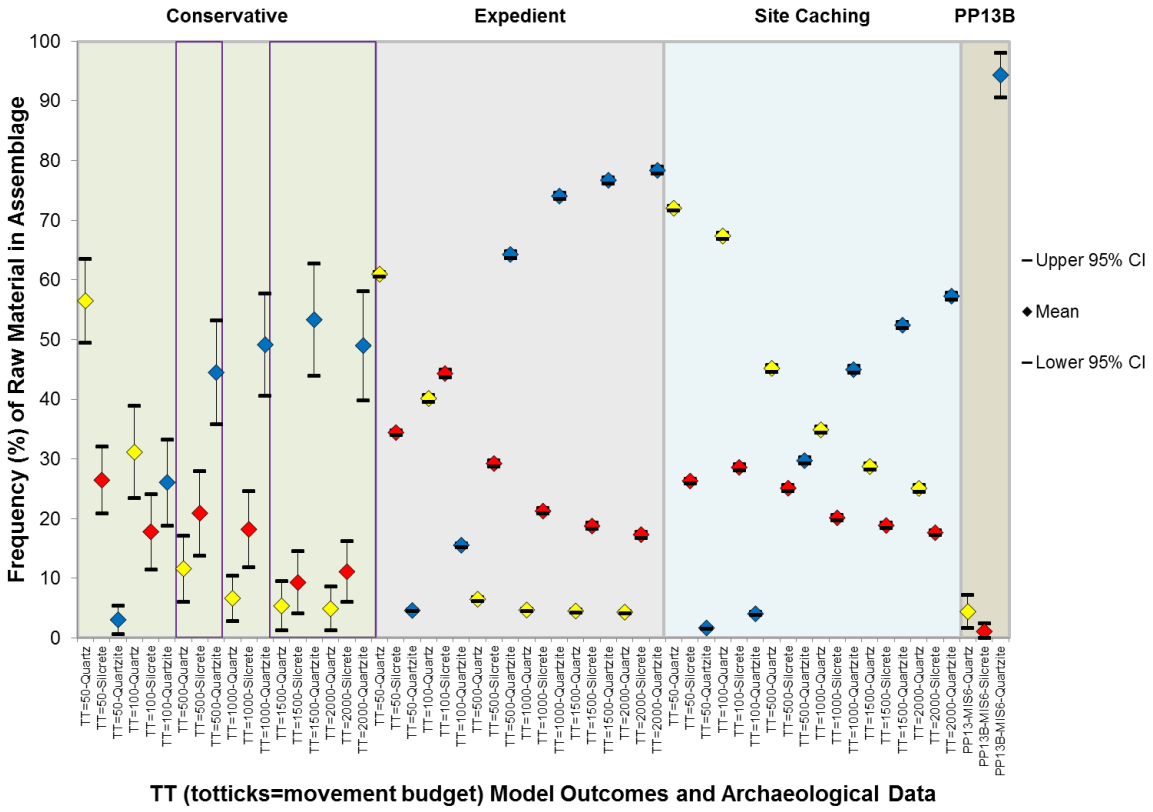

Figure 105. Comparison between OFAT4 outcomes using different movement budgets (TT values) for expedient, conservative, and site caching behaviors during MIS6 model conditions with a Paleo-Agulhas plain silcrete source where the agent moves to the closest locality when the movement budget (totticks) is exhausted and bootstrapped MIS6 archaeological raw material frequency data from PP13B. Plot shows the mean and the upper and lower 95% confidence intervals for the raw materials deposited at the both the simulated PP locality and at PP13B. Purple bar indicates a ranking match.

The simulation of site caching behavior shows that none of the raw material frequencies matches the archaeological frequencies from PP13B under any movement budget. Together, the results of simulating all three foraging behaviors show that not at

any time do all three materials match the archaeological frequencies under the same movement budget.

Although there is no positive frequency match there is a ranking match between conservative behavior using a movement budget of TT=1000 and TT=2000 and MIS6 archaeological frequencies from PP13B (**Supplementary Table B156**). The purple bars in **Figure 105** indicate the ranking matches. These ranking matches are not a good fit. This is because the model quartzite frequency is 44.5% to 53% of the model assemblage while the archaeological quartzite frequency is 94.3% of the MIS6 assemblage at PP13B. Additionally, silcrete is overpredicted. The model silcrete frequency is 11% to 21% of the assemblage while the archaeological silcrete frequency is 1.1% of the assemblage at PP13B.

Similar to simulations where Pinnacle Point is the exclusive locality accessible to the forager, what the results of all simulations when Pinnacle Point is one of three localities under all five model-conditions suggest is that simulating different foraging behaviors that are based on ethnographic observations and archaeological data do not produce raw material frequency outputs that match the archaeological frequencies. However, as with the simulations where Pinnacle Point is the exclusive locality, simulations of expedient behavior during MIS6 conditions without a Paleo-Agulhas plain silcrete source using movement budgets between TT=1000 and TT=2000 do produce a coherent raw material frequency output that matches the archaeological frequencies from PP13B. A ranking match result during MIS6 conditions without a Paleo-Agulhas plain silcrete source between expedient behavior and archaeological frequencies from PP13B supports the findings of the frequency match results.

There are several other positive ranking matches during MIS5 and MIS6 conditions. However, except for the ranking match during MIS6 conditions without a Paleo-Agulhas plain silcrete source when Pinnacle Points is the exclusive locality all the other ranking matches is based on raw material frequencies that either overpredicts or underpredicts the raw material frequencies present in the archaeological record. For this reason they are not discussed further in this study but it should be kept in mind.

Given the results of OFAT1, OFAT2, OFAT3, the initial conclusion of the evaluation of H_1 can be modified somewhat. H_1 has support from simulations conducted in OFAT3. Specifically, this pertains to the results from simulations of expedient behavior during simulations when Pinnacle Point is the exclusive locality and simulations when Pinnacle Point is just one of three localities during MIS6 conditions without a Paleo-Agulhas plain silcrete source. The results show that if one assumes that there are no silcrete sources on the Paleo-Agulhas plain during MIS6 the model outcomes statistically match up with the archaeological frequencies from PP13B.

What the results suggest is a mobility strategy and foraging movement that saw the forager utilize the three sites in random fashion but only in 10 to 20 day intervals. The forager would move out on the landscape and would not return to any of the three sites before 10 to 20 days had passed and then the sites would be reoccupied. Because MIS6 is a strong glacial phase where the coastline is on average 42 km away, this means that the coastline was removed from the present location making Pinnacle Point, Cape St. Blaze, and Vleesbaai all inland localities. A movement strategy where these localities where only returned to every 10-20 days can potentially imply movement between the coast and interior or latitudinal movement along the coast and small inward moves to these

localities when the forager found itself randomly close to one of them. A movement system to intercept the coast at particular times is a possibility, perhaps to be close to the coast at spring tides to reap significant coastal resources (Marean 2014). However, what is important to note here is that the forager in the OAM moves randomly in any direction and does not adhere to any particular strategy about where and when to be close to the coast. More precisely, the 10-20 day strategy could also mean movement between the inland localities of the Mossel Bay region and other even more interior-located localities.

Regardless of where the forager moves, the result suggests that when the forager moves across the landscape it did so in an expedient fashion in relation to raw material discard. Expedient behavior is often linked to scenarios where the forager has decreased its residential mobility by making less frequent moves thus becoming more sedentary (Parry and Kelly, 1987; Riel-Salvatore and Barton, 2004). On the face of it, this suggests that the expedient pattern does not hold because the model outcomes only match the archaeological pattern when the forager is allowed a movement budget where it can move very frequently before returning to any of the sites. However, it is not known if that is too frequent and it could be that the modeled behavior during increased movement budgets and the accessibility of three localities do not resemble actual residential mobility and thus instead resembles more restricted residential mobility.

Additionally, there are some requirements that have been proposed that are needed to be met to be able to expediently use and discard raw materials (Nelson (1991). 1) there has to be a plan to stockpile or cache raw materials or at least an anticipation of undertaking activities where raw materials are located (Bamforth, 1986; Parry and Kelly, 1987). 2) There has to be time to manufacture needed tools as a part of the activity of

their use, which implies that there is no time-stress involved with the activity (Torrence, 1983). 3) There have to be increased occupations or regular reuse of the places where raw materials are available in order to take advantage of the stockpile or cache of raw materials (Parry and Kelly, 1987).

The first and second point can be investigated by looking at whether raw material packages at these localities exhibit evidence for more complete or tested raw material packages such as complete cobbles and manuports/hammerstones, lower core-reduction intensity, and minimal retouch and maintenance of tools. All these would indicate that the raw material packages were not reduced, maintained, and used in a conservatory manner and that raw materials were potentially left for future occupations. Only PP13B has an MIS6 record of the three localities in question (see *Chapter 7*).

The MIS6 record from PP13B indicates expedient behavior based on the ratio of retouched pieces to artifact volumetric density. The MIS6 record has a higher artifact volumetric density compared to the MIS5 record but it has a similar frequency of retouched pieces. This suggests a more expedient use of raw materials during MIS6 compared to MIS5. However, the MIS6 record has fewer manuports/hammerstones compared to the overlaying MIS5 record, and the MIS6 artifacts are shorter and narrower than the artifacts from the MIS5 record. Additionally, the MIS6 artifacts have a higher mean cutting edge to mass ratio indicating a more conservative approach to reduction of the raw materials (c.f. Mackay, 2008). Together this suggests that MIS6 record indicates more conservative and later-stage reduction of the available raw materials. Assuming that the raw material packages that were brought into PP13B during MIS5 and MIS6 were of similar sizes this means that raw material packages during MIS6 were more often

reduced compared MIS5 packages and when the packages were reduced the focus was on getting more cutting edge from each raw material package compared to in the MIS5 record. This type of conservative approach to reducing the raw materials most likely resulted in later stages of reduction of the raw material packages, which in turn resulted in the production of stone tools with smaller sizes.

However, questions remain whether this expedient behavior in combination with random walk is realistic in the Mossel Bay region. This goes to the third point where it is argued that there have to be increased occupations and regular reuse of the places where raw materials are available in order to take advantage of the stockpiling. One way to evaluate whether the expedient random walk is realistic is to measure how much time the forager walks around in the landscape without raw material in the landscape. **Figure 106** shows the frequency of time without raw material in the toolkit at different movement budgets when the forager is conducting expedient foraging during MIS6 conditions without a Paleo-Agulhas silcrete source. Under a scenario where Pinnacle Point is the exclusive locality, the forager spends ~48 to ~59 % of the time without raw materials in the toolkit (**Figure 106** and **Table 59**). The number decreases when Pinnacle Point is only one of three localities. Then the forager spends around ~29 to ~56% of the time without raw material in the toolkit (**Figure 106** and **Table 59**). Is it realistic that the forager spends between ~30 to ~60 % of the time it is moving about the landscape without any raw materials in the toolkit?

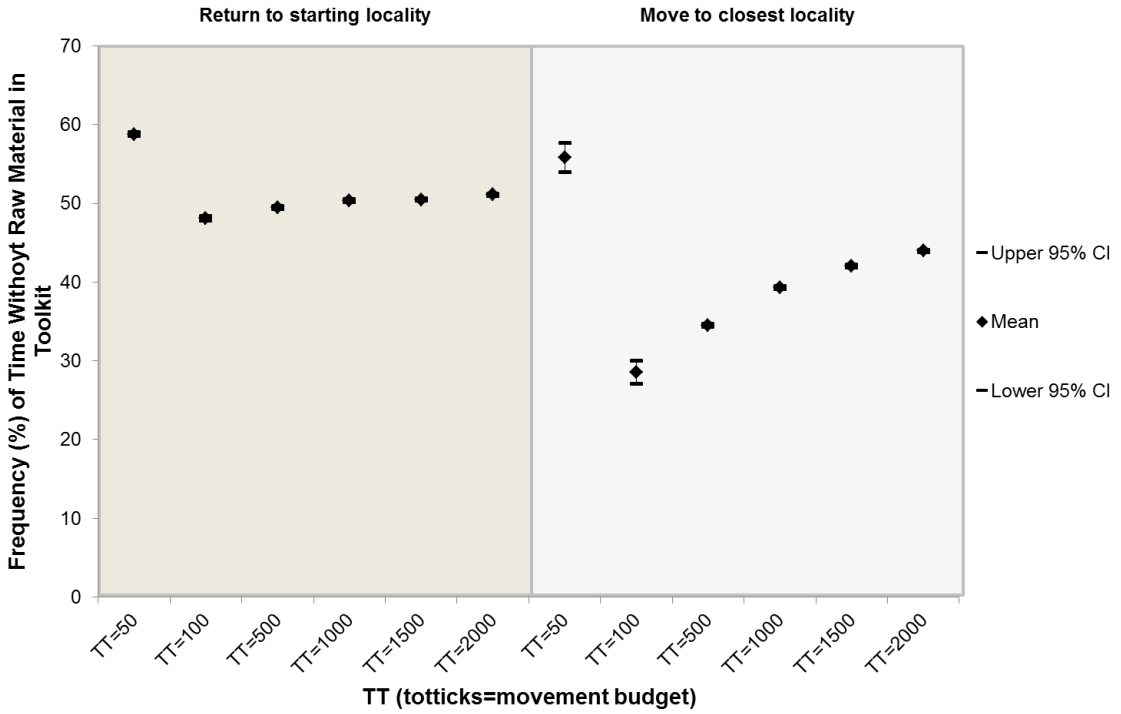

Figure 106. Plot with means and 95% confidence intervals showing the distribution of the frequency of time without raw material in toolkit at different movement budgets (TT=totticks) during MIS6 conditions without a Paleo-Agulhas plain silcrete source. Star with capped whiskers is the mean with the 95% confidence interval (CI).

Table 59. Frequency (%) of time without raw materials in toolkit descriptive statistics during MIS6 conditions without a Paleo-Agulhas plain silcrete source.

	Return to starting locality						Move to closest locality					
	TT=50	TT=100	TT=500	TT=1000	TT=1500	TT=2000	TT=50	TT=100	TT=500	TT=1000	TT=1500	TT=2000
n (number of simulated assemblages)	100	100	100	100	100	100	100	100	100	100	100	100
First Quartile	57.917	47.286	48.734	49.947	49.863	50.574	57.405	23.293	33.827	38.528	41.431	43.331
Min	55.537	44.471	46.062	47.415	48.207	48.792	9.626	9.258	31.719	36.482	39.993	42.174

Median	58.686	47.986	49.359	50.343	50.469	51.078	58.442	29.148	34.477	39.210	41.942	43.924
Mean	58.796	48.079	49.486	50.368	50.486	51.094	55.815	28.541	34.516	39.296	42.067	43.944
Max	62.067	51.541	51.945	52.232	53.287	53.572	62.257	43.461	37.185	41.253	44.162	46.612
Third Quartile	59.665	48.867	50.189	51.089	51.071	51.692	59.575	34.168	35.328	40.229	42.709	44.488
SD	1.338	1.354	1.049	0.986	0.936	0.892	9.360	7.285	1.137	1.041	0.952	0.789
SE	0.134	0.135	0.105	0.099	0.094	0.089	0.936	0.729	0.114	0.104	0.095	0.079
Margin of error (95% CI)	0.262	0.265	0.206	0.193	0.184	0.175	1.835	1.428	0.223	0.204	0.187	0.155
Upper 95% CI	59.059	48.344	49.691	50.562	50.670	51.269	57.649	29.969	34.739	39.499	42.253	44.099
Lower 95% CI	58.534	47.813	49.280	50.175	50.303	50.919	53.980	27.113	34.293	39.092	41.880	43.789

Oestmo, Janssen, and Marean (2016) argued based on their simulations that if the agent does, in fact, return regularly to places where raw materials are cached then it can be realistic to go extended periods without raw materials. To obtain a robust answer here

one needs to investigate whether the MIS6 record from PP13B reflects stockpiling behavior, which allowed the forager to return there to replenish.

OAM Hypothesis 1 evaluation summary

The initial test of whether random walk in regards to raw material sources is a realistic procurement strategy for stone raw materials in the Mossel Bay region suggests that is realistic with less than 1% of the time without material in the toolkit. However, the result of simulations using the base settings of assumptions suggests that the OAM does not explain the raw material pattern at Pinnacle Point. Further, the results of the OFAT2 and 3 show that when Pinnacle Point is just one of three accessible localities, or that if single model assumptions such as probability of discard on the landscape or at the locality, or the size of the toolkit are altered, the model outcomes do not match up with the archaeological raw material frequencies. This mostly holds true in OFAT4 where three different foraging behaviors based on ethnographic observations and archaeological data produce model outcomes that do not match the archaeological frequencies. However, simulations of expedient behavior during MIS6 conditions without a Paleo-Agulhas plain silcrete source regardless of whether Pinnacle Point is an exclusive site or one of three produce raw material frequencies that statistically match the archaeological frequencies. A ranking match during MIS6 conditions without a Paleo-Agulhas plain silcrete source between expedient behavior using a movement budget of TT=2000 and archaeological frequencies from PP13B strengthens the frequency match outcome.

However, it can be argued that expedient behavior in the Mossel Bay region is unrealistic due to the amount of time the forager moves about the landscape without raw

materials in the toolkit. This is especially true if no stone is cached at a central location and the random walk takes the forager away from such central locations without returning frequently. The MIS6 stone tool record at PP13B does not present clear-cut evidence for stockpiling or caching behavior. Future research needs to be focused on whether the raw material pattern observed at PP13B during MIS6 does, in fact, represent stockpiling or caching behavior.

The failure to find conclusive evidence to support the OAM in any of the model conditions at the MIS scale suggests that "Non preference-based" or 'pure' encounter-based procurement models that involve embedded procurement of raw materials either based on arguments linked to natural availability as advocated by Volman (1981) and Brown (2011), or based on arguments linked to changes in mobility strategy or ranging behavior of foragers as advocated by Ambrose and Lorenz (1990), and later McCall (2007), and McCall and Thomas (2012), are not supported.

Finally, what these results mean is that other factors than just opportunistic acquisition account for the raw material patterns observed in the Pinnacle Point record. That does not mean that embedded procurement can be ruled out completely because a deliberate choice of a raw material can also happen during embedded procurement when a source is encountered. The opposite model to the OAM is one where raw materials are selected based on a criteria or a ranking. Either this selection can happen while moving about the landscape and the forager encounters raw material sources and then makes a choice, or the selection can happen when the forager is at a home base or campsite and directly moves to a source to procure a wanted raw material. Below the evaluation of the

two hypotheses drawn from the two variants of the Active-Choice Model (ACM) will be presented: ACM-P and ACM-R.

CHAPTER 9: ACTIVE-CHOICE MODEL RESULTS

Introduction

Below I will first summarize the obtained measurements and estimates of Active-Choice Model (ACM) variables. Starting with the currency variables, *e* (cutting edge per total flaked core mass) and *d* (cutting edge durability (time to dullness)), then looking at the actual currency (*e* * *d*). This followed by the presentation of the t_s (travel and search time-cost), t_p (procurement time-cost), m_1 (heat-treatment wood fuel travel and search time-cost), m_2 (heat-treatment time-cost), and m_3 (flake manufacturing time-cost) variables. Finally, in the first section of this chapter the net-return rates under all model conditions for both the ACM-P (sequential encounter and embedded procurement; travel and search time-cost excluded) and ACM-R (simultaneous encounter and direct procurement; travel and search time-cost included) variants are presented.

ACM experiment results

e variable – Cutting Edge (cm)/Total Flaked Core Mass (kg)

Figure 107 and **Table 60** show that heat-treated silcrete blocks have significantly higher *e* value of cutting edge per mass (cm/kg) compared to both untreated silcrete and quartzite (**Supplementary Tables B157-B159** show raw data for each experimental raw material block). This result follows several studies that show that silcrete yields a higher cutting edge per mass value than quartzite in archaeological assemblages (Brown 2011, Mackay 2008, Schmidt and Mackay 2016). Quartzite blocks have the second highest mean *e* value but it is statistically similar to the mean *e* value of untreated silcrete blocks (**Table 60**). Schmidt and Mackay (2016) argued that a reason for heat-treatment of

silcrete is to increase the cutting edge per mass. The experimental result presented here supports that assertion showing that by heat-treating the silcrete it is possible, on average, to increases the e value output by 172.2 cm of cutting edge per mass (kg).

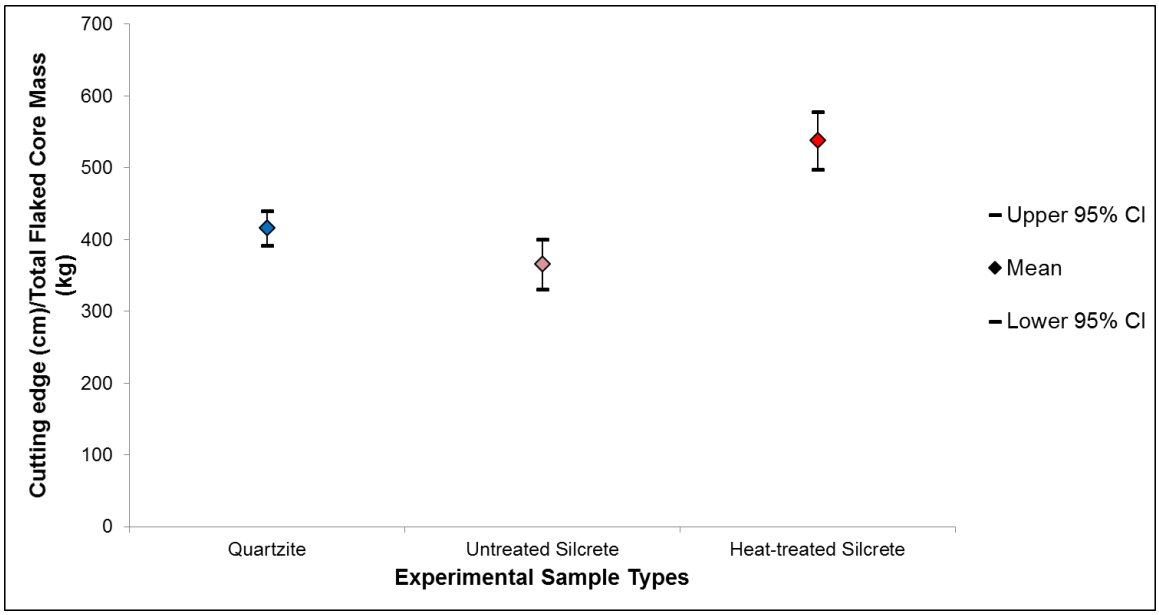

Figure 107. Plot with means and 95% confidence intervals showing the distribution of the *e* variable (available cutting edge per mass) data (Cutting Edge (cm)/ Total Flaked Core Mass (kg)) for all experimental sample types. Star with capped whiskers are the mean with the 95% confidence interval (CI). The CI was created by bootstrapping the standard error 10000 times.

Table 60. Summary statistics and bootstrap test results for *e* variable (available cutting edge per mass) for all experimental sample types.

	Quartzite	Untreated Silcrete	Heat-treated Silcrete
n sample blocks	20	8	8
First Quartile	366.4	323.75	480.9
Min	352.66	275.22	445.94
Median	404.95	381.74	548.87
Mean	415.7	365.44	537.66
Max	546.36	426.38	614.8
Third Quartile	474.23	410.27	591.1
SD	56.67	51.51	59.61
Bootstrapped SE*	12.22	17.56	20.4
Margin of error (95% CI)	23.95	34.42	39.99
Bootstrapped Upper 95% CI*	439.65	399.87	577.65
Bootstrapped Lower 95% CI*	391.75	331.02	497.67

*Samples bootstrapped 10000 times.

d variable – Cutting edge durability (time to dullness (minutes))

Figure 108 and **Table 61** show that heat-treated silcrete has cutting edges that last significantly longer before dulling (d variable value – minutes) compared to untreated silcrete and quartzite (**Supplementary Tables B160-162** show raw data for each experimental raw material block). Untreated silcrete blocks have the second highest mean *d* value but it is statistically similar to the mean *e* value of quartzite blocks (**Table 61**).

Given the fact that quartzite and untreated silcrete have similar overlapping fracture toughness values (Sevillano 1997) it is not surprising that they have similar *d* variable values. However, it is surprising that after heat-treatment, silcrete edges last almost one more minute longer before dulling compared to quartzite and untreated silcrete. This surprising result will be elaborated on more when discussing the evaluation of the ACM hypotheses (*Chapter 12*).

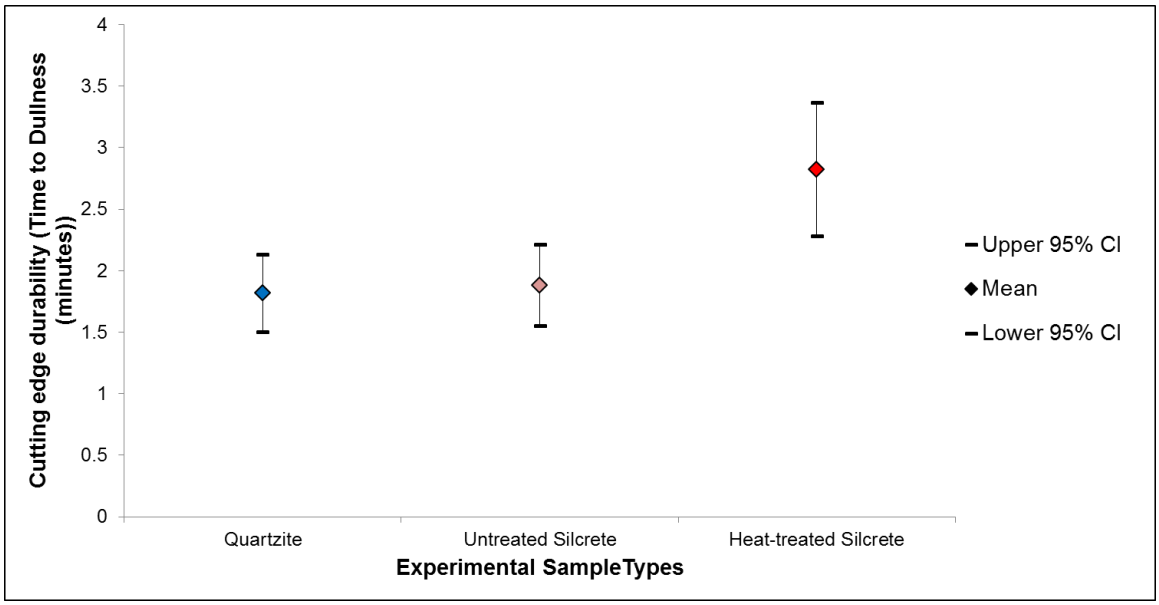

Figure 108. Plot with means and 95% confidence intervals showing the distribution of the *d* variable (cutting edge durability) data (time to dullness (minutes)) for all experimental sample types. Star with capped whiskers are the mean with the 95% confidence interval (CI). The CI was created by bootstrapping the standard error 10000 times.

Table 61. Summary statistics and bootstrap test results for the *d* variable (raw material durability – time to dullness (minutes)) for all experimental sample types.

	Quartzite	Untreated Silcrete	Heat-treated Silcrete
n samples	54	28	35
First Quartile	0.833	1.167	1.500
Min	0.083	0.583	0.083
Median	1.500	1.750	3.000
Mean	1.819	1.881	2.824
Max	4.000	3.500	6.500
Third Quartile	3.000	2.875	4.000
SD	1.187	0.899	1.659
Bootstrapped SE*	0.160	0.169	0.277
margin of error	0.314	0.330	0.543
Bootstrapped Upper 95% CI*	2.134	2.211	3.367
Bootstrapped Lower 95% CI*	1.505	1.551	2.281

*Samples bootstrapped 10000 times.

*e * d currency – Cutting Edge per Mass* Cutting Edge Durability*

Figure 109 and **Table 62** show that heat-treated silcrete has a significantly greater mean *e * d* currency value compared to untreated silcrete and quartzite (**Supplementary Tables B163-B165** show the raw data for each experimental raw material block). Quartzite blocks have the second highest mean *e * d* currency value but it is statistically similar to the mean *e * d* currency value of untreated silcrete blocks (**Table 62**). By heat-treating silcrete it is possible to more than double the assumed currency compared to untreated silcrete and quartzite. More specifically, given the results of the *e* and *d* variable experiments, this means that if silcrete is the choice and you heat-treat it you get increased flakeability and edge sharpness in addition to edge durability.

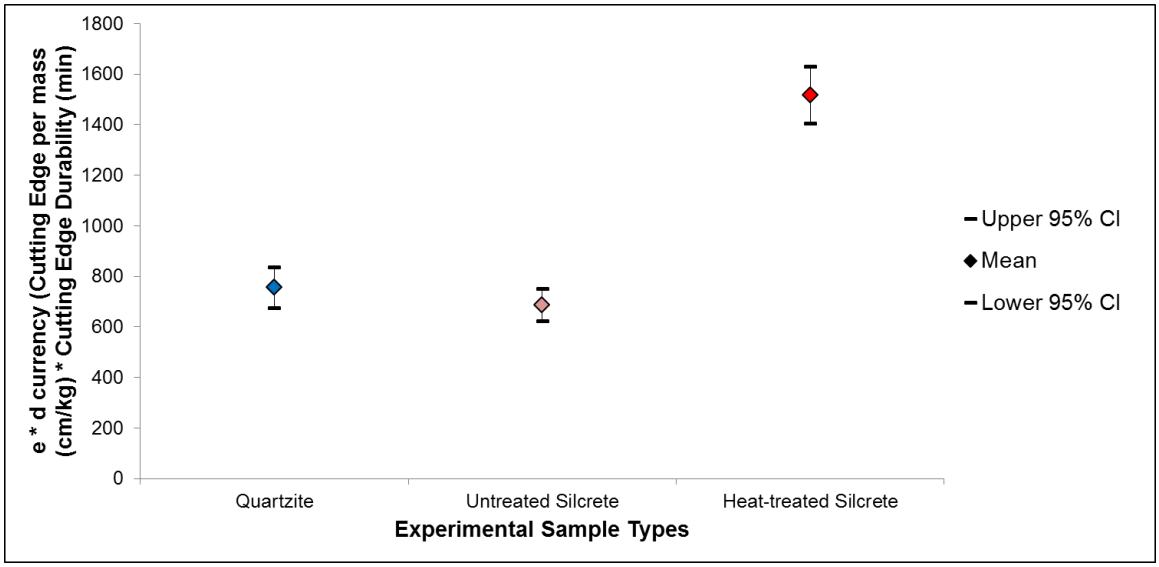

Figure 109. Plot with means and 95% confidence intervals showing the distribution of the *e * d currency* (cutting edge per mass * durability) data (CE/M * Minutes) for all experimental sample types. Star with capped whiskers are the mean with the 95% confidence interval (CI). The CI was created by bootstrapping the standard error 10000 times.

Table 62. Summary statistics and bootstrap test results for the *e * d currency* (Cutting edge per mass * cutting edge durability) for all experimental sample types.

	Quartzite	Untreated Silcrete	Heat-treated Silcrete
	20	8	8
First Quartile	572.4925	608.9475	1357.963
Min	551.03	517.68	1259.25
Median	726.5	718.04	1549.9
Mean	755.831	687.385	1518.249
Max	1106.37	802.01	1736.07
Third Quartile	960.3025	771.695	1669.155
Standard Deviation	191.8367	96.88077	168.3226
Bootstrapped SE	41.61719	33.04335	57.8113
Margin of error (95% CI)	81.56969	64.76497	113.3101
Bootstrapped Upper 95% CI mean	837.4007	752.15	1631.559
Bootstrapped Lower 95% CI mean	674.2613	622.62	1404.939

*Samples bootstrapped 10000 times.

t_s variable – Travel and search time (minutes)

MIS4 conditions

Figure 110 and **Table 63** show that under MIS4 conditions without a Paleo-Agulhas plain silcrete source, the untreated and heat-treated silcrete blocks have significantly higher travel and search time-costs (t_s values) compared to quartzite. The t_s values of untreated and heat-treated silcrete are statistically similar (**Supplementary Tables B166-B168** show the raw data for each experimental raw material block). However, when MIS4 conditions with a Paleo-Agulhas plain silcrete source is assumed both the untreated and heat-treated silcrete blocks have significantly lower travel and search time-cost values compared to quartzite (**Supplementary Tables B166 & B169-B170** show the raw data for each experimental raw material block). Again, the t_s values of untreated and heat-treated silcrete are statistically similar (**Table 63**).

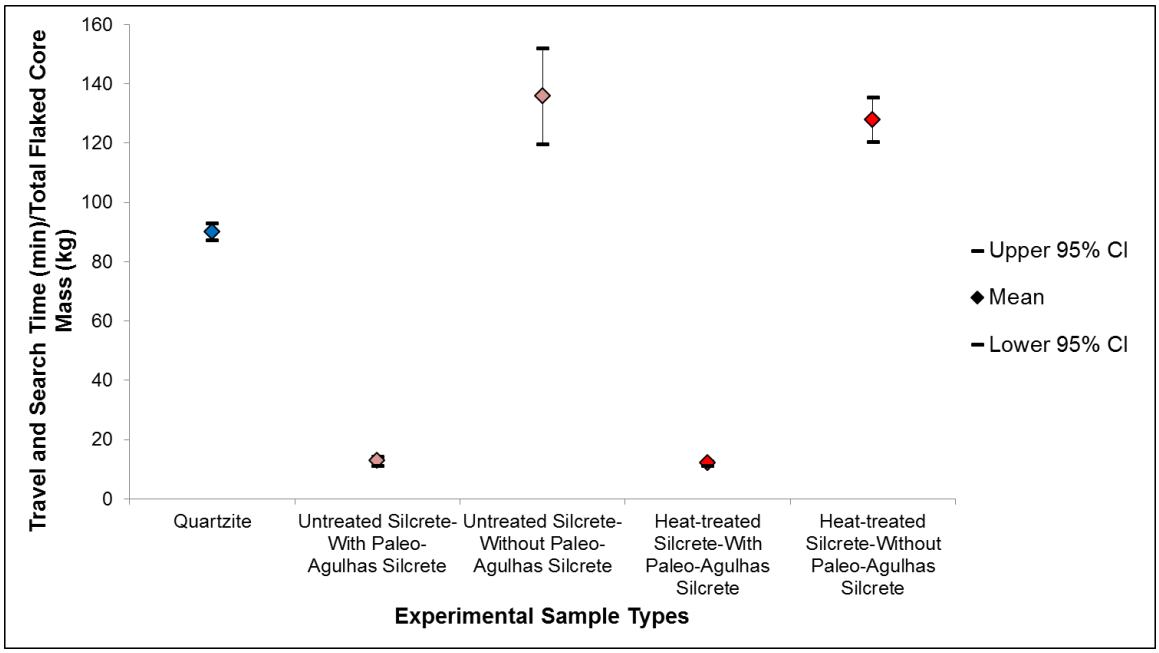

Figure 110. Plot with means and 95% confidence intervals showing the distribution of the t_s variable (travel and search time-cost) data (procurement time (min)/Total Flaked Core Mass (kg)) for all experimental sample types during MIS4 conditions. Star with capped whiskers are the mean with the 95% confidence interval (CI). The CI was created by bootstrapping the standard error 10000 times.

Table 63. Summary statistics and bootstrap test results for the *ts* variable (travel and search time-cost) for all experimental sample types during MIS4 conditions.

	Quartzite	Untreated Silcrete-With Paleo-Agulhas Silcrete	Untreated Silcrete-Without Paleo-Agulhas Silcrete	Heat-treated Silcrete-With Paleo-Agulhas Silcrete	Heat-treated Silcrete-Without Paleo-Agulhas Silcrete
n sample blocks	20	8	8	8	8
First Quartile	84.35	11.00	116.88	11.36	120.65
Min	73.46	9.48	100.66	10.60	112.62
Median	91.64	12.73	135.19	11.84	125.75
Mean	90.19	12.79	135.83	12.04	127.92
Max	100.90	16.22	172.34	14.19	150.73
Third Quartile	95.15	14.85	157.75	12.49	132.65
SD	6.92	2.27	24.17	1.07	11.34
Bootstrapped SE*	1.50	0.78	8.26	0.36	3.84
Margin of error (95% CI)	2.93	1.53	16.19	0.71	7.52
Bootstrapped Upper 95% CI*	93.12	14.31	152.02	12.75	135.44
Bootstrapped Lower 95% CI*	87.26	11.26	119.64	11.33	120.40

*Samples bootstrapped 10000 times.

MIS5 conditions

Figure 111 and **Table 64** show that under MIS5 conditions, the untreated and heat-treated silcrete blocks have significantly higher travel and search time-costs (t_s values) compared to quartzite. The t_s values of untreated and heat-treated silcrete are statistically similar (**Supplementary Tables B171-B173** show the raw data for each experimental raw material block).

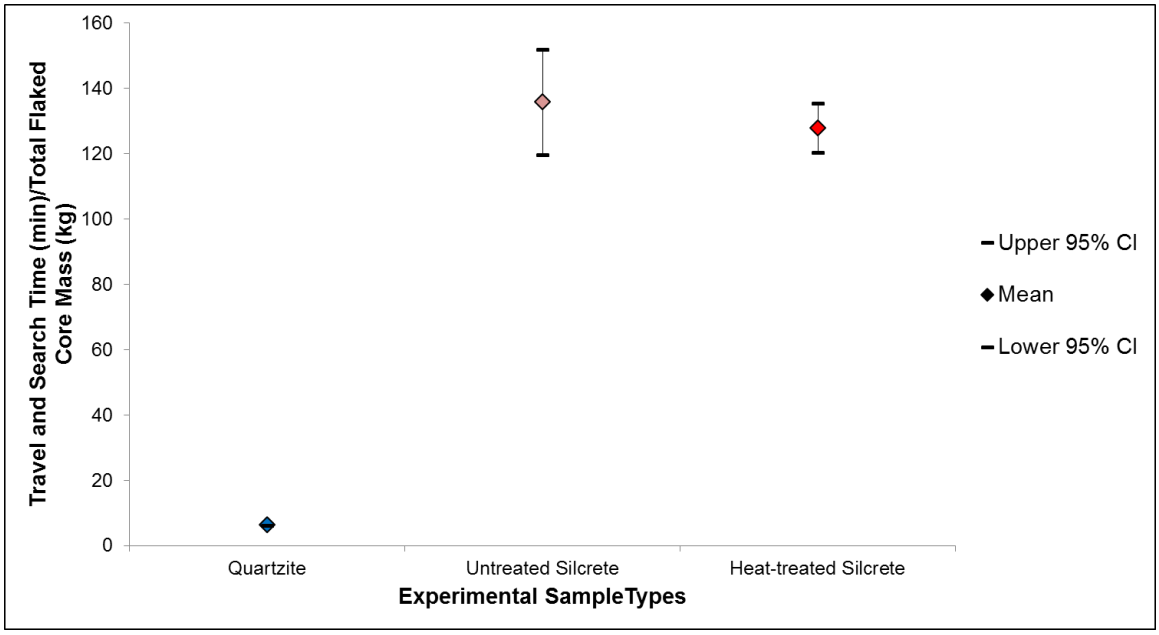

Figure 111. Plot with means and 95% confidence intervals showing the distribution of the t_s variable (travel and search time-cost) data (procurement time (min)/Total Flaked Core Mass (kg)) for all experimental sample types during MIS5 conditions. Star with capped whiskers are the mean with the 95% confidence interval (CI). The CI was created by bootstrapping the standard error 10000 times.

Table 64. Summary statistics and bootstrap test results for the *ts* variable (travel and search time-cost) for all experimental sample types during inter-glacial conditions.

	Quartzite	Untreated Silcrete	Heat-treated Silcrete
n sample blocks	20	8	8
First Quartile	5.95	116.88	120.65
Min	5.18	100.66	112.62
Median	6.47	135.19	125.75
Mean	6.36	135.83	127.92
Max	7.12	172.34	150.73
Third Quartile	6.72	157.75	132.65
SD	0.49	24.17	11.34
Bootstrapped SE*	0.11	8.26	3.84
Margin of error (95% CI)	0.21	16.19	7.52
Bootstrapped Upper 95% CI*	6.57	152.02	135.44
Bootstrapped Lower 95% CI*	6.16	119.64	120.40

*Samples bootstrapped 10000 times.

MIS6 conditions

Figure 112 and **Table 65** show that under MIS6 conditions without a Paleo-Agulhas plain silcrete source, the untreated and heat-treated silcrete blocks have significantly higher travel and search time-costs (t_s values) compared to quartzite.

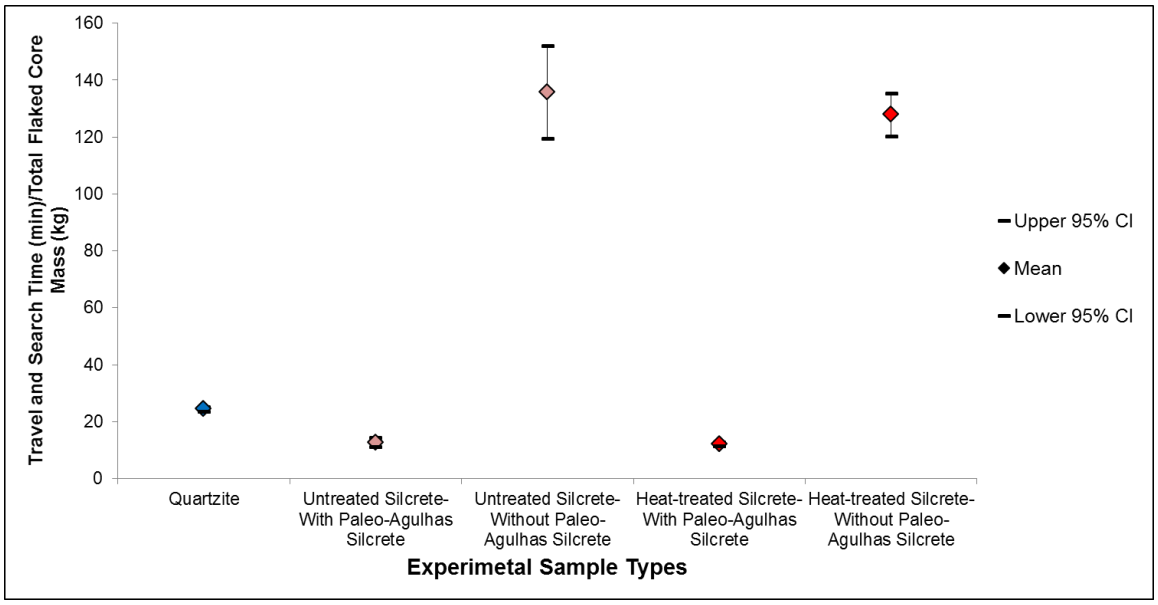

Figure 112. Plot with means and 95% confidence intervals showing the distribution of the t_s variable (travel and search time-cost) data (procurement time (min)/Total Flaked Core Mass (kg)) for all experimental sample types during MIS6 conditions. Star with capped whiskers are the mean with the 95% confidence interval (CI). The CI was created by bootstrapping the standard error 10000 times.

The t_s values of untreated and heat-treated silcrete are statistically similar (**Supplementary Tables B174 & B169-B170** show the raw data for each experimental raw material block). However, when MIS6 conditions with a Paleo-Agulhas plain silcrete source is assumed both the untreated and heat-treated silcrete blocks have significantly lower time-cost values compared to quartzite (**Supplementary Tables B174 & B169-B170** show the raw data for each experimental raw material block). Again, the t_s values of untreated and heat-treated silcrete are statistically similar (**Table 65**). An interesting observation is that the mean travel and search time-costs (t_s values) of quartzite is much

lower during MIS6 conditions (24.5 minutes) compared to MIS4 conditions (90.2 minutes).

Table 65. Summary statistics and bootstrap test results for the *ts* variable (travel and search time-cost) for all experimental sample types during MIS6 conditions.

	Quartzite	Untreated Silcrete-With Paleo-Agulhas Silcrete	Untreated Silcrete-Without Paleo-Agulhas Silcrete	Heat-treated Silcrete-With Paleo-Agulhas Silcrete	Heat-treated Silcrete-Without Paleo-Agulhas Silcrete
n sample blocks	20	8	8	8	8
First Quartile	22.88	11.00	116.88	11.36	120.65
Min	19.92	9.48	100.66	10.60	112.62
Median	24.86	12.73	135.19	11.84	125.75
Mean	24.46	12.79	135.83	12.04	127.92
Max	27.36	16.22	172.34	14.19	150.73
Third Quartile	25.81	14.85	157.75	12.49	132.65
SD	1.877	2.274	24.174	1.068	11.338
Bootstrapped SE*	0.404	0.779	8.260	0.360	3.837
Margin of error (95% CI)	0.792	1.527	16.190	0.705	7.521
Bootstrapped Upper 95% CI*	25.25	14.31	152.02	12.75	135.44
Bootstrapped Lower 95% CI*	23.67	11.26	119.64	11.33	120.40

*Samples bootstrapped 10000 times.

t_p variable – Procurement time (minutes)

Figure 113 and **Table 66** show that untreated and heat-treated silcrete have significantly higher procurement time-cost (t_p values) compared to quartzite. The t_p values of untreated and heat-treated silcrete are statistically similar (**Supplementary Tables B175-B177** show the raw data for each experimental raw material block).

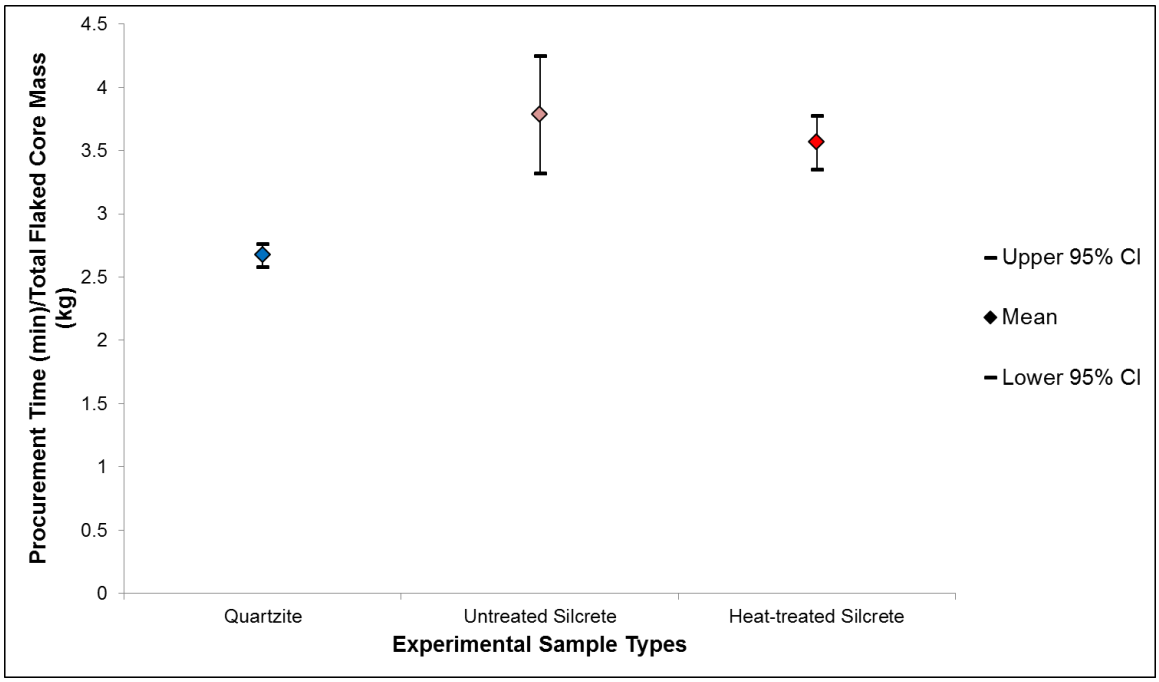

Figure 113. Plot with means and 95% confidence intervals showing the distribution of the t_p variable (procurement time-cost) data (procurement time (min)/ Total Flaked Core Mass (kg)) for all experimental sample types. Star with capped whiskers are the mean with the 95% confidence interval (CI). The CI was created by bootstrapping the standard error 10000 times.

Table 66. Summary statistics and bootstrap test results of t_p variable (procurement time-cost) for all experimental sample types.

	Quartzite	Untreated Silcrete	Heat-treated Silcrete
n sample blocks	20	8	8
First Quartile	2.493	3.255	3.368
Min	2.190	2.810	3.140
Median	2.710	3.770	3.505
Mean	2.674	3.786	3.566
Max	3.010	4.800	4.200
Third Quartile	2.840	4.400	3.698
Standard Deviation	0.213	0.673	0.315
Bootstrapped SE*	0.047	0.235	0.109
Margin of error (95% CI)	0.092	0.462	0.214
Bootstrapped Upper 95% CI*	2.766	4.248	3.780
Bootstrapped Lower 95% CI*	2.581	3.325	3.353

*Samples bootstrapped 10000 times.

m variable – manufacturing time (minutes)

m_1 variable – Heat-treatment wood fuel travel and search time (minutes)

Figure 114 and **Table 67** show that under MIS4 conditions, silcrete assumed to be heat-treated using the exposed method and the silcrete assumed to be heat-treated using the insulated methods have statistically similar travel and search time-cost for wood fuel (m_1) (**Supplementary Tables B178 & B179** show the raw data for each experimental raw material block). During MIS5 and MIS6 conditions, the insulated silcrete has significantly higher m_1 values compared to silcrete heat-treated with the exposed method (**Supplementary Tables B180-B183** show the raw data for each experimental raw material block).

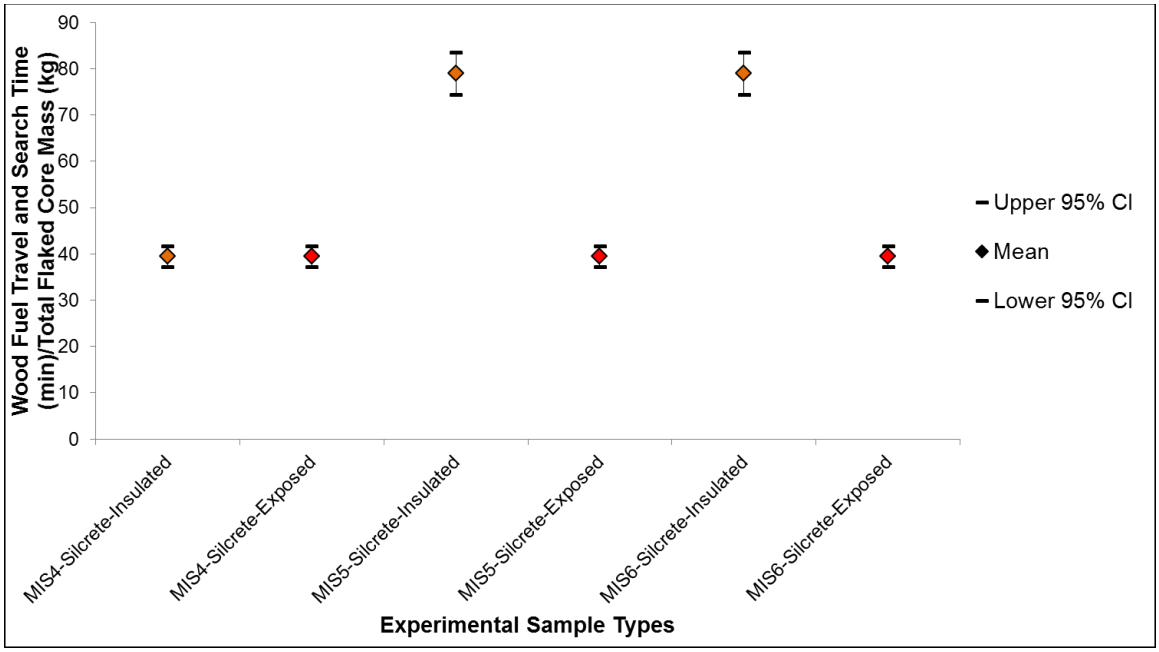

Figure 114. Plot with means and 95% confidence intervals showing the distribution of the *m1* variable (wood fuel travel and search time-cost) data (Wood Fuel Travel and Search Time (min)/Total Flaked Core Mass (kg)) for heat-treated silcrete sample types. Star with capped whiskers are the mean with the 95% confidence interval (CI). The CI was created by bootstrapping the standard error 10000 times.

Table 67. Summary statistics and bootstrap test results of m_1 variable (wood fuel travel and search time-cost) for heat-treated silcrete.

	MIS4-Silcrete-Insulated	MIS4-Silcrete-Exposed	IG-Silcrete-Insulated	IG-Silcrete-Exposed	MIS6-Silcrete-Insulated	MIS6-Silcrete-Exposed
N sample blocks	8	8	8	8	8	8
First Quartile	37.26	37.26	74.52	37.26	74.52	37.26
Min	34.78	34.78	69.56	34.78	69.56	34.78
Median	38.83	38.83	77.67	38.83	77.67	38.83
Mean	39.50	39.50	79.01	39.50	79.01	39.50
Max	46.55	46.55	93.10	46.55	93.10	46.55
Third Quartile	40.96	40.96	81.93	40.96	81.93	40.96
SD	3.501	3.501	7.003	3.501	7.003	3.501
Bootstrapped SE*	1.171	1.167	2.344	1.172	2.325	1.172
Margin of error (95% CI)	2.295	2.288	4.594	2.297	4.556	2.298
Bootstrapped Upper 95% CI*	41.80	41.79	83.60	41.80	83.56	41.80
Bootstrapped Lower 95% CI*	37.21	37.22	74.41	37.21	74.45	37.21

*Samples bootstrapped 10000 times.

m_2 variable – Heat-treatment time (minutes)

Figure 115 and **Table 68** show that silcrete assumed to be heat-treated using the exposed method have significantly higher heat-treatment cost (m_2 value) compared to silcrete assumed to be heat-treated using the insulated method (**Supplementary Tables B184-B185** show the raw data for each experimental raw material block).

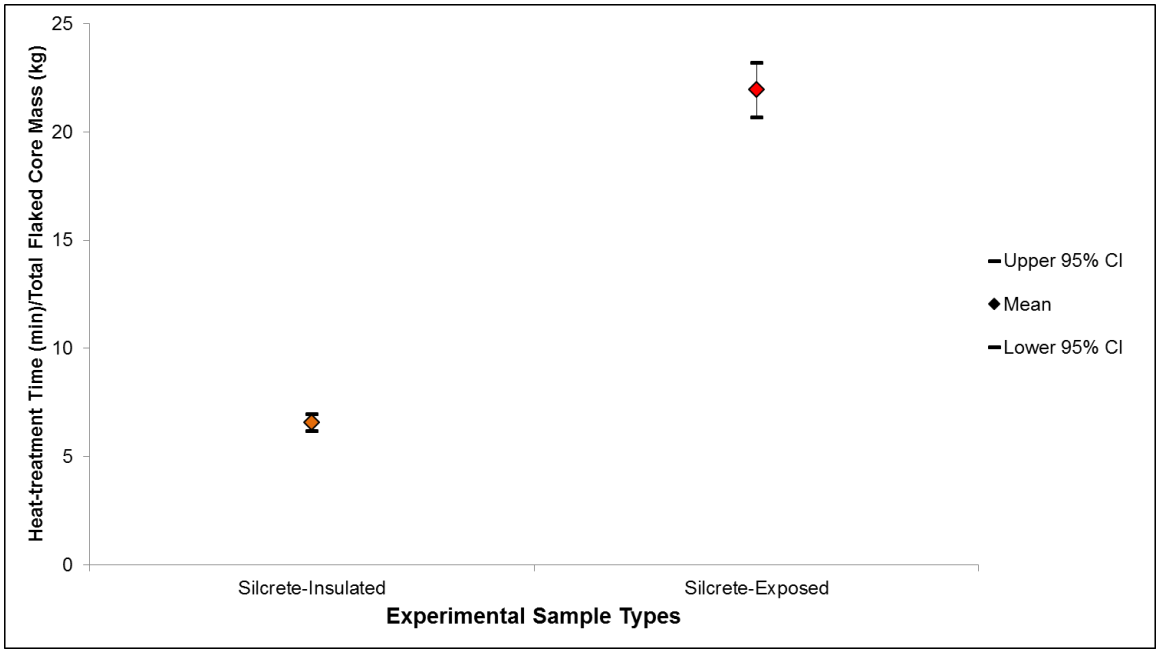

Figure 115. Plot with means and 95% confidence intervals showing the distribution of the *m2* variable (heat-treatment time-cost) data (Heat-treatment Time (min)/Total Flaked Core Mass (kg)) for heat-treated silcrete sample types. Star with capped whiskers are the mean with the 95% confidence interval (CI). The CI was created by bootstrapping the standard error 10000 times.

Table 68. Summary statistics and bootstrap test results of m_2 variable (heat-treatment time-cost) for heat-treated silcrete.

	Silcrete-Insulated	Silcrete-Exposed
n sample blocks	8	8
First Quartile	6.210	20.699
Min	5.797	19.322
Median	6.472	21.574
Mean	6.584	21.946
Max	7.758	25.860
Third Quartile	6.827	22.858
SD	0.584	1.945
Bootstrapped SE*	0.194	0.649
Margin of error (95% CI)	0.379	1.272
Bootstrapped Upper 95% CI*	6.963	23.219
Bootstrapped Lower 95% CI*	6.204	20.674

*Samples bootstrapped 10000 times.

m_3 variable – Flake manufacturing time (minutes)

Figure 106 and **Table 69** show that quartzite has significantly higher flake manufacturing time-cost (m_3 values) compared to heat-treated silcrete. However, untreated silcrete has statistically similar m_3 values to both heat-treated silcrete and quartzite (**Supplementary Tables B186-B188** show the raw data for each experimental raw material block).

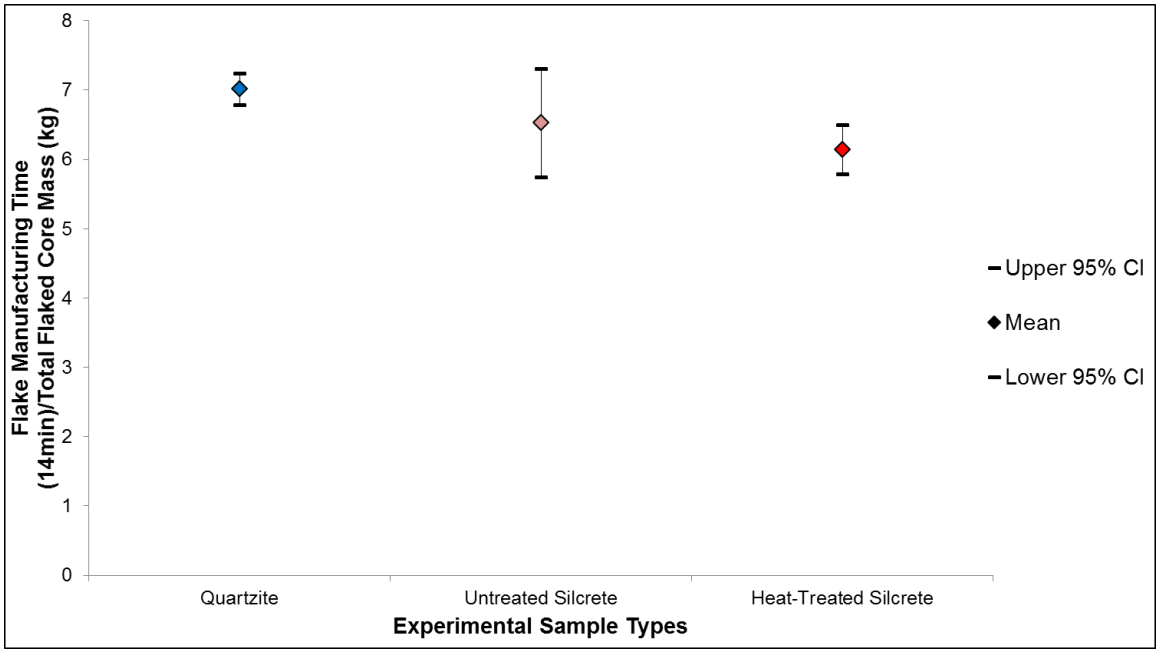

Figure 116. Plot with means and 95% confidence intervals showing the distribution of the *m3* variable (flake manufacturing time-cost) data (flake manufacturing time (14min)/ Total Flaked Core Mass (kg)) for all experimental sample types. Star with capped whiskers are the mean with the 95% confidence interval (CI). The CI was created by bootstrapping the standard error 10000 times.

Table 69. Summary statistics and bootstrap test results of m_3 variable (flake manufacturing time-cost) for all experimental sample types.

	Quartzite	Untreated Silcrete	Heat-Treated Silcrete
n sample blocks	20	8	8
First Quartile	6.560	5.615	5.796
Min	5.714	4.836	5.410
Median	7.128	6.494	6.041
Mean	7.015	6.525	6.145
Max	7.848	8.279	7.241
Third Quartile	7.401	7.580	6.372
Standard Deviation	0.539	1.161	0.545
Bootstrapped SE*	0.116	0.398	0.182
Margin of error (95% CI)	0.227	0.781	0.357
Bootstrapped Upper 95% CI*	7.242	7.306	6.502
Bootstrapped Lower 95% CI*	6.788	5.744	5.788

*Samples bootstrapped 10000 times.

Experiment results summary

Heat-treated silcrete has the highest cutting edge per mass value (*e* variable) and the highest value of edge durability (*d* variable – time to dullness (minutes)). Combined this makes heat-treated silcrete have the highest value of the assumed currency (*e* * *d*). Quartzite and untreated silcrete have statistically similar *e* variable values and *d* variable values making them have statistically similar values of the assumed currency.

Both untreated and heat-treated silcrete under assumed MIS4 and MIS6 conditions without a Paleo-Agulhas plain silcrete source have the highest travel and search time-costs (t_s variable). Conversely, both untreated and heat-treated silcrete under assumed MIS4 and MIS6 conditions with a Paleo-Agulhas plain silcrete source have the lowest t_s variable values. Under MIS5 conditions, quartzite has the lowest travel and search time-cost (t_s variable). Both untreated and heat-treated silcrete have higher procurement time-costs (t_p variable) compared to quartzite.

When looking at manufacturing time-costs (m), silcrete assumed to have been heat-treated using the insulated method have the highest wood fuel travel and search time-cost (m_1 variable) during MIS5 and MIS6. However, during MIS4 both heat-treatment methods have equal m_1 variable values. Silcrete assumed to have been heat-treated using the exposed methods has the highest actual heat-treatment time-cost (m_2 variable). Heat-treated silcrete has a significantly lower flake manufacturing time-cost (m_3 variable) compared to quartzite but it is not significantly lower than the m_3 value of untreated silcrete.

By obtaining these ACM variables, the net-return rates of raw material selection can now be calculated. In the next chapter below, the net-return rates for the ACM-P and ACM-R variants will be presented. The net-return rates from each model variant will be used to create rankings of raw materials. The rankings will be used to test Hypothesis 2 and 3 by comparing the rankings to archaeological raw material frequencies.

CHAPTER 10: ACTIVE-CHOICE MODEL – HYPOTHESES EVALUATION

Introduction

In this chapter, the evaluation of Hypothesis 2 (H_2) and Hypothesis 3 (H_3) from the Active-Choice Model (ACM) is presented. The ACM-P (active-choice without travel and search costs) net-return rates are used to evaluate Hypothesis 2 (H_2), while ACM-R (active-choice with travel and search costs) net-return rates are used to evaluate Hypothesis 3 (H_3). This is followed by the presentation of the model outcomes under the three different model condition variables to understand whether changes in individual time-costs drive the net-return rates and thus can explain the archaeological raw material frequencies. First, net-return rates from the different model condition variables are presented, which allows for a ranking that can be used compare to archaeological frequencies. Then, the comparison to the archaeological frequencies allows for testing of the predicted relationships between time-costs and model condition variables presented in *Chapter 5*.

Active-Choice Model – Testing Hypotheses 2 and 3

ACM-P net-return rates – Hypothesis 2

An observation when looking across all model conditions is that quartzite and untreated silcrete have significantly higher net-return rates than either type of heat-treated silcrete (exposed and insulated) (**Figure 117** and **Table 70**). Under MIS4 conditions quartzite and untreated silcrete, while having statistically similar net-return rates have significantly higher net-return rates (Pq and Ps) compared to both exposed and insulated heat-treated silcrete. The net-return rate of silcrete heat-treated using the insulated method is

significantly higher than silcrete heat-treated using the exposed method (MIS4 raw data in **Supplementary Tables B189** and **B190**).

Under MIS5 and MIS6 conditions (**Figure 117** and **Table 70**), quartzite and untreated silcrete, while having statistically similar net-return rates have significantly higher net-return rates (Pq and Ps) compared to both exposed and insulated heat-treated silcrete. However, compared to MIS 4 conditions the net-return rate of exposed silcrete is significantly higher than insulated silcrete (MIS5 raw data in **Supplementary Tables B189** and **B191**: MIS6 data in **Supplementary Tables B189** and **B192**).

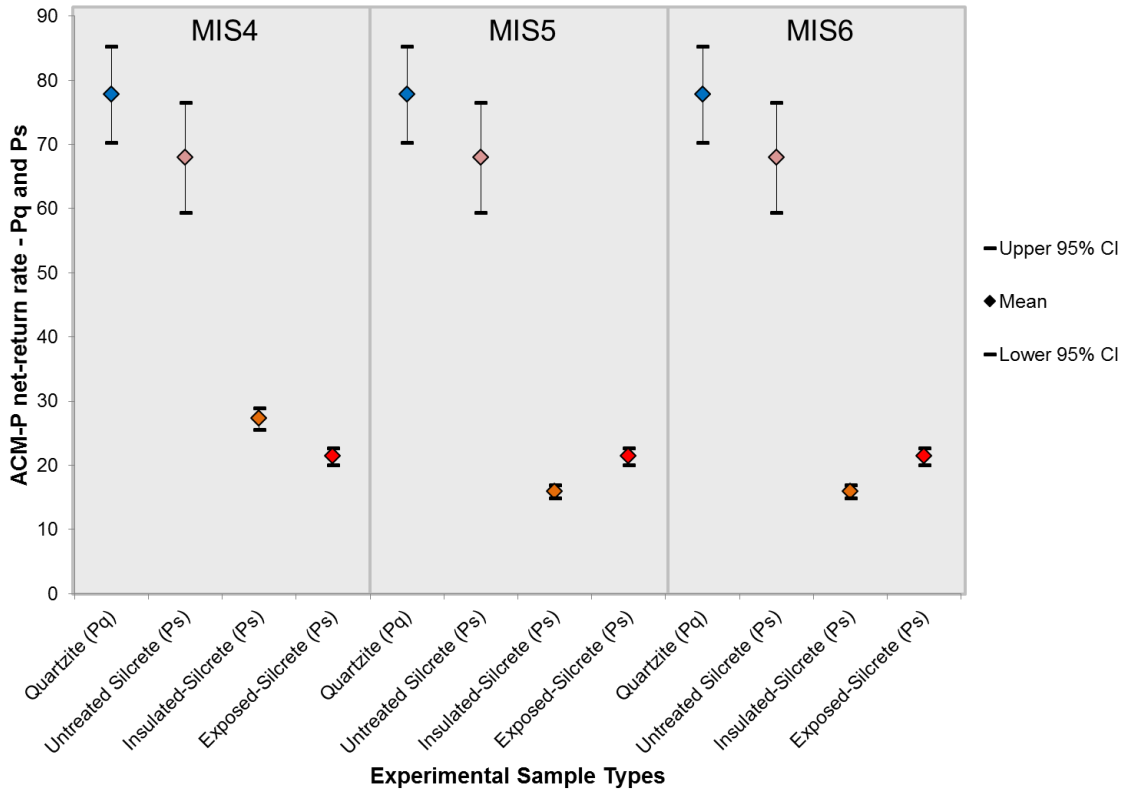

Figure 117. Plot with means and 95% confidence intervals showing the distribution of the ACM-P net-return rates for all experimental sample types during MIS4, MIS5, and MIS6 conditions. Star with capped whiskers is the mean with the 95% confidence interval (CI). The CI was created by bootstrapping the standard error 10000 times.

Table 70. Summary statistics and bootstrap test results of ACM-P net-return rates (for all experimental sample types during MIS4, MIS5, and MIS6 conditions.

	MIS4			MIS5			MIS6		
	Exposed-Silcrete (Ps)	Insulated-Silcrete (Ps)	Untreated Silcrete (Ps)	Exposed-Silcrete (Ps)	Insulated-Silcrete (Ps)	Untreated Silcrete (Ps)	Exposed-Silcrete (Ps)	Insulated-Silcrete (Ps)	Untreated Silcrete (Ps)
	Quartzite (Pq)			Quartzite (Pq)			Quartzite (Pq)		
n sample blocks	8	8	8	8	8	8	20	8	8
First Quartile	20.165	25.718	55.835	20.165	15.053	55.835	62.528	15.053	55.835
Min	18.250	23.280	53.820	18.250	13.630	53.820	54.240	13.630	53.820
Median	21.440	27.340	66.060	21.440	16.010	66.060	76.510	16.010	66.060
Mean	21.373	27.258	67.983	21.373	15.959	67.983	77.797	15.959	67.983
Max	25.230	32.180	89.160	25.230	18.840	89.160	108.390	18.840	89.160
Third Quartile	22.405	28.573	79.600	22.405	16.728	79.600	94.483	16.728	79.600
SD	2.045	2.608	12.720	2.045	1.527	12.720	17.701	1.527	12.720

Bootstrapped SE*	0.687	0.515	4.356	3.846	0.687	0.515	4.359	3.841	0.689	0.877	4.356	3.846
Margin of error (95% CI)	1.347	1.010	8.538	7.538	1.347	1.010	8.544	7.529	1.351	1.718	8.538	7.538
Bootstrapped Upper 95% CI*	22.719	16.969	76.521	85.335	22.719	16.969	76.527	85.326	22.723	28.976	76.521	85.335
Bootstrapped Lower 95% CI*	20.026	14.949	59.444	70.258	20.026	14.949	59.438	70.267	20.022	25.539	59.444	70.258

*Samples bootstrapped 10000 times.

Hypothesis 2 (H_2) is drawn from the ACM-P variant of the Active-Choice Model (ACM), and states that the archaeological stone raw material usage frequency is due to the selection of the raw material with the highest post-encounter net-return of cm-min tool cutting edge (P) unless waiting to encounter the high profitability stone source will lead the forager to run out of tool material. The prediction is that the forager will select the raw material with highest post-encounter P rate. Foragers will switch from one raw material to another depending on which material has the highest P rate.

To evaluate Hypothesis 2 (H_2), raw material rankings based on net-return rates from each model condition are compared to the archaeological frequencies from the respective Marine Isotope Stage (MIS). It is important to note that here the overall net-return rates are evaluated whereas model outcomes from the different model condition variables only consider time-costs under question to compile net-return rates. What that means is, for example, that net-return rates computed when considering the vegetation

type variable for each model conditions are potentially different from the ACM-P net-return rates when all relevant time-costs are included. However, the model outcomes under the different model condition variables will help understand if any time-cost explains the archaeological raw materials frequencies at Pinnacle Point.

Table 71 shows the ranking of raw materials based on the overall ACM-P net-return rates compared to the archaeological frequencies under different model conditions. For H_2 to be supported, the raw material with the highest rank based on net-return rate should be the same as the raw material with the highest frequency. In addition, the material with the second highest rank should be the same as the raw material with the second highest frequency.

Table 71. Comparison between a raw material ranking based on ACM-P net-return rates and archaeological data from MIS4, MIS5, and MIS6.

ACM-P Results-Ranked*				**Archaeological Data**			
MIS4				**MIS4**			
Quartzite	Untreated Silcrete	Insulated -Silcrete	Exposed-Silcrete	Quartzite (%)	Silcrete Overall (%)	Untreated Silcrete (%)	Heat-treated Silcrete (%)
1 (77.8)	***1*** (68)	***2*** (27.3)	***3*** (21.4)	44.6*	40*	16.9	83.1
MIS5				**MIS5**			
Quartzite	Untreated Silcrete	Insulated -Silcrete	Exposed-Silcrete	Quartzite (%)	Silcrete Overall (%)	Untreated Silcrete (%)	Heat-treated Silcrete (%)
1 (77.8)	***1*** (68)	***3*** (16)	***2*** (21.4)	77.2	13.1	11.6	88.4
MIS6				**MIS6**			
Quartzite	Untreated Silcrete	Insulated -Silcrete	Exposed-Silcrete	Quartzite (%)	Silcrete Overall (%)	Untreated Silcrete (%)	Heat-treated Silcrete (%)
1 (77.8)	***1*** (68)	***3*** (16)	***2*** (21.4)	94.3	1.1	NA	NA

* Ranking based on which raw materials have the highest mean Pq or Ps (in parenthesis). Similar rankings in the table are due to statistically similar Pq or Rs. MIS4, MIS5, and MIS6 Archaeological raw material frequencies from bootstrapped data in Figure 50 and Table 19.

During all three model-conditions, quartzite and untreated silcrete have the highest rankings, which are all based on statistically similar net-return rates (**Table 71**).

During both MIS6 and MIS5 quartzite has the highest archaeological frequency, which does not match the tied ACM-P ranking of quartzite and untreated silcrete. During MIS4 quartzite and silcrete have statistically similar archaeological frequencies, which do match the tied ranking of quartzite and untreated silcrete based on net-return rates. However, the archaeological data show that 83.1% of the silcrete is heat-treated. Therefore, while the ACM-P net-return rates can explain the dual selection of quartzite and untreated silcrete it does not explain why you would heat-treat the silcrete.

Taken together, the ACM-P net-return rates show little support for Hypothesis 2 (H_2). The lack of support for H_2 limits the support for a scenario where during embedded procurement (e.g. Binford 1979, Binford and Stone 1985) a forager strategically selects the raw material with the highest net-return rate of cm*min cutting edge available in the environment. This result suggests that the response to the climatic and environmental conditions throughout the Pinnacle Point sequence was not a combination of a mobility system that disregarded the location of raw material sources (embedded procurement) to target food resources and the selection of raw materials that could be used to produce extractive technology for such resources.

However, this result does not rule out the ACM completely as the ACM-R (simultaneous encounter and direct procurement) variant can still explain the raw material pattern. In the ACM-R the time-cost resulting from travel and search for a raw material is included. This makes the distribution of raw material sources on the landscape very important because it is very feasible that increased time-cost to travel and search for a raw material can negatively affect the willingness to select that raw material. It also can

be that the ACM-P can explain the pattern if a different currency is assumed, which will be addressed below in separate sections.

ACM-R net-return rates – Hypothesis 3

Figure 118 and **Table 72** show that under MIS4 conditions without a Paleo-Agulhas plain silcrete source quartzite and untreated silcrete, while having statistically similar net-return rates, have significantly lower net-return rates (Rq and Rs) compared to both exposed and insulated heat-treated silcrete. The net-return rate of silcrete heat-treated using the exposed is statistically similar to silcrete heat-treated using the insulated method (**Supplementary Tables B193-B194** show the raw data for each experimental raw material block).

During MIS4 conditions with a Paleo-Agulhas plain silcrete source untreated silcrete have significantly higher net-return rates (Rq and Rs) compared to both exposed and insulated heat-treated silcrete, and quartzite (**Figure 118** and **Table 72)**. The net-return rate of silcrete heat-treated using the exposed method is significantly lower than silcrete heat-treated using the insulated method (**Supplementary Tables B193 & B195** show the raw data for each experimental raw material block).

Quartzite has significantly higher net-return rates (Rq and Rs) compared to both types of heat-treated silcrete (exposed and insulated), and untreated silcrete during MIS5 conditions (**Figure 118** and **Table 72)**. Untreated silcrete has a significantly lower net-return compared to both types of heat-treated silcrete, while the net-return rate of silcrete heat-treated using the exposed method is statistically similar to silcrete heat-treated using

the insulated method (**Supplementary Tables B196-B197** show the raw data for each experimental raw material block).

Under MIS6 conditions without a Paleo-Agulhas plain silcrete source quartzite has significantly higher net-return rates (Rq and Rs) compared to both types of heat-treated silcrete (exposed and insulated), and untreated silcrete (**Figure 118** and **Table 72**). Untreated silcrete has a significantly lower net-return compared to both types of heat-treated silcrete, while the net-return rate of silcrete heat-treated using the exposed is statistically similar to silcrete heat-treated using the insulated method (**Supplementary Tables B198-B199** show the raw data for each experimental raw material block).

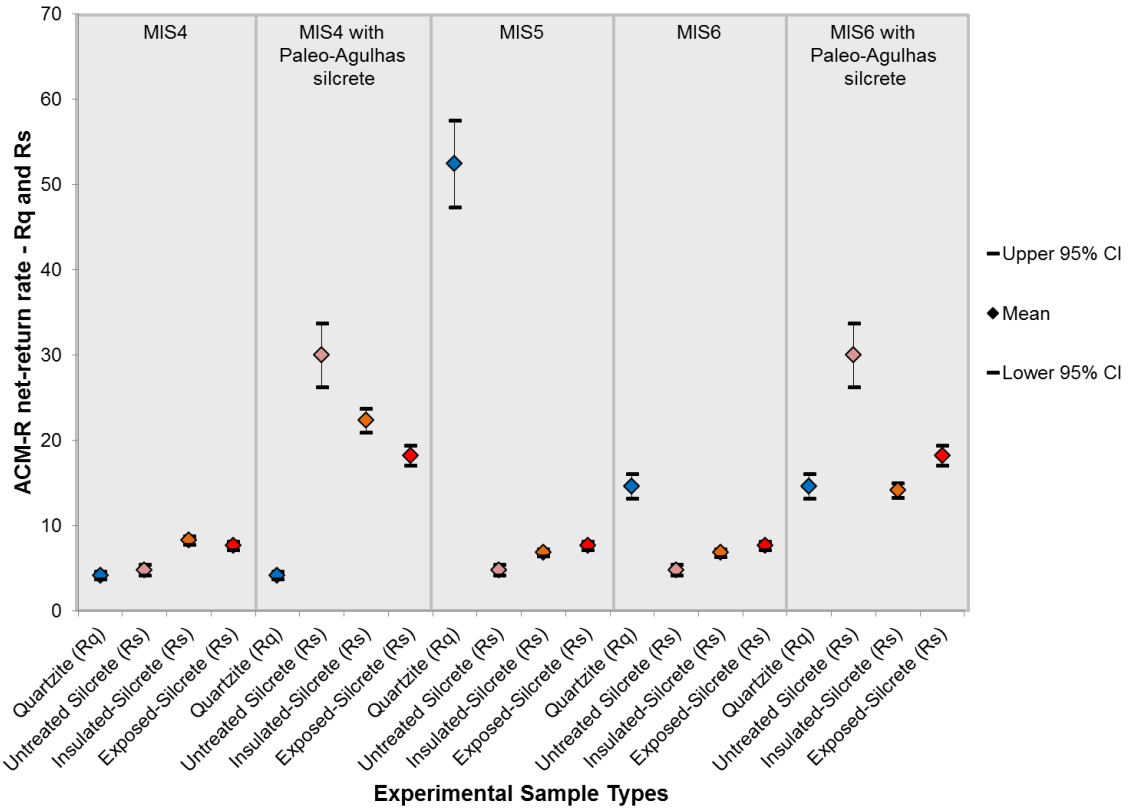

Figure 118. Plot with means and 95% confidence intervals showing the distribution of the ACM-R net-return rates (for all experimental sample types) during all model conditions. Star with capped whiskers is the mean with the 95% confidence interval (CI). The CI was created by bootstrapping the standard error 10000 times.

Figure 118 and **Table 72** show that under MIS6 conditions with a Paleo-Agulhas plain silcrete source untreated silcrete have significantly higher net-return rates (Rq and Rs) compared to both types of heat-treated silcrete (exposed and insulated), and quartzite. Silcrete assumed to be heat-treated using the insulated method have a significantly higher net-return compared to silcrete heat-treated using the exposed method, and quartzite, while the net-return rate of silcrete heat-treated using the exposed method is statistically similar to quartzite (**Supplementary Tables B198 & B200** show the raw data for each experimental raw material block).

Table 72. Summary statistics and bootstrap test results of ACM-R net-return rates (for all experimental sample types) during all model conditions.

MIS6 with Paleo-Agulhas Plain silcrete	**Exposed-Silcrete (Rs)**	8	17.192
	Insulated-Silcrete (Rs)	8	13.335
	Untreated Silcrete (Rs)	8	24.637
	Quartzite (Rq)	20	11.724
MIS6 without Paleo-Agulhas Plain silcrete	**Exposed-Silcrete (Rs)**	8	7.207
	Insulated-Silcrete (Rs)	8	6.428
	Untreated Silcrete (Rs)	8	3.940
	Quartzite (Rq)	20	11.724
MIS5	**Exposed-Silcrete (Rs)**	8	7.207
	Insulated-Silcrete (Rs)	8	6.428
	Untreated Silcrete (Rs)	8	3.940
	Quartzite (Rq)	20	42.185
MIS4 with Paleo-Agulhas Plain silcrete	**Exposed-Silcrete (Rs)**	8	17.192
	Insulated-Silcrete (Rs)	8	21.071
	Untreated Silcrete (Rs)	8	24.637
	Quartzite (Rq)	20	3.299
MIS4 without Paleo-Agulhas Plain silcrete	**Exposed-Silcrete (Rs)**	8	7.207
	Insulated-Silcrete (Rs)	8	7.810
	Untreated Silcrete (Rs)	8	3.940
	Quartzite (Rq)	20	3.299
		n sample blocks	First Quartile

15.562	18.281	18.223	21.513	19.103	1.744	0.588	1.152
12.071	14.179	14.135	16.687	14.817	1.353	0.457	0.896
23.749	29.149	29.998	39.343	35.124	5.613	1.918	3.759
10.203	14.391	14.614	20.386	17.772	3.346	0.727	1.424
6.524	7.664	7.640	9.019	8.008	0.731	0.246	0.483
5.819	6.835	6.813	8.043	7.142	0.652	0.221	0.432
3.798	4.661	4.797	6.291	5.617	0.898	0.307	0.602
10.203	14.391	14.614	20.386	17.772	3.346	0.727	1.424
6.524	7.664	7.640	9.019	8.008	0.731	0.247	0.483
5.819	6.835	6.813	8.043	7.142	0.652	0.220	0.431
3.798	4.661	4.797	6.291	5.617	0.898	0.307	0.601
36.608	51.636	52.476	73.149	63.767	11.969	2.601	5.097
15.562	18.281	18.223	21.513	19.103	1.744	0.590	1.157
19.073	22.405	22.335	26.367	23.413	2.137	0.722	1.416
23.749	29.149	29.998	39.343	35.124	5.613	1.909	3.742
2.876	4.124	4.171	5.617	5.118	0.987	0.215	0.421
6.524	7.664	7.640	9.019	8.008	0.731	0.246	0.483
7.070	8.305	8.278	9.773	8.678	0.792	0.267	0.524
3.798	4.661	4.797	6.291	5.617	0.898	0.307	0.603
2.876	4.124	4.171	5.617	5.118	0.987	0.215	0.421
Min	Median	Mean	Max	Third Quartile	SD	Bootstrapped SE*	Margin of error (95% CI)

19.376	17.071		
15.031	13.238		
33.756	26.239		
16.038	13.189		
8.123	7.157		
7.246	6.381		
5.399	4.195		
16.038	13.189		
8.123	7.156		
7.245	6.382		
5.398	4.196		
57.573	47.379		
19.381	17.066		
23.750	20.919		
33.739	26.256		
4.592	3.750		
8.123	7.157		
8.802	7.755		
5.400	4.194		
4.592	3.750		
Bootstrapped Upper 95% CI*	Bootstrapped Lower 95% CI*		

*Samples bootstrapped 10000 times.

Hypothesis 3 (H_3) drawn from the ACM-R model variant states that the archaeological stone raw material usage frequency is due to the selection of the raw material with the highest net-return rate of cm-min tool cutting edge (R) when all travel and search time-costs are considered. It predicts that the raw material with highest R rate will be selected, and the switch from one raw material to another depends on which material has the highest R rate given the current environmental conditions.

The evaluation of H_3 proceeds in the same way as with H_2: raw material rankings based on net-return rates from each model condition are compared to the archaeological frequencies from the respective marine isotope stage. Again, it is important to note that here the overall net-return rates are evaluated whereas model outcomes from the different model condition variables only consider time-costs under question to compile net-return rates. For ACM-R net-return rates, what that means is that the ACM-R net-return rates computed when considering the coastline position and raw material source distribution

variable and the mobility rate and strategy variable for each model conditions are potentially different from the ACM-R net-return rates when all relevant time-costs are included.

Table 73 shows the ranking of raw materials based on the overall ACM-R net-return rates compared to the archaeological frequencies under different model conditions. For H_3 to be supported, the raw material with the highest rank based on net-return rate should be the same as the raw material with the highest frequency, and so forth.

If it is assumed that there is not a silcrete source on the Paleo-Agulhas plain during MIS4 both potential types of heat-treated silcrete have the highest rankings followed by quartzite and untreated silcrete, which also have tied rankings due to statistically similar net-return rates. The ranking does not match the archaeological frequencies, which have statistically similar frequencies of quartzite and silcrete of which 83.1% is heat-treated (**Table 73**). This result does not support H_3.

During MIS4 conditions with a Paleo-Agulhas plain silcrete source, untreated silcrete has the highest ranking followed by silcrete heat-treated by the insulated method (**Table 73**). This result does not match the archaeological frequency pattern where quartzite and silcrete, which is dominated by heat-treated silcrete (83.1%), have statistically similar frequencies. The result of the model outcome from simulations of MIS4 conditions with a Paleo-Agulhas plain silcrete source and the raw material frequencies from MIS4 does not support H_3.

During MIS5 conditions there is a match between net-return rankings and archaeological raw material frequencies (**Table 73**). Quartzite has the highest ranking and it has the highest frequency in the archaeological record. Heat-treated silcrete has the

second highest ranking and the highest frequency in the archaeological record because 88.4% of the silcrete has been heat-treated. The MIS5 result supports H_3.

Table 73. Comparison between a raw material ranking based on ACM- R net-return rates and archaeological data from MIS4, MIS5, and MIS6.

ACM-R Results-Ranked*				**Archaeological Data**			
MIS4 without a Paleo-Agulhas plain silcrete source				**MIS4**			
Quartzite	Untreated Silcrete	Insulated -Silcrete	Exposed-Silcrete	Quartzite (%)	Silcrete Overall (%)	Untreated Silcrete (%)	Heat-treated Silcrete (%)
2 (4.2)	***2*** (4.8)	***1*** (8.3)	***1*** (7.6)	44.6*	40*	16.9	83.1
MIS4 with a Paleo-Agulhas plain silcrete source				**MIS4**			
Quartzite	Untreated Silcrete	Insulated -Silcrete	Exposed-Silcrete	Quartzite (%)	Silcrete Overall (%)	Untreated Silcrete (%)	Heat-treated Silcrete (%)
4 (4.2)	***1*** (30)	***2*** (22.3)	***3*** (18.2)	44.6*	40*	16.9	83.1
MIS5				**MIS5**			
Quartzite	Untreated Silcrete	Insulated -Silcrete	Exposed-Silcrete	Quartzite (%)	Silcrete Overall (%)	Untreated Silcrete (%)	Heat-treated Silcrete (%)
1 (52.5)	***3*** (4.8)	***2*** (6.8)	***2*** (7.6)	77.2	13.1	11.6	88.4
MIS6 without a Paleo-Agulhas plain silcrete source				**MIS6**			
Quartzite	Untreated Silcrete	Insulated -Silcrete	Exposed-Silcrete	Quartzite (%)	Silcrete Overall (%)	Untreated Silcrete (%)	Heat-treated Silcrete (%)
1 (14.6)	***3*** (4.8)	***2*** (6.8)	***2*** (7.6)	94.3	1.1	NA	NA
MIS6 with a Paleo-Agulhas plain silcrete source				**MIS6**			
Quartzite	Untreated Silcrete	Insulated -Silcrete	Exposed-Silcrete	Quartzite (%)	Silcrete Overall (%)	Untreated Silcrete (%)	Heat-treated Silcrete (%)
3 (14.6)	***1*** (30)	***3*** (14.1)	***2*** (18.2)	94.3	1.1	NA	NA

* Ranking based on which raw materials have the highest mean Rq or Rs (in parenthesis). Similar rankings in the table are due to statistically similar Rq or Rs. MIS4, MIS5, and MIS6 archaeological raw material frequencies from bootstrapped data in Figure 50 and Table 19.

When one assumes that a Paleo-Agulhas plain silcrete source is not present during MIS6, the highest ranked raw material is quartzite. This result matches the archaeological

data where quartzite has the highest frequency (**Table 73**). The match between model outcome and raw material frequency from MIS6 conditions supports H_3.

During MIS6 conditions with a Paleo-Agulhas plain silcrete source, untreated silcrete has the highest ranking (**Table 73**). This ranking does not match with the archaeological data from MIS6, which shows that quartzite has the highest frequency. This result does not support Hypothesis 3.

What the support for Hypothesis 3 (H_3) during MIS5 conditions and MIS6 conditions without a Paleo-Agulhas silcrete source minimally suggests is that the foragers are strategically selecting the raw material with the highest net-return of cm*min cutting edge that is available in the environment. This suggests that stone tool raw materials played an important part in the technological organization because the forager traveled and searched for raw materials at added cost. Support for H_3 suggests that the response to climatic and environmental conditions during MIS5 and MIS6 was a mobility system that involved targeted stone tool raw material procurement bouts (c.f. Gould, 1985; Gould and Saggers, 1985) to select specific stone raw materials needed to manufacture tools to obtain food resources and/or performing processing tasks. This, in turn, suggests that the foragers had increased knowledge about the characteristics of the raw materials and how to utilize them.

Testing Hypothesis 2 and 3 summary

Quartzite and untreated silcrete have significantly higher net-return rates compared to either type of heat-treated silcrete when investigating the ACM-P net-return rates. This pattern holds under MIS4, MIS5 and MIS6 conditions. The ranking of ACM-P net-return

rates did not match the archaeological frequencies during any model conditions, which limits support for Hypothesis 2.

The net-return rates change after adding travel and search time-cost (t_s variable) to the equation when considering the ACM-R. Under MIS4 conditions without a Paleo-Agulhas plain silcrete source, heat-treated silcrete under both assumed heat-treatment methods have statistically similar net-return rates that both are significantly higher than quartzite and untreated silcrete, which in turn also have statistically similar net-return rates. When one assumes that there is an available silcrete source on the Paleo-Agulhas plain during MIS4 then untreated silcrete have a significantly higher net-return rate compared to both types of heat-treated silcrete, while quartzite has a significantly lower net-return rate compared to both untreated and heat-treated silcrete. Important to note is that silcrete (heat-treated with the insulated method) has a significantly higher net-return rate compared to the exposed method.

Conversely, during MIS5 conditions quartzite has a significantly higher net-return rate compared to both types of heat-treated silcrete and untreated silcrete. Both types of heat-treated silcrete have statistically similar net-return rates that are both significantly higher than the net-return rate of untreated silcrete. This pattern also holds under MIS6 conditions without a Paleo-Agulhas plain silcrete source.

If a Paleo-Agulhas plain silcrete source is assumed to be present during MIS6 then untreated silcrete has a significantly higher net-return rate compared to quartzite and both types of heat-treated silcrete (exposed and insulated). Silcrete heat-treated using the exposed method has a significantly higher net-return rate compared to silcrete heat-

treated using the insulated method and quartzite, which have statistically similar net-return rates.

Support was found for Hypothesis 3 (H_3) during MIS5 conditions and MIS6 conditions without a Paleo-Agulhas silcrete source. The raw material ranking made from ACM-R net-return rates match the archaeological frequencies at Pinnacle Point. This suggests that quartzite was strategically selected during both MIS5 and MIS6 due to having the highest net-return rate of cutting edge per mass multiplied by the duration that the edges last before dulling. This result supports the 'Utilitarian' model of raw material selection and change (c.f. Mackay 2008).

Next follows the presentation of the model outcomes under the different model conditions variables (coastline position and raw material source distribution, vegetation type, mobility rate and strategy) to understand whether changes in individual time-costs drive the net-return rates and thus explain the archaeological raw material frequencies. First, net-return rates from the different model condition variables are presented, which allows for a ranking that can be used compare to archaeological frequencies. Then, the comparison to the archaeological frequencies allows for testing of predicted relationships between time-costs and model condition variable presented in *Chapter 5*.

In the following section, only the relevant model variables will be used keeping all other variables constant. For the coastline position and raw material source distribution variable only the travel and search time-cost (t_s variable) is considered in the denominator side of the ACM equation. For the vegetation type variable, only the wood fuel travel and search time-cost (m_1) and heat-treatment time-cost (m_2) are considered,

while for the mobility rate and strategy variable only flake manufacturing time-cost (m_3) is considered.

ACM – Model condition variable outcomes

Coastline position and raw material source distribution

Heat-treated silcrete have the highest net-return during MIS4 conditions without a Paleo-Agulhas plain silcrete source, while untreated silcrete and quartzite have statistically similar frequencies during conditions without a Paleo-Agulhas silcrete source (**Figure 119** and **Table 74**; raw data from MIS 4 conditions without a Paleo-Agulhas plain silcrete source in **Supplementary Tables B201-B202**). During MIS4 conditions without a Paleo-Agulhas plain silcrete source, heat-treated silcrete has the highest net-return rate followed by untreated silcrete then quartzite (raw data in **Supplementary Tables B201** and **B203**).

During MIS5 conditions quartzite has the highest net-return rate followed by heat-treated silcrete then untreated silcrete (**Figure 119** and **Table 74;** MIS5 conditions raw data in **Supplementary Tables B204-B205**). This result also holds during MIS6 conditions without a Paleo-Agulhas plain silcrete source. Quartzite has a significantly higher net-return rate compared to both untreated and heat-treated silcrete. All net-return rates are significantly different from each other (**Figure 106** and **Table 74**; raw data in **Supplementary Tables B206-B207**).

During MIS6 conditions with a Paleo-Agulhas plain silcrete source, heat-treated silcrete has a significantly higher net-return rate compared to both untreated silcrete ad quartzite. Untreated silcrete has a significantly higher net-return rate than quartzite (**Figure 119** and **Table 74**; raw data in **Supplementary Tables B206** and **B208**).

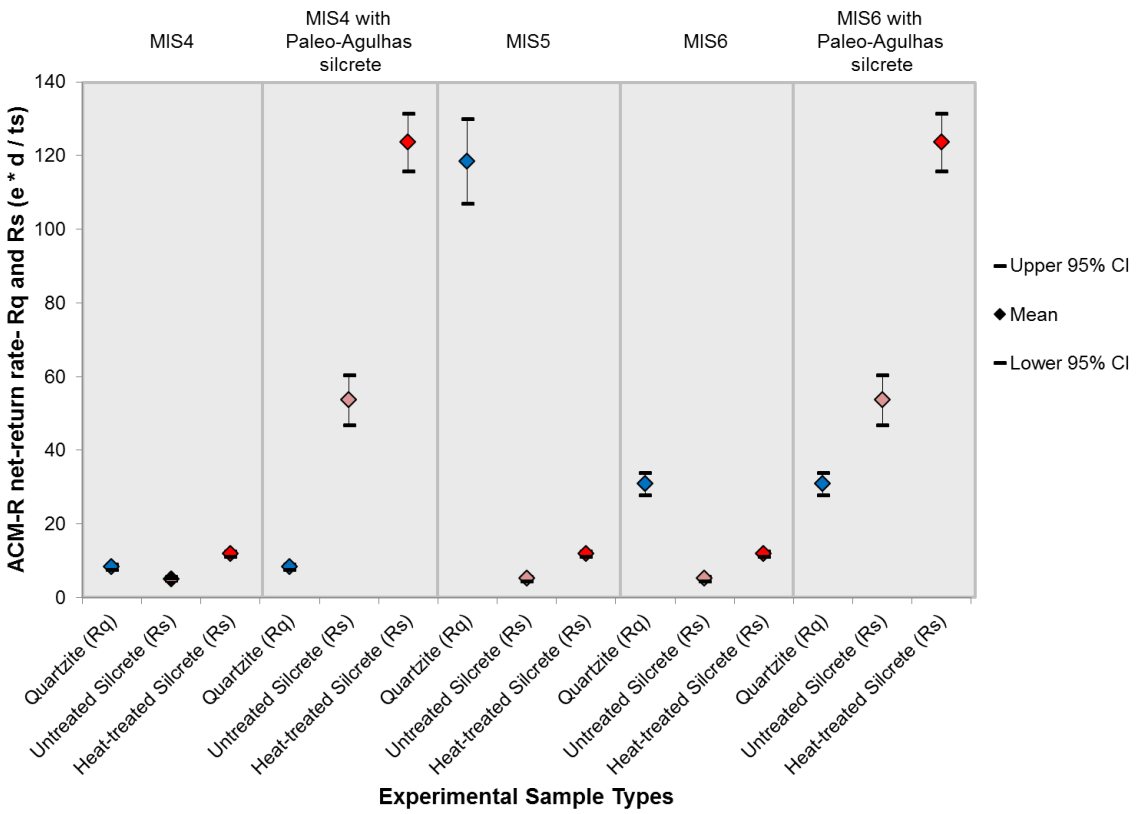

Figure 119. Plot with means and 95% confidence intervals showing the distribution of the ACM-R net-return rates (Rq and Rs) when only t_s time-cost (travel and search time) is considered (for all experimental sample types) during all model conditions. Star with capped whiskers is the mean with the 95% confidence interval (CI). The CI was created by bootstrapping the standard error 10000 times.

Table 74. Summary statistics and bootstrap test results of ACM-R net-return rates (Rq and Rs) when only t_s time-cost (travel and search time) is considered during all model conditions.

	MIS4 without a Paleo-Agulhas plain silcrete			MIS4 with a Paleo-Agulhas plain silcrete			MIS5			MIS6 without a Paleo-Agulhas plain silcrete			MIS6 with a Paleo-Agulhas plain silcrete		
	Quartzite (Rq)	Untreated Silcrete (Rs)	Heat-treated Silcrete (Rs)	Quartzite (Rq)	Untreated Silcrete (Rs)	Heat-treated Silcrete (Rs)	Quartzite (Rq)	Untreated Silcrete (Rs)	Heat-treated Silcrete (Rs)	Quartzite (Rq)	Untreated Silcrete (Rs)	Heat-treated Silcrete (Rs)	Quartzite (Rq)	Untreated Silcrete (Rs)	Heat-treated Silcrete (Rs)

8	116.680	105.618	124.068	123.677	146.005	129.647	11.835	4.003
8	44.092	42.504	52.169	53.687	70.413	62.862	10.046	3.432
20	24.671	21.528	30.366	30.827	43.017	37.499	7.068	1.535
8	11.217	10.154	11.927	11.890	14.036	12.464	1.138	0.383
8	4.239	4.086	5.016	5.161	6.769	6.044	0.966	0.330
20	24.671	21.528	30.366	30.827	43.017	37.499	7.068	1.535
8	11.217	10.154	11.927	11.890	14.036	12.464	1.138	0.383
8	4.239	4.086	5.016	5.161	6.769	6.044	0.966	0.330
20	94.830	82.751	116.721	118.494	165.348	144.142	27.167	5.900
8	116.680	105.618	124.068	123.677	146.005	129.647	11.835	3.988
8	44.092	42.504	52.169	53.687	70.413	62.862	10.046	3.433
20	6.691	5.839	8.236	8.361	11.666	10.170	1.917	0.416
8	11.217	10.154	11.927	11.890	14.036	12.463	1.138	0.385
8	4.239	4.086	5.015	5.161	6.769	6.043	0.966	0.330
20	6.691	5.839	8.235	8.360	11.666	10.170	1.917	0.416
n sample blocks	First Quartile	Min	Median	Mean	Max	Third Quartile	SD	Bootstrapped SE*

7.846	131.523	115.831		
6.727	60.414	46.959		
3.008	33.835	27.819		
0.751	12.641	11.138		
0.647	5.808	4.514		
3.008	33.835	27.819		
0.751	12.641	11.139		
0.647	5.808	4.514		
11.565	130.059	106.930		
7.817	131.494	115.860		
6.729	60.416	46.958		
0.816	9.177	7.544		
0.755	12.645	11.134		
0.647	5.808	4.514		
0.816	9.177	7.544		

Margin of error (95% CI)	Bootstrapped Upper 95% CI*	Bootstrapped Lower 95% CI*

*Samples bootstrapped 10000 times.

Table 75 compares the archaeological raw material frequencies from Pinnacle Point with ACM-R net-return rates when only travel and search time-cost (t_s variable) is considered in the denominator part of the equation. A comparison to the archaeological frequency data shows that the predicted relationship between travel and search time-cost (t_s) and the coastline position and raw material source distribution variable (with: **Figure 25;** without: **Figure 26**) during MIS4 conditions with or without a Paleo-Agulhas plain silcrete source is not supported. The archaeological frequency data show that quartzite and silcrete have statistically similar frequencies, while the model ranking shows that

heat-treated silcrete has the highest frequency (**Table 75**). This suggests that travel and search time-cost (t_s) does not explain raw material frequencies at Pinnacle Point during MIS4.

The predicted relationship (**Figure 25** and **Figure 26**) for MIS5 conditions is supported. The archaeological frequency data show that quartzite has the highest frequency while the highest ranked raw material is quartzite (**Table 75**). This suggests that during MIS5 travel and search time-cost (t_s) explains the raw material frequencies at Pinnacle Point.

A comparison between the archaeological frequency data to the ranked raw materials from MIS6 conditions without a Paleo-Agulhas plain silcrete source shows that the predicted relationship (**Figure 25**) is supported. The archaeological data show that quartzite has the highest frequency during MIS6, while the highest ranked raw material during MIS6 conditions with a Paleo-Agulhas plain silcrete source is quartzite. This suggests that during MIS6 travel and search time-cost (t_s) explains the raw material frequencies at Pinnacle Point.

A comparison of archaeological frequency data to the ranked raw materials from MIS6 conditions with a Paleo-Agulhas plain silcrete source shows that the predicted relationship (**Figure 26**) is not supported. Heat-treated silcrete have the highest net-return rate but the highest quartzite has the highest frequency in the archaeological record (**Table 75**). This suggests that travel and search time-cost does not explain raw material frequencies during MIS6 if it is assumed that a silcrete source is present on the Paleo-Agulhas plain silcrete source.

Table 75. Comparison between ranked raw materials resulting from testing predictions drawn from the coastline position and raw material source distribution variable and archaeological data.

ACM Results-Ranked*			Archaeological Data			
MIS4 Without a Paleo-Agulhas plain silcrete source			**MIS4***			
Quartzite	Untreated Silcrete	Heat-treated Silcrete	Quartzite	Silcrete Overall	Untreated Silcrete	Heat-treated Silcrete
2 (8.4)	***3*** (5.2)	***1*** (11.9)	(44.6%)	(40.0%)	16.9	83.1
MIS4 With a Paleo-Agulhas plain silcrete source			**MIS4***			
Quartzite	Untreated Silcrete	Heat-treated Silcrete	Quartzite	Silcrete Overall	Untreated Silcrete	Heat-treated Silcrete
3 (8.4)	***2*** (53.7)	***1*** (123.7)	(44.6%)	(40.0%)	16.9	83.1
MIS5			**MIS5***			
Quartzite	Untreated Silcrete	Heat-treated Silcrete	Quartzite	Silcrete Overall	Untreated Silcrete	Heat-treated Silcrete
1 (118.5)	***3*** (5.2)	***2*** (11.9)	(77.2%)	(13.1%)	11.6	88.4
MIS6 Without a Paleo-Agulhas plain silcrete source			**MIS6***			
Quartzite	Untreated Silcrete	Heat-treated Silcrete	Quartzite	Silcrete Overall	Untreated Silcrete	Heat-treated Silcrete
1 (30.8)	***3*** (5.2)	***2*** (11.9)	(94.3%)	(1.1%)	NA	NA
MIS6 With a Paleo-Agulhas plain silcrete source			**MIS6***			
Quartzite	Untreated Silcrete	Heat-treated Silcrete	Quartzite	Silcrete Overall	Untreated Silcrete	Heat-treated Silcrete
3 (30.8)	***2*** (53.7)	***1*** (123.7)	(94.3%)	(1.1%)	NA	NA

Ranking based on which raw materials have the highest mean Rq or Rs (in parenthesis). Similar rankings in table are due to statistically similar Rq or Rs. MIS4, MIS5, and MIS6 archaeological raw material frequencies from bootstrapped data in Figure 50 and Table 19.

The outcome of testing the predicted relationship between travel and search time-cost (t_s) and the coastline position and raw material source distribution variable shows that during both MIS5 conditions and MIS6 conditions without a Paleo-Agulhas plain silcrete source travel and search time-cost (t_s) does drives the net-return rates of raw materials so that it explains the archaeological raw material frequencies. When the coast is near during MIS5 conditions the travel and search time-cost (t_s) decreases enough for quartzite to drive the net-return rate above silcrete. In other words, the distribution of coastal cobble beaches in close vicinity to Pinnacle Point during MIS5 conditions

facilitates decreased travel and search time to procure quartzite and this drives the selection of quartzite. Similarly, during MIS6 conditions the close proximity of a wave-ravinement surface to Pinnacle Point facilitates decreased travel and search time to procure quartzite. This result lends support to Torrence's (1989, 1983) assertion that the frequencies of quartzite and silcrete are driven by the cost of procuring the raw materials. The raw material that is the least costly to procure will be selected if the quality of the raw material is good enough for the forager.

Vegetation type

During MIS4, MIS5, and MIS6 conditions quartzite and untreated silcrete have the highest net-return rates, and the net-return rates are statistically similar (**Figure 120** and **Table 76)**. During MIS4 silcrete heat-treated using insulated method has a significantly higher net-return compared to silcrete heat-treated using the exposed method (raw data from MIS 4 conditions can be found in **Supplementary Tables B209-B210)**. During MIS5 and MIS6 conditions, silcrete heat-treated using the exposed method has a significantly higher net-return rate compared to silcrete heat-treated using the insulated method (raw data from MIS5 conditions in **Supplementary Tables B209** and **B211**; MIS6 conditions: **Supplementary Tables B209** and **B212**).

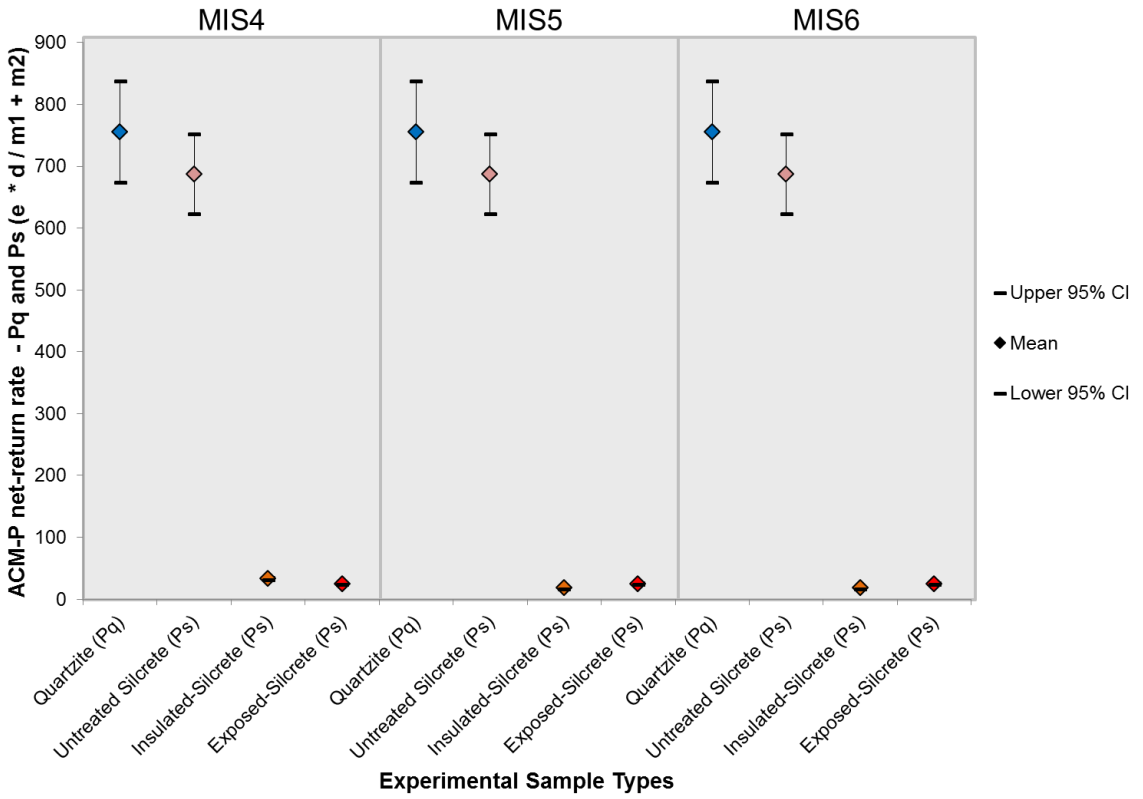

Figure 120. Plot with means and 95% confidence intervals showing the distribution of the ACM-P net-return rates (Pq and Ps) when only m_1 (wood fuel travel and search time) and m_2 time-costs (heat-treatment time) are considered (for all experimental sample types) during all model conditions. Star with capped whiskers are the mean with the 95% confidence interval (CI). The CI was created by bootstrapping the standard error 10000 times.

Table 76. Summary statistics and bootstrap test results of ACM-P net-return rates (Pq and Ps) when only m_1 (wood fuel travel and search time) and m_2 time-costs (heat-treatment time) are considered during all model conditions.

	MIS4				MIS5				MIS6			
	Quartzite (Pq)	Untreated Silcrete (Ps)	Insulated-Silcrete (Ps)	Exposed-Silcrete (Ps)	Quartzite (Pq)	Untreated Silcrete (Ps)	Insulated-Silcrete (Ps)	Exposed-Silcrete (Ps)	Quartzite (Pq)	Untreated Silcrete (Ps)	Insulated-Silcrete (Ps)	Exposed-Silcrete (Ps)
n sample blocks	20	8	8	8	20	8	8	8	20	8	8	8

23.350	21.136	24.829	24.750	29.218	25.945	2.368	0.805	1.578	26.328	23.172
16.764	15.175	17.825	17.769	20.977	18.627	1.700	0.578	1.133	18.902	16.636
608.949	517.679	718.038	687.385	802.006	771.698	96.880	32.957	64.595	751.980	622.789
572.493	551.030	726.500	755.831	1106.370	960.303	191.837	41.652	81.637	837.468	674.194
23.350	21.136	24.829	24.750	29.218	25.945	2.368	0.805	1.578	26.328	23.172
16.764	15.175	17.825	17.769	20.977	18.627	1.700	0.578	1.133	18.902	16.636
608.949	517.679	718.038	687.385	802.006	771.698	96.880	32.957	64.595	751.980	622.789
572.493	551.030	726.500	755.831	1106.370	960.303	191.837	41.652	81.637	837.468	674.194
23.350	21.136	24.829	24.750	29.218	25.945	2.368	0.805	1.578	26.328	23.172
31.133	28.182	33.105	33.000	38.958	34.593	3.158	1.064	2.086	35.086	30.914
608.949	517.679	718.038	687.385	802.006	771.698	96.880	32.957	64.595	751.980	622.789
572.493	551.030	726.500	755.831	1106.370	960.303	191.837	41.652	81.637	837.468	674.194

First Quartile | Min | Median | Mean | Max | Third Quartile | SD | Bootstrapped SE* | Margin of error (95% CI) | Bootstrapped Upper 95% CI* | Bootstrapped Lower 95% CI*

*Samples bootstrapped 10000 times.

Table 77 compares the archaeological raw material frequencies from Pinnacle Point with ACM-P net-return rates when wood fuel travel and search time-cost (m_1 variable) and heat-treatment time-cost (m_2 variable) are considered in the denominator part of the equation. A comparison to the archaeological frequency data shows that the predicted relationship between wood fuel travel and search time-cost (m_1) and heat-treatment time-cost (m_2) and the vegetation type variable (**Figure 27**) during MIS4 conditions is not supported. The archaeological raw material frequency data show that quartzite and silcrete (overall) have statistically similar raw material frequencies (**Table 77**). However, 83.1% of the silcrete has been heat-treated and only 16.9% are untreated. This does not fit with the ranking, which shows statistically similar net-return rates for quartzite and untreated silcrete (**Table 77**). This result suggests that wood fuel travel and search time-cost (m_1) and heat-treatment time-cost (m_2) do not explain the archaeological raw material frequencies at Pinnacle Point during MIS4.

A comparison between the archaeological frequency data to the ranked raw materials from MIS5 and MIS6 conditions show that the predicted relationships (**Figure 27**) are not supported. The archaeological data show that quartzite has the highest frequency during MIS5 and MIS6, while the highest ranked raw materials during MIS5 and MIS6 are quartzite and untreated silcrete that have statistically similar net-return rates (**Table 77**). This result suggests that wood fuel travel and search time-cost (m_1) and heat-treatment time-cost (m_2) do not explain raw material frequencies during MIS5 and MIS6. The result for all model conditions limits support for the "Wood-fuel availability" model proposed by Brown and Marean (2010).

Table 77. Comparison between ranked raw materials resulting from testing predictions drawn from the vegetation type variable and archaeological data.

ACM Results-Ranked*				Archaeological Data			
MIS4				**MIS4***			
Quartzite	Untreated Silcrete	Insulated-Silcrete	Exposed-Silcrete	Quartzite	Silcrete Overall	Untreated Silcrete	Heat-treated Silcrete
1 (755.8)	***1*** (687.4)	***2*** (33)	***3*** (24.8)	(44.6%*)	(40%*)	16.9%	83.1%
MIS5				**MIS5***			
Quartzite	Untreated Silcrete	Insulated-Silcrete	Exposed-Silcrete	Quartzite	Silcrete Overall	Untreated Silcrete	Heat-treated Silcrete
1 (755.5)	***1*** (687.4)	***3*** (17.8)	***2*** (24.8)	(77.2%)	(13.1%)	11.6%	88.4%
MIS6				**MIS6***			
Quartzite	Untreated Silcrete	Insulated-Silcrete	Exposed-Silcrete	Quartzite	Silcrete Overall	Untreated Silcrete	Heat-treated Silcrete
1 (755.5)	***1*** (687.4)	***3*** (17.8)	***2*** (24.8)	(94.3%)	(1.1%)	NA	NA

* Ranking based on which raw materials have the highest mean Rq or Rs (in parenthesis). Similar rankings in table are due to statistically similar Pq or Ps. *MIS4, MIS5, and MIS6 archaeological raw material frequencies from bootstrapped data in Figure 50 and Table 19.

Mobility rate and strategy

During MIS4 conditions heat-treated silcrete has a significantly higher net-return rate compared to both untreated silcrete and quartzite. Quartzite and untreated silcrete have statistically similar net-return rates (**Figure 121** and **Table 78;** raw data in **Supplementary Tables B213-B214)**.

Table 79 compares the MIS4 archaeological raw material frequencies from PP5-6 with ACM net-return rates resulting from MIS4 conditions when only the flake manufacturing time-cost (m_3 variable) is considered in the denominator part of the equation. The predicted relationship between flake manufacturing time-cost (m_3) and the mobility rate and strategy variable (**Figure 28**) during MIS4 conditions is not supported. The archaeological data show that quartzite and silcrete (83.1% of the silcrete has been heat-treated and 16.9% is untreated) have statistically similar frequencies during MIS4, while the highest ranked raw material during MIS4 is heat-treated silcrete (**Table 79**).

This result suggests that the higher cutting edge per mass outcome (*e* variable) of heat-treated silcrete and flake manufacture time-cost (m_3) do not explain raw material frequencies during MIS4 at Pinnacle Point. This result limits support for assertions made by Gould and Saggers (1985, 1985) that foragers select raw material specifically for their qualities.

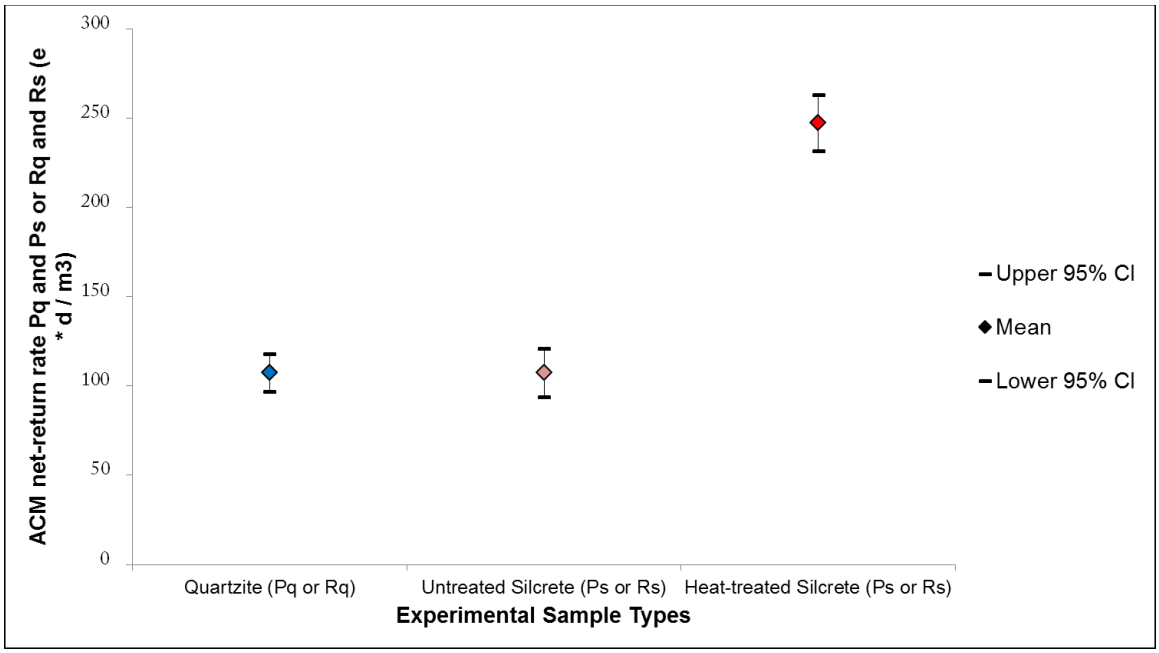

Figure 121. Plot with means and 95% confidence intervals showing the distribution of the ACM net-return rates (Pq and Ps or Rq and Rs) when only m_3 time-cost (flaking manufacturing time) is considered for all experimental sample types during MIS4 conditions. Star with capped whiskers is the mean with the 95% confidence interval (CI). The CI was created by bootstrapping the standard error 10000 times.

Table 78. Summary statistics and bootstrap test results of ACM net-return rates (Pq and Ps or Rq and Rs) when only m_3 time-cost (flaking manufacturing time) is considered for all experimental sample types during MIS4 conditions.

	Quartzite (Pq or Rq)	Untreated Silcrete (Ps or Rs)	Heat-treated Silcrete (Ps or Rs)
n sample blocks	20	8	8
First Quartile	86.028	88.235	233.500
Min	75.070	85.060	211.360
Median	105.880	104.400	248.285
Mean	107.491	107.438	247.501
Max	149.990	140.910	292.180
Third Quartile	130.755	125.798	259.445

SD	24.643	20.103	23.683
Bootstrapped SE*	5.345	6.887	8.013
Margin of error (95% CI)	10.475	13.499	15.706
Bootstrapped Upper 95% CI*	117.966	120.937	263.207
Bootstrapped Lower 95% CI*	97.015	93.938	231.795

*Samples bootstrapped 10000 times.

Table 79. Comparison between ranked raw materials resulting from testing predictions drawn from the mobility rate and strategy variable and archaeological data.

ACM Results-Ranked*			**Archaeological Raw Material Frequencies-MIS4**			
Quartzite	Untreated Silcrete	Heat-treated Silcrete	Quartzite	Silcrete Overall	Untreated Silcrete	Heat-treated Silcrete
2 (107.5)	***2*** (107.9)	***1*** (247.5)	(44.6%)	(40%)	16.9	83.1

[a] Ranking based on which raw materials have the highest mean Rq or Rs (in parenthesis). Similar rankings in table are due to statistically similar Rq or Rs.* MIS4 archaeological raw material frequencies from bootstrapped data in Figure 50 and Table 19.

ACM model condition variable results summary

The model outcomes under the three different model condition variables presented above show that the only predicted relationship that was supported was travel and search time-cost (t_s) explaining raw material frequencies during MIS5 conditions and MIS6 conditions without a Paleo-Agulhas plain silcrete source (**Table 80**). This suggests that during MIS5 and MIS6 the selection of quartzite was driven by the lower travel and search time-cost (t_s) of acquiring the quartzite. The low cost of quartzite was in turn affected by the position of the coastline and the distribution of raw material sources. During MIS6, if one assumes that no silcrete sources are present on the Paleo-Agulhas plain, the close proximity of an extensive cobble-rich wave-ravinement surface to Pinnacle Point lowered the travel and search cost for quartzite enough to increase the net-return rate above silcrete. When the coastline moved closer during MIS5 and was configured similarly to today's conditions, abundant cobble beaches kept the travel and search time-cost for quartzite low keeping the net-return rate of quartzite above silcrete.

While changes in coastline position and raw material source distribution explains raw material patterns during MIS5 and MIS6, the result shows that neither change in vegetation type or mobility rate and strategy directly explain the raw material frequencies during any Marine Isotope Stage at Pinnacle Point.

Table 80. Summary of whether model outcomes are the same as archaeological raw material frequencies

Model Condition Variable	Model Condition	Prediction Supported
Coastline Position and Raw Material Distribution	MIS4 without a Paleo-Agulhas Silcrete Source	Not Supported
Coastline Position and Raw Material Distribution	MIS4 with a Paleo-Agulhas Silcrete Source	Not Supported
Coastline Position and Raw Material Distribution	MIS5	Supported
Coastline Position and Raw Material Distribution	MIS6 without a Paleo-Agulhas Silcrete Source	Supported
Coastline Position and Raw Material Distribution	MIS6 with a Paleo-Agulhas Silcrete Source	Not Supported
Vegetation Type	MIS4-Exposed	Not Supported
Vegetation Type	MIS4-Insulated	Not Supported
Vegetation Type	MIS5-Exposed	Not Supported
Vegetation Type	MIS5-Insulated	Not Supported
Vegetation Type	MIS6-Exposed	Not Supported
Vegetation Type	MIS6-Insulated	Not Supported
Mobility Rate and Strategy	MIS4	Not Supported

During MIS4 conditions with or without a Paleo-Agulhas plain silcrete source, travel and search time-cost (t_s) does not explain the raw material frequency pattern at Pinnacle Point. The model predicts more heat-treated silcrete than is observed in the archaeological record. The pattern observed during MIS4 is not explained by a change in vegetation type either. The lower time-cost accrued by traveling and searching for wood fuel (m_1) to heat-treat silcrete and the act of heat-treatment (m_2) regardless of method (exposed or insulated) during MIS4 conditions do not increase the net-return rate of heat-

treated silcrete above quartzite. The model outcome, in fact, predicts that quartzite and untreated silcrete should be equally represented in the archaeological record, which is not the case; heat-treated silcrete and quartzite have statistically similar frequencies. The MIS4 pattern is also not explained by a change in mobility rate and strategy. The lower cost of flake manufacturing of heat-treated silcrete and the higher output of cutting edge per mass (*e* variable) from heat-treated silcrete results in the model predicting more heat-treated silcrete than what is observed in the archaeological record.

ACM sensitivity analysis – Changing assumed currency

The results above show that neither the ACM-P (sequential encounter and embedded procurement; travel and search cost not included) nor ACM-R (simultaneous encounter and direct procurement; travel and search cost is included) explains the raw material frequency patterns observed in MIS4 with or without a Paleo-Agulhas plain silcrete source. A common explanation for why an Optimal Foraging Theory (OFT) model does not explain an observed pattern is that the assumed currency that the forager is seeking to rate maximize is incorrect (Stephens and Krebs 1986, Bird and O'Connell 2006). Given that neither ACM-P nor the ACM-R explains the raw material pattern during MIS4 when the original currency is used, below the result evaluating both hypotheses again using two different alternative currencies will be presented.

The first alternative currency assumes that the forager seeks to maximize available cutting edge of blades produced multiplied by the duration of use before dulling (cutting edge of complete blades (cm) / total flaked core mass (kg) * *d* (minutes)). In other words, the forager seeks to maximize the amount of cutting edge of blades made

from a core mass, and the forager wants the cutting edge on those blades to last as long as possible. The second alternative currency assumes that the forager seeks to maximize the amount of produced blades for a given raw material mass, and that the forager wants the cutting edge on those blades to last as long as possible (count of complete blade (n=) /total flaked core mass (kg) * *d* (minutes)).

Both these currencies are plausible due to the increase in blade production in MIS4 at PP5-6 and the fact that a majority of the blades during MIS4 are made on silcrete (see *Chapter 7*) (Brown et al. 2012, Brown et al. 2009, Wilkins et al. 2017). Below first the ACM-P and ACM-R net-return rates for the two alternative currencies are presented. The net-return rates are used to create rankings that are compared to the archaeological raw material frequencies. This comparison is used to test Hypothesis 2 and 3. This is followed by a presentation of the model outcomes under the different model condition variables to understand whether changes in individual time-costs drive the net-return rates, in turn explaining the archaeological raw material frequencies at Pinnacle Point.

Maximizing cutting edge of complete blades per mass multiplied by duration of use before dulling

ACM-P net-return rates – Testing Hypothesis 2

As with the original currency when looking across all model conditions quartzite and untreated silcrete have significantly higher net-return rates than either type of heat-treated silcrete (exposed and insulated) (**Figure 122** and **Supplementary Table B215**). Under MIS4 conditions the net-return rate of insulated silcrete is significantly higher than exposed silcrete, while under MIS5 and MIS6 conditions the net-return rates of exposed

silcrete are significantly higher than insulated silcrete (**Supplementary Tables B216-B219** show the raw data for each experimental raw material block).

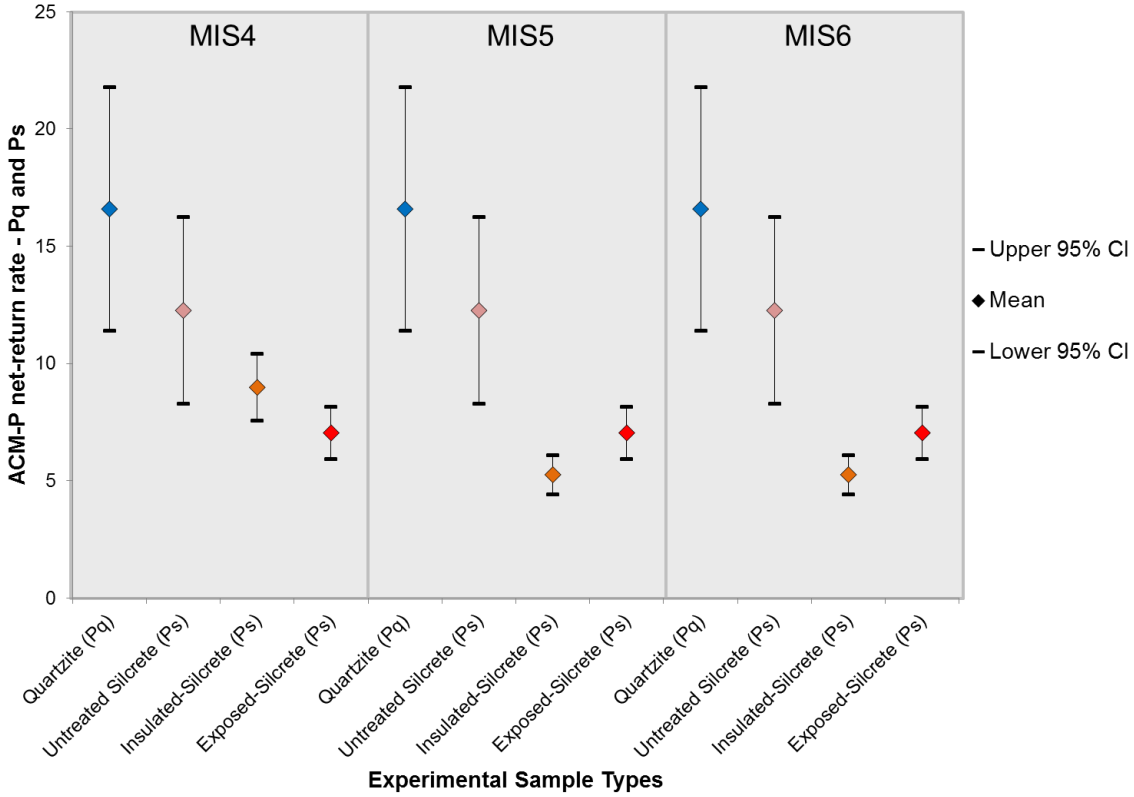

Figure 122. Plot with means and 95% confidence intervals showing the distribution of the ACM-P net-return rates (for all experimental sample types) during MIS4, MIS5, and MIS6 conditions. Star with capped whiskers is the mean with the 95% confidence intervals (CI). The CI was created by bootstrapping the standard error 10000 times.

Table 81 shows the ranking of raw materials based on the overall ACM-P net-return rates compared to the archaeological frequencies under different model conditions. For Hypothesis 2 (H_2) to be supported, the raw material with the highest rank based on net-return rate should be same as the raw material with the highest frequency, and so forth. During both MIS6 and MIS5 quartzite has the highest frequencies at Pinnacle Point, which does not match the tied ranking of quartzite and untreated silcrete (**Table 81**). During MIS4 quartzite and silcrete have statistically similar frequencies, which do

match the tied ranking of quartzite and untreated silcrete based on net-return rates (**Table 81**). However, the archaeological data show that 83.1% of the silcrete is heat-treated.

Therefore, while the ACM-P net-return rates can explain the dual selection of quartzite and untreated silcrete it does not explain why you would heat-treat the silcrete. These results are the same as when using the original currency. Compared to the original currency, the net-return rates of untreated silcrete and both types of heat-treated silcrete have moved closer to each other.

Table 81. Comparison between a raw material ranking based on ACM-P net-return rates and archaeological data from MIS4, MIS5, and MIS6.

ACM-P Results-Ranked*				Archaeological Data			
MIS4				**MIS4**			
Quartzite	Untreated Silcrete	Insulated-Silcrete	Exposed-Silcrete	Quartzite (%)	Silcrete Overall (%)	Untreated Silcrete (%)	Heat-treated Silcrete (%)
1 (16.6)	***1.5*** (12.3)	***1.5*** (9)	***2*** (7)	44.6*	40*	16.9	83.1
MIS5				**MIS5**			
Quartzite	Untreated Silcrete	Insulated-Silcrete	Exposed-Silcrete	Quartzite (%)	Silcrete Overall (%)	Untreated Silcrete (%)	Heat-treated Silcrete (%)
1 (16.6)	***1*** (12.3)	***2*** (5.3)	***2*** (7)	77.2	13.1	11.6	88.4
MIS6				**MIS6**			
Quartzite	Untreated Silcrete	Insulated-Silcrete	Exposed-Silcrete	Quartzite (%)	Silcrete Overall (%)	Untreated Silcrete (%)	Heat-treated Silcrete (%)
1 (16.6)	***1*** (12.3)	***2*** (5.3)	***2*** (7)	94.3	1.1	NA	NA

* Ranking based on which raw materials have the highest mean Rq or Rs (in parenthesis). Similar rankings in the table are due to statistically similar Pq or Ps. MIS4, MIS5, MIS6 archaeological raw material frequencies from bootstrapped data in Figure 50 and Table 19.

As with the original currency, taken together, the ACM-P net-return rates show no support for Hypothesis 2 (H_2). The lack of support for H_2 limits the support for a scenario where during embedded procurement a forager strategically select raw material and produce blades with the highest net-return of cm*min cutting edge on blades.

Nevertheless, the ACM-R variant can still explain the raw material frequency pattern. In the ACM-R the time-cost resulting from travel and search for a raw material is included.

ACM-R net-return rates – Testing Hypothesis 3

During MIS4 conditions without a Paleo-Agulhas plain silcrete source both types of heat-treated silcrete (exposed and insulated) have the highest net-return rates that are statistically similar (**Figure 123** and **Supplementary Table B220**; raw data in **Supplementary Tables B221-B222)**, whereas during MIS4 conditions with at Paleo-Agulhas plain silcrete source untreated silcrete, and both types of heat-treated silcrete (exposed and insulated) have the highest net-return rates that are statistically similar (**Supplementary Table B220**; raw data in **Supplementary B221** and **B223)**.

MIS5 condition model outcomes show that quartzite has the highest net-return rate while both types of heat-treated silcrete (exposed and insulated) have the second highest net-return rates, which are statistically similar (**Figure 123** and **Supplementary Table B220**; raw data in **Supplementary Tables B224-B225**).

Model outcomes from MIS6 conditions without a Paleo-Agulhas plain silcrete source show that quartzite and both types of heat-treated silcrete (exposed and insulated) have the highest net-return rates, which all are statistically similar (**Figure 123** and **Supplementary Table B220**; raw data in **Supplementary Tables B226-B227**). During MIS6 conditions with a Paleo-Agulhas plain silcrete source, untreated silcrete and silcrete heat-treated using the exposed method have the highest net-return rates, which are statistically similar. However, their net-return rates are also statistically similar to silcrete

heat-treated using the insulated method and quartzite (**Figure 123** and **Supplementary Table B220**; raw data in **Supplementary Tables B226** and **B228**).

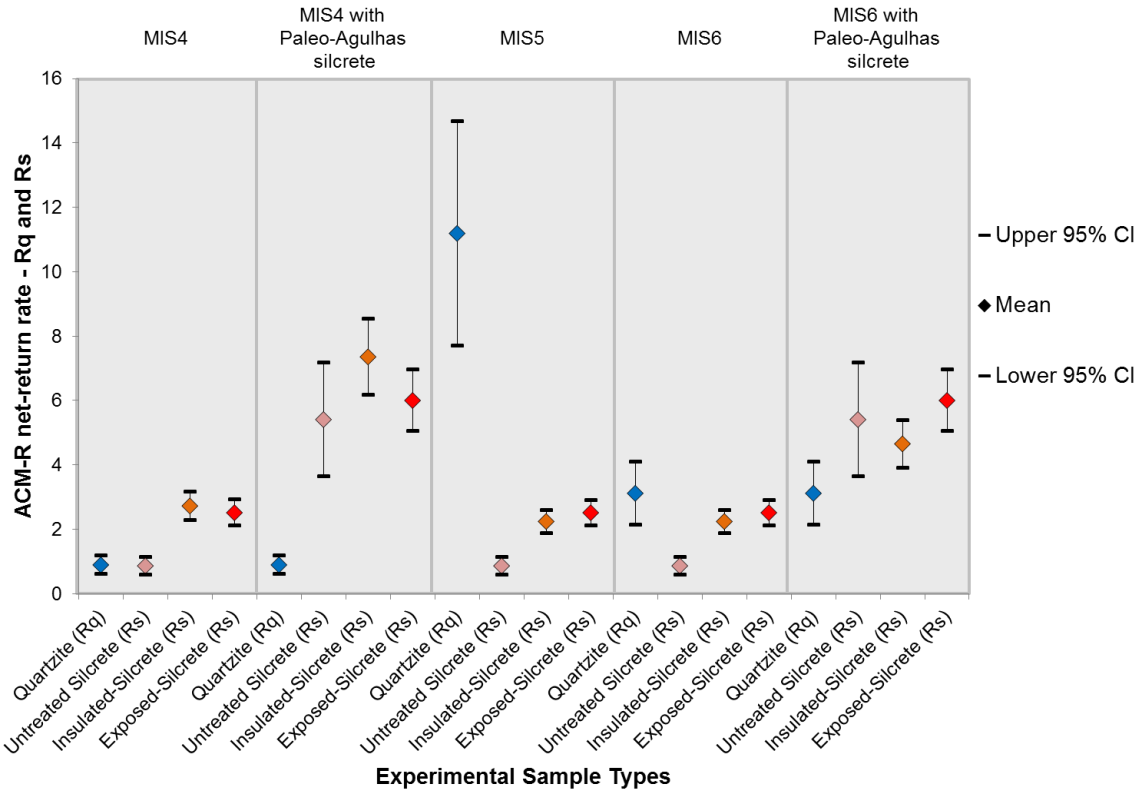

Figure 123. Plot with means and 95% confidence intervals showing the distribution of the ACM-R net-return rates (for all experimental sample types) during all model conditions. Star with capped whiskers is the mean with the 95% confidence intervals (CI). The CI was created by bootstrapping the standard error 10000 times.

Table 82 shows the ranking of raw materials based on the overall ACM-R net-return rates compared to the archaeological frequencies under different model conditions. For Hypothesis 3 (H_3) to be supported, the raw material with the highest rank based on net-return rate should be same as the raw material with the highest frequency, and so forth. Hypothesis 3 is only supported by the result from MIS5 conditions. During MIS4 and MIS6 conditions, the archaeological raw material frequencies do not match the raw material rankings.

Table 82. Comparison between a raw material ranking based on ACM- R net-return rates and archaeological data from MIS4, MIS5, and MIS6.

ACM-R Results-Ranked*				Archaeological Data			
MIS4 without a Paleo-Agulhas plain silcrete source				**MIS4**			
Quartzite	Untreated Silcrete	Insulated -Silcrete	Exposed-Silcrete	Quartzite (%)	Silcrete Overall (%)	Untreated Silcrete (%)	Heat-treated Silcrete (%)
2 (0.9)	***2*** (0.9)	***1*** (2.7)	***1*** (2.5)	44.6*	40*	16.9	83.1
MIS4 with a Paleo-Agulhas plain silcrete source				**MIS4**			
Quartzite	Untreated Silcrete	Insulated -Silcrete	Exposed-Silcrete	Quartzite (%)	Silcrete Overall (%)	Untreated Silcrete (%)	Heat-treated Silcrete (%)
2 (0.9)	***1*** (5.4)	***1***(7.4)	***1*** (6)	44.6*	40*	16.9	83.1
MIS5				**MIS5**			
Quartzite	Untreated Silcrete	Insulated -Silcrete	Exposed-Silcrete	Quartzite (%)	Silcrete Overall (%)	Untreated Silcrete (%)	Heat-treated Silcrete (%)
1 (11.2)	***3*** (0.9)	***2*** (2.2)	***2*** (2.5)	77.2	13.1	11.6	88.4
MIS6 without a Paleo-Agulhas plain silcrete source				**MIS6**			
Quartzite	Untreated Silcrete	Insulated -Silcrete	Exposed-Silcrete	Quartzite (%)	Silcrete Overall (%)	Untreated Silcrete (%)	Heat-treated Silcrete (%)
1 (3.1)	***2*** (0.9)	***1*** (2.2)	***1*** (2.5)	94.3	1.1	NA	NA
MIS6 with a Paleo-Agulhas plain silcrete source				**MIS6**			
Quartzite	Untreated Silcrete	Insulated -Silcrete	Exposed-Silcrete	Quartzite (%)	Silcrete Overall (%)	Untreated Silcrete (%)	Heat-treated Silcrete (%)
1.5 (3.1)	***1*** (5.4)	***1*** (4.7)	***1*** (6)	94.3	1.1	NA	NA

*Ranking based on which raw materials have the highest mean Rq or Rs (in parenthesis). Similar rankings in the table are due to statistically similar Rq or Rs. MIS4, MIS5, and MIS6 archaeological raw material frequencies from bootstrapped data in Figure 50 and Table 19.

What the support for H_3 during MIS5 conditions minimally suggests is that the foragers are strategically selecting the raw material with the highest net-return of cm*min cutting edge that is available in the environment. This result suggests that raw materials played an important role the overall technological organization because raw materials were procured at an added cost. The direct procurement of raw materials suggests planning of activities because the procurement of the raw materials had to be integrated

into the overall mobility strategy. Thus, the result suggests that during MIS5 a part of the response to climatic and environmental conditions was to utilize specific stone raw materials obtained during direct procurement trips (c.f. Gould, 1985; Gould and Saggers, 1985) and to manufacture technology to obtain food resources and/or perform processing tasks. This, in turn, suggests increased knowledge about raw material properties and how to best use the raw materials.

Hypothesis 2 and 3 evaluation summary

The ranking of ACM-P net-return rates did not match the archaeological frequencies during any model conditions, which limits support for Hypothesis 2. However, there is support for Hypothesis 3 during MIS5 conditions. This suggests that quartzite was strategically selected during MIS5 due to having the highest net-return rate of cutting edge per mass on blades multiplied by the duration that the edges of those blades last before dulling. This result suggests that both the original currency (cutting edge per mass on all stone tool types multiplied by the duration that the edges on those stone tools last before dulling) and this alternative currency can explain the raw material frequencies in the MIS5 record at Pinnacle Point. This result, as with the orginal currency, supports the 'Utilitarian' model of raw material selection and change (c.f. Mackay 2008).

Next follows the presentation of the model outcomes under the different model conditions variables (coastline positions and raw material source distribution, vegetation type, and mobility rate and strategy) to understand whether changes in individual time-costs drive the net-return rates and thus explain the archaeological raw material frequencies. First, net-return rates from the different model condition variables are

presented, which allows for a ranking that can be used compare to archaeological frequencies. Then, the comparison to the archaeological frequencies allows for testing predicted relationships between time-costs and model condition variables presented in *Chapter 5*.

ACM – Model condition variable outcomes

Coastline position and raw material source distribution

Heat-treated silcrete have the highest net-return during MIS4 conditions with or without a Paleo-Agulhas plain silcrete source, while untreated silcrete and quartzite have statistically similar frequencies (**Supplementary Figure A16** and **Supplementary Table B229**; Raw data from MIS 4 conditions without a Paleo-Agulhas plain silcrete source: **Supplementary Tables B230-B231**; MIS 4 conditions with a Paleo-Agulhas plain silcrete source: **Supplementary Tables B232-B233**).

During MIS5 conditions quartzite has the highest net-return rate followed by heat-treated silcrete (**Supplementary Figure A16** and **Supplementary Table B229;** MIS5 conditions raw data: **Supplementary Tables B234-B235**).

Quartzite and heat-treated silcrete have statistically similar net-return rates during MIS6 conditions without a Paleo-Agulhas plain silcrete source, while during MIS6 conditions with a Paleo-Agulhas plain silcrete source heat-treated silcrete has the highest net-return rate. Quartzite and untreated silcrete have statistically similar net-return rates (**Supplementary Figure A16** and **Supplementary Table B229**; MIS6 conditions without a Paleo-Agulhas plain silcrete source raw data in **Supplementary Tables B236-**

B237; MIS6 conditions with a Paleo-Agulhas plain silcrete source: **Supplementary Tables B238-B239**).

A comparison to the archaeological frequency data shows that the predicted relationships between travel and search time-cost (t_s) and coastline position and raw material source distribution (with: **Figure 25;** without: **Figure 26**) during MIS4 conditions with or without a Paleo-Agulhas plain silcrete source are not supported. The archaeological frequency data show that quartzite and silcrete have statistically similar frequencies, while the model ranking shows that heat-treated silcrete has the highest frequency (**Supplementary Table B240**). This suggests that travel and search time-cost (t_s) does not explain raw material frequencies at Pinnacle Point during MIS4.

The predicted relationship (**Figure 25** and **Figure 26**) for MIS5 conditions is supported. The archaeological frequency data show that quartzite has the highest frequency while the highest ranked raw material is quartzite (**Supplementary Table B240**). This suggests that during MIS5 travel and search time-cost (t_s) explains the raw material frequencies at Pinnacle Point when using this alternative currency. This lends support to Torrence's (1989, 1983) argument that procurement cost of raw materials drive selection if the quality of the raw material that is selected is sufficiently good.

A comparison between the archaeological frequency data to the ranked raw materials from MIS6 conditions with or without a Paleo-Agulhas plain silcrete source shows that the predicted relationships (with: **Figure 25**; without: **Figure 26**) are not supported. The archaeological data show that quartzite has the highest frequency during MIS6, while the highest ranked raw material during MIS6 conditions with a Paleo-Agulhas plain silcrete source is heat-treated silcrete whereas during MIS6 conditions

without a Paleo-Agulhas silcrete source quartzite and heat-treated silcrete have the highest but statistically similar net-return rates (**Supplementary Table B240**). This suggests that travel and search time-cost does not explain raw material frequencies during MIS6 when using this alternative currency.

The results of testing the predicted relationships between travel and search time cost and the coastline position and raw material source distribution variable show that only during MIS5 conditions does travel and search time-cost (t_s) drives the net-return rates of raw materials so that it explains the archaeological raw material frequencies. When the coast is near during MIS5 conditions the t_s time-cost decreases enough for quartzite to drive the net-return rate above silcrete. In other words, the distribution of coastal cobble beaches in close vicinity to Pinnacle Point during MIS5 conditions facilitates decreased travel and search time to procure quartzite and this drives the selection of quartzite.

Vegetation type

During MIS4, MIS5, and MIS6 conditions quartzite and untreated silcrete have the highest net-return rates, and the net-return rates are statistically similar (**Supplementary Figure A17** and **Supplementary Table B241;** Raw data from MIS 4 conditions can be found in **Supplementary Tables B242**-**B243**; MIS5 and MIS6 conditions: **Supplementary Tables B242** and **B244**).

A comparison to the archaeological frequency data shows that the predicted relationship between wood fuel travel and search time-cost (m_1) and heat-treatment time-cost (m_2) and the vegetation type variable (**Figure 27**) during MIS4 conditions is not

supported. The archaeological raw material frequency data show that quartzite and silcrete (overall) have statistically similar raw material frequencies (**Supplementary Table B245**). However, 83.1% of the silcrete has been heat-treated and only 16.9% are untreated. This does not fit with the ranking, which shows statistically similar net-return rates for quartzite and untreated silcrete (**Supplementary Table B245**). This result suggests that wood fuel travel and search time-cost (m_1) and heat-treatment time-cost (m_2) do not explain the archaeological raw material frequencies at Pinnacle Point during MIS4 when using this alternative currency. A comparison between the archaeological frequency data to the ranked raw materials from MIS5 and MIS6 conditions show that the predicted relationships (**Figure 27**) are not supported. The archaeological data show that quartzite has the highest frequency during MIS5 and MIS6, while the highest ranked raw materials during MIS5 and MIS6 are quartzite and untreated silcrete that have statistically similar net-return rates (**Supplementary Table B245**). This result suggests that wood fuel travel and search time-cost (m_1) and heat-treatment time-cost (m_2) do not explain raw material frequencies during MIS5 and MIS6 when using this alternative currency. The result from all model condition again limits support for the "Wood-fuel availability" model proposed by Brown and Marean (2010).

Mobility rate and strategy

During MIS4 conditions heat-treated silcrete has the highest net-return rate followed by quartzite and untreated silcrete, which have statistically similar net-return rates **Supplementary Figure A18** and **Supplementary Table B246;** Raw data in **Supplementary Tables B247-B248)**.

A comparison between the archaeological frequency data to the ranked raw materials from MIS4 conditions shows that the predicted relationship between flake manufacturing time-cost (m_3) and the mobility rate and strategy variable (**Figure 28**) is not supported. The archaeological data show that quartzite and silcrete (overall; where 83.1% of the silcrete has been heat-treated and 16.9% is untreated) have statistically similar frequencies during MIS4, while the highest ranked raw material during MIS4 is heat-treated silcrete (**Supplementary Table B249**). This result suggests that the higher cutting edge per mass outcome (*e* variable) of heat-treated silcrete and flake manufacture time-cost (m_3) do not directly explain raw material frequencies during MIS4 at Pinnacle Point when using this alternative currency. Again, this result limits support for arguments made by Gould and Saggers (1985, 1985) that foragers select raw material specifically for their qualities.

ACM – Model condition variable outcomes summary

The model outcomes under the three different model condition variables presented above show that the only predicted relationship that was supported was travel and search time-cost (t_s) explaining raw material frequencies during MIS5 conditions. This suggests, similar to the Hypothesis 3 (H_3) evaluation using the original currency that during MIS5 the selection of quartzite was driven by the lower travel and search time-cost (t_s) of acquiring the quartzite. The low cost of quartzite was in turn affected by the position of the coastline and the distribution of raw material sources. As with the original currency, when using this alternative currency neither change in vegetation type or mobility rate and strategy explain the net-return rates of the raw materials.

As with the original currency, the results above show that when changing the currency to maximizing the amount of cutting edge per mass from blades multiplied by duration of use neither the ACM-P (sequential encounter and embedded procurement; travel and search cost not included) nor ACM-R (simultaneous encounter and direct procurement; travel and search cost is included) explain the raw material frequency patterns observed in MIS4 with or without a Paleo-Agulhas plain silcrete source. Below the currency is changed again to investigate whether a simpler currency where maximizing the number of blades produced per mass multiplied by the duration of use is what the forager is seeking when selecting raw materials.

Maximizing number of complete blades produced per core multiplied by duration of use before dulling

ACM-P net-return rates – Testing Hypothesis 2

During MIS 4 conditions the net-return rate of insulated silcrete is statistically similar to both quartzite and untreated silcrete, while exposed silcrete is statistically similar to insulated silcrete (**Figure 124** and **Tables 83**; raw data for MIS4 conditions in **Supplementary Tables B250-B251**). When looking at MIS5 and MIS 6 conditions quartzite and untreated silcrete have only significantly higher net-return rates than exposed silcrete, while insulated silcrete has the lowest net-return (**Figure 124** and **Table 83**; raw data for MIS5 conditions in **Supplementary Tables B250** and **B252**; MIS6 conditions: **Supplementary Tables B250** and **B253**).

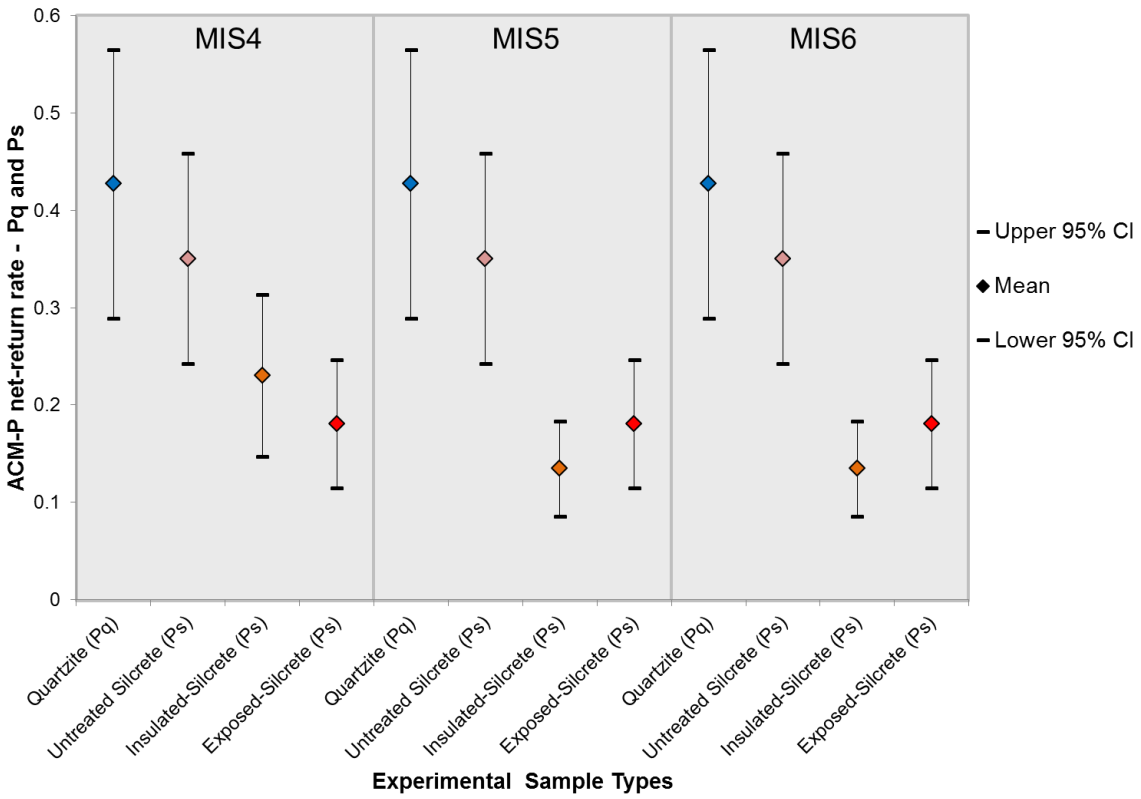

Figure 124. Plot with means and 95% confidence intervals showing the distribution of the ACM-P net-return rates for all experimental sample types during MIS4, MIS5, and MIS6 conditions. Star with capped whiskers is the mean with the 95% confidence interval (CI). The CI was created by bootstrapping the standard error 10000 times.

Table 83. Summary statistics and bootstrap test results of ACM-P net-return rates (for all experimental sample types during MIS4, MIS5, and MIS6 conditions.

	MIS4				MIS5				MIS6			
	Quartzite (Pq)	Untreated Silcrete (Ps)	Insulated-Silcrete (Ps)	Exposed-Silcrete (Ps)	Quartzite (Pq)	Untreated Silcrete (Ps)	Insulated-Silcrete (Ps)	Exposed-Silcrete (Ps)	Quartzite (Pq)	Untreated Silcrete (Ps)	Insulated-Silcrete (Ps)	Exposed-Silcrete (Ps)
n sample blocks	20	8	8	8	20	8	8	8	20	8	8	8

First Quartile	0.161	0.191	0.106	0.083	0.161	0.191	0.062	0.083	0.161	0.191	0.062	0.083
Min	0.000	0.170	0.067	0.052	0.000	0.170	0.039	0.052	0.000	0.170	0.039	0.052
Median	0.374	0.340	0.233	0.183	0.374	0.340	0.137	0.183	0.374	0.340	0.137	0.183
Mean	0.427	0.351	0.230	0.181	0.427	0.351	0.135	0.181	0.427	0.351	0.135	0.181
Max	1.150	0.595	0.422	0.331	1.150	0.595	0.247	0.331	1.150	0.595	0.247	0.331
Third Quartile	0.706	0.489	0.339	0.266	0.706	0.489	0.198	0.266	0.706	0.489	0.198	0.266
Standard Deviation	0.326	0.160	0.124	0.098	0.326	0.160	0.073	0.098	0.326	0.160	0.073	0.098
Bootstrapped SE*	0.070	0.055	0.042	0.034	0.070	0.055	0.025	0.034	0.070	0.055	0.025	0.034
Margin of error (95% CI)	0.138	0.108	0.083	0.066	0.138	0.108	0.049	0.066	0.138	0.108	0.049	0.066
Bootstrapped Upper 95% CI*	0.565	0.458	0.314	0.247	0.565	0.458	0.184	0.246	0.565	0.458	0.184	0.246
Bootstrapped Lower 95% CI*	0.289	0.243	0.147	0.115	0.289	0.243	0.086	0.115	0.289	0.243	0.086	0.115

*Samples bootstrapped 10000 times.

Table 84 shows the comparison between the ranking of raw material based on net-return rates and archaeological raw material frequencies. For Hypothesis 2 (H_2) to be supported, the raw material with the highest rank based on net-return rate should be the same as the raw material with the highest frequency, and so forth.

Table 84. Comparison between a raw material ranking based on ACM- P net-return rates and archaeological data from MIS4, MIS5, and MIS6.

ACM-P Results-Ranked				Archaeological Data			
MIS4				**MIS4**			
Quartzite	Untreated Silcrete	Insulated-Silcrete	Exposed-Silcrete	Quartzite (%)	Silcrete Overall (%)	Untreated Silcrete (%)	Heat-treated Silcrete (%)
1 (0.4)	***1*** (0.4)	***1*** (0.2)	***1.5*** (0.2)	44.6*	40*	16.9	83.1
MIS5				**MIS5**			
Quartzite	Untreated Silcrete	Insulated-Silcrete	Exposed-Silcrete	Quartzite (%)	Silcrete Overall (%)	Untreated Silcrete (%)	Heat-treated Silcrete (%)
1 (0.4)	***1*** (0.4)	***2*** (0.1)	***1.5*** (0.2)	77.2	13.1	11.6	88.4
MIS6				**MIS6**			
Quartzite	Untreated Silcrete	Insulated-Silcrete	Exposed-Silcrete	Quartzite (%)	Silcrete Overall (%)	Untreated Silcrete (%)	Heat-treated Silcrete (%)
1 (0.4)	***1*** (0.4)	***2*** (0.1)	***1.5*** (0.2)	94.3	1.1	NA	NA

*Ranking based on which raw materials have the highest mean Rq or Rs (in parenthesis). Similar rankings in the table are due to statistically similar Pq or Ps. MIS4, MIS5, and MIS6 archaeological raw material frequencies from bootstrapped data in Figure 50 and Table 19.

During both MIS6 and MIS5, quartzite has the highest frequencies at PP, which does not match the tied ranking of quartzite and untreated silcrete (**Table 84**). However, during MIS4 quartzite and silcrete have statistically similar frequencies where heat-treated silcrete accounts for 83.1% of the silcrete. The tied ranking based on net-return rates of quartzite, untreated silcrete, and insulated silcrete matches the archaeological frequencies (**Table 84**). Therefore, under the assumption that the forager seeks to maximize the amount of blades produced from a given core and the forager wants those blades to last as long as possible in terms of edge durability, the ACM-P net-return rates

can explain the dual selection of quartzite and silcrete during MIS4 conditions at Pinnacle Point.

As with the original currency and the first alternative currency, the ACM-P net-return rates show no support for Hypothesis 2 (H_2) during MIS5 or MIS6 conditions. However, the ACM-P results do support H_2 during MIS4 conditions. The support for H_2 during MIS4 indicates a scenario where during embedded procurement where other life style constraints (for example, foraging for food resources, social interactions) control the mobility strategy and foraging movement a forager strategically selects a raw material that could produce the highest net-return of produced blades per core multiplied by duration of use when encountered. Thus, support for H_2 suggests that the response to climatic and environmental conditions during MIS4 was relatively complex. There was a need for a mobility system that targeted food resources (disregarding the location of lithic raw material sources) that at the same time relied on investment in specific stone raw materials and technology that could be used to extract such resources. Given this positive result, can support for Hypothesis 3 (H_3) also be found for MIS4 conditions using the same alternative currency?

ACM-R net-return rates -Testing Hypothesis 3

Figure 125 shows that during MIS4 conditions without a Paleo-Agulhas plain silcrete source that both types of heat-treated silcrete (exposed and insulated) have the highest net-return rates that are statistically similar (**Supplementary Table B254**; raw data in **Supplementary Tables B255-B256)**, whereas during MIS4 conditions with at Paleo-Agulhas plain silcrete source untreated silcrete, and both types of heat-treated silcrete

(exposed and insulated) have the highest net-return rates that are statistically similar (**Supplementary Table B254**; raw data in **Supplementary Tables B255** and **B257)**.

During MIS5 conditions quartzite has the highest net-return rate while both types of heat-treated silcrete (exposed and insulated) have the second highest net-return rates, which are statistically similar (**Figure 125** and **Supplementary Table B254**; raw data in **Supplementary Tables B258-B259**).

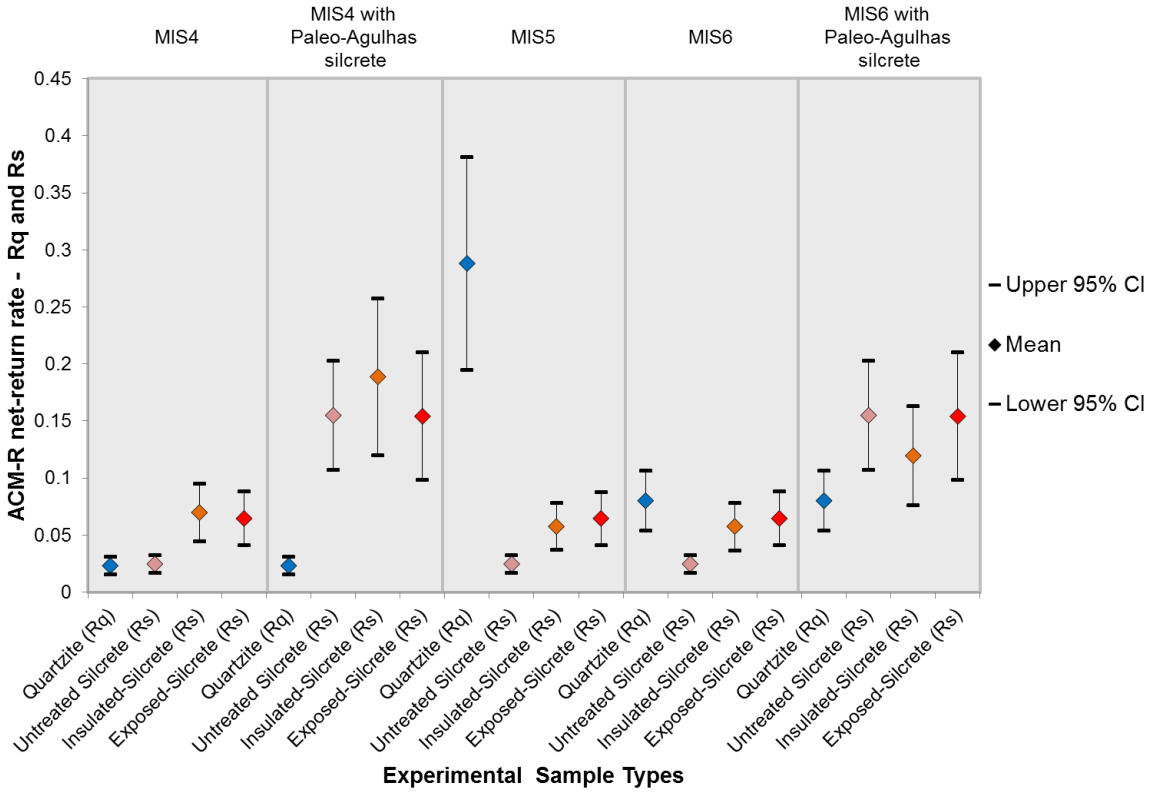

Figure 125. Plot with means and 95% confidence intervals showing the distribution of the ACM-R net-return rates (for all experimental sample types) during all model conditions. Star with capped whiskers is the mean with the 95% confidence intervals (CI). The CI was created by bootstrapping the standard error 10000 times.

Model outcomes from MIS6 conditions without a Paleo-Agulhas plain silcrete source show that quartzite and both types of heat-treated silcrete (exposed and insulated) have the highest net-return rates, which all are statistically similar (**Figure 125** and

Supplementary Table B254; raw data in **Supplementary Tables B260-B261**). During MIS6 conditions with a Paleo-Agulhas plain silcrete source, untreated silcrete and silcrete heat-treated using the exposed method have the highest net-return rates, which are statistically similar. However, their net-return rates are also statistically similar to silcrete heat-treated using the insulated method and quartzite (**Figure 125** and **Supplementary Table B254**; raw data in **Supplementary Tables B260** and **B262**).

Table 85 shows the ranking of raw materials based on the overall ACM-R net-return rates compared to the archaeological frequencies under different model conditions. For Hypothesis 3 (H_3) to be supported, the raw material with the highest rank based on net-return rate should be same as the raw material with the highest frequency, and so forth. Similar to the evaluation using the first alternative currency, Hypothesis 3 is only supported by the result from MIS5 conditions. During MIS4 and MIS6 conditions, the archaeological raw material frequencies do not match the raw material rankings.

Again there is support for H_3 during MIS5 conditions, which minimally suggests that the foragers are strategically selecting the raw material with the highest net-return of cm*min cutting edge that is available in the environment. As with the original and first alternative currency, this result suggests that raw materials played an important role the overall technological organization because raw materials were procured at an added cost. Further, the direct procurement of raw materials suggests planning of activities because the procurement of the raw materials had to be integrated into the overall mobility strategy. Thus, the result suggests that during MIS5 a part of the response to climatic and environmental conditions was to utilize specific stone raw materials obtained during direct procurement trips and to manufacture technology to obtain food resources and/or

perform processing tasks. This, in turn, suggests increased knowledge about raw material properties and how to best use the raw materials.

Table 85. Comparison between a raw material ranking based on ACM- R net-return rates and archaeological data from MIS4, MIS5, and MIS6.

ACM Results-Ranked*				Archaeological Data			
MIS4 without a Paleo-Agulhas plain silcrete source				**MIS4**			
Quartzite	Untreated Silcrete	Insulated -Silcrete	Exposed-Silcrete	Quartzite (%)	Silcrete Overall (%)	Untreated Silcrete (%)	Heat-treated Silcrete (%)
2 (0.02)	***2*** (0.02)	***1*** (0.07)	***1*** (0.06)	44.6*	40*	16.9	83.1
MIS4 with a Paleo-Agulhas plain silcrete source				**MIS4**			
Quartzite	Untreated Silcrete	Insulated -Silcrete	Exposed-Silcrete	Quartzite (%)	Silcrete Overall (%)	Untreated Silcrete (%)	Heat-treated Silcrete (%)
3 (0.02)	***1*** (0.2)	***1*** (0.2)	***1*** (0.2)	44.6*	40*	16.9	83.1
MIS5				**MIS5**			
Quartzite	Untreated Silcrete	Insulated -Silcrete	Exposed-Silcrete	Quartzite (%)	Silcrete Overall (%)	Untreated Silcrete (%)	Heat-treated Silcrete (%)
1 (0.3)	***3*** (0.02)	***2*** (0.06)	***2*** (0.06)	77.2	13.1	11.6	88.4
MIS6 without a Paleo-Agulhas plain silcrete source				**MIS6**			
Quartzite	Untreated Silcrete	Insulated -Silcrete	Exposed-Silcrete	Quartzite (%)	Silcrete Overall (%)	Untreated Silcrete (%)	Heat-treated Silcrete (%)
1 (0.08)	***2*** (0.02)	***1*** (0.06)	***1*** (0.6)	94.3	1.1	NA	NA
MIS6 with a Paleo-Agulhas plain silcrete source				**MIS6**			
Quartzite	Untreated Silcrete	Insulated -Silcrete	Exposed-Silcrete	Quartzite (%)	Silcrete Overall (%)	Untreated Silcrete (%)	Heat-treated Silcrete (%)
1.5 (0.08)	***1*** (0.2)	***1.5*** (0.1)	***1*** (0.2)	94.3	1.1	NA	NA

*Ranking based on which raw materials have the highest mean Rq or Rs (in parenthesis). Similar rankings in the table are due to statistically similar Rq or Rs. MIS4, MIS5, and MIS6 archaeological raw material frequencies from bootstrapped data in Figure 50 and Table 19.

Hypothesis 2 and 3 evaluation summary

The results above show that only during MIS5 as with the first alternative currency does the raw material ranking made from ACM-R net-return rates match the archaeological frequencies, which supports Hypothesis 3 (H_3). This result suggests that both the original currency (cutting edge per mass on all stone tool types multiplied by the duration that the edges on those stone tools last before dulling) and both alternative currencies can explain

the raw material frequencies in the MIS5 record at Pinnacle Point. Again, this result supports the 'Utilitarian' model of raw material selection and change (c.f. Mackay 2008). However, as with the original currency and the first alternative currency, the results above show that when changing the currency to maximizing the amount blades produced per core mass multiplied by the duration that the edges of those blades last before dulling the ACM-R does not explain the raw material frequency patterns observed in the MIS4 record at Pinnacle Point.

However, compared to evaluations of Hypothesis 2 (H_2) using the original currency or the first alternative currency, when the currency (maximizing the number of blades produced per core mass multiplied by the duration that the edges of those blades last before dulling) was changed again the ranking of ACM-P net-return rates during MIS4 conditions does match the raw material frequency pattern observed during MIS4 at Pinnacle Point. This supports Hypothesis 2. Further, this result supports the 'Utilitarian' model of raw material selection and change (c.f. Mackay 2008). Additionally, it suggests encounters of raw material sources during embedded procurement (c.f. Binford 1979).

As with the first alternative currency, next follows the presentation of the model outcomes under the different model conditions variables to understand whether changes in individual time-costs drive the raw material net-return rates, in turn explaining the material frequencies at Pinnacle Point. First, net-return rates from the different model condition variables are presented, which allows for a ranking that can be used compare to archaeological frequencies. Then, the comparison to the archaeological frequencies allows for testing of predicted relationships between time-costs and model condition variables presented in *Chapter 5*.

ACM - Model condition variable outcomes

Coastline position and raw material source distribution

Heat-treated silcrete have the highest net-return during MIS4 conditions with or without a Paleo-Agulhas plain silcrete source, while untreated silcrete and quartzite have statistically similar frequencies (**Supplementary Figure A19** and **Supplementary Table B263**; Raw data from MIS 4 conditions without a Paleo-Agulhas plain silcrete source: **Supplementary Tables B264-B265**; MIS 4 conditions with a Paleo-Agulhas plain silcrete source: **Supplementary Tables B264** and **B266**).

During MIS5 conditions quartzite has the highest net-return rate followed by heat-treated silcrete (**Supplementary Figure A19** and **Supplementary Table B263;** raw data in **Supplementary Tables B267-B268**).

Quartzite and heat-treated silcrete have statistically similar net-return rates during MIS6 conditions without a Paleo-Agulhas plain silcrete source, while during MIS6 conditions with a Paleo-Agulhas plain silcrete source heat-treated silcrete has the highest net-return rate followed by quartzite and untreated silcrete that have statistically similar net-return rates (**Supplementary Figure A19** and **Supplementary Table B263**; MIS6 conditions without a Paleo-Agulhas plain silcrete source raw data in **Supplementary Tables B269-B270**; MIS6 conditions with a Paleo-Agulhas plain silcrete source: **Supplementary Tables B269** and **B271**).

A comparison to the archaeological frequency data shows that the predicted relationships between travel and search time-cost (t_s) and the coastline position and raw material source distribution variable during MIS4 conditions with or without a Paleo-Agulhas plain silcrete source is not supported (with: **Figure 25;** without: **Figure 26**). The

archaeological frequency data show that quartzite and silcrete have statistically similar frequencies, while the model ranking shows that heat-treated silcrete has the highest frequency (**Supplementary Table B272**). This suggests that travel and search time-cost (t_s) does not explain archaeological raw material frequencies during MIS4 at Pinnacle Point when using this alternative currency.

The predicted relationship (**Figure 25** and **Figure 26**) for MIS5 conditions is supported. The archaeological frequency data show that quartzite has the highest frequency while the highest ranked raw material is quartzite (**Supplementary Table B272**). This suggests that during MIS5 travel and search time-cost (t_s) explains archaeological raw material frequencies in the MIS4 record at Pinnacle Point when using this alternative currency. As with original currency and the first alternative currency this result supports the assertion made by Torrence's (1989, 1983) that the cost of procurement explains why raw materials are selected if the quality of the raw material is good enough.

The predicted relationships (with: **Figure 25**; without: **Figure 26**) for MIS6 conditions with or without a Paleo-Agulhas plain silcrete source are not supported. A comparison between the archaeological frequency data to the ranked raw materials show that quartzite has the highest frequency during MIS6 at Pinnacle Point, while the highest ranked raw material during MIS6 conditions with a Paleo-Agulhas plain silcrete source is heat-treated silcrete whereas during MIS6 conditions without a Paleo-Agulhas silcrete source quartzite and heat-treated silcrete have statistically similar net-return rates (**Supplementary Table B272**). This suggests that travel and search time-cost does not

explain archaeological raw material frequencies during MIS6 at Pinnacle Point when using this alternative currency.

Similar to using the first alternative currency, the results of testing the predicted relationships between the travel and search time-cost (t_s) and the coastline position and raw material source distribution variable show that only during MIS5 conditions does travel and search time-cost (t_s) explain the archaeological raw material frequencies at Pinnacle Point. When the coast is near during MIS5 conditions the t_s time-cost decreases enough for quartzite to drive the net-return rate above silcrete. In other words, the distribution of coastal cobble beaches in close vicinity to Pinnacle Point during MIS5 conditions facilitates decreased travel and search time to procure quartzite and this drives the selection of quartzite.

Vegetation type

During MIS4, MIS5, and MIS6 conditions quartzite and untreated silcrete have the highest net-return rates, and the net-return rates are statistically similar. Both types of heat-treated silcrete (exposed and insulated) have statistically similar net-return rates during all model conditions (**Supplementary Figure A20** and **Supplementary Table B273;** Raw data from MIS 4 conditions can be found in **Supplementary Tables B274-B275**; MIS5 raw data in **Supplementary Tables B274** and **B276**; MIS6 raw data in **Supplementary Tables B274** and **B277**).

A comparison to the archaeological frequency data shows that the predicted relationship between wood fuel travel and search time-cost (m_1) and heat-treatment time-cost (m_2) and the vegetation type variable (**Figure 27**) during MIS4 conditions is not

supported. The archaeological raw material frequency data show that quartzite and silcrete (83.1% of the silcrete has been heat-treated and only 16.9% are untreated) have statistically similar raw material frequencies (**Supplementary Table B278**). This does not fit with the ranking, which shows statistically similar net-return rates for quartzite and untreated silcrete (**Supplementary Table B278**). This result suggests that wood fuel travel and search time-cost (m_1) and heat-treatment time-cost (m_2) do not explain the archaeological raw material frequencies at Pinnacle Point during MIS4 when using this alternative currency. A comparison between the archaeological frequency data to the ranked raw materials from MIS5 and MIS6 conditions show that the predicted relationships (**Figure 27**) are not supported. The archaeological data show that quartzite has the highest frequency during MIS5 and MIS6, while the highest ranked raw materials during MIS5 and MIS6 are quartzite and untreated silcrete that have statistically similar net-return rates (**Supplementary Table B278**). This result suggests that wood fuel travel and search time-cost (m_1) and heat-treatment time-cost (m_2) do not explain raw material frequencies during MIS5 and MIS6 at Pinnacle Point when using this alternative currency. As with the original currency and the first alternative currency, the result from all model conditions limits support for the "Wood-fuel availability" model (Brown and Marean 2010).

Mobility rate and strategy

During MIS4 conditions heat-treated silcrete has the highest net-return rate followed by quartzite and untreated silcrete, which have statistically similar net-return rates **Supplementary Figure A21**and **Supplementary Table B279;** Raw data in

Supplementary Tables B280-B281). This result is the same as the test using the original currency and the first alternative currency.

When comparing the archaeological frequency data to the ranked raw materials from MIS4 conditions it shows that the predicted relationship between flake manufacturing time-cost (m_3) and the mobility rate and strategy variable (**Figure 28**) is not supported. The archaeological data show that quartzite and silcrete (83.1% of the silcrete has been heat-treated and 16.9% is untreated) have statistically similar frequencies during MIS4, while the highest ranked raw material during MIS4 is heat-treated silcrete (**Supplementary Table B282**). This result suggests that the higher cutting edge per mass outcome (*e* variable) of heat-treated silcrete and flake manufacture time-cost (m_3) do not directly explain raw material frequencies during MIS4 at Pinnacle Point when using this alternative currency. Again, similar to using the original currency and the first alternative currency this result limits support for assertions made by Gould and Saggers (1985, 1985) that foragers select raw material specifically for their qualities.

ACM model condition variable outcomes summary

The model outcomes under the three different model condition variables presented above show that the only predicted relationship that was supported was travel and search time-cost (t_s) explaining raw material frequencies during MIS5 conditions. This suggests, similar to the evaluation of Hypothesis 3 (H_3) using the original currency and the alternative currency that during MIS5 the selection of quartzite was driven by the lower travel and search time-cost (t_s) of acquiring the quartzite. The position of the coastline and the distribution of raw material sources affected the cost of the quartzite.

The positive result comparing ACM-P net-return rates from MIS4 conditions to archaeological frequencies from the MIS4 record at Pinnacle Point suggests strategic selection of both quartzite and heat-treated silcrete. This suggests a complex raw material selection process. The vegetation type variable model outcomes under MIS4 conditions show that when heat-treatment time-costs (m_1 and m_2) are the only time-costs considered both types of heat-treated silcrete has significantly lower net-return rates compared to quartzite and untreated silcrete. Conversely, the mobility rate and strategy variable model outcome under MIS4 conditions shows that when considering only the flake manufacturing time-cost (m_3), heat-treated silcrete has a significantly higher net-return rate compared to quartzite and untreated silcrete. However, the higher net-return rate of heat-treated silcrete using only the m_3 time-cost results not only because the time-cost of m_3 is lower in heat-treated silcrete but also because by heat-treating silcrete the values of *e* (count of complete blades per mass) and *d* (duration of use before the edges of those blades dulls) both increases and are higher than quartzite and untreated silcrete.

When combined, when considering all time-costs (**Figure 111** and **Table 83**), including procurement time-cost (t_p), heat-treatment wood fuel travel and search time-cost (m_1), heat-treatment time-cost (m_2), and flake manufacturing time-cost (m_3) heat-treated silcrete (when assuming the insulated method) has a net-return rate that is statistically similar to quartzite and untreated silcrete.

What the conflicting results of heat-treatment time-costs (m_1 and m_2) and flake manufacturing time-cost (m_3) suggest is that what drives the net-return rate for heat-treated silcrete up is the higher gross-value of the assumed currency (count of blades multiplied by the duration of use) and a lower flake-manufacturing time-cost (m_3). The

net-return rates of quartzite and untreated silcrete is driven by the lack of heat-treatment time-costs and the higher flake-manufacturing time-costs. Together, the lack of having to invest in heat-treatment in quartzite and the gained currency value and decreased flake-manufacturing time-cost in heat-treated silcrete is what results in a tied ranking, which in turn potentially explains the raw material frequencies in the MIS4 record at Pinnacle Point.

Summary of evaluations using two alternative currencies

The evaluations using the two alternative currencies show that comparison between ACM-R net-return rates and archaeological frequencies during MIS5 conditions support hypothesis 3 (H_3), which is the same result as when using the original currency. This strongly suggests that quartzite was selected due to having the highest net-return rate during MIS5 conditions because regardless of currency quartzite has the highest ranking. The modeling outcome of the coastline position and raw material source distribution variable shows that travel and search time-cost (ts) of quartzite is significantly lower than the travel and search time-cost of silcrete, which in turn increases the net-return rate of all three types of assumed currencies for quartzite to rise above the net-return rate of silcrete. The benefit of selecting quartzite was its low travel and search time-cost regardless of currency but the trade-off was that it did not have the highest gross-return rate of any of the assumed currencies. This result supports the argument made by Torrence's (1989, 1983) that cost of procurement explains why raw materials are selected if the quality of the raw material is good enough.

Unlike the evaluation using the original currency, when evaluating the two alternative currencies there was no support for Hypothesis 3 (H_3) during MIS6 conditions without a Paleo-Agulhas plain silcrete source. This suggests that currencies linked to blade production were not sought to be maximized during MIS6 at Pinnacle Point. Rather, the result using the original currency suggests that quartzite was strategically selected because it could offer, when conducting a non-blade focused flaking strategy, the highest net-return of cutting edge per mass multiplied by the duration that those edges could be used before dulling. This fits well with the MIS6 record at PP13B, which suggests little blade production compared to later periods such as the MIS4 record at PP5-6 (Thompson, Williams, and Minichillo 2010 also see *Chapter 7* above).

Support for H_2 was found during simulation of MIS4 conditions when comparing the ranking of raw materials based on ACM-P net-return rates and archaeological frequencies while using the assumption that the forager seeks to maximize the number of blades that can be produced per core mass multiplied by the duration of use. A lower flake manufacturing time-cost when producing heat-treated silcrete tools compared to higher flake manufacturing time-costs when producing quartzite toold in addtition to the lack of heat-treatment cost for quartzite resulted in tied net-return rates. The tied ranking of heat-treated silcrete with quartzite provided the forager with raw material that yielded the highest possible gross value of the assumed currency, which in turn allowed the forager to produce blades in a more standardized fashion, including microlithic technology (Brown et al. 2012).

CHAPTER 11: ISSUES AND PROBLEMS PERTAINING TO THE ACM AND OAM

Introduction

Before putting the raw material selection in the MIS6 to MIS4 sequence at Pinnacle Point in a broader context in terms of both theoretical work and the overall technological organization in MSA record at Pinnacle Point it is important to highlight issues and problems facing the analysis and discussion just presented. These issues include the scale of analysis, the assumption of perfect knowledge about the environment, energy cost as another factor when selecting a raw material, and assumptions about time-costs. They will all be discussed below.

Before discussing those issues it is worth restating a potential criticism that can be directed at mathematically-based models, which is that they are often simple views of a complex world and they have assumptions that are often simplified (Surovell 2009: 21). However, simple models are a first necessary step of scientific development (Winterhalder and Smith 1992). This study advocates that one should test simpler models first such as the OAM and the ACM to see if they explain human behavior before attempting to explain human behavior using more complex chains of arguments. Such complex models are inherently hard to evaluate on an empirical basis, resulting in a potential situation where a negative model outcome can be hard to explain because of poorly measured or understood variables (Smith 1991, Surovell 2009).

Scale of analysis

An obvious potential criticism of this study is the scale of analysis, which uses Marine Isotope Stages as the time-periods to investigate behavior. Such a coarse-grain approach based on the MIS scale has the potential to erase all climatic and environmental fluctuations occurring within each stage (Wilkins et al. 2017). There is a lot of debate about the paleoenvironmental conditions within each MIS, especially MIS4 (Bar-Matthews et al. 2010, Chase 2010, Marean et al. 2014). One can also argue that the issue of distance to coastline, for example, should be investigated in much finer detail to better understand fluctuation in behavior (Fisher et al. 2010).

Although Marine Isotope Stages most certainly consists of variability, they do reflect a global trend. Marine Isotope Stages are by definition a climatic framework deduced by a dataset (e.g. deep-sea oxygen isotopes) that is completely independent from archaeological investigations. They signal a trend towards either warmer or cooler global temperatures. This makes Marine Isotope Stages useful for summarizing coarse-grained, long-term, time-averaged environmental conditions (Wilkins et al. 2017). Given this, there is precedent for making interpretations about behavioral variability in the MSA at the scale of MIS (e.g. Ambrose and Lorenz 1990, Compton 2011, Deacon and Brooker 1976, Deacon 1978, Foley and Lahr 1997, Henshilwood and Marean 2003, Karkanas et al. 2015, Mackay, Stewart, and Chase 2014, McCall and Thomas 2012, Mellars 2006). Additionally, for the purpose of this study the MIS scale provides a palimpsest of human behavior over a long time-period that is more suited to investigating human adaptations to environmental or climatic context (Barton and Riel-Salvatore 2014, Riel-Salvatore and Barton 2004).

Another related issue to the scale of analysis and use of Marine Isotope Stages to look at long-term adaptation to environmental and climatic condition is that other factors other than external environmental forces can act as the causal mechanism behind changes in behavioral variability. Other researchers have focused on other potential causal mechanisms such as information transmission dynamics, socio-cultural factors, and hyper-flexibility, ratcheting, and other multi-dimensional models (Clark 2013, Conard and Will 2015, Kandel et al. 2015, Lombard 2016, 2012, Porraz, Parkington, et al. 2013)

Considering this, it is important to note that they are discussing behaviors linked to several phenomena at once such as complete technological packages such as bow and arrow technology, heat-treatment, or symbolic artifact, etc. The focus of this study is on one independent behavior, raw material selection. Other studies in the past that have taken a 'selectionist' approach to technological behavior have combined too many variables that are included in a total package of technology. I propose that the selection of raw materials using a 'selectionist' approach is feasible because when a forager goes out on the landscape it has to select raw materials before it can construct a bow and arrow combination, or a stone-tipped spear. Put differently, the forager cannot go out on the landscape and search for fully assembled bows hanging in trees that they can subsequently procure and use. By applying an OFT approach to raw material selection one is focusing on the outermost base of the chain of behaviors linked to stone tool technology and behavior. Since the raw materials are individual types with potential differences much like food resources, one can rank them based on net-returns rates in a given environmental and climatic context.

Assumption of perfect knowledge

Another important issue to discuss with OFT models is that they assume that the forager has perfect knowledge about the environment (Stephen and Krebs 1986). This assumption is most likely false. However, one has to take into consideration that by cultural transmission over generations that a landscape in which a band or ethnolinguistic group lives would be very familiar to them. In fact, not being familiar with the surroundings would most likely be detrimental to survival. This issue is interlinked with the concept of risk. The concept of risk, when associated with OFT models, refers to variation in outcome (Smith 1991: 53). It pertains to situations where the outcomes are variable, regardless of whether the forager has complete knowledge or information about the probability of outcomes (Smith 1991). Smith (1991: 54-55) noted that risk theory has at least three predictions concerning foraging strategies: 1) risk should vary as a function of the prospects facing the forager. When resources are scarce, or there is competition the forager should be risk-seeking, while if the conditions are more moderate, the forager should be risk-averse. If the resources are abundant, the forager should be indifferent to risk. 2) There should be differences between individuals in their approach to risk. 3) Activities such as sharing and storage that happen after a resource has been procured can have an effect on the significance of risk. Given these three predictions, if running out of cutting edge and sharp durable edges is the utility then foragers that are faced with a budget that is negative (average rate of procured cutting edge and sharp durable edges is less than what is needed) should be risk-seeking, while foragers that face a budget that is positive (average rate of procured cutting edge and sharp durable edges is greater than what is needed) should be risk-averse (Smith 2011).

Only considering time-cost

A third issue is the fact that in the ACM only time-cost was considered without considering energy cost when the forager is making decisions about raw materials. Future studies need to include both time and energy as costs when calculating net-return rates. Normally, OFT models focus on energy as the currency that the forager seeks to maximize by minimizing time spent acquiring that energy. However, in this study the currency is not linked to food in a direct manner. That means it is extra costly to the forager to conduct this type of activity because when selecting a raw material it will not directly gain energy. Put simply, one cannot eat a rock to gain energy. A forager can do as much as it can to procure the material with the highest net-return rate, which results in minimized opportunity costs so it can focus on gaining energy through food-related foraging. Simultaneously, the forager when searching for, procuring and manufacturing stone tools from the selected raw material also uses up valuable energy needed to survive. Therefore, to make the ACM more realistic one should incorporate both time and energy as costs to model how the forager makes decisions in a given environmental and climatic context.

Assumptions about time-cost

All assumptions about the individual time-costs can be questioned in relation to the calculation of the ACM-P and ACM-R net-return rates. However, most would probably here not differentially affect quartzite and silcrete.

Travel and search time-cost (t_s) assumptions

The assumption that the forager moves 3.5 km/hr is based on how the Hadza move in east Africa (Marlowe 2010, Marlowe 2006). Their environment is not a perfect analogy to the environment on the South African coast but the well-studied Hadza gives use an estimate of how fast an African hunter-gatherer can move when foraging in a woody savannah-like environment. It is important to note however that by changing the speed of which a forager moves it does not affect the result of the net-return rates other than increasing or decreasing the time-cost for all raw materials at the same time.

Procurement time-cost (t_p) assumptions

The time-cost for procuring raw materials from both primary and secondary sources is based on systematic surveys. These time-costs can potentially be reduced due to the expertise that a forager would possess due the fact that their life most likely depended on having good materials to conduct a whole range of tasks. However, silcrete primary sources could have provided the forager with a challenge in terms of obtaining packages of raw materials suitable for transport. Today we use sledgehammers and rock hammers to break big boulders apart to obtain samples for analysis and experiments. However, in the past these types of tools obviously would not have been available. There is one example from Australia that illustrates however how a forager could have broken off smaller parts of a big boulder using fire (Binford and O'Connell 1984). The obvious implication of this type of behavior is that the time-cost associated with procuring silcrete would have increased. Future studies can investigate the time-cost involved in such an

operation to create smaller packages of stone and then the time-cost can be plugged into both the ACM-P and ACM-R to calculate net-return rates.

Flake manufacturing time-cost (m_3) assumptions

Amount of manufacturing time-cost (m_3) is likely correlated with the skill or expertise of the knapper. Thus, it is possible to predict that when the expertise of a knapper increases it potentially leads to greater minimizing of waste that is created from a given mass of raw material. In addition, an experienced knapper is more likely able to handle several different raw materials, meaning that the knapper knows tricks or techniques to knap individual types of raw materials. In this study, only one knapper was used to limit the variation in the manufacturing time-cost. Given this, future studies should involve more knappers to look at the variability of manufacturing time-cost that can arise from different expertise and experience levels. Such time-costs can then be quantified and plugged into the ACM-P and ACM-R models to calculate net-return rates.

Heat-treatment wood fuel travel and search time-cost (m_1) and heat-treatment time-cost (m_2) assumptions

The final set of time-costs are the ones linked to travel and search for wood fuel to heat-treat silcrete (m_1) and the actual act of heat-treatment itself (m_2). Changing these two time-costs will have different effects on quartzite and silcrete because it only pertains to silcrete. Increasing or decreasing the time-costs associated with silcrete will likely have big effects on the relative net-return rates of silcrete compared to quartzite.

While there is no debate over whether early modern humans in South Africa understood and used heat treatment perhaps as early as 160 ka (Brown et al. 2009, Schmidt 2016, Wadley and Prinsloo 2014), there is significant debate over what method was used (Brown and Marean 2010, Brown et al. 2009, Schmidt 2016, Schmidt and Mackay 2016, Schmidt et al. 2015, Schmidt et al. 2013, Wadley and Prinsloo 2014, Wadley 2013b). One method, the sand bath method or insulation method (Brown et al. 2009, Wadley and Prinsloo 2014: 50), implies "planning, patience, and considerable expertise and understanding of the natural properties of the products" that are being handled; it is suggestive of "analog reasoning and the ability to envisage action removed from view" (Wadley and Prinsloo 2014: 50). Similarly to the production of compound adhesives (Charrié-Duhaut et al. 2013, Wadley 2010), the heat-treatment of stone tool raw materials uses innovative processes, such as controlled pyrotechnology, to transform natural products, and is strongly suggestive of the first evidence of modern human's controlled use of fire to transform naturally available materials (Schmidt 2016). If the insulation method was used, it suggests all these abilities as early as 160 ka.

The alternative method called the ember method or exposed method (Schmidt and Mackay 2016, Schmidt 2016, Schmidt et al. 2015, Schmidt et al. 2013), is a much less complex process. This method implies less planning and patience, but it is debated whether it also implies less expertise and understanding about the natural properties of the products being handled (Schmidt 2016, Schmidt et al. 2015, Wadley and Prinsloo 2014).

Knowledge and utilization of heat-treatment may have been decisive in the evolutionary history of anatomically modern humans (Wadley and Prinsloo 2014); it is

argued that knapping of heat-treated rock requires decreased force and allows increased accuracy in obtaining a desired outcome such as shape, or the maximization of currency (Brown et al. 2009, Crabtree and Butler 1964, Domanski, Webb, and Boland 1994, Mercieca and Hiscock 2008, Purdy and Brooks 1971, Schmidt and Mackay 2016, Schmidt et al. 2012). It follows that stone tool heat-treatment is a transformative technology that generates discernable links between complex cognition and material culture (Wadley and Prinsloo 2014: 50). In addition, heat-treatment would have been interconnected with the overall technological organization of a forager group, a potentially important step in the overall chain of production of stone tools (Mercieca and Hiscock 2008, Schmidt 2016, Schmidt and Mackay 2016, Wadley and Prinsloo 2014). Thus, it remains of great importance to understand the procedures used to heat-treat stone tools, and the degree of complexity and investment associated with the procedures (Mercieca and Hiscock 2008, Schmidt 2016, Wadley and Prinsloo 2014). Moreover, given the mineralogical alterations that occur during raw material heat treatment for stone tool production, the identification and understanding of the processes associated with this behavior is critical to understanding and reconstructing raw material acquisition as heat-treated stone will have a different chemical signature to its source material (Nash, Coulson, Staurset, Smith, et al. 2013). Research on heat-treatment including the procedures linked to it, the benefits and cost to MSA foragers, and the reasons for its invention, poses important questions according to Schmidt (2016: 1): when and why did MSA foragers start using heat-treatment? What does it tell us about their technological toolkit? Additionally, does heat-treatment imply complex cognition and social learning processes? Schmidt (2016: 1) contended that answering these questions will shed light on

human behavioral, social, and cognitive processes during key periods of our evolution. I agree.

Research focusing on the South African MSA record has yielded an increasing amount of evidence for heat-treatment of silcrete (an abundant rock type on the west and south coast of South Africa) (Brown et al. 2012, Brown et al. 2009, Mourre, Villa, and Henshilwood 2010, Schmidt and Mackay 2016, Schmidt 2016, Schmidt et al. 2015, Schmidt et al. 2013, Wadley and Prinsloo 2014, Wadley 2013b). As mentioned above, in this context, two heat-treatment procedures have been suggested. Some authors (Brown and Marean 2010, Brown et al. 2009, Wadley and Prinsloo 2014, Wadley 2013b) have proposed that heat-treatment was a complicated, resource and time-consuming activity that relied on slow and indirect heating of silcrete in a sand-bath (insulated) below a campfire, also called a 'slow and steady' strategy (Mercieca and Hiscock 2008). In the ethnographic and archaeological record, there are observations of such a strategy from North America, Europe, and Australia (Akerman 1979, Arthur 2010, Eriksen 1997, Griffiths et al. 1987, Mandeville and Flenniken 1974). The sand-bath method or insulation method creates slow heating rates and low temperature that decreases the chance of unwanted overheating of the rocks (Wadley and Prinsloo 2014). Experiments show that the maximum temperatures reached in the subsurface sediments directly covering the silcrete are in the range of 300-400°C, which has been achieved by using between 9 to 20 kg of wood-fuel (Brown et al. 2009, Wadley and Prinsloo 2014). It has been proposed that this method reduces risk in terms of raw material fracturing and cracking in situations when raw materials are distant and effort is invested in preform production (Wadley and Prinsloo 2014). However, this strategy is potentially time-

intensive because the raw materials are placed under the fire itself and can only be taken out after the fire has burned out and the sand has cooled (Schmidt 2016). This could require an investment in time of up to a full day or more to let the silcrete cool (Brown et al. 2009, Eriksen 1997). This assertion that the sand-bath method is time-intensive has been challenged by (Wadley and Prinsloo 2014) who argued that the sand-bath method allows for simultaneous use of a fire for both domestic use and heat-treatment negating the construction of a special fire. The sand-bath method does require more wood fuel per heated stone because the sediment around the buried rocks consumes most of the radiated heat below the fire. As presented earlier, Brown and Marean (2010) hypothesized that silcrete's appearance and disappearance in the MSA record is constrained by the abundance of wood fuel. How much wood is available in the environment is proposed to be driven by the relative distribution of summer rain in this predominantly winter rainfall region. Summer rain brings in more acacia trees and thus better wood-fuel than the bushland of the winter rainfall regime (Brown and Marean 2010).

Conversely, Schmidt and colleagues (Schmidt 2016, Schmidt et al. 2015, Schmidt et al. 2013) have proposed that silcrete was heat-treated using embers from a regular domestic hearth (exposed), also called a 'fast' strategy (Mercieca and Hiscock 2008). In the ember method or exposed method, the silcrete is either placed under a pile of embers that has been pulled aside from the regular fire or the silcrete is pushed into the ash cone below the burning fire. Both approaches put the silcrete in direct contact with burning fuel (Wadley and Prinsloo 2014, Schmidt 2016, Schmidt et al. 2015). Maximum temperatures reached varies with experiments yielding temperatures ranging from ~350 to ~570°C when using the ember pile approach and ranging between ~390 to ~760°C

when using the ash cone approach. Based on structural and crystallographic research, Schmidt and colleagues (Schmidt et al. 2013) argued that the properties of silcrete do not require a slow heating rate compared to other rock raw materials and it can be heated relatively quickly (Schmidt 2016, Schmidt et al. 2015, Schmidt et al. 2013). The implication of the ember method is that it requires minimal time investment because of the faster heating cycle and no extra investment in wood fuels since the embers directly heat the rocks thus energy is not expended heating the subsurface sediments (Schmidt 2016). However, even with the ember (exposed) approach the silcrete was left in place for ~4.5 hours following heat-treatment to avoid rapid cooling (Schmidt et al. 2015). The ember method could also utilize a regular campfire that is simultaneously used for cooking, heating, and other social activities (Schmidt 2016).

Given the potential differences in planning depth, time investment, wood fuel cost, risk, and material outcome between a 'slow and steady' strategy (insulated method) and 'fast' strategy (exposed method), Mercieca and Hiscock (2008: 2638) proposed that the selection of a specific heat-treatment strategy could alternate depending on the context. The fast strategy (ember or ash cone method or exposed method) would be used by groups that rely on increased residential mobility, encounter difficulties with scheduling activities, are unable to plan tool production in advance of anticipated need, find themselves in regions without abundant suitable stone for knapping, and require incidental heat-treatment of small pieces of rock. In such situations, a method that required little time investment and little wood fuel cost would be preferred (Mercieca and Hiscock 2008: 2638). On the other hand, they proposed that the 'slow and steady' approach (sand-bath method or insulated method) would be used when groups are more

sedentary, obtain stone tool raw materials through logistic forays or via exchange, anticipate future events and can produce tools long in advance of use, require large-scale production perhaps to support more people, need larger preforms for tool production, or are using raw materials that are susceptible to thermal shock leading to raw material failure. In such a scenario, the potentially increased time-investment and wood fuel cost would be tolerable (Mercieca and Hiscock, 2008: 2638).

To summarize, more research is needed to fully understand the costs in terms of time and energy involved with heat-treatment of silcrete. As noted above, heat-treatment only pertains to silcrete thus only affects the net-return of silcrete and not quartzite, and can potentially swing the net-return rate of silcrete above or below quartzite due to increased or decreased heat-treatment time-costs. By conducting more modeling to investigate changes in wood fuel abundance in an integrated Paleoscape approach (Marean et al. 2015) one can potentially obtain estimates of the cost to procure wood fuels during changing glacial to interglacial conditions. If such an approach is successful, obtained numbers can be plugged into the ACM and new net-return rates for silcrete can be presented.

The main point about discussing these issues above is two-fold: 1) you have to be aware of them, and consider them going forward. The ACM is not a final model to answer all questions about raw material selection. It is a model, from which new hypotheses and predictions can be drawn again at a later stage when more data are available; 2) Related, the model is set up so that when better estimates of time-costs are obtained, through either theoretical work or experimental work, such numbers can be plugged into the equation to recalculate net-return rates. This means that support that this

study found for respective hypotheses drawn from the ACM might be falsified later when more data that are accurate is obtained.

CHAPTER 12: SYNTHESIS AND DISCUSSION

Introduction

Brown (2011), Wilkins et al. (2017), and this study (*Chapter 7*) demonstrate that there are significant technological differences between silcrete and quartzite stone tools at Pinnacle Point (PP), especially at PP5-6. The differences include patterns of procurement (outcrop versus secondary), how the raw materials are prepared (blade production versus prepared core), size of the debitage and tools (length and width), production of formal tools such as microliths, and how conservative the material is handled in terms of cutting edge per mass.

In addition, Brown (2011: 262) pointed out that there are three innovations that happen in the Pinnacle Point record, especially at PP5-6, which indicate potential differences in the roles that the major types of raw materials play at PP5-6. The first innovation is pyro-technology or heat-treatment technology, and the cost associated with it. Heat-treatment appears much earlier in the record, as far back as MIS6 at PP13B, compared to the prominent shift in raw material use that happens at PP5-6- in the ALBS-SADBS Lower to SADBS Upper transition during MIS4. It is hard to separate the technological decision to use silcrete from the investment in heat-treatment because it is likely that almost all silcrete that has been observed in the Pinnacle Point record, starting in MIS6 at PP13B has been heat-treated (Brown, 2011). Even when quartzite dominates an assemblage, heated silcrete appears in low frequencies. The second innovation or important behavioral change, Brown (2011) noted, is the selection of silcrete from outcrop sources during MIS4, which is a significant shift from earlier periods (Wilkins et al. 2017). The third innovation is the adaptation and production of small blades and

segments constituting microlithic technology made on fine-grained raw materials. Brown (2011: 262) proposed that each of these innovations represents investments in more time-intensive technologies.

Brown (2011: 262) added that when considering technological investment one should question whether one technology replaced another, or whether different technologies represent parallel classes that performed different roles within a larger resource procurement system (Bettinger, Winterhalder, and McElreath 2006). In light of this, Brown (2011: 262) noted that even though all the aforementioned innovations are associated with silcrete, there is evidence of quartzite and silcrete selection side by side throughout the Pinnacle Point sequence. Additionally, there is a consistency in many attributes listed above for both quartzite and silcrete throughout the Pinnacle Point sequence (Brown, 2011). That includes that silcrete is usually heat-treated even when not associated with backed blades and microlithic technology. Although no thorough analysis exists about the amount of heat-treatment in the PP13B record, the foundational paper by Brown and colleagues (2009) showed that there is evidence of heat-treatment during MIS6 at PP13B. The analysis presented above (*Chapter 7*), the analysis by Brown (2011) and Wilkins et al. (2017) all show that silcrete tools consistently have smaller mean dimensions in terms of length and width compared to quartzite tools except for in the LC-MSA Lower. The analyses also show that silcrete consistently yields more cutting edge per mass compared to quartzite.

Brown (2011) found that his ‘site-context’ model did not predict all technological investments because it did not take into account all costs and benefits that raw material selection is associated with in addition to distance to source. This study provides

estimates of such costs and benefits associated with raw material selection and highlights why raw material selection changed.

MIS6 record – Opportunistic acquisition or strategic choice?

For MIS6 conditions, two different results are available for the model evaluations above, one from the Opportunistic Acquisition Model (OAM) and one from the Active-Choice Model (ACM). No conclusive evidence was found to support Hypothesis 1 (H_1) drawn from the OAM under any model condition. An extensive sensitivity analysis showed that only when you assumed that the forager engages in expedient behavior during MIS6 conditions without a Paleo-Agulhas plain silcrete source did the model outcomes match the archaeological frequencies. However, a subsequent check to see how much of the time the forager spends without raw material in the toolkit suggests that it is unrealistic that the forager engages in expedient behavior in the Mossel Bay Region without consistently returning to a stone cache (c.f. Oestmo, Janssen, and Marean 2016). As noted above (see *Chapter 8*: more in-depth discussion about the results), future research should focus on whether the MIS6 record from PP13B reflects stockpiling or caching behavior.

However, the net-return rate outcome using the original currency from ACM-R variant supports Hypothesis 3 (H_3). As noted above, the support for H_3 during MIS6 conditions without a Paleo-Agulhas silcrete source minimally suggests that the foragers are strategically selecting the raw material with the highest net-return rate of cm*min cutting edge that is available in the environment. This suggests that stone tool raw materials played an important part in the technological organization because raw materials were travel and searched for at added cost. Heat-treated silcrete has the highest

gross value of the assumed currency (cutting edge per mass multiplied by the duration of use), while quartzite has the highest net-return rate. Given that, the selection of quartzite implies that assumed currency value of quartzite was good enough. The MIS6 result suggests that a part of the response to the climatic and environmental context during MIS6 was reliance on specific raw materials and technology to obtain food resources and/or performing processing tasks. This, in turn, suggests increased knowledge about raw material characteristics and how to utilize them during MIS6.

During MIS6 conditions, the coastline was on average 42 km away from the Pinnacle Point sites (Fisher et al. 2010). On the exposed Paleo-Agulhas plain, wave-ravinement surfaces containing quartzite were present (Cawthra et al. 2015). The closest quartzite source in the form of a wave-ravinement surface was 1.4 km from Pinnacle Point, while the closest primary context silcrete was 8.5 km away at Rietvlei. In addition, following Brown (2011), it is assumed that any previously deposited interglacial cobble beaches became depleted in high-quality raw materials and/or buried. The speleothem record suggests that the vegetation was stable C3 throughout MIS6 (Braun et al. ms), while the faunal assemblage from PP13B and PP30 suggest that there was a mosaic habitat that consisted of both C3 and C4 vegetation (Rector and Reed 2010). On the Paleo-Agulhas plain, a migration system consisting of ungulates was most likely operating in the form of a disperse-congregate system, or an east-west migration (Copeland et al. 2015). The longer distance to the coast during MIS6 likely meant that the groups living at Pinnacle Point lost access to predictable coastal resources within the daily foraging radius. However, the wide coastal plain offered more space for an increase in the population of migratory animals (Marean 2016). This increased width of the

coastal shelf makes the migratory animals a dense but unpredictable resource. The combination of less access to migratory animals and no daily access to predictable coastal resources could have put pressure on increasing the frequency of residential moves to find resources either on the plain or at the coast. Once at Pinnacle Point, the forager strategically chose quartzite because the travel and search time-cost (t_s) made the net-return rate rise above untreated and heat-treated silcrete. After procurement, the quartzite was expediently handled and discarded as observed in the low flaking efficiency, low frequency of blades, and the low ratio of retouch frequency to artifact density in MIS6 assemblages at PP13B (see *Chapter 7*). This supports the prediction made by Barton and Riel-Salvatore (2014) that an increase in access to raw materials decreases the frequency of retouched lithics.

Traveling and searching for a raw material suggests planning of the stone procurement activities because travel and search time needs to be included in the greater foraging mobility strategy. Hence, support for H_3 suggests that the response to climatic and environmental conditions during MIS6 was a mobility system that involved targeted stone tool raw material procurement bouts (c.f. Gould, 1985; Gould and Saggers, 1985) to select the raw material that yielded the highest value of a wanted utility. Further, this echoes arguments made by Torrence (1989, 1983) that the least costly raw material should be selected that meets the need of the forager in terms of desired flaking quality. It also supports the 'Utilitarian' variant of the Preference-based model category (c.f. Mackay 2008).

Given the assumed currency (cutting edge per mass multiplied by the duration of use), quartzite should always be selected, while silcrete should be the second priority. In

the archaeological record (see *Chapter 7*) from PP13B during MIS6 there is evidence for the selection of silcrete and other materials. At PP13B in some of the MIS6 stratigraphic aggregates silcrete constitutes ~2.5 to ~5% of the total assemblages in terms of weight. There is no significant difference in flaking efficiency between quartzite and silcrete in the MIS6 record, and the tools are of similar size, which suggests that silcrete was used in a similar fashion to quartzite.

However, the selection of silcrete given the assumed currency and the environmental and climatic context implies that opportunity cost was not minimized in those cases. Given that the raw material sources, especially primary sources of silcrete have a very low depletion rate (e.g. erosion rates) and can be seen as infinite with respect to the lifespan of a human, the implication of not selecting the raw material with the highest net-return rate under a given environmental or climatic context can be that they were selected for other reasons unrelated to an utilitarian-based net-return rate. Such selection might indicate that silcrete, through either direct or embedded procurement, were selected due to other needs such as symbolic (Clendon 1999, Gould et al. 1971, Wurz 1999) or stylistics needs (Close 2002, Mackay 2011, Sackett 1986, 1982). Both hypothetical explanations for raw material change are variants in the 'Preference-based change' model category presented in *Chapter 2*. However, it is difficult to predict what is being selected when selection of raw materials for style or symbolic needs is being conducted.

MIS5 – direct procurement of quartzite

During MIS5, the coastline was close to or at present location, easily within the daily foraging radius of a hunter-gatherer. Estimates by Fisher et al. (2010) put the coastline on average 1km away during MIS5. Cobble beaches occur directly adjacent to the Pinnacle Point sites, and at Dana Bay, Mossel Bay Point, Fransmanhoek, and Kanon Beach. Dynamic forces such as ocean swells, tidal forces, and storm surges help produce and replenish hi-energy cobble beaches (Brown 2011). The closest primary context quartzite was 5.3 km from Pinnacle Point, while the closest primary context silcrete was 8.5 km away at Rietvleei. As during MIS6 and in the later MIS4, quartz was available in close vicinity (100-200 meters) to the Pinnacle Point complex as veins in the local Skurweberg Formation.

During the peak interglacial in MIS5e there where warm temperatures and the prevailing rainfall regime on the south coast was summer-rainfall (Braun et al. ms). However, post-MIS5e the temperature decreased during the MIS5 and the prevailing rainfall regime changed to winter rainfall (Bar-Matthews et al. 2010, Braun et al. ms). A vegetation type called Fynbos, which is dominated by C3 photosynthesis, accompanied this winter-rainfall regime (Rebelo et al. 2006). The C3 dominant Fynbos was depleted in trees (O'Brien 1993, Van Wyk and Van Wyk 1997). The C3 signal is also supported by the faunal assemblage from PP13B and PP30 (Rector and Reed 2010). The Paleo-Agulhas plain narrowed, hypothetically restricting the abundance of migratory animals (Marean 2016). This potentially forced the foragers to perform an increased number of moves between inland and coastal areas, only moving to intercept coastal resources during low spring tides.

Given the proximity of cobble beaches during MIS5, one expects that quartzite will be selected. Indeed, support for Hypothesis 3 (H_3) was also found under MIS5 conditions. This suggests that the foragers during MIS5 conditions selected the raw material with the highest net-return rate of cutting edge per mass multiplied by the duration of use before dulling that was available on the landscape. This supports the 'Utilitarian model' of raw material selection and change (c.f. Mackay 2008). Similar to MIS6 conditions, this was quartzite. Coastline position and raw material distribution variable model outcomes show that what drove the net-return rate of quartzite to go above the net-return rate of untreated and heat-treated silcrete was the low travel and search time-cost (t_s). Because travel and search time-cost is included in the ACM-R this suggests that stone tool raw materials played an important part in the technological organization because raw materials were traveled and searched for at added cost. As with the support for H_3 during MIS6 conditions, the result for MIS5 conditions also suggests that the response to the climatic and environmental conditions was to rely on specific stone raw materials obtained during direct procurement (c.f. Gould, 1985; Gould and Saggers, 1985) and to manufacture technology to obtain food resources and/or performing processing tasks, which suggests increased knowledge about the properties of the raw materials and how best to use them. Further, as with quartzite during MIS6, the tools made on quartzite during MIS5 also reflects expedient behavior witnessed in the low flaking efficiency (even lower than MIS6), low frequency of blades, and a low ratio of retouch frequency to artifact density (see *Chapter 7*). This again follows the prediction by Barton and Riel-Salvatore (2014) that states that easy access to raw materials decreases the frequency of retouched lithics.

Brown (2011) pointed out that untreated silcrete has similar properties to quartzite. This assertion is supported by experimental work conducted in this study (*Chapter 9*). Quartzite and untreated silcrete have both statistically similar *e* values (cutting edge per mass) and *d* values (duration of use). Given this, if the quality of the raw material was the strict driver (with no attention to the cost of procurement) of which raw material should be selected and not the net-return rate of cutting edge per mass multiplied by the duration of use we should see more untreated silcrete. However, Brown (2011) pointed out, in line with the results of this study, that it would be less costly for a forager to select quartzite over untreated silcrete because of the abundant quartzite cobble beaches in the vicinity of Pinnacle Point. However, the small amount of heat-treated silcrete present at PP13B during MIS5 and a surprisingly increased amount of silcrete present in the YBSR stratigraphic aggregate at PP5-6 could have been brought to Pinnacle Point by residential moves from the interior where people were provisioned (c.f. Kuhn, 2004) with small and lightweight tools (Brown, 2011). Interior sources of silcrete are plentiful starting 8.5km away from Pinnacle Point. However, silcrete could also have been procured when encountered in small frequencies at the cobble beaches, which is supported by field observations by this author and Brown.

Given the assumed currency (cutting edge per mass multiplied by the duration of use before dulling), quartzite should always be selected during MIS5 conditions, while silcrete should be the second priority. In the archaeological record (see *Chapter 7*) from PP13B, PP9, and PP5-6 during MIS5 there is evidence for the selection of silcrete and other materials. At PP13B during MIS5 and at PP9, silcrete and these other raw materials are present in low quantities. However, at PP13B in some of the MIS5 stratigraphic

aggregates silcrete constitutes 5 to ~10% of the total assemblages in terms of weight. At PP5-6 during MIS5, overall silcrete constitutes 27.7% of the assemblage in terms of weight (kg). Within the YBSR stratigraphic aggregate (a combination of sub-aggregates) at the base of the PP5-6 archaeological sequence, the quantity of silcrete ranges from 9.5% to 48.2% of the total assemblages in terms of weight within each sub-aggregate. Compared to the silcrete in the MIS6 record however, the silcrete in the MIS5 record was handled more conservatively. Proportionally, more silcrete was used to create blades, while the silcrete lithics are also smaller (see *Chapter 7*).

Selection of silcrete given the assumed currency and the environmental and climatic context implies that opportunity cost was not minimized. As with MIS6 conditions, the implication of not selecting the raw material with the highest net-return rate under a given environmental or climatic context can be that silcrete was selected for other reasons unrelated to a utilitarian-based net-return rate. Such selection could mean that silcrete, obtained through direct or embedded procurement, was selected due to other needs such as symbolic (Clendon 1999, Gould et al. 1971, Wurz 1999), or stylistics needs (Close 2002, Mackay 2011, Sackett 1986, 1982).

Following Mackay et al.'s (2014) argument for evidence of 'place provisioning' in the Howiesons Poort, Wilkins et al. (2017) argues that foraging behavior during MIS5, and also MIS6, I will add, represents provisioning of individuals (c.f. Kuhn, 2004). In such a scenario, silcrete was transported across the landscape, to a lesser extent, and in smaller quantities compared to the later MIS4 period. The transport happened on a needs-basis with less long-term planning involved (Wilkins et al. 2017). Such an explanation is

consistent with the lack of earlier stages of reduction of silcrete lithics in MIS5 at PP5-6 (Wilkins et al. 2017).

The support for H_3 during both MIS5 and MIS6 conditions without a Paleo-Agulhas plain silcrete source suggests similar procurement systems for stone tool raw materials under two different environmental conditions. The biggest difference seems to be the distance to coastline. However, the MIS6 record from PP13B shows that shellfish was procured, which indicates that the coastline was within 10km at least at some parts of MIS6 (Fisher et al. 2010). That being said, on average the Paleo-Agulhas plain was wider and more exposed during MIS6 so the environmental context around PP13B would have been different. Nevertheless, what this study suggests is that the raw material selection response was the same during both periods. If the argument made by Wilkins et al. (2017) holds, that raw material selection during MIS5 and MIS6 indicates provisioning of individuals, it, in turn, suggests that people were more mobile. By provisioning individuals, the foragers were anticipating uncertainty related to raw material access when moving about the landscape. This can further indicate time-stress to intercept food resources. If there was time-stress during both periods, this would favor selecting the raw material with the highest net-return rate because it would lead to the least amount of cost related to opportunity to pursue other activities. Quartzite in this light must be seen as selected not because it offered the best quality but because it was good enough and cost the least (c.f. Torrence 1989, 1983), while silcrete was perhaps procured while moving, provisioned to the person and reduced in a different manner indicated by smaller size, more blade production, and harvested for more cutting edge per mass (*Chapter 7*).

MIS4 record – The rise of silcrete, microliths, and conservative behavior

Support for Hypothesis 2 (H_2) was only found when using an alternative currency during MIS4 conditions without a Paleo-Agulhas plain silcrete source. The alternative currency that was assumed was that the forager wanted to maximize the number of complete blades produced per core mass, and the forager wanted the cutting edge of those blades to last as long as possible. This is different from the original currency where it was assumed that the forager wanted to maximize cutting edge on all tool types per a given core mass, and that the forager wanted the cutting edges of all those tools to last as long as possible. A reason why the alternative currency might be working is because in the MIS5 to MIS4 transition at PP5-6 there is a shift to blade production focusing on small blades and an emerging microlithic technology mostly made on heat-treated silcrete that lasts until MIS3 (Brown et al. 2012, Wilkins et al. 2017).

MIS4 conditions see a shift back towards glacial conditions. However, the glacial conditions are not as strong as during MIS6. Estimates from Fisher et al. (2010) put the coastline on average 15km from Pinnacle Point during MIS4, which is within or near the daily foraging radius of hunter-gatherers. There is evidence of shellfish in the MIS4 record throughout suggesting that the site was occupied consistently when the site was close enough to the coast for that type of procurement (Brown 2011). The closest primary context quartzite source was 5.3 km away, while the closest primary silcrete was 8.5 km away at Rietvlei. This is the same distance and sources as during MIS5 and MIS6. There are wave-ravinement surfaces on the Paleo-Agulhas plain offering an increased abundance of quartzite accessible on the landscape (Cawthra et al 2015). The lack of dynamic ocean swells, tidal forces, and storms to replenish cobble beaches that formed

during interglacial MIS5 resulted in those cobble beaches becoming depleted in high-quality raw materials by normal foraging activity and/or burial (Brown 2011). Compared to MIS5, the proportions of summer rain increased accompanied by a vegetation type that included more C4 grasses and more trees such as acacias (Bar-Matthews et al. 2010, Braun et al. ms). The Paleo-Agulhas plain expanded again compared to MIS5 but not as much as during MIS6. However, the increase in C4 grasses and an expanded coastal plain most likely reintroduced the migratory animal system present during MIS6 (Copeland et al. 2015, Marean 2010). However, because the coastal plain was kept relatively narrow compared to MIS6 conditions, this allowed the foragers to have access to larger populations of migratory animals compared to the preceding MIS5 (Marean 2016), and access to predictable coastal resources. This increased the attractiveness of the Pinnacle Point location.

The support for H_2 during MIS4 indicates a scenario where during embedded procurement where other lifestyle constraints (e.g. food resource gathering and social behavior) controlled the mobility strategy and foraging movement, the MIS4 foragers strategically selected a raw material that could produce the highest post-encounter net-return rate of blades produced per core multiplied by duration of use when encountered. Thus, the support for H_2 during MIS4 is an example of how raw material procurement is embedded within the greater mobility strategy (Binford, 1979; Binford and Stone, 1985).

However, because quartzite and heat-treated silcrete have a tied rank and have statistically similar raw material frequencies in the PP5-6 record during MIS4 it suggests a complex situation of foraging decisions and strategies. When looking at the MIS4 record from PP5-6 (see *Chapter 7*), during the ALBS (90.9%), SADBS Lower (65.5%),

OBS1 (67.2%), and OBS2 (45.1%) stratigraphic aggregates quartzite dominates, while during the SADBS Upper (61.9%) and the SGS (48.8%) stratigraphic aggregate silcrete dominates. The variability between major stratigraphic aggregates and the variability within each aggregate potentially indicates changes in how the forager used the landscape, specifically in which direction the forager moved or came from. Variability can also indicate how the site was used differently.

A hypothetical explanation for this shifting raw material selection when both dominating raw materials have a tied ranking is that by heat-treating, which although cost is high, nevertheless creates a raw material for which the flake manufacturing time-cost is low enough compared to quartzite and untreated silcrete to equal the net-return rates. Put differently, the reason for the tied ranking has to do with both heat-treatment time-cost of silcrete and the rate and strategy of mobility.

Hence, support for H_2 suggests that the response to MIS4 climatic and environmental conditions was a combination of a mobility system and foraging movement that practiced embedded procurement of stone tool raw materials when targeting food resources (c.f. Binford 1979) and the selection of raw materials when encountered that both could be used to extract such resources and allowed the forager to spend more time on other activities because the opportunity costs were minimized. The dual selection of quartzite and silcrete depended on which one was encountered. If quartzite was encountered the forager would use it raw, while if silcrete was encountered, time-cost had to be front-loaded to achieve a net-return rate that was similar to quartzite. The changing selection of the raw materials had potentially different effects on the associated technology.

For example, the dominance of silcrete is accompanied by an increase in blade production in SADBS Upper stratigraphic aggregate at PP5-6. This suggests a different technological focus where silcrete was selected because it had the tied highest ranking but it also lent itself, due to physical properties such as flakeability to produce blades and microlithic technology, and for maximizing cutting edge produced per core (Brown et al. 2012, Mackay 2008).

The experimental work presented above (*Chapter 9*) shows that by heat-treating silcrete it is possible to more than double the amount of cutting edge per mass multiplied by the duration of use (e*d) that one can get out of a core compared to untreated silcrete and quartzite. More specifically, this means that if silcrete is procured and you heat-treat it you get increased flakeability and edge sharpness (Rick and Chappell 1983) in addition to edge durability. Additionally, heat-treatment of silcrete also results in fewer step fractures during manufacture in comparison to unheated stone (Mandeville and Flenniken 1974). Brown (2011) noted that change in color or luster also may have been desirable.

The increase in flakeability attained by heat-treating is not surprising because the silcrete becomes more fine-grained meaning that one has more control over the flaking outcomes (Brown et al. 2009). However, given that more fine-grained materials have sharper edges that are more brittle, heat-treatment of silcrete should reduce edge toughness (Crabtree 1967, Wilke, Flenniken, and Ozbun 1991) because of the decreased fracture toughness and/or increased Young's Modulus often associated with fine-grained materials (Beauchamp and Purdy 1986, Brown et al. 2009, Domanski, Webb, and Boland 1994). It is surprising that after heat-treatment, the edge of the silcrete lasts almost one more minute before dulling compared to quartzite and untreated silcrete.

Additionally, because finer-grained materials allow better control of flaking properties this allows for production of thinner flakes with edges that are more acute. Given that edge toughness is also positively correlated with edge angle, where a decrease in the edge angle (more acute) decreases edge toughness (McCormick and Almond 1990), it is also surprising that heat-treated silcrete has more durable edges than untreated silcrete and quartzite. Given that heat-treated silcrete has much lower fracture toughness than quartzite and untreated silcrete it should have decreased edge strength compared to those materials. This result goes against the relationships outlined in **Table 1.**

In the experiment, (see *Chapter 9*), edge angles of quartzite and untreated silcrete have an exponential relationship with time to dullness, which should give them an advantage over heat-treated silcrete when more acute edge angles are considered. However, the edge of heat-treated silcrete nevertheless lasts significantly longer than untreated silcrete and quartzite. Given that the abrasion on the edge conducting this study runs on and parallel to the edge, future studies will have to investigate whether strain perpendicular to the edge might better follow the predicted relationship between fracture toughness and edge strength.

Conversely, when quartzite was selected it was used in a prepared-core flaking strategy to create convergent-points, flakes, and blades. Although the gross utility of quartzite was not as high as heat-treated silcrete, the net-return rate, mostly driven by the lack of heat-treatment cost, made quartzite good enough for use.

As with the discussion of the Hypothesis 3 (H_3) results when using the original currency presented above, an implication of seeking raw materials with the highest net-return rate is that if raw materials show up in the archaeological record that do not have

the highest net-return rate, the selection of those raw materials did not minimize opportunity-cost for the forager. However, this time, compared to MIS5 and MIS6 conditions, quartzite and heat-treated silcrete have a tied ranking, which means that it did not matter which raw material was selected because both would minimize opportunity cost in a similar way. However, there are other raw materials present in the MIS4 record from PP5-6 such as quartz and chalcedony, which sometimes dominate individual sub-aggregates (see *Chapter 7*). However, because net-return rates were not calculated for those raw materials it is hard to judge whether selecting them would have had implications for opportunity-cost.

Nevertheless, it is important to note again that by selecting a raw material in disregard of the raw material that has the highest net-return rate could suggest that foragers made specific trips or utilized embedded procurement to procure these raw materials due to symbolic (Clendon 1999, Gould et al. 1971, Wurz 1999), or stylistics needs (Close 2002, Mackay 2011, Sackett 1986, 1982).

The ACM result in support for H_2 during MIS4 suggests that the mobility strategy changed compared to during MIS6 and MIS5 conditions. Because inhabitants of PP5-6 during MIS4 consistently foraged for shellfish and returned with them to PP5-6 (Wilkins et al. 2017), it suggests a mobility strategy that consistently intercepted the coast. Marean (2010) proposed that the reliance of coastal ecosystems and the interception of spring low tides provides the forager with logistical challenges because net-return rates are the highest during spring tides, and so you want to be at the coast when that happens twice a month. During neap tide, Marean (2010) proposed, the foragers should place residential camps further inland to obtain the best net-return rates from terrestrial food resources.

However, there is risk involved with intercept hunting of animals. The risk involved with intercept hunting on the Paleo-Agulhas plain or in interior areas in the Mossel Bay region is the failure to obtain such resources during temporally constrained availability of the prey species arising from seasonal migrations and the risk of using non-projectile weapons against dangerous animals such as Buffalo (Bousman 1993, Brown 2011).

Brown (2011) proposed that due to potential scheduling conflicts arising between shellfish harvesting during spring low tides (c.f. Marean, 2010) and the intercept of migratory animals a scenario may have been created where the forager was pressured to use a procurement strategy that would provision PP5-6 with silcrete. The pressure would come from time-constraints and a risk of raw material supply failure (Bamforth and Bleed 1997). This potential provision strategy, which is what Kuhn (1992; 2004) termed place provisioning would have made sure PP5-6 would always be supplied with adequate amounts of stone tool raw materials (Wilkins et al. 2017). The suggested change in mobility pattern during MIS4 in conjunction with a place provisioning strategy could explain the change in the overall technological composition of the assemblage from MIS5 to MIS4. The change is best exemplified by the transition from a mostly prepared-core technology to a technology with a significant prismatic blade production component that included microlithic technology (Brown et al. 2012, Wilkins et al. 2017, see also *Chapter 7*). Barton and Riel-Salvatore (2014) found that model assemblages exhibited changes in assemblage composition only when mobility system was changed in conjunction with either place or individual provisioning. Their result suggests that changes in mobility system by itself cannot explain changes in assemblage composition but that whether a site was provisioned or the individual foragers were provisioned has to be taken into

account. Pop (2015) predicted, using his adjusted neutral model of stone procurement, that there should be a sharp decline in raw material abundance at a site with increasing distance to source leading to large sites (high frequency of discarded raw materials) only being formed at or very near to raw material sources. The formation of a large site with abundant discarded materials that is not located at or very near a raw material source indicates non-random and biased movement on the part of the foragers. PP5-6 is not situated on top of primary or secondary sources of either quartzite or silcrete during MIS4, which suggests that the increased use of PP5-6 and discard of quartzite and silcrete during MIS4 at PP5-6 was due to a specific mobility strategy.

When silcrete was the supplied material, it offered the opportunity to create a standardized blade technology and a means to conserve material. Blade technology has been argued to be linked to flaking efficiency and raw material conservation due to higher output of cutting edge compared to flakes (Andrefsky 1994, Bar-Yosef and Kuhn 1999, Clark 1987). However, this has been contested by experimental work, and when different measures of efficiency have been used. When the whole process of blade making and retouch is taken into consideration then blades do not have more cutting edge and higher cutting edge per mass ratios than flakes (Eren, Greenspan, and Sampson 2008). In addition, blade cores do not produce more useable blanks then bifacial cores (Jennings, Pevny, and Dickens 2010). Moreover, Muller and Clarkson (2016) proposed based on extensive experimental work that the increase in prismatic blades, Levallois technology, and small foliate bifaces during the MSA and Middle Paleolithic is correlated with the most significant increase in efficiency in the global stone tool record. In this light, blade technology is a way of increasing flaking efficiency but small foliate bifaces

and Levallois technology can also achieve comparable efficiency. The increase in blade production in MIS4 at PP5-6 is correlated with an increase in cutting edge per mass ratios on silcrete stone tools, which suggests that compared to the preceding MIS5, conserving raw material seem to be a priority (Wilkins et al. 2017).

Wilkins et al. (2017) point out that the need to maximize flaking efficiency when using silcrete is potentially linked to three different causes: 1) increased distance to raw material sources; 2) changes in mobility; and 3) increased group or population size that can be combined with changes in mobility. Because all different raw material types at PP5-6 exhibit increased flaking efficiency during MIS4, the first explanation can be ruled out. The source distribution was most likely similar in the following MIS3 compared to MIS4 but during MIS3 the overall flaking efficiency for silcrete declined even though the distance to the closest silcrete source remained the same (Wilkins et al. 2017, also see *Chapter 7*). The two latter explanations are more plausible, either by themselves or as a combination of both.

An increase in conservative raw material practices and more blade production during MIS4 might have been due to the need to conserve a limited silcrete supply (Wilkins et al. 2017). The supply might have been restricted due to decreased residential mobility as Wilkins et al. (2017) propose. This proposition is based on the rational that when local raw material availability is low and/or depleted, hunter-gatherers that are less mobile will react by increasing flaking efficiency (Andrefsky Jr 1994, Riel-Salvatore and Barton 2004). Such an argument with decreased residential mobility and increased sedentariness runs counter to Ambrose and Lorenz's (1990) hypothesis that foragers during MIS4 increased their mobility (Wilkins et al. 2017).

The raw material quality in silcrete that could facilitate blade production and increased cutting edge per mass ratios could only be achieved after heat-treatment. This means that the cost to gain that outcome had to be front-loaded (Brown et al. 2009). However, by changing the procurement strategy by routing movement on the landscape by silcrete sources to procure silcrete, and sources of wood and then provisioning that to PP5-6, the cost of such heat-treatment could be lowered since all activities could be undertaken at the same place (Brown 2011). This assertion is supported by the observation that the MIS4 record exhibits a higher frequency of silcrete pieces that lack visible luster that indicates heat-treatment and exhibits cortex, which both suggest that there was increased reduction of pre-heat-treatment nodules prior to heat-treatment during MIS4 at PP5-6 than during MIS5 (Wilkins et al. 2017).

The ACM results presented above appear to support such a procurement strategy. During embedded procurement, the forager would take the highest ranked raw material when encountering one, which was either quartzite or silcrete. The changing frequencies of both materials in the record suggests that when silcrete is dominant the forager moved from an area of the landscape that had a higher abundance of silcrete, while when quartzite is dominant the movement came from a direction where quartzite was more abundant. What this can indicate is that when more heat-treated silcrete is observed in the sequence, most of the movement on the landscape was towards the interior or perpendicular to the coast in the interior, while when quartzite is most frequent, most of the movement on the landscape was outwards onto the Paleo-Agulhas plain or perpendicular to the coast close to the actual coastline. Support for this type of scenario is that during MIS4, there was a significant increase in the frequency of outcrop cortex on

silcrete, which indicates that the silcrete came from the interior, while the cortex type on quartzite remains dominated by cobble cortex (Brown 2011, Wilkins et al. 2017, also see *Chapter 7*).

The increase observed in blade production, increase in raw material conservation, and the advent of microlithic technology, which suggests projectile technology (Brown et al. 2012) was facilitated by the increased selection of silcrete and subsequent heat-treatment. The risk of failure to intercept animals when not procuring coastal resources would have been another pressure to develop technology that was more reliable so that tools would not fail when animals were encountered (Bleed 1986). The innovation of projectile technology was potentially one appropriate answer to a situation where the cost of failure was high (Elston and Brantingham 2002).

However, a question arises as to why innovation of projectile technology did not happen during MIS6 when intercept hunting must have also been a part of the mobility strategy. MIS6 conditions would have been similar to MIS4 conditions. The Paleo-Agulhas plain would have been expansive with potential migratory animals and the archaeological record shows that these early modern human foragers did intercept the coast because shellfish remains are present even in the LC-MSA Lower. However, there is a big difference between the shellfish record from the MIS6 and the MIS4. Although the MIS6 record shows intercept forays with the coast, it is only the MIS5 and in MIS4 records that showcase evidence for a 'true' coastal adaptation as indicated mostly by shell-supported matrixes in the observed stratigraphy (Marean 2015). The support for H_3 during MIS6 suggest that raw material selection played an important part in the technological organization because raw materials were actively chosen based on net-

return rates. As noted above, the selection of the material with the highest net-return rate implies that opportunity-cost was minimized. This suggests that other activities were prioritized. Additionally, the limited evidence for early stage reduction and conservation of raw materials suggest that PP13B was not a locality that was used often or for longer time-periods. This further suggests that perhaps those residential moves were frequent and that people were provisioned with raw materials and not sites.

Taken together, the indications that MIS6 foragers engaged in increased residential moves, was not fully involved in a coastal adaptation, decreased opportunity-cost by selecting the material with the highest net-return rate, and provisioned their people instead of localities suggest that they should have a greater reason to want to use technologies that would decrease the risk of failure to intercept animals while moving frequently. Future research needs to focus on why composite technologies such as projectile weapons were not invented earlier given such conditions.

I propose the following chain of events that led to the advent and innovation of microlithic technology and possible projectile technology during MIS4. The environmental context during MIS4 made PP5-6 very attractive. This is supported by work by Armstrong (2016) that showed that foragers at PP5-6 did not utilize small mammals, considered lower rank, but instead only focused on larger mammals and shellfish, considered higher quality resources. Further, this suggested to Armstrong (2016) that the foragers at PP5-6 could afford to only go after the higher quality resources because PP5-6 was situated in a higher yield environment. Additionally, work by Karkanas and colleagues (2014) showed that more people used the site for longer times

or that there was an increased use of the site on a regular basis during MIS4 compared to MIS5.

A potential foraging behavior outcome of living in an attractive environmental context with dense (migratory animals and coastal resources such as shellfish) and predictable resources (coastal resources) is elevated territoriality (Dyson-Hudson and Smith 1978). Under such circumstances, there is also commonly a decrease in mobility (Harpending and Davis 1977). Further, when a forager is faced with predictable resources the technology should reflect over-designed reliable hunting weapons (Bleed 1986). Wilkins et al. (2017) note that environments with predictable and dense resources often provide greater carrying capacity supporting larger populations and/or group sizes. The evidence from MIS4 occupations at PP5-6 is consistent with a model of increased resource predictability and density compared to earlier MIS5 occupations and later MIS3 occupations (Wilkins et al. 2017).

The attractiveness, I propose, could only be maintained if the forager switched between coastal foraging during spring low tides and intercept hunting during neap tides on a regular basis. However, it needs to be noted that that intercept hunting opportunity is potentially highly seasonal due to movement of prey (Bousman 1993, Brown 2011).The intercept hunting did not require a new technology to succeed but projectile technology would lower the risk of failure when a prey was encountered. To make projectile technology, raw materials that allowed for better control over flaking properties was needed and certain types of tools had to be made. Blade technology and heat-treatment was already invented prior to MIS4 (Brown et al. 2009). Having that knowledge, what the foragers sought was to maximize the number of blades that they could produce for a

given unit of raw material, and they wanted the edges of those blades to last as long as possible. The differential movement to intercept either coastal resources or migrating prey made the forager move past both quartzite and silcrete sources depending on the direction of movement, and because both raw materials provided similar net-return rates, they were both procured and provisioned to the locality when encountered. When the raw material happened to be silcrete, it allowed the foragers to produce needed tools for intercept hunting that would lower risk of failure.

However, attractiveness, associated mobility strategy, and efforts to minimize risk in terms of failure to effectively procure prey when encountered cannot explain fully why we see investment in costly projectile technology during MIS4 and not in MIS6 when intercept hunting most likely was even more prevalent. Another possibility is the need for innovation of a new technology to be able to procure lower ranked prey that was harder to acquire using non-projectile weapons or other simpler technologies. The reason for having to attack lower ranking prey could be due to a population increase that required more resources to be obtained to meet the calorie requirement of the group. However, work by Armstrong (2016) as noted above suggested that foragers at PP5-6 did not utilize smaller mammals, which are considered lower quality in terms of yield.

Future studies should focus on why it is that microlithic technology was invented in MIS4 and not in MIS6 when seemingly the attractiveness and the environmental conditions of the region would have been similar. However, one notable difference is that during MIS6 there was strong winter rainfall, while during MIS4 there was prevailing summer rainfall. This would have resulted in different vegetation regimes, which in turn could have yielded different animals on the Paleo-Agulhas plain or at least different

abundances of animals. The different types of animals or abundances during MIS6 might not have required a composite microlithic technology to minimize the risk of failure to procure prey when encountered.

Brown (2011) proposed that the combination of potentially direct procurement of silcrete, heat-treatment (Brown et al., 2009), and production of small standardized blades and microliths (Brown et al., 2012) during MIS4 demonstrates that the cognitive ability to create composite technology was in place by 70 ka. This argument has also been echoed by Wadley (2013b, 2010, 2008). Brown (2011: 283) and Marean (2010a) proposed that long-chain composite technologies include a series of linked steps or processes that can occur at different points on the landscape and requires independent planning and scheduling so that a final integrated finished product is produced.

The MIS4 record highlights several such steps and processes that in the end potentially created a composite projectile technology including active choice of silcrete during embedded procurement, heat-treatment of such selected silcrete to improve flaking ability but also perhaps edge durability, and production of standardized blades and microliths. In addition, the steps to create a composite projectile technology would include collection of wood fuels to heat-treat the silcrete, organic materials for arrow shafts and bow structure, sinew or twine for bowstring, and resin or other binding-agents to join components together.

The Active-Choice Model presented in this study allows for an analytical and logic-driven investigation of the independent steps and processes needed to create a composite technology or more simple technologies for that matter. Each resource (wood, resin, twine, bone etc.) needed to build a package of technology can be subjected to the

same ACM equations presented above. For example, one can switch out stone as the resource sought with wood intended to be used to build a bow. In such a scenario, one can argue that the assumed currency that the forager seeks to maximize is wood strength and flexibility. Given several known species of wood available in an environment, the ACM can be used to predict under what environmental and climatic conditions or behavioral conditions the forager would switch from one type of wood to another to build a bow. Assuming that the forager will engage in optimal or near-optimal behavior to the solve problems it faces, the net-return rate of an assumed currency should drive the selection of different resources. This way the ACM can be used to estimate the net-return rate of different resources that a forager needs to build its technology, and we will obtain a fuller picture of the web of decisions that forager faced during important parts of modern human origins.

It is important to note the model framework presented in this study needs to be applied on a site-by-site basis. This study lays out all the methodological steps needed to build a situation-specific agent-based model that can be used to test hypotheses related to neutral procurement of stone or to calculate or obtain estimates of variables needed to calculate net-return rates of raw materials. As reviewed above (*Chapter 3*) the change in preference from coarse-grained quartzite to fine-grained heat-treated silcrete or other CCS stone raw materials are visible at all major MSA sites in the Cape Region in South Africa. Well-studied sites such as Diepkloof Rock Shelter, where comprehensive raw material surveys have been conducted to establish potential sources on the landscape, are primed to employ the model framework presented in this study.

CHAPTER 13: CONCLUSIONS

The exhaustive evaluation of the Opportunistic Acquisition Model (OAM) suggests limited support for the hypothesis that raw material frequencies observed in the MSA record at Pinnacle Point (PP) are due to opportunistic encounters of raw material sources when randomly walking in the environment. There is, however, one exception. During MIS6 conditions without a Paleo-Agulhas plain silcrete source, the model frequencies match the archaeological frequencies at PP13B if the forager engages in expedient behavior. However, this behavior is potentially not realistic as the forager would spend between 30 and 60% of the time without raw materials in the toolkit. An argument can be made that it is a realistic behavior if the forager regularly returns to a locality where stone is stockpiled or cached. However, the MIS6 stone tool assemblage at PP13B does not offer conclusive evidence that it represents stockpiling or site-caching behavior. A future study should be aimed at resolving this issue.

One goal of this dissertation was to create a model framework that can be applied to any record. The failure to find conclusive support for the OAM using the Pinnacle Point record does not mean that it will not be found supported in a different context surrounding a different archaeological record. This means that the OAM, which simulated embedded and opportunistic procurement of raw materials, can still explain raw material selection at other sites. The methods laid out in this study can guide researchers in how to build their own situation-specific agent-based model to be able to test the OAM using their own data.

In contrast to the OAM results, this study has shown that the early modern humans living in the Mossel Bay region strategically selected raw materials that offered

the highest net-return rate of a desired currency. This result supports a utilitarian model of raw material selection and change (c.f. Mackay 2008). During MIS6 at PP13B, the net-return rate of quartzite was higher than silcrete even after heat-treatment because of the presence of a wave-ravinement surface close to Pinnacle Point during lower sea levels that offered abundant quartzite cobbles facilitating easy procurement. The selection of the raw material with the highest net-return rate implies that opportunity cost was minimized. This allowed the forager to spend more time on other pressing activities, while at the same time using a material for tasks without compromising suitability. The MIS6 foragers faced an expanded Paleo-Agulhas plain with a diverse ecosystem and potentially migrating ungulates in addition to the rich coastline. This most likely made them move frequently to conduct intercept hunting and to take advantage of rich coastal resources when available. A mobility strategy that supplied the individual with raw materials that was procured at minimal cost was likely operating.

During MIS5, the foragers at Pinnacle Point faced a coastal environment with the coastline close to or at the current configuration. The abundant cobble sources in the form of cobble beaches in vicinity to Pinnacle Point offered the foragers easily accessible raw materials. Although the coastline was closer during MIS5, shellfish remains from PP13B during MIS6 suggest that the site was occupied when the coast was within 10km. This makes the environmental context similar. As during MIS6, the low travel and search cost of quartzite drove the net-return rate of quartzite to exceed silcrete. The selection of quartzite during MIS5 suggests similar procurement systems for raw materials during MIS5 and MIS6 regardless of environmental conditions.

The raw material selection during MIS6 and MIS5 indicates provisioning of people, which can suggest that they were more mobile. The provision of people helps minimize risk related to shortfall resulting from finding new materials when moving about the landscape. Quartzite selection during these two periods indicates that quartzite was not selected because it had the best quality but because it was good enough and was the least costly in terms of net-return rate (c.f. Torrence 1989, 1983). However, because the currency assumed to be sought by the foragers is based on physical properties of the raw materials, the result from MIS5 and MIS6 conditions suggests that part of the response to climatic and environmental conditions was reliance on quartzite obtained through direct procurement (c.f. Gould, 1985; Gould and Saggers, 1985) and to manufacture technology to obtain food resources and/or conduct processing tasks thus suggesting knowledge about physical properties of raw materials and how to utilize them.

In MIS4, the increase in silcrete, the increase in procurement from outcrop sources, the increase in blade production, and the emergence of microlithic technology were underpinned by a raw material procurement strategy where both quartzite and silcrete was selected due to tied net-return rates. The foragers sought to maximize the number of blades they could produce per core, and they wanted the edges of those blades to last as long as possible. The low flake manufacturing cost and high gross value of the assumed currency for silcrete and the high flaking manufacturing cost and lack of heat-treatment cost for quartzite resulted in tied net-return rates. The raw materials were selected during embedded procurement where the mobility strategy was not dictated by locations of raw material sources (c.f. Binford 1979). Once encountered, both materials could be selected because they provided the same payoff. Both raw materials were

conservatively handled and discarded at site in a system that indicates place provisioning. However, the quality of heat-treated silcrete made it amenable to produce microlithic technology. Microlithic technology limited the risk of failure when conducting intercept hunting. In summary, the response to climatic and environmental conditions during MIS4 was relatively complex combining a mobility system that targeted food resources with a reliance on investment in specific stone raw materials and technology that would facilitate the extraction of the resources.

This study offers a new model framework to study human resource-choice behavior. The model framework can be used for different resources and under any archaeological context. It offers a researcher the tools to understand whether opportunistic behavior or strategic choice has driven the frequency of a raw material to be dominant in the given archaeological record. The two different behaviors have different implications for the role and importance the resource had in the technological organization of the foragers. This study indicates that raw material selection played an important role in the technological organization of the MSA foragers at Pinnacle Point. Further, this study suggests that external environmental-linked factors affected human behavior during MIS6 and MIS5. The position of the coastline and the distribution of sources on the landscape during these two periods drove the profitability of quartzite up. Whereas during MIS4, human behavior in terms of flaking manufacturing and heat-treatment, and the physical properties of the different raw material drove the profitability of the raw materials. Finally, the results presented in this study limit the support for other 'Preference-based' models that propose that raw material change at the MIS5 to MIS4 transition in the MSA is linked to symbolic value (Wurz 2009), or trade and/or exchange

(Deacon 1989). However, it is hard to rule out these models. Each site needs to be looked at individually.

REFERENCES

Akerman, K. 2007. "To Make a Point: Ethnographic Reality and the Ethnographic and Experimental Replication of Australian Macroblades Known as Leilira." *Australian Archaeology* 64:23-34.

Akerman, K. 1979. "Heat and lithic technology in the Kimberleys, W. A." *Archaeology & Physical Anthropology in Oceania* 14:144-151.

Akerman, K., R. Fullagar, and A. van Gijn. 2002. "Weapons and wunan: production, function and exchange of Kimberley points." *Australian Aboriginal Studies* 2002 (1):13-42.

Albert, R.M., and C.W. Marean. 2012. "The Exploitation of Plant Resources by Early Homo sapiens: The Phytolith Record from Pinnacle Point 13B Cave, South Africa." *Geoarchaeology: An International Journal* 27:363-384.

Alexander, R. M. 1996. *Optima for Animals*. Princeton, NJ: Princeton University Press.

Allan, J. C., R. Hart, and J. V. Tranquili. 2006. "The use of Passive Integrated Transponder (PIT) tags to trace cobble transport in a mixed sand and gravel beach on the high-energy Oregon coast, USA." *Marine Geology* 232:63-86.

Alvard, M. S., and L. Kuznar. 2001. "Deferred harvests: The transition from hunting to animal husbandry." *American Anthropologist* 103:295-311.

Ambrose, S. H. 2001. "Paleolithic Technology and Human Evolution." *Science* 291:1748-1753.

Ambrose, S. H. 2002. "Small Things Remembered: Origins of Early Microlithic Industries in Sub-Saharan Africa." *Archeological Papers of the American Anthropological Association* 12 (1):9-29. doi: 10.1525/ap3a.2002.12.1.9.

Ambrose, S. H. 2006. "Howiesons Poort lithic raw material procurement patterns and the evolution of modern human behavior: a response to Minichillo (2006)." *Journal of human evolution* 50 (3):365-369. doi: 10.1016/j.jhevol.2005.12.006.

Ambrose, S. H., and K. G. Lorenz. 1990. "Social and ecological models for the middle stone age in southern Africa." In *The emergence of modern humans: an archaeological perspective*, edited by P. Mellars, 3-33. Edinburgh: Edinburgh University Press.

Andrefsky Jr, W. 1994. "Raw-Material Availability and the Organization of Technology." *American Antiquity* 59 (1):21-34. doi: 10.2307/3085499.

Andrefsky, W. 1991. "Inferring trends in prehistoric settlement behavior from lithic production technology in the southern plains." *North American Archaeology* 12 (2):129-144.

Andrefsky, W. 1994. "The geological occurrence of lithic material and stone tool production strategies." *Geoarchaeology* 9 (5):375-391. doi: 10.1002/gea.3340090503.

Archer, W., G. Gunz, K. L. van Niekerk, C. S. Henshilwood, and S. P. McPherron. 2015. "Diachronic Change within the Still Bay at Blombos Cave, South Africa." *PLoS ONE* 10 (7):1-25.

Armstrong, A. 2016. "Small mammal utilization by Middle Stone Age humans at Die Kelders Cave 1 and Pinnacle Point Site 5-6, Western Cape Province, South Africa." *Journal of Human Evolution* 101:17-44.

Arthur, K. W. 2010. "Feminine Knowledge and Skill Reconsidered: Women and Flaked Stone Tools." *American Anthropologist* 112 (2):228-243. doi: 10.1111/j.1548-1433.2010.01222.x.

Atkinson, B. K. 1984. "Subcritical crack growth in geological materials." *Journal of Geophysical Research* 89:4077-4114.

Axelrod, R., and L. Tesfatsion. 2006. "Appendix A A Guide for Newcomers to Agent-Based Modeling in the Social Sciences." *Handbook of Computational Economics* 2:1647-1659.

Bamforth, D. B. 1986. "Technological Efficiency and Tool Curation." *American Antiquity* 51 (1):38-50. doi: 10.2307/280392.

Bamforth, D. B. 1990. "Settlement, raw material, and lithic procurement in the central Mojave Desert." *Journal of Anthropological Archaeology* 9 (1):70-104. doi: 10.1016/0278-4165(90)90006-Y.

Bamforth, D. B. 1991. "Technological Organization and Hunter-Gatherer Land Use: A California Example." *American Antiquity* 56 (2):216-234. doi: 10.2307/281416.

Bamforth, D. B., and P. Bleed. 1997. "Technology, Flaked Stone Technology, and Risk." *Archeological Papers of the American Anthropological Association* 7 (1):109-139. doi: 10.1525/ap3a.1997.7.1.109.

Bandura, A. 1977. *Social Learning Theory*. Englewood Cliffs, NJ: Prentice Hall.

Bar-Matthews, M., C. W. Marean, Z. Jacobs, P. Karkanas, E. C. Fisher, A. I. R. Herries, K. Brown, H. M. Williams, J. Bernatchez, A. Ayalon, and P. J. Nilssen. 2010. "A high resolution and continuous isotopic speleothem record of paleoclimate and

paleoenvironment from 90 to 53 ka from Pinnacle Point on the south coast of South Africa." *Quaternary Science Reviews* 29 (17–18):2131-2145. doi: 10.1016/j.quascirev.2010.05.009.

Bar-Yosef, O. 1991. "Raw Material explotation in the Levantine Epi-Paleolithic." In *Raw material economies among prehistoric hunter-gatherers*, edited by A. Montet-White and S. Holen. Lawrence: University of Kansas.

Bar-Yosef, O., and S. Kuhn. 1999. "The big deal about blades: laminar technologies and human evolution." *American Anthropologist* 101:322-328.

Barham, L., and P. Mitchell. 2008. *The first Africans: African archaeology from the earliest tool makers to most recent foragers*. Cambridge: Cambridge University Press.

Barlow, K. R., and D. Metcalfe. 1996. "Plant utility indices: Two Great Basin examples." *Journal of Archaeological Science* 23:351-371.

Barton, C. M. 1990. "Beyond Style and Function: A View from the Middle Paleolithic." *American Anthropologist* 92 (1):57-72. doi: 10.1525/aa.1990.92.1.02a00040.

Barton, C. M. 1991. "Retouched Tools, Fact or Fiction? Paradigms for Interpreting Paleolithic Chipped Stone." In *Perspectives on the Past: Theoretical Biases in Mediterranean Hunter-Gatherer Research*, edited by G. A. Clark, 143-163. Philadelphia: University of Pennsylvania Press.

Barton, C. M. 1998. "Looking Back from the World's End: Paleolithic Settlement and Mobility at Gibraltar." In *Las Culturas del Pleistoceno Superior en Andalucia*, edited by J. L. Sanchidritin Torti and M. D. S. Vallejo, 13-22. Cordoba: Patronato de la Cueva de Nerja.

Barton, C. M., and J. Riel-Salvatore. 2014. "The formation of lithic assemblages." *Journal of Archaeological Science* 46:334-352.

Barton, C. M., J. Riel-Salvatore, J. M. Anderies, and G. Popescu. 2011. "Modeling Human Ecodynamics and Biocultural Interactions in the Late Pleistocene of Western Eurasia." *Human Ecology* 39 (6):705-725. doi: 10.1007/s10745-011-9433-8.

Bartumeus, F., F. Peters, S. Pueyo, C. Marrase, and J. Catalan. 2003. "Helical Levy walks: Adjusting searching statistics to resource availability in microzooplankton." *Proceedings of the National Academy of Sciences* 100:12771-12775.

Basgall, M. 1987. "Resource intensification among hunter-gatherers: Acorn economies in prehistoric California." *Research in Economic Anthropology* 9:21-52.

Bayham, F. E. 1979. "Factors influencing the Archaic pattern of animal exploitation." *Kiva* 44:219-235.

Beardsley, R. K., P. Holder, A. D. Krieger, B. J. Meggers, J. B. Rinaldo, and P. Kutsche. 1956. "Functional and Evolutionary Implications of Community Patterning." *Memoirs of the Society for American Archaeology* (11):129-157. doi: 10.2307/25146638.

Beaton, J. B. 1991a. "Colonizing continents: Some problems from Australia and the Americas." In *The First Americans: Search and Research*, edited by T. D. Dillehay and D. J. Meltzer, 209–230. Baton Rouge, LA: CRC Press.

Beaton, J. M. 1991b. "Extensification and intensification in central California prehistory." *Antiquity* 65:947-951.

Beauchamp, E. K. , and B. A. Purdy. 1986. "Decrease in fracture toughness of chert by heat treatment." *Journal of Materials Science* 21:1963-1966.

Beaumont, P. B., H. de Villiers, and J. C. Vogel. 1978. "Modern man in sub-saharan africa prior to 49,000 years B.P.: a review and evaluation with particular reference to Border Cave." *South African Journal of Science* 74:409-419.

Beck, C., A. K. Taylor, and G. T. Jones. 2002. "Rocks are heavy: Transport costs and Paleoarchaic quarry behavior in the Great Basin " *Journal of Anthropological Archaeology* 21:481–507.

Bell, G. 2001. "Neutral Macroecology." *Science* 293:2413-2418.

Bernatchez, J. A. 2010. "Taphonomic implications of orientation of plotted finds from Pinnacle Point 13B (Mossel Bay, Western Cape Province, South Africa)." *Journal of Human Evolution* 59 (3–4):274-288. doi: 10.1016/j.jhevol.2010.07.005.

Bettinger, R. L., and M. A. Baumhoff. 1982. "The Numic spread: Great Basin cultures in competition." *American Antiquity* 47:485-503.

Bettinger, R. L., R. Mahli, and H. McCarthy. 1997. "Central place models of acorn and mussel processing." *Journal of Archaeological Science* 24:887-899.

Bettinger, R. L., B. Winterhalder, and R. McElreath. 2006. "A simple model of technological intensification." *Journal of Archaeological Science* 33:538-545.

Bicchieri, M. G. 1972. *Hunters and gatheres today*. Edited by M. G. Bicchieri. Prospect Heights, IL: Waveland.

Binford, L. R. 1973. "Interassemblage variability - the mousterian and the "functional" argument." In *The explanation of culture change: Models in prehistory*, edited by C. Renfrew, 227-254. London: Duckworth.

Binford, L. R. 1977. "Forty-seven trips: a case study in the character of archaeological formation processes." In *Stone Tools as Cultural Markers*, edited by R. V. S. Wright, 24-36. Canberra: Australian Institute of Aboriginal Studies.

Binford, L. R. 1978. *Nunamiut Ethnoarchaeology*. New York, NY: Academic Press.

Binford, L. R. 1979. "Organization and Formation Processes: Looking at Curated Technologies." *Journal of Anthropological Research* 35 (3):255-273.

Binford, L. R. 1980. "Willow Smoke and Dogs' Tails: Hunter-Gatherer Settlement Systems and Archaeological Site Formation." *American Antiquity* 45 (1):4-20. doi: 10.2307/279653.

Binford, L. R. 2001. *Constructing Frames of Reference: An Analytical Method for Archaeological Theory Building Using Ethnographic and Environmental Data Sets*. Berkeley: University of California Press.

Binford, L. R., and S. R. Binford. 1966. "A preliminary analysis of functional variability in the Mousterian of Levallois facies." *American anthropologist* 68 (2):238-295.

Binford, L. R., and J. F. O'Connell. 1984. "An Alyawara Day: The Stone Quarry." *Journal of Anthropological Research* 40 (3):406-432.

Binford, L. R., and N. M. Stone. 1985. ""Righteous Rocks" and Richard Gould: Some Observations on Misguided "Debate"." *American Antiquity* 50 (1):151-153. doi: 10.2307/280641.

Biran, A., J. Abbot, and R. Mace. 2004. "Families and Firewood: A Comparative Analysis of the Costs and Benefits of Children in Firewood Collection and Use in Two Rural Communities in Sub-Saharan Africa." *Human Ecology* 32 (1):1-25.

Bird, D. W., and J. F. O'Connell. 2006. "Behavioral Ecology and Archaeology." *Journal of Archaeological Research* 14 (2):143-188. doi: 10.1007/s10814-006-9003-6.

Bird, D. W., J. L. Richardson, P. M. Veth, and A. J. Barham. 2002. "Explaining Shellfish Variability in Middens on the Meriam Islands, Torres Strait, Australia." *Journal of Archaeological Science* 29 (5):457-469. doi: 10.1006/jasc.2001.0734.

Bird, R.B., E. Smith, and D.W. Bird. 2001. "The hunting handicap: costly signaling in human foraging strategies." *Behavioral Ecology and Sociobiology* 50 (1):9-19.

Bishop, C. A. 1983. "Comment on Smith 1983a." *Current Anthropology* 24.

Bleed, P. 1986. "The Optimal Design of Hunting Weapons: Maintainability or Reliability." *American Antiquity* 51 (4). doi: 10.2307/280862.

Bleed, P. 2001. "Trees or Chains, Links or Branches: Conceptual Alternatives for Consideration of Stone Tool Production and Other Sequential Activities." *Journal of Archaeological Method and Theory* 8 (1):101-127. doi: 10.1023/A:1009526016167.

Blumenschine, R. J., F. T. Masao, J. C. Tactikos, and J. I. Ebert. 2008. "Effects of distance from stone source on landscape-scale variation in Oldowan artifact assemblages in the Paleo-Olduvai Basin, Tanzania." *Journal of Archaeological Science* 35 (1):76-86. doi: 10.1016/j.jas.2007.02.009.

Bonabeau, E. 2002. "Agent-based modeling: Methods and techniques for simulating human systems." *Proceedings of the National Academy of Sciences* 99 (90003):7280-7287. doi: 10.1073/pnas.082080899.

Bordes, F. 1973. "On the chronology and contemporaneity of different paleolithic cultures in France." In *The explanation of culture change*, 217-226.

Bordes, F., and D. de Sonneville-Bordes. 1970. "The significance of variability in Palaeolithic assemblages." *World Archaeology* 2 (1):61-73.

Bordes, F., J. Kelley, and J. Cinq-Mars. 1969. "Reflections on Typology and Techniques in the Palaeolithic." *Arctic Anthropology* 6 (1):1-29. doi: 10.2307/40315681.

Botkin, S. 1980. "Effects of human exploitation on shellfish populations at Malibu Creek, California." In *Modeling Change in Prehistoric Subsistence Economies*, edited by T. Earle and A. L. Christenson, 121–139. New York: Academic Press.

Bouey, P. D. 1987. "The intensification of hunter-gatherer economies in the southern North Coast Ranges of California." *Research in Economic Anthropology* 9:53-101.

Bousman, C. B. 1993. "HUNTER-GATHERER ADAPTATIONS, ECONOMIC RISK AND TOOL DESIGN." *LITHIC TECHNOLOGY* 18 (1&2):59-86.

Boyer, D., O. Miramontes, G. Ramos-Fernandez, J. L. Mateos, and G. Cocho. 2004. "Modeling the searching behavior of social monkeys." *Physica A: Statistical Mechanics and Its Applications* 342:329-335.

Brantingham, P. J. 2003. "A Neutral Model of Stone Raw Material Procurement." *American Antiquity* 68 (3):487-509. doi: 10.2307/3557105.

Brantingham, P. J. 2006. "Measuring Forager Mobility." *Current Anthropology* 47 (3):435-459. doi: 10.1086/503062.

Brantingham, P. J., and S. L. Kuhn. 2001. "Constraints on Levallois Core Technology: A Mathematical Model." *Journal of Archaeological Science* 28 (7):747-761. doi: 10.1006/jasc.2000.0594.

Brantingham, P. J., J. W. Olsen, J. A. Rech, and A. I. Krivoshapkin. 2000. "Raw Material Quality and Prepared Core Technologies in Northeast Asia." *Journal of Archaeological Science* 27 (3):255-271. doi: 10.1006/jasc.1999.0456.

Braun, D. R. 2005. "Examining flake Production Strategies: Examples from the Middle Paleolithic of Southwest Asia." *Lithic Technology* 30 (2):107-125.

Braun, D. R., T. Plummer, P. Ditchfield, J. V. Ferraro, D. Maina, L. C. Bishop, and R. Potts. 2008. "Oldowan behavior and raw material transport: perspectives from the Kanjera Formation." *Journal of Archaeological Science* 35 (8):2329-2345. doi: 10.1016/j.jas.2008.03.004.

Braun, D. R., T. Plummer, J. V. Ferraro, P. Ditchfield, and L. C. Bishop. 2009. "Raw material quality and Oldowan hominin toolstone preferences: evidence from Kanjera South, Kenya." *Journal of Archaeological Science* 36 (7):1605-1614. doi: 10.1016/j.jas.2009.03.025.

Braun, D. R., M. J. Rogers, J. W. K. Harris, and S. J. Walker. 2008. "Landscape-scale variation in hominin tool use: Evidence from the Developed Oldowan." *Journal of Human Evolution* 55 (6):1053-1063. doi: 10.1016/j.jhevol.2008.05.020.

Braun, K., M. Bar-Matthews, R. Zahn, A. Matthews, A. Ayalon, R. M. Cowling, P. Karkanas, E. C. Fisher, T. Zilbermana, K. Dyez, and C. W. Marean. ms. "A record of climate and environment between 463 and 41 ka from speleothem stable isotopic compositions at Pinnacle Point on the South African south coast." Manuscript under review.

Bright, J., A. Ugan, and L. Hunsaker. 2002. "The effect of handling time on subsistence technology." *World Archaeology* 34 (1):164-181. doi: 10.1080/00438240220134304.

Broeke, G. T., G. van Voorna, and A. Ligtenberg. 2016. "Which Sensitivity Analysis Method Should I Use for My Agent-Based Model?" *Journal of Artificial Societies and Social Simulation* 19 (1):5.

Broughton, J. M. 1994. "Declines in foraging efficiency during the late Holocene: The archaeological mammal evidence from San Francisco Bay, California." *Journal of Anthropological Archaeology* 13:371-401.

Broughton, J. M. 1997. "Widening diet breadth, declining foraging efficiency, and prehistoric harvest pressure: Icthyofaunal evidence from the Emeryville Shellmound." *Antiquity* 71:845-862.

Broughton, J. M. 1999. *Resource Depression and Intensification During the Late Holocene, San Francisco Bay: Evidence from the Emeryville Shellmound Vertebrate Fauna*. Berkeley: University of California Anthropological Records 32.

Broughton, J. M. 2002. "Prey spatial structure and behavior affect archaeological tests of optimal foraging models: Examples from the Emeryville Shellmound vertebrate fauna." *World Archaeology* 34:60-83.

Broughton, J. M. 2004. *Prehistoric Human Impacts on California Birds: Evidence from the Emeryville Shellmound Avifauna, Ornithological Monographs 56*. Washington, DC: American Ornithologists' Union.

Broughton, J. M., and D. K. Grayson. 1993. "Diet breadth, adaptive change, and the White Mountains faunas." *Journal of Archaeological Science* 20:331-336.

Brouwer, I. D., J. C. Hoorweg, and M. J. Van Liere. 1997. "When Households Run Out of Fuel: Responses of Rural Households to Decreasing Fuelwood Availability, Ntcheu District, Malawi." *World Development* 25 (2):255-266.

Brown, K., and C. Marean. 2010. "Wood Fuel Availability for Heat Treatment Drives the Rise and Fall of Silcrete as a Raw Material in the Middle Stone Age of South Africa." In *In: Abstracts of the PaleoAnthropology Society 2010 Meetings.*, A0001-A0040. PaleoAnthropology.

Brown, K. S. 1999. "Raw material selection and flake production in the Middle Stone Age of Southern Africa: Die Kelders Cave I and Montagu Cave." State University of New York at Stony Brook.

Brown, K. S. 2011. "The Sword in the Stone: Lithic Raw Material Explotation in the Middle Stone Age at Pinnacle Point Site 5-6, Southern Cape, South Africa." University of Cape Town, Department of Archaeology.

Brown, K. S., C. W. Marean, A. I. R. Herries, Z. Jacobs, C. Tribolo, D. Braun, D. L. Roberts, M. C. Meyer, and J. Bernatchez. 2009. "Fire As an Engineering Tool of Early Modern Humans." *Science* 325 (5942):859-862. doi: 10.1126/science.1175028.

Brown, K. S., C. W. Marean, Z. Jacobs, B. J. Schoville, S. Oestmo, E. C. Fisher, J. Bernatchez, P. Karkanas, and T. Matthews. 2012. "An early and enduring advanced technology originating 71,000 years ago in South Africa." *Nature* 491 (7425):590-3. doi: 10.1038/nature11660.

Bräuer, G., H. J. Deacon, and F. Zipfel. 1992. "Comment on the new maxillary finds from Klasies River, South Africa." *Journal of Human Evolution* 23 (5):419-422. doi: DOI: 10.1016/0047-2484(92)90089-R</p>.

Butzer, K. W. 1978. "Sediment Stratigraphy of the Middle Stone Age Sequence at Klasies River Mouth, Tsitsikama Coast, South Africa." *The South African Archaeological Bulletin* 33 (128):141-151.

Butzer, K. W., P. B. Beaumont, and J. C. Vogel. 1978. "Lithostratigraphy of Border Cave, KwaZulu, South Africa: a Middle Stone Age sequence beginning c. 195,000 b.p." *Journal of Archaeological Science* 5 (4):317-341. doi: DOI: 10.1016/0305-4403(78)90052-3</p>.

Cannon, M. D. 2000. "Large mammal relative abundance in Pithouse and Pueblo period archaeofaunas from southwestern New Mexico: Resource depression in the Mimbres-Mogollon?" *Journal of Anthropological Archaeology* 19:317-347.

Cannon, M. D. 2003. "A model of central place forager prey choice and an application to faunal remains from the Mimbres Valley, New Mexico." *Journal of Anthropological Archaeology* 22:1-25.

Cariboni, J., D. Gatelli, R. Liska, and A. Saltelli. 2007. "The role of sensitivity analysis in ecological modelling." *Ecological modelling* 203 (1):167-182.

Carter, P. L., P. J. Mitchell, and P. Vinnicombe. 1988. *Sehonghong: The Middle and Later Stone Age Industrial Sequence at a Lesotho Rock-Shelter*: British Archaeological Reports (BAR).

Cashdan, E. 1992. "The spatial organization of habitat use." In *Evolutionary ecology and human behavior*, edited by B. Winterhalder and E. A. Smith, 237–266. New York: Aldine de Gruyter.

Catuneanu, O., H. Wopfner, P. G. Eriksson, B. Cairncross, B. S. Rubidge, R. M. H. Smith, and P. J. Hancox. 2005. "The Karoo basins of south-central Africa." *Journal of African Earth Sciences* 43:211-353.

Cawthra, H. C. 2014. "The marine geology of Mossel Bay, South Africa." University of Cape Town.

Cawthra, H. C., M. D. Bateman, A. S. Carr, J. S. Compton, and P. J. Holmes. 2014. "Understanding Late Quaternary change at the land–ocean interface: a synthesis of the evolution of the Wilderness coastline, South Africa." *Quaternary Science Reviews* 99:210-223.

Cawthra, H. C., R. Uken, and M. N. Ovechkina. 2012. "New insights into the geological evolution of the Durban Bluff and adjacent Blood Reef, South Africa." *South African Journal of Geology* 115 (3):291-308.

Cawthra, H.C., J.S. Compton, E.C. Fisher, M.R. MacHutchon, and C.W. Marean. 2015. "Submerged shorelines and landscape features offshore of Mossel Bay, South Africa." *Geological Society, London, Special Publications* 411:SP411-11.

Charnov, E. L. 1976. "Optimal Foraging, the Marginal Value Theorem." *Theoretical Population Biology* 9:129-136.

Charnov, E. L., and G. H. Orians. 1973. *Optimal foraging: Some theoretical explorations*. Salt Lake City: Mimeo, Department of Biology, University of Utah.

Charrié-Duhaut, A., G. Porraz, C. R. Cartwright, M. Igreja, J. Connan, C. Poggenpoel, and P.-J. Texier. 2013. "First molecular identification of a hafting adhesive in the Late Howiesons Poort at Diepkloof Rock Shelter (Western Cape, South Africa)." *Journal of Archaeological Science* 40:3506-3518. doi: 10.1016/j.jas.2012.12.026.

Chase, B. M. 2010. "South African palaeoenvironments during marine oxygen isotope stage 4: a context for the Howiesons Poort and Still Bay industries." *Journal of Archaeological Science* 37:1359-1366.

Ciravolo, A. E. 2016. "Glass shards at Pinnacle Point rock shelter 5-~6, South Africa: Are they from the last super-~eruption of Toba?" M.S., University of Nevada, Las Vegas.

Clark, J. D. 1980. "Raw material and African lithic technology." *Man and Environment* 4:44-55.

Clark, J. D., Y. Beyene, G. WoldeGabriel, W. K. Hart, P. R. Renne, H. Gilbert, A. Defleur, G. Suwa, S. Katoh, K. R. Ludwig, J.-R. Boisserie, B. Asfaw, and T. D. White. 2003. "Stratigraphic, chronological and behavioural contexts of Pleistocene Homo sapiens from Middle Awash, Ethiopia." *Nature* 423 (6941):747-752. doi: 10.1038/nature01670.

Clark, J. D., and H. Kurashina. 1979. "An analysis of Earlier Stone Age bifaces from Gadeb (Locality 8E), Northern Bale Highlands, Ethiopia." *South African Archaeological Bulletin* 34:93-109.

Clark, J. E. 1987. "Politics, prismatic blades, and Mesoamerican civilization." *The organization of core technology*:259-284.

Clark, J. L. 2013. "Exploring the relationship between climate change and the decline of the Howieson's Poort at Sibudu Cave (South Africa)." In *Zooarchaeology and*

modern human origins: human hunting behavior during the later Pleistocene, edited by J. L. Clark and J. D. Speth, 9-18. Dordrecht: Springer Science.

Clark, J.D. 1972. "Palaeolithic butchery practices." In *Man, settlement and urbanism*, edited by P. J. Ucko, R. Tringham and G. W. Dimleby, 149-156. London: Gerald Duckworth & CO.

Clendon, M. 1999. "Worora Gender Metaphores and Australian Prehistory." *Anthropological Linguistics* 41 (3):308-355.

Close, A. E. 2002. "Backed bladelets are a foreign country." In *Thinking Small: Global Perspectives on Microlithization*, edited by R. G. Elston and S. L. Kuhn, 31-44.

Cochrane, G.W.G., J.A. Webb, T. Doelman, and P.J. Habgood. 2016. "Elemental differences: Geochemical identification of aboriginal silcrete sources in the Arcadia Valley, eastern Australia." *Journal of Archaeological Science: Reports* Accepted Manuscript, In Press.

Collard, M., B. Buchanan, J. Morin, and A. Costopoulos. 2011. "What drives the evolution of hunter–gatherer subsistence technology? A reanalysis of the risk hypothesis with data from the Pacific Northwest." *Philosophical Transactions of the Royal Society B: Biological Sciences* 366 (1567):1129-1138. doi: 10.1098/rstb.2010.0366.

Collard, M., B. Buchanan, M. J. O'Brien, and J. Scholnick. 2013. "Risk, mobility or population size? Drivers of technological richness among contact-period western North American hunter-gatherers." *Philosophical Transactions of the Royal Society B: Biological Sciences* 368:1630.

Collard, M., B. Buchanan, and M. J. O'Brien. 2013. "Population Size as an Explanation for Patterns in the Paleolithic Archaeological Record: More Caution Is Needed." *Current Anthropology* 54 (S8):388-396.

Collard, M., A. Ruttle, B. Buchanan, and M. J. O'Brien. 2012. "Risk of Resource Failure and Toolkit Variation in Small-Scale Farmers and Herders." *PLoS ONE* 7 (7). doi: 10.1371/journal.pone.0040975.

Collins, S. 2008. "Experimental investigations into edge performance and its implications for stone artifact reduction modelling." *Journal of Archaeological Science* 35:2164-2170.

Compton, J.S. 2011. "Pleistocene sea-level fluctuations and human evolution on the southern coastal plain of South Africa." *Quaternary Science Reviews* 30 (5–6):506-527. doi: 10.1016/j.quascirev.2010.12.012.

Conard, N. J. , G. Porraz, and L. Wadley. 2012. "What is in a name? Characterising the "Post-Howiesons Poort" at Sibudu." *South African Archaeological Bulletin* 67:180-199.

Conard, N. J., and M. Will. 2015. "Examining the causes and consequences of short-term behavioral change during the Middle Stone Age at Sibudu, South Africa." *PLoS ONE* 10 (6):e0130001.

Coon, S.C. 1971. *The hunting peoples*. New York: Nick Lyons Books.

Copeland, S. R., H. C. Cawthra, E. C. Fisher, J. A. Lee-Thorp, R. M. Cowling, P. J. L. Roux, J. Hodgkins, and C. W. Marean. 2015. "Strontium Isotope Investigation of Ungulate Movement Patterns on the Pleistocene Paleo-Agulhas Plain of the Greater Cape Floristic Region, South Africa." *Quaternary Science Reviews* 141:65-84.

Corkill, T. 1999. "Here and there: links between stone sources and Aboriginal archaeological sites in Sydney, Australia." M.A. Thesis, , University of Sydney.

Cotterell, B., and J. Kamminga. 1992. *Mechanics of Pre-industrial Technology: An Introduction to the Mechanics of Ancient and Traditional Material Culture*. Cambridge: Cambridge University Press.

Crabtree, D. E. 1967. "Notes on experiments in flintknapping: 3 The Flintknapper's raw materials." *Tebiwa* 10:8-24.

Crabtree, D. E., and B. R. Butler. 1964. "Notes on experiments in flint knapping: 1. Heat treatment of silica minerals." *Tebiwa* 7:1-6.

Davis, Z. J., and J. J. Shea. 1998. "Quantifying Lithic Curation: An Experimental Test of Dibble and Pelcin's Original Flake-Tool Mass Predictor." *Journal of Archaeological Science* 25 (7):603-610. doi: 10.1006/jasc.1997.0255.

Dawkins, R. 2006. *The Selfish Gene: 30th Anniversary Edition*: Oxford University Press.

Day, M. H. 1969. "Omo human skeleton remains." *Nature* 222 (5199).

de la Peña, P., and L. Wadley. 2014. "Quartz Knapping Strategies in the Howiesons Poort at Sibudu (KwaZulu-Natal, South Africa)." *PLoS ONE* 9 (7):1-23.

Deacon, H. J. 1979. "Excavations at Boomplaas cave - a sequence through the upper Pleistocene and Holocene in South Africa." *World Archaeology* 10 (3):241-257. doi: 10.1080/00438243.1979.9979735.

Deacon, H. J. 1989. "Late Pleistocene palaeoecology and archaeology in the southern Cape, South Africa." In *The Human Revolution*, edited by P. Mellars and C. Stringer, 547-564. Princeton: Princeton University Press.

Deacon, H. J. 1995a. "Two Late Pleistocene-Holocene Archaeological Depositories from the Southern Cape, South Africa." *The South African Archaeological Bulletin* 50 (162):121-131.

Deacon, H. J. 2001. "Modern human emergence: an African archeological perspective." In *Humanity from African Naissance to Coming Millennia - Colloquia in Human Biology and Palaeoanthropology*, edited by T. P.V, R. M. A, M. C. J and D. G. A, 217-226. Florence: Florence University Press.

Deacon, H. J., and M. Brooker. 1976. "The Holocene and Upper Pleistocene sequence in the southern cape." *Annals of the South African Museum* 71:203-214.

Deacon, H. J., and J. Deacon. 1999. *Human Beginnings in South Africa: Uncovering the Secrets of the Stone Age*. Cape Town: David Phillip Publishers.

Deacon, H. J., J. Deacon, and M. Brooke. 1976. "Four Painted Stones from Boomplaas Cave, Oudtshoorn District." *The South African Archaeological Bulletin* 31 (123/124):141-145.

Deacon, H. J., J. Deacon, A. Scholtz, J. F. Thackeray, J. S. Brink, and J. C. Vogel. 1983. Correlation of Palaeoenvironmental data form Late Pleistocene and Holocene deposits at Boomplaas Cave, southern Cape.

Deacon, H. J., and V. B. Geleijnse. 1988. "The Stratigraphy and Sedimentology of the Main Site Sequence, Klasies River, South Africa." *The South African Archaeological Bulletin* 43 (147):5-14.

Deacon, J. 1972. "Wilton: an assessment after fifty years." *South African Archaeological Bulletin* 27:10-48.

Deacon, J. 1978. "Changing patterns in the Late Pleistocene/Early Holocene prehistory of southern Africa as seen from the Nelson Bay Cave stone artifact sequence." *Quaternary Research* 10:84-111.

Deacon, J. 1995b. "An Unsolved Mystery at the Howieson's Poort Name Site." *The South African Archaeological Bulletin* 50 (162):110-120.

Deino, A. L., and S. McBrearty. 2002. "40 Ar/ 39 Ar dating of the Kapthurin Formation, Baringo, Kenya." *Journal of Human Evolution* 42:185-210.

Delagnes, A., and H. Roche. 2005. "Late Pliocene hominid knapping skills: The case of Lokalalei 2C, West Turkana, Kenya." *Journal of Human Evolution* 48:435-472.

Delre, S. A., W. Jager, T. H. A. Bijmolt, and M. A. Janssen. 2010. "Will It Spread or Not? The Effects of Social Influences and Network Topology on Innovation Diffusion." *J PROD. INNOV. MANAG.* 27:267-282.

Dibble, H. L. 1997. "Platform variability and flake morphology: A comparison of experimental and archaeological data and implications for interpreting prehistoric lithic technological strategies." *Lithic Technology* 22 (2):150-170.

Dibble, H. L., and M. C. Bernard. 1980. "A comparative study of basic edge angle measurement techniques." *American Antiquity* 45:857-865.

Dibble, H. L., P. G. Chase, S. P. McPherron, and A. Tuffreau. 1997. "Testing The Reality of a "Living Floor" with Archaeological Data." *American Antiquity* 62 (4):629-651.

Dibble, H. L., and Z. Rezek. 2009. "Introducing a new experimental design for controlled studies of flake formation: results for exterior platform angle, platform depth, angle of blow, velocity, and force." *Journal of Archaeological Science* 36:1945-1954.

Dibble, H. L., U. A. Schurmans, R. P. Iovita, and M. V. McLaughlin. 2005. "The Measurement and Interpretation of Cortex in Lithic Assemblages." *American Antiquity* 70 (3):545-560. doi: 10.2307/40035313.

Dibble, H.L. , V. Aldeias, E. Alvarez-Fernandez, B. A. B. Blackwell, E. Hallett-Desguez, Z. Jacobs, P. Goldberg, S. C. Lin, A. Morala, M. C. Meyer, D. I. Olszewski, K. Reed, D. Reed, D. Richter, R. G. Roberts, D. M. Sandgathe, U. A. Schurmans, A. R. Skinner, T. E. Steele, and M. El-Hajraoui. 2012. "New excavations at the Site of Contrebandiers Cave, Morocco." *PaleoAnthropology*:145-201.

Diehl, M. W. 1997. "Rational behavior, the adoption of agriculture, and the organization of subsistence during the Late Archaic Period in the Greater Tucson Basin." In *Rediscovering Darwin: Evolutionary Theory in Archaeological Explanation*, edited by C. M. Barton and G. A. Clark, 251–265. Washington, DC: American Anthropological Association.

Ditchfield, K., S. Holdaway, M. S. Allen, and A. McAlister. 2014. "Measuring stone artefact transport: the experimental demonstration and pilot application of a new method to a prehistoric adze workshop, southern Cook Islands." *Journal of Archaeological Science* 50:512-523.

Domanski, M., and J. A. Webb. 1992. "Effect of heat treatment on siliceous rocks used in prehistoric lithic technology." *Journal of Archaeological Science* 19 (6):601-614. doi: 10.1016/0305-4403(92)90031-W.

Domanski, M., J. A. Webb, and J. Boland. 1994. "MECHANICAL PROPERTIES OF STONE ARTEFACT MATERIALS AND THE EFFECT OF HEAT TREATMENT*." *Archaeometry* 36 (2):177-208. doi: 10.1111/j.1475-4754.1994.tb00963.x.

Dominguez, S. 2002. "Optimal gardening strategies: Maximizing the input and retention ofwater in prehistoric gridded fields in north central New Mexico." *World Archaeology* 34:131-163.

Douglass, M. J. 2010. "The Archaeological Potential of Informal Lithic Technologies: a Case Study of Assemblage Variability in Western New South Wales, Australia." Ph.D., University of Auckland.

Douglass, M. J., and S. J. Holdaway. 2011. "Quantifying stone raw material size distributions: investigating cortex proportions in lithic assemblages from western New South Wales." In *Changing Perspectives in Australian Archaeology, Part IV*, edited by J. Specht and R. Torrence, 45-57. Sydney: Australiam Museum.

Douglass, M. J., S. J. Holdaway, P. C. Fanning, and J. I. Shiner. 2008. "An assessment and archaeological application of cortex measurement in lithic assemblages." *American Antiquity* 73:513-526.

Dyson-Hudson, R., and E. A. Smith. 1978. "Human Territoriality: An Ecological Reassessment." *American Anthropologist* 80 (1):21-41. doi: 10.1525/aa.1978.80.1.02a00020.

d'Errico, F., and C. S. Henshilwood. 2007. "Additional evidence for bone technology in the southern African Middle Stone Age." *Journal of Human Evolution* 52 (2):142-163. doi: 10.1016/j.jhevol.2006.08.003.

d'Errico, F., C. Henshilwood, M. Vanhaeren, and K. van Niekerk. 2005. "Nassarius kraussianus shell beads from Blombos Cave: evidence for symbolic behaviour in the Middle Stone Age." *Journal of Human Evolution* 48 (1):3-24. doi: 10.1016/j.jhevol.2004.09.002.

Edwards, D. A., and J. F. O'Connell. 1995. "Broad spectrum diets in arid Australia." *Antiquity* 69:769-783.

Elston, R. G., and P. G. Brantingham. 2002. "Microlithic technology in northern Asia: A risk-minimizing strategy of the late Paleolithic and early Holocene." In *Thinking Small: Perspectives on Microlithization*, edited by R. G. Elston and S. L. Kuhn, 104–117. Washington, DC: American Anthropological Association.

Elston, R. G., and D. W. Zeanah. 2002. "Thinking outside the box: A new perspective on diet breadth and sexual division of labor in the Pre-archaic Great Basin." *World Archaeology* 34:103-130.

Emlen, J. . 1966. "The role of time and energy in food preference." *American Naturalist* 100:611-617.

Enloe, J.G. 2006. "Geological processes and site structure: assessing integrity at a Late Paleolithic open-air site in Northern France." *Geoarchaeology: An International Journal* 21:523-540.

Erdogan, F. 2000. "Fracture mechanics." *International Journal of Solids and Structures* 37 (1–2):171-183. doi: 10.1016/S0020-7683(99)00086-4.

Eren, M. I., A. Greenspan, and C. G. Sampson. 2008. "Are Upper Paleolithic blade cores more productive than Middle Paleolithic discoidal cores? A replication experiment." *Journal of Human Evolution* 55 (6):952-961. doi: DOI: 10.1016/j.jhevol.2008.07.009</p>.

Eren, M. I., and S. J. Lycett. 2016. "A Statistical Examination of Flake Edge Angles Produced During Experimental Lineal Levallois Reductions and Consideration of Their Functional Implications." *J Archaeol Method Theory* 23:379-398.

Eriksen, B. V., ed. 1997. *Implications of thermal pre-treatment of chert in the German Mesolithic*. Edited by R. Schild and Z. Sulgostowska, *Man and flint, Proceedings of the VII International Flint Symposium, Warszawa-Ostrowiec Swietokrzyski, September 1995* Warsaw: Institute of Archaeology and Ethnology Polish Academy of Sciences.

Erlandson, J. M. 1991. "Shellfish and seeds as optimal resources: Early Holocene subsistence on the Santa Barbara Coast." In *Hunter-Gatherers of Early Holocene Coastal California*, edited by J. M. Erlandson and R. H. Colton, 101-111. Los Angeles: Institute of Archaeology, University of California.

Esteban, I., J. C. De Vynck, E. Singels, J. Vlok, C. W. Marean, R. M. Cowling, E. C. Fisher, D. Cabanes, and R. M. Albert. 2016. "Modern soil phytolith assemblages used as proxies for Paleoscape reconstruction on the south coast of South Africa." *Quaternary International* In Press. doi: http://dx.doi.org/10.1016/j.quaint.2016.01.037.

Fagundes, N. J. R., N. Ray, M. Beaumont, S. Neuenschwander, F. M. Salzano, S. L. Bonatto, and L. Excoffier. 2007. "Statistical evaluation of alternative models of human evolution." *Proceedings of the National Academy of Sciences* 104 (45):17614-17619. doi: 10.1073/pnas.0708280104.

Feathers, J. K. 2002. "Luminescence Dating in Less Than Ideal Conditions: Case Studies from Klasies River Main Site and Duinefontein, South Africa." *Journal of Archaeological Science* 29:177-194.

Feathers, J. K., and D. A. Bush. 2000. "Luminescence dating of Middle Stone Age Deposits at Die Kelders." *Journal of Human Evolution* 38:91-119.

Ferré, E. C., and L. Améglio. 2000. "Preserved magnetic fabrics vs. annealed microstructures in the syntectonic recrystallized George granite, South Africa." *Journal of Structural Geology* 22:1199-1219.

Fisher, E. C., M. Bar-Matthews, A. Jerardino, and C. W. Marean. 2010. "Middle and Late Pleistocene paleoscape modeling along the southern coast of South Africa." *Quaternary Science Reviews* 29 (11–12):1382-1398. doi: 10.1016/j.quascirev.2010.01.015.

Fleuret, P. C., and A. K. Fleuret. 1978. "Fuelwood Use in a Peasant Community: A Tanzanian Case Study." *The Journal of Developing Areas* 12 (3):315-322.

Foley, R., and M. M. Lahr. 1997. "Mode 3 Technologies and the Evolution of Modern Humans." *Cambridge Archaeological Journal* 7 (1):3-36. doi: 10.1017/S0959774300001451.

Foster, H. T. II 2003. "Dynamic optimization of horticulture among the Muscogee Creek Indians of the southeastern United States." *Journal of Anthropological Archaeology* 22:411-424.

Frankel, J. J. 1952. "Silcrete near Albertinia, Cape Province." *South African Journal of Science* 49:173-182.

Franklin, J., A.J. Potts, E.C. Fisher, R.M. Cowling, and C.W. Marean. 2015. "Paleodistribution modeling in archaeology and paleoanthropology." *Quaternary Science Reviews* 110:1-14.

Féblot-Augustins, J. 1993. "Mobility Strategies in the Late Middle Palaeolithic of Central Europe and Western Europe: Elements of Stability and Variability." *Journal of Anthropological Archaeology* 12 (3):211-265. doi: 10.1006/jaar.1993.1007.

Féblot-Augustins, J. 1997. "Middle and Upper Palaeolithic raw material transfers in western and central Europe: assessing the pace of change." *Journal of Middle Atlantic Archaeology* 13:57-90.

Gilbert, N. 2007. *Agent-Based Models*. Los Angles: Sage.

Glassow, M. A. 1996. *Purisimeno Chumash Prehistory*. New York: Harcourt Brace.

Glassow, M. A., and L. R. Wilcoxin. 1988. "Coastal adaptations near Point Conception, California, with particular regard to shellfish exploitation." *American Antiquity* 53:36-51.

Goldman-Neuman, T., and E. Hovers. 2012. "Raw material selectivity in Late Pliocene Oldowan sites in the Makaamitalu Basin, Hadar, Ethiopia." *Journal of Human Evolution* 62:353-366.

Goodman, M. E. 1944. "The Physical Properties of Stone Tool Materials." *American Antiquity* 9 (4):415-433. doi: 10.2307/275093.

Goodwin, A. J. H. 1928. "The Middle Stone Age." *Annals of the South African Museum* XXVII:95-145.

Goodwin, A. J. H. 1929. "The Stone Ages in South Africa." *Journal of the International African Institute* 2 (2):174-182.

Goodwin, A. J. H., and B. Peers. 1953. "Two Caves at Kalk Bay, Cape Peninsula." *The South African Archaeological Bulletin* 8 (31):59-77.

Goodwin, A. J. H., and C. Van Riet Lowe. 1929. "The Stone Age cultures of South Africa." *Annals of the South African Museum* 27:1-28.

Goodyear, A.C. 1989. "A hypothesis for the use of cryptocrystalline raw materials among the paleoindian groups of North America." In *Eastern Paleoindian Lithic Resource Use*, edited by C. Ellis and J. Lathrop, 1-9. Boulder: Westview Press.

Gotelli, N. J., and G. R. Graves. 1996. *Null Models in Ecology*. Washington, D.C.: Smithsonian Institution Press.

Goudie, A. S. 2006. "The Schmidt Hammer in geomorphological research." *Progress in Physical Geography* 30 (6):703-718. doi: 10.1177/0309133306071954.

Gould, R. A. 1978. "The anthropology of human residues." *American Anthropologist* 80 (4):815-835.

Gould, R. A. 1985. "The Empiricist Strikes Back: Reply to Binford." *American Antiquity* 50 (3). doi: 10.2307/280326.

Gould, R. A., and S. Saggers. 1985. "Lithic Procurement in Central Australia: A Closer Look at Binford's Idea of Embeddedness in Archaeology." *American Antiquity* 50 (1):117-136. doi: 10.2307/280637.

Gould, R.A., D.A. Koster, and A. Sontz. 1971. "The lithic assemblage of the Western Desert Aborigines of Australia." *American Antiquity* 36 (2):149-168.

Grayson, D. K. 1991. "Alpine faunas from the White Mountains, California: Adaptive change in the Great Basin? ." *Journal of Archaeological Science* 18:483-506.

Green, A. N. 2009. "The marine geology of the northern KwaZulu-Natal continental shelf, South Africa." Unpublished PhD thesis, University of KwaZulu-Natal, South Africa.

Gremillion, K. J. 2004. "Seed processing and the origins of food production in Eastern North America." *American Antiquity* 69:215-233.

Griffiths, D. R. , C. A. Bergman, C. J. Clayton, K. Ohnuma, G. V. Robins, and N. J. Seeley, eds. 1987. *Experimental investigations of the heat treatment of flint*. Edited by G. De. G. Sieveking and M. H. Newcomer, *The Human Uses of Flint and Chert*. Cambridge: Cambridge University Press.

Grimm, V., U. Berger, D. L. DeAngelis, J. G. Polhill, J. Giske, and S. F. Railsback. 2010. "The ODD protocol: A review and first update." *Ecological Modelling* 221:2760-2768.

Grine, F. E., R. G. Klein, and T. Volman. 1991. "Dating, archaeology and human fossils from the Middle Stone Age levels of Die Kelders, South Africa." *Journal of Human Evolution* 21:363-395. doi: DOI: 10.1016/0047-2484(91)90113-A</p>.

Gronau, I., M. J. Hubisz, B. Gulko, C. G. Danko, and A. Siepel. 2011. "Bayesian inference of ancient human demography from individual genome sequences." *Nature Genetics* 43 (10):1031-1034. doi: 10.1038/ng.937.

Grün, R., and P. Beaumont. 2001. "Border Cave revisited: a revised ESR chronology." *Journal of Human Evolution* 40 (6):467-482. doi: 10.1006/jhev.2001.0471.

Grün, R., P. B. Beaumont, and C. B. Stringer. 1990. "ESR dating evidence for early modern humans at Border Cave in South Africa." *Nature* 344:537-539.

Grün, R., P. Beaumont, P. V. Tobias, and S. Eggins. 2003. "On the age of Border Cave 5 human mandible." *Journal of Human Evolution* 45:155-167.

Gurven, M., K. Hill, R. Hames, T. Kameda, R. McDermott, K. Lupo, C. Kiahtipes, S. Ragir, A. Rosas, M. Gurven, and K. Hill. 2009. "Why do men hunt? A reevaluation of "man the hunter" and the sexual division of labor." *Current Anthropology* 50 (1):51-74.

Géneste, J. M. 1985. "Analyse lithique d'industries moustériennes du Périgord: une approche technologique du comportement des groups humains au Paléolithique moyen." University of Bordeaux I.

Harmand, S. 2009. "Variability in raw material selectivity at the Late Pliocene sites of Lokalalei, West Turkana, Kenya." In *Interdisciplinary Approaches to the Oldowan*, edited by E. Hovers and D.R. Braun, 85-97. Netherlands: Springer.

Harmand, S., J. E. Lewis, C. S. Feibel, C. J. Lepre, S. Prat, A. Lenoble, X. Boës, R. L. Quinn, M. Brenet, A. Arroyo, N. Taylor, S. Clément, G. Daver, J-P. Brugal, L. Leakey, R. A. Mortlock, J. D. Wright, S. Lokorodi, C. Kirwa, D. V. Kent, and H. Roche. 2015. "3.3-million-year-old stone tools from Lomekwi 3, West Turkana, Kenya." *Nature* 521:310–315.

Harpending, H., and H. Davis. 1977. "Some Implications for Hunter-Gatherer Ecology Derived from the Spatial Structure of Resources." *World Archaeology* 8:275-286.

Harper, P. T. N. 1997. "The Middle Stone Age sequences at Rose Cottage Cave: A search for continuity and discontinuity." *South African Journal of Science* 93 (10):470-475.

Hawkes, K., K. Hill, and J. F. O'Connell. 1982. "Why hunters gather: Optimal foraging and the Ache of eastern Paraguay." *American Ethnologist* 9:379-398.

Hawkes, K., and J. F. O'Connell. 1992. "On optimal foraging models and subsistence transitions." *Current Anthropology* 33:63-65.

Hay, E. R. 1984. "Sediment Dynamics on the Continental Shelf between Durban and Port St. Johns (south-east African continental margin). ." *Bulletin of the Joint Geological Survey/University of Cape Town Marine Geoscience Unit* 13:238.

Heider, K. G. 1967. "Archaeological Assumptions and Ethnographical Facts: A Cautionary Tale from New Guinea." *Southwestern Journal of Anthropology* 23 (1):52-64.

Henn, B. M., C. R. Gignoux, M. Jobin, J. M. Granka, J. M. Macpherson, J. M. Kidd, L. Rodríguez-Botigué, S. Ramachandran, L. Hon, A. Brisbin, A. A. Lin, P. A. Underhill, D. Comas, K. K. Kidd, P. J. Norman, P. Parham, C. D. Bustamante, J. L. Mountain, and M. W. Feldman. 2011. "Hunter-gatherer genomic diversity suggests a southern African origin for modern humans." *Proceedings of the National Academy of Sciences of the United States of America* 108:5154-5162.

Henrich, J. 2004. "Cultural group selection, coevolutionary processes and large-scale cooperation." *Journal of Economic Behavior & Organization* 53 (1):3-35.

Henshilwood, C., F. d'Errico, M. Vanhaeren, K. van Niekerk, and Z. Jacobs. 2004. "Middle Stone Age Shell Beads from South Africa." *Science* 304 (5669):404-404. doi: 10.1126/science.1095905.

Henshilwood, C. S., and B. Dubreuil. 2011. "The Still Bay and Howiesons Poort, 77–59 ka: Symbolic Material Culture and the Evolution of the Mind during the African Middle Stone Age." *Current Anthropology* 52 (3):361-400. doi: 10.1086/660022.

Henshilwood, C. S., F. d'Errico, K. L. van Niekerk, Y. Coquinot, Z. Jacobs, S. E. Lauritzen, M. Menu, and R. García-Moreno. 2011. "A 100,000-Year-Old Ochre-Processing Workshop at Blombos Cave, South Africa." *Science* 334 (6053):219-222. doi: 10.1126/science.1211535.

Henshilwood, C. S., F. d'Errico, and I. Watts. 2009. "Engraved ochres from the Middle Stone Age levels at Blombos Cave, South Africa." *Journal of Human Evolution* 57 (1):27-47. doi: 10.1016/j.jhevol.2009.01.005.

Henshilwood, C. S., F. d'Errico, R. Yates, Z. Jacobs, C. Tribolo, G. A. T. Duller, N. Mercier, J. C. Sealy, H. Valladas, I. Watts, and A. G. Wintle. 2002. "Emergence of Modern Human Behavior: Middle Stone Age Engravings from South Africa." *Science* 295 (5558):1278-1280. doi: 10.1126/science.1067575.

Henshilwood, C. S., and C. W. Marean. 2003. "The Origin of Modern Human Behavior: Critique of the Models and Their Test Implications." *Current Anthropology* 44 (5):627-651. doi: 10.1086/377665.

Henshilwood, C. S., J. C. Sealy, R. Yates, K. Cruz-Uribe, P. Goldberg, F. E. Grine, R. G. Klein, C. Poggenpoel, K. van Niekerk, and I. Watts. 2001. "Blombos Cave, Southern Cape, South Africa: Preliminary Report on the 1992–1999 Excavations of the Middle Stone Age Levels." *Journal of Archaeological Science* 28 (4):421-448. doi: 10.1006/jasc.2000.0638.

Henshilwood, C.S. 2012. "Late Pleistocene Techno-traditions in Southern Africa: A Review of the Still Bay and Howiesons Poort, c. 75–59 ka." *Journal of World Prehistory* 25:205-237.

Henshilwood, C.S., K.L. van Niekerk, S. Wurz, A. Delagnes, S.J. Armitage, R.F. Rifkin, K. Douze, P. Keene, M.M. Haaland, J. Reynard, E. Discamps, and S.S. Mienies. 2014. "Klipdrift Shelter, southern Cape, South Africa: Preliminary Report on the Howiesons Poort layers." *Journal of Archaeological Science* 45:284-303. doi: 10.1016/j.jas.2014.01.033.

Herries, A. I. R. 2011. "A Chronological Perspective on the Acheulian and Its Transition to the Middle Stone Age in Southern Africa: The Question of the Fauresmith." *International Journal of Evolutionary Biology* 2011:1-25. doi: 10.4061/2011/961401.

Herries, A. I. R., D. Curnoe, and J. W. Adams. 2009. "A multi-disciplinary seriation of early Homo and Paranthropus bearing palaeocaves in southern Africa."

Quaternary International 202 (1-2):14-28. doi: DOI: 10.1016/j.quaint.2008.05.017</p>.

Herries, A. I. R., and E. C. Fisher. 2010. "Multidimensional GIS modeling of magnetic mineralogy as a proxy for fire use and spatial patterning: Evidence from the Middle Stone Age bearing sea cave of Pinnacle Point 13B (Western Cape, South Africa)." *Journal of Human Evolution* 59 (3–4):306-320. doi: 10.1016/j.jhevol.2010.07.012.

Hildebrandt, W. R., and T. L. Jones. 1992. "Evolution of marine mammal hunting: A view from the California and Oregon coasts." *Journal of Anthropological Archaeology* 11:360-401.

Hill, K., and K. Hawkes. 1983. "Neo-tropical hunting among the Ache of eastern Paraguay." In *Adaptive Responses of Native Amazonians*,, edited by R. B. Hames and W. T. Vickers, 129–188. New York: Academic Press.

Hill, K., H. Kaplan, K. Hawkes, and A. M. Hurtado. 1987. "Foraging decisions among Ache hunter-gatherers: New data and implications for optimal foraging theory. ." *Ethology and Sociobiology* 8:1–36.

Hiscock, P., A. Turq, J. P. Faivre, and L. Bourguignon. 2009. "Quina Procurement and Tool Production." In *Lithic Materials and Paleolithic Societies*, edited by Brian Adams and Brooke S. Blades, 232-246. Wiley-Blackwell.

JMP PRO 12.1.0 (64-bit). SAS Institute Inc.

Hofman, J. L., ed. 1987. *Hopewell blades from Twenhafel: Distinguishing local and foreign core technology, The Organization of Core Technology*. Boulder, CO: Westview Press.

Holdaway, S. J., M. J. Douglass, and P. C. Fanning. 2013. "A new ecological framework for understanding human-environment interaction in arid Australia." In *Archaeology in Environment and Technology: Intersections and Transformations*, edited by D. Frankel, J. M. Webb and S. Lawrence, 51-68. Routledge.

Holdaway, S. J., J. I. Shiner, P. C. Fanning, and M. J. Douglass. 2008. "Assemblage formation as a result of raw material acquisition in western New South Wales, Australia." *Lithic Technology* 33:73-85.

Holdaway, S. J., W. Wendrich, and R. Phillipps. 2010. "Identifying low-level food producers: detecting mobility from lithics." *Antiquity* 84:185-194.

Hublin, J-J. 1992. "Recent Human Evolution in Northwestern Africa." *Philosophical Transactions of the Royal Society of London. Series B: Biological Sciences* 337 (1280):185-191. doi: 10.1098/rstb.1992.0096.

Igreja, M., and G. Porraz. 2013. "Functional insights into the innovative Early Howiesons Poort technology at Diepkloof Rock Shelter, Western Cape, South Africa." *Journal of Archaeological Science* 40:3474-3491.

Inskeep, R.R., and G. Avery. 1987. *Nelson Bay Cave, Cape Province, South Africa : the Holocene levels*. Vol. 357. Oxford: BAR.

Isaac, G. L. 1975. "Middle Pleistocene stratigraphy and cultural patterns in East Africa." In *After the Australopithecines: Stratigraphy, Ecology, and Culture Change in the Middle Pleistocene*, edited by K. W. Butzer and G. L. Isaac, 495-542. The Hague: Mouton.

Isaac, G. L. 1986. "Foundation stones; early artifacts as indicators of activities and abilities." In *Stone Age Prehistory: Studies in Memory of Charles McBurney*, edited by G. N. Bailey and P. Callow, 221-242. Cambridge: Cambridge University Press.

Jacobs, Z. 2010. "An OSL chronology for the sedimentary deposits from Pinnacle Point Cave 13B—A punctuated presence." *Journal of Human Evolution* 59 (3–4):289-305. doi: 10.1016/j.jhevol.2010.07.010.

Jacobs, Z., G. A. T. Duller, and A. G. Wintle. 2003. "Optical dating of dune sand from Blombos Cave, South Africa: II--single grain data." *Journal of Human Evolution* 44 (5):613-625. doi: DOI: 10.1016/S0047-2484(03)00049-6</p>.

Jacobs, Z., G. A. T. Duller, A. G. Wintle, and C. S. Henshilwood. 2006. "Extending the chronology of deposits at Blombos Cave, South Africa, back to 140 ka using optical dating of single and multiple grains of quartz." *Journal of Human Evolution* 51 (3):255-273. doi: 10.1016/j.jhevol.2006.03.007.

Jacobs, Z., E. H. Hayes, R. G. Roberts, R. F. Galbraith, and C. S. Henshilwood. 2012. "An improved OSL chronology for the Still Bay layers at Blombos Cave, South Africa: Further tests of single-grain dating procedures and a re-evaluation of the timing of the Still Bay industry across southern Africa." *Journal of Archaeological Science* 40 (1):579-594. doi: 10.1016/j.jas.2012.06.037.

Jacobs, Z., and R. G. Roberts. 2008. "Testing Times: Old and New Chronologies for the Howieson's Poort and Still Bay Industries in Environmental Context." *South African Archaeological Society Goodwin Series* 10.

Jacobs, Z., and R. G. Roberts. 2015. "An improved single grain OSL chronology for the sedimentary deposits from Diepkloof Rockshelter, Western Cape, South Africa." *Journal of Archaeological Science* 63: 175-192

Jacobs, Z., and R. G. Roberts. 2017. “Single-grain OSL chronologies for the Still Bay and Howieson's Poort industries and the transition between them: Further analyses and statistical modelling.” Journal of Human Evolution 107: 1-13.

Jacobs, Z., R. G. Roberts, R. F. Galbraith, H. J. Deacon, R. Grün, A. Mackay, P. Mitchell, R. Vogelsang, and L. Wadley. 2008a. "Ages for the Middle Stone Age of Southern Africa: Implications for Human Behavior and Dispersal." *Science* 322 (5902):733-735. doi: 10.1126/science.1162219.

Jacobs, Z., R. G. Roberts, R. F. Galbraith, H. J. Deacon, R. Grün, A. Mackay, P. Mitchell, R. Vogelsang, and L. Wadley. 2008b. "Supporting Online Material for "Ages for the Middle Stone Age of Southern Africa: Implications for Human Behavior and Dispersal"." *Science* 322.

Jacobs, Z., A. G. Wintle, and G. A. T. Duller. 2003. "Optical dating of dune sand from Blombos Cave, South Africa: I--multiple grain data." *Journal of Human Evolution* 44 (5):599-612. doi: DOI: 10.1016/S0047-2484(03)00048-4</p>.

Jacobs, Z., A. G. Wintle, G. A. T. Duller, R. G. Roberts, and L. Wadley. 2008. "New ages for the post-Howiesons Poort, late and final Middle Stone Age at Sibudu, South Africa." *Journal of Archaeological Science* 35:1790-1807.

Janssen, M.A., and S. Oestmo. 2013. "A Neutral Model of Stone Raw Material Procurement (Version 1)." *CoMSES Computational Model Library* Retrieved from: http://www.openabm.org/model/3957/version/1.

Janssen, M.A., and E. Ostrom. 2006. "Empirically Based, Agent-based models." *Ecology and Society* 11 (2):37.

Jelinek, A. J. 1991. "Observations on reduction patterns and raw materials in some Middle Paleolithic industries in the Perigord." In *Raw material economies among prehistoric hunter-gatherers*, edited by A. Montet-White and S. Holen, 7-32. Lawrence: University of Kansas Publications in Anthropology 19.

Jennings, T. A., C. D. Pevny, and W. A. Dickens. 2010. "A biface and blade core efficiency experiment: implications for Early Paleoindian technological organization." *Journal of Archaeological Science* 37:2155-2164.

Jerardino, A. 2007. "Excavations at a Hunter-Gatherer Site Know as ‘Grootrif G’ Shell Midden, Lamberts Bay, Western Cape Province." *South African Archaeological Bulletin* 62:162-170.

Jerardino, A., and C. W. Marean. 2010. "Shellfish gathering, marine paleoecology and modern human behavior: perspectives from cave PP13B, Pinnacle Point, South Africa." *Journal of Human Evolution* 59 (3–4):412-424. doi: 10.1016/j.jhevol.2010.07.003.

Jochim, M. 1983. "Optimization models in context." In *Archaeological hammers and theories,* edited by A. S. Keene and J. A. Moore, 157-172. New York: Academic Press.

Johnson, C. R., and S. McBrearty. 2010. "500,000 year old blades from the Kapthurin Formation, Kenya." *Journal of Human Evolution* 58 (2):193-200. doi: 10.1016/j.jhevol.2009.10.001.

Johnson, M. R., C. J. van Vuuran, J. N. J. Visser, D. I. Cole, H. de V. Wickens, A. D. M. Christie, D. L. Roberts, and G. Brandle. 2006. "Sedimentary rocks of the Karoo Supergroup." In *The Geology of South Africa,* edited by B. Thomas, 461-500. Johannesburg: Geological Society of South Africa.

Johnson, M. R., C. J. Van Vuuren, W. F. Hegenberger, R. Key, and U. Show. 1996. "Stratigraphy of the Karoo Supergroup in southern Africa: an overview." *Journal of African Earth Sciences* 23:3-15.

Jolly, K. 1947. "Preliminary Note on New Excavations at Skildergat, Fish Hoek." *The South African Archaeological Bulletin* 2 (5):11-12.

Jolly, K. 1948. "The Development of the Cape Middle Stone Age in the Skildegat Cave, Fish Hoek." *The South African Archaeological Bulletin* 3 (12):106-107.

Jones, P. R. 1979. "Effects of Raw Materials on Biface Manufacture." *Science* 204 (4395):835-836. doi: 10.1126/science.204.4395.835.

Jones, T. L., and J. R. Richman. 1995. "On mussels: Mytilus californicus as a prehistoric resource." *North American Archaeologist* 16:33-58.

Jouzel, J., V. Masson-Delmotte, O. Cattani, G. Dreyfus, S. Falourd, G. Hoffmann, B. Minster, J. Nouet, J. M. Barnola, J. Chappellaz, H. Fischer, J. C. Gallet, S. Johnsen, M. Leuenberger, L. Loulergue, D. Luethi, H. Oerter, F. Parrenin, G. Raisbeck, D. Raynaud, A. Schilt, J. Schwander, E. Selmo, R. Souchez, R. Spahni, B. Stauffer, J. P. Steffensen, B. Stenni, T. F. Stocker, J. L. Tison, M. Werner, and E. W. Wolff. 2007. "Orbital and Millennial Antarctic Climate Variability over the Past 800,000 Years." *Science* 317 (5839):793-796. doi: 10.1126/science.1141038.

Kahraman, S., and M. Fener. 2007. "Predicting the Los Angeles abrasion loss of rock aggregates from the uniaxial compressive strength." *Materials Letters* 61 (26):4861-4865. doi: 10.1016/j.matlet.2007.06.003.

Kandel, A. W., M. Bolus, K. Bretzke, A. A. Bruch, M. N. Haidle, C. Hertler, and M. Märker. 2015. "Increasing behavioral flexibility? An integrative macro-scale

approach to understanding the Middle Stone Age of southern Africa." *Journal of Archaeological Method & Theory* doi:10.1007/s10816-015-9254-y:1-46.

Kaplan, J. 1990. "The Umhlatuzana Rock Shelter Sequence: 100 000 years of Stone Age history." *Natal Museum Journal of Humanities* 2:1-94.

Kaplan, J. M. 1989. "45000 Years of Hunter-Gatherer History in Natal as Seen from Umhlatuzana Rock Shelter." *Goodwin Series* 6 (Goodwin's Legacy):7-16.

Karkanas, P., K. S. Brown, E. C. Fisher, Z. Jacobs, and C. W. Marean. 2015. "Interpreting human behavior from depositional rates and combustion features through the study of sedimentary microfacies at site Pinnacle Point 5-6, South Africa." *Journal of human evolution* 85:1-21.

Karkanas, P., and P. Goldberg. 2010. "Site formation processes at Pinnacle Point Cave 13B (Mossel Bay, Western Cape Province, South Africa): resolving stratigraphic and depositional complexities with micromorphology." *Journal of Human Evolution* 59 (3–4):256-273. doi: 10.1016/j.jhevol.2010.07.001.

Keegan, W. 1986. "The optimal foraging analysis of horticultural production." *American Anthropologist* 88:92-107.

Keegan, W. 1995. "Modeling dispersal in the prehistoric West Indies." *World Archaeology* 26:400-420.

Keegan, W., and B. Butler. 1987. "The microeconomic logic of horticultural intensification in the Eastern Woodlands." In *Emergent Horticultural Economies of the Eastern Woodlands*, edited by W. Keegan, 109-127. Carbondale: Center for Archaeological Investigations, Southern Illinois University.

Keegan, W., and J. Diamond. 1987. "Colonization of islands by humans: A biogeographical perspective." In *Advances in Archaeological Method and Theory, Vol. 10*, edited by M. B. Schiffer, 49-92. New York: Academic Press.

Keene, A. S. 1983. "Biology, behavior, and borrowing: a critical examination of optimal foraging theory in archaeology." In *Archaeological hammers and theories*, edited by A. S. Keene and J. A. Moore, 137-155. New York: Academic Press.

Keller, C. M. 1970. "C14 Dates: Montagu Cave." *The South African Archaeological Bulletin* 25 (97).

Keller, C. M. 1973. *Montague Cave in Prehistory: A descriptive analysis*. Berkley: University of California Press.

Kelly, R. L. 1995. *The Foraging Spectrum: Diversity in Hunter-Gatherer Lifeways*. Washington: Smithsonian Institution Press.

Kelly, R. L. 1999. "Hunter-gatherer foraging and the colonization of the Western Hemisphere." *Anthropologie* 37:143-153.

Kelly, Robert L. 1983. "Hunter-Gatherer Mobility Strategies." *Journal of Anthropological Research* 39 (3):277-306.

Kelly, Robert L. 1988. "The Three Sides of a Biface." *American Antiquity* 53 (4). doi: 10.2307/281115.

Kelly, Robert L. 1992. "Mobility/Sedentism: Concepts, Archaeological Measures, and Effects." *Annual Review of Anthropology* 21:43-66.

Kennett, D. J. 2005. *The Island Chumash: Behavioral Ecology of a Maritime Society*. Berkeley: University of California Press.

Kennett, D. J., A. Anderson, and B. Winterhalder. 2006. "The ideal free distribution, food production and the colonization of Oceania." In *Human Behavioral Ecology and the Origins of Food Production*, edited by D. J. Kennett and B. Winterhalder, 265-288. Berkeley: University of California Press.

Kennett, D. J., and J. P. Kennett. 2000. "Competitive and cooperative responses to climatic instability in southern California." *American Antiquity* 65:379-395.

Kennett, D. J., and B. Winterhalder, eds. 2006. *Human Behavioral Ecology and the Origins of Food Production*. Berkeley: University of California Press.

Key, A, J. M., and S. J. Lycett. 2015. "EDGE ANGLE AS A VARIABLY INFLUENTIAL FACTOR IN FLAKE CUTTING EFFICIENCY: AN EXPERIMENTAL INVESTIGATION OF ITS RELATIONSHIP WITH TOOL SIZE AND LOADING." *Archaeometry* 57 (5):911-927.

King, L. C. 1948. "On the ages of African land-surfaces." *Journal of the Geological Society* 104:439-459.

Klein, R. G. 1970. "Problems in the Study of the Middle Stone Age of South Africa." *The South African Archaeological Bulletin* 25 (99/100):127-135. doi: 10.2307/3888136.

Klein, R. G. 1972. "The Late Quaternary mammalian fauna of Nelson Bay Cave (Cape Province, South Africa): its implications for megafaunal extinctions and environmental and cultural change." *Quaternary Research* 2:135-142.

Klein, R. G. 2000. "Archeology and the evolution of human behavior." *Evolutionary Anthropology: Issues, News, and Reviews* 9 (1):17-36. doi: 10.1002/(SICI)1520-6505(2000)9:1<17::AID-EVAN3>3.0.CO;2-A.

Knecht, H. 1993. "Early Upper Paleolithic approaches to bone and antler projectile technology." In *Hunting and Animal Exploitation in the Later Paleolithic and Mesolithic of Eurasia, Archeological Papers No. 4*, edited by G. L. Peterkin, H. M. Bricker and P. Mellars, 33–47. Washington, DC: American Anthropological Association.

Krebs, J. R., and N. B. Davies. 1984. *Behavioural Ecology: An evolutionary Approach*. Oxford: Blackwell.

Kuhn, S. L. 1989. "Hunter-gatherer foraging organization and strategies of artifact replacement and discard." In *Experiments in lithic technology*, edited by D. S. Amick and R. P. Mauldin, 33-47. Oxford: British Archaeological Reports International Series.

Kuhn, S. L. 1991. "“Unpacking” reduction: Lithic raw material economy in the mousterian of west-central Italy." *Journal of Anthropological Archaeology* 10 (1):76-106. doi: 10.1016/0278-4165(91)90022-P.

Kuhn, S. L. 1992. "On Planning and Curated Technologies in the Middle Paleolithic." *Journal of Anthropological Research* 48 (3):185-214.

Kuhn, S. L. 1994. "A Formal Approach to the Design and Assembly of Mobile Toolkits." *American Antiquity* 59 (3):426-442. doi: 10.2307/282456.

Kuhn, S. L. 1995. *Mousterian Lithic Technology: An Ecological Perspective*. Princeton: Princeton University Press.

Kuhn, S. L. 2004. "Upper Paleolithic raw material economies at Üçağızlı cave, Turkey." *Journal of Anthropological Archaeology* 23 (4):431-448. doi: 10.1016/j.jaa.2004.09.001.

Kuhn, S. L., and M. C. Stiner. 2001. "The antiquity of hunter-gatherers." In *Hunter-Gatherers: An Interdisciplinary Perspective*, edited by C. Panter-Brick, R. H. Layton and P. Rowley-Conwy, 99-142. Cambridge University Press: Cambridge.

Kuman, K. A. 1989. "Florisbad and #Gi: The contribution of open-air sites to study of the Middle Stone Age in southern Africa." University of Pennsylvania, Anthropology.

Lavrenov, I. V. 1998. "The wave energy concentration at the Agulhas current off South Africa." *Natural Hazards* 17:117-127.

Layton, R. H., R. A. Foley, and E. Williams. 1991. "The transition between hunting and gathering and the specialized husbandry of resources. ." *Current Anthropology* 32:255-274.

Leakey, M.D. 1971. *Olduvai Gorge Vol. 3*. Cambridge: Cambridge University Press.

Lee, R. B. 1979. *The !Kung San: Men, Women and Work in a Foraging Society*. Cambridge: Cambridge University Press.

Lee, R. B., and I. DeVore. 1968. *Man the hunter*. Edited by R. B. Lee and I. DeVore. Chicago: Aldine Press.

Lenoble, A., and P. Bertran. 2004. "Fabric of Palaeolithic levels: methods and implications for site formation processes." *Journal of Archaeological Science* 31 (4):457-469. doi: 10.1016/j.jas.2003.09.013.

Lenoble, A., P. Bertran, and F. Lacrampe. 2008. "Solifluction-induced modifications of archaeological levels: simulation based on experimental data from a modern periglacial slope and application to French Palaeolithic sites." *Journal of Archaeological Science* 35 (1):99-110. doi: 10.1016/j.jas.2007.02.011.

Lepre, C. J., H. Roche, D. V. Kent, S. Harmand, R. L. Quinn, J-P. Brugal, P-J. Texier, A. Lenoble, and C. S. Feibel. 2011. "An earlier origin for the Acheulian." *Nature* 477:82-85.

Lin, S. C. H., M. J. Douglass, S. J. Holdaway, and B. Floyd. 2010. "The application of 3D laser scanning technology to the assessment of ordinal and mechanical cortex quantification in lithic analysis." *Journal of Archaeological Science* 37:694-702.

Lin, S. C., S. P McPherron, and H. L. Dibble. 2015. "Establishing statistical confidence in Cortex Ratios within and among lithic assemblages: a case study of the Middle Paleolithic of southwestern France." *Journal of Archaeological Science* 59:89-109.

Lombard, M. 2004. "Distribution Patterns of Organic Residues on Middle Stone Age Points From Sibudu Cave, KwaZulu-Natal, South Africa." *South African Archaeological Bulletin* 59:37-44.

Lombard, M. 2005. "Evidence of hunting and hafting during the Middle Stone Age at Sibidu Cave, KwaZulu-Natal, South Africa: a multianalytical approach." *Journal of Human Evolution* 48:279-300.

Lombard, M. 2006. "First impressions of the functions and hafting technology of Still Bay pointed artefacts from Sibudu Cave." *Southern African Humanities* 18 (1):27-41.

Lombard, M. 2008a. "Finding resolution for the Howiesons Poort through the microscope: micro-residue analysis of segments from Sibudu Cave, South Africa." *Journal of Archaeological Science* 35:26-41.

Lombard, M. 2008b. "FROM TESTING TIMES TO HIGH RESOLUTION: THE LATE PLEISTOCENE MIDDLE STONE AGE OF SOUTH AFRICA AND BEYOND." *Goodwin Series* 10:180-188.

Lombard, M. 2012. "Thinking through the Middle Stone Age of sub-Saharan Africa." *Quaternary International* 270:140-155. doi: 10.1016/j.quaint.2012.02.033.

Lombard, M. 2016. "Mountaineering or ratcheting? Stone Age hunting weapons as proxy for the evolution of human technological, behavioral and cognitive flexibility." In *The nature of culture*, edited by Haidle M. N., Conard N. J. and Bolus M., 135-146. New York: Springer.

Lombard, M., and J. Pargeter. 2008. "Hunting with Howiesons Poort segments: pilot experimental study and the functional interpretation of archaeological tools." *Journal of Archaeological Science* 35:2523-2531.

Lombard, M., L. Wadley, J. Deacon, S. Wurz, I. Parsons, M. Mohapi, J. Swart, and P. Mitchell. 2012. "South African and Lesotho Stone Age Sequence Updated (I)." *South African Archaeological Bulletin* 67 (195):120-144.

Lombard, M., L. Wadley, Z. Jacobs, M. Mohapi, and R. G. Roberts. 2010. "Still Bay and serrated points from Umhlatuzana Rock Shelter, Kwazulu-Natal, South Africa." *Journal of Archaeological Science* 37 (7):1773-1784. doi: 10.1016/j.jas.2010.02.015.

Louw, A. W. 1969. "Bushman Rock Shelter, Ohrigstad, Eastern Transvaal: A Preliminary Investigation, 1965." *The South African Archaeological Bulletin* 24 (94):39-51
.

Luedtke, B. E. 1992. *An archaeologist's guide to chert and flint, Archaeological Research Tools*. Los Angeles: Institute of Archaeology, University of California, Los Angeles.

Lupo, K. D. 2001. "On the archaeological resolution of body part transport patterns: An ethnoarchaeological example from East African hunter-gatherers." *Journal of Anthropological Archaeology* 20:361-378.

Lupo, K. D., and D. Schmitt. 1997. "Experiments in bone boiling: Nutritional yields and archaeological reflections." *Anthropozoologica* 25-26:137-144.

MacArthur, R., and E. Pianka. 1966. "On optimal use of a patchy environment." *American Naturalist* 100:603-609.

Mackay, A. 2006. "A Characterization of the MSA Stone Artefact Assemblage from the 1984 Excavations at Klein Kliphuis, Western Cape." *The South African Archaeological Bulletin* 61 (184):181-188. doi: 10.2307/20474926.

Mackay, A. 2008. "A method for estimating edge length from flake dimensions: use and implications for technological change in the southern African MSA." *Journal of Archaeological Science* 35 (3):614-622. doi: 10.1016/j.jas.2007.05.013.

Mackay, A. 2009. "History and Selection in the Late Pleistocene Archaeology of the Western Cape, South Africa." The Australian National University.

Mackay, A. 2011. "Potentially stylistic differences between backed artefacts from two nearby sites occupied ~60,000 years before present in South Africa." *Journal of Anthropological Archaeology* 30 (2):235-245. doi: 10.1016/j.jaa.2011.03.002.

Mackay, A., and B. Marwick. 2011. "Costs and benefits in technological decision making under variable conditions: examples from the late Pleistocene in southern Africa." In *Keeping your Edge: Recent Approaches to the Organisation of Stone Artefact Technology*, edited by B. Marwick and A. Mackay, 119-134. Oxford: Archaeopress.

Mackay, A., B. A. Stewart, and B. M. Chase. 2014. "Coalescence and fragmentation in the late Pleistocene archaeology of southernmost Africa." *Journal of Human Evolution* Accepted Manuscript, In Press.

Mackay, A., and A. Welz. 2008. "Engraved ochre from a Middle Stone Age context at Klein Kliphuis in the Western Cape of South Africa." *Journal of Archaeological Science* 35 (6):1521-1532. doi: 10.1016/j.jas.2007.10.015.

Madubansi, M., and C. M. Shackleton. 2007. "Changes in fuelwood use and selection following electrification in the Bushbuckridge lowveld, South Africa." *Journal of Environmental Management* 83:416-426.

Magne, M. P. R. 2001. "Debitage analysis as a scientific tool for archaeological knowledge." In *Lithic Debitage, Context, Form, Meaning*, edited by W. Andrefsky, 21-30. Salt Lake City: The University of Utah Press.

Malan, B. D. 1955. "The Archaeology of the Tunnel Cave and Skildergat Kop, Fish Hoek, Cape of Good Hope." *The South African Archaeological Bulletin* 10 (37):3-9.

Malan, J., and J. Viljoen. 2008. "Southern Cape Geology: Evolution of a Rifted Margin. Field Excursion FT07 Guidebook." *Prepared for the American Association of Petroleum Geologists International Conference and Exhibition, 26-29th of October, 2008 Cape Town, South Africa*.

Mandeville, M. D., and J. Flenniken. 1974. "A comparison of the flaking qualities of Nehawka chert before and after thermal pretreatment." *Plains Anthropologist* 19:146-148.

Mannino, M. A., and K. D. Thomas. 2002. "Depletion of a resource? The impact of prehistoric human foraging on intertidal mollusk communities and its significance for human settlement, mobility and dispersal." *World Archaeology* 33:452-474.

Marean, C. 2010a. "When the Sea Saved Humanity." *Scientific American Magazine*, 2010, 54-61.

Marean, C. W. 2000. "The Middle Stone Age at Die Kelders Cave 1, South Africa." *Journal of Human Evolution* 38 (1):3-5. doi: DOI: 10.1006/jhev.1999.0348</p>.

Marean, C. W. 2010b. "Pinnacle Point Cave 13B (Western Cape Province, South Africa) in context: The Cape Floral kingdom, shellfish, and modern human origins." *Journal of Human Evolution* 59 (3–4):425-443. doi: 10.1016/j.jhevol.2010.07.011.

Marean, C. W. 2014. "The origins and significance of coastal resource use in Africa and Western Eurasia." *Journal of Human Evolution* 77 (The Role of Freshwater and Marine Resources in the Evolution of the Human Diet, Brain and Behavior):17-40.

Marean, C. W. 2016. "The transition to foraging for dense and predictable resources and its impact on the evolution of modern humans." *Phil. Trans. R. Soc. B* DOI: 10.1098/rstb.2015.0239.

Marean, C. W., R. J. Anderson, M. Bar-Matthews, K. Braun, H. C. Cawthra, R. M. Cowling, F. Engelbrecht, K. J. Esler, E. Fisher, J. Franklin, K. Hill, M. Janssen, A. J. Potts, and R. Zahn. 2015. "A new research strategy for integrating studies of paleoclimate, paleoenvironment, and paleoanthropology." *Evolutionary Anthropology: Issues, News, and Reviews* 24 (2):62-72.

Marean, C. W., and Z. Assefa. 2005. "The Middle and Upper Pleistocene African record for the biological and behavioral origins of modern humans." In *African Archaeology*, edited by A. B. Stahl. New York: Blackwell.

Marean, C. W., M. Bar-Matthews, J. Bernatchez, E. Fisher, P. Goldberg, A. I. R. Herries, Z. Jacobs, A. Jerardino, P. Karkanas, T. Minichillo, P. J. Nilssen, E. Thompson, I. Watts, and H. M. Williams. 2007. "Early human use of marine resources and pigment in South Africa during the Middle Pleistocene." *Nature* 449 (7164):905-908. doi: 10.1038/nature06204.

Marean, C. W., M. Bar-Matthews, E. Fisher, P. Goldberg, A. Herries, P. Karkanas, P. J. Nilssen, and E. Thompson. 2010. "The stratigraphy of the Middle Stone Age sediments at Pinnacle Point Cave 13B (Mossel Bay, Western Cape Province, South Africa)." *Journal of Human Evolution* 59 (3–4):234-255. doi: 10.1016/j.jhevol.2010.07.007.

Marean, C. W., P. Goldberg, G. Avery, F. E. Grine, and R. G. Klein. 2000. "Middle Stone Age Stratigraphy and Excavations at Die Kelders Cave 1 (Western Cape Province, South Africa): the 1992, 1993, and 1995 Field Seasons." *Journal of Human Evolution* 38 (1):7-42. doi: 10.1006/jhev.1999.0349.

Marean, C. W., P. J. Nilssen, K. Brown, A. Jerardino, and D. Stynder. 2004. "Paleoanthropological investigations of Middle Stone Age sites at Pinnacle Point, Mossel Bay (South Africa): Archaeology and hominid remains from the 2000 Field Season." *PaleoAnthropology*:14-83.

Marean, C.W., H.C. Cawthra, R.M. Cowling, K.J. Esler, E. Fisher, A. Milewski, A.J. Potts, E. Singels, and J. De Vynck. 2014. "Stone Age people in a changing South African Greater Cape Floristic Region." In *Fynbos: Ecology, Evolution, and Conservation of a Megadiverse Region*, edited by N. Allsopp, J.F. Colville and G.A. Verboom. Oxford University Press.

Marean, C.W., and N. Cleghorn. 2003. "Large mammal skeletal element transport: Applying foraging theory in a complex taphonomic system." *Journal of Taphonomy* 1:15-42.

Marker, M. E. , and M. J. McFarlane. 1997. "Cartographic analysis of the African surface complex between Albertinia and Mossel Bay, Southern Cape, South Africa." *South African Journal of Geology* 100:185-194.

Marlowe, F. 2010. *The Hadza: hunter-gatherers of Tanzania (Vol. 3)*: Univ of California Press.

Marlowe, F. W. 2006. "14 Central place provisioning, the Hadza as an example." In *Feeding ecology in apes and other primates*, edited by G. Hohmann, M. M. Robbins and C. Boesch, 359-377.

Mason, R. J. 1957. "The Transvaal Middle Stone Age and Statistical Analysis." *The South African Archaeological Bulletin* 12 (48):119-137.

Matthews, T., C. W. Marean, and P. J. Nilssen. 2009. "Micromammals from the Middle Stone Age (92 - 167 ka) at Cave PP13B, Pinnacle Point, south coast, South Africa." *Paleontologia Africana* 44:112-120.

Matthews, T., A. Rector, Z. Jacobs, A. I. R. Herries, and C. W. Marean. 2011. "Environmental implications of micromammals accumulated close to the MIS 6 to MIS 5 transition at Pinnacle Point Cave 9 (Mossel Bay, Western Cape Province, South Africa)." *Palaeogeography, Palaeoclimatology, Palaeoecology* 302:213-229.

Maynard Smith, J. 1978. "Optimization theory in evolution." *Annual Review of Ecology and Systematics* 9:31-56.

McBrearty, S., and A. S. Brooks. 2000. "The revolution that wasn't: a new interpretation of the origin of modern human behavior." *Journal of Human Evolution* 39 (5):453-563. doi: 10.1006/jhev.2000.0435.

McCall, G. S. 2006. "Multivariate perspectives on change and continuity in the Middle Stone Age lithics from Klasies River Mouth, South Africa." *Journal of Human Evolution* 51 (4):429-439. doi: 10.1016/j.jhevol.2006.06.003.

McCall, G. S. 2007. "Behavioral ecological models of lithic technological change during the later Middle Stone Age of South Africa." *Journal of Archaeological Science* 34 (10):1738-1751. doi: 10.1016/j.jas.2006.12.015.

McCall, G. S. 2012. "Ethnoarchaeology and the Organization of Lithic Technology." *Journal of Archaeological Research* 20:157-203.

McCall, G. S., and J. T. Thomas. 2012. "Still Bay and Howiesons Poort foraging strategies: recent research and models of culture change." *African Archaeological Review* 29:7-50.

McCormick, N. J. 1985. "Edge flaking as a measure of material performance." *Metals and Materials Letters* 8:154-156.

McCormick, N. J., and E. A. Almond. 1990. "Edge flaking of brittle materials." *Journal of Hard Materials* 1:25-52.

McNabb, J., and A. Sinclair. 2009. *The Cave of Hearths: Makapan middle pleistocene research project*. Oxford: ArchaeoPress.

McPherron, S. J. P., H. L. Dibble, and P. Goldberg. 2005. "Z." *Geoarchaeology: An International Journal* 20 (3):243-262.

McPherron, S. P., Z. Alemseged, C. W. Marean, J. G. Wynn, D. Reed, D. Geraads, R. Bobe, and H. A. Bearat. 2010. "Evidence for stone-tool-assisted consumption of animal tissues before 3.39 million years ago at Dikika, Ethiopia." *Nature* 466 (7308):857-860.

Mellars, P. 2006. "Why did modern humans disperse from Africa 60,000 years ago? A new model." *Proceedings of the National Academy of Sciences* 103:9381-9386.

Mellars, P.A. 1996. *The Neandertal Legacy: An Archaeological Perspective from Western Europe*. Princeton: Princeton University Press.

Meltzer, D. J. 2002. "What do you do when no one's been there before? Thoughts on the exploration and colonization of new lands." In *The First Americans: The Pleistocene Colonization of the New World*, edited by N. Jablonski, 27-58. Memoirs No. 27, California Academy of Sciences: San Francisco.

Mercieca, A., and P. Hiscock. 2008. "Experimental insights into alternative strategies of lithic heat treatment." *Journal of Archaeological Science* 35:2634–2639.

Metcalfe, D., and K. R. Barlow. 1992. "A Model for Exploring the Optimal Trade-off between Field Processing and Transport." *American Anthropologist* 94 (2):340-356. doi: 10.1525/aa.1992.94.2.02a00040.

Milliken, S. 1998. "The role of raw material availability in technological organization: a case study from the southeast Italian Late Palaeolithic." In *The Organization of Lithic Technology in Late Glacial and Early Postglacial Europe*, edited by S. Milliken, 63-82. Oxford: British Archaeological Reports.

Milo, R. G. 1994. "Human-animal interactions in southern African prehistory: a microscopic study of bone damage signatures." University of Chicago, Department of Anthropology.

Minichillo, T. 2005. "Middle Stone Age Lithic Study, South Africa: An Examination of Modern Human Origins." University of Washington, Department of Anthropology.

Minichillo, T. 2006. "Raw material use and behavioral modernity: Howiesons Poort lithic foraging strategies." *Journal of Human Evolution* 50 (3):359-364. doi: 10.1016/j.jhevol.2005.08.013.

Mitchell, P. 2002. *The Archaeology of Southern Africa*. Cambridge: Cambridge University Press.

Mitchell, P. J. 1995. "Revisiting the Robberg: New Results and a Revision of Old Ideas at Sehonghong Rock Shelter." *South African Archaeological Bulletin* 50:28-38.

Mitchell, P. J. 1996. "The late Quaternary of the Lesotho highlands, southern Africa: Preliminary results and future potential of ongoing research at Sehonghong shelter." *Quaternary International* 33:35-43. doi: DOI: 10.1016/1040-6182(95)00097-6</p>.

Mitchell, P. J., and J. M. Steinberg. 1992. "Ntloana Tsoana: A Middle Stone Age Sequence from Western Lesotho." *The South African Archaeological Bulletin* 47 (155):26-33.

Mourre, V., P. Villa, and C. S. Henshilwood. 2010. "Early Use of Pressure Flaking on Lithic Artifacts at Blombos Cave, South Africa." *Science* 330 (6004):659-662. doi: 10.1126/science.1195550.

Mucina, L., and M. C. Rutherford. 2006. *The Vegetation of South Africa, Lesotho and Swaziland, Strelitzia 19*. Pretoria: The South African National Biodiversity Institute.

Muller, A., and C. Clarkson. 2016. "Identifying Major Transitions in the Evolution of Lithic Cutting Edge Production Rates." *PLoS ONE* http://dx.doi.org/10.1371/journal.pone.0167244.

Murdock, G. P. 1967. "Ethnographic Atlas: A Summary." *Ethnology* 6 (2):109-236. doi: 10.2307/3772751.

Nagaoka, L. 2002. "The effects of resource depression on foraging efficiency, diet breadth, and patch use in southern New Zealand." *Journal of Anthropological Archaeology* 21:419-442.

Nash, D., S. Coulson, S. Staurset, M. Smith, and J. Ullyott. 2013. "Provenancing silcrete in the Cape coastal zone: Implications for Middle Stone Age research in South Africa." *Journal of human evolution* 65 (5):682-688.

Nash, D. J., S. Coulson, S. Staurset, J. S. Ullyott, M. Babutsi, L. Hopkinson, and M. P. Smith. 2013. "Provenancing of silcrete raw materials indicates long-distance transport to Tsodilo Hills, Botswana, during the Middle Stone Age." *J Hum Evol* 64 (4):280-8. doi: 10.1016/j.jhevol.2013.01.010.

Nash, D. J., S. Coulson, S. Staurset, J. S. Ullyott, M. Babutsi, and M. P. Smith. 2016. "Going the distance: Mapping mobility in the Kalahari Desert during the Middle Stone Age through multi-site geochemical provenancing of silcrete artefacts." *J Hum Evol* 96:113-33. doi: 10.1016/j.jhevol.2016.05.004.

Neeley, M. P., and C. M. Barton. 1994. "A new approach to interpreting late Pleistocene microlith industries in southwest Asia." *Antiquity* 68:275-288.

Nelson, M. C. 1991. "The Study of Technological Organization." *Archaeological Method and Theory* 3:57-100.

Nelson, N. C. 1916. "Flint working by Ishi." In *R.F. Heizer, T. Kroeber (Eds.), Ishi the Last Yahi A Documentary History*, 168-172. Berkeley: University of California Press.

Noll, M. P. 2000. "Components of Acheulean lithic assemblage variability at Olorgesailie, Kenya." University of Illinois at Urbana-Champaign, Google Scholar.

Nordfjord, S. , J. A. Goff, J. A. Austin, and L. S. Duncan. 2009. "Shallow stratigraphy and complex transgressive ravinement on the New Jersey middle and outer continental shelf." *Marine Geology* 266 (1):232-243.

O'Brien, E.M. 1993. "Climatic Gradients in Woody Plant Species Richness: Towards an Explanation Based on an Analysis of Southern Africa's Woody Flora." *J. Biogeography* 20:181-198.

Oestmo, S., M. A. Janssen, and C. W. Marean. 2016. "Testing Brantingham's Neutral Model: The Effect of Spatial Clustering on Stone Raw Material Procurement." In *Simulating Prehistoric and Ancient Worlds*, edited by J.A. Barceló and F. Del Castillo, 175-188. Springer.

Oestmo, S., and C.W. Marean. 2015. "Excavation and survey at Pinnacle Point." In *Field Archaeology from Around the World: Ideas and Approaches*, edited by M. Carver, B. Gaydarska and S. Monton-Subias, 123-126. New York: Springer.

Oestmo, S., B.J. Schoville, J. Wilkins, and C.W. Marean. 2014. "A Middle Stone Age Paleoscape near the Pinnacle Point caves, Vleesbaai, South Africa." *Quaternary International* 350:147-168.

Orians, G. H., and N. E. Pearson. 1979. "On the theory of central place foraging." In *Analysis of Ecological Systems*, edited by D. J. Horn, R. D. Mitchell and C. R. Stairs, 154–177. Columbus: Ohio State University Press.

Ortega Y Gasset, J. 1972. *Meditations on hunting*. New York: Charles Scribner's Sons.

Orton, J. 2008. "A useful measure of the desirability of different raw materials for retouch within and between assemblages: the raw material retouch index (RMRI)." *Journal of Archaeological Science* 35:1090-1094.

Oswalt, W. 1973. *Habitat and Technology*. New York: Holt, Rinehart and Winston.

O'Connell, J. F., and K. Hawkes. 1981. "Alyawara plant use and optimal foraging theory." In *Hunter-Gatherer Foraging Strategies*, edited by B. Winterhalder and E. A. Smith, 99-125. Chicago: University of Chicago Press.

O'Connell, J. F., K. T. Jones, and S. R. Simms. 1982. "Some thoughts on prehistoric archaeology in the Great Basin." In *Man and Environment in the Great Basin, Papers II*, edited by D. B. Madsen and J. F. O'Connell, 227-240. Washington, DC: Society for American Archaeology.

O'Connell, J. F., and B. Marshall. 1989. "Analysis of kangaroo body part transport among the Alyawara of central Australia." *Journal of Archaeological Science* 16:393-405.

Parker, D. 2011. "The Complexity of Lithic Simplicity: Computer Simulation of Lithic Assemblage Formation in Western New South Wales, Australia." M.A., University of Auckland.

Parkington, J., J.-Ph. Rigaud, C. Poggenpoel, G. Porraz, and P.-J. Texier. 2013. "Introduction to the project and excavation of Diepkloof Rock Shelter (Western Cape, South Africa): a view on the Middle Stone Age." *Journal of Archaeological Science* 40:3369-3375.

Parry, W. J., and R. L. Kelly. 1987. "Expedient Core Technology and Sedentism." In *The Organization of Core Technology*, edited by J. Johnson and C. Morrow, 285-304. Boulder, Co: Westview Press.

Partridge, T. C., G. A. Botha, and I. G. Haddon. 2006. "Cenozoic deposits of the interior." In *The Geology of South Africa*, edited by B. Thomas, 585-604. Johannesburg: Geological Society of South Africa.

Partridge, T. C., and R. R. Maud. 1987. "Geomorphic Evolution of southern Africa since the Mesozoic." *South African Journal of Geology* 90 (2):179-208.

Pelcin, A. W. 1998. "The threshold effect of platform width: A reply to Davis and Shea." *Journal of Archaeological Science* 25:615-620.

Perlman, S. M. 1980. "An optimum diet model, coastal variability, and hunter-gatherer behavior." *Advances in Archaeological Method and Theory* 3:257-310.

Phillipps, R. S. 2012. "Documenting Socio-economic Variability in the Egyptian Neolithic through Stone Artefact Analysis." Ph.D., University of Auckland.

Pickering, R., Z. Jacobs, A. I. R. Herries, P. Karkanas, M. Bar-Matthews, J. D. Woodhead, P. Kappen, E. Fisher, and C. W. Marean. 2013. "Paleoanthropologically significant South African sea caves dated to 1.1–1.0 million years using a combination of U–Pb, TT-OSL and palaeomagnetism." *Quaternary Science Reviews* 65:39-52.

Piperno, D. R., and D. M. Pearsall. 1998. *The Origins of Agriculture in the Lowland Neotropics*. San Diego, CA: Academic Press.

Pop, C. M. 2015. "Simulating Lithic Raw Material Variability in Archaeological Contexts: A Re-evaluation and Revision of Brantingham's Neutral Model." *Journal of Archaeological Method and Theory* 23 (4).

Porat, N., M. Chazan, R. Grün, M. Aubert, V. Eisenmann, and L. K. Horwitz. 2010. "New radiometric ages for the Fauresmith industry from Kathu Pan, southern

Africa: Implications for the Earlier to Middle Stone Age transition." *Journal of Archaeological Science* 37 (2):269-283. doi: 10.1016/j.jas.2009.09.038.

Porcasi, J. F., T. L. Jones, and L. M. Raab. 2000. "Trans-Holocene marine mammal exploitation on San Clemente Island, California: A tragedy of the commons revisited." *Journal of Anthropological Archaeology* 19:200-220.

Porraz, G., J. E. Parkington, J.-P. Rigaud, C. M. Miller, C. Poggenpoel, C. Tribolo, W. Archer, C. R. Cartwright, A. Charrié-Duhaut, L. Dayet, M. Igreja, N. Mercier, P. Schmidt, C. Verna, and P.-J. Texier. 2013. "The MSA sequence of Diepkloof and the history of southern African Late Pleistocene populations." *Journal of Archaeological Science* 40:3542-3552. doi: 10.1016/j.jas.2013.02.024.

Porraz, G., P.-J. Texier, W. Archer, M. Piboule, J.-P. Rigaud, and C. Tribolo. 2013. "Technological successions in the Middle Stone Age sequence of Diepkloof Rock Shelter, Western Cape, South Africa." *Journal of Archaeological Science* 40:3376-3400. doi: 10.1016/j.jas.2013.02.012.

Porraz, G., P.-J. Texier, J.-P. Rigaud, J. Parkington, C. Poggenpoel, and D. L. Roberts. 2008. "Preliminary characterization of a Middle Stone Age lithic assemblage preceding the 'classic' Howieson's Poort complex at Diepkloof rock shelter, Western Cape Province, South Africa." *South African Archaeological Society, Goodwin Series* 10:105-121.

Posamentier, H. W. 2002. "Ancient shelf ridges-A potentially significant component of the transgressive systems tract: Case study from offshore northwest Java." *AAPG bulletin* 86 (1):75-106.

Potts, R. 1988. *Early hominid activities at Olduvai Gorge*. New York: Aldine de Gruyter.

Potts, R. 1991. "Why the Oldowan? Plio-Pleistocene tool making and the transport of resources." *Journal of Anthropological Research* 47:153-176.

Purdy, B. A., and H. K. Brooks. 1971. "Thermal Alternation of Silica Minerals: An Archaeological Approach." *Science, New Series* 173 (3994):322-325.

Raab, L. M. 1992. "An optimal foraging analysis of prehistoric shellfish collecting on San Clemente Island, California." *Journal of Ethnobiology* 12:63-80.

Raab, L. M. 1996. "Debating prehistory in coastal southern California: Resource intensification versus political economy." *Journal of California and Great Basin Anthropology* 18:64-80.

Raab, L. M., and K. Bradford. 1997. "Making nature answer to interpretivism: Response to J. E. Arnold, R. H. Colten, and S. Pletka." *American Antiquity* 62:340-341.

Raab, L. M., and D. O. Larson. 1997. "Medieval climatic anomaly and punctuated cultural evolution in coastal southern California." *American Antiquity* 63:319-336.

Raab, L. M., J. F. Porcasi, K. Bradford, and A. Yatsko. 1995. "Debating cultural evolution: Regional implications of fishing intensification at Eel Point, San Clemente Island." *Pacific Coast Archaeological Quarterly* 31:3-27.

Raab, L. M., and A. Yatsko. 1992. "Ancient maritime adaptations of the California Bight: A perspective from San Clemente Island." In *Essays on the Prehistory of Maritime California*, edited by T. L. Jones, 173–193. Davis: Center for Archaeological Research, University of California.

Raichlen, D.A., B.M. Wood, A.D. Gordon, A.Z. Mabulla, F.W. Marlowe, and H. Pontzer. 2014. "Evidence of Lévy walk foraging patterns in human hunter–gatherers." *Proceedings of the National Academy of Sciences* 111 (2):728-733.

Railsback, S. F., and V. Grimm. 2012. *Agent-Based and Individual-Based Modeling: A Practical Introduction*. Princeton and Oxford: Princeton University Press.

Ramos-Fernandez, G., J. L. Mateos, O. Miramontes, G. Cocho, H. Larralde, and B. Ayala-Orozco. 2004. "Levy walk patterns in the foraging movements of spider monkeys (Ateles geoffroyi)." *Behavioral Ecology and Sociobiology* 55:223-230.

Rebelo, A. G., C. Boucher, N. Helme, L. Mucina, and M. C. Rutherford. 2006. "Fynbos Biome." In *The Vegetation of South Africa, Lesotho and Swaziland*, edited by L. Mucina and M. C. Rutherford, 52-219. Pretoria: South African National Biodiversity Institute.

Rector, A. L., and K. E. Reed. 2010. "Middle and late Pleistocene faunas of Pinnacle Point and their paleoecological implications." *Journal of Human Evolution* 59 (3–4):340-357. doi: 10.1016/j.jhevol.2010.07.002.

Redding, R. 1988. "A general explanation of subsistence change: From hunting and gathering to food production." *Journal of Anthropological Archaeology* 7:56-97.

Relethford, J. H. 2008. "Genetic evidence and the modern human origins debate." *Heredity* 100:555-563.

Renfrew, C. 1969. "Trade and Culture Process in European Prehistory." *Current Anthropology* 10:151-169.

Rick, J. W., and S. Chappell. 1983. "Thermal alteration of silica materials in technological and functional perspective." *Lithic Technology* 12:69-80.

Riel-Salvatore, J., and C. M. Barton. 2004. "Late Pleistocene Technology, Economic Behavior, and Land-Use Dynamics in Southern Italy." *American Antiquity* 69 (2):257-274. doi: 10.2307/4128419.

Riel-Salvatore, J., G. Popescu, and C. M. Barton. 2008. "Standing at the gates of Europe: Human behavior and biogeography in the Southern Carpathians during the Late Pleistocene." *Journal of Anthropological Archaeology* 27 (4):399-417. doi: 10.1016/j.jaa.2008.02.002.

Rigaud, J.-P., P.-J. Texier, J. Parkington, and C. Poggenpoel. 2006. "Stillbay and Howiesons Poort stone tool techno-complexes. South African Middle Stone Age chronology and its implications." *Comptes Rendus Palevol* 5:829-849.

Roberts, D. L. 2003. "Age, Genesis and Significance of South African Coastal Belt Silcretes." *Council for Geoscience, South Africa* Memoir 95.

Roberts, D. L. , G. A. Botha, R. R. Maud, and J. Pether. 2006. "Coastal Cenozoic Deposits." In *The Geology of South Africa*, edited by B. Thomas, 605-628. Johannesburg: Geological Society of South Africa.

Roberts, D.L., P. Karkanas, Z. Jacobs, C.W. Marean, and R.G. Roberts. 2012. "Melting ice sheets 400,000 yr ago raised sealevel by 13 m: Past analogue for future trends." *Earth and Planetary Science Letters* 357-358:226–237.

Roche, H. 1999. "Early hominid stone tool production and technical skill 2.34[thinsp]Myr ago in West Turkana, Kenya." *Nature* 399:57-60.

Rogers, J. 1980. "First Report on the Cenozoic Sediments between Cape Town and Elands Bay." *Geological Survey of South Africa Open File* 136.

Russell, K. W. 1988. *After Eden: The Behavioral Ecology of Food Production in the Near East and North Africa, BAR International Series 391*. Oxford: British Archaeological Reports.

Sackett, J. R. 1982. "Approaches to style in lithic archaeology." *Journal of Anthropological Archaeology* 1:59-112.

Sackett, J. R. 1986. "Style, Function, and Assemblage Variability: A Reply to Binford." *American Antiquity* 51 (3). doi: 10.2307/281759.

Sahlins, M. D. 1976. *The Use and Abuse of Biology: An Anthropological Critiue of Sociobiology*. Ann Arbor: University of Michigan Press.

Salau, K., M.L. Schoon, J.A. Baggio, and M.A. Janssen. 2012. "Varying effects of connectivity and dispersal on interacting species dynamics." *Ecological Modelling* 242:81-91.

Saltelli, A., S. Tarantola, F. Campolongo, and M. Ratto. 2004. *Sensitivity analysis in practice: A guide to assessing scientific models*: John Wiley & Sons.

Sampson, C. G. 1972. *The stone age industries of the Orange River Scheme and South Africa*: National Museum.

Sampson, C. G. 1974. *The Stone Age Archaeology of Southern Africa*. New York: Academic Press.

Schick, K.D., and N. Toth. 1993. *Making Silent Stones Speak: Human Evolution and the Dawn of Technology*. New York: Simon and Schuster.

Schiffer, M. B. 1975. "Archaeology as Behavioral Science." *American Anthropologist* 77 (4):836-848. doi: 10.1525/aa.1975.77.4.02a00060.

Schmidt, P. 2016. "The 'Sand-Bath' and Lithic Heat Treatment in the South African Middle Stone Age: Myth or Reality?" *African Archaeological Review* DOI 10.1007/s10437-016-9217-z:1-7.

Schmidt, P., and A. Mackay. 2016. "Why Was Silcrete Heat-Treated in the Middle Stone Age? An Early Transformative Technology in the Context of Raw Material Use at Mertenhof Rock Shelter, South Africa." *PLOS ONE* DOI:10.1371/journal.pone.0149243:1-16.

Schmidt, P., S. Masseb, G. Laurent, A. Slodczyk, E. Le Bourhis, C. Perrenoud, J. Livage, and F. Fröhlich. 2012. "Crystallographic and structural transformations of sedimentary chalcedony in flint upon heat treatment." *Journal of Archaeological Science* 39:135-144.

Schmidt, P., G. Porraz, L. Bellot-Gurlet, E. February, B. Ligouis, C. Paris, P-J. Texier, J. E. Parkington, C. E. Miller, K. C. Nickel, and N. J. Conard. 2015. "A previously undescribed organic residue sheds light on heat treatment in the Middle Stone Age." *Journal of Human Evolution* 85:22-34.

Schmidt, P., G. Porraz, A. Slodczyk, L. Bellot-gurlet, W. Archer, and C. E. Miller. 2013. "Heat treatment in the South African Middle Stone Age: temperature induced transformations of silcrete and their technological implications." *Journal of Archaeological Science* 40:3519-3531. doi: 10.1016/j.jas.2012.10.016.

Schoville, B. J. , and K. S. Brown. 2010. "Comparing lithic assemblage edge damage distributions: examples from the Late Pleistocene and preliminary experimental results." *Vis-à-vis: Explorations in Anthropology* 10:34-49.

Schrire, C. 2009. *Past and Present in Hunter-Gatherer Studies*. Walnut Creek: Left Coast Press.

Schrire, C., and J. Deacon. 1989. "The indigenous artefacts from Oudepost I, a colonial outpost of the VOC at Saldanha Bay, Cape." *South African Archaeological Bulletin* 44:105-113.

Schwarcz, H. P., and W. J. Rink. 2000. "ESR dating of the Die Kelders Cave 1 Site, South Africa." *Journal of Human Evolution* 38:121-128.

Schweitzer, F. R. 1970. "A Preliminary Report of Excavations of a Cave at Die Kelders." *The South African Archaeological Bulletin* 25 (99/100):136-138.

Schweitzer, F. R. 1974. "Archaeological Evidence for Sheep at the Cape." *The South African Archaeological Bulletin* 29 (115/116):75-82.

Schweitzer, F. R. 1979. "Excavations at Die Kelders, Cape Province, South Africa: the Holocene deposits." *Annals of the South African Museum* 78:101-233.

Semaw, S. 1997. "2.5-million-year-old stone tools from Gona, Ethiopia." *Nature* 385:333-336.

Semaw, S. 2000. "The world's oldest stone artefacts from Gona, Ethiopia: Their implications for understanding stone technology and patterns of human evolution between 2.6-1.5 million years ago." *Journal of Archaeological Science* 27:1197-1214.

Semaw, S., M.J. Rogers, J. Quade, P.R. Renne, R.F. Butler, M. Domínguez-Rodrigo, D. Stout, W. S. Hart, T. Pickering, and S. W. Simpson. 2003. "2.6-Million-year-old stone tools and associated bones from OGS-6 and OGS-7, Gona, Afar, Ethiopia." *Journal of Human Evolution* 45:169-177.

Sevillano, J. G. 1997. "Lithic tool making by Amazonian palaeoindians: a case-study on materials selection." *Journal of Materials Science Letters* 16:465-468.

Shackley, M.S. 1998. "Gamma rays, X-rays and stone tools: some recent advances in archaeological geochemistry." *Journal of Archaeological Science* 25:259-270.

Sharon, G. 2008. "The impact of raw material on Acheulian large flake production." *Journal of Archaeological Science* 35 (5):1329-1344. doi: 10.1016/j.jas.2007.09.004.

Shea, J. J. 2008. "The Middle Stone Age archaeology of the Lower Omo Valley Kibish Formation: Excavations, lithic assemblages, and inferred patterns of early Homo sapiens behavior." *Journal of Human Evolution* 55 (3):448-485. doi: 10.1016/j.jhevol.2008.05.014.

Shea, J. J. 2011. "Homo sapiens Is as Homo sapiens Was." *Current Anthropology* 52 (1):1-35.

Sheets, P., and G. Muto. 1972. "Pressure Blades and Total Cutting Edge: An Experiment in Lithic Technology." *Science* 175:632-634.

Shlesinger, M. F., G. M. Zaslavsky, and J. Klafter. 1993. "Strange kinetics." *Nature* 363:31-37.

Shone, R. W. 2006. "Onshore Post-Karoo Mesozoic Deposits." In *The Geology of South Africa*, edited by B. Thomas, 541-552. Johannesburg: Geological Society of South Africa.

Shott, M. J. 1986. "Technological Organization and Settlement Mobility: An Ethnographic Examination." *Journal of Anthropological Research* 42 (1):15-51.

Simms, S. R. 1987. *Behavioral Ecology and Hunter-Gatherer Foraging: An Example from the Great Basin, BAR International Series 381*. Oxford: British Archaeological Reports.

Singer, R., and J. Wymer. 1982. *The Middle Stone Age at Klasies River Mouth in South Africa*. Chicago: University of Chicago Press.

Smith, A. B., K. Sadr, J. Gribble, and R. Yates. 1991. "Excavations in the south-western Cape, South Africa, and the archaeological identity of prehistoric hunter-gatherers within the last 2000 Years." *South African Archaeological Bulletin* 46:71-91.

Smith, E. , A. Ciravolo, M. Ren, P. Karkanas, C. W. Marean, E. C. Fisher, N. Cleghorn, and C. Lane. 2015. "Cryptotephra Discovered at Pinnacle Point Site 5-6 May Correlate with the 74 ka Eruption of Toba in Indonesia: Implications for Resolving the Dating Controversy for Middle Stone Age Sites in Southern Africa." Society for American Archaeology, San Francisco, April 15-19.

Smith, E. A. 1991. *Inujjuamiut Foraging Strategies: Evolutionary Ecology of Arctic Hunting Economy*. New York: Aldine de Gruyter.

Smith, E. A. . 1981. "The application of optimal foraging theory to the analysis of hunter-gatherer group size." In *Hunter-Gatherer Foraging Strategies: Ethnographic and Archaeological Analyses*, edited by B. Winterhalder and E. A. Smith, 36-65. Chicago: University of Chicago Press.

Smith, E. A., and R. Boyd. 1990. "Risk and Reciprocity: Hunter-gatherer socioecology and the evolutionary theory of games." In *Risk and Uncertainty in Tribal and Peasant Economies*, edited by E. Cashdan. Boulder, CO: Westview Press.

Soltis, J., R. Boyd, and P.J. Richerson. 1995. "Can group-functional behaviors evolve by cultural group selection?: An empirical test." *Current Anthropology* 36 (3):473-494.

Soriano, S., P. Villa, and L. Wadley. 2007. "Blade technology and tool forms in the Middle Stone Age of South Africa: the Howiesons Poort and post-Howiesons Poort at Rose Cottage Cave." *Journal of Archaeological Science* 34 (5):681-703. doi: 10.1016/j.jas.2006.06.017.

Stephens, D., and J. Krebs. 1986. *Foraging Theory*. Princeton: Princeton University Press.

Stiner, M. C., and N. D. Munro. 2002. "Approaches to prehistoric diet breadth, demography and prey ranking systems in time and space." *Journal of Archaeological Method and Theory* 9:181-214.

Stiner, M. C., N. D. Munro, and T. A. Surovell. 2000. "The Tortoise and the Hare: Small-Game Use, the Broad-Spectrum Revolution, and Paleolithic Demography." *Current Anthropology* 41 (1):39-73.

Stiner, M. C., N. D. Munro, T. A. Surovell, E. Tchernov, and O. Bar-Yosef. 1999. "Paleolithic population growth pulses evidenced by small animal exploitation." *Science* 283:190-194.

Stout, D. 2002. "Skill and Cognition in Stone Tool Production: An Ethnographic Case Study from Irian Jaya." *Current Anthropology* 43 (5):693-722. doi: 10.1086/342638.

Stout, D., J. Quade, S. Semaw, M. J. Rogers, and N. E. Levin. 2005. "Raw material selectivity of the earliest stone toolmakers at Gona, Afar, Ethiopia." *Journal of Human Evolution* 48 (4):365-380. doi: 10.1016/j.jhevol.2004.10.006.

Stout, D., S. Semaw, M. J. Rogers, and D. Cauche. 2010. "Technological variation in the earliest Oldowan from Gona, Afar, Ethiopia." *Journal of Human Evolution* 58:474-491.

Stow, D.A.V. 2007. *Sedimentary Rocks in the Field: A Colour Guide*. London: Mason Publishing.

Summerfield, M. A. 1983. "Silcrete as a Palaeoclimatic Indicator: Evidence from Southern Africa." *Palaeogeography, Palaeoclimatology, Palaeoecology* 41:65-79.

Summerfield, M. A. . 1981. "The nature and occurrence of silcrete, southern Cape Province, South Africa." In *Report Number 28*, 1-36. University of Oxford: School of Geography.

Surovell, T. A. 2003. "The behavioral ecology of Folsom lithic technology." University of Arizona.

Surovell, T. A. 2009. *Toward A Behavioral Ecology of Lithic Technology: Cases From Paleoindian Archaeology*. Tucson: The University Of Arizona Press.

Szuter, C., and F. Bayham. 1989. "Sedentism and prehistoric animal procurement among desert horticulturalists of the North American Southwest." In *Farmers as Hunters: The implications of Sedentism*, edited by S. Kent, 67-78. Albuquerque: University of New Mexico Press.

Tabuti, J. R. S., S. S. Dhilliona, and K. A. Lye. 2003. "Firewood use in Bulamogi County, Uganda:species selection, harvesting and consumption patterns." *Biomass and Bioenergy* 25:581-596.

Talma, A. S. , and J. C. Vogel. 1992. "Late Quaternary paleotemperatures derived from a speleothem from Cango Caves, Cape Province, South Africa." *Quaternary Research* 37:201-213.

Thackeray, A. I. 2000. "Middle Stone Age artefacts from the 1993 and 1995 excavations of Die Kelders Cave 1, South Africa." *Journal of Human Evolution* 38 (1):147-168. doi: 10.1006/jhev.1999.0354.

Thackeray, A. I., and A. J. Kelly. 1988. "A Technological and Typological Analysis of Middle Stone Age Assemblages Antecedent to the Howiesons Poort at Klasies River Main Site." *The South African Archaeological Bulletin* 43 (147):15-26.

Thamm, A. G., and M. R. Johnson. 2006. "The Cape Supergroup." In *The Geology of South Africa*, edited by M. R. Johnson, C. R. Anhauesser and R. J. Thomas, 443-460. Pretoria: Geological Society of South Africa, Johannesburg/Council for Geoscience.

Thiele, J. C., W. Kurth, and V. Grimm. 2014. "Facilitating Parameter Estimation and Sensitivity Analysis of Agent-Based Models: A Cookbook Using NetLogo and R." *Journal of Artificial Societies and Social Simulation* 17 (3):11.

Thompson, E., and C. W. Marean. 2008. "The Mossel Bay Lithic Variant: 120 Years of Middle Stone Age Research From Cape St Blaize Cave to Pinnacle Point." *Goodwin Series* 10:90-104.

Thompson, E., H. M. Williams, and T. Minichillo. 2010. "Middle and late Pleistocene Middle Stone Age lithic technology from Pinnacle Point 13B (Mossel Bay, Western Cape Province, South Africa)." *Journal of Human Evolution* 59 (3–4):358-377. doi: 10.1016/j.jhevol.2010.07.009.

Tobias, P. V. 1949. "The Excavation of Mwulu's Cave, Potgietersrust District." *The South African Archaeological Bulletin* 4 (13):2-13.

Torrence, R. 1983. "Time Budgeting and Hunter-Gatherer Technology." In *Hunter-Gatherer Economy in Prehistory*, edited by G. Bailey, 11-22. Cambridge: Cambridge University Press.

Torrence, R. 1986. *Production and Exchange of Stone Tools*. Cambridge: Cambridge University Press.

Torrence, R. 1989. *Time, Energy and Stone Tools, New Directions in Archaeology*. Cambridge: Cambridge University Press.

Toth, N. 1985. "The Oldowan reassessed: A close look at early stone artifacts." *Journal of Archaeological Science* 12 (2):101-120. doi: DOI: 10.1016/0305-4403(85)90056-1</p>.

Tribolo, C. 2003. "Apport Des Methodes De La Luminescence A La Chronologie Des Techno-Facies Du Middle Stone Age Associes Aux Premiers Hommes Moderns Du Sud De l'Afrique." L'université Bordeaux.

Tribolo, C., N. Mercier, E. Douville, J.-L. Joron, J.-L. Reyss, D. Rufer, N. Cantin, Y. Lefrais, C. E. Miller, G. Porraz, J. Parkington, J.-P. Rigaud, and P.-J. Texier. 2013. "OSL and TL dating of the Middle Stone Age sequence at Diepkloof Rock Shelter (South Africa): a clarification." *Journal of Archaeological Science* 40:3401-3411. doi: 10.1016/j.jas.2012.12.001.

Tribolo, C., N. Mercier, H. Valladas, J. L. Joron, P. Guibert, Y. Lefrais, M. Selo, P.-J. Texier, J.-Ph. Rigaud, G. Porraz, C. Poggenpoel, J. Parkington, J.-P. Texier, and A. Lenoble. 2009. "Thermoluminescence dating of a Stillbay–Howiesons Poort sequence at Diepkloof Rock Shelter (Western Cape, South Africa)." *Journal of Archaeological Science* 36 (3):730-739. doi: 10.1016/j.jas.2008.10.018.

Tryon, C.A., and S. McBrearty. 2002. "Tephrostratigraphy and the Acheulian to Middle Stone Age transition in the Kapthurin Formation, Kenya." *Journal of Human Evolution* 42:211-235.

Ugan, A., J. Bright, and A. Rogers. 2003. "When is Technology worth the Trouble?" *Journal of Archaeological Science* 30:1315-1329.

van Riet Lowe, C. 1954. "The Cave of Hearths." *South African Archaeological Bulletin* 9:25-29.

Van Wyk, B., and P. Van Wyk. 1997. *Field guide to trees of southern Africa*: Struik.

Viljoen, J.H.A., and J.A. Malan. 1993. *Die Geologie van die Gebiede 3421 BB Mosselbaai en 3422 AA Herbertsdale*. Pretoria: Department of Mineral and Energy Affairs.

Villa, P., M. Soressi, C. S. Henshilwood, and V. Mourre. 2009. "The Still Bay points of Blombos Cave (South Africa)." *Journal of Archaeological Science* 36:441-460.

Villa, P., S. Soriano, N. Teyssandier, and S. Wurz. 2010. "The Howiesons Poort and MSA III at Klasies River main site, Cave 1A." *Journal of Archaeological Science* 37:630-655. doi: DOI: 10.1016/j.jas.2009.10.028</p>.

Viswanathan, G. M., V. Afanasyev, S. V. Buldyrev, E. J. Murphy, P. A. Prince, and H. E. Stanley. 1996. "Levy flight search patterns of wandering albatrosses." *Nature* 381:413-415.

Viswanathan, G. M., F. Bartumeus, S. V. Buldyrev, J. Catalan, U. L. Fulco, S. Havlin, M. G. E. da Luz, M. L. Lyra, E. P. Raposo, and H. E. Stanley. 2002. "Levy flight random searches in biological phenomena." *Physica A: Statistical Mechanics and Its Applications* 314:208-213.

Viswanathan, G. M., S. V. Buldyrev, S. Havlin, M. G. E. da Luz, E. P. Raposo, and H. E. Stanley. 1999. "Optimizing the success of random searches." *Nature* 401:911-914.

Vogel, J. C. 1969. "Radiocarbon Dating of Bushman Rock Shelter, Ohrigstad District." *The South African Archaeological Bulletin* 24 (94).

Volman, T. P. 1981. "The Middle Stone Age in the Southern Cape." University of Chicago, Department of Anthropology.

Volman, T. P. 1984. "Early prehistory of southern Africa." In *Southern African Prehistory and Paleoenvironments*, edited by R. G. Klein, 169-220. Rotterdam: Balkema.

Waddington, K.D., and L. Holden. 1979. "Optimal foraging: on flower selection of bees." *American Naturalist* 114:179-196.

Wadley, L. 1996. "The Robberg Industry of Rose Cottage Cave, eastern Free State: the technology, spatial patterns and environment." *South African Archaeological Bulletin* 51:64-74.

Wadley, L. 1997. "Rose Cottage Cave: Archaeological work 1987 to 1997." *South African Journal of Science* 93 (10).

Wadley, L. 2000. "The early Holocene layers of Rose Cottage Cave, Eastern Free State: Technology, spatial patterns and environment." *South African Archaeological Bulletin* 55:18-31.

Wadley, L. 2005. "A Typological Study of the Final Middle Stone Age Stone Tools from Sibudu Cave, KwaZulu-Natal." *South African Archaeological Bulletin* 60 (182):51-63.

Wadley, L. 2007. "Announcing a Still Bay industry at Sibudu Cave, South Africa." *Journal of Human Evolution* 52:681-689.

Wadley, L. 2010. "Compound-adhesive manufacture as a behavioral proxy for complex cognition in the Middle Stone Age." *Current Anthropology* 51 (Supplement 1):S111-S119.

Wadley, L. 2013a. "MIS 4 and MIS 3 occupations in Sibudu, KwaZulu-Natal, South Africa." *South African Archaeological Bulletin* 68:41-51.

Wadley, L. 2013b. "Recognizing complex cognition through innovative technology in Stone Age and Palaeolithic Sites." *Cambridge Archaeological Journal* 23:163-183.

Wadley, L. , and Z. Jacobs. 2006. "Sibudu Cave: background to the excavations, stratigraphy and dating." *South African Humanities* 18:1-26.

Wadley, L., and P. Harper. 1989. "Rose Cottage Cave Revisited: Malan's Middle Stone Age Collection." *The South African Archaeological Bulletin* 44 (149):23-32.

Wadley, L., and Z. Jacobs. 2004. "Sibudu Cave, KwaZulu-Natal: Background to the excavations of Middle Stone Age and Iron Age occupations." *South African Journal of Science* 100:145-151.

Wadley, L., and M. Mohapi. 2008. "A Segment is not a Monolith: evidence from the Howiesons Poort of Sibudu, South Africa." *Journal of Archaeological Science* 35 (9):2594-2605. doi: DOI: 10.1016/j.jas.2008.04.017</p>.

Wadley, L., and L. C. Prinsloo. 2014. "Experimental heat treatment of silcrete implies analogical reasoning in the Middle Stone Age." *Journal of Human Evolution*:In press.

Walker, F., and M. Mathias. 1946. "The petrology of two granite-slate contacts at Cape Town, South Africa." *Quarterly Journal of the Geological Society* 102:499-521.

Watts, I. 2010. "The pigments from Pinnacle Point Cave 13B, Western Cape, South Africa." *Journal of Human Evolution* 59:392-411.

Webb, J. A., and M. Domanski. 2008. "THE RELATIONSHIP BETWEEN LITHOLOGY, FLAKING PROPERTIES AND ARTEFACT MANUFACTURE FOR AUSTRALIAN SILCRETES*." *Archaeometry* 50 (4):555-575. doi: 10.1111/j.1475-4754.2007.00381.x.

Wendt, W. E. 1974. "Art Mobilier aus der Apollo 11 Grotte in Sudwest-Afrika." *Acta Praehistorica et archaeologica* 5:1-42.

Wendt, W. E. 1976. "'Art Mobilier' from the Apollo 11 Cave, South West Africa: Africa's Oldest Dated Works of Art." *The South African Archaeological Bulletin* 31 (121/122):5-11.

Whallon, R. 2006. "Social networks and information: Non-"utilitarian" mobility among hunter-gatherers." *Journal of Anthropological Archaeology* 25:259-270.

White, T. D., B. Asfaw, D. DeGusta, H. Gilbert, G. D. Richards, G. Suwa, and F. C. Howell. 2003. "Pleistocene Homo sapiens from Middle Awash, Ethiopia." *Nature* 423 (6941):742-747. doi: 10.1038/nature01669.

Wilensky, U. 1999. "NetLogo." *http://ccl.northwestern.edu/netlogo/. Center for Connected Learning and Computer-Based Modeling, Northwestern University, Evanston, IL.*

Wilke, P. J. , J. J. Flenniken, and T. L. Ozbun. 1991. "Clovis Technology at the Anzick Site, Montana." *Journal of California and Great Basin Anthropology* 13:242-272.

Wilkins, J., K. S. Brown, S. Oestmo, T. Pereira, K. L. Ranhorn, B. J. Schoville, and C. W. Marean. 2017. "Lithic technological responses to Late Pleistocene glacial cycling at Pinnacle Point Site 5-6, South Africa." *PLoS ONE* 12 (3): e0174051.

Wilkins, J., K. S. Brown, S. Oestmo, T. Pereira, K. Ranhorn, B. J. Schoville, and C. W. Marean. 2014. https://www.academia.edu/6703567/Pinnacle_Point_5-6_Lithic_Analytical_Methods_E4_Codes_and_Trait_Definitions.

Wilkins, J., and M. Chazan. 2012. "Blade production ~500 thousand years ago at Kathu Pan 1, South Africa: support for a multiple origins hypothesis for early Middle Pleistocene blade technologies." *Journal of Archaeological Science* In Press:1-18.

Wilkins, J., B. J. Schoville, K. S. Brown, and M. Chazan. 2012. "Evidence for Early Hafted Hunting Technology." *Science* 338 (6109):942-946. doi: 10.1126/science.1227608.

Will, M., G. D. Bader, and N. J. Conard. 2014. "Characterizing the Late Pleistocene MSA Lithic Technology of Sibudu, KwaZulu-Natal, South Africa." *PLOS ONE* 9 (5):1-27.

Winterhalder, B. 1981. "Foraging strategies in the boreal environment: an analysis of Cree hunting and gathering." In *Hunter-gatherer foraging strategies: ethnographic and archeological analyses*, edited by B. Winterhalder and E. A. Smith, 66-98. Chicago: University of Chicago Press.

Winterhalder, B., and C. Goland. 1997. "An evolutionary ecology perspective on diet choice, risk, and plant domestication." In *Plants, People, and Landscapes: Studies in Paleoethnobotany*, edited by K. Gremillion, 123-160. University of Alabama Press: Tuscaloosa.

Winterhalder, B., and E. A. Smith. 1992. "Evolutionary Ecology and the social sciences." In *Evolutionary ecology and Human behavior*, edited by E. A. Smith and B. Winterhalder. New York: Aldine de Gruyter.

Winterhalder, B., and E. A. Smith. 2000. "Analyzing Adaptive Strategies: Human Behavioral Ecology at Twenty-Five." *Evolutionary Anthropology* 9:51-72.

Wolgemuth, E. 1996. "Resource intensification in prehistoric central California: Evidence from archaeobotanical data." *Journal of California and Great Basin Anthropology* 18:81-103.

Wright, K. I. 1994. "Ground-stone tools and hunter-gatherer subsistence in southwest Asia: Implications for the transition to farming." *American Antiquity* 59:238-263.

Wurz, S. 1999. "The Howiesons Poort Backed Artefacts from Klasies River: An Argument for Symbolic Behaviour." *The South African Archaeological Bulletin* 54 (169):38-50.

Wurz, S. 2000. "The Middle Stone Age at Klasies River, South Africa." University of Stellenbosch.

Wurz, S. 2002. "Variability in the Middle Stone Age Lithic Sequence, 115,000-60,000 Years Ago at Klasies River, South Africa." *Journal of Archaeological Science* 29 (9):1001-1015. doi: DOI: 10.1006/jasc.2001.0799</p>.

Wurz, S. 2013. "Technological Trends in the Middle Stone Age of South Africa between MIS 7 and MIS 3." *Current Anthropology* In press.

Wurz, S., N. J. le Roux, S. Gardner, and H. J. Deacon. 2003. "Discriminating between the end products of the earlier Middle Stone Age sub-stages at Klasies River using biplot methodology." *Journal of Archaeological Science* 30:1107-1126. doi: DOI: 10.1016/S0305-4403(03)00009-8</p>.

Yesner, D. R. 1989. "Effects of prehistoric Aleut exploitation on sea-mammal populations." *Arctic Anthropology* 25:28-43.

Zeanah, D. 2000. "Transport costs, central place foraging and hunter-gatherer alpine land use strategies." In *Intermountain Archaeologies*, edited by D. Madsen and M. Metcalf, 1-14. Salt Lake City: Anthropological Papers 122, University of Utah.

Zeanah, D. 2004. "Sexual division of labor and central place foraging: A model for the Carson Desert of western Nevada." *Journal of Anthropological Anthropology* 23:1-32.

APPENDIX A

SUPPLEMENTARY FIGURES

CHAPTER 8- OPPORTUNISTIC ACQUISITION MODEL – HYPOTHESIS EVALUATION AND SENSITIVITY ANALYSIS

Is random walk a realistic lithic raw material procurement strategy?

MIS4 without a Paleo-Agulhas plain silcrete

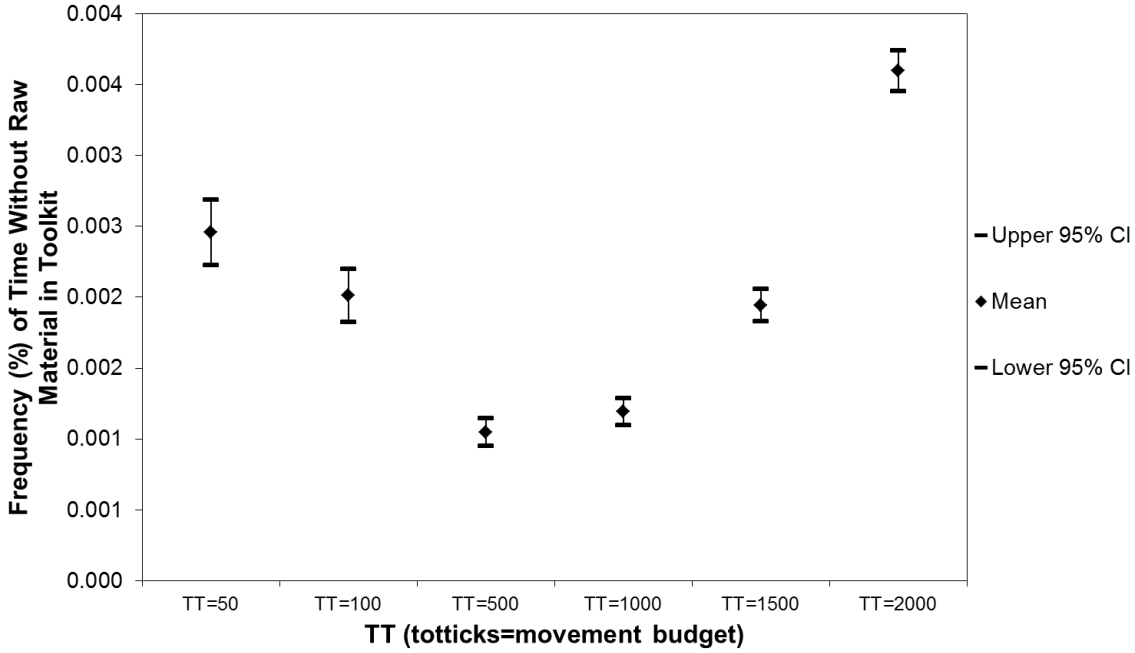

Figure A1. Plot with means and 95% confidence intervals showing the distribution of the frequency of time without raw material in toolkit at different movement budgets (TT=totticks) during MIS4 conditions without a Paleo-Agulhas plain silcrete source. Star with capped whiskers is the mean with the 95% confidence interval (CI).

MIS4 with a Paleo-Agulhas plain silcrete

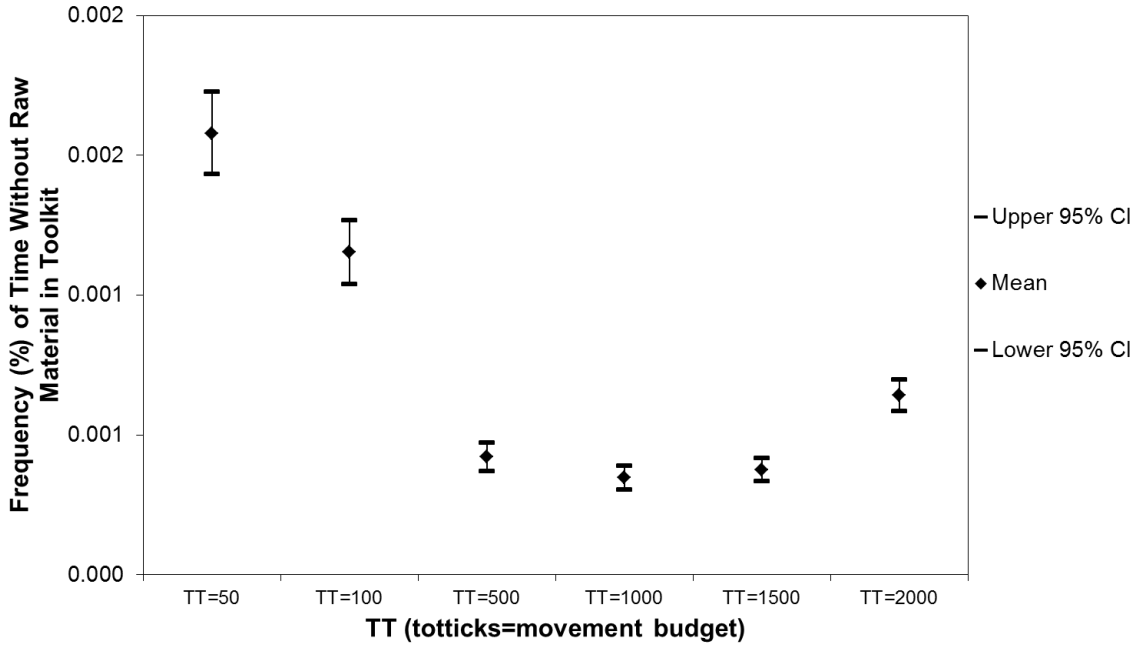

Figure A2. Plot with means and 95% confidence intervals showing the distribution of the frequency of time without raw material in toolkit at different movement budgets (TT=totticks) during MIS4 conditions with a Paleo-Agulhas plain silcrete source. Star with capped whiskers is the mean with the 95% confidence interval (CI).

MIS5

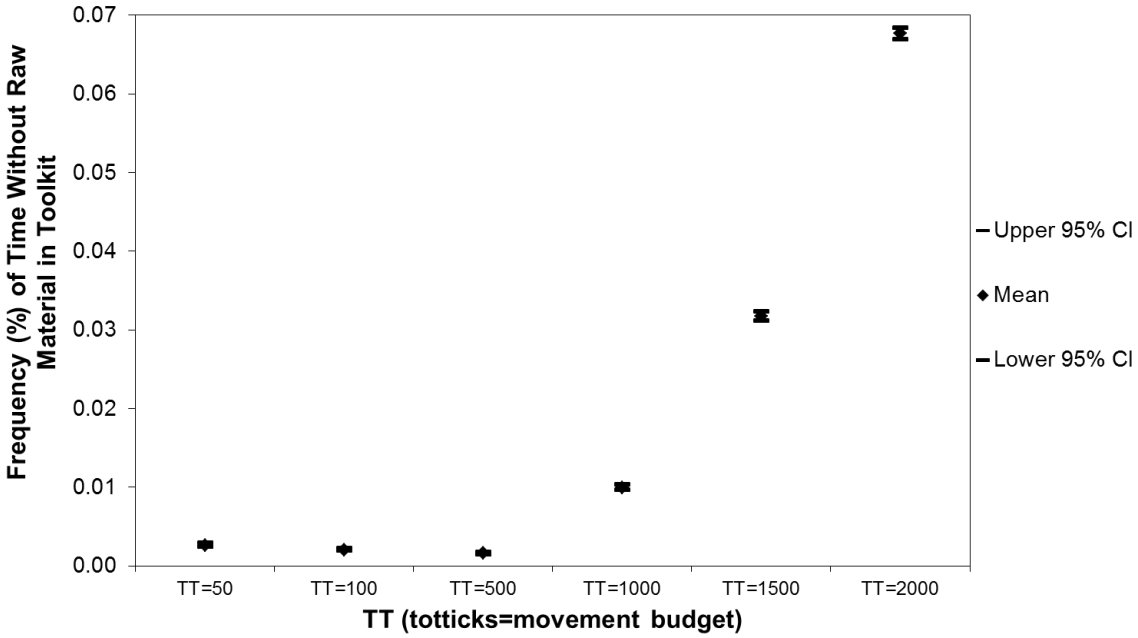

Figure A3. Plot with means and 95% confidence intervals showing the distribution of the frequency of time without raw material in toolkit at different movement budgets (TT=totticks) during MIS5 conditions. Star with capped whiskers is the mean with the 95% confidence interval (CI).

MIS6 without a Paleo-Agulhas plain silcrete

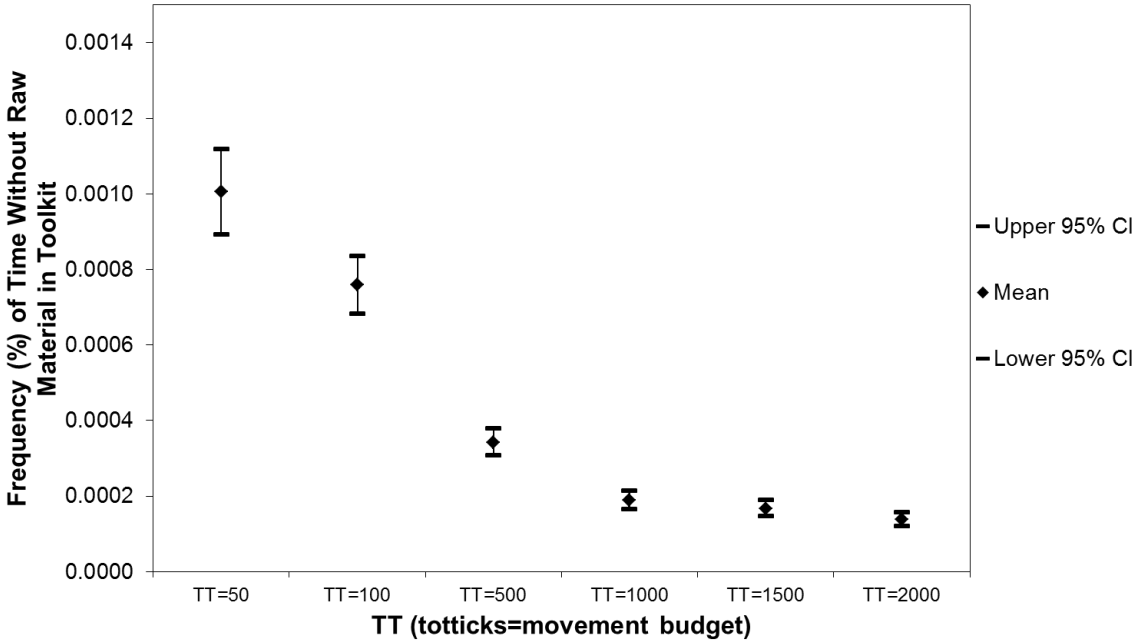

Figure A4. Plot with means and 95% confidence intervals showing the distribution of the frequency of time without raw material in toolkit at different movement budgets (TT=totticks) during MIS6 conditions without a Paleo-Agulhas plain silcrete source. Star with capped whiskers is the mean with the 95% confidence interval (CI).

MIS6 without a Paleo-Agulhas plain silcrete

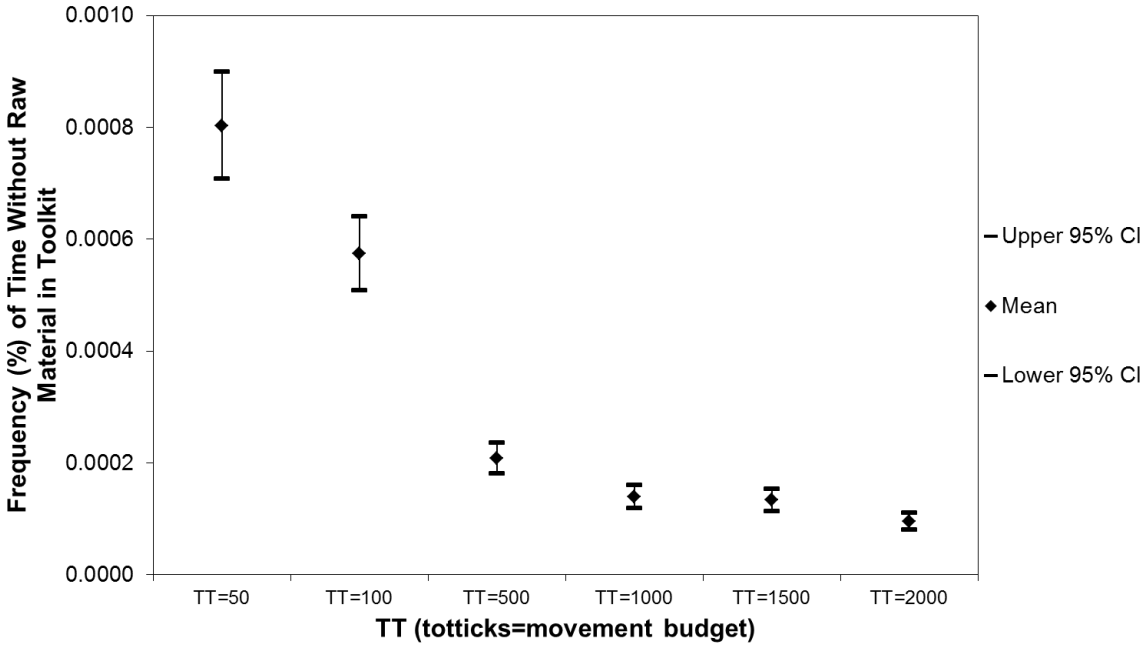

Figure A5. Plot with means and 95% confidence intervals showing the distribution of the frequency of time without raw material in toolkit at different movement budgets (TT=totticks) during MIS6 conditions with a Paleo-Agulhas plain silcrete source. Star with capped whiskers is the mean with the 95% confidence interval (CI).

OFAT3 – Changing Discard probabilities and toolkit size

Return to starting location simulations

MIS4 without a Paleo-Agulhas plain silcrete source

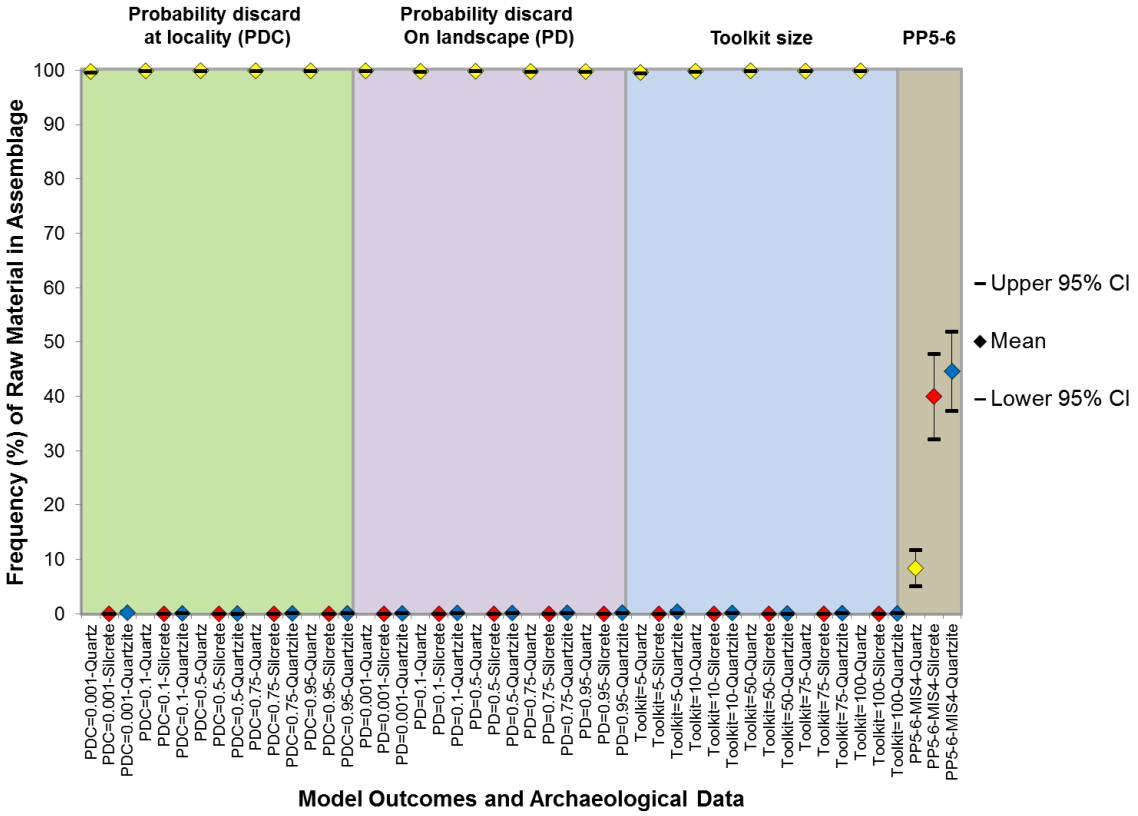

Figure A6. Comparison between OFAT3 outcomes using different PDC (Probability discard on landscape), PD (Probability discard at locality), and toolkit (toolkit size) values during MIS4 model conditions without a Paleo-Agulhas plain silcrete source from same-day return simulations (TT=100) where the agent returns to the starting locality (PP) and bootstrapped MIS4 archaeological raw material frequency data from PP5-6. Plot shows the mean and the upper and lower 95% confidence intervals for the raw materials deposited at the both the simulated PP locality and at PP5-6.

MIS4 with a Paleo-Agulhas plain silcrete source

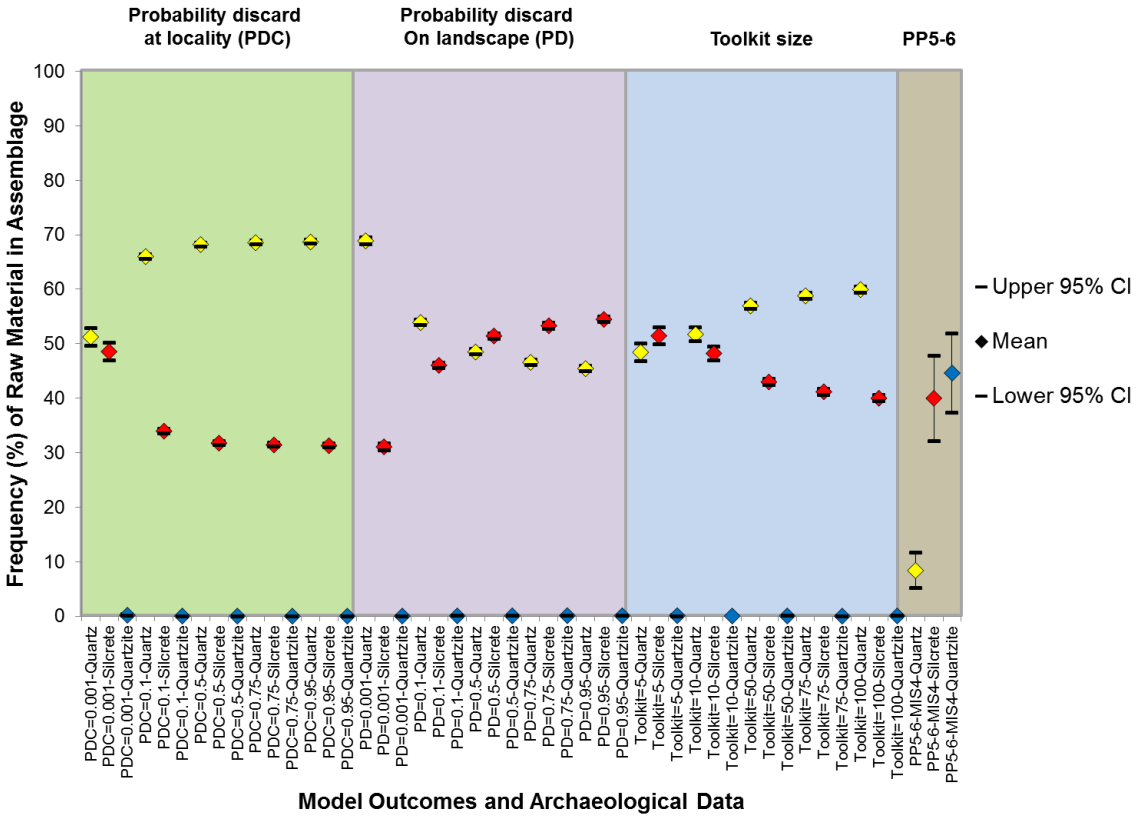

Figure A7. Comparison between OFAT3 outcomes using different PDC (Probability discard on landscape), PD (Probability discard at locality), and toolkit (toolkit size) values during MIS4 model conditions with a Paleo-Agulhas plain silcrete source. from same-day return simulations (TT=100) where the agent returns to the starting locality (PP) and bootstrapped MIS4 archaeological raw material frequency data from PP5-6. Plot shows the mean and the upper and lower 95% confidence intervals for the raw materials deposited at the both the simulated PP locality and at PP5-6.

MIS5 conditions

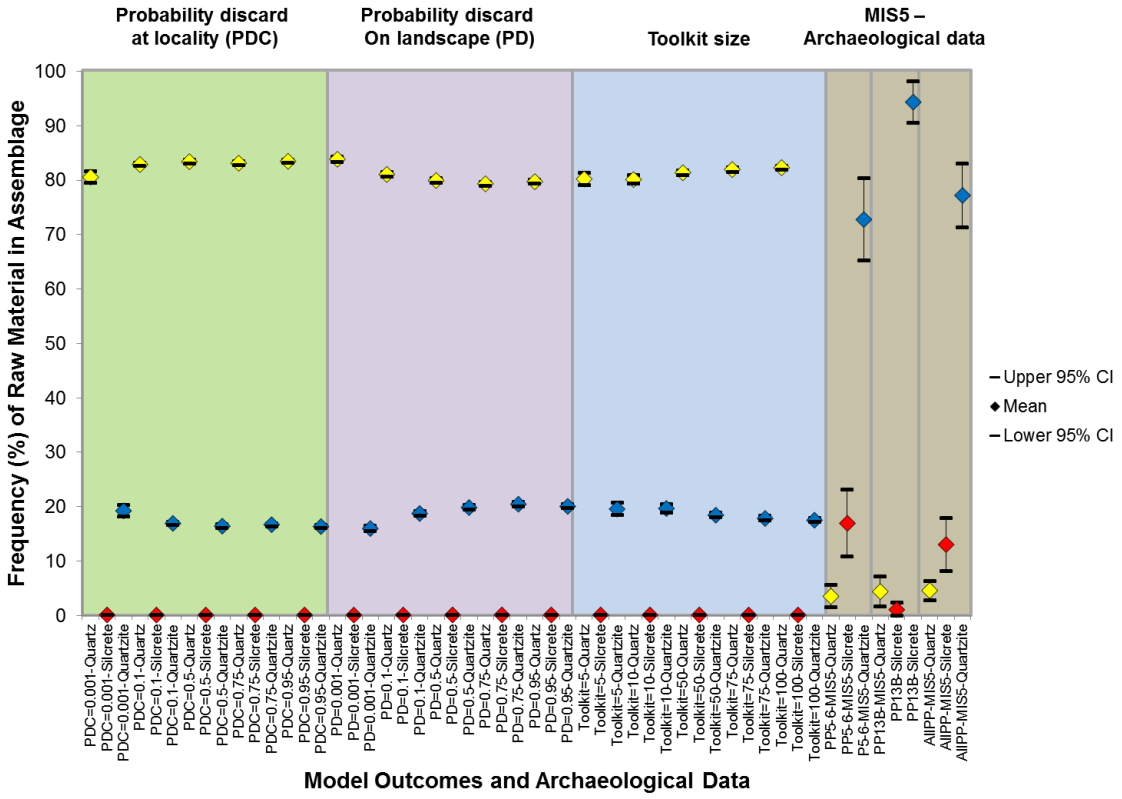

Figure A8. Comparison between OFAT3 outcomes using different PDC (Probability discard on landscape), PD (Probability discard at locality), and toolkit (toolkit size) values during MIS5 model conditions from same-day return simulations (TT=100) where the agent returns to the starting locality (PP) and bootstrapped MIS5 archaeological raw material frequency data from PP5-6, PP13B, and all MIS5 assemblages from the PP sequence including PP5-6, PP13B, PP9B, and PP9C. Plot shows the mean and the upper and lower 95% confidence intervals for the raw materials deposited at the both the simulated PP locality and at PP5-6, PP9B, PP9C, and PP13B.

MIS6 without a Paleo-Agulhas plain silcrete source

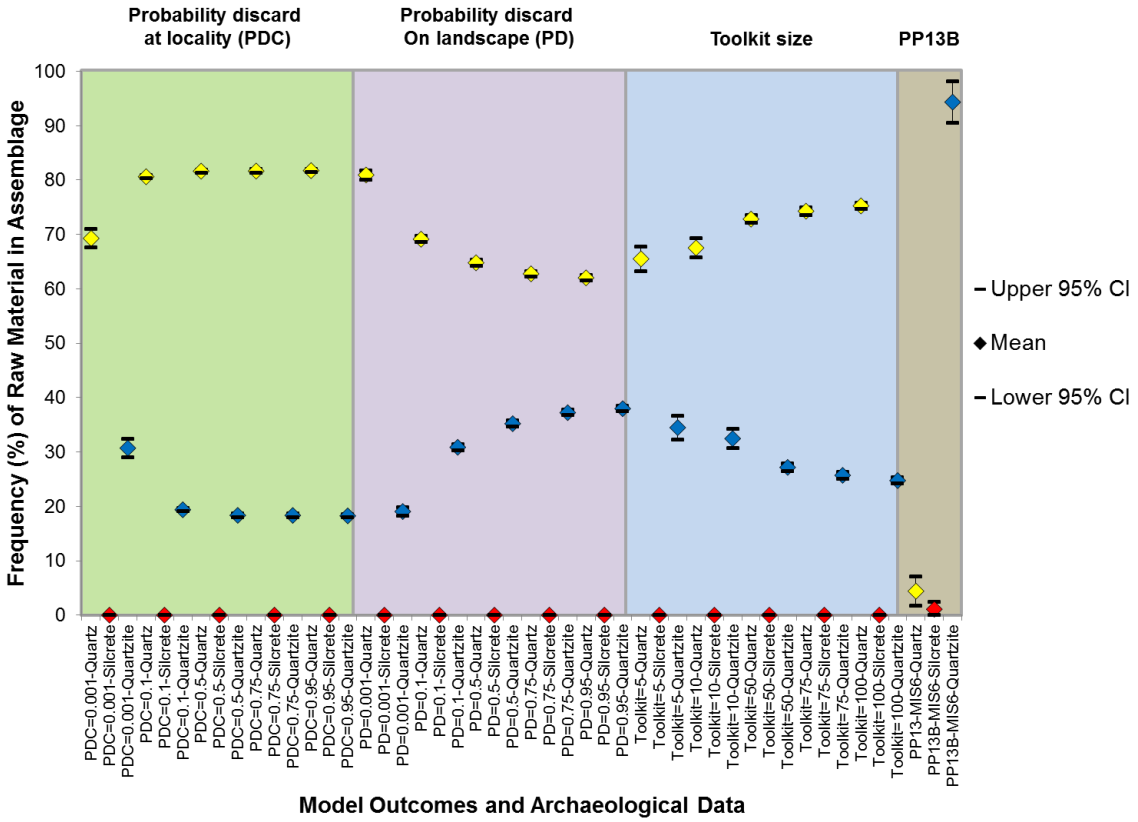

Figure A9. Comparison between OFAT3 outcomes using different PDC (Probability discard on landscape), PD (Probability discard at locality), and toolkit (toolkit size) values during MIS6 model conditions without a Paleo-Agulhas plain silcrete source from same-day return simulations (TT=100) where the agent returns to the starting locality (PP) and bootstrapped MIS6 archaeological raw material frequency data from PP13B. Plot shows the mean and the upper and lower 95% confidence intervals for the raw materials deposited at the both the simulated PP locality and at PP13B.

MIS6 with a Paleo-Agulhas plain silcrete source

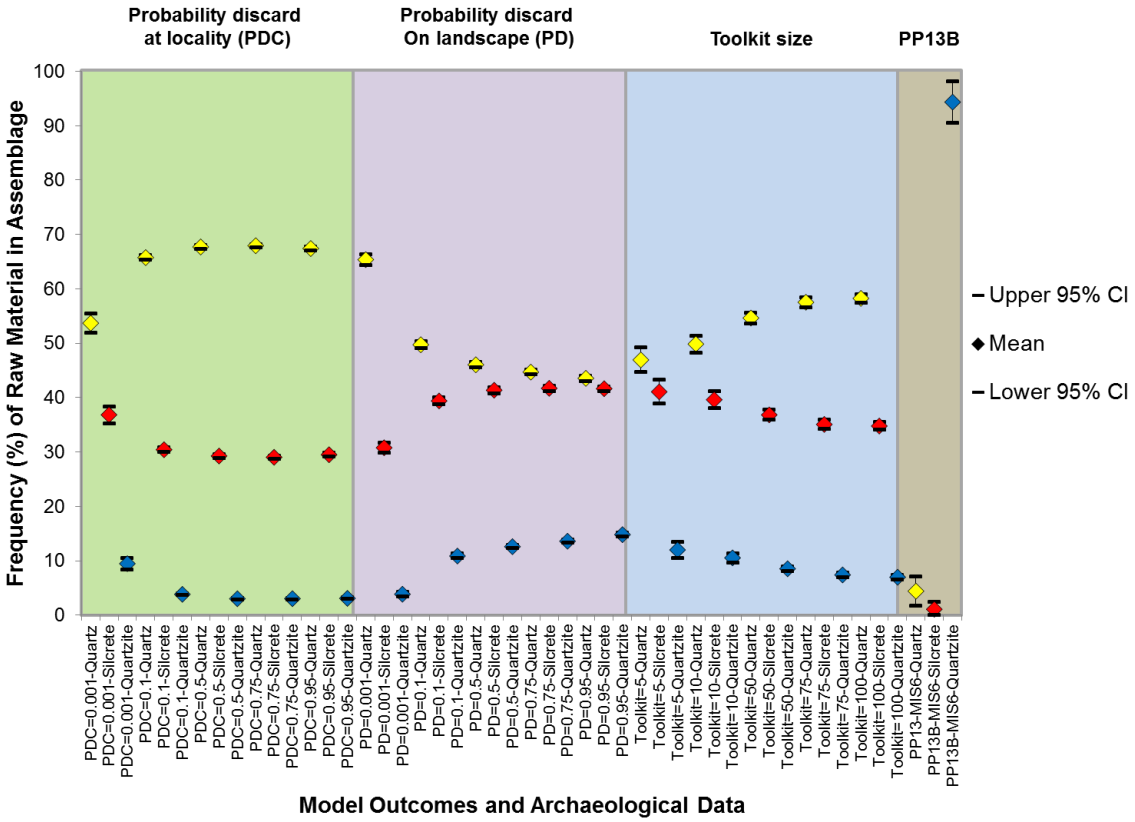

Figure A10. Comparison between OFAT3 outcomes using different PDC (Probability discard on landscape), PD (Probability discard at locality), and toolkit (toolkit size) values during MIS6 model conditions with a Paleo-Agulhas plain silcrete source from same-day return simulations (TT=100) where the agent returns to the starting locality (PP) and bootstrapped MIS6 archaeological raw material frequency data from PP13B. Plot shows the mean and the upper and lower 95% confidence intervals for the raw materials deposited at the both the simulated PP locality and at PP13B.

Move to closest locality simulations

MIS4 without a Paleo-Agulhas plain silcrete source

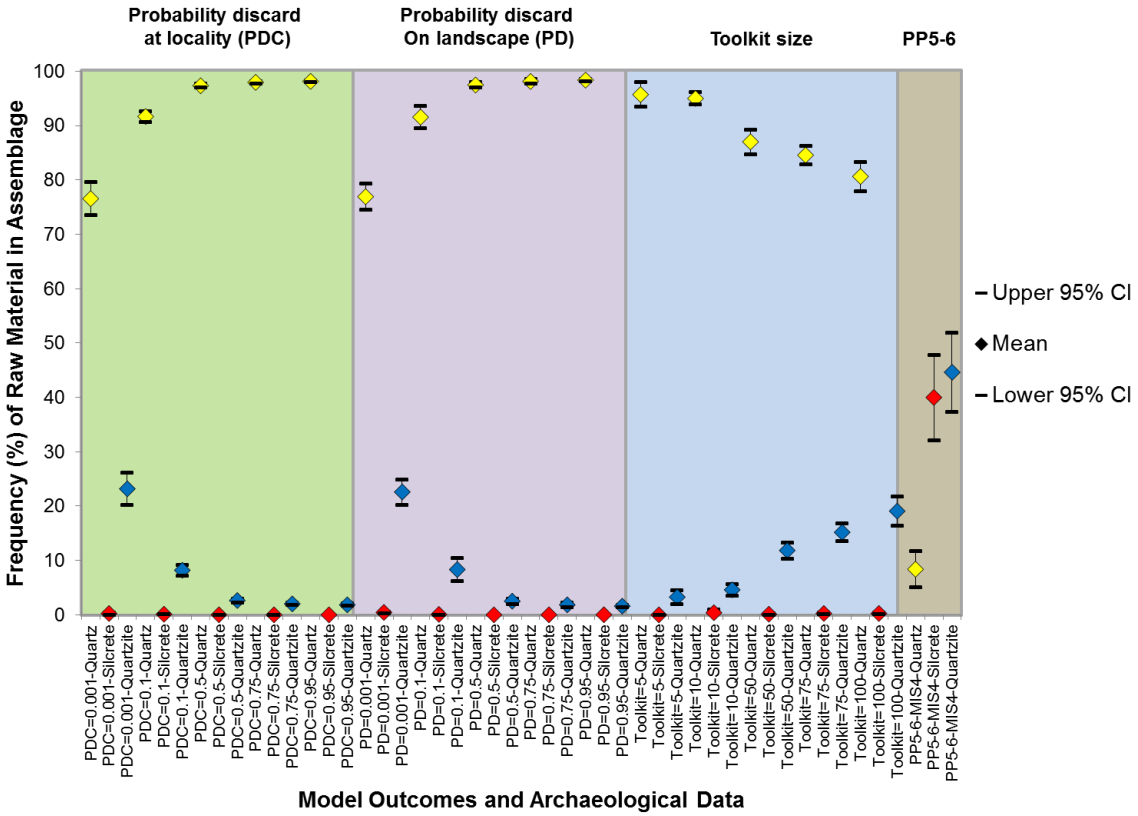

Figure A11. Comparison between OFAT3 outcomes using different PDC (Probability discard on landscape), PD (Probability discard at locality), and toolkit (toolkit size) values during MIS4 model conditions without a Paleo-Agulhas plain silcrete source from same-day returns simulations (TT=100) where the agent moves to the closest locality when the movement budget (totticks) is exhausted and bootstrapped MIS4 archaeological raw material frequency data from PP5-6. Plot shows the mean and the upper and lower 95% confidence intervals for the raw materials deposited at the both the simulated PP locality and at PP5-6.

MIS4 with a Paleo-Agulhas plain silcrete source

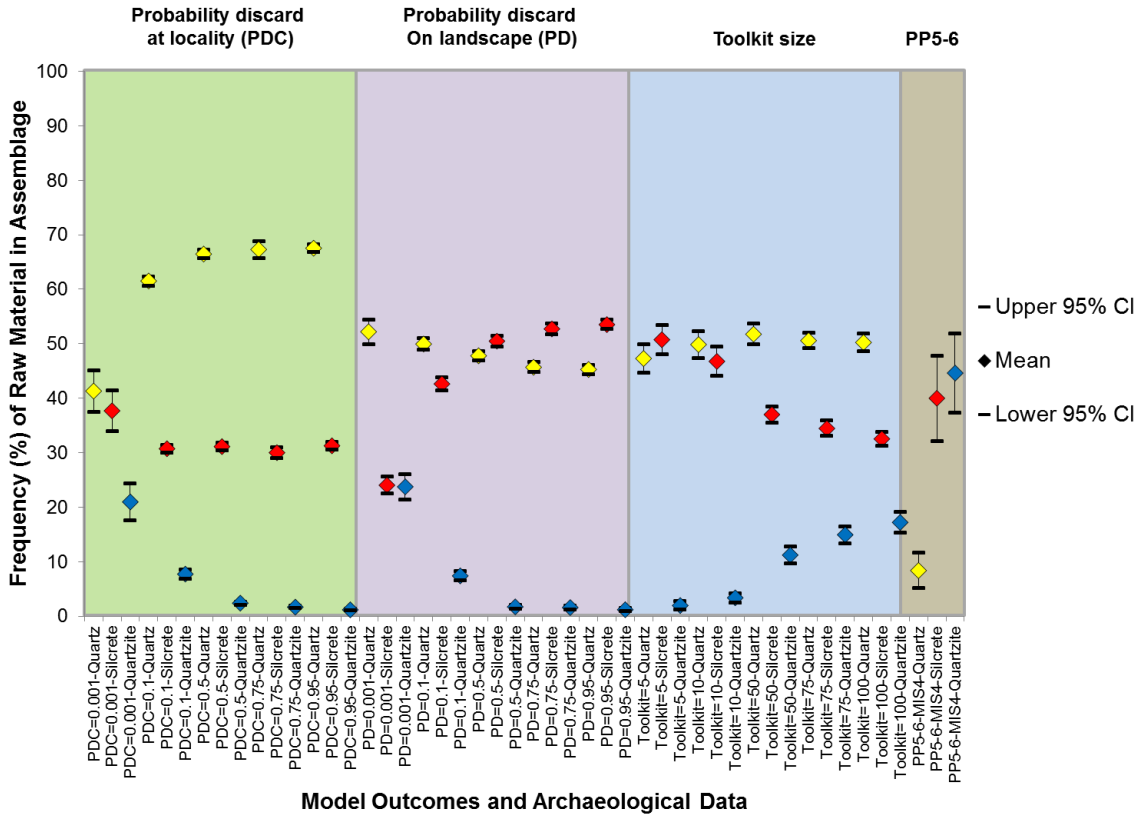

Figure A12. Comparison between OFAT3 outcomes using different PDC (Probability discard on landscape), PD (Probability discard at locality), and toolkit (toolkit size) values during MIS4 model conditions with a Paleo-Agulhas plain silcrete source from same-day returns simulations (TT=100) where the agent moves to the closest locality when the movement budget (totticks) is exhausted and bootstrapped MIS4 archaeological raw material frequency data from PP5-6. Plot shows the mean and the upper and lower 95% confidence intervals for the raw materials deposited at the both the simulated PP locality and at PP5-6.

MIS5 conditions

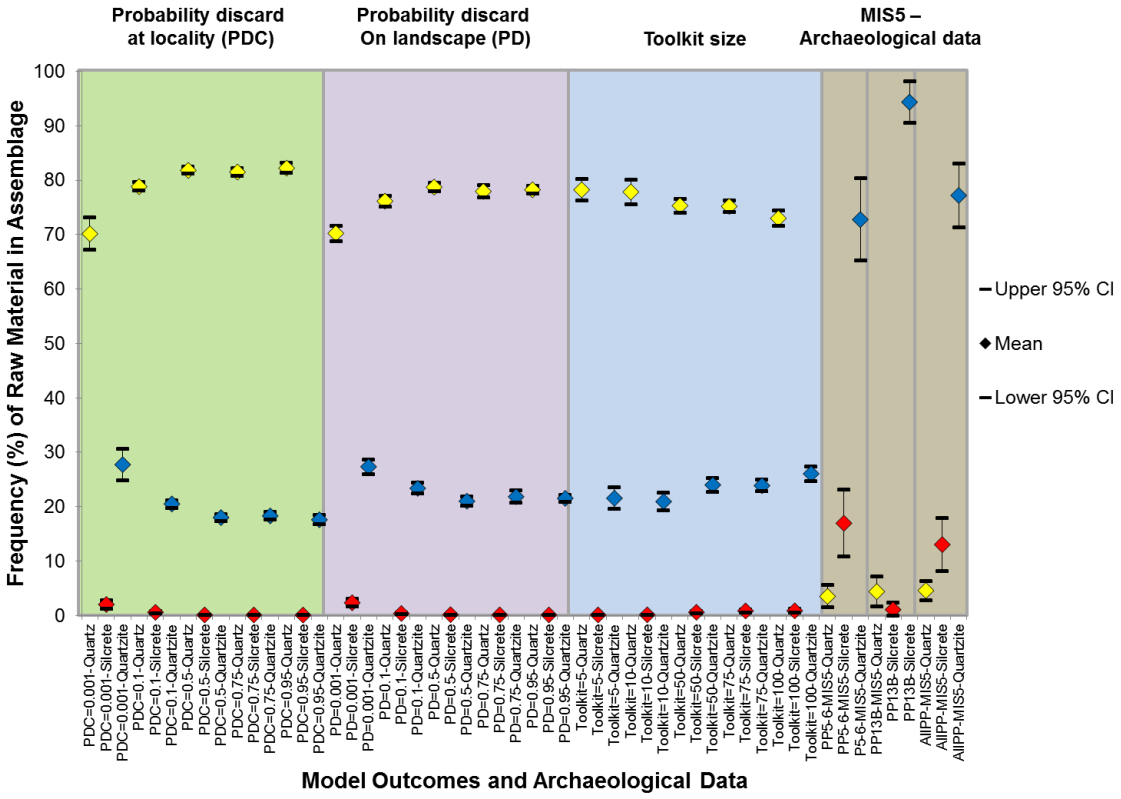

Figure A13. Comparison between OFAT3 outcomes using different PDC (Probability discard on landscape), PD (Probability discard at locality), and toolkit (toolkit size) values during MIS5 model conditions from same-day returns simulations (TT=100) where the agent moves to the closest locality when the movement budget (totticks) is exhausted and bootstrapped MIS5 archaeological raw material frequency data from PP5-6, PP13B, and all MIS5 assemblages from the PP sequence including PP5-6, PP13B, PP9B, and PP9C. Plot shows the mean and the upper and lower 95% confidence intervals for the raw materials deposited at the both the simulated PP locality and at PP5-6, PP9B, PP9C, and PP13B.

MIS6 without a Paleo-Agulhas plain silcrete source

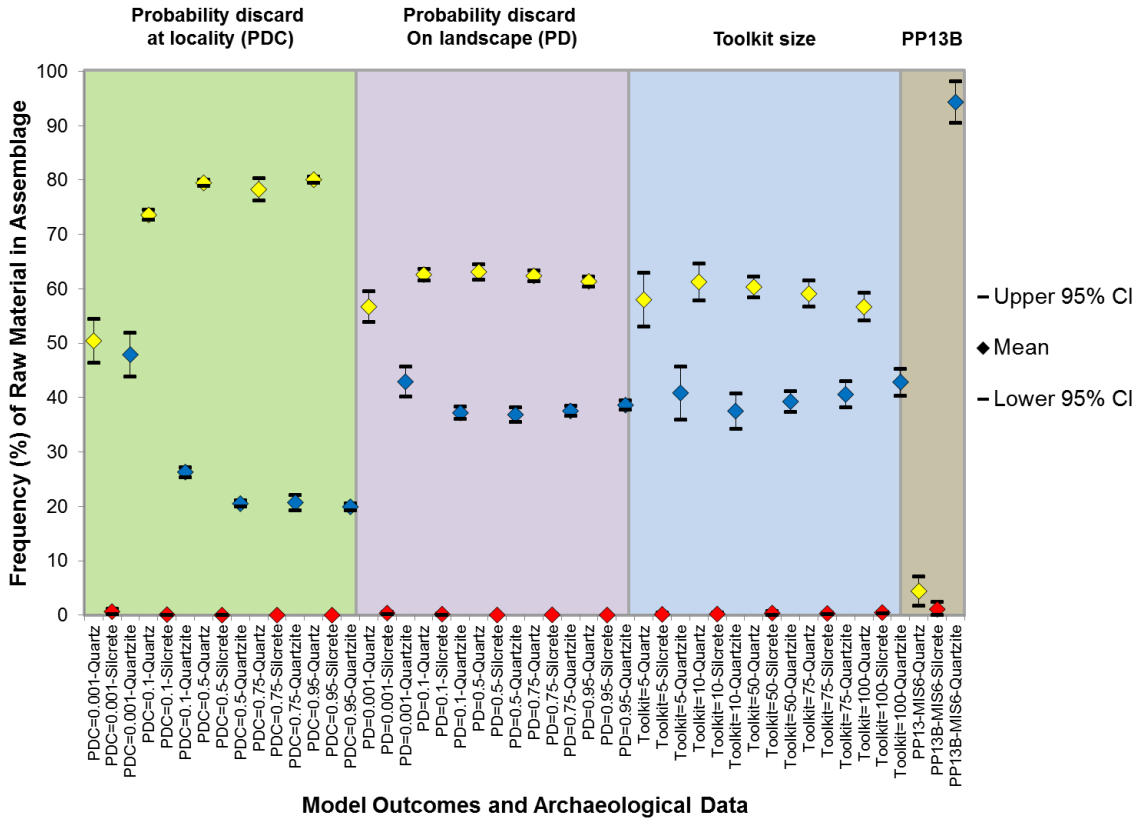

Figure A14. Comparison between model outcomes using different PDC (Probability discard on landscape), PD (Probability discard at locality), and toolkit (toolkit size) values during MIS6 model conditions without a Paleo-Agulhas plain silcrete source from same-day returns simulations (TT=100) where the agent moves to the closest locality when the movement budget (totticks) is exhausted and bootstrapped MIS6 archaeological raw material frequency data from PP13B. Plot shows the mean and the upper and lower 95% confidence intervals for the raw materials deposited at the both the simulated PP locality and at PP13B.

MIS6 with a Paleo-Agulhas plain silcrete source

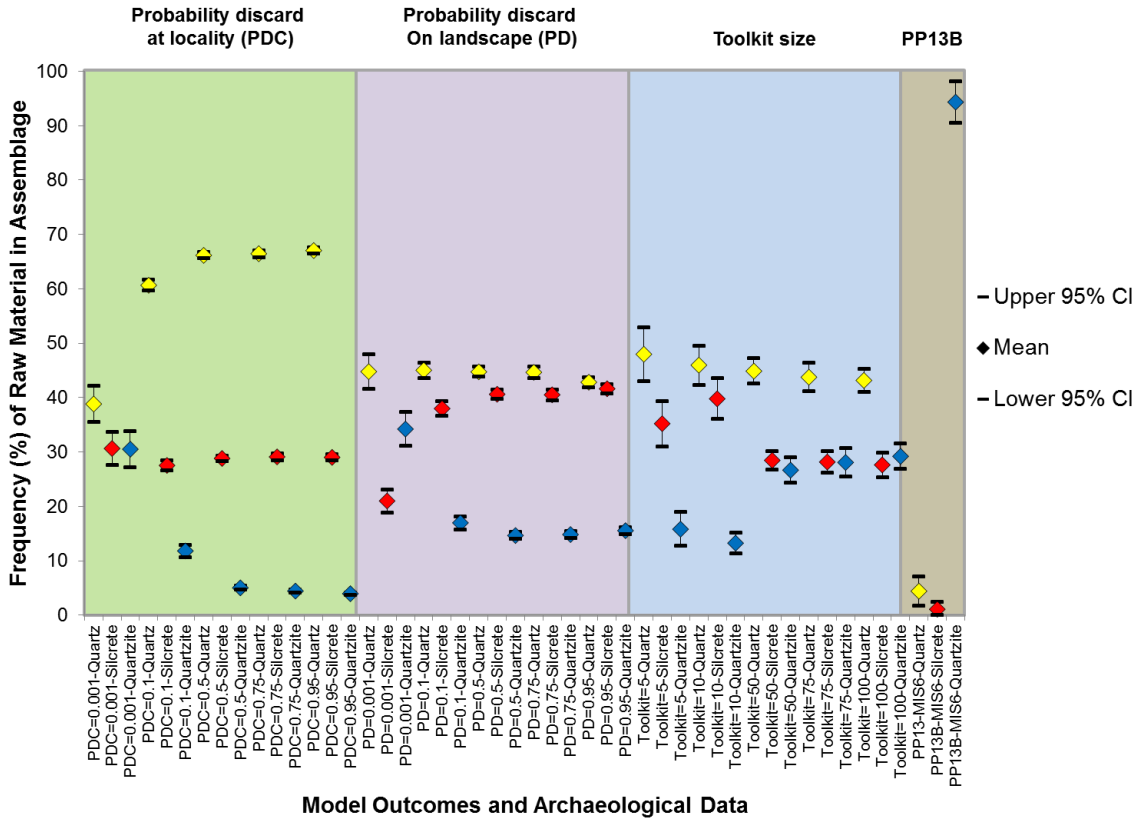

Figure A15. Comparison between OFAT3 outcomes using different PDC (Probability discard on landscape), PD (Probability discard at locality), and toolkit (toolkit size) values during MIS6 model conditions with a Paleo-Agulhas plain silcrete source from same-day returns simulations (TT=100) where the agent moves to the closest locality when the movement budget (totticks) is exhausted and bootstrapped MIS6 archaeological raw material frequency data from PP13B. Plot shows the mean and the upper and lower 95% confidence intervals for the raw materials deposited at the both the simulated PP locality and at PP13B.

CHAPTER 11: ACTIVE-CHOICE MODEL – CHANGING ASSUMED CURRENCY

Maximizing cutting edge of complete blades per mass multiplied by duration of use before dulling

ACM – Model condition variable outcomes

Coastline position and raw material source distribution

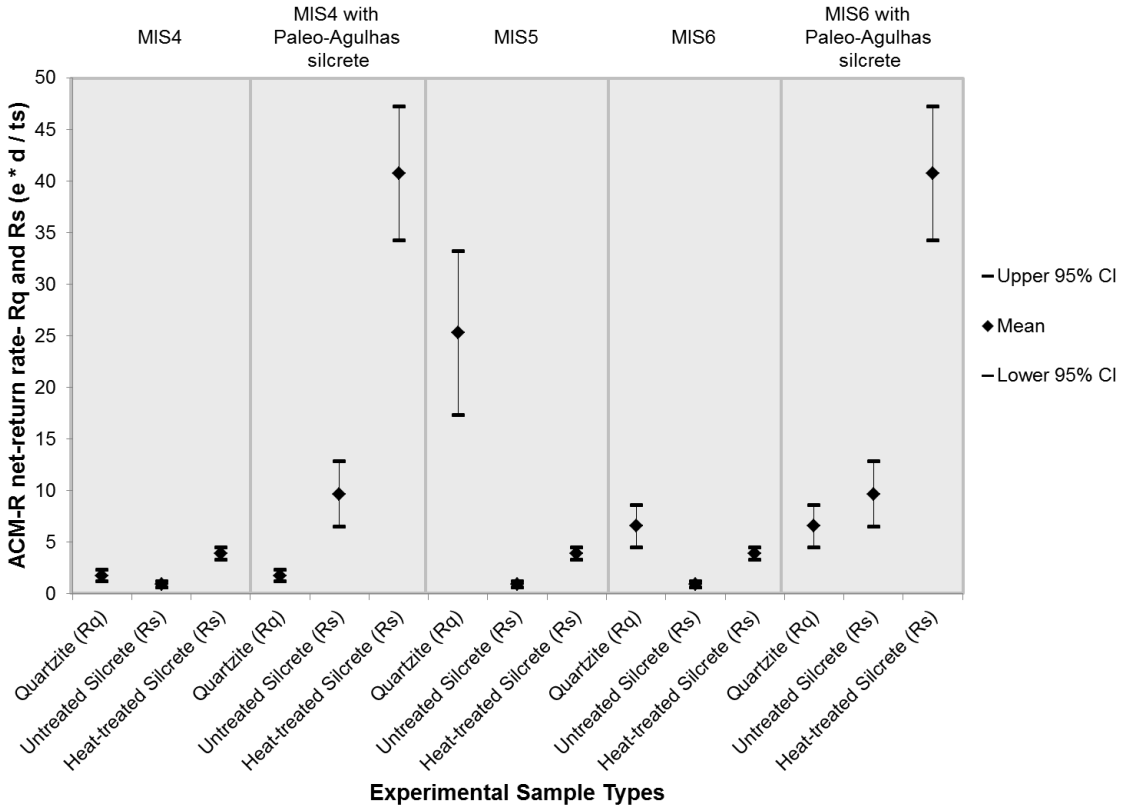

Figure A16. Plot with means and 95% confidence intervals showing the distribution of the ACM-R net-return rates (Rq and Rs) when only t_s time-cost (travel and search time) is considered (for all experimental sample types) during all model conditions. Star with capped whiskers is the mean with the 95% confidence intervals (CI). The CI was created by bootstrapping the standard error 10000 times.

Vegetation type

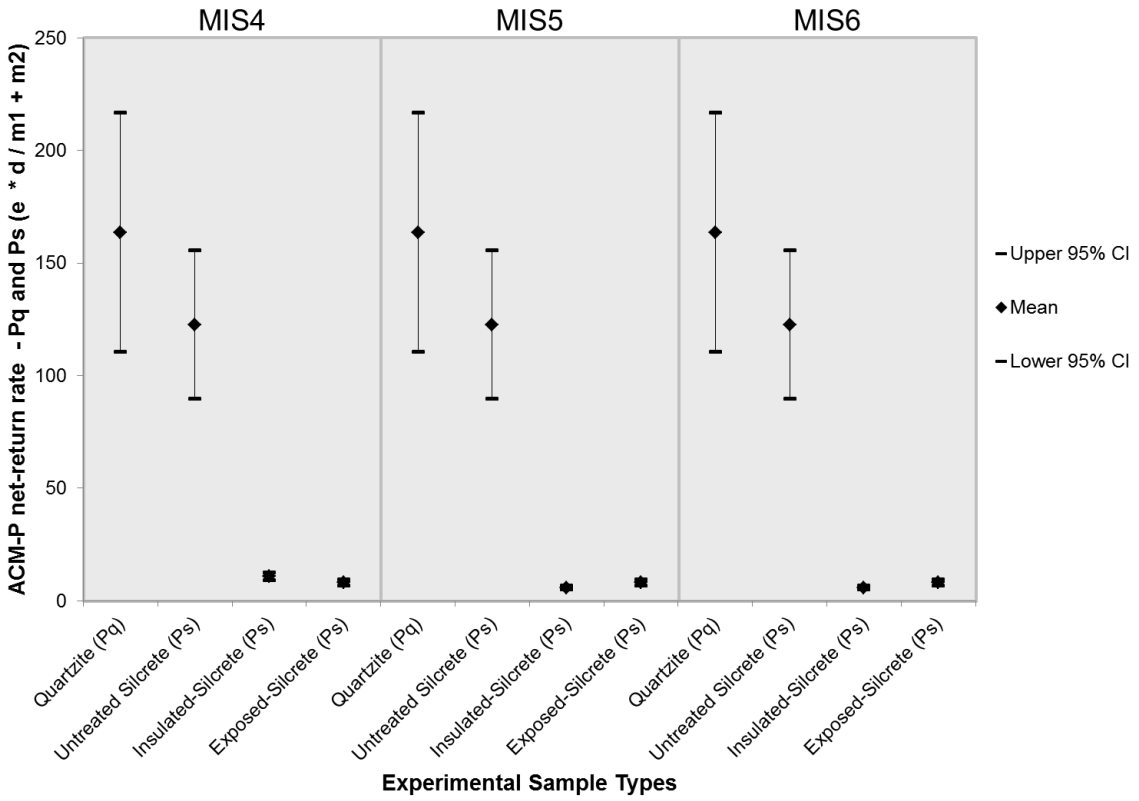

Figure A17. Plot with means and 95% confidence intervals showing the distribution of the ACM-P net-return rates (Pq and Ps) when only m_1 (wood fuel travel and search time) and m_2 time-costs (heat-treatment time) are considered (for all experimental sample types) during all model conditions. Star with capped whiskers is the mean with the 95% confidence intervals (CI). The CI was created by bootstrapping the standard error 10000 times.

Mobility rate and strategy

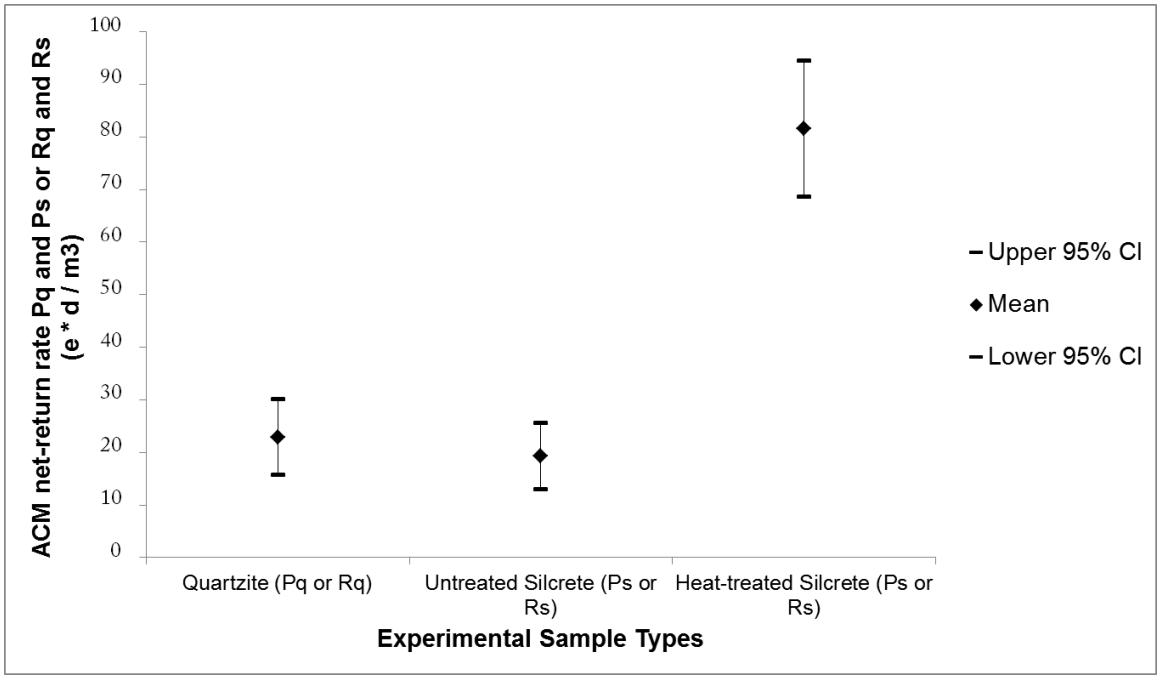

Figure A18. Plot with means and 95% confidence intervals showing the distribution of the ACM net-return rates (Pq and Ps or Rq and Rs) when only m_3 time-cost (flaking manufacturing time) is considered (for all experimental sample types) during MIS4 conditions. Star with capped whiskers is the mean with the 95% confidence intervals (CI). The CI was created by bootstrapping the standard error 10000 times.

Maximizing number of complete blades produced per core multiplied by duration of use before dulling

ACM – Model condition variable outcomes

Coastline position and raw material distribution

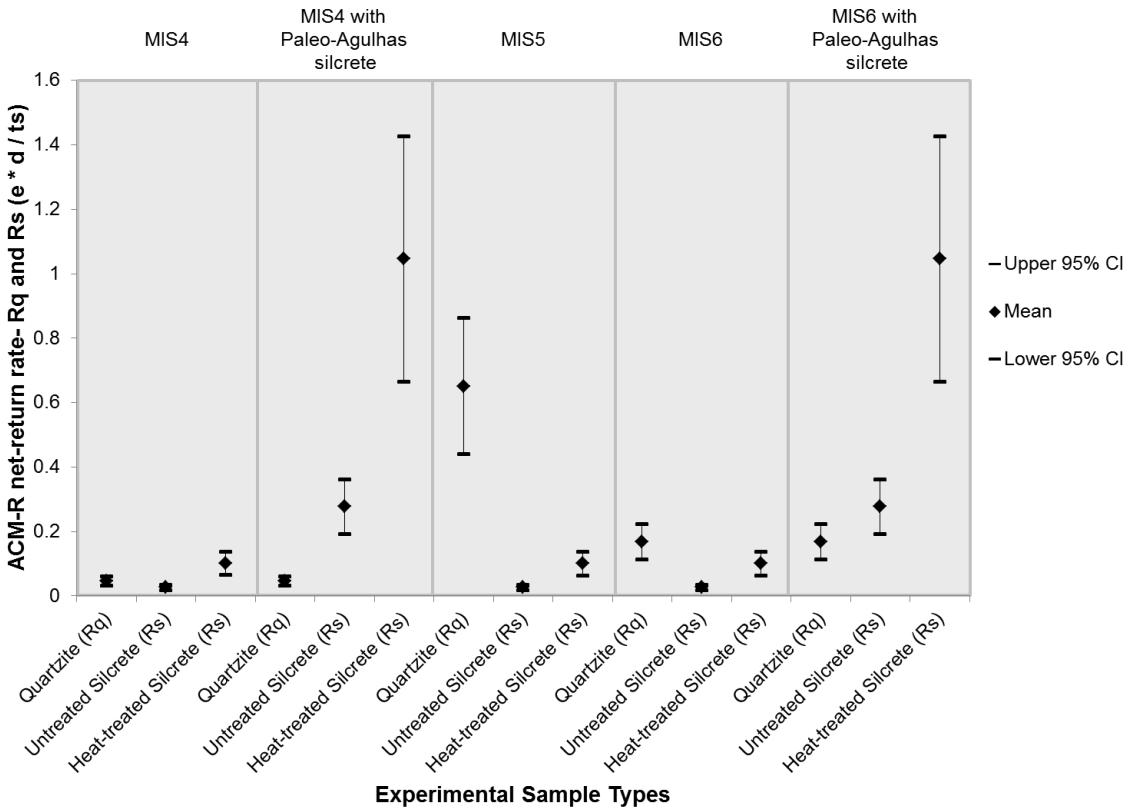

Figure A19. Plot with means and 95% confidence intervals showing the distribution of the ACM-R net-return rates (Rq and Rs) when only t_s time-cost (travel and search time) is considered (for all experimental sample types) during all model conditions. Star with capped whiskers is the mean with the 95% confidence intervals (CI). The CI was created by bootstrapping the standard error 10000 times.

Vegetation type

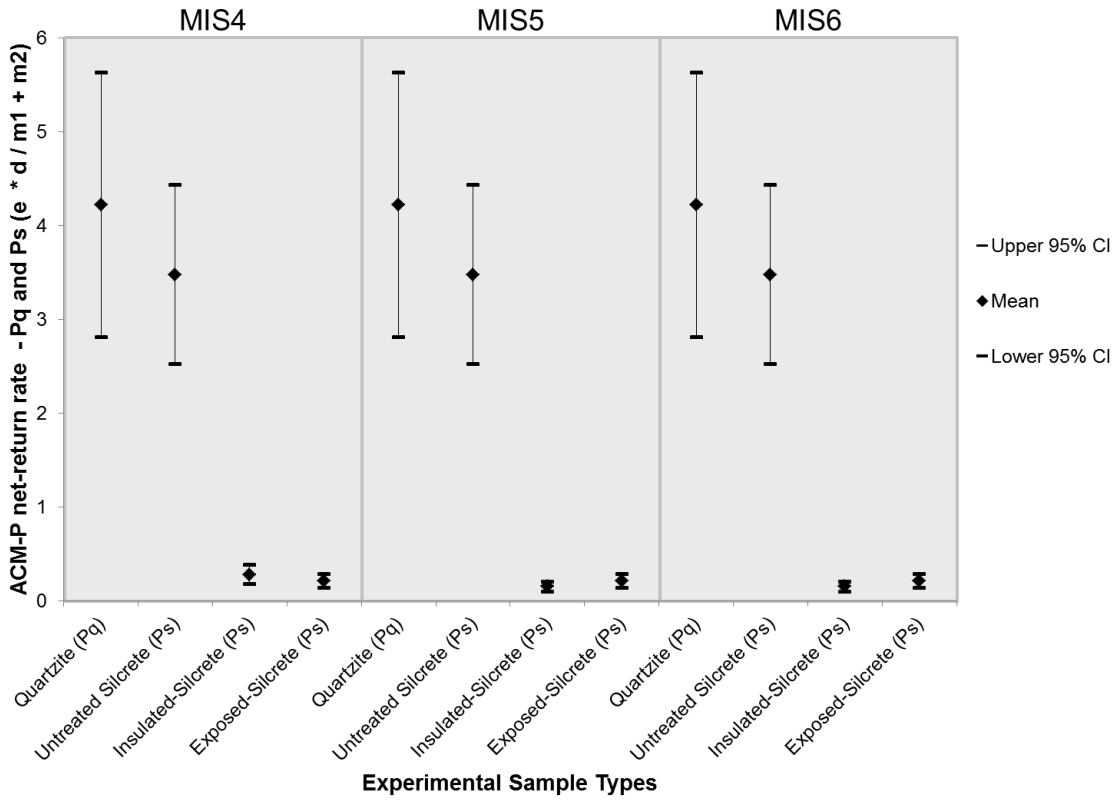

Figure A20. Plot with means and 95% confidence intervals showing the distribution of the ACM-P net-return rates (Pq and Ps) when only m_1 (wood fuel travel and search time) and m_2 time-costs (heat-treatment time) are considered (for all experimental sample types) during all model conditions. Star with capped whiskers is the mean with the 95% confidence intervals (CI). The CI was created by bootstrapping the standard error 10000 times.

Mobility rate and strategy

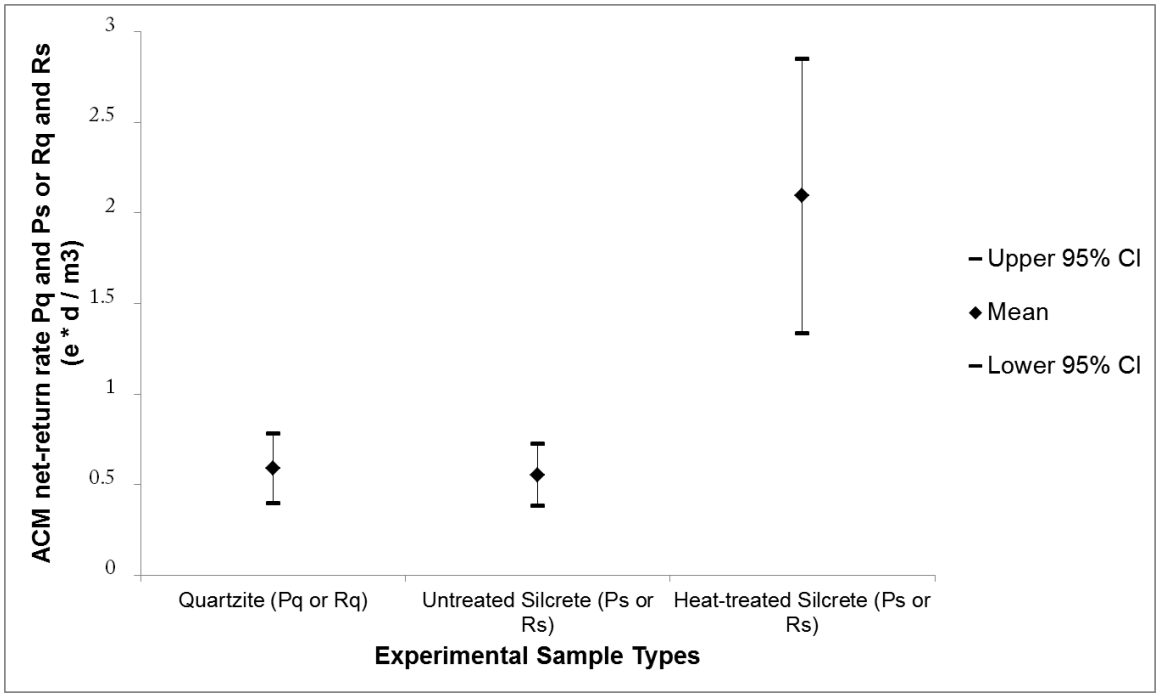

Figure A21. Plot with means and 95% confidence intervals showing the distribution of the ACM net-return rates (Pq and Ps or Rq and Rs) when only m_3 time-cost (flaking manufacturing time) is considered (for all experimental sample types) during MIS4 conditions. Star with capped whiskers is the mean with the 95% confidence intervals (CI). The CI was created by bootstrapping the standard error 10000 times.

APPENDIX B

SUPPLEMENTARY TABLES

CHAPTER 7 – PINNACLE POINT ARCHAEOLOGICAL RECORD

By Marine Isotope Stage

Maximum Dimension

Table B1. Maximum Dimension (mm) descriptive statistics for all stone artifact classes made on all raw material types by site and MIS designation.

	PP5-6-MIS3	PP5-6-MIS4	PP5-6-MIS5	PP9B-MIS5	PP9C-MIS5	PP13B-MIS5	PP13B-MIS6
N	5027	8958	3098	68	86	3684	1890
Min	2.43	1.00	2.00	10.00	9.00	3.00	5.00
Max	153.45	100.00	116.07	102.00	106.00	164.00	175.00
Mean	21.06	19.61	31.36	40.50	40.16	38.44	29.82
Std. error	0.19	0.11	0.29	2.59	2.38	0.35	0.42
Variance	190.44	115.47	262.15	455.18	487.81	439.99	326.87
Stand. dev	13.80	10.75	16.19	21.33	22.09	20.98	18.08
Median	17.32	17.00	28.00	37.00	38.50	34.00	25.00
25 prcntil	12.24	12.89	19.85	23.25	21.75	22.00	16.00
75 prcntil	25.46	24.00	39.00	55.00	54.75	52.00	39.00

Table B2. Maximum Dimension (mm) test results for all stone artifact classes made on all raw material types by site and MIS designation.

All raw materials: Maximum Dimension (mm)			**Total *n* = 22811**	**Kruskal-Wallis H: 4311**		***p* (Significant ≤0.05) <0.00001**	
Uncorrected Mann-Whitney pairwise comparisons - (*p*):							
Site/MIS Designation	PP5-6-MIS3	PP5-6-MIS4	PP5-6-MIS5	PP9B-MIS5	PP9C-MIS5	PP13B-MIS5	PP13B-MIS6
PP5-6-MIS3		0.017	<0.00001	<0.00001	<0.00001	<0.00001	<0.00001
PP5-6-MIS4	0.017		<0.00001	<0.00001	<0.00001	<0.00001	<0.00001
PP5-6-MIS5	<0.00001	<0.00001		0.0002	0.0003	<0.00001	<0.00001
PP9B-MIS5	<0.00001	<0.00001	0.0002		0.8514	0.3641	<0.00001
PP9C-MIS5	<0.00001	<0.00001	0.0003	0.8514		0.5336	0.00001
PP13B-MIS5	<0.00001	<0.00001	<0.00001	0.3641	0.5336		<0.00001
PP13B-MIS6	<0.00001	<0.00001	<0.00001	<0.00001	0.00001	<0.00001	

Values shaded in grey are significant (≤0.05).

Maximum Dimension – quartzite versus silcrete

Table B3. Maximum Dimension (mm) descriptive statistics for all stone artifact classes made on all raw material types by site and MIS designation.

	PP5-6-MIS3-Q	PP5-6-MIS3-S	PP5-6-MIS4-Q	PP5-6-MIS4-S	PP5-6-MIS5-Q	PP5-6-MIS5-S	PP9B-MIS5-Q	PP9C-MIS5-Q	PP13B-MIS5-Q	PP13B-MIS5-S	PP13B-MIS6-Q	PP13B-MIS6-S
N	2007	3121	1654	5500	2007	772	52	63	2939	108	1468	80
Min	4.24	2.43	1.00	1.00	2.00	2.59	13.00	9.00	3.00	6.00	6.00	14.00
Max	153.45	78.14	100.00	85.00	116.07	79.36	102.00	106.00	164.00	104.00	175.00	77.00
Mean	38.51	17.35	27.89	18.45	34.79	25.20	42.06	44.79	41.29	33.57	31.69	31.64
Std. error	0.47	0.16	0.36	0.12	0.38	0.44	2.99	2.72	0.39	1.67	0.49	1.55
Variance	436.30	78.15	220.02	74.12	291.99	148.26	464.76	465.84	453.52	300.45	354.52	191.15
Stand. dev	20.89	8.84	14.83	8.61	17.09	12.18	21.56	21.58	21.30	17.33	18.83	13.83
Median	38.00	15.20	24.00	17.00	31.00	22.55	39.00	43.00	38.00	32.00	26.00	27.00
25 prcntil	21.18	11.10	17.00	13.00	22.54	15.87	25.00	31.00	24.00	21.25	17.00	21.00
75 prcntil	50.34	21.28	36.00	22.35	43.73	32.53	55.75	58.00	55.00	44.25	42.00	39.75

Table B4. Maximum Dimension (mm) test results for all stone artifact classes made on quartzite (Q) and silcrete (S) by site and MIS designation.

Quartzite and Silcrete: Maximum Dimension (mm)			**Total *n* = 19771**			**Kruskal-Wallis H: 5976**			***p* (Significant ≤0.05) <0.00001**			
Uncorrected Mann-Whitney pairwise comparisons - (*p*):												
Site/MIS Designation	PP5-6-MIS3-Q	PP5-6-MIS3-S	PP5-6-MIS4-Q	PP5-6-MIS4-S	PP5-6-MIS5-Q	PP5-6-MIS5-S	PP9B-MIS5-Q	PP9C-MIS5-Q	PP13B-MIS5-Q	PP13B-MIS5-S	PP13B-MIS6-Q	PP13B-MIS6-S
PP5-6-MIS3-Q		<0.00001	<0.00001	<0.00001	<0.00001	<0.00001	0.2245	0.02	<0.00001	0.02	<0.00001	0.01
PP5-6-MIS3-S	<0.00001		<0.00001	<0.00001	<0.00001	<0.00001	<0.00001	<0.00001	<0.00001	<0.00001	<0.00001	<0.00001
PP5-6-MIS4-Q	<0.00001	<0.00001		<0.00001	<0.00001	0.0009	<0.00001	<0.00001	<0.00001	0.00017	0.00001	0.0036
PP5-6-MIS4-S	<0.00001	<0.00001	<0.00001		<0.00001	<0.00001	<0.00001	<0.00001	<0.00001	<0.00001	<0.00001	<0.00001
PP5-6-MIS5-Q	<0.00001	<0.00001	<0.00001	<0.00001		<0.00001	0.01	0.00009	<0.00001	0.4632	<0.00001	0.1272
PP5-6-MIS5-S	<0.00001	<0.00001	0.0009	<0.00001	<0.00001		<0.00001	<0.00001	<0.00001	<0.00001	<0.00001	0.00003
PP9B-MIS5-Q	0.2245	<0.00001	<0.00001	<0.00001	0.01	<0.00001		0.3821	0.7937	0.01	0.00016	0.005
PP9C-MIS5-Q	0.02061	<0.00001	<0.00001	<0.00001	0.00009	<0.00001	0.3821		0.1702	0.0006	<0.00001	0.00019
PP13B-MIS5-Q	<0.00001	<0.00001	<0.00001	<0.00001	<0.00001	<0.00001	0.7937	0.1702		0.00018	<0.00001	0.00007
PP13B-MIS5-S	0.02	<0.00001	0.0002	<0.00001	0.4632	<0.00001	0.01	0.0006	0.0002		0.06	0.5125
PP13B-MIS6-Q	<0.00001	<0.00001	0.00001	<0.00001	<0.00001	<0.00001	0.0002	<0.00001	<0.00001	0.06		0.2189
PP13B-MIS6-S	0.01	<0.00001	0.0036	<0.00001	0.1272	0.00003	0.005	0.0002	0.00007	0.5125	0.2189	

Values shaded in grey are significant (≤0.05). Q=Quartzite; S=Silcrete.

Maximum Thickness

Table B5. Maximum thickness (mm) descriptive statistics for all stone artifact classes made on all raw material types by site and MIS designation.

	PP5-6-MIS3	PP5-6-MIS4	PP5-6-MIS5	PP9B-MIS5	PP9C-MIS5	PP13B-MIS5	PP13B-MIS6
N	4866	6791	2709	68	85	2935	1683
Min	0.27	0.23	0.76	1.00	1.00	1.00	1.00
Max	38.89	59.97	40.85	31.00	51.00	59.00	60.00
Mean	4.59	4.23	7.61	9.25	8.81	9.56	7.59
Std. error	0.05	0.04	0.09	0.70	0.86	0.14	0.16
Variance	13.47	12.46	23.26	33.71	63.56	55.74	41.54
Stand. dev	3.67	3.53	4.82	5.81	7.97	7.47	6.45
Median	3.57	3.00	6.57	8.00	7.00	7.00	6.00
25 prcntil	2.23	2.00	4.10	5.00	4.50	5.00	4.00
75 prcntil	5.73	5.00	9.58	12.00	10.50	11.00	9.00

Table B6. Maximum thickness (mm) test results for all stone artifact classes made on all raw material types by site and MIS designation.

All raw materials: Maximum Thickness (mm)			**Total *n* = 19137**	**Kruskal-Wallis H: 3981**		***p* (Significant ≤0.05) <0.00001**	
Uncorrected Mann-Whitney pairwise comparisons - (*p*):							
Site/MIS Designation	PP5-6-MIS3	PP5-6-MIS4	PP5-6-MIS5	PP9B-MIS5	PP9C-MIS5	PP13B-MIS5	PP13B-MIS6
PP5-6-MIS3		<0.00001	<0.00001	<0.00001	<0.00001	<0.00001	<0.00001
PP5-6-MIS4	<0.00001		<0.00001	<0.00001	<0.00001	<0.00001	<0.00001
PP5-6-MIS5	<0.00001	<0.00001		0.01	0.4740	<0.00001	0.00001
PP9B-MIS5	<0.00001	<0.00001	0.01		0.1629	0.5720	0.0007
PP9C-MIS5	<0.00001	<0.00001	0.4740	0.1629		0.1218	0.062
PP13B-MIS5	<0.00001	<0.00001	<0.00001	0.5720	0.1218		<0.00001
PP13B-MIS6	<0.00001	<0.00001	0.00001	0.0007	0.062	<0.00001	

Values shaded in grey are significant (≤0.05).

Maximum Thickness – quartzite versus silcrete

Table B7. Maximum thickness (mm) descriptive statistics for all stone artifact classes made on quartzite (Q) and silcrete (S) by site and MIS designation.

	PP5-6-MIS3-Q	PP5-6-MIS3-S	PP5-6-MIS4-Q	PP5-6-MIS4-S	PP5-6-MIS5-Q	PP5-6-MIS5-S	PP9B-MIS5-Q	PP9C-MIS5-Q	PP13B-MIS5-Q	PP13B-MIS5-S	PP13B-MIS6-Q	PP13B-MIS6-S
N	1279	3062	1194	4097	1658	751	52	62	2372	88	1310	73
Min	0.66	0.27	0.77	0.23	1.00	0.76	1.00	2.00	1.00	1.00	1.00	2.00
Max	38.89	36.79	59.97	55.00	40.85	27.48	31.00	51.00	59.00	40.00	60.00	16.00
Mean	6.72	3.73	6.45	3.83	8.59	5.78	9.44	10.19	9.95	6.92	7.90	6.30
Std. error	0.13	0.05	0.14	0.05	0.13	0.14	0.74	1.11	0.16	0.61	0.19	0.36
Variance	21.88	7.98	23.75	9.04	26.17	13.69	28.84	76.52	59.65	33.06	46.69	9.21
Stand. dev	4.68	2.82	4.87	3.01	5.12	3.70	5.37	8.75	7.72	5.75	6.83	3.04
Median	5.46	3.00	5.00	3.00	7.47	4.90	9.00	8.00	8.00	5.50	6.00	6.00
25 prcntil	3.63	1.97	3.40	2.00	5.00	3.21	6.00	5.75	5.00	4.00	4.00	4.00
75 prcntil	8.53	4.64	8.00	4.69	10.72	7.21	12.00	12.00	12.00	8.00	9.00	8.00

Table B8. Maximum thickness (mm) test results for all stone artifact classes made on quartzite (Q) and silcrete (S) by site and MIS designation.

Quartzite and Silcrete: Maximum Thickness (mm)	**Total *n* = 15998**	**Kruskal-Wallis H: 4564**	***p* (Significant ≤0.05) <0.00001**

Uncorrected Mann-Whitney pairwise comparisons - (*p*):

Site/MIS Designation	PP5-6-MIS3-Q	PP5-6-MIS3-S	PP5-6-MIS4-Q	PP5-6-MIS4-S	PP5-6-MIS5-Q	PP5-6-MIS5-S	PP9B-MIS5-Q	PP9C-MIS5-Q	PP13B-MIS5-Q	PP13B-MIS5-S	PP13B-MIS6-Q	PP13B-MIS6-S
PP5-6-MIS3-Q		<0.00001	0.066	<0.00001	<0.00001	0.00003	0.00001	0.00001	<0.00001	0.9930	0.00029	0.6778
PP5-6-MIS3-S	<0.00001		<0.00001	0.3138	<0.00001	<0.00001	<0.00001	<0.00001	<0.00001	<0.00001	<0.00001	<0.00001
PP5-6-MIS4-Q	0.066	<0.00001		<0.00001	<0.00001	0.01	<0.00001	<0.00001	<0.00001	0.4950	<0.00001	0.2625

PP5-6-MIS4-S	<0.00001	0.3138	<0.00001		<0.00001	<0.00001	>0.00001	0.1149	0.3758	0.0025	<0.00001
PP5-6-MIS5-Q	<0.00001	<0.00001	<0.00001	<0.00001		<0.00001	>0.00001	<0.00001	<0.00001	<0.00001	<0.00001
PP5-6-MIS5-S	0.00003	<0.00001	0.01	<0.00001	<0.00001		<0.00001	<0.00001	<0.00001	<0.00001	0.082
PP9B-MIS5-Q	0.00001	<0.00001	<0.00001	<0.00001	0.1149	<0.00001		0.5798	0.5798	0.4459	0.0001
PP9C-MIS5-Q	0.00001	<0.00001	<0.00001	<0.00001	0.3758	<0.00001	0.5798		0.8651	0.8651	0.0003
PP13B-MIS5-Q	<0.00001	<0.00001	<0.00001	<0.00001	0.003	<0.00001	0.4459	0.8651		<0.00001	<0.00001
PP13B-MIS5-S	0.9930	<0.00001	0.4950	<0.00001	0.00001	0.08	0.0001	0.0003	<0.00001		0.1752
PP13B-MIS6-Q	0.00029	<0.00001	<0.00001	<0.00001	<0.00001	<0.00001	0.0007	0.001	<0.00001	0.1752	
PP13B-MIS6-S	0.6778	<0.00001	0.2625	<0.00001	0.00004	0.03	0.0001	0.0005	<0.00001	0.7273	0.3670

Values shaded in grey are significant (≤0.05). Q=Quartzite; S=Silcrete.

Technological Length

Table B9. Technological length (mm) descriptive statistics for all complete flakes and blades made on all raw materials by site and MIS designation.

	PP5-6-MIS3	PP5-6-MIS4	PP5-6-MIS5	PP9B-MIS5	PP9C-MIS5	PP13B-MIS5	PP13B-MIS6
N	886	2282	1135	24	43	1313	620
Min	1.56	1.41	2.11	11.00	6.00	5.00	5.00
Max	143.04	98.00	117.72	101.00	104.00	121.00	119.00
Mean	22.88	19.99	31.05	41.71	40.98	43.09	32.05
Std. error	0.53	0.23	0.48	4.24	3.18	0.55	0.70
Variance	250.69	121.57	258.15	431.52	435.26	393.08	307.27
Stand. dev	15.83	11.03	16.07	20.77	20.86	19.83	17.53
Median	18.40	17.00	27.00	44.00	36.00	41.00	28.00
25 prcntil	13.08	12.10	19.00	23.50	25.00	28.00	18.00
75 prcntil	27.42	25.00	40.00	57.75	53.00	56.00	43.00

Table B10. Technological length (mm) test results for all complete flakes and blades made on all raw materials by site and MIS designation.

All raw materials: Technological Length (mm)			**Total *n* = 6303**	**Kruskal-Wallis H: 1623**		***p* (Significant ≤0.05) <0.00001**	
Uncorrected Mann-Whitney pairwise comparisons - (*p*):							
Site/MIS Designation	PP5-6-MIS3	PP5-6-MIS4	PP5-6-MIS5	PP9B-MIS5	PP9C-MIS5	PP13B-MIS5	PP13B-MIS6
PP5-6-MIS3		0.0007	<0.00001	<0.00001	<0.00001	<0.00001	<0.00001
PP5-6-MIS4	0.0007		<0.00001	<0.00001	<0.00001	<0.00001	<0.00001
PP5-6-MIS5	<0.00001	<0.00001		0.007	0.0008	<0.00001	0.5557
PP9B-MIS5	<0.00001	<0.00001	0.007		0.7735	0.7726	0.015
PP9C-MIS5	<0.00001	<0.00001	0.0008	0.7735		0.3562	0.003
PP13B-MIS5	<0.00001	<0.00001	<0.00001	0.7726	0.3562		<0.00001
PP13B-MIS6	<0.00001	<0.00001	0.5557	0.015	0.003	<0.00001	

Values shaded in grey are significant (≤0.05).

Technological Length – quartzite versus silcrete

Table B11. Technological length (mm) descriptive statistics for all complete flakes and blades made on quartzite (Q) and silcrete (S) by site and MIS designation.

	PP5-6-MIS3-Q	PP5-6-MIS3-S	PP5-6-MIS4-Q	PP5-6-MIS4-S	PP5-6-MIS5-Q	PP5-6-MIS5-S	PP9B-MIS5-Q	PP9C-MIS5-Q	PP13B-MIS5-Q	PP13B-MIS5-S	PP13B-MIS6-Q	PP13B-MIS6-S
N	249	535	510	1416	742	299	24	34	1158	47	520	41
Min	5.72	1.56	5.03	1.41	7.00	2.11	11.00	6.00	5.00	12.00	5.00	9.00
Max	143.04	75.56	98.00	74.00	117.72	78.77	101.00	104.00	121.00	85.00	119.00	74.00

Mean	33.73	18.11	26.95	18.32	33.27	26.95	41.71	44.50	44.52	36.89	32.89	31.63
Std. error	1.38	0.43	0.65	0.24	0.63	0.75	4.24	3.74	0.59	2.50	0.79	2.04
Variance	473.58	97.50	216.45	78.46	294.01	168.80	431.52	475.05	402.57	292.88	328.11	170.84
Stand. dev	21.76	9.87	14.71	8.86	17.15	12.99	20.77	21.80	20.06	17.11	18.11	13.07
Median	27.86	15.98	24.00	16.69	29.00	25.32	44.00	41.00	43.00	36.00	29.00	29.00
25 prcntil	18.00	11.00	16.00	12.00	20.98	17.00	23.50	27.75	29.00	22.00	18.00	21.00
75 prcntil	42.56	22.75	35.45	23.00	42.36	35.30	57.75	57.25	58.00	50.00	44.00	40.50

Table B12. Technological length (mm) test results for all complete flakes and blades made on quartzite (Q) and silcrete (S) by site and MIS designation.

Quartzite and Silcrete: Technological Length (mm)	**Total *n* = 5575**		**Kruskal-Wallis H: 1737**			**p (Significant ≤0.05) <0.00001**					
Uncorrected Mann-Whitney pairwise comparisons - (p):											
Site/MIS Designation	PP5-6-MIS3-Q	PP5-6-MIS3-S	PP5-6-MIS4-Q	PP5-6-MIS4-S	PP5-6-MIS5-Q	PP5-6-MIS5-S	PP9B-MIS5-Q	PP9C-MIS5-Q	PP13B-MIS5-Q	PP13B-MIS5-S	PP13B-MIS6-Q	PP13B-MIS6-S
PP5-6-MIS3-Q		<0.00001	0.00019	<0.00001	0.2963	0.004	0.03	0.001	<0.00001	0.063	0.7772	0.6331
PP5-6-MIS3-S	<0.00001		<0.00001	0.1806	<0.00001	<0.00001	<0.00001	<0.00001	<0.00001	<0.00001	<0.00001	<0.00001
PP5-6-MIS4-Q	0.00019	<0.00001		<0.00001	<0.00001	0.4877	0.0002	<0.00001	<0.00001	0.00004	<0.00001	0.01
PP5-6-MIS4-S	<0.00001	0.1806	<0.00001		<0.00001	<0.00001	<0.00001	<0.00001	<0.00001	<0.00001	<0.00001	<0.00001
PP5-6-MIS5-Q	0.2963	<0.00001	<0.00001	<0.00001		<0.00001	0.036	0.001	<0.00001	0.1107	0.3933	0.9859
PP5-6-MIS5-S	0.004	<0.00001	0.4877	<0.00001	<0.00001		0.00027	<0.00001	<0.00001	0.0001	0.00005	0.02

PP9B-MIS5-Q	0.03	<0.00001	0.0002	<0.00001	0.036	0.00027		0.7283	0.5246	0.2956	0.027	0.03
PP9C-MIS5-Q	0.001	<0.00001	<0.00001	<0.00001	0.001	<0.00001	0.7283		0.8540	0.1316	0.001	0.007
PP13B-MIS5-Q	<0.00001	<0.00001	<0.00001	<0.00001	<0.00001	<0.00001	0.5246	0.8540		0.009	<0.00001	0.00002
PP13B-MIS5-S	0.063	<0.00001	0.00004	<0.00001	0.1107	0.0001	0.2956	0.1316	0.009		0.08	0.1847
PP13B-MIS6-Q	0.7772	<0.00001	<0.00001	<0.00001	0.3933	0.00005	0.027	0.001	<0.00001	0.08		0.8692
PP13B-MIS6-S	0.6331	<0.00001	0.01	<0.00001	0.9859	0.02	0.03	0.007	0.00002	0.1847	0.8692	

Values shaded in grey are significant (≤0.05). Q=Quartzite; S=Silcrete.

Technological Width

Table B13. Technological width (mm) descriptive statistics for all complete flakes and blades made on all raw materials by site and MIS designation.

	PP5-6-MIS3	PP5-6-MIS4	PP5-6-MIS5	PP9B-MIS5	PP9C-MIS5	PP13B-MIS5	PP13B-MIS6
N	887	2281	1138	25	43	1328	632
Min	3.10	1.53	4.07	11.00	12.00	6.00	3.00
Max	81.94	74.71	80.00	117.00	62.00	104.00	83.00
Mean	17.19	14.75	24.42	33.84	30.23	32.07	26.99
Std. error	0.35	0.18	0.34	4.52	1.57	0.39	0.56
Variance	106.45	72.67	135.09	510.22	105.99	198.18	195.25
Stand. dev	10.32	8.52	11.62	22.59	10.30	14.08	13.97
Median	14.46	12.13	22.19	28	29	30	25
25 prcntil	10.25	9.00	16.00	24.00	23.00	22.00	16.25
75 prcntil	21.01	18.00	30.00	34.00	35.00	40.00	35.00

Table B14. Technological width (mm) test results for all complete flakes and blades made on all raw materials by site and MIS designation.

All raw materials: Technological Width (mm)			**Total *n* = 6334**	**Kruskal-Wallis H: 2023**		***p* (Significant ≤0.05) <0.00001**	
Uncorrected Mann-Whitney pairwise comparisons - (*p*):							
Site/MIS Designation	PP5-6-MIS3	PP5-6-MIS4	PP5-6-MIS5	PP9B-MIS5	PP9C-MIS5	PP13B-MIS5	PP13B-MIS6
PP5-6-MIS3		<0.00001	<0.00001	<0.00001	<0.00001	<0.00001	<0.00001
PP5-6-MIS4	<0.00001		<0.00001	<0.00001	<0.00001	<0.00001	<0.00001
PP5-6-MIS5	<0.00001	<0.00001		0.007	0.00008	<0.00001	0.0007
PP9B-MIS5	<0.00001	<0.00001	0.007		0.8635	0.6631	0.1081
PP9C-MIS5	<0.00001	<0.00001	0.00008	0.8635		0.5793	0.02
PP13B-MIS5	<0.00001	<0.00001	<0.00001	0.6631	0.5793		<0.00001
PP13B-MIS6	<0.00001	<0.00001	0.0007	0.1081	0.02	<0.00001	

Values shaded in grey are significant (≤0.05).

Technological Width – quartzite versus silcrete

Table B15. Technological width (mm) descriptive statistics for all complete flakes and blades made on quartzite (Q) and silcrete (S) by site and MIS designation.

	PP5-6-MIS3-Q	**PP5-6-MIS3-S**	**PP5-6-MIS4-Q**	**PP5-6-MIS4-S**	**PP5-6-MIS5-Q**	**PP5-6-MIS5-S**	**PP9B-MIS5-Q**	**PP9C-MIS5-Q**	**PP13B-MIS5-Q**	**PP13B-MIS5-S**	**PP13B-MIS6-Q**	**PP13B-MIS6-S**
N	249	536	509	1415	744	300	25	34	1172	47	530	42
Min	4.0	3.1	5.0	1.5	5.0	4.1	11.0	16.0	6.0	10.0	3.0	8.0
Max	81.9	53.0	74.7	63.0	80.0	47.5	117.0	62.0	98.0	104.0	83.0	57.0
Mean	24.3	14.0	22.3	12.5	27.0	18.6	33.8	32.2	32.9	26.9	27.6	26.4
Std. error	0.841	0.308	0.486	0.163	0.448	0.441	4.518	1.741	0.413	2.360	0.622	1.665
Variance	176.1	50.8	120.2	37.5	149.1	58.3	510.2	103.0	200.2	261.7	205.1	116.4
Stand. dev	13.3	7.1	11.0	6.1	12.2	7.6	22.6	10.1	14.1	16.2	14.3	10.8
Median	22.0	12.2	20.0	11.0	24.8	17.3	28.0	30.5	31.0	23.0	25.0	25.0
25 prcntil	15.1	9.3	14.0	8.4	18.0	13.1	24.0	26.0	23.0	16.0	17.0	18.5
75 prcntil	28.6	17.0	28.0	15.0	34.0	22.8	34.0	37.0	41.0	32.0	35.0	33.3

Table B16. Technological width (mm) test results for all complete flakes and blades made on quartzite (Q) and silcrete (S) by site and MIS designation.

Quartzite and Silcrete: Technological width (mm)					Total *n* = 5603		Kruskal-Wallis H: 2334			*p* (Significant ≤0.05) <0.00001		
Uncorrected Mann-Whitney pairwise comparisons - (*p*):												
Site/MIS Designation	PP5-6-MIS3-Q	PP5-6-MIS3-S	PP5-6-MIS4-Q	PP5-6-MIS4-S	PP5-6-MIS5-Q	PP5-6-MIS5-S	PP9B-MIS5-Q	PP9C-MIS5-Q	PP13B-MIS5-Q	PP13B-MIS5-S	PP13B-MIS6-Q	PP13B-MIS6-S
PP5-6-MIS3-Q		<0.00001	0.1444	<0.00001	0.00009	<0.00001	0.0035	0.00001	<0.00001	0.2812	0.0007	0.08
PP5-6-MIS3-S	<0.00001		<0.00001	0.00001	<0.00001	<0.00001	<0.00001	<0.00001	<0.00001	<0.00001	<0.00001	<0.00001
PP5-6-MIS4-Q	0.1444	<0.00001		<0.00001	<0.00001	0.00001	0.00049	<0.00001	<0.00001	0.058	<0.00001	0.009
PP5-6-MIS4-S	<0.00001	0.00001	<0.00001		<0.00001	<0.00001	<0.00001	<0.00001	<0.00001	<0.00001	<0.00001	<0.00001
PP5-6-MIS5-Q	0.00009	<0.00001	<0.00001	<0.00001		<0.00001	0.1049	0.0017	<0.00001	0.3894	0.9598	0.9738
PP5-6-MIS5-S	<0.00001	<0.00001	0.00001	<0.00001	<0.00001		<0.00001	<0.00001	<0.00001	0.00009	<0.00001	<0.00001
PP9B-MIS5-Q	0.004	<0.00001	0.00049	<0.00001	0.1049	<0.00001		0.3690	0.4439	0.06924	0.1642	0.1611
PP9C-MIS5-Q	0.00001	<0.00001	<0.00001	<0.00001	0.002	<0.00001	0.3690		0.9900	0.0038	0.007	0.008

PP13B-MIS5-Q	<0.00001	<0.00001	<0.00001	<0.00001	<0.00001	<0.00001	0.4439	0.9900		0.0003	<0.00001	0.002
PP13B-MIS5-S	0.2812	<0.00001	0.058	<0.00001	0.3894	0.00009	0.07	0.0038	0.0003		0.5221	0.5593
PP13B-MIS6-Q	0.00073	<0.00001	<0.00001	<0.00001	0.9598	<0.00001	0.1642	0.007	<0.00001	0.5221		0.9590
PP13B-MIS6-S	0.08	<0.00001	0.009	<0.00001	0.9738	<0.00001	0.16110	0.008	0.002	0.5593	0.9590	

Values shaded in grey are significant (≤0.05). Q=Quartzite; S=Silcrete.

Cutting edge per mass

Table B17. Cutting edge / Mass (CE/M) test results for all raw materials by site and MIS designation.

All raw materials: Cutting Edge / Mass values			**Total *n* = 6261**	**Kruskal-Wallis H: 1801**		***p* (Significant ≤0.05) <0.00001**	
Uncorrected Mann-Whitney pairwise comparisons - (*p*):							
Site/MIS Designation	PP5-6-MIS3	PP5-6-MIS4	PP5-6-MIS5	PP9B-MIS5	PP9C-MIS5	PP13B-MIS5	PP13B-MIS6
PP5-6-MIS3		<0.00001	<0.00001	<0.00001	<0.00001	<0.00001	<0.00001
PP5-6-MIS4	<0.00001		<0.00001	<0.00001	<0.00001	<0.00001	<0.00001
PP5-6-MIS5	<0.00001	<0.00001		0.08	0.007	<0.00001	0.8635
PP9B-MIS5	<0.00001	<0.00001	0.08		0.9063	0.8355	0.1184
PP9C-MIS5	<0.00001	<0.00001	0.007	0.9063		0.7435	0.02
PP13B-MIS5	<0.00001	<0.00001	<0.00001	0.8355	0.7435		<0.00001
PP13B-MIS6	<0.00001	<0.00001	0.8635	0.1184	0.02	<0.00001	

Values shaded in grey are significant (≤0.05).

Cutting edge per mass – quartzite versus silcrete

Table B18. Cutting edge / Mass (CE/M) test results for quartzite and silcrete by site and MIS designation.

Quartzite and Silcrete: Cutting Edge / Mass values					**Total *n* = 5540**		**Kruskal-Wallis H: 2186**			***p* (Significant ≤0.05) <0.00001**		
Uncorrected Mann-Whitney pairwise comparisons - (*p*):												
Site/MIS Designation	PP5-6-MIS3-Q	PP5-6-MIS3-S	PP5-6-MIS4-Q	PP5-6-MIS4-S	PP5-6-MIS5-Q	PP5-6-MIS5-S	PP9B-MIS5-Q	PP9C-MIS5-Q	PP13B-MIS5-Q	PP13B-MIS5-S	PP13B-MIS6-Q	PP13B-MIS6-S
PP5-6-MIS3-Q		<0.00001	0.018	<0.00001	0.00011	<0.00001	0.07	0.0010	<0.00001	0.9238	0.2190	0.8329
PP5-6-MIS3-S	<0.00001		<0.00001	0.1247	<0.00001	<0.00001	<0.00001	<0.00001	<0.00001	<0.00001	<0.00001	<0.00001
PP5-6-MIS4-Q	0.018	<0.00001		<0.00001	<0.00001	0.0006	0.007	0.00001	<0.00001	0.2392	0.00001	0.3032
PP5-6-MIS4-S	<0.00001	0.1247	<0.00001		<0.00001	<0.00001	0.00000	<0.00001	<0.00001	<0.00001	<0.00001	<0.00001
PP5-6-MIS5-Q	0.0001	<0.00001	<0.00001	<0.00001		<0.00001	0.4719	0.06	<0.00001	0.035	0.0029	0.03
PP5-6-MIS5-S	<0.00001	<0.00001	0.0006	<0.00001	<0.00001		0.00006	<0.00001	<0.00001	0.003	<0.00001	0.007
PP9B-MIS5-Q	0.07	<0.00001	0.007	<0.00001	0.4719	0.00006		0.6471	0.6033	0.07	0.1719	0.07
PP9C-MIS5-Q	0.00098	<0.00001	0.00001	<0.00001	0.059	<0.00001	0.6471		0.8874	0.003	0.01	0.003

PP13B-MIS5-Q	<0.00001	<0.00001	<0.00001	<0.00001	<0.00001	<0.00001	0.6033	0.8874		0.0002	<0.00001	0.0002
PP13B-MIS5-S	0.9238	<0.00001	0.2392	<0.00001	0.035	0.003	0.07	0.003	0.0002		0.4500	0.9068
PP13B-MIS6-Q	0.2190	<0.00001	0.00001	<0.00001	0.0029	<0.00001	0.1719	0.01	<0.00001	0.4500		0.3676
PP13B-MIS6-S	0.8329	<0.00001	0.3032	<0.00001	0.03	0.007	0.07	0.003	0.0002	0.9068	0.3676	

Values shaded in grey are significant (≤0.05). Q=Quartzite; S=Silcrete.

By Stratigraphic Aggregate/Unit

Raw Material Type

PP13B

Table B19. Count of raw material type at PP13B by stratigraphic aggregate.

Stratigraphic Aggregate/Unit	Other (n=)	Chert or Chalcedony (n=)	Quartz (n=)	Silcrete (n=)	Quartzite (n=)	Total (n=)
LB Sand 1	3	1	43	22	287	356
DB Sand 2	3	0	22	3	221	249
LB Sand 2	1	0	9	5	42	57
DB Sand 3	13	3	96	13	549	674
Shelly Brown Sand	0	1	30	3	165	199
Roof Spall-Upper	7	2	88	21	846	964
Roof Spall-Lower	4	0	59	7	233	303
LBG Sand 1	2	1	37	5	419	464
LC-MSA Upper	1	1	2	9	46	59
LC-MSA Middle	0	2	20	20	142	184
DB Sand 4a	0	0	2	0	34	36
LBG Sand 2	2	1	10	0	73	86
DB Sand 4b	0	1	6	3	37	47
DB Sand 4c	0	0	2	0	20	22
LC-MSA Lower	12	4	226	74	1206	1522
LB Silt-G	0	0	0	0	16	16
LB Silt	2	0	7	1	81	91

Total (n=)	50	17	659	186	4417	5329

PP9B and PP9C

Table B20. Count of raw material type at PP9B and PP9C.

Cave site	Other (n=)	Chert or Chalcedony (n=)	Quartz (n=)	Silcrete (n=)	Quartzite (n=)	Total (n=)
PP9B	1	0	15	0	52	68
PP9C	0	0	19	4	63	86
Total (n=)	1	0	34	4	115	154

PP5-6

Table B21. Count of raw material type at PP5-6 by stratigraphic aggregate.

Stratigraphic Aggregate	Other	Chert or Chalcedony	Quartz	Silcrete	Quartzite	Total
RBSR	18	67	26	259	182	552
NWR	1	4	10	111	149	275
BBCSR/BAS	100	99	165	2015	930	3309
OBS2	11	200	379	473	131	1194
SGS	5	31	37	198	68	339
OBS1	5	60	318	190	152	725
SADBS Upper	19	102	136	2990	536	3783
SADBS Lower	5	12	12	131	134	294
ALBS	5	6	2	49	254	316
LBSR	45	49	164	628	1925	2811
YBSR	38	19	4	143	76	280
Total (n=)	252	649	1253	7187	4537	13878

PP5-6 sub-aggregate raw material frequencies

Table B22. Count of raw material type at PP5-6 by MIS5 sub-aggregates.

Stratigraphic Aggregate	Sub-aggregate	Other (n=)	Chert or Chalcedony (n=)	Quartz (n=)	Silcrete (n=)	Quartzite (n=)	Total (n=)
LBSR	Jed 2	8	11	3	20	1028	1070
LBSR	Jed 1	0	2	3	5	112	122
LBSR	Ludumo Red	6	0	1	12	131	150
LBSR	Ludumo Sand and Roofspall	1	0	1	1	19	22
LBSR	Martin Red	0	0	0	0	13	13
LBSR	Hope Red	4	0	0	19	5	28
LBSR	Lwando Shell	3	0	0	2	61	66
LBSR	Aaron Sand and Roofspall	2	1	0	7	23	33
LBSR	Kyle Shell	0	0	0	105	17	122
LBSR	Adrian Sand and Roofspall	2	0	1	15	9	27
LBSR	Adrian Shell	1	1	4	3	28	37

LBSR	Leba Shell	2	5	14	5	74	100
LBSR	Cobus Shell	0	0	3	1	6	10
LBSR	Luke Sand and Roofspall	0	0	0	1	45	46
LBSR	Luke Shell	3	0	6	3	71	83
LBSR	Sondra Sand and Roofspall	3	0	0	40	24	67
LBSR	Sondra Red	0	2	5	68	32	107
LBSR	Logan Sand and Roofspall 1	1	2	10	41	20	74
LBSR	Logan Sand and Roofspall 2	0	0	3	73	6	82
LBSR	Logan Red	1	9	36	23	45	114
LBSR	Arnold Sand and Roofspall	0	1	1	0	19	21
LBSR	Arnold Red	2	0	27	1	19	49
LBSR	Simen Sand and Roofspall	1	0	11	3	7	22
LBSR	Simen Red	0	1	12	31	26	70
LBSR	Tove Sand and Roofspall	0	2	6	46	8	62
LBSR	Tove Red	4	10	7	94	60	175
YBSR	Lee	0	0	0	6	8	14
YBSR	Meghan Sand and Roofspall	3	0	0	5	9	17
YBSR	Elizabeth Sand and Roofspall	17	6	2	99	25	149
YBSR	Bryant	7	9	1	12	23	52
YBSR	Kirsty	11	3	1	16	7	38
Total (n=)		82	65	158	757	1980	3042

Table B23. Count of raw material type at PP5-6 by MIS4 sub-aggregates.

Stratigraphic Aggregate	Sub-aggregate	Other (n=)	Chert or Chalcedony (n=)	Quartz (n=)	Silcrete (n=)	Quartzite (n=)	Total (n=)
OBS2	Emma Sand (n=53)	0	6	9	31	7	53
OBS2	Andy (n=135)	0	17	89	17	12	135
OBS2	Elizabeth (n=97)	1	19	24	35	18	97
OBS2	Kevin Sand (n=47)	0	47	0	0	0	47
OBS2	Sarah (n=488)	5	104	215	104	60	488
OBS2	Hans (n=219)	3	2	10	194	10	219
OBS2	Chantal (n=20)	0	0	2	18	0	20
OBS2	Alicen (=99)	1	4	12	67	15	99
OBS2	Josh (n=33)	1	0	17	6	9	33
SGS	Zuri Upper (n=37)	2	3	6	11	15	37
SGS	Zuri Lower (n=68)	0	5	1	53	9	68
SGS	Jinga Upper (n=56)	1	9	8	24	14	56
SGS	Jinga Middle (n=40)	1	1	4	28	6	40
SGS	Jinga Lower Dark 3 (n=120)	1	8	15	76	20	120
SGS	Jinga Lower Dark 2 (n=16)	0	5	2	5	4	16
OBS1	Lizelle 2 (n=35)	2	2	10	6	15	35
OBS1	Lizelle 1 (n=20)	0	4	7	3	6	20
OBS1	Orfer (n=114)	0	15	38	20	41	114

OBS1	Chris (n=55)	1	11	14	12	17	55
OBS1	Celeste (n=87)	1	5	35	4	42	87
OBS1	Sasha (n=33)	1	1	22	8	1	33
OBS1	Spencer (n=301)	0	16	172	86	27	301
OBS1	Joanne 1 (n=77)	0	6	18	51	2	77
SADBS Upper	Joanne (n=372)	2	15	39	254	62	372
SADBS Upper	Bettina (n=339)	4	22	17	260	36	339
SADBS Upper	House (n=92)	0	2	17	53	20	92
SADBS Upper	Kim (n=58)	0	1	5	46	6	58
SADBS Upper	Enrico (n=161)	1	11	10	120	19	161
SADBS Upper	Gert (n=717)	6	22	26	562	101	717
SADBS Upper	Holly (n=193)	0	3	4	139	47	193
SADBS Upper	Sydney (n=1492)	6	26	14	1224	222	1492
SADBS Upper	Thandesizwe (n=356)	0	0	4	331	21	356
SADBS Lower	Erich (n=79)	1	0	0	58	20	79
SADBS Lower	Jocelyn (n=215)	4	12	12	73	114	215
ALBS	Conrad Sand (n=19)	1	3	0	13	2	19
ALBS	Conrad Shell (n=54)	1	2	1	22	28	54
ALBS	Conrad Cobble and Sand (n=243)	3	1	1	14	224	243
Total (n=)		50	410	880	4028	1272	6640

Table B24. Raw material type tallied by artifact mass (kg) for PP5-6 DBCS sub-aggregates.

Sub-aggregate	Other (kg)	Chert or Chalcedony (kg)	Quartz (kg)	Silcrete (kg)	Quartzite (kg)	Total (kg)
Ollie	0.000	0.004	0.000	0.066	0.015	0.085
Leonides	0.000	0.002	0.001	0.010	0.001	0.013
Miller	0.040	0.121	0.031	1.087	1.683	2.962
Colleen	0.000	0.002	0.001	0.011	0.012	0.025
Sorel	0.011	0.023	0.005	0.366	0.246	0.652
Coco	0.002	0.044	0.007	0.195	0.258	0.507
Sam	0.002	0.008	0.026	0.029	0.046	0.110
Quinn Upper	0.018	0.019	0.004	0.104	0.225	0.371
Quinn Lower B	0.017	0.054	0.017	0.061	0.316	0.465
Total (kg)	0.090	0.275	0.092	1.931	2.802	5.191

Table B25. Count of raw material type for PP5-6 DBCS sub-aggregates.

Sub-aggregate	Other (n=)	Chert or Chalcedony (n=)	Quartz (n=)	Silcrete (n=)	Quartzite (n=)	Total (n=)
Ollie	0	8	0	89	4	101
Leonides	0	2	2	14	1	19
Miller	18	105	37	791	168	1119
Colleen	0	1	2	18	4	25
Sorel	7	28	11	241	78	365

Coco	2	40	14	154	37	247
Sam	1	23	31	26	8	89
Quinn Upper	7	33	8	85	35	168
Quinn Lower B	7	56	16	60	44	183
Total (n=)	42	296	121	1478	379	2316

Table B26. Count of raw material type at PP5-6 by MIS3 sub-aggregates.

Stratigraphic Aggregate	Sub-aggregate	Other (n=)	Chert or Chalcedony (n=)	Quartz (n=)	Silcrete (n=)	Quartzite (n=)	Total (n=)
RBSR	Denise	0	0	4	2	20	26
RBSR	Takis	18	67	22	256	162	523
NWR	Dark Brown Silty Sand	0	1	3	84	119	207
NWR	Compact Brown and Red Sand	1	1	5	23	27	57
NWR	Coarse Grained Dark Brown Sand	0	2	2	4	3	11
BBCSR/BAS	Ellis	52	6	12	1258	539	1867
BBCSR/BAS	Nkosi	5	2	8	32	131	178
BBCSR/BAS	Sydwell	2	0	4	29	73	108
BBCSR/BAS	Emily	19	35	95	278	94	521
BBCSR/BAS	James	1	1	13	9	12	36
BBCSR/BAS	Zenobia	21	55	33	409	81	599
Total (n=)		119	170	201	2384	1261	4133

Technological length

PP13B

Table B27. Technological length (mm) descriptive statistics for all complete flakes and blades made on all raw materials at PP13B by stratigraphic aggregate.

	LB Sand 1	DB Sand 2	LB Sand 2	DB Sand 3	Shelly Brown Sand	Roof Spall-Upper	Roof Spall-Lower	LBG Sand 1	LC-MSA Upper	LC-MSA Middle	LBG Sand 2	DB Sand 4b	LC-MSA Lower	LB Silt
N	154	119	31	301	53	346	73	146	27	64	25	20	535	20

Min	Max	Mean	Std. error	Variance	Stand. dev	Median	25 prcntil	75 prcntil
10	96	39.75	4.346732	377.8816	19.43918	42.5	25.25	48.75
5.0	119.0	30.8	0.7	297.9	17.3	27.0	17.0	41.0
12.0	68.0	41.6	3.521	247.9	15.7	42.5	29.5	52.5
15.0	83.0	38.4	3.362	282.6	16.8	36.0	25.0	50.5
8.0	88.0	42.0	2.419	374.6	19.4	37.5	30.3	57.0
9.0	105.0	33.2	4.586	567.9	23.8	24.0	17.0	52.0
6.0	92.0	45.7	1.661	402.7	20.1	44.0	29.8	59.3
9.0	98.0	46.5	2.618	500.2	22.4	47.0	28.0	63.5
5.0	101.0	40.3	1.049	380.6	19.5	38.0	24.0	53.0
7.0	84.0	37.4	2.745	399.2	20.0	35.0	21.5	51.5
5.0	104.0	44.3	1.123	379.6	19.5	42.0	29.0	57.5
15.0	85.0	45.9	3.672	418.0	20.4	40.0	30.0	53.0
11.0	121.0	45.9	1.710	348.0	18.7	47.0	31.0	56.0
10.0	96.0	44.7	1.515	353.3	18.8	43.0	30.0	56.0

Table B28. Technological length (mm) test results for all complete flakes and blades made on all raw materials at PP13B by stratigraphic aggregate.

All raw materials: Technological Length (mm)						**Total *n* = 1914**		**Kruskal-Wallis H: 199**			**p (Significant ≤0.05) <0.00001**			
Uncorrected Mann-Whitney pairwise comparisons - (*p*):														
Stratigraphic aggregate	LB Sand 1	DB Sand 2	LB Sand 2	DB Sand 3	Shelly Brown Sand	Roof-Spall Upper	Roof Spall Lower	LBG Sand 1	LC-MSA Upper	LC-MSA Middle	LBG Sand 2	DB Sand 4b	LC-MSA Lower	LB Silt
LB Sand 1		0.5211	0.9809	0.7331	0.01	0.009	0.5975	0.7442	0.0008	0.3639	0.097	0.6437	<0.00001	0.2514
DB Sand 2	0.5211		0.6079	0.3024	0.005	0.002	0.8904	0.6941	0.0006	0.2055	0.057	0.3383	<0.00001	0.096
LB Sand 2	0.9809	0.6079		0.7257	0.059	0.1371	0.8395	0.9461	0.005	0.4112	0.1585	0.7648	0.00002	0.4066
DB Sand 3	0.7331	0.3024	0.7257		0.01	0.005	0.4915	0.4687	0.0007	0.4527	0.1369	0.7173	<0.00001	0.3617
Shelly Brown Sand	0.01	0.005	0.06	0.01		0.2774	0.02	0.008	0.1455	0.1692	0.6683	0.2253	0.02	0.5080
Roof-Spall Upper	0.009	0.002	0.1371	0.0047	0.2774		0.03	0.004	0.02	0.4138	0.7536	0.5017	<0.00001	0.9991
Roof Spall Lower	0.5975	0.8904	0.8395	0.4915	0.02	0.03		0.8670	0.005	0.2564	0.1092	0.4743	<0.00001	0.2258
LBG Sand 1	0.7442	0.6941	0.9461	0.4687	0.008	0.004	0.8670		0.001	0.2348	0.08	0.4582	<0.00001	0.2507

LC-MSA Upper	0.00081	0.0006	0.005	0.0007	0.1455	0.02	0.005	0.001		0.01	0.06	0.04	0.9187	0.1403
LC-MSA Middle	0.3639	0.2055	0.4112	0.4527	0.1692	0.4138	0.2564	0.2348	0.01		0.3684	0.9038	<0.00001	0.6666
LBG Sand 2	0.097	0.057	0.1585	0.1369	0.6683	0.7536	0.1092	0.08	0.06	0.3684		0.4304	0.01	0.8369
DB Sand 4b	0.6437	0.3383	0.7648	0.7173	0.2253	0.5017	0.4743	0.4582	0.04	0.9038	0.4304		0.002	0.7556
LC-MSA Lower	<0.00001	<0.00001	0.00002	<0.00001	0.017	<0.00001	<0.00001	<0.00001	0.9187	<0.00001	0.01	0.002		0.02
LB Silt	0.2514	0.096	0.4066	0.3617	0.5080	0.9991	0.2258	0.2507	0.1403	0.6666	0.8369	0.7556	0.02	

Values shaded in grey are significant (≤0.05).

PP9B and PP9C

Table B29. Technological length (mm) descriptive statistics for all complete flakes and blades made on all raw materials by cave site.

	PP9B-MIS5	PP9C-MIS5
N	24	43
Min	11	6
Max	101	104
Mean	41.71	40.98
Std. error	4.24	3.18
Variance	431.52	435.26
Stand. dev	20.77	20.86
Median	44	36
25 prcntil	23.5	25
75 prcntil	57.75	53

Table B30. Technological length (mm) test results for all complete flakes and blades made on all raw materials by cave site.

All Raw Materials: Technological Length (mm)	Total *n* = 67	Mann-Whitney U: 493.5	*p* (Significant ≤0.05) 0.77352
Uncorrected Mann-Whitney pairwise comparisons - (*p*):			
Stratigraphic aggregate/Unit	PP9B-MIS5	PP9C-MIS5	
PP9B-MIS5		0.7735	
PP9C-MIS5	0.7735		

PP5-6

Table B31. Technological length (mm) descriptive statistics for all complete flakes and blades made on all raw materials at PP5-6 by stratigraphic aggregate

	RBSR	NWR	BCCSR	OBS2	SGS	OBS1	SADBS Upper	SADBS Lower	ALBS	LBSR	YBSR
N	180	77	476	237	85	188	1078	72	108	1015	117
Min	1.6	6	2.5	1.4	3.0	3.5	5.0	8.0	8.0	5.0	2.1
Max	111.4	82	143.0	53.6	53.0	72.0	72.0	68.0	98.0	117.7	76.8
Mean	28.7	26.8	22.1	16.6	20.3	20.4	19.3	25.1	29.3	31.5	26.8
Std. error	1.4	1.9	0.7	0.6	1.1	0.9	0.3	1.6	1.5	0.5	1.3
Variance	341.2	286.1	235.9	96.3	110.1	138.5	87.8	173.6	233.0	263.5	195.3
Stand. dev	18.5	16.9	15.4	9.8	10.5	11.8	9.4	13.2	15.3	16.2	14.0
Median	25.0	21	17.7	14.2	18.5	18.0	17.0	20.0	27.6	27.8	25.1
25 prcntil	17.0	15.5	13.1	9.7	11.4	12.0	13.0	14.0	18.0	19.3	16.5
75 prcntil	32.7	34	26.0	21.1	26.5	26.0	24.0	34.8	39.0	40.5	31.9

Table B32. Technological length (mm) test results for all complete flakes and blades made on all raw materials at PP5-6 by stratigraphic aggregate.

All raw materials: Technological Length (mm)	**Total *n* = 3633**	**Kruskal-Wallis H: 564.4**	***p* (Significant ≤0.05) <0.00001**

Uncorrected Mann-Whitney pairwise comparisons - (*p*):

Stratigraphic aggregate	RBSR	NWR	BCCSR/BAS	OBS2	SGS	OBS1	SADBS Upper	SADBS Lower	ALBS	LBSR	YBSR
RBSR		0.2131	<0.00001	<0.00001	0.00006	<0.00001	<0.00001	0.2443	0.2432	0.003	0.8818
NWR	0.2131		0.009	<0.00001	0.02	0.006	0.0003	0.8181	0.08	0.001	0.3714
BCCSR/BAS	<0.00001	0.009		<0.00001	0.7968	0.4877	0.09	0.017	<0.00001	<0.00001	0.00001
OBS2	<0.00001	<0.00001	<0.00001		0.002	0.0002	<0.00001	<0.00001	<0.00001	<0.00001	<0.00001
SGS	0.00006	0.025	0.7968	0.002		0.8354	0.5873	0.03	0.00001	<0.00001	0.00046
OBS1	<0.00001	0.006	0.4877	0.0002	0.8354		0.6767	0.0048	<0.00001	<0.00001	0.00001
SADBS Upper	<0.00001	0.0003	0.09	<0.00001	0.5873	0.6767		0.0004	<0.00001	<0.00001	<0.00001
SADBS Lower	0.2443	0.8181	0.017	<0.00001	0.03	0.0048	0.0004		0.048	0.0003	0.4473

ALBS	0.2432	0.08	<0.00001	<0.00001	0.00001	<0.00001	<0.00001	0.048		0.2375	0.1751							
LBSR	0.0025	0.001	<0.00001	<0.00001	<0.00001	<0.00001	<0.00001	0.0003	0.2375		0.003							
YBSR	0.8818	0.3714	0.00001	<0.00001	0.00046	0.00001	<0.00001	0.4473	0.1751	0.003								

Values shaded in grey are significant (≤0.05).

Technological length – quartzite versus silcrete

PP13B

Table B33. Technological length (mm) descriptive statistics for all complete flakes and blades made on quartzite (Q) and silcrete (S) at PP13B by stratigraphic aggregate.

	LB Sand 1-Q	LB Sand 1-S	DB Sand 2-Q	LB Sand 2-Q	DB Sand 3-Q	Shelly Brown Sand-Q	Roof Spall-Upper-Q	Roof Spall-Upper-S	Roof Spall-Lower-Q	LBG Sand 1-Q	LC-MSA Upper-Q	LC-MSA Middle-Q	LBG Sand 2-Q	DB Sand 4b-Q	LC-MSA Lower-Q	LC-MSA Lower-S	LB Silt-Q
N	131	12	108	23	260	44	312	10	68	139	19	55	23	15	445	38	19
Min	10.0	14.0	11.0	19.0	5.0	7.0	5.0	16.0	9.0	6.0	9.0	8.0	15.0	12.0	5.0	9.0	10
Max	96.0	84.0	121.0	85.0	104.0	84.0	101.0	52.0	98.0	92.0	105.0	88.0	83.0	68.0	119.0	74.0	96
Mean	45.8	44.7	47.4	46.7	46.2	38.6	41.3	30.2	48.0	46.7	37.1	43.5	38.8	41.1	31.7	30.9	40.9

Std. error	Variance	Stand. dev	Median	25 prcntil	75 prcntil
4.4	371.2	19.3	43	26	49
2.153	176.2	13.3	28.0	20.8	40.3
0.847	319.6	17.9	28.0	17.0	43.0
4.619	320.1	17.9	42.0	24.0	55.0
3.649	306.2	17.5	36.0	25.0	52.0
2.667	391.3	19.8	41.0	31.0	58.0
6.300	754.2	27.5	25.0	14.0	60.0
1.690	396.8	19.9	46.0	32.0	60.0
2.682	489.3	22.1	48.0	31.3	64.8
3.806	144.8	12.0	27.5	20.0	40.3
1.126	395.7	19.9	39.0	25.0	56.0
3.227	458.2	21.4	36.0	20.5	55.8
1.226	390.8	19.8	44.0	32.0	60.0
3.810	333.9	18.3	40.0	37.0	53.0
1.796	348.4	18.7	48.0	35.0	56.0
5.276	334.1	18.3	44.0	31.5	55.0
1.666	363.7	19.1	45.0	32.0	58.0

Table B34. Technological length (mm) test results for all complete flakes and blades made on quartzite (Q) and silcrete (S) at PP13B by stratigraphic aggregate.

Quartzite and Silcrete: Technological Length (mm)									**Total *n* = 1721**	**Kruskal-Wallis H: 185.8**	***p* (Significant ≤0.05) <0.00001**				
Uncorrected Mann-Whitney pairwise comparisons - (*p*):															
Stratigraphic aggregate	LB Sand 1-Q	LB Sand 1-S	DB Sand 2-Q	LB Sand 2-Q	DB Sand 3-Q	Shelly Brown Sand-Q	Roof Spall-Upper-Q	Roof Spall-Upper-S	Roof Spall-Lower-Q	LBG Sand 1-Q	LC-MSA Upper-Q	LC-MSA Middle-Q	LBG Sand 2-Q	DB Sand 4b-Q	LC-MSA Lower-Q	LC-MSA Lower-S	LB Silt-Q
LB Sand 1-Q		0.8899	0.4475	0.9737	0.9626	0.03	0.018	0.009	0.4891	0.7338	0.04	0.4812	0.08	0.4487	<0.00001	0.00001	0.2753

0.4775	0.09	0.4184	0.3094	0.5692	0.9813	0.1132	0.1954	0.2683	0.4219	0.6469
0.01	<0.00001	0.0007	<0.00001	0.1759	0.002	0.9090	0.00009	<0.00001	0.9595	0.001
0.01	<0.00001	0.0001	<0.00001	0.044	<0.00001	0.9071	<0.00001	<0.00001	0.8033	0.00001
0.6427	0.2446	0.5206	0.3907	0.5365	0.8844	0.1138	0.3347	0.3087	0.3400	0.7527
0.3475	0.04	0.1038	0.08	0.8018	0.6196	0.2241	0.07	0.07	0.3240	0.2542
0.8188	0.2285	0.5037	0.4068	0.2112	0.3657	0.04	0.2751	0.3304	0.1391	
0.2159	0.04	0.07	0.03	0.4539	0.1534	0.9817	0.04	0.04		0.1391
0.8607	0.5858	0.9350	0.7398	0.02	0.005	0.008	0.7164		0.04	0.3304
0.5898	0.8114	0.7319	0.5602	0.03	0.02	0.01		0.7164	0.04	0.2751
0.048	0.002	0.02	0.009	0.3670	0.08		0.01	0.008	0.9817	0.04
0.4876	0.002	0.1625	0.002	0.3334		0.08	0.02	0.005	0.1534	0.3657
0.2989	0.01	0.09	0.02		0.3334	0.3670	0.03	0.02	0.4539	0.2112
0.9222	0.4270	0.8482		0.02	0.002	0.009	0.5602	0.7398	0.03	0.4068
1.0	0.5351		0.8482	0.09	0.1625	0.02	0.7319	0.9350	0.07	0.5037
0.6428		0.5351	0.4270	0.01	0.002	0.002	0.8114	0.5858	0.04	0.2285
	0.6428	1.0000	0.9222	0.2989	0.4876	0.048	0.5898	0.8607	0.2159	0.8188
0.8899	0.4475	0.9737	0.9626	0.03	0.02	0.009	0.4891	0.7338	0.04	0.4812
LB Sand 1-S	DB Sand 2-Q	LB Sand 2-Q	DB Sand 3-Q	Shelly Brown Sand-Q	Roof Spall-Upper-Q	Roof Spall-Upper-S	Roof Spall-Lower-Q	LBG Sand 1-Q	LC-MSA Upper-Q	LC-MSA Middle-Q

	LBG Sand 2-Q	DB Sand 4b-Q	LC-MSA Lower-Q	LC-MSA Lower-S	LB Silt-Q
YBSR-S	0.7137	0.9723	0.02	0.03	
YBSR-Q	0.09	0.05	0.7254		0.03
LBSR-S	0.03	0.03		0.7254	0.02
LBSR-Q	0.7423		0.03	0.05	0.9723
ALBS-S		0.7423	0.03	0.09	0.7137
ALBS-Q	0.2542	0.7527	0.00001	0.001	0.6469
SADBS Lower-Q	0.3240	0.3400	0.8033	0.9595	0.4219
SADBS Lower-S	0.07	0.3087	<0.00001	<0.00001	0.2683
SADBS Upper-Q	0.07	0.3347	<0.00001	0.00009	0.1954
SADBS Upper-S	0.2241	0.1138	0.9071	0.9090	0.1132
OBS1-S	0.6196	0.8844	<0.00001	0.002	0.9813
OBS1-Q	0.8018	0.5365	0.04	0.1759	0.5692
OBS2-Q	0.08	0.3907	<0.00001	<0.00001	0.3094
OBS2-S	0.1038	0.5206	0.0001	0.0007	0.4184
SGS-Q	0.04	0.2446	<0.00001	<0.00001	0.09
SGS-S	0.3475	0.6427	0.01	0.01	0.4775
BCCSR-Q	0.08	0.4487	<0.00001	0.00001	0.2753
BCCSR-S	0.1038	0.5206	0.0001	0.0007	0.4184
NWR-S	0.8018	0.5365	0.04	0.1759	0.5692
NWR-Q	0.6196	0.8844	<0.00001	0.002	0.9813
RBSR-S	0.2241	0.1138	0.9071	0.9090	0.1132
RBSR-Q	0.07	0.3347	<0.00001	0.00009	0.1954

Values shaded in grey are significant (≤0.05). Q=Quartzite; S=Silcrete.

PP5-6

Table B35. Technological length (mm) descriptive statistics for all complete flakes and blades made on quartzite (Q) and silcrete (S) at PP5-6 by stratigraphic aggregate.

	N	Min	Max
YBSR-S	56	2.1	72.6
YBSR-Q	34	10.8	76.8
LBSR-S	242	5.0	78.8
LBSR-Q	706	7.0	117.7
ALBS-S	16	10.5	48.0
ALBS-Q	89	8.0	98.0
SADBS Lower-S	24	8.0	64.0
SADBS Lower-Q	38	9.0	68.0
SADBS Upper-S	849	5.0	50.0
SADBS Upper-Q	170	6.0	72.0
OBS1-S	56	3.5	41.5
OBS1-Q	63	5.3	72.0
SGS-S	52	7.9	40.0
SGS-Q	18	5.0	53.0
OBS2-S	110	1.4	53.6
OBS2-Q	36	6.1	50.2
BCCSR-S	285	2.5	75.6
BCCSR-Q	134	5.7	143.0
NWR-S	38	6	54
NWR-Q	38	9	82
RBSR-S	90	1.6	53.9
RBSR-Q	57	12.0	111.4

Mean	Std. error	Variance	Stand. dev	Median	25 prcntil	75 prcntil
21.8	1.5	132.8	11.5	21.9	12.4	27.7
35.2	2.8	266.1	16.3	30.5	24.5	46.6
28.0	0.8	168.3	13.0	26.1	17.5	37.0
33.2	0.6	296.3	17.2	29.0	20.7	42.1
25.6	2.9	136.1	11.7	23.1	15.9	30.5
30.2	1.7	251.0	15.8	28.0	18.0	39.5
21.3	2.7	170.6	13.1	16.5	13.3	28.5
28.4	2.2	177.4	13.3	30.0	17.0	36.3
18.1	0.3	57.1	7.6	17.0	13.0	22.0
25.4	1.1	205.8	14.3	22.5	15.0	33.3
17.9	1.2	78.5	8.9	17.8	10.6	25.3
27.0	1.9	222.1	14.9	25.0	16.0	33.0
19.9	1.3	83.9	9.2	17.0	11.9	26.8
24.6	3.4	208.2	14.4	21.8	13.0	37.0
17.6	1.0	113.9	10.7	15.0	9.7	23.1
21.7	1.9	126.3	11.2	18.4	14.0	29.7
17.9	0.6	98.0	9.9	15.8	11.5	21.6
32.0	1.9	459.8	21.4	26.6	17.1	40.1
19.5	1.6	98.0	9.9	17.5	11	24.25
34.5	3.1	371.2	19.3	30.5	19.75	49.25
22.7	1.2	131.8	11.5	22.1	15.0	29.1
40.1	3.2	599.1	24.5	30.7	24.1	50.8

Table B36. Technological length (mm) test results for all complete flakes and blades made on quartzite (Q) and silcrete (S) at PP5-6 by stratigraphic aggregate.

Quartzite and Silcrete: Technological Length (mm)				**Total *n* = 3201**		**Kruskal-Wallis H: 680.8**		**p (Significant ≤0.05) <0.00001**
Uncorrected Mann-Whitney pairwise comparisons - (*p*):								
Stratigraphic aggregate	RBSR-Q	RBSR-S	NWR-Q	NWR-S	BCCSR/BAS-Q	BCCSR/BAS-S	OBS2-Q	OBS2-S
RBSR-Q		<0.00001	0.2435	<0.00001	0.01	<0.00001	0.00001	<0.00001
RBSR-S	<0.00001		0.0019	0.1058	0.001	0.00002	0.5799	0.0004
NWR-Q	0.2435	0.0019		0.00019	0.3504	<0.00001	0.0029	<0.00001
NWR-S	<0.00001	0.1058	0.00019		0.0001	0.1809	0.4328	0.1373
BCCSR/BAS-Q	0.01	0.001	0.3504	0.0001		<0.00001	0.005	<0.00001
BCCSR/BAS-S	<0.00001	0.00002	<0.00001	0.1809	<0.00001		0.03	0.4347
OBS2-Q	0.00001	0.5799	0.003	0.4328	0.0049	0.03		0.027
OBS2-S	<0.00001	0.0004	<0.00001	0.1373	<0.00001	0.4347	0.027	
SGS-Q	0.008	0.7698	0.07	0.2920	0.1812	0.054	0.5509	0.044
SGS-S	<0.00001	0.1499	0.00015	0.8157	0.00004	0.08	0.5899	0.07
OBS1-Q	0.001	0.1072	0.07	0.006	0.1998	<0.00001	0.09	0.00001
OBS1-S	<0.00001	0.015	0.00001	0.5607	<0.00001	0.7197	0.1378	0.5592
SADBS Upper-Q	<0.00001	0.3355	0.008	0.019	0.006	<0.00001	0.2047	<0.00001
SADBS Upper-S	<0.00001	0.00007	<0.00001	0.5612	<0.00001	0.053	0.08	0.051
SADBS Lower-Q	0.039	0.02	0.1992	0.0017	0.7692	<0.00001	0.02	<0.00001
SADBS Lower-S	0.00002	0.3052	0.003	0.9078	0.004	0.2447	0.5765	0.1284
ALBS-Q	0.028	0.0008	0.3472	0.00009	0.9232	<0.00001	0.003	<0.00001
ALBS-S	0.017	0.4118	0.1725	0.058	0.3563	0.003	0.2626	0.006
LBSR-Q	0.06	<0.00001	0.8970	<0.00001	0.09	<0.00001	0.00002	<0.00001
LBSR-S	0.0008	0.001	0.1122	0.00005	0.4750	<0.00001	0.004	<0.00001
YBSR-Q	0.7335	0.00003	0.5843	0.00001	0.09	<0.00001	0.00016	<0.00001
YBSR-S	<0.00001	0.6536	0.002	0.2525	0.001	0.003	0.9809	0.0079

0.5665	0.3809	0.059	0.06	0.1933	0.01	0.009	0.5815	0.0005	0.2552	<0.00001
0.03	<0.00001	0.01	<0.00001	0.0004	<0.00001	0.1104	0.0003	0.1165	0.027	0.3076
0.2700	0.00002	0.3146	<0.00001	0.007	<0.00001	0.8903	0.003	0.3854	0.5011	0.00039
0.03	<0.00001	0.004	<0.00001	<0.00001	<0.00001	0.1275	0.00004	0.1709	0.08	
0.7042	0.08	0.8596	0.017	0.6374	0.005	0.5192	0.1545	0.2927		0.08
0.1772	0.00003	0.1709	<0.00001	0.007	<0.00001	0.7301	0.003		0.2927	0.1709
0.3800	0.9421	0.047	0.3185	0.1174	0.4950	0.01		0.003	0.1545	0.00004
0.4042	0.0016	0.3473	0.00009	0.1099	<0.00001		0.01	0.7301	0.5192	0.1275
0.09	0.3128	<0.00001	0.7167	<0.00001		<0.00001	0.4950	<0.00001	0.005	<0.00001
0.8429	0.02	0.3807	0.0006		<0.00001	0.1099	0.1174	0.007	0.6374	<0.00001
0.1068	0.2683	0.0003		0.0006	0.7167	0.00009	0.3185	<0.00001	0.017	<0.00001
0.5854	0.01		0.0003	0.3807	<0.00001	0.3473	0.047	0.1709	0.8596	0.004
0.2851		0.01	0.2683	0.02	0.3128	0.0016	0.9421	0.00003	0.08	<0.00001
	0.2851	0.5854	0.1068	0.8429	0.09	0.4042	0.3800	0.1772	0.7042	0.03
0.044	0.07	0.00001	0.5592	<0.00001	0.051	<0.00001	0.1284	<0.00001	0.006	<0.00001
0.5509	0.5899	0.09	0.1378	0.2047	0.08	0.02	0.5765	0.003	0.2626	0.00002
0.054	0.08	<0.00001	0.7197	<0.00001	0.053	<0.00001	0.2447	<0.00001	0.003	<0.00001
0.1812	0.00004	0.1998	<0.00001	0.0057	<0.00001	0.7692	0.0037	0.9232	0.3563	0.09
0.2920	0.8157	0.0058	0.5607	0.019	0.5612	0.0017	0.9078	0.00009	0.058	<0.00001
0.07	0.00015	0.07	0.00001	0.008	<0.00001	0.1992	0.0026	0.3472	0.1725	0.8970
0.7698	0.1499	0.1072	0.015	0.3355	0.00007	0.02	0.3052	0.0008	0.4118	<0.00001
0.008	<0.00001	0.001	<0.00001	<0.00001	<0.00001	0.039	0.00002	0.028	0.017	0.06
SGS-Q	SGS-S	OBS1-Q	OBS1-S	Upper-Q	Upper-S	Lower-Q	Lower-S	ALBS-Q	ALBS-S	LBSR-Q

LBSR-S	YBSR-Q	YBSR-S
0.0008	0.7335	<0.00001
0.001	0.00003	0.6536
0.1122	0.5843	0.002
0.00005	0.00001	0.2525
0.4750	0.09	0.001
<0.00001	<0.00001	0.003
0.004	0.00016	0.9809
<0.00001	<0.00001	0.008
0.2700	0.03	0.5665
0.00002	<0.00001	0.3809
0.3146	0.01	0.059
<0.00001	<0.00001	0.06
0.007	0.0004	0.1933
<0.00001	<0.00001	0.01
0.8903	0.1104	0.009
0.003	0.0003	0.5815
0.3854	0.1165	0.0005
0.5011	0.027	0.2552
0.00039	0.3076	<0.00001
	0.018	0.0007
0.018		0.00003
0.0007	0.00003	

Values shaded in grey are significant (≤0.05). Q=Quartzite; S=Silcrete.

Cutting edge per mass

PP13B

Table B37. Cutting edge / Mass (CE/M) descriptive statistics for all raw materials at PP13B by stratigraphic aggregate.

	N	Min	Max	Mean
LB Sand 1	154	1.9	105.0	16.4
DB Sand 2	118	2.0	130.0	15.7
LB Sand 2	30	2.8	92.0	19.0
DB Sand 3	301	1.9	270.0	19.6
Shelly Brown Sand	53	3.2	80.0	23.8
Roof Spall-Upper	345	2.2	133.3	21.1
Roof Spall-Lower	72	2.8	195.0	25.5
LBG Sand 1	145	1.8	230.0	16.8
LC-MSA Upper	27	4.0	280.0	45.7
LC-MSA Middle	63	1.7	145.0	20.7
LBG Sand 2	25	1.4	44.5	15.2
DB Sand 4b	20	2.9	58.0	14.3
LC-MSA Lower	523	1.2	340.0	35.6
LB Silt	20	1.6	90.0	15.8

Std. error	1.5	1.5	3.6	1.6	3.1	1.1	4.1	2.3	11.5	3.0	2.6	3.6	1.9	5.0
Variance	324.4	277.8	387.9	739.8	494.6	440.7	1237.5	799.5	3585.0	583.3	164.5	252.9	1900.8	495.3
Stand. dev	18.0	16.7	19.7	27.2	22.2	21.0	35.2	28.3	59.9	24.2	12.8	15.9	43.6	22.3
Median	10.2	10.7	13.0	11.7	15.8	13.1	14.6	7.2	27.3	12.3	9.6	7.9	19.5	7.2
25 prcntil	6.1	6.5	5.8	6.8	9.0	8.2	7.9	4.0	9.9	7.2	5.5	5.2	10.2	4.3
75 prcntil	18.1	17.5	21.5	21.9	30.2	25.5	30.5	16.7	59.0	24.2	25.6	18.1	44.4	14.9

Table B38. Cutting edge / Mass (CE/M) test results for all raw materials at PP13B by stratigraphic aggregate.

All raw materials: Cutting Edge / Mass values					**Total *n* = 1896**			**Kruskal-Wallis H: 164.1**			**p (Significant ≤0.05) <0.00001**			
Uncorrected Mann-Whitney pairwise comparisons - (*p*):														
Stratigraphic aggregate	LB Sand 1	DB Sand 2	LB Sand 2	DB Sand 3	Shelly Brown Sand	Roof Spall-Upper	Roof Spall-Lower	LBG Sand 1	LC-MSA Upper	LC-MSA Middle	LBG Sand 2	DB Sand 4b	LC-MSA Lower	LB Silt
LB Sand 1		0.6419	0.3695	0.1094	0.0047	0.0002	0.02	0.006	0.0001	0.1874	0.9122	0.4998	<0.00001	0.1562
DB Sand 2	0.6419		0.4729	0.2959	0.0095	0.003	0.05	0.003	0.0002	0.3346	0.8048	0.3287	<0.00001	0.1006

	LB Sand 2	DB Sand 3	Shelly Brown Sand	Roof Spall-Upper	Roof Spall-Lower	LBG Sand 1	LC-MSA Upper	LC-MSA Middle	LBG Sand 2	DB Sand 4b	LC-MSA Lower
0.1201	0.01	<0.00001	0.09	<0.00001	0.007	<0.00001	0.3568	0.0006	0.001	0.0006	
0.2805	0.1332	0.02	0.02	0.02	0.052	0.4434	0.001	0.1461	0.6894		0.0006
0.5373	0.4370	0.07	0.07	0.08	0.1432	0.2271	0.004	0.3177		0.6894	0.001
0.8792	0.6909	0.1693	0.08	0.3291	0.4095	0.001	0.008		0.3177	0.1461	0.0006
0.02	0.0005	0.08	0.007	0.03	0.00001			0.008	0.004	0.001	0.3568
0.03	0.00001	0.00002	<0.00001	0.00007		0.00001	0.00001	0.001	0.2271	0.4434	<0.00001
0.5063	0.1514	0.5274	0.9828		0.00007	0.03	0.03	0.4095	0.1432	0.052	0.007
0.4142	0.01	0.4038		0.9828	<0.00001	0.007	0.07	0.3291	0.08	0.02	<0.00001
0.2232	0.046		0.4038	0.5274	0.00002	0.08	0.00046	0.1693	0.07	0.02	0.09
0.9299		0.05	0.01	0.1514	0.00001	0.00046	0.00019	0.6909	0.4370	0.1332	<0.00001
	0.9299	0.2232	0.4142	0.5063	0.03	0.02	0.02	0.8792	0.5373	0.2805	0.01
0.4729	0.2959	0.0095	0.003	0.045	0.003	0.00019	0.00019	0.3346	0.8048	0.3287	<0.00001
0.3695	0.1094	0.005	0.0002	0.02	0.006	0.003	0.0001	0.1874	0.9122	0.4998	<0.00001

LB sIlt	0.1562	0.1006	0.1201	0.04	0.006	0.005	0.01	0.9423	0.001	0.049	0.4307	0.6359	0.0002	

Values shaded in grey are significant (≤0.05).

PP9B and PP9C

Table B39. Cutting edge / Mass (CE/M) descriptive statistics for all raw materials at PP9.

	PP9B	**PP9C**
N	24	43
Min	3.45	3.43
Max	130	130
Mean	24.58	17.81
Std. error	6.78	3.12
Variance	1102.31	419.12
Stand. dev	33.20	20.47
Median	11.01	13.12
25 prcntil	8.17	7.73
75 prcntil	22.94	19.13

Table B40. Cutting edge / Mass (CE/M) test results for all raw materials at PP9B and PP9C.

All raw materials: Cutting Edge / Mass values	**Total *n* = 67**	**Mann-Whitney U: 506.5**	***p* (Significant ≤0.05) 0.90631**
Uncorrected Mann-Whitney pairwise comparisons - (*p*):			
Cave site	PP9B	PP9C	
PP9B		0.906	
PP9C	0.906		

PP5-6

Table B41. Cutting edge / Mass (CE/M) descriptive statistics for all raw materials at PP5-6 by stratigraphic aggregate

	RBSR	NWR	BCCSR/BAS	OBS2	SGS	OBS1	SADBS Upper	SADBS Lower	ALBS	LBSR	YBSR
N	180	76	476	236	85	188	1070	72	108	1014	117
Min	1.3	2.3	2.1	0.2	2.2	2.6	2.8	1.6	2.5	1.5	2.3
Max	397.7	340.0	704.8	905.5	593.8	805.7	473.8	340.0	150.0	900.0	245.3
Mean	55.0	61.3	75.3	129.1	86.7	80.7	91.2	57.1	35.5	30.2	43.4
Std. error	5.0	8.2	3.5	9.8	10.8	8.1	2.3	7.4	3.4	1.5	4.4
Variance	4505.8	5119.1	5896.3	22615.1	9977.0	12273.5	5712.4	3966.5	1240.8	2357.3	2262.5
Stand. dev	67.1	71.5	76.8	150.4	99.9	110.8	75.6	63.0	35.2	48.6	47.6
Median	32.2	34.0	50.6	72.4	50.8	43.7	70.0	40.6	21.4	17.3	23.0

25 prcntil	13.4	18.2	24.1	28.7	23.7	19.5	37.2	16.2	8.8	9.2	11.7
75 prcntil	76.6	74.5	99.7	165.9	107.1	96.9	120.0	68.3	52.8	34.8	59.3

Table B42. Cutting edge / Mass (CE/M) test results for all raw materials at PP5-6 by stratigraphic aggregate

All raw materials: Cutting Edge / Mass Values	**Total *n* = 3622**			**Kruskal-Wallis H: 844.9**			**p (Significant ≤0.05) <0.00001**		
Uncorrected Mann-Whitney pairwise comparisons - (p):									
Stratigraphic aggregate	RBSR	NWR	BCCSR/BAS	OBS2	SGS	OBS1	SADBS Upper	SADBS Lower	ALBS	LBSR	YBSR
RBSR		0.39900	<0.00001	<0.00001	0.0009	0.01	<0.00001	0.3640	0.016	<0.00001	0.1814
NWR	0.3990		0.017	0.00002	0.03	0.1842	<0.00001	0.9878	0.004	<0.00001	0.046
BCCSR/BAS	<0.00001	0.017		0.0001	0.6871	0.2159	<0.00001	0.01	<0.00001	<0.00001	<0.00001
OBS2	<0.00001	0.00002	0.0001		0.036	0.0001	0.3346	0.00002	<0.00001	<0.00001	<0.00001
SGS	0.0009	0.0343	0.6871	0.036		0.2479	0.026	0.037	<0.00001	<0.00001	0.00002
OBS1	0.01	0.18420	0.2159	0.0001	0.2479		<0.00001	0.1830	<0.00001	<0.00001	0.00008

SADBS Upper	<0.00001	<0.00001	<0.00001	<0.00001	<0.00001	<0.00001		<0.00001	0.026	0.3346	<0.00001	<0.00001	<0.00001
SADBS Lower	0.054	<0.00001	0.0049		0.1830	<0.00001		0.037	0.00002	0.01	0.9878	0.3640
ALBS	0.2373	0.08		0.0049	<0.00001	<0.00001	<0.00001	<0.00001	<0.00001	<0.00001	0.004	0.016
LBSR	0.0006		0.08	<0.00001	<0.00001	<0.00001	<0.00001	<0.00001	<0.00001	<0.00001	<0.00001	<0.00001
YBSR		0.0006	0.2373	0.054	<0.00001	0.00008	0.00002	<0.00001	<0.00001	<0.00001	0.046	0.1814

Values shaded in grey are significant (≤0.05).

Cutting edge per mass –quartzite versus silcrete

PP13B

Table B43. Cutting edge / Mass (CE/M) descriptive statistics for quartzite and silcrete at PP13B by stratigraphic aggregate.

	LB Sand 1-Q	LB Sand 1-S	DB Sand 2-Q	LB Sand 2-Q	DB Sand 3-Q	Shelly Brown Sand-Q	Roof Spall-Upper-Q	Roof Spall-Upper-S	Roof Spall-Lower-Q	LBG Sand 1-Q	LC-MSA Upper-Q	LC-MSA Middle-Q	LBG Sand 2-Q	DB Sand 4b-Q	LC-MSA Lower-Q	LC-MSA Lower-S	LB Silt-Q
N	131	12	107	22	260	44	311	10	67	138	19	54	23	15	437	38	19
Min	1.9	4.1	2.0	2.8	2.0	3.2	2.2	6.7	2.8	1.8	4.0	1.7	1.4	2.9	1.2	3.9	1.615

Max	Mean	Std. error	Variance	Stand. dev	Median	25 prcntil	75 prcntil
90	14.05	4.908	457.7	21.39	7.083	4.183	10.74
85.0	29.0	3.6	504.6	22.5	22.7	11.3	45.0
340.0	34.1	1.9	1659.2	40.7	18.1	10.0	43.8
58.0	16.5	4.6	318.7	17.9	8.8	4.9	19.8
44.5	15.7	2.8	176.5	13.3	9.6	5.3	26.9
145.0	19.3	3.3	581.1	24.1	11.0	6.2	22.4
280.0	51.1	16.1	4917.9	70.1	24.2	8.8	61.3
230.0	16.2	2.4	819.5	28.6	6.5	3.8	14.7
195.0	24.7	4.4	1270.1	35.6	12.7	7.5	28.7
65.7	32.9	6.7	449.7	21.2	24.4	17.8	55.2
133.3	20.7	1.2	444.5	21.1	12.7	8.1	24.8
80.0	23.2	3.3	471.8	21.7	16.1	8.8	27.1
270.0	18.6	1.6	665.7	25.8	11.1	6.6	21.5
58.6	14.8	3.0	191.6	13.8	11.9	5.8	15.6
130.0	15.3	1.7	293.0	17.1	10.4	6.4	16.8
100.0	22.4	7.7	712.1	26.7	11.9	9.0	26.0
105.0	15.0	1.4	265.1	16.3	9.1	5.5	17.1

Table B44. Cutting edge / Mass (CE/M) test results for quartzite and silcrete at PP13B by stratigraphic aggregate.

Quartzite and Silcrete: Cutting Edge / Mass values							Total *n* = 1707			Kruskal-Wallis H: 166.4				*p* (Significant ≤0.05) <0.00001			
Uncorrected Mann-Whitney pairwise comparisons - (*p*):																	
Stratigraphic aggregate	LB Sand 1-Q	LB Sand 1-S	DB Sand 2-Q	LB Sand 2-Q	DB Sand 3-Q	Shelly Brown Sand-Q	Roof Spall-Upper-Q	Roof Spall-Upper-S	Roof Spall-Lower-Q	LBG Sand 1-Q	LC-MSA Upper-Q	LC-MSA Middle-Q	LBG Sand 2-Q	DB Sand 4b-Q	LC-MSA Lower-Q	LC-MSA Lower-S	LB Silt-Q
LB Sand 1-Q		0.1484	0.4372	0.5905	0.07	0.002	0.00006	0.001	0.01	0.01	0.002	0.2025	0.8038	0.8290	<0.00001	0.00001	0.1611
LB Sand 1-S	0.1484		0.2605	0.3773	0.4383	0.6970	0.9711	0.08	0.9728	0.02	0.3011	0.5060	0.3755	0.3172	0.2347	0.1557	0.04
DB Sand 2-Q	0.4372	0.2605		0.8781	0.3320	0.009	0.003	0.002	0.055	0.002	0.005	0.4907	0.9951	0.9007	<0.00001	0.00004	0.07
LB Sand 2-Q	0.5905	0.3773	0.8781		0.6780	0.08	0.1865	0.006	0.2638	0.07	0.03	0.6676	0.9728	0.9630	0.006	0.005	0.1396
DB Sand 3-Q	0.07	0.4383	0.3320	0.6780		0.04	0.008	0.005	0.1572	0.00001	0.008	0.9049	0.6070	0.5204	<0.00001	0.0002	0.03
Shelly Brown Sand-Q	0.002	0.6970	0.009	0.08	0.04		0.3631	0.09	0.4493	0.00002	0.2194	0.1027	0.1086	0.1152	0.1635	0.1261	0.003
Roof Spall-Upper-Q	0.00006	0.9711	0.003	0.1865	0.008	0.3631		0.02	0.9190	<0.00001	0.056	0.1905	0.1367	0.1667	<0.00001	0.007	0.002
Roof Spall-Upper-S	0.001	0.08	0.002	0.006	0.005	0.09	0.02		0.03	0.0004	0.9087	0.01	0.02	0.01	0.3113	0.4388	0.002

Roof Spall-Lower-Q	LBG Sand 1-Q	LC-MSA Upper-Q	LC-MSA Middle-Q	LBG Sand 2-Q	DB Sand 4b-Q	LC-MSA Lower-Q	LC-MSA Lower-S	LB Silt-Q
0.01	0.01	0.002	0.2025	0.8038	0.8290	<0.00001	0.00001	0.1611
0.9728	0.02	0.3011	0.5060	0.3755	0.3172	0.2347	0.1557	0.04
0.055	0.002	0.005	0.4907	0.9951	0.9007	<0.00001	0.00004	0.07
0.2638	0.07	0.03	0.6676	0.9728	0.9630	0.006	0.005	0.1396
0.1572	0.00001	0.008	0.9049	0.6070	0.5204	<0.00001	0.0002	0.03
0.4493	0.00002	0.2194	0.1027	0.1086	0.1152	0.1635	0.1261	0.003
0.9190	<0.00001	0.056	0.1905	0.1367	0.1667	<0.00001	0.007	0.002
0.03	0.0004	0.9087	0.01	0.02	0.01	0.3113	0.4388	0.002
	0.00006	0.09	0.3295	0.2401	0.2751	0.008	0.02	0.008
0.00006		0.0002	0.003	0.1801	0.2280	<0.00001	<0.00001	0.0004
0.09	0.0002		0.03	0.02	0.02	0.5360	0.6660	0.004
0.3295	0.003	0.03		0.5893	0.5754	0.0005	0.003	0.046
0.2401	0.1801	0.02	0.5893		0.9286	0.004	0.008	0.3121
0.2751	0.2280	0.02	0.5754	0.9286		0.02	0.01	0.3672
0.008	<0.00001	0.5360	0.0005	0.004	0.02		0.6191	0.00008
0.02	<0.00001	0.6660	0.003	0.008	0.01	0.6191		0.0004
0.008	0.9936	0.004	0.046	0.3121	0.3672	0.00008	0.0004	

Values shaded in grey are significant (≤0.05). Q=Quartzite; S=Silcrete.

PP5-6

Table B45. Cutting edge / Mass (CE/M) descriptive statistics for quartzite and silcrete at PP5-6 by stratigraphic aggregate.

	N	Min	Max	Mean	Std. error	Variance	Stand. dev	Median
YBSR-S	56	6.8	245.3	60.4	7.2	2905.5	53.9	40.9
YBSR-Q	34	2.3	72.0	15.4	2.1	148.1	12.2	13.3
LBSR-S	241	3.0	567.1	45.6	3.7	3309.7	57.5	28.8
LBSR-Q	706	1.5	260.0	23.0	0.9	634.9	25.2	14.3
ALBS-S	16	6.2	97.1	59.5	6.7	728.2	27.0	63.0
ALBS-Q	89	2.5	146.7	30.4	3.5	1090.4	33.0	19.3
SADBS Lower-S	24	1.6	340.0	95.7	17.8	7600.6	87.2	62.1
SADBS Lower-Q	38	4.7	115.0	33.6	4.9	898.6	30.0	22.3
SADBS Upper-S	842	8.5	473.8	99.7	2.6	5888.3	76.7	76.7
SADBS Upper-Q	169	2.8	300.0	55.4	4.7	3735.6	61.1	31.6
OBS1-S	56	7.6	805.7	135.9	22.9	29315.4	171.2	64.8
OBS1-Q	63	2.6	169.4	33.5	4.6	1327.5	36.4	18.6
SGS-S	52	5.2	593.8	93.8	14.5	10917.1	104.5	61.8
SGS-Q	18	2.2	390.2	63.6	22.8	9388.7	96.9	30.0
OBS2-S	110	3.3	905.5	133.2	14.6	23436.9	153.1	79.3
OBS2-Q	36	0.2	166.1	36.6	6.2	1381.5	37.2	24.4
BCCSR/BAS-S	285	4.5	704.8	95.2	5.0	7253.7	85.2	68.4
BCCSR/BAS-Q	134	2.1	274.2	37.3	3.9	1989.3	44.6	20.7
NWR-S	37	11.6	340.0	89.9	13.7	6965.7	83.5	65.7
NWR-Q	38	2.3	250.0	33.1	7.2	1961.9	44.3	20.2
RBSR-S	90	1.3	397.7	70.3	7.5	5075.0	71.2	47.7
RBSR-Q	57	2.7	115.0	22.9	3.2	599.7	24.5	14.3

25 prcntil	75 prcntil
5.9	26.7
20.2	89.2
9.1	42.0
28.2	115.4
10.9	48.2
40.2	133.2
9.5	58.0
29.0	164.8
9.9	71.1
23.2	122.5
10.2	42.3
31.7	178.3
15.7	73.6
45.6	126.7
10.8	45.3
41.8	126.7
7.9	40.6
40.2	81.3
8.0	29.3
16.4	50.1
8.4	19.1
19.5	82.0

Table B46. Cutting edge / Mass (CE/M) test results for quartzite and silcrete at PP5-6 by stratigraphic aggregate.

Quartzite and Silcrete: Cutting Edge / Mass Values			Total *n* = 3191	Kruskal-Wallis H: 1171	*p* (Significant ≤0.05) <0.00001
Uncorrected Mann-Whitney pairwise comparisons - (*p*):					
Stratigraphic aggregate	RBSR-Q	RBSR-S	NWR-Q	NWR-S	BCCSR-Q	BCCSR-S
RBSR-Q		<0.00001	0.1081	<0.00001	0.01	<0.00001
RBSR-S	<0.00001		0.0001	0.1543	<0.00001	0.0007
NWR-Q	0.1081	0.0001		<0.00001	0.5219	<0.00001
NWR-S	<0.00001	0.1543	<0.00001		<0.00001	0.4728
BCCSR/BAS-Q	0.01	<0.00001	0.5219	<0.00001		<0.00001
BCCSR/BAS-S	<0.00001	0.0007	<0.00001	0.4728	<0.00001	
OBS2-Q	0.06	0.0017	0.6614	0.00018	0.9620	<0.00001
OBS2-S	<0.00001	0.002	<0.00001	0.3521	<0.00001	0.5110
SGS-Q	0.04	0.1272	0.3479	0.02	0.4742	0.0016
SGS-S	<0.00001	0.1604	0.00001	0.7644	<0.00001	0.2769
OBS1-Q	0.036	0.00002	0.8609	<0.00001	0.5801	<0.00001
OBS1-S	<0.00001	0.017	<0.00001	0.5352	<0.00001	0.7799
SADBS Upper-Q	<0.00001	0.02	0.01	0.001	0.003	<0.00001
SADBS Upper-S	<0.00001	<0.00001	<0.00001	0.1248	<0.00001	0.07
SADBS Lower-Q	0.01	0.001	0.4451	0.00004	0.8233	<0.00001
SADBS Lower-S	<0.00001	0.0995	0.00004	0.7011	0.00001	0.9025
ALBS-Q	0.1682	<0.00001	0.6337	<0.00001	0.1928	<0.00001
ALBS-S	0.00002	0.6118	0.0007	0.6770	0.0008	0.2490
LBSR-Q	0.5859	<0.00001	0.08	<0.00001	0.00004	<0.00001
LBSR-S	<0.00001	0.0004	0.02	0.00001	0.0099	<0.00001
YBSR-Q	0.4830	<0.00001	0.027	<0.00001	0.001	<0.00001
YBSR-S	<0.00001	0.5394	0.001	0.056	0.0004	0.00028

0.01	0.002	0.2193	0.09	0.0007	0.007	0.1736	<0.00001	0.009	0.049	0.00002
0.02	<0.00001	0.01	<0.00001	0.01	<0.00001	<0.00001	<0.00001	0.0029	<0.00001	0.047
0.1712	<0.00001	0.8334	0.00002	0.006	<0.00001	0.3137	<0.00001	0.1509	0.0001	0.0002
0.03	<0.00001	0.04	<0.00001	0.01	<0.00001	<0.00001	<0.00001	0.004	<0.00001	0.096
0.007	0.1718	0.09	0.6592	0.001	0.3641	0.07	0.056	0.003	0.4395	0.00029
0.3875	<0.00001	0.2026	<0.00001	0.4170	<0.00001	0.0001	<0.00001	0.1719	<0.00001	
0.0007	0.6953	0.019	0.6309	0.00002	0.7970	0.0028	0.5159	0.0001		<0.00001
0.8499	<0.00001	0.6295	0.00007	0.4681	<0.00001	0.09	<0.00001		0.0001	0.1719
<0.00001	0.8469	0.0003	0.058	<0.00001	0.6080	<0.00001		<0.00001	0.5159	<0.00001
0.08	<0.00001	0.6436	0.001	0.0049	0.00002		<0.00001	0.09	0.0028	0.0001
0.00002	0.9252	0.007	0.3118	<0.00001		0.00002	0.6080	<0.00001	0.7970	<0.00001
0.7794	<0.00001	0.3545	<0.00001		<0.00001	0.0049	<0.00001	0.4681	0.00002	0.4170
0.00025	0.1959	0.039		<0.00001	0.3118	0.001	0.058	0.00007	0.6309	<0.00001
0.6010	0.006		0.039	0.3545	0.007	0.6436	0.0003	0.6295	0.019	0.2026
<0.00001		0.0056	0.1959	<0.00001	0.9252	<0.00001	0.8469	<0.00001	0.6953	<0.00001
	<0.00001	0.6010	0.00025	0.7794	0.00002	0.08	<0.00001	0.8499	0.0007	0.3875
<0.00001	0.5110	0.0016	0.2769	<0.00001	0.7799	<0.00001	0.07	<0.00001	0.9025	<0.00001
0.9620	<0.00001	0.4742	<0.00001	0.5801	<0.00001	0.003	<0.00001	0.8233	0.00001	0.1928
0.0002	0.3521	0.025	0.7644	<0.00001	0.5352	0.001	0.1248	0.00004	0.7011	<0.00001
0.6614	<0.00001	0.3479	0.00001	0.8609	<0.00001	0.01	<0.00001	0.4451	0.00004	0.6337
0.0017	0.002	0.1272	0.1604	0.00002	0.017	0.02	<0.00001	0.001	0.0995	<0.00001
0.06	<0.00001	0.04	<0.00001	0.036	<0.00001	<0.00001	<0.00001	0.01	<0.00001	0.1682
OBS2-Q	OBS2-S	SGS-Q	SGS-S	OBS1-Q	OBS1-S	Upper-Q	Upper-S	Lower-Q	Lower-S	ALBS-Q

0.3195	<0.00001	0.02	<0.00001		
<0.00001	0.2613	<0.00001		<0.00001	
0.004	<0.00001		<0.00001	0.02	
<0.00001		<0.00001	0.2613	<0.00001	
	<0.00001	0.004	<0.00001	0.3195	
0.00029	0.096	0.0002	0.047	0.00002	
0.4395	<0.00001	0.00010	<0.00001	0.049	
0.003	0.004	0.1509	0.003	0.009	
0.056	<0.00001	<0.00001	<0.00001	<0.00001	
0.07	<0.00001	0.3137	<0.00001	0.1736	
0.3641	<0.00001	<0.00001	<0.00001	0.007	
0.001	0.01	0.006	0.01	0.0007	
0.6592	<0.00001	0.00002	<0.00001	0.09	
0.09	0.035	0.8334	0.01	0.2193	
0.1718	<0.00001	<0.00001	<0.00001	0.0016	
0.007	0.03	0.1712	0.02	0.01	
0.2490	<0.00001	<0.00001	<0.00001	0.00028	
0.0008	0.00004	0.0099	0.001	0.0004	
0.6770	<0.00001	0.00001	<0.00001	0.056	
0.0007	0.08	0.02	0.027	0.001	
0.6118	<0.00001	0.0004	<0.00001	0.5394	
0.00002	0.5859	<0.00001	0.4830	<0.00001	
ALBS-S	LBSR-Q	LBSR-S	YBSR-Q	YBSR-S	

Values shaded in grey are significant (≤0.05). Q=Quartzite; S=Silcrete

CHAPTER 8: OAM HYPOTHSIS EVALUATION AND SENSITIVY ANALYSIS

Hypothesis 1 Evaluation

Hypothesis 1 – Same-day return outcomes

MIS4 without a Paleo-Agulhas plain silcrete source

Table B47. Comparison between ranked model frequencies from same-day return simulations of MIS4 conditions without a Paleo-Agulhas plain silcrete source and ranked MIS4 archaeological frequencies from PP5-6.

Raw material	MIS4 without a Paleo-Agulhas plain silcrete source*	MIS4-PP5-6
Quartz	1	2
Silcrete	3	1
Quartzite	2	1

* Ranking based on which raw materials have the highest mean frequency. Similar rankings in the table are due to statistically similar frequencies. Ranking based on MIS4 archaeological raw material frequencies from bootstrapped data in Figure 50 and Table 19. Similar rankings in the table are due to statistically similar frequencies.

MIS4 with a Paleo-Agulhas plain silcrete source

Table B48. Comparison between ranked model frequencies from same-day return simulations of MIS4 conditions with a Paleo-Agulhas plain silcrete source and ranked MIS4 archaeological frequencies from PP5-6.

Raw material	MIS4 with a Paleo-Agulhas plain silcrete source*	MIS4-PP5-6
Quartz	1	2
Silcrete	2	1
Quartzite	3	1

* Ranking based on which raw materials have the highest mean frequency. Similar rankings in the table are due to statistically similar frequencies. Ranking based on MIS4 archaeological raw material frequencies from bootstrapped data in Figure 50 and Table 19. Similar rankings in the table are due to statistically similar frequencies.

MIS5

Table B49. Comparison between ranked model frequencies from same-day return simulations of MIS5 conditions and ranked MIS5 archaeological frequencies from PP5-6, PP13B, PP9B, and PP9C.

Raw material	MIS5 conditions*	MIS5-PP5-6	MIS5-PP13B	MIS5-All PP
Quartz	1	3	2	3
Silcrete	3	2	2	2
Quartzite	2	1	1	1

* Ranking based on which raw materials have the highest mean frequency. Similar rankings in the table are due to statistically similar frequencies. Ranking based on MIS5 archaeological raw material frequencies from bootstrapped data in Figure 50 and Table 19. Similar rankings in the table are due to statistically similar frequencies.

MIS6 without a Paleo-Agulhas plain silcrete source

Table B50. Comparison between ranked model frequencies from same-day return simulations of MIS6 conditions without a Paleo-Agulhas plain silcrete source and ranked MIS6 archaeological frequencies from PP13B.

Raw material	MIS6 without a Paleo-Agulhas plain silcrete source*	MIS6-PP13B
Quartz	1	2
Silcrete	3	2
Quartzite	2	1

* Ranking based on which raw materials have the highest mean frequency. Similar rankings in the table are due to statistically similar frequencies. Ranking based on MIS6 archaeological raw material frequencies from bootstrapped data in Figure 50 and Table 19. Similar rankings in the table are due to statistically similar frequencies.

MIS6 with a Paleo-Agulhas plain silcrete source

Table B51. Comparison between ranked model frequencies from same-day return simulations of MIS6 conditions with a Paleo-Agulhas plain silcrete source and ranked MIS6 archaeological frequencies from PP13B.

Raw material	MIS6 with a Paleo-Agulhas plain silcrete source*	MIS6-PP13B
Quartz	1	2
Silcrete	2	2
Quartzite	3	1

* Ranking based on which raw materials have the highest mean frequency. Similar rankings in the table are due to statistically similar frequencies. Ranking based on MIS6 archaeological raw material frequencies from bootstrapped data in Figure 50 and Table 19. Similar rankings in the table are due to statistically similar frequencies.

OFAT1 modeling outcomes - Effect of increased movement budget

Table B52. Comparison between ranked model frequencies from OFAT1 simulations of MIS4 conditions without a Paleo-Agulhas plain silcrete source and ranked MIS4 archaeological frequencies from PP5-6.

	MIS4 without a Paleo-Agulhas plain silcrete source*						Archaeology
Raw Material	TT=50	TT=100	TT=500	TT=1000	TT=1500	TT=2000	MIS4-PP5-6
Quartz	1	1	1	1	2	2	2
Silcrete	2	3	3	3	3	3	1
Quartzite	2	2	2	2	1	1	1

* Ranking based on which raw materials have the highest mean frequency. Similar rankings in the table are due to statistically similar frequencies. Ranking based on MIS4 archaeological raw material frequencies from bootstrapped data in Figure 50 and Table 19. Similar rankings in the table are due to statistically similar frequencies.

Table B53. Comparison between ranked model frequencies from OFAT1 simulations of MIS4 conditions with a Paleo-Agulhas plain silcrete source and ranked MIS4 archaeological frequencies from PP5-6.

	MIS4 with a Paleo-Agulhas plain silcrete source*						Archaeology
Raw Material	**TT=50**	**TT=100**	**TT=500**	**TT=1000**	**TT=1500**	**TT=2000**	**MIS4-PP5-6**
Quartz	1	1	2	2	3	3	2
Silcrete	2	2	1	1	1	1	1
Quartzite	3	3	3	3	2	2	1

* Ranking based on which raw materials have the highest mean frequency. Similar rankings in the table are due to statistically similar frequencies. Ranking based on MIS4 archaeological raw material frequencies from bootstrapped data in Figure 50 and Table 19. Similar rankings in the table are due to statistically similar frequencies.

TableB54. Comparison between ranked model frequencies from OFAT1 simulations of MIS5 conditions and ranked MIS5 archaeological frequencies from PP5-6, PP13B, PP9B, and PP9C.

	MIS5 conditions*						Archaeology		
Raw Material	**TT=50**	**TT=100**	**TT=500**	**TT=1000**	**TT=1500**	**TT=2000**	**MIS5-PP5-6**	**MIS5-PP13B**	**MIS5-All PP**
Quartz	1	1	1	1	1	2	3	2	3
Silcrete	3	3	3	3	3	3	2	2	2
Quartzite	2	2	2	2	2	1	1	1	1

* Ranking based on which raw materials have the highest mean frequency. Similar rankings in the table are due to statistically similar frequencies. Ranking based on MIS5 archaeological raw material frequencies from bootstrapped data in Figure 50 and Table 19. Similar rankings in the table are due to statistically similar frequencies.

TableB55. Comparison between ranked model frequencies from OFAT1 simulations of MIS6 conditions without a Paleo-Agulhas plain silcrete source and ranked MIS6 archaeological frequencies from PP13B.

	MIS6 without a Paleo-Agulhas plain silcrete source						Archaeology
Raw Material	**TT=50**	**TT=100**	**TT=500**	**TT=1000**	**TT=1500**	**TT=2000**	**MIS6-PP13B**
Quartz	1	1	2	2	2	2	2
Silcrete	3	3	3	3	3	3	2
Quartzite	2	2	1	1	1	1	1

* Ranking based on which raw materials have the highest mean frequency. Similar rankings in the table are due to statistically similar frequencies. Ranking based on MIS6 archaeological raw material frequencies from bootstrapped data in Figure 50 and Table 19. Similar rankings in the table are due to statistically similar frequencies.

Table B56. Comparison between ranked model frequencies from OFAT1 simulations of MIS6 conditions with a Paleo-Agulhas plain silcrete source and ranked MIS6 archaeological frequencies from PP13B.

	MIS6 with a Paleo-Agulhas plain silcrete source						Archaeology
Raw Material	**TT=50**	**TT=100**	**TT=500**	**TT=1000**	**TT=1500**	**TT=2000**	**MIS6-PP13B**
Quartz	1	1	1	3	3	3	2
Silcrete	2	2	2	2	2	2	2
Quartzite	3	3	3	1	1	1	1

* Ranking based on which raw materials have the highest mean frequency. Similar rankings in the table are due to statistically similar frequencies. Ranking based on MIS6 archaeological raw material frequencies from bootstrapped data in Figure 50 and Table 19. Similar rankings in the table are due to statistically similar frequencies.

Is random walk a realistic raw material procurement strategy?

MIS4 without a Paleo-Agulhas plain silcrete source

Table B57. Frequency (%) of time without raw materials in toolkit descriptive statistics during MIS4 conditions without a Paleo-Agulhas plain silcrete source.

	TT=50	TT=100	TT=500	TT=1000	TT=1500	TT=2000
n (number of simulated assemblages)	1000	1000	1000	1000	1000	1000
First Quartile	0.000000	0.000000	0.000000	0.000000	0.000532	0.001847
Min	0.000000	0.000000	0.000000	0.000000	0.000000	0.000000
Median	0.000000	0.000989	0.000199	0.000599	0.001531	0.003145
Mean	0.002456	0.002011	0.001048	0.001192	0.001943	0.003598
Max	0.031341	0.027695	0.008973	0.009980	0.012646	0.013080
Third Quartile	0.003918	0.002967	0.001595	0.001896	0.002862	0.005130
SD	0.003726	0.003043	0.001560	0.001510	0.001820	0.002315
SE	0.000118	0.000096	0.000049	0.000048	0.000058	0.000073
Margin of error (95% CI)	0.000231	0.000189	0.000097	0.000094	0.000113	0.000144
Upper 95% CI	0.002687	0.002199	0.001145	0.001285	0.002055	0.003741
Lower 95% CI	0.002225	0.001822	0.000951	0.001098	0.001830	0.003454

Table B58. Frequency (%) of time without raw material in toolkit test results during MIS4 conditions without a Paleo-Agulhas plain silcrete source.

MIS4 without a Paleo-Agulhas Plain Silcrete Source-Frequency (%) of time without raw material in toolkit	**Total *n* =6000**	**Kruskal-Wallis H: 926.4**		***p* (Significant ≤0.05) <0.00001**	
Uncorrected Mann-Whitney pairwise comparisons - (*p*):					
	TT=50	TT=100	TT=500	TT=1000	TT=1500	TT=2000
TT=50		0.5127	0.0001	0.2390	<0.00001	<0.00001
TT=100	0.5127		0.00001	0.1789	<0.00001	<0.00001
TT=500	0.0001	0.00001		0.00001	<0.00001	<0.00001
TT=1000	0.2390	0.1789	0.00001		<0.00001	<0.00001
TT=1500	<0.00001	<0.00001	<0.00001	<0.00001		<0.00001
TT=2000	<0.00001	<0.00001	<0.00001	<0.00001	<0.00001	

Values shaded in grey are significant (≤0.05).

MIS4 with a Paleo-Agulhas plain silcrete source

Table B59. Frequency (%) of time without raw materials in toolkit descriptive statistics during MIS4 conditions without a Paleo-Agulhas plain silcrete source.

	TT=50	TT=100	TT=500	TT=1000	TT=1500	TT=2000
n (number of simulated assemblages)	1000	1000	1000	1000	1000	1000
First Quartile	0.000000	0.000000	0.000000	0.000000	0.000000	0.000000
Min	0.000000	0.000000	0.000000	0.000000	0.000000	0.000000

Median	0.000000	0.000000	0.000000	0.000000	0.000067	0.000200
Mean	0.001579	0.001153	0.000421	0.000347	0.000375	0.000642
Max	0.015671	0.012858	0.008175	0.004990	0.005591	0.006241
Third Quartile	0.001959	0.001978	0.000399	0.000299	0.000399	0.000949
SD	0.002372	0.001835	0.000829	0.000687	0.000680	0.000904
SE	0.000075	0.000058	0.000026	0.000022	0.000022	0.000029
Margin of error (95% CI)	0.000147	0.000114	0.000051	0.000043	0.000042	0.000056
Upper 95% CI	0.001726	0.001267	0.000473	0.000390	0.000417	0.000698
Lower 95% CI	0.001432	0.001040	0.000370	0.000305	0.000333	0.000586

Table B60. Frequency (%) of time without raw material in toolkit test results during MIS4 conditions without a Paleo-Agulhas plain silcrete source.

MIS4 with a Paleo-Agulhas Plain Silcrete Source-Frequency (%) of time without raw material in toolkit	**Total *n* = 6000**	**Kruskal-Wallis H: 150.1**		***p* (Significant ≤0.05) <0.00001**	
Uncorrected Mann-Whitney pairwise comparisons - (*p*):					
	TT=50	TT=100	TT=500	TT=1000	TT=1500	TT=2000
TT=50		0.2448	<0.00001	<0.00001	0.00001	0.6866
TT=100	0.2448		<0.00001	<0.00001	0.00010	0.053
TT=500	<0.00001	<0.00001		0.6519	0.008	<0.00001
TT=1000	<0.00001	<0.00001	0.6519		0.06	<0.00001
TT=1500	0.00001	0.0001	0.008	0.06		<0.00001
TT=2000	0.6866	0.053	<0.00001	<0.00001	<0.00001	

Values shaded in grey are significant (≤0.05).

MIS5

Table B61. Frequency (%) of time without raw materials in toolkit descriptive statistics during MIS5 conditions.

	TT=50	**TT=100**	**TT=500**	**TT=1000**	**TT=1500**	**TT=2000**
n (number of simulated assemblages)	1000	1000	1000	1000	1000	1000
First Quartile	0.000000	0.000000	0.000000	0.005589	0.025025	0.058812
Min	0.000000	0.000000	0.000000	0.000000	0.009651	0.030255
Median	0.001959	0.000989	0.000399	0.008982	0.030882	0.067349
Mean	0.002662	0.002074	0.001628	0.009980	0.031737	0.067671
Max	0.021547	0.020771	0.016550	0.036228	0.069484	0.105791
Third Quartile	0.003918	0.002967	0.002592	0.013373	0.037854	0.075811
SD	0.003598	0.003016	0.002352	0.005815	0.009369	0.012073
SE	0.000114	0.000095	0.000074	0.000184	0.000296	0.000382
Margin of error (95% CI)	0.000223	0.000187	0.000146	0.000360	0.000581	0.000748
Upper 95% CI	0.002885	0.002261	0.001774	0.010340	0.032317	0.068419
Lower 95% CI	0.002439	0.001887	0.001482	0.009620	0.031156	0.066923

Table B62. Frequency (%) of time without raw material in toolkit test results during MIS5 conditions.

MIS5-Frequency (%) of time without raw material in toolkit		**Total *n* = 6000**	**Kruskal-Wallis H: 4824**		***p* (Significant ≤0.05) <0.00001**	
Uncorrected Mann-Whitney pairwise comparisons - (*p*):						
	TT=50	TT=100	TT=500	TT=1000	TT=1500	TT=2000
TT=50		0.1020	0.003	<0.00001	<0.00001	<0.00001
TT=100	0.1020		0.6146	<0.00001	<0.00001	<0.00001
TT=500	0.003	0.6146		<0.00001	<0.00001	<0.00001
TT=1000	<0.00001	<0.00001	<0.00001		<0.00001	<0.00001
TT=1500	<0.00001	<0.00001	<0.00001	<0.00001		<0.00001
TT=2000	<0.00001	<0.00001	<0.00001	<0.00001	<0.00001	

Values shaded in grey are significant (≤0.05).

MIS6 without a Paleo-Agulhas plain silcrete source

Table B63. Frequency (%) of time without raw materials in toolkit descriptive statistics during MIS6 conditions without a Paleo-Agulhas plain silcrete source.

	TT=50	**TT=100**	**TT=500**	**TT=1000**	**TT=1500**	**TT=2000**
n (number of simulated assemblages)	1000	1000	1000	1000	1000	1000
First Quartile	0.000000	0.000000	0.000000	0.000000	0.000000	0.000000
Min	0.000000	0.000000	0.000000	0.000000	0.000000	0.000000
Median	0.000000	0.000000	0.000000	0.000000	0.000000	0.000000
Mean	0.001005	0.000759	0.000342	0.000189	0.000168	0.000139
Max	0.013712	0.007913	0.005184	0.003094	0.002862	0.001997
Third Quartile	0.001959	0.000989	0.000399	0.000200	0.000133	0.000100
SD	0.001824	0.001237	0.000572	0.000393	0.000355	0.000299
SE	0.000058	0.000039	0.000018	0.000012	0.000011	0.000009
Margin of error (95% CI)	0.000113	0.000077	0.000035	0.000024	0.000022	0.000019
Upper 95% CI	0.001118	0.000835	0.000377	0.000213	0.000190	0.000157
Lower 95% CI	0.000892	0.000682	0.000307	0.000164	0.000146	0.000120

Table B64. Frequency (%) of time without raw material in toolkit test results during MIS6 conditions without a Paleo-Agulhas plain silcrete source.

MIS6 without a Paleo-Agulhas Plain Silcrete Source-Frequency (%) of time without raw material in toolkit		**Total *n* = 6000**	**Kruskal-Wallis H: 42.49**		***p* (Significant ≤0.05) <0.00001**	
Uncorrected Mann-Whitney pairwise comparisons - (*p*):						
	TT=50	TT=100	TT=500	TT=1000	TT=1500	TT=2000
TT=50		0.1297	0.7004	0.059	0.3396	0.4555
TT=100	0.1297		0.026	<0.00001	<0.00001	<0.00001
TT=500	0.7004	0.026		<0.00001	<0.00001	<0.00001
TT=1000	0.059	<0.00001	<0.00001		0.8326	0.3708

TT=1500	0.3396	<0.00001	<0.00001	0.8326		0.2820
TT=2000	0.4555	<0.00001	<0.00001	0.3708	0.2820	

Values shaded in grey are significant (≤0.05).

MIS6 with a Paleo-Agulhas plain silcrete source

Table B65. Frequency (%) of time without raw materials in toolkit descriptive statistics during MIS6 conditions witha Paleo-Agulhas plain silcrete source.

	TT=50	TT=100	TT=500	TT=1000	TT=1500	TT=2000
n (number of simulated assemblages)	1000	1000	1000	1000	1000	1000
First Quartile	0.000000	0.000000	0.000000	0.000000	0.000000	0.000000
Min	0.000000	0.000000	0.000000	0.000000	0.000000	0.000000
Median	0.000000	0.000000	0.000000	0.000000	0.000000	0.000000
Mean	0.000803	0.000575	0.000208	0.000140	0.000133	0.000096
Max	0.011753	0.008902	0.003390	0.002894	0.003594	0.001548
Third Quartile	0.001959	0.000989	0.000199	0.000100	0.000067	0.000050
SD	0.001543	0.001062	0.000446	0.000332	0.000325	0.000245
SE	0.000049	0.000034	0.000014	0.000010	0.000010	0.000008
Margin of error (95% CI)	0.000096	0.000066	0.000028	0.000021	0.000020	0.000015
Upper 95% CI	0.000899	0.000640	0.000236	0.000160	0.000153	0.000111
Lower 95% CI	0.000707	0.000509	0.000180	0.000119	0.000113	0.000081

Table B66. Frequency (%) of time without raw material in toolkit test results during MIS6 conditions with a Paleo-Agulhas plain silcrete source.

MIS6 with a Paleo-Agulhas Plain Silcrete Source-Frequency (%) of time without raw material in toolkit		**Total *n* =6000**	**Kruskal-Wallis H: 15.46**		***p* (Significant ≤0.05) <0.00001**	
Uncorrected Mann-Whitney pairwise comparisons - (*p*):						
	TT=50	TT=100	TT=500	TT=1000	TT=1500	TT=2000
TT=50		0.4512	0.1011	0.1464	0.6343	0.2667
TT=100	0.4512		0.0005	0.00007	0.002	0.00009
TT=500	0.1011	0.0005		0.2828	0.6290	0.047
TT=1000	0.1464	0.00007	0.2828		0.7497	0.2943
TT=1500	0.6343	0.002	0.6290	0.7497		0.01838
TT=2000	0.2667	0.00009	0.047	0.2943	0.01838	

Values shaded in grey are significant (≤0.05).

OFAT 2 - Pinnacle Point only one of three localities to return too

MIS4 without a Paleo-Agulhas plain silcrete source

Table B67. Summary statistics and test results for OFAT2 modeling MIS4 conditions without a Paleo-Agulhas plain silcrete source compared to MIS4 archaeological raw material frequency data from PP5-6.

	TT=50-Quartz	**TT=100-Quartz**	**TT=500-Quartz**	**TT=1000-Quartz**	**TT=1500-Quartz**	**TT=2000-Quartz**	**PP5-6-MIS4-Quartz**
n (number of simulated assemblages)	1000	1000	1000	1000	1000	1000	46
First Quartile	100.00	76.83	31.93	23.18	18.74	16.27	1.21
Min	0.00	31.84	20.05	15.79	10.96	8.84	0.00
Median	100.00	83.52	35.29	25.65	21.31	18.60	3.73
Mean	99.73	82.22	35.25	25.79	21.31	18.62	8.39
Max	100.00	100.00	48.69	40.24	32.32	28.79	66.11
Third Quartile	100.00	88.88	38.29	28.18	23.72	20.89	10.53
SD	3.30	9.54	4.75	3.71	3.52	3.42	11.83
SE	0.10	0.30	0.15	0.12	0.11	0.11	1.67*
Margin of error (95% CI)	0.20	0.59	0.29	0.23	0.22	0.21	3.28
Upper 95% CI	99.93	82.81	35.54	26.02	21.53	18.84	11.66*
Lower 95% CI	99.53	81.63	34.95	25.56	21.09	18.41	5.11*
	TT=50-Silcrete	**TT=100-Silcrete**	**TT=500-Silcrete**	**TT=1000-Silcrete**	**TT=1500-Silcrete**	**TT=2000-Silcrete**	**PP5-6-MIS4-Silcrete**
n (number of simulated assemblages)	1000	1000	1000	1000	1000	1000	46
First Quartile	0.00	0.00	3.05	4.63	5.70	6.32	13.79
Min	0.00	0.00	0.00	1.06	0.56	0.00	0.00
Median	0.00	0.00	3.94	5.81	6.94	7.84	39.13
Mean	0.00	0.29	4.12	5.91	7.11	7.91	40.00
Max	0.00	6.53	11.06	12.24	15.50	15.82	96.55
Third Quartile	0.00	0.36	5.09	7.07	8.43	9.37	62.77
SD	0.00	0.64	1.65	1.90	2.10	2.27	27.52
SE	0.00	0.02	0.05	0.06	0.07	0.07	4.01*
Margin of error (95% CI)	0.00	0.04	0.10	0.12	0.13	0.14	7.85
Upper 95% CI	0.00	0.33	4.22	6.03	7.24	8.05	47.85*
Lower 95% CI	0.00	0.25	4.02	5.80	6.98	7.77	32.15*
	TT=50-Quartzite	**TT=100-Quartzite**	**TT=500-Quartzite**	**TT=1000-Quartzite**	**TT=1500-Quartzite**	**TT=2000-Quartzite**	**PP5-6-MIS4-Quartzite**
n (number of simulated assemblages)	1000	1000	1000	1000	1000	1000	46
First Quartile	0.00	10.80	57.58	65.61	68.93	70.87	5.19
Min	0.00	0.00	47.14	55.96	58.29	61.59	0.00
Median	0.00	16.12	60.65	68.37	71.66	73.43	43.00

Mean	0.17	17.49	60.64	68.30	71.58	73.46	44.63
Max	11.11	65.91	75.00	80.11	81.82	85.21	96.45
Third Quartile	0.00	22.77	63.89	70.87	74.35	76.15	68.24
SD	0.96	9.39	4.71	3.80	3.83	3.72	25.54
SE	0.03	0.30	0.15	0.12	0.12	0.12	3.71*
Margin of error (95% CI)	0.06	0.58	0.29	0.24	0.24	0.23	7.27
Upper 95% CI	0.23	18.07	60.93	68.53	71.82	73.69	51.90*
Lower 95% CI	0.11	16.91	60.34	68.06	71.35	73.23	37.35*

*Margins of error (95% CI) for archaeological data were obtained by bootstrapping the standard errors 10000 times.

Table B68. Comparison between ranked model frequencies from OFAT2 simulations of MIS4 conditions without a Paleo-Agulhas plain silcrete source and ranked MIS4 archaeological frequencies from PP5-6.

	MIS4 without a Paleo-Agulhas plain silcrete source*						Archaeology
Raw Material	**TT=50**	**TT=100**	**TT=500**	**TT=1000**	**TT=1500**	**TT=2000**	**MIS4-PP5-6**
Quartz	1	1	2	2	2	2	2
Silcrete	3	3	3	3	3	3	1
Quartzite	2	2	1	1	1	1	1

* Ranking based on which raw materials have the highest mean frequency. Similar rankings in the table are due to statistically similar frequencies. Ranking based on MIS4 archaeological raw material frequencies from bootstrapped data in Figure 50 and Table 19. Similar rankings in the table are due to statistically similar frequencies.

MIS4 with a Paleo-Agulhas plain silcrete source

Table B69. Summary statistics and test results for OFAT2 modeling of MIS4 conditions with a Paleo-Agulhas plain silcrete source compared to MIS4 archaeological raw material frequency data from PP5-6.

	TT=50-Quartz	**TT=100-Quartz**	**TT=500-Quartz**	**TT=1000-Quartz**	**TT=1500-Quartz**	**TT=2000-Quartz**	**PP5-6-MIS4-Quartz**
n (number of simulated assemblages)	1000	1000	1000	1000	1000	1000	46
First Quartile	66.15	46.08	16.34	11.49	9.35	7.76	1.21
Min	0.00	0.00	8.40	5.97	3.54	3.03	0.00
Median	68.59	51.24	18.37	13.49	10.88	9.32	3.73
Mean	68.35	50.60	18.56	13.45	11.04	9.50	8.39
Max	100.00	100.00	29.22	23.67	20.38	18.38	66.11
Third Quartile	71.02	55.51	20.68	15.27	12.63	11.05	10.53
SD	5.82	8.55	3.27	2.75	2.51	2.36	11.83
SE	0.18	0.27	0.10	0.09	0.08	0.07	1.67*
Margin of error (95% CI)	0.36	0.53	0.20	0.17	0.16	0.15	3.28
Upper 95% CI	68.71	51.13	18.77	13.62	11.19	9.65	11.66*
Lower 95% CI	67.99	50.07	18.36	13.28	10.88	9.36	5.11*
	TT=50-Silcrete	**TT=100-Silcrete**	**TT=500-Silcrete**	**TT=1000-Silcrete**	**TT=1500-Silcrete**	**TT=2000-Silcrete**	**PP5-6-MIS4-Silcrete**
n (number of simulated	1000	1000	1000	1000	1000	1000	46

assemblages)							
First Quartile	28.81	28.95	29.52	30.24	30.07	29.61	13.79
Min	0.00	0.00	19.70	22.24	20.84	19.49	0.00
Median	31.28	33.53	32.03	32.82	32.72	32.35	39.13
Mean	31.25	32.79	32.15	32.81	32.71	32.44	40.00
Max	71.23	100.00	44.97	44.35	44.62	44.60	96.55
Third Quartile	33.69	37.07	34.82	35.34	35.22	35.19	62.77
SD	5.16	7.33	3.82	3.77	3.89	3.90	27.52
SE	0.16	0.23	0.12	0.12	0.12	0.12	4.01*
Margin of error (95% CI)	0.32	0.45	0.24	0.23	0.24	0.24	7.85
Upper 95% CI	31.57	33.25	32.39	33.05	32.95	32.68	47.85*
Lower 95% CI	30.93	32.34	31.92	32.58	32.46	32.20	32.15*
	TT=50-Quartzite	**TT=100-Quartzite**	**TT=500-Quartzite**	**TT=1000-Quartzite**	**TT=1500-Quartzite**	**TT=2000-Quartzite**	**PP5-6-MIS4-Quartzite**
n (number of simulated assemblages)	1000	1000	1000	1000	1000	1000	46
First Quartile	0.00	10.24	46.19	51.03	53.23	55.24	5.19
Min	0.00	0.00	37.23	42.03	44.81	44.86	0.00
Median	0.00	14.81	49.23	53.70	56.30	58.06	43.00
Mean	0.20	16.30	49.28	53.74	56.26	58.06	44.63
Max	44.44	75.00	62.79	67.02	69.14	68.99	96.45
Third Quartile	0.00	20.90	52.28	56.27	59.16	61.04	68.24
SD	1.75	8.85	4.45	4.06	4.20	4.11	25.54
SE	0.06	0.28	0.14	0.13	0.13	0.13	3.71*
Margin of error (95% CI)	0.11	0.55	0.28	0.25	0.26	0.26	7.27
Upper 95% CI	0.31	16.85	49.56	53.99	56.52	58.31	51.90*
Lower 95% CI	0.09	15.75	49.01	53.49	56.00	57.80	37.35*

*Margins of error (95% CI) for archaeological data were obtained by bootstrapping the standard errors 10000 times.

Table B70. Comparison between ranked model frequencies from OFAT2 simulations of MIS4 conditions with a Paleo-Agulhas plain silcrete source and ranked MIS4 archaeological frequencies from PP5-6.

	MIS4 with a Paleo-Agulhas plain silcrete source*						**Archaeology**
Raw Material	**TT=50**	**TT=100**	**TT=500**	**TT=1000**	**TT=1500**	**TT=2000**	**MIS4-PP5-6**
Quartz	1	1	3	3	3	3	2
Silcrete	2	2	2	2	2	2	1
Quartzite	3	3	1	1	1	1	1

* Ranking based on which raw materials have the highest mean frequency. Similar rankings in the table are due to statistically similar frequencies. Ranking based on MIS4 archaeological raw material frequencies from bootstrapped data in Figure 50 and Table 19. Similar rankings in the table are due to statistically similar frequencies.

MIS5

Table B71. Summary statistics and test results for OFAT2 modeling of MIS5 conditions compared to MIS5 archaeological raw material frequency data from PP5-6, PP13B, PP9B, and PP9C.

	TT=50-Quartz	TT=100-Quartz	TT=500-Quartz	TT=1000-Quartz	TT=1500-Quartz	TT=2000-Quartz	PP5-6-MIS5-Quartz	PP13B-MIS5-Quartz	AllPP-MIS5-Quartz
n (number of assemblages)	1000	1000	1000	1000	1000	1000	31	7	43
First Quartile	82.79	70.10	40.19	32.75	28.09	24.92	0.00	1.71	0.10
Min	0.00	44.40	29.91	22.69	20.36	17.69	0.00	0.00	0.00
Median	84.39	73.91	42.58	35.24	30.10	27.16	0.89	2.15	2.65
Mean	84.12	73.50	42.60	35.14	30.26	27.17	3.53	4.41	4.61
Max	100.00	100.00	54.30	47.46	41.37	38.95	24.87	9.39	24.87
Third Quartile	86.00	77.40	45.30	37.41	32.37	29.28	3.92	9.33	6.95
SD	5.11	6.47	3.81	3.43	3.25	3.32	5.94	3.91	6.03
SE	0.16	0.20	0.12	0.11	0.10	0.10	1.03	1.40	0.90*
Margin of error (95% CI)	0.32	0.40	0.24	0.21	0.20	0.21	2.03	2.74	1.76
Upper 95% CI	84.43	73.90	42.84	35.35	30.46	27.38	5.56	7.15	6.37*
Lower 95% CI	83.80	73.10	42.36	34.93	30.05	26.96	1.51	1.68	2.85*
	TT=50-Silcrete	**TT=100-Silcrete**	**TT=500-Silcrete**	**TT=1000-Silcrete**	**TT=1500-Silcrete**	**TT=2000-Silcrete**	**PP5-6-MIS5-Silcrete**	**PP13B-Silcrete**	**AllPP-MIS5-Silcrete**
n (number of assemblages)	1000	1000	1000	1000	1000	1000	31	7	4.30E+01
First Quartile	0.08	0.10	13.35	17.64	20.13	22.09	1.45	0.00	0.95
Min	0.00	0.00	7.71	10.61	12.97	15.29	0.00	0.00	0.00
Median	0.09	0.14	15.25	19.61	22.41	24.11	10.19	0.00	6.44
Mean	0.09	1.32	15.45	19.74	22.49	24.25	16.97	1.09	13.05
Max	0.89	43.35	27.15	34.05	32.97	35.67	64.83	5.01	64.83
Third Quartile	0.10	1.84	17.36	21.66	24.67	26.34	32.95	2.55	21.21
SD	0.03	2.51	3.11	3.14	3.26	3.23	17.85	1.97	16.45
SE	0.00	0.08	0.10	0.10	0.10	0.10	3.14	0.68	2.46*
Margin of error (95% CI)	0.00	0.16	0.19	0.19	0.20	0.20	6.16	1.34	4.82
Upper 95% CI	0.10	1.48	15.64	19.93	22.69	24.45	23.12	2.42	17.86*
Lower 95% CI	0.09	1.16	15.25	19.54	22.29	24.05	10.81	0.00	8.23*
	TT=50-Quartzite	**TT=100-Quartzite**	**TT=500-Quartzite**	**TT=1000-Quartzite**	**TT=1500-Quartzite**	**TT=2000-Quartzite**	**P5-6-MIS5-Quartzite**	**PP13B-Silcrete**	**AllPP-MIS5-Quartzite**

n (number of assemblages)	1000	1000	1000	1000	1000	1000	31	7	43
First Quartile	13.84	21.40	39.15	42.50	44.68	46.02	60.24	87.62	64.30
Min	0.00	0.00	30.45	33.61	36.01	36.50	26.94	87.62	26.94
Median	15.44	24.91	41.80	44.94	47.29	48.61	76.11	97.85	83.74
Mean	15.53	25.11	41.88	45.05	47.18	48.50	72.77	94.34	77.20
Max	58.63	55.04	56.20	59.54	58.41	61.19	100.00	100.00	100.00
Third Quartile	17.02	28.53	44.52	47.51	49.70	50.98	92.83	98.29	92.83
SD	3.49	6.15	3.82	3.57	3.67	3.87	21.79	5.37	20.01
SE	0.11	0.19	0.12	0.11	0.12	0.12	3.85	1.92	3.00*
Margin of error (95% CI)	0.22	0.38	0.24	0.22	0.23	0.24	7.55	3.76	5.87
Upper 95% CI	15.74	25.49	42.12	45.27	47.40	48.74	80.32	98.10	83.07*
Lower 95% CI	15.31	24.73	41.65	44.83	46.95	48.26	65.21	90.58	71.33*

*Margins of error (95% CI) for archaeological data were obtained by bootstrapping the standard errors 10000 times.

Table B72. Comparison between ranked model frequencies from OFAT2 simulations of MIS5 conditions and ranked MIS5 archaeological frequencies from PP13B, PP9B, PP9C, and PP5-6.

	MIS5 conditions*						Archaeology		
Raw Material	**TT=50**	**TT=100**	**TT=500**	**TT=1000**	**TT=1500**	**TT=2000**	**MIS5-PP5-6**	**MIS5-PP13B**	**MIS5-All PP**
Quartz	1	1	1	2	2	2	3	2	3
Silcrete	3	3	3	3	3	3	2	2	2
Quartzite	2	2	2	1	1	1	1	1	1

* Ranking based on which raw materials have the highest mean frequency. Similar rankings in the table are due to statistically similar frequencies. Ranking based on MIS5 archaeological raw material frequencies from bootstrapped data in Figure 50 and Table 19. Similar rankings in the table are due to statistically similar frequencies.

MIS6 without a Paleo-Agulhas plain silcrete source

Table B73. Summary statistics and test results for OFAT2 modeling of MIS6 conditions without a Paleo-Agulhas plain silcrete source compared to MIS6 archaeological raw material frequency data from PP13B.

	TT=50-Quartz	**TT=100-Quartz**	**TT=500-Quartz**	**TT=1000-Quartz**	**TT=1500-Quartz**	**TT=2000-Quartz**	**PP13-MIS6-Quartz**
n (number of assemblages)	1000	1000	1000	1000	1000	1000	7
First Quartile	84.62	50.01	16.01	11.03	9.17	7.93	1.71
Min	0.00	0.00	7.28	4.75	2.18	1.14	0.00
Median	86.91	58.09	18.95	13.40	11.20	9.90	2.15
Mean	86.16	57.01	18.97	13.58	11.40	10.06	4.41
Max	100.00	100.00	34.55	27.02	23.96	22.32	9.39
Third Quartile	88.92	65.15	21.92	16.04	13.44	12.13	9.33
SD	6.30	12.51	4.36	3.58	3.22	3.17	3.91

SE	0.20	0.40	0.14	0.11	0.10	0.10	1.40*
Margin of error (95% CI)	0.39	0.78	0.27	0.22	0.20	0.20	2.74
Upper 95% CI	86.55	57.79	19.24	13.80	11.60	10.26	7.15*
Lower 95% CI	85.77	56.24	18.70	13.36	11.20	9.86	1.68*
	TT=50-Silcrete	**TT=100-Silcrete**	**TT=500-Silcrete**	**TT=1000-Silcrete**	**TT=1500-Silcrete**	**TT=2000-Silcrete**	**PP13B-MIS6-Silcrete**
n (number of assemblages)	1000	1000	1000	1000	1000	1000	7
First Quartile	0.00	0.00	2.72	4.18	5.16	6.06	0.00
Min	0.00	0.00	0.00	0.00	0.98	0.87	0.00
Median	0.00	0.00	4.02	5.77	6.91	7.88	0.00
Mean	0.00	0.41	4.23	5.99	7.16	8.11	1.09
Max	0.00	14.14	14.56	15.84	16.50	18.56	5.01
Third Quartile	0.00	0.50	5.55	7.60	9.00	10.00	2.55
SD	0.00	0.99	2.11	2.53	2.69	2.86	1.97
SE	0.00	0.03	0.07	0.08	0.08	0.09	0.68*
Margin of error (95% CI)	0.00	0.06	0.13	0.16	0.17	0.18	1.34
Upper 95% CI	0.00	0.47	4.36	6.14	7.33	8.28	2.42*
Lower 95% CI	0.00	0.35	4.10	5.83	6.99	7.93	0.00*
	TT=50-Quartzite	**TT=100-Quartzite**	**TT=500-Quartzite**	**TT=1000-Quartzite**	**TT=1500-Quartzite**	**TT=2000-Quartzite**	**PP13B-MIS6-Quartzite**
n (number of assemblages)	1000	1000	1000	1000	1000	1000	7
First Quartile	11.06	34.62	74.02	77.67	78.87	79.32	87.62
Min	0.00	0.00	61.95	63.46	65.14	69.95	87.62
Median	13.07	41.47	76.86	80.58	81.57	81.96	97.85
Mean	13.64	42.58	76.80	80.44	81.44	81.83	94.34
Max	51.16	100.00	89.25	93.26	93.26	95.40	100.00
Third Quartile	15.38	49.35	80.00	83.33	84.28	84.69	98.29
SD	5.02	12.36	4.52	4.22	4.04	4.06	5.37
SE	0.16	0.39	0.14	0.13	0.13	0.13	1.92*
Margin of error (95% CI)	0.31	0.77	0.28	0.26	0.25	0.25	3.76
Upper 95% CI	13.95	43.35	77.08	80.70	81.69	82.08	98.10*
Lower 95% CI	13.33	41.81	76.52	80.17	81.19	81.58	90.58*

*Margins of error (95% CI) for archaeological data were obtained by bootstrapping the standard errors 10000 times.

Table B74. Comparison between ranked model frequencies from OFAT2 simulations of MIS6 conditions without a Paleo-Agulhas plain silcrete source and ranked MIS6 archaeological frequencies from PP13B.

	MIS6 without a Paleo-Agulhas plain silcrete source*						Archaeology
Raw Material	**TT=50**	**TT=100**	**TT=500**	**TT=1000**	**TT=1500**	**TT=2000**	**MIS6-PP13B**
Quartz	1	1	2	2	2	2	2
Silcrete	3	3	3	3	3	3	2
Quartzite	2	2	1	1	1	1	1

* Ranking based on which raw materials have the highest mean frequency. Similar rankings in the table are due to statistically similar frequencies. Ranking based on MIS6 archaeological raw material frequencies from bootstrapped data in Figure 50 and Table 19. Similar rankings in the table are due to statistically similar frequencies.

MIS6 with a Paleo-Agulhas plain silcrete source

Table B75. Summary statistics and test results for OFAT2 modeling of MIS6 conditions with a Paleo-Agulhas plain silcrete source compared to MIS6 archaeological raw material frequency data from PP13B.

	TT=50-Quartz	**TT=100-Quartz**	**TT=500-Quartz**	**TT=1000-Quartz**	**TT=1500-Quartz**	**TT=2000-Quartz**	**PP13-MIS6-Quartz**
n (number of assemblages)	1000	1000	1000	1000	1000	1000	7
First Quartile	64.21	38.11	12.02	8.39	7.06	5.87	1.71
Min	0.00	0.00	1.09	1.92	0.05	0.05	0.00
Median	68.09	45.29	14.42	10.72	9.14	7.72	2.15
Mean	67.24	44.83	14.58	10.73	9.21	7.96	4.41
Max	100.00	100.00	28.60	24.04	23.42	20.88	9.39
Third Quartile	70.99	51.77	17.11	12.77	11.05	9.73	9.33
SD	8.89	11.71	3.87	3.19	3.11	2.93	3.91
SE	0.28	0.37	0.12	0.10	0.10	0.09	1.40*
Margin of error (95% CI)	0.55	0.73	0.24	0.20	0.19	0.18	2.74
Upper 95% CI	67.79	45.56	14.82	10.93	9.40	8.14	7.15*
Lower 95% CI	66.69	44.10	14.34	10.53	9.02	7.77	1.68*
	TT=50-Silcrete	**TT=100-Silcrete**	**TT=500-Silcrete**	**TT=1000-Silcrete**	**TT=1500-Silcrete**	**TT=2000-Silcrete**	**PP13B-MIS6-Silcrete**
n (number of assemblages)	1000	1000	1000	1000	1000	1000	7
First Quartile	26.25	20.61	19.67	19.20	19.27	19.25	0.00
Min	0.00	0.00	9.16	8.10	8.67	7.02	0.00
Median	29.07	25.65	22.56	22.18	22.01	21.87	0.00
Mean	29.68	26.16	22.68	22.27	22.14	22.04	1.09
Max	100.00	100.00	37.52	36.63	36.87	36.73	5.01
Third Quartile	32.52	31.20	25.59	25.34	24.91	24.93	2.55
SD	8.36	9.11	4.36	4.49	4.11	4.44	1.97
SE	0.26	0.29	0.14	0.14	0.13	0.14	0.68*
Margin of error (95% CI)	0.52	0.56	0.27	0.28	0.25	0.28	1.34
Upper 95% CI	30.20	26.73	22.95	22.55	22.40	22.31	2.42*

Lower 95% CI	29.16	25.60	22.41	21.99	21.89	21.76	0.00*
	TT=50-Quartzite	**TT=100-Quartzite**	**TT=500-Quartzite**	**TT=1000-Quartzite**	**TT=1500-Quartzite**	**TT=2000-Quartzite**	**PP13B-MIS6-Quartzite**
n (number of assemblages)	1000	1000	1000	1000	1000	1000	7
First Quartile	1.88	21.13	58.97	63.64	65.22	66.67	87.62
Min	0.00	0.00	46.02	52.34	53.21	51.49	87.62
Median	2.64	27.95	62.73	67.11	68.82	70.09	97.85
Mean	3.08	28.91	62.74	67.00	68.65	70.01	94.34
Max	72.73	88.24	79.81	81.25	82.98	86.49	100.00
Third Quartile	3.47	35.57	66.35	70.59	72.03	73.42	98.29
SD	3.94	12.07	5.25	4.99	4.83	5.09	5.37
SE	0.12	0.38	0.17	0.16	0.15	0.16	1.92*
Margin of error (95% CI)	0.24	0.75	0.33	0.31	0.30	0.32	3.76
Upper 95% CI	3.33	29.65	63.07	67.31	68.95	70.32	98.10*
Lower 95% CI	2.84	28.16	62.42	66.69	68.35	69.69	90.58*

*Margins of error (95% CI) for archaeological data were obtained by bootstrapping the standard errors 10000 times.

Table B76. Comparison between ranked model frequencies from OFAT2 simulations of MIS6 conditions with a Paleo-Agulhas plain silcrete source and ranked MIS6 archaeological frequencies from PP13B.

	MIS6 with a Paleo-Agulhas plain silcrete source*						**Archaeology**
Raw Material	**TT=50**	**TT=100**	**TT=500**	**TT=1000**	**TT=1500**	**TT=2000**	**MIS6-PP13B**
Quartz	1	1	3	3	3	3	2
Silcrete	2	3	2	2	2	2	2
Quartzite	3	2	1	1	1	1	1

* Ranking based on which raw materials have the highest mean frequency. Similar rankings in the table are due to statistically similar frequencies. Ranking based on MIS6 archaeological raw material frequencies from bootstrapped data in Figure 50 and Table 19. Similar rankings in the table are due to statistically similar frequencies.

OFAT 3 - Changing Discard probabilities and toolkit size

Return to starting locality

MIS4 without a Paleo-Agulhas plain silcrete source - Discard probability at locality (PDC-ProbDiscardCamp parameter)

Table B77. Summary statistics and test results for OFAT3 modeling of MIS4 conditions without a Paleo-Agulhas plain silcrete source compared to MIS4 archaeological raw material frequency data from PP5-6.

	PDC=0.001-Quartz	**PDC=0.1-Quartz**	**PDC=0.5-Quartz**	**PDC=0.75-Quartz**	**PDC=0.95-Quartz**	**PP5-6-MIS4-Quartz**
n (number of simulated assemblages)	1000	1000	1000	1000	1000	46
First Quartile	100.00	99.84	99.90	99.84	99.82	1.21
Min	88.89	99.27	99.51	99.13	99.45	0.00
Median	100.00	100.00	100.00	100.00	100.00	3.73

Mean	99.79	99.91	99.94	99.92	99.91	8.39
Max	100.00	100.00	100.00	100.00	100.00	66.11
Third Quartile	100.00	100.00	100.00	100.00	100.00	10.53
SD	1.21	0.16	0.12	0.13	0.14	11.83
SE	0.12	0.02	0.01	0.01	0.01	1.67*
Margin of error (95% CI)	0.24	0.03	0.02	0.03	0.03	3.28
Upper 95% CI	100.03	99.94	99.96	99.95	99.94	11.66*
Lower 95% CI	99.55	99.88	99.91	99.90	99.88	5.11*
	PDC=0.001-Silcrete	**PDC=0.1-Silcrete**	**PDC=0.5-Silcrete**	**PDC=0.75-Silcrete**	**PDC=0.95-Silcrete**	**PP5-6-MIS4-Silcrete**
n (number of simulated assemblages)	1000	1000	1000	1000	1000	46
First Quartile	0.00	0.00	0.00	0.00	0.00	13.79
Min	0.00	0.00	0.00	0.00	0.00	0.00
Median	0.00	0.00	0.00	0.00	0.00	39.13
Mean	0.00	0.00	0.00	0.00	0.00	40.00
Max	0.00	0.00	0.00	0.00	0.00	96.55
Third Quartile	0.00	0.00	0.00	0.00	0.00	62.77
SD	0.00	0.00	0.00	0.00	0.00	27.52
SE	0.00	0.00	0.00	0.00	0.00	4.01*
Margin of error (95% CI)	0.00	0.00	0.00	0.00	0.00	7.85
Upper 95% CI	0.00	0.00	0.00	0.00	0.00	47.85*
Lower 95% CI	0.00	0.00	0.00	0.00	0.00	32.15*
	PDC=0.001-Quartzite	**PDC=0.1-Quartzite**	**PDC=0.5-Quartzite**	**PDC=0.75-Quartzite**	**PDC=0.95-Quartzite**	**PP5-6-MIS4-Quartzite**
n (number of simulated assemblages)	1000	1000	1000	1000	1000	46
First Quartile	0.00	0.00	0.00	0.00	0.00	5.19
Min	0.00	0.00	0.00	0.00	0.00	0.00
Median	0.00	0.00	0.00	0.00	0.00	43.00
Mean	0.21	0.09	0.06	0.08	0.09	44.63
Max	11.11	0.73	0.49	0.87	0.55	96.45
Third Quartile	0.00	0.16	0.10	0.16	0.18	68.24
SD	1.21	0.16	0.12	0.13	0.14	25.54
SE	0.12	0.02	0.01	0.01	0.01	3.71*
Margin of error (95% CI)	0.24	0.03	0.02	0.03	0.03	7.27
Upper 95% CI	0.45	0.12	0.09	0.10	0.12	51.90*
Lower 95% CI	0.00	0.06	0.04	0.05	0.06	37.35*

*Margins of error (95% CI) for archaeological data were obtained by bootstrapping the standard errors 10000 times.

MIS4 without a Paleo-Agulhas plain silcrete source – Discard probability on landscape (PD-ProbDiscard parameter)

Table B78. Summary statistics and test results for OFAT3 modeling of MIS4 conditions without a Paleo-Agulhas plain silcrete source compared to MIS4 archaeological raw material frequency data from PP5-6.

	PD=0.001-Quartz	**PD=0.1-Quartz**	**PD=0.5-Quartz**	**PD=0.75-Quartz**	**PD=0.95-Quartz**	**PP5-6-MIS4-Quartz**
n (number of simulated assemblages)	1000	1000	1000	1000	1000	46
First Quartile	99.85	99.69	99.69	99.62	99.62	1.21
Min	99.22	98.84	98.78	99.07	98.61	0.00
Median	100.00	100.00	100.00	100.00	100.00	3.73
Mean	99.91	99.83	99.84	99.80	99.79	8.39
Max	100.00	100.00	100.00	100.00	100.00	66.11
Third Quartile	100.00	100.00	100.00	100.00	100.00	10.53
SD	0.17	0.27	0.25	0.26	0.32	11.83
SE	0.02	0.03	0.02	0.03	0.03	1.67*
Margin of error (95% CI)	0.03	0.05	0.05	0.05	0.06	3.28
Upper 95% CI	99.95	99.88	99.89	99.85	99.85	11.66*
Lower 95% CI	99.88	99.78	99.80	99.74	99.73	5.11*
	PD=0.001-Silcrete	**PD=0.1-Silcrete**	**PD=0.5-Silcrete**	**PD=0.75-Silcrete**	**PD=0.95-Silcrete**	**PP5-6-MIS4-Silcrete**
n (number of simulated assemblages)	1000	1000	1000	1000	1000	46
First Quartile	0.00	0.00	0.00	0.00	0.00	13.79
Min	0.00	0.00	0.00	0.00	0.00	0.00
Median	0.00	0.00	0.00	0.00	0.00	39.13
Mean	0.00	0.00	0.00	0.00	0.00	40.00
Max	0.00	0.00	0.00	0.00	0.00	96.55
Third Quartile	0.00	0.00	0.00	0.00	0.00	62.77
SD	0.00	0.00	0.00	0.00	0.00	27.52
SE	0.00	0.00	0.00	0.00	0.00	4.01*
Margin of error (95% CI)	0.00	0.00	0.00	0.00	0.00	7.85
Upper 95% CI	0.00	0.00	0.00	0.00	0.00	47.85*
Lower 95% CI	0.00	0.00	0.00	0.00	0.00	32.15*
	PD=0.001-Quartzite	**PD=0.1-Quartzite**	**PD=0.5-Quartzite**	**PD=0.75-Quartzite**	**PD=0.95-Quartzite**	**PP5-6-MIS4-Quartzite**
n (number of simulated assemblages)	1000	1000	1000	1000	1000	46
First Quartile	0.00	0.00	0.00	0.00	0.00	5.19
Min	0.00	0.00	0.00	0.00	0.00	0.00
Median	0.00	0.00	0.00	0.00	0.00	43.00
Mean	0.09	0.17	0.16	0.20	0.21	44.63
Max	0.78	1.16	1.22	0.93	1.39	96.45
Third Quartile	0.15	0.31	0.31	0.38	0.38	68.24

SD	0.17	0.27	0.25	0.26	0.32	25.54
SE	0.02	0.03	0.02	0.03	0.03	3.71*
Margin of error (95% CI)	0.03	0.05	0.05	0.05	0.06	7.27
Upper 95% CI	0.12	0.22	0.20	0.26	0.27	51.90*
Lower 95% CI	0.05	0.12	0.11	0.15	0.15	37.35*

*Margins of error (95% CI) for archaeological data were obtained by bootstrapping the standard errors 10000 times.

MIS4 without a Paleo-Agulhas plain silcrete source– Toolkit size (Toolkit parameter)

Table B79. Summary statistics and test results for OFAT3 modeling of MIS4 conditions without a Paleo-Agulhas plain silcrete source compared to MIS4 archaeological raw material frequency data from PP5-6.

	Toolkit=5-Quartz	**Toolkit=10-Quartz**	**Toolkit=50-Quartz**	**Toolkit=75-Quartz**	**Toolkit=100-Quartz**	**PP5-6-MIS4-Quartz**
n (number of simulated assemblages)	1000	1000	1000	1000	1000	46
First Quartile	100.00	100.00	100.00	99.80	99.85	1.21
Min	95.00	97.87	98.79	97.43	99.22	0.00
Median	100.00	100.00	100.00	100.00	100.00	3.73
Mean	99.62	99.83	99.92	99.87	99.92	8.39
Max	100.00	100.00	100.00	100.00	100.00	66.11
Third Quartile	100.00	100.00	100.00	100.00	100.00	10.53
SD	1.10	0.50	0.19	0.32	0.15	11.83
SE	0.11	0.05	0.02	0.03	0.01	1.67*
Margin of error (95% CI)	0.22	0.10	0.04	0.06	0.03	3.28
Upper 95% CI	99.84	99.93	99.96	99.94	99.95	11.66*
Lower 95% CI	99.41	99.74	99.88	99.81	99.89	5.11*
	Toolkit=5-Silcrete	**Toolkit=10-Silcrete**	**Toolkit=50-Silcrete**	**Toolkit=75-Silcrete**	**Toolkit=100-Silcrete**	**PP5-6-MIS4-Silcrete**
n (number of simulated assemblages)	1000	1000	1000	1000	1000	46
First Quartile	0.00	0.00	0.00	0.00	0.00	13.79
Min	0.00	0.00	0.00	0.00	0.00	0.00
Median	0.00	0.00	0.00	0.00	0.00	39.13
Mean	0.00	0.00	0.00	0.00	0.00	40.00
Max	0.00	0.00	0.00	0.00	0.00	96.55
Third Quartile	0.00	0.00	0.00	0.00	0.00	62.77
SD	0.00	0.00	0.00	0.00	0.00	27.52
SE	0.00	0.00	0.00	0.00	0.00	4.01*
Margin of error (95% CI)	0.00	0.00	0.00	0.00	0.00	7.85
Upper 95% CI	0.00	0.00	0.00	0.00	0.00	47.85*
Lower 95% CI	0.00	0.00	0.00	0.00	0.00	32.15*
	Toolkit=5-Quartzite	**Toolkit=10-Quartzite**	**Toolkit=50-Quartzite**	**Toolkit=75-Quartzite**	**Toolkit=100-Quartzite**	**PP5-6-MIS4-Quartzite**

n (number of simulated assemblages)	1000	1000	1000	1000	1000	46
First Quartile	0.00	0.00	0.00	0.00	0.00	5.19
Min	0.00	0.00	0.00	0.00	0.00	0.00
Median	0.00	0.00	0.00	0.00	0.00	43.00
Mean	0.38	0.17	0.08	0.13	0.08	44.63
Max	5.00	2.13	1.21	2.57	0.78	96.45
Third Quartile	0.00	0.00	0.00	0.20	0.15	68.24
SD	1.10	0.50	0.19	0.32	0.15	25.54
SE	0.11	0.05	0.02	0.03	0.01	3.71*
Margin of error (95% CI)	0.22	0.10	0.04	0.06	0.03	7.27
Upper 95% CI	0.59	0.26	0.12	0.19	0.11	51.90*
Lower 95% CI	0.16	0.07	0.04	0.06	0.05	37.35*

*Margins of error (95% CI) for archaeological data were obtained by bootstrapping the standard errors 10000 times.

Table B80. Comparison between ranked model frequencies from OFAT3 simulations of MIS4 conditions without a Paleo-Agulhas plain silcrete source and ranked MIS4 archaeological frequencies from PP5-6.

	Discard probability at locality (PDC)*					**Archaeology**
Raw Material	**0.001**	**0.1**	**0.5**	**0.75**	**0.95**	**MIS4-PP5-6**
Quartz	1	1	1	1	1	2
Silcrete	2	3	3	3	3	1
Quartzite	2	2	2	2	2	1
	Discard probability on landscape (PD)*					**Archaeology**
Raw Material	**0.001**	**0.1**	**0.5**	**0.75**	**0.95**	**MIS4-PP5-6**
Quartz	1	1	1	1	1	2
Silcrete	3	3	3	3	3	1
Quartzite	2	2	2	2	2	1
	Toolkit size*					**Archaeology**
Raw Material	**5**	**10**	**50**	**75**	**100**	**MIS4-PP5-6**
Quartz	1	1	1	1	1	2
Silcrete	3	3	3	3	3	1
Quartzite	2	2	2	2	2	1

* Ranking based on which raw materials have the highest mean frequency. Similar rankings in the table are due to statistically similar frequencies. Ranking based on MIS4 archaeological raw material frequencies from bootstrapped data in Figure 50 and Table 19. Similar rankings in the table are due to statistically similar frequencies.

MIS4 with a Paleo-Agulhas plain silcrete source- Discard probability at locality (PDC-ProbDiscardCamp parameter)

Table B81. Summary statistics and test results for OFAT3 modeling of MIS4 conditions with a Paleo-Agulhas plain silcrete source compared to MIS4 archaeological raw material frequency data from PP5-6.

	PDC=0.001-Quartz	**PDC=0.1-Quartz**	**PDC=0.5-Quartz**	**PDC=0.75-Quartz**	**PDC=0.95-Quartz**	**PP5-6-MIS4-Quartz**
n (number of simulated assemblages)	1000	1000	1000	1000	1000	46
First Quartile	44.85	64.70	67.08	67.43	67.49	1.21
Min	34.88	60.99	64.41	63.54	63.62	0.00
Median	51.09	66.19	68.17	68.67	68.68	3.73
Mean	51.26	66.00	68.21	68.55	68.69	8.39
Max	71.43	70.16	72.91	72.62	73.50	66.11
Third Quartile	57.37	67.30	69.24	70.03	69.68	10.53
SD	8.24	1.92	1.65	1.89	1.80	11.83
SE	0.82	0.19	0.16	0.19	0.18	1.67*
Margin of error (95% CI)	1.61	0.38	0.32	0.37	0.35	3.28
Upper 95% CI	52.87	66.37	68.53	68.92	69.04	11.66*
Lower 95% CI	49.64	65.62	67.89	68.18	68.33	5.11*
	PDC=0.001-Silcrete	**PDC=0.1-Silcrete**	**PDC=0.5-Silcrete**	**PDC=0.75-Silcrete**	**PDC=0.95-Silcrete**	**PP5-6-MIS4-Silcrete**
n (number of simulated assemblages)	1000	1000	1000	1000	1000	46
First Quartile	42.63	32.70	30.70	29.97	30.20	13.79
Min	28.21	29.78	27.09	27.38	26.50	0.00
Median	48.91	33.67	31.83	31.27	31.31	39.13
Mean	48.56	33.97	31.76	31.43	31.30	40.00
Max	63.83	39.01	35.35	36.46	36.38	96.55
Third Quartile	55.15	35.29	32.92	32.57	32.47	62.77
SD	8.28	1.93	1.64	1.89	1.80	27.52
SE	0.83	0.19	0.16	0.19	0.18	4.01*
Margin of error (95% CI)	1.62	0.38	0.32	0.37	0.35	7.85
Upper 95% CI	50.18	34.35	32.09	31.80	31.65	47.85*
Lower 95% CI	46.94	33.59	31.44	31.06	30.94	32.15*
	PDC=0.001-Quartzite	**PDC=0.1-Quartzite**	**PDC=0.5-Quartzite**	**PDC=0.75-Quartzite**	**PDC=0.95-Quartzite**	**PP5-6-MIS4-Quartzite**
n (number of simulated assemblages)	1000	1000	1000	1000	1000	46
First Quartile	0.00	0.00	0.00	0.00	0.00	5.19
Min	0.00	0.00	0.00	0.00	0.00	0.00
Median	0.00	0.00	0.00	0.00	0.00	43.00
Mean	0.18	0.03	0.03	0.01	0.02	44.63
Max	2.94	0.41	0.24	0.28	0.21	96.45
Third Quartile	0.00	0.03	0.01	0.00	0.00	68.24

SD	0.63	0.07	0.06	0.05	0.05	25.54
SE	0.06	0.01	0.01	0.00	0.00	3.71*
Margin of error (95% CI)	0.12	0.01	0.01	0.01	0.01	7.27
Upper 95% CI	0.31	0.04	0.04	0.02	0.03	51.90*
Lower 95% CI	0.06	0.02	0.01	0.01	0.01	37.35*

*Margins of error (95% CI) for archaeological data were obtained by bootstrapping the standard errors 10000 times.

MIS4 with a Paleo-Agulhas plain silcrete source– Discard probability on landscape (PD-ProbDiscard parameter)

Table B82. Summary statistics and test results for OFAT3 modeling of MIS4 conditions with a Paleo-Agulhas plain silcrete source compared to MIS4 archaeological raw material frequency data from PP5-6.

	PD=0.001-Quartz	**PD=0.1-Quartz**	**PD=0.5-Quartz**	**PD=0.75-Quartz**	**PD=0.95-Quartz**	**PP5-6-MIS4-Quartz**
n (number of simulated assemblages)	1000	1000	1000	1000	1000	46
First Quartile	66.33	52.40	46.65	44.58	43.63	1.21
Min	60.94	46.77	40.81	40.61	41.06	0.00
Median	69.04	53.85	48.46	46.37	45.81	3.73
Mean	68.88	53.90	48.50	46.59	45.43	8.39
Max	76.43	59.08	53.74	54.08	50.94	66.11
Third Quartile	71.21	55.80	50.35	48.38	46.87	10.53
SD	3.40	2.46	2.52	2.66	2.29	11.83
SE	0.34	0.25	0.25	0.27	0.23	1.67*
Margin of error (95% CI)	0.67	0.48	0.49	0.52	0.45	3.28
Upper 95% CI	69.55	54.38	48.99	47.11	45.88	11.66*
Lower 95% CI	68.22	53.42	48.00	46.07	44.99	5.11*
	PD=0.001-Silcrete	**PD=0.1-Silcrete**	**PD=0.5-Silcrete**	**PD=0.75-Silcrete**	**PD=0.95-Silcrete**	**PP5-6-MIS4-Silcrete**
n (number of simulated assemblages)	1000	1000	1000	1000	1000	46
First Quartile	28.77	44.14	49.56	51.53	52.97	13.79
Min	23.57	40.90	46.26	45.19	49.06	0.00
Median	30.94	46.05	51.43	53.44	54.01	39.13
Mean	31.09	46.04	51.43	53.31	54.48	40.00
Max	39.06	53.23	59.06	59.28	58.94	96.55
Third Quartile	33.67	47.57	53.24	55.24	56.34	62.77
SD	3.39	2.46	2.52	2.67	2.28	27.52
SE	0.34	0.25	0.25	0.27	0.23	4.01*
Margin of error (95% CI)	0.67	0.48	0.49	0.52	0.45	7.85
Upper 95% CI	31.75	46.53	51.93	53.83	54.93	47.85*
Lower 95% CI	30.42	45.56	50.94	52.79	54.03	32.15*
	PD=0.001-Quartzite	**PD=0.1-Quartzite**	**PD=0.5-Quartzite**	**PD=0.75-Quartzite**	**PD=0.95-Quartzite**	**PP5-6-MIS4-Quartzite**
n (number of simulated assemblages)	1000	1000	1000	1000	1000	46

First Quartile	0.00	0.00	0.00	0.00	0.00	5.19
Min	0.00	0.00	0.00	0.00	0.00	0.00
Median	0.00	0.00	0.00	0.00	0.00	43.00
Mean	0.03	0.06	0.07	0.10	0.09	44.63
Max	0.61	0.54	0.76	0.73	0.73	96.45
Third Quartile	0.00	0.14	0.13	0.13	0.12	68.24
SD	0.10	0.12	0.13	0.16	0.16	25.54
SE	0.01	0.01	0.01	0.02	0.02	3.71*
Margin of error (95% CI)	0.02	0.02	0.03	0.03	0.03	7.27
Upper 95% CI	0.05	0.08	0.10	0.13	0.12	51.90*
Lower 95% CI	0.01	0.04	0.05	0.07	0.06	37.35*

*Margins of error (95% CI) for archaeological data were obtained by bootstrapping the standard errors 10000 times.

MIS4 with a Paleo-Agulhas plain silcrete source– Toolkit size (Toolkit parameter)

Table B83. Summary statistics and test results for OFAT3 modeling of MIS4 conditions with a Paleo-Agulhas plain silcrete source compared to MIS4 archaeological raw material frequency data from PP5-6.

	Toolkit=5-Quartz	**Toolkit=10-Quartz**	**Toolkit=50-Quartz**	**Toolkit=75-Quartz**	**Toolkit=100-Quartz**	**PP5-6-MIS4-Quartz**
n (number of simulated assemblages)	1000	1000	1000	1000	1000	46
First Quartile	44.87	47.93	54.97	56.31	57.76	1.21
Min	28.13	33.33	45.71	51.46	53.32	0.00
Median	48.89	52.44	57.44	58.38	60.10	3.73
Mean	48.44	51.73	56.95	58.79	59.95	8.39
Max	70.00	65.52	65.02	65.30	65.15	66.11
Third Quartile	53.64	56.38	58.74	61.12	61.84	10.53
SD	8.24	6.60	3.17	2.97	2.65	11.83
SE	0.82	0.66	0.32	0.30	0.26	1.67*
Margin of error (95% CI)	1.62	1.29	0.62	0.58	0.52	3.28
Upper 95% CI	50.06	53.02	57.57	59.37	60.46	11.66*
Lower 95% CI	46.83	50.43	56.33	58.21	59.43	5.11*
	Toolkit=5-Silcrete	**Toolkit=10-Silcrete**	**Toolkit=50-Silcrete**	**Toolkit=75-Silcrete**	**Toolkit=100-Silcrete**	**PP5-6-MIS4-Silcrete**
n (number of simulated assemblages)	1000	1000	1000	1000	1000	46
First Quartile	46.20	43.62	41.19	38.88	38.03	13.79
Min	30.00	34.48	34.67	34.70	34.73	0.00
Median	50.51	47.56	42.56	41.62	39.82	39.13
Mean	51.46	48.23	42.99	41.19	40.00	40.00
Max	71.88	66.67	54.29	48.54	46.68	96.55
Third Quartile	55.13	51.94	45.03	43.69	42.19	62.77
SD	8.23	6.58	3.17	2.97	2.66	27.52

SE	0.82	0.66	0.32	0.30	0.27	4.01*
Margin of error (95% CI)	1.61	1.29	0.62	0.58	0.52	7.85
Upper 95% CI	53.07	49.52	43.62	41.78	40.52	47.85*
Lower 95% CI	49.84	46.95	42.37	40.61	39.48	32.15*
	Toolkit=5-Quartzite	**Toolkit=10-Quartzite**	**Toolkit=50-Quartzite**	**Toolkit=75-Quartzite**	**Toolkit=100-Quartzite**	**PP5-6-MIS4-Quartzite**
n (number of simulated assemblages)	1000	1000	1000	1000	1000	46
First Quartile	0.00	0.00	0.00	0.00	0.00	5.19
Min	0.00	0.00	0.00	0.00	0.00	0.00
Median	0.00	0.00	0.00	0.00	0.00	43.00
Mean	0.10	0.04	0.05	0.01	0.05	44.63
Max	3.03	2.53	0.79	0.21	0.61	96.45
Third Quartile	0.00	0.00	0.00	0.00	0.10	68.24
SD	0.48	0.28	0.16	0.05	0.11	25.54
SE	0.05	0.03	0.02	0.01	0.01	3.71*
Margin of error (95% CI)	0.10	0.06	0.03	0.01	0.02	7.27
Upper 95% CI	0.19	0.09	0.08	0.02	0.07	51.90*
Lower 95% CI	0.00	-0.02	0.02	0.00	0.03	37.35*

*Margins of error (95% CI) for archaeological data were obtained by bootstrapping the standard errors 10000 times.

Table B84. Comparison between ranked model frequencies from OFAT3 simulations of MIS4 conditions with a Paleo-Agulhas plain silcrete source and ranked MIS4 archaeological frequencies from PP5-6.

	Discard probability at locality (PDC)*					**Archaeology**
Raw Material	**0.001**	**0.1**	**0.5**	**0.75**	**0.95**	**MIS4-PP5-6**
Quartz	1	1	1	1	1	2
Silcrete	1	2	2	2	2	1
Quartzite	2	3	3	3	3	1
	Discard probability on landscape (PD)*					**Archaeology**
Raw Material	**0.001**	**0.1**	**0.5**	**0.75**	**0.95**	**MIS4-PP5-6**
Quartz	1	1	2	2	2	2
Silcrete	2	2	1	1	1	1
Quartzite	3	3	3	3	3	1
	Toolkit size*					**Archaeology**
Raw Material	**5**	**10**	**50**	**75**	**100**	**MIS4-PP5-6**
Quartz	1	1	1	1	1	2
Silcrete	1	2	2	2	2	1
Quartzite	2	3	3	3	3	1

* Ranking based on which raw materials have the highest mean frequency. Similar rankings in the table are due to statistically similar frequencies. Ranking based on MIS4 archaeological raw material frequencies from bootstrapped data in Figure 50 and Table 19. Similar rankings in the table are due to statistically similar frequencies.

MIS5 conditions - Discard probability at locality (PDC-ProbDiscardCamp parameter)

Table B85. Summary statistics and test results for OFAT3 modeling of MIS5 conditions compared to MIS5 archaeological raw material frequency data from PP5-6, PP13B, PP9B, and PP9C.

	PDC=0.001-Quartz	PDC=0.1-Quartz	PDC=0.5-Quartz	PDC=0.75-Quartz	PDC=0.95-Quartz	PP5-6-MIS5-Quartz	PP13B-MIS5-Quartz	AllPP-MIS5-Quartz
n (number of assemblages)	1000	1000	1000	1000	1000	31	7	43
First Quartile	77.04	81.78	82.44	82.05	82.39	0.00	1.71	0.10
Min	64.69	79.20	80.14	79.84	80.47	0.00	0.00	0.00
Median	80.10	83.02	83.50	83.01	83.41	0.89	2.15	2.65
Mean	80.56	82.89	83.40	83.12	83.47	3.53	4.41	4.61
Max	92.89	86.35	87.17	87.17	86.72	24.87	9.39	24.87
Third Quartile	84.81	84.00	84.45	84.18	84.69	3.92	9.33	6.95
SD	5.26	1.62	1.59	1.49	1.54	5.94	3.91	6.03
SE	0.53	0.16	0.16	0.15	0.15	1.03*	1.40*	0.90*
Margin of error (95% CI)	1.03	0.32	0.31	0.29	0.30	2.03	2.74	1.76
Upper 95% CI	81.59	83.20	83.71	83.41	83.77	5.56*	7.15*	6.37*
Lower 95% CI	79.53	82.57	83.09	82.83	83.17	1.51*	1.68*	2.85*
	PDC=0.001-Silcrete	**PDC=0.1-Silcrete**	**PDC=0.5-Silcrete**	**PDC=0.75-Silcrete**	**PDC=0.95-Silcrete**	**PP5-6-MIS5-Silcrete**	**PP13B-Silcrete**	**AllPP-MIS5-Silcrete**
n (number of assemblages)	1000	1000	1000	1000	1000	31	7	4.30E+01
First Quartile	0.09	0.10	0.09	0.10	0.09	1.45	0.00	0.95
Min	0.04	0.08	0.08	0.08	0.08	0.00	0.00	0.00
Median	0.12	0.10	0.10	0.10	0.10	10.19	0.00	6.44
Mean	0.12	0.10	0.10	0.10	0.10	16.97	1.09	13.05
Max	0.21	0.13	0.12	0.12	0.12	64.83	5.01	64.83
Third Quartile	0.14	0.11	0.11	0.11	0.11	32.95	2.55	21.21
SD	0.03	0.01	0.01	0.01	0.01	17.85	1.97	16.45
SE	0.00	0.00	0.00	0.00	0.00	3.14*	0.68*	2.46*
Margin of error (95% CI)	0.01	0.00	0.00	0.00	0.00	6.16	1.34	4.82
Upper 95% CI	0.12	0.11	0.10	0.10	0.10	23.12*	2.42*	17.86*
Lower 95% CI	0.11	0.10	0.10	0.10	0.10	10.81*	0.00*	8.23*
	PDC=0.001-Quartzite	**PDC=0.1-Quartzite**	**PDC=0.5-Quartzite**	**PDC=0.75-Quartzite**	**PDC=0.95-Quartzite**	**P5-6-MIS5-Quartzite**	**PP13B-Quartzite**	**AllPP-MIS5-Quartzite**
n (number of assemblages)	1000	1000	1000	1000	1000	31	7	43

First Quartile	15.04	15.84	15.40	15.66	15.15	60.24	87.62	64.30
Min	7.04	13.51	12.71	12.70	13.15	26.94	87.62	26.94
Median	19.70	16.81	16.33	16.82	16.43	76.11	97.85	83.74
Mean	19.25	16.94	16.43	16.71	16.36	72.77	94.34	77.20
Max	34.95	20.59	19.66	19.96	19.34	100.00	100.00	100.00
Third Quartile	22.73	18.03	17.39	17.77	17.43	92.83	98.29	92.83
SD	5.20	1.60	1.57	1.47	1.52	21.79	5.37	20.01
SE	0.52	0.16	0.16	0.15	0.15	3.85*	1.92*	3.00*
Margin of error (95% CI)	1.02	0.31	0.31	0.29	0.30	7.55	3.76	5.87
Upper 95% CI	20.27	17.26	16.74	17.00	16.66	80.328	98.10*	83.07*
Lower 95% CI	18.23	16.63	16.13	16.42	16.06	65.21*	90.58*	71.33*

*Margins of error (95% CI) for archaeological data were obtained by bootstrapping the standard errors 10000 times.

MIS5 Conditions– Discard probability on landscape (PD-ProbDiscard parameter)

Table B86. Summary statistics and test results for OFAT3 modeling of MIS5 conditions compared to MIS5 archaeological raw material frequency data from PP5-6, PP13B, PP9B, and PP9C.

	PD=0.001 -Quartz	**PD=0.1- Quartz**	**PD=0.5- Quartz**	**PD=0.75- Quartz**	**PD=0.95- Quartz**	**PP5-6- MIS5- Quartz**	**PP13B- MIS5- Quartz**	**AllPP- MIS5- Quartz**
n (number of assemblages)	1000	1000	1000	1000	1000	31	7	43
First Quartile	81.81	79.49	78.61	77.97	78.31	0.00	1.71	0.10
Min	77.53	75.95	75.01	74.86	74.81	0.00	0.00	0.00
Median	84.27	81.29	79.97	79.25	79.93	0.89	2.15	2.65
Mean	83.84	81.05	79.95	79.33	79.73	3.53	4.41	4.61
Max	89.03	85.50	86.64	84.16	85.82	24.87	9.39	24.87
Third Quartile	85.67	82.55	81.53	80.87	80.91	3.92	9.33	6.95
SD	2.51	2.05	2.17	1.99	1.94	5.94	3.91	6.03
SE	0.25	0.20	0.22	0.20	0.19	1.03*	1.40*	0.90*
Margin of error (95% CI)	0.49	0.40	0.43	0.39	0.38	2.03	2.74	1.76
Upper 95% CI	84.33	81.46	80.37	79.72	80.11	5.56*	7.15*	6.37*
Lower 95% CI	83.35	80.65	79.52	78.94	79.35	1.51*	1.68*	2.85*
	PD=0.001 -Silcrete	**PD=0.1- Silcrete**	**PD=0.5- Silcrete**	**PD=0.75- Silcrete**	**PD=0.95- Silcrete**	**PP5-6- MIS5- Silcrete**	**PP13B- Silcrete**	**AllPP- MIS5- Silcrete**
n (number of assemblages)	1000	1000	1000	1000	1000	31	7	4.30E+01
First Quartile	0.09	0.11	0.11	0.12	0.12	1.45	0.00	0.95
Min	0.07	0.09	0.08	0.10	0.09	0.00	0.00	0.00
Median	0.09	0.11	0.12	0.13	0.12	10.19	0.00	6.44
Mean	0.10	0.11	0.12	0.12	0.12	16.97	1.09	13.05

Max	0.14	0.15	0.15	0.15	0.15	64.83	5.01	64.83
Third Quartile	0.11	0.12	0.13	0.13	0.13	32.95	2.55	21.21
SD	0.02	0.01	0.01	0.01	0.01	17.85	1.97	16.45
SE	0.00	0.00	0.00	0.00	0.00	3.14*	0.68*	2.46*
Margin of error (95% CI)	0.00	0.00	0.00	0.00	0.00	6.16	1.34	4.82
Upper 95% CI	0.10	0.12	0.12	0.13	0.12	23.12*	2.42*	17.86*
Lower 95% CI	0.09	0.11	0.12	0.12	0.12	10.81*	0.00*	8.23*
	PD=0.001-Quartzite	**PD=0.1-Quartzite**	**PD=0.5-Quartzite**	**PD=0.75-Quartzite**	**PD=0.95-Quartzite**	**P5-6-MIS5-Quartzite**	**PP13B-Quartzite**	**AllPP-MIS5-Quartzite**
n (number of assemblages)	1000	1000	1000	1000	1000	31	7	43
First Quartile	14.18	17.27	18.28	18.94	18.90	60.24	87.62	64.30
Min	10.86	14.35	13.23	15.69	14.04	26.94	87.62	26.94
Median	15.57	18.52	19.83	20.54	19.86	76.11	97.85	83.74
Mean	16.00	18.75	19.85	20.46	20.07	72.77	94.34	77.20
Max	22.24	23.81	24.73	24.88	24.94	100.00	100.00	100.00
Third Quartile	18.01	20.31	21.17	21.81	21.47	92.83	98.29	92.83
SD	2.49	2.03	2.15	1.97	1.92	21.79	5.37	20.01
SE	0.25	0.20	0.21	0.20	0.19	3.85*	1.92*	3.00*
Margin of error (95% CI)	0.49	0.40	0.42	0.39	0.38	7.55	3.76	5.87
Upper 95% CI	16.49	19.15	20.27	20.85	20.44	80.32*	98.10*	83.07*
Lower 95% CI	15.51	18.36	19.43	20.08	19.69	65.21*	90.58*	71.33*

*Margins of error (95% CI) for archaeological data were obtained by bootstrapping the standard errors 10000 times.

MIS5 conditions– Toolkit size (Toolkit parameter)

Table B87. Summary statistics and test results for OFAT3 modeling of MIS5 conditions compared to MIS5 archaeological raw material frequency data from PP5-6, PP13B, PP9B, and PP9C.

	Toolkit=5-Quartz	**Toolkit=10-Quartz**	**Toolkit=50-Quartz**	**Toolkit=75-Quartz**	**Toolkit=100-Quartz**	**PP5-6-MIS5-Quartz**	**PP13B-MIS5-Quartz**	**AllPP-MIS5-Quartz**
n (number of assemblages)	1000	1000	1000	1000	1000	31	7	43
First Quartile	76.21	77.42	79.86	80.48	81.16	0.00	1.71	0.10
Min	65.96	70.28	75.23	75.85	77.87	0.00	0.00	0.00
Median	79.67	80.10	81.34	81.92	82.54	0.89	2.15	2.65
Mean	80.23	80.12	81.36	81.96	82.30	3.53	4.41	4.61
Max	96.25	89.08	85.84	87.51	85.85	24.87	9.39	24.87
Third Quartile	84.29	83.23	83.17	83.52	83.62	3.92	9.33	6.95
SD	5.92	4.01	2.34	2.17	1.92	5.94	3.91	6.03
SE	0.59	0.40	0.23	0.22	0.19	1.03*	1.40*	0.90*

Margin of error (95% CI)	1.16	0.79	0.46	0.43	0.38	2.03	2.74	1.76
Upper 95% CI	81.39	80.91	81.82	82.39	82.67	5.56*	7.15*	6.37*
Lower 95% CI	79.06	79.34	80.91	81.54	81.92	1.51*	1.68*	2.85*
	Toolkit=5-Silcrete	**Toolkit=10-Silcrete**	**Toolkit=50-Silcrete**	**Toolkit=75-Silcrete**	**Toolkit=100-Silcrete**	**PP5-6-MIS5-Silcrete**	**PP13B-Silcrete**	**AllPP-MIS5-Silcrete**
n (number of assemblages)	1000	1000	1000	1000	1000	31	7	4.30E+01
First Quartile	0.09	0.10	0.10	0.10	0.10	1.45	0.00	0.95
Min	0.02	0.07	0.09	0.08	0.09	0.00	0.00	0.00
Median	0.12	0.12	0.11	0.11	0.11	10.19	0.00	6.44
Mean	0.12	0.12	0.11	0.11	0.11	16.97	1.09	13.05
Max	0.21	0.18	0.15	0.15	0.13	64.83	5.01	64.83
Third Quartile	0.14	0.14	0.12	0.12	0.11	32.95	2.55	21.21
SD	0.04	0.02	0.01	0.01	0.01	17.85	1.97	16.45
SE	0.00	0.00	0.00	0.00	0.00	3.14*	0.68*	2.46*
Margin of error (95% CI)	0.01	0.00	0.00	0.00	0.00	6.16	1.34	4.82
Upper 95% CI	0.13	0.12	0.12	0.11	0.11	23.12*	2.42*	17.86*
Lower 95% CI	0.11	0.12	0.11	0.11	0.10	10.81*	0.00*	8.23*
	Toolkit=5-Quartzite	**Toolkit=10-Quartzite**	**Toolkit=50-Quartzite**	**Toolkit=75-Quartzite**	**Toolkit=100-Quartzite**	**P5-6-MIS5-Quartzite**	**PP13B-Quartzite**	**AllPP-MIS5-Quartzite**
n (number of assemblages)	1000	1000	1000	1000	1000	31	7	43
First Quartile	15.55	16.60	16.66	16.32	16.22	60.24	87.62	64.30
Min	3.72	10.81	14.02	12.36	14.01	26.94	87.62	26.94
Median	20.12	19.70	18.47	17.90	17.28	76.11	97.85	83.74
Mean	19.58	19.68	18.45	17.85	17.53	72.77	94.34	77.20
Max	33.70	29.42	24.52	23.90	21.91	100.00	100.00	100.00
Third Quartile	23.55	22.35	19.94	19.32	18.66	92.83	98.29	92.83
SD	5.86	3.97	2.31	2.15	1.90	21.79	5.37	20.01
SE	0.59	0.40	0.23	0.21	0.19	3.85*	1.92*	3.00*
Margin of error (95% CI)	1.15	0.78	0.45	0.42	0.37	7.55	3.76	5.87
Upper 95% CI	20.73	20.45	18.90	18.28	17.90	80.32*	98.10*	83.07*
Lower 95% CI	18.43	18.90	17.99	17.43	17.15	65.21*	90.58*	71.33*

*Margins of error (95% CI) for archaeological data were obtained by bootstrapping the standard errors 10000 times.

Table B88. Comparison between ranked model frequencies from OFAT3 simulations of MIS5 conditions and ranked MIS5 archaeological frequencies from PP13B, PP9B, PP9C, and PP5-6.

	Discard probability at locality (PDC)*					Archaeology		
Raw Material	**0.001**	**0.1**	**0.5**	**0.75**	**0.95**	**MIS5-PP5-6**	**MIS5-PP13B**	**MIS5-All PP**
Quartz	1	1	1	1	1	3	2	3
Silcrete	3	3	3	3	3	2	2	2
Quartzite	2	2	2	2	2	1	1	1
	Discard probability on landscape (PD)*					**Archaeology**		
Raw Material	**0.001**	**0.1**	**0.5**	**0.75**	**0.95**	**MIS5-PP5-6**	**MIS5-PP13B**	**MIS5-All PP**
Quartz	1	1	1	1	1	3	2	3
Silcrete	3	3	3	3	3	2	2	2
Quartzite	2	2	2	2	2	1	1	1
	Toolkit size*					**Archaeology**		
Raw Material	**5**	**10**	**50**	**75**	**100**	**MIS5-PP5-6**	**MIS5-PP13B**	**MIS5-All PP**
Quartz	1	1	1	1	1	3	2	3
Silcrete	3	3	3	3	3	2	2	2
Quartzite	2	2	2	2	2	1	1	1

* Ranking based on which raw materials have the highest mean frequency. Similar rankings in the table are due to statistically similar frequencies. Ranking based on MIS5 archaeological raw material frequencies from bootstrapped data in Figure 50 and Table 19. Similar rankings in the table are due to statistically similar frequencies.

MIS6 without a Paleo-Agulhas plain silcrete source- Discard probability at locality (PDC-ProbDiscardCamp parameter)

Table B89. Summary statistics and test results for OFAT3 modeling of MIS6 conditions without a Paleo-Agulhas plain silcrete source compared to MIS6 archaeological raw material frequency data from PP13B.

	PDC=0.001-Quartz	**PDC=0.1-Quartz**	**PDC=0.5-Quartz**	**PDC=0.75-Quartz**	**PDC=0.95-Quartz**	**PP13-MIS6-Quartz**
n (number of assemblages)	1000	1000	1000	1000	1000	7
First Quartile	62.86	79.31	80.62	80.64	80.72	1.71
Min	46.43	77.35	77.72	77.46	78.12	0.00
Median	69.88	80.65	81.68	81.63	81.77	2.15
Mean	69.28	80.62	81.65	81.66	81.75	4.41
Max	87.10	84.35	85.42	85.05	84.94	9.39
Third Quartile	75.68	81.80	82.78	82.66	82.82	9.33
SD	8.62	1.66	1.59	1.56	1.34	3.91
SE	0.86	0.17	0.16	0.16	0.13	1.40*
Margin of error (95% CI)	1.69	0.33	0.31	0.31	0.26	2.74
Upper 95% CI	70.97	80.95	81.96	81.97	82.01	7.158
Lower 95% CI	67.59	80.29	81.34	81.36	81.48	1.68*

	PDC=0.001-Silcrete	PDC=0.1-Silcrete	PDC=0.5-Silcrete	PDC=0.75-Silcrete	PDC=0.95-Silcrete	PP13B-MIS6-Silcrete
n (number of assemblages)	1000	1000	1000	1000	1000	7
First Quartile	0.00	0.00	0.00	0.00	0.00	0.00
Min	0.00	0.00	0.00	0.00	0.00	0.00
Median	0.00	0.00	0.00	0.00	0.00	0.00
Mean	0.00	0.00	0.00	0.00	0.00	1.09
Max	0.00	0.00	0.00	0.00	0.00	5.01
Third Quartile	0.00	0.00	0.00	0.00	0.00	2.55
SD	0.00	0.00	0.00	0.00	0.00	1.97
SE	0.00	0.00	0.00	0.00	0.00	0.68*
Margin of error (95% CI)	0.00	0.00	0.00	0.00	0.00	1.34
Upper 95% CI	0.00	0.00	0.00	0.00	0.00	2.42*
Lower 95% CI	0.00	0.00	0.00	0.00	0.00	0.00*
	PDC=0.001-Quartzite	**PDC=0.1-Quartzite**	**PDC=0.5-Quartzite**	**PDC=0.75-Quartzite**	**PDC=0.95-Quartzite**	**PP13B-MIS6-Quartzite**
n (number of assemblages)	1000	1000	1000	1000	1000	7
First Quartile	24.32	18.20	17.22	17.34	17.18	87.62
Min	12.90	15.65	14.58	14.95	15.06	87.62
Median	30.12	19.35	18.32	18.37	18.23	97.85
Mean	30.72	19.38	18.35	18.34	18.25	94.34
Max	53.57	22.65	22.28	22.54	21.88	100.00
Third Quartile	37.14	20.69	19.38	19.36	19.28	98.29
SD	8.62	1.66	1.59	1.56	1.34	5.37
SE	0.86	0.17	0.16	0.16	0.13	1.92*
Margin of error (95% CI)	1.69	0.33	0.31	0.31	0.26	3.76
Upper 95% CI	32.41	19.71	18.66	18.64	18.52	98.10*
Lower 95% CI	29.03	19.05	18.04	18.03	17.99	90.58*

*Margins of error (95% CI) for archaeological data were obtained by bootstrapping the standard errors 10000 times.

MIS6 without a Paleo-Agulhas plain silcrete source– Discard probability on landscape (PD-ProbDiscard parameter)

Table B90. Summary statistics and test results for OFAT3 modeling of MIS6 conditions without a Paleo-Agulhas plain silcrete source compared to MIS6 archaeological raw material frequency data from PP13B.

	PD=0.001-Quartz	PD=0.1-Quartz	PD=0.5-Quartz	PD=0.75-Quartz	PD=0.95-Quartz	PP13-MIS6-Quartz
n (number of assemblages)	1000	1000	1000	1000	1000	7
First Quartile	78.55	67.21	63.20	61.32	60.27	1.71
Min	68.77	63.04	54.14	55.98	56.33	0.00
Median	82.14	69.24	65.11	62.61	62.17	2.15
Mean	80.94	69.13	64.79	62.76	62.03	4.41

Max	88.24	75.96	70.41	70.10	67.76	9.39
Third Quartile	84.03	71.16	66.83	64.21	63.87	9.33
SD	4.24	2.83	2.90	2.53	2.57	3.91
SE	0.42	0.28	0.29	0.25	0.26	1.40*
Margin of error (95% CI)	0.83	0.56	0.57	0.50	0.50	2.74
Upper 95% CI	81.78	69.69	65.36	63.26	62.53	7.15*
Lower 95% CI	80.11	68.58	64.23	62.27	61.53	1.68*
	PD=0.001-Silcrete	**PD=0.1-Silcrete**	**PD=0.5-Silcrete**	**PD=0.75-Silcrete**	**PD=0.95-Silcrete**	**PP13B-MIS6-Silcrete**
n (number of assemblages)	1000	1000	1000	1000	1000	7
First Quartile	0.00	0.00	0.00	0.00	0.00	0.00
Min	0.00	0.00	0.00	0.00	0.00	0.00
Median	0.00	0.00	0.00	0.00	0.00	0.00
Mean	0.00	0.00	0.00	0.00	0.00	1.09
Max	0.00	0.00	0.00	0.00	0.00	5.01
Third Quartile	0.00	0.00	0.00	0.00	0.00	2.55
SD	0.00	0.00	0.00	0.00	0.00	1.97
SE	0.00	0.00	0.00	0.00	0.00	0.68*
Margin of error (95% CI)	0.00	0.00	0.00	0.00	0.00	1.34
Upper 95% CI	0.00	0.00	0.00	0.00	0.00	2.42*
Lower 95% CI	0.00	0.00	0.00	0.00	0.00	0.00*
	PD=0.001-Quartzite	**PD=0.1-Quartzite**	**PD=0.5-Quartzite**	**PD=0.75-Quartzite**	**PD=0.95-Quartzite**	**PP13B-MIS6-Quartzite**
n (number of assemblages)	1000	1000	1000	1000	1000	7
First Quartile	15.97	28.84	33.17	35.79	36.13	87.62
Min	11.76	24.04	29.59	29.90	32.24	87.62
Median	17.86	30.76	34.89	37.39	37.83	97.85
Mean	19.06	30.87	35.21	37.24	37.97	94.34
Max	31.23	36.96	45.86	44.02	43.67	100.00
Third Quartile	21.45	32.79	36.80	38.68	39.73	98.29
SD	4.24	2.83	2.90	2.53	2.57	5.37
SE	0.42	0.28	0.29	0.25	0.26	1.92*
Margin of error (95% CI)	0.83	0.56	0.57	0.50	0.50	3.76
Upper 95% CI	19.89	31.42	35.77	37.73	38.47	98.10*
Lower 95% CI	18.22	30.31	34.64	36.74	37.47	90.58*

*Margins of error (95% CI) for archaeological data were obtained by bootstrapping the standard errors 10000 times.

MIS6 without a Paleo-Agulhas plain silcrete source– Toolkit size (Toolkit parameter)

Table B91. Summary statistics and test results for OFAT3 modeling of MIS6 conditions without a Paleo-Agulhas plain silcrete source compared to MIS6 archaeological raw material frequency data from PP13B.

	Toolkit=5-Quartz	**Toolkit=10-Quartz**	**Toolkit=50-Quartz**	**Toolkit=75-Quartz**	**Toolkit=100-Quartz**	**PP13-MIS6-Quartz**
n (number of assemblages)	1000	1000	1000	1000	1000	7
First Quartile	57.28	60.72	70.15	72.26	73.09	1.71
Min	33.33	41.67	62.36	61.02	65.98	0.00
Median	66.67	67.61	72.39	74.30	75.55	2.15
Mean	65.52	67.53	72.83	74.29	75.25	4.41
Max	93.75	89.19	81.18	81.23	82.44	9.39
Third Quartile	72.73	73.17	75.36	76.76	77.71	9.33
SD	11.35	9.00	3.85	3.46	3.04	3.91
SE	1.14	0.90	0.39	0.35	0.30	1.40*
Margin of error (95% CI)	2.23	1.76	0.75	0.68	0.60	2.74
Upper 95% CI	67.74	69.30	73.59	74.97	75.85	7.15*
Lower 95% CI	63.29	65.77	72.08	73.61	74.66	1.68*
	Toolkit=5-Silcrete	**Toolkit=10-Silcrete**	**Toolkit=50-Silcrete**	**Toolkit=75-Silcrete**	**Toolkit=100-Silcrete**	**PP13B-MIS6-Silcrete**
n (number of assemblages)	1000	1000	1000	1000	1000	7
First Quartile	0.00	0.00	0.00	0.00	0.00	0.00
Min	0.00	0.00	0.00	0.00	0.00	0.00
Median	0.00	0.00	0.00	0.00	0.00	0.00
Mean	0.00	0.00	0.00	0.00	0.00	1.09
Max	0.00	0.00	0.00	0.00	0.00	5.01
Third Quartile	0.00	0.00	0.00	0.00	0.00	2.55
SD	0.00	0.00	0.00	0.00	0.00	1.97
SE	0.00	0.00	0.00	0.00	0.00	0.68*
Margin of error (95% CI)	0.00	0.00	0.00	0.00	0.00	1.34
Upper 95% CI	0.00	0.00	0.00	0.00	0.00	2.42*
Lower 95% CI	0.00	0.00	0.00	0.00	0.00	0.00*
	Toolkit=5-Quartzite	**Toolkit=10-Quartzite**	**Toolkit=50-Quartzite**	**Toolkit=75-Quartzite**	**Toolkit=100-Quartzite**	**PP13B-MIS6-Quartzite**
n (number of assemblages)	1000	1000	1000	1000	1000	7
First Quartile	27.27	26.83	24.64	23.24	22.29	87.62
Min	6.25	10.81	18.82	18.77	17.56	87.62
Median	33.33	32.39	27.61	25.70	24.45	97.85
Mean	34.48	32.47	27.17	25.71	24.75	94.34
Max	66.67	58.33	37.64	38.98	34.02	100.00
Third Quartile	42.72	39.28	29.85	27.74	26.91	98.29
SD	11.35	9.00	3.85	3.46	3.04	5.37

SE	1.14	0.90	0.39	0.35	0.30	1.92*
Margin of error (95% CI)	2.23	1.76	0.75	0.68	0.60	3.76
Upper 95% CI	36.71	34.23	27.92	26.39	25.34	98.10*
Lower 95% CI	32.26	30.70	26.41	25.03	24.15	90.58*

*Margins of error (95% CI) for archaeological data were obtained by bootstrapping the standard errors 10000 times.

Table B92. Comparison between ranked model frequencies from OFAT3 simulations of MIS6 conditions without a Paleo-Agulhas plain silcrete source and ranked MIS6 archaeological frequencies from PP13B.

	Discard probability at locality (PDC)*					**Archaeology**
Raw Material	**0.001**	**0.1**	**0.5**	**0.75**	**0.95**	**MIS6-PP13B**
Quartz	1	1	1	1	1	2
Silcrete	3	3	3	3	3	2
Quartzite	2	2	2	2	2	1
	Discard probability on landscape (PD)*					**Archaeology**
Raw Material	**0.001**	**0.1**	**0.5**	**0.75**	**0.95**	**MIS6-PP13B**
Quartz	1	1	1	1	1	2
Silcrete	3	3	3	3	3	2
Quartzite	2	2	2	2	2	1
	Toolkit size*					**Archaeology**
Raw Material	**5**	**10**	**50**	**75**	**100**	**MIS6-PP13B**
Quartz	1	1	1	1	1	2
Silcrete	3	3	3	3	3	2
Quartzite	2	2	2	2	2	1

* Ranking based on which raw materials have the highest mean frequency. Similar rankings in the table are due to statistically similar frequencies. Ranking based on MIS6 archaeological raw material frequencies from bootstrapped data in Figure 50 and Table 19. Similar rankings in the table are due to statistically similar frequencies.

MIS6 with a Paleo-Agulhas plain silcrete source- Discard probability at locality (PDC-ProbDiscardCamp parameter)

Table B93. Summary statistics and test results for OFAT3 modeling of MIS6 conditions with a Paleo-Agulhas plain silcrete source compared to MIS6 archaeological raw material frequency data from PP13B.

	PDC=0.001-Quartz	**PDC=0.1-Quartz**	**PDC=0.5-Quartz**	**PDC=0.75-Quartz**	**PDC=0.95-Quartz**	**PP13-MIS6-Quartz**
n (number of assemblages)	1000	1000	1000	1000	1000	7
First Quartile	47.22	64.48	66.42	66.82	66.10	1.71
Min	32.61	60.13	63.20	64.16	62.85	0.00
Median	52.45	65.65	67.88	67.84	67.34	2.15
Mean	53.69	65.75	67.71	67.94	67.41	4.41
Max	75.68	70.31	71.66	72.54	71.54	9.39
Third Quartile	60.24	67.20	68.89	68.99	68.66	9.33

SD	8.83	2.07	1.64	1.56	1.91	3.91
SE	0.88	0.21	0.16	0.16	0.19	1.40*
Margin of error (95% CI)	1.73	0.41	0.32	0.30	0.37	2.74
Upper 95% CI	55.42	66.16	68.03	68.24	67.79	7.15*
Lower 95% CI	51.96	65.35	67.39	67.63	67.04	1.68*
	PDC=0.001-Silcrete	**PDC=0.1-Silcrete**	**PDC=0.5-Silcrete**	**PDC=0.75-Silcrete**	**PDC=0.95-Silcrete**	**PP13B-MIS6-Silcrete**
n (number of assemblages)	1000	1000	1000	1000	1000	7
First Quartile	30.52	29.26	28.09	28.22	27.95	0.00
Min	21.62	25.45	24.54	24.42	25.00	0.00
Median	36.85	30.23	29.21	29.05	29.72	0.00
Mean	36.84	30.42	29.27	29.03	29.50	1.09
Max	55.17	35.93	34.30	32.61	33.49	5.01
Third Quartile	41.98	31.92	30.45	29.97	30.85	2.55
SD	7.89	2.06	1.73	1.48	1.91	1.97
SE	0.79	0.21	0.17	0.15	0.19	0.68*
Margin of error (95% CI)	1.55	0.40	0.34	0.29	0.37	1.34
Upper 95% CI	38.39	30.83	29.61	29.32	29.87	2.42*
Lower 95% CI	35.29	30.02	28.93	28.74	29.13	0.00*
	PDC=0.001-Quartzite	**PDC=0.1-Quartzite**	**PDC=0.5-Quartzite**	**PDC=0.75-Quartzite**	**PDC=0.95-Quartzite**	**PP13B-MIS6-Quartzite**
n (number of assemblages)	1000	1000	1000	1000	1000	7
First Quartile	6.03	3.22	2.54	2.57	2.57	87.62
Min	0.00	2.16	1.12	1.57	1.85	87.62
Median	8.66	3.68	3.00	2.95	3.07	97.85
Mean	9.47	3.83	3.02	3.03	3.09	94.34
Max	25.93	6.38	4.97	4.81	5.00	100.00
Third Quartile	12.00	4.44	3.49	3.47	3.51	98.29
SD	5.31	0.78	0.71	0.65	0.67	5.37
SE	0.53	0.08	0.07	0.06	0.07	1.92*
Margin of error (95% CI)	1.04	0.15	0.14	0.13	0.13	3.76
Upper 95% CI	10.51	3.98	3.16	3.16	3.22	98.10*
Lower 95% CI	8.42	3.67	2.88	2.90	2.96	90.58*

*Margins of error (95% CI) for archaeological data were obtained by bootstrapping the standard errors 10000 times.

MIS6 with a Paleo-Agulhas plain silcrete source– Discard probability on landscape (PD-ProbDiscard parameter)

Table B94. Summary statistics and test results for OFAT3 modeling of MIS6 conditions with a Paleo-Agulhas plain silcrete source compared to MIS6 archaeological raw material frequency data from PP13B.

	PD=0.001-Quartz	**PD=0.1-Quartz**	**PD=0.5-Quartz**	**PD=0.75-Quartz**	**PD=0.95-Quartz**	**PP13-MIS6-Quartz**
n (number of assemblages)	1000	1000	1000	1000	1000	7
First Quartile	84.62	47.04	44.35	43.22	41.56	1.71
Min	0.00	42.22	39.49	39.34	38.11	0.00
Median	86.91	50.07	46.41	44.79	43.51	2.15
Mean	86.16	49.73	46.04	44.70	43.55	4.41
Max	100.00	61.42	54.63	50.94	50.78	9.39
Third Quartile	88.92	51.49	47.85	46.17	45.26	9.33
SD	6.30	3.49	2.77	2.31	2.58	3.91
SE	0.20	0.35	0.28	0.23	0.26	1.40*
Margin of error (95% CI)	0.39	0.68	0.54	0.45	0.50	2.74
Upper 95% CI	86.55	50.42	46.59	45.15	44.05	7.15*
Lower 95% CI	85.77	49.05	45.50	44.24	43.04	1.68*
	PD=0.001-Silcrete	**PD=0.1-Silcrete**	**PD=0.5-Silcrete**	**PD=0.75-Silcrete**	**PD=0.95-Silcrete**	**PP13B-MIS6-Silcrete**
n (number of assemblages)	1000	1000	1000	1000	1000	7
First Quartile	26.75	36.85	39.68	40.20	40.34	0.00
Min	20.35	31.50	33.99	36.52	34.84	0.00
Median	29.94	39.27	41.04	41.51	41.50	0.00
Mean	30.78	39.40	41.36	41.71	41.65	1.09
Max	41.12	46.40	46.98	47.96	46.23	5.01
Third Quartile	35.03	41.51	43.37	43.09	43.18	2.55
SD	4.98	3.11	2.74	2.37	2.07	1.97
SE	0.50	0.31	0.27	0.24	0.21	0.68*
Margin of error (95% CI)	0.98	0.61	0.54	0.46	0.41	1.34
Upper 95% CI	31.75	40.01	41.90	42.17	42.05	2.42*
Lower 95% CI	29.80	38.79	40.82	41.25	41.24	0.00*
	PD=0.001-Quartzite	**PD=0.1-Quartzite**	**PD=0.5-Quartzite**	**PD=0.75-Quartzite**	**PD=0.95-Quartzite**	**PP13B-MIS6-Quartzite**
n (number of assemblages)	1000	1000	1000	1000	1000	7
First Quartile	2.63	9.13	11.72	12.66	13.48	87.62
Min	1.29	6.28	8.60	8.42	9.79	87.62
Median	3.39	10.77	12.61	13.61	14.72	97.85
Mean	3.85	10.87	12.60	13.59	14.81	94.34
Max	14.80	16.01	15.88	16.67	19.43	100.00
Third Quartile	4.34	12.32	13.44	14.72	16.16	98.29

SD	2.30	2.13	1.63	1.55	1.89	5.37
SE	0.23	0.21	0.16	0.15	0.19	1.92*
Margin of error (95% CI)	0.45	0.42	0.32	0.30	0.37	3.76
Upper 95% CI	4.30	11.29	12.92	13.90	15.18	98.10*
Lower 95% CI	3.40	10.45	12.28	13.29	14.44	90.58*

*Margins of error (95% CI) for archaeological data were obtained by bootstrapping the standard errors 10000 times.

MIS6 with a Paleo-Agulhas plain silcrete source– Toolkit size (Toolkit parameter)

Table B95. Summary statistics and test results for OFAT3 modeling of MIS6 conditions with a Paleo-Agulhas plain silcrete source compared to MIS6 archaeological raw material frequency data from PP13B.

	Toolkit=5-Quartz	**Toolkit=10-Quartz**	**Toolkit=50-Quartz**	**Toolkit=75-Quartz**	**Toolkit=100-Quartz**	**PP13-MIS6-Quartz**
n (number of assemblages)	1000	1000	1000	1000	1000	7
First Quartile	39.13	46.20	51.34	55.04	55.70	1.71
Min	15.00	25.93	42.94	43.91	44.75	0.00
Median	46.15	48.81	55.00	57.32	58.55	2.15
Mean	46.93	49.85	54.64	57.53	58.25	4.41
Max	73.33	71.05	65.50	67.25	65.55	9.39
Third Quartile	55.56	54.94	58.74	60.14	61.05	9.33
SD	11.62	7.84	4.90	4.56	3.93	3.91
SE	1.16	0.78	0.49	0.46	0.39	1.40*
Margin of error (95% CI)	2.28	1.54	0.96	0.89	0.77	2.74
Upper 95% CI	49.21	51.39	55.60	58.43	59.02	7.15*
Lower 95% CI	44.66	48.31	53.68	56.64	57.48	1.68*
	Toolkit=5-Silcrete	**Toolkit=10-Silcrete**	**Toolkit=50-Silcrete**	**Toolkit=75-Silcrete**	**Toolkit=100-Silcrete**	**PP13B-MIS6-Silcrete**
n (number of assemblages)	1000	1000	1000	1000	1000	7
First Quartile	34.91	34.05	33.71	31.74	32.17	0.00
Min	10.53	22.22	21.05	26.83	26.67	0.00
Median	41.42	40.00	36.94	34.57	34.37	0.00
Mean	41.07	39.61	36.83	35.07	34.77	1.09
Max	66.67	62.96	46.86	49.82	47.22	5.01
Third Quartile	47.77	44.62	39.97	37.69	36.96	2.55
SD	11.02	7.73	4.70	4.20	3.72	1.97
SE	1.10	0.77	0.47	0.42	0.37	0.68*
Margin of error (95% CI)	2.16	1.51	0.92	0.82	0.73	1.34
Upper 95% CI	43.23	41.13	37.75	35.90	35.50	2.42*
Lower 95% CI	38.91	38.10	35.91	34.25	34.04	0.00*
	Toolkit=5-Quartzite	**Toolkit=10-Quartzite**	**Toolkit=50-Quartzite**	**Toolkit=75-Quartzite**	**Toolkit=100-Quartzite**	**PP13B-MIS6-Quartzite**
n (number of assemblages)	1000	1000	1000	1000	1000	7

First Quartile	5.64	7.74	6.57	5.84	5.66	87.62
Min	0.00	2.50	3.13	2.72	3.96	87.62
Median	11.54	10.26	8.40	7.28	6.72	97.85
Mean	12.00	10.54	8.53	7.40	6.98	94.34
Max	32.00	24.32	15.69	13.58	13.44	100.00
Third Quartile	15.79	13.29	9.91	8.78	8.02	98.29
SD	7.68	4.21	2.44	1.89	1.92	5.37
SE	0.77	0.42	0.24	0.19	0.19	1.92*
Margin of error (95% CI)	1.51	0.83	0.48	0.37	0.38	3.76
Upper 95% CI	13.50	11.36	9.01	7.77	7.35	98.10*
Lower 95% CI	10.49	9.71	8.05	7.02	6.60	90.58*

*Margins of error (95% CI) for archaeological data were obtained by bootstrapping the standard errors 10000 times.

Table B96. Comparison between ranked model frequencies from OFAT3 simulations of MIS6 conditions with a Paleo-Agulhas plain silcrete source and ranked MIS6 archaeological frequencies from PP13B.

	Discard probability at locality (PDC)*					**Archaeology**
Raw Material	**0.001**	**0.1**	**0.5**	**0.75**	**0.95**	**MIS6-PP13B**
Quartz	1	1	1	1	1	2
Silcrete	2	2	2	2	2	2
Quartzite	3	3	3	3	3	1
	Discard probability on landscape (PD)*					**Archaeology**
Raw Material	**0.001**	**0.1**	**0.5**	**0.75**	**0.95**	**MIS6-PP13B**
Quartz	1	1	1	1	1	2
Silcrete	2	2	2	2	2	2
Quartzite	3	3	3	3	3	1
	Toolkit size*					**Archaeology**
Raw Material	**5**	**10**	**50**	**75**	**100**	**MIS6-PP13B**
Quartz	1	1	1	1	1	2
Silcrete	2	2	2	2	2	2
Quartzite	3	3	3	3	3	1

* Ranking based on which raw materials have the highest mean frequency. Similar rankings in the table are due to statistically similar frequencies. Ranking based on MIS6 archaeological raw material frequencies from bootstrapped data in Figure 50 and Table 19. Similar rankings in the table are due to statistically similar frequencies.

Move to closest locality

MIS4 without a Paleo-Agulhas plain silcrete source– Discard probability at locality (PDC-ProbDiscardCamp parameter)

Table B97. Summary statistics and test results for OFAT3 modeling of MIS4 conditions without a Paleo-Agulhas plain silcrete source compared to MIS4 archaeological raw material frequency data from PP5-6.

	PDC=0.001-Quartz	**PDC=0.1-Quartz**	**PDC=0.5-Quartz**	**PDC=0.75-Quartz**	**PDC=0.95-Quartz**	**PP5-6-MIS4-Quartz**
n (number of simulated assemblages)	1000	1000	1000	1000	1000	46
First Quartile	69.23	89.86	96.69	97.34	97.58	1.21
Min	25.00	70.42	90.34	94.20	94.56	0.00
Median	77.78	92.33	97.63	98.19	98.23	3.73
Mean	76.57	91.68	97.35	97.98	98.16	8.39
Max	100.00	100.00	100.00	100.00	100.00	66.11
Third Quartile	88.24	95.13	98.33	98.75	98.84	10.53
SD	15.32	4.95	1.70	1.16	1.08	11.83
SE	1.53	0.49	0.17	0.12	0.11	1.67*
Margin of error (95% CI)	3.00	0.97	0.33	0.23	0.21	3.28
Upper 95% CI	79.57	92.65	97.68	98.20	98.37	11.66*
Lower 95% CI	73.56	90.71	97.02	97.75	97.95	5.11*
	PDC=0.001-Silcrete	**PDC=0.1-Silcrete**	**PDC=0.5-Silcrete**	**PDC=0.75-Silcrete**	**PDC=0.95-Silcrete**	**PP5-6-MIS4-Silcrete**
n (number of simulated assemblages)	1000	1000	1000	1000	1000	46
First Quartile	0.00	0.00	0.00	0.00	0.00	13.79
Min	0.00	0.00	0.00	0.00	0.00	0.00
Median	0.00	0.00	0.00	0.00	0.00	39.13
Mean	0.25	0.11	0.01	0.01	0.00	40.00
Max	8.25	0.72	0.36	0.16	0.03	96.55
Third Quartile	0.00	0.15	0.00	0.00	0.00	62.77
SD	1.15	0.20	0.06	0.03	0.00	27.52
SE	0.11	0.02	0.01	0.00	0.00	4.01*
Margin of error (95% CI)	0.22	0.04	0.01	0.01	0.00	7.85
Upper 95% CI	0.47	0.15	0.03	0.01	0.00	47.85*
Lower 95% CI	0.02	0.07	0.00	0.00	0.00	32.15*
	PDC=0.001-Quartzite	**PDC=0.1-Quartzite**	**PDC=0.5-Quartzite**	**PDC=0.75-Quartzite**	**PDC=0.95-Quartzite**	**PP5-6-MIS4-Quartzite**
n (number of simulated assemblages)	1000	1000	1000	1000	1000	46
First Quartile	11.76	4.81	1.64	1.25	1.16	5.19
Min	0.00	0.00	0.00	0.00	0.00	0.00
Median	22.22	7.64	2.35	1.81	1.76	43.00
Mean	23.19	8.21	2.64	2.02	1.84	44.63

Max	75.00	29.58	9.34	5.80	5.44	96.45
Third Quartile	30.77	10.12	3.25	2.66	2.42	68.24
SD	15.16	4.94	1.69	1.16	1.08	25.54
SE	1.52	0.49	0.17	0.12	0.11	3.71*
Margin of error (95% CI)	2.97	0.97	0.33	0.23	0.21	7.27
Upper 95% CI	26.16	9.17	2.97	2.25	2.05	51.90*
Lower 95% CI	20.22	7.24	2.31	1.79	1.63	37.35*

*Margins of error (95% CI) for archaeological data were obtained by bootstrapping the standard errors 10000 times.

MIS4 without a Paleo-Agulhas plain silcrete source – Discard probability on landscape (PD-ProbDiscard parameter)

Table B98. Summary statistics and test results for OFAT3 modeling of MIS4 conditions without a Paleo-Agulhas plain silcrete source compared to MIS4 archaeological raw material frequency data from PP5-6.

	PD=0.001-Quartz	**PD=0.1-Quartz**	**PD=0.5-Quartz**	**PD=0.75-Quartz**	**PD=0.95-Quartz**	**PP5-6-MIS4-Quartz**
n (number of simulated assemblages)	1000	1000	1000	1000	1000	46
First Quartile	69.89	90.99	96.62	97.76	97.89	1.21
Min	50.00	0.00	84.62	87.88	94.23	0.00
Median	78.77	93.36	98.15	98.51	98.59	3.73
Mean	76.94	91.58	97.49	98.14	98.39	8.39
Max	100.00	100.00	100.00	100.00	100.00	66.11
Third Quartile	85.98	95.44	99.15	99.30	99.12	10.53
SD	12.16	10.62	2.55	1.98	1.18	11.83
SE	1.22	1.06	0.26	0.20	0.12	1.67*
Margin of error (95% CI)	2.38	2.08	0.50	0.39	0.23	3.28
Upper 95% CI	79.33	93.66	97.99	98.53	98.62	11.66*
Lower 95% CI	74.56	89.49	96.99	97.75	98.16	5.11*
	PD=0.001-Silcrete	**PD=0.1-Silcrete**	**PD=0.5-Silcrete**	**PD=0.75-Silcrete**	**PD=0.95-Silcrete**	**PP5-6-MIS4-Silcrete**
n (number of simulated assemblages)	1000	1000	1000	1000	1000	46
First Quartile	0.00	0.00	0.00	0.00	0.00	13.79
Min	0.00	0.00	0.00	0.00	0.00	0.00
Median	0.00	0.00	0.00	0.00	0.00	39.13
Mean	0.45	0.08	0.00	0.02	0.02	40.00
Max	4.08	2.83	0.36	1.51	1.04	96.55
Third Quartile	0.65	0.00	0.00	0.00	0.00	62.77
SD	0.81	0.33	0.04	0.15	0.12	27.52
SE	0.08	0.03	0.00	0.02	0.01	4.01*
Margin of error (95% CI)	0.16	0.06	0.01	0.03	0.02	7.85
Upper 95% CI	0.61	0.15	0.01	0.04	0.04	47.85*
Lower 95% CI	0.29	0.02	0.00	0.00	0.00	32.15*

	PD=0.001-Quartzite	PD=0.1-Quartzite	PD=0.5-Quartzite	PD=0.75-Quartzite	PD=0.95-Quartzite	PP5-6-MIS4-Quartzite
n (number of simulated assemblages)	1000	1000	1000	1000	1000	46
First Quartile	13.95	4.55	0.85	0.70	0.88	5.19
Min	0.00	0.00	0.00	0.00	0.00	0.00
Median	20.37	6.55	1.85	1.49	1.35	43.00
Mean	22.60	8.34	2.51	1.84	1.60	44.63
Max	50.00	100.00	15.38	12.12	5.77	96.45
Third Quartile	28.52	9.01	3.38	2.24	2.09	68.24
SD	11.93	10.55	2.55	1.97	1.17	25.54
SE	1.19	1.06	0.26	0.20	0.12	3.71*
Margin of error (95% CI)	2.34	2.07	0.50	0.39	0.23	7.27
Upper 95% CI	24.94	10.41	3.01	2.23	1.83	51.90*
Lower 95% CI	20.27	6.27	2.01	1.46	1.37	37.35*

*Margins of error (95% CI) for archaeological data were obtained by bootstrapping the standard errors 10000 times.

MIS4 without a Paleo-Agulhas plain silcrete source – Toolkit size (Toolkit parameter)

Table B99. Summary statistics and test results for OFAT3 modeling of MIS4 conditions without a Paleo-Agulhas plain silcrete source compared to MIS4 archaeological raw material frequency data from PP5-6.

	Toolkit=5-Quartz	Toolkit=10-Quartz	Toolkit=50-Quartz	Toolkit=75-Quartz	Toolkit=100-Quartz	PP5-6-MIS4-Quartz
n (number of simulated assemblages)	1000	1000	1000	1000	1000	46
First Quartile	94.44	91.78	83.50	78.90	76.85	1.21
Min	0.00	75.00	0.00	60.00	26.37	0.00
Median	100.00	96.49	88.65	85.99	84.07	3.73
Mean	95.73	95.01	87.03	84.57	80.66	8.39
Max	100.00	100.00	100.00	100.00	100.00	66.11
Third Quartile	100.00	100.00	93.46	90.33	88.23	10.53
SD	11.58	5.94	11.59	8.75	13.64	11.83
SE	1.16	0.59	1.16	0.87	1.36	1.67*
Margin of error (95% CI)	2.27	1.16	2.27	1.71	2.67	3.28
Upper 95% CI	98.00	96.17	89.30	86.28	83.33	11.66*
Lower 95% CI	93.45	93.84	84.76	82.85	77.99	5.11*
	Toolkit=5-Silcrete	**Toolkit=10-Silcrete**	**Toolkit=50-Silcrete**	**Toolkit=75-Silcrete**	**Toolkit=100-Silcrete**	**PP5-6-MIS4-Silcrete**
n (number of simulated assemblages)	1000	1000	1000	1000	1000	46
First Quartile	0.00	0.00	0.00	0.00	0.00	13.79
Min	0.00	0.00	0.00	0.00	0.00	0.00
Median	0.00	0.00	0.00	0.00	0.00	39.13
Mean	0.00	0.39	0.12	0.25	0.25	40.00

Max	0.00	24.75	2.25	7.07	5.21	96.55
Third Quartile	0.00	0.00	0.00	0.00	0.31	62.77
SD	0.00	2.84	0.39	0.87	0.65	27.52
SE	0.00	0.28	0.04	0.09	0.07	4.01*
Margin of error (95% CI)	0.00	0.56	0.08	0.17	0.13	7.85
Upper 95% CI	0.00	0.95	0.20	0.42	0.38	47.85*
Lower 95% CI	0.00	0.00	0.04	0.08	0.13	32.15*
	Toolkit=5-Quartzite	**Toolkit=10-Quartzite**	**Toolkit=50-Quartzite**	**Toolkit=75-Quartzite**	**Toolkit=100-Quartzite**	**PP5-6-MIS4-Quartzite**
n (number of simulated assemblages)	1000	1000	1000	1000	1000	46
First Quartile	0.00	0.00	6.21	9.45	11.74	5.19
Min	0.00	0.00	0.00	0.00	0.00	0.00
Median	0.00	3.39	11.12	13.68	15.74	43.00
Mean	3.27	4.60	11.85	15.18	19.09	44.63
Max	33.33	25.00	37.70	40.00	69.70	96.45
Third Quartile	5.42	6.84	15.84	20.71	22.30	68.24
SD	6.39	5.56	7.63	8.47	13.41	25.54
SE	0.64	0.56	0.76	0.85	1.34	3.71*
Margin of error (95% CI)	1.25	1.09	1.50	1.66	2.63	7.27
Upper 95% CI	4.53	5.69	13.35	16.84	21.71	51.90*
Lower 95% CI	2.02	3.51	10.35	13.52	16.46	37.35*

*Margins of error (95% CI) for archaeological data were obtained by bootstrapping the standard errors 10000 times.

Table B100. Comparison between ranked model frequencies from OFAT3 simulations of MIS4 conditions without a Paleo-Agulhas plain silcrete source and ranked MIS4 archaeological frequencies from PP5-6.

	Discard probability at locality (PDC)*					**Archaeology**
Raw Material	**0.001**	**0.1**	**0.5**	**0.75**	**0.95**	**MIS4-PP5-6**
Quartz	1	1	1	1	1	2
Silcrete	3	3	3	3	3	1
Quartzite	2	2	2	2	2	1
	Discard probability on landscape (PD)*					**Archaeology**
Raw Material	**0.001**	**0.1**	**0.5**	**0.75**	**0.95**	**MIS4-PP5-6**
Quartz	1	1	1	1	1	2
Silcrete	3	3	3	3	3	1
Quartzite	2	2	2	2	2	1
	Toolkit size*					**Archaeology**
Raw Material	**5**	**10**	**50**	**75**	**100**	**MIS4-PP5-6**
Quartz	1	1	1	1	1	2
Silcrete	3	3	3	3	3	1

Quartzite	2	2	2	2	2	1

* Ranking based on which raw materials have the highest mean frequency. Similar rankings in the table are due to statistically similar frequencies. Ranking based on MIS4 archaeological raw material frequencies from bootstrapped data in Figure 50 and Table 19. Similar rankings in the table are due to statistically similar frequencies.

MIS4 with a Paleo-Agulhas plain silcrete source– Discard probability at locality (PDC-ProbDiscardCamp parameter)

Table B101. Summary statistics and test results for OFAT3 modeling of MIS4 conditions with a Paleo-Agulhas plain silcrete source compared to MIS4 archaeological raw material frequency data from PP5-6.

	PDC=0.001-Quartz	**PDC=0.1-Quartz**	**PDC=0.5-Quartz**	**PDC=0.75-Quartz**	**PDC=0.95-Quartz**	**PP5-6-MIS4-Quartz**
n (number of simulated assemblages)	1000	1000	1000	1000	1000	46
First Quartile	30.46	58.77	64.60	65.88	65.43	1.21
Min	0.00	51.52	42.36	0.00	56.32	0.00
Median	41.67	61.70	66.96	67.92	67.99	3.73
Mean	41.32	61.52	66.47	67.31	67.54	8.39
Max	100.00	77.27	79.26	98.41	75.27	66.11
Third Quartile	53.40	64.09	68.13	69.62	69.56	10.53
SD	19.31	4.42	3.73	8.00	3.33	11.83
SE	1.93	0.44	0.37	0.80	0.33	1.67*
Margin of error (95% CI)	3.79	0.87	0.73	1.57	0.65	3.28
Upper 95% CI	45.11	62.39	67.20	68.87	68.19	11.66*
Lower 95% CI	37.54	60.66	65.74	65.74	66.89	5.11*
	PDC=0.001-Silcrete	**PDC=0.1-Silcrete**	**PDC=0.5-Silcrete**	**PDC=0.75-Silcrete**	**PDC=0.95-Silcrete**	**PP5-6-MIS4-Silcrete**
n (number of simulated assemblages)	1000	1000	1000	1000	1000	46
First Quartile	28.57	28.42	29.42	28.40	29.16	13.79
Min	0.00	19.05	20.74	0.00	24.73	0.00
Median	36.18	31.03	30.85	30.55	31.19	39.13
Mean	37.70	30.74	31.13	30.02	31.28	40.00
Max	100.00	38.18	51.75	39.50	40.82	96.55
Third Quartile	45.74	32.98	32.80	32.71	33.19	62.77
SD	18.87	3.61	3.29	5.20	3.31	27.52
SE	1.89	0.36	0.33	0.52	0.33	4.01*
Margin of error (95% CI)	3.70	0.71	0.64	1.02	0.65	7.85
Upper 95% CI	41.40	31.45	31.77	31.03	31.93	47.85*
Lower 95% CI	34.00	30.03	30.48	29.00	30.63	32.15*
	PDC=0.001-Quartzite	**PDC=0.1-Quartzite**	**PDC=0.5-Quartzite**	**PDC=0.75-Quartzite**	**PDC=0.95-Quartzite**	**PP5-6-MIS4-Quartzite**
n (number of simulated assemblages)	1000	1000	1000	1000	1000	46
First Quartile	9.09	4.62	1.52	1.02	0.59	5.19
Min	0.00	0.00	0.00	0.00	0.00	0.00

Median	16.67	7.30	2.05	1.42	1.05	43.00
Mean	20.97	7.74	2.40	1.68	1.18	44.63
Max	100.00	22.80	7.94	6.23	4.20	96.45
Third Quartile	29.41	9.47	2.91	1.98	1.59	68.24
SD	17.21	4.17	1.47	1.11	0.81	25.54
SE	1.72	0.42	0.15	0.11	0.08	3.71*
Margin of error (95% CI)	3.37	0.82	0.29	0.22	0.16	7.27
Upper 95% CI	24.35	8.55	2.69	1.90	1.34	51.90*
Lower 95% CI	17.60	6.92	2.11	1.46	1.02	37.35*

*Margins of error (95% CI) for archaeological data were obtained by bootstrapping the standard errors 10000 times.

MIS4 with a Paleo-Agulhas plain silcrete source– Discard probability on landscape (PD-ProbDiscard parameter)

Table B102. Summary statistics and test results for OFAT3 modeling of MIS4 conditions with a Paleo-Agulhas plain silcrete source compared to MIS4 archaeological raw material frequency data from PP5-6.

	PD=0.001-Quartz	**PD=0.1-Quartz**	**PD=0.5-Quartz**	**PD=0.75-Quartz**	**PD=0.95-Quartz**	**PP5-6-MIS4-Quartz**
n (number of simulated assemblages)	1000	1000	1000	1000	1000	46
First Quartile	46.40	47.03	45.37	43.18	42.12	1.21
Min	7.69	33.33	32.46	30.61	33.66	0.00
Median	54.56	49.87	48.46	45.33	44.79	3.73
Mean	52.21	49.96	47.80	45.69	45.28	8.39
Max	73.08	65.52	59.30	61.32	59.83	66.11
Third Quartile	60.14	53.09	50.45	47.85	48.00	10.53
SD	11.44	5.21	4.61	4.60	4.39	11.83
SE	1.14	0.52	0.46	0.46	0.44	1.67*
Margin of error (95% CI)	2.24	1.02	0.90	0.90	0.86	3.28
Upper 95% CI	54.45	50.98	48.70	46.59	46.14	11.66*
Lower 95% CI	49.96	48.94	46.89	44.79	44.42	5.11*
	PD=0.001-Silcrete	**PD=0.1-Silcrete**	**PD=0.5-Silcrete**	**PD=0.75-Silcrete**	**PD=0.95-Silcrete**	**PP5-6-MIS4-Silcrete**
n (number of simulated assemblages)	1000	1000	1000	1000	1000	46
First Quartile	19.69	38.91	48.15	50.00	50.47	13.79
Min	3.90	27.27	32.56	33.96	40.17	0.00
Median	24.01	43.65	50.28	53.19	54.22	39.13
Mean	24.04	42.63	50.48	52.72	53.52	40.00
Max	53.85	66.67	66.67	67.35	66.34	96.55
Third Quartile	28.88	46.09	53.02	55.39	56.76	62.77
SD	7.86	5.92	4.83	4.91	4.38	27.52
SE	0.79	0.59	0.48	0.49	0.44	4.01*
Margin of error (95% CI)	1.54	1.16	0.95	0.96	0.86	7.85

Upper 95% CI	25.58	43.79	51.43	53.68	54.38	47.85*
Lower 95% CI	22.50	41.47	49.54	51.76	52.66	32.15*
	PD=0.001-Quartzite	**PD=0.1-Quartzite**	**PD=0.5-Quartzite**	**PD=0.75-Quartzite**	**PD=0.95-Quartzite**	**PP5-6-MIS4-Quartzite**
n (number of simulated assemblages)	1000	1000	1000	1000	1000	46
First Quartile	16.34	4.40	0.87	0.62	0.49	5.19
Min	1.96	0.00	0.00	0.00	0.00	0.00
Median	21.33	6.81	1.51	1.26	0.91	43.00
Mean	23.75	7.41	1.72	1.59	1.20	44.63
Max	70.13	18.46	9.09	14.81	8.82	96.45
Third Quartile	28.07	9.71	2.21	1.87	1.47	68.24
SD	12.02	4.23	1.51	1.87	1.28	25.54
SE	1.20	0.42	0.15	0.19	0.13	3.71*
Margin of error (95% CI)	2.36	0.83	0.30	0.37	0.25	7.27
Upper 95% CI	26.11	8.24	2.02	1.95	1.45	51.90*
Lower 95% CI	21.40	6.58	1.42	1.22	0.95	37.35*

*Margins of error (95% CI) for archaeological data were obtained by bootstrapping the standard errors 10000 times.

MIS4 with a Paleo-Agulhas plain silcrete source – Toolkit size (Toolkit parameter)

Table B103. Summary statistics and test results for OFAT3 modeling of MIS4 conditions with a Paleo-Agulhas plain silcrete source compared to MIS4 archaeological raw material frequency data from PP5-6.

	Toolkit=5-Quartz	**Toolkit=10-Quartz**	**Toolkit=50-Quartz**	**Toolkit=75-Quartz**	**Toolkit=100-Quartz**	**PP5-6-MIS4-Quartz**
n (number of simulated assemblages)	1000	1000	1000	1000	1000	46
First Quartile	40.42	42.19	47.15	47.09	44.36	1.21
Min	0.00	0.00	19.07	31.43	25.20	0.00
Median	48.20	50.00	51.06	50.74	51.84	3.73
Mean	47.29	49.86	51.76	50.58	50.24	8.39
Max	80.00	85.71	100.00	94.12	65.71	66.11
Third Quartile	55.42	56.22	55.64	53.56	56.06	10.53
SD	13.56	12.79	9.71	7.30	8.27	11.83
SE	1.36	1.28	0.97	0.73	0.83	1.67*
Margin of error (95% CI)	2.66	2.51	1.90	1.43	1.62	3.28
Upper 95% CI	49.95	52.36	53.67	52.02	51.86	11.66*
Lower 95% CI	44.64	47.35	49.86	49.15	48.62	5.11*
	Toolkit=5-Silcrete	**Toolkit=10-Silcrete**	**Toolkit=50-Silcrete**	**Toolkit=75-Silcrete**	**Toolkit=100-Silcrete**	**PP5-6-MIS4-Silcrete**
n (number of simulated assemblages)	1000	1000	1000	1000	1000	46
First Quartile	41.96	40.16	34.42	30.39	28.52	13.79
Min	20.00	0.00	0.00	5.88	8.00	0.00

Median	50.00	47.59	37.68	34.84	33.09	39.13
Mean	50.74	46.77	37.02	34.46	32.55	40.00
Max	87.50	100.00	53.02	51.82	49.99	96.55
Third Quartile	58.44	54.55	41.46	39.68	36.77	62.77
SD	13.78	13.53	7.72	7.20	6.62	27.52
SE	1.38	1.35	0.77	0.72	0.66	4.01*
Margin of error (95% CI)	2.70	2.65	1.51	1.41	1.30	7.85
Upper 95% CI	53.44	49.42	38.53	35.87	33.84	47.85*
Lower 95% CI	48.04	44.12	35.50	33.05	31.25	32.15*
	Toolkit=5-Quartzite	**Toolkit=10-Quartzite**	**Toolkit=50-Quartzite**	**Toolkit=75-Quartzite**	**Toolkit=100-Quartzite**	**PP5-6-MIS4-Quartzite**
n (number of simulated assemblages)	1000	1000	1000	1000	1000	46
First Quartile	0.00	0.00	6.10	9.75	10.17	5.19
Min	0.00	0.00	0.00	0.00	0.00	0.00
Median	0.00	2.25	9.71	13.59	16.57	43.00
Mean	1.96	3.38	11.22	14.95	17.21	44.63
Max	16.67	25.00	45.24	36.96	62.00	96.45
Third Quartile	0.00	5.20	15.54	19.93	24.17	68.24
SD	3.91	4.44	7.81	7.89	9.68	25.54
SE	0.39	0.44	0.78	0.79	0.97	3.71*
Margin of error (95% CI)	0.77	0.87	1.53	1.55	1.90	7.27
Upper 95% CI	2.73	4.25	12.75	16.50	19.11	51.90*
Lower 95% CI	1.19	2.51	9.69	13.41	15.32	37.35*

*Margins of error (95% CI) for archaeological data were obtained by bootstrapping the standard errors 10000 times.

Table B104. Comparison between ranked model frequencies from OFAT3 simulations of MIS4 conditions with a Paleo-Agulhas plain silcrete source and ranked MIS4 archaeological frequencies from PP5-6.

	Discard probability at locality (PDC)*					**Archaeology**
Raw Material	**0.001**	**0.1**	**0.5**	**0.75**	**0.95**	**MIS4-PP5-6**
Quartz	1	1	1	1	1	2
Silcrete	1	2	2	2	2	1
Quartzite	2	3	3	3	3	1
	Discard probability on landscape (PD)*					**Archaeology**
Raw Material	**0.001**	**0.1**	**0.5**	**0.75**	**0.95**	**MIS4-PP5-6**
Quartz	1	1	2	2	2	2
Silcrete	2	2	1	1	1	1
Quartzite	2	3	3	3	3	1
	Toolkit size*					**Archaeology**
Raw Material	**5**	**10**	**50**	**75**	**100**	**MIS4-PP5-6**

Quartz	1	1	1	1	1	2
Silcrete	1	1	2	2	2	1
Quartzite	2	2	3	3	3	1

* Ranking based on which raw materials have the highest mean frequency. Similar rankings in the table are due to statistically similar frequencies. Ranking based on MIS4 archaeological raw material frequencies from bootstrapped data in Figure 50 and Table 19. Similar rankings in the table are due to statistically similar frequencies.

MIS5 conditions– Discard probability at locality (PDC-ProbDiscardCamp parameter)

Table B105. Summary statistics and test results for OFAT3 modeling of MIS5 conditions compared to MIS5 archaeological raw material frequency data from PP5-6, PP13B, PP9B, and PP9C.

	PDC=0.001-Quartz	**PDC=0.1-Quartz**	**PDC=0.5-Quartz**	**PDC=0.75-Quartz**	**PDC=0.95-Quartz**	**PP5-6-MIS5-Quartz**	**PP13B-MIS5-Quartz**	**AllPP-MIS5-Quartz**
n (number of assemblages)	1000	1000	1000	1000	1000	31	7	43
First Quartile	63.26	76.45	80.21	80.30	81.01	0.00	1.71	0.10
Min	0.00	70.02	72.75	64.80	52.62	0.00	0.00	0.00
Median	70.90	78.79	82.01	82.01	82.64	0.89	2.15	2.65
Mean	70.15	78.82	81.81	81.50	82.22	3.53	4.41	4.61
Max	100.00	88.67	98.51	86.92	100.00	24.87	9.39	24.87
Third Quartile	77.82	81.62	83.83	83.90	84.29	3.92	9.33	6.95
SD	15.04	3.89	3.31	3.78	4.57	5.94	3.91	6.03
SE	1.50	0.39	0.33	0.38	0.46	1.03*	1.40*	0.90*
Margin of error (95% CI)	2.95	0.76	0.65	0.74	0.90	2.03	2.74	1.76
Upper 95% CI	73.10	79.58	82.45	82.24	83.12	5.56*	7.15*	6.37*
Lower 95% CI	67.20	78.06	81.16	80.76	81.32	1.51*	1.68*	2.85*
	PDC=0.001-Silcrete	**PDC=0.1-Silcrete**	**PDC=0.5-Silcrete**	**PDC=0.75-Silcrete**	**PDC=0.95-Silcrete**	**PP5-6-MIS5-Silcrete**	**PP13B-Silcrete**	**AllPP-MIS5-Silcrete**
n (number of assemblages)	1000	1000	1000	1000	1000	31	7	4.30E+01
First Quartile	0.08	0.09	0.09	0.09	0.09	1.45	0.00	0.95
Min	0.00	0.07	0.01	0.07	0.00	0.00	0.00	0.00
Median	0.11	0.14	0.10	0.10	0.10	10.19	0.00	6.44
Mean	2.05	0.60	0.12	0.12	0.10	16.97	1.09	13.05
Max	24.83	6.04	0.84	0.75	0.29	64.83	5.01	64.83
Third Quartile	2.94	0.86	0.12	0.11	0.11	32.95	2.55	21.21
SD	4.02	0.87	0.09	0.08	0.03	17.85	1.97	16.45
SE	0.40	0.09	0.01	0.01	0.00	3.14*	0.68*	2.46*
Margin of error (95% CI)	0.79	0.17	0.02	0.02	0.01	6.16	1.34	4.82
Upper 95% CI	2.84	0.77	0.14	0.13	0.11	23.12*	2.42*	17.86*

Lower 95% CI	1.26	0.43	0.10	0.10	0.10	10.81*	0.00*	8.23*
	PDC=0.001-Quartzite	**PDC=0.1-Quartzite**	**PDC=0.5-Quartzite**	**PDC=0.75-Quartzite**	**PDC=0.95-Quartzite**	**P5-6-MIS5-Quartzite**	**PP13B-Quartzite**	**AllPP-MIS5-Quartzite**
n (number of assemblages)	1000	1000	1000	1000	1000	31	7	43
First Quartile	19.79	18.06	15.99	15.95	15.56	60.24	87.62	64.30
Min	0.00	11.21	1.47	12.95	0.00	26.94	87.62	26.94
Median	26.47	20.89	17.83	17.79	17.20	76.11	97.85	83.74
Mean	27.74	20.52	18.01	18.32	17.61	72.77	94.34	77.20
Max	100.00	29.57	27.02	34.85	46.90	100.00	100.00	100.00
Third Quartile	34.48	22.62	19.60	19.52	18.82	92.83	98.29	92.83
SD	14.67	3.65	3.27	3.73	4.52	21.79	5.37	20.01
SE	1.47	0.37	0.33	0.37	0.45	3.85*	1.92*	3.00*
Margin of error (95% CI)	2.88	0.72	0.64	0.73	0.89	7.55	3.76	5.87
Upper 95% CI	30.61	21.23	18.65	19.05	18.50	80.32*	98.10*	83.07*
Lower 95% CI	24.86	19.80	17.37	17.59	16.72	65.21*	90.58*	71.33*

*Margins of error (95% CI) for archaeological data were obtained by bootstrapping the standard errors 10000 times.

MIS5 conditions – Discard probability on landscape (PD-ProbDiscard parameter)

Table B106. Summary statistics and test results for OFAT3 modeling of MIS5 conditions compared to MIS5 archaeological raw material frequency data from PP5-6, PP13B, PP9B, and PP9C.

	PD=0.001-Quartz	**PD=0.1-Quartz**	**PD=0.5-Quartz**	**PD=0.75-Quartz**	**PD=0.95-Quartz**	**PP5-6-MIS5-Quartz**	**PP13B-MIS5-Quartz**	**AllPP-MIS5-Quartz**
n (number of assemblages)	1000	1000	1000	1000	1000	31	7	43
First Quartile	65.54	73.77	75.98	75.91	75.74	0.00	1.71	0.10
Min	47.66	59.12	67.02	33.67	69.81	0.00	0.00	0.00
Median	71.84	76.69	78.65	78.72	78.40	0.89	2.15	2.65
Mean	70.24	76.16	78.73	77.94	78.24	3.53	4.41	4.61
Max	86.09	87.02	100.00	87.04	85.54	24.87	9.39	24.87
Third Quartile	75.52	79.82	81.00	80.68	80.42	3.92	9.33	6.95
SD	7.19	4.99	4.25	5.85	3.31	5.94	3.91	6.03
SE	0.72	0.50	0.43	0.59	0.33	1.03*	1.40*	0.90*
Margin of error (95% CI)	1.41	0.98	0.83	1.15	0.65	2.03	2.74	1.76
Upper 95% CI	71.64	77.13	79.56	79.09	78.89	5.56*	7.15*	6.37*
Lower 95% CI	68.83	75.18	77.90	76.79	77.59	1.51*	1.68*	2.85*
	PD=0.001-Silcrete	**PD=0.1-Silcrete**	**PD=0.5-Silcrete**	**PD=0.75-Silcrete**	**PD=0.95-Silcrete**	**PP5-6-MIS5-Silcrete**	**PP13B-Silcrete**	**AllPP-MIS5-Silcrete**

n (number of assemblages)	1000	1000	1000	1000	1000	31	7	4.30E+01
First Quartile	0.08	0.10	0.11	0.11	0.12	1.45	0.00	0.95
Min	0.05	0.03	0.00	0.08	0.08	0.00	0.00	0.00
Median	0.94	0.12	0.12	0.12	0.13	10.19	0.00	6.44
Mean	2.36	0.39	0.17	0.13	0.13	16.97	1.09	13.05
Max	24.80	3.78	5.45	0.40	0.18	64.83	5.01	64.83
Third Quartile	3.70	0.17	0.14	0.14	0.14	32.95	2.55	21.21
SD	3.53	0.69	0.53	0.04	0.02	17.85	1.97	16.45
SE	0.35	0.07	0.05	0.00	0.00	3.14*	0.68*	2.46*
Margin of error (95% CI)	0.69	0.13	0.10	0.01	0.00	6.16	1.34	4.82
Upper 95% CI	3.05	0.52	0.28	0.14	0.13	23.12*	2.42*	17.86*
Lower 95% CI	1.67	0.25	0.07	0.12	0.12	10.81*	0.00*	8.23*
	PD=0.001-Quartzite	**PD=0.1-Quartzite**	**PD=0.5-Quartzite**	**PD=0.75-Quartzite**	**PD=0.95-Quartzite**	**P5-6-MIS5-Quartzite**	**PP13B-Quartzite**	**AllPP-MIS5-Quartzite**
n (number of assemblages)	1000	1000	1000	1000	1000	31	7	43
First Quartile	21.89	19.68	18.84	19.13	19.39	60.24	87.62	64.30
Min	12.37	12.85	0.00	12.83	14.31	26.94	87.62	26.94
Median	26.93	23.14	21.14	21.07	21.39	76.11	97.85	83.74
Mean	27.35	23.38	21.02	21.84	21.55	72.77	94.34	77.20
Max	46.97	40.60	32.68	65.67	29.90	100.00	100.00	100.00
Third Quartile	32.33	25.78	23.79	23.85	24.03	92.83	98.29	92.83
SD	6.91	4.99	4.13	5.79	3.28	21.79	5.37	20.01
SE	0.69	0.50	0.41	0.58	0.33	3.85*	1.92*	3.00*
Margin of error (95% CI)	1.35	0.98	0.81	1.13	0.64	7.55	3.76	5.87
Upper 95% CI	28.71	24.36	21.83	22.98	22.19	80.32*	98.10*	83.07*
Lower 95% CI	26.00	22.41	20.21	20.71	20.91	65.21*	90.58*	71.33*

*Margins of error (95% CI) for archaeological data were obtained by bootstrapping the standard errors 10000 times.

MIS5 conditions – Toolkit size (Toolkit parameter)

Table B107. Summary statistics and test results for OFAT3 modeling of MIS5 conditions compared to MIS5 archaeological raw material frequency data from PP5-6, PP13B, PP9B, and PP9C.

	Toolkit=5-Quartz	**Toolkit=10-Quartz**	**Toolkit=50-Quartz**	**Toolkit=75-Quartz**	**Toolkit=100-Quartz**	**PP5-6-MIS5-Quartz**	**PP13B-MIS5-Quartz**	**AllPP-MIS5-Quartz**
n (number of assemblages)	1000	1000	1000	1000	1000	31	7	43
First Quartile	72.04	74.09	72.17	72.73	69.33	0.00	1.71	0.10
Min	50.25	0.00	54.08	57.61	47.10	0.00	0.00	0.00
Median	78.12	77.68	75.89	75.16	74.03	0.89	2.15	2.65

Mean	78.24	77.84	75.32	75.19	73.00	3.53	4.41	4.61
Max	100.00	100.00	95.48	92.57	94.10	24.87	9.39	24.87
Third Quartile	86.07	84.69	79.12	78.24	78.12	3.92	9.33	6.95
SD	10.24	11.38	6.39	5.55	7.24	5.94	3.91	6.03
SE	1.02	1.14	0.64	0.55	0.72	1.03	1.40	0.90*
Margin of error (95% CI)	2.01	2.23	1.25	1.09	1.42	2.03	2.74	1.76
Upper 95% CI	80.25	80.07	76.57	76.28	74.42	5.56	7.15	6.37*
Lower 95% CI	76.23	75.61	74.06	74.11	71.58	1.51	1.68	2.85*
	Toolkit=5-Silcrete	**Toolkit=10-Silcrete**	**Toolkit=50-Silcrete**	**Toolkit=75-Silcrete**	**Toolkit=100-Silcrete**	**PP5-6-MIS5-Silcrete**	**PP13B-Silcrete**	**AllPP-MIS5-Silcrete**
n (number of assemblages)	1000	1000	1000	1000	1000	31	7	4.30E+01
First Quartile	0.08	0.08	0.09	0.10	0.09	1.45	0.00	0.95
Min	0.00	0.00	0.03	0.04	0.00	0.00	0.00	0.00
Median	0.13	0.11	0.12	0.12	0.10	10.19	0.00	6.44
Mean	0.12	0.14	0.61	0.86	0.88	16.97	1.09	13.05
Max	0.30	2.70	5.48	5.22	7.18	64.83	5.01	64.83
Third Quartile	0.16	0.15	0.73	1.25	0.65	32.95	2.55	21.21
SD	0.06	0.26	1.02	1.28	1.60	17.85	1.97	16.45
SE	0.01	0.03	0.10	0.13	0.16	3.14	0.68	2.46*
Margin of error (95% CI)	0.01	0.05	0.20	0.25	0.31	6.16	1.34	4.82
Upper 95% CI	0.14	0.19	0.81	1.11	1.19	23.12	2.42	17.86*
Lower 95% CI	0.11	0.09	0.41	0.61	0.57	10.81	0.00	8.23*
	Toolkit=5-Quartzite	**Toolkit=10-Quartzite**	**Toolkit=50-Quartzite**	**Toolkit=75-Quartzite**	**Toolkit=100-Quartzite**	**P5-6-MIS5-Quartzite**	**PP13B-Quartzite**	**AllPP-MIS5-Quartzite**
n (number of assemblages)	1000	1000	1000	1000	1000	31	7	43
First Quartile	13.81	14.79	20.56	20.90	21.66	60.24	87.62	64.30
Min	0.00	0.00	4.48	7.35	5.84	26.94	87.62	26.94
Median	21.68	21.55	23.05	24.14	25.51	76.11	97.85	83.74
Mean	21.55	20.95	24.01	23.88	26.06	72.77	94.34	77.20
Max	49.25	42.76	45.76	39.47	52.82	100.00	100.00	100.00
Third Quartile	27.69	25.47	27.34	26.16	29.06	92.83	98.29	92.83
SD	10.14	8.42	6.42	5.44	6.89	21.79	5.37	20.01
SE	1.01	0.84	0.64	0.54	0.69	3.85	1.92	3.00*
Margin of error (95% CI)	1.99	1.65	1.26	1.07	1.35	7.55	3.76	5.87
Upper 95% CI	23.54	22.60	25.26	24.95	27.41	80.32	98.10	83.07*
Lower 95%	19.57	19.30	22.75	22.82	24.71	65.21	90.58	71.33*

CI								

*Margins of error (95% CI) for archaeological data were obtained by bootstrapping the standard errors 10000 times.

Table B108. Comparison between ranked model frequencies from OFAT3 simulations of MIS5 conditions and ranked MIS5 archaeological frequencies from PP13B, PP9B, PP9C, and PP5-6.

	Discard probability at locality (PDC)*					Archaeology		
Raw Material	**0.001**	**0.1**	**0.5**	**0.75**	**0.95**	**MIS5-PP5-6**	**MIS5-PP13B**	**MIS5-All PP**
Quartz	1	1	1	1	1	3	2	3
Silcrete	3	3	3	3	3	2	2	2
Quartzite	2	2	2	2	2	1	1	1
	Discard probability on landscape (PD)*					**Archaeology**		
Raw Material	**0.001**	**0.1**	**0.5**	**0.75**	**0.95**	**MIS5-PP5-6**	**MIS5-PP13B**	**MIS5-All PP**
Quartz	1	1	1	1	1	3	2	3
Silcrete	3	3	3	3	3	2	2	2
Quartzite	2	2	2	2	2	1	1	1
	Toolkit size*					**Archaeology**		
Raw Material	**5**	**10**	**50**	**75**	**100**	**MIS5-PP5-6**	**MIS5-PP13B**	**MIS5-All PP**
Quartz	1	1	1	1	1	3	2	3
Silcrete	3	3	3	3	3	2	2	2
Quartzite	2	2	2	2	2	1	1	1

* Ranking based on which raw materials have the highest mean frequency. Similar rankings in the table are due to statistically similar frequencies. Ranking based on MIS5 archaeological raw material frequencies from bootstrapped data in Figure 50 and Table 19. Similar rankings in the table are due to statistically similar frequencies.

MIS6 without a Paleo-Agulhas plain silcrete source– Discard probability at locality (PDC-ProbDiscardCamp parameter)

Table B109. Summary statistics and test results for OFAT3 modeling of MIS6 conditions without a Paleo-Agulhas plain silcrete source compared to MIS6 archaeological raw material frequency data from PP13B.

	PDC=0.001-Quartz	**PDC=0.1-Quartz**	**PDC=0.5-Quartz**	**PDC=0.75-Quartz**	**PDC=0.95-Quartz**	**PP13-MIS6-Quartz**
n (number of assemblages)	1000	1000	1000	1000	1000	7
First Quartile	38.85	70.82	77.47	77.68	78.64	1.71
Min	0.00	61.85	69.15	0.00	65.48	0.00
Median	50.93	73.78	80.05	79.90	80.46	2.15
Mean	50.45	73.59	79.49	78.28	80.08	4.41
Max	100.00	83.43	86.93	85.30	87.09	9.39
Third Quartile	64.12	77.04	81.09	81.75	81.78	9.33
SD	20.78	4.78	2.72	10.42	3.04	3.91
SE	2.08	0.48	0.27	1.04	0.30	1.40*
Margin of error (95% CI)	4.07	0.94	0.53	2.04	0.60	2.74

Upper 95% CI	54.52	74.53	80.02	80.32	80.67	7.15*
Lower 95% CI	46.37	72.65	78.95	76.24	79.48	1.68*
	PDC=0.001-Silcrete	**PDC=0.1-Silcrete**	**PDC=0.5-Silcrete**	**PDC=0.75-Silcrete**	**PDC=0.95-Silcrete**	**PP13B-MIS6-Silcrete**
n (number of assemblages)	1000	1000	1000	1000	1000	7
First Quartile	0.00	0.00	0.00	0.00	0.00	0.00
Min	0.00	0.00	0.00	0.00	0.00	0.00
Median	0.00	0.00	0.00	0.00	0.00	0.00
Mean	0.65	0.10	0.01	0.00	0.00	1.09
Max	19.80	1.47	0.20	0.14	0.09	5.01
Third Quartile	0.00	0.12	0.00	0.00	0.00	2.55
SD	2.69	0.23	0.03	0.02	0.01	1.97
SE	0.27	0.02	0.00	0.00	0.00	0.68*
Margin of error (95% CI)	0.53	0.05	0.01	0.00	0.00	1.34
Upper 95% CI	1.18	0.15	0.02	0.01	0.00	2.42*
Lower 95% CI	0.13	0.06	0.00	0.00	0.00	0.00*
	PDC=0.001-Quartzite	**PDC=0.1-Quartzite**	**PDC=0.5-Quartzite**	**PDC=0.75-Quartzite**	**PDC=0.95-Quartzite**	**PP13B-MIS6-Quartzite**
n (number of assemblages)	1000	1000	1000	1000	1000	7
First Quartile	33.33	22.88	18.91	18.20	18.22	87.62
Min	0.00	16.57	13.07	0.00	12.91	87.62
Median	46.90	26.22	19.95	20.07	19.54	97.85
Mean	47.90	26.31	20.50	20.72	19.92	94.34
Max	100.00	38.15	30.85	81.69	34.52	100.00
Third Quartile	60.00	28.96	22.53	22.20	21.36	98.29
SD	20.61	4.72	2.71	7.11	3.04	5.37
SE	2.06	0.47	0.27	0.71	0.30	1.92*
Margin of error (95% CI)	4.04	0.93	0.53	1.39	0.60	3.76
Upper 95% CI	51.94	27.23	21.04	22.11	20.52	98.10*
Lower 95% CI	43.86	25.38	19.97	19.32	19.33	90.58*

*Margins of error (95% CI) for archaeological data were obtained by bootstrapping the standard errors 10000 times.

MIS6 without a Paleo-Agulhas plain silcrete source– Discard probability on landscape (PD-ProbDiscard parameter)

Table B110. Summary statistics and test results for OFAT3 modeling of MIS6 conditions without a Paleo-Agulhas plain silcrete source compared to MIS6 archaeological raw material frequency data from PP13B.

	PD=0.001-Quartz	**PD=0.1-Quartz**	**PD=0.5-Quartz**	**PD=0.75-Quartz**	**PD=0.95-Quartz**	**PP13-MIS6-Quartz**
n (number of assemblages)	1000	1000	1000	1000	1000	7
First Quartile	48.64	58.78	60.81	58.88	58.77	1.71
Min	0.00	42.32	16.67	51.42	46.81	0.00

Median	57.41	62.76	63.77	61.78	61.42	2.15
Mean	56.71	62.62	63.12	62.39	61.36	4.41
Max	85.71	75.00	75.76	76.34	78.43	9.39
Third Quartile	67.30	66.44	67.15	65.53	63.56	9.33
SD	14.40	5.63	7.05	4.71	4.63	3.91
SE	1.44	0.56	0.71	0.47	0.46	1.40*
Margin of error (95% CI)	2.82	1.10	1.38	0.92	0.91	2.74
Upper 95% CI	59.53	63.73	64.50	63.31	62.27	7.15*
Lower 95% CI	53.89	61.52	61.74	61.47	60.46	1.68*
	PD=0.001-Silcrete	**PD=0.1-Silcrete**	**PD=0.5-Silcrete**	**PD=0.75-Silcrete**	**PD=0.95-Silcrete**	**PP13B-MIS6-Silcrete**
n (number of assemblages)	1000	1000	1000	1000	1000	7
First Quartile	0.00	0.00	0.00	0.00	0.00	0.00
Min	0.00	0.00	0.00	0.00	0.00	0.00
Median	0.00	0.00	0.00	0.00	0.00	0.00
Mean	0.37	0.18	0.03	0.06	0.01	1.09
Max	3.81	2.63	1.49	4.95	0.66	5.01
Third Quartile	0.00	0.00	0.00	0.00	0.00	2.55
SD	0.91	0.43	0.16	0.50	0.09	1.97
SE	0.09	0.04	0.02	0.05	0.01	0.68*
Margin of error (95% CI)	0.18	0.08	0.03	0.10	0.02	1.34
Upper 95% CI	0.55	0.26	0.06	0.16	0.03	2.42*
Lower 95% CI	0.19	0.09	0.00	0.00	0.00	0.00*
	PD=0.001-Quartzite	**PD=0.1-Quartzite**	**PD=0.5-Quartzite**	**PD=0.75-Quartzite**	**PD=0.95-Quartzite**	**PP13B-MIS6-Quartzite**
n (number of assemblages)	1000	1000	1000	1000	1000	7
First Quartile	32.21	33.50	32.85	34.35	36.44	87.62
Min	14.29	25.00	24.24	23.66	21.57	87.62
Median	42.04	37.16	36.23	38.22	38.58	97.85
Mean	42.92	37.20	36.85	37.55	38.62	94.34
Max	100.00	56.41	83.33	48.58	53.19	100.00
Third Quartile	51.05	41.05	39.19	41.12	41.23	98.29
SD	14.24	5.61	7.05	4.75	4.62	5.37
SE	1.42	0.56	0.70	0.48	0.46	1.92*
Margin of error (95% CI)	2.79	1.10	1.38	0.93	0.91	3.76
Upper 95% CI	45.71	38.30	38.24	38.48	39.53	98.10*
Lower 95% CI	40.13	36.10	35.47	36.62	37.72	90.58*

*Margins of error (95% CI) for archaeological data were obtained by bootstrapping the standard errors 10000 times.

MIS6 without a Paleo-Agulhas plain silcrete source – Toolkit size (Toolkit parameter)

Table B111. Summary statistics and test results for OFAT3 modeling of MIS6 conditions without a Paleo-Agulhas plain silcrete source compared to MIS6 archaeological raw material frequency data from PP13B.

	Toolkit=5-Quartz	**Toolkit=10-Quartz**	**Toolkit=50-Quartz**	**Toolkit=75-Quartz**	**Toolkit=100-Quartz**	**PP13-MIS6-Quartz**
n (number of assemblages)	1000	1000	1000	1000	1000	7
First Quartile	40.71	56.35	54.66	52.36	50.01	1.71
Min	0.00	0.00	38.24	8.00	8.11	0.00
Median	61.81	63.64	59.70	60.92	58.03	2.15
Mean	58.00	61.27	60.35	59.10	56.69	4.41
Max	100.00	100.00	100.00	94.74	87.10	9.39
Third Quartile	75.00	70.59	65.07	66.19	63.81	9.33
SD	25.27	17.26	9.95	12.25	12.84	3.91
SE	2.53	1.73	0.99	1.23	1.28	1.40*
Margin of error (95% CI)	4.95	3.38	1.95	2.40	2.52	2.74
Upper 95% CI	62.95	64.66	62.30	61.50	59.21	7.15*
Lower 95% CI	53.04	57.89	58.40	56.70	54.17	1.68*
	Toolkit=5-Silcrete	**Toolkit=10-Silcrete**	**Toolkit=50-Silcrete**	**Toolkit=75-Silcrete**	**Toolkit=100-Silcrete**	**PP13B-MIS6-Silcrete**
n (number of assemblages)	1000	1000	1000	1000	1000	7
First Quartile	0.00	0.00	0.00	0.00	0.00	0.00
Min	0.00	0.00	0.00	0.00	0.00	0.00
Median	0.00	0.00	0.00	0.00	0.00	0.00
Mean	0.14	0.20	0.38	0.31	0.47	1.09
Max	14.14	9.90	14.14	3.41	7.33	5.01
Third Quartile	0.00	0.00	0.00	0.00	0.82	2.55
SD	1.41	1.22	1.56	0.70	0.97	1.97
SE	0.14	0.12	0.16	0.07	0.10	0.68*
Margin of error (95% CI)	0.28	0.24	0.31	0.14	0.19	1.34
Upper 95% CI	0.42	0.44	0.68	0.45	0.66	2.42*
Lower 95% CI	0.00	0.00	0.07	0.17	0.28	0.00*
	Toolkit=5-Quartzite	**Toolkit=10-Quartzite**	**Toolkit=50-Quartzite**	**Toolkit=75-Quartzite**	**Toolkit=100-Quartzite**	**PP13B-MIS6-Quartzite**
n (number of assemblages)	1000	1000	1000	1000	1000	7
First Quartile	25.00	28.78	34.30	33.45	35.47	87.62
Min	0.00	0.00	0.00	5.26	12.90	87.62
Median	37.50	35.71	39.98	39.08	41.28	97.85
Mean	40.86	37.53	39.27	40.59	42.84	94.34
Max	100.00	100.00	61.76	92.00	91.89	100.00
Third Quartile	56.75	43.21	44.44	46.98	49.14	98.29
SD	24.87	16.63	9.81	12.25	12.60	5.37

SE	2.49	1.66	0.98	1.22	1.26	1.92*
Margin of error (95% CI)	4.87	3.26	1.92	2.40	2.47	3.76
Upper 95% CI	45.74	40.79	41.19	42.99	45.31	98.10*
Lower 95% CI	35.99	34.27	37.35	38.19	40.37	90.58*

*Margins of error (95% CI) for archaeological data were obtained by bootstrapping the standard errors 10000 times.

Table B112. Comparison between ranked model frequencies from OFAT3 simulations of MIS6 conditions without a Paleo-Agulhas plain silcrete source and ranked MIS6 archaeological frequencies from PP13B.

	Discard probability at locality (PDC)*					Archaeology
Raw Material	**0.001**	**0.1**	**0.5**	**0.75**	**0.95**	**MIS6-PP13B**
Quartz	1	1	1	1	1	2
Silcrete	2	3	3	3	3	2
Quartzite	1	2	2	2	2	1
	Discard probability on landscape (PD)*					**Archaeology**
Raw Material	**0.001**	**0.1**	**0.5**	**0.75**	**0.95**	**MIS6-PP13B**
Quartz	1	1	1	1	1	2
Silcrete	3	3	3	3	3	2
Quartzite	2	2	2	2	2	1
	Toolkit size*					**Archaeology**
Raw Material	**5**	**10**	**50**	**75**	**100**	**MIS6-PP13B**
Quartz	1	1	1	1	1	2
Silcrete	3	3	3	3	3	2
Quartzite	2	2	2	2	2	1

* Ranking based on which raw materials have the highest mean frequency. Similar rankings in the table are due to statistically similar frequencies. Ranking based on MIS6 archaeological raw material frequencies from bootstrapped data in Figure 50 and Table 19. Similar rankings in the table are due to statistically similar frequencies.

MIS6 with a Paleo-Agulhas plain silcrete source – Discard probability at locality (PDC-ProbDiscardCamp parameter)

Table B113. Summary statistics and test results for OFAT3 modeling of MIS6 conditions with a Paleo-Agulhas plain silcrete source compared to MIS6 archaeological raw material frequency data from PP13B.

	PDC=0.001-Quartz	**PDC=0.1-Quartz**	**PDC=0.5-Quartz**	**PDC=0.75-Quartz**	**PDC=0.95-Quartz**	**PP13-MIS6-Quartz**
n (number of assemblages)	1000	1000	1000	1000	1000	7
First Quartile	28.57	58.11	64.56	64.71	65.04	1.71
Min	0.00	44.01	59.05	59.21	58.72	0.00
Median	37.27	61.13	65.93	66.59	67.12	2.15
Mean	38.83	60.66	66.16	66.46	67.04	4.41
Max	100.00	69.68	76.52	78.55	75.42	9.39
Third Quartile	50.00	64.15	67.75	68.17	69.36	9.33
SD	17.07	4.89	2.89	3.21	3.04	3.91

SE	1.71	0.49	0.29	0.32	0.30	1.40*
Margin of error (95% CI)	3.35	0.96	0.57	0.63	0.60	2.74
Upper 95% CI	42.18	61.62	66.73	67.09	67.64	7.15*
Lower 95% CI	35.49	59.70	65.59	65.83	66.45	1.68*
	PDC=0.001-Silcrete	**PDC=0.1-Silcrete**	**PDC=0.5-Silcrete**	**PDC=0.75-Silcrete**	**PDC=0.95-Silcrete**	**PP13B-MIS6-Silcrete**
n (number of assemblages)	1000	1000	1000	1000	1000	7
First Quartile	20.00	25.32	27.41	27.53	26.49	0.00
Min	0.00	10.58	21.99	19.75	22.81	0.00
Median	29.29	28.04	28.75	28.90	28.94	0.00
Mean	30.65	27.53	28.82	29.11	29.02	1.09
Max	100.00	42.92	36.11	39.02	36.99	5.01
Third Quartile	39.47	30.03	30.12	31.03	31.02	2.55
SD	15.31	4.46	2.67	3.34	3.05	1.97
SE	1.53	0.45	0.27	0.33	0.31	0.68*
Margin of error (95% CI)	3.00	0.87	0.52	0.65	0.60	1.34
Upper 95% CI	33.65	28.41	29.34	29.76	29.61	2.42*
Lower 95% CI	27.65	26.66	28.30	28.45	28.42	0.00*
	PDC=0.001-Quartzite	**PDC=0.1-Quartzite**	**PDC=0.5-Quartzite**	**PDC=0.75-Quartzite**	**PDC=0.95-Quartzite**	**PP13B-MIS6-Quartzite**
n (number of assemblages)	1000	1000	1000	1000	1000	7
First Quartile	18.64	7.51	3.96	3.65	3.26	87.62
Min	0.00	2.62	0.16	0.00	0.36	87.62
Median	30.00	10.81	4.71	4.28	4.04	97.85
Mean	30.52	11.81	5.02	4.43	3.94	94.34
Max	75.00	29.58	11.22	10.09	6.68	100.00
Third Quartile	43.53	13.93	5.79	5.08	4.67	98.29
SD	16.83	5.71	1.75	1.46	1.13	5.37
SE	1.68	0.57	0.17	0.15	0.11	1.92*
Margin of error (95% CI)	3.30	1.12	0.34	0.29	0.22	3.76
Upper 95% CI	33.82	12.93	5.36	4.71	4.17	98.10*
Lower 95% CI	27.22	10.69	4.68	4.14	3.72	90.58*

*Margins of error (95% CI) for archaeological data were obtained by bootstrapping the standard errors 10000 times.

MIS6 with a Paleo-Agulhas plain silcrete source– Discard probability on landscape (PD-ProbDiscard parameter)

Table B114. Summary statistics and test results for OFAT3 modeling of MIS6 conditions with a Paleo-Agulhas plain silcrete source compared to MIS6 archaeological raw material frequency data from PP13B.

	PD=0.001-Quartz	**PD=0.1-Quartz**	**PD=0.5-Quartz**	**PD=0.75-Quartz**	**PD=0.95-Quartz**	**PP13-MIS6-Quartz**
n (number of assemblages)	1000	1000	1000	1000	1000	7
First Quartile	33.59	41.80	42.01	42.02	39.95	1.71
Min	0.00	12.50	34.13	26.97	30.67	0.00
Median	44.12	45.04	45.15	44.82	43.19	2.15
Mean	44.79	45.03	44.74	44.65	42.83	4.41
Max	100.00	63.81	57.05	56.86	58.54	9.39
Third Quartile	57.99	49.42	47.70	47.38	45.85	9.33
SD	16.38	7.13	4.64	5.24	4.82	3.91
SE	1.64	0.71	0.46	0.52	0.48	1.40*
Margin of error (95% CI)	3.21	1.40	0.91	1.03	0.94	2.74
Upper 95% CI	48.00	46.43	45.65	45.68	43.78	7.15*
Lower 95% CI	41.58	43.64	43.83	43.63	41.89	1.68*
	PD=0.001-Silcrete	**PD=0.1-Silcrete**	**PD=0.5-Silcrete**	**PD=0.75-Silcrete**	**PD=0.95-Silcrete**	**PP13B-MIS6-Silcrete**
n (number of assemblages)	1000	1000	1000	1000	1000	7
First Quartile	13.41	33.46	38.00	38.26	38.24	0.00
Min	0.00	18.60	29.73	26.89	31.71	0.00
Median	19.87	38.18	40.88	40.08	42.11	0.00
Mean	21.00	38.00	40.62	40.52	41.63	1.09
Max	55.36	58.06	51.17	57.30	53.33	5.01
Third Quartile	26.16	41.93	43.74	43.03	44.46	2.55
SD	10.85	6.58	4.31	5.09	4.26	1.97
SE	1.08	0.66	0.43	0.51	0.43	0.68*
Margin of error (95% CI)	2.13	1.29	0.84	1.00	0.83	1.34
Upper 95% CI	23.12	39.28	41.46	41.52	42.47	2.42*
Lower 95% CI	18.87	36.71	39.78	39.52	40.80	0.00*
	PD=0.001-Quartzite	**PD=0.1-Quartzite**	**PD=0.5-Quartzite**	**PD=0.75-Quartzite**	**PD=0.95-Quartzite**	**PP13B-MIS6-Quartzite**
n (number of assemblages)	1000	1000	1000	1000	1000	7
First Quartile	22.60	13.33	12.27	12.96	13.34	87.62
Min	0.00	5.56	7.81	5.88	6.50	87.62
Median	32.47	15.47	14.29	14.64	15.45	97.85
Mean	34.22	16.97	14.64	14.83	15.54	94.34
Max	100.00	37.50	24.32	25.00	25.52	100.00
Third Quartile	42.98	19.53	16.17	16.66	17.96	98.29

SD	16.01	6.07	3.27	3.34	3.44	5.37
SE	1.60	0.61	0.33	0.33	0.34	1.92*
Margin of error (95% CI)	3.14	1.19	0.64	0.65	0.67	3.76
Upper 95% CI	37.36	18.16	15.28	15.48	16.21	98.10*
Lower 95% CI	31.08	15.78	14.00	14.17	14.86	90.58*

*Margins of error (95% CI) for archaeological data were obtained by bootstrapping the standard errors 10000 times.

MIS6 with a Paleo-Agulhas plain silcrete source – Toolkit size (Toolkit parameter)

Table B115. Summary statistics and test results for OFAT3 modeling of MIS6 conditions with a Paleo-Agulhas plain silcrete source compared to MIS6 archaeological raw material frequency data from PP13B.

	Toolkit=5-Quartz	**Toolkit=10-Quartz**	**Toolkit=50-Quartz**	**Toolkit=75-Quartz**	**Toolkit=100-Quartz**	**PP13-MIS6-Quartz**
n (number of assemblages)	1000	1000	1000	1000	1000	7
First Quartile	34.37	37.50	38.89	34.84	37.58	1.71
Min	0.00	0.00	14.74	0.00	16.67	0.00
Median	50.00	47.73	45.76	42.87	43.66	2.15
Mean	47.98	45.97	44.87	43.76	43.16	4.41
Max	100.00	100.00	85.71	84.62	81.25	9.39
Third Quartile	61.81	57.14	52.94	51.29	50.55	9.33
SD	25.01	18.47	11.85	13.33	10.67	3.91
SE	2.50	1.85	1.19	1.33	1.07	1.40*
Margin of error (95% CI)	4.90	3.62	2.32	2.61	2.09	2.74
Upper 95% CI	52.88	49.59	47.20	46.37	45.25	7.15*
Lower 95% CI	43.08	42.35	42.55	41.15	41.07	1.68*
	Toolkit=5-Silcrete	**Toolkit=10-Silcrete**	**Toolkit=50-Silcrete**	**Toolkit=75-Silcrete**	**Toolkit=100-Silcrete**	**PP13B-MIS6-Silcrete**
n (number of assemblages)	1000	1000	1000	1000	1000	7
First Quartile	22.44	28.72	24.22	21.43	20.38	0.00
Min	0.00	0.00	12.50	0.00	4.35	0.00
Median	36.93	38.68	27.47	27.26	26.24	0.00
Mean	35.22	39.79	28.46	28.17	27.63	1.09
Max	100.00	100.00	59.09	55.56	71.88	5.01
Third Quartile	50.00	49.50	32.92	34.58	34.35	2.55
SD	21.34	19.20	8.36	10.34	11.53	1.97
SE	2.13	1.92	0.84	1.03	1.15	0.68*
Margin of error (95% CI)	4.18	3.76	1.64	2.03	2.26	1.34
Upper 95% CI	39.40	43.55	30.10	30.19	29.89	2.42*
Lower 95% CI	31.04	36.02	26.82	26.14	25.37	0.00*
	Toolkit=5-Quartzite	**Toolkit=10-Quartzite**	**Toolkit=50-Quartzite**	**Toolkit=75-Quartzite**	**Toolkit=100-Quartzite**	**PP13B-MIS6-Quartzite**
n (number of assemblages)	1000	1000	1000	1000	1000	7

First Quartile	0.00	5.42	18.68	19.74	21.30	87.62
Min	0.00	0.00	0.00	0.00	2.17	87.62
Median	13.39	12.50	25.57	27.42	29.21	97.85
Mean	15.80	13.25	26.66	28.08	29.21	94.34
Max	100.00	35.71	60.00	100.00	60.87	100.00
Third Quartile	25.00	20.00	31.99	34.67	36.05	98.29
SD	15.87	9.81	12.05	13.58	11.99	5.37
SE	1.59	0.98	1.20	1.36	1.20	1.92*
Margin of error (95% CI)	3.11	1.92	2.36	2.66	2.35	3.76
Upper 95% CI	18.91	15.17	29.03	30.74	31.55	98.10*
Lower 95% CI	12.69	11.32	24.30	25.42	26.86	90.58*

*Margins of error (95% CI) for archaeological data were obtained by bootstrapping the standard errors 10000 times.

Table B116. Comparison between ranked model frequencies from OFAT3 simulations of MIS6 conditions with a Paleo-Agulhas plain silcrete source and ranked MIS6 archaeological frequencies from PP13B.

	Discard probability at locality (PDC)*					**Archaeology**
Raw Material	**0.001**	**0.1**	**0.5**	**0.75**	**0.95**	**MIS6-PP13B**
Quartz	1	1	1	1	1	2
Silcrete	2	2	2	2	2	2
Quartzite	2	3	3	3	3	1
	Discard probability on landscape (PD)*					**Archaeology**
Raw Material	**0.001**	**0.1**	**0.5**	**0.75**	**0.95**	**MIS6-PP13B**
Quartz	1	1	1	1	1	2
Silcrete	3	2	2	2	1	2
Quartzite	2	3	3	3	2	1
	Toolkit size*					**Archaeology**
Raw Material	**5**	**10**	**50**	**75**	**100**	**MIS6-PP13B**
Quartz	1	1	1	1	1	2
Silcrete	2	1	2	2	2	2
Quartzite	3	2	2	2	2	1

* Ranking based on which raw materials have the highest mean frequency. Similar rankings in the table are due to statistically similar frequencies. Ranking based on MIS6 archaeological raw material frequencies from bootstrapped data in Figure 50 and Table 19. Similar rankings in the table are due to statistically similar frequencies.

OFAT 4 - Changing Raw Material consumption and discard strategy
Return to starting locality

MIS4 without a Paleo-Agulhas plain silcrete source - Conservative Behavior

Table B117. Summary statistics and test results for OFAT4 modeling of MIS4 conditions without a Paleo-Agulhas plain silcrete source compared to MIS4 archaeological raw material frequency data from PP5-6.

	TT=50-Quartz	**TT=100-Quartz**	**TT=500-Quartz**	**TT=1000-Quartz**	**TT=1500-Quartz**	**TT=2000-Quartz**	**PP5-6-MIS4-Quartz**
n (number of simulated assemblages)	1000	1000	1000	1000	1000	1000	46
First Quartile	100.00	100.00	57.14	40.00	20.40	17.62	1.21
Min	0.00	80.00	0.00	0.00	0.00	0.00	0.00
Median	100.00	100.00	78.89	60.00	50.00	37.69	3.73
Mean	99.00	99.80	74.49	58.08	41.31	37.91	8.39
Max	100.00	100.00	100.00	100.00	100.00	100.00	66.11
Third Quartile	100.00	100.00	100.00	80.00	60.15	50.16	10.53
SD	10.00	2.00	25.93	29.97	27.53	28.05	11.83
SE	1.00	0.20	2.59	3.00	2.75	2.81	1.67*
Margin of error (95% CI)	1.96	0.39	5.08	5.87	5.40	5.50	3.28
Upper 95% CI	100.96	100.19	79.57	63.96	46.71	43.40	11.66*
Lower 95% CI	97.04	99.41	69.40	52.21	35.92	32.41	5.11*
	TT=50-Silcrete	**TT=100-Silcrete**	**TT=500-Silcrete**	**TT=1000-Silcrete**	**TT=1500-Silcrete**	**TT=2000-Silcrete**	**PP5-6-MIS4-Silcrete**
n (number of simulated assemblages)	1000	1000	1000	1000	1000	1000	46
First Quartile	0.00	0.00	0.00	0.00	0.00	0.00	13.79
Min	0.00	0.00	0.00	0.00	0.00	0.00	0.00
Median	0.00	0.00	0.00	0.00	0.00	0.00	39.13
Mean	0.00	0.00	0.00	2.58	4.99	6.61	40.00
Max	0.00	0.00	0.00	49.50	49.50	99.00	96.55
Third Quartile	0.00	0.00	0.00	0.00	0.00	8.28	62.77
SD	0.00	0.00	0.00	8.07	11.43	14.65	27.52
SE	0.00	0.00	0.00	0.81	1.14	1.47	4.01*
Margin of error (95% CI)	0.00	0.00	0.00	1.58	2.24	2.87	7.85
Upper 95% CI	0.00	0.00	0.00	4.16	7.23	9.48	47.85*
Lower 95% CI	0.00	0.00	0.00	1.00	2.75	3.74	32.15*
	TT=50-Quartzite	**TT=100-Quartzite**	**TT=500-Quartzite**	**TT=1000-Quartzite**	**TT=1500-Quartzite**	**TT=2000-Quartzite**	**PP5-6-MIS4-Quartzite**
n (number of simulated assemblages)	1000	1000	1000	1000	1000	1000	46
First Quartile	0.00	0.00	0.00	16.67	33.333	34.37	5.19
Min	0.00	0.00	0.00	0.00	0.000	0.00	0.00

Median	0.00	0.00	20.00	33.33	50.000	50.00	43.00
Mean	0.00	0.20	24.51	36.33	52.694	53.48	44.63
Max	0.00	20.00	100.00	100.00	100.000	100.00	96.45
Third Quartile	0.00	0.00	42.86	50.00	66.667	73.71	68.24
SD	0.00	2.00	24.94	28.38	28.463	29.72	25.54
SE	0.00	0.20	2.49	2.84	2.846	2.97	3.71*
Margin of error (95% CI)	0.00	0.39	4.89	5.56	5.579	5.82	7.27
Upper 95% CI	0.00	0.59	29.40	41.90	58.272	59.30	51.90*
Lower 95% CI	0.00	0.00	19.63	30.77	47.115	47.65	37.35*

*Margins of error (95% CI) for archaeological data were obtained by bootstrapping the standard errors 10000 times.

MIS4 without a Paleo-Agulhas plain silcrete source – Expedient behavior

Table B118. Summary statistics and test results for OFAT4 modeling of MIS4 conditions without a Paleo-Agulhas plain silcrete source compared to MIS4 archaeological raw material frequency data from PP5-6.

	TT=50-Quartz	**TT=100-Quartz**	**TT=500-Quartz**	**TT=1000-Quartz**	**TT=1500-Quartz**	**TT=2000-Quartz**	**PP5-6-MIS4-Quartz**
n (number of simulated assemblages)	1000	1000	1000	1000	1000	1000	46
First Quartile	100.00	99.51	21.16	8.32	5.51	4.44	1.21
Min	100.00	98.25	17.25	6.25	3.26	3.25	0.00
Median	100.00	99.66	22.90	9.67	6.10	4.90	3.73
Mean	100.00	99.67	23.19	9.51	6.29	5.04	8.39
Max	100.00	100.00	30.48	14.19	10.52	7.78	66.11
Third Quartile	100.00	100.00	25.22	10.57	7.10	5.55	10.53
SD	0.00	0.40	3.00	1.59	1.21	0.87	11.83
SE	0.00	0.04	0.30	0.16	0.12	0.09	1.67*
Margin of error (95% CI)	0.00	0.08	0.59	0.31	0.24	0.17	3.28
Upper 95% CI	100.00	99.75	23.78	9.82	6.53	5.21	11.66*
Lower 95% CI	100.00	99.59	22.60	9.20	6.05	4.87	5.11*
	TT=50-Silcrete	**TT=100-Silcrete**	**TT=500-Silcrete**	**TT=1000-Silcrete**	**TT=1500-Silcrete**	**TT=2000-Silcrete**	**PP5-6-MIS4-Silcrete**
n (number of simulated assemblages)	1000	1000	1000	1000	1000	1000	46
First Quartile	0.00	0.00	0.91	2.77	3.12	3.95	13.79
Min	0.00	0.00	0.00	0.93	1.30	1.62	0.00
Median	0.00	0.00	1.64	3.38	3.95	4.64	39.13
Mean	0.00	0.00	1.67	3.44	4.05	4.65	40.00
Max	0.00	0.00	4.21	7.05	7.71	6.85	96.55
Third Quartile	0.00	0.00	2.21	4.02	4.78	5.37	62.77
SD	0.00	0.00	0.95	1.06	1.29	1.03	27.52
SE	0.00	0.00	0.10	0.11	0.13	0.10	4.01*

Margin of error (95% CI)	0.00	0.00	0.19	0.21	0.25	0.20	7.85
Upper 95% CI	0.00	0.00	1.85	3.65	4.30	4.85	47.85*
Lower 95% CI	0.00	0.00	1.48	3.23	3.80	4.44	32.15*
	TT=50-Quartzite	**TT=100-Quartzite**	**TT=500-Quartzite**	**TT=1000-Quartzite**	**TT=1500-Quartzite**	**TT=2000-Quartzite**	**PP5-6-MIS4-Quartzite**
n (number of simulated assemblages)	1000	1000	1000	1000	1000	1000	46
First Quartile	0.00	0.00	73.09	85.77	88.78	89.43	5.19
Min	0.00	0.00	67.70	81.76	83.72	87.73	0.00
Median	0.00	0.34	75.28	87.17	89.87	90.31	43.00
Mean	0.00	0.33	75.14	87.05	89.66	90.31	44.63
Max	0.00	1.75	81.59	91.32	93.56	93.91	96.45
Third Quartile	0.00	0.49	77.51	88.41	91.02	90.91	68.24
SD	0.00	0.40	3.00	1.95	1.98	1.25	25.54
SE	0.00	0.04	0.30	0.19	0.20	0.13	3.71*
Margin of error (95% CI)	0.00	0.08	0.59	0.38	0.39	0.25	7.27
Upper 95% CI	0.00	0.41	75.73	87.43	90.05	90.55	51.90*
Lower 95% CI	0.00	0.25	74.55	86.67	89.27	90.06	37.35*

*Margins of error (95% CI) for archaeological data were obtained by bootstrapping the standard errors 10000 times.

MIS4 without a Paleo-Agulhas plain silcrete source – Site caching

Table B119. Summary statistics and test results for OFAT4 modeling of MIS4 conditions without a Paleo-Agulhas plain silcrete source compared to MIS4 archaeological raw material frequency data from PP5-6.

	TT=50-Quartz	**TT=100-Quartz**	**TT=500-Quartz**	**TT=1000-Quartz**	**TT=1500-Quartz**	**TT=2000-Quartz**	**PP5-6-MIS4-Quartz**
n (number of simulated assemblages)	1000	1000	1000	1000	1000	1000	46
First Quartile	100.00	100.00	88.73	79.57	75.17	73.19	1.21
Min	100.00	99.56	87.05	77.34	73.18	70.51	0.00
Median	100.00	100.00	89.43	80.49	76.12	74.04	3.73
Mean	100.00	99.95	89.54	80.46	76.20	73.99	8.39
Max	100.00	100.00	93.55	83.07	78.82	76.17	66.11
Third Quartile	100.00	100.00	90.17	81.23	77.33	74.91	10.53
SD	0.00	0.10	1.21	1.15	1.29	1.22	11.83
SE	0.00	0.01	0.12	0.11	0.13	0.12	1.67*
Margin of error (95% CI)	0.00	0.02	0.24	0.22	0.25	0.24	3.28
Upper 95% CI	100.00	99.97	89.78	80.68	76.46	74.23	11.66*
Lower 95% CI	100.00	99.93	89.30	80.23	75.95	73.75	5.11*
	TT=50-Silcrete	**TT=100-Silcrete**	**TT=500-Silcrete**	**TT=1000-Silcrete**	**TT=1500-Silcrete**	**TT=2000-Silcrete**	**PP5-6-MIS4-Silcrete**
n (number of simulated assemblages)	1000	1000	1000	1000	1000	1000	46

First Quartile	0.00	0.00	0.26	1.28	2.03	2.40	13.79
Min	0.00	0.00	0.00	0.29	1.09	1.49	0.00
Median	0.00	0.00	0.40	1.55	2.31	2.69	39.13
Mean	0.00	0.00	0.42	1.54	2.33	2.77	40.00
Max	0.00	0.00	0.97	2.72	3.30	3.96	96.55
Third Quartile	0.00	0.00	0.53	1.79	2.72	3.15	62.77
SD	0.00	0.00	0.24	0.38	0.51	0.51	27.52
SE	0.00	0.00	0.02	0.04	0.05	0.05	4.01*
Margin of error (95% CI)	0.00	0.00	0.05	0.07	0.10	0.10	7.85
Upper 95% CI	0.00	0.00	0.46	1.61	2.43	2.87	47.85*
Lower 95% CI	0.00	0.00	0.37	1.47	2.23	2.68	32.15*
	TT=50-Quartzite	**TT=100-Quartzite**	**TT=500-Quartzite**	**TT=1000-Quartzite**	**TT=1500-Quartzite**	**TT=2000-Quartzite**	**PP5-6-MIS4-Quartzite**
n (number of simulated assemblages)	1000	1000	1000	1000	1000	1000	46
First Quartile	0.00	0.00	9.48	17.16	20.66	22.39	5.19
Min	0.00	0.00	6.44	14.48	18.63	20.71	0.00
Median	0.00	0.00	10.12	18.14	21.53	23.19	43.00
Mean	0.00	0.05	10.05	18.00	21.47	23.24	44.63
Max	0.00	0.44	12.58	20.87	24.53	26.89	96.45
Third Quartile	0.00	0.00	10.77	18.91	22.32	24.03	68.24
SD	0.00	0.10	1.15	1.17	1.15	1.20	25.54
SE	0.00	0.01	0.12	0.12	0.12	0.12	3.71*
Margin of error (95% CI)	0.00	0.02	0.23	0.23	0.23	0.23	7.27
Upper 95% CI	0.00	0.07	10.27	18.23	21.69	23.47	51.90*
Lower 95% CI	0.00	0.03	9.82	17.77	21.24	23.00	37.35*

*Margins of error (95% CI) for archaeological data were obtained by bootstrapping the standard errors 10000 times.

Table B120. Comparison between ranked model frequencies from OFAT4 simulations of MIS4 conditions without a Paleo-Agulhas plain silcrete source and ranked MIS4 archaeological frequencies from PP5-6.

			Conservative*				**Archaeology**
Raw Material	**TT=50**	**TT=100**	**TT=500**	**TT=1000**	**TT=1500**	**TT=2000**	**MIS4-PP5-6**
Quartz	1	1	1	1	2	2	2
Silcrete	2	3	3	3	3	3	1
Quartzite	2	2	2	2	1	1	1
			Expedient*				**Archaeology**
Raw Material	**TT=50**	**TT=100**	**TT=500**	**TT=1000**	**TT=1500**	**TT=2000**	**MIS4-PP5-6**
Quartz	1	1	2	2	2	2	2
Silcrete	2	3	3	3	3	3	1
Quartzite	2	2	1	1	1	1	1
			Site Caching*				**Archaeology**

Raw Material	TT=50	TT=100	TT=500	TT=1000	TT=1500	TT=2000	MIS4-PP5-6
Quartz	1	1	1	1	1	1	2
Silcrete	2	3	3	3	3	3	1
Quartzite	2	2	2	2	2	2	1

* Ranking based on which raw materials have the highest mean frequency. Similar rankings in the table are due to statistically similar frequencies. Ranking based on MIS4 archaeological raw material frequencies from bootstrapped data in Figure 50 and Table 19. Similar rankings in the table are due to statistically similar frequencies.

MIS4 with a Paleo-Agulhas plain silcrete source - Conservative Behavior

Table B121. Summary statistics and test results for OFAT4 modeling of MIS4 conditions with a Paleo-Agulhas plain silcrete source compared to MIS4 archaeological raw material frequency data from PP5-6.

	TT=50-Quartz	TT=100-Quartz	TT=500-Quartz	TT=1000-Quartz	TT=1500-Quartz	TT=2000-Quartz	PP5-6-MIS4-Quartz
n (number of simulated assemblages)	1000	1000	1000	1000	1000	1000	46
First Quartile	50.00	33.33	25.00	0.00	0.03	0.00	1.21
Min	0.00	0.00	0.00	0.00	0.00	0.00	0.00
Median	66.67	50.00	40.00	16.67	20.00	16.67	3.73
Mean	63.57	51.92	43.55	22.00	23.01	18.52	8.39
Max	100.00	100.00	100.00	100.00	100.00	100.00	66.11
Third Quartile	85.71	75.00	60.00	36.46	36.46	33.33	10.53
SD	29.54	28.12	28.07	25.03	21.12	20.57	11.83
SE	2.95	2.81	2.81	2.50	2.11	2.06	1.67*
Margin of error (95% CI)	5.79	5.51	5.50	4.91	4.14	4.03	3.28
Upper 95% CI	69.36	57.43	49.05	26.91	27.15	22.55	11.66*
Lower 95% CI	57.78	46.41	38.05	17.09	18.87	14.49	5.11*
	TT=50-Silcrete	**TT=100-Silcrete**	**TT=500-Silcrete**	**TT=1000-Silcrete**	**TT=1500-Silcrete**	**TT=2000-Silcrete**	**PP5-6-MIS4-Silcrete**
n (number of simulated assemblages)	1000	1000	1000	1000	1000	1000	46
First Quartile	3.57	25.00	27.08	33.33	25.00	25.86	13.79
Min	0.00	0.00	0.00	0.00	0.00	0.00	0.00
Median	33.33	50.00	50.00	50.00	42.22	49.50	39.13
Mean	35.43	47.08	44.47	52.44	46.10	46.10	40.00
Max	100.00	100.00	100.00	100.00	100.00	100.00	96.55
Third Quartile	50.00	65.63	61.88	75.00	61.88	60.00	62.77
SD	29.05	28.03	28.06	29.84	27.11	27.53	27.52
SE	2.91	2.80	2.81	2.98	2.71	2.75	4.01*
Margin of error (95% CI)	5.69	5.49	5.50	5.85	5.31	5.39	7.85
Upper 95% CI	41.12	52.58	49.97	58.28	51.42	51.49	47.85*
Lower 95% CI	29.73	41.59	38.98	46.59	40.79	40.70	32.15*
	TT=50-Quartzite	**TT=100-Quartzite**	**TT=500-Quartzite**	**TT=1000-Quartzite**	**TT=1500-Quartzite**	**TT=2000-Quartzite**	**PP5-6-MIS4-Quartzite**

n (number of simulated assemblages)	1000	1000	1000	1000	1000	1000	46
First Quartile	0.00	0.00	0.00	0.00	0.00	16.67	5.19
Min	0.00	0.00	0.00	0.00	0.00	0.00	0.00
Median	0.00	0.00	0.00	25.00	33.33	33.33	43.00
Mean	0.00	0.00	8.98	23.56	29.89	35.38	44.63
Max	0.00	0.00	75.00	100.00	100.00	100.00	96.45
Third Quartile	0.00	0.00	16.07	40.00	44.05	50.00	68.24
SD	0.00	0.00	14.99	23.45	23.86	26.67	25.54
SE	0.00	0.00	1.50	2.34	2.39	2.67	3.71*
Margin of error (95% CI)	0.00	0.00	2.94	4.60	4.68	5.23	7.27
Upper 95% CI	0.00	0.00	11.91	28.16	34.57	40.61	51.90*
Lower 95% CI	0.00	0.00	6.04	18.97	25.22	30.15	37.35*

*Margins of error (95% CI) for archaeological data were obtained by bootstrapping the standard errors 10000 times.

MIS4 with a Paleo-Agulhas plain silcrete source – Expedient behavior

Table B122. Summary statistics and test results for OFAT4 modeling of MIS4 conditions with a Paleo-Agulhas plain silcrete source compared to MIS4 archaeological raw material frequency data from PP5-6.

	TT=50-Quartz	**TT=100-Quartz**	**TT=500-Quartz**	**TT=1000-Quartz**	**TT=1500-Quartz**	**TT=2000-Quartz**	**PP5-6-MIS4-Quartz**
n (number of simulated assemblages)	1000	1000	1000	1000	1000	1000	46
First Quartile	61.03	41.96	7.30	4.33	3.34	2.82	1.21
Min	56.69	39.85	5.62	3.16	2.02	1.99	0.00
Median	62.39	42.58	7.92	4.79	3.74	3.22	3.73
Mean	62.37	42.82	8.12	4.88	3.71	3.22	8.39
Max	66.49	45.66	11.10	7.40	5.24	4.28	66.11
Third Quartile	63.69	43.70	8.76	5.39	4.07	3.61	10.53
SD	1.68	1.25	1.14	0.79	0.61	0.52	11.83
SE	0.17	0.13	0.11	0.08	0.06	0.05	1.67*
Margin of error (95% CI)	0.33	0.25	0.22	0.16	0.12	0.10	3.28
Upper 95% CI	62.70	43.07	8.34	5.04	3.83	3.32	11.66*
Lower 95% CI	62.04	42.58	7.89	4.73	3.59	3.11	5.11*
	TT=50-Silcrete	**TT=100-Silcrete**	**TT=500-Silcrete**	**TT=1000-Silcrete**	**TT=1500-Silcrete**	**TT=2000-Silcrete**	**PP5-6-MIS4-Silcrete**
n (number of simulated assemblages)	1000	1000	1000	1000	1000	1000	46
First Quartile	36.31	56.23	62.58	41.90	31.74	26.00	13.79
Min	33.51	54.06	57.06	38.08	27.45	22.23	0.00
Median	37.61	57.19	64.16	43.37	33.36	27.53	39.13
Mean	37.63	57.07	63.99	43.41	33.29	27.68	40.00
Max	43.31	60.15	69.64	49.82	39.12	32.40	96.55

Third Quartile	38.97	57.93	65.54	44.85	34.64	29.26	62.77
SD	1.68	1.26	2.34	2.39	2.28	2.14	27.52
SE	0.17	0.13	0.23	0.24	0.23	0.21	4.01*
Margin of error (95% CI)	0.33	0.25	0.46	0.47	0.45	0.42	7.85
Upper 95% CI	37.96	57.32	64.44	43.88	33.74	28.09	47.85*
Lower 95% CI	37.30	56.83	63.53	42.94	32.84	27.26	32.15*
	TT=50-Quartzite	**TT=100-Quartzite**	**TT=500-Quartzite**	**TT=1000-Quartzite**	**TT=1500-Quartzite**	**TT=2000-Quartzite**	**PP5-6-MIS4-Quartzite**
n (number of simulated assemblages)	1000	1000	1000	1000	1000	1000	46
First Quartile	0.00	0.00	26.33	50.16	61.43	67.69	5.19
Min	0.00	0.00	23.80	44.08	56.75	63.82	0.00
Median	0.00	0.00	27.82	51.43	62.87	69.24	43.00
Mean	0.00	0.10	27.90	51.70	63.00	69.11	44.63
Max	0.00	0.61	35.89	57.60	68.99	74.49	96.45
Third Quartile	0.00	0.20	29.35	53.53	64.53	70.45	68.24
SD	0.00	0.13	2.20	2.50	2.40	2.18	25.54
SE	0.00	0.01	0.22	0.25	0.24	0.22	3.71*
Margin of error (95% CI)	0.00	0.03	0.43	0.49	0.47	0.43	7.27
Upper 95% CI	0.00	0.13	28.33	52.19	63.47	69.53	51.90*
Lower 95% CI	0.00	0.08	27.47	51.21	62.53	68.68	37.35*

*Margins of error (95% CI) for archaeological data were obtained by bootstrapping the standard errors 10000 times.

MIS4 with a Paleo-Agulhas plain silcrete source – Site caching

Table B123. Summary statistics and test results for OFAT4 modeling of MIS4 conditions with a Paleo-Agulhas plain silcrete source compared to MIS4 archaeological raw material frequency data from PP5-6.

	TT=50-Quartz	**TT=100-Quartz**	**TT=500-Quartz**	**TT=1000-Quartz**	**TT=1500-Quartz**	**TT=2000-Quartz**	**PP5-6-MIS4-Quartz**
n (number of simulated assemblages)	1000	1000	1000	1000	1000	1000	46
First Quartile	72.07	67.93	61.03	58.70	57.68	56.16	1.21
Min	69.28	62.39	58.36	56.65	54.34	53.62	0.00
Median	73.21	68.70	62.42	60.01	58.59	57.34	3.73
Mean	73.10	68.94	62.40	59.93	58.44	57.38	8.39
Max	76.28	72.95	66.76	64.21	61.68	61.14	66.11
Third Quartile	74.07	70.09	63.54	61.01	59.32	58.23	10.53
SD	1.47	1.75	1.68	1.62	1.44	1.46	11.83
SE	0.15	0.17	0.17	0.16	0.14	0.15	1.67*
Margin of error (95% CI)	0.29	0.34	0.33	0.32	0.28	0.29	3.28
Upper 95% CI	73.39	69.28	62.73	60.24	58.72	57.66	11.66*
Lower 95% CI	72.81	68.60	62.07	59.61	58.16	57.09	5.11*

	TT=50-Silcrete	TT=100-Silcrete	TT=500-Silcrete	TT=1000-Silcrete	TT=1500-Silcrete	TT=2000-Silcrete	PP5-6-MIS4-Silcrete
n (number of simulated assemblages)	1000	1000	1000	1000	1000	1000	46
First Quartile	25.93	29.91	33.60	34.58	34.88	34.93	13.79
Min	23.72	27.05	31.10	31.13	31.19	32.47	0.00
Median	26.79	31.23	34.92	35.45	35.65	36.06	39.13
Mean	26.90	31.03	34.90	35.35	35.68	35.97	40.00
Max	30.72	37.61	39.19	39.57	39.95	39.83	96.55
Third Quartile	27.93	32.07	36.01	36.18	36.52	37.12	62.77
SD	1.47	1.75	1.74	1.60	1.41	1.42	27.52
SE	0.15	0.17	0.17	0.16	0.14	0.14	4.01*
Margin of error (95% CI)	0.29	0.34	0.34	0.31	0.28	0.28	7.85
Upper 95% CI	27.19	31.38	35.24	35.66	35.96	36.25	47.85*
Lower 95% CI	26.61	30.69	34.56	35.03	35.40	35.69	32.15*
	TT=50-Quartzite	TT=100-Quartzite	TT=500-Quartzite	TT=1000-Quartzite	TT=1500-Quartzite	TT=2000-Quartzite	PP5-6-MIS4-Quartzite
n (number of simulated assemblages)	1000	1000	1000	1000	1000	1000	46
First Quartile	0.00	0.00	2.35	4.18	5.41	6.14	5.19
Min	0.00	0.00	1.35	3.17	3.92	5.18	0.00
Median	0.00	0.00	2.65	4.75	5.89	6.57	43.00
Mean	0.00	0.03	2.70	4.73	5.88	6.66	44.63
Max	0.00	0.27	3.97	6.35	8.40	8.40	96.45
Third Quartile	0.00	0.00	3.05	5.15	6.37	7.18	68.24
SD	0.00	0.06	0.57	0.68	0.73	0.71	25.54
SE	0.00	0.01	0.06	0.07	0.07	0.07	3.71*
Margin of error (95% CI)	0.00	0.01	0.11	0.13	0.14	0.14	7.27
Upper 95% CI	0.00	0.04	2.81	4.86	6.02	6.80	51.90*
Lower 95% CI	0.00	0.01	2.59	4.59	5.74	6.52	37.35*

*Margins of error (95% CI) for archaeological data were obtained by bootstrapping the standard errors 10000 times.

Table B124. Comparison between ranked model frequencies from OFAT4 simulations of MIS4 conditions with a Paleo-Agulhas plain silcrete source and ranked MIS4 archaeological frequencies from PP5-6.

			Conservative*				Archaeology
Raw Material	**TT=50**	**TT=100**	**TT=500**	**TT=1000**	**TT=1500**	**TT=2000**	**MIS4-PP5-6**
Quartz	1	1	1	2	2	3	2
Silcrete	2	1	1	1	1	1	1
Quartzite	3	2	2	2	2	2	1
			Expedient*				**Archaeology**
Raw Material	**TT=50**	**TT=100**	**TT=500**	**TT=1000**	**TT=1500**	**TT=2000**	**MIS4-PP5-6**
Quartz	1	2	3	3	3	3	2

Silcrete	2	1	1	2	2	2	1
Quartzite	3	3	2	1	1	1	1

	Site Caching*						Archaeology
Raw Material	**TT=50**	**TT=100**	**TT=500**	**TT=1000**	**TT=1500**	**TT=2000**	**MIS4-PP5-6**
Quartz	1	1	1	1	1	1	2
Silcrete	2	2	2	2	2	2	1
Quartzite	3	3	3	3	3	3	1

* Ranking based on which raw materials have the highest mean frequency. Similar rankings in the table are due to statistically similar frequencies. Ranking based on MIS4 archaeological raw material frequencies from bootstrapped data in Figure 50 and Table 19. Similar rankings in the table are due to statistically similar frequencies.

MIS5 Conditions - Conservative Behavior

Table B125. Summary statistics and test results for OFAT4 modeling of MIS5 conditions compared to MIS5 archaeological raw material frequency data from PP5-6, PP13B, PP9B, and PP9C.

	TT=50-Quartz	**TT=100-Quartz**	**TT=500-Quartz**	**TT=1000-Quartz**	**TT=1500-Quartz**	**TT=2000-Quartz**	**PP5-6-MIS5-Quartz**	**PP13B-MIS5-Quartz**	**AllPP-MIS5-Quartz**
n (number of assemblages)	1000	1000	1000	1000	1000	1000	31	7	43
First Quartile	66.83	68.02	52.03	50.03	33.50	30.18	0.00	1.71	0.10
Min	0.00	0.00	0.00	0.33	0.00	0.00	0.00	0.00	0.00
Median	83.42	83.42	75.13	60.25	50.13	50.06	0.89	2.15	2.65
Mean	80.27	80.25	70.47	59.60	46.78	44.63	3.53	4.41	4.61
Max	100.00	100.00	100.00	100.00	100.00	100.00	24.87	9.39	24.87
Third Quartile	100.00	100.00	87.55	75.13	66.67	60.20	3.92	9.33	6.95
SD	22.68	24.18	24.65	27.19	28.44	25.97	5.94	3.91	6.03
SE	2.27	2.42	2.47	2.72	2.84	2.60	1.03*	1.40*	0.90*
Margin of error (95% CI)	4.45	4.74	4.83	5.33	5.57	5.09	2.03	2.74	1.76
Upper 95% CI	84.72	84.99	75.30	64.93	52.36	49.72	5.56*	7.15*	6.37*
Lower 95% CI	75.82	75.51	65.63	54.27	41.21	39.54	1.51*	1.68*	2.85*
	TT=50-Silcrete	**TT=100-Silcrete**	**TT=500-Silcrete**	**TT=1000-Silcrete**	**TT=1500-Silcrete**	**TT=2000-Silcrete**	**PP5-6-MIS5-Silcrete**	**PP13B-Silcrete**	**AllPP-MIS5-Silcrete**
n (number of assemblages)	1000	1000	1000	1000	1000	1000	31	7	4.30E+01
First Quartile	0.00	0.00	0.00	0.00	0.09	0.20	1.45	0.00	0.95
Min	0.00	0.00	0.00	0.00	0.00	0.00	0.00	0.00	0.00
Median	0.10	0.09	0.15	0.20	0.30	14.23	10.19	0.00	6.44
Mean	0.11	0.11	1.05	6.42	12.50	17.25	16.97	1.09	13.05
Max	0.45	0.60	33.00	49.80	99.00	99.00	64.83	5.01	64.83
Third	0.20	0.15	0.24	0.60	20.04	27.48	32.95	2.55	21.21

Quartile									
SD	0.12	0.13	4.72	13.25	20.30	20.72	17.85	1.97	16.45
SE	0.01	0.01	0.47	1.33	2.03	2.07	3.14*	0.68*	2.46*
Margin of error (95% CI)	0.02	0.03	0.93	2.60	3.98	4.06	6.16	1.34	4.82
Upper 95% CI	0.13	0.13	1.98	9.02	16.47	21.31	23.12*	2.42*	17.86*
Lower 95% CI	0.08	0.08	0.13	3.83	8.52	13.18	10.81*	0.00*	8.23*
	TT=50-Quartzite	**TT=100-Quartzite**	**TT=500-Quartzite**	**TT=1000-Quartzite**	**TT=1500-Quartzite**	**TT=2000-Quartzite**	**P5-6-MIS5-Quartzite**	**PP13B-Quartzite**	**AllPP-MIS5-Quartzite**
n (number of assemblages)	1000	1000	1000	1000	1000	1000	31	7	43
First Quartile	0.00	0.00	0.00	16.48	19.70	20.00	60.24	87.62	64.30
Min	0.00	0.00	0.00	0.00	0.00	0.00	26.94	87.62	26.94
Median	16.42	14.07	24.63	32.83	36.37	39.40	76.11	97.85	83.74
Mean	17.55	17.57	26.39	33.87	37.63	37.04	72.77	94.34	77.20
Max	73.88	98.50	98.50	99.00	100.00	99.25	100.00	100.00	100.00
Third Quartile	32.83	24.63	39.63	49.25	56.26	49.72	92.83	98.29	92.83
SD	19.51	21.19	22.23	25.50	26.79	26.38	21.79	5.37	20.01
SE	1.95	2.12	2.22	2.55	2.68	2.64	3.85*	1.92*	3.00*
Margin of error (95% CI)	3.82	4.15	4.36	5.00	5.25	5.17	7.55	3.76	5.87
Upper 95% CI	21.38	21.73	30.75	38.87	42.88	42.21	80.32*	98.10*	83.07*
Lower 95% CI	13.73	13.42	22.04	28.87	32.38	31.87	65.21*	90.58*	71.33*

*Margins of error (95% CI) for archaeological data were obtained by bootstrapping the standard errors 10000 times.

MIS5 conditions – Expedient behavior

Table B126. Summary statistics and test results for OFAT4 modeling of MIS5 conditions compared to MIS5 archaeological raw material frequency data from PP5-6, PP13B, PP9B, and PP9C.

	TT=50-Quartz	**TT=100-Quartz**	**TT=500-Quartz**	**TT=1000-Quartz**	**TT=1500-Quartz**	**TT=2000-Quartz**	**PP5-6-MIS5-Quartz**	**PP13B-MIS5-Quartz**	**AllPP-MIS5-Quartz**
n (number of assemblages)	1000	1000	1000	1000	1000	1000	31	7	43
First Quartile	81.89	74.49	37.44	25.24	22.49	21.72	0.00	1.71	0.10
Min	79.04	72.10	30.41	19.88	18.25	18.46	0.00	0.00	0.00
Median	82.71	75.76	41.49	27.06	24.13	23.40	0.89	2.15	2.65
Mean	82.75	75.67	41.15	27.37	24.14	23.33	3.53	4.41	4.61
Max	85.62	80.43	52.88	35.58	33.09	30.15	24.87	9.39	24.87
Third Quartile	83.81	76.77	43.80	29.60	25.70	24.71	3.92	9.33	6.95

SD	1.42	1.64	4.31	3.08	2.63	2.31	5.94	3.91	6.03
SE	0.14	0.16	0.43	0.31	0.26	0.23	1.03*	1.40*	0.90*
Margin of error (95% CI)	0.28	0.32	0.84	0.60	0.52	0.45	2.03	2.74	1.76
Upper 95% CI	83.03	75.99	41.99	27.97	24.65	23.78	5.56*	7.15*	6.37*
Lower 95% CI	82.47	75.35	40.30	26.76	23.62	22.87	1.51*	1.68*	2.85*
	TT=50-Silcrete	**TT=100-Silcrete**	**TT=500-Silcrete**	**TT=1000-Silcrete**	**TT=1500-Silcrete**	**TT=2000-Silcrete**	**PP5-6-MIS5-Silcrete**	**PP13B-Silcrete**	**AllPP-MIS5-Silcrete**
n (number of assemblages)	1000	1000	1000	1000	1000	1000	31	7	4.30E+01
First Quartile	0.10	0.14	4.04	13.48	18.25	22.90	1.45	0.00	0.95
Min	0.09	0.12	1.79	8.04	11.31	13.42	0.00	0.00	0.00
Median	0.10	0.15	4.80	15.44	21.12	25.29	10.19	0.00	6.44
Mean	0.10	0.15	5.24	15.35	21.07	25.68	16.97	1.09	13.05
Max	0.13	0.17	11.64	22.87	36.73	37.15	64.83	5.01	64.83
Third Quartile	0.11	0.15	6.03	17.57	23.32	28.40	32.95	2.55	21.21
SD	0.01	0.01	1.90	3.20	3.88	4.03	17.85	1.97	16.45
SE	0.00	0.00	0.19	0.32	0.39	0.40	3.14*	0.68*	2.46*
Margin of error (95% CI)	0.00	0.00	0.37	0.63	0.76	0.79	6.16	1.34	4.82
Upper 95% CI	0.11	0.15	5.61	15.98	21.83	26.47	23.12*	2.42*	17.86*
Lower 95% CI	0.10	0.14	4.86	14.73	20.31	24.89	10.81*	0.00*	8.23*
	TT=50-Quartzite	**TT=100-Quartzite**	**TT=500-Quartzite**	**TT=1000-Quartzite**	**TT=1500-Quartzite**	**TT=2000-Quartzite**	**P5-6-MIS5-Quartzite**	**PP13B-Quartzite**	**AllPP-MIS5-Quartzite**
n (number of assemblages)	1000	1000	1000	1000	1000	1000	31	7	43
First Quartile	16.03	23.00	50.53	54.79	52.14	47.82	60.24	87.62	64.30
Min	14.24	19.38	43.75	46.57	41.95	42.55	26.94	87.62	26.94
Median	17.12	24.00	53.00	57.04	55.11	51.31	76.11	97.85	83.74
Mean	17.07	24.09	53.51	57.21	54.73	50.94	72.77	94.34	77.20
Max	20.75	27.62	63.81	66.65	64.45	61.17	100.00	100.00	100.00
Third Quartile	17.92	25.26	56.45	59.73	57.37	53.74	92.83	98.29	92.83
SD	1.41	1.63	4.21	3.81	4.01	4.08	21.79	5.37	20.01
SE	0.14	0.16	0.42	0.38	0.40	0.41	3.85*	1.92*	3.00*
Margin of error (95% CI)	0.28	0.32	0.83	0.75	0.79	0.80	7.55	3.76	5.87
Upper 95% CI	17.35	24.41	54.33	57.96	55.52	51.74	80.32*	98.10*	83.07*
Lower 95% CI	16.80	23.77	52.68	56.46	53.95	50.14	65.21*	90.58*	71.33*

*Margins of error (95% CI) for archaeological data were obtained by bootstrapping the standard errors 10000 times.

MIS5 conditions – Site caching

Table B127. Summary statistics and test results for OFAT4 modeling of MIS5 conditions compared to MIS5 archaeological raw material frequency data from PP5-6, PP13B, PP9B, and PP9C.

	TT=50-Quartz	TT=100-Quartz	TT=500-Quartz	TT=1000-Quartz	TT=1500-Quartz	TT=2000-Quartz	PP5-6-MIS5-Quartz	PP13B-MIS5-Quartz	AllPP-MIS5-Quartz
n (number of assemblages)	1000	1000	1000	1000	1000	1000	31	7	43
First Quartile	84.45	83.16	76.79	72.32	69.82	68.04	0.00	1.71	0.10
Min	82.08	81.67	75.07	70.31	67.41	65.45	0.00	0.00	0.00
Median	85.42	84.21	78.06	73.61	71.00	69.04	0.89	2.15	2.65
Mean	85.43	84.13	78.06	73.48	70.85	69.05	3.53	4.41	4.61
Max	88.08	87.30	81.43	77.94	73.99	72.56	24.87	9.39	24.87
Third Quartile	86.36	85.06	79.01	74.84	71.82	70.24	3.92	9.33	6.95
SD	1.32	1.38	1.43	1.58	1.41	1.45	5.94	3.91	6.03
SE	0.13	0.14	0.14	0.16	0.14	0.14	1.03*	1.40*	0.908
Margin of error (95% CI)	0.26	0.27	0.28	0.31	0.28	0.28	2.03	2.74	1.76
Upper 95% CI	85.69	84.40	78.34	73.79	71.13	69.34	5.56*	7.15*	6.37*
Lower 95% CI	85.17	83.86	77.78	73.17	70.58	68.77	1.51*	1.68*	2.85*
	TT=50-Silcrete	**TT=100-Silcrete**	**TT=500-Silcrete**	**TT=1000-Silcrete**	**TT=1500-Silcrete**	**TT=2000-Silcrete**	**PP5-6-MIS5-Silcrete**	**PP13B-Silcrete**	**AllPP-MIS5-Silcrete**
n (number of assemblages)	1000	1000	1000	1000	1000	1000	31	7	4.30E+01
First Quartile	0.08	0.09	0.52	2.17	3.61	4.76	1.45	0.00	0.95
Min	0.07	0.08	0.24	1.47	2.54	3.47	0.00	0.00	0.00
Median	0.09	0.10	0.67	2.48	4.15	5.23	10.19	0.00	6.44
Mean	0.09	0.10	0.72	2.50	4.07	5.25	16.97	1.09	13.05
Max	0.11	0.11	1.33	3.65	6.05	6.86	64.83	5.01	64.83
Third Quartile	0.09	0.10	0.90	2.82	4.45	5.70	32.95	2.55	21.21
SD	0.01	0.01	0.26	0.49	0.68	0.66	17.85	1.97	16.45
SE	0.00	0.00	0.03	0.05	0.07	0.07	3.14*	0.68*	2.46*
Margin of error (95% CI)	0.00	0.00	0.05	0.10	0.13	0.13	6.16	1.34	4.82
Upper 95% CI	0.09	0.10	0.78	2.60	4.20	5.38	23.12*	2.42*	17.86*
Lower 95% CI	0.09	0.09	0.67	2.41	3.93	5.12	10.81*	0.00*	8.23*
	TT=50-Quartzite	**TT=100-Quartzite**	**TT=500-Quartzite**	**TT=1000-Quartzite**	**TT=1500-Quartzite**	**TT=2000-Quartzite**	**P5-6-MIS5-Quartzite**	**PP13B-Quartzite**	**AllPP-MIS5-Quartzite**

n (number of assemblages)	1000	1000	1000	1000	1000	1000	31	7	43
First Quartile	13.50	14.79	20.20	22.78	23.98	24.54	60.24	87.62	64.30
Min	11.80	12.58	17.99	19.58	20.76	22.28	26.94	87.62	26.94
Median	14.43	15.63	21.13	23.85	24.94	25.67	76.11	97.85	83.74
Mean	14.43	15.71	21.14	23.93	25.00	25.62	72.77	94.34	77.20
Max	17.74	18.14	24.08	27.18	28.51	28.62	100.00	100.00	100.00
Third Quartile	15.39	16.67	22.31	25.13	26.04	26.84	92.83	98.29	92.83
SD	1.30	1.36	1.40	1.54	1.47	1.41	21.79	5.37	20.01
SE	0.13	0.14	0.14	0.15	0.15	0.14	3.85*	1.92*	3.00*
Margin of error (95% CI)	0.26	0.27	0.27	0.30	0.29	0.28	7.55	3.76	5.87
Upper 95% CI	14.68	15.98	21.41	24.24	25.28	25.89	80.32*	98.10*	83.07*
Lower 95% CI	14.17	15.45	20.86	23.63	24.71	25.34	65.21*	90.58*	71.33*

*Margins of error (95% CI) for archaeological data were obtained by bootstrapping the standard errors 10000 times.

Table B128. Comparison between ranked model frequencies from OFAT4 simulations of MIS5 conditions and ranked MIS5 archaeological frequencies from PP13B, PP9B, PP9C, and PP5-6.

	Conservative*						Archaeology		
Raw Material	**TT=50**	**TT=100**	**TT=500**	**TT=1000**	**TT=1500**	**TT=2000**	**MIS5-PP5-6**	**MIS5-PP13B**	**MIS5-All PP**
Quartz	1	1	1	1	1	1	3	2	3
Silcrete	3	3	3	3	2	2	2	2	2
Quartzite	2	2	2	2	1	1	1	1	1

	Expedient*						Archaeology		
Raw Material	**TT=50**	**TT=100**	**TT=500**	**TT=1000**	**TT=1500**	**TT=2000**	**MIS5-PP5-6**	**MIS5-PP13B**	**MIS5-All PP**
Quartz	1	1	2	2	2	3	3	2	3
Silcrete	3	3	3	3	3	2	2	2	2
Quartzite	2	2	1	1	1	1	1	1	1

	Site Caching*						Archaeology		
Raw Material	**TT=50**	**TT=100**	**TT=500**	**TT=1000**	**TT=1500**	**TT=2000**	**MIS5-PP5-6**	**MIS5-PP13B**	**MIS5-All PP**
Quartz	1	1	1	1	1	1	3	2	3
Silcrete	3	3	3	3	3	3	2	2	2
Quartzite	2	2	2	2	2	2	1	1	1

* Ranking based on which raw materials have the highest mean frequency. Similar rankings in the table are due to statistically similar frequencies. Ranking based on MIS5 archaeological raw material frequencies from bootstrapped data in Figure 50 and Table 19. Similar rankings in the table are due to statistically similar frequencies. Grey shading indicates a ranking match.

MIS6 without a Paleo-Agulhas plain silcrete source - Conservative Behavior

Table B129. Summary statistics and test results for OFAT4 modeling of MIS6 conditions without a Paleo-Agulhas plain silcrete source compared to MIS6 archaeological raw material frequency data from PP13B.

	TT=50-Quartz	**TT=100-Quartz**	**TT=500-Quartz**	**TT=1000-Quartz**	**TT=1500-Quartz**	**TT=2000-Quartz**	**PP13-MIS6-Quartz**
n (number of assemblages)	1000	1000	1000	1000	1000	1000	7
First Quartile	72.32	57.14	20.00	3.37	0.00	0.00	1.71
Min	0.00	0.00	0.00	0.00	0.00	0.00	0.00
Median	100.00	73.21	33.33	30.95	25.00	16.67	2.15
Mean	82.22	67.28	38.74	34.89	27.03	20.92	4.41
Max	100.00	100.00	100.00	100.00	100.00	100.00	9.39
Third Quartile	100.00	84.29	59.29	50.00	40.00	33.33	9.33
SD	24.44	27.80	27.48	30.24	27.06	23.99	3.91
SE	2.44	2.78	2.75	3.02	2.71	2.40	1.40*
Margin of error (95% CI)	4.79	5.45	5.39	5.93	5.30	4.70	2.74
Upper 95% CI	87.01	72.73	44.13	40.82	32.33	25.62	7.15*
Lower 95% CI	77.43	61.83	33.36	28.97	21.73	16.22	1.68*
	TT=50-Silcrete	**TT=100-Silcrete**	**TT=500-Silcrete**	**TT=1000-Silcrete**	**TT=1500-Silcrete**	**TT=2000-Silcrete**	**PP13B-MIS6-Silcrete**
n (number of assemblages)	1000	1000	1000	1000	1000	1000	7
First Quartile	0.00	0.00	0.00	0.00	0.00	0.00	0.00
Min	0.00	0.00	0.00	0.00	0.00	0.00	0.00
Median	0.00	0.00	0.00	0.00	0.00	0.00	0.00
Mean	0.00	0.00	0.33	1.67	4.94	4.08	1.09
Max	0.00	0.00	33.00	49.50	66.00	49.50	5.01
Third Quartile	0.00	0.00	0.00	0.00	0.00	0.00	2.55
SD	0.00	0.00	3.30	7.14	13.11	10.60	1.97
SE	0.00	0.00	0.33	0.71	1.31	1.06	0.68*
Margin of error (95% CI)	0.00	0.00	0.65	1.40	2.57	2.08	1.34
Upper 95% CI	0.00	0.00	0.98	3.07	7.50	6.16	2.42*
Lower 95% CI	0.00	0.00	0.00	0.27	2.37	2.00	0.00*
	TT=50-Quartzite	**TT=100-Quartzite**	**TT=500-Quartzite**	**TT=1000-Quartzite**	**TT=1500-Quartzite**	**TT=2000-Quartzite**	**PP13B-MIS6-Quartzite**
n (number of assemblages)	1000	1000	1000	1000	1000	1000	7
First Quartile	0.00	12.95	40.00	50.00	50.00	50.00	87.62
Min	0.00	0.00	0.00	0.00	0.00	0.00	87.62
Median	0.00	25.00	64.58	66.67	75.00	78.89	97.85
Mean	14.78	29.72	59.93	61.44	68.03	74.00	94.34
Max	100.00	100.00	100.00	100.00	100.00	100.00	100.00
Third Quartile	25.00	40.00	80.00	85.12	100.00	100.00	98.29
SD	19.83	25.67	27.60	31.46	28.45	26.00	5.37

SE	1.98	2.57	2.76	3.15	2.84	2.60	1.928
Margin of error (95% CI)	3.89	5.03	5.41	6.17	5.58	5.10	3.76
Upper 95% CI	18.67	34.75	65.34	67.60	73.61	79.10	98.10*
Lower 95% CI	10.90	24.69	54.52	55.27	62.46	68.90	90.58*

*Margins of error (95% CI) for archaeological data were obtained by bootstrapping the standard errors 10000 times.

MIS6 without a Paleo-Agulhas plain silcrete source – Expedient behavior

Table B130. Summary statistics and test results for OFAT4 modeling of MIS6 conditions without a Paleo-Agulhas plain silcrete source compared to MIS6 archaeological raw material frequency data from PP13B.

	TT=50-Quartz	**TT=100-Quartz**	**TT=500-Quartz**	**TT=1000-Quartz**	**TT=1500-Quartz**	**TT=2000-Quartz**	**PP13-MIS6-Quartz**
n (number of assemblages)	1000	1000	1000	1000	1000	1000	7
First Quartile	80.27	53.63	7.11	3.94	3.35	2.96	1.71
Min	77.93	50.53	5.37	2.87	2.41	2.48	0.00
Median	81.46	54.89	7.66	4.51	3.75	3.29	2.15
Mean	81.52	54.93	7.72	4.51	3.75	3.31	4.41
Max	85.15	61.20	9.72	7.14	5.02	4.99	9.39
Third Quartile	82.86	56.10	8.34	5.03	4.20	3.56	9.33
SD	1.63	1.84	0.83	0.76	0.56	0.49	3.91
SE	0.16	0.18	0.08	0.08	0.06	0.05	1.40*
Margin of error (95% CI)	0.32	0.36	0.16	0.15	0.11	0.10	2.74
Upper 95% CI	81.83	55.29	7.88	4.66	3.86	3.41	7.15*
Lower 95% CI	81.20	54.57	7.56	4.36	3.64	3.22	1.68*
	TT=50-Silcrete	**TT=100-Silcrete**	**TT=500-Silcrete**	**TT=1000-Silcrete**	**TT=1500-Silcrete**	**TT=2000-Silcrete**	**PP13B-MIS6-Silcrete**
n (number of assemblages)	1000	1000	1000	1000	1000	1000	7
First Quartile	0.00	0.00	0.30	1.32	2.12	2.84	0.00
Min	0.00	0.00	0.00	0.67	0.91	1.96	0.00
Median	0.00	0.00	0.52	1.68	2.57	3.33	0.00
Mean	0.00	0.00	0.55	1.76	2.65	3.41	1.09
Max	0.00	0.00	1.46	3.37	4.43	5.24	5.01
Third Quartile	0.00	0.00	0.77	2.18	3.19	3.98	2.55
SD	0.00	0.00	0.34	0.57	0.71	0.72	1.97
SE	0.00	0.00	0.03	0.06	0.07	0.07	0.68*
Margin of error (95% CI)	0.00	0.00	0.07	0.11	0.14	0.14	1.34
Upper 95% CI	0.00	0.00	0.62	1.87	2.79	3.55	2.42*
Lower 95% CI	0.00	0.00	0.49	1.65	2.51	3.27	0.00*
	TT=50-Quartzite	**TT=100-Quartzite**	**TT=500-Quartzite**	**TT=1000-Quartzite**	**TT=1500-Quartzite**	**TT=2000-Quartzite**	**PP13B-MIS6-Quartzite**
n (number of assemblages)	1000	1000	1000	1000	1000	1000	7
First Quartile	17.14	43.90	91.11	93.12	93.09	92.58	87.62

Min	14.85	38.80	88.83	91.25	91.22	90.49	87.62
Median	18.54	45.11	91.78	93.91	93.69	93.36	97.85
Mean	18.48	45.07	91.73	93.74	93.60	93.27	94.34
Max	22.07	49.47	93.94	95.69	95.70	95.19	100.00
Third Quartile	19.73	46.37	92.42	94.55	94.24	93.90	98.29
SD	1.63	1.84	0.92	0.99	0.85	0.93	5.37
SE	0.16	0.18	0.09	0.10	0.08	0.09	1.92*
Margin of error (95% CI)	0.32	0.36	0.18	0.19	0.17	0.18	3.76
Upper 95% CI	18.80	45.43	91.91	93.93	93.77	93.46	98.10*
Lower 95% CI	18.17	44.71	91.55	93.54	93.44	93.09	90.58*

*Margins of error (95% CI) for archaeological data were obtained by bootstrapping the standard errors 10000 times.

MIS6 without a Paleo-Agulhas plain silcrete source – Site caching

Table B131. Summary statistics and test results for OFAT4 modeling of MIS6 conditions without a Paleo-Agulhas plain silcrete source compared to MIS6 archaeological raw material frequency data from PP13B.

	TT=50-Quartz	**TT=100-Quartz**	**TT=500-Quartz**	**TT=1000-Quartz**	**TT=1500-Quartz**	**TT=2000-Quartz**	**PP13-MIS6-Quartz**
n (number of assemblages)	1000	1000	1000	1000	1000	1000	7
First Quartile	87.64	80.62	69.78	66.35	64.77	63.50	1.71
Min	85.20	78.20	67.68	63.68	60.82	60.69	0.00
Median	88.54	81.91	71.05	67.13	65.74	64.38	2.15
Mean	88.54	81.83	70.99	67.43	65.69	64.54	4.41
Max	91.89	85.14	74.67	71.98	69.07	67.95	9.39
Third Quartile	89.35	82.85	72.20	68.56	66.79	65.81	9.33
SD	1.41	1.46	1.49	1.58	1.53	1.46	3.91
SE	0.14	0.15	0.15	0.16	0.15	0.15	1.40*
Margin of error (95% CI)	0.28	0.29	0.29	0.31	0.30	0.29	2.74
Upper 95% CI	88.82	82.11	71.28	67.74	65.99	64.83	7.15*
Lower 95% CI	88.26	81.54	70.69	67.12	65.39	64.26	1.68*
	TT=50-Silcrete	**TT=100-Silcrete**	**TT=500-Silcrete**	**TT=1000-Silcrete**	**TT=1500-Silcrete**	**TT=2000-Silcrete**	**PP13B-MIS6-Silcrete**
n (number of assemblages)	1000	1000	1000	1000	1000	1000	7
First Quartile	0.00	0.00	0.14	0.87	1.47	1.82	0.00
Min	0.00	0.00	0.00	0.35	0.58	0.94	0.00
Median	0.00	0.00	0.32	1.05	1.68	2.09	0.00
Mean	0.00	0.00	0.33	1.11	1.72	2.14	1.09
Max	0.00	0.00	1.17	2.26	2.92	3.33	5.01
Third Quartile	0.00	0.00	0.47	1.35	2.00	2.43	2.55
SD	0.00	0.00	0.22	0.36	0.41	0.45	1.97
SE	0.00	0.00	0.02	0.04	0.04	0.05	0.68*
Margin of error	0.00	0.00	0.04	0.07	0.08	0.09	1.34

(95% CI)							
Upper 95% CI	0.00	0.00	0.38	1.18	1.80	2.22	2.42*
Lower 95% CI	0.00	0.00	0.29	1.04	1.64	2.05	0.00*
	TT=50-Quartzite	**TT=100-Quartzite**	**TT=500-Quartzite**	**TT=1000-Quartzite**	**TT=1500-Quartzite**	**TT=2000-Quartzite**	**PP13B-MIS6-Quartzite**
n (number of assemblages)	1000	1000	1000	1000	1000	1000	7
First Quartile	10.65	17.15	27.47	30.39	31.49	32.07	87.62
Min	8.11	14.86	25.15	27.43	28.87	30.14	87.62
Median	11.46	18.09	28.56	31.66	32.63	33.71	97.85
Mean	11.46	18.17	28.68	31.46	32.59	33.32	94.34
Max	14.80	21.80	32.20	35.61	37.24	37.22	100.00
Third Quartile	12.36	19.38	29.96	32.49	33.57	34.29	98.29
SD	1.41	1.46	1.51	1.58	1.52	1.49	5.37
SE	0.14	0.15	0.15	0.16	0.15	0.15	1.92*
Margin of error (95% CI)	0.28	0.29	0.30	0.31	0.30	0.29	3.76
Upper 95% CI	11.74	18.46	28.98	31.77	32.89	33.61	98.10*
Lower 95% CI	11.18	17.89	28.38	31.16	32.29	33.03	90.58*

*Margins of error (95% CI) for archaeological data were obtained by bootstrapping the standard errors 10000 times.

Table B132. Comparison between ranked model frequencies from OFAT4 simulations of MIS6 conditions without a Paleo-Agulhas plain silcrete source and ranked MIS6 archaeological frequencies from PP13B.

			Conservative*				**Archaeology**
Raw Material	**TT=50**	**TT=100**	**TT=500**	**TT=1000**	**TT=1500**	**TT=2000**	**MIS6-PP13B**
Quartz	1	1	2	2	2	2	2
Silcrete	3	3	3	3	3	3	2
Quartzite	2	2	1	1	1	1	1
			Expedient*				**Archaeology**
Raw Material	**TT=50**	**TT=100**	**TT=500**	**TT=1000**	**TT=1500**	**TT=2000**	**MIS6-PP13B**
Quartz	1	1	2	2	2	2	2
Silcrete	3	3	3	3	3	2	2
Quartzite	2	2	1	1	1	1	1
			Site Caching*				**Archaeology**
Raw Material	**TT=50**	**TT=100**	**TT=500**	**TT=1000**	**TT=1500**	**TT=2000**	**MIS6-PP13B**
Quartz	1	1	1	1	1	1	2
Silcrete	3	3	3	3	3	3	2
Quartzite	2	2	2	2	2	2	1

* Ranking based on which raw materials have the highest mean frequency. Similar rankings in the table are due to statistically similar frequencies. Ranking based on MIS6 archaeological raw material frequencies from bootstrapped data in Figure 50 and Table 19. Similar rankings in the table are due to statistically similar frequencies. Grey shading indicates a ranking match.

MIS6 with a Paleo-Agulhas plain silcrete source - Conservative Behavior

Table B133. Summary statistics and test results for OFAT4 modeling of MIS6 conditions with a Paleo-Agulhas plain silcrete source compared to MIS6 archaeological raw material frequency data from PP13B.

	TT=50-Quartz	**TT=100-Quartz**	**TT=500-Quartz**	**TT=1000-Quartz**	**TT=1500-Quartz**	**TT=2000-Quartz**	**PP13-MIS6-Quartz**
n (number of assemblages)	1000	1000	1000	1000	1000	1000	7
First Quartile	33.33	29.76	3.82	0.00	0.00	0.00	1.71
Min	0.00	0.00	0.00	0.00	0.00	0.00	0.00
Median	50.00	50.00	33.33	25.00	25.00	16.67	2.15
Mean	51.31	46.78	31.06	24.95	23.89	19.31	4.41
Max	100.00	100.00	100.00	100.00	100.00	100.00	9.39
Third Quartile	75.00	66.67	50.00	33.33	33.63	33.33	9.33
SD	32.18	29.87	25.88	25.17	20.66	22.42	3.91
SE	3.55	2.99	2.59	2.52	2.07	2.24	1.40*
Margin of error (95% CI)	6.96	5.85	5.07	4.93	4.05	4.39	2.74
Upper 95% CI	58.27	52.63	36.13	29.88	27.94	23.71	7.15*
Lower 95% CI	44.35	40.92	25.99	20.02	19.84	14.92	1.68*
	TT=50-Silcrete	**TT=100-Silcrete**	**TT=500-Silcrete**	**TT=1000-Silcrete**	**TT=1500-Silcrete**	**TT=2000-Silcrete**	**PP13B-MIS6-Silcrete**
n (number of assemblages)	1000	1000	1000	1000	1000	1000	7
First Quartile	0.00	20.00	16.67	0.00	0.00	0.00	0.00
Min	0.00	0.00	0.00	0.00	0.00	0.00	0.00
Median	40.00	33.33	35.42	28.50	25.00	26.71	0.00
Mean	39.96	38.94	38.63	29.38	27.85	30.19	1.09
Max	100.00	100.00	100.00	100.00	100.00	100.00	5.01
Third Quartile	60.00	55.36	50.00	50.00	47.99	49.75	2.55
SD	32.60	27.68	31.53	24.44	25.01	28.37	1.97
SE	3.60	2.77	3.15	2.44	2.50	2.84	0.68*
Margin of error (95% CI)	7.06	5.43	6.18	4.79	4.90	5.56	1.34
Upper 95% CI	47.01	44.37	44.81	34.17	32.75	35.76	2.42*
Lower 95% CI	32.90	33.51	32.45	24.59	22.94	24.63	0.00*
	TT=50-Quartzite	**TT=100-Quartzite**	**TT=500-Quartzite**	**TT=1000-Quartzite**	**TT=1500-Quartzite**	**TT=2000-Quartzite**	**PP13B-MIS6-Quartzite**
n (number of assemblages)	1000	1000	1000	1000	1000	1000	7
First Quartile	0.00	0.00	0.00	25.00	25.00	33.33	87.62
Min	0.00	0.00	0.00	0.00	0.00	0.00	87.62
Median	0.00	0.00	26.79	43.65	50.00	50.00	97.85
Mean	5.07	9.28	29.31	44.67	47.27	49.49	94.34
Max	100.00	66.67	100.00	100.00	100.00	100.00	100.00
Third Quartile	0.00	19.17	48.61	65.00	66.67	66.67	98.29
SD	14.43	14.39	27.28	28.35	27.33	28.20	5.37

SE	1.59	1.44	2.73	2.83	2.73	2.82	1.92*
Margin of error (95% CI)	3.12	2.82	5.35	5.56	5.36	5.53	3.76
Upper 95% CI	8.20	12.10	34.66	50.22	52.62	55.02	98.10*
Lower 95% CI	1.95	6.46	23.96	39.11	41.91	43.97	90.58*

*Margins of error (95% CI) for archaeological data were obtained by bootstrapping the standard errors 10000 times.

MIS6 with a Paleo-Agulhas plain silcrete source – Expedient behavior

Table B134. Summary statistics and test results for OFAT4 modeling of MIS6 conditions with a Paleo-Agulhas plain silcrete source compared to MIS6 archaeological raw material frequency data from PP13B.

	TT=50-Quartz	**TT=100-Quartz**	**TT=500-Quartz**	**TT=1000-Quartz**	**TT=1500-Quartz**	**TT=2000-Quartz**	**PP13-MIS6-Quartz**
n (number of assemblages)	1000	1000	1000	1000	1000	1000	7
First Quartile	60.36	39.42	5.33	3.09	2.71	2.32	1.71
Min	57.23	36.97	4.35	1.98	1.73	1.73	0.00
Median	61.31	40.28	5.84	3.47	2.97	2.59	2.15
Mean	61.36	40.38	5.91	3.49	2.96	2.63	4.41
Max	65.91	44.03	8.68	4.94	4.27	3.57	9.39
Third Quartile	62.68	41.16	6.45	3.87	3.20	2.96	9.33
SD	1.78	1.40	0.80	0.56	0.49	0.43	3.91
SE	0.18	0.14	0.08	0.06	0.05	0.04	1.40*
Margin of error (95% CI)	0.35	0.28	0.16	0.11	0.10	0.08	2.74
Upper 95% CI	61.71	40.66	6.07	3.60	3.06	2.71	7.15*
Lower 95% CI	61.01	40.10	5.75	3.38	2.87	2.54	1.68*
	TT=50-Silcrete	**TT=100-Silcrete**	**TT=500-Silcrete**	**TT=1000-Silcrete**	**TT=1500-Silcrete**	**TT=2000-Silcrete**	**PP13B-MIS6-Silcrete**
n (number of assemblages)	1000	1000	1000	1000	1000	1000	7
First Quartile	33.04	43.67	26.79	18.38	15.58	13.54	0.00
Min	29.47	41.37	23.74	15.04	13.25	11.67	0.00
Median	34.00	44.78	27.75	19.44	16.51	14.48	0.00
Mean	34.14	44.71	27.81	19.27	16.53	14.53	1.09
Max	37.96	48.09	31.52	22.77	18.98	17.90	5.01
Third Quartile	35.38	45.53	28.99	20.00	17.46	15.64	2.55
SD	1.65	1.44	1.56	1.49	1.26	1.33	1.97
SE	0.17	0.14	0.16	0.15	0.13	0.13	0.68*
Margin of error (95% CI)	0.32	0.28	0.31	0.29	0.25	0.26	1.34
Upper 95% CI	34.46	44.99	28.11	19.56	16.78	14.79	2.42*
Lower 95% CI	33.81	44.43	27.50	18.97	16.28	14.27	0.00*
	TT=50-Quartzite	**TT=100-Quartzite**	**TT=500-Quartzite**	**TT=1000-Quartzite**	**TT=1500-Quartzite**	**TT=2000-Quartzite**	**PP13B-MIS6-Quartzite**
n (number of assemblages)	1000	1000	1000	1000	1000	1000	7
First Quartile	4.04	14.28	65.06	76.38	79.66	81.72	87.62

Min	3.06	12.68	62.47	73.66	77.56	79.46	87.62
Median	4.45	14.81	66.20	77.23	80.48	82.94	97.85
Mean	4.51	14.91	66.28	77.24	80.51	82.85	94.34
Max	5.91	17.70	71.52	82.07	83.77	85.91	100.00
Third Quartile	4.99	15.45	67.48	78.11	81.41	83.85	98.29
SD	0.61	0.91	1.73	1.64	1.30	1.41	5.37
SE	0.06	0.09	0.17	0.16	0.13	0.14	1.92*
Margin of error (95% CI)	0.12	0.18	0.34	0.32	0.25	0.28	3.76
Upper 95% CI	4.63	15.09	66.62	77.56	80.76	83.12	98.10*
Lower 95% CI	4.39	14.73	65.94	76.92	80.25	82.57	90.58*

*Margins of error (95% CI) for archaeological data were obtained by bootstrapping the standard errors 10000 times.

MIS6 with a Paleo-Agulhas plain silcrete source – Site caching

Table B135. Summary statistics and test results for OFAT4 modeling of MIS6 conditions with a Paleo-Agulhas plain silcrete source compared to MIS6 archaeological raw material frequency data from PP13B.

	TT=50-Quartz	**TT=100-Quartz**	**TT=500-Quartz**	**TT=1000-Quartz**	**TT=1500-Quartz**	**TT=2000-Quartz**	**PP13-MIS6-Quartz**
n (number of assemblages)	1000	1000	1000	1000	1000	1000	7
First Quartile	70.41	66.86	60.19	58.06	56.72	55.85	1.71
Min	67.03	63.68	57.68	54.12	54.08	53.41	0.00
Median	71.53	68.35	61.46	59.03	58.04	56.80	2.15
Mean	71.73	68.13	61.35	59.05	58.04	57.04	4.41
Max	77.25	71.61	66.26	62.64	62.79	61.60	9.39
Third Quartile	72.89	69.32	62.50	60.08	59.20	58.22	9.33
SD	1.85	1.67	1.67	1.56	1.70	1.64	3.91
SE	0.18	0.17	0.17	0.16	0.17	0.16	1.40*
Margin of error (95% CI)	0.36	0.33	0.33	0.31	0.33	0.32	2.74
Upper 95% CI	72.09	68.46	61.67	59.35	58.37	57.36	7.15*
Lower 95% CI	71.37	67.80	61.02	58.74	57.70	56.72	1.68*
	TT=50-Silcrete	**TT=100-Silcrete**	**TT=500-Silcrete**	**TT=1000-Silcrete**	**TT=1500-Silcrete**	**TT=2000-Silcrete**	**PP13B-MIS6-Silcrete**
n (number of assemblages)	1000	1000	1000	1000	1000	1000	7
First Quartile	25.30	27.73	30.54	31.19	31.14	31.24	0.00
Min	21.36	25.03	26.52	28.82	28.37	28.30	0.00
Median	26.72	28.89	31.81	32.06	32.15	32.30	0.00
Mean	26.57	29.04	31.69	32.15	32.09	32.25	1.09
Max	30.63	33.66	35.68	36.44	35.96	35.58	5.01
Third Quartile	27.93	30.21	32.93	33.24	33.22	33.42	2.55
SD	1.77	1.67	1.71	1.51	1.50	1.41	1.97
SE	0.18	0.17	0.17	0.15	0.15	0.14	0.68*
Margin of error	0.35	0.33	0.34	0.30	0.29	0.28	1.34

(95% CI)							
Upper 95% CI	26.91	29.37	32.03	32.44	32.38	32.52	2.42*
Lower 95% CI	26.22	28.72	31.36	31.85	31.79	31.97	0.00*
	TT=50-Quartzite	**TT=100-Quartzite**	**TT=500-Quartzite**	**TT=1000-Quartzite**	**TT=1500-Quartzite**	**TT=2000-Quartzite**	**PP13B-MIS6-Quartzite**
n (number of assemblages)	1000	1000	1000	1000	1000	1000	7
First Quartile	1.41	2.48	6.23	8.10	9.285	10.09	87.62
Min	0.66	1.69	4.56	6.17	8.082	7.68	87.62
Median	1.70	2.80	6.91	8.78	9.874	10.78	97.85
Mean	1.70	2.83	6.96	8.80	9.877	10.71	94.34
Max	3.02	4.12	8.91	11.13	12.723	13.56	100.00
Third Quartile	2.01	3.20	7.59	9.49	10.472	11.50	98.29
SD	0.50	0.50	0.90	0.93	0.959	1.05	5.37
SE	0.05	0.05	0.09	0.09	0.096	0.11	1.92*
Margin of error (95% CI)	0.10	0.10	0.18	0.18	0.188	0.21	3.76
Upper 95% CI	1.80	2.93	7.14	8.99	10.065	10.92	98.10*
Lower 95% CI	1.60	2.73	6.79	8.62	9.689	10.51	90.58*

*Margins of error (95% CI) for archaeological data were obtained by bootstrapping the standard errors 10000 times.

Table B136. Comparison between ranked model frequencies from OFAT4 simulations of MIS6 conditions with a Paleo-Agulhas plain silcrete source and ranked MIS6 archaeological frequencies from PP13B.

			Conservative*				**Archaeology**
Raw Material	**TT=50**	**TT=100**	**TT=500**	**TT=1000**	**TT=1500**	**TT=2000**	**MIS6-PP13B**
Quartz	1	1	1	2	2	3	2
Silcrete	1	1	1	2	2	2	2
Quartzite	2	2	1	1	1	1	1
			Expedient*				**Archaeology**
Raw Material	**TT=50**	**TT=100**	**TT=500**	**TT=1000**	**TT=1500**	**TT=2000**	**MIS6-PP13B**
Quartz	1	3	3	3	3	3	2
Silcrete	2	1	2	2	2	2	2
Quartzite	3	3	1	1	1	1	1
			Site Caching*				**Archaeology**
Raw Material	**TT=50**	**TT=100**	**TT=500**	**TT=1000**	**TT=1500**	**TT=2000**	**MIS6-PP13B**
Quartz	1	1	1	1	1	1	2
Silcrete	2	2	2	2	2	2	2
Quartzite	3	3	3	3	3	3	1

* Ranking based on which raw materials have the highest mean frequency. Similar rankings in the table are due to statistically similar frequencies. Ranking based on MIS6 archaeological raw material frequencies from bootstrapped data in Figure 50 and Table 19. Similar rankings in the table are due to statistically similar frequencies. Grey shading indicates a ranking match.

Move to closest locality

MIS4 without a Paleo-Agulhas plain silcrete source – Conservative Behavior

Table B137. Summary statistics and test results for OFAT4 modeling of MIS4 conditions without a Paleo-Agulhas plain silcrete source compared to MIS4 archaeological raw material frequency data from PP5-6.

	TT=50-Quartz	TT=100-Quartz	TT=500-Quartz	TT=1000-Quartz	TT=1500-Quartz	TT=2000-Quartz	PP5-6-MIS4-Quartz
n (number of simulated assemblages)	1000	1000	1000	1000	1000	1000	46
First Quartile	100.00	0.00	0.00	0.00	0.00	0.00	1.21
Min	0.00	0.00	0.00	0.00	0.00	0.00	0.00
Median	100.00	46.43	0.00	0.00	0.00	0.00	3.73
Mean	95.00	43.55	25.72	18.88	14.70	7.92	8.39
Max	100.00	100.00	100.00	100.00	100.00	100.00	66.11
Third Quartile	100.00	100.00	50.00	45.83	0.63	0.00	10.53
SD	21.90	42.52	36.33	31.82	30.24	22.77	11.83
SE	2.19	4.25	3.63	3.18	3.02	2.28	1.67*
Margin of error (95% CI)	4.29	8.33	7.12	6.24	5.93	4.46	3.28
Upper 95% CI	99.29	51.88	32.84	25.11	20.63	12.39	11.66*
Lower 95% CI	90.71	35.21	18.60	12.64	8.78	3.46	5.11*
	TT=50-Silcrete	**TT=100-Silcrete**	**TT=500-Silcrete**	**TT=1000-Silcrete**	**TT=1500-Silcrete**	**TT=2000-Silcrete**	**PP5-6-MIS4-Silcrete**
n (number of simulated assemblages)	1000	1000	1000	1000	1000	1000	46
First Quartile	0.00	0.00	0.00	0.00	0.00	0.00	13.79
Min	0.00	0.00	0.00	0.00	0.00	0.00	0.00
Median	0.00	0.00	0.00	0.00	0.00	0.00	39.13
Mean	0.00	0.00	4.04	4.46	3.80	5.53	40.00
Max	0.00	0.00	99.00	99.00	99.00	99.00	96.55
Third Quartile	0.00	0.00	0.00	0.00	0.00	0.00	62.77
SD	0.00	0.00	14.39	15.53	14.99	20.38	27.52
SE	0.00	0.00	1.44	1.55	1.50	2.04	4.01*
Margin of error (95% CI)	0.00	0.00	2.82	3.04	2.94	3.99	7.85
Upper 95% CI	0.00	0.00	6.86	7.50	6.73	9.52	47.85*
Lower 95% CI	0.00	0.00	1.22	1.41	0.86	1.53	32.15*
	TT=50-Quartzite	**TT=100-Quartzite**	**TT=500-Quartzite**	**TT=1000-Quartzite**	**TT=1500-Quartzite**	**TT=2000-Quartzite**	**PP5-6-MIS4-Quartzite**
n (number of simulated assemblages)	1000	1000	1000	1000	1000	1000	46
First Quartile	0.00	0.00	0.00	0.00	0.00	0.00	5.19
Min	0.00	0.00	0.00	0.00	0.00	0.00	0.00
Median	0.00	0.00	50.00	58.33	50.00	66.67	43.00

Mean	1.00	28.45	43.23	55.67	50.50	53.55	44.63
Max	100.00	100.00	100.00	100.00	100.00	100.00	96.45
Third Quartile	0.00	50.00	100.00	100.00	100.00	100.00	68.24
SD	10.00	37.17	42.11	44.06	45.64	46.81	25.54
SE	1.00	3.72	4.21	4.41	4.56	4.68	3.71*
Margin of error (95% CI)	1.96	7.29	8.25	8.64	8.95	9.17	7.27
Upper 95% CI	2.96	35.74	51.49	64.30	59.45	62.72	51.90*
Lower 95% CI	0.00	21.17	34.98	47.03	41.55	44.38	37.35*

*Margins of error (95% CI) for archaeological data were obtained by bootstrapping the standard errors 10000 times.

MIS4 without a Paleo-Agulhas plain silcrete source – Expedient Behavior

Table B138. Summary statistics and test results for OFAT4 modeling of MIS4 conditions without a Paleo-Agulhas plain silcrete source compared to MIS4 archaeological raw material frequency data from PP5-6.

	TT=50-Quartz	**TT=100-Quartz**	**TT=500-Quartz**	**TT=1000-Quartz**	**TT=1500-Quartz**	**TT=2000-Quartz**	**PP5-6-MIS4-Quartz**
n (number of simulated assemblages)	1000	1000	1000	1000	1000	1000	46
First Quartile	100.00	97.59	32.49	20.19	17.06	14.78	1.21
Min	99.22	92.59	22.64	13.50	8.46	9.35	0.00
Median	100.00	98.53	37.96	25.28	21.62	17.70	3.73
Mean	99.97	98.18	38.24	25.38	21.66	18.43	8.39
Max	100.00	100.00	57.93	44.07	38.14	35.82	66.11
Third Quartile	100.00	99.14	42.91	30.00	25.61	20.87	10.53
SD	0.12	1.43	6.88	6.55	6.15	5.36	11.83
SE	0.01	0.14	0.69	0.65	0.62	0.54	1.67*
Margin of error (95% CI)	0.02	0.28	1.35	1.28	1.21	1.05	3.28
Upper 95% CI	99.99	98.46	39.58	26.66	22.87	19.48	11.66*
Lower 95% CI	99.95	97.90	36.89	24.10	20.46	17.38	5.11*
	TT=50-Silcrete	**TT=100-Silcrete**	**TT=500-Silcrete**	**TT=1000-Silcrete**	**TT=1500-Silcrete**	**TT=2000-Silcrete**	**PP5-6-MIS4-Silcrete**
n (number of simulated assemblages)	1000	1000	1000	1000	1000	1000	46
First Quartile	0.00	0.00	0.00	0.00	0.00	0.00	13.79
Min	0.00	0.00	0.00	0.00	0.00	0.00	0.00
Median	0.00	0.00	0.00	0.00	0.00	0.00	39.13
Mean	0.00	0.00	0.22	0.47	0.21	0.17	40.00
Max	0.00	0.00	2.89	3.95	3.17	1.66	96.55
Third Quartile	0.00	0.00	0.00	0.64	0.00	0.00	62.77
SD	0.00	0.00	0.54	0.85	0.54	0.40	27.52
SE	0.00	0.00	0.05	0.08	0.05	0.04	4.01*
Margin of error (95% CI)	0.00	0.00	0.11	0.17	0.11	0.08	7.85

Upper 95% CI	0.00	0.00	0.32	0.64	0.32	0.25	47.85*
Lower 95% CI	0.00	0.00	0.11	0.30	0.10	0.09	32.15*
	TT=50-Quartzite	**TT=100-Quartzite**	**TT=500-Quartzite**	**TT=1000-Quartzite**	**TT=1500-Quartzite**	**TT=2000-Quartzite**	**PP5-6-MIS4-Quartzite**
n (number of simulated assemblages)	1000	1000	1000	1000	1000	1000	46
First Quartile	0.00	0.86	56.84	69.37	74.02	78.98	5.19
Min	0.00	0.00	41.43	55.93	61.86	64.18	0.00
Median	0.00	1.47	62.04	74.27	78.24	82.25	43.00
Mean	0.03	1.82	61.55	74.15	78.13	81.40	44.63
Max	0.78	7.41	77.36	86.50	91.54	90.65	96.45
Third Quartile	0.00	2.41	67.32	79.16	82.73	85.09	68.24
SD	0.12	1.43	6.99	6.55	6.20	5.32	25.54
SE	0.01	0.14	0.70	0.65	0.62	0.53	3.71*
Margin of error (95% CI)	0.02	0.28	1.37	1.28	1.22	1.04	7.27
Upper 95% CI	0.05	2.10	62.92	75.43	79.34	82.44	51.90*
Lower 95% CI	0.01	1.54	60.18	72.87	76.91	80.36	37.35*

*Margins of error (95% CI) for archaeological data were obtained by bootstrapping the standard errors 10000 times.

MIS4 without a Paleo-Agulhas plain silcrete source – Site Caching

Table B139. Summary statistics and test results for OFAT4 modeling of MIS4 conditions without a Paleo-Agulhas plain silcrete source compared to MIS4 archaeological raw material frequency data from PP5-6.

	TT=50-Quartz	**TT=100-Quartz**	**TT=500-Quartz**	**TT=1000-Quartz**	**TT=1500-Quartz**	**TT=2000-Quartz**	**PP5-6-MIS4-Quartz**
n (number of simulated assemblages)	1000	1000	1000	1000	1000	1000	46
First Quartile	100.00	97.56	63.72	44.74	36.62	30.95	1.21
Min	99.30	91.34	59.27	39.74	31.18	24.47	0.00
Median	100.00	98.43	65.34	46.88	38.39	33.05	3.73
Mean	99.98	97.97	65.50	46.78	38.31	33.08	8.39
Max	100.00	100.00	72.15	53.52	44.17	41.69	66.11
Third Quartile	100.00	98.81	67.76	48.87	40.07	35.07	10.53
SD	0.11	1.48	2.96	3.00	2.47	3.16	11.83
SE	0.01	0.15	0.30	0.30	0.25	0.32	1.67*
Margin of error (95% CI)	0.02	0.29	0.58	0.59	0.48	0.62	3.28
Upper 95% CI	100.00	98.26	66.08	47.37	38.79	33.70	11.66*
Lower 95% CI	99.96	97.68	64.91	46.20	37.82	32.46	5.11*
	TT=50-Silcrete	**TT=100-Silcrete**	**TT=500-Silcrete**	**TT=1000-Silcrete**	**TT=1500-Silcrete**	**TT=2000-Silcrete**	**PP5-6-MIS4-Silcrete**
n (number of simulated assemblages)	1000	1000	1000	1000	1000	1000	46
First Quartile	0.00	0.00	0.36	1.48	2.13	2.67	13.79

Min	0.00	0.00	0.00	0.31	0.68	0.68	0.00
Median	0.00	0.00	0.70	1.89	2.66	3.33	39.13
Mean	0.00	0.00	0.77	1.95	2.68	3.46	40.00
Max	0.00	0.00	2.41	4.20	4.76	8.25	96.55
Third Quartile	0.00	0.00	1.13	2.37	3.17	4.10	62.77
SD	0.00	0.00	0.59	0.76	0.80	1.14	27.52
SE	0.00	0.00	0.06	0.08	0.08	0.11	4.01*
Margin of error (95% CI)	0.00	0.00	0.12	0.15	0.16	0.22	7.85
Upper 95% CI	0.00	0.00	0.88	2.10	2.84	3.69	47.85*
Lower 95% CI	0.00	0.00	0.65	1.80	2.53	3.24	32.15*
	TT=50-Quartzite	**TT=100-Quartzite**	**TT=500-Quartzite**	**TT=1000-Quartzite**	**TT=1500-Quartzite**	**TT=2000-Quartzite**	**PP5-6-MIS4-Quartzite**
n (number of simulated assemblages)	1000	1000	1000	1000	1000	1000	46
First Quartile	0.00	1.19	31.36	49.30	57.17	60.91	5.19
Min	0.00	0.00	27.54	44.83	53.75	55.66	0.00
Median	0.00	1.57	33.71	51.23	58.58	63.27	43.00
Mean	0.02	2.03	33.74	51.27	59.01	63.46	44.63
Max	0.70	8.66	40.22	58.18	66.28	71.62	96.45
Third Quartile	0.00	2.44	35.65	53.37	60.87	65.83	68.24
SD	0.11	1.48	2.91	2.97	2.60	3.36	25.54
SE	0.01	0.15	0.29	0.30	0.26	0.34	3.71*
Margin of error (95% CI)	0.02	0.29	0.57	0.58	0.51	0.66	7.27
Upper 95% CI	0.04	2.32	34.31	51.85	59.52	64.12	51.90*
Lower 95% CI	0.00	1.74	33.17	50.69	58.50	62.80	37.35*

*Margins of error (95% CI) for archaeological data were obtained by bootstrapping the standard errors 10000 times.

Table B140. Comparison between ranked model frequencies from OFAT4 simulations of MIS4 conditions without a Paleo-Agulhas plain silcrete source and ranked MIS4 archaeological frequencies from PP5-6.

			Conservative*				**Archaeology**
Raw Material	**TT=50**	**TT=100**	**TT=500**	**TT=1000**	**TT=1500**	**TT=2000**	**MIS4-PP5-6**
Quartz	1	1	2	2	2	2	2
Silcrete	2	3	3	3	3	2	1
Quartzite	2	2	1	1	1	1	1
			Expedient*				**Archaeology**
Raw Material	**TT=50**	**TT=100**	**TT=500**	**TT=1000**	**TT=1500**	**TT=2000**	**MIS4-PP5-6**
Quartz	1	1	2	2	2	2	2
Silcrete	2	3	3	3	3	3	1
Quartzite	2	2	1	1	1	1	1
			Site Caching*				**Archaeology**
Raw Material	**TT=50**	**TT=100**	**TT=500**	**TT=1000**	**TT=1500**	**TT=2000**	**MIS4-PP5-6**

Quartz	1	1	1	2	2	2	2
Silcrete	2	3	3	3	3	3	1
Quartzite	2	2	2	1	1	1	1

* Ranking based on which raw materials have the highest mean frequency. Similar rankings in the table are due to statistically similar frequencies. Ranking based on MIS4 archaeological raw material frequencies from bootstrapped data in Figure 50 and Table 19. Similar rankings in the table are due to statistically similar frequencies.

MIS4 with a Paleo-Agulhas plain silcrete source – Conservative Behavior

Table B141. Summary statistics and test results for OFAT4 modeling of MIS4 conditions with a Paleo-Agulhas plain silcrete source compared to MIS4 archaeological raw material frequency data from PP5-6.

	TT=50-Quartz	**TT=100-Quartz**	**TT=500-Quartz**	**TT=1000-Quartz**	**TT=1500-Quartz**	**TT=2000-Quartz**	**PP5-6-MIS4-Quartz**
n (number of simulated assemblages)	1000	1000	1000	1000	1000	1000	46
First Quartile	33.33	0.00	0.00	0.00	0.00	0.00	1.21
Min	0.00	0.00	0.00	0.00	0.00	0.00	0.00
Median	66.67	0.00	0.00	0.00	0.00	0.00	3.73
Mean	61.57	30.51	10.76	5.46	7.88	3.61	8.39
Max	100.00	100.00	100.00	100.00	100.00	100.00	66.11
Third Quartile	100.00	57.50	0.50	0.00	0.19	0.00	10.53
SD	34.66	39.96	25.09	16.63	19.87	16.04	11.83
SE	3.56	4.00	2.51	1.66	1.99	1.60	1.67*
Margin of error (95% CI)	6.97	7.83	4.92	3.26	3.90	3.14	3.28
Upper 95% CI	68.54	38.34	15.68	8.72	11.78	6.75	11.66*
Lower 95% CI	54.60	22.67	5.84	2.20	3.99	0.46	5.11*
	TT=50-Silcrete	**TT=100-Silcrete**	**TT=500-Silcrete**	**TT=1000-Silcrete**	**TT=1500-Silcrete**	**TT=2000-Silcrete**	**PP5-6-MIS4-Silcrete**
n (number of simulated assemblages)	1000	1000	1000	1000	1000	1000	46
First Quartile	0.00	0.00	0.00	0.00	0.00	0.00	13.79
Min	0.00	0.00	0.00	0.00	0.00	0.00	0.00
Median	25.00	0.00	0.00	0.00	0.00	0.00	39.13
Mean	30.01	24.18	22.09	19.29	23.55	17.98	40.00
Max	100.00	100.00	100.00	100.00	100.00	100.00	96.55
Third Quartile	50.00	50.00	47.08	33.33	49.94	33.00	62.77
SD	31.40	36.05	35.39	33.83	35.18	33.45	27.52
SE	3.22	3.60	3.54	3.38	3.52	3.35	4.01*
Margin of error (95% CI)	6.31	7.07	6.94	6.63	6.89	6.56	7.85
Upper 95% CI	36.32	31.24	29.02	25.92	30.45	24.53	47.85*
Lower 95% CI	23.69	17.11	15.15	12.66	16.66	11.42	32.15*
	TT=50-Quartzite	**TT=100-Quartzite**	**TT=500-Quartzite**	**TT=1000-Quartzite**	**TT=1500-Quartzite**	**TT=2000-Quartzite**	**PP5-6-MIS4-Quartzite**
n (number of simulated	1000	1000	1000	1000	1000	1000	46

assemblages)							
First Quartile	0.00	0.00	0.00	0.00	0.00	0.00	5.19
Min	0.00	0.00	0.00	0.00	0.00	0.00	0.00
Median	0.00	0.00	0.00	29.17	50.00	29.17	43.00
Mean	1.05	15.32	37.15	41.25	43.57	43.42	44.63
Max	50.00	100.00	100.00	100.00	100.00	100.00	96.45
Third Quartile	0.00	15.00	100.00	100.00	100.00	100.00	68.24
SD	7.22	30.47	42.88	44.37	42.42	45.48	25.54
SE	0.74	3.05	4.29	4.44	4.24	4.55	3.71*
Margin of error (95% CI)	1.45	5.97	8.40	8.70	8.32	8.91	7.27
Upper 95% CI	2.50	21.29	45.55	49.95	51.88	52.33	51.90*
Lower 95% CI	0.00	9.35	28.75	32.55	35.25	34.50	37.35*

*Margins of error (95% CI) for archaeological data were obtained by bootstrapping the standard errors 10000 times.

MIS4 with a Paleo-Agulhas plain silcrete source – Expedient Behavior

Table B142. Summary statistics and test results for OFAT4 modeling of MIS4 conditions with a Paleo-Agulhas plain silcrete source compared to MIS4 archaeological raw material frequency data from PP5-6.

	TT=50-Quartz	**TT=100-Quartz**	**TT=500-Quartz**	**TT=1000-Quartz**	**TT=1500-Quartz**	**TT=2000-Quartz**	**PP5-6-MIS4-Quartz**
n (number of simulated assemblages)	1000	1000	1000	1000	1000	1000	46
First Quartile	60.73	40.86	7.81	6.28	5.81	5.70	1.21
Min	45.56	28.66	4.95	3.74	2.95	3.90	0.00
Median	61.94	42.29	9.38	7.50	7.11	7.00	3.73
Mean	61.95	42.18	9.43	7.72	7.15	7.14	8.39
Max	68.51	50.81	14.92	16.13	11.12	11.23	66.11
Third Quartile	63.31	43.92	10.85	8.95	8.48	8.35	10.53
SD	2.58	2.76	2.10	2.03	1.89	1.83	11.83
SE	0.26	0.28	0.21	0.20	0.19	0.18	1.67*
Margin of error (95% CI)	0.50	0.54	0.41	0.40	0.37	0.36	3.28
Upper 95% CI	62.46	42.72	9.84	8.12	7.52	7.50	11.66*
Lower 95% CI	61.45	41.64	9.02	7.32	6.78	6.78	5.11*
	TT=50-Silcrete	**TT=100-Silcrete**	**TT=500-Silcrete**	**TT=1000-Silcrete**	**TT=1500-Silcrete**	**TT=2000-Silcrete**	**PP5-6-MIS4-Silcrete**
n (number of simulated assemblages)	1000	1000	1000	1000	1000	1000	46
First Quartile	36.69	55.27	70.12	60.35	54.07	49.36	13.79
Min	31.49	47.40	62.11	52.93	42.29	39.41	0.00
Median	38.06	57.11	72.33	63.80	56.70	53.07	39.13
Mean	38.04	57.00	71.88	63.35	57.00	52.44	40.00
Max	54.44	67.46	80.69	73.14	71.12	63.77	96.55

Third Quartile	39.27	58.53	74.44	66.40	59.50	56.24	62.77
SD	2.58	2.63	3.89	4.43	4.70	5.11	27.52
SE	0.26	0.26	0.39	0.44	0.47	0.51	4.01*
Margin of error (95% CI)	0.50	0.52	0.76	0.87	0.92	1.00	7.85
Upper 95% CI	38.54	57.51	72.64	64.22	57.93	53.45	47.85*
Lower 95% CI	37.53	56.48	71.11	62.48	56.08	51.44	32.15*
	TT=50-Quartzite	**TT=100-Quartzite**	**TT=500-Quartzite**	**TT=1000-Quartzite**	**TT=1500-Quartzite**	**TT=2000-Quartzite**	**PP5-6-MIS4-Quartzite**
n (number of simulated assemblages)	1000	1000	1000	1000	1000	1000	46
First Quartile	0.00	0.40	16.05	26.18	32.89	36.78	5.19
Min	0.00	0.00	10.68	21.21	23.77	25.09	0.00
Median	0.00	0.70	18.04	28.25	35.69	40.85	43.00
Mean	0.01	0.82	18.69	28.93	35.85	40.41	44.63
Max	0.29	3.88	32.94	40.61	48.91	56.69	96.45
Third Quartile	0.00	1.06	20.74	31.67	39.13	43.29	68.24
SD	0.04	0.62	3.94	4.33	4.56	5.16	25.54
SE	0.00	0.06	0.39	0.43	0.46	0.52	3.71*
Margin of error (95% CI)	0.01	0.12	0.77	0.85	0.89	1.01	7.27
Upper 95% CI	0.01	0.94	19.46	29.78	36.74	41.43	51.90*
Lower 95% CI	0.00	0.70	17.92	28.08	34.95	39.40	37.35*

*Margins of error (95% CI) for archaeological data were obtained by bootstrapping the standard errors 10000 times.

MIS4 with a Paleo-Agulhas plain silcrete source – Site Caching

Table B143. Summary statistics and test results for OFAT4 modeling of MIS4 conditions with a Paleo-Agulhas plain silcrete source compared to MIS4 archaeological raw material frequency data from PP5-6.

	TT=50-Quartz	**TT=100-Quartz**	**TT=500-Quartz**	**TT=1000-Quartz**	**TT=1500-Quartz**	**TT=2000-Quartz**	**PP5-6-MIS4-Quartz**
n (number of simulated assemblages)	1000	1000	1000	1000	1000	1000	46
First Quartile	71.56	66.04	44.40	32.83	27.04	23.45	1.21
Min	68.92	58.32	40.11	27.80	22.34	18.82	0.00
Median	72.53	68.09	46.11	34.89	29.27	25.22	3.73
Mean	72.98	68.02	46.23	34.81	29.19	25.26	8.39
Max	78.49	76.44	53.88	41.61	35.99	31.55	66.11
Third Quartile	74.38	70.06	48.39	36.98	31.60	26.87	10.53
SD	2.10	2.97	2.84	2.82	2.78	2.41	11.83
SE	0.21	0.30	0.28	0.28	0.28	0.24	1.67*
Margin of error (95% CI)	0.41	0.58	0.56	0.55	0.55	0.47	3.28
Upper 95% CI	73.40	68.60	46.79	35.36	29.74	25.73	11.66*
Lower 95% CI	72.57	67.44	45.67	34.25	28.65	24.79	5.11*

	TT=50-Silcrete	TT=100-Silcrete	TT=500-Silcrete	TT=1000-Silcrete	TT=1500-Silcrete	TT=2000-Silcrete	PP5-6-MIS4-Silcrete
n (number of simulated assemblages)	1000	1000	1000	1000	1000	1000	46
First Quartile	25.62	28.87	25.60	21.12	19.03	17.70	13.79
Min	21.51	23.56	20.51	17.07	14.76	14.21	0.00
Median	27.47	30.44	27.22	23.03	21.20	19.21	39.13
Mean	27.01	30.69	27.17	23.11	20.82	19.43	40.00
Max	31.08	41.68	32.78	27.55	28.17	25.65	96.55
Third Quartile	28.44	32.87	28.86	25.22	22.44	21.24	62.77
SD	2.11	2.94	2.43	2.50	2.48	2.44	27.52
SE	0.21	0.29	0.24	0.25	0.25	0.24	4.01*
Margin of error (95% CI)	0.41	0.58	0.48	0.49	0.49	0.48	7.85
Upper 95% CI	27.42	31.27	27.64	23.59	21.30	19.91	47.85*
Lower 95% CI	26.60	30.12	26.69	22.62	20.33	18.95	32.15*
	TT=50-Quartzite	**TT=100-Quartzite**	**TT=500-Quartzite**	**TT=1000-Quartzite**	**TT=1500-Quartzite**	**TT=2000-Quartzite**	**PP5-6-MIS4-Quartzite**
n (number of simulated assemblages)	1000	1000	1000	1000	1000	1000	46
First Quartile	0.00	0.72	24.75	40.07	47.93	53.71	5.19
Min	0.00	0.00	21.88	35.67	41.89	47.92	0.00
Median	0.00	1.17	26.37	41.75	49.93	55.29	43.00
Mean	0.01	1.29	26.60	42.09	49.99	55.31	44.63
Max	0.33	3.42	32.53	50.46	60.90	62.81	96.45
Third Quartile	0.00	1.62	28.53	43.87	51.78	57.16	68.24
SD	0.04	0.78	2.40	2.80	3.29	2.97	25.54
SE	0.00	0.08	0.24	0.28	0.33	0.30	3.71*
Margin of error (95% CI)	0.01	0.15	0.47	0.55	0.65	0.58	7.27
Upper 95% CI	0.02	1.44	27.07	42.64	50.64	55.89	51.90*
Lower 95% CI	0.00	1.13	26.13	41.54	49.35	54.72	37.35*

*Margins of error (95% CI) for archaeological data were obtained by bootstrapping the standard errors 10000 times.

Table B144. Comparison between ranked model frequencies from OFAT4 simulations of MIS4 conditions with a Paleo-Agulhas plain silcrete source and ranked MIS4 archaeological frequencies from PP5-6.

			Conservative*				**Archaeology**
Raw Material	**TT=50**	**TT=100**	**TT=500**	**TT=1000**	**TT=1500**	**TT=2000**	**MIS4-PP5-6**
Quartz	1	1	1.5	3	3	3	2
Silcrete	2	1	1	2	2	2	1
Quartzite	3	1.5	1	1	1	1	1
			Expedient*				**Archaeology**
Raw Material	**TT=50**	**TT=100**	**TT=500**	**TT=1000**	**TT=1500**	**TT=2000**	**MIS4-PP5-6**
Quartz	1	2	3	3	3	3	2

Silcrete	2	1	1	1	1	1	1
Quartzite	3	3	2	2	2	2	1

	Site Caching*						Archaeology
Raw Material	**TT=50**	**TT=100**	**TT=500**	**TT=1000**	**TT=1500**	**TT=2000**	**MIS4-PP5-6**
Quartz	1	1	1	2	2	2	2
Silcrete	2	2	2	3	3	3	1
Quartzite	3	3	2	1	1	1	1

* Ranking based on which raw materials have the highest mean frequency. Similar rankings in the table are due to statistically similar frequencies. Ranking based on MIS4 archaeological raw material frequencies from bootstrapped data in Figure 50 and Table 19. Similar rankings in the table are due to statistically similar frequencies.

MIS5 conditions – Conservative Behavior

Table B145. Summary statistics and test results for OFAT4 modeling of MIS5 conditions compared to MIS5 archaeological raw material frequency data from PP5-6, PP13B, PP9B, and PP9C.

	TT=50-Quartz	**TT=100-Quartz**	**TT=500-Quartz**	**TT=1000-Quartz**	**TT=1500-Quartz**	**TT=2000-Quartz**	**PP5-6-MIS5-Quartz**	**PP13B-MIS5-Quartz**	**AllPP-MIS5-Quartz**
n (number of assemblages)	1000	1000	1000	1000	1000	1000	31	7	43
First Quartile	66.83	0.00	0.34	0.06	0.00	0.00	0.00	1.71	0.10
Min	0.00	0.00	0.00	0.00	0.00	0.00	0.00	0.00	0.00
Median	83.42	50.25	29.23	1.00	0.50	0.75	0.89	2.15	2.65
Mean	76.37	51.61	34.76	29.44	15.91	22.20	3.53	4.41	4.61
Max	100.00	100.00	100.00	100.00	100.00	100.00	24.87	9.39	24.87
Third Quartile	100.00	100.00	50.50	50.25	19.00	33.96	3.92	9.33	6.95
SD	30.65	41.79	38.02	36.38	29.44	32.36	5.94	3.91	6.03
SE	3.07	4.18	3.80	3.64	2.94	3.24	1.03*	1.40*	0.90*
Margin of error (95% CI)	6.01	8.19	7.45	7.13	5.77	6.34	2.03	2.74	1.76
Upper 95% CI	82.38	59.80	42.21	36.57	21.68	28.55	5.56*	7.15*	6.37*
Lower 95% CI	70.37	43.42	27.30	22.31	10.13	15.86	1.51*	1.68*	2.85*
	TT=50-Silcrete	**TT=100-Silcrete**	**TT=500-Silcrete**	**TT=1000-Silcrete**	**TT=1500-Silcrete**	**TT=2000-Silcrete**	**PP5-6-MIS5-Silcrete**	**PP13B-Silcrete**	**AllPP-MIS5-Silcrete**
n (number of assemblages)	1000	1000	1000	1000	1000	1000	31	7	4.30E+01
First Quartile	0.00	0.00	0.00	0.00	0.00	0.00	1.45	0.00	0.95
Min	0.00	0.00	0.00	0.00	0.00	0.00	0.00	0.00	0.00
Median	0.00	0.00	0.15	0.00	0.30	0.25	10.19	0.00	6.44
Mean	0.09	3.73	17.87	20.96	22.64	22.94	16.97	1.09	13.05
Max	0.60	66.00	99.00	99.00	99.00	99.00	64.83	5.01	64.83
Third	0.15	0.20	33.00	38.14	49.50	49.50	32.95	2.55	21.21

Quartile									
SD	0.12	12.99	28.27	33.12	33.57	31.96	17.85	1.97	16.45
SE	0.01	1.30	2.83	3.31	3.36	3.20	3.14*	0.68*	2.46*
Margin of error (95% CI)	0.02	2.55	5.54	6.49	6.58	6.26	6.16	1.34	4.82
Upper 95% CI	0.11	6.28	23.42	27.46	29.21	29.20	23.12*	2.42*	17.86*
Lower 95% CI	0.06	1.19	12.33	14.47	16.06	16.67	10.81*	0.00*	8.23*
	TT=50-Quartzite	**TT=100-Quartzite**	**TT=500-Quartzite**	**TT=1000-Quartzite**	**TT=1500-Quartzite**	**TT=2000-Quartzite**	**P5-6-MIS5-Quartzite**	**PP13B-Quartzite**	**AllPP-MIS5-Quartzite**
n (number of assemblages)	1000	1000	1000	1000	1000	1000	31	7	43
First Quartile	0.00	0.00	0.00	0.00	0.00	0.00	60.24	87.62	64.30
Min	0.00	0.00	0.00	0.00	0.00	0.00	26.94	87.62	26.94
Median	0.00	0.00	33.33	49.25	49.25	33.08	76.11	97.85	83.74
Mean	14.48	28.61	35.32	41.55	41.38	36.82	72.77	94.34	77.20
Max	98.50	100.00	100.00	100.00	100.00	100.00	100.00	100.00	100.00
Third Quartile	24.63	50.00	66.04	66.60	98.50	66.54	92.83	98.29	92.83
SD	19.26	36.57	37.70	40.03	41.42	40.15	21.79	5.37	20.01
SE	1.93	3.66	3.77	4.00	4.14	4.01	3.85*	1.92*	3.00*
Margin of error (95% CI)	3.78	7.17	7.39	7.85	8.12	7.87	7.55	3.76	5.87
Upper 95% CI	18.26	35.78	42.71	49.39	49.50	44.68	80.32*	98.10*	83.07*
Lower 95% CI	10.71	21.45	27.93	33.70	33.26	28.95	65.21*	90.58*	71.33*

*Margins of error (95% CI) for archaeological data were obtained by bootstrapping the standard errors 10000 times.

MIS5 conditions – Expedient Behavior

Table B146. Summary statistics and test results for OFAT4 modeling of MIS5 conditions compared to MIS5 archaeological raw material frequency data from PP5-6, PP13B, PP9B, and PP9C.

	TT=50-Quartz	**TT=100-Quartz**	**TT=500-Quartz**	**TT=1000-Quartz**	**TT=1500-Quartz**	**TT=2000-Quartz**	**PP5-6-MIS5-Quartz**	**PP13B-MIS5-Quartz**	**AllPP-MIS5-Quartz**
n (number of assemblages)	1000	1000	1000	1000	1000	1000	31	7	43
First Quartile	81.63	73.90	52.87	54.31	57.26	57.78	0.00	1.71	0.10
Min	73.21	65.62	40.98	46.14	38.74	44.37	0.00	0.00	0.00
Median	82.75	75.51	59.12	60.40	61.63	62.94	0.89	2.15	2.65
Mean	82.76	75.24	58.15	60.32	61.52	62.62	3.53	4.41	4.61
Max	88.02	80.31	71.74	78.91	77.33	76.99	24.87	9.39	24.87
Third Quartile	84.06	77.04	62.46	64.34	66.64	66.97	3.92	9.33	6.95

SD	2.10	2.70	6.72	6.99	7.69	6.89	5.94	3.91	6.03
SE	0.21	0.27	0.67	0.70	0.77	0.69	1.03*	1.40*	0.90*
Margin of error (95% CI)	0.41	0.53	1.32	1.37	1.51	1.35	2.03	2.74	1.76
Upper 95% CI	83.18	75.77	59.46	61.69	63.03	63.97	5.56*	7.15*	6.37*
Lower 95% CI	82.35	74.71	56.83	58.95	60.01	61.27	1.51*	1.68*	2.85*
	TT=50-Silcrete	**TT=100-Silcrete**	**TT=500-Silcrete**	**TT=1000-Silcrete**	**TT=1500-Silcrete**	**TT=2000-Silcrete**	**PP5-6-MIS5-Silcrete**	**PP13B-Silcrete**	**AllPP-MIS5-Silcrete**
n (number of assemblages)	1000	1000	1000	1000	1000	1000	31	7	4.30E+01
First Quartile	0.10	0.14	0.23	0.24	0.20	0.21	1.45	0.00	0.95
Min	0.07	0.11	0.16	0.12	0.13	0.14	0.00	0.00	0.00
Median	0.10	0.14	0.36	1.06	0.26	0.93	10.19	0.00	6.44
Mean	0.10	0.14	0.98	1.50	1.29	1.70	16.97	1.09	13.05
Max	0.16	0.20	5.75	5.17	8.50	7.60	64.83	5.01	64.83
Third Quartile	0.11	0.15	1.60	2.65	2.05	2.71	32.95	2.55	21.21
SD	0.01	0.02	1.10	1.41	1.79	1.92	17.85	1.97	16.45
SE	0.00	0.00	0.11	0.14	0.18	0.19	3.14*	0.68*	2.46*
Margin of error (95% CI)	0.00	0.00	0.22	0.28	0.35	0.38	6.16	1.34	4.82
Upper 95% CI	0.11	0.15	1.20	1.77	1.64	2.07	23.12*	2.42*	17.86*
Lower 95% CI	0.10	0.14	0.77	1.22	0.94	1.32	10.81*	0.00*	8.23*
	TT=50-Quartzite	**TT=100-Quartzite**	**TT=500-Quartzite**	**TT=1000-Quartzite**	**TT=1500-Quartzite**	**TT=2000-Quartzite**	**P5-6-MIS5-Quartzite**	**PP13B-Silcrete**	**AllPP-MIS5-Quartzite**
n (number of assemblages)	1000	1000	1000	1000	1000	1000	31	7	43
First Quartile	15.78	22.74	35.83	33.46	31.38	29.42	60.24	87.62	64.30
Min	11.86	19.49	27.98	20.89	20.77	22.30	26.94	87.62	26.94
Median	17.07	24.26	40.25	38.10	37.08	36.04	76.11	97.85	83.74
Mean	17.06	24.52	40.72	38.04	37.05	35.54	72.77	94.34	77.20
Max	26.52	34.05	58.45	53.37	57.95	51.48	100.00	100.00	100.00
Third Quartile	18.18	25.84	45.91	43.63	42.13	40.42	92.83	98.29	92.83
SD	2.08	2.67	6.75	7.03	7.46	6.69	21.79	5.37	20.01
SE	0.21	0.27	0.68	0.70	0.75	0.67	3.85*	1.92*	3.00*
Margin of error (95% CI)	0.41	0.52	1.32	1.38	1.46	1.31	7.55	3.76	5.87
Upper 95% CI	17.47	25.04	42.04	39.42	38.51	36.85	80.32*	98.10*	83.07*
Lower 95% CI	16.66	24.00	39.39	36.66	35.59	34.23	65.21*	90.58*	71.33*

*Margins of error (95% CI) for archaeological data were obtained by bootstrapping the standard errors 10000 times.

MIS5 conditions – Site Caching

Table B147. Summary statistics and test results for OFAT4 modeling of MIS5 conditions compared to MIS5 archaeological raw material frequency data from PP5-6, PP13B, PP9B, and PP9C.

	TT=50-Quartz	TT=100-Quartz	TT=500-Quartz	TT=1000-Quartz	TT=1500-Quartz	TT=2000-Quartz	PP5-6-MIS5-Quartz	PP13B-MIS5-Quartz	AllPP-MIS5-Quartz
n (number of assemblages)	1000	1000	1000	1000	1000	1000	31	7	43
First Quartile	84.13	81.17	61.51	47.83	41.96	37.79	0.00	1.71	0.10
Min	80.72	72.57	54.59	44.77	36.09	33.21	0.00	0.00	0.00
Median	85.41	82.42	62.91	50.87	43.95	39.38	0.89	2.15	2.65
Mean	85.38	82.34	62.84	50.51	43.81	39.57	3.53	4.41	4.61
Max	91.96	89.97	69.25	56.67	49.52	46.30	24.87	9.39	24.87
Third Quartile	86.59	83.65	64.67	52.85	45.73	41.41	3.92	9.33	6.95
SD	1.88	2.26	2.69	2.93	2.56	2.58	5.94	3.91	6.03
SE	0.19	0.23	0.27	0.29	0.26	0.26	1.03*	1.40*	0.90*
Margin of error (95% CI)	0.37	0.44	0.53	0.57	0.50	0.50	2.03	2.74	1.76
Upper 95% CI	85.75	82.79	63.37	51.08	44.31	40.07	5.56*	7.15*	6.37*
Lower 95% CI	85.01	81.90	62.31	49.93	43.31	39.06	1.51*	1.68*	2.85*
	TT=50-Silcrete	**TT=100-Silcrete**	**TT=500-Silcrete**	**TT=1000-Silcrete**	**TT=1500-Silcrete**	**TT=2000-Silcrete**	**PP5-6-MIS5-Silcrete**	**PP13B-Silcrete**	**AllPP-MIS5-Silcrete**
n (number of assemblages)	1000	1000	1000	1000	1000	1000	31	7	4.30E+01
First Quartile	0.08	0.09	1.99	8.26	13.32	16.56	1.45	0.00	0.95
Min	0.05	0.06	1.22	5.94	8.99	14.03	0.00	0.00	0.00
Median	0.09	0.10	2.80	9.79	14.54	17.81	10.19	0.00	6.44
Mean	0.09	0.10	2.78	9.69	14.49	17.86	16.97	1.09	13.05
Max	0.12	0.14	5.01	15.15	18.44	24.01	64.83	5.01	64.83
Third Quartile	0.10	0.11	3.42	10.86	15.75	19.08	32.95	2.55	21.21
SD	0.01	0.01	0.95	1.82	1.79	1.91	17.85	1.97	16.45
SE	0.00	0.00	0.10	0.18	0.18	0.19	3.14*	0.68*	2.46*
Margin of error (95% CI)	0.00	0.00	0.19	0.36	0.35	0.37	6.16	1.34	4.82
Upper 95% CI	0.09	0.10	2.97	10.04	14.85	18.23	23.12*	2.42*	17.86*
Lower 95% CI	0.09	0.10	2.60	9.33	14.14	17.48	10.81*	0.00*	8.23*
	TT=50-Quartzite	**TT=100-Quartzite**	**TT=500-Quartzite**	**TT=1000-Quartzite**	**TT=1500-Quartzite**	**TT=2000-Quartzite**	**P5-6-MIS5-Quartzite**	**PP13B-Quartzite**	**AllPP-MIS5-Quartzite**

n (number of assemblages)	1000	1000	1000	1000	1000	1000	31	7	43
First Quartile	13.28	16.20	32.68	37.46	39.83	40.64	60.24	87.62	64.30
Min	7.96	9.93	28.21	35.16	34.99	35.65	26.94	87.62	26.94
Median	14.44	17.41	34.23	39.37	41.59	42.46	76.11	97.85	83.74
Mean	14.47	17.49	34.30	39.73	41.62	42.51	72.77	94.34	77.20
Max	19.08	27.20	42.16	45.92	50.02	48.45	100.00	100.00	100.00
Third Quartile	15.71	18.65	35.94	41.37	43.53	44.49	92.83	98.29	92.83
SD	1.86	2.24	2.69	2.69	2.75	2.77	21.79	5.37	20.01
SE	0.19	0.22	0.27	0.27	0.27	0.28	3.85*	1.92*	3.00*
Margin of error (95% CI)	0.36	0.44	0.53	0.53	0.54	0.54	7.55	3.76	5.87
Upper 95% CI	14.84	17.93	34.83	40.26	42.16	43.05	80.32*	98.10*	83.07*
Lower 95% CI	14.11	17.05	33.77	39.20	41.09	41.96	65.21*	90.58*	71.33*

*Margins of error (95% CI) for archaeological data were obtained by bootstrapping the standard errors 10000 times.

Table B148. Comparison between ranked model frequencies from OFAT4 simulations of MIS5 conditions and ranked MIS5 archaeological frequencies from PP13B, PP9B, PP9C, and PP5-6.

	Conservative*						**Archaeology**		
Raw Material	**TT=50**	**TT=100**	**TT=500**	**TT=1000**	**TT=1500**	**TT=2000**	**MIS5-PP5-6**	**MIS5-PP13B**	**MIS5-All PP**
Quartz	1	1	1	1	2	1.5	3	2	3
Silcrete	3	3	2	1	2	1	2	2	2
Quartzite	2	2	1	1.5	1	1	1	1	1
	Expedient*						**Archaeology**		
Raw Material	**TT=50**	**TT=100**	**TT=500**	**TT=1000**	**TT=1500**	**TT=2000**	**MIS5-PP5-6**	**MIS5-PP13B**	**MIS5-All PP**
Quartz	1	1	1	1	1	1	3	2	3
Silcrete	3	3	3	3	3	3	2	2	2
Quartzite	2	2	2	2	2	2	1	1	1
	Site Caching*						**Archaeology**		
Raw Material	**TT=50**	**TT=100**	**TT=500**	**TT=1000**	**TT=1500**	**TT=2000**	**MIS5-PP5-6**	**MIS5-PP13B**	**MIS5-All PP**
Quartz	1	1	1	1	1	2	3	2	3
Silcrete	3	3	3	3	3	3	2	2	2
Quartzite	2	2	2	2	2	1	1	1	1

* Ranking based on which raw materials have the highest mean frequency. Similar rankings in the table are due to statistically similar frequencies. Ranking based on MIS5 archaeological raw material frequencies from bootstrapped data in Figure 50 and Table 19. Similar rankings in the table are due to statistically similar frequencies. Grey shading indicates a ranking match.

MIS6 without a Paleo-Agulhas plain silcrete source – Conservative Behavior

Table B149. Summary statistics and test results for OFAT4 modeling of MIS6 conditions without a Paleo-Agulhas plain silcrete source compared to MIS6 archaeological raw material frequency data from PP13B.

	TT=50-Quartz	**TT=100-Quartz**	**TT=500-Quartz**	**TT=1000-Quartz**	**TT=1500-Quartz**	**TT=2000-Quartz**	**PP13-MIS6-Quartz**
n (number of assemblages)	1000	1000	1000	1000	1000	1000	7
First Quartile	57.14	0.00	0.00	0.00	0.00	0.00	1.71
Min	0.00	0.00	0.00	0.00	0.00	0.00	0.00
Median	84.52	50.00	0.00	0.00	0.00	0.00	2.15
Mean	75.08	44.96	12.85	11.11	7.75	9.12	4.41
Max	100.00	100.00	100.00	100.00	100.00	100.00	9.39
Third Quartile	100.00	100.00	0.31	0.00	0.00	0.00	9.33
SD	32.13	43.07	27.71	26.95	23.62	24.12	3.91
SE	3.21	4.31	2.77	2.69	2.36	2.41	1.40*
Margin of error (95% CI)	6.30	8.44	5.43	5.28	4.63	4.73	2.74
Upper 95% CI	81.38	53.40	18.28	16.39	12.38	13.85	7.15*
Lower 95% CI	68.79	36.52	7.42	5.82	3.12	4.39	1.68*
	TT=50-Silcrete	**TT=100-Silcrete**	**TT=500-Silcrete**	**TT=1000-Silcrete**	**TT=1500-Silcrete**	**TT=2000-Silcrete**	**PP13B-MIS6-Silcrete**
n (number of assemblages)	1000	1000	1000	1000	1000	1000	7
First Quartile	0.00	0.00	0.00	0.00	0.00	0.00	0.00
Min	0.00	0.00	0.00	0.00	0.00	0.00	0.00
Median	0.00	0.00	0.00	0.00	0.00	0.00	0.00
Mean	0.00	0.00	3.38	2.31	5.31	3.83	1.09
Max	0.00	0.00	99.00	99.00	99.00	99.00	5.01
Third Quartile	0.00	0.00	0.00	0.00	0.00	0.00	2.55
SD	0.00	0.00	15.47	11.91	19.20	16.08	1.97
SE	0.00	0.00	1.55	1.19	1.92	1.61	0.68*
Margin of error (95% CI)	0.00	0.00	3.03	2.33	3.76	3.15	1.34
Upper 95% CI	0.00	0.00	6.41	4.64	9.08	6.98	2.42*
Lower 95% CI	0.00	0.00	0.35	0.00	1.55	0.68	0.00*
	TT=50-Quartzite	**TT=100-Quartzite**	**TT=500-Quartzite**	**TT=1000-Quartzite**	**TT=1500-Quartzite**	**TT=2000-Quartzite**	**PP13B-MIS6-Quartzite**
n (number of assemblages)	1000	1000	1000	1000	1000	1000	7
First Quartile	0.00	0.00	0.00	0.00	0.00	0.00	87.62
Min	0.00	0.00	0.00	0.00	0.00	0.00	87.62
Median	0.00	0.00	50.00	100.00	100.00	100.00	97.85
Mean	15.92	33.04	48.77	66.58	62.93	64.05	94.34
Max	100.00	100.00	100.00	100.00	100.00	100.00	100.00
Third Quartile	25.00	65.00	100.00	100.00	100.00	100.00	98.29
SD	22.23	39.87	45.79	43.51	45.48	44.30	5.37

SE	2.22	3.99	4.58	4.35	4.55	4.43	1.92*
Margin of error (95% CI)	4.36	7.81	8.98	8.53	8.91	8.68	3.76
Upper 95% CI	20.27	40.85	57.74	75.11	71.85	72.73	98.10*
Lower 95% CI	11.56	25.22	39.79	58.06	54.02	55.37	90.58*

*Margins of error (95% CI) for archaeological data were obtained by bootstrapping the standard errors 10000 times.

MIS6 without a Paleo-Agulhas plain silcrete source – Expedient Behavior

Table B150. Summary statistics and test results for OFAT4 modeling of MIS6 conditions without a Paleo-Agulhas plain silcrete source compared to MIS6 archaeological raw material frequency data from PP13B.

	TT=50-Quartz	**TT=100-Quartz**	**TT=500-Quartz**	**TT=1000-Quartz**	**TT=1500-Quartz**	**TT=2000-Quartz**	**PP13-MIS6-Quartz**
n (number of assemblages)	1000	1000	1000	1000	1000	1000	7
First Quartile	80.61	52.25	7.63	5.11	4.80	5.07	1.71
Min	75.11	45.26	5.06	3.31	3.05	2.70	0.00
Median	81.81	54.85	8.57	6.13	5.98	6.07	2.15
Mean	81.74	54.57	8.78	6.31	6.00	6.21	4.41
Max	85.50	61.71	12.64	12.91	9.32	10.04	9.39
Third Quartile	82.96	56.61	9.91	6.95	7.15	7.32	9.33
SD	1.78	3.08	1.66	1.63	1.50	1.54	3.91
SE	0.18	0.31	0.17	0.16	0.15	0.15	1.40*
Margin of error (95% CI)	0.35	0.60	0.32	0.32	0.29	0.30	2.74
Upper 95% CI	82.09	55.18	9.10	6.62	6.30	6.51	7.15*
Lower 95% CI	81.39	53.97	8.45	5.99	5.71	5.91	1.68*
	TT=50-Silcrete	**TT=100-Silcrete**	**TT=500-Silcrete**	**TT=1000-Silcrete**	**TT=1500-Silcrete**	**TT=2000-Silcrete**	**PP13B-MIS6-Silcrete**
n (number of assemblages)	1000	1000	1000	1000	1000	1000	7
First Quartile	0.00	0.00	0.00	0.00	0.00	0.00	0.00
Min	0.00	0.00	0.00	0.00	0.00	0.00	0.00
Median	0.00	0.00	0.00	0.00	0.00	0.00	0.00
Mean	0.00	0.00	0.07	0.05	0.13	0.06	1.09
Max	0.00	0.00	0.74	0.92	1.43	0.60	5.01
Third Quartile	0.00	0.00	0.05	0.00	0.23	0.00	2.55
SD	0.00	0.00	0.15	0.14	0.25	0.15	1.97
SE	0.00	0.00	0.01	0.01	0.02	0.01	0.68*
Margin of error (95% CI)	0.00	0.00	0.03	0.03	0.05	0.03	1.34
Upper 95% CI	0.00	0.00	0.10	0.08	0.18	0.09	2.42*
Lower 95% CI	0.00	0.00	0.04	0.02	0.08	0.03	0.00*
	TT=50-Quartzite	**TT=100-Quartzite**	**TT=500-Quartzite**	**TT=1000-Quartzite**	**TT=1500-Quartzite**	**TT=2000-Quartzite**	**PP13B-MIS6-Quartzite**
n (number of assemblages)	1000	1000	1000	1000	1000	1000	7
First Quartile	17.04	43.39	90.00	92.98	92.77	92.68	87.62

Min	14.50	38.29	87.36	87.09	90.22	89.81	87.62
Median	18.19	45.15	91.36	93.85	93.90	93.93	97.85
Mean	18.26	45.43	91.15	93.64	93.86	93.73	94.34
Max	24.89	54.74	94.94	96.26	96.83	97.30	100.00
Third Quartile	19.39	47.75	92.35	94.73	95.08	94.79	98.29
SD	1.78	3.08	1.66	1.63	1.54	1.54	5.37
SE	0.18	0.31	0.17	0.16	0.15	0.15	1.92*
Margin of error (95% CI)	0.35	0.60	0.33	0.32	0.30	0.30	3.76
Upper 95% CI	18.61	46.03	91.48	93.96	94.16	94.03	98.10*
Lower 95% CI	17.91	44.82	90.83	93.32	93.56	93.43	90.58*

*Margins of error (95% CI) for archaeological data were obtained by bootstrapping the standard errors 10000 times.

MIS6 without a Paleo-Agulhas plain silcrete source – Site Caching

Table B151. Summary statistics and test results for OFAT4 modeling of MIS6 conditions without a Paleo-Agulhas plain silcrete source compared to MIS6 archaeological raw material frequency data from PP13B.

	TT=50-Quartz	**TT=100-Quartz**	**TT=500-Quartz**	**TT=1000-Quartz**	**TT=1500-Quartz**	**TT=2000-Quartz**	**PP13-MIS6-Quartz**
n (number of assemblages)	1000	1000	1000	1000	1000	1000	7
First Quartile	87.61	79.16	51.36	37.65	30.44	27.04	1.71
Min	84.55	74.47	47.83	31.63	25.32	22.02	0.00
Median	88.61	80.99	53.41	39.78	32.66	28.75	2.15
Mean	88.65	80.75	53.44	39.53	32.59	28.55	4.41
Max	100.00	89.09	59.09	46.66	41.88	34.09	9.39
Third Quartile	89.61	82.58	55.68	41.66	34.53	29.97	9.33
SD	1.82	2.84	2.77	3.20	3.10	2.22	3.91
SE	0.18	0.28	0.28	0.32	0.31	0.22	1.40*
Margin of error (95% CI)	0.36	0.56	0.54	0.63	0.61	0.43	2.74
Upper 95% CI	89.01	81.31	53.99	40.16	33.19	28.98	7.15*
Lower 95% CI	88.30	80.20	52.90	38.90	31.98	28.11	1.68*
	TT=50-Silcrete	**TT=100-Silcrete**	**TT=500-Silcrete**	**TT=1000-Silcrete**	**TT=1500-Silcrete**	**TT=2000-Silcrete**	**PP13B-MIS6-Silcrete**
n (number of assemblages)	1000	1000	1000	1000	1000	1000	7
First Quartile	0.00	0.00	0.31	1.25	1.75	2.27	0.00
Min	0.00	0.00	0.00	0.32	0.38	1.28	0.00
Median	0.00	0.00	0.57	1.70	2.30	2.75	0.00
Mean	0.00	0.00	0.63	1.75	2.40	2.90	1.09
Max	0.00	0.00	2.31	3.41	4.76	4.99	5.01
Third Quartile	0.00	0.00	0.85	2.19	2.98	3.60	2.55
SD	0.00	0.00	0.52	0.65	0.87	0.90	1.97
SE	0.00	0.00	0.05	0.07	0.09	0.09	0.68*
Margin of error	0.00	0.00	0.10	0.13	0.17	0.18	1.34

(95% CI)							
Upper 95% CI	0.00	0.00	0.73	1.87	2.57	3.08	2.42*
Lower 95% CI	0.00	0.00	0.53	1.62	2.23	2.73	0.00*
	TT=50-Quartzite	**TT=100-Quartzite**	**TT=500-Quartzite**	**TT=1000-Quartzite**	**TT=1500-Quartzite**	**TT=2000-Quartzite**	**PP13B-MIS6-Quartzite**
n (number of assemblages)	1000	1000	1000	1000	1000	1000	7
First Quartile	10.39	17.42	43.81	56.30	62.82	67.03	87.62
Min	0.00	10.91	40.25	51.41	56.50	63.21	87.62
Median	11.39	19.01	45.81	58.55	65.09	68.51	97.85
Mean	11.35	19.25	45.93	58.72	65.01	68.55	94.34
Max	15.45	25.53	51.85	66.30	72.65	75.74	100.00
Third Quartile	12.39	20.84	47.67	60.67	67.01	69.95	98.29
SD	1.82	2.84	2.79	3.21	3.11	2.21	5.37
SE	0.18	0.28	0.28	0.32	0.31	0.22	1.92*
Margin of error (95% CI)	0.36	0.56	0.55	0.63	0.61	0.43	3.76
Upper 95% CI	11.70	19.80	46.47	59.35	65.62	68.98	98.10*
Lower 95% CI	10.99	18.69	45.38	58.10	64.40	68.12	90.58*

*Margins of error (95% CI) for archaeological data were obtained by bootstrapping the standard errors 10000 times.

Table B152. Comparison between ranked model frequencies from OFAT4 simulations of MIS6 conditions without a Paleo-Agulhas plain silcrete source and ranked MIS6 archaeological frequencies from PP13B.

				Conservative*			**Archaeology**
Raw Material	**TT=50**	**TT=100**	**TT=500**	**TT=1000**	**TT=1500**	**TT=2000**	**MIS6-PP13B**
Quartz	1	1	2	2	2	2	2
Silcrete	3	2	3	3	2	2	2
Quartzite	2	1	1	1	1	1	1
				Expedient*			**Archaeology**
Raw Material	**TT=50**	**TT=100**	**TT=500**	**TT=1000**	**TT=1500**	**TT=2000**	**MIS6-PP13B**
Quartz	1	1	2	2	2	2	2
Silcrete	3	3	3	3	3	3	2
Quartzite	2	2	1	1	1	1	1
				Site Caching*			**Archaeology**
Raw Material	**TT=50**	**TT=100**	**TT=500**	**TT=1000**	**TT=1500**	**TT=2000**	**MIS6-PP13B**
Quartz	1	1	1	2	2	2	2
Silcrete	3	3	3	3	3	3	2
Quartzite	2	2	2	1	1	1	1

* Ranking based on which raw materials have the highest mean frequency. Similar rankings in the table are due to statistically similar frequencies. Ranking based on MIS6 archaeological raw material frequencies from bootstrapped data in Figure 50 and Table 19. Similar rankings in the table are due to statistically similar frequencies. Grey shading indicates a ranking match.

MIS6 with a Paleo-Agulhas plain silcrete source – Conservative Behavior

Table B153. Summary statistics and test results for OFAT4 modeling of MIS6 conditions with a Paleo-Agulhas plain silcrete source compared to MIS6 archaeological raw material frequency data from PP13B.

	TT=50-Quartz	**TT=100-Quartz**	**TT=500-Quartz**	**TT=1000-Quartz**	**TT=1500-Quartz**	**TT=2000-Quartz**	**PP13-MIS6-Quartz**
n (number of assemblages)	1000	1000	1000	1000	1000	1000	7
First Quartile	33.33	0.00	0.00	0.00	0.00	0.00	1.71
Min	0.00	0.00	0.00	0.00	0.00	0.00	0.00
Median	60.00	0.00	0.00	0.00	0.00	0.00	2.15
Mean	56.50	31.13	11.60	6.65	5.37	4.90	4.41
Max	100.00	100.00	100.00	100.00	100.00	100.00	9.39
Third Quartile	96.43	60.00	0.00	0.00	0.00	0.00	9.33
SD	35.65	39.34	28.14	19.56	20.90	18.69	3.91
SE	3.56	3.93	2.81	1.96	2.09	1.87	1.40*
Margin of error (95% CI)	6.99	7.71	5.52	3.83	4.10	3.66	2.74
Upper 95% CI	63.48	38.84	17.12	10.48	9.47	8.56	7.15*
Lower 95% CI	49.51	23.42	6.09	2.81	1.27	1.23	1.68*
	TT=50-Silcrete	**TT=100-Silcrete**	**TT=500-Silcrete**	**TT=1000-Silcrete**	**TT=1500-Silcrete**	**TT=2000-Silcrete**	**PP13B-MIS6-Silcrete**
n (number of assemblages)	1000	1000	1000	1000	1000	1000	7
First Quartile	0.00	0.00	0.00	0.00	0.00	0.00	0.00
Min	0.00	0.00	0.00	0.00	0.00	0.00	0.00
Median	25.00	0.00	0.00	0.00	0.00	0.00	0.00
Mean	26.45	17.80	20.91	18.20	9.30	11.10	1.09
Max	100.00	100.00	100.00	100.00	100.00	100.00	5.01
Third Quartile	50.00	31.25	33.33	33.33	0.00	0.00	2.55
SD	28.50	32.40	36.11	32.46	26.72	26.12	1.97
SE	2.85	3.24	3.61	3.25	2.67	2.61	0.68*
Margin of error (95% CI)	5.59	6.35	7.08	6.36	5.24	5.12	1.34
Upper 95% CI	32.04	24.15	27.99	24.56	14.53	16.22	2.42*
Lower 95% CI	20.86	11.45	13.84	11.84	4.06	5.98	0.00*
	TT=50-Quartzite	**TT=100-Quartzite**	**TT=500-Quartzite**	**TT=1000-Quartzite**	**TT=1500-Quartzite**	**TT=2000-Quartzite**	**PP13B-MIS6-Quartzite**
n (number of assemblages)	1000	1000	1000	1000	1000	1000	7
First Quartile	0.00	0.00	0.00	0.00	0.00	0.00	87.62
Min	0.00	0.00	0.00	0.00	0.00	0.00	87.62
Median	0.00	0.00	50.00	50.00	75.00	50.00	97.85
Mean	3.05	26.07	44.48	49.15	53.33	49.00	94.34
Max	100.00	100.00	100.00	100.00	100.00	100.00	100.00
Third Quartile	0.00	50.00	100.00	100.00	100.00	100.00	98.29
SD	12.29	36.79	44.23	43.63	48.24	46.77	5.37

SE	1.23	3.68	4.42	4.36	4.82	4.68	1.92*
Margin of error (95% CI)	2.41	7.21	8.67	8.55	9.46	9.17	3.76
Upper 95% CI	5.46	33.28	53.15	57.70	62.79	58.17	98.10*
Lower 95% CI	0.64	18.86	35.81	40.60	43.88	39.83	90.58*

*Margins of error (95% CI) for archaeological data were obtained by bootstrapping the standard errors 10000 times.

MIS6 with a Paleo-Agulhas plain silcrete source – Expedient Behavior

Table B154. Summary statistics and test results for OFAT4 modeling of MIS6 conditions with a Paleo-Agulhas plain silcrete source compared to MIS6 archaeological raw material frequency data from PP13B.

	TT=50-Quartz	**TT=100-Quartz**	**TT=500-Quartz**	**TT=1000-Quartz**	**TT=1500-Quartz**	**TT=2000-Quartz**	**PP13-MIS6-Quartz**
n (number of assemblages)	1000	1000	1000	1000	1000	1000	7
First Quartile	59.40	38.51	5.59	3.69	3.67	3.47	1.71
Min	53.49	28.42	3.23	2.00	2.06	2.22	0.00
Median	61.04	40.32	6.46	4.59	4.41	4.27	2.15
Mean	60.96	40.14	6.49	4.68	4.52	4.32	4.41
Max	65.17	46.43	9.92	8.01	8.46	7.87	9.39
Third Quartile	62.26	41.82	7.34	5.25	5.42	4.97	9.33
SD	2.03	2.71	1.35	1.25	1.18	1.13	3.91
SE	0.20	0.27	0.14	0.13	0.12	0.11	1.40*
Margin of error (95% CI)	0.40	0.53	0.27	0.25	0.23	0.22	2.74
Upper 95% CI	61.36	40.67	6.75	4.93	4.75	4.55	7.15*
Lower 95% CI	60.57	39.61	6.22	4.44	4.29	4.10	1.68*
	TT=50-Silcrete	**TT=100-Silcrete**	**TT=500-Silcrete**	**TT=1000-Silcrete**	**TT=1500-Silcrete**	**TT=2000-Silcrete**	**PP13B-MIS6-Silcrete**
n (number of assemblages)	1000	1000	1000	1000	1000	1000	7
First Quartile	32.94	42.41	26.98	19.24	16.92	15.49	0.00
Min	30.10	37.57	23.21	16.32	13.55	11.64	0.00
Median	34.28	43.90	29.33	21.20	18.78	16.78	0.00
Mean	34.42	44.32	29.23	21.26	18.76	17.31	1.09
Max	40.41	60.21	34.97	25.87	26.83	26.29	5.01
Third Quartile	35.83	46.17	31.17	23.04	20.78	19.34	2.55
SD	1.96	3.01	2.77	2.29	2.56	2.62	1.97
SE	0.20	0.30	0.28	0.23	0.26	0.26	0.68*
Margin of error (95% CI)	0.38	0.59	0.54	0.45	0.50	0.51	1.34
Upper 95% CI	34.81	44.91	29.78	21.71	19.26	17.83	2.42*
Lower 95% CI	34.04	43.73	28.69	20.82	18.26	16.80	0.00*
	TT=50-Quartzite	**TT=100-Quartzite**	**TT=500-Quartzite**	**TT=1000-Quartzite**	**TT=1500-Quartzite**	**TT=2000-Quartzite**	**PP13B-MIS6-Quartzite**
n (number of assemblages)	1000	1000	1000	1000	1000	1000	7
First Quartile	4.18	14.68	61.80	71.96	74.65	76.51	87.62

Min	3.30	11.37	56.29	67.44	71.12	69.02	87.62
Median	4.55	15.68	64.21	74.03	76.89	79.00	97.85
Mean	4.61	15.54	64.28	74.05	76.72	78.36	94.34
Max	7.14	19.69	70.73	80.56	82.42	84.98	100.00
Third Quartile	4.95	16.46	66.49	76.23	78.59	80.46	98.29
SD	0.64	1.69	2.95	2.68	2.59	2.89	5.37
SE	0.06	0.17	0.30	0.27	0.26	0.29	1.92*
Margin of error (95% CI)	0.13	0.33	0.58	0.53	0.51	0.57	3.76
Upper 95% CI	4.74	15.87	64.86	74.58	77.23	78.93	98.10*
Lower 95% CI	4.49	15.21	63.70	73.53	76.21	77.80	90.58*

*Margins of error (95% CI) for archaeological data were obtained by bootstrapping the standard errors 10000 times.

MIS6 with a Paleo-Agulhas plain silcrete source – Site Caching

Table B155. Summary statistics and test results for OFAT4 modeling of MIS6 conditions with a Paleo-Agulhas plain silcrete source compared to MIS6 archaeological raw material frequency data from PP13B.

	TT=50-Quartz	**TT=100-Quartz**	**TT=500-Quartz**	**TT=1000-Quartz**	**TT=1500-Quartz**	**TT=2000-Quartz**	**PP13-MIS6-Quartz**
n (number of assemblages)	1000	1000	1000	1000	1000	1000	7
First Quartile	70.65	65.77	43.81	32.63	27.21	23.05	1.71
Min	68.01	58.36	37.42	29.27	22.03	19.16	0.00
Median	72.01	67.50	45.47	35.04	28.72	25.02	2.15
Mean	72.02	67.37	45.18	34.89	28.73	25.07	4.41
Max	78.91	74.93	52.85	42.65	35.64	32.54	9.39
Third Quartile	73.27	68.97	46.91	36.93	30.27	27.29	9.33
SD	1.91	2.64	2.89	2.82	2.37	2.79	3.91
SE	0.19	0.26	0.29	0.28	0.24	0.28	1.40*
Margin of error (95% CI)	0.37	0.52	0.57	0.55	0.46	0.55	2.74
Upper 95% CI	72.40	67.88	45.75	35.44	29.20	25.62	7.15*
Lower 95% CI	71.65	66.85	44.62	34.34	28.27	24.52	1.68*
	TT=50-Silcrete	**TT=100-Silcrete**	**TT=500-Silcrete**	**TT=1000-Silcrete**	**TT=1500-Silcrete**	**TT=2000-Silcrete**	**PP13B-MIS6-Silcrete**
n (number of assemblages)	1000	1000	1000	1000	1000	1000	7
First Quartile	25.14	26.58	23.57	18.62	17.04	16.15	0.00
Min	19.32	20.55	17.39	14.83	13.49	11.60	0.00
Median	26.39	28.85	25.13	20.16	18.66	17.67	0.00
Mean	26.30	28.58	25.10	20.14	18.85	17.65	1.09
Max	30.16	37.75	30.09	25.59	24.46	22.14	5.01
Third Quartile	27.72	30.11	26.81	21.66	20.88	19.19	2.55
SD	1.87	2.76	2.41	2.30	2.45	2.11	1.97
SE	0.19	0.28	0.24	0.23	0.25	0.21	0.68*
Margin of error	0.37	0.54	0.47	0.45	0.48	0.41	1.34

(95% CI)							
Upper 95% CI	26.67	29.12	25.57	20.59	19.33	18.06	2.42*
Lower 95% CI	25.93	28.04	24.63	19.68	18.37	17.23	0.00*
	TT=50-Quartzite	**TT=100-Quartzite**	**TT=500-Quartzite**	**TT=1000-Quartzite**	**TT=1500-Quartzite**	**TT=2000-Quartzite**	**PP13B-MIS6-Quartzite**
n (number of assemblages)	1000	1000	1000	1000	1000	1000	7
First Quartile	1.38	3.06	27.91	43.12	50.33	55.89	87.62
Min	0.44	1.85	25.07	37.22	45.75	48.50	87.62
Median	1.64	4.01	29.39	44.54	52.57	57.33	97.85
Mean	1.68	4.05	29.72	44.98	52.42	57.29	94.34
Max	3.07	8.52	36.95	53.88	58.22	64.27	100.00
Third Quartile	1.98	4.78	31.46	47.06	54.28	59.14	98.29
SD	0.50	1.31	2.60	2.95	2.71	2.78	5.37
SE	0.05	0.13	0.26	0.29	0.27	0.28	1.92*
Margin of error (95% CI)	0.10	0.26	0.51	0.58	0.53	0.55	3.76
Upper 95% CI	1.77	4.31	30.22	45.56	52.95	57.83	98.10*
Lower 95% CI	1.58	3.79	29.21	44.40	51.89	56.74	90.58*

*Margins of error (95% CI) for archaeological data were obtained by bootstrapping the standard errors 10000 times.

Table B156. Comparison between ranked model frequencies from OFAT4 simulations of MIS6 conditions with a Paleo-Agulhas plain silcrete source and ranked MIS6 archaeological frequencies from PP13B.

			Conservative*				**Archaeology**
Raw Material	**TT=50**	**TT=100**	**TT=500**	**TT=1000**	**TT=1500**	**TT=2000**	**MIS6-PP13B**
Quartz	1	1	2	3	2	2	2
Silcrete	2	1.5	2	2	2	2	2
Quartzite	3	1	1	1	1	1	1
			Expedient*				**Archaeology**
Raw Material	**TT=50**	**TT=100**	**TT=500**	**TT=1000**	**TT=1500**	**TT=2000**	**MIS6-PP13B**
Quartz	1	2	3	3	3	3	2
Silcrete	2	1	2	2	2	2	2
Quartzite	3	3	1	1	1	1	1
			Site Caching*				**Archaeology**
Raw Material	**TT=50**	**TT=100**	**TT=500**	**TT=1000**	**TT=1500**	**TT=2000**	**MIS6-PP13B**
Quartz	1	1	1	2	2	2	2
Silcrete	2	2	3	3	3	3	2
Quartzite	3	3	2	1	1	1	1

* Ranking based on which raw materials have the highest mean frequency. Similar rankings in the table are due to statistically similar frequencies. Ranking based on MIS6 archaeological raw material frequencies from bootstrapped data in Figure 50 and Table 19. Similar rankings in the table are due to statistically similar frequencies.

e variable

Table B157. *e* variable measurements for quartzite experimental blocks.

Block	Raw Material	Total Cutting Edge Measured (cm)	Total Flaked Core Mass (kg)	e variable-Cutting Edge (cm)/Total Flaked Core Mass (kg)
D11-1-85C1	Quartzite	955.2	2.00	478.557
D11-1-91A1	Quartzite	807.3	1.96	411.411
D11-1-91A2	Quartzite	911.7	2.17	419.309
D11-1-91B3	Quartzite	898.3	1.88	476.610
D11-1-91B5	Quartzite	1037.0	2.22	467.058
D11-1-91C3	Quartzite	809.5	1.96	412.547
D11-1-94B2	Quartzite	905.9	1.83	495.620
D11-1-94B3	Quartzite	974.7	1.78	546.357
D11-1-94D2	Quartzite	797.3	1.966	405.526
D11-1-97C	Quartzite	887.2	1.83	483.986
C9-1-1B8	Quartzite	774.8	1.92	403.491
C9-1-1B9	Quartzite	769.9	2.06	373.662
D11-1-100A	Quartzite	758.8	2.15	353.094
D11-1-90D1	Quartzite	864.1	2.45	352.656
D11-1-95A	Quartzite	725.6	2.03	357.187
D11-1-95B	Quartzite	790.4	2.16	365.895
D11-1-97A1	Quartzite	708.2	1.93	367.896
D11-1-98B1	Quartzite	773.4	1.91	404.358
D11-1-98C1	Quartzite	781.2	2.09	373.660
D11-1-98D	Quartzite	672.6	1.84	365.042

Table B158. *e* variable measurements for untreated silcrete experimental blocks.

Block	Sample Type	Raw Material	Total Cutting Edge Measured (cm)	Total Flaked Core Mass (kg)	*e* variable-Cutting Edge (cm)/Total Flaked Core Mass (kg)
D9-1-10a	Untreated	Silcrete	633.1	1.98	319.72
D9-1-12a	Untreated	Silcrete	860.8	2.25	382.64
D9-1-12c	Untreated	Silcrete	757.3	1.81	419.07
E3-1-1A	Untreated	Silcrete	695	2.07	335.82
E3-1-5n	Untreated	Silcrete	1048.8	2.46	426.38
E3-1-5o	Untreated	Silcrete	961.5	2.50	383.86
E3-1-6b	Untreated	Silcrete	644	1.69	380.84
I14-2-16a	Untreated	Silcrete	796.8	2.90	275.22

Table B159. *e* variable measurements for heat-treated silcrete experimental blocks.

Block	Sample Type	Raw Material	Total Cutting Edge Measured (cm)	Total Flaked Core Mass (kg)	*e* variable-Cutting Edge (cm)/Total Flaked Core Mass (kg)
D9-1-10b	Heat-treated	Silcrete	1047.9	2.35	445.94
D9-1-12b	Heat-treated	Silcrete	1239.2	2.20	563.25
D9-1-12d	Heat-treated	Silcrete	1156.8	2.29	505.97
E3-1-1b	Heat-treated	Silcrete	1160.2	1.93	600.05
E3-1-5p	Heat-treated	Silcrete	1222.8	2.59	472.54
E3-1-6a	Heat-treated	Silcrete	1239.1	2.20	564.24
E3-1-6c	Heat-treated	Silcrete	1302	2.44	534.48
I14-2-16l	Heat-treated	Silcrete	1448.6	2.36	614.80

d variable

Table B160. *d* variable measurements for quartzite experimental blocks.

Block	Raw Material	*d* variable - Time to Edge Dullness (min)-Average per block	*d* variable - Time to dullness (min)-Average of all samples	*d* variable - Time to dullness (min)-Average by source	*d* variable - Time to dullness (min)-Average 0-40 degree angles
C9-1-1B8	Quartzite	1.00	0.74	0.91	1.56
C9-1-1B9	Quartzite	0.82	0.74	0.91	1.56
D11-1-100A	Quartzite	0.50	0.74	0.66	1.56
D11-1-90D1	Quartzite	1.39	0.74	0.66	1.56
D11-1-95A	Quartzite	0.26	0.74	0.66	1.56
D11-1-95B	Quartzite	0.71	0.74	0.66	1.56
D11-1-97A1	Quartzite	0.99	0.74	0.66	1.56
D11-1-98B1	Quartzite	0.29	0.74	0.66	1.56
D11-1-98C1	Quartzite	0.17	0.74	0.66	1.56
D11-1-98D	Quartzite	0.96	0.74	0.66	1.56
D11-1-85C1	Quartzite	0.50	1.26	1.26	2.03
D11-1-91A1	Quartzite	1.02	1.26	1.26	2.03
D11-1-91A2	Quartzite	0.52	1.26	1.26	2.03
D11-1-91B3	Quartzite	1.93	1.26	1.26	2.03
D11-1-91B5	Quartzite	0.50	1.26	1.26	2.03
D11-1-91C3	Quartzite	1.14	1.26	1.26	2.03
D11-1-94B2	Quartzite	2.18	1.26	1.26	2.03
D11-1-94B3	Quartzite	1.51	1.26	1.26	2.03
D11-1-94D2	Quartzite	1.92	1.26	1.26	2.03
D11-1-97C	Quartzite	1.31	1.26	1.26	2.03

Table B161. *d* variable measurements for untreated silcrete experimental blocks.

Block	Sample Type	Raw Material	d variable - Time to Edge Dullness (min)- Average per block	d variable - Time to dullness (min)- Average of all samples	d variable - Time to dullness (min)- Average by source	d variable - Time to dullness (min)- Average 0-40 degree angles
D9-1-10a	Untreated	Silcrete	0.67	1.08	1.20	1.88
D9-1-12a	Untreated	Silcrete	1.49	1.08	1.20	1.88
D9-1-12c	Untreated	Silcrete	1.56	1.08	1.20	1.88
E3-1-1A	Untreated	Silcrete	1.52	1.08	1.07	1.88
E3-1-5n	Untreated	Silcrete	1.60	1.08	1.07	1.88
E3-1-5o	Untreated	Silcrete	0.87	1.08	1.07	1.88
E3-1-6b	Untreated	Silcrete	0.47	1.08	1.07	1.88
I14-2-16a	Untreated	Silcrete	0.78	1.08	0.78	1.88

Table B162. *d* variable measurements for heat-treated silcrete experimental blocks.

Block	Sample Type	Raw Material	d variable - Time to Edge Dullness (min)- Average per block	d variable - Time to dullness (min)- Average of all samples	d variable - Time to dullness (min)- Average by source	d variable - Time to dullness (min)- Average 0-40 degree angles
D9-1-10b	Heat-treated	Silcrete	0.61	1.90	1.30	2.82
D9-1-12b	Heat-treated	Silcrete	1.95	1.90	1.30	2.82
D9-1-12d	Heat-treated	Silcrete	1.33	1.90	1.30	2.82
E3-1-1b	Heat-treated	Silcrete	1.76	1.90	1.96	2.82
E3-1-5p	Heat-treated	Silcrete	2.79	1.90	1.96	2.82
E3-1-6a	Heat-treated	Silcrete	1.88	1.90	1.96	2.82
E3-1-6c	Heat-treated	Silcrete	1.57	1.90	1.96	2.82
I14-2-16l	Heat-treated	Silcrete	2.79	1.90	2.79	2.82

e * *d* currency

Table B163. *e* * *d* currency calculations for quartzite experimental blocks.

Block	Raw Material	Total Cutting Edge Measured (cm)	Total Flaked Core Mass(kg)	e (CE(cm)/Total Flaked Core Mass (kg))	d variable - Time to dullness (min)- Average 0-40 degree angles	Cutting Edge * Durability (e * d)
C9-1-1B8	Quartzite	774.80	1.92	403.49	1.56	630.46
C9-1-1B9	Quartzite	769.90	2.06	373.66	1.56	583.85
D11-1-100A	Quartzite	758.80	2.15	353.09	1.56	551.71
D11-1-90D1	Quartzite	864.10	2.45	352.66	1.56	551.03
D11-1-95A	Quartzite	725.60	2.03	357.19	1.56	558.10
D11-1-95B	Quartzite	790.40	2.16	365.90	1.56	571.71

D11-1-97A1	Quartzite	708.20	1.93	367.90	1.56	574.84
D11-1-98B1	Quartzite	773.40	1.91	404.36	1.56	631.81
D11-1-98C1	Quartzite	781.20	2.09	373.66	1.56	583.84
D11-1-98D	Quartzite	672.60	1.84	365.04	1.56	570.38
D11-1-85C1	Quartzite	955.20	2.00	478.56	2.03	969.08
D11-1-91A1	Quartzite	807.30	1.96	411.41	2.03	833.11
D11-1-91A2	Quartzite	911.70	2.17	419.31	2.03	849.10
D11-1-91B3	Quartzite	898.30	1.88	476.61	2.03	965.14
D11-1-91B5	Quartzite	1037.00	2.22	467.06	2.03	945.79
D11-1-91C3	Quartzite	809.50	1.96	412.55	2.03	835.41
D11-1-94B2	Quartzite	905.90	1.83	495.62	2.03	1003.63
D11-1-94B3	Quartzite	974.70	1.78	546.36	2.03	1106.37
D11-1-94D2	Quartzite	797.30	1.97	405.53	2.03	821.19
D11-1-97C	Quartzite	887.20	1.83	483.99	2.03	980.07

Table B164. *e * d* currency calculations for untreated silcrete experimental blocks.

Block	Sample Type	Raw Material	Total Cutting Edge Measured (cm)	Total Flaked Core Mass (kg)	e (CE(cm)/Total Flaked Core Mass (kg))	d variable - Time to dullness (min)- Average 0-40 degree angles	Cutting Edge * Durability (e * d)
D9-1-10a	Untreated	Silcrete	633.10	1.98	319.72	1.88	601.38
D9-1-12a	Untreated	Silcrete	860.80	2.25	382.64	1.88	719.74
D9-1-12c	Untreated	Silcrete	757.30	1.81	419.07	1.88	788.25
E3-1-1A	Untreated	Silcrete	695.00	2.07	335.82	1.88	631.65
E3-1-5n	Untreated	Silcrete	1048.80	2.46	426.38	1.88	802.01
E3-1-5o	Untreated	Silcrete	961.50	2.50	383.86	1.88	722.03
E3-1-6b	Untreated	Silcrete	644.00	1.69	380.84	1.88	716.34
I14-2-16a	Untreated	Silcrete	796.80	2.90	275.22	1.88	517.68

Table B165. *e * d* currency calculations for heat-treated silcrete experimental blocks.

Block	Sample Type	Raw Material	Total Cutting Edge Measured (cm)	Total Flaked Core Mass (kg)	e (CE(cm)/Total Flaked Core Mass (kg))	d variable - Time to dullness (min)- Average 0-40 degree angles	Cutting Edge * Durability (e * d)
D9-1-10b	Heat-Treated	Silcrete	1047.90	2.35	445.94	2.82	1259.25
D9-1-12b	Heat-Treated	Silcrete	1239.20	2.20	563.25	2.82	1590.52
D9-1-12d	Heat-Treated	Silcrete	1156.80	2.29	505.97	2.82	1428.77
E3-1-1b	Heat-Treated	Silcrete	1160.20	1.93	600.05	2.82	1694.44
E3-1-5p	Heat-Treated	Silcrete	1222.80	2.59	472.54	2.82	1334.36
E3-1-6a	Heat-Treated	Silcrete	1239.10	2.20	564.24	2.82	1593.30

E3-1-6c	Heat-Treated	Silcrete	1302.00	2.44	534.48	2.82	1509.28
I14-2-16l	Heat-Treated	Silcrete	1448.60	2.36	614.80	2.82	1736.07

t_s variable

MIS4 conditions – quartzite

Table B166. t_s variable measurements for quartzite experimental blocks during MIS4 conditions.

Block	Raw Material	Travel and search time (min)	Total Flaked Core Mass (kg)	ts variable -Travel and search time (min)/Total Flaked Core Mass (kg)
D11-1-85C1	Quartzite	180.0	2.00	90.18
D11-1-91A1	Quartzite	180.0	1.96	91.73
D11-1-91A2	Quartzite	180.0	2.17	82.79
D11-1-91B3	Quartzite	180.0	1.88	95.50
D11-1-91B5	Quartzite	180.0	2.22	81.07
D11-1-91C3	Quartzite	180.0	1.96	91.73
D11-1-94B2	Quartzite	180.0	1.83	98.48
D11-1-94B3	Quartzite	180.0	1.78	100.90
D11-1-94D2	Quartzite	180.0	1.97	91.55
D11-1-97C	Quartzite	180.0	1.83	98.19
C9-1-1B8	Quartzite	180.0	1.92	93.74
C9-1-1B9	Quartzite	180.0	2.06	87.36
D11-1-100A	Quartzite	180.0	2.15	83.76
D11-1-90D1	Quartzite	180.0	2.45	73.46
D11-1-95A	Quartzite	180.0	2.03	88.61
D11-1-95B	Quartzite	180.0	2.16	83.33
D11-1-97A1	Quartzite	180.0	1.93	93.51
D11-1-98B1	Quartzite	180.0	1.91	94.11
D11-1-98C1	Quartzite	180.0	2.09	86.10
D11-1-98D	Quartzite	180.0	1.84	97.69

MIS4 and MIS6 conditions without a Paleo-Agulhas plain silcrete source – silcrete

Table B167. t_s variable measurements for untreated silcrete experimental blocks during MIS4 and MIS6 conditions without a Paleo-Agulhas plain silcrete source.

Block	Sample Type	Raw Material	Travel and search time (min)	Weight Total Flaked (kg)	ts variable - Travel and search time (min)/Weight Total Flaked (kg)
D9-1-10a	Untreated	Silcrete	291.4	1.98	147.18
D9-1-12a	Untreated	Silcrete	291.4	2.25	129.55
D9-1-12c	Untreated	Silcrete	291.4	1.81	161.27

E3-1-1A	Untreated	Silcrete	291.4	2.07	140.82
E3-1-5n	Untreated	Silcrete	291.4	2.46	118.48
E3-1-5o	Untreated	Silcrete	291.4	2.50	116.35
E3-1-6b	Untreated	Silcrete	291.4	1.69	172.34
I14-2-16a	Untreated	Silcrete	291.4	2.90	100.66

Table B168. t_s variable measurements for heat-treated silcrete experimental blocks during MIS4 and MIS6 conditions without a Paleo-Agulhas plain silcrete source.

Block	Sample Type	Raw Material	Travel and search time (min)	Total Flaked Core Mass (kg))	ts variable - Travel and search time (min)/ Total Flaked Core Mass (kg)
D9-1-10b	Heat-treated	Silcrete	291.4	2.35	124.02
D9-1-12b	Heat-treated	Silcrete	291.4	2.20	132.47
D9-1-12d	Heat-treated	Silcrete	291.4	2.29	127.47
E3-1-1b	Heat-treated	Silcrete	291.4	1.93	150.73
E3-1-5p	Heat-treated	Silcrete	291.4	2.59	112.62
E3-1-6a	Heat-treated	Silcrete	291.4	2.20	132.71
E3-1-6c	Heat-treated	Silcrete	291.4	2.44	119.64
I14-2-16l	Heat-treated	Silcrete	291.4	2.36	123.69

MIS4 and MIS 6conditions with a Paleo-Agulhas plain silcrete source – silcrete

Table B169. t_s variable measurements for untreated silcrete experimental blocks during MIS4 and MIS6 conditions with a Paleo-Agulhas plain silcrete source.

Block	Sample Type	Raw Material	Travel and search time (min)	Total Flaked Core Mass (kg)	ts variable - Travel and search time (min)/Total Flaked Core Mass (kg)
D9-1-10a	Untreated	Silcrete	28.0	1.98	13.85
D9-1-12a	Untreated	Silcrete	28.0	2.25	12.19
D9-1-12c	Untreated	Silcrete	28.0	1.81	15.18
E3-1-1A	Untreated	Silcrete	28.0	2.07	13.26
E3-1-5n	Untreated	Silcrete	28.0	2.46	11.15
E3-1-5o	Untreated	Silcrete	28.0	2.50	10.95
E3-1-6b	Untreated	Silcrete	28.0	1.69	16.22
I14-2-16a	Untreated	Silcrete	28.0	2.90	9.48

Table B170. t_s variable measurements for heat-treated silcrete experimental blocks during MIS4 and MIS6 conditions with a Paleo-Agulhas plain silcrete source.

Block	Sample Type	Raw Material	Travel and search time (min)	Total Flaked Core Mass (kg)	ts variable - Travel and search time (min)/Total Flaked Core Mass (kg)
D9-1-10b	Heated	Silcrete	28.0	2.35	11.67
D9-1-12b	Heated	Silcrete	28.0	2.20	12.47
D9-1-12d	Heated	Silcrete	28.0	2.29	12.00
E3-1-1b	Heated	Silcrete	28.0	1.93	14.19
E3-1-5p	Heated	Silcrete	28.0	2.59	10.60
E3-1-6a	Heated	Silcrete	28.0	2.20	12.49
E3-1-6c	Heated	Silcrete	28.0	2.44	11.26
I14-2-16l	Heated	Silcrete	28.0	2.36	11.64

MIS5 conditions

Table B171. t_s variable measurements for quartzite experimental blocks during MIS5 conditions.

Block	Raw Material	Travel and search time (min)	Total Flaked Core Mass (kg)	ts variable -Travel and search time (min)/Total Flaked Core Mass (kg)
D11-1-85C1	Quartzite	12.7	2.00	6.36
D11-1-91A1	Quartzite	12.7	1.96	6.47
D11-1-91A2	Quartzite	12.7	2.17	5.84
D11-1-91B3	Quartzite	12.7	1.88	6.74
D11-1-91B5	Quartzite	12.7	2.22	5.72
D11-1-91C3	Quartzite	12.7	1.96	6.47
D11-1-94B2	Quartzite	12.7	1.83	6.95
D11-1-94B3	Quartzite	12.7	1.78	7.12
D11-1-94D2	Quartzite	12.7	1.97	6.46
D11-1-97C	Quartzite	12.7	1.83	6.93
C9-1-1B8	Quartzite	12.7	1.92	6.61
C9-1-1B9	Quartzite	12.7	2.06	6.16
D11-1-100A	Quartzite	12.7	2.15	5.91
D11-1-90D1	Quartzite	12.7	2.45	5.18
D11-1-95A	Quartzite	12.7	2.03	6.25
D11-1-95B	Quartzite	12.7	2.16	5.88
D11-1-97A1	Quartzite	12.7	1.93	6.60
D11-1-98B1	Quartzite	12.7	1.91	6.64
D11-1-98C1	Quartzite	12.7	2.09	6.07
D11-1-98D	Quartzite	12.7	1.84	6.89

Table B172. t_s variable measurements for untreated silcrete experimental blocks during MIS5 conditions.

Block	Sample Type	Raw Material	Travel and search time (min)	Total Flaked Core Mass (kg)	ts variable - Travel and search time (min)/ Total Flaked Core Mass (kg)
D9-1-10a	Untreated	Silcrete	291.4	1.98	147.18
D9-1-12a	Untreated	Silcrete	291.4	2.25	129.55
D9-1-12c	Untreated	Silcrete	291.4	1.81	161.27
E3-1-1A	Untreated	Silcrete	291.4	2.07	140.82
E3-1-5n	Untreated	Silcrete	291.4	2.46	118.48
E3-1-5o	Untreated	Silcrete	291.4	2.50	116.35
E3-1-6b	Untreated	Silcrete	291.4	1.69	172.34
I14-2-16a	Untreated	Silcrete	291.4	2.90	100.66

Table B173. t_s variable measurements for heat-treated silcrete experimental blocks during MIS5 conditions.

Block	Sample Type	Raw Material	Travel and search time (min)	Total Flaked Core Mass (kg))	ts variable - Travel and search time (min)/ Total Flaked Core Mass (kg)
D9-1-10b	Heat-treated	Silcrete	291.4	2.35	124.02
D9-1-12b	Heat-treated	Silcrete	291.4	2.20	132.47
D9-1-12d	Heat-treated	Silcrete	291.4	2.29	127.47
E3-1-1b	Heat-treated	Silcrete	291.4	1.93	150.73
E3-1-5p	Heat-treated	Silcrete	291.4	2.59	112.62
E3-1-6a	Heat-treated	Silcrete	291.4	2.20	132.71
E3-1-6c	Heat-treated	Silcrete	291.4	2.44	119.64
I14-2-16l	Heat-treated	Silcrete	291.4	2.36	123.69

MIS6 conditions – quartzite

Table B174. t_s variable measurements for heat-treated silcrete experimental blocks during MIS6 conditions.

Block	Raw Material	Travel and search time (min)	Total Flaked Core Mass (kg)	ts variable -Travel and search time (min)/Total Flaked Core Mass (kg)
C9-1-1B8	Quartzite	48.8	1.92	25.42
C9-1-1B9	Quartzite	48.8	2.06	23.69
D11-1-100A	Quartzite	48.8	2.15	22.72
D11-1-90D1	Quartzite	48.8	2.45	19.92
D11-1-95A	Quartzite	48.8	2.03	24.03
D11-1-95B	Quartzite	48.8	2.16	22.60
D11-1-97A1	Quartzite	48.8	1.93	25.36

D11-1-98B1	Quartzite	48.8	1.91	25.52
D11-1-98C1	Quartzite	48.8	2.09	23.35
D11-1-98D	Quartzite	48.8	1.84	26.49
D11-1-85C1	Quartzite	48.8	2.00	24.46
D11-1-91A1	Quartzite	48.8	1.96	24.88
D11-1-91A2	Quartzite	48.8	2.17	22.45
D11-1-91B3	Quartzite	48.8	1.88	25.90
D11-1-91B5	Quartzite	48.8	2.22	21.99
D11-1-91C3	Quartzite	48.8	1.96	24.88
D11-1-94B2	Quartzite	48.8	1.83	26.71
D11-1-94B3	Quartzite	48.8	1.78	27.36
D11-1-94D2	Quartzite	48.8	1.97	24.83
D11-1-97C	Quartzite	48.8	1.83	26.63

t_p variable

Table B175. t_p variable measurements for quartzite experimental blocks.

Block	Raw Material	Procurement Time (min)	Total Flaked Core Mass (kg)	tp variable - Procurement Time (min)/Total Flaked Core Mass (kg)
D11-1-85C1	Quartzite	5.37	2.00	2.69
D11-1-91A1	Quartzite	5.37	1.96	2.74
D11-1-91A2	Quartzite	5.37	2.17	2.47
D11-1-91B3	Quartzite	5.37	1.88	2.85
D11-1-91B5	Quartzite	5.37	2.22	2.42
D11-1-91C3	Quartzite	5.37	1.96	2.74
D11-1-94B2	Quartzite	5.37	1.83	2.94
D11-1-94B3	Quartzite	5.37	1.78	3.01
D11-1-94D2	Quartzite	5.37	1.97	2.73
D11-1-97C	Quartzite	5.37	1.83	2.93
C9-1-1B8	Quartzite	5.00	1.92	2.60
C9-1-1B9	Quartzite	5.00	2.06	2.43
D11-1-100A	Quartzite	5.37	2.15	2.50
D11-1-90D1	Quartzite	5.37	2.45	2.19
D11-1-95A	Quartzite	5.37	2.03	2.65
D11-1-95B	Quartzite	5.37	2.16	2.49
D11-1-97A1	Quartzite	5.37	1.93	2.79
D11-1-98B1	Quartzite	5.37	1.91	2.81
D11-1-98C1	Quartzite	5.37	2.09	2.57
D11-1-98D	Quartzite	5.37	1.84	2.92

Table B176. t_p variable measurements for untreated silcrete experimental blocks.

Block	Sample Type	Raw Material	Procurement Time (min)	Total Flaked Core Mass (kg)	*tp* variable - Procurement Time (min)/Total Flaked Core Mass (kg)
D9-1-10a	Untreated	Silcrete	8.125	1.98	4.10
D9-1-12a	Untreated	Silcrete	8.125	2.25	3.61
D9-1-12c	Untreated	Silcrete	8.125	1.81	4.50
E3-1-1A	Untreated	Silcrete	8.125	2.07	3.93
E3-1-5n	Untreated	Silcrete	8.125	2.46	3.30
E3-1-5o	Untreated	Silcrete	8.125	2.50	3.24
E3-1-6b	Untreated	Silcrete	8.125	1.69	4.80
I14-2-16a	Untreated	Silcrete	8.125	2.90	2.81

Table B177. t_p variable measurements for heat-treated silcrete experimental blocks.

Block	Sample Type	Raw Material	Procurement Time (min)	Total Flaked Core Mass (kg)	*tp* variable - Procurement Time (min)/Total Flaked Core Mass (kg)
D9-1-10b	Heat-treated	Silcrete	8.125	2.35	3.46
D9-1-12b	Heat-treated	Silcrete	8.125	2.20	3.69
D9-1-12d	Heat-treated	Silcrete	8.125	2.29	3.55
E3-1-1b	Heat-treated	Silcrete	8.125	1.93	4.20
E3-1-5p	Heat-treated	Silcrete	8.125	2.59	3.14
E3-1-6a	Heat-treated	Silcrete	8.125	2.20	3.70
E3-1-6c	Heat-treated	Silcrete	8.125	2.44	3.34
I14-2-16l	Heat-treated	Silcrete	8.125	2.36	3.45

$\underline{m_1}$ variable

MIS4

Table B178. m_1 variable measurements for heat-treated silcrete experimental blocks assuming the insulated heating scenario during MIS4 conditions.

Block	Sample Type	Raw Material	Heating Scenario	Wood Fuel Search and Travel Time (min)	Total Flaked Core Mass (kg)	*m1*-Wood Fuel Search and Travel Time (min)/Total Flaked Core Mass (kg)
D9-1-10b	Heat-treated	Silcrete	Insulated	90.00	2.35	38.30
D9-1-12b	Heat-treated	Silcrete	Insulated	90.00	2.20	40.91
D9-1-12d	Heat-treated	Silcrete	Insulated	90.00	2.29	39.37
E3-1-1b	Heat-treated	Silcrete	Insulated	90.00	1.93	46.55
E3-1-5p	Heat-treated	Silcrete	Insulated	90.00	2.59	34.78
E3-1-6a	Heat-treated	Silcrete	Insulated	90.00	2.20	40.98
E3-1-6c	Heat-treated	Silcrete	Insulated	90.00	2.44	36.95

I14-2-16l	Heat-treated	Silcrete	Insulated	90.00	2.36	38.20

Table B179. m_1 variable measurements for heat-treated silcrete experimental blocks assuming the exposed heating scenario during MIS4 conditions.

Block	Sample Type	Raw Material	Heating Scenario	Wood Fuel Search and Travel Time (min)	Total Flaked Core Mass (kg)	*m1*-Wood Fuel Search and Travel Time (min)/Total Flaked Core Mass (kg)
D9-1-10b	Heat-treated	Silcrete	Exposed	90.00	2.35	38.30
D9-1-12b	Heat-treated	Silcrete	Exposed	90.00	2.20	40.91
D9-1-12d	Heat-treated	Silcrete	Exposed	90.00	2.29	39.37
E3-1-1b	Heat-treated	Silcrete	Exposed	90.00	1.93	46.55
E3-1-5p	Heat-treated	Silcrete	Exposed	90.00	2.59	34.78
E3-1-6a	Heat-treated	Silcrete	Exposed	90.00	2.20	40.98
E3-1-6c	Heat-treated	Silcrete	Exposed	90.00	2.44	36.95
I14-2-16l	Heat-treated	Silcrete	Exposed	90.00	2.36	38.20

MIS5

Table B180. m_1 variable measurements for heat-treated silcrete experimental blocks assuming the insulated heating scenario during MIS5 conditions.

Block	Sample Type	Raw Material	Heating Scenario	Wood Fuel Search and Travel Time (min)	Total Flaked Core Mass (kg)	*m1*-Wood Fuel Search and Travel Time (min)/Total Flaked Core Mass (kg)
D9-1-10b	Heat-treated	Silcrete	Insulated	180	2.3	76.60
D9-1-12b	Heat-treated	Silcrete	Insulated	180	2.2	81.82
D9-1-12d	Heat-treated	Silcrete	Insulated	180	2.3	78.73
E3-1-1b	Heat-treated	Silcrete	Insulated	180	1.9	93.10
E3-1-5p	Heat-treated	Silcrete	Insulated	180	2.6	69.56
E3-1-6a	Heat-treated	Silcrete	Insulated	180	2.2	81.96
E3-1-6c	Heat-treated	Silcrete	Insulated	180	2.4	73.89
I14-2-16l	Heat-treated	Silcrete	Insulated	180	2.4	76.39

Table B181. m_1 variable measurements for heat-treated silcrete experimental blocks assuming the exposed heating scenario during MIS5 conditions.

Block	Sample Type	Raw Material	Heating Scenario	Wood Fuel Search and Travel Time (min)	Total Flaked Core Mass (kg)	*m1*-Wood Fuel Search and Travel Time (min)/Total Flaked Core Mass (kg)
D9-1-10b	Heat-treated	Silcrete	Exposed	90	2.3	38.30
D9-1-12b	Heat-treated	Silcrete	Exposed	90	2.2	40.91
D9-1-12d	Heat-treated	Silcrete	Exposed	90	2.3	39.37
E3-1-1b	Heat-treated	Silcrete	Exposed	90	1.9	46.55
E3-1-5p	Heat-treated	Silcrete	Exposed	90	2.6	34.78
E3-1-6a	Heat-treated	Silcrete	Exposed	90	2.2	40.98

E3-1-6c	Heat-treated	Silcrete	Exposed	90	2.4	36.95
I14-2-16l	Heat-treated	Silcrete	Exposed	90	2.4	38.20

MIS6

Table B182. m_1 variable measurements for heat-treated silcrete experimental blocks assuming the insulated heating scenario during MIS6 conditions.

Block	Sample Type	Raw Material	Heating Scenario	Wood Fuel Search and Travel Time (min)	Total Flaked Core Mass (kg)	*m1*-Wood Fuel Search and Travel Time (min)/Total Flaked Core Mass (kg)
D9-1-10b	Heat-treated	Silcrete	Insulated	180	2.35	76.60
D9-1-12b	Heat-treated	Silcrete	Insulated	180	2.20	81.82
D9-1-12d	Heat-treated	Silcrete	Insulated	180	2.29	78.73
E3-1-1b	Heat-treated	Silcrete	Insulated	180	1.93	93.10
E3-1-5p	Heat-treated	Silcrete	Insulated	180	2.59	69.56
E3-1-6a	Heat-treated	Silcrete	Insulated	180	2.20	81.96
E3-1-6c	Heat-treated	Silcrete	Insulated	180	2.44	73.89
I14-2-16l	Heat-treated	Silcrete	Insulated	180	2.36	76.39

Table B183. m_1 variable measurements for heat-treated silcrete experimental blocks assuming the exposed heating scenario during MIS6 conditions.

Block	Sample Type	Raw Material	Heating Scenario	Wood Fuel Search and Travel Time (min)	Total Flaked Core Mass (kg)	*m1*-Wood Fuel Search and Travel Time (min)/Total Flaked Core Mass (kg)
D9-1-10b	Heat-treated	Silcrete	Exposed	90	2.35	38.30
D9-1-12b	Heat-treated	Silcrete	Exposed	90	2.20	40.91
D9-1-12d	Heat-treated	Silcrete	Exposed	90	2.29	39.37
E3-1-1b	Heat-treated	Silcrete	Exposed	90	1.93	46.55
E3-1-5p	Heat-treated	Silcrete	Exposed	90	2.59	34.78
E3-1-6a	Heat-treated	Silcrete	Exposed	90	2.20	40.98
E3-1-6c	Heat-treated	Silcrete	Exposed	90	2.44	36.95
I14-2-16l	Heat-treated	Silcrete	Exposed	90	2.36	38.20

<u>m_2 variable</u>

Table B184. m_2 variable measurements for heat-treated silcrete experimental blocks assuming the insulated heating scenario.

Block	Sample Type	Raw Material	Heating Scenario	Heat-treatment time (min)	Total Flaked Core Mass (kg)	*m2*-Heat-treatment Time (min)/Total Flaked Core Mass (kg)
D9-1-10b	Heat-treated	Silcrete	Insulated	15	2.35	6.38
D9-1-12b	Heat-treated	Silcrete	Insulated	15	2.20	6.82
D9-1-12d	Heat-treated	Silcrete	Insulated	15	2.29	6.56
E3-1-1b	Heat-treated	Silcrete	Insulated	15	1.93	7.76
E3-1-5p	Heat-treated	Silcrete	Insulated	15	2.59	5.80

E3-1-6a	Heat-treated	Silcrete	Insulated	15	2.20	6.83
E3-1-6c	Heat-treated	Silcrete	Insulated	15	2.44	6.16
I14-2-16l	Heat-treated	Silcrete	Insulated	15	2.36	6.37

Table B185. m_2 variable measurements for heat-treated silcrete experimental blocks assuming the exposed heating scenario.

Block	Sample Type	Raw Material	Heating Scenario	Heat-treatment time (min)	Total Flaked Core Mass (kg)	*m2*-Heat-treatment Time (min)/Total Flaked Core Mass (kg)
D9-1-10b	Heat-treated	Silcrete	Exposed	50	2.35	21.28
D9-1-12b	Heat-treated	Silcrete	Exposed	50	2.20	22.73
D9-1-12d	Heat-treated	Silcrete	Exposed	50	2.29	21.87
E3-1-1b	Heat-treated	Silcrete	Exposed	50	1.93	25.86
E3-1-5p	Heat-treated	Silcrete	Exposed	50	2.59	19.32
E3-1-6a	Heat-treated	Silcrete	Exposed	50	2.20	22.77
E3-1-6c	Heat-treated	Silcrete	Exposed	50	2.44	20.53
I14-2-16l	Heat-treated	Silcrete	Exposed	50	2.36	21.22

m_3 variable

Table B186. m_3 variable measurements for quartzite experimental blocks.

Block	Raw Material	Flaking Time (min)	Total Flaked Core Mass (kg)	m3 variable - Time (14min)/Total Flaked Core Mass (kg)
C9-1-1B8	Quartzite	14	1.92	7.29
C9-1-1B9	Quartzite	14	2.06	6.79
D11-1-100A	Quartzite	14	2.15	6.51
D11-1-90D1	Quartzite	14	2.45	5.71
D11-1-95A	Quartzite	14	2.03	6.89
D11-1-95B	Quartzite	14	2.16	6.48
D11-1-97A1	Quartzite	14	1.93	7.27
D11-1-98B1	Quartzite	14	1.91	7.32
D11-1-98C1	Quartzite	14	2.09	6.70
D11-1-98D	Quartzite	14	1.84	7.60
D11-1-85C1	Quartzite	14	2.00	7.01
D11-1-91A1	Quartzite	14	1.96	7.13
D11-1-91A2	Quartzite	14	2.17	6.44
D11-1-91B3	Quartzite	14	1.88	7.43
D11-1-91B5	Quartzite	14	2.22	6.31
D11-1-91C3	Quartzite	14	1.96	7.13
D11-1-94B2	Quartzite	14	1.83	7.66
D11-1-94B3	Quartzite	14	1.78	7.85

D11-1-94D2	Quartzite	14	1.97	7.12
D11-1-97C	Quartzite	14	1.83	7.64

Table B187. m_3 variable measurements for untreated silcrete experimental blocks.

Block	Sample Type	Raw Material	Flaking Time (min)	Total Flaked Core Mass (kg)	*m3* variable - Time (14min)/Total Flaked Core Mass (kg)
D9-1-10a	Untreated	Silcrete	14	1.98	7.07
D9-1-12a	Untreated	Silcrete	14	2.25	6.22
D9-1-12c	Untreated	Silcrete	14	1.81	7.75
E3-1-1A	Untreated	Silcrete	14	2.07	6.76
E3-1-5n	Untreated	Silcrete	14	2.46	5.69
E3-1-5o	Untreated	Silcrete	14	2.50	5.59
E3-1-6b	Untreated	Silcrete	14	1.69	8.28
I14-2-16a	Untreated	Silcrete	14	2.90	4.84

Table B188. m_3 variable measurements for heat-treated silcrete experimental blocks.

Block	Sample Type	Raw Material	Flaking Time (min	Total Flaked Core Mass (kg)	*m3* variable - Time (14min)/Total Flaked Core Mass (kg)
D9-1-10b	Heat-treated	Silcrete	14	2.35	5.96
D9-1-12b	Heat-treated	Silcrete	14	2.20	6.36
D9-1-12d	Heat-treated	Silcrete	14	2.29	6.12
E3-1-1b	Heat-treated	Silcrete	14	1.93	7.24
E3-1-5p	Heat-treated	Silcrete	14	2.59	5.41
E3-1-6a	Heat-treated	Silcrete	14	2.20	6.38
E3-1-6c	Heat-treated	Silcrete	14	2.44	5.75
I14-2-16l	Heat-treated	Silcrete	14	2.36	5.94

CHAPTER 10: ACTIVE-CHOICE MODEL HYPOTHESES EVALUATION

ACM-P net-return rates

MIS4, MIS5, and MIS6 conditions – Quartzite

Table B189. ACM-P net-return rates (Pq) for quartzite experimental blocks during MIS4, MIS5, MIS 6 conditions.

Model Conditions	Block	Raw Material	Cutting Edge * Durability (e * d)	tp (procurement time (min))	m3 (flake manufacture time (min))	Pq
MIS4, MIS5, & MIS6	C9-1-1B8	Quartzite	630.455	2.604	7.291	63.717
MIS4, MIS5, & MIS6	C9-1-1B9	Quartzite	583.846	2.427	6.795	63.314
MIS4, MIS5, & MIS6	D11-1-100A	Quartzite	551.710	2.501	6.515	61.196
MIS4, MIS5, & MIS6	D11-1-90D1	Quartzite	551.026	2.193	5.714	69.688
MIS4, MIS5, & MIS6	D11-1-95A	Quartzite	558.104	2.646	6.892	58.518
MIS4, MIS5, & MIS6	D11-1-95B	Quartzite	571.712	2.488	6.481	63.744
MIS4, MIS5, & MIS6	D11-1-97A1	Quartzite	574.838	2.792	7.273	57.115
MIS4, MIS5, & MIS6	D11-1-98B1	Quartzite	631.810	2.810	7.320	62.373
MIS4, MIS5, & MIS6	D11-1-98C1	Quartzite	583.844	2.571	6.696	63.002
MIS4, MIS5, & MIS6	D11-1-98D	Quartzite	570.377	2.917	7.598	54.244
MIS4, MIS5, & MIS6	D11-1-85C1	Quartzite	969.078	2.693	7.014	99.837
MIS4, MIS5, & MIS6	D11-1-91A1	Quartzite	833.108	2.739	7.135	84.379
MIS4, MIS5, & MIS6	D11-1-91A2	Quartzite	849.101	2.472	6.439	95.291
MIS4, MIS5, & MIS6	D11-1-91B3	Quartzite	965.135	2.851	7.428	93.890
MIS4, MIS5, & MIS6	D11-1-91B5	Quartzite	945.793	2.421	6.306	108.387
MIS4, MIS5, & MIS6	D11-1-91C3	Quartzite	835.408	2.739	7.135	84.609
MIS4, MIS5, & MIS6	D11-1-94B2	Quartzite	1003.631	2.940	7.659	94.685
MIS4, MIS5, & MIS6	D11-1-94B3	Quartzite	1106.372	3.012	7.848	101.876
MIS4, MIS5, & MIS6	D11-1-94D2	Quartzite	821.190	2.733	7.121	83.334
MIS4, MIS5, & MIS6	D11-1-97C	Quartzite	980.072	2.932	7.637	92.730

MIS4 conditions – Silcrete

Table B190. ACM-P net-return rates (Ps) for heat-treated silcrete assuming both the insulated and exposed heating scenarios and untreated silcrete experimental blocks during MIS4 conditions.

Model Conditions	Heating Scenario	Block	Raw Material	Cutting Edge * Durability (e * d)	tp (procurement time (min))	m1 (Wood fuel Travel and Search time (min))	m2 (Heat-treatment time (min))	m3 (Flake manufacture time (min))	Ps
MIS4	Insulated	D9-1-10b	Silcrete	1259.248	3.458	38.300	6.383	5.958	23.277
MIS4	Insulated	D9-1-12b	Silcrete	1590.524	3.693	40.908	6.818	6.363	27.526
MIS4	Insulated	D9-1-12d	Silcrete	1428.770	3.554	39.365	6.561	6.123	25.696
MIS4	Insulated	E3-1-1b	Silcrete	1694.441	4.202	46.548	7.758	7.241	25.771
MIS4	Insulated	E3-1-5p	Silcrete	1334.362	3.140	34.780	5.797	5.410	27.162
MIS4	Insulated	E3-1-6a	Silcrete	1593.300	3.700	40.982	6.830	6.375	27.524
MIS4	Insulated	E3-1-6c	Silcrete	1509.278	3.335	36.946	6.158	5.747	28.921
MIS4	Insulated	I14-2-16l	Silcrete	1736.073	3.448	38.197	6.366	5.942	32.178
MIS4	Exposed	D9-1-10b	Silcrete	1259.248	3.458	38.300	21.278	5.958	18.252
MIS4	Exposed	D9-1-12b	Silcrete	1590.524	3.693	40.908	22.727	6.363	21.584
MIS4	Exposed	D9-1-12d	Silcrete	1428.770	3.554	39.365	21.869	6.123	20.149
MIS4	Exposed	E3-1-1b	Silcrete	1694.441	4.202	46.548	25.860	7.241	20.208
MIS4	Exposed	E3-1-5p	Silcrete	1334.362	3.140	34.780	19.322	5.410	21.298
MIS4	Exposed	E3-1-6a	Silcrete	1593.300	3.700	40.982	22.768	6.375	21.582
MIS4	Exposed	E3-1-6c	Silcrete	1509.278	3.335	36.946	20.525	5.747	22.678
MIS4	Exposed	I14-2-16l	Silcrete	1736.073	3.448	38.197	21.220	5.942	25.231
MIS4	Untreated	D9-1-10a	Silcrete	601.381	4.103	0	0	7.070	53.823
MIS4	Untreated	D9-1-12a	Silcrete	719.735	3.612	0	0	6.223	73.181
MIS4	Untreated	D9-1-12c	Silcrete	788.254	4.496	0	0	7.747	64.382
MIS4	Untreated	E3-1-1A	Silcrete	631.653	3.926	0	0	6.765	59.085
MIS4	Untreated	E3-1-5n	Silcrete	802.006	3.303	0	0	5.692	89.164
MIS4	Untreated	E3-1-5o	Silcrete	722.028	3.244	0	0	5.589	81.742
MIS4	Untreated	E3-1-6b	Silcrete	716.341	4.805	0	0	8.279	54.750
MIS4	Untreated	I14-2-16a	Silcrete	517.679	2.806	0	0	4.836	67.740

MIS5 conditions – Silcrete

Table B191. ACM-P net-return rates (Ps) for heat-treated silcrete assuming both the insulated and exposed heating scenarios and untreated silcrete experimental blocks during MIS5 conditions.

Model Conditions	Heating Scenario	Block	Raw Material	Cutting Edge * Durability (e * d)	tp (procurement time-cost(min))	m1 (Wood fuel Travel and Search time (min))	m2 (Heat-treatment time (min))	m3 (Flake manufacture time (min))	Ps
MIS5	Insulated	D9-1-10b	Silcrete	1259.248	3.458	76.600	6.383	5.958	13.628
MIS5	Insulated	D9-1-12b	Silcrete	1590.524	3.693	81.816	6.818	6.363	16.116
MIS5	Insulated	D9-1-12d	Silcrete	1428.770	3.554	78.730	6.561	6.123	15.045
MIS5	Insulated	E3-1-1b	Silcrete	1694.441	4.202	93.096	7.758	7.241	15.089
MIS5	Insulated	E3-1-5p	Silcrete	1334.362	3.140	69.559	5.797	5.410	15.903
MIS5	Insulated	E3-1-6a	Silcrete	1593.300	3.700	81.965	6.830	6.375	16.115
MIS5	Insulated	E3-1-6c	Silcrete	1509.278	3.335	73.892	6.158	5.747	16.933
MIS5	Insulated	I14-2-16l	Silcrete	1736.073	3.448	76.394	6.366	5.942	18.840
MIS5	Exposed	D9-1-10b	Silcrete	1259.248	3.458	38.300	21.278	5.958	18.252
MIS5	Exposed	D9-1-12b	Silcrete	1590.524	3.693	40.908	22.727	6.363	21.584
MIS5	Exposed	D9-1-12d	Silcrete	1428.770	3.554	39.365	21.869	6.123	20.149
MIS5	Exposed	E3-1-1b	Silcrete	1694.441	4.202	46.548	25.860	7.241	20.208
MIS5	Exposed	E3-1-5p	Silcrete	1334.362	3.140	34.780	19.322	5.410	21.298
MIS5	Exposed	E3-1-6a	Silcrete	1593.300	3.700	40.982	22.768	6.375	21.582
MIS5	Exposed	E3-1-6c	Silcrete	1509.278	3.335	36.946	20.525	5.747	22.678
MIS5	Exposed	I14-2-16l	Silcrete	1736.073	3.448	38.197	21.220	5.942	25.231
MIS5	Untreated	D9-1-10a	Silcrete	601.381	4.103	0	0	7.070	53.823
MIS5	Untreated	D9-1-12a	Silcrete	719.735	3.612	0	0	6.223	73.181
MIS5	Untreated	D9-1-12c	Silcrete	788.254	4.496	0	0	7.747	64.382
MIS5	Untreated	E3-1-1A	Silcrete	631.653	3.926	0	0	6.765	59.085
MIS5	Untreated	E3-1-5n	Silcrete	802.006	3.303	0	0	5.692	89.164
MIS5	Untreated	E3-1-5o	Silcrete	722.028	3.244	0	0	5.589	81.742
MIS5	Untreated	E3-1-6b	Silcrete	716.341	4.805	0	0	8.279	54.750
MIS5	Untreated	I14-2-16a	Silcrete	517.679	2.806	0	0	4.836	67.740

MIS6 conditions – Silcrete

Table B192. ACM-P net-return rates (Ps) for heat-treated silcrete assuming both the insulated and exposed heating scenarios and untreated silcrete experimental blocks during MIS6 conditions.

Model Conditions	Heating Scenario	Block	Raw Material	Cutting Edge * Durability (e * d)	tp (procurement time (min))	m1 (Wood fuel Travel and Search time (min))	m2 (Heat-treatment time (min))	m3 (Flake manufacture time (min))	Ps
MIS6	Insulated	D9-1-10b	Silcrete	1259.248	3.458	76.600	6.383	5.958	13.628
MIS6	Insulated	D9-1-12b	Silcrete	1590.524	3.693	81.816	6.818	6.363	16.116
MIS6	Insulated	D9-1-12d	Silcrete	1428.770	3.554	78.730	6.561	6.123	15.045
MIS6	Insulated	E3-1-1b	Silcrete	1694.441	4.202	93.096	7.758	7.241	15.089
MIS6	Insulated	E3-1-5p	Silcrete	1334.362	3.140	69.559	5.797	5.410	15.903
MIS6	Insulated	E3-1-6a	Silcrete	1593.300	3.700	81.965	6.830	6.375	16.115
MIS6	Insulated	E3-1-6c	Silcrete	1509.278	3.335	73.892	6.158	5.747	16.933
MIS6	Insulated	I14-2-16l	Silcrete	1736.073	3.448	76.394	6.366	5.942	18.840
MIS6	Exposed	D9-1-10b	Silcrete	1259.248	3.458	38.300	21.278	5.958	18.252
MIS6	Exposed	D9-1-12b	Silcrete	1590.524	3.693	40.908	22.727	6.363	21.584
MIS6	Exposed	D9-1-12d	Silcrete	1428.770	3.554	39.365	21.869	6.123	20.149
MIS6	Exposed	E3-1-1b	Silcrete	1694.441	4.202	46.548	25.860	7.241	20.208
MIS6	Exposed	E3-1-5p	Silcrete	1334.362	3.140	34.780	19.322	5.410	21.298
MIS6	Exposed	E3-1-6a	Silcrete	1593.300	3.700	40.982	22.768	6.375	21.582
MIS6	Exposed	E3-1-6c	Silcrete	1509.278	3.335	36.946	20.525	5.747	22.678
MIS6	Exposed	I14-2-16l	Silcrete	1736.073	3.448	38.197	21.220	5.942	25.231
MIS6	Untreated	D9-1-10a	Silcrete	601.381	4.103	0	0	7.070	53.823
MIS6	Untreated	D9-1-12a	Silcrete	719.735	3.612	0	0	6.223	73.181
MIS6	Untreated	D9-1-12c	Silcrete	788.254	4.496	0	0	7.747	64.382
MIS6	Untreated	E3-1-1A	Silcrete	631.653	3.926	0	0	6.765	59.085
MIS6	Untreated	E3-1-5n	Silcrete	802.006	3.303	0	0	5.692	89.164
MIS6	Untreated	E3-1-5o	Silcrete	722.028	3.244	0	0	5.589	81.742
MIS6	Untreated	E3-1-6b	Silcrete	716.341	4.805	0	0	8.279	54.750
MIS6	Untreated	I14-2-16a	Silcrete	517.679	2.806	0	0	4.836	67.740

ACM-R net-return rates

MIS4 conditions with or without a Paleo-Agulhas plain silcrete source

Table B193. ACM-R net-return rates (Rq) for quartzite experimental blocks during MIS4 conditions with or without a Paleo-Agulhas plain silcrete source.

Model Conditions	Block	Raw Material	Cutting Edge * Durability (e * d)	*ts* (Travel and search time (min))	*tp* (procurement time (min))	*m*3 (flake manufacture time (min))	Rq
MIS4-Without Paleo-Agulhas Silcrete	C9-1-1B8	Quartzite	630.455	93.738	2.604	93.738	3.317
MIS4-Without Paleo-Agulhas Silcrete	C9-1-1B9	Quartzite	583.846	87.361	2.427	87.361	3.296
MIS4-Without Paleo-Agulhas Silcrete	D11-1-100A	Quartzite	551.710	83.760	2.501	83.760	3.245
MIS4-Without Paleo-Agulhas Silcrete	D11-1-90D1	Quartzite	551.026	73.462	2.193	73.462	3.695
MIS4-Without Paleo-Agulhas Silcrete	D11-1-95A	Quartzite	558.104	88.608	2.646	88.608	3.103
MIS4-Without Paleo-Agulhas Silcrete	D11-1-95B	Quartzite	571.712	83.326	2.488	83.326	3.380
MIS4-Without Paleo-Agulhas Silcrete	D11-1-97A1	Quartzite	574.838	93.506	2.792	93.506	3.029
MIS4-Without Paleo-Agulhas Silcrete	D11-1-98B1	Quartzite	631.810	94.110	2.810	94.110	3.307
MIS4-Without Paleo-Agulhas Silcrete	D11-1-98C1	Quartzite	583.844	86.097	2.571	86.097	3.341
MIS4-Without Paleo-Agulhas Silcrete	D11-1-98D	Quartzite	570.377	97.692	2.917	97.692	2.876
MIS4-Without Paleo-Agulhas Silcrete	D11-1-85C1	Quartzite	969.078	90.180	2.693	93.738	5.193
MIS4-Without Paleo-Agulhas Silcrete	D11-1-91A1	Quartzite	833.108	91.730	2.739	87.361	4.582
MIS4-Without Paleo-Agulhas Silcrete	D11-1-91A2	Quartzite	849.101	82.786	2.472	83.760	5.024
MIS4-Without Paleo-Agulhas Silcrete	D11-1-91B3	Quartzite	965.135	95.502	2.851	73.462	5.617
MIS4-Without Paleo-Agulhas Silcrete	D11-1-91B5	Quartzite	945.793	81.071	2.421	88.608	5.496
MIS4-Without Paleo-Agulhas Silcrete	D11-1-91C3	Quartzite	835.408	91.734	2.739	83.326	4.699
MIS4-Without Paleo-Agulhas Silcrete	D11-1-94B2	Quartzite	1003.631	98.479	2.940	93.506	5.149
MIS4-Without Paleo-Agulhas Silcrete	D11-1-94B3	Quartzite	1106.372	100.897	3.012	94.110	5.587
MIS4-Without Paleo-Agulhas Silcrete	D11-1-94D2	Quartzite	821.190	91.552	2.733	86.097	4.552
MIS4-Without Paleo-Agulhas Silcrete	D11-1-97C	Quartzite	980.072	98.194	2.932	97.692	4.930

MIS4 conditions without a Paleo-Agulhas plain silcrete source

Table B194. ACM-R net-return rates (Rs) for heat-treated silcrete assuming both the insulated and exposed heating scenarios and untreated silcrete experimental blocks during MIS4 conditions without a Paleo-Agulhas plain silcrete source.

Model Conditions	Heating Scenario	Block	Raw Material	Cutting Edge * Durability (e * d)	*ts* (Travel and search time (min))	*tp* (procurement time (min))	*m1* (Wood fuel travel and search time (min))	*m2* (heat-treatment time (min))	*m3* (flake manufacture time (min))	Rs
MIS4-Without Paleo-Agulhas Silcrete	Insulated	D9-1-10b	Silcrete	1259.248	124.021	3.458	38.300	6.383	5.958	7.070
MIS4-Without Paleo-Agulhas Silcrete	Insulated	D9-1-12b	Silcrete	1590.524	132.465	3.693	40.908	6.818	6.363	8.360
MIS4-Without Paleo-Agulhas Silcrete	Insulated	D9-1-12d	Silcrete	1428.770	127.470	3.554	39.365	6.561	6.123	7.804
MIS4-Without Paleo-Agulhas Silcrete	Insulated	E3-1-1b	Silcrete	1694.441	150.729	4.202	46.548	7.758	7.241	7.827
MIS4-Without Paleo-Agulhas Silcrete	Insulated	E3-1-5p	Silcrete	1334.362	112.622	3.140	34.780	5.797	5.410	8.250
MIS4-Without Paleo-Agulhas Silcrete	Insulated	E3-1-6a	Silcrete	1593.300	132.707	3.700	40.982	6.830	6.375	8.360
MIS4-Without Paleo-Agulhas Silcrete	Insulated	E3-1-6c	Silcrete	1509.278	119.636	3.335	36.946	6.158	5.747	8.784
MIS4-Without Paleo-Agulhas Silcrete	Insulated	I14-2-16l	Silcrete	1736.073	123.687	3.448	38.197	6.366	5.942	9.773
MIS4-Without Paleo-Agulhas Silcrete	Exposed	D9-1-10b	Silcrete	1259.248	124.021	3.458	38.300	21.278	5.958	6.524
MIS4-Without Paleo-Agulhas Silcrete	Exposed	D9-1-12b	Silcrete	1590.524	132.465	3.693	40.908	22.727	6.363	7.715
MIS4-Without Paleo-Agulhas Silcrete	Exposed	D9-1-12d	Silcrete	1428.770	127.470	3.554	39.365	21.869	6.123	7.202
MIS4-Without Paleo-Agulhas Silcrete	Exposed	E3-1-1b	Silcrete	1694.441	150.729	4.202	46.548	25.860	7.241	7.223
MIS4-Without Paleo-	Exposed	E3-1-5p	Silcrete	1334.362	112.622	3.140	34.780	19.322	5.410	7.613

Agulhas Silcrete										
MIS4-Without Paleo-Agulhas Silcrete	Exposed	E3-1-6a	Silcrete	1593.300	132.707	3.700	40.982	22.768	6.375	7.715
MIS4-Without Paleo-Agulhas Silcrete	Exposed	E3-1-6c	Silcrete	1509.278	119.636	3.335	36.946	20.525	5.747	8.106
MIS4-Without Paleo-Agulhas Silcrete	Exposed	I14-2-16l	Silcrete	1736.073	123.687	3.448	38.197	21.220	5.942	9.019
MIS4-Without Paleo-Agulhas Silcrete	Untreated	D9-1-10a	Silcrete	601.381	147.177	4.103	0	0	7.070	3.798
MIS4-Without Paleo-Agulhas Silcrete	Untreated	D9-1-12a	Silcrete	719.735	129.548	3.612	0	0	6.223	5.164
MIS4-Without Paleo-Agulhas Silcrete	Untreated	D9-1-12c	Silcrete	788.254	161.272	4.496	0	0	7.747	4.543
MIS4-Without Paleo-Agulhas Silcrete	Untreated	E3-1-1A	Silcrete	631.653	140.817	3.926	0	0	6.765	4.169
MIS4-Without Paleo-Agulhas Silcrete	Untreated	E3-1-5n	Silcrete	802.006	118.480	3.303	0	0	5.692	6.291
MIS4-Without Paleo-Agulhas Silcrete	Untreated	E3-1-5o	Silcrete	722.028	116.350	3.244	0	0	5.589	5.768
MIS4-Without Paleo-Agulhas Silcrete	Untreated	E3-1-6b	Silcrete	716.341	172.344	4.805	0	0	8.279	3.863
MIS4-Without Paleo-Agulhas Silcrete	Untreated	I14-2-16a	Silcrete	517.679	100.664	2.806	0	0	4.836	4.780

MIS4 conditions with a Paleo-Agulhas plain silcrete source

Table B195. ACM-R net-return rates (Rs) for heat-treated silcrete assuming both the insulated and exposed heating scenarios and untreated silcrete experimental blocks during MIS4 conditions with a Paleo-Agulhas plain silcrete source.

Model Conditions	Heating Scenario	Block	Raw Material	Cutting Edge * Durability (e * d)	*ts* (Travel and search time (min))	*tp* (procurement time (min))	*m*1 (Woodfuel search time (min))	*m*2 (heat-treatment time (min))	*m*3 (flake manufacture time (min))	Rs
MIS4-With Paleo-Agulhas Silcrete	Insulated	D9-1-10b	Silcrete	1259.248	11.923	3.458	38.300	6.383	5.958	19.073
MIS4-With Paleo-Agulhas Silcrete	Insulated	D9-1-12b	Silcrete	1590.524	12.734	3.693	40.908	6.818	6.363	22.555
MIS4-With Paleo-Agulhas Silcrete	Insulated	D9-1-12d	Silcrete	1428.770	12.254	3.554	39.365	6.561	6.123	21.055
MIS4-With Paleo-Agulhas Silcrete	Insulated	E3-1-1b	Silcrete	1694.441	14.490	4.202	46.548	7.758	7.241	21.117
MIS4-With Paleo-Agulhas Silcrete	Insulated	E3-1-5p	Silcrete	1334.362	10.827	3.140	34.780	5.797	5.410	22.257
MIS4-With Paleo-Agulhas Silcrete	Insulated	E3-1-6a	Silcrete	1593.300	12.758	3.700	40.982	6.830	6.375	22.553
MIS4-With Paleo-Agulhas Silcrete	Insulated	E3-1-6c	Silcrete	1509.278	11.501	3.335	36.946	6.158	5.747	23.698
MIS4-With Paleo-Agulhas Silcrete	Insulated	I14-2-16l	Silcrete	1736.073	11.891	3.448	38.197	6.366	5.942	26.367
MIS4-With Paleo-Agulhas Silcrete	Exposed	D9-1-10b	Silcrete	1259.248	11.923	3.458	38.300	21.278	5.958	15.562
MIS4-With Paleo-Agulhas Silcrete	Exposed	D9-1-12b	Silcrete	1590.524	12.734	3.693	40.908	22.727	6.363	18.403
MIS4-With Paleo-Agulhas Silcrete	Exposed	D9-1-12d	Silcrete	1428.770	12.254	3.554	39.365	21.869	6.123	17.180
MIS4-With Paleo-	Exposed	E3-1-1b	Silcrete	1694.441	14.490	4.202	46.548	25.860	7.241	17.230

Agulhas Silcrete										
MIS4-With Paleo-Agulhas Silcrete	Exposed	E3-1-5p	Silcrete	1334.362	10.827	3.140	34.780	19.322	5.410	18.160
MIS4-With Paleo-Agulhas Silcrete	Exposed	E3-1-6a	Silcrete	1593.300	12.758	3.700	40.982	22.768	6.375	18.402
MIS4-With Paleo-Agulhas Silcrete	Exposed	E3-1-6c	Silcrete	1509.278	11.501	3.335	36.946	20.525	5.747	19.336
MIS4-With Paleo-Agulhas Silcrete	Exposed	I14-2-16l	Silcrete	1736.073	11.891	3.448	38.197	21.220	5.942	21.513
MIS4-With Paleo-Agulhas Silcrete	Untreated	D9-1-10a	Silcrete	601.381	14.149	4.103	0	0	7.070	23.749
MIS4-With Paleo-Agulhas Silcrete	Untreated	D9-1-12a	Silcrete	719.735	12.454	3.612	0	0	6.223	32.291
MIS4-With Paleo-Agulhas Silcrete	Untreated	D9-1-12c	Silcrete	788.254	15.504	4.496	0	0	7.747	28.408
MIS4-With Paleo-Agulhas Silcrete	Untreated	E3-1-1A	Silcrete	631.653	13.537	3.926	0	0	6.765	26.071
MIS4-With Paleo-Agulhas Silcrete	Untreated	E3-1-5n	Silcrete	802.006	11.390	3.303	0	0	5.692	39.343
MIS4-With Paleo-Agulhas Silcrete	Untreated	E3-1-5o	Silcrete	722.028	11.185	3.244	0	0	5.589	36.069
MIS4-With Paleo-Agulhas Silcrete	Untreated	E3-1-6b	Silcrete	716.341	16.568	4.805	0	0	8.279	24.158
MIS4-With Paleo-Agulhas Silcrete	Untreated	I14-2-16a	Silcrete	517.679	9.677	2.806	0	0	4.836	29.890

MIS5 conditions

Table B196. ACM-R net-return rates (Rq) for quartzite experimental blocks during MIS5 conditions.

Model Conditions	Block	Raw Material	Cutting Edge * Durability (e * d)	*t*s (Travel and search time (min))	*t*p (procurement time (min))	*m*3 (flake manufacture time (min))	Rq
MIS5	C9-1-1B8	Quartzite	630.455	5.538	2.604	6.614	42.728
MIS5	C9-1-1B9	Quartzite	583.846	5.161	2.427	6.164	42.458
MIS5	D11-1-100A	Quartzite	551.710	4.948	2.501	5.910	41.300
MIS5	D11-1-90D1	Quartzite	551.026	4.340	2.193	5.183	47.031
MIS5	D11-1-95A	Quartzite	558.104	5.234	2.646	6.252	39.493
MIS5	D11-1-95B	Quartzite	571.712	4.922	2.488	5.879	43.020
MIS5	D11-1-97A1	Quartzite	574.838	5.524	2.792	6.597	38.546

MIS5	D11-1-98B1	Quartzite	631.810	5.559	2.810	6.640	42.095
MIS5	D11-1-98C1	Quartzite	583.844	5.086	2.571	6.075	42.519
MIS5	D11-1-98D	Quartzite	570.377	5.771	2.917	6.893	36.608
MIS5	D11-1-85C1	Quartzite	969.078	5.327	2.693	6.363	67.379
MIS5	D11-1-91A1	Quartzite	833.108	5.419	2.739	6.472	56.946
MIS5	D11-1-91A2	Quartzite	849.101	4.890	2.472	5.841	64.310
MIS5	D11-1-91B3	Quartzite	965.135	5.642	2.851	6.738	63.365
MIS5	D11-1-91B5	Quartzite	945.793	4.789	2.421	5.720	73.149
MIS5	D11-1-91C3	Quartzite	835.408	5.419	2.739	6.472	57.101
MIS5	D11-1-94B2	Quartzite	1003.631	5.818	2.940	6.948	63.901
MIS5	D11-1-94B3	Quartzite	1106.372	5.960	3.012	7.119	68.754
MIS5	D11-1-94D2	Quartzite	821.190	5.408	2.733	6.460	56.241
MIS5	D11-1-97C	Quartzite	980.072	5.801	2.932	6.928	62.582

Table B197. ACM-R net-return rates (Rs) for heat-treated silcrete assuming both the insulated and exposed heating scenarios and untreated silcrete experimental blocks during MIS5 conditions.

Model Conditions	Heating Scenario	Block	Raw Material	Cutting Edge * Durability (e * d)	*ts* (Travel and search time (min))	*tp* (procurement time (min))	*m1* (Wood fuel travel and search time-cost(min))	*m2* (heat-treatment time (min))	*m3* (flake manufacture time (min))	Rs
MIS5	Insulated	D9-1-10b	Silcrete	1259.248	124.021	3.458	76.600	6.383	5.958	5.819
MIS5	Insulated	D9-1-12b	Silcrete	1590.524	132.465	3.693	81.816	6.818	6.363	6.881
MIS5	Insulated	D9-1-12d	Silcrete	1428.770	127.470	3.554	78.730	6.561	6.123	6.423
MIS5	Insulated	E3-1-1b	Silcrete	1694.441	150.729	4.202	93.096	7.758	7.241	6.442
MIS5	Insulated	E3-1-5p	Silcrete	1334.362	112.622	3.140	69.559	5.797	5.410	6.790
MIS5	Insulated	E3-1-6a	Silcrete	1593.300	132.707	3.700	81.965	6.830	6.375	6.880
MIS5	Insulated	E3-1-6c	Silcrete	1509.278	119.636	3.335	73.892	6.158	5.747	7.229
MIS5	Insulated	I14-2-16l	Silcrete	1736.073	123.687	3.448	76.394	6.366	5.942	8.043
MIS5	Exposed	D9-1-10b	Silcrete	1259.248	124.021	3.458	38.300	21.278	5.958	6.524
MIS5	Exposed	D9-1-12b	Silcrete	1590.524	132.465	3.693	40.908	22.727	6.363	7.715
MIS5	Exposed	D9-1-12d	Silcrete	1428.770	127.470	3.554	39.365	21.869	6.123	7.202
MIS5	Exposed	E3-1-1b	Silcrete	1694.441	150.729	4.202	46.548	25.860	7.241	7.223

MIS5	Exposed	E3-1-5p	Silcrete	1334.362	112.622	3.140	34.780	19.322	5.410	7.613
MIS5	Exposed	E3-1-6a	Silcrete	1593.300	132.707	3.700	40.982	22.768	6.375	7.715
MIS5	Exposed	E3-1-6c	Silcrete	1509.278	119.636	3.335	36.946	20.525	5.747	8.106
MIS5	Exposed	I14-2-16l	Silcrete	1736.073	123.687	3.448	38.197	21.220	5.942	9.019
MIS5	Untreated	D9-1-10a	Silcrete	601.381	147.177	4.103	0	0	7.070	3.798
MIS5	Untreated	D9-1-12a	Silcrete	719.735	129.548	3.612	0	0	6.223	5.164
MIS5	Untreated	D9-1-12c	Silcrete	788.254	161.272	4.496	0	0	7.747	4.543
MIS5	Untreated	E3-1-1A	Silcrete	631.653	140.817	3.926	0	0	6.765	4.169
MIS5	Untreated	E3-1-5n	Silcrete	802.006	118.480	3.303	0	0	5.692	6.291
MIS5	Untreated	E3-1-5o	Silcrete	722.028	116.350	3.244	0	0	5.589	5.768
MIS5	Untreated	E3-1-6b	Silcrete	716.341	172.344	4.805	0	0	8.279	3.863
MIS5	Untreated	I14-2-16a	Silcrete	517.679	100.664	2.806	0	0	4.836	4.780

MIS6 conditions with or without a Paleo-Agulhas plain silcrete source

Table B198. ACM-R net-return rates (Rq) for quartzite experimental blocks during MIS6 conditions with or without a Paleo-Agulhas plain silcrete source.

Model Conditions	Block	Raw Material	Cutting Edge * Durability (e * d)	*t*s (Travel and search time (min))	*t*p (procurement time (min))	*m*3 (flake manufacture time (min))	Rq
MIS6-Without Paleo-Agulhas Silcrete	C9-1-1B8	Quartzite	630.455	25.422	2.604	25.422	11.796
MIS6-Without Paleo-Agulhas Silcrete	C9-1-1B9	Quartzite	583.846	23.693	2.427	23.693	11.721
MIS6-Without Paleo-Agulhas Silcrete	D11-1-100A	Quartzite	551.710	22.716	2.501	22.716	11.510
MIS6-Without Paleo-Agulhas Silcrete	D11-1-90D1	Quartzite	551.026	19.923	2.193	19.923	13.107
MIS6-Without Paleo-Agulhas Silcrete	D11-1-95A	Quartzite	558.104	24.031	2.646	24.031	11.006
MIS6-Without Paleo-Agulhas Silcrete	D11-1-95B	Quartzite	571.712	22.598	2.488	22.598	11.989
MIS6-Without Paleo-Agulhas Silcrete	D11-1-97A1	Quartzite	574.838	25.359	2.792	25.359	10.743
MIS6-Without Paleo-Agulhas Silcrete	D11-1-98B1	Quartzite	631.810	25.523	2.810	25.523	11.732
MIS6-Without Paleo-Agulhas Silcrete	D11-1-98C1	Quartzite	583.844	23.350	2.571	23.350	11.850
MIS6-Without Paleo-Agulhas Silcrete	D11-1-98D	Quartzite	570.377	26.494	2.917	26.494	10.203
MIS6-Without Paleo-Agulhas Silcrete	D11-1-85C1	Quartzite	969.078	24.457	2.693	24.457	18.778
MIS6-Without Paleo-Agulhas Silcrete	D11-1-91A1	Quartzite	833.108	24.878	2.739	24.878	15.871
MIS6-Without Paleo-Agulhas Silcrete	D11-1-91A2	Quartzite	849.101	22.452	2.472	22.452	17.923
MIS6-Without Paleo-Agulhas Silcrete	D11-1-91B3	Quartzite	965.135	25.901	2.851	25.901	17.659
MIS6-Without Paleo-Agulhas Silcrete	D11-1-91B5	Quartzite	945.793	21.987	2.421	21.987	20.386
MIS6-Without Paleo-Agulhas Silcrete	D11-1-91C3	Quartzite	835.408	24.879	2.739	24.879	15.914
MIS6-Without Paleo-Agulhas Silcrete	D11-1-94B2	Quartzite	1003.631	26.708	2.940	26.708	17.809
MIS6-Without Paleo-	D11-1-	Quartzite	1106.372	27.364	3.012	27.364	19.161

Agulhas Silcrete	94B3						
MIS6-Without Paleo-Agulhas Silcrete	D11-1-94D2	Quartzite	821.190	24.829	2.733	24.829	15.674
MIS6-Without Paleo-Agulhas Silcrete	D11-1-97C	Quartzite	980.072	26.631	2.932	26.631	17.441

MIS6 conditions without a Paleo-Agulhas plain silcrete source

Table B199. ACM-R net-return rates (Rs) for heat-treated silcrete assuming both the insulated and exposed heating scenarios and untreated silcrete experimental blocks during MIS6 conditions without a Paleo-Agulhas plain silcrete source.

Model Conditions	Heating Scenario	Block	Raw Material	Cutting Edge * Durability (e * d)	*ts* (Travel and search time (min))	*tp* (procurement time (min))	*m*1 (Wood fuel Travel and search time (min))	*m*2 (heat-treatment time (min))	*m*3 (flake manufacture time (min))	Rs
MIS6-Without Paleo-Agulhas Silcrete	Insulated	D9-1-10b	Silcrete	1259.248	124.021	3.458	76.600	6.383	5.958	5.819
MIS6-Without Paleo-Agulhas Silcrete	Insulated	D9-1-12b	Silcrete	1590.524	132.465	3.693	81.816	6.818	6.363	6.881
MIS6-Without Paleo-Agulhas Silcrete	Insulated	D9-1-12d	Silcrete	1428.770	127.470	3.554	78.730	6.561	6.123	6.423
MIS6-Without Paleo-Agulhas Silcrete	Insulated	E3-1-1b	Silcrete	1694.441	150.729	4.202	93.096	7.758	7.241	6.442
MIS6-Without Paleo-Agulhas Silcrete	Insulated	E3-1-5p	Silcrete	1334.362	112.622	3.140	69.559	5.797	5.410	6.790
MIS6-Without Paleo-Agulhas Silcrete	Insulated	E3-1-6a	Silcrete	1593.300	132.707	3.700	81.965	6.830	6.375	6.880
MIS6-Without Paleo-Agulhas Silcrete	Insulated	E3-1-6c	Silcrete	1509.278	119.636	3.335	73.892	6.158	5.747	7.229
MIS6-Without Paleo-Agulhas Silcrete	Insulated	I14-2-16l	Silcrete	1736.073	123.687	3.448	76.394	6.366	5.942	8.043
MIS6-Without Paleo-Agulhas Silcrete	Exposed	D9-1-10b	Silcrete	1259.248	124.021	3.458	38.300	21.278	5.958	6.524
MIS6-Without Paleo-Agulhas Silcrete	Exposed	D9-1-12b	Silcrete	1590.524	132.465	3.693	40.908	22.727	6.363	7.715
MIS6-Without Paleo-Agulhas Silcrete	Exposed	D9-1-12d	Silcrete	1428.770	127.470	3.554	39.365	21.869	6.123	7.202

MIS6-Without Paleo-Agulhas Silcrete	Exposed	E3-1-1b	Silcrete	1694.441	150.729	4.202	46.548	25.860	7.241	7.223
MIS6-Without Paleo-Agulhas Silcrete	Exposed	E3-1-5p	Silcrete	1334.362	112.622	3.140	34.780	19.322	5.410	7.613
MIS6-Without Paleo-Agulhas Silcrete	Exposed	E3-1-6a	Silcrete	1593.300	132.707	3.700	40.982	22.768	6.375	7.715
MIS6-Without Paleo-Agulhas Silcrete	Exposed	E3-1-6c	Silcrete	1509.278	119.636	3.335	36.946	20.525	5.747	8.106
MIS6-Without Paleo-Agulhas Silcrete	Exposed	I14-2-16l	Silcrete	1736.073	123.687	3.448	38.197	21.220	5.942	9.019
MIS6-Without Paleo-Agulhas Silcrete	Untreated	D9-1-10a	Silcrete	601.381	147.177	4.103	0	0	7.070	3.798
MIS6-Without Paleo-Agulhas Silcrete	Untreated	D9-1-12a	Silcrete	719.735	129.548	3.612	0	0	6.223	5.164
MIS6-Without Paleo-Agulhas Silcrete	Untreated	D9-1-12c	Silcrete	788.254	161.272	4.496	0	0	7.747	4.543
MIS6-Without Paleo-Agulhas Silcrete	Untreated	E3-1-1A	Silcrete	631.653	140.817	3.926	0	0	6.765	4.169
MIS6-Without Paleo-Agulhas Silcrete	Untreated	E3-1-5n	Silcrete	802.006	118.480	3.303	0	0	5.692	6.291
MIS6-Without Paleo-Agulhas Silcrete	Untreated	E3-1-5o	Silcrete	722.028	116.350	3.244	0	0	5.589	5.768
MIS6-Without Paleo-Agulhas Silcrete	Untreated	E3-1-6b	Silcrete	716.341	172.344	4.805	0	0	8.279	3.863
MIS6-Without Paleo-Agulhas Silcrete	Untreated	I14-2-16a	Silcrete	517.679	100.664	2.806	0	0	4.836	4.780

MIS6 conditions with a Paleo-Agulhas plain silcrete source

Table B200. ACM-R net-return rates (Rs) for heat-treated silcrete assuming both the insulated and exposed heating scenarios and untreated silcrete experimental blocks during MIS6 conditions with a Paleo-Agulhas plain silcrete source.

Model Conditions	Heating Scenario	Block	Raw Material	Cutting Edge * Durability (e * d)	*ts* (Travel and search time (min))	*tp* (procurement time (min))	*m1* (Wood fuel search time (min))	*m2* (heat-treatment time (min))	*m3* (flake manufacture time (min))	Rs
MIS6-With Paleo-Agulhas Silcrete	Insulated	D9-1-10b	Silcrete	1259.248	11.923	3.458	76.600	6.383	5.958	12.071
MIS6-With Paleo-Agulhas Silcrete	Insulated	D9-1-12b	Silcrete	1590.524	12.734	3.693	81.816	6.818	6.363	14.274
MIS6-With Paleo-Agulhas	Insulated	D9-1-12d	Silcrete	1428.770	12.254	3.554	78.730	6.561	6.123	13.325

Silcrete										
MIS6-With Paleo-Agulhas Silcrete	Insulated	E3-1-1b	Silcrete	1694.441	14.490	4.202	93.096	7.758	7.241	13.364
MIS6-With Paleo-Agulhas Silcrete	Insulated	E3-1-5p	Silcrete	1334.362	10.827	3.140	69.559	5.797	5.410	14.086
MIS6-With Paleo-Agulhas Silcrete	Insulated	E3-1-6a	Silcrete	1593.300	12.758	3.700	81.965	6.830	6.375	14.273
MIS6-With Paleo-Agulhas Silcrete	Insulated	E3-1-6c	Silcrete	1509.278	11.501	3.335	73.892	6.158	5.747	14.998
MIS6-With Paleo-Agulhas Silcrete	Insulated	I14-2-16l	Silcrete	1736.073	11.891	3.448	76.394	6.366	5.942	16.687
MIS6-With Paleo-Agulhas Silcrete	Exposed	D9-1-10b	Silcrete	1259.248	11.923	3.458	38.300	21.278	5.958	15.562
MIS6-With Paleo-Agulhas Silcrete	Exposed	D9-1-12b	Silcrete	1590.524	12.734	3.693	40.908	22.727	6.363	18.403
MIS6-With Paleo-Agulhas Silcrete	Exposed	D9-1-12d	Silcrete	1428.770	12.254	3.554	39.365	21.869	6.123	17.180
MIS6-With Paleo-Agulhas Silcrete	Exposed	E3-1-1b	Silcrete	1694.441	14.490	4.202	46.548	25.860	7.241	17.230
MIS6-With Paleo-Agulhas Silcrete	Exposed	E3-1-5p	Silcrete	1334.362	10.827	3.140	34.780	19.322	5.410	18.160
MIS6-With Paleo-Agulhas Silcrete	Exposed	E3-1-6a	Silcrete	1593.300	12.758	3.700	40.982	22.768	6.375	18.402
MIS6-With Paleo-Agulhas Silcrete	Exposed	E3-1-6c	Silcrete	1509.278	11.501	3.335	36.946	20.525	5.747	19.336
MIS6-With Paleo-Agulhas Silcrete	Exposed	I14-2-16l	Silcrete	1736.073	11.891	3.448	38.197	21.220	5.942	21.513
MIS6-With Paleo-Agulhas Silcrete	Untreated	D9-1-10a	Silcrete	601.381	14.149	4.103	0	0	7.070	23.749
MIS6-With Paleo-Agulhas Silcrete	Untreated	D9-1-12a	Silcrete	719.735	12.454	3.612	0	0	6.223	32.291
MIS6-With Paleo-Agulhas Silcrete	Untreated	D9-1-12c	Silcrete	788.254	15.504	4.496	0	0	7.747	28.408
MIS6-With Paleo-Agulhas Silcrete	Untreated	E3-1-1A	Silcrete	631.653	13.537	3.926	0	0	6.765	26.071
MIS6-With Paleo-Agulhas Silcrete	Untreated	E3-1-5n	Silcrete	802.006	11.390	3.303	0	0	5.692	39.343
MIS6-With Paleo-Agulhas Silcrete	Untreated	E3-1-5o	Silcrete	722.028	11.185	3.244	0	0	5.589	36.069
MIS6-With Paleo-Agulhas Silcrete	Untreated	E3-1-6b	Silcrete	716.341	16.568	4.805	0	0	8.279	24.158
MIS6-With Paleo-Agulhas Silcrete	Untreated	I14-2-16a	Silcrete	517.679	9.677	2.806	0	0	4.836	29.890

ACM – Model condition variable outcomes

Coastline position and raw material source distribution

MIS4 with or without a Paleo-Agulhas plain silcrete source

Table B201. ACM-R net-return rates (Rq) for quartzite experimental blocks when only t_s time-cost (travel and search time) is considered during MIS4 conditions with or without a Paleo-Agulhas plain silcrete source.

Block	Raw Material	e (CE(cm)/Total Flaked Core Mass (kg))	d (durability (min)	ts-Travel and search time (min)/Total Flaked Core Mass (kg)	Rq (e * d / ts)
C9-1-1B8	Quartzite	403.49	1.56	93.74	6.726
C9-1-1B9	Quartzite	373.66	1.56	87.36	6.683
D11-1-100A	Quartzite	353.09	1.56	83.76	6.587
D11-1-90D1	Quartzite	352.66	1.56	73.46	7.501
D11-1-95A	Quartzite	357.19	1.56	88.61	6.299
D11-1-95B	Quartzite	365.90	1.56	83.33	6.861
D11-1-97A1	Quartzite	367.90	1.56	93.51	6.148
D11-1-98B1	Quartzite	404.36	1.56	94.11	6.714
D11-1-98C1	Quartzite	373.66	1.56	86.10	6.781
D11-1-98D	Quartzite	365.04	1.56	97.69	5.839
D11-1-85C1	Quartzite	478.56	2.03	90.18	10.746
D11-1-91A1	Quartzite	411.41	2.03	91.73	9.082
D11-1-91A2	Quartzite	419.31	2.03	82.79	10.257
D11-1-91B3	Quartzite	476.61	2.03	95.50	10.106
D11-1-91B5	Quartzite	467.06	2.03	81.07	11.666
D11-1-91C3	Quartzite	412.55	2.03	91.73	9.107
D11-1-94B2	Quartzite	495.62	2.03	98.48	10.191
D11-1-94B3	Quartzite	546.36	2.03	100.90	10.965
D11-1-94D2	Quartzite	405.53	2.03	91.55	8.970
D11-1-97C	Quartzite	483.99	2.03	98.19	9.981

MIS4 without a Paleo-Agulhas plain silcrete source

Table B202. ACM-R net-return rates (Rs) for heat-treated silcrete assuming both the insulated and exposed heating scenarios and untreated silcrete experimental blocks when only t_s time-cost (travel and search time) is considered during MIS4 conditions without a Paleo-Agulhas plain silcrete source.

Block	Sample Type	Raw Material	e (Cutting Edge (cm)/Total Flaked Core Mass (kg))	d (durability (min)	ts-Travel and search time (min)/Total Flaked Core Mass (kg)	Rs (e * d / ts)
D9-1-10b	Heat-treated	Silcrete	445.94	2.82	124.02	10.154

D9-1-12b	Heat-treated	Silcrete	563.25	2.82	132.47	12.007
D9-1-12d	Heat-treated	Silcrete	505.97	2.82	127.47	11.209
E3-1-1b	Heat-treated	Silcrete	600.05	2.82	150.73	11.242
E3-1-5p	Heat-treated	Silcrete	472.54	2.82	112.62	11.848
E3-1-6a	Heat-treated	Silcrete	564.24	2.82	132.71	12.006
E3-1-6c	Heat-treated	Silcrete	534.48	2.82	119.64	12.616
I14-2-16l	Heat-treated	Silcrete	614.80	2.82	123.69	14.036
D9-1-10a	Untreated	Silcrete	319.72	1.88	147.18	4.086
D9-1-12a	Untreated	Silcrete	382.64	1.88	129.55	5.556
D9-1-12c	Untreated	Silcrete	419.07	1.88	161.27	4.888
E3-1-1A	Untreated	Silcrete	335.82	1.88	140.82	4.486
E3-1-5n	Untreated	Silcrete	426.38	1.88	118.48	6.769
E3-1-5o	Untreated	Silcrete	383.86	1.88	116.35	6.206
E3-1-6b	Untreated	Silcrete	380.84	1.88	172.34	4.156
I14-2-16a	Untreated	Silcrete	275.22	1.88	100.66	5.143

MIS4 with a Paleo-Agulhas plain silcrete source

Table B203. ACM-R net-return rates (Rs) for heat-treated silcrete assuming both the insulated and exposed heating scenarios and untreated silcrete experimental blocks when only t_s time-cost (travel and search time) is considered during MIS4 conditions with a Paleo-Agulhas plain silcrete source.

Block	Sample Type	Raw Material	e (Cutting Edge (cm)/Total Flaked Core Mass (kg))	d (durability (min)	ts-Travel and search time (min)/Total Flaked Core Mass (kg)	Rs (e * d / ts)
D9-1-10b	Heat-treated	Silcrete	445.94	2.82	11.92	105.618
D9-1-12b	Heat-treated	Silcrete	563.25	2.82	12.73	124.899
D9-1-12d	Heat-treated	Silcrete	505.97	2.82	12.25	116.594
E3-1-1b	Heat-treated	Silcrete	600.05	2.82	14.49	116.937
E3-1-5p	Heat-treated	Silcrete	472.54	2.82	10.83	123.246
E3-1-6a	Heat-treated	Silcrete	564.24	2.82	12.76	124.889
E3-1-6c	Heat-treated	Silcrete	534.48	2.82	11.50	131.229
I14-2-16l	Heat-treated	Silcrete	614.80	2.82	11.89	146.005
D9-1-10a	Untreated	Silcrete	319.72	1.88	14.15	42.504
D9-1-12a	Untreated	Silcrete	382.64	1.88	12.45	57.791
D9-1-12c	Untreated	Silcrete	419.07	1.88	15.50	50.843
E3-1-1A	Untreated	Silcrete	335.82	1.88	13.54	46.660
E3-1-5n	Untreated	Silcrete	426.38	1.88	11.39	70.413
E3-1-5o	Untreated	Silcrete	383.86	1.88	11.19	64.552
E3-1-6b	Untreated	Silcrete	380.84	1.88	16.57	43.236
I14-2-16a	Untreated	Silcrete	275.22	1.88	9.68	53.495

MIS5

Table B204. ACM-R net-return rates (Rq) for quartzite experimental blocks when only t_s time-cost (travel and search time) is considered during MIS5 conditions.

Block	Raw Material	e (Cutting Edge (cm)/Total Flaked Core Mass (kg))	d (durability (min)	ts-Travel and search time (min)/Total Flaked Core Mass (kg)	Rq (e * d / ts)
C9-1-1B8	Quartzite	403.49	1.56	6.61	95.325
C9-1-1B9	Quartzite	373.66	1.56	6.16	94.722
D11-1-100A	Quartzite	353.09	1.56	5.91	93.356
D11-1-90D1	Quartzite	352.66	1.56	5.18	106.312
D11-1-95A	Quartzite	357.19	1.56	6.25	89.272
D11-1-95B	Quartzite	365.90	1.56	5.88	97.244
D11-1-97A1	Quartzite	367.90	1.56	6.60	87.131
D11-1-98B1	Quartzite	404.36	1.56	6.64	95.153
D11-1-98C1	Quartzite	373.66	1.56	6.07	96.112
D11-1-98D	Quartzite	365.04	1.56	6.89	82.751
D11-1-85C1	Quartzite	478.56	2.03	6.36	152.306
D11-1-91A1	Quartzite	411.41	2.03	6.47	128.723
D11-1-91A2	Quartzite	419.31	2.03	5.84	145.369
D11-1-91B3	Quartzite	476.61	2.03	6.74	143.233
D11-1-91B5	Quartzite	467.06	2.03	5.72	165.348
D11-1-91C3	Quartzite	412.55	2.03	6.47	129.074
D11-1-94B2	Quartzite	495.62	2.03	6.95	144.445
D11-1-94B3	Quartzite	546.36	2.03	7.12	155.415
D11-1-94D2	Quartzite	405.53	2.03	6.46	127.129
D11-1-97C	Quartzite	483.99	2.03	6.93	141.463

Table B205. ACM-R net-return rates (Rs) for heat-treated silcrete assuming both the insulated and exposed heating scenarios and untreated silcrete experimental blocks when only t_s time-cost (travel and search time) is considered during MIS5 conditions.

Block	Sample Type	Raw Material	e (Cutting Edge (cm)/Total Flaked Core Mass (kg))	d (durability (min)	ts-Travel and search time (min)/Total Flaked Core Mass (kg)	Rs (e * d / ts)
D9-1-10b	Heat-treated	Silcrete	445.94	2.82	124.02	10.154
D9-1-12b	Heat-treated	Silcrete	563.25	2.82	132.47	12.007
D9-1-12d	Heat-treated	Silcrete	505.97	2.82	127.47	11.209
E3-1-1b	Heat-treated	Silcrete	600.05	2.82	150.73	11.242
E3-1-5p	Heat-treated	Silcrete	472.54	2.82	112.62	11.848
E3-1-6a	Heat-treated	Silcrete	564.24	2.82	132.71	12.006
E3-1-6c	Heat-treated	Silcrete	534.48	2.82	119.64	12.616

I14-2-16l	Heat-treated	Silcrete	614.80	2.82	123.69	14.036
D9-1-10a	Untreated	Silcrete	319.72	1.88	147.18	4.086
D9-1-12a	Untreated	Silcrete	382.64	1.88	129.55	5.556
D9-1-12c	Untreated	Silcrete	419.07	1.88	161.27	4.888
E3-1-1A	Untreated	Silcrete	335.82	1.88	140.82	4.486
E3-1-5n	Untreated	Silcrete	426.38	1.88	118.48	6.769
E3-1-5o	Untreated	Silcrete	383.86	1.88	116.35	6.206
E3-1-6b	Untreated	Silcrete	380.84	1.88	172.34	4.156
I14-2-16a	Untreated	Silcrete	275.22	1.88	100.66	5.143

MIS6 with or without a Paleo-Agulhas plain silcrete source

Table B206. ACM-R net-return rates (Rq) for quartzite experimental blocks when only t_s time-cost (travel and search time) is considered during MIS6 conditions with or without a Paleo-Agulhas plain silcrete source.

Block	Raw Material	e (Cutting Edge (cm)/Total Flaked Core Mass (kg))	d (durability (min)	ts-Travel and search time (min)/Total Flaked Core Mass (kg)	Rq (e * d / ts)
C9-1-1B8	Quartzite	403.49	1.56	25.42	24.799
C9-1-1B9	Quartzite	373.66	1.56	23.69	24.643
D11-1-100A	Quartzite	353.09	1.56	22.72	24.287
D11-1-90D1	Quartzite	352.66	1.56	19.92	27.658
D11-1-95A	Quartzite	357.19	1.56	24.03	23.225
D11-1-95B	Quartzite	365.90	1.56	22.60	25.299
D11-1-97A1	Quartzite	367.90	1.56	25.36	22.668
D11-1-98B1	Quartzite	404.36	1.56	25.52	24.755
D11-1-98C1	Quartzite	373.66	1.56	23.35	25.004
D11-1-98D	Quartzite	365.04	1.56	26.49	21.528
D11-1-85C1	Quartzite	478.56	2.03	24.46	39.623
D11-1-91A1	Quartzite	411.41	2.03	24.88	33.488
D11-1-91A2	Quartzite	419.31	2.03	22.45	37.819
D11-1-91B3	Quartzite	476.61	2.03	25.90	37.263
D11-1-91B5	Quartzite	467.06	2.03	21.99	43.017
D11-1-91C3	Quartzite	412.55	2.03	24.88	33.579
D11-1-94B2	Quartzite	495.62	2.03	26.71	37.578
D11-1-94B3	Quartzite	546.36	2.03	27.36	40.432
D11-1-94D2	Quartzite	405.53	2.03	24.83	33.073
D11-1-97C	Quartzite	483.99	2.03	26.63	36.803

MIS6 without a Paleo-Agulhas plain silcrete source

Table B207. ACM-R net-return rates (Rs) for heat-treated silcrete assuming both the insulated and exposed heating scenarios and untreated silcrete experimental blocks when only t_s time-cost (travel and search time) is considered during MIS6 conditions without a Paleo-Agulhas plain silcrete source.

Block	Sample Type	Raw Material	e (Cutting Edge (cm)/Total Flaked Core Mass (kg))	d (durability (min)	ts-Travel and search time (min)/Total Flaked Core Mass (kg)	Rs (e * d / ts)
D9-1-10b	Heat-treated	Silcrete	445.94	2.82	124.02	10.154
D9-1-12b	Heat-treated	Silcrete	563.25	2.82	132.47	12.007
D9-1-12d	Heat-treated	Silcrete	505.97	2.82	127.47	11.209
E3-1-1b	Heat-treated	Silcrete	600.05	2.82	150.73	11.242
E3-1-5p	Heat-treated	Silcrete	472.54	2.82	112.62	11.848
E3-1-6a	Heat-treated	Silcrete	564.24	2.82	132.71	12.006
E3-1-6c	Heat-treated	Silcrete	534.48	2.82	119.64	12.616
I14-2-16l	Heat-treated	Silcrete	614.80	2.82	123.69	14.036
D9-1-10a	Untreated	Silcrete	319.72	1.88	147.18	4.086
D9-1-12a	Untreated	Silcrete	382.64	1.88	129.55	5.556
D9-1-12c	Untreated	Silcrete	419.07	1.88	161.27	4.888
E3-1-1A	Untreated	Silcrete	335.82	1.88	140.82	4.486
E3-1-5n	Untreated	Silcrete	426.38	1.88	118.48	6.769
E3-1-5o	Untreated	Silcrete	383.86	1.88	116.35	6.206
E3-1-6b	Untreated	Silcrete	380.84	1.88	172.34	4.156
I14-2-16a	Untreated	Silcrete	275.22	1.88	100.66	5.143

MIS6 with a Paleo-Agulhas plain silcrete source

Table B208. ACM-R net-return rates (Rs) for heat-treated silcrete assuming both the insulated and exposed heating scenarios and untreated silcrete experimental blocks when only t_s time-cost (travel and search time) is considered during MIS6 conditions with a Paleo-Agulhas plain silcrete source.

Block	Sample Type	Raw Material	e (Cutting Edge (cm)/Total Flaked Core Mass (kg))	d (durability (min)	ts-Travel and search time (min)/Total Flaked Core Mass (kg)	Rs (e * d / ts)
D9-1-10b	Heat-treated	Silcrete	445.94	2.82	11.92	105.618
D9-1-12b	Heat-treated	Silcrete	563.25	2.82	12.73	124.899
D9-1-12d	Heat-treated	Silcrete	505.97	2.82	12.25	116.594
E3-1-1b	Heat-treated	Silcrete	600.05	2.82	14.49	116.937
E3-1-5p	Heat-treated	Silcrete	472.54	2.82	10.83	123.246
E3-1-6a	Heat-treated	Silcrete	564.24	2.82	12.76	124.889

E3-1-6c	Heat-treated	Silcrete	534.48	2.82	11.50	131.229
I14-2-16l	Heat-treated	Silcrete	614.80	2.82	11.89	146.005
D9-1-10a	Untreated	Silcrete	319.72	1.88	14.15	42.504
D9-1-12a	Untreated	Silcrete	382.64	1.88	12.45	57.791
D9-1-12c	Untreated	Silcrete	419.07	1.88	15.50	50.843
E3-1-1A	Untreated	Silcrete	335.82	1.88	13.54	46.660
E3-1-5n	Untreated	Silcrete	426.38	1.88	11.39	70.413
E3-1-5o	Untreated	Silcrete	383.86	1.88	11.19	64.552
E3-1-6b	Untreated	Silcrete	380.84	1.88	16.57	43.236
I14-2-16a	Untreated	Silcrete	275.22	1.88	9.68	53.495

Vegetation type
Quartzite MIS4, MIS5, and MIS6

Table B209. ACM-P net-return rates (Pq) for quartzite experimental blocks when only m_1 (wood fuel travel and search time) and m_2 time-costs (heat-treatment time) are considered during MIS4, MIS5, and MIS6 conditions.

Block	Raw Material	e (Cutting Edge (cm)/Total Flaked Core Mass (kg))	d (durability (min)	m1-Wood Fuel travel and search time (min)/Total Flaked Core Mass (kg)	m2-Heat-treatment time (min)/Total Flaked core Mass (kg)	Pq (e *d/m1+m2)
C9-1-1B8	Quartzite	403.49	1.56	0	0	630.46
C9-1-1B9	Quartzite	373.66	1.56	0	0	583.85
D11-1-100A	Quartzite	353.09	1.56	0	0	551.71
D11-1-90D1	Quartzite	352.66	1.56	0	0	551.03
D11-1-95A	Quartzite	357.19	1.56	0	0	558.10
D11-1-95B	Quartzite	365.90	1.56	0	0	571.71
D11-1-97A1	Quartzite	367.90	1.56	0	0	574.84
D11-1-98B1	Quartzite	404.36	1.56	0	0	631.81
D11-1-98C1	Quartzite	373.66	1.56	0	0	583.84
D11-1-98D	Quartzite	365.04	1.56	0	0	570.38
D11-1-85C1	Quartzite	478.56	2.03	0	0	969.08
D11-1-91A1	Quartzite	411.41	2.03	0	0	833.11
D11-1-91A2	Quartzite	419.31	2.03	0	0	849.10
D11-1-91B3	Quartzite	476.61	2.03	0	0	965.14
D11-1-91B5	Quartzite	467.06	2.03	0	0	945.79
D11-1-91C3	Quartzite	412.55	2.03	0	0	835.41
D11-1-94B2	Quartzite	495.62	2.03	0	0	1003.63
D11-1-94B3	Quartzite	546.36	2.03	0	0	1106.37
D11-1-94D2	Quartzite	405.53	2.03	0	0	821.19
D11-1-97C	Quartzite	483.99	2.03	0	0	980.07

MIS4 Silcrete

Table B210. ACM-P net-return rates (Ps) for heat-treated silcrete assuming both the insulated and exposed heating scenarios and untreated silcrete experimental blocks when only m_1 (wood fuel travel and search time) and m_2 time-costs (heat-treatment time) are considered during MIS5 conditions.

Block	Heating Scenario	Raw Material	e (Cutting Edge (cm)/Total Flaked Core Mass (kg))	d (durability (min)	m1-Wood Fuel travel and search time (min)/Total Flaked Core Mass (kg)	m2-Heat-treatment time (min)/Total Flaked core Mass (kg)	Ps (e *d/m1+m2)
D9-1-10b	Insulated	Silcrete	445.94	2.82	38.300	6.383	28.182
D9-1-12b	Insulated	Silcrete	563.25	2.82	40.908	6.818	33.326
D9-1-12d	Insulated	Silcrete	505.97	2.82	39.365	6.561	31.110
E3-1-1b	Insulated	Silcrete	600.05	2.82	46.548	7.758	31.202
E3-1-5p	Insulated	Silcrete	472.54	2.82	34.780	5.797	32.885
E3-1-6a	Insulated	Silcrete	564.24	2.82	40.982	6.830	33.324
E3-1-6c	Insulated	Silcrete	534.48	2.82	36.946	6.158	35.015
I14-2-16l	Insulated	Silcrete	614.80	2.82	38.197	6.366	38.958
D9-1-10b	Exposed	Silcrete	445.94	2.82	38.300	21.278	21.136
D9-1-12b	Exposed	Silcrete	563.25	2.82	40.908	22.727	24.995
D9-1-12d	Exposed	Silcrete	505.97	2.82	39.365	21.869	23.333
E3-1-1b	Exposed	Silcrete	600.05	2.82	46.548	25.860	23.401
E3-1-5p	Exposed	Silcrete	472.54	2.82	34.780	19.322	24.664
E3-1-6a	Exposed	Silcrete	564.24	2.82	40.982	22.768	24.993
E3-1-6c	Exposed	Silcrete	534.48	2.82	36.946	20.525	26.261
I14-2-16l	Exposed	Silcrete	614.80	2.82	38.197	21.220	29.218
D9-1-10a	Untreated	Silcrete	319.72	1.88	0	0	601.381
D9-1-12a	Untreated	Silcrete	382.64	1.88	0	0	719.735
D9-1-12c	Untreated	Silcrete	419.07	1.88	0	0	788.254
E3-1-1A	Untreated	Silcrete	335.82	1.88	0	0	631.653
E3-1-5n	Untreated	Silcrete	426.38	1.88	0	0	802.006
E3-1-5o	Untreated	Silcrete	383.86	1.88	0	0	722.028
E3-1-6b	Untreated	Silcrete	380.84	1.88	0	0	716.341
I14-2-16a	Untreated	Silcrete	275.22	1.88	0	0	517.679

MIS5 Silcrete

Table B211. ACM-P net-return rates (Ps) for heat-treated silcrete assuming both the insulated and exposed heating scenarios and untreated silcrete experimental blocks when only m_1 (wood fuel travel and search time) and m_2 time-costs (heat-treatment time) are considered during MIS5 conditions.

Block	Heating Scenario	Raw Material	e (Cutting Edge (cm)/Total Flaked Core Mass (kg))	d (durability (min)	m1-Wood Fuel travel and search time (min)/Total Flaked Core Mass (kg)	m2-Heat-treatment time (min)/Total Flaked core Mass (kg)	Ps (e *d/m1+m2)
D9-1-10b	Insulated	Silcrete	445.94	2.82	76.600	6.383	15.175
D9-1-12b	Insulated	Silcrete	563.25	2.82	81.816	6.818	17.945
D9-1-12d	Insulated	Silcrete	505.97	2.82	78.730	6.561	16.752
E3-1-1b	Insulated	Silcrete	600.05	2.82	93.096	7.758	16.801
E3-1-5p	Insulated	Silcrete	472.54	2.82	69.559	5.797	17.707
E3-1-6a	Insulated	Silcrete	564.24	2.82	81.965	6.830	17.943
E3-1-6c	Insulated	Silcrete	534.48	2.82	73.892	6.158	18.854
I14-2-16l	Insulated	Silcrete	614.80	2.82	76.394	6.366	20.977
D9-1-10b	Exposed	Silcrete	445.94	2.82	38.300	21.278	21.136
D9-1-12b	Exposed	Silcrete	563.25	2.82	40.908	22.727	24.995
D9-1-12d	Exposed	Silcrete	505.97	2.82	39.365	21.869	23.333
E3-1-1b	Exposed	Silcrete	600.05	2.82	46.548	25.860	23.401
E3-1-5p	Exposed	Silcrete	472.54	2.82	34.780	19.322	24.664
E3-1-6a	Exposed	Silcrete	564.24	2.82	40.982	22.768	24.993
E3-1-6c	Exposed	Silcrete	534.48	2.82	36.946	20.525	26.261
I14-2-16l	Exposed	Silcrete	614.80	2.82	38.197	21.220	29.218
D9-1-10a	Untreated	Silcrete	319.72	1.88	0	0	601.381
D9-1-12a	Untreated	Silcrete	382.64	1.88	0	0	719.735
D9-1-12c	Untreated	Silcrete	419.07	1.88	0	0	788.254
E3-1-1A	Untreated	Silcrete	335.82	1.88	0	0	631.653
E3-1-5n	Untreated	Silcrete	426.38	1.88	0	0	802.006
E3-1-5o	Untreated	Silcrete	383.86	1.88	0	0	722.028
E3-1-6b	Untreated	Silcrete	380.84	1.88	0	0	716.341
I14-2-16a	Untreated	Silcrete	275.22	1.88	0	0	517.679

MIS6 Silcrete

Table B212. ACM-P net-return rates (Ps) for heat-treated silcrete assuming both the insulated and exposed heating scenarios and untreated silcrete experimental blocks when only m_1 (wood fuel travel and search time) and m_2 time-costs (heat-treatment time) are considered during MIS6 conditions.

Block	Heating Scenario	Raw Material	e (Cutting Edge (cm)/Total Flaked Core Mass (kg))	d (durability (min)	m1-Wood Fuel travel and search time (min)/Total Flaked Core Mass (kg)	m2-Heat-treatment time (min)/Total Flaked core Mass (kg)	Ps (e *d/m1+m2)
D9-1-10b	Insulated	Silcrete	445.94	2.82	76.600	6.383	15.175
D9-1-12b	Insulated	Silcrete	563.25	2.82	81.816	6.818	17.945
D9-1-12d	Insulated	Silcrete	505.97	2.82	78.730	6.561	16.752
E3-1-1b	Insulated	Silcrete	600.05	2.82	93.096	7.758	16.801
E3-1-5p	Insulated	Silcrete	472.54	2.82	69.559	5.797	17.707
E3-1-6a	Insulated	Silcrete	564.24	2.82	81.965	6.830	17.943
E3-1-6c	Insulated	Silcrete	534.48	2.82	73.892	6.158	18.854
I14-2-16l	Insulated	Silcrete	614.80	2.82	76.394	6.366	20.977
D9-1-10b	Exposed	Silcrete	445.94	2.82	38.300	21.278	21.136
D9-1-12b	Exposed	Silcrete	563.25	2.82	40.908	22.727	24.995
D9-1-12d	Exposed	Silcrete	505.97	2.82	39.365	21.869	23.333
E3-1-1b	Exposed	Silcrete	600.05	2.82	46.548	25.860	23.401
E3-1-5p	Exposed	Silcrete	472.54	2.82	34.780	19.322	24.664
E3-1-6a	Exposed	Silcrete	564.24	2.82	40.982	22.768	24.993
E3-1-6c	Exposed	Silcrete	534.48	2.82	36.946	20.525	26.261
I14-2-16l	Exposed	Silcrete	614.80	2.82	38.197	21.220	29.218
D9-1-10a	Untreated	Silcrete	319.72	1.88	0	0	601.381
D9-1-12a	Untreated	Silcrete	382.64	1.88	0	0	719.735
D9-1-12c	Untreated	Silcrete	419.07	1.88	0	0	788.254
E3-1-1A	Untreated	Silcrete	335.82	1.88	0	0	631.653
E3-1-5n	Untreated	Silcrete	426.38	1.88	0	0	802.006
E3-1-5o	Untreated	Silcrete	383.86	1.88	0	0	722.028
E3-1-6b	Untreated	Silcrete	380.84	1.88	0	0	716.341
I14-2-16a	Untreated	Silcrete	275.22	1.88	0	0	517.679

Mobility rate and strategy

MIS4

Table B213. ACM net-return rates (Pq or Rq) for quartzite experimental blocks when only m_3 time-cost (flake manufacturing time) is considered during MIS4 conditions.

Block	Raw Material	e (CE(cm)/Total Flaked Core Mass (kg))	d (durability (min)	m3-FlakingTime (14min)/Total Flaked Core Mass (kg)	Pq or Rq
C9-1-1B8	Quartzite	403.49	1.56	7.29	86.47
C9-1-1B9	Quartzite	373.66	1.56	6.79	85.93
D11-1-100A	Quartzite	353.09	1.56	6.51	84.69
D11-1-90D1	Quartzite	352.66	1.56	5.71	96.44
D11-1-95A	Quartzite	357.19	1.56	6.89	80.98
D11-1-95B	Quartzite	365.90	1.56	6.48	88.21
D11-1-97A1	Quartzite	367.90	1.56	7.27	79.04
D11-1-98B1	Quartzite	404.36	1.56	7.32	86.32
D11-1-98C1	Quartzite	373.66	1.56	6.70	87.19
D11-1-98D	Quartzite	365.04	1.56	7.60	75.07
D11-1-85C1	Quartzite	478.56	2.03	7.01	138.16
D11-1-91A1	Quartzite	411.41	2.03	7.13	116.77
D11-1-91A2	Quartzite	419.31	2.03	6.44	131.87
D11-1-91B3	Quartzite	476.61	2.03	7.43	129.93
D11-1-91B5	Quartzite	467.06	2.03	6.31	149.99
D11-1-91C3	Quartzite	412.55	2.03	7.13	117.09
D11-1-94B2	Quartzite	495.62	2.03	7.66	131.03
D11-1-94B3	Quartzite	546.36	2.03	7.85	140.98
D11-1-94D2	Quartzite	405.53	2.03	7.12	115.32
D11-1-97C	Quartzite	483.99	2.03	7.64	128.33

Table B214. ACM net-return rates (Ps or Rs) for untreated and heat-treated silcrete experimental blocks when only m_3 time-cost (flake manufacturing time) is considered during MIS4 conditions.

Block	Sample Type	Raw Material	e (Cutting Edge (cm)/Total Flaked Core Mass (kg))	d (durability (min)	m3-FlakingTime (14min)/Total Flaked Core Mass (kg)	Ps or Rs
D9-1-10b	Heat-treated	Silcrete	445.94	2.82	5.96	211.36
D9-1-12b	Heat-treated	Silcrete	563.25	2.82	6.36	249.95
D9-1-12d	Heat-treated	Silcrete	505.97	2.82	6.12	233.33
E3-1-1b	Heat-treated	Silcrete	600.05	2.82	7.24	234.01
E3-1-5p	Heat-treated	Silcrete	472.54	2.82	5.41	246.64
E3-1-6a	Heat-treated	Silcrete	564.24	2.82	6.38	249.93

E3-1-6c	Heat-treated	Silcrete	534.48	2.82	5.75	262.61
I14-2-16l	Heat-treated	Silcrete	614.80	2.82	5.94	292.18
D9-1-10a	Untreated	Silcrete	319.72	1.88	7.07	85.06
D9-1-12a	Untreated	Silcrete	382.64	1.88	6.22	115.65
D9-1-12c	Untreated	Silcrete	419.07	1.88	7.75	101.75
E3-1-1A	Untreated	Silcrete	335.82	1.88	6.76	93.38
E3-1-5n	Untreated	Silcrete	426.38	1.88	5.69	140.91
E3-1-5o	Untreated	Silcrete	383.86	1.88	5.59	129.18
E3-1-6b	Untreated	Silcrete	380.84	1.88	8.28	86.52
I14-2-16a	Untreated	Silcrete	275.22	1.88	4.84	107.05

ACTIVE-CHOICE MODEL – CHANGING ASSUMED CURRENCY

Maximizing cutting edge of blades multiplied by duration of use (cutting edge of complete blades (cm) / total flaked core mass (kg) * d (minutes))

ACM-P net-return rates

Table B215. Summary statistics and test results of ACM-P net-return rates ((for all experimental sample types) during MIS4, MIS5, and MIS6 conditions.

	MIS4				MIS5				MIS6			
	Quartzite (Pq)	Untreated Silcrete (Ps)	Insulated-Silcrete (Ps)	Exposed-Silcrete (Ps)	Quartzite (Pq)	Untreated Silcrete (Ps)	Insulated-Silcrete (Ps)	Exposed-Silcrete (Ps)	Quartzite (Pq)	Untreated Silcrete (Ps)	Insulated-Silcrete (Ps)	Exposed-Silcrete (Ps)
n sample blocks	20	8	8	8	20	8	8	8	20	8	8	8
First Quartile	6.886	7.700	7.021	5.505	6.886	7.700	4.111	5.505	6.886	7.700	4.111	5.505
Min	2.282	5.458	6.839	5.363	2.282	5.458	4.004	5.363	2.282	5.458	4.004	5.363
Median	14.600	10.533	8.576	6.724	14.600	10.533	5.021	6.724	14.600	10.533	5.021	6.724

Mean	7.041	10.144	8.227	1.677	0.572	1.121	8.162	5.920
	5.257	7.574	6.144	1.252	0.426	0.836	6.093	4.421
	12.261	21.687	18.083	5.932	2.038	3.994	16.255	8.267
	16.589	43.982	24.251	12.276	2.647	5.189	21.778	11.400
Max	7.041	10.144	8.227	1.677	0.572	1.121	8.162	5.920
	8.980	12.937	10.493	2.139	0.730	1.431	10.410	7.549
	12.261	21.687	18.083	5.932	2.031	3.981	16.242	8.280
	16.589	43.982	24.251	12.276	2.647	5.189	21.778	11.400
Third Quartile	7.041	10.144	8.227	1.677	0.572	1.121	8.162	5.920
	5.257	7.574	6.144	1.252	0.426	0.836	6.093	4.421
	12.261	21.687	18.083	5.932	2.038	3.994	16.255	8.267
	16.589	43.982	24.251	12.276	2.647	5.189	21.778	11.400
Standard Deviation	7.041	10.144	8.227	1.677	0.572	1.121	8.162	5.920
	5.257	7.574	6.144	1.252	0.426	0.836	6.093	4.421
	12.261	21.687	18.083	5.932	2.038	3.994	16.255	8.267
	16.589	43.982	24.251	12.276	2.647	5.189	21.778	11.400
Bootstrapped SE*	7.041	10.144	8.227	1.677	0.572	1.121	8.162	5.920
	8.980	12.937	10.493	2.139	0.730	1.431	10.410	7.549
	12.261	21.687	18.083	5.932	2.031	3.981	16.242	8.280
	16.589	43.982	24.251	12.276	2.647	5.189	21.778	11.400
Margin of error (95% CI)	7.041	10.144	8.227	1.677	0.572	1.121	8.162	5.920
	8.980	12.937	10.493	2.139	0.730	1.431	10.410	7.549
	12.261	21.687	18.083	5.932	2.031	3.981	16.242	8.280
	16.589	43.982	24.251	12.276	2.647	5.189	21.778	11.400
Bootstrapped Upper 95% CI*	7.041	10.144	8.227	1.677	0.572	1.121	8.162	5.920
	8.980	12.937	10.493	2.139	0.730	1.431	10.410	7.549
	12.261	21.687	18.083	5.932	2.031	3.981	16.242	8.280
	16.589	43.982	24.251	12.276	2.647	5.189	21.778	11.400
Bootstrapped Lower 95% CI*	7.041	10.144	8.227	1.677	0.572	1.121	8.162	5.920
	8.980	12.937	10.493	2.139	0.730	1.431	10.410	7.549
	12.261	21.687	18.083	5.932	2.031	3.981	16.242	8.280
	16.589	43.982	24.251	12.276	2.647	5.189	21.778	11.400

*Samples bootstrapped 10000 times.

MIS4, MIS5, and MIS6 conditions

Table B216. ACM-P net-return rates (Pq) for quartzite experimental blocks during MIS4, MIS5, and MIS6 conditions.

Model Conditions	Block	Raw Material	Cutting Edge Complete Blades (cm)	Total Flaked Core Mass (kg)	CE Blades (cm) / Total Flaked Core Mass (kg)	Cutting Edge * Durability (e * d)	Pq
MIS4, MIS5, and MIS6	C9-1-1B8	Quartzite	92.6	1.920	48.223	75.349	7.615
MIS4, MIS5, and MIS6	C9-1-1B9	Quartzite	83.2	2.060	40.380	63.094	6.842
MIS4, MIS5, and MIS6	D11-1-100A	Quartzite	156	2.149	72.592	113.425	12.581

MIS4, MIS5, and MIS6	D11-1-90D1	Quartzite	52.3	2.450	21.345	33.351	4.218
MIS4, MIS5, and MIS6	D11-1-95A	Quartzite	68.9	2.031	33.917	52.995	5.557
MIS4, MIS5, and MIS6	D11-1-95B	Quartzite	89.5	2.160	41.432	64.737	7.218
MIS4, MIS5, and MIS6	D11-1-97A1	Quartzite	28.3	1.925	14.701	22.971	2.282
MIS4, MIS5, and MIS6	D11-1-98B1	Quartzite	87	1.913	45.486	71.072	7.016
MIS4, MIS5, and MIS6	D11-1-98C1	Quartzite	92.7	2.091	44.340	69.281	7.476
MIS4, MIS5, and MIS6	D11-1-98D	Quartzite	77.8	1.843	42.225	65.976	6.274
MIS4, MIS5, and MIS6	D11-1-85C1	Quartzite	420.8	1.996	210.822	426.914	43.982
MIS4, MIS5, and MIS6	D11-1-91A1	Quartzite	202.4	1.962	103.146	208.870	21.155
MIS4, MIS5, and MIS6	D11-1-91A2	Quartzite	250.2	2.174	115.072	233.021	26.151
MIS4, MIS5, and MIS6	D11-1-91B3	Quartzite	322.3	1.885	171.002	346.280	33.687
MIS4, MIS5, and MIS6	D11-1-91B5	Quartzite	174	2.220	78.368	158.696	18.186
MIS4, MIS5, and MIS6	D11-1-91C3	Quartzite	170.3	1.962	86.790	175.750	17.800
MIS4, MIS5, and MIS6	D11-1-94B2	Quartzite	206.6	1.828	113.031	228.889	21.594
MIS4, MIS5, and MIS6	D11-1-94B3	Quartzite	240.5	1.784	134.809	272.989	25.137
MIS4, MIS5, and MIS6	D11-1-94D2	Quartzite	159	1.966	80.871	163.764	16.619
MIS4, MIS5, and MIS6	D11-1-97C	Quartzite	386.4	1.833	210.789	426.848	40.387

MIS4 conditions

Table B217. ACM-P net-return rates (Ps) for heat-treated silcrete assuming both the insulated and exposed heating scenarios and untreated silcrete experimental blocks during MIS4 conditions.

Model Conditions	Heating Scenario	Block	Raw Material	Cutting Edge Complete Blades (cm)	Total Flaked Core Mass (kg)	CE Blades (cm) / Total Flaked Core Mass (kg)	Cutting Edge * Durability (e * d)	Ps
MIS4	Insulated	D9-1-10b	Silcrete	311.700	2.350	132.646	374.566	6.924
MIS4	Insulated	D9-1-12b	Silcrete	329.100	2.200	149.586	422.403	7.310
MIS4	Insulated	D9-1-12d	Silcrete	307.900	2.286	134.672	380.289	6.839
MIS4	Insulated	E3-1-1b	Silcrete	479.300	1.933	247.894	700.005	10.647
MIS4	Insulated	E3-1-5p	Silcrete	362.400	2.588	140.046	395.463	8.050
MIS4	Insulated	E3-1-6a	Silcrete	409.700	2.196	186.561	526.814	9.101
MIS4	Insulated	E3-1-6c	Silcrete	451.500	2.436	185.345	523.378	10.029
MIS4	Insulated	I14-2-16l	Silcrete	582.400	2.356	247.176	697.977	12.937
MIS4	Exposed	D9-1-10b	Silcrete	311.700	2.350	132.646	374.566	5.429
MIS4	Exposed	D9-1-12b	Silcrete	329.100	2.200	149.586	422.403	5.732
MIS4	Exposed	D9-1-12d	Silcrete	307.900	2.286	134.672	380.289	5.363
MIS4	Exposed	E3-1-1b	Silcrete	479.300	1.933	247.894	700.005	8.348

MIS4	Exposed	E3-1-5p	Silcrete	362.400	2.588	140.046	395.463	6.312
MIS4	Exposed	E3-1-6a	Silcrete	409.700	2.196	186.561	526.814	7.136
MIS4	Exposed	E3-1-6c	Silcrete	451.500	2.436	185.345	523.378	7.864
MIS4	Exposed	I14-2-16l	Silcrete	582.400	2.356	247.176	697.977	10.144
MIS4	Untreated	D9-1-10a	Silcrete	89.500	1.980	45.198	85.016	7.609
MIS4	Untreated	D9-1-12a	Silcrete	179.700	2.250	79.881	150.251	15.277
MIS4	Untreated	D9-1-12c	Silcrete	97.000	1.807	53.677	100.965	8.246
MIS4	Untreated	E3-1-1A	Silcrete	150.800	2.070	72.865	137.055	12.820
MIS4	Untreated	E3-1-5n	Silcrete	223.700	2.460	90.944	171.061	19.018
MIS4	Untreated	E3-1-5o	Silcrete	255.100	2.505	101.844	191.565	21.687
MIS4	Untreated	E3-1-6b	Silcrete	93.800	1.691	55.470	104.337	7.974
MIS4	Untreated	I14-2-16a	Silcrete	64.200	2.895	22.175	41.711	5.458

MIS5 conditions

Table B218. ACM-P net-return rates (Ps) for heat-treated silcrete assuming both the insulated and exposed heating scenarios and untreated silcrete experimental blocks during MIS5 conditions.

Model Conditions	Heating Scenario	Block	Raw Material	Cutting Edge Complete Blades (cm)	Total Flaked Core Mass (kg)	CE Blades (cm) / Total Flaked Core Mass (kg)	Cutting Edge * Durability (e * d)	Ps
MIS5	Insulated	D9-1-10b	Silcrete	311.700	2.350	132.646	374.566	4.054
MIS5	Insulated	D9-1-12b	Silcrete	329.100	2.200	149.586	422.403	4.280
MIS5	Insulated	D9-1-12d	Silcrete	307.900	2.286	134.672	380.289	4.004
MIS5	Insulated	E3-1-1b	Silcrete	479.300	1.933	247.894	700.005	6.234
MIS5	Insulated	E3-1-5p	Silcrete	362.400	2.588	140.046	395.463	4.713
MIS5	Insulated	E3-1-6a	Silcrete	409.700	2.196	186.561	526.814	5.328
MIS5	Insulated	E3-1-6c	Silcrete	451.500	2.436	185.345	523.378	5.872
MIS5	Insulated	I14-2-16l	Silcrete	582.400	2.356	247.176	697.977	7.574
MIS5	Exposed	D9-1-10b	Silcrete	311.700	2.350	132.646	374.566	5.429
MIS5	Exposed	D9-1-12b	Silcrete	329.100	2.200	149.586	422.403	5.732
MIS5	Exposed	D9-1-12d	Silcrete	307.900	2.286	134.672	380.289	5.363
MIS5	Exposed	E3-1-1b	Silcrete	479.300	1.933	247.894	700.005	8.348
MIS5	Exposed	E3-1-5p	Silcrete	362.400	2.588	140.046	395.463	6.312
MIS5	Exposed	E3-1-6a	Silcrete	409.700	2.196	186.561	526.814	7.136
MIS5	Exposed	E3-1-6c	Silcrete	451.500	2.436	185.345	523.378	7.864
MIS5	Exposed	I14-2-16l	Silcrete	582.400	2.356	247.176	697.977	10.144
MIS5	Untreated	D9-1-10a	Silcrete	89.500	1.980	45.198	85.016	7.609
MIS5	Untreated	D9-1-12a	Silcrete	179.700	2.250	79.881	150.251	15.277
MIS5	Untreated	D9-1-12c	Silcrete	97.000	1.807	53.677	100.965	8.246
MIS5	Untreated	E3-1-1A	Silcrete	150.800	2.070	72.865	137.055	12.820
MIS5	Untreated	E3-1-5n	Silcrete	223.700	2.460	90.944	171.061	19.018

MIS5	Untreated	E3-1-5o	Silcrete	255.100	2.505	101.844	191.565	21.687
MIS5	Untreated	E3-1-6b	Silcrete	93.800	1.691	55.470	104.337	7.974
MIS5	Untreated	I14-2-16a	Silcrete	64.200	2.895	22.175	41.711	5.458

MIS6 conditions

Table B219. ACM-P net-return rates (Ps) for heat-treated silcrete assuming both the insulated and exposed heating scenarios and untreated silcrete experimental blocks during MIS6 conditions.

Model Conditions	Heating Scenario	Block	Raw Material	Cutting Edge Complete Blades (cm)	Total Flaked Core Mass (kg)	CE Blades (cm) / Total Flaked Core Mass (kg)	Cutting Edge * Durability (e * d)	Ps-e x d
MIS6	Insulated	D9-1-10b	Silcrete	311.700	2.350	132.646	374.566	4.054
MIS6	Insulated	D9-1-12b	Silcrete	329.100	2.200	149.586	422.403	4.280
MIS6	Insulated	D9-1-12d	Silcrete	307.900	2.286	134.672	380.289	4.004
MIS6	Insulated	E3-1-1b	Silcrete	479.300	1.933	247.894	700.005	6.234
MIS6	Insulated	E3-1-5p	Silcrete	362.400	2.588	140.046	395.463	4.713
MIS6	Insulated	E3-1-6a	Silcrete	409.700	2.196	186.561	526.814	5.328
MIS6	Insulated	E3-1-6c	Silcrete	451.500	2.436	185.345	523.378	5.872
MIS6	Insulated	I14-2-16l	Silcrete	582.400	2.356	247.176	697.977	7.574
MIS6	Exposed	D9-1-10b	Silcrete	311.700	2.350	132.646	374.566	5.429
MIS6	Exposed	D9-1-12b	Silcrete	329.100	2.200	149.586	422.403	5.732
MIS6	Exposed	D9-1-12d	Silcrete	307.900	2.286	134.672	380.289	5.363
MIS6	Exposed	E3-1-1b	Silcrete	479.300	1.933	247.894	700.005	8.348
MIS6	Exposed	E3-1-5p	Silcrete	362.400	2.588	140.046	395.463	6.312
MIS6	Exposed	E3-1-6a	Silcrete	409.700	2.196	186.561	526.814	7.136
MIS6	Exposed	E3-1-6c	Silcrete	451.500	2.436	185.345	523.378	7.864
MIS6	Exposed	I14-2-16l	Silcrete	582.400	2.356	247.176	697.977	10.144
MIS6	Untreated	D9-1-10a	Silcrete	89.500	1.980	45.198	85.016	7.609
MIS6	Untreated	D9-1-12a	Silcrete	179.700	2.250	79.881	150.251	15.277
MIS6	Untreated	D9-1-12c	Silcrete	97.000	1.807	53.677	100.965	8.246
MIS6	Untreated	E3-1-1A	Silcrete	150.800	2.070	72.865	137.055	12.820
MIS6	Untreated	E3-1-5n	Silcrete	223.700	2.460	90.944	171.061	19.018
MIS6	Untreated	E3-1-5o	Silcrete	255.100	2.505	101.844	191.565	21.687
MIS6	Untreated	E3-1-6b	Silcrete	93.800	1.691	55.470	104.337	7.974
MIS6	Untreated	I14-2-16a	Silcrete	64.200	2.895	22.175	41.711	5.458

ACM-R net-return rates

Table B220. Summary statistics and test results of ACM-R net-return rates ((for all experimental sample types) during all model conditions.

	n sample blocks	First Quartile	Min	Median	Mean	Max
MIS6 with Paleo-Agulhas plain silcrete						
Exposed-Silcrete (Rs)	8	4.694	4.573	5.733	6.003	8.649
Insulated-Silcrete (Rs)	8	3.641	3.547	4.447	4.657	6.709
Untreated Silcrete (Rs)	8	3.398	2.408	4.648	5.410	9.570
Quartzite (Rq)	20	1.280	0.429	2.746	3.118	8.272
MIS6 without Paleo-Agulhas plain silcrete						
Exposed-Silcrete (Rs)	8	1.968	1.917	2.404	2.517	3.626
Insulated-Silcrete (Rs)	8	1.755	1.710	2.144	2.245	3.234
Untreated Silcrete (Rs)	8	0.544	0.385	0.744	0.865	1.530
Quartzite (Rq)	20	1.280	0.429	2.746	3.118	8.272
MIS5						
Exposed-Silcrete (Rs)	8	1.968	1.917	2.404	2.517	3.626
Insulated-Silcrete (Rs)	8	1.755	1.710	2.144	2.245	3.234
Untreated Silcrete (Rs)	8	0.544	0.385	0.744	0.865	1.530
Quartzite (Rq)	20	4.625	1.540	9.854	11.193	29.683
MIS4 with Paleo-Agulhas plain silcrete						
Exposed-Silcrete (Rs)	8	4.694	4.573	5.733	6.003	8.649
Insulated-Silcrete (Rs)	8	5.752	5.604	7.027	7.358	10.601
Untreated Silcrete (Rs)	8	3.398	2.408	4.648	5.410	9.570
Quartzite (Rq)	20	0.360	0.121	0.788	0.895	2.288
MIS4 without Paleo-Agulhas plain silcrete						
Exposed-Silcrete (Rs)	8	1.968	1.917	2.404	2.517	3.626
Insulated-Silcrete (Rs)	8	2.132	2.077	2.605	2.727	3.929
Untreated Silcrete (Rs)	8	0.544	0.385	0.744	0.865	1.530
Quartzite (Rq)	20	0.360	0.121	0.788	0.895	2.288

7.015	1.430	0.487	0.954	6.958	5.049
5.441	1.109	0.377	0.739	5.396	3.917
7.979	2.618	0.902	1.767	7.178	3.643
4.561	2.311	0.497	0.975	4.093	2.143
2.941	0.599	0.204	0.399	2.916	2.117
2.623	0.535	0.182	0.356	2.601	1.889
1.276	0.419	0.143	0.281	1.147	0.584
4.561	2.311	0.497	0.975	4.093	2.143
2.941	0.599	0.204	0.400	2.917	2.117
2.623	0.535	0.181	0.355	2.600	1.890
1.276	0.419	0.143	0.281	1.146	0.585
16.367	8.288	1.782	3.493	14.686	7.699
7.015	1.430	0.487	0.954	6.957	5.050
8.598	1.753	0.599	1.174	8.532	6.184
7.979	2.618	0.899	1.762	7.172	3.649
1.328	0.668	0.144	0.282	1.177	0.612
2.941	0.599	0.206	0.404	2.921	2.113
3.187	0.650	0.221	0.433	3.161	2.294
1.276	0.419	0.144	0.282	1.147	0.583
1.328	0.668	0.144	0.282	1.177	0.612
Third Quartile	SD	Bootstrapped SE*	Margin of error (95% CI)	Bootstrapped Upper 95% CI*	Bootstrapped Lower 95% CI*

*Samples bootstrapped 10000 times.

MIS4 conditions with or without a Paleo-Agulhas plain silcrete source

Table B221. ACM-R net-return rates (Rq) for quartzite experimental blocks during MIS4 conditions with or without a Paleo-Agulhas plain silcrete source.

Model Conditions	Block	Raw Material	Cutting Edge Complete Blades (cm)	Total Flaked Core Mass (kg)	CE Blades (cm) / Total Flaked Core Mass (kg)	Cutting Edge * Durability (e * d)	Rq
MIS4	C9-1-1B8	Quartzite	92.600	1.920	48.223	75.349	0.396
MIS4	C9-1-1B9	Quartzite	83.200	2.060	40.380	63.094	0.356
MIS4	D11-1-100A	Quartzite	156.000	2.149	72.592	113.425	0.667
MIS4	D11-1-90D1	Quartzite	52.300	2.450	21.345	33.351	0.224
MIS4	D11-1-95A	Quartzite	68.900	2.031	33.917	52.995	0.295
MIS4	D11-1-95B	Quartzite	89.500	2.160	41.432	64.737	0.383
MIS4	D11-1-97A1	Quartzite	28.300	1.925	14.701	22.971	0.121
MIS4	D11-1-98B1	Quartzite	87.000	1.913	45.486	71.072	0.372
MIS4	D11-1-98C1	Quartzite	92.700	2.091	44.340	69.281	0.396
MIS4	D11-1-98D	Quartzite	77.800	1.843	42.225	65.976	0.333
MIS4	D11-1-85C1	Quartzite	420.800	1.996	210.822	426.914	2.288
MIS4	D11-1-91A1	Quartzite	202.400	1.962	103.146	208.870	1.149
MIS4	D11-1-91A2	Quartzite	250.200	2.174	115.072	233.021	1.379
MIS4	D11-1-91B3	Quartzite	322.300	1.885	171.002	346.280	2.015
MIS4	D11-1-91B5	Quartzite	174.000	2.220	78.368	158.696	0.922
MIS4	D11-1-91C3	Quartzite	170.300	1.962	86.790	175.750	0.988
MIS4	D11-1-94B2	Quartzite	206.600	1.828	113.031	228.889	1.174
MIS4	D11-1-94B3	Quartzite	240.500	1.784	134.809	272.989	1.379
MIS4	D11-1-94D2	Quartzite	159.000	1.966	80.871	163.764	0.908
MIS4	D11-1-97C	Quartzite	386.400	1.833	210.789	426.848	2.147

MIS4 conditions without a Paleo-Agulhas plain silcrete source

Table B222. ACM-R net-return rates (Rs) for heat-treated silcrete assuming both the insulated and exposed heating scenarios and untreated silcrete experimental blocks during MIS4 conditions without a Paleo-Agulhas plain silcrete source.

Model Conditions	Heating Scenario	Block	Raw Material	Cutting Edge Complete Blades (cm)	Total Flaked Core Mass (kg)	CE Blades (cm) / Total Flaked Core Mass (kg)	Cutting Edge * Durability (e * d)	Rs
MIS4-Without Paleo-Agulhas Silcrete	Insulated	D9-1-10b	Silcrete	311.700	2.350	132.646	374.566	2.103
MIS4-Without Paleo-Agulhas Silcrete	Insulated	D9-1-12b	Silcrete	329.100	2.200	149.586	422.403	2.220
MIS4-Without Paleo-Agulhas Silcrete	Insulated	D9-1-12d	Silcrete	307.900	2.286	134.672	380.289	2.077
MIS4-Without Paleo-Agulhas Silcrete	Insulated	E3-1-1b	Silcrete	479.300	1.933	247.894	700.005	3.234
MIS4-Without Paleo-	Insulated	E3-1-	Silcrete	362.400	2.588	140.046	395.463	2.445

Agulhas Silcrete		5p						
MIS4-Without Paleo-Agulhas Silcrete	Insulated	E3-1-6a	Silcrete	409.700	2.196	186.561	526.814	2.764
MIS4-Without Paleo-Agulhas Silcrete	Insulated	E3-1-6c	Silcrete	451.500	2.436	185.345	523.378	3.046
MIS4-Without Paleo-Agulhas Silcrete	Insulated	I14-2-16l	Silcrete	582.400	2.356	247.176	697.977	3.929
MIS4-Without Paleo-Agulhas Silcrete	Exposed	D9-1-10b	Silcrete	311.700	2.350	132.646	374.566	1.941
MIS4-Without Paleo-Agulhas Silcrete	Exposed	D9-1-12b	Silcrete	329.100	2.200	149.586	422.403	2.049
MIS4-Without Paleo-Agulhas Silcrete	Exposed	D9-1-12d	Silcrete	307.900	2.286	134.672	380.289	1.917
MIS4-Without Paleo-Agulhas Silcrete	Exposed	E3-1-1b	Silcrete	479.300	1.933	247.894	700.005	2.984
MIS4-Without Paleo-Agulhas Silcrete	Exposed	E3-1-5p	Silcrete	362.400	2.588	140.046	395.463	2.256
MIS4-Without Paleo-Agulhas Silcrete	Exposed	E3-1-6a	Silcrete	409.700	2.196	186.561	526.814	2.551
MIS4-Without Paleo-Agulhas Silcrete	Exposed	E3-1-6c	Silcrete	451.500	2.436	185.345	523.378	2.811
MIS4-Without Paleo-Agulhas Silcrete	Exposed	I14-2-16l	Silcrete	582.400	2.356	247.176	697.977	3.626
MIS4-Without Paleo-Agulhas Silcrete	Untreated	D9-1-10a	Silcrete	89.500	1.980	45.198	85.016	0.537
MIS4-Without Paleo-Agulhas Silcrete	Untreated	D9-1-12a	Silcrete	179.700	2.250	79.881	150.251	1.078
MIS4-Without Paleo-Agulhas Silcrete	Untreated	D9-1-12c	Silcrete	97.000	1.807	53.677	100.965	0.582
MIS4-Without Paleo-Agulhas Silcrete	Untreated	E3-1-1A	Silcrete	150.800	2.070	72.865	137.055	0.905
MIS4-Without Paleo-Agulhas Silcrete	Untreated	E3-1-5n	Silcrete	223.700	2.460	90.944	171.061	1.342
MIS4-Without Paleo-Agulhas Silcrete	Untreated	E3-1-5o	Silcrete	255.100	2.505	101.844	191.565	1.530
MIS4-Without Paleo-Agulhas Silcrete	Untreated	E3-1-6b	Silcrete	93.800	1.691	55.470	104.337	0.563
MIS4-Without Paleo-Agulhas Silcrete	Untreated	I14-2-16a	Silcrete	64.200	2.895	22.175	41.711	0.385

MIS4 conditions with a Paleo-Agulhas plain silcrete source

Table B223. ACM-R net-return rates (Rs) for heat-treated silcrete assuming both the insulated and exposed heating scenarios and untreated silcrete experimental blocks during MIS4 conditions with a Paleo-Agulhas plain silcrete source.

Model Conditions	Heating Scenario	Block	Raw Material	Cutting Edge Complete Blades (cm)	Total Flaked Core Mass (kg)	CE Blades (cm) / Total Flaked Core Mass (kg)	Cutting Edge * Durability (e * d)	Rs
MIS4-With Paleo-Agulhas Silcrete	Insulated	D9-1-10b	Silcrete	311.700	2.350	132.646	374.566	5.673
MIS4-With Paleo-Agulhas Silcrete	Insulated	D9-1-12b	Silcrete	329.100	2.200	149.586	422.403	5.990
MIS4-With Paleo-Agulhas Silcrete	Insulated	D9-1-12d	Silcrete	307.900	2.286	134.672	380.289	5.604
MIS4-With Paleo-Agulhas Silcrete	Insulated	E3-1-1b	Silcrete	479.300	1.933	247.894	700.005	8.724
MIS4-With Paleo-Agulhas Silcrete	Insulated	E3-1-5p	Silcrete	362.400	2.588	140.046	395.463	6.596
MIS4-With Paleo-Agulhas Silcrete	Insulated	E3-1-6a	Silcrete	409.700	2.196	186.561	526.814	7.457

MIS4-With Paleo-Agulhas Silcrete	Insulated	E3-1-6c	Silcrete	451.500	2.436	185.345	523.378	8.218
MIS4-With Paleo-Agulhas Silcrete	Insulated	I14-2-16l	Silcrete	582.400	2.356	247.176	697.977	10.601
MIS4-With Paleo-Agulhas Silcrete	Exposed	D9-1-10b	Silcrete	311.700	2.350	132.646	374.566	4.629
MIS4-With Paleo-Agulhas Silcrete	Exposed	D9-1-12b	Silcrete	329.100	2.200	149.586	422.403	4.887
MIS4-With Paleo-Agulhas Silcrete	Exposed	D9-1-12d	Silcrete	307.900	2.286	134.672	380.289	4.573
MIS4-With Paleo-Agulhas Silcrete	Exposed	E3-1-1b	Silcrete	479.300	1.933	247.894	700.005	7.118
MIS4-With Paleo-Agulhas Silcrete	Exposed	E3-1-5p	Silcrete	362.400	2.588	140.046	395.463	5.382
MIS4-With Paleo-Agulhas Silcrete	Exposed	E3-1-6a	Silcrete	409.700	2.196	186.561	526.814	6.084
MIS4-With Paleo-Agulhas Silcrete	Exposed	E3-1-6c	Silcrete	451.500	2.436	185.345	523.378	6.705
MIS4-With Paleo-Agulhas Silcrete	Exposed	I14-2-16l	Silcrete	582.400	2.356	247.176	697.977	8.649
MIS4-With Paleo-Agulhas Silcrete	Untreated	D9-1-10a	Silcrete	89.500	1.980	45.198	85.016	3.357
MIS4-With Paleo-Agulhas Silcrete	Untreated	D9-1-12a	Silcrete	179.700	2.250	79.881	150.251	6.741
MIS4-With Paleo-Agulhas Silcrete	Untreated	D9-1-12c	Silcrete	97.000	1.807	53.677	100.965	3.639
MIS4-With Paleo-Agulhas Silcrete	Untreated	E3-1-1A	Silcrete	150.800	2.070	72.865	137.055	5.657
MIS4-With Paleo-Agulhas Silcrete	Untreated	E3-1-5n	Silcrete	223.700	2.460	90.944	171.061	8.392
MIS4-With Paleo-Agulhas Silcrete	Untreated	E3-1-5o	Silcrete	255.100	2.505	101.844	191.565	9.570
MIS4-With Paleo-Agulhas Silcrete	Untreated	E3-1-6b	Silcrete	93.800	1.691	55.470	104.337	3.519
MIS4-With Paleo-Agulhas Silcrete	Untreated	I14-2-16a	Silcrete	64.200	2.895	22.175	41.711	2.408

MIS5 conditions

Table B224. ACM-R net-return rates (Rq) for quartzite experimental blocks during MIS5 conditions.

Model Conditions	Block	Raw Material	Cutting Edge Complete Blades (cm)	Total Flaked Core Mass (kg)	CE Blades (cm) / Total Flaked Core Mass (kg)	Cutting Edge * Durability (e * d)	Rq-e x d
MIS5	C9-1-1B8	Quartzite	92.600	1.920	48.223	75.349	5.107
MIS5	C9-1-1B9	Quartzite	83.200	2.060	40.380	63.094	4.588
MIS5	D11-1-100A	Quartzite	156.000	2.149	72.592	113.425	8.491
MIS5	D11-1-90D1	Quartzite	52.300	2.450	21.345	33.351	2.847
MIS5	D11-1-95A	Quartzite	68.900	2.031	33.917	52.995	3.750
MIS5	D11-1-95B	Quartzite	89.500	2.160	41.432	64.737	4.871
MIS5	D11-1-97A1	Quartzite	28.300	1.925	14.701	22.971	1.540
MIS5	D11-1-98B1	Quartzite	87.000	1.913	45.486	71.072	4.735
MIS5	D11-1-98C1	Quartzite	92.700	2.091	44.340	69.281	5.045
MIS5	D11-1-98D	Quartzite	77.800	1.843	42.225	65.976	4.235
MIS5	D11-1-85C1	Quartzite	420.800	1.996	210.822	426.914	29.683
MIS5	D11-1-91A1	Quartzite	202.400	1.962	103.146	208.870	14.277

MIS5	D11-1-91A2	Quartzite	250.200	2.174	115.072	233.021	17.649
MIS5	D11-1-91B3	Quartzite	322.300	1.885	171.002	346.280	22.735
MIS5	D11-1-91B5	Quartzite	174.000	2.220	78.368	158.696	12.274
MIS5	D11-1-91C3	Quartzite	170.300	1.962	86.790	175.750	12.013
MIS5	D11-1-94B2	Quartzite	206.600	1.828	113.031	228.889	14.573
MIS5	D11-1-94B3	Quartzite	240.500	1.784	134.809	272.989	16.965
MIS5	D11-1-94D2	Quartzite	159.000	1.966	80.871	163.764	11.216
MIS5	D11-1-97C	Quartzite	386.400	1.833	210.789	426.848	27.256

Table B225. ACM-R net-return rates (Rs) for heat-treated silcrete assuming both the insulated and exposed heating scenarios and untreated silcrete experimental blocks during MIS5 conditions.

Model Conditions	Heating Scenario	Block	Raw Material	Cutting Edge Complete Blades (cm)	Total Flaked Core Mass (kg)	CE Blades (cm) / Total Flaked Core Mass (kg)	Cutting Edge * Durability (e * d)	Rs
MIS5	Insulated	D9-1-10b	Silcrete	311.700	2.350	132.646	374.566	1.731
MIS5	Insulated	D9-1-12b	Silcrete	329.100	2.200	149.586	422.403	1.827
MIS5	Insulated	D9-1-12d	Silcrete	307.900	2.286	134.672	380.289	1.710
MIS5	Insulated	E3-1-1b	Silcrete	479.300	1.933	247.894	700.005	2.661
MIS5	Insulated	E3-1-5p	Silcrete	362.400	2.588	140.046	395.463	2.012
MIS5	Insulated	E3-1-6a	Silcrete	409.700	2.196	186.561	526.814	2.275
MIS5	Insulated	E3-1-6c	Silcrete	451.500	2.436	185.345	523.378	2.507
MIS5	Insulated	I14-2-16l	Silcrete	582.400	2.356	247.176	697.977	3.234
MIS5	Exposed	D9-1-10b	Silcrete	311.700	2.350	132.646	374.566	1.941
MIS5	Exposed	D9-1-12b	Silcrete	329.100	2.200	149.586	422.403	2.049
MIS5	Exposed	D9-1-12d	Silcrete	307.900	2.286	134.672	380.289	1.917
MIS5	Exposed	E3-1-1b	Silcrete	479.300	1.933	247.894	700.005	2.984
MIS5	Exposed	E3-1-5p	Silcrete	362.400	2.588	140.046	395.463	2.256
MIS5	Exposed	E3-1-6a	Silcrete	409.700	2.196	186.561	526.814	2.551
MIS5	Exposed	E3-1-6c	Silcrete	451.500	2.436	185.345	523.378	2.811
MIS5	Exposed	I14-2-16l	Silcrete	582.400	2.356	247.176	697.977	3.626
MIS5	Untreated	D9-1-10a	Silcrete	89.500	1.980	45.198	85.016	0.537
MIS5	Untreated	D9-1-12a	Silcrete	179.700	2.250	79.881	150.251	1.078
MIS5	Untreated	D9-1-12c	Silcrete	97.000	1.807	53.677	100.965	0.582
MIS5	Untreated	E3-1-1A	Silcrete	150.800	2.070	72.865	137.055	0.905
MIS5	Untreated	E3-1-5n	Silcrete	223.700	2.460	90.944	171.061	1.342
MIS5	Untreated	E3-1-5o	Silcrete	255.100	2.505	101.844	191.565	1.530
MIS5	Untreated	E3-1-6b	Silcrete	93.800	1.691	55.470	104.337	0.563
MIS5	Untreated	I14-2-16a	Silcrete	64.200	2.895	22.175	41.711	0.385

MIS6 conditions with or without a Paleo-Agulhas plain silcrete source

Table B226. ACM-R net-return rates (Rq) for quartzite experimental blocks during MIS6 conditions with or without a Paleo-Agulhas plain silcrete source.

Model Conditions	Block	Raw Material	Cutting Edge Complete Blades (cm)	Total Flaked Core Mass (kg)	CE Blades (cm) / Total Flaked Core Mass (kg)	Cutting Edge * Durability (e * d)	Rq
MIS6	C9-1-1B8	Quartzite	92.600	1.920	48.223	75.349	1.410
MIS6	C9-1-1B9	Quartzite	83.200	2.060	40.380	63.094	1.267
MIS6	D11-1-100A	Quartzite	156.000	2.149	72.592	113.425	2.366
MIS6	D11-1-90D1	Quartzite	52.300	2.450	21.345	33.351	0.793
MIS6	D11-1-95A	Quartzite	68.900	2.031	33.917	52.995	1.045
MIS6	D11-1-95B	Quartzite	89.500	2.160	41.432	64.737	1.358
MIS6	D11-1-97A1	Quartzite	28.300	1.925	14.701	22.971	0.429
MIS6	D11-1-98B1	Quartzite	87.000	1.913	45.486	71.072	1.320
MIS6	D11-1-98C1	Quartzite	92.700	2.091	44.340	69.281	1.406
MIS6	D11-1-98D	Quartzite	77.800	1.843	42.225	65.976	1.180
MIS6	D11-1-85C1	Quartzite	420.800	1.996	210.822	426.914	8.272
MIS6	D11-1-91A1	Quartzite	202.400	1.962	103.146	208.870	3.979
MIS6	D11-1-91A2	Quartzite	250.200	2.174	115.072	233.021	4.919
MIS6	D11-1-91B3	Quartzite	322.300	1.885	171.002	346.280	6.336
MIS6	D11-1-91B5	Quartzite	174.000	2.220	78.368	158.696	3.421
MIS6	D11-1-91C3	Quartzite	170.300	1.962	86.790	175.750	3.348
MIS6	D11-1-94B2	Quartzite	206.600	1.828	113.031	228.889	4.061
MIS6	D11-1-94B3	Quartzite	240.500	1.784	134.809	272.989	4.728
MIS6	D11-1-94D2	Quartzite	159.000	1.966	80.871	163.764	3.126
MIS6	D11-1-97C	Quartzite	386.400	1.833	210.789	426.848	7.596

MIS6 conditions without a Paleo-Agulhas plain silcrete source

Table B227. ACM-R net-return rates (Rs) for heat-treated silcrete assuming both the insulated and exposed heating scenarios and untreated silcrete experimental blocks during MIS6 conditions without a Paleo-Agulhas plain silcrete source.

Model Conditions	Heating Scenario	Block	Raw Material	Cutting Edge Complete Blades (cm)	Total Flaked Core Mass (kg)	CE Blades (cm) / Total Flaked Core Mass (kg)	Cutting Edge * Durability (e * d)	Rs
MIS6-Without Paleo-Agulhas Silcrete	Insulated	D9-1-10b	Silcrete	311.700	2.350	132.646	374.566	1.731
MIS6-Without Paleo-Agulhas Silcrete	Insulated	D9-1-12b	Silcrete	329.100	2.200	149.586	422.403	1.827
MIS6-Without Paleo-Agulhas Silcrete	Insulated	D9-1-12d	Silcrete	307.900	2.286	134.672	380.289	1.710
MIS6-Without Paleo-Agulhas Silcrete	Insulated	E3-1-1b	Silcrete	479.300	1.933	247.894	700.005	2.661

MIS6-Without Paleo-Agulhas Silcrete	Insulated	E3-1-5p	Silcrete	362.400	2.588	140.046	395.463	2.012
MIS6-Without Paleo-Agulhas Silcrete	Insulated	E3-1-6a	Silcrete	409.700	2.196	186.561	526.814	2.275
MIS6-Without Paleo-Agulhas Silcrete	Insulated	E3-1-6c	Silcrete	451.500	2.436	185.345	523.378	2.507
MIS6-Without Paleo-Agulhas Silcrete	Insulated	I14-2-16l	Silcrete	582.400	2.356	247.176	697.977	3.234
MIS6-Without Paleo-Agulhas Silcrete	Exposed	D9-1-10b	Silcrete	311.700	2.350	132.646	374.566	1.941
MIS6-Without Paleo-Agulhas Silcrete	Exposed	D9-1-12b	Silcrete	329.100	2.200	149.586	422.403	2.049
MIS6-Without Paleo-Agulhas Silcrete	Exposed	D9-1-12d	Silcrete	307.900	2.286	134.672	380.289	1.917
MIS6-Without Paleo-Agulhas Silcrete	Exposed	E3-1-1b	Silcrete	479.300	1.933	247.894	700.005	2.984
MIS6-Without Paleo-Agulhas Silcrete	Exposed	E3-1-5p	Silcrete	362.400	2.588	140.046	395.463	2.256
MIS6-Without Paleo-Agulhas Silcrete	Exposed	E3-1-6a	Silcrete	409.700	2.196	186.561	526.814	2.551
MIS6-Without Paleo-Agulhas Silcrete	Exposed	E3-1-6c	Silcrete	451.500	2.436	185.345	523.378	2.811
MIS6-Without Paleo-Agulhas Silcrete	Exposed	I14-2-16l	Silcrete	582.400	2.356	247.176	697.977	3.626
MIS6-Without Paleo-Agulhas Silcrete	Untreated	D9-1-10a	Silcrete	89.500	1.980	45.198	85.016	0.537
MIS6-Without Paleo-Agulhas Silcrete	Untreated	D9-1-12a	Silcrete	179.700	2.250	79.881	150.251	1.078
MIS6-Without Paleo-Agulhas Silcrete	Untreated	D9-1-12c	Silcrete	97.000	1.807	53.677	100.965	0.582
MIS6-Without Paleo-Agulhas Silcrete	Untreated	E3-1-1A	Silcrete	150.800	2.070	72.865	137.055	0.905
MIS6-Without Paleo-Agulhas Silcrete	Untreated	E3-1-5n	Silcrete	223.700	2.460	90.944	171.061	1.342
MIS6-Without Paleo-Agulhas Silcrete	Untreated	E3-1-5o	Silcrete	255.100	2.505	101.844	191.565	1.530
MIS6-Without Paleo-Agulhas Silcrete	Untreated	E3-1-6b	Silcrete	93.800	1.691	55.470	104.337	0.563
MIS6-Without Paleo-Agulhas Silcrete	Untreated	I14-2-16a	Silcrete	64.200	2.895	22.175	41.711	0.385

MIS6 conditions with a Paleo-Agulhas plain silcrete source

Table B228. ACM-R net-return rates (Rs) for heat-treated silcrete assuming both the insulated and exposed heating scenarios and untreated silcrete experimental blocks during MIS6 conditions with a Paleo-Agulhas plain silcrete source.

Model Conditions	Heating Scenario	Block	Raw Material	Cutting Edge Complete Blades (cm)	Total Flaked Blade Mass (kg)	CE Blades (cm) / Total Flaked Blade Mass (kg)	Cutting Edge * Durability (e * d)	Rs
MIS6-With Paleo-Agulhas Silcrete	Insulated	D9-1-10b	Silcrete	311.700	2.350	132.646	374.566	3.591
MIS6-With Paleo-Agulhas Silcrete	Insulated	D9-1-12b	Silcrete	329.100	2.200	149.586	422.403	3.791
MIS6-With Paleo-Agulhas Silcrete	Insulated	D9-1-12d	Silcrete	307.900	2.286	134.672	380.289	3.547
MIS6-With Paleo-Agulhas Silcrete	Insulated	E3-1-1b	Silcrete	479.300	1.933	247.894	700.005	5.521
MIS6-With Paleo-Agulhas Silcrete	Insulated	E3-1-5p	Silcrete	362.400	2.588	140.046	395.463	4.175

MIS6-With Paleo-Agulhas Silcrete	Insulated	E3-1-6a	Silcrete	409.700	2.196	186.561	526.814	4.719
MIS6-With Paleo-Agulhas Silcrete	Insulated	E3-1-6c	Silcrete	451.500	2.436	185.345	523.378	5.201
MIS6-With Paleo-Agulhas Silcrete	Insulated	I14-2-16l	Silcrete	582.400	2.356	247.176	697.977	6.709
MIS6-With Paleo-Agulhas Silcrete	Exposed	D9-1-10b	Silcrete	311.700	2.350	132.646	374.566	4.629
MIS6-With Paleo-Agulhas Silcrete	Exposed	D9-1-12b	Silcrete	329.100	2.200	149.586	422.403	4.887
MIS6-With Paleo-Agulhas Silcrete	Exposed	D9-1-12d	Silcrete	307.900	2.286	134.672	380.289	4.573
MIS6-With Paleo-Agulhas Silcrete	Exposed	E3-1-1b	Silcrete	479.300	1.933	247.894	700.005	7.118
MIS6-With Paleo-Agulhas Silcrete	Exposed	E3-1-5p	Silcrete	362.400	2.588	140.046	395.463	5.382
MIS6-With Paleo-Agulhas Silcrete	Exposed	E3-1-6a	Silcrete	409.700	2.196	186.561	526.814	6.084
MIS6-With Paleo-Agulhas Silcrete	Exposed	E3-1-6c	Silcrete	451.500	2.436	185.345	523.378	6.705
MIS6-With Paleo-Agulhas Silcrete	Exposed	I14-2-16l	Silcrete	582.400	2.356	247.176	697.977	8.649
MIS6-With Paleo-Agulhas Silcrete	Untreated	D9-1-10a	Silcrete	89.500	1.980	45.198	85.016	3.357
MIS6-With Paleo-Agulhas Silcrete	Untreated	D9-1-12a	Silcrete	179.700	2.250	79.881	150.251	6.741
MIS6-With Paleo-Agulhas Silcrete	Untreated	D9-1-12c	Silcrete	97.000	1.807	53.677	100.965	3.639
MIS6-With Paleo-Agulhas Silcrete	Untreated	E3-1-1A	Silcrete	150.800	2.070	72.865	137.055	5.657
MIS6-With Paleo-Agulhas Silcrete	Untreated	E3-1-5n	Silcrete	223.700	2.460	90.944	171.061	8.392
MIS6-With Paleo-Agulhas Silcrete	Untreated	E3-1-5o	Silcrete	255.100	2.505	101.844	191.565	9.570
MIS6-With Paleo-Agulhas Silcrete	Untreated	E3-1-6b	Silcrete	93.800	1.691	55.470	104.337	3.519
MIS6-With Paleo-Agulhas Silcrete	Untreated	I14-2-16a	Silcrete	64.200	2.895	22.175	41.711	2.408

ACM – Model condition variable outcomes

Coastline position and raw material source distribution

Table B229. Summary statistics and test results of ACM-R net-return rates (Rq and Rs) when only t_s time-cost (travel and search time) is considered during all model conditions.

	MIS4 without Paleo-Agulhas plain silcrete			MIS4 with Paleo-Agulhas plain silcrete			MIS5			MIS6 without Paleo-Agulhas plain silcrete			MIS6 with Paleo-Agulhas plain silcrete		
	Quartzite (Rq)	Untreated Silcrete (Rs)	Heat-treated Silcrete (Rs)	Quartzite (Rq)	Untreated Silcrete (Rs)	Heat-treated Silcrete (Rs)	Quartzite (Rq)	Untreated Silcrete (Rs)	Heat-treated Silcrete (Rs)	Quartzite (Rq)	Untreated Silcrete (Rs)	Heat-treated Silcrete (Rs)	Quartzite (Rq)	Untreated Silcrete (Rs)	Heat-treated Silcrete (Rs)

8	31.855	31.033	38.910	40.744	58.700	47.609	9.704	3.303
8	6.081	4.310	8.318	9.683	17.127	14.281	4.685	1.608
20	2.694	0.906	5.795	6.578	17.456	9.625	4.877	1.055
8	3.062	2.983	3.741	3.917	5.643	4.577	0.933	0.318
8	0.585	0.414	0.800	0.931	1.646	1.373	0.450	0.154
20	2.694	0.906	5.795	6.578	17.456	9.625	4.877	1.055
8	3.062	2.983	3.741	3.917	5.643	4.577	0.933	0.317
8	0.585	0.414	0.800	0.931	1.646	1.373	0.450	0.154
20	10.353	3.482	22.273	25.286	67.096	36.996	18.745	4.045
8	31.855	31.033	38.910	40.744	58.700	47.609	9.704	3.316
8	6.081	4.310	8.318	9.683	17.127	14.281	4.685	1.614
20	0.730	0.246	1.572	1.784	4.734	2.611	1.323	0.286
8	3.062	2.983	3.741	3.917	5.643	4.577	0.933	0.316
8	0.585	0.414	0.800	0.931	1.646	1.373	0.450	0.154
20	0.730	0.246	1.572	1.784	4.734	2.611	1.323	0.286
n sample blocks	First Quartile	Min	Median	Mean	Max	Third Quartile	SD	Bootstrapped SE*

6.474	47.219	34.270	0.623	4.540	3.293	0.621	4.538	3.296
3.153	12.835	6.530	0.303	1.233	0.628	0.302	1.233	0.629
2.067	8.645	4.511	2.067	8.645	4.511	7.928	33.214	17.357
Margin of error (95% CI)	Bootstrapped Upper 95% CI*	Bootstrapped Lower 95% CI*	0.620	4.537	3.297	0.560	2.344	1.224
			0.302	1.233	0.628	3.164	12.847	6.519
			0.560	2.344	1.224	6.500	47.245	34.244

*Samples bootstrapped 10000 times.

MIS4 without a Paleo-Agulhas plain silcrete source

Table B230. ACM-R net-return rates (Rq) for quartzite experimental blocks when only t_s time-cost (travel and search time) is considered during MIS4 conditions without a Paleo-Agulhas plain silcrete source.

Block	Raw Material	Cutting Edge Complete Blades (cm)	Total Flaked Core Mass (kg)	CE Blades (cm) / Total Flaked Core Mass (kg)	Cutting Edge * Durability (e * d)	ts-Travel and search time (min)/Total Flaked Core Mass (kg)	Rq
C9-1-1B8	Quartzite	92.600	1.920	48.223	75.349	93.74	0.804
C9-1-1B9	Quartzite	83.200	2.060	40.380	63.094	87.36	0.722
D11-1-100A	Quartzite	156.000	2.149	72.592	113.425	83.76	1.354
D11-1-90D1	Quartzite	52.300	2.450	21.345	33.351	73.46	0.454
D11-1-95A	Quartzite	68.900	2.031	33.917	52.995	88.61	0.598
D11-1-95B	Quartzite	89.500	2.160	41.432	64.737	83.33	0.777
D11-1-97A1	Quartzite	28.300	1.925	14.701	22.971	93.51	0.246

D11-1-98B1	Quartzite	87.000	1.913	45.486	71.072	94.11	0.755
D11-1-98C1	Quartzite	92.700	2.091	44.340	69.281	86.10	0.805
D11-1-98D	Quartzite	77.800	1.843	42.225	65.976	97.69	0.675
D11-1-85C1	Quartzite	420.800	1.996	210.822	426.914	90.18	4.734
D11-1-91A1	Quartzite	202.400	1.962	103.146	208.870	91.73	2.277
D11-1-91A2	Quartzite	250.200	2.174	115.072	233.021	82.79	2.815
D11-1-91B3	Quartzite	322.300	1.885	171.002	346.280	95.50	3.626
D11-1-91B5	Quartzite	174.000	2.220	78.368	158.696	81.07	1.958
D11-1-91C3	Quartzite	170.300	1.962	86.790	175.750	91.73	1.916
D11-1-94B2	Quartzite	206.600	1.828	113.031	228.889	98.48	2.324
D11-1-94B3	Quartzite	240.500	1.784	134.809	272.989	100.90	2.706
D11-1-94D2	Quartzite	159.000	1.966	80.871	163.764	91.55	1.789
D11-1-97C	Quartzite	386.400	1.833	210.789	426.848	98.19	4.347

Table B231. ACM-R net-return rates (Rs) for heat-treated silcrete assuming both the insulated and exposed heating scenarios and untreated silcrete experimental blocks when only t_s time-cost (travel and search time) is considered during MIS4 conditions without a Paleo-Agulhas plain silcrete source.

Block	Sample Type	Raw Material	Cutting Edge Complete Blades (cm)	Total Flaked Core Mass (kg)	CE Blades (cm) / Total Flaked Core Mass (kg)	Cutting Edge * Durability (e * d)	ts-Travel and search time (min)/Total Flaked Core Mass (kg)	Rs
D9-1-10b	Heat-treated	Silcrete	311.700	2.350	132.646	374.566	124.02	3.020
D9-1-12b	Heat-treated	Silcrete	329.100	2.200	149.586	422.403	132.47	3.189
D9-1-12d	Heat-treated	Silcrete	307.900	2.286	134.672	380.289	127.47	2.983
E3-1-1b	Heat-treated	Silcrete	479.300	1.933	247.894	700.005	150.73	4.644
E3-1-5p	Heat-treated	Silcrete	362.400	2.588	140.046	395.463	112.62	3.511
E3-1-6a	Heat-treated	Silcrete	409.700	2.196	186.561	526.814	132.71	3.970
E3-1-6c	Heat-treated	Silcrete	451.500	2.436	185.345	523.378	119.64	4.375
I14-2-16l	Heat-treated	Silcrete	582.400	2.356	247.176	697.977	123.69	5.643
D9-1-10a	Untreated	Silcrete	89.500	1.980	45.198	85.016	147.18	0.578
D9-1-12a	Untreated	Silcrete	179.700	2.250	79.881	150.251	129.55	1.160
D9-1-12c	Untreated	Silcrete	97.000	1.807	53.677	100.965	161.27	0.626
E3-1-1A	Untreated	Silcrete	150.800	2.070	72.865	137.055	140.82	0.973
E3-1-5n	Untreated	Silcrete	223.700	2.460	90.944	171.061	118.48	1.444
E3-1-5o	Untreated	Silcrete	255.100	2.505	101.844	191.565	116.35	1.646
E3-1-	Untreate	Silcrete	93.800	1.691	55.470	104.337	172.34	0.605

6b	d							
I14-2-16a	Untreated	Silcrete	64.200	2.895	22.175	41.711	100.66	0.414

MIS4 with a Paleo-Agulhas plain silcrete source

Table B232. ACM-R net-return rates (Rq) for quartzite experimental blocks when only t_s time-cost (travel and search time) is considered during MIS4 conditions with a Paleo-Agulhas plain silcrete source.

Block	Raw Material	Cutting Edge Complete Blades (cm)	Total Flaked Core Mass (kg)	CE Blades (cm) / Total Flaked Core Mass (kg)	Cutting Edge * Durability (e * d)	ts-Travel and search time (min)/Total Flaked Core Mass (kg)	Rq
C9-1-1B8	Quartzite	92.600	1.920	48.223	75.349	93.738	0.804
C9-1-1B9	Quartzite	83.200	2.060	40.380	63.094	87.361	0.722
D11-1-100A	Quartzite	156.000	2.149	72.592	113.425	83.760	1.354
D11-1-90D1	Quartzite	52.300	2.450	21.345	33.351	73.462	0.454
D11-1-95A	Quartzite	68.900	2.031	33.917	52.995	88.608	0.598
D11-1-95B	Quartzite	89.500	2.160	41.432	64.737	83.326	0.777
D11-1-97A1	Quartzite	28.300	1.925	14.701	22.971	93.506	0.246
D11-1-98B1	Quartzite	87.000	1.913	45.486	71.072	94.110	0.755
D11-1-98C1	Quartzite	92.700	2.091	44.340	69.281	86.097	0.805
D11-1-98D	Quartzite	77.800	1.843	42.225	65.976	97.692	0.675
D11-1-85C1	Quartzite	420.800	1.996	210.822	426.914	90.180	4.734
D11-1-91A1	Quartzite	202.400	1.962	103.146	208.870	91.730	2.277
D11-1-91A2	Quartzite	250.200	2.174	115.072	233.021	82.786	2.815
D11-1-91B3	Quartzite	322.300	1.885	171.002	346.280	95.502	3.626
D11-1-91B5	Quartzite	174.000	2.220	78.368	158.696	81.071	1.958
D11-1-91C3	Quartzite	170.300	1.962	86.790	175.750	91.734	1.916
D11-1-94B2	Quartzite	206.600	1.828	113.031	228.889	98.479	2.324
D11-1-94B3	Quartzite	240.500	1.784	134.809	272.989	100.897	2.706
D11-	Quartzite	159.000	1.966	80.871	163.764	91.552	1.789

1-94D2							
D11-1-97C	Quartzite	386.400	1.833	210.789	426.848	98.194	4.347

Table B233. ACM-R net-return rates (Rs) for heat-treated silcrete assuming both the insulated and exposed heating scenarios and untreated silcrete experimental blocks when only t_s time-cost (travel and search time) is considered during MIS4 conditions with a Paleo-Agulhas plain silcrete source.

Block	Sample Type	Raw Material	Cutting Edge Complete Blades (cm)	Total Flaked Core Mass (kg)	CE Blades (cm) / Total Flaked Core Mass (kg)	Cutting Edge * Durability (e * d)	*ts*-Travel and search time (min)/Total Flaked Core Mass (kg)	Rs
D9-1-10b	Heat-treated	Silcrete	311.700	2.350	132.646	374.566	11.923	31.416
D9-1-12b	Heat-treated	Silcrete	329.100	2.200	149.586	422.403	12.734	33.170
D9-1-12d	Heat-treated	Silcrete	307.900	2.286	134.672	380.289	12.254	31.033
E3-1-1b	Heat-treated	Silcrete	479.300	1.933	247.894	700.005	14.490	48.309
E3-1-5p	Heat-treated	Silcrete	362.400	2.588	140.046	395.463	10.827	36.526
E3-1-6a	Heat-treated	Silcrete	409.700	2.196	186.561	526.814	12.758	41.294
E3-1-6c	Heat-treated	Silcrete	451.500	2.436	185.345	523.378	11.501	45.507
I14-2-16l	Heat-treated	Silcrete	582.400	2.356	247.176	697.977	11.891	58.700
D9-1-10a	Untreated	Silcrete	89.500	1.980	45.198	85.016	14.149	6.009
D9-1-12a	Untreated	Silcrete	179.700	2.250	79.881	150.251	12.454	12.065
D9-1-12c	Untreated	Silcrete	97.000	1.807	53.677	100.965	15.504	6.512
E3-1-1A	Untreated	Silcrete	150.800	2.070	72.865	137.055	13.537	10.124
E3-1-5n	Untreated	Silcrete	223.700	2.460	90.944	171.061	11.390	15.019
E3-1-5o	Untreated	Silcrete	255.100	2.505	101.844	191.565	11.185	17.127
E3-1-6b	Untreated	Silcrete	93.800	1.691	55.470	104.337	16.568	6.297
I14-2-16a	Untreated	Silcrete	64.200	2.895	22.175	41.711	9.677	4.310

MIS5

Table B234. ACM-R net-return rates (Rq) for quartzite experimental blocks when only t_s time-cost (travel and search time) is considered during MIS5 conditions.

Block	Raw Material	Cutting Edge Complete Blades (cm)	Total Flaked Core Mass (kg)	CE Blades (cm) / Total Flaked Core Mass (kg)	Cutting Edge * Durability (e * d)	ts-Travel and search time (min)/Total Flaked Core Mass (kg)	Rq
C9-1-1B8	Quartzite	92.600	1.920	48.223	75.349	6.61	11.393
C9-1-1B9	Quartzite	83.200	2.060	40.380	63.094	6.16	10.236
D11-1-100A	Quartzite	156.000	2.149	72.592	113.425	5.91	19.193

D11-1-90D1	Quartzite	52.300	2.450	21.345	33.351	5.18	6.435
D11-1-95A	Quartzite	68.900	2.031	33.917	52.995	6.25	8.477
D11-1-95B	Quartzite	89.500	2.160	41.432	64.737	5.88	11.011
D11-1-97A1	Quartzite	28.300	1.925	14.701	22.971	6.60	3.482
D11-1-98B1	Quartzite	87.000	1.913	45.486	71.072	6.64	10.704
D11-1-98C1	Quartzite	92.700	2.091	44.340	69.281	6.07	11.405
D11-1-98D	Quartzite	77.800	1.843	42.225	65.976	6.89	9.572
D11-1-85C1	Quartzite	420.800	1.996	210.822	426.914	6.36	67.096
D11-1-91A1	Quartzite	202.400	1.962	103.146	208.870	6.47	32.272
D11-1-91A2	Quartzite	250.200	2.174	115.072	233.021	5.84	39.894
D11-1-91B3	Quartzite	322.300	1.885	171.002	346.280	6.74	51.390
D11-1-91B5	Quartzite	174.000	2.220	78.368	158.696	5.72	27.744
D11-1-91C3	Quartzite	170.300	1.962	86.790	175.750	6.47	27.154
D11-1-94B2	Quartzite	206.600	1.828	113.031	228.889	6.95	32.942
D11-1-94B3	Quartzite	240.500	1.784	134.809	272.989	7.12	38.347
D11-1-94D2	Quartzite	159.000	1.966	80.871	163.764	6.46	25.352
D11-1-97C	Quartzite	386.400	1.833	210.789	426.848	6.93	61.611

Table B235. ACM-R net-return rates (Rs) for heat-treated silcrete assuming both the insulated and exposed heating scenarios and untreated silcrete experimental blocks when only t_s time-cost (travel and search time) is considered during MIS5 conditions.

Block	Sample Type	Raw Material	Cutting Edge Complete Blades (cm)	Total Flaked Core Mass (kg)	CE Blades (cm) / Total Flaked Core Mass (kg)	Cutting Edge * Durability (e * d)	ts-Travel and search time (min)/Total Flaked Core Mass (kg)	Rs
D9-1-10b	Heat-treated	Silcrete	311.700	2.350	132.646	374.566	124.02	3.020
D9-1-12b	Heat-treated	Silcrete	329.100	2.200	149.586	422.403	132.47	3.189
D9-1-12d	Heat-treated	Silcrete	307.900	2.286	134.672	380.289	127.47	2.983
E3-1-1b	Heat-treated	Silcrete	479.300	1.933	247.894	700.005	150.73	4.644
E3-1-5p	Heat-treated	Silcrete	362.400	2.588	140.046	395.463	112.62	3.511
E3-1-6a	Heat-treated	Silcrete	409.700	2.196	186.561	526.814	132.71	3.970
E3-1-6c	Heat-treated	Silcrete	451.500	2.436	185.345	523.378	119.64	4.375
I14-2-16l	Heat-treated	Silcrete	582.400	2.356	247.176	697.977	123.69	5.643
D9-1-10a	Untreated	Silcrete	89.500	1.980	45.198	85.016	147.18	0.578
D9-1-12a	Untreated	Silcrete	179.700	2.250	79.881	150.251	129.55	1.160
D9-1-	Untreated	Silcrete	97.000	1.807	53.677	100.965	161.27	0.626

12c								
E3-1-1A	Untreated	Silcrete	150.800	2.070	72.865	137.055	140.82	0.973
E3-1-5n	Untreated	Silcrete	223.700	2.460	90.944	171.061	118.48	1.444
E3-1-5o	Untreated	Silcrete	255.100	2.505	101.844	191.565	116.35	1.646
E3-1-6b	Untreated	Silcrete	93.800	1.691	55.470	104.337	172.34	0.605
I14-2-16a	Untreated	Silcrete	64.200	2.895	22.175	41.711	100.66	0.414

MIS6 without a Paleo-Agulhas plain silcrete source

Table B236. ACM-R net-return rates (Rq) for quartzite experimental blocks when only t_s time-cost (travel and search time) is considered during MIS6 conditions without a Paleo-Agulhas plain silcrete source.

Block	Raw Material	Cutting Edge Complete Blades (cm)	Total Flaked Core Mass (kg)	CE Blades (cm) / Total Flaked Core Mass (kg)	Cutting Edge * Durability (e * d)	*ts*-Travel and search time (min)/Total Flaked Core Mass (kg)	Rq
C9-1-1B8	Quartzite	92.600	1.920	48.223	75.349	25.42	2.964
C9-1-1B9	Quartzite	83.200	2.060	40.380	63.094	23.69	2.663
D11-1-100A	Quartzite	156.000	2.149	72.592	113.425	22.72	4.993
D11-1-90D1	Quartzite	52.300	2.450	21.345	33.351	19.92	1.674
D11-1-95A	Quartzite	68.900	2.031	33.917	52.995	24.03	2.205
D11-1-95B	Quartzite	89.500	2.160	41.432	64.737	22.60	2.865
D11-1-97A1	Quartzite	28.300	1.925	14.701	22.971	25.36	0.906
D11-1-98B1	Quartzite	87.000	1.913	45.486	71.072	25.52	2.785
D11-1-98C1	Quartzite	92.700	2.091	44.340	69.281	23.35	2.967
D11-1-98D	Quartzite	77.800	1.843	42.225	65.976	26.49	2.490
D11-1-85C1	Quartzite	420.800	1.996	210.822	426.914	24.46	17.456
D11-1-91A1	Quartzite	202.400	1.962	103.146	208.870	24.88	8.396
D11-1-91A2	Quartzite	250.200	2.174	115.072	233.021	22.45	10.379
D11-1-91B3	Quartzite	322.300	1.885	171.002	346.280	25.90	13.370
D11-1-91B5	Quartzite	174.000	2.220	78.368	158.696	21.99	7.218
D11-1-91C3	Quartzite	170.300	1.962	86.790	175.750	24.88	7.064
D11-1-94B2	Quartzite	206.600	1.828	113.031	228.889	26.71	8.570
D11-1-94B3	Quartzite	240.500	1.784	134.809	272.989	27.36	9.976
D11-1-94D2	Quartzite	159.000	1.966	80.871	163.764	24.83	6.596
D11-1-97C	Quartzite	386.400	1.833	210.789	426.848	26.63	16.029

Table B237. ACM-R net-return rates (Rs) for heat-treated silcrete assuming both the insulated and exposed heating scenarios and untreated silcrete experimental blocks when only t_s time-cost (travel and search time) is considered during MIS6 conditions without a Paleo-Agulhas plain silcrete source.

Block	Sample Type	Raw Material	Cutting Edge Complete Blades (cm)	Total Flaked Core Mass (kg)	CE Blades (cm) / Total Flaked Core Mass (kg)	Cutting Edge * Durability (e * d)	ts-Travel and search time (min)/Total Flaked Core Mass (kg)	Rs
D9-1-10b	Heat-treated	Silcrete	311.700	2.350	132.646	374.566	124.02	3.020
D9-1-12b	Heat-treated	Silcrete	329.100	2.200	149.586	422.403	132.47	3.189
D9-1-12d	Heat-treated	Silcrete	307.900	2.286	134.672	380.289	127.47	2.983
E3-1-1b	Heat-treated	Silcrete	479.300	1.933	247.894	700.005	150.73	4.644
E3-1-5p	Heat-treated	Silcrete	362.400	2.588	140.046	395.463	112.62	3.511
E3-1-6a	Heat-treated	Silcrete	409.700	2.196	186.561	526.814	132.71	3.970
E3-1-6c	Heat-treated	Silcrete	451.500	2.436	185.345	523.378	119.64	4.375
I14-2-16l	Heat-treated	Silcrete	582.400	2.356	247.176	697.977	123.69	5.643
D9-1-10a	Untreated	Silcrete	89.500	1.980	45.198	85.016	147.18	0.578
D9-1-12a	Untreated	Silcrete	179.700	2.250	79.881	150.251	129.55	1.160
D9-1-12c	Untreated	Silcrete	97.000	1.807	53.677	100.965	161.27	0.626
E3-1-1A	Untreated	Silcrete	150.800	2.070	72.865	137.055	140.82	0.973
E3-1-5n	Untreated	Silcrete	223.700	2.460	90.944	171.061	118.48	1.444
E3-1-5o	Untreated	Silcrete	255.100	2.505	101.844	191.565	116.35	1.646
E3-1-6b	Untreated	Silcrete	93.800	1.691	55.470	104.337	172.34	0.605
I14-2-16a	Untreated	Silcrete	64.200	2.895	22.175	41.711	100.66	0.414

MIS6 with a Paleo-Agulhas plain silcrete source

Table B238. ACM-R net-return rates (Rq) for quartzite experimental blocks when only t_s time-cost (travel and search time) is considered during MIS6 conditions with a Paleo-Agulhas plain silcrete source.

Block	Raw Material	Cutting Edge Complete Blades (cm)	Total Flaked Core Mass (kg)	CE Blades (cm) / Total Flaked Core Mass (kg)	Cutting Edge * Durability (e * d)	ts-Travel and search time (min)/Total Flaked Core Mass (kg)	Rq
C9-1-1B8	Quartzite	92.600	1.920	48.223	75.349	25.42	2.964
C9-1-1B9	Quartzite	83.200	2.060	40.380	63.094	23.69	2.663
D11-1-100A	Quartzite	156.000	2.149	72.592	113.425	22.72	4.993
D11-1-90D1	Quartzite	52.300	2.450	21.345	33.351	19.92	1.674
D11-1-	Quartzite	68.900	2.031	33.917	52.995	24.03	2.205

95A							
D11-1-95B	Quartzite	89.500	2.160	41.432	64.737	22.60	2.865
D11-1-97A1	Quartzite	28.300	1.925	14.701	22.971	25.36	0.906
D11-1-98B1	Quartzite	87.000	1.913	45.486	71.072	25.52	2.785
D11-1-98C1	Quartzite	92.700	2.091	44.340	69.281	23.35	2.967
D11-1-98D	Quartzite	77.800	1.843	42.225	65.976	26.49	2.490
D11-1-85C1	Quartzite	420.800	1.996	210.822	426.914	24.46	17.456
D11-1-91A1	Quartzite	202.400	1.962	103.146	208.870	24.88	8.396
D11-1-91A2	Quartzite	250.200	2.174	115.072	233.021	22.45	10.379
D11-1-91B3	Quartzite	322.300	1.885	171.002	346.280	25.90	13.370
D11-1-91B5	Quartzite	174.000	2.220	78.368	158.696	21.99	7.218
D11-1-91C3	Quartzite	170.300	1.962	86.790	175.750	24.88	7.064
D11-1-94B2	Quartzite	206.600	1.828	113.031	228.889	26.71	8.570
D11-1-94B3	Quartzite	240.500	1.784	134.809	272.989	27.36	9.976
D11-1-94D2	Quartzite	159.000	1.966	80.871	163.764	24.83	6.596
D11-1-97C	Quartzite	386.400	1.833	210.789	426.848	26.63	16.029

Table B239. ACM-R net-return rates (Rs) for heat-treated silcrete assuming both the insulated and exposed heating scenarios and untreated silcrete experimental blocks when only t_s time-cost (travel and search time) is considered during MIS6 conditions with a Paleo-Agulhas plain silcrete source.

Block	Sample Type	Raw Material	Cutting Edge Complete Blades (cm)	Total Flaked Core Mass (kg)	CE Blades (cm) / Total Flaked Core Mass (kg)	Cutting Edge * Durability (e * d)	ts-Travel and search time (min)/Total Flaked Core Mass (kg)	Rs
D9-1-10b	Heat-treated	Silcrete	311.700	2.350	132.646	374.566	11.92	31.416
D9-1-12b	Heat-treated	Silcrete	329.100	2.200	149.586	422.403	12.73	33.170
D9-1-12d	Heat-treated	Silcrete	307.900	2.286	134.672	380.289	12.25	31.033
E3-1-1b	Heat-treated	Silcrete	479.300	1.933	247.894	700.005	14.49	48.309
E3-1-5p	Heat-treated	Silcrete	362.400	2.588	140.046	395.463	10.83	36.526
E3-1-6a	Heat-treated	Silcrete	409.700	2.196	186.561	526.814	12.76	41.294
E3-1-6c	Heat-treated	Silcrete	451.500	2.436	185.345	523.378	11.50	45.507
I14-2-16l	Heat-treated	Silcrete	582.400	2.356	247.176	697.977	11.89	58.700
D9-1-10a	Untreated	Silcrete	89.500	1.980	45.198	85.016	14.15	6.009
D9-1-12a	Untreated	Silcrete	179.700	2.250	79.881	150.251	12.45	12.065
D9-1-	Untreated	Silcrete	97.000	1.807	53.677	100.965	15.50	6.512

12c								
E3-1-1A	Untreated	Silcrete	150.800	2.070	72.865	137.055	13.54	10.124
E3-1-5n	Untreated	Silcrete	223.700	2.460	90.944	171.061	11.39	15.019
E3-1-5o	Untreated	Silcrete	255.100	2.505	101.844	191.565	11.19	17.127
E3-1-6b	Untreated	Silcrete	93.800	1.691	55.470	104.337	16.57	6.297
I14-2-16a	Untreated	Silcrete	64.200	2.895	22.175	41.711	9.68	4.310

Table B240. Comparison between a raw material ranking based on ACM- R net-return rates and archaeological data from MIS4, MIS5, and MIS6.

ACM-R Results-Ranked*			**Archaeological Data**			
MIS4 Without a Paleo-Agulhas plain silcrete source			**MIS4***			
Quartzite	Untreated Silcrete	Heat-treated Silcrete	Quartzite (%)	Silcrete Overall (%)	Untreated Silcrete (%)	Heat-treated Silcrete (%)
2 (1.8)	***2*** (0.9)	***1*** (3.9)	44.6	40.0	16.9	83.1
MIS4 With a Paleo-Agulhas plain silcrete source			**MIS4***			
Quartzite	Untreated Silcrete	Heat-treated Silcrete	Quartzite (%)	Silcrete Overall (%)	Untreated Silcrete (%)	Heat-treated Silcrete (%)
3 (1.8)	***2*** (9.7)	***1*** (40.7)	44.6	40.0	16.9	83.1
MIS5			**MIS5***			
Quartzite	Untreated Silcrete	Heat-treated Silcrete	Quartzite (%)	Silcrete Overall (%)	Untreated Silcrete (%)	Heat-treated Silcrete (%)
1 (25.3)	***3*** (0.9)	***2*** (3.9)	77.2	13.1	11.6	88.4
MIS6 Without a Paleo-Agulhas plain silcrete source			**MIS6***			
Quartzite	Untreated Silcrete	Heat-treated Silcrete	Quartzite (%)	Silcrete Overall (%)	Untreated Silcrete (%)	Heat-treated Silcrete (%)
1 (6.6)	***2*** (0.9)	***1*** (3.9)	94.3	1.1	NA	NA
MIS6 With a Paleo-Agulhas plain silcrete source			**MIS6***			
Quartzite	Untreated Silcrete	Heat-treated Silcrete	Quartzite (%)	Silcrete Overall (%)	Untreated Silcrete (%)	Heat-treated Silcrete (%)
2 (6.6)	***2*** (9.7)	***1*** (40.7)	92.4	2.5	NA	NA

* Ranking based on which raw materials have the highest mean Rq or Rs (in parenthesis).Similar ranking in table is due to statistically similar Rq or Rs. * MIS4, MIS5, and MIS6 archaeological raw material frequencies from bootstrapped data in Figure 50 and Table 19.

Vegetation type variable

Table B241. Summary Statistics and test results of ACM-P net-return rates (Pq and Ps) when only m_1 (wood fuel travel and search time) and m_2 time-costs (heat-treatment time) are considered during all model conditions.

	MIS4			MIS5			MIS6		
	Exposed-Silcrete (Ps)	Insulated-Silcrete (Ps)	Untreated Silcrete (Ps)	Exposed-Silcrete (Ps)	Insulated-Silcrete (Ps)	Untreated Silcrete (Ps)	Exposed-Silcrete (Ps)	Insulated-Silcrete (Ps)	Untreated Silcrete (Ps)
	Quartzite (Pq)			Quartzite (Pq)			Quartzite (Pq)		
n sample blocks	8	8	20	8	8	20	8	8	20
First Quartile	6.210	8.280	41.711	6.210	4.459	41.711	6.210	4.459	41.711
Min	7.787	10.382	120.696	7.787	5.591	120.696	7.787	5.591	120.696
Median	8.154	10.872	122.745	8.154	5.854	122.745	8.154	5.854	122.745
Mean	11.747	15.663	191.565	11.747	8.434	191.565	11.747	8.434	191.565
Max	9.528	12.703	165.859	9.528	6.840	165.859	9.528	6.840	165.859
Third Quartile	1.942	2.589	49.041	1.942	1.394	49.041	1.942	1.394	49.041
	125.953			125.953			125.953		

SD	20.000	8.000	8.000	8.000	20.000	8.000	8.000	8.000	20.000	8.000	8.000	8.000
Bootstrapped SE*	53.263	32.818	1.735	1.296	53.263	32.818	0.929	1.296	53.263	32.818	0.929	1.296
Margin of error (95% CI)	216.977	155.563	12.606	9.450	216.977	155.563	6.783	9.450	216.977	155.563	6.783	9.450
Bootstrapped Upper 95% CI*	163.714	122.745	10.872	8.154	163.714	122.745	5.854	8.154	163.714	122.745	5.854	8.154
Bootstrapped Lower 95% CI*	110.450	89.928	9.137	6.858	110.450	89.928	4.926	6.858	110.450	89.928	4.926	6.858

*Samples bootstrapped 10000 times.

Quartzite MIS4, MIS5, and MIS6

Table B242. ACM-P net-return rates (Pq) for quartzite experimental blocks when only m_1 (wood fuel travel and search time) and m_2 time-costs (heat-treatment time) are considered during MIS4, MIS5, and MIS6 conditions.

Block	Raw Material	Cutting Edge Complete Blades (cm)	Total Flaked Core Mass (kg)	CE Blades (cm) / Total Flaked Core Mass (kg)	Cutting Edge * Durability (e * d)	*m*1-Wood Fuel travel and search time (min)/Total Flaked Core Mass (kg)	*m*2-Heat-treatment time (min)/Total Flaked core Mass (kg)	Pq
C9-1-1B8	Quartzite	92.6	1.920	48.223	75.349	0	0	75.349
C9-1-1B9	Quartzite	83.2	2.060	40.380	63.094	0	0	63.094
D11-1-100A	Quartzite	156	2.149	72.592	113.425	0	0	113.425
D11-1-90D1	Quartzite	52.3	2.450	21.345	33.351	0	0	33.351
D11-1-95A	Quartzite	68.9	2.031	33.917	52.995	0	0	52.995
D11-1-95B	Quartzite	89.5	2.160	41.432	64.737	0	0	64.737
D11-1-97A1	Quartzite	28.3	1.925	14.701	22.971	0	0	22.971
D11-1-98B1	Quartzite	87	1.913	45.486	71.072	0	0	71.072
D11-1-98C1	Quartzite	92.7	2.091	44.340	69.281	0	0	69.281
D11-1-98D	Quartzite	77.8	1.843	42.225	65.976	0	0	65.976

D11-1-85C1	Quartzite	420.8	1.996	210.822	426.914	0	0	426.914
D11-1-91A1	Quartzite	202.4	1.962	103.146	208.870	0	0	208.870
D11-1-91A2	Quartzite	250.2	2.174	115.072	233.021	0	0	233.021
D11-1-91B3	Quartzite	322.3	1.885	171.002	346.280	0	0	346.280
D11-1-91B5	Quartzite	174	2.220	78.368	158.696	0	0	158.696
D11-1-91C3	Quartzite	170.3	1.962	86.790	175.750	0	0	175.750
D11-1-94B2	Quartzite	206.6	1.828	113.031	228.889	0	0	228.889
D11-1-94B3	Quartzite	240.5	1.784	134.809	272.989	0	0	272.989
D11-1-94D2	Quartzite	159	1.966	80.871	163.764	0	0	163.764
D11-1-97C	Quartzite	386.4	1.833	210.789	426.848	0	0	426.848

MIS4 Silcrete

Table B243. ACM-P net-return rates (Ps) for heat-treated silcrete assuming both the insulated and exposed heating scenarios and untreated silcrete experimental blocks when only m_1 (wood fuel travel and search time) and m_2 time-costs (heat-treatment time) are considered during MIS5 conditions.

Block	Heating Scenario	Raw Material	Cutting Edge Complete Blades (cm)	Total Flaked Core Mass (kg)	CE Blades (cm) / Total Flaked Core Mass (kg)	Cutting Edge * Durability (e * d)	*m*1-Wood Fuel travel and search time (min)/Total Flaked Core Mass (kg)	*m*2-Heat-treatment time (min)/Total Flaked core Mass (kg)	Ps
D9-1-10b	Insulated	Silcrete	311.700	2.350	132.646	374.566	38.300	6.383	8.383
D9-1-12b	Insulated	Silcrete	329.100	2.200	149.586	422.403	40.908	6.818	8.851
D9-1-12d	Insulated	Silcrete	307.900	2.286	134.672	380.289	39.365	6.561	8.280
E3-1-1b	Insulated	Silcrete	479.300	1.933	247.894	700.005	46.548	7.758	12.890
E3-1-5p	Insulated	Silcrete	362.400	2.588	140.046	395.463	34.780	5.797	9.746
E3-1-6a	Insulated	Silcrete	409.700	2.196	186.561	526.814	40.982	6.830	11.018
E3-1-6c	Insulated	Silcrete	451.500	2.436	185.345	523.378	36.946	6.158	12.142
I14-2-16l	Insulated	Silcrete	582.400	2.356	247.176	697.977	38.197	6.366	15.663
D9-1-10b	Exposed	Silcrete	311.700	2.350	132.646	374.566	38.300	21.278	6.287
D9-1-12b	Exposed	Silcrete	329.100	2.200	149.586	422.403	40.908	22.727	6.638
D9-1-12d	Exposed	Silcrete	307.900	2.286	134.672	380.289	39.365	21.869	6.210
E3-1-1b	Exposed	Silcrete	479.300	1.933	247.894	700.005	46.548	25.860	9.668
E3-1-5p	Exposed	Silcrete	362.400	2.588	140.046	395.463	34.780	19.322	7.310
E3-1-	Exposed	Silcrete	409.700	2.196	186.561	526.814	40.982	22.768	8.264

6a									
E3-1-6c	Exposed	Silcrete	451.500	2.436	185.345	523.378	36.946	20.525	9.107
I14-2-16l	Exposed	Silcrete	582.400	2.356	247.176	697.977	38.197	21.220	11.747
D9-1-10a	Untreated	Silcrete	89.500	1.980	45.198	85.016	0.000	0.000	85.016
D9-1-12a	Untreated	Silcrete	179.700	2.250	79.881	150.251	0.000	0.000	150.251
D9-1-12c	Untreated	Silcrete	97.000	1.807	53.677	100.965	0.000	0.000	100.965
E3-1-1A	Untreated	Silcrete	150.800	2.070	72.865	137.055	0.000	0.000	137.055
E3-1-5n	Untreated	Silcrete	223.700	2.460	90.944	171.061	0.000	0.000	171.061
E3-1-5o	Untreated	Silcrete	255.100	2.505	101.844	191.565	0.000	0.000	191.565
E3-1-6b	Untreated	Silcrete	93.800	1.691	55.470	104.337	0.000	0.000	104.337
I14-2-16a	Untreated	Silcrete	64.200	2.895	22.175	41.711	0.000	0.000	41.711

MIS5and MIS6 Silcrete

Table B244. ACM-P net-return rates (Ps) for heat-treated silcrete assuming both the insulated and exposed heating scenarios and untreated silcrete experimental blocks when only m_1 (wood fuel travel and search time) and m_2 time-costs (heat-treatment time) are considered during MIS5 and MIS6 conditions.

Block	Heating Scenario	Raw Material	Cutting Edge Complete Blades (cm)	Total Flaked Core Mass (kg)	CE Blades (cm) / Total Flaked Core Mass (kg)	Cutting Edge * Durability (e * d)	m1-Wood Fuel travel and search time (min)/Total Flaked Core Mass (kg)	m2-Heat-treatment time (min)/Total Flaked core Mass (kg)	Ps
D9-1-10b	Insulated	Silcrete	311.700	2.350	132.646	374.566	76.600	6.383	4.514
D9-1-12b	Insulated	Silcrete	329.100	2.200	149.586	422.403	81.816	6.818	4.766
D9-1-12d	Insulated	Silcrete	307.900	2.286	134.672	380.289	78.730	6.561	4.459
E3-1-1b	Insulated	Silcrete	479.300	1.933	247.894	700.005	93.096	7.758	6.941
E3-1-5p	Insulated	Silcrete	362.400	2.588	140.046	395.463	69.559	5.797	5.248
E3-1-6a	Insulated	Silcrete	409.700	2.196	186.561	526.814	81.965	6.830	5.933
E3-1-6c	Insulated	Silcrete	451.500	2.436	185.345	523.378	73.892	6.158	6.538
I14-2-16l	Insulated	Silcrete	582.400	2.356	247.176	697.977	76.394	6.366	8.434
D9-1-10b	Exposed	Silcrete	311.700	2.350	132.646	374.566	38.300	21.278	6.287
D9-1-12b	Exposed	Silcrete	329.100	2.200	149.586	422.403	40.908	22.727	6.638
D9-1-12d	Exposed	Silcrete	307.900	2.286	134.672	380.289	39.365	21.869	6.210
E3-1-1b	Exposed	Silcrete	479.300	1.933	247.894	700.005	46.548	25.860	9.668
E3-1-5p	Exposed	Silcrete	362.400	2.588	140.046	395.463	34.780	19.322	7.310

E3-1-6a	Exposed	Silcrete	409.700	2.196	186.561	526.814	40.982	22.768	8.264
E3-1-6c	Exposed	Silcrete	451.500	2.436	185.345	523.378	36.946	20.525	9.107
I14-2-16l	Exposed	Silcrete	582.400	2.356	247.176	697.977	38.197	21.220	11.747
D9-1-10a	Untreated	Silcrete	89.500	1.980	45.198	85.016	0	0	85.016
D9-1-12a	Untreated	Silcrete	179.700	2.250	79.881	150.251	0	0	150.251
D9-1-12c	Untreated	Silcrete	97.000	1.807	53.677	100.965	0	0	100.965
E3-1-1A	Untreated	Silcrete	150.800	2.070	72.865	137.055	0	0	137.055
E3-1-5n	Untreated	Silcrete	223.700	2.460	90.944	171.061	0	0	171.061
E3-1-5o	Untreated	Silcrete	255.100	2.505	101.844	191.565	0	0	191.565
E3-1-6b	Untreated	Silcrete	93.800	1.691	55.470	104.337	0	0	104.337
I14-2-16a	Untreated	Silcrete	64.200	2.895	22.175	41.711	0	0	41.711

Table B245. Comparison between a raw material ranking based on ACM- P net-return rates and archaeological data from MIS4, MIS5, and MIS6.

ACM-P Results-Ranked*				**Archaeological Data**			
MIS4				**MIS4***			
Quartzite	Untreated Silcrete	Insulated-Silcrete	Exposed-Silcrete	Quartzite (%)	Silcrete Overall (%)	Untreated Silcrete (%)	Heat-treated Silcrete (%)
1 (163.7)	***1*** (122.7)	***2*** (10.9)	***3*** (8.2)	44.6*	40*	16.9	83.1
MIS5				**MIS5***			
Quartzite	Untreated Silcrete	Insulated-Silcrete	Exposed-Silcrete	Quartzite (%)	Silcrete Overall (%)	Untreated Silcrete (%)	Heat-treated Silcrete (%)
1 (163.7)	***1*** (122.7)	***3*** (5.9)	***2*** (8.2)	77.2	13.1	11.6	88.4
MIS6				**MIS6***			
Quartzite	Untreated Silcrete	Insulated-Silcrete	Exposed-Silcrete	Quartzite (%)	Silcrete Overall (%)	Untreated Silcrete (%)	Heat-treated Silcrete (%)
1 (163.7)	***1*** (122.7)	***3*** (5.9)	***2*** (8.2)	94.3	1.1	NA	NA

* Ranking based on which raw materials have the highest mean Rq or Rs (in parenthesis).Similar ranking in table is due to statistically similar Rq or Rs. *MIS4, MIS5, and MIS6 archaeological raw material frequencies from bootstrapped data in Figure 50 and Table 19.

Mobility rate and strategy variable

Table B246. Summary Statistics and test results of ACM net-return rates (Pq and Ps or Rq and Rs) when only m_3 time-cost (flaking manufacturing time) is considered (for all experimental sample types) during MIS4 conditions.

	Quartzite (Pq or Rq)	**Untreated Silcrete (Ps or Rs)**	**Heat-treated Silcrete (Ps or Rs)**
n sample blocks	20	8	8
First Quartile	9.395	12.165	63.748
Min	3.160	8.630	62.100
Median	20.205	16.645	77.870

Mean	22.939	19.375	81.539
Max	60.870	34.270	117.470
Third Quartile	33.563	28.573	95.278
SD	17.005	9.373	19.419
Bootstrapped SE*	3.675	3.212	6.618
Margin of error (95% CI)	7.204	6.295	12.970
Bootstrapped Upper 95% CI*	30.142	25.670	94.509
Bootstrapped Lower 95% CI*	15.735	13.080	68.568

*Samples bootstrapped 10000 times.

MIS4

Table B247. ACM-P net-return rates (Pq) for quartzite experimental blocks when only m_3 time-cost (flake manufacturing time) is considered during MIS4 conditions.

Block	Raw Material	Cutting Edge Complete Blades (cm)	Total Flaked Core Mass (kg)	CE Blades (cm) / Total Flaked Core Mass (kg)	Cutting Edge * Durability (e * d)	*m*3-FlakingTime (14min)/Total Flaked Core Mass (kg)	Pq or Rq
C9-1-1B8	Quartzite	92.600	1.920	48.223	75.349	7.29	10.33
C9-1-1B9	Quartzite	83.200	2.060	40.380	63.094	6.79	9.29
D11-1-100A	Quartzite	156.000	2.149	72.592	113.425	6.51	17.41
D11-1-90D1	Quartzite	52.300	2.450	21.345	33.351	5.71	5.84
D11-1-95A	Quartzite	68.900	2.031	33.917	52.995	6.89	7.69
D11-1-95B	Quartzite	89.500	2.160	41.432	64.737	6.48	9.99
D11-1-97A1	Quartzite	28.300	1.925	14.701	22.971	7.27	3.16
D11-1-98B1	Quartzite	87.000	1.913	45.486	71.072	7.32	9.71
D11-1-98C1	Quartzite	92.700	2.091	44.340	69.281	6.70	10.35
D11-1-98D	Quartzite	77.800	1.843	42.225	65.976	7.60	8.68
D11-1-85C1	Quartzite	420.800	1.996	210.822	426.914	7.01	60.87
D11-1-91A1	Quartzite	202.400	1.962	103.146	208.870	7.13	29.28
D11-1-91A2	Quartzite	250.200	2.174	115.072	233.021	6.44	36.19
D11-1-91B3	Quartzite	322.300	1.885	171.002	346.280	7.43	46.62
D11-1-91B5	Quartzite	174.000	2.220	78.368	158.696	6.31	25.17
D11-1-91C3	Quartzite	170.300	1.962	86.790	175.750	7.13	24.63
D11-1-94B2	Quartzite	206.600	1.828	113.031	228.889	7.66	29.88
D11-1-94B3	Quartzite	240.500	1.784	134.809	272.989	7.85	34.79
D11-1-94D2	Quartzite	159.000	1.966	80.871	163.764	7.12	23.00
D11-1-97C	Quartzite	386.400	1.833	210.789	426.848	7.64	55.89

Table B248. ACM-P net-return rates (Ps) for untreated and heat-treated silcrete experimental blocks when only m_3 time-cost (flake manufacturing time) is considered during MIS4 conditions.

Block	Sample Type	Raw Material	Cutting Edge Complete Blades (cm)	Total Flaked Core Mass (kg)	CE Blades (cm) / Total Flaked Core Mass (kg)	Cutting Edge * Durability (e * d)	*m*3-FlakingTime (14min)/Total Flaked Core Mass (kg)	Ps or Rs
D9-1-10b	Heat-treated	Silcrete	311.700	2.350	132.646	374.566	5.96	62.87
D9-1-12b	Heat-treated	Silcrete	329.100	2.200	149.586	422.403	6.36	66.38
D9-1-12d	Heat-treated	Silcrete	307.900	2.286	134.672	380.289	6.12	62.10
E3-1-1b	Heat-treated	Silcrete	479.300	1.933	247.894	700.005	7.24	96.68
E3-1-5p	Heat-treated	Silcrete	362.400	2.588	140.046	395.463	5.41	73.10
E3-1-6a	Heat-treated	Silcrete	409.700	2.196	186.561	526.814	6.38	82.64
E3-1-6c	Heat-treated	Silcrete	451.500	2.436	185.345	523.378	5.75	91.07
I14-2-16l	Heat-treated	Silcrete	582.400	2.356	247.176	697.977	5.94	117.47
D9-1-10a	Untreated	Silcrete	89.500	1.980	45.198	85.016	7.07	12.02
D9-1-12a	Untreated	Silcrete	179.700	2.250	79.881	150.251	6.22	24.14
D9-1-12c	Untreated	Silcrete	97.000	1.807	53.677	100.965	7.75	13.03
E3-1-1A	Untreated	Silcrete	150.800	2.070	72.865	137.055	6.76	20.26
E3-1-5n	Untreated	Silcrete	223.700	2.460	90.944	171.061	5.69	30.05
E3-1-5o	Untreated	Silcrete	255.100	2.505	101.844	191.565	5.59	34.27
E3-1-6b	Untreated	Silcrete	93.800	1.691	55.470	104.337	8.28	12.60
I14-2-16a	Untreated	Silcrete	64.200	2.895	22.175	41.711	4.84	8.63

Table B249. Comparison between a raw material ranking based on ACM net-return rates and archaeological data from MIS4.

ACM Results-Ranked	Quartzite	***2*** (22.9)
	Untreated Silcrete	***2*** (19.4)
	Heat-treated Silcrete	***1*** (81.6)
Archaeological Raw Material Data – MIS4*	Quartzite (%)	44.6*
	Silcrete Overall (%)	40*
	Untreated Silcrete (%)	16.9
	Heat-treated Silcrete (%)	83.1

* Ranking based on which raw materials have the highest mean Rq or Rs (in parenthesis).Similar ranking in table is due to statistically similar Rq or Rs. *MIS4 archaeological raw material frequencies from bootstrapped data in Figure 50 and Table 19.

Maximizing number of blades per core multiplied by duration of use (count of complete blade (n=) / total flaked core mass (kg) * d (minutes))

ACM-P net-return rates

MIS4, MIS5, and MIS6 conditions

Table B250. ACM-P net-return rates (Pq) for quartzite experimental blocks during MIS4, MIS5, and MIS6 conditions.

Model Conditions	Block	Raw Material	Count Complete Blades (n=)	Total Flaked Core Mass (kg)	Count Complete Blades (n=)/Total Flaked Core Mass (kg)	Count Blades * Durability (e * d)	Pq
MIS4, MIS5, & MIS6	C9-1-1B8	Quartzite	2	1.920	1.042	1.627	0.164
MIS4, MIS5, & MIS6	C9-1-1B9	Quartzite	4	2.060	1.941	3.033	0.329
MIS4, MIS5, & MIS6	D11-1-100A	Quartzite	1	2.149	0.465	0.727	0.081
MIS4, MIS5, & MIS6	D11-1-90D1	Quartzite	1	2.450	0.408	0.638	0.081
MIS4, MIS5, & MIS6	D11-1-95A	Quartzite	2	2.031	0.985	1.538	0.161
MIS4, MIS5, & MIS6	D11-1-95B	Quartzite	2	2.160	0.926	1.447	0.161
MIS4, MIS5, & MIS6	D11-1-97A1	Quartzite	0	1.925	0.000	0.000	0.000
MIS4, MIS5, & MIS6	D11-1-98B1	Quartzite	3	1.913	1.568	2.451	0.242
MIS4, MIS5, & MIS6	D11-1-98C1	Quartzite	3	2.091	1.435	2.242	0.242
MIS4, MIS5, & MIS6	D11-1-98D	Quartzite	1	1.843	0.543	0.848	0.081
MIS4, MIS5, & MIS6	D11-1-85C1	Quartzite	8	1.996	4.008	8.116	0.836
MIS4, MIS5, & MIS6	D11-1-91A1	Quartzite	6	1.962	3.058	6.192	0.627
MIS4, MIS5, & MIS6	D11-1-91A2	Quartzite	8	2.174	3.679	7.451	0.836
MIS4, MIS5, & MIS6	D11-1-91B3	Quartzite	11	1.885	5.836	11.818	1.150
MIS4, MIS5, & MIS6	D11-1-91B5	Quartzite	4	2.220	1.802	3.648	0.418
MIS4, MIS5, & MIS6	D11-1-91C3	Quartzite	5	1.962	2.548	5.160	0.523
MIS4, MIS5, & MIS6	D11-1-94B2	Quartzite	5	1.828	2.736	5.539	0.523
MIS4, MIS5, & MIS6	D11-1-94B3	Quartzite	8	1.784	4.484	9.081	0.836
MIS4, MIS5, & MIS6	D11-1-94D2	Quartzite	5	1.966	2.543	5.150	0.523
MIS4, MIS5, & MIS6	D11-1-97C	Quartzite	7	1.833	3.819	7.733	0.732

MIS4

Table B251. ACM-P net-return rates (Ps) for heat-treated silcrete assuming both the insulated and exposed heating scenarios and untreated silcrete experimental blocks during MIS4 conditions.

Model Conditions	Heating Scenario	Block	Raw Material	Count Complete Blades (n=)	Total Flaked Core Mass (kg)	Count Complete Blades (n=) / Total Flaked Core Mass (kg)	Count Blades * Durability (e * d)	Ps
MIS4	Insulated	D9-1-10b	Silcrete	7	2.350	2.979	8.412	0.155
MIS4	Insulated	D9-1-12b	Silcrete	3	2.200	1.364	3.851	0.067
MIS4	Insulated	D9-1-12d	Silcrete	4	2.286	1.750	4.940	0.089
MIS4	Insulated	E3-1-1b	Silcrete	13	1.933	6.724	18.986	0.289
MIS4	Insulated	E3-1-5p	Silcrete	10	2.588	3.864	10.912	0.222
MIS4	Insulated	E3-1-6a	Silcrete	16	2.196	7.286	20.574	0.355
MIS4	Insulated	E3-1-6c	Silcrete	19	2.436	7.800	22.025	0.422
MIS4	Insulated	I14-2-16l	Silcrete	11	2.356	4.668	13.183	0.244
MIS4	Exposed	D9-1-10b	Silcrete	7	2.350	2.979	8.412	0.122
MIS4	Exposed	D9-1-12b	Silcrete	3	2.200	1.364	3.851	0.052
MIS4	Exposed	D9-1-12d	Silcrete	4	2.286	1.750	4.940	0.070
MIS4	Exposed	E3-1-1b	Silcrete	13	1.933	6.724	18.986	0.226
MIS4	Exposed	E3-1-5p	Silcrete	10	2.588	3.864	10.912	0.174
MIS4	Exposed	E3-1-6a	Silcrete	16	2.196	7.286	20.574	0.279
MIS4	Exposed	E3-1-6c	Silcrete	19	2.436	7.800	22.025	0.331
MIS4	Exposed	I14-2-16l	Silcrete	11	2.356	4.668	13.183	0.192
MIS4	Untreated	D9-1-10a	Silcrete	3	1.980	1.515	2.850	0.255
MIS4	Untreated	D9-1-12a	Silcrete	7	2.250	3.112	5.853	0.595
MIS4	Untreated	D9-1-12c	Silcrete	2	1.807	1.107	2.082	0.170
MIS4	Untreated	E3-1-1A	Silcrete	5	2.070	2.416	4.544	0.425
MIS4	Untreated	E3-1-5n	Silcrete	5	2.460	2.033	3.823	0.425
MIS4	Untreated	E3-1-5o	Silcrete	6	2.505	2.395	4.506	0.510
MIS4	Untreated	E3-1-6b	Silcrete	2	1.691	1.183	2.225	0.170
MIS4	Untreated	I14-2-16a	Silcrete	3	2.895	1.036	1.949	0.255

MIS5 conditions

Table B252. ACM-P net-return rates (Ps) for heat-treated silcrete assuming both the insulated and exposed heating scenarios and untreated silcrete experimental blocks during MIS5 conditions.

Model Conditions	Heating Scenario	Block	Raw Material	Count Complete Blades (n=)	Total Flaked Core Mass (kg)	Count Complete Blades (n=) / Total Flaked Core Mass (kg)	Count Blades * Durability (e * d)	Ps
MIS5	Insulated	D9-1-10b	Silcrete	7	2.350	2.979	8.412	0.091
MIS5	Insulated	D9-1-12b	Silcrete	3	2.200	1.364	3.851	0.039
MIS5	Insulated	D9-1-12d	Silcrete	4	2.286	1.750	4.940	0.052
MIS5	Insulated	E3-1-1b	Silcrete	13	1.933	6.724	18.986	0.169
MIS5	Insulated	E3-1-5p	Silcrete	10	2.588	3.864	10.912	0.130
MIS5	Insulated	E3-1-6a	Silcrete	16	2.196	7.286	20.574	0.208
MIS5	Insulated	E3-1-6c	Silcrete	19	2.436	7.800	22.025	0.247
MIS5	Insulated	I14-2-16l	Silcrete	11	2.356	4.668	13.183	0.143
MIS5	Exposed	D9-1-10b	Silcrete	7	2.350	2.979	8.412	0.122
MIS5	Exposed	D9-1-12b	Silcrete	3	2.200	1.364	3.851	0.052
MIS5	Exposed	D9-1-12d	Silcrete	4	2.286	1.750	4.940	0.070
MIS5	Exposed	E3-1-1b	Silcrete	13	1.933	6.724	18.986	0.226
MIS5	Exposed	E3-1-5p	Silcrete	10	2.588	3.864	10.912	0.174
MIS5	Exposed	E3-1-6a	Silcrete	16	2.196	7.286	20.574	0.279
MIS5	Exposed	E3-1-6c	Silcrete	19	2.436	7.800	22.025	0.331
MIS5	Exposed	I14-2-16l	Silcrete	11	2.356	4.668	13.183	0.192
MIS5	Untreated	D9-1-10a	Silcrete	3	1.980	1.515	2.850	0.255
MIS5	Untreated	D9-1-12a	Silcrete	7	2.250	3.112	5.853	0.595
MIS5	Untreated	D9-1-12c	Silcrete	2	1.807	1.107	2.082	0.170
MIS5	Untreated	E3-1-1A	Silcrete	5	2.070	2.416	4.544	0.425
MIS5	Untreated	E3-1-5n	Silcrete	5	2.460	2.033	3.823	0.425
MIS5	Untreated	E3-1-5o	Silcrete	6	2.505	2.395	4.506	0.510
MIS5	Untreated	E3-1-6b	Silcrete	2	1.691	1.183	2.225	0.170
MIS5	Untreated	I14-2-16a	Silcrete	3	2.895	1.036	1.949	0.255

MIS6 conditions

Table B253. ACM-P net-return rates (Ps) for heat-treated silcrete assuming both the insulated and exposed heating scenarios and untreated silcrete experimental blocks during MIS6 conditions.

Model Conditions	Heating Scenario	Block	Raw Material	Count Complete Blades (n=)	Total Flaked Core Mass (kg)	Count Complete Blades (n=) / Total Flaked Core Mass (kg)	Count Blades * Durability (e * d)	Ps
MIS6	Insulated	D9-1-10b	Silcrete	7	2.350	2.979	8.412	0.091
MIS6	Insulated	D9-1-12b	Silcrete	3	2.200	1.364	3.851	0.039
MIS6	Insulated	D9-1-12d	Silcrete	4	2.286	1.750	4.940	0.052
MIS6	Insulated	E3-1-1b	Silcrete	13	1.933	6.724	18.986	0.169
MIS6	Insulated	E3-1-5p	Silcrete	10	2.588	3.864	10.912	0.130
MIS6	Insulated	E3-1-6a	Silcrete	16	2.196	7.286	20.574	0.208
MIS6	Insulated	E3-1-6c	Silcrete	19	2.436	7.800	22.025	0.247
MIS6	Insulated	I14-2-16l	Silcrete	11	2.356	4.668	13.183	0.143
MIS6	Exposed	D9-1-10b	Silcrete	7	2.350	2.979	8.412	0.122
MIS6	Exposed	D9-1-12b	Silcrete	3	2.200	1.364	3.851	0.052
MIS6	Exposed	D9-1-12d	Silcrete	4	2.286	1.750	4.940	0.070
MIS6	Exposed	E3-1-1b	Silcrete	13	1.933	6.724	18.986	0.226
MIS6	Exposed	E3-1-5p	Silcrete	10	2.588	3.864	10.912	0.174
MIS6	Exposed	E3-1-6a	Silcrete	16	2.196	7.286	20.574	0.279
MIS6	Exposed	E3-1-6c	Silcrete	19	2.436	7.800	22.025	0.331
MIS6	Exposed	I14-2-16l	Silcrete	11	2.356	4.668	13.183	0.192
MIS6	Untreated	D9-1-10a	Silcrete	3	1.980	1.515	2.850	0.255
MIS6	Untreated	D9-1-12a	Silcrete	7	2.250	3.112	5.853	0.595
MIS6	Untreated	D9-1-12c	Silcrete	2	1.807	1.107	2.082	0.170
MIS6	Untreated	E3-1-1A	Silcrete	5	2.070	2.416	4.544	0.425
MIS6	Untreated	E3-1-5n	Silcrete	5	2.460	2.033	3.823	0.425
MIS6	Untreated	E3-1-5o	Silcrete	6	2.505	2.395	4.506	0.510
MIS6	Untreated	E3-1-6b	Silcrete	2	1.691	1.183	2.225	0.170
MIS6	Untreated	I14-2-16a	Silcrete	3	2.895	1.036	1.949	0.255

ACM-R net-return rates

Table B254. Summary statistics and test results of ACM-R net-return rates ((for all experimental sample types) during all model conditions.

		n sample blocks	First Quartile	Min	Median	Mean	Max
MIS4 without Paleo-Agulhas plain silcrete	**Quartzite (Rq)**	20	0.009	0.000	0.019	0.023	0.069
	Untreated Silcrete (Rs)	8	0.014	0.012	0.024	0.025	0.042
	Insulated-Silcrete (Rs)	8	0.032	0.020	0.071	0.070	0.128
	Exposed-Silcrete (Rs)	8	0.030	0.019	0.065	0.065	0.118
MIS4 with Paleo-Agulhas plain silcrete	**Quartzite (Rq)**	20	0.009	0.000	0.019	0.023	0.069
	Untreated Silcrete (Rs)	8	0.085	0.075	0.151	0.155	0.263
	Insulated-Silcrete (Rs)	8	0.087	0.055	0.191	0.189	0.346
	Exposed-Silcrete (Rs)	8	0.070	0.045	0.156	0.154	0.282
MIS5	**Quartzite (Rq)**	20	0.109	0.000	0.252	0.288	0.776
	Untreated Silcrete (Rs)	8	0.014	0.012	0.024	0.025	0.042
	Insulated-Silcrete (Rs)	8	0.026	0.017	0.059	0.058	0.105
	Exposed-Silcrete (Rs)	8	0.030	0.019	0.065	0.065	0.118
MIS6 without Paleo-Agulhas plain silcrete	**Quartzite (Rq)**	20	0.030	0.000	0.070	0.080	0.216
	Untreated Silcrete (Rs)	8	0.014	0.012	0.024	0.025	0.042
	Insulated-Silcrete (Rs)	8	0.026	0.017	0.059	0.058	0.105
	Exposed-Silcrete (Rs)	8	0.030	0.019	0.065	0.065	0.118
MIS6 with Paleo-Agulhas plain silcrete	**Quartzite (Rq)**	20	0.030	0.000	0.070	0.080	0.216
	Untreated Silcrete (Rs)	8	0.085	0.075	0.151	0.155	0.263
	Insulated-Silcrete (Rs)	8	0.055	0.035	0.121	0.120	0.219
	Exposed-Silcrete (Rs)	8	0.070	0.045	0.156	0.154	0.282

0.227	0.083	0.028	0.056	0.210	0.098
0.176	0.064	0.022	0.043	0.163	0.076
0.216	0.071	0.024	0.048	0.203	0.107
0.133	0.061	0.013	0.026	0.106	0.054
0.095	0.035	0.012	0.023	0.088	0.041
0.085	0.031	0.011	0.021	0.078	0.037
0.035	0.011	0.004	0.008	0.032	0.017
0.133	0.061	0.013	0.026	0.106	0.054
0.095	0.035	0.012	0.023	0.088	0.041
0.085	0.031	0.011	0.021	0.078	0.037
0.035	0.011	0.004	0.008	0.032	0.017
0.476	0.220	0.047	0.093	0.381	0.195
0.227	0.083	0.028	0.056	0.210	0.098
0.278	0.102	0.035	0.069	0.258	0.120
0.216	0.071	0.024	0.048	0.203	0.107
0.038	0.018	0.004	0.008	0.031	0.015
0.095	0.035	0.012	0.023	0.088	0.041
0.103	0.038	0.013	0.025	0.095	0.045
0.035	0.011	0.004	0.008	0.032	0.017
0.038	0.018	0.004	0.008	0.031	0.015
Third Quartile	SD	Bootstrapped SE*	Margin of error (95% CI)	Bootstrapped Upper 95% CI*	Bootstrapped Lower 95% CI*

*Samples bootstrapped 10000 times.

MIS4 conditions with or without a Paleo-Agulhas plain silcrete source

Table B255. ACM-R net-return rates (Rq) for quartzite experimental blocks during MIS4 conditions with or without a Paleo-Agulhas plain silcrete source.

Model Conditions	Block	Raw Material	Count Complete Blades (n=)	Total Flaked Core Mass (kg)	Count Complete Blades (n=) / Total Flaked Core Mass (kg)	Count Blades * Durability (e * d)	Rq
MIS4	C9-1-1B8	Quartzite	2	1.920	1.042	1.627	0.009
MIS4	C9-1-1B9	Quartzite	4	2.060	1.941	3.033	0.017
MIS4	D11-1-100A	Quartzite	1	2.149	0.465	0.727	0.004
MIS4	D11-1-90D1	Quartzite	1	2.450	0.408	0.638	0.004
MIS4	D11-1-95A	Quartzite	2	2.031	0.985	1.538	0.009
MIS4	D11-1-95B	Quartzite	2	2.160	0.926	1.447	0.009
MIS4	D11-1-97A1	Quartzite	0	1.925	0.000	0.000	0.000
MIS4	D11-1-98B1	Quartzite	3	1.913	1.568	2.451	0.013
MIS4	D11-1-98C1	Quartzite	3	2.091	1.435	2.242	0.013
MIS4	D11-1-98D	Quartzite	1	1.843	0.543	0.848	0.004
MIS4	D11-1-85C1	Quartzite	8	1.996	4.008	8.116	0.043
MIS4	D11-1-91A1	Quartzite	6	1.962	3.058	6.192	0.034
MIS4	D11-1-91A2	Quartzite	8	2.174	3.679	7.451	0.044
MIS4	D11-1-91B3	Quartzite	11	1.885	5.836	11.818	0.069
MIS4	D11-1-91B5	Quartzite	4	2.220	1.802	3.648	0.021
MIS4	D11-1-91C3	Quartzite	5	1.962	2.548	5.160	0.029
MIS4	D11-1-94B2	Quartzite	5	1.828	2.736	5.539	0.028
MIS4	D11-1-94B3	Quartzite	8	1.784	4.484	9.081	0.046
MIS4	D11-1-94D2	Quartzite	5	1.966	2.543	5.150	0.029
MIS4	D11-1-97C	Quartzite	7	1.833	3.819	7.733	0.039

MIS4 conditions without a Paleo-Agulhas plain silcrete source

Table B256. ACM-R net-return rates (Rs) for heat-treated silcrete assuming both the insulated and exposed heating scenarios and untreated silcrete experimental blocks during MIS4 conditions without a Paleo-Agulhas plain silcrete source.

Model Conditions	Heating Scenario	Block	Raw Material	Count Complete Blades (n=)	Total Flaked Core Mass (kg)	Count Complete Blades (n=) / Total Flaked Core Mass (kg)	Count Blades * Durability (e * d)	Rs
MIS4-Without Paleo-Agulhas Silcrete	Insulated	D9-1-10b	Silcrete	7	2.350	2.979	8.412	0.047
MIS4-Without Paleo-Agulhas Silcrete	Insulated	D9-1-12b	Silcrete	3	2.200	1.364	3.851	0.020
MIS4-Without Paleo-Agulhas Silcrete	Insulated	D9-1-12d	Silcrete	4	2.286	1.750	4.940	0.027

MIS4-Without Paleo-Agulhas Silcrete	Insulated	E3-1-1b	Silcrete	13	1.933	6.724	18.986	0.088
MIS4-Without Paleo-Agulhas Silcrete	Insulated	E3-1-5p	Silcrete	10	2.588	3.864	10.912	0.067
MIS4-Without Paleo-Agulhas Silcrete	Insulated	E3-1-6a	Silcrete	16	2.196	7.286	20.574	0.108
MIS4-Without Paleo-Agulhas Silcrete	Insulated	E3-1-6c	Silcrete	19	2.436	7.800	22.025	0.128
MIS4-Without Paleo-Agulhas Silcrete	Insulated	I14-2-16l	Silcrete	11	2.356	4.668	13.183	0.074
MIS4-Without Paleo-Agulhas Silcrete	Exposed	D9-1-10b	Silcrete	7	2.350	2.979	8.412	0.044
MIS4-Without Paleo-Agulhas Silcrete	Exposed	D9-1-12b	Silcrete	3	2.200	1.364	3.851	0.019
MIS4-Without Paleo-Agulhas Silcrete	Exposed	D9-1-12d	Silcrete	4	2.286	1.750	4.940	0.025
MIS4-Without Paleo-Agulhas Silcrete	Exposed	E3-1-1b	Silcrete	13	1.933	6.724	18.986	0.081
MIS4-Without Paleo-Agulhas Silcrete	Exposed	E3-1-5p	Silcrete	10	2.588	3.864	10.912	0.062
MIS4-Without Paleo-Agulhas Silcrete	Exposed	E3-1-6a	Silcrete	16	2.196	7.286	20.574	0.100
MIS4-Without Paleo-Agulhas Silcrete	Exposed	E3-1-6c	Silcrete	19	2.436	7.800	22.025	0.118
MIS4-Without Paleo-Agulhas Silcrete	Exposed	I14-2-16l	Silcrete	11	2.356	4.668	13.183	0.068
MIS4-Without Paleo-Agulhas Silcrete	Untreated	D9-1-10a	Silcrete	3	1.980	1.515	2.850	0.018
MIS4-Without Paleo-Agulhas Silcrete	Untreated	D9-1-12a	Silcrete	7	2.250	3.112	5.853	0.042
MIS4-Without Paleo-Agulhas Silcrete	Untreated	D9-1-12c	Silcrete	2	1.807	1.107	2.082	0.012
MIS4-Without Paleo-Agulhas Silcrete	Untreated	E3-1-1A	Silcrete	5	2.070	2.416	4.544	0.030
MIS4-Without Paleo-Agulhas Silcrete	Untreated	E3-1-5n	Silcrete	5	2.460	2.033	3.823	0.030
MIS4-Without Paleo-Agulhas Silcrete	Untreated	E3-1-5o	Silcrete	6	2.505	2.395	4.506	0.036
MIS4-Without Paleo-Agulhas Silcrete	Untreated	E3-1-6b	Silcrete	2	1.691	1.183	2.225	0.012
MIS4-Without Paleo-Agulhas Silcrete	Untreated	I14-2-16a	Silcrete	3	2.895	1.036	1.949	0.018

MIS4 conditions with a Paleo-Agulhas plain silcrete source

Table B257. ACM-R net-return rates (Rs) for heat-treated silcrete assuming both the insulated and exposed heating scenarios and untreated silcrete experimental blocks during MIS4 conditions with a Paleo-Agulhas plain silcrete source.

Model Conditions	Heating Scenario	Block	Raw Material	Count Complete Blades (n=)	Total Flaked Core Mass (kg)	Count Complete Blades (n=) / Total Flaked Core Mass (kg)	Count Blades * Durability (e * d)	Rs
MIS4-With Paleo-Agulhas Silcrete	Insulated	D9-1-10b	Silcrete	7	2.350	2.979	8.412	0.127
MIS4-With Paleo-Agulhas Silcrete	Insulated	D9-1-12b	Silcrete	3	2.200	1.364	3.851	0.055
MIS4-With Paleo-Agulhas Silcrete	Insulated	D9-1-12d	Silcrete	4	2.286	1.750	4.940	0.073
MIS4-With Paleo-Agulhas Silcrete	Insulated	E3-1-1b	Silcrete	13	1.933	6.724	18.986	0.237

MIS4-With Paleo-Agulhas Silcrete	Insulated	E3-1-5p	Silcrete	10	2.588	3.864	10.912	0.182
MIS4-With Paleo-Agulhas Silcrete	Insulated	E3-1-6a	Silcrete	16	2.196	7.286	20.574	0.291
MIS4-With Paleo-Agulhas Silcrete	Insulated	E3-1-6c	Silcrete	19	2.436	7.800	22.025	0.346
MIS4-With Paleo-Agulhas Silcrete	Insulated	I14-2-16l	Silcrete	11	2.356	4.668	13.183	0.200
MIS4-With Paleo-Agulhas Silcrete	Exposed	D9-1-10b	Silcrete	7	2.350	2.979	8.412	0.104
MIS4-With Paleo-Agulhas Silcrete	Exposed	D9-1-12b	Silcrete	3	2.200	1.364	3.851	0.045
MIS4-With Paleo-Agulhas Silcrete	Exposed	D9-1-12d	Silcrete	4	2.286	1.750	4.940	0.059
MIS4-With Paleo-Agulhas Silcrete	Exposed	E3-1-1b	Silcrete	13	1.933	6.724	18.986	0.193
MIS4-With Paleo-Agulhas Silcrete	Exposed	E3-1-5p	Silcrete	10	2.588	3.864	10.912	0.149
MIS4-With Paleo-Agulhas Silcrete	Exposed	E3-1-6a	Silcrete	16	2.196	7.286	20.574	0.238
MIS4-With Paleo-Agulhas Silcrete	Exposed	E3-1-6c	Silcrete	19	2.436	7.800	22.025	0.282
MIS4-With Paleo-Agulhas Silcrete	Exposed	I14-2-16l	Silcrete	11	2.356	4.668	13.183	0.163
MIS4-With Paleo-Agulhas Silcrete	Untreated	D9-1-10a	Silcrete	3	1.980	1.515	2.850	0.113
MIS4-With Paleo-Agulhas Silcrete	Untreated	D9-1-12a	Silcrete	7	2.250	3.112	5.853	0.263
MIS4-With Paleo-Agulhas Silcrete	Untreated	D9-1-12c	Silcrete	2	1.807	1.107	2.082	0.075
MIS4-With Paleo-Agulhas Silcrete	Untreated	E3-1-1A	Silcrete	5	2.070	2.416	4.544	0.188
MIS4-With Paleo-Agulhas Silcrete	Untreated	E3-1-5n	Silcrete	5	2.460	2.033	3.823	0.188
MIS4-With Paleo-Agulhas Silcrete	Untreated	E3-1-5o	Silcrete	6	2.505	2.395	4.506	0.225
MIS4-With Paleo-Agulhas Silcrete	Untreated	E3-1-6b	Silcrete	2	1.691	1.183	2.225	0.075
MIS4-With Paleo-Agulhas Silcrete	Untreated	I14-2-16a	Silcrete	3	2.895	1.036	1.949	0.113

MIS5 conditions

Table B258. ACM-R net-return rates (Rq) for quartzite experimental blocks during MIS5 conditions.

Model Conditions	Block	Raw Material	Count Complete Blades (n=)	Total Flaked Core Mass (kg)	Count Complete Blades (n=)/Total Flaked Core Mass (kg)	Count Blades * Durability (e * d)	Rq
MIS5	C9-1-1B8	Quartzite	2	1.920	1.042	1.627	0.110
MIS5	C9-1-1B9	Quartzite	4	2.060	1.941	3.033	0.221
MIS5	D11-1-100A	Quartzite	1	2.149	0.465	0.727	0.054
MIS5	D11-1-90D1	Quartzite	1	2.450	0.408	0.638	0.054
MIS5	D11-1-95A	Quartzite	2	2.031	0.985	1.538	0.109
MIS5	D11-1-95B	Quartzite	2	2.160	0.926	1.447	0.109
MIS5	D11-1-97A1	Quartzite	0	1.925	0.000	0.000	0.000
MIS5	D11-1-98B1	Quartzite	3	1.913	1.568	2.451	0.163
MIS5	D11-1-98C1	Quartzite	3	2.091	1.435	2.242	0.163

MIS5	D11-1-98D	Quartzite	1	1.843	0.543	0.848	0.054
MIS5	D11-1-85C1	Quartzite	8	1.996	4.008	8.116	0.564
MIS5	D11-1-91A1	Quartzite	6	1.962	3.058	6.192	0.423
MIS5	D11-1-91A2	Quartzite	8	2.174	3.679	7.451	0.564
MIS5	D11-1-91B3	Quartzite	11	1.885	5.836	11.818	0.776
MIS5	D11-1-91B5	Quartzite	4	2.220	1.802	3.648	0.282
MIS5	D11-1-91C3	Quartzite	5	1.962	2.548	5.160	0.353
MIS5	D11-1-94B2	Quartzite	5	1.828	2.736	5.539	0.353
MIS5	D11-1-94B3	Quartzite	8	1.784	4.484	9.081	0.564
MIS5	D11-1-94D2	Quartzite	5	1.966	2.543	5.150	0.353
MIS5	D11-1-97C	Quartzite	7	1.833	3.819	7.733	0.494

Table B259. ACM-R net-return rates (Rs) for heat-treated silcrete assuming both the insulated and exposed heating scenarios and untreated silcrete experimental blocks during MIS5 conditions.

Model Conditions	Heating Scenario	Block	Raw Material	Count Complete Blades (n=)	Total Flaked Core Mass (kg)	Count Complete Blades (n=) / Total Flaked Core Mass (kg)	Count Blades * Durability (e * d)	Rs
MIS5	Insulated	D9-1-10b	Silcrete	7	2.350	2.979	8.412	0.039
MIS5	Insulated	D9-1-12b	Silcrete	3	2.200	1.364	3.851	0.017
MIS5	Insulated	D9-1-12d	Silcrete	4	2.286	1.750	4.940	0.022
MIS5	Insulated	E3-1-1b	Silcrete	13	1.933	6.724	18.986	0.072
MIS5	Insulated	E3-1-5p	Silcrete	10	2.588	3.864	10.912	0.056
MIS5	Insulated	E3-1-6a	Silcrete	16	2.196	7.286	20.574	0.089
MIS5	Insulated	E3-1-6c	Silcrete	19	2.436	7.800	22.025	0.105
MIS5	Insulated	I14-2-16l	Silcrete	11	2.356	4.668	13.183	0.061
MIS5	Exposed	D9-1-10b	Silcrete	7	2.350	2.979	8.412	0.044
MIS5	Exposed	D9-1-12b	Silcrete	3	2.200	1.364	3.851	0.019
MIS5	Exposed	D9-1-12d	Silcrete	4	2.286	1.750	4.940	0.025
MIS5	Exposed	E3-1-1b	Silcrete	13	1.933	6.724	18.986	0.081
MIS5	Exposed	E3-1-5p	Silcrete	10	2.588	3.864	10.912	0.062
MIS5	Exposed	E3-1-6a	Silcrete	16	2.196	7.286	20.574	0.100
MIS5	Exposed	E3-1-6c	Silcrete	19	2.436	7.800	22.025	0.118
MIS5	Exposed	I14-2-16l	Silcrete	11	2.356	4.668	13.183	0.068
MIS5	Untreated	D9-1-10a	Silcrete	3	1.980	1.515	2.850	0.018
MIS5	Untreated	D9-1-12a	Silcrete	7	2.250	3.112	5.853	0.042

MIS5	Untreated	D9-1-12c	Silcrete	2	1.807	1.107	2.082	0.012
MIS5	Untreated	E3-1-1A	Silcrete	5	2.070	2.416	4.544	0.030
MIS5	Untreated	E3-1-5n	Silcrete	5	2.460	2.033	3.823	0.030
MIS5	Untreated	E3-1-5o	Silcrete	6	2.505	2.395	4.506	0.036
MIS5	Untreated	E3-1-6b	Silcrete	2	1.691	1.183	2.225	0.012
MIS5	Untreated	I14-2-16a	Silcrete	3	2.895	1.036	1.949	0.018

MIS6 conditions with or without a Paleo-Agulhas plain silcrete source

Table B260. ACM-R net-return rates (Rq) for quartzite experimental blocks during MIS6 conditions with or without a Paleo-Agulhas plain silcrete source.

Model Conditions	Block	Raw Material	Count Complete Blades (n=)	Total Flaked Core Mass (kg)	Count Complete Blades (n=) / Total Flaked Core Mass (kg)	Count Blades * Durability (e * d)	Rq
MIS6	C9-1-1B8	Quartzite	2	1.920	1.042	1.627	0.030
MIS6	C9-1-1B9	Quartzite	4	2.060	1.941	3.033	0.061
MIS6	D11-1-100A	Quartzite	1	2.149	0.465	0.727	0.015
MIS6	D11-1-90D1	Quartzite	1	2.450	0.408	0.638	0.015
MIS6	D11-1-95A	Quartzite	2	2.031	0.985	1.538	0.030
MIS6	D11-1-95B	Quartzite	2	2.160	0.926	1.447	0.030
MIS6	D11-1-97A1	Quartzite	0	1.925	0.000	0.000	0.000
MIS6	D11-1-98B1	Quartzite	3	1.913	1.568	2.451	0.046
MIS6	D11-1-98C1	Quartzite	3	2.091	1.435	2.242	0.046
MIS6	D11-1-98D	Quartzite	1	1.843	0.543	0.848	0.015
MIS6	D11-1-85C1	Quartzite	8	1.996	4.008	8.116	0.157
MIS6	D11-1-91A1	Quartzite	6	1.962	3.058	6.192	0.118
MIS6	D11-1-91A2	Quartzite	8	2.174	3.679	7.451	0.157
MIS6	D11-1-91B3	Quartzite	11	1.885	5.836	11.818	0.216
MIS6	D11-1-91B5	Quartzite	4	2.220	1.802	3.648	0.079
MIS6	D11-1-91C3	Quartzite	5	1.962	2.548	5.160	0.098
MIS6	D11-1-94B2	Quartzite	5	1.828	2.736	5.539	0.098
MIS6	D11-1-94B3	Quartzite	8	1.784	4.484	9.081	0.157
MIS6	D11-1-94D2	Quartzite	5	1.966	2.543	5.150	0.098
MIS6	D11-1-97C	Quartzite	7	1.833	3.819	7.733	0.138

MIS6 conditions without a Paleo-Agulhas plain silcrete source

Table B261. ACM-R net-return rates (Rs) for heat-treated silcrete assuming both the insulated and exposed heating scenarios and untreated silcrete experimental blocks during MIS6 conditions without a Paleo-Agulhas plain silcrete source.

Model Conditions	Heating Scenario	Block	Raw Material	Count Complete Blades (n=)	Total Flaked Core Mass (kg)	Count Complete Blades (n=) / Total Flaked Core Mass (kg)	Count Blades * Durability (e * d)	Rs
MIS6-Without Paleo-Agulhas Silcrete	Insulated	D9-1-10b	Silcrete	7	2.350	2.979	8.412	0.039
MIS6-Without Paleo-Agulhas Silcrete	Insulated	D9-1-12b	Silcrete	3	2.200	1.364	3.851	0.017
MIS6-Without Paleo-Agulhas Silcrete	Insulated	D9-1-12d	Silcrete	4	2.286	1.750	4.940	0.022
MIS6-Without Paleo-Agulhas Silcrete	Insulated	E3-1-1b	Silcrete	13	1.933	6.724	18.986	0.072
MIS6-Without Paleo-Agulhas Silcrete	Insulated	E3-1-5p	Silcrete	10	2.588	3.864	10.912	0.056
MIS6-Without Paleo-Agulhas Silcrete	Insulated	E3-1-6a	Silcrete	16	2.196	7.286	20.574	0.089
MIS6-Without Paleo-Agulhas Silcrete	Insulated	E3-1-6c	Silcrete	19	2.436	7.800	22.025	0.105
MIS6-Without Paleo-Agulhas Silcrete	Insulated	I14-2-16l	Silcrete	11	2.356	4.668	13.183	0.061
MIS6-Without Paleo-Agulhas Silcrete	Exposed	D9-1-10b	Silcrete	7	2.350	2.979	8.412	0.044
MIS6-Without Paleo-Agulhas Silcrete	Exposed	D9-1-12b	Silcrete	3	2.200	1.364	3.851	0.019
MIS6-Without Paleo-Agulhas Silcrete	Exposed	D9-1-12d	Silcrete	4	2.286	1.750	4.940	0.025
MIS6-Without Paleo-Agulhas Silcrete	Exposed	E3-1-1b	Silcrete	13	1.933	6.724	18.986	0.081
MIS6-Without Paleo-Agulhas Silcrete	Exposed	E3-1-5p	Silcrete	10	2.588	3.864	10.912	0.062
MIS6-Without Paleo-Agulhas Silcrete	Exposed	E3-1-6a	Silcrete	16	2.196	7.286	20.574	0.100
MIS6-Without Paleo-Agulhas Silcrete	Exposed	E3-1-6c	Silcrete	19	2.436	7.800	22.025	0.118
MIS6-Without Paleo-Agulhas Silcrete	Exposed	I14-2-16l	Silcrete	11	2.356	4.668	13.183	0.068
MIS6-Without Paleo-Agulhas Silcrete	Untreated	D9-1-10a	Silcrete	3	1.980	1.515	2.850	0.018
MIS6-Without Paleo-Agulhas Silcrete	Untreated	D9-1-12a	Silcrete	7	2.250	3.112	5.853	0.042
MIS6-Without Paleo-Agulhas Silcrete	Untreated	D9-1-12c	Silcrete	2	1.807	1.107	2.082	0.012
MIS6-Without Paleo-Agulhas Silcrete	Untreated	E3-1-1A	Silcrete	5	2.070	2.416	4.544	0.030
MIS6-Without Paleo-Agulhas Silcrete	Untreated	E3-1-5n	Silcrete	5	2.460	2.033	3.823	0.030
MIS6-Without Paleo-Agulhas Silcrete	Untreated	E3-1-5o	Silcrete	6	2.505	2.395	4.506	0.036
MIS6-Without Paleo-Agulhas Silcrete	Untreated	E3-1-6b	Silcrete	2	1.691	1.183	2.225	0.012
MIS6-Without Paleo-Agulhas Silcrete	Untreated	I14-2-16a	Silcrete	3	2.895	1.036	1.949	0.018

MIS6 conditions with a Paleo-Agulhas plain silcrete source

Table B262. ACM-R net-return rates (Rs) for heat-treated silcrete assuming both the insulated and exposed heating scenarios and untreated silcrete experimental blocks during MIS6 conditions with a Paleo-Agulhas plain silcrete source.

Model Conditions	Heating Scenario	Block	Raw Material	Count Complete Blades (n=)	Total Flaked Core Mass (kg)	Count Complete Blades (n=) / Total Flaked Core Mass (kg)	Count Blades * Durability (e * d)	Rs
MIS6-With Paleo-Agulhas Silcrete	Insulated	D9-1-10b	Silcrete	7	2.350	2.979	8.412	0.081
MIS6-With Paleo-Agulhas Silcrete	Insulated	D9-1-12b	Silcrete	3	2.200	1.364	3.851	0.035
MIS6-With Paleo-Agulhas Silcrete	Insulated	D9-1-12d	Silcrete	4	2.286	1.750	4.940	0.046
MIS6-With Paleo-Agulhas Silcrete	Insulated	E3-1-1b	Silcrete	13	1.933	6.724	18.986	0.150
MIS6-With Paleo-Agulhas Silcrete	Insulated	E3-1-5p	Silcrete	10	2.588	3.864	10.912	0.115
MIS6-With Paleo-Agulhas Silcrete	Insulated	E3-1-6a	Silcrete	16	2.196	7.286	20.574	0.184
MIS6-With Paleo-Agulhas Silcrete	Insulated	E3-1-6c	Silcrete	19	2.436	7.800	22.025	0.219
MIS6-With Paleo-Agulhas Silcrete	Insulated	I14-2-16l	Silcrete	11	2.356	4.668	13.183	0.127
MIS6-With Paleo-Agulhas Silcrete	Exposed	D9-1-10b	Silcrete	7	2.350	2.979	8.412	0.104
MIS6-With Paleo-Agulhas Silcrete	Exposed	D9-1-12b	Silcrete	3	2.200	1.364	3.851	0.045
MIS6-With Paleo-Agulhas Silcrete	Exposed	D9-1-12d	Silcrete	4	2.286	1.750	4.940	0.059
MIS6-With Paleo-Agulhas Silcrete	Exposed	E3-1-1b	Silcrete	13	1.933	6.724	18.986	0.193
MIS6-With Paleo-Agulhas Silcrete	Exposed	E3-1-5p	Silcrete	10	2.588	3.864	10.912	0.149
MIS6-With Paleo-Agulhas Silcrete	Exposed	E3-1-6a	Silcrete	16	2.196	7.286	20.574	0.238
MIS6-With Paleo-Agulhas Silcrete	Exposed	E3-1-6c	Silcrete	19	2.436	7.800	22.025	0.282
MIS6-With Paleo-Agulhas Silcrete	Exposed	I14-2-16l	Silcrete	11	2.356	4.668	13.183	0.163
MIS6-With Paleo-Agulhas Silcrete	Untreated	D9-1-10a	Silcrete	3	1.980	1.515	2.850	0.113
MIS6-With Paleo-Agulhas Silcrete	Untreated	D9-1-12a	Silcrete	7	2.250	3.112	5.853	0.263
MIS6-With Paleo-Agulhas Silcrete	Untreated	D9-1-12c	Silcrete	2	1.807	1.107	2.082	0.075
MIS6-With Paleo-Agulhas Silcrete	Untreated	E3-1-1A	Silcrete	5	2.070	2.416	4.544	0.188
MIS6-With Paleo-Agulhas Silcrete	Untreated	E3-1-5n	Silcrete	5	2.460	2.033	3.823	0.188
MIS6-With Paleo-Agulhas Silcrete	Untreated	E3-1-5o	Silcrete	6	2.505	2.395	4.506	0.225
MIS6-With Paleo-Agulhas Silcrete	Untreated	E3-1-6b	Silcrete	2	1.691	1.183	2.225	0.075
MIS6-With Paleo-Agulhas Silcrete	Untreated	I14-2-16a	Silcrete	3	2.895	1.036	1.949	0.113

ACM – Model condition variable outcomes

Coastline position and raw material distribution variable

Table B263. Summary Statistics and test results of ACM-R net-return rates (Rq and Rs) when only t_s time-cost (travel and search time) is considered during all model conditions.

	MIS4 without Paleo-Agulhas plain silcrete			MIS4 with Paleo-Agulhas plain silcrete			MIS5			MIS6 without Paleo-Agulhas plain silcrete			MIS6 with Paleo-Agulhas plain silcrete		
	Heat-treated Silcrete (Rs)	Untreated Silcrete (Rs)	Quartzite (Rq)	Heat-treated Silcrete (Rs)	Untreated Silcrete (Rs)	Quartzite (Rq)	Heat-treated Silcrete (Rs)	Untreated Silcrete (Rs)	Quartzite (Rq)	Heat-treated Silcrete (Rs)	Untreated Silcrete (Rs)	Quartzite (Rq)	Heat-treated Silcrete (Rs)	Untreated Silcrete (Rs)	Quartzite (Rq)
n sample blocks	8	8	20	8	8	20	8	8	20	8	8	20	8	8	20
First Quartile	0.046	0.015	0.017	0.479	0.151	0.017	0.046	0.015	0.246	0.046	0.015	0.064	0.479	0.151	0.064
Min	0.029	0.013	0.000	0.302	0.134	0.000	0.029	0.013	0.000	0.029	0.013	0.000	0.302	0.134	0.000
Median	0.102	0.026	0.040	1.059	0.269	0.040	0.102	0.026	0.565	0.102	0.026	0.147	1.059	0.269	0.147
Mean	0.101	0.027	0.046	1.046	0.277	0.046	0.101	0.027	0.651	0.101	0.027	0.169	1.046	0.277	0.169
Max	0.184	0.045	0.124	1.915	0.470	0.124	0.184	0.045	1.754	0.184	0.045	0.456	1.915	0.470	0.456

1.537	0.565	0.194	0.380	1.426	0.666	
0.386	0.127	0.044	0.086	0.363	0.191	
0.280	0.129	0.028	0.055	0.224	0.114	
0.148	0.054	0.019	0.036	0.137	0.064	
0.037	0.012	0.004	0.008	0.035	0.018	
0.280	0.129	0.028	0.055	0.224	0.114	
0.148	0.054	0.019	0.037	0.137	0.064	
0.037	0.012	0.004	0.008	0.035	0.018	
1.076	0.497	0.108	0.211	0.862	0.440	
1.537	0.565	0.194	0.380	1.426	0.666	
0.386	0.127	0.044	0.085	0.362	0.192	
0.076	0.035	0.008	0.015	0.061	0.031	
0.148	0.054	0.018	0.036	0.137	0.064	
0.037	0.012	0.004	0.008	0.035	0.018	
0.076	0.035	0.008	0.015	0.061	0.031	
Third Quartile	SD	Bootstrapped SE*	Margin of error (95% CI)	Bootstrapped Upper 95% CI*	Bootstrapped Lower 95% CI*	

*Samples bootstrapped 10000 times.

MIS4 with or without a Paleo-Agulhas plain silcrete source

Table B264. ACM-R net-return rates (Rq) for quartzite experimental blocks when only t_s time-cost (travel and search time) is considered during MIS4 conditions with or without a Paleo-Agulhas plain silcrete source.

Block	Raw Material	Count Complete Blades (n=)	Total Flaked Core Mass (kg)	Count Complete Blades (n=) / Total Flaked Core Mass (kg)	Count Blades * Durability (e * d)	ts-Travel and search time (min) / Total Flaked Core Mass (kg)	Rq
C9-1-1B8	Quartzite	2	1.920	1.042	1.627	93.74	0.017
C9-1-1B9	Quartzite	4	2.060	1.941	3.033	87.36	0.035
D11-1-100A	Quartzite	1	2.149	0.465	0.727	83.76	0.009
D11-1-90D1	Quartzite	1	2.450	0.408	0.638	73.46	0.009
D11-1-95A	Quartzite	2	2.031	0.985	1.538	88.61	0.017
D11-1-95B	Quartzite	2	2.160	0.926	1.447	83.33	0.017
D11-1-97A1	Quartzite	0	1.925	0.000	0.000	93.51	0.000
D11-1-98B1	Quartzite	3	1.913	1.568	2.451	94.11	0.026
D11-1-98C1	Quartzite	3	2.091	1.435	2.242	86.10	0.026
D11-1-98D	Quartzite	1	1.843	0.543	0.848	97.69	0.009
D11-1-85C1	Quartzite	8	1.996	4.008	8.116	90.18	0.090
D11-1-91A1	Quartzite	6	1.962	3.058	6.192	91.73	0.068
D11-1-91A2	Quartzite	8	2.174	3.679	7.451	82.79	0.090
D11-1-91B3	Quartzite	11	1.885	5.836	11.818	95.50	0.124
D11-1-91B5	Quartzite	4	2.220	1.802	3.648	81.07	0.045
D11-1-91C3	Quartzite	5	1.962	2.548	5.160	91.73	0.056
D11-1-94B2	Quartzite	5	1.828	2.736	5.539	98.48	0.056
D11-1-94B3	Quartzite	8	1.784	4.484	9.081	100.90	0.090
D11-1-94D2	Quartzite	5	1.966	2.543	5.150	91.55	0.056
D11-1-97C	Quartzite	7	1.833	3.819	7.733	98.19	0.079

MIS4 with or without a Paleo-Agulhas plain silcrete source

Table B265. ACM-R net-return rates (Rs) for heat-treated silcrete assuming both the insulated and exposed heating scenarios and untreated silcrete experimental blocks when only t_s time-cost (travel and search time) is considered during MIS4 conditions without a Paleo-Agulhas plain silcrete source.

Block	Sample Type	Raw Material	Count Complete Blades (n=)	Total Flaked Core Mass (kg)	Count Complete Blades (n=) / Total Flaked Core Mass (kg)	Count Blades * Durability (e * d)	ts-Travel and search time (min) / Total Flaked Core Mass (kg)	Rs
D9-1-10b	Heat-treated	Silcrete	7	2.350	2.979	8.412	124.02	0.068
D9-1-12b	Heat-treated	Silcrete	3	2.200	1.364	3.851	132.47	0.029

D9-1-12d	Heat-treated	Silcrete	4	2.286	1.750	4.940	127.47	0.039
E3-1-1b	Heat-treated	Silcrete	13	1.933	6.724	18.986	150.73	0.126
E3-1-5p	Heat-treated	Silcrete	10	2.588	3.864	10.912	112.62	0.097
E3-1-6a	Heat-treated	Silcrete	16	2.196	7.286	20.574	132.71	0.155
E3-1-6c	Heat-treated	Silcrete	19	2.436	7.800	22.025	119.64	0.184
I14-2-16l	Heat-treated	Silcrete	11	2.356	4.668	13.183	123.69	0.107
D9-1-10a	Untreated	Silcrete	3	1.980	1.515	2.850	147.18	0.019
D9-1-12a	Untreated	Silcrete	7	2.250	3.112	5.853	129.55	0.045
D9-1-12c	Untreated	Silcrete	2	1.807	1.107	2.082	161.27	0.013
E3-1-1A	Untreated	Silcrete	5	2.070	2.416	4.544	140.82	0.032
E3-1-5n	Untreated	Silcrete	5	2.460	2.033	3.823	118.48	0.032
E3-1-5o	Untreated	Silcrete	6	2.505	2.395	4.506	116.35	0.039
E3-1-6b	Untreated	Silcrete	2	1.691	1.183	2.225	172.34	0.013
I14-2-16a	Untreated	Silcrete	3	2.895	1.036	1.949	100.66	0.019

MIS4 with a Paleo-Agulhas plain silcrete source

Table B266. ACM-R net-return rates (Rs) for heat-treated silcrete assuming both the insulated and exposed heating scenarios and untreated silcrete experimental blocks when only t_s time-cost (travel and search time) is considered during MIS4 conditions with a Paleo-Agulhas plain silcrete source.

Block	Sample Type	Raw Material	Count Complete Blades (n=)	Total Flaked Core Mass (kg)	Count Complete Blades (n=) / Total Flaked Core Mass (kg)	Count Blades * Durability (e * d)	ts-Travel and search time (min) / Total Flaked Core Mass (kg)	Rs
D9-1-10b	Heat-treated	Silcrete	7	2.350	2.979	8.412	11.923	0.706
D9-1-12b	Heat-treated	Silcrete	3	2.200	1.364	3.851	12.734	0.302
D9-1-12d	Heat-treated	Silcrete	4	2.286	1.750	4.940	12.254	0.403
E3-1-1b	Heat-treated	Silcrete	13	1.933	6.724	18.986	14.490	1.310
E3-1-5p	Heat-treated	Silcrete	10	2.588	3.864	10.912	10.827	1.008
E3-1-6a	Heat-treated	Silcrete	16	2.196	7.286	20.574	12.758	1.613
E3-1-6c	Heat-treated	Silcrete	19	2.436	7.800	22.025	11.501	1.915
I14-2-16l	Heat-treated	Silcrete	11	2.356	4.668	13.183	11.891	1.109
D9-1-10a	Untreated	Silcrete	3	1.980	1.515	2.850	14.149	0.201
D9-1-12a	Untreated	Silcrete	7	2.250	3.112	5.853	12.454	0.470
D9-1-12c	Untreated	Silcrete	2	1.807	1.107	2.082	15.504	0.134
E3-1-1A	Untreated	Silcrete	5	2.070	2.416	4.544	13.537	0.336

E3-1-5n	Untreated	Silcrete	5	2.460	2.033	3.823	11.390	0.336
E3-1-5o	Untreated	Silcrete	6	2.505	2.395	4.506	11.185	0.403
E3-1-6b	Untreated	Silcrete	2	1.691	1.183	2.225	16.568	0.134
I14-2-16a	Untreated	Silcrete	3	2.895	1.036	1.949	9.677	0.201

MIS5

Table B267. ACM-R net-return rates (Rq) for quartzite experimental blocks when only t_s time-cost (travel and search time) is considered during MIS5 conditions.

Block	Raw Material	Count Complete Blades (n=)	Total Flaked Core Mass (kg)	Count Complete Blades (n=) / Total Flaked Core Mass (kg)	Count Blades * Durability (e * d)	ts-Travel and search time (min) / Total Flaked Core Mass (kg)	Rq
C9-1-1B8	Quartzite	2	1.920	1.042	1.627	6.61	0.246
C9-1-1B9	Quartzite	4	2.060	1.941	3.033	6.16	0.492
D11-1-100A	Quartzite	1	2.149	0.465	0.727	5.91	0.123
D11-1-90D1	Quartzite	1	2.450	0.408	0.638	5.18	0.123
D11-1-95A	Quartzite	2	2.031	0.985	1.538	6.25	0.246
D11-1-95B	Quartzite	2	2.160	0.926	1.447	5.88	0.246
D11-1-97A1	Quartzite	0	1.925	0.000	0.000	6.60	0.000
D11-1-98B1	Quartzite	3	1.913	1.568	2.451	6.64	0.369
D11-1-98C1	Quartzite	3	2.091	1.435	2.242	6.07	0.369
D11-1-98D	Quartzite	1	1.843	0.543	0.848	6.89	0.123
D11-1-85C1	Quartzite	8	1.996	4.008	8.116	6.36	1.276
D11-1-91A1	Quartzite	6	1.962	3.058	6.192	6.47	0.957
D11-1-91A2	Quartzite	8	2.174	3.679	7.451	5.84	1.276
D11-1-91B3	Quartzite	11	1.885	5.836	11.818	6.74	1.754
D11-1-91B5	Quartzite	4	2.220	1.802	3.648	5.72	0.638
D11-1-91C3	Quartzite	5	1.962	2.548	5.160	6.47	0.797
D11-1-94B2	Quartzite	5	1.828	2.736	5.539	6.95	0.797
D11-1-94B3	Quartzite	8	1.784	4.484	9.081	7.12	1.276
D11-1-94D2	Quartzite	5	1.966	2.543	5.150	6.46	0.797
D11-1-97C	Quartzite	7	1.833	3.819	7.733	6.93	1.116

Table B268. ACM-R net-return rates (Rs) for heat-treated silcrete assuming both the insulated and exposed heating scenarios and untreated silcrete experimental blocks when only t_s time-cost (travel and search time) is considered during MIS5 conditions.

Block	Sample Type	Raw Material	Count Complete Blades (n=)	Total Flaked Core Mass (kg)	Count Complete Blades (n=) / Total Flaked Core Mass (kg)	Count Blades * Durability (e * d)	ts-Travel and search time (min) / Total Flaked Core Mass (kg)	Rs
D9-1-10b	Heat-treated	Silcrete	7	2.350	2.979	8.412	124.02	0.068
D9-1-12b	Heat-treated	Silcrete	3	2.200	1.364	3.851	132.47	0.029
D9-1-12d	Heat-treated	Silcrete	4	2.286	1.750	4.940	127.47	0.039
E3-1-1b	Heat-treated	Silcrete	13	1.933	6.724	18.986	150.73	0.126
E3-1-5p	Heat-treated	Silcrete	10	2.588	3.864	10.912	112.62	0.097
E3-1-6a	Heat-treated	Silcrete	16	2.196	7.286	20.574	132.71	0.155
E3-1-6c	Heat-treated	Silcrete	19	2.436	7.800	22.025	119.64	0.184
I14-2-16l	Heat-treated	Silcrete	11	2.356	4.668	13.183	123.69	0.107
D9-1-10a	Untreated	Silcrete	3	1.980	1.515	2.850	147.18	0.019
D9-1-12a	Untreated	Silcrete	7	2.250	3.112	5.853	129.55	0.045
D9-1-12c	Untreated	Silcrete	2	1.807	1.107	2.082	161.27	0.013
E3-1-1A	Untreated	Silcrete	5	2.070	2.416	4.544	140.82	0.032
E3-1-5n	Untreated	Silcrete	5	2.460	2.033	3.823	118.48	0.032
E3-1-5o	Untreated	Silcrete	6	2.505	2.395	4.506	116.35	0.039
E3-1-6b	Untreated	Silcrete	2	1.691	1.183	2.225	172.34	0.013
I14-2-16a	Untreated	Silcrete	3	2.895	1.036	1.949	100.66	0.019

MIS6 with or without a Paleo-Agulhas plain silcrete source

Table B269. ACM-R net-return rates (Rq) for quartzite experimental blocks when only t_s time-cost (travel and search time) is considered during MIS6 conditions without with a Paleo-Agulhas plain silcrete source.

Block	Raw Material	Count Complete Blades (n=)	Total Flaked Core Mass (kg)	Count Complete Blades (n=) / Total Flaked Core Mass (kg)	Count Blades * Durability (e * d)	*t*s-Travel and search time (min) / Total Flaked Core Mass (kg)	Rq
C9-1-1B8	Quartzite	2	1.920	1.042	1.627	25.42	0.064
C9-1-1B9	Quartzite	4	2.060	1.941	3.033	23.69	0.128
D11-1-100A	Quartzite	1	2.149	0.465	0.727	22.72	0.032
D11-1-90D1	Quartzite	1	2.450	0.408	0.638	19.92	0.032
D11-1-95A	Quartzite	2	2.031	0.985	1.538	24.03	0.064
D11-1-95B	Quartzite	2	2.160	0.926	1.447	22.60	0.064

D11-1-97A1	Quartzite	0	1.925	0.000	0.000	25.36	0.000
D11-1-98B1	Quartzite	3	1.913	1.568	2.451	25.52	0.096
D11-1-98C1	Quartzite	3	2.091	1.435	2.242	23.35	0.096
D11-1-98D	Quartzite	1	1.843	0.543	0.848	26.49	0.032
D11-1-85C1	Quartzite	8	1.996	4.008	8.116	24.46	0.332
D11-1-91A1	Quartzite	6	1.962	3.058	6.192	24.88	0.249
D11-1-91A2	Quartzite	8	2.174	3.679	7.451	22.45	0.332
D11-1-91B3	Quartzite	11	1.885	5.836	11.818	25.90	0.456
D11-1-91B5	Quartzite	4	2.220	1.802	3.648	21.99	0.166
D11-1-91C3	Quartzite	5	1.962	2.548	5.160	24.88	0.207
D11-1-94B2	Quartzite	5	1.828	2.736	5.539	26.71	0.207
D11-1-94B3	Quartzite	8	1.784	4.484	9.081	27.36	0.332
D11-1-94D2	Quartzite	5	1.966	2.543	5.150	24.83	0.207
D11-1-97C	Quartzite	7	1.833	3.819	7.733	26.63	0.290

MIS6 without a Paleo-Agulhas plain silcrete source

Table B270. ACM-R net-return rates (Rs) for heat-treated silcrete assuming both the insulated and exposed heating scenarios and untreated silcrete experimental blocks when only t_s time-cost (travel and search time) is considered during MIS6 conditions without a Paleo-Agulhas plain silcrete source.

Block	Sample Type	Raw Material	Count Complete Blades (n=)	Total Flaked Core Mass (kg)	Count Complete Blades (n=) / Total Flaked Core Mass (kg)	Count Blades * Durability (e * d)	ts-Travel and search time (min) / Total Flaked Core Mass (kg)	Rs
D9-1-10b	Heat-treated	Silcrete	7	2.350	2.979	8.412	124.02	0.068
D9-1-12b	Heat-treated	Silcrete	3	2.200	1.364	3.851	132.47	0.029
D9-1-12d	Heat-treated	Silcrete	4	2.286	1.750	4.940	127.47	0.039
E3-1-1b	Heat-treated	Silcrete	13	1.933	6.724	18.986	150.73	0.126
E3-1-5p	Heat-treated	Silcrete	10	2.588	3.864	10.912	112.62	0.097
E3-1-6a	Heat-treated	Silcrete	16	2.196	7.286	20.574	132.71	0.155
E3-1-6c	Heat-treated	Silcrete	19	2.436	7.800	22.025	119.64	0.184
I14-2-16l	Heat-treated	Silcrete	11	2.356	4.668	13.183	123.69	0.107
D9-1-10a	Untreated	Silcrete	3	1.980	1.515	2.850	147.18	0.019
D9-1-12a	Untreated	Silcrete	7	2.250	3.112	5.853	129.55	0.045
D9-1-12c	Untreated	Silcrete	2	1.807	1.107	2.082	161.27	0.013

E3-1-1A	Untreated	Silcrete	5	2.070	2.416	4.544	140.82	0.032
E3-1-5n	Untreated	Silcrete	5	2.460	2.033	3.823	118.48	0.032
E3-1-5o	Untreated	Silcrete	6	2.505	2.395	4.506	116.35	0.039
E3-1-6b	Untreated	Silcrete	2	1.691	1.183	2.225	172.34	0.013
I14-2-16a	Untreated	Silcrete	3	2.895	1.036	1.949	100.66	0.019

MIS6 with a Paleo-Agulhas plain silcrete source

Table B271. ACM-R net-return rates (Rs) for heat-treated silcrete assuming both the insulated and exposed heating scenarios and untreated silcrete experimental blocks when only t_s time-cost (travel and search time) is considered during MIS6 conditions with a Paleo-Agulhas plain silcrete source.

Block	Sample Type	Raw Material	Count Complete Blades (n=)	Total Flaked Core Mass (kg)	Count Complete Blades (n=)/Total Flaked Core Mass (kg)	Count Blades * Durability (e * d)	ts-Travel and search time (min)/Total Flaked Core Mass (kg)	Rs
D9-1-10b	Heat-treated	Silcrete	7	2.350	2.979	8.412	11.92	0.706
D9-1-12b	Heat-treated	Silcrete	3	2.200	1.364	3.851	12.73	0.302
D9-1-12d	Heat-treated	Silcrete	4	2.286	1.750	4.940	12.25	0.403
E3-1-1b	Heat-treated	Silcrete	13	1.933	6.724	18.986	14.49	1.310
E3-1-5p	Heat-treated	Silcrete	10	2.588	3.864	10.912	10.83	1.008
E3-1-6a	Heat-treated	Silcrete	16	2.196	7.286	20.574	12.76	1.613
E3-1-6c	Heat-treated	Silcrete	19	2.436	7.800	22.025	11.50	1.915
I14-2-16l	Heat-treated	Silcrete	11	2.356	4.668	13.183	11.89	1.109
D9-1-10a	Untreated	Silcrete	3	1.980	1.515	2.850	14.15	0.201
D9-1-12a	Untreated	Silcrete	7	2.250	3.112	5.853	12.45	0.470
D9-1-12c	Untreated	Silcrete	2	1.807	1.107	2.082	15.50	0.134
E3-1-1A	Untreated	Silcrete	5	2.070	2.416	4.544	13.54	0.336
E3-1-5n	Untreated	Silcrete	5	2.460	2.033	3.823	11.39	0.336
E3-1-5o	Untreated	Silcrete	6	2.505	2.395	4.506	11.19	0.403
E3-1-6b	Untreated	Silcrete	2	1.691	1.183	2.225	16.57	0.134
I14-2-16a	Untreated	Silcrete	3	2.895	1.036	1.949	9.68	0.201

Table B272. Comparison between a raw material ranking based on ACM- R net-return rates and archaeological data from MIS4, MIS5, and MIS6.

ACM-R Results-Ranked*			Archaeological Data			
MIS4 Without a Paleo-Agulhas plain silcrete source			**MIS4**			
Quartzite	Untreated Silcrete	Heat-treated Silcrete	Quartzite (%)	Silcrete Overall (%)	Untreated Silcrete (%)	Heat-treated Silcrete (%)
2 (0.05)	***2*** (0.03)	***1*** (0.1)	44.6	40.0	16.9	83.1
MIS4 With a Paleo-Agulhas plain silcrete source			**MIS4**			
Quartzite	Untreated Silcrete	Heat-treated Silcrete	Quartzite (%)	Silcrete Overall (%)	Untreated Silcrete (%)	Heat-treated Silcrete (%)
3 (0.05)	***2*** (0.3)	***1*** (1.05)	44.6	40.0	16.9	83.1
MIS5			**MIS5**			
Quartzite	Untreated Silcrete	Heat-treated Silcrete	Quartzite (%)	Silcrete Overall (%)	Untreated Silcrete (%)	Heat-treated Silcrete (%)
1 (0.7)	***3*** (0.03)	***2*** (0.1)	77.2	13.1	11.6	88.4
MIS6 Without a Paleo-Agulhas plain silcrete source			MIS6			
Quartzite	Untreated Silcrete	Heat-treated Silcrete	Quartzite (%)	Silcrete Overall (%)	Untreated Silcrete (%)	Heat-treated Silcrete (%)
1 (0.2)	***2*** (0.03)	***1*** (0.1)	94.3	1.1	NA	NA
MIS6 With a Paleo-Agulhas plain silcrete source			MIS6			
Quartzite	Untreated Silcrete	Heat-treated Silcrete	Quartzite (%)	Silcrete Overall (%)	Untreated Silcrete (%)	Heat-treated Silcrete (%)
2 (0.2)	***2*** (0.3)	***1*** (1.05)	92.4	2.5	NA	NA

*Ranking based on which raw materials have the highest mean Rq or Rs (in parenthesis).Similar ranking in table is due to statistically similar Rq or Rs. MIS4, MIS5, and MIS6 archaeological raw material frequencies from bootstrapped data in Figure 50 and Table 19.

Vegetation type variable

Table B273. Summary Statistics and test results of ACM-P net-return rates (Pq and Ps) when only m_1 (wood fuel travel and search time) and m_2 time-costs (heat-treatment time) are considered during all model conditions.

	MIS4				MIS5				MIS6			
	Quartzite (Pq)	**Untreated Silcrete (Ps)**	**Insulated-Silcrete (Ps)**	**Exposed-Silcrete (Ps)**	**Quartzite (Pq)**	**Untreated Silcrete (Ps)**	**Insulated-Silcrete (Ps)**	**Exposed-Silcrete (Ps)**	**Quartzite (Pq)**	**Untreated Silcrete (Ps)**	**Insulated-Silcrete (Ps)**	**Exposed-Silcrete (Ps)**
n sample blocks	20	8	8	8	20	8	8	8	20	8	8	8

0.061	0.212	0.209	0.383	0.308	0.113	8.000	0.076	0.285	0.209	0.134
0.043	0.152	0.150	0.275	0.221	0.081	8.000	0.055	0.205	0.150	0.096
1.949	3.337	3.479	5.853	4.535	1.424	8.000	0.954	4.433	3.479	2.525
0.000	3.341	4.222	11.818	7.136	3.335	20.000	1.413	5.635	4.222	2.809
0.061	0.212	0.209	0.383	0.308	0.113	8.000	0.076	0.285	0.209	0.134
0.043	0.152	0.150	0.275	0.221	0.081	8.000	0.055	0.205	0.150	0.096
1.949	3.337	3.479	5.853	4.535	1.424	8.000	0.954	4.433	3.479	2.525
0.000	3.341	4.222	11.818	7.136	3.335	20.000	1.413	5.635	4.222	2.809
0.061	0.212	0.209	0.383	0.308	0.113	8.000	0.076	0.285	0.209	0.134
0.081	0.283	0.279	0.511	0.410	0.151	8.000	0.101	0.380	0.279	0.178
1.949	3.337	3.479	5.853	4.535	1.424	8.000	0.954	4.433	3.479	2.525
0.000	3.341	4.222	11.818	7.136	3.335	20.000	1.413	5.635	4.222	2.809

First Quartile | Min | Median | Mean | Max | Third Quartile | SD | Bootstrapped SE* | Margin of error (95% CI) | Bootstrapped Upper 95% CI* | Bootstrapped Lower 95% CI*

*Samples bootstrapped 10000 times.

Quartzite MIS4, MIS5, and MIS6

Table B274. ACM-P net-return rates (Pq) for quartzite experimental blocks when only m_1 (wood fuel travel and search time) and m_2 time-costs (heat-treatment time) are considered during MIS4, MIS5, and MIS6 conditions.

Block	Raw Material	Count Complete Blades (n=)	Total Flaked Core Mass (kg)	Count Complete Blades (n=) / Total Flaked Core Mass (kg)	Count Blades * Durability (e * d)	m1-Wood Fuel travel and search time (min) / Total Flaked Core Mass (kg)	m2-Heat-treatment time (min) / Total Flaked core Mass (kg)	Pq
C9-1-1B8	Quartzite	2	1.920	1.042	1.627	0	0	1.627
C9-1-1B9	Quartzite	4	2.060	1.941	3.033	0	0	3.033
D11-1-100A	Quartzite	1	2.149	0.465	0.727	0	0	0.727
D11-1-90D1	Quartzite	1	2.450	0.408	0.638	0	0	0.638
D11-1-95A	Quartzite	2	2.031	0.985	1.538	0	0	1.538
D11-1-95B	Quartzite	2	2.160	0.926	1.447	0	0	1.447
D11-1-97A1	Quartzite	0	1.925	0.000	0.000	0	0	0.000
D11-1-98B1	Quartzite	3	1.913	1.568	2.451	0	0	2.451
D11-1-98C1	Quartzite	3	2.091	1.435	2.242	0	0	2.242
D11-1-98D	Quartzite	1	1.843	0.543	0.848	0	0	0.848
D11-1-85C1	Quartzite	8	1.996	4.008	8.116	0	0	8.116
D11-1-91A1	Quartzite	6	1.962	3.058	6.192	0	0	6.192
D11-1-91A2	Quartzite	8	2.174	3.679	7.451	0	0	7.451
D11-1-91B3	Quartzite	11	1.885	5.836	11.818	0	0	11.818
D11-1-91B5	Quartzite	4	2.220	1.802	3.648	0	0	3.648
D11-1-91C3	Quartzite	5	1.962	2.548	5.160	0	0	5.160
D11-1-94B2	Quartzite	5	1.828	2.736	5.539	0	0	5.539
D11-1-94B3	Quartzite	8	1.784	4.484	9.081	0	0	9.081
D11-1-94D2	Quartzite	5	1.966	2.543	5.150	0	0	5.150
D11-1-97C	Quartzite	7	1.833	3.819	7.733	0	0	7.733

MIS4 Silcrete

Table B275. ACM-P net-return rates (Ps) for heat-treated silcrete assuming both the insulated and exposed heating scenarios and untreated silcrete experimental blocks when only m_1 (wood fuel travel and search time) and m_2 time-costs (heat-treatment time) are considered during MIS5 conditions.

Block	Heating Scenario	Raw Material	Count Complete Blades (n=)	Total Flaked Core Mass (kg)	Count Complete Blades (n=) / Total Flaked Core Mass (kg)	Count Blades * Durability (e * d)	m1-Wood Fuel travel and search time (min) / Total Flaked Core Mass (kg)	m2-Heat-treatment time (min) / Total Flaked core Mass (kg)	Ps
D9-1-10b	Insulated	Silcrete	7	2.350	2.979	8.412	38.300	6.383	0.188
D9-1-12b	Insulated	Silcrete	3	2.200	1.364	3.851	40.908	6.818	0.081
D9-1-12d	Insulated	Silcrete	4	2.286	1.750	4.940	39.365	6.561	0.108
E3-1-1b	Insulated	Silcrete	13	1.933	6.724	18.986	46.548	7.758	0.350
E3-1-5p	Insulated	Silcrete	10	2.588	3.864	10.912	34.780	5.797	0.269
E3-1-6a	Insulated	Silcrete	16	2.196	7.286	20.574	40.982	6.830	0.430
E3-1-6c	Insulated	Silcrete	19	2.436	7.800	22.025	36.946	6.158	0.511
I14-2-16l	Insulated	Silcrete	11	2.356	4.668	13.183	38.197	6.366	0.296
D9-1-10b	Exposed	Silcrete	7	2.350	2.979	8.412	38.300	21.278	0.141
D9-1-12b	Exposed	Silcrete	3	2.200	1.364	3.851	40.908	22.727	0.061
D9-1-12d	Exposed	Silcrete	4	2.286	1.750	4.940	39.365	21.869	0.081
E3-1-1b	Exposed	Silcrete	13	1.933	6.724	18.986	46.548	25.860	0.262
E3-1-5p	Exposed	Silcrete	10	2.588	3.864	10.912	34.780	19.322	0.202
E3-1-6a	Exposed	Silcrete	16	2.196	7.286	20.574	40.982	22.768	0.323
E3-1-6c	Exposed	Silcrete	19	2.436	7.800	22.025	36.946	20.525	0.383
I14-2-16l	Exposed	Silcrete	11	2.356	4.668	13.183	38.197	21.220	0.222
D9-1-10a	Untreated	Silcrete	3	1.980	1.515	2.850	0.000	0.000	2.850
D9-1-12a	Untreated	Silcrete	7	2.250	3.112	5.853	0.000	0.000	5.853
D9-1-12c	Untreated	Silcrete	2	1.807	1.107	2.082	0.000	0.000	2.082
E3-1-1A	Untreated	Silcrete	5	2.070	2.416	4.544	0.000	0.000	4.544
E3-1-5n	Untreated	Silcrete	5	2.460	2.033	3.823	0.000	0.000	3.823
E3-1-5o	Untreated	Silcrete	6	2.505	2.395	4.506	0.000	0.000	4.506
E3-1-6b	Untreated	Silcrete	2	1.691	1.183	2.225	0.000	0.000	2.225
I14-2-16a	Untreated	Silcrete	3	2.895	1.036	1.949	0.000	0.000	1.949

MIS5 Silcrete

Table B276. ACM-P net-return rates (Ps) for heat-treated silcrete assuming both the insulated and exposed heating scenarios and untreated silcrete experimental blocks when only m_1 (wood fuel travel and search time) and m_2 time-costs (heat-treatment time) are considered during MIS5 conditions.

Block	Heating Scenario	Raw Material	Count Complete Blades (n=)	Total Flaked Core Mass (kg)	Count Complete Blades (n=) / Total Flaked Core Mass (kg)	Count Blades * Durability (e * d)	m1-Wood Fuel travel and search time (min) / Total Flaked Core Mass (kg)	m2-Heat-treatment time (min) / Total Flaked core Mass (kg)	Ps
D9-1-10b	Insulated	Silcrete	7	2.350	2.979	8.412	76.600	6.383	0.101
D9-1-12b	Insulated	Silcrete	3	2.200	1.364	3.851	81.816	6.818	0.043
D9-1-12d	Insulated	Silcrete	4	2.286	1.750	4.940	78.730	6.561	0.058
E3-1-1b	Insulated	Silcrete	13	1.933	6.724	18.986	93.096	7.758	0.188
E3-1-5p	Insulated	Silcrete	10	2.588	3.864	10.912	69.559	5.797	0.145
E3-1-6a	Insulated	Silcrete	16	2.196	7.286	20.574	81.965	6.830	0.232
E3-1-6c	Insulated	Silcrete	19	2.436	7.800	22.025	73.892	6.158	0.275
I14-2-16l	Insulated	Silcrete	11	2.356	4.668	13.183	76.394	6.366	0.159
D9-1-10b	Exposed	Silcrete	7	2.350	2.979	8.412	38.300	21.278	0.141
D9-1-12b	Exposed	Silcrete	3	2.200	1.364	3.851	40.908	22.727	0.061
D9-1-12d	Exposed	Silcrete	4	2.286	1.750	4.940	39.365	21.869	0.081
E3-1-1b	Exposed	Silcrete	13	1.933	6.724	18.986	46.548	25.860	0.262
E3-1-5p	Exposed	Silcrete	10	2.588	3.864	10.912	34.780	19.322	0.202
E3-1-6a	Exposed	Silcrete	16	2.196	7.286	20.574	40.982	22.768	0.323
E3-1-6c	Exposed	Silcrete	19	2.436	7.800	22.025	36.946	20.525	0.383
I14-2-16l	Exposed	Silcrete	11	2.356	4.668	13.183	38.197	21.220	0.222
D9-1-10a	Untreated	Silcrete	3	1.980	1.515	2.850	0	0	2.850
D9-1-12a	Untreated	Silcrete	7	2.250	3.112	5.853	0	0	5.853
D9-1-12c	Untreated	Silcrete	2	1.807	1.107	2.082	0	0	2.082
E3-1-1A	Untreated	Silcrete	5	2.070	2.416	4.544	0	0	4.544
E3-1-5n	Untreated	Silcrete	5	2.460	2.033	3.823	0	0	3.823
E3-1-5o	Untreated	Silcrete	6	2.505	2.395	4.506	0	0	4.506
E3-1-6b	Untreated	Silcrete	2	1.691	1.183	2.225	0	0	2.225
I14-2-16a	Untreated	Silcrete	3	2.895	1.036	1.949	0	0	1.949

MIS6 Silcrete

Table B277. ACM-P net-return rates (Ps) for heat-treated silcrete assuming both the insulated and exposed heating scenarios and untreated silcrete experimental blocks when only m_1 (wood fuel travel and search time) and m_2 time-costs (heat-treatment time) are considered during MIS6 conditions.

Block	Heating Scenario	Raw Material	Count Complete Blades (n=)	Total Flaked Core Mass (kg)	Count Complete Blades (n=) / Total Flaked Core Mass (kg)	Count Blades * Durability (e * d)	m1-Wood Fuel travel and search time (min) / Total Flaked Core Mass (kg)	m2-Heat-treatment time (min) / Total Flaked core Mass (kg)	Ps
D9-1-10b	Insulated	Silcrete	7	2.350	2.979	8.412	76.600	6.383	0.101
D9-1-12b	Insulated	Silcrete	3	2.200	1.364	3.851	81.816	6.818	0.043
D9-1-12d	Insulated	Silcrete	4	2.286	1.750	4.940	78.730	6.561	0.058
E3-1-1b	Insulated	Silcrete	13	1.933	6.724	18.986	93.096	7.758	0.188
E3-1-5p	Insulated	Silcrete	10	2.588	3.864	10.912	69.559	5.797	0.145
E3-1-6a	Insulated	Silcrete	16	2.196	7.286	20.574	81.965	6.830	0.232
E3-1-6c	Insulated	Silcrete	19	2.436	7.800	22.025	73.892	6.158	0.275
I14-2-16l	Insulated	Silcrete	11	2.356	4.668	13.183	76.394	6.366	0.159
D9-1-10b	Exposed	Silcrete	7	2.350	2.979	8.412	38.300	21.278	0.141
D9-1-12b	Exposed	Silcrete	3	2.200	1.364	3.851	40.908	22.727	0.061
D9-1-12d	Exposed	Silcrete	4	2.286	1.750	4.940	39.365	21.869	0.081
E3-1-1b	Exposed	Silcrete	13	1.933	6.724	18.986	46.548	25.860	0.262
E3-1-5p	Exposed	Silcrete	10	2.588	3.864	10.912	34.780	19.322	0.202
E3-1-6a	Exposed	Silcrete	16	2.196	7.286	20.574	40.982	22.768	0.323
E3-1-6c	Exposed	Silcrete	19	2.436	7.800	22.025	36.946	20.525	0.383
I14-2-16l	Exposed	Silcrete	11	2.356	4.668	13.183	38.197	21.220	0.222
D9-1-10a	Untreated	Silcrete	3	1.980	1.515	2.850	0	0	2.850
D9-1-12a	Untreated	Silcrete	7	2.250	3.112	5.853	0	0	5.853
D9-1-12c	Untreated	Silcrete	2	1.807	1.107	2.082	0	0	2.082
E3-1-1A	Untreated	Silcrete	5	2.070	2.416	4.544	0	0	4.544
E3-1-5n	Untreated	Silcrete	5	2.460	2.033	3.823	0	0	3.823
E3-1-5o	Untreated	Silcrete	6	2.505	2.395	4.506	0	0	4.506
E3-1-6b	Untreated	Silcrete	2	1.691	1.183	2.225	0	0	2.225
I14-2-16a	Untreated	Silcrete	3	2.895	1.036	1.949	0	0	1.949

Table B278. Comparison between a raw material ranking based on ACM- P net-return rates and archaeological data from MIS4, MIS5, and MIS6.

ACM-P Results-Ranked*				Archaeological Data			
MIS4				**MIS4**			
Quartzite	Untreated Silcrete	Insulated-Silcrete	Exposed-Silcrete	Quartzite (%)	Silcrete Overall (%)	Untreated Silcrete (%)	Heat-treated Silcrete (%)
1 (4.2)	***1*** (3.5)	***2*** (0.3)	***3*** (0.2)	44.6*	40*	16.9	83.1
MIS5				**MIS5**			
Quartzite	Untreated Silcrete	Insulated-Silcrete	Exposed-Silcrete	Quartzite (%)	Silcrete Overall (%)	Untreated Silcrete (%)	Heat-treated Silcrete (%)
1 (4.2)	***1*** (3.5)	***3*** (0.2)	***3*** (0.2)	77.2	13.1	11.6	88.4
MIS6				**MIS6**			
Quartzite	Untreated Silcrete	Insulated-Silcrete	Exposed-Silcrete	Quartzite (%)	Silcrete Overall (%)	Untreated Silcrete (%)	Heat-treated Silcrete (%)
1 (4.2)	***1*** (3.5)	***3*** (0.2)	***3*** (0.2)	94.3	1.1	NA	NA

*Ranking based on which raw materials have the highest mean Rq or Rs (in parenthesis).Similar ranking in table is due to statistically similar Rq or Rs. MIS4, MIS5, and MIS6 archaeological raw material frequencies from bootstrapped data in Figure 50 and Table 19.

Mobility rate and strategy variable

Table B279. Summary Statistics and test results of ACM net-return rates (Pq and Ps or Rq and Rs) when only m_3 time-cost (flaking manufacturing time) is considered (for all experimental sample types) during MIS4 conditions.

	Quartzite (Pq or Rq)	Untreated Silcrete (Ps or Rs)	Heat-treated Silcrete (Ps or Rs)
n sample blocks	20	8	8
First Quartile	0.220	0.303	0.960
Min	0.000	0.270	0.610
Median	0.515	0.535	2.120
Mean	0.590	0.554	2.094
Max	1.590	0.940	3.830
Third Quartile	0.975	0.775	3.078
SD	0.452	0.254	1.129
Bootstrapped SE*	0.098	0.087	0.387
Margin of error (95% CI)	0.192	0.170	0.759
Bootstrapped Upper 95% CI*	0.781	0.724	2.853
Bootstrapped Lower 95% CI*	0.398	0.383	1.335

*Samples bootstrapped 10000 times.

MIS4

Table B280. ACM-P net-return rates (Pq) for quartzite experimental blocks when only m_3 time-cost (flake manufacturing time) is considered during MIS4 conditions.

Block	Raw Material	Count Complete Blades (n=)	Total Flaked Core Mass (kg)	Count Complete Blades (n=) / Total Flaked Core Mass (kg)	Count Blades * Durability (e * d)	m3-FlakingTime (14min) / Total Flaked Core Mass (kg)	Pq or Rq
C9-1-1B8	Quartzite	2	1.920	1.042	1.627	7.29	0.22
C9-1-1B9	Quartzite	4	2.060	1.941	3.033	6.79	0.45
D11-1-100A	Quartzite	1	2.149	0.465	0.727	6.51	0.11
D11-1-90D1	Quartzite	1	2.450	0.408	0.638	5.71	0.11
D11-1-95A	Quartzite	2	2.031	0.985	1.538	6.89	0.22
D11-1-95B	Quartzite	2	2.160	0.926	1.447	6.48	0.22
D11-1-97A1	Quartzite	0	1.925	0.000	0.000	7.27	0.00
D11-1-98B1	Quartzite	3	1.913	1.568	2.451	7.32	0.33
D11-1-98C1	Quartzite	3	2.091	1.435	2.242	6.70	0.33
D11-1-98D	Quartzite	1	1.843	0.543	0.848	7.60	0.11
D11-1-85C1	Quartzite	8	1.996	4.008	8.116	7.01	1.16
D11-1-91A1	Quartzite	6	1.962	3.058	6.192	7.13	0.87
D11-1-91A2	Quartzite	8	2.174	3.679	7.451	6.44	1.16
D11-1-91B3	Quartzite	11	1.885	5.836	11.818	7.43	1.59
D11-1-91B5	Quartzite	4	2.220	1.802	3.648	6.31	0.58
D11-1-91C3	Quartzite	5	1.962	2.548	5.160	7.13	0.72
D11-1-94B2	Quartzite	5	1.828	2.736	5.539	7.66	0.72
D11-1-94B3	Quartzite	8	1.784	4.484	9.081	7.85	1.16
D11-1-94D2	Quartzite	5	1.966	2.543	5.150	7.12	0.72
D11-1-97C	Quartzite	7	1.833	3.819	7.733	7.64	1.01

Table B281. ACM-P net-return rates (Ps) for untreated and heat-treated silcrete experimental blocks when only m_3 time-cost (flake manufacturing time) is considered during MIS4 conditions.

Block	Sample Type	Raw Material	Count Complete Blades (n=)	Total Flaked Core Mass (kg)	Count Complete Blades (n=) / Total Flaked Core Mass (kg)	Count Blades * Durability (e * d)	m3-FlakingTime (14min) / Total Flaked Core Mass (kg)	Ps or Rs
D9-1-10b	Heat-treated	Silcrete	7	2.350	2.979	8.412	5.96	1.41
D9-1-12b	Heat-treated	Silcrete	3	2.200	1.364	3.851	6.36	0.61
D9-1-12d	Heat-treated	Silcrete	4	2.286	1.750	4.940	6.12	0.81
E3-1-1b	Heat-treated	Silcrete	13	1.933	6.724	18.986	7.24	2.62
E3-1-5p	Heat-treated	Silcrete	10	2.588	3.864	10.912	5.41	2.02
E3-1-6a	Heat-treated	Silcrete	16	2.196	7.286	20.574	6.38	3.23
E3-1-6c	Heat-treated	Silcrete	19	2.436	7.800	22.025	5.75	3.83
I14-2-16l	Heat-treated	Silcrete	11	2.356	4.668	13.183	5.94	2.22
D9-1-10a	Untreated	Silcrete	3	1.980	1.515	2.850	7.07	0.40
D9-1-12a	Untreated	Silcrete	7	2.250	3.112	5.853	6.22	0.94
D9-1-12c	Untreated	Silcrete	2	1.807	1.107	2.082	7.75	0.27
E3-1-1A	Untreated	Silcrete	5	2.070	2.416	4.544	6.76	0.67
E3-1-5n	Untreated	Silcrete	5	2.460	2.033	3.823	5.69	0.67
E3-1-5o	Untreated	Silcrete	6	2.505	2.395	4.506	5.59	0.81
E3-1-6b	Untreated	Silcrete	2	1.691	1.183	2.225	8.28	0.27
I14-2-16a	Untreated	Silcrete	3	2.895	1.036	1.949	4.84	0.40

Table B282. Comparison between a raw material ranking based on ACM net-return rates and archaeological data from MIS4.

ACM Results-Ranked*	Quartzite	***2*** (0.6)
	Untreated Silcrete	***2*** (0.6)
	Heat-treated Silcrete	***1*** (2.1)
Archaeological Raw Material Data – MIS4	Quartzite (%)	44.6*
	Silcrete Overall (%)	40*
	Untreated Silcrete (%)	16.9
	Heat-treated Silcrete (%)	83.1

*Ranking based on which raw materials have the highest mean Rq or Rs (in parenthesis).Similar ranking in table is due to statistically similar Rq or Rs. MIS4 archaeological raw material frequency from bootstrapped data in Figure 50 and Table 19.

APPENDIX C

RANDOM WALK MODEL ODD

Model description

This is a model description following the ODD protocol (Grimm et al. 2010) of the neutral model of raw material procurement by Brantingham (2003).

Overview:

Purpose:
To show that a simple model of random encounters of materials can produce distributions as found in the archaeological record.

State variables and scales:
One agent is foraging according a random walk and has a toolkit of fixed size. Material sources are randomly distributed on the landscape (**Figure 1**). The landscape has 250,000 cells and 5,000 material sources. The model stops if the agent reaches the edge of the landscape.

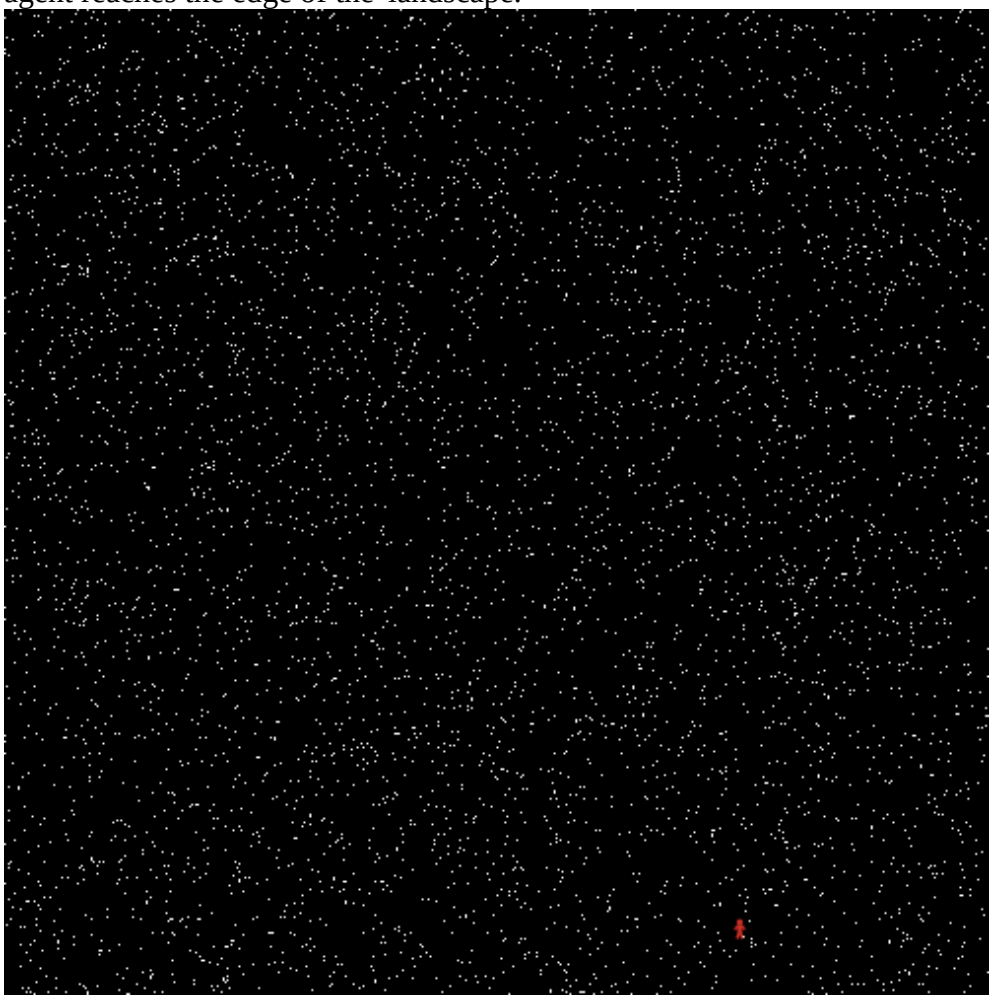

Figure C1. Landscape with randomly distributed material sources and one forager (red figure at bottom left).

Process overview and scheduling:

Figure 2 shows the main structure of the scheduling of activities in the model. One agent with a mobile toolkit of fixed capacity is randomly placed on the environment. At each time step, the agent moves to one of the nearest eight neighboring cells or stays in the present cell, with equal probability (=1/9). Each time step a fixed amount of raw material is consumed dependent only upon its frequency in the mobile toolkit. If a raw material source is encountered, the toolkit is re-provisioned up to its maximum capacity before moving again at random. If no raw material source is encountered, the forager moves immediately at random. Simulations are run until 200 unique raw material sources are encountered, or the edge of the simulation world is reached.

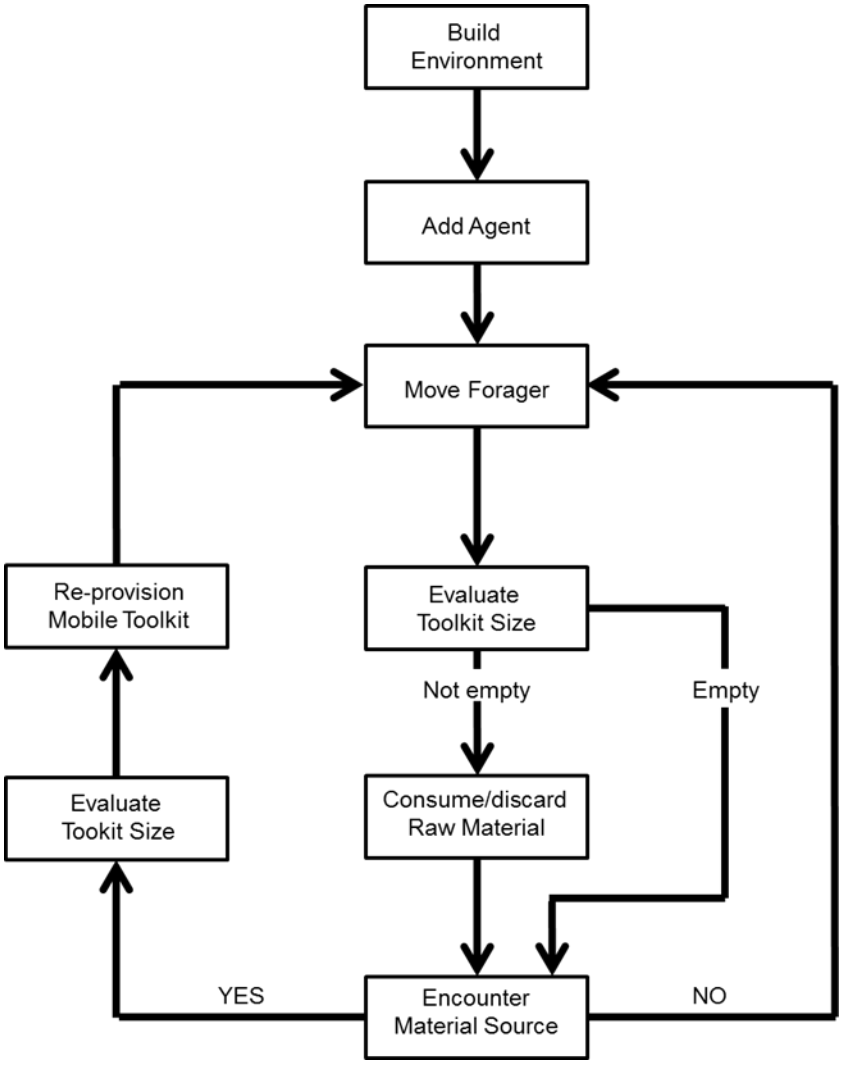

Figure C2. Neutral model scheduling. Figure recreated from "Figure 5. Structural and dynamic components of a neutral model of stone raw material procurement." In Brantingham (2003).

Design Concepts:

Basic principles: **Which general concepts, theories, hypotheses, or modeling approaches are underlying the model's design?**

There is debate whether changes in stone tool raw material frequencies in an archaeological assemblage can be considered a reliable proxy for human forager adaptive variability (Brantingham 2003, Feblot-Augustins 1993, Kuhn 2005, Mellars 1996). Brantingham (2003) points out that a commonly made argument is that raw material richness, transport distances, and the character of transported technologies should signal four behaviors. First, it should signal raw material selection variation due to material quality and abundance. Then, secondly, it should signal time and energy cost optimization associated with raw material procurement from spatially dispersed sources. Thirdly, it should signal planning depth that combines raw material procurement with other forager activities such as food procurement. Fourth and finally, it should signal risk minimization resulting in raw material transportation strategies focusing on quantities and forms that are energetically economical and least likely to fail. To test if raw material richness, transport distance, and the character of transported technologies is the result of adaptive behavior, Brantingham (2003: 487) presents a behaviorally neutral agent-based model that involves "…a forager engaged in a random walk within a uniform environment." The neutral model relies on the core principle (Brantingham, 2003: 491) "that all same-level components of a system are equivalent both in terms of their innate behaviors and the impact that the environment has on the expression of those behaviors." Brantingham's (2003: 491) model provides a baseline for comparison where archaeologists can be certain that "observed patterns in raw material richness, transport distance, and both quantity- distance and reduction intensity-distance relationships" is not the result of adaptation.

Emergence: **What key results or outputs of the model are modeled as emerging from the adaptive traits, or behaviors, of individuals?**

Distribution of frequencies of distances of material is part of the tool box compared to the source of the material. This is an indication how far material may travel. Distribution of richness of material sources in the toolbox.

Adaptation: **What adaptive traits do the individuals have? What rules do they have for making decisions or changing behavior in response to changes in themselves or their environment?**

Agent moves randomly and do not learn, adapt or evolve.

Objectives: **If adaptive traits explicitly act to increase some measure of the individual's success at meeting some objective, what exactly is that objective and how is it measured?**

There are no adaptive traits.

Learning: **Many individuals or agents (but also organizations and institutions) change their adaptive traits over time as a consequence of their experience? If so, how?**

Agent does not learn.

Prediction: **Prediction is fundamental to successful decision-making; if an agent's adaptive traits or learning procedures are based on estimating future consequences of decisions, how do agents predict the future conditions (either environmental or internal) they will experience?**

Agent does not predict.

Sensing: **What internal and environmental state variables are individuals assumed to sense and consider in their decisions?**

Agent can sense whether there are material source on the cell it occupies. The agent can sense the amount and distribution of materials in its tool box.

Interaction: **What kinds of interactions among agents are assumed? Are there direct interactions in which individuals encounter and affect others, or are interactions indirect, e.g., via competition for a mediating resource?**

There is only one agent.

Stochasticity: **What processes are modeled by assuming they are random or partly random?**

Agents move randomly, and decisions on use of material are done randomly. Material is distributed randomly on the landscape.

Collectives: **Do the individuals form or belong to aggregations that affect, and are affected by, the individuals?**

No

Observation: **What data are collected from the ABM for testing, understanding, and analyzing it, and how and when are they collected?**

Distribution of distance of material traveled and richness of material sources in the toolbox.

Details:

Initialization: **What is the initial state of the model world, i.e., at time t = 0 of a simulation run?**

Table C1 provides the parameters as used in the model.

Table C1.Neutral model parameters.

Variable description	Variable	Units	Baseline Parameter Setting/Range
Simulated world size in X Dimension	X	grid cells	500
Simulated world size in Y Dimension	Y	grid cells	500
x-coordinate position of raw material/forager	x	grid cells	random from uniform = [1,500]
y-coordinate position of raw material/forager	y	grid cells	random from uniform = [1,500]
Number of unique raw material sources	*n*	sources	5000
Raw material type label	*i*		1, 2,.....5000
Quantity of material from source i in mobile toolkit	v_i	arbitrary units	minimum = 1; Maximum = 100
Total material of all types in mobile toolkit; maximum toolkit capacity	Σv_i	arbitrary units	minimum = 1; Maximum = 100
Amount of material collected from source *i*	a_i	arbitrary units	minimum = 1; Maximum = 100
Probability of consuming material of type *i* in mobile toolkit	c_i		(0.0, 1.0)
An observed number of simulation time steps	*N*	time steps	
Estimated distance traveled in *N* time steps; effective foraging radius	*d*	grid cells	minimum = 1; Maximum = 707
Maximum forager move length at each time step	*l*	grid cells	1
Raw material consumption rate	*r*	arbitrary units / time step	1
Raw material richness in mobile toolkit	*k*	number of types	minimum = 0; Maximum = 100
Quantity of material discarded in making room for newly procured material	q_i	arbitrary units	minimum = 1; Maximum = 100
Most abundant material in the mobile toolkit at a given time step	max $[v_i]$	arbitrary units	minimum = 1; Maximum = 100

*Table recreated from "Table 1. Variables and Baseline Parameter Settings." In Brantingham (2003).

Input data: **Does the model use input from external sources such as data files or other models to represent processes that change over time?**

No

Submodels: **What, in detail, are the submodels that represent the processes listed in 'Process overview and scheduling'? What are the model parameters, their dimensions, and reference values? How were submodels designed or chosen, and how were they parameterized and then tested?**

The mobile toolkit is simulated as a vector vi where each element represents the amount of stone raw material in the toolkit of unique type i. The maximum size of the toolkit is 100, and the sum of the elements of vi (Σi vi) has to be smaller or equal to 100. The amount of material added to the toolbox when a material source is encountered is 100 - Σi vi, meaning that the toolbox is filled up to the maximum capacity. Every time step one unit of material is consumed from the tool box. The probability that material source i is consumed is vi /Σi vi, meaning that it is relative to the frequency of available materials. Material sources do not deplete in the environment during the duration of the simulation.

Model implementation

The model is implemented in Netlogo 5.0.3

Some results of replication

Below are some typical results of the model. The first figure shows the number of material sources in the tool box during the simulation of 8229 time steps. The middle figure shows the distribution of ticks having a certain number of different material sources in the tool box, and the bottom figure shows the distribution of material away from the source while still in the toolbox.

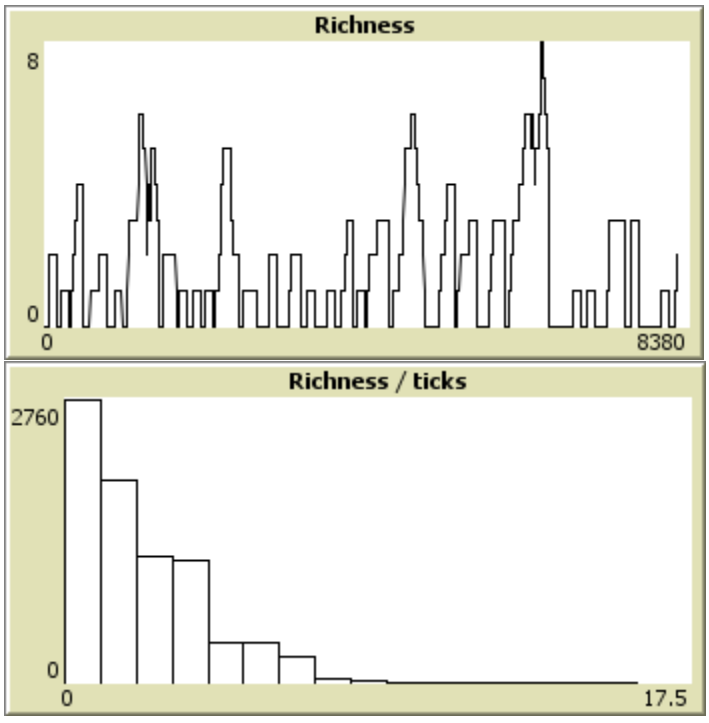

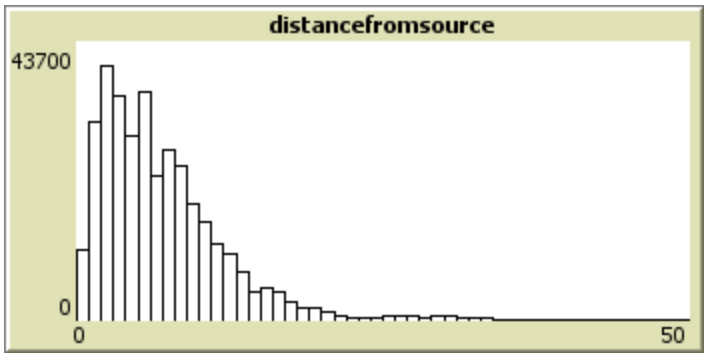

Figure C3. Neutral model simulation results.

References

Brantingham, P. J. 2003. A Neutral Model of Stone Raw Material Procurement, *American Antiquity* 68(3): 487–509.

Grimm, V., U. Berger, D.L. DeAngelis, J.G. Polhill, J. Giske, and S.F. Railsback. 2010.The
ODD protocol: A review and first update. *Ecological Modeling* 221(23): 2760-2768.

Feblot-Augustins, J. 1993. Mobility Strategies in the Late Middle Palaeolithic of Central Europe and Western Europe: Elements of Stability and Variability. Journal ofAnthropological Archaeology 12:211-265.

Kuhn, S. L. 1995. Mousterian Lithic Technology: An Ecological Perspective. Princeton University Press, Princeton.

Mellars, P. A. 1996. The Neandertal Legacy: An Archaeological Perspective from Western Europe. Princeton University Press, Princeton.

APPENDIX D

SPATIAL DISTRIBUTION MODEL ODD

Model description

This is a model description following the ODD protocol (Grimm et al. 2010) of a study (Oestmo et al. 2016) investigating what effect spatial clustering has on the outcome of the neutral model of raw material procurement by Brantingham (2003).

Overview:

Purpose:
To examine what effect that spatial clustering have on the neutral model outcome.

State variables and scales:
One agent is foraging according a random walk, wiggling walk, or seeking walk and has a toolkit of a fixed size. Materials are distributed on the landscape according to a probability of clustering p_r ('prandom'). If p_r is set to 1 the raw materials are distributed in a random way across the landscape. If p_r is set to 0 the raw material are distributed together in one central cluster on the landscape. The landscape has 250,000 cells and there are 5,000 material sources with either 5000 unique raw material types or 20 unique raw material types. The model stops when 35000 time steps have been run.

Process overview and scheduling:

Figure D1 shows the main structure of the scheduling of activities in the model. One agent with a mobile toolkit of fixed capacity is randomly placed on the environment. If the threshold is set to 0, at each time step, the agent moves to one of the nearest eight neighboring cells or stays in the present cell, with equal probability (=1/9). Each time step a fixed amount of raw material is consumed dependent only upon its frequency in the mobile toolkit. If a raw material source is encountered, the toolkit is re-provisioned up to its maximum capacity before moving again at random. If no raw material source is encountered, the forager moves immediately at random. If the 'threshold' function is set to a value >0 and the forager has a quantity of raw material in the toolkit equal to that value the forager will seek to the closest raw material source to replenish the toolkit. When the quantity of raw material is above the threshold the agent moves at random, discarding a material every time step, and when encountering a source the toolkit is re-provisioned up to maximum capacity. Simulations are run until 35000 time steps have been simulated.

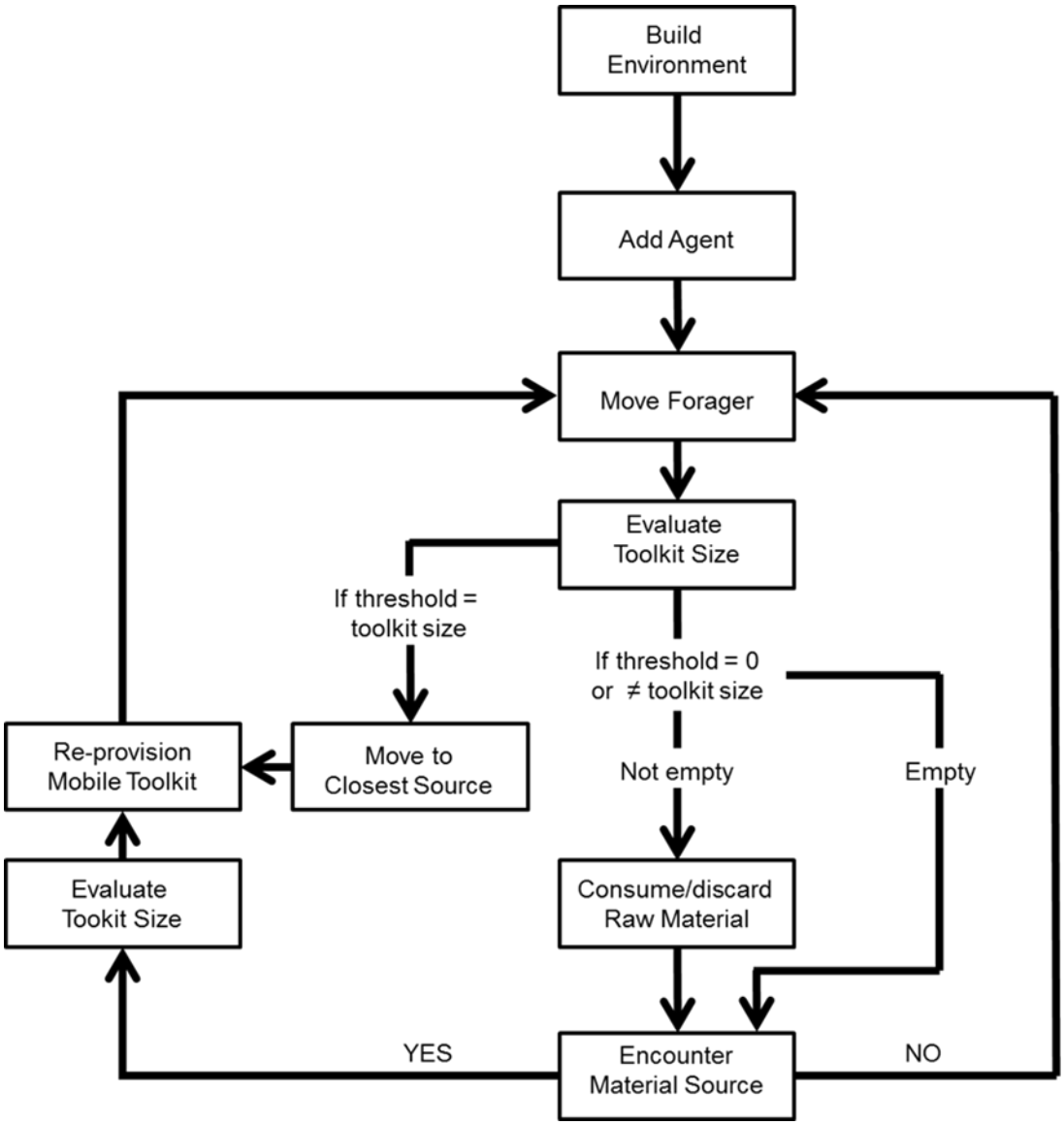

Figure D1. Spatial clustering model scheduling.

Design Concepts:

Basic principles: **Which general concepts, theories, hypotheses, or modeling approaches are underlying the model's design?**

Brantingham (2003) points out that a valid criticism of the neutral model approach is that random walk in the environment can be considered an unrealistic foraging behavior; that a forager would never ignore the difference between raw material types. Additionally, he states that future evaluations of the neutral model should be conducted using a real landscape with real source locations. This model partly addresses both by looking at the effect that spatial clustering or raw material sources have on the neutral model outcome. Spatial clustering of raw

material sources simulates a more realistic scenario because raw material sources are located on the landscape according to geological structures and geophysical processes, which often results in same type raw material sources clustering together on the landscape. One key measure that is collected in the model to evaluate the effect that spatial clustering has is time without raw material in toolkit. Another limitation of the original neutral model that is addressed is the unrealistic assumption that there are 5000 unique raw material types distributed across the landscape. It is more realistic that 1-25 raw material types are distributed among 5000 sources, which in turn are distributed across the landscape according to geological structures and geophysical processes.

Emergence: **What key results or outputs of the model are modeled as emerging from the adaptive traits, or behaviors, of individuals?**

Distribution of frequencies of distances of material as part of the toolkit compared to the source of the material. This is an indication how far material may travel. Distribution of richness of material sources in the toolbox. Time without raw material in toolkit.

Adaptation: **What adaptive traits do the individuals have? What rules do they have for making decisions or changing behavior in response to changes in themselves or their environment?**

Agent moves either in random, wiggle, or seeking behavior and do not learn, adapt or evolve.

Objectives: **If adaptive traits explicitly act to increase some measure of the individual's success at meeting some objective, what exactly is that objective and how is it measured?**

There are no adaptive traits.

Learning: **Many individuals or agents (but also organizations and institutions) change their adaptive traits over time as a consequence of their experience? If so, how?**

The agent does not learn.

Prediction: **Prediction is fundamental to successful decision-making; if an agent's adaptive traits or learning procedures are based on estimating future consequences of decisions, how do agents predict the future conditions (either environmental or internal) they will experience?**

The agent does not predict.

Sensing: **What internal and environmental state variables are individuals assumed to sense and consider in their decisions?**

Agent can sense whether there are material source on the cell it occupies. The agent can sense the amount and distribution of materials in its toolkit. If threshold value is set to <0 and the forager has a quantity of raw material in toolkit equal to that value the forager can sense which raw material source is closest and will directly move there.

Interaction: **What kinds of interactions among agents are assumed? Are there direct interactions in which individuals encounter and affect others, or are interactions indirect, e.g., via competition for a mediating resource?**

There is only one agent.

Stochasticity: **What processes are modeled by assuming they are random or partly random?**

When the movement is set to random the agent moves randomly. Decisions on use of material are done randomly. When the p_r value is set to 1 raw materials are distributed randomly on the landscape.

Collectives: **Do the individuals form or belong to aggregations that affect, and are affected by, the individuals?**

No

Observation: **What data are collected from the ABM for testing, understanding, and analyzing it, and how and when are they collected?**

Distribution of distance of material traveled and richness of material sources in the toolbox. Time without raw material in toolkit.

Details:

Initialization: **What is the initial state of the model world, i.e., at time t = 0 of a simulation run?**

Table D1 provides the parameters as used in the model.

Table D1: Spatial clustering model variables/parameters

Variable description	Variable	Units	Model Variables/Range
Simulated world size in *X* dimension	X	grid cells	500
Simulated world size in *Y* dimension	Y	grid cells	500
x-coordinate position of raw material/foragers	x	grid cells	Sources locations depending on prandom function; Forager randomly placed
y-coordinate position of raw material/foragers	y	grid cells	Sources locations depending on prandom function; Forager randomly placed
Number of agents moving about the landscape	fixed	arbitrary units	1
Toolkit size	space 100 - sumv	arbitrary units	0-100
Type of movement strategy	randomwalk	arbitrary units	equalchance; wiggling
Threshold of seeking more raw materials	threshold	arbitrary units	0-100
Raw material scenario	nrmaterials	arbitrary units	5000; 20
Source distribution on the landscape	distribution	arbitrary units	random; clustered
Probability of clustering of source locations	prandom	arbitrary units	0-1.000
Number of unique raw material sources	materialsources	arbitrary units	0-5000
Raw material type/source label if nrmaterials=20	materialtype	materialtype	0, 1, 2…20
Raw material unit from any source	i	arbitrary units	1
Quantity of material from source *i* in mobile toolkit	v_i	arbitrary units	Minimum = 0; maximum = 100
Total material of all types in mobile tool kit	sumv	arbitrary units	Minimum = 0; maximum = 100
Probability of discarding material of source *i* in toolkit	vi /Σi vi	arbitrary units	0-100
Probability of discarding materialtype in toolkit, min and max amount	∑materialtype / sumv	arbitrary units	Minimum = 0; maximum = 100
Maximum forager move length at each time step	l	grid cells	1
Distance traveled in *N* time steps; per maximum move length	N	grid cells	1

Input data: **Does the model use input from external sources such as data files or other models to represent processes that change over time?**

No

Submodels: **What, in detail, are the submodels that represent the processes listed in 'Process overview and scheduling'? What are the model parameters, their dimensions, and reference values? How were submodels designed or chosen, and how were they parameterized and then tested?**

The mobile toolkit is simulated as a vector vi where each element represents the amount of stone raw material from individual sources in the toolkit of unique type i and by raw material types denoted by materialtype. The maximum size of the toolkit is 100, and the sum of the elements of vi (Σi vi) has to be smaller or equal to 100. The amount of material added to the toolbox when a material source is encountered is 100 - Σi vi, meaning that the toolbox is filled up to the maximum capacity. Every time step one unit of material is consumed from the tool box. The probability that material source i is consumed is vi /Σi vi, meaning that it is relative to the frequency of available materials. Material sources do not deplete in the environment during the duration of the simulation. If threshold is set to <0 the forager will seek to closest raw material location if the quantity of raw material in toolkit is equal to the threshold value.

Model implementation

The model is implemented in Netlogo 5.3.1.

References

Brantingham, P. J. 2003. A Neutral Model of Stone Raw Material Procurement, *American Antiquity* 68(3): 487–509.

Grimm, V., U. Berger, D.L. DeAngelis, J.G. Polhill, J. Giske, and S.F. Railsback. 2010. The
ODD protocol: A review and first update. *Ecological Modeling* 221(23): 2760-2768.

Oestmo, S., Janssen, M.A., Marean, C.W. 2016. Testing Brantingham's Neutral Model: The Effect of Spatial Clustering on Stone Raw Material Procurement, in: Barceló, J.A., Del Castillo, F. (eds.), Simulating Prehistoric and Ancient Worlds, Springer, pp. 175-188.

APPENDIX E

E4 CODE – FLAKING EXPERIMENT

[E4]
Filename=MeasurementData.mdb
Delaytime=1
Table=MeasurementData
Re-edit=Yes
BackColor=12038291

[FlakingExperimentSample]
Type=Menu
Prompt=Is the sample from flaking experiment?
Menu=True False
Length=10

[Block]
Type=Text
Prompt=Enter Block Name or Unknown:
Length=10

[SampleType]
Type=Menu
Prompt=What is sample type?
Menu=AG WG H UT
Length=25
Comment=AG, Against the grain/against the banding
Comment=WG, With the grain/Planar with banding
Comment=H, Heat-treated
Comment=UT, Untreated

[RawMaterial]
Type=Menu
Prompt=Select the Raw Material:
Menu=Quartzite Silcrete
Length=25
Carry=True

[SampleNumber]
Type=Text
Prompt=Enter Sample Number:
Length=10
Comment=D11-1-98A-3, or Q1-WG etc

[SubSampleLetter]
Type=Text
Prompt=Enter SubSample letter:
Length=10

Comment=a,b,c and so on

[UniqueID]
Type=Numeric
Prompt=Unique Value for each sample
Length=10
Unique=True

[LithicArtifactClass]
Type=Menu
Prompt=Select the Lithic Artifact Class:
Menu=CompFlake FlakeFrag BladeBLadeFrag Shatter Core Waste
Length=25

[UnretouchedPoint?]
Type=Menu
Prompt=Is this piece a Point or Point Fragment?:
Menu=No Yes Indeterminate
Length=15
Condition1=LithicArtifactClass CompFlake FlakeFrag BladeBladeFrag

[Completeness]
Type=Menu
Prompt=Enter the Portion of the Artifact that is Present.
Menu=Complete Proximal Fragment Distal Mesial LeftLateral RightLateral ProxLeftLat ProxRightLat DistalLeftLat DistalRightLat MesialLeftLat MesialRightLat
Length=25
Condition1=LithicArtifactClass NOT CompFlake Shatter Core Waste

[CortexArea]
Type=Menu
Prompt=Enter the Estimated Cortex Area of DORSAL surface, or the entire surface of Shatter or core
Menu=0% 1-20% 21-40% 41-60% 61-80% 81-99% 100%
Length=10
Condition1=LithicArtifactClass NOT Waste

[PlatformCortex]
Type=Menu
Prompt=Is there Platform Cortex?:
Menu=No YesComplete YesPartial
Length=20
Condition1=LithicArtifactClass CompFlake OR
Condition2=Completeness Complete Proximal LeftLateral RightLateral ProxLeftLat ProxRightLat

[CortexChatterMarks]
Type=Menu
Prompt=Select whether there are Chatter Marks present, or not:
Menu=No Yes Indeterminate
Length=20
Condition1=CortexArea NOT 0% OR
Condition2=PlatformCortex YesComplete YesPartial

[CortexRoundness]
Type=Menu
Prompt=Select the Roundness of the Cortex Edges:
Menu=Angular SubangularSubrounded Rounded Indeterminate Cut
Length=20
Condition1=CortexArea NOT 0% OR
Condition2=PlatformCortex YesComplete YesPartial

[CortexLocation]
Type=Menu
Prompt=Select where the Majority of Cortex is Located:
Menu=WholeDorsal Proximal Distal Mesial LeftLateral RightLateral ProxLeftLat ProxRightLat DistalLeftLat DistalRightLat MesialLeftLat MesialRightLat Indeterminate
Length=20
Condition1=CortexArea NOT 0% AND
Condition2=LithicArtifactClass NOT Shatter Core Waste

[VisibleLuster]
Type=Menu
Prompt=Is there a Visible Heat-treatment Luster?:
Menu=Yes No Indeterminate
Length=20
Condition1=RawMaterial Silcrete

[PreHeatArea]
Type=Menu
Prompt=Enter the Estimated PreHeatTreatment Area of DORSAL surface, or the entire surface of Shatter
Menu=0% 1-20% 21-40% 41-60% 61-80% 81-99% 100%
Length=10
Condition1=RawMaterial Silcrete AND
Condition2=VisibleLuster Yes

[PlatformPreHeatSurface]
Type=Menu
Prompt=Is there a PreHeatTreatment Surface on the Platform?:
Menu=No YesComplete YesPartial
Length=20

Condition1=RawMaterial Silcrete AND
Condition2=VisibleLuster Yes AND
Condition3=LithicArtifactClass CompFlake OR
Condition4=Completeness Complete Proximal LeftLateral RightLateral ProxLeftLat ProxRightLat

[PreHeatTreatmentLocation]
Type=Menu
Prompt=Select where the Majority of PreHeatTreatment Surface is Located:
Menu=WholeDorsal Proximal Distal Mesial LeftLateral RightLateral ProxLeftLat ProxRightLat DistalLeftLat DistalRightLat MesialLeftLat MesialRightLat Indeterminate
Length=20
Condition1=RawMaterial Silcrete AND
Condition2=VisibleLuster Yes AND
Condition3=PreHeatArea NOT 0% AND
Condition4=LithicArtifactClass NOT Shatter Core HammerManuportGrindstone

[DorsalScarCount]
Type=Numeric
Prompt=Enter the Number of Dorsal Scars Greater than 6mm:
Length=5
Condition1=LithicArtifactClass NOT Shatter Core Waste Extra AND
Condition2=CortexArea NOT 100%

[DorsalDirection]
Type=Menu
Prompt=Enter the Dorsal Scar Directionality:
Menu=Radial Subradial Bidirectional Unidirectional BiOrUni Indeterminate
Length=25
Condition1=LithicArtifactClass NOT Shatter Core Waste Extra AND
Condition2=CortexArea NOT 100% AND
Condition3=DorsalScarCount NOT 0 1

[ArisOrientation]
Type=Menu
Prompt=Enter the Aris (Scar Ridge) Orientation:
Menu=Parallel Convergent Indeterminate
Length=13
Condition1=DorsalDirection Bidirectional Unidirectional BiOrUni AND
Condition2=CortexArea NOT 100% AND
Condition3=DorsalScarCount NOT 0 1 2

[ProfileShape]
Type=Menu
Prompt=Enter the Profile Shape:
Menu=Flat Curved Twisted Indeterminate

Length=13
Condition1=LithicArtifactClass CompFlake OR
Condition2=Completeness Complete Proximal LeftLateral RightLateral ProxLeftLateral ProxRightLat

[Mass]
Type=Numeric
Prompt=Enter the Mass (g):
Length=10

[MaxLength]
Type=Instrument
Prompt=Enter the Maximum Length (mm):
Length=10
Condition1=LithicArtifactClass NOT Waste

[MaxWidth]
Type=Instrument
Prompt=Enter the Maximum Width (mm):
Length=10
Condition1=LithicArtifactClass NOT Waste

[TechLength]
Type=Instrument
Prompt=Enter the Technological Length (mm):
Length=10
Condition1=LithicArtifactClass CompFlake OR
Condition2=Completeness Complete LeftLateral RightLateral

[MaxTechWidth]
Type=Instrument
Prompt=Enter the Max Technological Width (mm):
Length=10
Condition1=LithicArtifactClass CompFlake OR
Condition2=Completeness Complete Proximal Mesial

[MaxThickness]
Type=Instrument
Prompt=Enter the Max Thickness (mm):
Length=10
Condition1=LithicArtifactClass NOT Waste

[MidThickness]
Type=Instrument
Prompt=Enter the Thickness at the Midpoint (mm):
Length=10

Condition1=LithicArtifactClass CompFlake OR
Condition2=Completeness Complete LeftLateral RightLateral

[PlatformWidth]
Type=Instrument
Prompt=Enter Width of the Platform (mm):
Length=10
Condition1=LithicArtifactClass CompFlake OR
Condition2=Completeness Complete Proximal

[PlatformThickness]
Type=Instrument
Prompt=Enter Thickness of the Platform (mm):
Length=10
Condition1=LithicArtifactClass CompFlake OR
Condition2=Completeness Complete Proximal LeftLateral RightLateral ProxLeftLat ProxRightLat

[ExteriorPlatAngle]
Type=Numeric
Prompt=Enter Exterior Platform Angle (degrees):
Length=10
Condition1=LithicArtifactClass CompFlake OR
Condition2=Completeness Complete Proximal LeftLateral RightLateral ProxLeftLat ProxRightLat

[FlakeTermination]
Type=Menu
Prompt=Select the Termination Type:
Menu=Feather Hinge Step HingeOrStep PartialHingeOrStep Overshoot Indeterminate
Length=25
Comment=Feather,acute angle, sharp
Comment=Hinge,curved up towards the dorsal surface
Comment=Step,abrupt right angle break
Comment=HingeOrStep,difficult to classify as Hinge or Step, but one of the two
Comment=PartialHingeOrStep,in profile, termination hinged or stepped on the ventral side and is feathered on the dorsal side
Comment=Overshoot,preserves core relict edge or opposite platform, plunging or not plunging
Comment=Indeterminate,difficult to classify or absent
Condition1=LithicArtifactClass CompFlake OR
Condition2=Completeness Complete Distal DistalLeftLat DistalRightLat

[PlatformPrep]
Type=Menu
Prompt=Select the Platform Preparation:

Menu=NotPrepared FacetedWithBulb ResidualFacetWithoutBulb Indeterminate
Length=35
Condition1=LithicArtifactClass CompFlake OR
Condition2=Completeness Complete Proximal LeftLateral RightLateral ProxLeftLat ProxRightLat AND
Condition3=PlatFormCortex NOT YesComplete

[NumberPlatformScars]
Type=Text
Prompt=Enter the Number of Platform Scars (greater than 1 mm):
Length=4
Condition1=LithicArtifactClass CompFlake OR
Condition2=Completeness Complete Proximal LeftLateral RightLateral ProxLeftLat ProxRightLat AND
Condition3=PlatformPrep NOT NotPrepared Indeterminate

[DorsalPrep]
Type=Menu
Prompt=Select the Type of DORSAL Preparation:
Menu=None HingedRemovals LongFeatherRemovals LateralNotching Indeterminate
Length=25
Condition1=LithicArtifactClass CompFlake OR
Condition2=Completeness Complete Proximal LeftLateral RightLateral ProxLeftLat ProxRightLat

[PlatAbrasion]
Type=Menu
Prompt=Is there Platform Abrasion visible?:
Menu=No Yes Indeterminate
Length=15
Condition1=LithicArtifactClass CompFlake OR
Condition2=Completeness Complete Proximal LeftLateral RightLateral ProxLeftLat ProxRightLat

[FractureInitiationPoint]
Type=Menu
Prompt=Where is the Fracture Initiation Point Located?:
Menu=NotExpressed Centered Lateral Indeterminate
Length=15
Condition1=LithicArtifactClass CompFlake OR
Condition2=Completeness Complete Proximal

[PlatformDelineation]
Type=Menu
Prompt=Select the Platform Delineation with the Ventral Surface?:

Menu=RegCurve OverhangCurveNoBreak OverhangCurveBreak Double Rectillinear Indeterminate
Length=20
Comment=RegCurve,platform on same plane as flake and bulb
Comment=OverhangCurveNoBreak,platform plane is more dorsal than rest of flake, delineation between platform and ventral surface is smooth
Comment=OverhangCurveBreak,delineation has a bump that sticks out where percussion point is
Comment=Double,there are two obvious percussion points
Comment=Rectillinear,delineation is not curved, but straight line
Comment=Indeterminate,difficult to classify
Condition1=LithicArtifactClass CompFlake OR
Condition2=Completeness Complete Proximal LeftLateral RightLateral ProxLeftLat ProxRightLat

[FissuringOnPlatform]
Type=Menu
Prompt=Select the Type of Fissuring, if any, on the Platform at the Percussion Point:
Menu=None CompleteFissure PartialFissure Indeterminate
Length=20
Condition1=LithicArtifactClass CompFlake OR
Condition2=Completeness Complete Proximal LeftLateral RightLateral ProxLeftLat ProxRightLat

[MarksVentralSurface]
Type=Menu
Prompt=Select the Type of Marks on the Ventral Surface, if any:
Menu=None RipplesUndulations ShatteredBulb HertzianCone Crushing Indeterminate
Length=18
Condition1=LithicArtifactClass CompFlake OR
Condition2=Completeness Complete Proximal LeftLateral RightLateral ProxLeftLat ProxRightLat

[Lipping]
Type=Menu
Prompt=Select the Size of Lip, if present:
Menu=NoLip SmallOrPartialLip LargeContinuousLip Indeterminate
Length=18
Condition1=LithicArtifactClass CompFlake OR
Condition2=Completeness Complete Proximal LeftLateral RightLateral ProxLeftLat ProxRightLat

[Bulb]
Type=Menu
Prompt=Is there a Bulb Visible?:
Menu=No Yes Indeterminate

Length=13
Condition1=LithicArtifactClass CompFlake OR
Condition2=Completeness Complete Proximal LeftLateral RightLateral ProxLeftLat ProxRightLat

[BulbLength]
Type=Instrument
Prompt=Enter the Length of the Bulb (mm):
Length=10
Condition1=Bulb Yes

[PlatformMorphology]
Type=Menu
Prompt=Select Platform Morphology:
Menu=NarrowLinear QuadrangularTrapezoid OvularOrTriangular NarrowCurved Punctiform ChapeauDeGendarme Indeterminate
Length=21
Condition1=LithicArtifactClass CompFlake OR
Condition2=Completeness Complete Proximal LeftLateral RightLateral ProxLeftLat ProxRightLat

[BandingOrientation]
Type=Menu
Prompt=How is the Axis of Percussion Oriented with respect to Visible Banding, if present?
Menu=NoBandingVisible With Through Oblique Against Indeterminate
Length=16
Comment=NoBandingVisible,NoBandingVisible - no bands are visible
Comment=With,With - bands will be visible on dorsal and ventral surfaces and parallel to flaking axis
Comment=Through,Through - bands are mainly visible in side view and run parallel to the flaking axis
Comment=Oblique,Oblique - bands are visible on the dorsal and ventral surfaces and are diagonal to the flaking axis
Comment=Against,Against - bands are visible on dorsal and lateral surfaces and are perpendicular to flaking axis
Comment=Indeterminate,Indeterminate - banding visible but difficult to interpret relationship to flaking axis
Condition1=RawMaterial Quartzite AND
Condition2=LithicArtifactClass CompFlake OR
Condition3=Completeness Complete Proximal Distal LeftLateral RightLateral ProxLeftLat ProxRightLat DistalLeftLat DistalRightLat MesialLeftLat MesialRightLat

[Comments]
Type=Text
Prompt=Enter Other Notes:

Length=50

[KyleComments]
Type=Text
Prompt=Enter Kyle Text from artifacts
Length=10

[CuttingEdgeLength]
Type=Numeric
Prompt=Enter the Cutting Edge Length (mm):
Length=10
Condition1=LithicArtifactClass Not Core Waste